

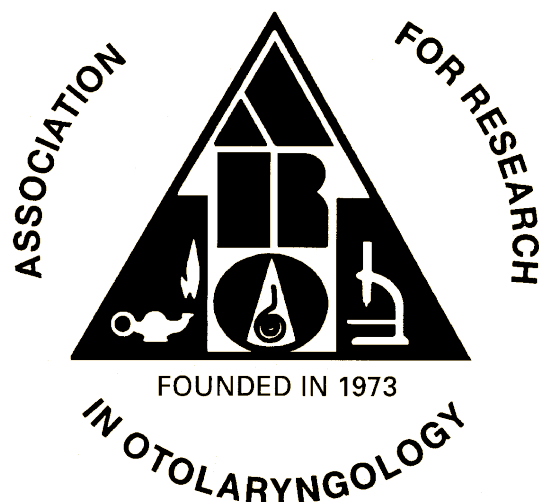
**ABSTRACTS OF THE THIRTY-FIFTH ANNUAL  
MIDWINTER RESEARCH MEETING**

# **ASSOCIATION FOR RESEARCH IN OTOLARYNGOLOGY**



February 25-29, 2012  
The Manchester Grand Hyatt Hotel  
San Diego, California, USA

**ABSTRACTS OF THE THIRTY-FIFTH ANNUAL  
MIDWINTER RESEARCH MEETING  
OF THE**



**February 25-29, 2012**

**San Diego, California, USA**

**Peter A. Santi, PhD**

*Editor*

Association for Research in Otolaryngology  
19 Mantua Road, Mt. Royal, NJ 08061 USA

## CONFERENCE OBJECTIVES

After attending the Scientific Meeting participants should be better able to:

1. Understand current concepts of the function of normal and diseased ears and other head and neck structures.
2. Understand current controversies in research methods and findings that bear on this understanding.
3. Understand what are considered to be the key research questions and promising areas of research in otolaryngology.

ISSN-0742-3152

The *Abstracts of the Association for Research in Otolaryngology* is published annually and consists of abstracts presented at the Annual MidWinter Research Meeting. A limited number of copies of this book and previous books of abstracts (1978-2011) are available.

Please address your order or inquiry to:  
**Association for Research in Otolaryngology**  
19 Mantua Road  
Mt. Royal, NJ 08061 USA

**General Inquiry**  
Phone (856) 423-0041 Fax (856) 423-3420  
E-Mail: [headquarters@aro.org](mailto:headquarters@aro.org)

**Meetings**  
E-Mail: [meetings@aro.org](mailto:meetings@aro.org)

This book was prepared from abstracts that were entered electronically by the authors. Authors submitted abstracts over the World Wide Web using Mira Digital Publishing's PaperCutter™ Online Abstract Management System. Any mistakes in spelling and grammar in the abstracts are the responsibility of the authors. The Program Committee performed the difficult task of reviewing and organizing the abstracts into sessions. The Program Committee Chair, Dr. Lawrence R. Lustig and the President, Dr. Debara L. Tucci constructed the final program. Mira electronically scheduled the abstracts and prepared Adobe Acrobat pdf files of the Program and Abstract Books. These abstracts and previous years' abstracts are available at: <http://www.aro.org>.

Citation of these abstracts in publications should be as follows:  
**Authors, year, title, Assoc. Res. Otolaryngol. Abs.: page number.**

For Example:

Eiju Kanagawa, 2012, Action of Substance P on the Recovery from the Acoustic Trauma. Abs.: 973.



### General Chair

Debara L. Tucci, MD (2011-2012)

### Program Organizing Committee

Lawrence R. Lustig, MD, Chair (2012-2014)  
Jeffrey R. Holt, PhD (2010-2012)  
Bohua Hu, PhD (2010-2012)  
Jeremy Gene Turner, PhD (2010-2012)  
Keiko Hirose, MD (2011-2013)  
Stefan Heller, PhD (2011-2013)  
Steve D.M. Brown, PhD (2011-2013)  
Alec N. Salt, PhD (2011-2013)  
Douglas Oliver, PhD (2011-2013)  
Yale E. Cohen, PhD (2012-2014)  
Lisa L. Hunter, PhD (2012-2014)  
Ruth Y. Litovsky, PhD (2012-2014)  
Gay R. Holstein, PhD (2012-2014)  
Julie Arenberg Bierer, PhD (2012-2014)  
Council Liaison: Lawrence R. Lustig, MD (2011-2014)  
spARO Representative: Thomas Welch

### Program Publications

Peter A. Santi, PhD, Editor (2009-2012)

### Animal Research Committee

Rickie R. Davis, PhD, Chair (2011-2013)  
Byung Yoon Choi, MD, PhD (2010-2012)  
Saima Riazuddin, PhD (2011-2013)  
Suhred M. Rajguru, PhD (2011-2013)  
Robert Keith Duncan, PhD (2012-2014)  
Sherri Marie Jones, PhD (2012-2014)  
Edward Lobarinas, PhD (2012-2014)  
Karen S. Pawlowski, PhD (2012-2014)  
Sorosh G. Sadeghi (2012-2014)  
Council Liaison: Peter A. Santi, PhD (2010-2012)  
spARO Representative: Ann Hickox

### Award of Merit Committee

M. Charles Liberman, PhD, Chair (2011-2013)  
Robert D. Frisina, PhD (2010-2012)  
Robert V. Shannon, PhD (2011-2013)  
Peter G. Gillespie, PhD (2011-2013)  
Judy R. Dubno, PhD (2011-2013)  
Karen B. Avraham, PhD (2012-2014)  
Jeffrey T. Corwin, PhD (2012-2014)  
Dan H. Sanes, PhD (2012-2014)  
Council Liaison: David J. Lim, MD (2010-2012)

### Diversity & Minority Affairs Committee

Howard W. Francis, MD, Chair (2011-2013)  
Catherine E. Carr, PhD (2010-2012)  
Diana I. Lurie, PhD (2010-2012)  
Neeliyath A. Ramakrishnan, PhD (2011-2013)  
Raju Metherate, PhD (2011-2013)  
Xiaorui Shi, MD, PhD (2011-2013)  
Dwayne D. Simmons, PhD (2012-2014)  
Avril Gene Holt, PhD (2012-2014)  
Frank Lin, M.D. PhD (2012-2014)  
Peter S. Steyger, PhD (2012-2014)  
Council Liaison: Dan H. Sanes, PhD (2011-2012)  
spARO Representative: Yoojin Chung, PhD

### External Relations Committee

Anne Luebke, PhD, Chair (2009-2014)  
Carey D. Balaban, PhD, Chair (2012-2014)  
Anna Lysakowski, PhD (2011-2014)  
Mario A. Svirsky, PhD (2011-2014)  
Charles Limb, MD (2011-2014)  
Paul D. Allen, PhD (2011-2014)  
spARO Representative: Adrian KC Lee

### Finance Committee

Dennis R. Trune, PhD, MBA, Chair (2010-2013)  
Jean Luc Puel, PhD (2011-2013)  
Steven Wan Cheung, MD (2011-2013)

### **International Committee**

Robert K. Shepherd, PhD, Australia, Chair (2012-2014)  
Joong Ho Ahn, MD, PhD (Korea), (2010-2012)  
Khalid M. Khan, PhD (Kuwait), (2010-2012)  
Rodrigo Martinez Monedero, MD (Spain), (2010-2012)  
Azal Zine, PhD (France), (2011-2013)  
Deniz Baskent, PhD (Netherlands), (2011-2013)  
Goran Laurell, MD (Sweden), (2011-2013)  
W. Wiktor Jedrzejczak (Poland), (2011-2013)  
James Fallon, PhD (Australia), (2011-2013)  
Takayuki Nakagawa, MD, PhD (Japan), (2012-2014)  
Tatsuya Yamasoba, MD, PhD (Japan), (2012-2014)  
M'hamed Grati, Eng., Ph.D. (USA), (2012-2014)  
Council Liaison: Robert K. Shepherd, PhD (2011-2014)  
spARO Representative: Simon Jones, PhD

### **JARO Editorial Board**

Paul B. Manis, PhD, Editor-in-Chief (2011-2016)  
Barbara G. Shinn-Cunningham, PhD (2009-2012)  
Laurence O. Trussell, PhD (2009-2012)  
Stefan Heller, PhD (2009-2012)  
John C. Middlebrooks, PhD (2009-2012)  
Charles C. Della Santina, MD, PhD (2009-2012)  
Tobias Moser, MD (2009-2012)  
Cythia F. Moss, PhD (2009-2012)  
Robert P. Carlyon, PhD (2010-2012)  
Laurel H. Carney, PhD (2010-2013)  
Nigel P. Cooper, PhD (2010-2013)  
Jennifer Melcher, PhD (2010-2013)  
Sunil Puria, PhD (2010-2013)  
Anthony J. Ricci, PhD (2010-2013)

### **Long Range Planning Committee**

Karina S. Cramer, PhD, Chair (2012-2014)  
Carey D. Balaban, PhD (2010-2012)  
Charley C. Della Santina, MD, PhD (2010-2012)  
Michael Anne Gratton, PhD (2010-2012)  
Steven H. Green, PhD (2011-2014)  
Andrej Kral, MD, PhD (2011-2013)  
Lina A. Reiss, PhD (2011-2013)  
Edwin W. Rubel, PhD (2012-2014)  
Konstantina M. Stankovic, MD, PhD (2012-2014)  
Council Liaison: Karina S. Cramer, PhD (2012-2014)  
President Elect: John C. Middlebrooks, PhD (2011-2012)  
International Committee Chair: Robert K. Shepherd (2011-2014)  
spARO Representative: Jasmine M. Grimsley, PhD

### **Membership Committee**

Colleen Garbe Le Prell, PhD, Chair (2012-2014)  
Stephane F. Maison, PhD (2010-2012)  
Mitsuya Suzuki, MD (2010-2012)  
spARO Representative: Jazz Bailey, PhD

### **Nominating Committee**

Karen B. Avraham, PhD, Chair (2011-2012)  
Karen Jo Doyle, MD, PhD (2011-2012)  
Anne E. Luebke, PhD (2011-2012)  
Leonard P. Rybak, MD, PhD (2011-2012)  
Joseph R. Santos-Sacchi, PhD (2011-2012)

### **Publications Committee**

Anil K. Lalwani, MD, Chair (2011-2013)  
Doris Kar-Wah Wu, PhD (2010-2012)  
Ana Belen Elgoyhen, PhD (2010-2012)  
John J. Galvin (2010-2012)  
Anil K. Lalwani, MD (2010-2012)  
Philip X. Joris, MD, PhD (2011-2013)  
Alan R. Palmer, PhD (2011-2013)  
Paul B. Manis, PhD (2011-2013)  
Elizabeth S. Olson, PhD (2011-2013)  
Paul A. Fuchs, PhD (2011-2013)  
Susan E. Shore, PhD (2012-2014)  
Thomas B. Friedman, PhD (2012-2014)  
Charles J. Limb, MD (2012-2014)  
JARO Editor: Paul B. Manis, PhD, ex officio  
Springer Representative: Ann Avouris, ex officio

*Secretary / Treasurer:* John P. Carey, MD, *ex officio*

*Council Liaison:* Peter A. Santi, PhD (2011-2012)

*spARO Representative:* Stephen David, PhD

*Springer Representative:* Ann Avouris, *ex officio*

*Secretary/Treasurer:* Karen Jo Doyle, MD, PhD, *ex officio*

*Council Liaison:* Peter A. Santi, PhD (3/10-2/11)

*spARO Representative:* Stephen David, PhD

### **Travel Awards**

Marlan R. Hansen, MD, *Chair* (2008-2014)  
Zubair M. Ahmed, PhD (2010-2012)  
Simone Kurt, PhD (2010-2012)  
Shu-Chen Peng, PhD (2010-2012)  
Daniel Lee, MD (2010-2012)  
Anh Nguyen-Huynh, MD, PhD (2010-2012)  
Alec N. Salt, PhD (2010-2012)  
Ronna P. Hertzano, MD, PhD (2011-2013)  
Alexander A. Spector, PhD (2011-2013)  
Dianne Durham, PhD (2012-2014)  
Avril Genee Holt, PhD (2012-2014)  
Yunxia Wang Lundberg, PhD (2012-2014)  
Yehoash Raphael, PhD (2012-2014)  
*spARO Representative:* Judith S. Kempfle, MD



## President's Message 2012

Welcome back to the West Coast and San Diego! We anticipate that the Manchester Grand Hyatt will be a great venue for the 35th Annual MidWinter Meeting of the Association for Research in Otolaryngology. The latest basic science, clinical and translational research will be presented and discussed in symposia, workshops, podiums and poster sessions over a period of five days. The list of symposia includes: Current Theories About the Generation of Otoacoustic Emissions and the Clinical Implications; Mechanisms and Circuitry Underlying Auditory Spectrotemporal Integration; Molecular Anatomy and Physiology of the Ribbon Synapse; New Insights on Vestibular Neuropharmacology: From Bench to Bedside; Real-World Hearing: Neural Coding and Perception; The Spiral Ganglion: Neurogenesis and Concepts for Regeneration; The Yin and Young of Sound Localization; Using Massively-Parallel Next Generation Sequencing Techniques to Advance Studies and Clinical Cares of Hearing Loss; and Vestibular Psychophysics. **Podium sessions** will include Auditory Prosthesis; External & Middle Ear Mechanics; Otoacoustic Emissions; Development; Basic Vestibular Research; Genetics; Inner Ear: Hair Cells: Hair Bundles & Mechanotransduction; Inner Ear Damage and Prevention; Regeneration; and Psychophysics: Auditory Attention, Masking and Segregation. Last but not least, a number of **workshops** will provide us with the latest technology and experimental techniques in our field: Interactive Workshop on 3D Reconstruction of the Ear; Facing Animal Rights Extremism: A Community Response; and Training/Career Development, as well as an Early Stage/New Investigator workshop.

We will open the meeting on Saturday morning with the **Presidential Symposium** titled "Listening with the Brain: Cochlear Implants and Central Auditory System Plasticity," with presentations by some of our most esteemed members and leaders in this field of research. The **Welcome Get-Together** will again be sponsored in part by Springer. Please join us at the ARO **Business Meeting** on Sunday evening, where an update of ARO events, honors and plans for the future will be discussed. This is an opportunity to be part of this wonderful organization and play a role in its activities. An added bonus will be the scavenger hunt; this year we will again be giving away gifts including an iPad, iPod Touch, and Amex Gift cards.

Join us for the **Presidential Lecture and Awards Ceremony** to honor the Award of Merit winner, David P. Corey. Dr. Corey will be introduced by Jeffrey R. Holt, followed by his lecture entitled "**Molecular Mechanics of the Transduction Apparatus in Hair Cells**" and the **Awards and Honors Reception**.

Graduate students and post-docs – don't forget to attend the spARO Town Hall and be part of this group and learn more about their activities at ARO.

Contributions from so many dedicated members make ARO the wonderful organization that it is. Our many committee members make ARO 'tick' and we thank you for your efforts, both during the year and at the meeting. We are thankful to the American Academy of Otolaryngology – Head and Neck Surgery Foundation, Hearing Health Foundation, American Academy of Audiology Foundation, and the Collegium Oto-Rhino-Laryngologicum Amicitiae Sacrum – US Group, Inc. for their donations to allow more students and fellows to attend the meeting with travel funds. We also thank the exhibitors for helping support the many activities of the meeting. In addition we thank the National Institute on Deafness and Other Communication Disorders of the National Institutes of Health for making the meeting possible. Also, a special note of thanks goes to Talley Management Group, for their superb administration of the meeting.

When you find some free time, head downtown to San Diego's Gaslamp District which is not far from the Manchester Grand Hyatt. There you will find shopping, restaurants and wine bars, and some of the finest craft beer selections around. Our parting social event will again be the Hair Ball, this year with the band *Hot Pursuit*, who were voted #1 out of 75 local bands in the San Diego area by residents. Bring your dancing shoes and watch your colleagues in another mode.

We continue to want your input to make the ARO MidWinter Meeting the best and most scientifically important meeting of the year. This meeting gives us the opportunity to be exposed to the cutting-edge research being performed in our field, interact with our colleagues, and meet old and new friends. The impact of ARO goes well beyond the meeting, to include its own journal, JARO, the leading journal in the subject category Otorhinolaryngology, and we encourage you to continue to send your exciting results for submission. And finally, be sure to check out the ARO website, which functions as a resource to members throughout the year.

I thank you for giving me the opportunity to chair my absolute favorite meeting of the year and for the privilege to have led this organization.

Debara L. Tucci  
President



**David P. Corey**  
**2012 Award of Merit Recipient**

## David P. Corey

### 2012 Recipient of the ARO Award of Merit

The Association for Research in Otolaryngology has chosen to honor David Paul Corey with the 2012 Award of Merit. This is a wonderful and obvious choice: David's scientific, intellectual, community service and mentoring contributions to Research in Otolaryngology have benefited both the field of auditory research and the ARO. David's research has advanced our field with numerous fundamental discoveries. In each case they exemplify the highest standards for quality scientific research. But David's discoveries extend beyond our immediate field and his work has contributed to many areas in the broader neuroscience community. David has also served as spokesman and broadly shared the praises and progress of our field bringing new attention and funding to the field. For all these reasons the society and its members have chosen to honor and thank David Corey for his invaluable contributions to our collective progress.

David's scientific career was launched at Amherst College in Massachusetts. At Amherst, David majored in physics (BA, 1974) honing his keen quantitative approach and indulging his passion for tinkering with scientific equipment. Unfulfilled with physics, however, David thought neuroscience might be interesting, and without introduction called Torsten Wiesel at Harvard Medical School to see if he might have an open technician job. Wiesel did not, but referred David to Ann Stuart's lab where David began his research career as a lab technician. This was an extraordinary break, because it connected David with both a field (sensory neuroscience) and an institution (Harvard Medical School) to which he would dedicate much of his career. It also introduced him to Jim Hudspeth, who was in Ann's laboratory and who was about to take a faculty job at Caltech, and who in turn introduced David to hair cells. David followed Jim to Caltech as a graduate student, and together they did pioneering physiology on single hair cells with direct mechanical stimulation. Caltech was also a hothouse for neuroscience, and a number of David's classmates and postdoctoral colleagues have become distinguished neuroscientists, including Steve Block, Ruth Anne Eatock, Steve Green, Eric Knudsen, Rich Lewis, Dan Margoliash, John Maunsell, and Bill Newsome. David thrived in this rich environment, working side by side with Jim, all while continuing to develop the equipment needed for the new experimental approach. Jim Hudspeth writes: "David was developing extracellular recordings, the basis of the 1983 papers on kinetics, for his thesis project: he proceeded from voltage recordings to voltage-clamped current recordings, then made the system more elaborate with series-resistance compensation, advanced piezoelectrical-bimorph stimulators, peeling of the otolithic membrane to isolate bundles of a common orientation, an elaborate perfusion system, and temperature control. Although I goaded him from time to time to get on with actually acquiring data, he persisted in gilding the lily with ever-more-elaborate technical nuances. Anyway, the end result was a spectacular success -- the basis of the gating-spring model and description of adaptation -- that thoroughly justified his effort" (Corey and Hudspeth, *J Neurosci*, 1983a,b).

While the significance of David's thesis work in Jim Hudspeth's lab is broadly recognized, it extends well beyond inner ear physiology. At that time, the notions of voltage-gated and ligand-gated ion channels were well established. But David and Jim were the first to present clear evidence for direct activation of a novel class of ion channels, those gated by mechanical force. David's hand-built equipment enabled the first measurements of the microsecond activation kinetics of hair-cell transduction. Based on the incredible speed -- far too fast for the second messenger cascades that typify phototransduction -- they proposed direct activation of mechanosensitive ion channels, and David developed an explicit biophysical theory for the gating. This provocative idea now forms the foundation of the broader field of mechanotransduction, which underlies not just auditory and vestibular transduction but also our senses of touch, proprioception, blood pressure regulation, and osmosensation. David graduated from Caltech in 1980 with seven publications, an impressive graduate career.

David then moved to Yale University to join Chuck Stevens as a post-doctoral fellow, where he continued to develop instrumentation. In Chuck's lab, David studied voltage-gated sodium and calcium channels (Aldrich, Corey and Stevens, *Nature*, 1983), but his major contribution may have been to help develop and teach the new field of patch clamping. He designed a patch clamp amplifier and a computer interface for minicomputers, both commercialized, and he directed the first Single-Channel Recording Course at Cold Spring Harbor.

David moved back to Boston to set up his own lab in 1984 at Massachusetts General Hospital and Harvard Medical School and was appointed an Assistant Investigator with the Howard Hughes Medical Institute. Although David's lab was primarily focused on hair cells, he allowed trainees the flexibility that Hudspeth had given him. David had a knack for attracting exceptional people and the wisdom to let them run with their own ideas. In many cases work in areas outside of hearing formed the foundation of a number of stellar careers which further extended David's influence on the broader field of neuroscience. Notable among these are Ben Barres, now Chair of Neurobiology at Stanford Medical School (glial cell physiology); Steve Cannon, past Chair of Neurology, UT Southwestern (sodium channels in inherited neurological disorders); Walter Koroshetz, deputy director of the National Institute of Neurological Disorders and Stroke (excitatory synapses); Emily Liman, Associate Professor of Neuroscience, USC (vomeronasal sensation); and Jaime García-Añoveros and Anne Duggan, Associate Professors of Neuroscience at Northwestern (ASIC channels in touch sensation).

Although these successes in related fields may have been tempting, David's passion for hair cell mechanotransduction has remained steadfast for 35 years, as evidenced by over 100 publications in journals such as *Cell*, *Nature*, *Science*, *Nature Neuroscience*, *Neuron*, *Journal of Neuroscience*, *the Biophysical Journal* and others. Among the numerous contributions to come from David's lab are the quantitative model for slow adaptation in vestibular hair cells (Assad and Corey, *J Neurosci*,

1992) followed by confirmation of myosin-1c as the slow adaptation motor (Holt et al., *Cell*, 2002); the discovery that removing  $\text{Ca}^{2+}$  simultaneously cuts tip links and abolishes mechanosensitivity (Assad et al., *Neuron*, 1991), followed later by the crystal structure of the tip-link protein cadherin-23 and finally the calcium-sensitive interface between cadherin-23 and protocadherin-15 (Sotomayor et al., *Neuron*, 2010); presentation of TRPA1 as a hair-cell transduction candidate (Corey et al., *Nature*, 2004), which—though not validated—was followed by work revealing several novel functions of TRPA1 (Kwan et al., *Neuron*, 2006; Kwan et al., *J. Neurosci*, 2009; Macpherson et al., *J. Neurosci*, 2007; Shigetomi et al., *Nat. Neurosci*, 2011); ten papers on cloning, identification and localization of unconventional myosins in hair cells (including Berg et al., *J. Cell Sci*, 2000; Garcia et al., *J. Neurosci*, 1998; Hasson et al., *JCB*, 1997; Solc et al., 1994) and numerous studies focused on biophysical characterization of hair-cell transduction and adaptation (Assad et al., *PNAS*, 1989; Cheung and Corey, *Biophysical J*, 2006; Holt et al., *J. Neurosci*, 1997; Shepherd and Corey, *J. Neurosci*, 1994;). Collectively, the publications from David's lab are of the highest quality, the writing is crystal clear, they generate vast numbers of citations (>10,000 to date), the work is well respected by colleagues and competitors alike and they form a foundation for the entire field of hair cell physiology.

David's excellent scientific guidance and superb mentoring skills catapulted the careers of numerous Corey Lab members, many of whom continue to work on hair cells. Past trainees include John Assad, Professor, Harvard Medical School; Gordon Shepherd, Jr., Associate Professor, Northwestern University; Zheng-Yi Chen, Associate Professor, Mass Eye and Ear Infirmary / Harvard Medical School; Heidi Rehm, Director of the Harvard Medical School Center for Hereditary Deafness; Jeffrey Holt, Associate Professor, Children's Hospital / Harvard Medical School; Gwenaëlle Géléoc, Assistant Professor, Children's Hospital / Harvard Medical School; Shuh-Yow Lin, Assistant Professor, UCSD; Melissa Vollrath, Assistant Professor, McGill University; and others.

Beyond David's direct scientific influences are many less tangible but also highly significant contributions. These include leadership roles as the Chair of Neurobiology at Harvard Medical School and service in the Biophysical Society, Society for General Physiologists, Society for Neuroscience and of course, ARO. In addition, David has played a major role in organizing a number of scientific meetings and symposia like the Molecular Biology of Hearing and Deafness meeting, the first Force-Gated Channels meeting, and an upcoming Mechanics of Hearing meeting. For someone who does not really enjoy attention, he seems to have a special interest in getting other people together to talk about science! David has also served critically important roles in guiding new funding to the field as a member of the advisory council at NIDCD and recently as chief liaison for the Bertarelli Program in Translational Neuroscience at Harvard Medical School.

Despite all the brilliant technical achievements, all the stellar publications, all the high praise and honors and all the transformative community service, when you ask anyone who has ever worked in David Corey's lab about their experience, you will first hear that David is the nicest, warmest, most supportive and best advisor they have ever had. The richness of David's character and his unwavering support for his trainees are universally recognized and appreciated. His trainees have noted: "David was incredibly generous and supportive in allowing me to pursue whatever scientific problems I was most passionate about" - Emily Liman. "David worked with us till the wee hours of the night and then went to the machine shop to make us an emergency replacement recording chamber when our first one failed. He likes to be a part of the science and has great enthusiasm for it" - Melissa Vollrath. "David taught me to always go to the heart of the question and not fiddle around the outsides" - Walter Koroshetz. "We know David as an outstanding scientist but it is important to remember his kindness and his extreme respect for coworkers - Valeria Piazza. "He is an excellent mentor and friend with great vision, virtue, integrity, and generosity. He recognizes everyone's strengths and tries his best to help us establish a scientific career. He is always supportive and his advice is always valuable." - Jun Shen. "I have many fond memories of David. First and foremost, he is an outstanding citizen in the scientific community and is amazingly generous in these competitive times"- Steve Cannon. "David represents the best characteristics you could ask for in a mentor. He always has your best interest as his priority. David is also the most talented teacher I have ever encountered: he has a fantastic ability to explain complicated issues"- Zheng-Yi Chen. "He's not just a good teacher - his enthusiasm is infectious" - Eunice Cheung. "The luckiest thing that ever happened to me in my life was having David Corey as a Ph.D. advisor and mentor" - Ben Barres. Colleagues echo these sentiments: "David is extraordinarily generous with his time and talents, often providing not just valued counsel but material help." - Ruth Anne Eatock.

Whether you are a close colleague or a peripheral admirer, David's sphere of influence is wide and he has benefited us all. The ARO and science in general are better off because of David Corey. For all these reasons and more, David Paul Corey has been selected as a most fitting recipient of the 2012 ARO Award of Merit.

JEFFREY R. HOLT

# Association for Research in Otolaryngology

Executive Offices

19 Mantua Road • Mt. Royal, New Jersey 08061

Phone: (856) 423-0041 • Fax: (856) 423-3420

Email: meetings@aro.org

## *ARO Officers for 2011-2012*

**President: Debara L. Tucci, MD (2011-2012)**

Duke University Medical Center  
Division of Otolaryngology-HNS  
Durham, NC 27710

**Secretary/Treasurer: John P. Carey, MD (2011-2014)**

Johns Hopkins School of Medicine  
Department of Otolaryngology-HNS  
601 North Caroline Street, Room 6255  
Baltimore, MD 21287-0910

**President Elect: John C. Middlebrooks, PhD (2011-2012)**

University of California at Irvine  
Department of Otolaryngology  
Irvine, CA 92697-5310

**Editor: Peter A. Santi, PhD (2009-2012)**

University of Minnesota  
Dept. of Otolaryngology  
Lions Research Building, Room 121  
2001 Sixth Street, SE  
Minneapolis, MN 55455

**Past President: Karen B. Avraham, PhD (2011-2012)**

Tel Aviv University,  
Sackler School of Medicine  
Dept. of Human Molecular Genetics &  
Biochemistry  
Ramat Aviv  
Tel Aviv 69978, Israel

**Historian: David J. Lim, MD**

House Ear Institute  
2100 W. Third Street, Fifth Floor  
Los Angeles, CA 90057

## *Council Members*

**Robin L. Davis, PhD (2009-2012)**

Rutgers University  
Cell Biology & Neuroscience  
604 Allison Road  
Piscataway, NJ 08854-8082

**Ruth Litovsky, PhD (2011-2014)**

University of Wisconsin  
Waisman Center 521  
1500 Highland Avenue  
Madison, WI 53705

**Dan H. Sanes, PhD (2010-2013)**

New York University  
Center for Neural Science  
4 Washington Place  
New York, NY 10003

# Association for Research in Otolaryngology

## Executive Offices

19 Mantua Road, Mt. Royal, NJ 08061 USA

Phone: (856) 423-0041 Fax: (856) 423-3420

E-Mail: [headquarters@aro.org](mailto:headquarters@aro.org)

Meetings E-mail: [meetings@aro.org](mailto:meetings@aro.org)

## Past Presidents

1973-74 David L. Hilding, MD  
1974-75 Jack Vernon, PhD  
1975-76 Robert A. Butler, PhD  
1976-77 David J. Lim, MD  
1977-78 Vicente Honrubia, MD  
1978-80 F. Owen Black, MD  
1980-81 Barbara Bohne, PhD  
1981-82 Robert H. Mathog, MD  
1982-83 Josef M. Miller, PhD  
1983-84 Maxwell Abramson, MD  
1984-85 William C. Stebbins, PhD  
1985-86 Robert J. Ruben, MD  
1986-87 Donald W. Nielsen, PhD  
1987-88 George A. Gates, MD  
1988-89 William A. Yost, PhD  
1989-90 Joseph B. Nadol, Jr., MD  
1990-91 Ilsa R. Schwartz, PhD  
1991-92 Jeffrey P. Harris, MD, PhD  
1992-93 Peter Dallos, PhD  
1993-94 Robert A. Dobie, MD  
1994-95 Allen F. Ryan, PhD  
1995-96 Bruce J. Gantz, MD  
1996-97 M. Charles Liberman, PhD  
1997-98 Leonard P. Rybak, MD, PhD  
1998-99 Edwin W. Rubel, PhD  
1999-00 Richard A. Chole, MD, PhD  
2000-01 Judy R. Dubno, PhD  
2001-02 Richard T. Miyamoto, MD  
2002-03 Donata Oertel, PhD  
2003-04 Edwin M. Monsell, MD, PhD  
2004-05 William E. Brownell, PhD  
2005-06 Lloyd B. Minor, MD  
2006-07 Robert V. Shannon, PhD  
2007-08 P. Ashley Wackym, MD  
2008-09 Paul A. Fuchs, PhD  
2009-10 Steven Rauch, MD  
2011-12 Karen B. Avraham, PhD

## Award of Merit Recipients

1978 Harold Schuknecht, MD  
1979 Merle Lawrence, PhD  
1980 Juergen Tonndorf, MD  
1981 Catherine Smith, PhD  
1982 Hallowell Davis, MD  
1983 Ernest Glen Wever, PhD  
1984 Teruzo Konishi, MD  
1985 Joseph Hawkins, PhD  
1986 Raphael Lorente de Nó, MD  
1987 Jerzy E. Rose, MD  
1988 Josef Zwislocki, PhD  
1989 Áke Flóck, PhD  
1990 Robert Kimura, PhD  
1991 William D. Neff, PhD  
1992 Jan Wersäll, PhD  
1993 David Lim, MD  
1994 Peter Dallos, PhD  
1995 Kirsten Osen, MD  
1996 Ruediger Thalmann, MD & Isolde Thalmann, PhD  
1997 Jay Goldberg, PhD  
1998 Robert Galambos, MD, PhD  
1999 Murray B. Sachs, PhD  
2000 David M. Green, PhD  
2001 William S. Rhode, PhD  
2002 A. James Hudspeth, MD, PhD  
2003 David T. Kemp, PhD  
2004 Donata Oertel, PhD  
2005 Edwin W. Rubel, PhD  
2006 Robert Fettiplace, PhD  
2007 Eric D. Young, PhD  
2008 Brian C. J. Moore, PhD  
2009 M. Charles Liberman, PhD  
2010 Professor Ian Russell  
2011 Robert V. Shannon, PhD  
2012 David P. Corey

# Table of Contents

Abstract Number

## Presidential Symposium

A:	Presidential Symposium: Listening With The Brain: Cochlear Implants and Central Auditory System Plasticity .....	1-5
----	--	-----

## Symposium

B:	The Spiral Ganglion: Neurogenesis and Concepts for Regeneration.....	6-11
----	--	------

## Podium

C:	Auditory Prosthesis .....	12-24
D:	External & Middle Ear Mechanics & Otoacoustic Emissions .....	25-37

## Poster

E1	Basic Vestibular Research I.....	38-61
E2	Clinical Vestibular I .....	62-71
E3	Aging: Human Studies .....	72-81
E4	Tinnitus: Auditory Cortex .....	82-88
E5	Speech: Physiology and Production .....	89-94
E6	Otoacoustic Emissions I.....	95-102
E7	Psychophysics: Complex Listening Environments and Echoes .....	103-113
E8	Sound Localization: Coding of Spatial Cues .....	114-123
E9	External & Middle Ear Mechanics I .....	124-134
E10	Inner Ear Physiology I.....	135-149
E11	Inner Ear: Damage: Methods for Inner Ear Research.....	150-157
E12	Inner Ear: Damage: Ototoxicity: Prevention .....	158-165
E13	Inner Ear: Genetic and Clinical Pathology .....	166-179
E14	Inner Hair: Hair Cells: Outer Hair Cells & Prestin .....	180-195
E15	Inner Ear: Mechanics: Models .....	196-208
E16	Auditory Pathways: Brainstem: Binaural .....	209-212
E17	Auditory Pathways: Brainstem: Development.....	213-216
E18	Auditory Pathways: Brainstem: Evoked Potentials.....	217-225
E19	Auditory Pathways: Brainstem: Hearing Loss.....	226-236
E20	Auditory Pathways: Brainstem: Mechanisms .....	237-246
E21	Auditory Pathways: Brainstem: Morphology .....	247-250
E22	Auditory Pathways: Brainstem: Plasticity.....	251-255

## NIDCD Workshops

F1	Training/Career Development Workshop .....	256
F2	Early Stage/New Investigator Workshop.....	256

## Symposium

G	The Yin and Young of Sound Localization.....	257-264
---	--	---------

## Podium

H	Development.....	265-274
I	Basic Vestibular Research II.....	275-288

## A Community Response

J	Facing Animal Rights Extremism: A Community Response .....	289
K	Molecular Anatomy and Physiology of the Ribbon Synapse .....	290-297

## Podium

L	Genetics .....	298-311
---	----------------	---------

Poster

M1	Clinical Otolaryngology .....	312-324
M2	Aging: Animal Models .....	325-340
M3	Regeneration I .....	341-357
M4	Tinnitus: Auditory Nerve to Midbrain .....	358-366
M5	Speech: Perception, Attention and Complex Signals .....	367-378
M6	Auditory Prosthesis: Bilateral Stimulation .....	379-386
M7	Auditory Prosthesis: Cognitive Effects & Music .....	387-390
M8	Auditory Prosthesis: Combined Electric & Acoustic Stimulation .....	391-393
M9	Auditory Prosthesis: Current Steering & Shaping .....	394-395
M10	Otoacoustic Emissions II .....	396-403
M11	Psychophysics: Perceptual Learning, Speech Unmasking and Attention .....	404-418
M12	Inner Ear Physiology II .....	419-431
M13	Inner Ear: Damage I .....	432-441
M14	Inner Ear: Hair Cells: Transduction .....	442-454
M15	Inner Ear: Membranes and Fluids .....	455-462
M16	Auditory Pathways: Cortex and Thalamus: Behavior .....	463-474
M17	Auditory Pathways: Cortex and Thalamus: Circuitry .....	475-487
M18	Auditory Pathways: Cortex and Thalamus: Complex Sound Processing .....	488-495
M19	Auditory Pathways: Cortex and Thalamus: From Normal to Aberrant Sound Processing .....	496-505
M20	Auditory Pathways: Cortex and Thalamus: Physiology .....	506-523
M21	Auditory Pathways: Cortex and Thalamus: Plasticity .....	524-529
M22	Auditory Pathways: Cortex and Thalamus: Scene Analysis .....	530-537

Symposium

N	Using Massively-Parallel Next Generation Sequencing Techniques to Advance Studies and Clinical Cares of Hearing Loss .....	538-544
O	Real-World Hearing: Neural Coding and Perception .....	545-550

Podium

P	Auditory Prosthesis II .....	551-565
---	------------------------------	---------

Symposium

Q	Vestibular Psychophysics .....	566-572
---	--------------------------------	---------

Podium

R	Inner Ear: Hair Cells: Hair Bundles & Mechanotransduction .....	573-585
---	---	---------

Poster

S1	Tinnitus .....	586-595
S2	Auditory Prosthesis: Implantable Hearing Aids & Round Window Stimulation .....	596-598
S3	Auditory Prosthesis: Modeling & Simulations .....	599-605
S4	Auditory Prosthesis: Optical Stimulation .....	606-610
S5	Auditory Prosthesis: Optimizing Methods .....	611-615
S6	Cochlear Drug Delivery .....	616-621
S7	Psychophysics: Peripheral Processing .....	622-631
S8	Psychophysics: Temporal Processing and Temporal Fine Structure .....	632-639
S9	Sound Localization: Speech Unmasking and the Precedence Effect .....	640-648
S10	Sound Localization: Strategies, Oculomotor and Audio-Visual .....	649-660
S11	Development I .....	661-687
S12	Regeneration II .....	689-703
S13	Inner Ear: Damage II .....	704-715
S14	Inner Ear: Acoustic Trauma: Prevention .....	716-734
S15	Inner Ear: Hair Cells: Ion Channels .....	735-745

S16	Inner Ear: Hair Cells: Synapses .....	746-760
S17	Auditory Nerve: Molecular Mechanisms.....	761-770
S18	Auditory Pathways: Midbrain: Binaural.....	771-780
S19	Auditory Pathways: Midbrain: Hearing Loss .....	781-782
S20	Auditory Pathways: Midbrain I .....	783-789
S21	Auditory Pathways: Midbrain II .....	790-798
<b>Presidential Lecture and Awards Ceremony</b>		
T	Presidential Lecture and Awards Ceremony.....	799
<b>Symposium</b>		
U	Mechanisms and Circuitry Underlying Auditory Spectrotemporal Integration.....	800-805
V	New Insights on Vestibular Neuropharmacology: From Bench to Bedside.....	806-813
<b>Podium</b>		
W	Inner Ear Damage and Prevention .....	814-828
<b>Workshop</b>		
X	Interactive Workshop on 3D Reconstruction of the Ear .....	829-835
<b>Symposium</b>		
Y	Current Theories About the Generation of Otoacoustic Emissions and the Clinical Implications.....	836-842
<b>Poster</b>		
Z1	Clinical Audiology: Assessment .....	843-851
Z2	Clinical Audiology .....	852-860
Z3	External & Middle Ear Mechanics: Pathology.....	861-869
Z4	External & Middle Ear: Otitis Media .....	870-881
Z5	Taste and Smell .....	882
Z6	Tinnitus: Clinical.....	883-890
Z7	Clinical Vestibular II .....	891-904
Z8	Development II.....	905-927
Z9	Genetics I .....	928-943
Z10	Inner Ear Physiology III.....	944-954
Z11	Inner Ear: Acoustic Trauma: Mechanisms .....	955-973
Z12	Inner Ear: Damage: Ototoxicity: Mechanisms .....	974-984
Z13	Inner Ear: Damage: Prevention and Treatment Strategies .....	985-998
Z14	Inn Ear: Hair Cells: Novel Approaches .....	999-1010
Z15	Inner Ear: Mechanics: Measurements .....	1011-1024
Z16	Auditory Nerve: Physiology.....	1025-1040
Z17	Psychophysics: Animal .....	1041-1048
Z18	Psychophysics: Potpourri .....	1049-1061
<b>Podium</b>		
AA	Regeneration.....	1062-1069
BB	Psychophysics: Auditory Attention, Masking and Segregation.....	1070



## **1 Hybrid Cochlear Implants: What Have We Learned About the Auditory System**

**Bruce Gantz<sup>1</sup>**, Christopher Turner<sup>1</sup>, Lina Reiss<sup>1</sup>, Kate Gfeller<sup>1</sup>

<sup>1</sup>*The University of Iowa Cochlear Implant Clinical Research Center*

Hybrid Cochlear Implants utilize residual acoustic hearing in combination with electric speech processing, in order to provide treatment to a group of patients for whom hearing aids did not help and for whom traditional cochlear implants were not recommended. This combination has been successful in providing important place of articulation information to those that have profound high frequency hearing loss at frequencies greater than 1500 Hz. Combined acoustic plus electric speech processing has enabled most of this group of volunteers to gain improved word understanding compared to their preoperative hearing with bilateral hearing aids. Using acoustic hearing along with electric hearing can provide better speech recognition in background noise than electric hearing alone. It appears that the preserved residual low frequency acoustic hearing preserves fine pitch discrimination not provided by electrical speech processing and enables improved melody recognition and localization of sound. These measures are very important in real life to the hearing impaired. Surprisingly, even with a very short electrode, where a wide range of speech frequencies is assigned to a short distance along the base of the cochlea, very high levels of electric-only speech recognition are possible. A related novel finding in this group of subjects is that alteration in place pitch perception over time up to 2 octaves can occur. The short electrode and its highly abnormal place-frequency mapping has allowed us to observe substantial plasticity in our adults patients. This finding has enabled us to explore less invasive electrodes in profoundly deaf infants to preserve cellular structure in the Organ of Corti in the event that auditory regeneration becomes a reality.

This research was sponsored in part by NIH grants DC 00242, DC 00377, RR00059, and the Cochlear Corporation

## **2 Sensorineural Hearing Loss and Cochlear Implants: Pathology, Atrophy and Plastic Change Within the Auditory Pathway**

**Robert Shepherd<sup>1</sup>**, Dexter Irvine<sup>1</sup>, Remy Pujol<sup>2</sup>, David Ryugo<sup>3</sup>, Lisa Pettingill<sup>1</sup>, Tom Landry<sup>1</sup>, Andrew Wise<sup>1</sup>, James Fallon<sup>1</sup>

<sup>1</sup>*Bionics Institute*, <sup>2</sup>*Universite de Montpellier*, <sup>3</sup>*Garvin Institute*

Sensorineural hearing loss (SNHL) is the most common form of deafness and is typically a result of the loss of sensory hair cells. This loss initiates a gradual degeneration of spiral ganglion neurons (SGNs) within the cochlea, altered synaptic morphology within the cochlear nucleus and shrinkage of neurons within the central auditory pathway. These deafness induced changes impact on the initiation and propagation of neural activity evoked by cochlear implants (CIs) as evidenced by altered neural response properties. Using neonatal models of

SNHL we have established that reactivation of the auditory pathway via chronic, behaviorally relevant electrical stimulation from a CI can partially reverse some of the deafness induced changes observed. In addition, we have developed techniques designed to preserve SGNs following SNHL via the delivery of exogenous neurotrophins in combination with a CI. We will review this work with respect to the potential clinical implications for the severe-profoundly deaf.

This work was funded by the NIH (HHS-N-263-2007-00053-C) and the Garnett Passe & Rodney Williams Memorial Foundation. The Bionics Institute acknowledges the support it receives from the Victorian Government through its Operational Infrastructure Support Program.

## **3 Auditory Development and Plasticity in Congenital Deafness**

**Andrej Kral<sup>1</sup>**

<sup>1</sup>*Medical University Hannover*

Congenitally deaf (white) cats (CDCs) are a model of human prelingual deafness. To investigate the impact of auditory experience on postnatal development of the auditory cortex, we compared cortical responses to cochlear implant (CI) stimulation in congenitally deaf animals and normal hearing controls. Developmental delays and alterations were observed (Kral et al., 2005, *Cereb Cortex* 15: 552-562), with functional synaptogenesis in the cortex being delayed from the 1st to the 3rd month p.n., together with a subsequent increased functional synaptic pruning (review in Kral & O'Donoghue 2010, *New England J Med* 383: 1438-1450). The changes correlated with developmental changes in the visual cortex as well as with the duration of sensitive periods in the auditory cortex of CDCs with chronic electrostimulation with a CI (review in Kral and Sharma, *Trends in Neurosci*, in press). Analysis of layer-specific activity indicated a functional de-coupling of the primary auditory cortex from top-down influences in deafness (review in Kral & Eggermont, 2007, *Brain Res Rev* 56: 259-269). To investigate the influence of other sensory systems on these effects, awake cats were trained in a battery of seven visual tasks (Lomber et al., 2010, *Nat Neurosci* 13:1421-1427). The deaf cats demonstrated supranormal performance in detection of visual stimuli in peripheral visual field and in movement detection (ibid.). Consequently, cooling probes were implanted over several cortical areas. The supranormal abilities reversibly disappeared when the posterior auditory field (PAF) and the dorsal zone (DZ) have been inactivated by cooling (ibid.). These data demonstrate a causal relationship between cross-modal reorganization in deafness and supranormal visual abilities, as well as a differential visual recruitment of different auditory areas. These reorganizations are in part due to abnormal heteromodal projections from several sources of the visual system (Barone, Lacassagne and Kral, in preparation).

#### **4 Learning to Hear with Bilateral Cochlear Implants: Effect of Degraded Signals on Spatial Hearing and Auditory Development** **Ruth Litovsky<sup>1</sup>**

<sup>1</sup>*University of Wisconsin-Madison*

Cochlear implants (CIs) are being provided at an increasing rate, in particular to young children. While many bilateral CI users attain spoken language skills that are well within the range of performance seen in normal-hearing (NH) peers, CI users generally perform significantly worse than NH children on tasks that involve functioning in realistic, complex listening environments. Namely, they are worse at speech understanding in noise, segregation of target from masking sounds and sound localization. This is despite the overwhelming positive reports regarding improvement in quality of life with two vs. one CIs. Our lab investigates binaural processing in bilateral CI users, with the goal of uncovering mechanisms that enhance performance, and factors that limit performance. This talk will focus on recent findings in (1) young children who are bilaterally implanted by age 1-3 years, (2) children who received their devices at an older age, and (3) adults who were either pre-lingually or post-lingually deaf prior to being implanted. Some of the factors we are taking into account include: CIs were not designed to provide binaural stimulation and are not synchronized across the two ears, CIs in two ears may be surgically mismatched by depth and therefore provide mismatched information to the two sets of channels, the two ears are likely to have mismatched neural survival, the CI processors and microphones do not preserve spatial cues with fidelity. Our research aims to understand what limitations exist in today's clinical processors and how we can restore binaural cues to CI users with fidelity using unique signal processing and research platforms. Towards this goal our behavioral studies on spatial hearing provide insight into mechanisms involved in auditory plasticity.

Work supported by NIH-NIDCD

#### **5 A "Top Down" or "Cognitive Neuroscience" Approach to Cochlear Implant Designs and Fittings**

**Blake Wilson<sup>1</sup>, Michael Dorman<sup>2</sup>, Marty Woldorff<sup>3</sup>, Debara L. Tucci<sup>1</sup>**

<sup>1</sup>*Duke University Medical Center*, <sup>2</sup>*Arizona State University*, <sup>3</sup>*Duke University*

The cochlear implant (CI) is one of the great success stories of modern medicine. A high level of function is provided for most patients. However, some patients still do not achieve excellent or even good results using the present-day devices. Accumulating evidence is pointing to differences in the processing abilities of the "auditory brain" among patients as a principal contributor to this remaining and still large variability in outcomes. In this talk, we will describe a new approach to the design of CIs that regards the brain as an important part of the prosthesis system and at least attempts to take the differences in brain function into account. The approach asks what the compromised brain needs as an input in order to perform optimally, as

opposed to the traditional approach of reproducing insofar as possible the normal patterns of activity within the auditory nerve. The talk will include (1) a brief review of the design and performance of the present-day CIs, (2) a summary of the evidence indicating the importance of the brain in determining outcomes with CIs, (3) the description of the new approach, and (4) a list of questions that are raised by the approach.

#### **6 The Spiral Ganglion: Neurogenesis and Concepts for Regeneration**

**Alain Dabdoub<sup>1</sup>, Robin Davis<sup>2</sup>**

<sup>1</sup>*UCSD School of Medicine*, <sup>2</sup>*Rutgers University*

Regenerating damaged or lost cells by re-initiating developmental processes is a central aim for many researchers. Promising progress continues to be made utilizing embryonic stem cells and induced pluripotent stem cells generated by reprogramming differentiated adult cells. More recently, the direct conversion of somatic cells and glial cells into neurons by forced expression of transcription factors also seems to hold promise for regenerative therapies. This Symposium will provide an overview of the potential uses of these strategies in regenerating the spiral ganglion neurons.

Loss of spiral ganglion neurons is permanent. Therefore in this Symposium, as a necessary step for regenerating spiral ganglion neurons, we will also describe their development - the genes involved in their neurogenesis, the influences of their environment and glial cells, and their organization and electrophysiological characteristics. The aim of this Symposium is to elucidate the properties of the spiral ganglion neurons, the target for regeneration. The regenerated neurons must reiterate the full richness of the spiral ganglion electrophysiological signature, their organization, and form synaptic connections to both the hair cells and cells within the cochlear nucleus. On the whole, this Symposium will provide an overview of the development and characteristics of the spiral ganglion neurons and explore cell-based therapies that would result in integrated and fully functional spiral ganglion neurons.

#### **7 Genetics and Stem Cell Based Therapy for Age-Related Macular Degeneration**

**Kang Zhang<sup>1</sup>**

<sup>1</sup>*Director, West China Hospital Eye Center, and Director, Institute for Genomic Medicine UCSD*

Age-related macular degeneration (AMD) is the most common cause of visual impairment of the elderly in the developed countries. AMD is a multi-factorial disease that involves interaction of genetic and environmental influences. Allelic variants of genes encoding members of the alternative complement pathway, including CFH, and C3 strongly influence an individual's risk of developing AMD. We and others demonstrated that HTRA1 locus at chromosome 10q26 also strongly impact AMD risk. We demonstrated that *HTRA1* was significantly associated with AMD in Caucasian and Chinese cohorts. We showed a disease haplotype increased HTRA1 expression in AMD patients. We showed in our AMD population that variations in CFH, HTRA1, and C3 contribute to a vast

majority of the genetic risk for AMD and are strongly predictive of advanced AMD and bilaterality. In addition, we showed *TLR3* plays a role in geographic atrophy. Smoking is the strongest identifiable environmental factor. Inducible pluripotent stem cells (iPS) can be obtained from individual patients and used to derive retinal photoreceptors and RPE for autologous cell based therapies. iPS will revolutionize our treatment and approach to all blinding degenerative diseases of the eye including AMD and glaucoma. The recent advance in genetics and stem cell therapy of AMD will allow identification the high risk patients for customized intervention and treatment in the near future.

## **8 Making Neurons from Glia and Pericytes: The Wizardry of Transcription Factors**

**Benedikt Berninger<sup>1,2</sup>**

<sup>1</sup>*Institute of Physiology LMU Munich*, <sup>2</sup>*Institute of Stem Cell Research, Helmholtz Zentrum München*

Cellular reprogramming of somatic cells into neurons by forced expression of transcription factors provides a novel alternative strategy for cell-based therapies of neurodegenerative processes. Over the past years we have examined the possibility of in vitro reprogramming astroglia isolated from the cerebral cortex of young mice into neurons by retroviral expression of distinct neurogenic transcription factors. While forced expression of Neurogenin-2 converts astroglia into synapse-forming glutamatergic neurons, Mash1 or Dlx2 induce a GABAergic neuron identity (Heinrich et al., PLoS Biology 2010). More recently we have investigated whether also somatic cells of the adult human brain are amenable to neurogenic reprogramming. We found that cultures of the adult human cerebral cortex are enriched in cells derived from brain pericytes as evidenced by their co-expression of PDGF receptor beta- and NG2. Interestingly, following forced expression of Sox2 and Mash1 pericyte-derived cells from the adult human cortex give rise to functional neurons, capable of repetitive action potential firing and receiving functional synaptic input from co-cultured neurons. This data show that neurogenic reprogramming can also be achieved from somatic cells residing within the adult human cerebral cortex holding out the prospect of recruiting endogenous cells for neural repair.

## **9 Evolution, Development and Molecular Composition of the Spiral Ganglion Neurons**

**Bernd Fritsch<sup>1</sup>**, Ning Pan<sup>1</sup>, Israt Jahan<sup>1</sup>, Jennifer Kersigo<sup>1</sup>, Benjamin Kopecky<sup>1</sup>, Jeremy Duncan<sup>1</sup>

<sup>1</sup>*University of Iowa*

Hair cells and neurons evolved from an ancestral single sensory cell that conducted sensory information via its own, unmyelinated axon to the CNS. Gene and cell duplication resulted in hair cells (Atoh1) and sensory neurons (Neurog1/Neurod1) and the addition of neural crest derived Schwann cells to form myelin. However, the downstream pathways are not fully segregated allowing neuronal precursors to assume a hair cell phenotype. For example, Mice lacking Neurod1 develop hair cells in sensory ganglia, suggesting that Neurod1 suppresses

Atoh1. Misexpression of Neurog1 under the Atoh1 locus (Atoh1tgNeurog1) cannot change the fate of hair cell precursors into neurons indicating that the ancestral developmental pathway of hair cells is molecularly stabilized through unknown processes that could help in hair cell regeneration. Nevertheless, Neurod1 also inhibits Atoh1 expression in hair cells, resulting in altered hair cell phenotypes when removed. Loss of Schwann cells in ErbB2 and Sox10 null mice results in distorted spiral ganglion cell distribution, loss of many neurons and aberrant projections. Schwann cells may, comparable to the role of glia cells in the CNS, guide neuronal migration and axonal projection. Further research is needed to define the molecular basis for the neuron/Schwann cell interaction to assist attempts aimed at regenerating neuronal processes to specific central and peripheral targets. Several molecules guiding neuritis have been identified. The last part of this presentation will present the role of Neurod1, Prox1 and neurotrophins in the development of patterned innervation. Importantly, double neurotrophin null mutants show that hair cells are nearly independent of innervation whereas all afferent and innervation is lost. These data show that the development of the sensory neuron and its projection patterns critically depend on the associated cells, the hair cell or peripheral target cell and the Schwann cells.

## **10 Distribution and Diversity of Spiral Ganglion Neuron Firing Features**

**Robin Davis<sup>1</sup>**

<sup>1</sup>*Rutgers University*

With the growth of cell replacement therapy as a viable means of treating peripheral auditory disorders, it has become increasingly important to understand fully the fundamental features and basic organization of the cells under study. For spiral ganglion neurons, this task has become more daunting as a number of investigators have shown that this seemingly simple cell class shows numerous physiological and synaptic specializations that vary systematically along the tonotopic axis of the cochlea. Within each region, moreover, the properties of individual neurons are heterogeneous; potentially representing at a single-cell level a form of parallel processing that may be important for coding aspects of an auditory stimulus such as sound intensity. By using a variety of different preparations we have obtained greater insight into the full spectrum of tonotopic features, the ion channels involved, and regulatory mechanisms that determine their distribution.

Evidence for the electrophysiological complexity of spiral ganglion neurons was found in their endogenous kinetic features (Adamson et al., *J. Comp. Neurol.* 2002). Neurons obtained from the high frequency cochlea region had rapid kinetics whereas neurons isolated from the low-frequency region were slower. Even synaptic proteins, such as AMPA receptors, showed predictable distribution patterns, both in neonatal and adult animals (Flores-Otero and Davis, *J. Comp. Neurol.* 2011). Use of a "gangliotopic" preparation (Liu and Davis, *J. Neurophysiol.* 2007) revealed that neuronal excitability is also tonotopically organized, but

with a distinctly different pattern. Neurons isolated from the mid-cochlear region had the highest and widest range of sensitivities, consistent with what one might expect from *in vivo* recordings.

To target neuron replacement knowledgeably, we are now building upon this foundation by evaluating the effects of extrinsic and intrinsic factors that shape the exquisite complexity of the spiral ganglion.

## **11 Stem Cells for the Replacement of Spiral Ganglion Neurons**

**Albert Edge<sup>1,2</sup>**

<sup>1</sup>*Department of Otolaryngology, Harvard Medical School,*

<sup>2</sup>*Eaton Peabody Laboratory, Massachusetts Eye and Ear Infirmary*

The synapse between hair cells and auditory neurons is sensitive to damage and methods to replace the afferent neurons are of therapeutic interest. We have used an *in vitro* organ of Corti explant to study genes that enhance regeneration of the afferent synapse and have used *in vivo* approaches to assess the functional replacement of the auditory nerve. In addition to their role during development several axonal guidance molecules may affect regrowth of fibers to hair cells from new neurons placed in the cochlea to regenerate the afferent innervation. Repulsive guidance molecule, RGMA, was expressed in the cochlea after birth, consistent with such a role. After adding newborn mouse spiral ganglion neurons to an organ of Corti explant that lacked afferent connections, contact of neural processes with hair cells and elaboration of postsynaptic densities at sites of the ribbon synapse were increased by treatment with a blocking antibody to RGMA. Expression of axonal guidance molecules with inhibitory roles thus appears to be detrimental to regeneration of afferent hair cell innervation and could explain why auditory neurons have a low capacity to regenerate peripheral processes. Transplantation of auditory neurons for functional replacement has been tested in a mouse model, in which type 1 spiral ganglion neurons were removed by ouabain. Loss of neurons was accompanied by loss of synaptic ribbons at hair cells and elevation of ABR threshold. Embryonic stem cells expressing tau-GFP were converted to neural progenitors and transplanted into the cochlear modiolus. A decrease in ABR thresholds was observed in transplanted as compared to non transplanted animals 3 months after transplantation, and cells positive for both neural markers and GFP had sent out extensive processes into the cochlear nucleus and the cochlea. The engrafted cells were positive for postsynaptic glutamatergic markers at the hair cell synapse and for presynaptic glutamatergic markers at the endings in the cochlear nucleus.

Supported by NIH grant DC007174

## **12 Context Effects on Pitch Contour Identification in Normal-Hearing Listeners and Cochlear-Implant Users**

**Krista Ashmore<sup>1</sup>, Xin Luo<sup>1</sup>**

<sup>1</sup>*Purdue University*

Studies have shown that the mean fundamental frequency (F0) of a preceding sentence has a contrastive effect on

lexical tone perception in normal-hearing (NH) listeners who speak tonal languages. The context effects may help listeners normalize the pitch variations in lexical tones produced by different talkers. In this study, English-speaking NH listeners and cochlear-implant (CI) users were tested on their abilities to identify flat- and rising-pitch contours with preceding flat-pitch contours. For NH listeners, pitch contours contained either F0 alone or the lowest four harmonics with the F0 ranging from 160 to 200 Hz. For CI users, pitch contours with the lowest four harmonics were presented via their clinical speech processors; an extended F0 range (100-300 Hz) was used to accommodate the poor pitch perception with CI. The results showed that for most NH and CI subjects, the F0 of preceding context had a contrastive effect on pitch contour identification (PCI), i.e., pitch contours were more likely to be identified as rising when the preceding context had a higher F0. The observed context effects were similar to those in lexical tone perception, although the target stimuli were not lexically meaningful, the context stimuli were only 500 ms long, and the subjects had no tonal language experience. The similar results in NH listeners and CI users suggest that the context effects were due to central auditory processing, regardless of the various peripheral auditory inputs. To better understand the underlying mechanisms, context effects on PCI were also tested in CI users via direct electric stimulation, using both place and temporal coding. Place-pitch contours were created by steering current between two adjacent apical electrodes, while temporal-pitch contours were created by varying amplitude-modulation frequencies (100-300 Hz). However, initial results of direct electric stimulation did not show consistent context effects and further investigation is warranted.

## **13 Self-Selection of Frequency Tables in Users of Bilateral Cochlear Implants**

**Matthew Fitzgerald<sup>1</sup>, Chin-Tuan Tan<sup>1</sup>, Katelyn Glassman<sup>1</sup>, Brandon Laflen<sup>1</sup>, Mario Svirsky<sup>1</sup>**

<sup>1</sup>*New York University Langone Medical Center*

Compared to monaural cochlear implants (CI), bilateral CIs provide many benefits including improved speech understanding in noise and sound localization. In current clinical practice for bilateral CIs, each CI is fit independently, with minor adjustments to ensure that loudness is balanced between ears. Such fitting procedures cannot account for between-ear mismatches in insertion depth or neural survival, which could lead to a given frequency stimulating different regions of the cochlea in each ear. Such between-ear differences can hinder sound-localization abilities and may also affect speech understanding if patients cannot adapt. It is possible that adjustments to the frequency table in one or both implants could, however, compensate for between-ear mismatches in site of stimulation. Unfortunately, no tool exists to allow audiologists to determine when adjustments to the frequency table may be necessary, and what adjustments would be appropriate. Thus, we have been developing a tool which allows for adjustment of the frequency table in real time. In using this tool, we assume that a patient may

benefit from reprogramming of the frequency table if they select a table in one ear that differs from the standard table used in the contralateral CI, especially when listening with both CIs simultaneously. We are testing this procedure in users of bilateral CIs, and observe that some listeners select a frequency table in one ear which differs from the standard. These selections sometimes shift when the contralateral CI is active, suggesting that listeners are combining information between the two ears when making their selections. We are currently investigating whether these selections are driven by listeners weighing some speech sounds more heavily than others, and whether the self-selected tables elicit percepts that are pitch-matched across the arrays.

Funding for this work was provided by NIH/NIDCD. Advanced Bionics provided equipment needed to perform the research.

#### **14 A Frequency-Place Map for Electrical Stimulation in Cochlear Implants: Change Over Time**

**Katrien Vermeire**<sup>1</sup>, Reinhold Schatzer<sup>2</sup>, Andrea Kleine Punte<sup>3</sup>, Paul Van de Heyning<sup>3</sup>, Maurits Voormolen<sup>3</sup>, Daniel Visser<sup>2</sup>, Andreas Krenmayr<sup>2,4</sup>, Mathias Kals<sup>2,4</sup>, Clemens Zierhofer<sup>2</sup>

<sup>1</sup>University Hospital Ghent, <sup>2</sup>University Innsbruck,

<sup>3</sup>University Hospital Antwerp, <sup>4</sup>MED-EL GmbH

##### Introduction

Recent studies by Vermeire et al. (2008), Dorman et al. (2007) and Boëx et al. (2006) have determined frequency-place maps for the electrically stimulated cochlea from unilateral CI subjects with contralateral hearing. Reiss et al (2007) showed that in Hybrid patients this electric pitch perception shifts in frequency, sometimes by two octaves downwards, during the first years of implant use.

The goal of this study was to look at the effect of experience on electric pitch sensations.

##### Methods

Five subjects with near-to-normal hearing in the contralateral ear have been provided with a MED-EL CI in the deaf ear in order to reduce intractable tinnitus. After loudness balancing, electric pitch percepts from unmodulated trains of biphasic pulses (1500 pulses per second, 50 µs/phase) were pitch-matched to contralateral acoustic pure tones. To look at the influence of experience, pitch-match experiments were performed, before the first fitting and after 1, 3, 6 and 12 months of CI experience. Matched acoustic frequencies were evaluated as a function of electrode insertion angles. Electrode placement and insertion angles were determined from high-resolution CT scans of the subjects' temporal bones (Xu et al., 2000).

##### Results

The mean frequency-place function is about one octave below Greenwood's map in the basal turn, deviating by a lesser amount and coming close to Greenwood's function for more deeply inserted electrodes. No systematic changes can be found over time.

##### Conclusion

The results of this study do not show an influence of experience on electric pitch sensation. This is not in

agreement with the results found by Reiss et al (2007). A possible explanation might be the fact that patients included in this study were all implanted with a standard electrode where the most apical electrode has a distance of 30.4mm from the marker ring, compared to the 10.5 mm for the hybrid electrode used in the study by Reiss (2007). Because of this deeper insertion there is less mismatch between the predicted pitch sensation (based on Greenwood's map) and the centre frequency of the filterbank of the electrode.

#### **15 Investigating Cochlear Implant Place-Pitch and Temporal-Pitch Perception Using Different Pitch Perception Tasks**

**Vijay Mohan Raaja Marimuthu**<sup>1</sup>, Brett Swanson<sup>2</sup>, Robert Mannell<sup>1</sup>

<sup>1</sup>Macquarie University, <sup>2</sup>Cochlear Limited. Sydney

Place and temporal cues to pitch can be studied independently in cochlear implant (CI) recipients. Temporal pitch has been shown to convey melody in CI recipients, but few studies have investigated place pitch alone. The present study investigated the role of place pitch and temporal pitch using different pitch perception tasks. Five post-lingually-deafened CI recipients, with at least one year of implant usage, participated in the study. The four experimental procedures were: 4AFC discrimination, 2AFC ranking, and 2AFC Modified Melodies test (backward and warp modification). The three stimulus types were: (1) Pure tones with base frequency of C5 (523 Hz), providing place cues only; (2) Harmonic tones with base frequency of C3 (131 Hz), providing temporal cues only; (3) Harmonic tones with base frequency of C4 (262 Hz). The stimuli were presented via loudspeaker at a comfortable loudness level. The recipients used their usual processor. The overall scores for discrimination and ranking were high for all three stimulus types, however, three subjects showed pitch reversals in ranking the C4 harmonic tones. In the Modified Melodies test, scores were similar for C5 pure tones and C3 harmonic tones, while scores using C4 harmonic tones were worse and mostly near chance. The C4 harmonic tones potentially offered temporal and place cues. However, their fundamental frequency range of 262 to 523 Hz was probably above the upper frequency limit of temporal pitch for most subjects, and the place pitch cues may have been ambiguous. This may explain the observed pitch reversals, which prevent good performance in a melody task. Scores with C5 pure tones were as good as those with C3 harmonic tones. This implies that place cues alone were sufficient to convey melody. These results are consistent with those from a previous study (Swanson et al., 2009), and support the hypothesis that cochlear implant recipients perceive place cues as pitch rather than brightness.

#### **16 Identification and Enumeration of Double Vowels in Cochlear Implant Users**

**Bomjun Kwon**<sup>1</sup>, Trevor Perry<sup>1</sup>

<sup>1</sup>The Ohio State University

When two vowels are presented simultaneously (a "double vowel"), normal hearing (NH) listeners utilize

spectral/temporal cues, such as fundamental frequency (F0) differences or onset differences, for better identification. This study examined the ability of cochlear implant (CI) users to use F0 and/or temporal onset differences in a double vowel identification task. In each trial of the testing, the subject was presented with either a double vowel consisting of two synthesized vowels from a set of 5 cardinal vowels or a single vowel, and responded with one or two responses. The vowels in double vowel trials had an F0 of either 100 or 300 Hz, and were temporally arranged with an onset difference of 0, 100, 300, or 800 ms. The results from 10 CI subjects were analyzed based on identification and enumeration of vowels (whether the presentation was one or two vowels). First, there was no effect of the F0 difference on performance, in contrast to findings in NH listeners. Second, the majority of subjects (9 of 10) showed vowel enumeration scores close to chance level, i.e., they did not have a clear sense of how many talkers they heard. Third, the onset difference appears to have a significant effect, as performance both in terms of identification and enumeration improves substantially with as little as 100 ms of delay. These results illustrate the importance of temporal cues for segregating one voice from another and the limited segregation based on spectral cues in CI listeners. Further data analysis indicates that the identification performance in the double vowel trials with correct enumeration could be comparable to that of NH listeners as reported in the literature. This leads to speculation that, given a priori knowledge about episodic context (such as the number of talkers), speech understanding in either selective or divided attention tasks under an impoverished spectral resolution could be achieved without segregating the voices [supported by NIH—R03DC009061].

### **17 A New Method for Determining Frequency Discrimination in Cats with Different Hearing Profiles**

**Yuri Benovitski<sup>1,2</sup>, James Fallon<sup>1</sup>, Peter Blamey<sup>1</sup>, Graeme Rathbone<sup>1,2</sup>**

<sup>1</sup>Bionics Institute, <sup>2</sup>La Trobe University

Animal behavioural studies make a significant contribution to research and provide vital information regarding physiological aspects in ways not possible with human subjects. However, behavioural experiments in animals can be difficult, prohibitively time consuming, and not all animals can learn the task with satisfactory performance levels.

We developed a novel behavioural experimental system to allow efficient animal training in response to audio stimuli, without employing negative re-enforcers such as electric shocks or food deprivation. Cats were required to perform a relatively simple task of moving toward and away from the device in accordance to the stimuli (a go / no-go task). Our new experimental setup proved to be effective with all subjects (n = 9) performing at > 90% correct on an easy task. Subjects were trained within several weeks and then generated 150 to 200 trials within 4 to 6 sessions per day. A frequency discrimination threshold of 330 Hz (8 kHz

reference) in a normal hearing cat measured with the current system was comparable with previously published results. Four partially deafened cats were trained with 6 different reference frequencies. Their performance decreased with increasing reference frequency, consistent with previous literature where performance is inversely proportional to frequency (i.e.  $df/f \sim \text{constant}$ ).

The system is relatively simple to set up and animals can be trained quickly. This method can be generalised to test a variety of different perceptual abilities such as rate and electrode discrimination. Additionally, it is possible to correlate data generated by this system with electrophysiological data collected from the same animal.

This work is funded by the National Institutes of Health (NIDCD, HHS-N-263-2007-00053-C) and The Department of Electronic Engineering, La-Trobe University. Bionics Institute acknowledges the support it receives from the Victorian Government through its Operational Infrastructure Support Program.

### **18 The Effects of Sound Coding and Training on the Perception of Prosody by Cochlear Implant Users**

**Chris James<sup>1,2</sup>, Mathieu Marx<sup>2</sup>, Olivier Deguine<sup>2</sup>, Marie-Laurence Laborde<sup>2</sup>, Bernard Fraysse<sup>2</sup>**

<sup>1</sup>Cochlear France SAS, <sup>2</sup>Hopital Purpan, Toulouse, France  
Novel sound coding for cochlear implants (CI) with enhanced spectral and temporal processing (STEP) was developed with the aim to improve the perception of prosodic information carried by voice pitch. A dual filter-bank approach was employed with a bank of narrow, good quality filters SP and a bank of parallel wide filters TE. SP filters reduced redundancy between channels and allowed better extraction of the low harmonics of voiced signals. TE filters had increased modulation bandwidth to better represent periodicity in the extracted temporal envelopes. Channel selection and current steering were provided by via SP filters while the amplitudes of regularly timed current pulses were modulated using the envelopes obtained via corresponding TE filters.

An enhancement ("Quick") was added to STEP with the aim to improve synchronization of neural responses to modulation frequency as opposed to carrier frequency (Middlebrooks 2008, J Neurophysiol 100: 92-107): The temporal envelopes of selected channels were oversampled and peak timings determined; peak-amplitude, peak-synchronized current pulses replaced regular pulses.

The new coding strategies were evaluated with 12 Nucleus CI recipients on two tests of prosody: Firstly a voice Emotion task, where subjects discriminated affectations of Anger, Fear, Joy, Sadness and Neutral tone for semantically neutral sentences. Secondly, a Question/Statement discrimination task where semantically neutral sentences were "natural", pitch-flattened or normalized for duration. This allowed determination of the use of pitch or duration cues in discriminating meaning. Speech recognition was evaluated in quiet and in noise, and sound quality judgments on a scale 0-10 collected for a number of different sound stimuli.

Subjects completed 3 visits: The second and third visits included a speech prosody training phase with a new strategy or subjects' usual ACE maxima strategy, in a balanced cross-over design. Preliminary results will be available at the time of the meeting.

### **19 Decoding Stimulus Identity Along the Ventral Auditory Stream in the Awake Primate: Implications for Cortical Neuroprostheses**

**Elliot Smith<sup>1</sup>, Bradley Greger<sup>1</sup>**  
<sup>1</sup>*University of Utah*

Hierarchical processing of visual and auditory sensory information is believed to occur in two streams: a "ventral" stream responsible for stimulus identity or quality and a "dorsal" stream responsible for processing spatial elements of a stimulus. Neuroanatomical evidence supports the presence of a ventral processing stream in auditory cortex extending from primary auditory cortex to the Belt and Parabelt auditory cortical areas and on to ventrolateral prefrontal cortex. There are few physiological studies of this stream. The goal of the present study was to examine early stages in this processing stream in order to better understand the possibility for a cortically based auditory neuroprosthetic. To examine information processing in the auditory object identification stream, we implanted two 96-channel microelectrode arrays in the superior temporal gyrus. One microelectrode array was implanted in the primary auditory cortex (AI) field of auditory cortex and the second was implanted in rostral Parabelt auditory cortex (PBr). Action potentials (APs) and local field potentials (LFPs) were simultaneously recorded on both electrode arrays while the monkey passively listened to species-specific vocalizations. As PBr is higher than AI in the object identity stream hierarchy, we hypothesized that neural responses in PBr would be better able to discriminate between individual vocalizations. To test this hypothesis we used linear discriminant analysis to decode vocalization identity from AP and LFP responses in AI and PBr. The decode was applied separately to both the LFP spectrograms and gaussian-smoothed peri-stimulus time histograms of AP responses. We used recordings from consecutive days as training and testing data. Only units from common channels and the same number of trials per class were included in each data set. Chance performance ranged from 50% for two classes, to 14% for seven classes. Decode performance in PBr ranged from 53% to 17% for LFP (N = 96 electrodes for training and testing data) and 56% to 17% for APs (N = 24 neurons for both training and testing data), while performance in AI ranged 78% to 48% for LFP (N = 96 electrodes for training and testing data), and 82% and 37% for APs (N = 12 neurons for both training and testing data) from two to seven classes. While linear analysis of LFP spectral elements and AP firing rates may not utilize the preferred features of PBr, temporal modulations in both signals are adequate for decoding stimuli in AI. This result suggests that PBr may utilize sparse, nonlinear or generally abstract feature coding.

### **20 The Adaptive Pattern of the Auditory N1 Peak Revealed by Standardized Low-Resolution Brain Electromagnetic Tomography in Cochlear Implant Users and Normal Hearing Listeners**

**Aniruddha Deshpande<sup>1</sup>, Fawen Zhang<sup>1</sup>**  
<sup>1</sup>*University of Cincinnati*

The N1 peak in the late auditory evoked potential (LAEP) rapidly decreases in amplitude following stimulus repetition, displaying an adaptive pattern. The present study explored the functional neural substrates that may underlie the N1 adaptive pattern using standardized Low Resolution Brain Electromagnetic Tomography (sLORETA) in 10 cochlear implant (CI) and 10 normal hearing (NH) subjects. Tone bursts (1 kHz) and speech syllable /da/ were presented in trains of 5; the inter-stimulus interval was 0.7 s and the inter-train interval was 15 s. The waveform analysis showed significant effects of stimulus type (/da/ vs. 1 kHz tone) and stimulus order (1st vs. 5th) but not of subject type (CI vs. NH) or interaction of these factors. The sLORETA data performed for the N1 in its latency range (70-160 ms) showed that, for NH listeners, S1 response evoked by 1 kHz tone displayed brain activation in broader cortical areas as compared to the S5 response. The sLORETA comparison maps between S1 and S5 response showed a significant activation in the frontal and parietal lobes for the 1 kHz tone but not for the /da/ stimuli in NH listeners and for both /da/ and 1 kHz tone in CI users. These results suggest that the N1 adaptive pattern evoked by 1 kHz tone is related to the adaptation and/or refractory features of neural structures. The parieto-frontal network might help sensitize the brain to novel stimuli by filtering out repetitive stimuli. This mechanism may be altered when stimulus is speech (i.e. /da/) or when subjects suffer from neural deficits following long-term deafness (i.e. in CI users). This study demonstrates that sLORETA may be useful for identifying generators of scalp-recorded event related potentials and for examining the physiological features of these generators. This technique could be especially useful for cortical source localization in individuals who cannot be examined with functional magnetic resonance imaging or magnetoencephalography (e.g. CI users).

### **21 Waveform and Pulse Rate Effect Behavioral Detection of Intracortical Microstimulation**

**Andrew Koviuniemi<sup>1</sup>, Jessica Brenner<sup>1</sup>, Oliver Regele<sup>1</sup>, Kevin Otto<sup>1</sup>**  
<sup>1</sup>*Purdue University*

Background: Sensory prostheses using intracortical electrical microstimulation require the consistent and efficient activation of neurons in the targeted cortical region. The objective of this research is to optimize pulse rate and stimulus waveform used to produce longitudinally stable sensory stimuli.

Methods: Rats, trained in a conditioned avoidance task to detect auditory stimuli, were implanted with a 16 site,

single shank, 100  $\mu\text{m}$  pitch, silicon microelectrode array in the primary auditory cortex of the right hemisphere. Once the rats recovered from surgery (~2 days) they were tested for detection of constant current, biphasic, charge balanced electrical stimuli. An adapted up-down task was employed to measure the detection threshold. With this procedure, rats were able to generate ~15-20 thresholds per day. Experiments were designed to explore the role of phase order (anode leading vs. cathode leading), phase asymmetry, phase delay and pulse rate, as well as any interaction between these four factors.

**Results:** Asymmetry conferred no benefit in terms of lowering the threshold for a given stimulus when measured in charge delivered per phase (the primary determining factor of the safety of electrical stimulation) when compared with symmetric cathode leading pulses of an equivalent cathode phase duration. The primary determinate of threshold level was cathode phase duration; however, symmetric, anode leading pulses always resulted in higher threshold levels when compared with cathode leading pulse of equivalent phase durations. Furthermore, the addition of a phase delay of greater than 200  $\mu\text{s}$  between the anode and cathode phase for an anode leading pulse brought the detection threshold to a level equivalent to the cathode leading pulse. Finally, detection threshold decreased logarithmically for the domain of 16 pulses per second (PPS) to 84 PPS but showed no change for pulse rate above this point up to 338 PPS.

**Ongoing studies:** We are currently working to determine the role of frequency and amplitude modulation in the discriminability of the electrical microstimulation.

## **[22] Dexamethasone Releasing Hydrogel for Hearing Preservation and Reduction of Fibrous Tissue Growth**

Mareike Hütten<sup>1,2</sup>, Roland Hessler<sup>3</sup>, Timo Stöver<sup>4</sup>, Karl-Heinz Esser<sup>2</sup>, Thomas Lenarz<sup>1</sup>, **Verena Scheper<sup>1</sup>**  
<sup>1</sup>Hannover Medical School, Hannover, Germany, <sup>2</sup>Institute of Zoology, University of Veterinary Medicine Hannover, Foundation, Germany, <sup>3</sup>MED-EL, Innsbruck, Austria, <sup>4</sup>Department of Otolaryngology, KGU Frankfurt am Main, Germany

**Objective:** Cochlear implants (CIs) are the treatment of choice for patients suffering from sensorineural hearing loss to regain a hearing perception. Postoperative immune reaction influences the CI efficiency by inducing fibroblast growth and thus increasing the impedances and reducing residual hearing. CIs functionalized with glucocorticoides like dexamethasone (DEX) could reduce the immune reaction, leading to decreased fibroblast growth and hearing loss, and thus improve the outcome of the implant. **Methods:** The chemistry and consistency of the hydrogel STAR-PEG-stat-PO allows it to be filled into a silicone reservoir and to incorporate active ingredients. The hydrogel was injected into the reservoir, saturated with DEX solution, and implanted into the inner ear of normal hearing guinea pigs. Animals receiving a hydrogel reservoir without drug and animals receiving DEX via an osmotic pump served as controls. In order to assess the

effects of the delivered DEX (35  $\mu\text{g/hr}$ ) on the animals' hearing, the hearing threshold was weekly measured via acoustically evoked auditory brainstem response over a period of 28 days. On day 28 cochleae were explanted, embedded in epoxy casting resin, and grinded in steps of 20  $\mu\text{m}$ . Subsequently fibrous tissue growth and spiral ganglion cells (SGC) were examined histologically.

**Results:** Compared to the control groups animals implanted with the DEX filled hydrogel reservoir showed significantly lower tissue growth around the implant and significantly better hearing thresholds. The SGC densities did not differ between groups.

**Conclusion:** Our results proof that the hydrogel reservoir is a promising drug delivery device to apply water-soluble drugs in therapeutically relevant doses into the inner ear for a sustained treatment period. Additionally we were able to prove that DEX is an appropriate drug to decrease fibrous tissue growth and to prevent residual hearing.

This study was supported by the EU (NanoEar, NMP4 – CT-2006-02556).

## **[23] Perception of Frequency-Modulation Patterns Based on Recovered-Envelope Cues for Cochlear Implant Users**

**Ward R. Drennan<sup>1</sup>**, D. Timothy Ives<sup>2</sup>, Jong Ho Won<sup>1</sup>, Elyse M. Jameyson<sup>1</sup>, Kaibao Nie<sup>1</sup>, Jay T. Rubinstein<sup>1</sup>, Christian Lorenzi<sup>2</sup>

<sup>1</sup>University of Washington, USA, <sup>2</sup>Ecole normale supérieure, CNRS, UPD, France

Amplitude-modulation (AM) and frequency-modulation (FM) patterns convey crucial information for speech identification. FM information is encoded into both temporal-envelope and temporal fine-structure cues via cochlear filtering and neural phase locking in the peripheral auditory system. Cochlear implant (CI) users provide a unique opportunity to assess the ability to use the temporal-envelope cues reconstructed from FM after peripheral filtering without any contribution of neural temporal fine-structure cues. This was achieved by measuring the sensitivity ( $d'$ ) of CI users in a discrimination task using complex patterns of FM applied to a 930-Hz sine carrier. Stimuli were passed either through a model of a cochlear filter or a clinical filter of the implant's processor, and presented through one electrode using an equivalent loudness. Overall, the results showed that CI users can use the reconstructed envelope cues as well as normal-hearing listeners to discriminate complex FM patterns when peripheral filtering mimics the normal filtering in the human cochlea. Speech identification capacities were also evaluated when speech sounds were submitted to several forms of distortion (masking noise, infinite peak clipping or amplitude compression) which severely degraded the speech AM cues. Preliminary results with CI users (N=4) suggest a strong relationship between the ability to detect AM cues from FM-AM conversion and the ability to understand speech in degraded conditions. This suggests that envelope reconstruction from FM is an important auditory mechanism contributing to the robust perception of speech sounds in degraded listening conditions.

This work was supported by NIH grants R01-DC010148, T32-DC000033, P30-DC004661, Starkey France and the V.M. Bloedel Traveling Scholars Fund.

## **[24] Sensitive Periods for Asymmetric Hearing: Developmental Effect of Unilateral Hearing Experience**

Andrej Kral<sup>1</sup>, Peter Hubka<sup>1</sup>, Rüdiger Land<sup>1</sup>, Jochen Tillein<sup>1,2</sup>

<sup>1</sup>*Institute of Audioneurotechnology, Medical University Hannover, Germany*, <sup>2</sup>*MedEl Company, Innsbruck, Austria*  
To study consequence of unilateral hearing experience at different ages, cortical plasticity in congenitally deaf cats (CDC) chronically stimulated with a cochlear implant (CI) for 2 and 5 months (csCDCs, n=5) and animals born with unilateral congenital deafness (UCD, n=2) were compared to naive CDCs (n=7) and normal hearing controls (n=7), all in adult age. As a measure of cortical reorganization, onset latency of local field potentials (LFPs) recorded at 75-150 recording positions in field A1 was determined at the cortex ipsilateral to the „trained“ (hearing or chronically stimulated) ear. A developmental comparison from additional 12 naive CDCs (age from day 8 p.n. to adult) demonstrated that LFP onset latency matured before month 2.0 in CDCs, similarly as in hearing cats (Eggermont, 1996, *Audit Neurosci* 2:309). All investigated animals were well above this age.

Comparison was between responses to the trained ear vs. the deaf ear, both stimulated with a CI (monopolar, biphasic pulse 200  $\mu$ s/phase). In UCDs the onset latency, paired-wise compared, was shorter for the ipsilateral (trained) ear (contra-ipsi=1.68 $\pm$ 0.25 ms median paired difference, p<0.001) and this difference was opposite to controls (-0.89 $\pm$ 0.49 ms, p<0.001). In naive CDCs, the paired difference was not significant (0.04 $\pm$ 0.29 ms). In csCDCs, the paired difference was similar to UCD and statistically significant only for the animals implanted at youngest ages (2.0 and 3.5 months). Nominally, the paired difference in latency anticorrelated significantly (r=-0.9512, p=0.0009) with onset of unilateral hearing experience and fell into the range observed in non-trained CDCs at the implantation age of ~ 4 months.

This demonstrates a sensitive period for aural representation at the cortex ipsilateral to the hearing ear. Paired difference in onset latency is a very sensitive measure of plasticity, saturating after few months of hearing experience.

Supported by Deutsche Forschungsgemeinschaft (Kr 3370/1-3).

## **[25] Three-Dimensional Vibration Measurements of the Human Eardrum and Middle Ear Ossicles**

Ryan Jackson<sup>1</sup>, Hongxue Cai<sup>1</sup>, Sunil Puria<sup>1</sup>

<sup>1</sup>*Stanford University, Otobiomechanics*

Why do larger mammals have an articulated malleus-incus joint? One possibility is that the mobile, saddle-shaped connection between these bones enables efficient high frequency sound conduction. Morphometric studies in our

lab suggest that the malleus and incus each rotate about independent axes and interact in a way that resembles a bevel gear at high frequencies. In addition, asymmetry in the eardrum may help to “twist” the malleus, which would further amplify an energetically favorable, gear-like effect (Puria and Steele, 2010). We are investigating these potential motions through three-dimensional laser Doppler vibrometry (3DLV-Polytec) and finite element modeling of the human middle ear. Here we will present the findings of our vibration measurements for fresh human temporal bones (n=4). For eardrum surface measurements, we considered both the in-plane and out-of-plane velocities of the entire eardrum in the 0.5 to 20 kHz range (SNR>20 dB). The velocity component along the focal axis approximates the out-of-plane velocity, and the two velocity components in the shared focal plane of the 3DLV lasers approximate the in-plane velocity. We found the shape, amplitude, number and position of measured eardrum surface waves in general agreement with other publications, which quantified out-of-plane motion only (e.g., Cheng et al., 2010). Though negligible at low frequency, the in-plane motion is, surprisingly, of the same order-of-magnitude as the out-of-plane motion beyond 4 kHz. The relative phase, of in-plane and out-of-plane motion is equal at low frequency, but beyond 6 kHz the in-plane significantly lags the out-of-plane motion suggesting a greater time delay. We are also applying our measurement technique to look at the relative, and possibly rotational, motion of the malleus, incus, and stapes as further evidence for a “gear” in the middle ear. [Work supported by R01 DC005960 and ARRA supplements to SP/CRS and F30DC010305 to RPJ from the NIDCD of NIH.]

## **[26] A Non-Linear Viscoelastic Model for the Tympanic Membrane**

Hamid Motallebzadeh<sup>1</sup>, Mathieu Charlebois<sup>1</sup>, W. Robert J. Funnell<sup>1</sup>, Sam J. Daniel<sup>1</sup>

<sup>1</sup>*McGill University*

Mathematical models of the middle ear help to interpret and predict its sound-transmission function and ultimately can be used to design new diagnostic tools and therapeutic techniques. Modelling the tympanic membrane in particular, and especially the definition of its material properties, is important and challenging.

The mechanical behaviour of the tympanic membrane displays both energy dissipation and non-linearity. Previous finite-element models of the tympanic membrane, however, have been either non-linear or viscoelastic but not both. In this study, we combine these two features by proposing a non-linear viscoelastic model. The non-linearity is represented by the Ogden hyperelastic model and the viscoelasticity is represented by a Prony's series. Our model output is compared with the relaxation curves and hysteresis loops observed in previous measurements performed on strips of tympanic membrane. In addition, a sensitivity analysis is performed to investigate the effects of the model parameters on the results, and the effect of strain rate is explored.

## **27** Ossicular Resonant Vibration of Human Temporal Bone Measured with Different Frequency Sound Stimulation

Juyong Chung<sup>1</sup>, Won Joon Song<sup>2</sup>, Wandoo Kim<sup>2</sup>, Jun Ho Lee<sup>1</sup>, Sun O Chang<sup>1</sup>, Seung Ha Oh<sup>1</sup>

<sup>1</sup>Department of Otolaryngology-Head and Neck Surgery, Seoul National University Hospital, Seoul, Korea,

<sup>2</sup>Department of Nature-Inspired Nanoconvergence Systems, Korea Institute of Machinery and Materials

Implantable hearing device is an emerging modality of rehabilitation for the hearing impaired patients. However a total implantable device has a couple of problems such as a subcutaneous microphone and a rechargeable battery. The study on vibration characteristics of human ossicle will give a valuable information on how to select proper sites for taking sound energy from the ossicular chain substituting the microphone. We investigated the vibrations of ossicles at the different points with different frequencies of pure tone stimulation. Sound-induced vibrations at malleus head (MH), 4 different points of incus body, long process (LP) of incus, and incudostapedial (IS) joint were measured in the fresh frozen temporal bones ( $n = 6$ ) using laser-Doppler vibrometry with or without IS joint separation, respectively. We analyzed the displacement transfer function (DTF, the ratio of ossicular displacement to the ear canal sound pressure) and the phase angle at 7 sites of ossicles over the frequency range (1-9kHz). At 1, 2kHz, the DTF of MH was the largest and at 3, 4kHz, that of anterosuperior part of incus body was the largest. At 5, 7kHz, the DTF of anterior part of incus body was the largest and at 9kHz, that of LP was the largest. The total resonant frequency of middle ear is around 3 or 4kHz in this study. After IS joint dislocation, the DTF of incus body, LP, and IS joint were significantly increased especially at 3, 5, 7kHz and the phase was changed. The phase patterns of MH and 4 points of incus body were similar each other, but they were different from those of LP and IS joint. In summary, the resonant vibration is variable at the different points. If the point is nearer to the tympanic membrane, the resonant vibration occurs in a lower frequency. The anterosuperior part of incus body showed relatively larger DTFs throughout the frequency range than the other points. This study is sponsored by a grant (20110001666) from National Research Foundation, Seoul, Korea.

## **28** Comparison of Umbo Velocity in Air and Bone Conduction

Christof Röösl<sup>1,2</sup>, David Chhan<sup>1</sup>, Chris Halpin<sup>3</sup>, John Rosowski<sup>1,2</sup>

<sup>1</sup>Eaton-Peabody Laboratory, Massachusetts Eye and Ear Infirmary, <sup>2</sup>Department of Otology and Laryngology, Harvard Medical School, <sup>3</sup>Department of Audiology, Massachusetts Eye and Ear Infirmary

Four different routes have been suggested for the transmission of bone conducted (BC) sound to the cochlea: a) The inertial effect of middle ear ossicles and inner ear fluid, b) sound radiated into the external ear, c) compression of the petrous bone, and d) sound transmitted through non osseous contents of the skull.

Several of these suspected BC paths are thought to stimulate the inner ear via relative motions between the ossicles and the bone surrounding the inner ear.

The motion of the umbo is assumed to be an indicator of stapes motion and therefore an indicator of those routes to the inner ear that depend on stapes motion. It was assessed in live human ears with normal middle ear function as defined by audiometric testing. Laser Doppler Vibrometry was used to measure air conduction (AC) and BC induced umbo velocity ( $V_u$ ) in both ears of 10 subjects, 20 ears total. Sound pressure in the ear canal (PEC) was measured simultaneously. For air conduction,  $V_u$  at threshold was calculated. For BC,  $\Delta V$  was defined as the difference between  $V_u$  and the tympanic ring velocity (an estimate of the skull velocity measured in the ear canal).  $\Delta V$  and PEC at BC threshold were calculated and compared to the corresponding air conduction measurements.

$\Delta V$  at BC threshold was significantly smaller than  $V_u$  at AC threshold between 500 Hz and 2000 Hz. This is consistent with the idea that the motion of the umbo is not the principal drive to BC hearing in this frequency range. Ear canal pressure at BC threshold tended to be smaller than for AC below 3000 Hz (with significant differences at 1000 Hz and 2000 Hz). Our results are most consistent with inertia of the ossicles and cochlear fluid driving BC hearing below 500 Hz, but with other mechanisms playing a significant role at higher frequencies. Sound radiated into the external ear canal might contribute to BC hearing at 3000 Hz and above.

## **29** Acoustics of the Ear Canal and Middle Ear Cavity Probed with High Spatial Resolution

Christopher Bergevin<sup>1</sup>, Elizabeth Olson<sup>1</sup>

<sup>1</sup>Columbia University

The tympanic membrane (TM) is a diaphanous cone-shaped structure integral in sound transmission to the inner ear. Given its highly complex mechanical response, the common description of the TM as a piston driven on one side appears too simple within the context of more modern theories of middle ear function. For example, various model classes incorporate traveling waves along the TM surface, or sound radiation on the backside of the TM into the middle ear cavity and the subsequent reflections from the back bony wall. Our present goal is to measure ear canal and middle ear cavity acoustics in order to determine the validity and relative importance of these considerations, and ultimately what they imply for TM function. We report data from gerbil (*Meriones unguiculatus*), using miniaturized pressure sensors (Olson, 1998 JASA 103:3445-3463) that allow for measurement in small spaces, sensitivity out to 60 kHz, and fine spatial resolution (on the order of 10  $\mu\text{m}$ ). Several salient results are noted here. First, the pressure measured across the TM (middle ear cavity relative to canal) close to the TM surface revealed a significant, frequency-dependent drop of  $\sim 10$ -30 dB. This finding argues against sound reflections from the back cavity wall having a significant effect upon TM motion. Second, pressure measured along the canal-side face of the TM, within  $\sim 20$ -30  $\mu\text{m}$  of the surface,

revealed variations on the order of 10 dB or less. Further study is needed to determine if these variations can be linked to the TM's complex wave-like motion. Lastly, postmortem experiments where the temporal bone is presumably drying out, indicate that the TM impedance can significantly affect canal acoustics, such as standing wave notch frequencies.

### **[30] Imaging and Vibrational Measurement of Middle-Ear Ossicles with Spectral-Domain Phase-Sensitive Optical Coherence Tomography**

Anh Nguyen-Huynh<sup>1</sup>, Hrehash Subhash<sup>2</sup>, Yuming Liu<sup>2</sup>, Ruikang Wang<sup>3</sup>, Alfred Nuttall<sup>1</sup>, Steven Jacques<sup>2</sup>

<sup>1</sup>Department of Otolaryngology, Oregon Health & Science University, <sup>2</sup>Department of Biomedical Engineering, Oregon Health & Science University, <sup>3</sup>Department of Biomedical Engineering, University of Washington

Optical coherence tomography (OCT) exploits interferometry of low-coherence infrared light to generate cross-sectional images with micron axial resolution. Analogous to the use of ultrasound, OCT has been used to image structures in the middle ear. We now report the first use of spectral-domain phase-sensitive OCT to measure vibration of the middle ear ossicles behind an intact tympanic membrane (TM). Our bench top system is a standard spectral domain OCT microscope based on a superluminescent diode operating at 1310-nm wavelength (48-nm bandwidth, 15- $\mu$ m axial resolution). Our method creates an axial scan of reflectance from each depth position  $z$  versus time for each  $x,y$  position chosen for analysis, acquired as  $R(z,t)$ . An auditory signal applied to the ear causes a structure of interest to vibrate, which is viewed as an oscillation of the  $z$  position of the reflective surface of the structure.

We have tested our system in unfixed human cadaveric ears. Both intact head and isolated temporal bone specimens were used. Sound stimuli were delivered at different frequencies and intensities from both far-field speaker and sound conductor close in to the TM. Under these conditions the OCT microscope was able to image the TM, malleus, incus, and stapes capitulum, and to measure the vibration amplitudes of these structures in response to sound. The OCT microscope was also able to image an experimentally produced fracture of the incus and to measure the differential vibration amplitudes of the proximal and distal segments.

Application of OCT to imaging and vibrational measurement of middle-ear ossicles has the potential to provide a non-invasive diagnostic tool that can localize and quantify the lesion(s) causing conductive hearing loss. In addition, the technology can also facilitate developing and testing of middle ear prostheses designed for optimal sound transmission.

This work was supported by NCRR grant KL2RR024141, NIDCD grants DC00105, DC010201, and DC010399.

### **[31] A Finite Element Model of Pediatric Ear for Sound Transmission from Ear Canal to Middle Ear**

Xiangming Zhang<sup>1</sup>, Rong Gan<sup>1</sup>

<sup>1</sup>University of Oklahoma

A 3-dimensional finite element (FE) model of pediatric ear was developed based on a set of histological sections of the 4-year old temporal bone. This model included the ear canal, tympanic membrane, ossicular chain with suspensory ligaments and muscles, and middle ear cavity, as the first step toward a comprehensive FE model of the pediatric ear with cochlea. The external ear canal had a cartilage layer on the canal wall and the middle ear soft tissues were assumed as nonlinear viscoelastic material. The cochlea was simplified as a mass and damping load connected to the stapes footplate. The geometry and physical parameters of the pediatric ear model were compared with published data for newborn and adult ears. Input sound of 90 dB SPL was applied in the ear canal at 2 or 20 mm away from the umbo. The acoustic-structure coupled analysis was conducted in the model over the frequency range of 0.2-8 kHz. The pediatric model was validated by comparing the model-derived energy absorbance (EA) curves with published clinical measurements. The model-derived middle ear transfer function (METF) was compared with the results from published FE models of newborn and adult ears. The effects of ear canal cartilage layer thickness and middle ear cavity volume on METF and EA were assessed. The effects of mechanical properties of tympanic membrane, incudostapedial joint and stapedial annular ligament on METF and EA were studied. (Work supported by NIH R01DC011585)

### **[32] Broad Generation Region for Tone-Pip-Evoked Otoacoustic Emissions in Chinchillas**

Jonathan Siegel<sup>1</sup>, Karolina Charaziak<sup>1</sup>

<sup>1</sup>Hugh Knowles Center, Roxelyn and Richard Pepper Dept. of Comm. Sci. and Disord, Northwestern Univ.

Otoacoustic emissions evoked by low-level transient stimuli are postulated to be generated by coherent linear reflection (CRF) (Shera and Guinan, 1999). We tested this hypothesis in chinchillas by evoking emission with 1 ms duration tone pips at 1 kHz, that CRF would predict to generate emissions only in the apical region of the cochlea. Separating the stimulus from the emission using a stimulus estimate measured at a higher stimulus level (the scale-subtract, or compression method) revealed an emission with a spectrum weighted toward frequencies below the center frequency of the tone pip and with a group delay similar to that of stimulus-frequency otoacoustic emissions (SFOAE) measured using pure tones and the suppression method. This skewed spectrum, and especially a large lobe at frequencies well below the center frequency of the probe, suggested the presence of an intermodulation-distortion band that cannot arise from a strictly linear mechanism. To probe the region of generation, we used continuous tone suppressors to separate the emission from the stimulus. Suppressor tones near the center frequency of the tone pip revealed

emissions that were similar to those using the scale-subtract method. Successively higher-frequency suppressors reveal emissions with 1) largest amplitude for suppressors in the range of 2-6 kHz and demonstrable for suppressors as high as 10 kHz, 2) successively shorter time-domain and group delays, 3) spectra that more closely resemble the stimulus. These attributes support the hypothesis that much of the emission is generated by a linear mechanism in a large region extending basally from the peak of the traveling wave and that the action of the suppressor is to remove emission generators evoked by the tone-pip and not to generate nonlinear artifacts in regions basal to the peak region. The original formulation of the CRF theory does not account for these results. Supported by NIH Grant DC-00419 and Northwestern University.

### **33 DPOAE Growth Behavior in Acute Otitis Media and Otitis Media with Effusion Models of Guinea Pigs**

**Xiying Guan<sup>1</sup>, Rong Z. Gan<sup>1</sup>**

<sup>1</sup>*School of Aerospace and Mechanical Engineering and Bioengineering Center, University of Oklahoma*

Acute otitis media (AOM) and otitis media with effusion (OME) are the most common middle ear diseases in young children and result in conductive hearing loss. Some animal studies reported that the inner ear function may be affected in otitis media (OM) and sensorineural hearing loss became an outcome of the OM. However, to what extent the inner ear function would change in OM needs further investigation. This study was designed to measure the input/output functions of distortion product otoacoustic emissions (DPOAE I/O-functions) in AOM and OME models of guinea pigs. If AOM or OME has an impact on inner ear, the non-linear behavior in DPOAE I/O-functions would possibly change. To test this hypothesis, DPOAE I/O-functions were recorded in a wide primary tone level range of  $f_2$  frequencies between 2 and 16 kHz ( $15 < L_2 < 65$  dB SPL,  $L_1 = 0.46L_2 + 41$  dB SPL;  $f_2/f_1 = 1.2$ ) in guinea pig ears. The AOM and OME were created by transbullar injection of *streptococcus pneumonia* type 3 ( $\sim 10^5$  CFU/ml in 0.1 ml saline) and lipopolysaccharide (100 ug/ml in 0.1 ml saline) into the left ear of the animal, respectively. DPOAE I/O-functions were measured three days post inoculation using TDT system III. The results from 6 AOM ears and 4 OME ears show that steepened DPOAE I/O-functions were observed at 2-16 kHz in two AOM ears, which suggested the loss of non-linear amplification of the inner ear. In 4 AOM and 4 OME ears, the non-linearity of DPOAE I/O-functions was observed at all tested frequencies except 16 kHz. This preliminary study concluded that the inner ear dysfunction was not likely to happen in the OME model, and there was a low chance that the inner ear non-linearity changed in the AOM model. Further studies are needed to investigate the inner ear function in the AOM model. (Supported by OCAST HR09-033 and NIH R01DC011585)

### **34 Understanding the Tone-Burst Otoacoustic Emission Latency Estimate**

**Sarah Verhulst<sup>1</sup>**

<sup>1</sup>*Technical University of Denmark*

Tone bursts are commonly used to determine the cochlear roundtrip time from tone burst otoacoustic emissions (TBOAEs). The TBOAE latency is typically around twice the cochlear travel time derived from the wave-V latency in auditory brainstem responses.

The TBOAE latency estimate suffers from a large variability, partly ascribed to the methods used to separate the stimulus from the emission onset. Recent studies furthermore question the underlying mechanisms (i.e., reflection source versus distortion source) behind the growth rates of consecutive emission bursts. This study investigates the cochlear mechanisms underlying the TBOAE latency estimate to explain the inter-subject variability and the components contributing to the estimate. A nonlinear time-domain model of the cochlea based on coherent reflection was adopted for this purpose.

Five recorded TBOAE level series were compared to simulated TBOAE level series for 20 subjects. The simulated subjects shared the underlying cochlear mechanics, but differed in the placement of the basilar-membrane irregularities responsible for coherent reflection. As stimulus level increased, shorter TBOAE latencies were found for both simulations and recordings. The shorter latencies were due to additionally evoked frequency components ascribed to spread of excitation or inter-modulation distortion, when stimulus level increased. Regardless of their origin, the closely spaced emission components led to TBOAE envelope maxima with shorter latencies than the envelope maxima of TBOAEs containing a single frequency. The simulated TBOAE envelopes were dominated by the interaction of multiple evoked frequency components, giving rise to a standard deviation of 2.5 ms on the simulated 1-kHz latency estimate. These results suggest that caution is advised when estimating the roundtrip time from TBOAE latencies, as it only describes the cochlear roundtrip time accurately when a single frequency component is evoked or tracked.

### **35 Visualization of Time-Course of OCB Acoustical Reflex Using SFOAE**

**Tatsuhiko Harada<sup>1</sup>**

<sup>1</sup>*International University of Health and Welfare Atami Hospital*

(Objective) To detect time-course change of stimulus frequency otoacoustic emission (SFOAE) due to olivocochlear bundle (OCB) reflex elicited with ipsilateral noise.

(Subjects and equipment) Normal hearing volunteers are participated. Three subjects had been measured at present. ER10C (Etymotic Research) and RP2.1 (Tucker Davis Technology) were used as receiver-stimulator and signal processor. Control of stimulus and recording, and processing of the recorded data were done with customized software made with LabVIEW v8.6 (National Instruments).

(Stimulus and processing) Sound stimuli were composed of 4 patterns: (1) probe tone + interrupting noise (2) reversed phase probe tone + interrupting noise (3) probe tone + suppressor tone (4) reversed phase probe tone + suppressor tone. In this study, probe tone was 4000Hz, suppressor tone was 3800Hz, and interrupting noise was composed of random phased tones from 400Hz to 3600Hz with the intervals of 0.75Hz. Recording period was 1342ms. The probe and the suppressor tones were whole length of recording, but interrupting noise was only from 200msec to 600msec after the onset of recording. Recording was repeated and averaged, and ((1)-(2))-((3)-(4)) was calculated. Band pass filtering with pass band from 3800Hz to 4200Hz was applied to the results, and root mean square of 10msec time length was calculated as instantaneous waveform amplitude.

(Results and conclusion) In all of the subjects showed that SFOAE levels decreased after the onset of interrupting noise but recovery of the level was delayed after the end of the noise. The duration to the recovery was shortened as the noise level decreased. With large probe tone (60dB SPL), the SFOAE level gradually decreased in addition to the effects of the noise. These can be regarded as OCB reflex elicited with noise and probe tone itself. In conclusion, this method is useful for visualizing OCB reflex.

### **[36] Dose-Related Effect of Cisplatin on Distortion Product Otoacoustic Emissions in Veterans**

**Kelly M. Reavis**<sup>1</sup>, Garnett P. McMillan<sup>1,2</sup>, Dawn Konrad-Martin<sup>1,2</sup>, Peter G. Jacobs<sup>1</sup>, Marilyn Dille<sup>1,2</sup>

<sup>1</sup>VA RR&D, National Center for Rehabilitative Auditory Research (NCRAR), <sup>2</sup>Oregon Health & Science University  
It is well known that therapeutic treatment with the chemotherapy agent cisplatin causes hearing loss and the risk for cisplatin-induced hearing loss is dose-dependent. The initial cochlear structures damaged by cisplatin include the outer hair cells (OHC) and the stria vascularis which provides the electrical drive to the OHCs. Distortion-product otoacoustic emissions (DPOAE) are well-suited to detect ototoxicity because of their physiological dependence on OHC function. The objective of this analysis was to estimate changes in DPOAE levels during cisplatin chemotherapy. DPOAE level data collected using fine frequency-step resolution were obtained in one ear from each of 19 Veterans tested as part of a prospective Veterans Affairs study investigating methods of ototoxicity monitoring. DPOAEs were measured over the course of cisplatin chemotherapy treatment. A total of 56 monitoring visits were included, with an average of 2.9 monitoring visits per patient. DPOAE primary frequency,  $f_2$ , was measured in 1/48th octave steps over the highest half-octave of obtainable emissions with  $f_2/f_1=1.22$  and  $L1/L2=65/65$  dB SPL. To investigate the effects of cisplatin on DPOAE levels, a model was fit to the mean DPOAE shift functions (derived by subtracting DPOAE level at a given monitoring visit from baseline level measurements) using unpenalized cubic B-spline regression. The model included both a population mean basis expansion to

identify average DPOAE level shifts induced by increasing cisplatin exposure and random subject-specific basis expansions to allow for individual variability in the effects of cisplatin. The model identified an overall pattern whereby DPOAE levels decreased with increasing cisplatin exposure; the decrease was more pronounced at the higher frequencies. The model is validated on an independent sample of seven recently tested cisplatin patients. The potential clinical utility of such a model is that, once validated, it can estimate the dose at which cisplatin will begin to affect a DPOAE-based proxy measure of OHC function in an individual patient.

### **[37] Comparisons of Transient-Evoked Otoacoustic Emissions at Ambient and Tympanometric-Peak Pressure, and the Use of Absorbed Power to Increase the Detection Bandwidth of Chirp-Evoked Emissions**

**Douglas Keefe**<sup>1</sup>, Lisa Hunter<sup>2</sup>, Patrick Feeney<sup>3,4</sup>, David Brown<sup>2</sup>, Denis Fitzpatrick<sup>1</sup>

<sup>1</sup>Boys Town National Research Hospital, <sup>2</sup>Cincinnati Children's Hospital Medical Center, <sup>3</sup>National Center for Rehabilitative Auditory Research, <sup>4</sup>Oregon Health & Science University

New transient-evoked otoacoustic emissions (TEOAEs) tests using click and chirp stimuli were devised to better assess cochlear status in clinical translational studies of hearing in infants and adults. Procedures were based on successive measurements of absorbance tympanometry, ambient absorbance, and TEOAE responses using the same ear-canal probe. Absorbance tympanometry measured the tympanometric peak pressure (TPP), which was averaged in some ears over ascending and descending sweeps of air pressure in the ear canal; subsequent TEOAE tests were compared between ambient and TPP conditions. Ambient absorbance measurement provided an in-the-ear calibration of a TEOAE chirp stimulus based on absorbed sound power. The calibrated chirp was further adjusted to increase the stimulus level at frequencies with elevated noise levels. TEOAEs were elicited over a bandwidth from 1 kHz to either 8 or 10 kHz using clicks and chirps with a local frequency linearly increasing or decreasing with time. Chirp-evoked TEOAEs with sufficiently long dwell times relative to OAE delays are functionally similar to swept stimulus-frequency OAE measurements, yet amenable to signal averaging and artifact rejection. Detection of a TEOAE at any frequency/time may be improved by considering both signal-to-noise ratio (SNR) and phase coherence. Measurement feasibility was demonstrated in adult ears and ears of infants from well-baby nurseries and neonatal intensive care units. Preliminary results suggest that TEOAE levels improved in adults when measured at TPP compared to ambient pressure; tests in infants raise special problems. When compared to TEOAEs recorded at constant voltage at the receiver or at constant ear-canal pressure, TEOAE testing at constant absorbed sound power has the potential to better detect cochlear responses at frequencies for which middle-ear absorption is inefficient, thereby improving the SNR and phase

coherence overall. [Research supported by NIDCD grant DC010202]

### **38 Offline Correction for Series Resistance in the Whole-Cell Recording of Ongoing Synaptic Activity**

Shilpa Chatlani<sup>1</sup>, Jay M. Goldberg<sup>2</sup>

<sup>1</sup>Johns Hopkins School of Medicine, <sup>2</sup>University of Chicago  
In studies of ongoing synaptic activity from calyx endings in the turtle posterior crista, we found that whole-cell recordings were facilitated by the use of higher impedance patch pipettes (6-8 M $\Omega$  in bath) and by keeping the pipette near the calyx membrane as seal formation gradually increased. The result was a high series resistance (RS  $\approx$  40 M $\Omega$ ) combined with a low membrane resistance (RM  $\approx$  40 M $\Omega$ ) and a high membrane capacitance (CM  $\approx$  40 pF). This combination leads to severe attenuation and some slowing of EPSCs. The customary way to compensate for these effects, injection of RS-scaled current into the pipette, has limitations. We have found that ongoing EPSCs can be completely corrected offline using simple, one-compartment circuit calculations. Corrections of voltage-clamp records can be checked by offline manipulation of EPSPs obtained in current clamp. Corrections based on EPSPs are too small, by about 30%, reflecting the imperfections of patch-clamp amplifiers when used in current clamp. The assumptions of the treatment, that EPSCs are adequately space clamped and do not activate ionic currents, need to be verified, as was done in our recordings. For our experimental conditions, EPSCs are attenuated threefold and slowed nearly twofold. Even modest series resistances ( $\approx$ 10 M $\Omega$ ) can lead to substantial effects so that individual recordings need to be corrected or, at the very least, specific values of RM, RS and CM need to be reported.

### **39 An *in Vivo* Model for Pharmacologic Investigations of the Vestibular Neuroepithelia**

Larry Hoffman<sup>1</sup>, Tanye Tang<sup>2</sup>, David Sultemeier<sup>1</sup>, Y. Sungtaek Ju<sup>2</sup>

<sup>1</sup>Geffen School of Medicine at UCLA, <sup>2</sup>UCLA

We have adapted and tested a new model for conducting *in vivo* pharmacologic investigations of the mammalian peripheral vestibular neuroepithelia using afferent neuron discharge as the output measure. The principal advances involve the use of a microfluidic delivery system enabling pressure modulation and flow measurement at the microliter-scale, and a MEMS-fabricated fluidic multiplexer that provided mixing of multiple fluid channels at the final stage prior to direct intraperilymphatic delivery. Chinchillas were anesthetized (Nembutal) and placed in a custom head restraint for electrophysiologic recording from the superior vestibular nerve. A 5mm length of stainless steel tubing (27 ga. thin wall) was glued into a small fenestra carefully made in the dorsalmost aspect of the bony superior semicircular canal within the middle ear. This perilymph access port was secured within the middle ear with a bonding agent, and enabled fluid delivery to the perilymph without occluding the superior canal. Solution

delivery temperature was closely monitored as it exited a custom inline heater prior to solution entry into the labyrinth, and within the superior canal. Solution flow through the labyrinth was enabled after perforating the round window membrane. Using artificial perilymph as the perfusate we verified the stability of afferent discharge at different flow rates, and have determined the optimal flow onset and termination profile that minimizes effects on afferent discharge. We also tested the kinetics of pharmacologic action on a sample of semicircular canal afferents with heterogeneous dynamics using AMPA receptor agonists and antagonists. The integrity of the neuroepithelia was verified through immunohistologic examination of hair cells (anti-Myosin VI) and afferent calyces (anti- $\beta$ 3-tubulin). This study demonstrates the efficacy of the delivery strategy and hardware developed for effective pharmacologic investigation of the vestibular neuroepithelia.

### **40 Endogenous and Exogenous Modulation of Synaptic Repair in Vestibular Peripheral Endorgans**

Sophie Gaboyard-Niay<sup>1</sup>, Aurore Brugeaud<sup>1</sup>, Cécile Travo<sup>2</sup>, Audrey Broussy<sup>1</sup>, Aurélie Saleur<sup>1</sup>, Christian Chabbert<sup>1,2</sup>

<sup>1</sup>Sensorion, <sup>2</sup>INSERM U1051

We recently delineated different stages from lesion to repair following excitotoxic injury of the vestibular peripheral endorgans in a rodent model using transtympanic injection of kainic acid (Gaboyard et al., ARO 2011). These steps are correlated to a precise time course of behavioral deficit development and recovery and, with histological damage determining deficit induction and structural synaptic plasticity underlying the recovery of vestibular function.

In the present study, we investigated whether epigenetic factors presumably underlying aging can modulate peripheral vestibular repair capacity, using 6 to 10 month-old old Wistar rats. While age did not influence the acute crisis stage following transtympanic injection of kainic acid, older animals displayed a significantly delayed recovery from induced vestibular deficits correlated with a significantly longer lasting period of structural synaptic repair.

We furthermore examined the mechanisms underlying the neuroprotective capacity of the anti-emetic ondansetron, recently shown to reduce lasting vestibular deficits following excitotoxic lesions *in vivo*. Ondansetron treatment following excitotoxic injury reduced the peak histological lesion, promoted faster resorption of terminal swellings and thus accelerated the synaptic repair and functional recovery.

These findings demonstrate the possibility for modulation of structural synaptic plasticity of peripheral vestibular synaptic terminals after injury. Indeed, this highlights the opportunities and potential to pharmacologically protect and/or promote recovery of vestibular function. Further investigations are necessary to determine the specific target of ondansetron in the vestibular tissue as well as

epigenetic modifications underlying the age-related decrease in repair capacity.

#### **[41] Topical Application of FGLM-NH2 and SSSR Facilitates Vestibular Functional Recovery Induced by AMPA**

Hideki Toyota<sup>1</sup>, Hiroaki Shimogori<sup>1</sup>, Kazuma Sugahara<sup>1</sup>, Hiroshi Yamashita<sup>1</sup>

<sup>1</sup>*Department of Otolaryngology, Graduate School of Medicine, Yamaguchi University*

Topical FGLM-NH2 and SSSR facilitates recovery from vestibular disorders induced by (□)  $\alpha$ -amino-3-hydroxy-5-methyl-isoxazole-4-propionic acid (AMPA) in guinea pigs and might offer a treatment strategy for patients with peripheral vestibular disorders.

The tetrapeptide FGLM-NH2 derived from Substance P (SP) can cure corneal disorders when combined with SSSR, a tetrapeptide derived from insulin-like growth factor-1 (IGF-1). We examined the influence of FGLM-NH2 and SSSR when locally applied to the unilateral inner ear of guinea pigs with vestibular disorder induced by AMPA.

Hartley white guinea pigs were assigned to groups administered with FGLM-NH2 +SSSR, artificial perilymph and no treatment. A hole was drilled adjacent to a round window and AMPA was infused into the hole to induce vestibular disorder. Thereafter, FGLM-NH2+SSSR or artificial perilymph was delivered via an osmotic pump inserted into the hole. We observed spontaneous nystagmus and measured vestibulo-ocular reflexes (VOR) using sinusoidal rotation tests. Two animals from each group were immunohistochemically examined at 24 h after treatment.

Spontaneous nystagmus decreased immediately after FGLM-NH2 +SSSR infusion, and the gain ratios were statistically higher than those in the control group at 3 and 7 days after treatment. Many synaptic ribbons were stained in the FGLM-NH2 +SSSR group compared with the untreated group.

Topical FGLM-NH2 and SSSR facilitates recovery from AMPA-induced vestibular disorders in guinea pigs.

#### **[42] Vestibular Research and AMPA**

shuhei yoshida<sup>1</sup>, hiroaki shimogori<sup>1</sup>, hideki toyota<sup>1</sup>, kazuma sugahara<sup>1</sup>, hiroshi yamashita<sup>1</sup>

<sup>1</sup>*Yamaguchi University*

Glutamate is the major excitatory neurotransmitter in the peripheral vestibular system, and a glutamate receptor, the (□)  $\alpha$ -amino-3-hydroxy-5-methyl-isoxazole-4-propionic acid (AMPA) receptor, is of primary importance in neuronal transmission in the vestibular periphery. It is well known that glutamate induces excitotoxicity in neuronal cells in brain ischemia. AMPA induces a transient, reversible disorder of inner ear hair cells and causes ischemia-like histologic changes in the cochlea. We have developed a model of partial vestibular dysfunction induced by topical application of AMPA. Though, this model has a potential to possess functional recovery, another physiological model showing permanent vestibular dysfunction is also necessary to investigate drug effects for inner ear

diseases. In this presentation, we will show the model-making process using AMPA in our laboratory.

#### **[43] Nicotinic ACh Receptors in the Turtle Posterior Semicircular Canal**

Xiaorong Xu Parks<sup>1</sup>, Donatella Contini<sup>1</sup>, Joseph Holt<sup>1</sup>

<sup>1</sup>*University of Rochester*

In turtle posterior semicircular crista, cholinergic efferent neurons terminate on type II hair cells, bouton afferents innervating type II hair cells and afferent calyces innervating type I hair cells. Sharp electrode recordings from canal afferents have revealed that efferent actions are quite diverse including rapid inhibition of bouton afferents and rapid excitation of calyx/dimorphic (CD) afferents. From such recordings, it has been inferred that efferent-mediated inhibition of bouton afferents is attributed to activation of  $\alpha$ 9/ $\alpha$ 10-containing nicotinic ACh receptors ( $\alpha$ 9/ $\alpha$ 10nAChRs) on type II hair cells. Calcium influx through  $\alpha$ 9/ $\alpha$ 10nAChRs subsequently recruits small-conductance, calcium-dependent potassium channels (SK) that hyperpolarize the hair cell and decrease transmitter release to inhibit afferent discharge. Efferent-mediated excitation of CD units is generated by activating nAChRs located on calyceal terminals that then directly depolarize the afferent. In order to describe the distinct cellular mechanisms underlying these efferent actions, we have been performing whole-cell patch clamp recordings from type II hair cells and calyx-bearing afferents in a split epithelial preparation of the posterior crista. This particular preparation allows us to easily visualize hair cells and calyx afferents as well as specify their location within the epithelium. Type II hair cells both in the central zone and near the non-sensory torus routinely respond to the application of 50-100 $\mu$ M ACh. This particular ACh response is antagonized by compounds known to block  $\alpha$ 9/ $\alpha$ 10nAChRs including ICS. Consistent with the downstream activation of SK channels, the ACh-sensitive current reverses around -90mV and is outward at more depolarized potentials. Cellular characterization of excitatory nAChRs on calyx afferents and further pharmacological analyses of  $\alpha$ 9/ $\alpha$ 10nAChRs and SK channels in type II hair cells are currently underway. (Supported by DC008981).

#### **[44] CGRP Is Expressed by Vestibular Efferents in Turtle Vestibular Organs**

Paivi Jordan<sup>1</sup>, Margaret Fettes<sup>1</sup>, Sarah Westendorf<sup>1</sup>, Anne Luebke<sup>1</sup>, Joseph Holt<sup>1</sup>

<sup>1</sup>*University of Rochester*

It is generally accepted that the predominant vestibular efferent transmitter is acetylcholine (ACh). The presence of dense core vesicles in efferent terminals, however, also suggests a role for peptidergic transmission in the vestibular periphery. The most compelling evidence to date implicates calcitonin gene-related peptide (CGRP), a 37-amino acid neuropeptide frequently co-expressed at cholinergic synapses including the neuromuscular junction (NMJ) and in auditory, lateral line and vestibular efferent neurons. We are currently investigating whether CGRP is involved in vestibular efferent function in the turtle posterior

crista. Our first approach utilized immunohistochemistry to identify if CGRP was expressed in the turtle vestibular periphery. A well-characterized CGRP antibody intensely labeled efferent terminals throughout the neuroepithelium of the semicircular canals, lagena, utricle, and saccule. In turtle cristae, CGRP staining was extensively co-localized with labeling for choline acetyltransferase (ChAT) where almost every ChAT-positive terminal was also CGRP-positive. CGRP labeling in the sensory epithelium did not appear restricted to any region or display any obvious zonal boundaries. Unlike mammals where CGRP-positive terminals are reported to mainly terminate on afferent dendrites and calyceal terminals, many CGRP-positive terminals in the turtle are also found along the base of type II hair cells. Despite the widespread expression of CGRP among efferent terminals in the turtle posterior crista, most of the observed efferent actions, seen following genuine efferent stimulation, are antagonized by cholinergic antagonists. What then might be the role of CGRP? Borrowing from studies of the NMJ, perhaps CGRP interacts with efferent neurotransmission either by modulating the presynaptic release of ACh or by modifying signaling through postsynaptic cholinergic receptors. The feasibility of such mechanisms will be discussed. (Supported by DC008981)

#### **[45] A Conductance-Based Model to Study How Ion Channels Regulate Firing Patterns in Mammalian Vestibular Ganglion Neurons**

A. Edward Hight<sup>1,2</sup>, Radha Kalluri<sup>1,2</sup>

<sup>1</sup>House Research Institute, <sup>2</sup>University of Southern California

Some mammalian vestibular afferents fire at irregular interspike intervals and others at regular intervals. The neurons have diverse complements of ion channels (e.g., Limon et al 2005; Iwasaki et al. 2008) that could shape in vivo firing patterns (Smith and Goldberg 1986, Highstein and Politoff, 1978). Based on in vitro recordings from dissociated rat and mice vestibular ganglion neurons, Kalluri et al. (2010) proposed that spike timing regularity in vivo is controlled by the size of low-voltage activated potassium currents ( $I_{KL}$ ). To examine the impact of  $I_{KL}$  on spike timing we implemented a single compartment Hodgkin-Huxley style model with four types of currents known to be present in the vestibular ganglion: low-voltage activated persistent potassium ( $I_{KL}$ ), transient-sodium, high-voltage activated potassium, and hyperpolarization activated cationic ( $I_h$ ) currents. Consistent with in vitro results, decreasing  $I_{KL}$  in the model depolarized resting potential, increased input resistance and membrane time constant, and converted step-evoked firing patterns from transient (one spike at the onset of the step) to sustained. Blocking  $I_{KL}$  with drugs induces spontaneous spiking in ganglion neurons that otherwise spike transiently; modeled neurons spiked spontaneously only when they contain large persistent inward currents (e.g.,  $I_h$ ). To test the impact of  $I_{KL}$  on spike timing regularity, we simulated responses to synaptic inputs. Arrival times, amplitudes, and time course of synaptic events were modeled on

recordings of synaptic activity from the bouton terminals of cochlear inner hair cells (e.g., Glowatski et al. 2009). In response to statistically identical synaptic drive, decreasing  $I_{KL}$  increased spike rates (10 to 100 Hz) and increased the regularity of spike intervals (coefficient of variation from 0.8 to 0.2). Future work will examine the influence of synaptic event time course, amplitude and statistics.

#### **[46] Relation Between Vestibular Afferents Sound Sensitivity and Peripheral Innervation Patterns in Rat Vestibular End Organs**

Hong Zhu<sup>1</sup>, Xuehui Tang<sup>1</sup>, Adel Maklad<sup>2</sup>, William Mustain<sup>1</sup>, Richard Rabbitt<sup>3,4</sup>, Steve Highstein<sup>4</sup>, Wu Zhou<sup>1,2</sup>

<sup>1</sup>Department of Otolaryngology, University of Mississippi Medical Center, Jackson MS, <sup>2</sup>Department of Neurobiology and Anatomical Sciences, University of Mississippi Medical Center, <sup>3</sup>Department of Bioengineering, University of Utah, Salt Lake City, UT, <sup>4</sup>Marine Biological Laboratory, Woods Hole, MA

Sound-evoked vestibular myogenic potentials in the sternocleidomastoid muscles (cVEMPs) have been used clinically to assess vestibular function (for a review, Rosengren et al., 2010). The cVEMP is typically interpreted as a test of saccule function based on the assumption that sound clicks primarily activate the saccule. Our recent neurophysiology studies, however, indicate that air-conducted clicks or tone bursts commonly used in clinical VEMP testing can activate other vestibular end organs, such as semicircular canals (Zhu et al, Click-evoked responses in vestibular afferents in rats. *J. Neurophysiol.* 106: (2) 754-763, 2011; Zhu et al., Air-conducted short tone bursts-evoked vestibular responses in rats. Abstract No. 579.05 Society of Neuroscience Meeting. Washington, DC, 2011). In the present study we used intra-axonal labeling to examine the peripheral innervation patterns of sound sensitive vestibular afferents in Sprague-Dawley rats. A total of 20 vestibular afferents (13 regular afferents and 7 irregular afferents) were electrophysiologically characterized and injected with biocytin. Afferent spike train responses to air-conducted clicks (80 dB SL re ABR threshold, 0.1 ms duration, rarefaction) were recorded. Sound sensitive irregularly discharging afferent neurons projecting to the horizontal canal crista ampullaris and to the utricular macula were found. Thus, both anatomical and electrophysiological evidence support that the sound stimuli used in current clinical VEMP tests activate otolith and canal sensory organs. These results suggest caution when interpreting clinical cVEMP results, and may provide insights into the development of VEMP diagnostic tests with higher specificity. {Partial support R01 DC008585 (WZ) and R01 DC006685 (RDR)}

#### **47 Immunohistochemical and Biomolecular Identification of Melatonin 1a and 1b Receptors in Rat Vestibular Nuclei**

Seong-Ki Ahn<sup>1</sup>, Roza Khalmuratova<sup>1</sup>, Young-Sool Hah<sup>2</sup>, Dong Gu Hur<sup>1</sup>, Hung-Soo Kang<sup>1</sup>, Carey D Balaban<sup>3</sup>

<sup>1</sup>Department of Otolaryngology, School of Medicine, Gyeong National University and University Hospital,

<sup>2</sup>Clinical research Institute, Gyeong National University Hospital, <sup>3</sup>Department of Otolaryngology, School of Medicine, University of Pittsburgh

**Objective:** The aim of this study was to examine the localizations and expressions of melatonin 1a (MT1a) and 1b (MT1b) receptors in rat vestibular nuclei by immunohistochemical staining and reverse transcriptase-polymerase chain reaction.

**Materials and methods:** Twenty male Sprague-Dawley rats were used in this study. Antibodies for the MT1a and MT1b receptors were used in 10 rats, respectively. A further 10 animals were sacrificed for RT-PCR. Tissues containing medial vestibular nuclei were selectively isolated from brain stem slices for RT-PCR.

**Results:** MT1a and MT1b receptor immunopositive neurons were found to be distributed throughout the four major vestibular nuclei. Both receptors were primarily detected in neuronal somata and their proximal dendrites. The presences of the mRNAs of the MT1a and MT1b receptors were confirmed by RT-PCR in medial vestibular nuclei and trigeminal ganglia.

**Conclusions:** The present study demonstrates, for the first time, that MT1a and MT1b receptors are localized and expressed in rat vestibular nuclei. This study provides additional insight into the role of melatonin receptors during vestibular signal processing.

#### **48 Anatomical and Physiological Characterization of Mouse Lateral Vestibular Nucleus Neurons**

Iain Stitt<sup>1</sup>, Hannah Drury<sup>1</sup>, Robert Callister<sup>1</sup>, Alan Brichta<sup>1</sup>, Rebecca Lim<sup>1</sup>

<sup>1</sup>University of Newcastle

**Background.** The lateral vestibular nucleus (LVN) plays an important role in the activation of vestibular-mediated behaviors such as the vestibulocollic and vestibulospinal reflexes and yet we know surprisingly little about LVN neurons, particularly in mice. As in other animals, a characteristic feature of mouse LVN is the presence of large diameter neurons (> 30  $\mu$ m) called Deiters' neurons. These neurons are thought to be the primary source of projection fibers from the LVN. However, our preliminary retrograde labeling studies show that spinal projection neurons can be smaller, with a mean soma diameter of  $20.2 \pm 1.8 \mu$ m (n = 15). Here we show significant anatomical and electrophysiological differences between Deiters' and small (< 17  $\mu$ m) putative interneurons in wild type mice.

**Methods.** C57/Bl6 mice (3 - 5 weeks old) were anaesthetized with Ketamine (100mg/kg) and decapitated. The brainstem was isolated and the region containing the

LVN was sectioned (250  $\mu$ m) and placed in an oxygenated recording chamber of Ringers solution at 28 deg C. Whole cell recordings in current- and voltage-clamp modes used KCH<sub>3</sub>SO<sub>4</sub> and CsCl internal solutions, respectively. All values are expressed as mean  $\pm$  S.E.

**Results.** More than 90% of Deiters' neurons and smaller LVN neurons are tonically active. However, discharge rates and action potential (AP) width were significantly different with Deiters' neurons having faster rates and narrower AP width (Rate:  $28.3 \pm 4.5$  Hz, n = 18 vs.  $15.6 \pm 1.3$  Hz, n = 23; p < 0.05 and AP width:  $0.52 \pm 0.03$  vs.  $1.16 \pm 0.09$ ). We also investigated differences in fast synaptic inhibition of these two LVN neuronal populations. Our results show that Deiters' GABA<sub>A</sub>ergic miniature inhibitory postsynaptic currents frequency was significantly higher ( $12.4 \pm 1.4$  Hz, n = 12 vs.  $1.5 \pm 0.4$  Hz n = 33; p < 0.001). In addition, intracellular labeling shows that Deiters' neurons appear to have more primary dendrites ( $8.0 \pm 1.0$ , n = 7 vs.  $4.7 \pm 0.9$ , n = 3).

#### **49 A Strategy for Identifying Cell Types and Marker Genes in Heterogenous Neuronal Populations by Single-Cell Transcript Profiling**

Takashi Kodama<sup>1,2</sup>, Shiloh Guerrero<sup>1,2</sup>, Minyoung Shin<sup>1,2</sup>, Setareh Moghadam<sup>3</sup>, Michael Faulstich<sup>1,2</sup>, Sascha du Lac<sup>1,2</sup>

<sup>1</sup>Salk Institute, <sup>2</sup>Howard Hughes Medical Institute,

<sup>3</sup>University of California, San Diego

Identification of marker genes that are exclusively expressed in specific neuronal populations is essential for genetically dissecting neural circuits. I will present a novel strategy to identify marker genes for functional cell types using single-cell transcript profiling. Comprehensive single-cell transcript profiles of transmitter-related and ion channel genes sort cells into functionally distinct groups, based on which cell types are defined. Subsequently, expression of marker gene candidates screened by Allen Mouse Brain Atlas are profiled on single-cell basis, and involved in the cell classification, by which proper marker genes for each cell type are identified.

We applied this strategy to neurons in the mouse medial vestibular nucleus (MVN), which mediates vestibular reflexes, relatively simple behaviors that can be modified with motor learning. I will demonstrate that ion channel transcript profiles can distinguish and predict subtle differences in intrinsic excitability among MVN neurons, allowing us to establish a functional cell classification scheme in combination with the expression of transmitter-related genes. With single-cell transcript profiles of marker gene candidates, 6 cell types and their marker genes are established in MVN. This strategy for identifying cell types and associated marker genes is applicable throughout the CNS and could facilitate employing molecular genetic tools to elucidate the roles of neuronal subpopulations in behaviors.

## **50 Vasovagal Responses (VVR) Induced by Otolith Stimulation in the Anesthetized Rat**

Sergei B Yakushin<sup>1</sup>, Adam Schaffner<sup>1</sup>, Yongqing Xiang<sup>2</sup>, Giorgio P Martinelli<sup>1</sup>, Dmitri Ogorodnikov<sup>1</sup>, Gay Holstein<sup>1</sup>, Theodore Raphan<sup>2</sup>, Bernard Cohen<sup>1</sup>

<sup>1</sup>Mount Sinai School of Medicine, <sup>2</sup>Brooklyn College of CUNY

The VVR in human subjects is frequently associated with vasovagal syncope (VVS) that can be a substantial medical problem. We recently determined that sinusoidal galvanic vestibular stimulation (sGVS) induces VVR in anesthetized rats, suggesting that the rat can be a model for studying various aspects of the human VVS (Cohen et al., 2011). The rat VVR is composed of transient decreases in arterial blood pressure (BP)  $\approx 80$  mmHg and heart rate (HR)  $\approx 70$  beat\*min<sup>-1</sup> which both spontaneously recover over a 3-6 min period. sGVS also induces oscillatory modulations of BP and HR in the low frequency range (Mayer waves) with dominant oscillations at twice of frequency of stimulation. Oscillatory modulations are maintained throughout the entire period of sGVS. In the present study we investigated whether similar changes in BP and HR could be induced by a pure otolith stimulus. Long-Evans rats were implanted with a head holder, a remote intra-aortic BP sensor or a photoplethysmography (PPG) sensor was attached to the paw. Animals were anesthetized with 2% isoflurane (4% induction), placed in the rat-holder with the head fixed approximately in the stereotaxic horizontal plane. PPG and/or BP were recorded for 5 min while the animal was at a resting position or tilted 90° in various orientations. HR was derived off-line from systoles of BP. Data were filtered by wavelet transform to determine transient responses and changes in the frequencies of the Mayer wave range. Shortly after the animals were tilted nose up, there was  $\approx 50$  mmHg drop in BP and  $\approx 90$  beat\*min<sup>-1</sup> drop in HR, which gradually returned to normal. There was a substantial increase in the power (mmHg<sup>2</sup>) of the Mayer wave frequencies associated with the transient response. The changes in BP and HR were similar if not identical to those induced by sGVS in the same rat. Nose down and side down tilts had no effects on BP and HR. Thus, the previously reported VVRs induced by sGVS are likely to be due to electrical activation of the same otolith receptors that being activated by tilt. This study also supports the hypotheses that the onset of the transient response of the VVR is closely associated with an increase in activity in the range of the Mayer waves (Nowak et al., 2008).

Support by NIH Grants: DC008846, DC004996 and DC05204

## **51 Visualization of Neurons in the Rat Vestibular Nuclei That Project to the Rostral Ventrolateral Medulla and Are Activated by Sinusoidal Galvanic Vestibular Stimulation**

Gay R. Holstein<sup>1</sup>, Giorgio P. Martinelli<sup>2</sup>, Victor L. Friedrich Jr.<sup>3</sup>, Dmitri Ogorodnikov<sup>2</sup>, Sergei B. Yakushin<sup>2</sup>, Bernard Cohen<sup>2</sup>

<sup>1</sup>Departments of Neurology and Neuroscience; Mount Sinai School of Medicine, <sup>2</sup>Department of Neurology; Mount Sinai School of Medicine, <sup>3</sup>Department of Neuroscience; Mount Sinai School of Medicine

Changes in posture to the upright position trigger rapid sympathetic responses including alterations in blood pressure (BP) and heart rate (HR). It is thought that arterial baroreceptors participate in a regulatory feedback mechanism that determines and stabilizes sympathetic tone through the baroreflex while signals from the vestibular end organs drive a faster, feedforward mechanism that counteracts the effects of a change in posture. This latter pathway is often called the vestibulo-sympathetic reflex (VSR). Primary afferents of the VSR are derived mostly from the otolith organs, and terminate on cells in the caudal vestibular nuclei (VN). These neurons, in turn, project to brainstem sites involved in the regulation of cardiovascular activity such as the rostral ventrolateral medulla (RVLM). In order to identify the vestibular neurons of the VSR, retrograde tracer (Fluoro-Gold) deposits were placed in the RVLM of rats 7 days prior to sacrifice. Two hr before euthanasia, the isoflurane-anesthetized rats received binaural sinusoidal galvanic vestibular stimulation (sGVS). The effects of this stimulus were assessed using a modification of photoplethysmography that we developed to determine HR and BP changes. Activated neurons were identified in tissue sections through the VN using an antibody against the immediate early gene protein product c-Fos. c-Fos immunolabeling in the VN of rats that showed a significant change in HR and BP associated with sGVS was significantly greater than that from rats with little or no sympathetic response to the stimulus. In addition, many of the c-Fos-immunofluorescent VN neurons contained Fluoro-Gold. This study demonstrates that c-Fos immunolabeling can be used to identify sGVS-activated VN neurons, and that many of these neurons send direct projections to the RVLM. It is likely that these latter cells mediate the VSR and may play a role in producing vasovagal responses (Cohen et al., 2011). Supported by NIH/NIDCD grant R01 DC008846.

## **52 Gravity-Dependent Adaptation of the Angular Vestibulo-Ocular Reflex (AVOR) Is Coded in the Fastigial Nucleus (FN)**

Olga Kolesnikova<sup>1</sup>, Theodore Raphan<sup>2</sup>, Bernard Cohen<sup>1</sup>, Sergei Yakushin<sup>1</sup>

<sup>1</sup>Mount Sinai School of Medicine, <sup>2</sup>Brooklyn College CUNY  
Adaptation of the gain of the aVOR in specific head orientation is comprised of two components. One, which we denote as global learning, is independent of head orientation relative to gravity. The other component represents local learning and is tuned to the head

orientation relative to gravity in which the adaptation took place. We recently demonstrated that gravity-independent and gravity-dependent components of the aVOR gain adaptation are coded by different groups of central vestibular neurons. The eye-head-velocity (EHV) neurons code only the gravity-independent component, while the gravity-dependent component is coded by position-vestibular-pause (PVP) neurons. It is generally accepted that the cerebellum is a critical structure for various types of learning. Since only EHV neurons are targeted by the flocculus (Lisberger, 1994), the cerebellar projections to PVP neurons that are critical for gravity-dependent gain changes have so far remained unknown. We previously demonstrated that the nodulus-uvula does not code gravity-dependent aVOR gain changes (Yakushin et al., 2003). The other major cerebellar input to the vestibular nuclei (VN) that has both canal and otolith-related activity comes from FN. To determine whether FN is important for the gravity-dependent learning observed in PVP neurons in VN, muscimol, a GABA<sub>A</sub>-agonist, was injected into caudal FN after the vertical aVOR gain was adaptively decreased for 2 hr in cynomolgus monkeys in side-down position. Gravity-dependent and gravity-independent gain changes obtained immediately after adaptation were compared to those after muscimol injection. Gravity-dependent adaptation was lost after FN was inactivated by muscimol. This demonstrates that cerebellar flocculus code only global (gravity-independent) learning of the aVOR gain and that the cerebellar pathway to PVP in VN through caudal FN is critical for coding contextual (gravity-dependent) learning of the aVOR gain. Thus, for the first time we have demonstrated that two separate areas of the cerebellum contribute to different aspects of aVOR gain adaptation.

Supported by DC04996 and DC05204.

### **[53] Ipsilesional Incremental Adaptation of the Angular Vestibulo-Ocular Reflex**

**Michael Schubert<sup>1</sup>**, Americo Migliaccio<sup>2</sup>

<sup>1</sup>*Johns Hopkins University*, <sup>2</sup>*Neuroscience Research Australia*

Unilateral vestibular hypofunction (UVH) causes marked asymmetry in the horizontal angular vestibulo-ocular reflex (aVOR) during rapid head rotations, with aVOR gain being lower for head rotations toward the lesion than for rotations in the opposite direction. Increasing ipsilesional aVOR gain and reducing the gain asymmetry is an important step toward improving gaze stability following UVH. We sought to determine if it was possible to induce unilateral aVOR adaptation in humans and to design a simple portable device (*Stable-Eyes*) to drive unilateral incremental adaptation.

We tested 3 subjects with UVH, 3 subjects with BVH, and 5 healthy controls using *Stable-Eyes*, which required contralesional aVOR gain (BVH/control subjects randomized left or right) to be 1x and ipsilesional aVOR gain to be 1.5x. Subjects faced a blank wall 114 cm ahead and aside from the laser target were in complete darkness. They were trained to rotate their head horizontally at low-amplitude (~5 deg) and high peak velocity (~150 deg/s).

Each random head rotation was followed by a 2 s rest period during which the subject centred their head and the laser target reset to straight-ahead. This was repeated for 15 mins. We measured pre- and post-adaptation, left and right aVOR gains using active head impulses.

For the subjects with UVH, the range of ipsilesional 1.5x adaptation varied from 5 – 43% with a large variability. In contrast, the control 1x side showed a reduction in mean aVOR gain (-9.1 ± 4.5%). These differences approached significance (p = 0.051). Data from the subjects with BVH was difficult to process (i.e. saccades occurring before the onset of the head rotation). In healthy controls, the mean increase in aVOR gain towards the 1.5x side was 23% ± 26.4 compared with a mean 4.4 ± 10% on the 1x side, also short of significance (p = 0.052). Our preliminary data indicate the presence of the human neural circuitry needed for unilateral aVOR adaptation. This exciting finding suggests we can boost the lesioned side without adversely affecting the normal side, and develop more focused rehabilitation protocols for UVH.

### **[54] 3-D Measurement of Linear Accelerations and Angular Velocities of the Head, Torso and Leg During Natural Activities**

**David Lasker<sup>1</sup>**, Michael Schubert<sup>1</sup>

<sup>1</sup>*Johns Hopkins University*

We measured 3-d linear acceleration and angular velocity of the head, torso and leg in 2 individuals during walking, running and climbing stairs during a 10 minute course. Linear accelerations were largest in the vertical direction during all activities. During walking the range of acceleration at the leg and torso ranged from 1-2 g (g=10 m/s), which increased to > 6 g during running and stair walking. These accelerations modulated at approximately 2 Hz. Interestingly, vertical g-forces measured at the head were significantly attenuated at less than 2 g during all activities. Pitch angular head motion also modulated at approximately 2 Hz. However, the peak angular vertical head velocities were generally < 50 deg/s during walking and < 100 deg/s during running and stair walking. In contrast, yaw head velocities reached magnitudes of 300-400 deg/s during over-ground walking and stair walking. Peak yaw head velocities reached 400-500 deg/s during running. These were due to active head movements made during gaze shifts. Our data suggest the linear forces at the head, across a broad spectrum of daily activities, are much lower than those forces at the torso or leg, presumably to preserve gaze stability.

## **55 Development of a Human-Implantable Multichannel Vestibular Prosthesis Via Modification of a Commercially Available Cochlear Implant**

Nicolas S. Valentin<sup>1</sup>, Chenkai Dai<sup>2</sup>, JoongHo Ahn<sup>2</sup>, Charles C. Della Santina<sup>1,2</sup>, Gene Y. Fridman<sup>2</sup>

<sup>1</sup>Johns Hopkins University Department of Biomedical Engineering, <sup>2</sup>Johns Hopkins University Department of Otolaryngology – Head & Neck Surgery

No adequate treatment options exist for individuals disabled by profound bilateral vestibular hypofunction despite rehabilitation exercises. We have successfully demonstrated lab-built multichannel vestibular prostheses (MVP) in chinchillas and monkeys, but translation to clinical application may be best accomplished via modification of a commercially available cochlear implant (CI) to mimic the function of our MVP.

We developed software and circuitry to sense head rotation and command a modified CI to deliver pulse commands at up to 1k pps to any of 9 electrodes implanted near vestibular nerve branches. We tested the device on 2 rhesus monkeys with bilateral vestibular hypofunction due to gentamicin ototoxicity. When the device delivered pulse-frequency-modulated biphasic current pulse trains encoding virtual sinusoidal head rotations about each SCC axis with velocities of 50-200°/s at 0.1-5Hz, 3D vestibulo-ocular reflex responses ranged from 3.76±1.57 to 194.79±19.97°/s peak with misalignment of 12.57±3.24 to 63.82±24.51°, similar to results obtained with our dedicated MVP designs.

When sensors are housed in an external headpiece, the headpiece must remain securely held to the head to faithfully transduce motion. We quantified normal and shear headpiece retention forces as a function of scalp thickness  $t$  and determined velocity and acceleration thresholds at which head/headpiece decoupling occurred. For  $t \leq 7$ mm, the headpiece remained attached during steps of yaw acceleration up to 10k°/s<sup>2</sup>; for  $t = 10$ mm, decoupling occurred at 1k°/s<sup>2</sup>. During 0.1-5Hz sinusoidal yaw head rotations with  $t \leq 6$ mm, the headpiece remained secure for velocities up to 1k°/s; for  $t = 10$ mm, decoupling thresholds were 480 and 220°/s at 0.1 and 5Hz, respectively.

A modified CI with sensors embedded in a magnetically coupled headpiece can yield neural stimulation performance similar to a dedicated MVP and sufficiently secure head/sensor coupling to restore 3D vestibular sensation during daily activities.

## **56 Multichannel Vestibular Prosthesis Restores Vergence-Mediated Changes in Vestibulo-Ocular Reflex of Rhesus Monkeys with Gentamicin-Induced Bilateral Vestibular Hypofunction**

Joong Ho Ahn<sup>1</sup>, David Lasker<sup>1</sup>, Dai Chenkai<sup>1</sup>, Charles Della Santina<sup>1</sup>

<sup>1</sup>Johns Hopkins Vestibular NeuroEngineering Lab

We investigated whether input from a multichannel vestibular prosthesis (MVP) drives central neural circuits

that effect vergence-mediated changes of the vestibulo-ocular reflex (VOR).

Using the scleral coil technique, we measured horizontal VOR responses to passive whole-body impulse rotations in darkness and during far (140 cm) and near (12 cm) target viewing in 3 Rhesus monkeys treated previously with bilateral intratympanic gentamicin (ITG). Each was tested with and without prosthetic stimulation delivered by a unilaterally implanted MVP that encoded head rotation via pulse-frequency-modulated stimulation targeting ampullary nerves. The MVP did not encode linear acceleration and did not deliberately stimulate otolithic endorgans. Motion stimuli were low amplitude (30°), high peak velocity (150°/s), high acceleration (1000°/s<sup>2</sup>), passive, whole-body yaw rotations administered about an Earth-vertical axis with rotation sense randomized.

Without MVP input, mean ( $\pm$ SD) VOR gain measured during steps of acceleration was 0.01  $\pm$  0.17 in total darkness, 0.09 $\pm$ 0.19 for far target viewing, and 0.11 $\pm$ 0.14 for near target. Mean response latency for these conditions was 181 $\pm$ 211, 243 $\pm$ 157, 349 $\pm$ 146 ms, respectively. With MVP input, VOR gain was 0.46 $\pm$ 0.38 in darkness, 0.54 $\pm$ 0.25 for far target, and 0.86 $\pm$ 0.29 for near target. Mean VOR latency with MVP input was 20 $\pm$ 5, 19 $\pm$ 2, and 17 $\pm$ 3 ms for rotation toward the implanted ear. When quantified in terms of the change in VOR gain from the darkness condition, near target VOR gain was significantly higher than far target VOR gain only when using the MVP ( $p < 0.05$ ).

In addition to helping restore a more normal VOR for far target viewing conditions, MVP input also recruits vergence-mediated increases in VOR gain during near-target viewing. Since this vergence-mediated increase occurs even when the MVP neither measures nor deliberately encodes linear acceleration, it may occur even without normal otolithic endorgan activity.

Support: NIDCD R01DC9255

## **57 Electrically-Evoked Compound Action Potentials and 3D Vestibulo-Ocular Reflex Are Correlated to Each Other and to Electrode Position in Rhesus Monkeys Using a Multichannel Vestibular Prosthesis**

Chenkai Dai<sup>1</sup>, Joong Ho Ahn<sup>1</sup>, Gene Y. Fridman<sup>1</sup>, Mehdi A. Rahman<sup>1,2</sup>, Charles C. Della Santina<sup>1,2</sup>

<sup>1</sup>Department of Otolaryngology - Head & Neck Surgery, Johns Hopkins School of Medicine, <sup>2</sup>Department of Biomedical Engineering, Johns Hopkins School of Medicine

Maximizing the selectivity and efficacy of vestibular nerve branch stimulation is a key goal in development of a multichannel vestibular prosthesis (MVP) intended to restore sensation of 3-dimensional head movement in individuals disabled by chronic bilateral loss of labyrinthine hair cell function. Optimal positioning of electrodes during implantation is essential to achieving this goal; however, intraoperative confirmation of proper placement in the labyrinth is complicated by the fact that the 3D electrically-evoked vestibulo-ocular reflex (eVOR) is suppressed during general anesthesia. Intraoperative measurement of

vestibular electrically-evoked compound action potentials (eCAPs) has been proposed as a solution to this dilemma, and this approach was recently demonstrated in monkeys by Nie *et al.*, but more data are needed to clarify relationships between eCAPs, electrode location, and post-operative 3D eVOR responses.

We characterized eCAPs and 3D VOR responses as functions of electrode location and stimulus parameters for 27 electrodes in 3 rhesus monkeys. Electrodes implanted in each ampulla were spaced at 200  $\mu\text{m}$  intervals and reconstructions of post-implantation CT scans were used to measure electrode locations with respect to anatomic landmarks.

We found that eCAP and 3D eVOR amplitudes were strongly correlated to each other and to stimulus current. Amplitudes of eCAPs and eVOR change significantly with 200-400  $\mu\text{m}$  changes in electrode location. In one monkey, revision surgery to reposition electrodes meant for the posterior semicircular canal but initially in the sacculle yielded significant improvements in eCAP amplitude, eVOR amplitude and 3D eVOR alignment. We conclude that eCAPs provide a useful intraoperative measure of electrode location, and variation of as little as 200  $\mu\text{m}$  in electrode position significantly affects the strength and selectivity of coupling between electrodes and a target branch of the rhesus vestibular nerve.

Support: NICDC R01DC9255

### **58 Repeated Unidirectional Rotations Reduce Vestibulo-Ocular Reflex Gain Asymmetry in Rhesus Monkeys Using a Unilateral Multichannel Vestibular Prosthesis**

Chenkai Dai<sup>1</sup>, David Laker<sup>1</sup>, Joong Ho Ahn<sup>1</sup>, Mehdi Rahman<sup>1</sup>, Gene Fridman<sup>1</sup>, Charles Della Santina<sup>1</sup>  
<sup>1</sup>Johns Hopkins University

Unilateral prosthetic stimulation in bilaterally vestibular-deficient (BVD) rhesus monkeys elicits vestibulo-ocular reflex (VOR) responses with marked asymmetry in gain during rapid head rotations. VOR gain is lower for head rotations toward the nonimplanted side (away from the prosthesis side) than for rotations in opposite direction. Reducing this gain asymmetry by enhancing contralateral responses would be an important step toward improving gaze stability in BVD individuals using a multichannel vestibular prosthesis (MVP).

We have previously shown that the central nervous system rapidly adapts to multichannel prosthetic stimuli, improving VOR gain and 3D eye/head alignment over the first week of MVP use. Ushio *et al.* recently showed that even in rhesus monkeys that appear to have reached a compensatory steady state long after unilateral labyrinthectomy, a training paradigm comprising repeated passive whole-body rotations toward the lesioned side boosts lesion-side VOR gain. Based on these previous findings, we hypothesized that (1) BVD rhesus monkeys using a unilaterally-implanted MVP would exhibit acute improvements in VOR asymmetry and head movement asymmetry when exposed to repeated unilateral rotations (UR) away from the MVP side; and (2) repeated training

with the UR paradigm would produce a lasting reduction in VOR gain asymmetry.

Three BVD monkeys that had previously undergone unilateral implantation, left ear MVP activation, and VOR characterization were exposed to a UR training paradigm comprising a 3 hr series of rightward whole-body passive rotations (1000°/s<sup>2</sup> to 150°/s plateau lasting 1s, then deceleration to zero and a 1.1 s rest) in light. The UR paradigm reduced gain asymmetry from range [0.76, 0.89] to range [0.32, 0.45] and the improved persisted when tested 14 days after training (tested in one monkey). These results suggest that an analogous rehabilitation paradigm could improve VOR asymmetry in humans using an MVP.

Support by NIDCD R01DC9255

### **59 Responses of Vestibular-Deficient Rhesus Monkeys to Prosthetic Stimulation Via a Multichannel Vestibular Prosthesis Are Enhanced When Multisensory Inputs Are Congruent**

Chenkai Dai<sup>1</sup>, Joong Ho Ahn<sup>1</sup>, Gene Fridman<sup>1</sup>, Mehdi Rahman<sup>1</sup>, Charles Della Santina<sup>1</sup>  
<sup>1</sup>Johns Hopkins University

Several studies have demonstrated the importance of multisensory integration in maintaining stable gaze. In particular, neural signals encoding smooth pursuit, optokinetic inputs, neck proprioception and motor efference appear to play roles augmenting an otherwise deficient vestibulo-ocular reflex (VOR) in animals with reduced labyrinthine sensation. We hypothesized that responses to stimuli delivered by a multichannel vestibular prosthesis (MVP) would be most robust when prosthetic inputs are congruent with other sensory input.

To test this hypothesis, we treated 4 rhesus monkeys bilaterally with ototoxic doses of gentamicin, implanted MVP electrodes in their left ears, and measured their eye movements in darkness using 3D scleral coils during four stimulus paradigms: (1) sinusoidal passive whole-body rotation with MVP stimuli held at constant rates (*mechanical-only condition*); (2) sinusoidal modulation of MVP stimulus pulse rates with the animal stationary (*MVP-only condition*); and (3) combined passive whole-body rotation and MVP pulse rate modulation.

We found gaze stabilization was more robust in the *combined condition* (VOR gain 0.4-0.6 at 1Hz, 50°/s peak velocity and 125 pps peak pulse rate) than in the *mechanical-only condition* (VOR gain ~0.05) or *MVP-only condition* (VOR gain ~0.1-0.2). Modulating MVP stimuli out of phase with actual body rotation velocity reduced responses. Since the only difference between the *MVP-only* and *combined* conditions was addition of a mechanical stimulus that could not alone generate a measurable VOR, these results suggest that the central nervous system integrates input from multiple sources (including residual natural labyrinth activity, electrically-evoked activity, proprioception and somatosensory inputs) in a nonlinear way, and that the most robust perception of head movement arises when all inputs are congruent.

Support: NIDCD R01DC9255

## **60** Regularity of Firing in Purkinje Cells in the Vestibulocerebellum

Chang-Hee Kim<sup>1,2</sup>, Yong-Gyu Kim<sup>1</sup>, Jun Kim<sup>1</sup>, Sang Jeong Kim<sup>1</sup>

<sup>1</sup>*Department of Physiology, Seoul National University College of Medicine,* <sup>2</sup>*Department of Otorhinolaryngology, Konkuk University College of Medicine*

We previously observed more diversity in firing pattern in Purkinje cells (PCs) of lobule X (vestibulocerebellum) compared to lobule III-V (spinocerebellum). Firing regularity has long been an issue of neuronal characterization in the vestibular circuitry, and previous studies have noted that PCs exhibit spike frequency adaptation as reported in other neuron types in the cortex or the spinal cord.

We compared the firing regularity and examined the extent of spike frequency adaptation (SFA) by measuring interspike interval (ISI) in tonic and gap firing neurons in lobule III-V and X.

Over the course of low frequency spike trains, tonic firing neurons in lobule III-V showed gradual lengthening of ISI due to SFA. In contrast, ISI showed little change during the propagation of spikes in tonic ( $n = 89$ ) and gap firing neurons ( $n = 48$ ) in lobule X. In high frequency spiking, tonic firing neurons in lobule III-V exhibited progressive SFA, whereas tonic and gap firing neurons in lobule X showed dramatic increase in ISI during the first four spikes and then stayed unchanged. Regularity of ISI was evaluated by measuring coefficient of variation (CV) of ISI. CVs of tonic firing neurons ( $8.9 \pm 0.5\%$ ) and gap firing neurons in lobule X ( $8.0 \pm 0.4\%$ ) were significantly smaller than that of tonic firing neurons in lobule III-V ( $26.1 \pm 2.8\%$ ) in low frequency firing.

These differences in firing regularity probably contribute to the signal processing of afferent inputs in lobule-specific fashion, and lack of SFA especially in low frequency firing in lobule X PCs, as a part of vestibulocerebellum, might be involved in a regular coordination of vestibular function by the cerebellar cortex in response to low stimulation.

## **61** Retrograde Tracing Studies of Vestibulo-Parabrachio-Amygdaloid Networks in Rats

Carey Balaban<sup>1</sup>, Wei Gao<sup>1</sup>

<sup>1</sup>*University of Pittsburgh*

This study uses trans-synaptic retrograde tracing methods to illustrate network organization of vestibular and nociceptive parabrachio-amygdaloid pathways and noradrenergic and serotonergic pathways that have been explored previously with traditional tracers that do not cross synapses. Common features of these pathways are hypothesized as an explanation for co-morbidity and interactions between anxiety disorders, migraine and balance disorders. Male Long-Evans rats were injected stereotaxically in the left and right central amygdaloid nucleus with either (1) different, standard fluorescent retrograde tracers (Fast Blue and Fluoro-Ruby) or two modified pseudorabies viruses (PRV-Bablu and PRV-152 that express distinct reporter proteins. Survival times ranged from 24-120 hours. Rats were perfused transcardially with buffered saline and paraformaldehyde-

lysine-sodium metaperiodate fixative and free-floating frozen sections were cut at 30 microns. PRV-Bablu and PRV-152 were visualized as described previously with either immunoperoxidase or indirect immunofluorescence methods (e.g. Neuroscience 133 (2005) 1047-1052). The Fluoro-Ruby, Fast Blue and PRV retrograde transport data revealed several novel features of ascending pathways. Firstly, despite the fact that vestibulo-parabrachial pathways are bilateral, distinct groups of parabrachial nucleus neurons give rise to the contralateral and ipsilateral projections to the central amygdaloid nucleus. Secondly, the ipsilateral and contralateral dorsal raphe nucleus projections to the amygdala originate almost exclusively from distinct groups of cells, which overlap with the locations of neurons that contribute collateralize of raphe-vestibular and raphe-amygdaloid connections (Neuroscience 140 (2006) 1067-1077). Thirdly, the caudal locus coeruleus (site of origin of the coeruleo-vestibular pathway) shows robust retrograde labeling from the amygdala. Fourthly, at longer survival times (72-120 hours), PRV labeled cells were present in the vestibular nuclei and neurons capping the ventral margin of the rostral spinal nucleus of the trigeminal tract. These findings provide a more detailed view of vestibular and nociceptive contributions to parabrachial nucleus-amygdaloid-insula networks that influence fear and anxiety responses. Supported by R01DC000739.

## **62** A Large Scale Survey and Retrospective Analysis of BPPV Cases

Oluwaseye Ayoola Ogun<sup>1</sup>, Kristen Janky<sup>1</sup>, Edward Cohn<sup>1</sup>, Yunxia (Yesha) Lundberg<sup>1</sup>

<sup>1</sup>*Boys Town National Research Hospital*

It is noted that benign paroxysmal positional vertigo (BPPV) can co-occur with a number of illnesses and procedures including hearing loss, infections, migraine, Meniere's disease, surgeries, anesthesia, etc. However, it is difficult to assess the relative prevalence of each type of association because many of the studies are reported by various groups from different countries using different patient populations and possibly varying diagnostic criteria. Our purpose in this study is to analyze one large patient population, all diagnosed with BPPV at Boys Town National Research Hospital (BTNRH) between 2002 and 2011 using established diagnostic criteria, to determine the gender differences and recurrence rate of BPPV, and to identify additional co-morbidities and possible genetic involvement in BPPV etiology. We have sent a survey invitation to 1377 adult BPPV patients (>18 years old) and performed a retrospective analysis of patients' records. From the first set of responses received ( $n=138$ ), 71.0% are females ( $n=98$ ) and 29.0% ( $n=40$ ) males, comparable to the gender ratio of 67.9% (935) females and 32.0% (442) males shown by BTNRH medical records of BPPV patients. Notably, 44.9% of the female participants report experiencing the first episode of BPPV after menopause, 33.3% having had hysterectomy, 22.2% oophorectomy, and only 9.9% being on a hormone replacement therapy. A total of 75.2% participants report having experienced recurrent BPPV, and 76.0% report being successfully

treated after each session. There are high incidences of allergies (42.5%), hearing loss or other ear problems (40.2%), high blood pressure (39.4%), high cholesterol (35.4%), muscular skeletal problems including osteoporosis/osteopenia (39.4%) and general headaches (31.5%). Migraines (22.1%), thyroid (18.1%) and gallbladder (15.8%) problems are also fairly common. Interestingly, 25.2% report a known family history of BPPV, 12.2% are on some type of special diet, and only 11.5% report an incident of head trauma prior to initial BPPV symptoms. The data identify additional factors associated with BPPV, and suggest possible influence of systemic factors in BPPV etiology.

### **63 Modification of Otolith Reflex Asymmetries Following Space Flight**

Andrew Clarke<sup>1</sup>, Uwe Schönfeld<sup>1</sup>, Scott Wood<sup>2,3</sup>  
<sup>1</sup>Charité Medical School, <sup>2</sup>USRA, <sup>3</sup>NASA JSC

We hypothesize that changes in otolith-mediated reflexes adapted for microgravity contribute to perceptual, gaze and postural disturbances upon return to Earth's gravity. Our goal was to determine pre- versus post-flight differences in unilateral otolith reflexes that reflect these adaptive changes. This study represents the first comprehensive examination of unilateral otolith function following space flight. Ten astronauts participated in unilateral otolith function tests three times pre-flight and up to four times after Shuttle flights from landing day through the subsequent 10 days. During unilateral centrifugation (UC,  $\pm 3.5\text{cm}$  at  $400^\circ/\text{s}$ ), utricular function was examined by the perceptual changes reflected by the subjective visual vertical (SVV) and by video-oculographic measurement of the otolith-mediated ocular counter-roll (OOR). Unilateral saccular reflexes were recorded by measurement of the collic Vestibular Evoked Myogenic Potential (cVEMP). Although data from a few subjects were not obtained early post-flight, a general increase in asymmetry of otolith responses was observed on landing day relative to pre-flight baseline, with a subsequent reversal in asymmetry within 2-3 days. Recovery to baseline levels was achieved within 10 days. This fluctuation in the asymmetry measures appeared strongest for SVV, in a consistent direction for OOR, and in an opposite direction for cVEMP. These results are consistent with our hypothesis that space flight results in adaptive changes in central nervous system processing of otolith input. Adaptation to microgravity may reveal asymmetries in otolith function upon to return to Earth that were not detected prior to the flight due to compensatory mechanisms.

### **64 Postural Stability When Leaning from Perceived Upright**

Robert Vanya<sup>1,2</sup>, John Grounds<sup>2,3</sup>, Scott Wood<sup>2,4</sup>  
<sup>1</sup>Wyle, <sup>2</sup>NASA JSC, <sup>3</sup>USRP, <sup>4</sup>USRA

The transition between quiet stance and gait requires the volitional movement of one's center of mass (COM) toward a limit of stability (LOS). The goal of this study was to measure the effect of leaning from perceived upright on postural stability when voluntarily maintaining fixed stance positions and during perturbations of the support surface.

The COM was derived from force plate data in 12 healthy subjects while standing with feet positioned so that lateral base of support was equal to foot length. For all conditions, arms were folded and subjects were instructed to lean without bending at the hips or lifting their feet. The LOS was determined during maximal voluntary leans with eyes open and closed. The COM was then displayed on a monitor located in front of the subject. Subjects were visually guided to lean toward a target position, maintain this position for 10s, return to upright, and then repeat the same targeted lean maneuver with eyes closed. Targets were randomly presented at  $2^\circ$  in 8 directions and between  $2\text{-}6^\circ$  in these same directions according to the asymmetric LOS. Subjects were then verbally guided to lean between  $2^\circ$  back and  $4^\circ$  forward prior to a perturbation of the support surface in either a forward or backward direction. The average LOS was  $5.8^\circ$  forward,  $2.9^\circ$  back, and  $4.8^\circ$  in left/right directions, with no significant difference between eyes open and closed. Center of pressure (COP) velocity increased as subjects maintained fixed stance positions farther from upright, with increased variability during eyes closed conditions. The time to stability and COP path length increased as subjects leaned opposite to the direction of the support surface perturbations. We conclude that postural stability is compromised as subjects lean away from perceived upright, except for perturbations that induce sway in the direction opposite the lean. The asymmetric LOS relative to perceived upright favors postural stability for COM movements in the forward direction.

### **65 Lower Limb Muscle Power and Balance Performance During Sit-To-Stand Movement in Fallers and Non-Fallers**

Chugn-Lan Kao<sup>1,2</sup>, Po-Yin Chen<sup>1,3</sup>, Shun-Hwa Wei<sup>2,4</sup>

<sup>1</sup>Department of Physical Medicine & Rehabilitation, Taipei Veterans General Hospital, <sup>2</sup>National Yang-Ming University, <sup>3</sup>Center of Geriatrics & Gerontology, Taipei Veterans General Hospital, <sup>4</sup>Institute of Physical Therapy and Assisted Technology, School of Biomedical Science and Engineering

Background: As a population ages, the accompanying dysfunction of the lower limbs affects people's quality of life and their ability to perform leisure activities. Improving the quickness of force generation in the lower limbs is one of the main strategies to decrease the risk of falls. Purposes: Develop an equipment to measure and differentiate the lower limbs muscle power and temporal parameters of vertical ground reaction forces during the sit-to stand (STS) movement in three groups (young adults, elderly non-fallers, and elderly fallers) of people. The primary goal was to identify elderly people who are at risk for fall. Methods: Healthy elderly adults (non-fallers;  $n=18$ ), elderly adults with a history of falling (fallers;  $n=16$ ) and healthy young adults (young adults;  $n=10$ ). The participants in the elderly adult groups were 65 years old or older. Mechanical and temporal parameters during STS movement, and clinical functional scales were measured. Results: The maximum lower limb muscle power was significantly greater in the group of non-fallers than that in

the group of fallers ( $p < 0.05$ ). The daily functional performance (balance, mobility, and self-confidence) was significantly better in the group of non-fallers than in the group of fallers ( $p < 0.05$ ). Discussion/Conclusion: The lower limb muscle power and STS movement temporal parameters can potentially be helpful in the assessment of balance and the risk of falls.

### **66 Efficacy of Habituation Training at Home for Benign Paroxysmal Positional Vertigo**

**Hidefumi Yamamoto<sup>1</sup>**, Kishiko Sunami<sup>1</sup>, Hideo Yamane<sup>1</sup>

<sup>1</sup>*Osaka City University Graduate School of Medicine*

#### **Objective**

Benign paroxysmal positional vertigo (BPPV) is a common vestibular disorder characterized by brief episodes of vertigo. Canalith repositioning maneuver and the Brandt-Daroff maneuver are known to be effective treatments for BPPV. We performed habituation training at home for the BPPV patients and investigated the efficacy and problems associated with the habituation training.

#### **Patients and Methods**

The study included 29 BPPV patients (12 patients under 65 years old and 17 patients over 65 years old); the patients were randomized and divided into the following 2 groups: (1) those treated by the Brandt-Daroff maneuver and (2) those treated by the Brandt-Daroff maneuver, in which the positioning maneuver was performed with movement between right ear-down position and left ear-down and positioning maneuver with movement between sitting position and hanging head position. The patients repeated these maneuvers twice a day; they were interviewed for the subjective signs and positioning nystagmus test 1 month after their first visit.

#### **Results**

Age had no correlation with the improvement of subjective signs. The improvement ratio in positioning nystagmus test was higher in patients under 65 years old than in patients over 65 years old. The procedure of habituation training did not improve the subjective signs and positioning nystagmus test.

#### **Conclusion**

Habituation training at home is as effective as the canalith repositioning maneuver in patients under 65 years old. However, because neck or spine disorders are more common in patients over 65 years old than in those under 65 years old, the former find it difficult to perform habituation training and show a tendency of refraining from habituation training because of the fear of moving head position. Hence, it is important to treat with canalith repositioning maneuver or explain the importance of moving head position in detail for BPPV patients over 65 years.

### **67 Cerebral Blood Flow Decreases Prior to Nausea During Off-Vertical Axis Rotation**

**Jorge Serrador<sup>1,2</sup>**, Melissa Blatt<sup>1</sup>, Michael Falvo<sup>1</sup>, Jessica Jasien<sup>1</sup>, Scott Wood<sup>3</sup>

<sup>1</sup>*War Related Illness & Injury Study Center, NJ VA Health Care System, East Orange, NJ*, <sup>2</sup>*Harvard Medical School,*

*Boston, MA*, <sup>3</sup>*NASA Johnson Space Centre & Universities Space Research Association, Houston, TX.*

Nausea and motion sickness are often debilitating symptoms associated with vestibular disorders. In addition, there is currently no objective measure of nausea. The goal of this work was to determine if changes in cerebral blood flow precede the development of nausea in motion sick susceptible subjects.

Fifteen healthy subjects (5 females,  $31.2 \pm 6.7$  years) participated. Cerebral flow velocity (CFV) in the middle cerebral artery (transcranial Doppler), blood pressure (Portapres) and end-tidal CO<sub>2</sub> were measured during a 20s off vertical axis rotation for 15 min at 0.1 Hz (360/sec) followed by 15 min of 0.2 Hz (720/sec). Rotation was terminated when subjects reported persistent moderate nausea or they completed 30 min. Rotation while upright did not significantly change cerebral blood flow, blood pressure or end-tidal CO<sub>2</sub>. Motion sick subjects showed a significant decrease of ~10% ( $P < 0.001$ ) in CFV during off vertical axis rotation compared to controls who demonstrated no change. CFV decreased linearly until plateauing at  $\sim 289 \pm 34$  sec prior to termination of rotation due to symptoms. There was a significant increase in blood pressure compared to baseline with no difference between groups (controls:  $+4.9 \pm 5.7$  mmHg, motion sick:  $+7.9 \pm 3.4$  mmHg,  $P < 0.001$ ). Subjects also had a small but significant decrease in end tidal CO<sub>2</sub> with no difference between groups (controls:  $-2.698 \pm 2.2$  mmHg, motion sick:  $-3.273 \pm 1.3$  mmHg,  $P < 0.001$ ).

These data indicate that cerebral hyperperfusion precedes the development of symptoms of motion sickness and that neither changes in blood pressure nor hypocapnia appear to be primary causes of this decrease. Further work is necessary to determine what role cerebral hypoperfusion plays in the development of nausea and motion sickness. However, this work suggests that cerebral blood flow may be considered as an objective indicator of motion sickness. Supported by NASA grant NNJ04HI13G (Serrador) and NIH grant R21DC009900 (Serrador).

### **68 Dose Deficit in Hippocampus Function Affect Path Integration and Distinction of Auditory Space Map in Human?**

**Kishiko Sunami<sup>1</sup>**, Hidefumi Yamamoto<sup>1</sup>, Hideo Yamane<sup>1</sup>, Naohiro Tsuyuguchi<sup>1</sup>, Michiharu Morino<sup>2</sup>

<sup>1</sup>*Osaka City University*, <sup>2</sup>*Tokyo Metropolitan neurological Hospital*

**Objective:** Perception of spatial orientation and self-motion can benefit from integration of multiple sensory cues including vestibular signals. Place cells were found in hippocampus areas CA1 and CA3, correlates of head orientation collectively map spatial locations. To elucidate hippocampus function related with spatial orientation in human, we examined the subject undergone hippocampectomy about path integration and sound localization test.

**Subjects and methods:** Data were obtained from 16 patients with hippocampus sclerosis and temporal lobe epilepsy. Eleven patients were also investigated after the amygdalohippocampectomy. To determine the path

integration, they were investigated by modified step test (Initially, in this test the subjects walked for 1 m on a straight road and then turned 90° to the right or to the left. Subsequently, they walked straight for 1 m with their eyes opened. And then they turned around and traced their track with their eyes closed. We measured the angle on their way back, and then subtracted 90° from that angle.). We also investigated sound lateralization test.

Results: The results of modified step test got worth after amygdalohippocampectomy. Sound is an important factor of a sense of direction. Space-specific neurons in the auditory space map gain spatial selectivity as a result of tuning to combinations of the interaural time difference (ITD) and interaural level difference (ILD). The insufficiency of sound lateralization test was detected in patients with temporal lobe epilepsy and hippocampal sclerosis, and this was also detected after the amygdalohippocampectomy.

Conclusions: The hippocampus should play a role in path integration and sound lateralization in human.

### **[69] Auditory Temporal Processing During Vestibulo-Ocular Stimulation and Postural Challenge in Older Subjects**

**Joseph Furman<sup>1</sup>, John Durrant<sup>1</sup>, Susan Fuhrman<sup>1</sup>, J. Richard Jennings<sup>1</sup>**

<sup>1</sup>University of Pittsburgh

We hypothesized that cognitive interference by vestibulo-ocular stimulation and a balance challenge would manifest as degraded temporal processing of auditory stimuli in older subjects. Two subject groups, Older (65-85, n=13, F=7, 75.1±/ 4.6) and Young (18-40, n=14, F=8, 24.9±/ 5.6), were screened to ensure normal auditory, visual, neurological, cognitive, vestibular, and motor function. Three auditory tasks were used: a within-channel gap detection task, a cross-channel gap detection task, and, as a control, a frequency difference task. All tasks used an adaptive one-up, two-down algorithm. Tasks were coupled with vestibulo-ocular stimulation, a postural challenge, and baseline seated conditions. Each subject performed each task in all conditions. Results were explored using several outcome measures including: 4-reversal mean, 3-minimum correct mean, and range from the minimum correct response to the maximum correct response occurring after the first minimum. A repeated measures ANOVA was used for each task with postural and vestibular conditions as within-subjects variables, and age group as a between-subject variable. Results showed that older subjects had significantly worse performance on the auditory tasks (p<0.001). However, condition had no effect and no significant interactions were found. Also, no significant effects were seen for changes from baseline for the vestibular and postural conditions. Sensory detection of a temporal gap in auditory input could not be shown to be influenced by concurrent vestibular stimulation or a postural challenge. This negative result differs from previous results based on reaction time tasks and suggests that balance-cognition interference is not a general effect of fatigue or distraction. Rather, our result adds support to the theory that balance-cognition

interference involves a bottleneck in sensory-motor processing.

This study was supported by NIH Grants AG 10009, AG 024827 and DC 05205.

### **[70] Cortical Involvement in Unilateral Vestibular Deficit: Early Metabolic Changes**

**Bianca Napolitano<sup>1</sup>, Alessandro Micarelli<sup>1</sup>, Marco Pagani<sup>2</sup>, Orazio Schillaci<sup>1</sup>, Barbara Di Pietro<sup>1</sup>, Agostino Chiaravalloti<sup>1</sup>, Fabrizio Ottaviani<sup>1</sup>, Ernesto Bruno<sup>1</sup>, Marco Alessandrini<sup>1</sup>**

<sup>1</sup>"Tor Vergata" University - Rome, <sup>2</sup>Institute of Cognitive Sciences and Technologies - CNR - Roma

The aim of the present study was to analyze the cortical metabolic changes in acute vestibular deficit due to Vestibular Neuritis (VN).

Six patients (M:F=2:4; mean age 48±7 yrs) affected by VN underwent a brain FDG-PET scan within 48 hours from the onset of symptoms (PET0; n=6) and after 1 month (PET1; n=5). Differences between PET0 and PET1 and FDG-PET data from a control group of 30 healthy subjects (CG) were analyzed by statistical parametric mapping (SPM2) introducing age and sex as nuisance variables. A further within-subject analysis was performed between PET0 (n=5) and PET1 (n=5). SPM t-maps were corrected either for multiple comparison with False Discovery Rate (p<0.05) or thresholded at p<0.001, uncorrected, at voxel level and corrected for multiple comparison at cluster level (p<0.001).

As compared to CG, PET0 patients showed a significant lower FDG uptake in several brain regions: bilateral visual (Brodmann Areas, BAs, 17, 18, 19), superior parietal lobule (BA 7) and posterior cingulate cortex, and a significantly higher FDG uptake in two brain regions: the right orbitofrontal cortex (BA 47) and temporal pole (BA 38). As compared to PET1, PET0 patients showed a significant hypometabolism in the left sensorimotor (BAs 2, 4, 6), posterior cingulate (BA 31) and parietal (BAs 7, 40) cortex and a significant hypermetabolism in right temporal lobe (BAs 20, 38) and thalamus.

The activation of different cortical areas suggests that more sites can be involved in different phases in the intricate mechanisms of the vestibular compensation.

These results introduce the activation of BA38, a cortical area likely responsible for emotional responsiveness, in PET0 patients as compared to both PET1 and CG patients and suggest this pattern is a peculiar feature of the early phase, i.e. this activation would be the cortical representation of the psychophysical discomfort related to early symptoms of the VN.

### **[71] The Role of Glucocorticoids and Antiviral Agents in Vestibular Neuritis with Respect to Recurrence**

**Hoseok Choi<sup>1</sup>, Changduk Han<sup>1</sup>, Jae Eun Kim<sup>1</sup>**

<sup>1</sup>Inha University

The role of glucocorticoids and antiviral agents in vestibular neuritis with respect to recurrence

**Objective:** Vestibular neuritis (VN) is known to be resolved with symptomatic treatment. We previously report that the recurrence rate of vestibular neuritis is about 10% without specific treatment. According to viral reaction etiology, the rate seems to be not low. Our hypothesis based on pathophysiology is that recurrence rate would reflect the disease severity and treatment outcome. The aim of this study is to support the evidence to need steroid or antiviral agents treatment.

**Methodology:** We thought BPPV, uncompensated state, second event VN and unexplained sustained dizziness after first VN as recurrence. Recurrence numbering were included in case of more than 1 month after first event. We set treatment group into 3 groups (steroid group, antiviral agent group, steroid and antiviral group) and later compared the recurrence rate with no specific treatment group.

**Result:** From Jan. 2007 to Jan. 2011 total VN recruitment was 423 patients. 28 of 311 patients (9.0%) without medication showed recurrence after 1 month later. 71 patients with steroid treatment showed 2.1% recurrence rate (15 patients). 12 patients with acyclovir treatment showed 0% recurrence rate. 10 patients with steroid and acyclovir treatment showed 0% recurrence rate. We got again similar recurrence rate (9.0%) to previous result (10%) in case of no treatment. The recurrence ratio without no treatment was not low.

**Conclusion:** According to viral etiology in VN the recurrence rate may reflect the severity of first event. That is because recurrence would come from sequelae of first vestibular organ damage. In many papers treatment outcome was evaluated with caloric test and hospital days. But the parameter is not really important considering the prognosis. Through follow up from 1 months to 2 years more we observed that the recurrence rate decreased with steroid or antiviral agents. With limitation of small sample numbers these data will support the rationale of treatment based on viral reaction in VN.

## **72 Perceptual and Cognitive Advantages in Adult Musicians Across the Life-Span**

**Alexandra Parbery-Clark<sup>1</sup>, Samira Anderson<sup>1</sup>, Emily Hittner<sup>1</sup>, Nina Kraus<sup>1</sup>**

<sup>1</sup>*Northwestern University*

There is growing evidence that younger and older adult musicians have more accurate auditory perceptual skills and greater auditory-based cognitive abilities than age-matched nonmusicians. Here we asked whether these effects are due to an advantage that is sustained and consistent throughout adult life or whether musical training actually offsets the aging trajectory. To this aim we measured auditory perceptual and cognitive abilities in 180 musicians and nonmusicians ranging from 18 – 77 years old. Outcomes reveal that musicians experience less age-related decline for certain perceptual and cognitive tasks (e.g., backward masking, frequency discrimination and auditory working memory). For other tasks, such as speech-in-noise perception (e.g., QuickSIN and HINT), the extent of the musician advantage remains constant across the lifespan. These results suggest that the impact of

musical experience on sensory-cognitive processes varies depending on the nature of the task, highlighting the multifaceted effects of music on the nervous system.

Supported by NSF 1057556

## **73 Association of Skin Color, Race/Ethnicity, and Hearing Loss Among Adults in the United States**

**Frank Lin<sup>1</sup>, Paige Maas<sup>1</sup>, Wade Chien<sup>1</sup>, John Carey<sup>1</sup>, Luigi Ferrucci<sup>2</sup>, Roland Thorpe<sup>1</sup>**

<sup>1</sup>*Johns Hopkins*, <sup>2</sup>*National Institute on Aging*

Epidemiologic studies of hearing loss in adults have demonstrated that the odds of hearing loss are substantially lower in black than in white individuals. The basis of this association is unknown. We hypothesized that skin pigmentation as a marker of melanocytic functioning mediates this observed association and that skin pigmentation is associated with hearing loss independent of race/ethnicity. We analyzed cross-sectional data from 1258 adults (20-59 years) in the 2003-4 cycle of the National Health and Nutritional Examination Survey who had assessment of Fitzpatrick skin type and pure tone audiometric testing. Audiometric thresholds in the worse hearing ear were used to calculate speech-frequency (0.5 – 4 kHz) and high-frequency (3-8 kHz) pure tone averages (PTA). Regression models were stratified by Fitzpatrick skin type or race/ethnicity to examine the association of each factor with hearing loss independent of the other. Models were adjusted for potential confounders as appropriate (demographic, medical, and noise exposure covariates). Among all participants, race/ethnicity was associated with hearing thresholds (black participants with the best hearing followed by Hispanics and then white individuals), but these associations were not significant in analyses stratified by skin color. In contrast, in race-stratified analyses, darker-skinned Hispanics had better hearing than lighter-skinned Hispanics by an average of -2.5 db HL (95% CI: -4.8 – -0.2) and -3.1 db HL (95% CI: -5.3 – -0.8) for speech and high-frequency PTA, respectively. Associations between skin color and hearing loss were not significant in white and black participants. Our results demonstrate that skin pigmentation as measured by Fitzpatrick skin type is independently associated with hearing loss in Hispanics and suggest that skin pigmentation likely mediates the strong association observed between race/ethnicity and hearing loss.

## **74 Study on Correlation Between “Kidney Deficiency” and Age-Related Hearing Loss Based on Serum Hormone Level and Gene Expression**

**Yang Dong<sup>1</sup>, Puzhao Liu<sup>2</sup>, Haiyan Song<sup>1</sup>, Yimin Wang<sup>1</sup>, Ming Li<sup>2</sup>, Jianrong Shi<sup>1</sup>**

<sup>1</sup>*Shanghai University of Traditional Chinese Medicine*,

<sup>2</sup>*Shanghai Yueyang Hospital*

Hearing loss was considered to be related to kidney in the theory of “Kidney controlling ears” in Traditional Chinese Medicine (TCM). This study was designed to investigate the correlation between “kidney deficiency” in TCM and

age-related hearing loss (ARHL) and the material basis. Hearing function was examined by pure tone test, and 20 persons were divided into control group (n=11) and ARHL group (n=9). The “kidney deficiency” accumulate point was got by form about “kidney deficiency” symptoms. The results showed that the “kidney deficiency” accumulate point of ARHL group was higher than control group. Pearson correlation analysis showed that “kidney deficiency” accumulate point was positively correlated with hearing threshold value ( $r=0.766$ ,  $P=0.000$ ). Chemiluminescence test showed that the levels of T3 and T4 were lower than control group, but had no significant difference. The levels of ACTH and cortisol in ARHL group were lower than that of control group, the differences were significant ( $P<0.01$ ,  $P<0.05$ ). The genechip expression analysis showed that the expressions of many glucocorticoid receptor target genes such as RGS2, ARL8B, IL11RA, Cdc42 and TSC22D3 had significant difference between ARHL group and control group. Realtime qPCR showed that TSC22D3 expression in ARHL group was five times lower than that of control group significantly ( $P<0.05$ ). All these results suggested that the glucocorticoid and its receptors might be the material basis of correlation between the “kidney deficiency” in TCM and ARHL. In addition, TSC22D3 gene played an important role.

Supported by Key Basic Research Program of Shanghai Science and technology Committee (09JC1413500) and Project of Leading Academic Discipline, Shanghai Education Committee (J50301).

### **75 The Influence of Age and High-Frequency Hearing Loss on Sensitivity to Temporal Fine Structure at Low Frequencies**

**Brian Moore**<sup>1</sup>, Brian Glasberg<sup>1</sup>, Martin Stoev<sup>1</sup>, Christian Fullgrabe<sup>2</sup>, Kathryn Hopkins<sup>3</sup>

<sup>1</sup>University of Cambridge, <sup>2</sup>MRC-IHR Nottingham,

<sup>3</sup>University of Manchester

Data in the literature suggest that sensitivity to temporal fine structure (TFS) at low frequencies may be adversely affected by hearing loss at high frequencies, even when absolute thresholds at low frequencies are within the normal range. However, in several previous studies the effects of hearing loss were confounded with the effects of age. Here, 39 subjects with ages from 61 to 83 yrs were tested using a test of sensitivity to changes in interaural phase, the TFS-LF test (Hopkins and Moore 2010), at 500 and 750 Hz. All subjects had normal or near-normal audiometric thresholds at low frequencies, but hearing thresholds varied across subjects at high frequencies. TFS scores were correlated with age ( $r = 0.74$  at 500 Hz and  $r = 0.58$  at 750 Hz). The TFS scores were not significantly correlated with absolute thresholds at the test frequencies. TFS scores for the test frequency of 750 Hz were weakly but significantly correlated with absolute thresholds at high frequencies ( $r = 0.29$  for 4000 Hz and  $r = 0.32$  for 8000 Hz). However, when the effect of age was partialled out, the correlations decreased and became non-significant ( $r = 0.085$  at 4000 Hz and  $r = 0.167$  at 8000 Hz). Thus, the data do not provide any clear support for the idea that

sensitivity to TFS at low frequencies is related to absolute threshold at high frequencies, independently of the effect of age.

Reference

HOPKINS K, MOORE BCJ. Development of a fast method for measuring sensitivity to temporal fine structure information at low frequencies. *Int. J. Audiol.* 49:940-946, 2010.

### **76 Neural Precision with Auditory Training in Older Adults**

**Samira Anderson**<sup>1</sup>, Alexandra Parbery-Clark<sup>1</sup>, Hee Jae Choi<sup>1</sup>, Nina Kraus<sup>1</sup>

<sup>1</sup>Northwestern University

Older adults are known to have impaired temporal resolution resulting from several factors, including loss of neural synchrony, delayed neural recovery, and decreased inhibition. As precise timing is required for speech perception, deficits in temporal encoding likely lead to impaired speech-in-noise perception. Amplification systems designed to provide audibility do not correct for these deficits. Animal models have demonstrated the plasticity of the auditory system in aging animals. For example, in older rats, age-related decreases in reliability of temporal coding and in cortical firing synchrony can be reversed by intense auditory training. We hypothesized that similar improvements in temporal processing are found in older adult humans who receive auditory training. Participants included older adults, ages 58 to 65, who were randomly assigned to one of two treatment groups. The experimental group completed 8 weeks of cognitive-based auditory training, and the control group completed 8 weeks of general interest education training. For both groups, participants engaged in 40 total hours of software-based training on personal computers. Pre- and post-test assessments included perceptual (audiometry and speech-in-noise performance), cognitive (memory and attention), and neurophysiological (brainstem responses to speech in quiet and noise) measures. Outcomes in the experimental group revealed improved neural precision, especially for frequencies corresponding to the first formant of speech. This improvement in temporal processing also related to improvements in speech-in-noise performance and auditory memory. The control group did not improve in these areas. These results speak to the efficacy of implementing auditory training when working with older adults who have trouble hearing in background noise. This work is supported by the NRSA Institutional Research Training Grant (T32 DC009399-01A10) and NIH (RO1 DC01510).

### **77 Evidence for Over-Recruitment of Executive Functions Among Older Adults During Multi-Talker Listening**

**Pádraig Thomas Kitterick**<sup>1</sup>, A. Quentin Summerfield<sup>1</sup>

<sup>1</sup>University of York

Many older people report difficulty and fatigue when trying to attend to one talker while other talkers are speaking at the same time. To examine the bases of their difficulties, we used magneto-encephalography (MEG) to map the

spatio-temporal sequence of brain activity during a multi-talker listening task performed by twelve younger and twelve older adult human listeners.

Participants lay supine in the MEG scanner and listened to phrases that had been recorded using a head-and-torso simulator. On each trial, seven phrases were presented from seven loudspeakers in a semi-circular array spaced at 30° intervals spanning from left to right. Phrases had the form 'Ready call-sign, go to color number now', with eight possible call-signs, four colors, and four numbers. The task was to listen out for the phrase containing the call-sign that had been assigned to each participant, and report the color and number in that phrase. We measured the additional activity evoked during two key moments: (1) while listeners attended to their target talker and (2) resisted distraction from a competing talker.

We found no difference between the groups in the level or timing of additional activity in brain networks associated with selective attention, including right superior temporal gyrus and left posterior parietal regions. We did find differences in networks associated with executive control, including bilateral prefrontal cortex and left anterior insula. The older group displayed significantly more additional activity in these areas than the younger group, who displayed no additional activity. At each key moment, the unique additional activity in the older group was synchronized with activity common to both groups.

These results are compatible with the idea that older listeners sustain performance in multi-talker listening by recruiting extended brain networks at moments of high cognitive demand. These additional resources may underpin the sense of fatigue reported by older listeners.

#### Acknowledgements

The data were collected as part of a studentship from RNID awarded to PTK. PTK is supported by the Wellcome Trust and the University of York.

### **[78] Changes in the Central Auditory System Accompanying Presbycusis Investigated by MRI**

**Oliver Profant**<sup>1,2</sup>, Zuzana Balogová<sup>1,2</sup>, Monika Dezortova<sup>3</sup>, Jan Betka<sup>2</sup>, Milan Hajek<sup>3</sup>, Josef Syka<sup>1</sup>

<sup>1</sup>*Inst Exp Med ASCR, Prague, Czech Rep.*, <sup>2</sup>*Dept. of ENT, 1st Medical Faculty of Charles University, FN Motol, Prague, Czech Rep.*, <sup>3</sup>*MR Unit IKEM, Prague, Czech Rep.*

The results of animal experiments show that one of the significant age-related changes concerns the deterioration of inhibitory transmission in the central auditory pathway, demonstrated, for example, by means of the immunocytochemical detection of glutamate decarboxylase. Similarly, decreases were found in the levels of calcium-binding proteins, such as calbindin, calretinin and parvalbumin. The decline in the function of the inhibitory system in the central auditory system is accompanied by a decline in the processing of the temporal parameters of acoustical signals, with the proof for this statement being supplied by both animal experiments and psychoacoustical measurements in man. In the present study we analyze the content of the essential transmitters and their metabolites in the human

auditory cortex and compare the results obtained in groups of young and elderly subjects (aged more than 65 years). We used for this purpose magnetic resonance spectroscopy, performed on a Siemens Trio 3 TESLA scanner. In all subjects the auditory function was assessed with high frequency audiometry and by the measurement of oto-acoustic emissions. According to the data obtained so far from 15 subjects of each group, the content of glutamate and acetyl-aspartate in the auditory cortex is decreased in the aged group.

Supported by grants AV0Z50390512, LC 554 and GACR P304/10/1872

### **[79] How Well Can Centenarians Hear?**

**Zhongping Mao**<sup>1</sup>, Lijun Zhao<sup>1</sup>, Lichun Pu<sup>1</sup>, David He<sup>2</sup>, Yaojing Jin<sup>1</sup>

<sup>1</sup>*Shaoxing Second Hospital, Shaoxing, P.R.China,*

<sup>2</sup>*Creighton University, Omaha, Nebraska*

With significant advancement of medicines and improvement of life conditions in the past two decades, the elderly population is rapidly expanding. There is a growing number of population aged 100 years and above. While many changes in the human body occur with physiological aging, as many as 35% to 50% of the population aged between 65 and 75 years have presbycusis. Presbycusis is a progressive age-related sensorineural hearing loss that can contribute to social isolation and loss of autonomy and is associated with anxiety, depression, and cognitive decline. There are many studies of the prevalence of age-related hearing loss in the United States, Europe, and Asia. However, no audiological assessment in the population aged 100 years and over has been done. Therefore, it is not clear how well people over the age of 100 can hear. For this aim, we measured middle ear impedance, pure tone audiometry and DPOAEs from 72 centenarians living in the city of Shaoxing, China, to evaluate their middle ear function and hearing thresholds. Subjects who have a family history of hearing loss and/or a past history of ototoxic drug use were excluded. Subjects with obvious abnormality in the external ear canal or tympanic membrane were also excluded. This study presents the first audiological assessment of how well centenarians can hear (Supported by a grant from the Department for Science and Technology of the City of Shaoxing, P. R. China).

### **[80] Subcortical Encoding of the Frequency of Pure Tones: Effects of Age and Cochlear Hearing Loss**

**Frederic Marmel**<sup>1</sup>, Deborah Linley<sup>1</sup>, Christopher Plack<sup>1</sup>, Robert Carlyon<sup>2</sup>, Hedwig Gockel<sup>2</sup>

<sup>1</sup>*Human Communication and Deafness Division, The University of Manchester, Manchester M13 9PL, UK,*

<sup>2</sup>*MRC Cognition and Brain Sciences Unit, Cambridge CB2 7EF, UK*

One difficulty when studying the effects of cochlear hearing loss (CHL) on auditory perception is that age is often a confound. Teasing apart the respective contributions of CHL and age may be crucial for our understanding of the difficulties that many older people experience on tasks

such as listening to speech in noisy backgrounds. In particular, aging has been shown to impair behavioral frequency discrimination as well as the subcortical encoding of temporal fine structure for participants with normal hearing (Clinard et al., 2010). In the present study, we measured frequency difference limens (FDLs) and electrophysiological frequency-following responses (FFRs) to pure tones in listeners spanning a wide range of ages (23-71) and audiometric thresholds (averaged thresholds between 250 Hz and 8 kHz ranged from -9 to 66 dB HL). Subcortical temporal encoding was assessed by calculating the signal-to-noise ratio and phase coherence of the FFR response at the stimulation frequency. Pearson's correlations revealed that age was predictive of FFR strength even when audiometric thresholds were partialled out, and that audiometric thresholds were predictive of FDLs even when age was partialled out. Furthermore, FFR strength correlated with the FDL. These results suggest that, to some extent, aging and CHL may be affecting separate aspects of the neural encoding of the frequency of pure tones.

### **81** Age-Related Decline in the Central Auditory Nervous System and Hearing Aid Benefit in Older Adults

**Adrian Fuente**<sup>1</sup>, Louise Hickson<sup>1</sup>

<sup>1</sup>*The University of Queensland*

This research aimed to investigate how age-related decline in the central auditory nervous system (CANS) relates to hearing aid benefit in older adults. A total of 60 older-adult hearing aid users were selected. Age-related decline in the CANS was investigated through the use of psychoacoustic tasks, including low-passed filtered double dichotic digits, backward and forward masking, gap detection, auditory pattern identification and binaural masking level difference. Working memory and attention were also studied, as they may influence the results in psychoacoustic tasks and speech discrimination in noise. Speech discrimination in noise was investigated using the words-in-noise (WIN) and hearing-in-noise (HINT) tests. The WIN and HINT were carried out in aided and unaided conditions. Hearing aid benefit was calculated as being the difference between the aided and unaided condition of the results obtained in the WIN and HINT tests. Simple linear regression analyses were carried out to examine associations between the WIN and HINT results (aided), hearing aid outcomes and the continuous variables of age, peripheral hearing levels and results for each of the psychoacoustic measures. Also, the continuous covariates of working memory and attention were compared to speech discrimination in noise measures and hearing aid outcomes, using simple linear regression. Multiple linear regressions were then performed to separately model the association between subjects' results from the WIN and HINT procedures (aided), each of the two outcome measures of hearing aid benefit and central auditory factors measured through psychoacoustic tasks and the covariates of age, peripheral hearing loss, working memory and attention. A total of four models were created. Results indicated that pure-tone thresholds and some of the psychoacoustic measures

were significantly associated with speech in noise performance and with hearing aid benefit. Cognitive aspects such as working memory were also significantly associated with speech in noise performance. Findings of this research provide further evidence of the association between age-related decline in the CANS and hearing aid benefit in older adults.

### **82** Gray Matter in the Human Brain: Differences Associated with Tinnitus and Hearing Loss

**Kristiana Boyen**<sup>1</sup>, Dave Langers<sup>1</sup>, Emile de Kleine<sup>1</sup>, Pim van Dijk<sup>1</sup>

<sup>1</sup>*Dept. of Otorhinolaryngology, University Medical Center Groningen, The Netherlands*

The underlying pathophysiology of tinnitus is poorly understood. Several studies support the hypothesis that neurophysiological mechanisms in the central auditory system play a crucial role in tinnitus generation. Such mechanisms must have a neuroanatomical basis. So, tinnitus may be related to particular neuroanatomical brain characteristics.

In the present study, Voxel-Based Morphometry was applied to identify regionally specific gray matter (GM) differences related to hearing loss and tinnitus. Structural MRI scans in 31 hearing-impaired subjects with tinnitus (PTA(1-2-4 kHz): 41±8 dB HL; age: 56±9), 16 hearing-impaired subjects without tinnitus (PTA: 45±10 dB HL; age: 63±10) and 24 normal-hearing healthy subjects (age: 58±6) were performed.

Testing for whole-brain differences showed that the tinnitus group had the largest total GM amount. In order to correct for these global differences between the groups, the images were standardized by dividing the GM value of each voxel of a particular image by the total GM of the subject. Then, we performed voxel-by-voxel comparisons and region of interest (ROI) analyses, in which the cortex was subdivided in Brodmann Areas (BAs). Both analysis methods mainly revealed significant GM increases in the temporal lobe and GM decreases in the frontal and occipital lobes for both hearing-impaired groups relative to the control group. In addition, the ROI analyses confirmed the involvement of the limbic system in tinnitus, but showed differences in relation to hearing loss as well. A tinnitus-related GM increase was revealed in the left primary auditory cortex (BA 41).

Our results show that hearing loss and tinnitus are associated with GM differences. The differences related to tinnitus are possibly a consequence of the tinnitus or, alternatively, may have caused the tinnitus. Understanding this causality relation between tinnitus and GM differences will be an important next step towards understanding tinnitus generation mechanisms.

### **83 Protein Profiles in Auditory Cortex and Hippocampus-Similarities and Differences**

**Senthilvelan Manohar<sup>1</sup>**, Richard Salvi<sup>1</sup>, Samson Jamesdaniel<sup>1</sup>, Donald Coling<sup>1</sup>

<sup>1</sup>*University at Buffalo*

The auditory cortex (AC) plays a key role in interpreting complex sounds; however, the biological significance of these signals likely involves structures outside the auditory pathway such as the hippocampus, a region involved in memory, emotion, and spatial navigation. For example, we found strong activation of AC and hippocampus when patients modulated their tinnitus. Moreover, acoustic trauma not only disturbs auditory function, but also disrupts the function of hippocampal place cells and suppresses hippocampal neurogenesis. Here, we report the results of a large scale screen that identified major differences in protein expression in rat AC versus hippocampus. Using an antibody microarray, we detected 698 and 623 proteins in AC and hippocampus respectively; 613 were expressed in both regions. Five proteins in AC and 93 in hippocampus were expressed at 5-fold higher levels than actin. Some of the most abundantly expressed proteins in the hippocampus were involved in apoptosis (e.g., casp4, casp7, casp9, Gzmb, Kpna1, Ing1, Ddx20 and Aifm1), plasticity and axon function (e.g., Prkce, Gsk3b, Csnk2b, L1cam, Map2k1, Inexa, Cnp and Atf2); many of these protein were expressed much lower levels in AC. Only a few apoptotic proteins (Cradd, Ripk2 and Adam17) were abundantly expressed in AC. The abundance of plasticity and axonal proteins in hippocampus may be related to the important role this structure plays in neuroplastic processes such memory and learning. The abundance of apoptotic proteins in hippocampus is likely related to two factors. First, many proliferating stem cells within the hippocampus are destined to undergo programmed cell death to prevent overpopulation. Second, the hippocampus is extremely sensitive to trauma and high levels of apoptotic proteins would aid in safely removing injured cells. Supported by grant from NIH (DC0090910; DC009219-01).

### **84 Pinpointing Tinnitus-Related Hyperactive Neurons in the Auditory Brain Structure**

**Na Zhu<sup>1</sup>**, Sean Wu<sup>1</sup>, Xueguo Zhang<sup>1</sup>, Jinsheng Zhang<sup>1</sup>

<sup>1</sup>*Wayne State University*

Pinpointing tinnitus-related hyperactive neurons in the auditory brain structure

A new methodology has been developed to pinpoint the locations of tinnitus related hyperactive neurons in the brain. The underlying principle of this method is a computational based scanning by using time-reversal algorithms, which enables one to trace the neural signals measured at the multichannel electrode recording sites and sensors back to the original neurons themselves. The spatial resolution of scanning can be as high as a few micrometers. To validate source localization results, benchmark tests were conducted on normal adult Sprague Dawley rats. For comparison purpose, spontaneous neural network signals were measured by using the multichannel electrode array implanted in the auditory cortex of the rats.

Electrical stimulation at a pre-selected position was then applied, and the corresponding neural responses during stimulations were measured and taken as the input data to time-reversal algorithms. The scanning results confirmed that the electric stimulation positions were correctly identified. Following the validation of benchmark tests, actual experiments were conducted to localize the source neurons that may contribute to the etiology of hyperactivity in the auditory cortex of animals that were behaviorally tested positive for tinnitus. Again, the measured data were used in time-reversal algorithms to pinpoint the exact locations of neural activities in the auditory cortex through fine scanning. Experimental results demonstrated that this new approach not only located the positions of hyperactive neurons, but also determined the strengths of the detected neural activities. Finally, neuromodulation through auditory cortex electrical stimulations was applied, and its impacts on suppressing tinnitus related neural activities were clearly observed. These experimental results demonstrated that this new technology may be used to accurately identify the sources of tinnitus-related activities in a brain structure.

### **85 Increased Excitability and Altered Morphology in Pyramidal Neurons After Long-Term, But Not Transient, Hearing Loss**

**Sungchil Yang<sup>1</sup>**, Wesley Jackson<sup>1</sup>, Benjamin D Weiner<sup>1</sup>, Shaowen Bao<sup>1</sup>

<sup>1</sup>*University of California at Berkeley, Helen Wills*

*Neuroscience Institute*

Hearing loss often causes tinnitus. The mechanisms underlying this type of tinnitus is not entirely clear. Although recent studies have investigated synaptic plasticity in the primary auditory cortex (AI) induced by transient and long-term hearing loss, parallel biophysical and morphological changes in AI remain largely unknown. Exposure to loud 4-kHz tone resulted in a threshold increase in the entire hearing range of the rat, and it gradually recovers in the low frequency, but not the high, range. When mapped ten days after the hearing lesion, two distinct cortical AI zones were observed, a low-CF zone displaying normal/lower threshold, enhance cortical responses and map expansion, and a high-CF zone showing higher threshold and map distortion. Membrane excitability of layer 2-3 pyramidal neurons, measured with patch-clamp recording, was increased only in the cortical hearing loss zone, but not the normal hearing zone. In addition, dendritic morphology and spine density of the pyramidal neurons were altered also only in hear loss zone, but not the hearing zone. These results indicate that membrane excitability and neuronal morphology are altered by long-term, but not transient, hearing loss. They also suggest that map expansion was mediated by functional changes of existing synapses.

## **86 Enhanced Neural Synchrony Within Auditory Cortex and Dorsal Cochlear Nucleus Following Bimodal Somatosensory-Auditory Stimulation Is Temporally Dependent**

Gregory Basura<sup>1</sup>, Seth Koehler<sup>1</sup>, Ishan Biswas<sup>1</sup>, Susan Shore<sup>1</sup>

<sup>1</sup>University of Michigan

Central auditory pathway neurons exhibit extensive plasticity that is influenced by activity-dependent inputs from other systems. Bimodal stimulation of dorsal cochlear nucleus (DCN) with sound and spinal trigeminal nucleus (Sp5) activation, alters pyramidal cell spike-timing (Shore, EJN, 2005; Koehler et al., EJN, 2011). Auditory cortex (AC), also receives somatosensory input to areas previously considered to be “unimodal” (Hackett et al., 2007). The fundamental mechanism underlying activity-dependent changes in auditory response properties to multimodal stimulation remains largely unexplored. The present study examined spontaneous activity and neural synchrony in DCN and AC following paired auditory-Sp5 stimulation in response to changes in order and timing of bimodal stimulation. Four-shank, 32-channel silicon electrodes were placed in guinea pig DCN and AC to simultaneously record spontaneous unit activity before and after bimodal stimulation with alternating pairing order (tone-Sp5 or Sp5-tone). Synchrony between neuron pairs was measured using cross-correlations and the z-score of the central peak (Vos Maex et al., 1999). Increased neural synchrony in both DCN and AC was observed only when Sp5 preceded sound, while synchrony decreased in both regions when the pairing order was reversed (tone-Sp5). Post-pairing increases in DCN and AC synchrony were isolated to each location, with no changes observed when compared across (DCN vs AC) regions. The changes in response properties to bimodal stimulation order observed here may reflect spike-timing dependent plasticity (Dahmen et al., 2008). These data demonstrate that neuronal firing properties within the central auditory circuit may be influenced by the temporal nature of converging sensory systems, which may be important in pathway aberrancy such as that observed in tinnitus.

## **87 Lack of Tonotopic Cortical Reorganization in Tinnitus**

Dave Langers<sup>1</sup>, Emile de Kleine<sup>1</sup>, Pim van Dijk<sup>1</sup>

<sup>1</sup>University Medical Center Groningen, the Netherlands

Tinnitus is a prevalent hearing disorder that can be characterized by the presence of a chronic sound percept in a silent environment. Tinnitus is known to arise in the brain, and one popular hypothesis regarding its pathophysiology asserts that tinnitus results from aberrant tonotopic reorganization, for example in response to peripheral hearing loss. This is thought to induce an overrepresentation of certain sound frequencies in the brain, giving rise to elevated levels of spontaneous activity or synchronicity that may subsequently lead to a sound percept (i.e. tinnitus).

In the present study we tested this hypothesis by mapping the tonotopic organization of the auditory cortices in twenty

tinnitus patients and twenty controls that were matched with regard to hearing loss. Functional magnetic resonance imaging was performed to measure the brain response to tone sequences presented at approx. 20-50 dB HL and ranging from 250 to 8000 Hz, while at the same time subjects were engaged in a visual/emotional task unrelated to the sound stimuli.

In spite of some inter-subject variability, the derived tonotopic maps were consistent with previous reports on the tonotopic organization in humans: multiple tonotopic progressions were found bilaterally, located on the anterior bank of Heschl's gyrus, on its posterior bank, and on the planum temporale. However, no systematic differences were observed between the average maps of the two subjects groups. In particular, no tonotopic overrepresentation of high sound frequencies was observed. To exclude that differences between groups may have been lost by averaging across subjects, we performed analyses on the tonotopic maps of all individual subjects by means of principal component analysis and through the use of linear classifiers. The two groups were shown not to be distinguishable beyond chance.

Our detailed results show that tinnitus in humans is not generally associated with large-scale reorganization of the tonotopic maps in auditory cortex. Although we cannot exclude the existence of subtle or variable reorganizations, or other differences that may have remained undetectable by means of non-invasive neuroimaging, these findings suggest that the hypothesis that tinnitus is caused by cortical plasticity needs to be revised.

## **88 Involvement of the Amygdala and Its Interactions with Auditory Centers in Noise-Induced Tinnitus**

Xueguo Zhang<sup>1</sup>, Edward Pace<sup>1</sup>, John Moran<sup>2</sup>, Jinsheng Zhang<sup>1</sup>

<sup>1</sup>Wayne State University, <sup>2</sup>Henry Ford Health System

The amygdala (AMG) receives heavy projections from auditory centers and is thought to play a key role in the pathology of tinnitus. The AMG also has abundant connections with the autonomic system and other structures of the limbic system, involving functions such as anxiety, stress, emotion and memory. However, the role of the AMG and its interactions with auditory structures in bothersome tinnitus remains unclear. In this study, we used intense tone exposure to induce tinnitus, conducted behavioral testing of tinnitus using gap detection acoustic startle reflex paradigm, tested memory using Morris water maze and anxiety using elevated plus maze. We also conducted electrophysiological recordings in the AMG, medial geniculate body (MGB) and auditory cortex (AC). The behavior data showed that in tinnitus(+) animals, memory deteriorated and anxiety increased. The electrophysiological data from the AMG of tinnitus(+) animals manifested much more complex responses compared to the AC. AMG neurons responded to sound with long latency, and their responses were synchronized with delayed responses of AC neurons (2nd peak response). Following the initial firing peak to sound, the 2nd peak in the AMG appeared in the control animals but

diminished in tinnitus(+) animals. The activity rates in response to sound were not significantly different between tinnitus(+) and tinnitus(-) animals. Neural network coherence analysis demonstrated broadly enhanced neural connectivity in the AC of tinnitus(+) animals. We also observed that neural connectivity within the AMG was less robust in tinnitus(+) than in tinnitus(-) animals. Finally, there was a similar enhancement of neural coherence in the MGB in both tinnitus(+) and tinnitus(-) animals. Electrical stimulation of the AMG decreased bursting activity in AC, AMG and MGB and lowered the short interspike interval in the AMG and MGB.

Tinnitus(+) animals demonstrated characteristic changes in AMG neurons. Electrical stimulation of the AMG produced profound changes in the AC, AMG and MGB. The electrical stimulation-induced changes may help explain AMG's involvement in the emotional component of tinnitus.

### **[89] Development of Vocalizations in the Pallid Bat, *Antrozous pallidus*: Insights from Mother-Pup Interactions**

**Bethany Chagnon<sup>1</sup>, Zoltan Fuzessery<sup>1</sup>**

<sup>1</sup>*University of Wyoming*

Vocalization development has been an important area of research for determining how bats acquire the ability to use echolocation as their primary means of spatial orientation. While much is known about the development of echolocation in a number of bat species, few studies have focused on the development of their social vocalizations. Here we used the pallid bat, *Antrozous pallidus*, as our model to illustrate the development of both echolocation and social calls in the context of mother-pup social interactions. The echolocation calls and the social vocalizations of bat pups were analyzed from post-natal day 1 to post-natal week 8. As shown in other species, pups showed an increase in the call frequency until adult-like features emerged. A decrease in the duration of the echolocation signal over time was also noted. Older pup echolocation call parameters were also examined for correlations between mother-pup, sibling, and non-related individual's calls. A number of social vocalizations were observed throughout development of the pups. These social vocalizations were characterized based on spectrotemporal features and syllable structure. Over this time course, the bats' vocal repertoire changed as they reached maturity. Our data suggest that, at one week of age, pallid bats use primarily simple, multiple-note calls that merge into a single complex FM sinusoidal vocalization used in mother-pups interactions. Our data support a form of vocal pre-patterning of more complex vocalizations that are seen most commonly later in development and in adulthood. Whether these findings reflect a form of vocal learning, or simply a maturation of the vocal production system, is unclear.

### **[90] Evidence for Environmental Input Into the Development of Vocalizations in *Eptesicus fuscus***

**Kimberly E. Miller<sup>1</sup>, Lindsey Kishline<sup>1</sup>, Jessica M. Thomas<sup>1</sup>, Zada Liu<sup>1</sup>, Ellen Covey<sup>1</sup>**

<sup>1</sup>*University of Washington*

The role of auditory tutors in learning of species-specific vocalizations has been extensively investigated in birds, but few studies have been performed on non-human mammals. Due to their complex social structure and large vocal repertoire, bats are an excellent mammalian model for audio-vocal learning. We investigated the question of whether the communication and/or echolocation calls of infant bats can be modified by exposure to altered versions of species-specific vocalizations during development. Infant *Eptesicus fuscus* were exposed to either normal echolocation and communication calls of their mothers, or digitally altered recordings of these same calls. The frequency range of the altered calls was modified to be half that of the typical calls. Both groups of bats remained with their mothers and conspecifics throughout development to prevent the stress of isolation. Bats exposed to altered vocalizations had earplugs inserted binaurally while with conspecifics. Echolocation calls of bats exposed to altered playback diverged in frequency range from those of control bats at 8-10 days, while social communication calls diverged at 14-17 days of age. Both call types were shifted downward by 5-10 kHz.

We have started to investigate the effects of altered input on development of tonotopic organization in the inferior colliculus (IC). Using electrophysiological recording, we mapped tonotopy within the ICs of experimental bats and sibling controls. Developing bats exposed to altered vocalizations had a slightly greater volume representing frequencies in the range of 30-40 kHz, with little evidence of responses to 70 kHz or greater.

The data strongly suggest that experience with tutor vocalizations shapes the characteristics of both communication and echolocation calls in developing bats and provides preliminary evidence that altered auditory experience may influence tonotopic representation in the central auditory system.

Research supported by NSF Grant IOS0719295.

### **[91] The Effects of Temporal Regularity on Auditory Brainstem Function**

**Adam Tierney<sup>1</sup>, Alexandra Parbery-Clark<sup>1</sup>, Nina Kraus<sup>1</sup>**

<sup>1</sup>*Northwestern University*

Syllables embedded within a spoken sentence tend to follow certain temporal regularities: for example, in English, longer stressed syllables are likely to precede shorter unstressed syllables. As a result, tracking the temporal regularity of speech can help the listener segregate acoustic streams into syllables, an essential step in learning to comprehend and produce speech. Prior research has shown that the presence of temporal regularity enhances performance on auditory tasks such as frequency discrimination. Biologically, temporal regularity leads to increased cortical firing rates and enhanced electrophysiological potentials. Does the

auditory brainstem contribute to the biological mechanism responsible for the processing of temporal regularities? Here we show that sounds presented at regular intervals give rise to larger brainstem onset responses than sounds presented at variable intervals. These results suggest that the presence of temporal regularity can pre-attentively affect processing throughout the auditory system. (supported by NIH T32 DC009399-02)

## **92 Neurophysiological Mechanisms of Word Segmentation**

**Antoine Shahin<sup>1</sup>, Mark Pitt<sup>1</sup>**

<sup>1</sup>*Ohio State University*

A fundamental problem in speech perception is word segmentation, identifying when one word ends (offset) and the next one begins (onset) — a nontrivial problem performed tens of times a minute when engaged in conversation. Without the ability to segment speech, spoken language would be largely incomprehensible. The problem of understanding the neural mechanisms of segmentation would be easy to solve if the acoustics of speech changed in predictable, invariant ways at word boundaries, for example, if silent gaps marked word boundaries. The acoustics of speech are not this simple, however. Acoustic cues to segmentation are elusive, especially in casual, everyday speech. Using electroencephalography (EEG) we examined the neurophysiological mechanisms that underlie speech segmentation. Native English speakers listened to segmentally ambiguous non-word phrases and decided whether they heard one or two utterances. The same process was repeated for when a 30 ms subliminal gap separated the two non-words. We found that individuals exhibited an increase in alpha band (8-14 Hz) activity immediately following non-word boundaries and also prior to their response when they segmented the spoken phrases compared to when they failed to segment. This effect occurred in the presence of and despite the subliminal gap. These findings demonstrate that word parsing may occur immediately following word boundaries and can last until a response is made.

## **93 Neural Correlates of Improvisation in Freestyle Rapping**

**Monica Lopez-Gonzalez<sup>1</sup>, Matthew Sachs<sup>2</sup>, Patpong Jiradejvong<sup>1</sup>, Charles Limb<sup>1,3</sup>**

<sup>1</sup>*Johns Hopkins University School of Medicine*, <sup>2</sup>*Harvard University*, <sup>3</sup>*Peabody Conservatory of Music*

Creativity plays a fundamental role in spontaneous musical performance. In this functional MRI study, we sought to identify the neural substrates that underlie freestyle rapping, a musical genre in which rap artists spontaneously improvise lyrics, typically to the accompaniment of a rhythmic beat. Eight professional freestyle rappers (mean age  $27.4 \pm 4.1$  s.d.) participated in this study. Two experimental paradigms were used during scanning, one of low complexity and one of high complexity; a fiberoptic active noise-cancelling microphone was used to record vocal output for all experiments. In the low complexity paradigm, subjects either generated simple

rhymes to a given cue word (experimental task) or repeated the cue word (control task). In the high complexity paradigm, subjects either incorporated a cue word into spontaneously improvised lyrics (experimental task) or recited a novel rap that was memorized prior to scanning (control task). All tasks were performed to rhythmic accompaniment at a fixed tempo. Statistical Parametric Mapping 8 was used to analyze all functional neuroimaging data. Imaging data contrast analyses of improvised conditions vs. non-generative conditions revealed heightened activity in left Broca's area, a classic perisylvian language area, as well as deactivation of dorsal prefrontal cortex. Additionally, there was increased sensorimotor cortex and cerebellar activation in both paradigms during improvisation tasks in comparison to control tasks. These data suggest that a complex network of brain regions that includes prefrontal, sensorimotor, and perisylvian language cortices is responsible for the generation of creative output during spontaneous freestyle rap.

## **94 Right Hemisphere Dominance of ERP Responses to Voice Pitch-Shifted Auditory Feedback in Singers with Absolute Pitch**

**Chuck Larson<sup>1</sup>, Nadine Ibrahim<sup>1</sup>, Oleg Korzyukov<sup>1</sup>, Roozbeh Behroozmand<sup>1</sup>**

<sup>1</sup>*Northwestern University*

The pitch-shift technique has been successfully used in recent years to study the neural mechanisms underlying the role of auditory feedback on voice control. Most studies have been done on normal participants without extensive training in music. To further our understanding of the neural mechanisms of voice control, the present study compared vocal and ERP responses to perturbations in voice auditory feedback in singers with and without "absolute pitch" ability. It has been previously shown using fMRI techniques that singers with absolute pitch have greater left hemisphere involvement while listening to variations in musical tones as compared with singers without absolute pitch ability. The present study tested the hypothesis that singers with absolute pitch would demonstrate greater left hemisphere neural activity in response to voice pitch-shifted auditory feedback. Event-related potentials (ERPs) were recorded in thirty four singers (11 absolute pitch, 12 relative pitch and 11 untrained non-musicians) while they sustained vowel sounds (ah) and their voice pitch feedback was shifted up or down (100 cents, 200 ms duration) in a randomized sequence. Results showed that the amplitude of the P200 ERP component was significantly larger for the singers with absolute pitch compared to the other two groups. Topographic scalp distributions showed that there was a right hemisphere dominance of the P200 response (200-250 ms peak) in the non-musicians and singers without absolute pitch. Singers with absolute pitch showed significantly larger ERPs in the left hemisphere compared to the other two groups. These findings support previous results of bilateral activations in singers with absolute pitch. The P200 ERP response may serve as an index of neural mechanisms related to musicality.

## **95 DPOAE STCs in Normal and Impaired Human Ears**

**Michael Gorga**<sup>1</sup>, Stephen Neely<sup>1</sup>, Alyson Gruhlke<sup>1,2</sup>, Cori Birkholz<sup>1,2</sup>, Judy Kopun<sup>1</sup>, Hongyang Tan<sup>1</sup>, Walt Jesteadt<sup>1</sup>  
<sup>1</sup>Boys Town National Research Hospital, <sup>2</sup>Department of Special Education and Communication Disorders, University of Nebraska-Lincoln

**ABSTRACT:** A fundamental attribute of the peripheral auditory system is its analytical ability in the frequency domain. Normal systems are characterized by sharp tuning while impaired systems have reduced frequency selectivity. This general description, however, may depend on the degree of hearing loss and the stimulus levels at which normal and impaired systems are assessed. This poster describes DPOAE suppression tuning curves (STC) in subjects with mild-to-moderate hearing loss (HL). STCs in normal-hearing (NH) subjects for  $f_2$  frequencies of 0.5 to 8.0 kHz (1/2 octave steps) and  $L_2$  levels from 10 to 60 dB SL (Gorga et al., 2011b) were compared to similar data for  $f_2$  frequencies of 2.0 to 5.6 kHz and  $L_2$  levels of 10 dB SL to as much as 50 dB SL in subjects with HL. The reduced range of frequencies evaluated in HL subjects was determined by the prevalence of HL as a function of frequency. The reduced range of  $L_2$  levels in HL subjects was a consequence of the interaction between the magnitude of HL and the output limit of our hardware. In NH subjects, well-defined STCs were observed, with both tip-to-tail (T-T) differences and  $Q_{ERB}$  decreasing as  $L_2$  increased. Similar patterns were observed in subjects with HL, although STCs could be measured over a reduced range of  $L_2$  levels in these subjects. When STCs in NH and HL subjects were compared for conditions in which  $L_2$  was held constant relative to behavioral threshold (i.e., dB SL), the HL ears showed reduced T-T differences and  $Q_{ERB}$ 's, with the deviation from normal increasing as the magnitude of HL increased. When the STCs from the two groups were compared for conditions in which  $L_2$  was held constant in absolute level (dB SPL), however, the STCs were nearly identical. This result suggests that, for subjects with mild-to-moderate HL, changes in measured STCs are more a result of the levels that must be used to make the measurements, and less a result of changes in cochlear frequency selectivity. [Work supported by the NIDCD R01 2251 and P30 4662].

## **96 Fast Method for Online Registration of Single Source DPOAE Input/output-Functions**

**Manfred Mauermann**<sup>1,2</sup>  
<sup>1</sup>Medical Physics, Carl von Ossietzky Universität Oldenburg, Germany, <sup>2</sup>Research Center Neurosensory Science, Carl von Ossietzky Universität Oldenburg, Germany

The interaction of the two cochlear sources of DPAOE is an important reason for the large variability of DPOAE input/output (I/O)-functions and impedes their potential use as individual predictors for cochlear compression. A better approach might be the use of I/O functions from a single DPOAE source - the initial distortion component (DCOAE)

- alone (Mauermann and Kollmeier, 2004; J. Acoust. Soc. Am. 116, 2199-2212). However, the measurement time that is needed to achieve single source DPOAE I/O functions with classical DPOAE paradigms is too high for the use in clinical studies. Long et al. (2008, J. Acoust. Soc. Am 124, 1613-1626) suggested a faster DPOAE paradigm using continuously sweeping primaries (DPOAE-sweep measurement) combined with an appropriate least squares fit (LSF) analysis. The LSF analysis even allows for a direct extraction of the distortion component alone when using sufficiently sharp filters (i.e., sufficiently broad analysis windows). The goal of the current study is to adapt, optimize and test this approach to obtain a fast and reliable measurement of single source DPOAE I/O functions. The DPOAE-sweep measurement was implemented including an online analysis which allows immediate decisions whether the recording of further epochs is needed or not. Single source DPOAE I/O functions ( $L_2$ : 25, 35, 45, 55, 65 dB SPL) were obtained from measurements with the DPOAE-sweep method and an LSF-analysis with sufficiently sharp filters. Data was recorded from six normal hearing participants for different measurement parameters to optimize the procedure. One essential outcome is that the measurement time for the online registration of a single source DPOAE I/O function in a narrow frequency band (1/3 octave bandwidth for primary sweeps, 2s/octave) lays typically in the range of 2-3 minutes (including measurements to check the stability of the probe fit). This time is clearly acceptable even for clinical studies.

## **97 DPOAE-Onset Latencies Suggest an Alternative to the Hypothesized Inverted Direction of Wave Propagation (IDWP) in the Cochlea**

**Glen Martin**<sup>1,2</sup>, Barden Stagner<sup>1</sup>, Brenda Lonsbury-Martin<sup>1,2</sup>

<sup>1</sup>VA Loma Linda Healthcare System, <sup>2</sup>Dept of Otolaryngology, Loma Linda University Medical Center  
Recently, there has been considerable debate regarding the mechanism whereby otoacoustic emissions (OAEs) are transmitted back to the cochlear base. This debate largely centers on whether or not OAEs are propagated to the ear canal by slow transverse traveling waves (TWs), or as fast longitudinal compression waves. Recent measurement of DPOAEs by Ren and associates appear to support the compression-wave notion in that they only found evidence for forward TWs. In another study, de Boer and colleagues replicated these results and proposed the notion of an 'inverted direction of wave propagation' (IDWP) in the cochlea to explain these findings. In the present study, DPOAE onset latencies, where the DPOAE can be visualized in the time domain, were collected in rabbits with and without an interference-tone placed 1/3-octave above  $f_2$  (1/3-oct IT) at several primary-tone levels and at a variety of  $f_2/f_1$  ratios including narrow (1.05) and more 'standard' (1.25) ones. DPOAE onset time waveforms were often complex, particularly at narrow  $f_2/f_1$  ratios, with the initial segment being out of phase with the steady-state portion. This complexity was often removed

by the 1/3-oct IT, which generally lengthened latencies. Overall, the existence of very short DPOAE onset latencies for very narrow  $f_2/f_1$  ratios and the lengthening effects of 1/3-oct ITs suggest that basal DPOAE components comprise the short-latency segment of the DPOAE time waveforms. In the above studies, these basal DPOAE components could have been interpreted as evidence for IDWP because their measurement sites were, in fact, apical to a region of significant DPOAE generation in which case the DPOAE wave would be seen as a forward propagating TW.

### **98 Three Different Measurement Techniques Find Significant DPOAE Components**

#### **Distributed Basal to $F_2$**

**Barden Stagner**<sup>1</sup>, Glen Martin<sup>1,2</sup>, Brenda Lonsbury-Martin<sup>1,2</sup>

<sup>1</sup>VA Loma Linda Healthcare System, <sup>2</sup>Dept of Otolaryngology, Loma Linda University Medical Center

Recent studies in our laboratory using humans and a variety of laboratory species indicate that significant DPOAE components are generated basal to  $f_2$  in the overlapping  $f_1$  and  $f_2$  traveling wave (TW) tails. These components should be maximized or minimized by  $L_1, L_2$  level combinations that affect the extent and amount of this basal overlap. When  $L_2$  is lowered with respect to  $L_1$  while employing the commonly used 'optimal'  $L_2 < L_1$  or 'scissors' paradigm, this manipulation aligns the tails of the TW envelopes and basal DPOAE components should be maximized. Conversely when  $L_1$  is lowered with respect to  $L_2$  ( $L_1 < L_2$ ) basal components should be minimized. Likewise, low level  $L_1 = L_2$  conditions should have fewer basal components as compared to high level  $L_1 = L_2$  primaries. To test these predictions regarding basal DPOAE components, DPOAE level/phase maps, onset latencies, and interference response areas were obtained from three rabbits using  $L_1, L_2 = 50, 65; 50, 50; 65, 50;$  or  $65, 65$  dB SPL. The results indicated that DPOAEs collected with  $L_2 < L_1$  or the higher level  $L_1 = L_2$  condition were dominated by basal-source DPOAE components originating above  $f_2$  as compared to the opposite situation with  $L_2 > L_1$  or with the lower level  $L_1 = L_2$  condition. DPOAE level/phase maps from the conditions that favored basal component generation showed complex phase patterns and wider phase banding resulting in shorter group delays. DPOAE onset latencies were also shorter and interference response area residuals showed more components generated above  $f_2$  for these same conditions. Taken together, these findings based upon these three independent measurement techniques are consistent with distributed basal DPOAE components that are generated in an amount roughly proportional to the overlap area of the  $f_1$  and  $f_2$  TW tails.

### **99 The Aging Cochlea**

**Carolina Abdala**<sup>1,2</sup>, Sumitrajit Dhar<sup>3,4</sup>, Srikanta Mishra<sup>1</sup>

<sup>1</sup>House Research Institute, <sup>2</sup>University of Southern California, <sup>3</sup>Northwestern University, Hugh Knowles Center, <sup>4</sup>Roxelyn & Richard Pepper Dept of Communication Sciences & Disorders

The  $2f_1 - f_2$  distortion product otoacoustic emission (DPOAE) was recorded from 0.5 to 4 kHz in 156 subjects spanning seven decades of life to describe age-related changes in cochlear function. DPOAE phase-gradient delays and IFFT-derived component magnitude and phase were measured to examine violations of scaling symmetry in the apical half of the cochlea, cochlear amplification and outer hair cell nonlinearity as a function of age. Results indicate: 1) The scaling "break" frequency around which DPOAE phase-gradient delays transition from invariant (mid-to-high frequencies) to prolonged (low frequencies) was centered at  $\sim 1.5$  kHz for all age groups; 2) Below 1.5 kHz, delays were significantly longer in newborns and systematically shortened with increasing age; 3) Infants showed the highest levels of reflection and steepest reflection-component phase slope and 4) Elderly exhibited significant reduction in distortion component amplitude as well as a relatively shallow phase slope for the reflection component. These findings indicate that the frequency range marking the putative apical-basal transition is constant throughout life. Below this frequency, in the unscaled apical region of the cochlea, DPOAE phase-gradient delays are prolonged by almost one millisecond in newborns relative to adults, suggesting immaturity in apical mechanics around the time of birth. In the basal half of the cochlea, newborns show robust amplification inferred from strong reflection; their steep phase slope for this component is likely explained by immature middle ear function. Aging is typified by substantially reduced nonlinear distortion and a relatively shallow reflection-component phase slope. One interpretation of these findings is that cochlear function becomes more linear with aging and tuning broadens. Notably, results suggest that normal, age-related changes in cochlear function impact emission types differently, supporting the idea that distortion- and reflection-type OAEs are sensitive to distinct cochlear properties.

### **100 Stability of Hearing Thresholds and $2f_1 - f_2$ Distortion Product Otoacoustic Emission Measures Up to 20 KHz in Adults**

**Gayla Poling**<sup>1</sup>, Jonathan Siegel<sup>1</sup>, Jungmee Lee<sup>1</sup>, Jungwha Lee<sup>2</sup>, Sumitrajit Dhar<sup>1</sup>

<sup>1</sup>Northwestern University, Roxelyn & Richard Pepper Dept of Com Sci & Dis, Hugh Knowles Center, <sup>2</sup>Northwestern University, Feinberg School of Medicine, Dept. of Preventive Medicine

Physiological changes in the auditory periphery due to aging and ototoxicity are initially evident and most prominent at frequencies above 8 kHz, corresponding to the base of the cochlea. The base appears to be most dependent on the cochlear amplifier for normal function. Thus any disruption of the outer hair cells has a significant impact on auditory function at these higher frequencies. In

addition to behavioral measures of hearing, distortion product otoacoustic emissions (DPOAEs) are a non-invasive, but objective measure of cochlear function known to be sensitive to minor changes in cochlear physiology (Brown et al., 1993; Rao & Long, 2011). Semi-periodic fluctuations in DPOAE level as a function of frequency, known as DPOAE fine structure, hold the promise of being an even more sensitive indicator of cochlear pathology than DPOAE level alone (Engdahl & Kemp, 1996). Although hearing thresholds and DPOAE levels have been found to be repeatable over short (days) and long (weeks) periods of time, less is known about the repeatability of DPOAE fine structure. Furthermore, limited information is available exploring stability of these measures above 8 kHz. This investigation aims to quantify the stability of hearing thresholds and DPOAE characteristics through 20 kHz in 43 individuals (10-65 yrs) with normal hearing ( $\leq 20$  dB HL through 4 kHz) who returned for a repeat evaluation ~6 months after initial test. Repeatability of 2f1-f2 DPOAE level and fine structure characteristics obtained using three stimulus level combinations (L1/L2= 55/40, 65/55, 75/75 dB SPL) as well as behavioral hearing thresholds will be compared between test sessions. Repeatability of hearing thresholds and DPOAE measures obtained with ear simulator and forward pressure calibration methods will also be evaluated. Discussion will focus on the stability and frequency dependency of the measures. [Research supported by NIDCD R01 DC008420 and Northwestern University]

### **[101] Fine Structure of Distortion Product Otoacoustic Emissions in Newborns, Infants, and Adults**

**Melissa Wheaton**<sup>1</sup>, Beth Prieve<sup>1</sup>, Glenis Long<sup>2</sup>, Carrick Talmadge<sup>3</sup>, Lisa Thomas<sup>1</sup>

<sup>1</sup>Communication Sciences & Disorders, Syracuse University, <sup>2</sup>Graduate Center, City University of New York, <sup>3</sup>National Center for Physical Acoustics, University of Mississippi

Examination of DPOAE fine-structure allows for extraction of components of otoacoustic emissions, which are generated through distinct mechanisms. Models have been developed to characterize the mechanisms and relate them to cochlear physiology. Consequently, DPOAE fine-structure is an excellent means for exploring peripheral auditory development in humans. Some literature attributes most of the differences in OAE levels from infants and adults to changes in the ear canal and middle ear (e.g., Keefe & Abdala, 2007), however, some differences remain unexplained. It is hypothesized that differences in DPOAE fine-structure between newborns, infants and adults are partially linked to cochlear changes. Fine-structure DPOAEs were measured in one ear of 11 healthy neonates, 8 infants, and in both ears of 11 adults. Primaries were equal-level and presented from 60 to 75 dB SPL in neonates, and from 50 to 75 dB SPL in infants and adults. A least-squares fit analysis (Long et al., 2008) allowed for simultaneous extraction of the stimulus and its OAE from the measured waveform, resulting in compound DPOAE level, as well as the level and phase of the

generator and reflection sub-components. Neonates and infants have greater mean generator and reflection levels than adults. Consistent with previous work on DPOAEs and TEOAEs (e.g., Prieve et al., 2009), the mean generator and reflection levels were higher in infants than neonates. The growth rates of the generator and reflection components, and the relationship between the two components are different in infants than in adults. Compared to adults, the slope of the generator component phase is steeper at low frequencies in newborns and infants than in adults, similar to that observed in previous studies (Abdala & Dhar, 2010). The changing physiology of the outer and middle ear as well as immaturities of the inner ear could contribute to the results observed. (Research funded by the March of Dimes Birth Defects Foundation).

### **[102] Effect of Middle-Ear-Muscle Reflex on Measures of Efferent-Induced Suppression of Distortion Product Otoacoustic Emissions**

**Simon Henin**<sup>1</sup>, Glenis Long<sup>1</sup>

<sup>1</sup>The Graduate Center of the City University of New York

The middle-ear-muscle (MEM) reflex is a bilateral contraction of the muscles of the middle ear evoked by loud sounds providing protective attenuation, primarily at low frequencies. The MEM reflex may be evoked bilaterally, such as when using contralateral acoustic stimulation (CAS) to elicit efferent activity. This would alter sound transmission through the middle ear and modify stimulus levels in the cochlea. Changes in stimulus level in the cochlea could produce changes in the OAE and potentially contaminate estimates of efferent function. The use of logarithmically sweeping primaries provides a fast and efficient method for measurement of distortion product otoacoustic emissions (DPOAEs) across frequency. When probe position is carefully monitored, evaluation of the changes in the sweeping primaries across frequency can be used to detect middle ear activation. Efferent-induced changes in DPOAE were measured simultaneously with changes in primary level due to MEM activation using CAS levels above and below commonly reported acoustic reflex thresholds. MEM activation was found to depend on the combined bilateral input level (e.g. both primary levels & CAS level) and the changes in primary level across frequency were consistent with a change in resonance frequency of the tympanic membrane. This change in resonance frequency resulted in a low-frequency region where the primary level in the ear canal was reduced (increased reflected energy) as expected, and a slightly higher frequency region in which the primary level was enhanced (decrease in reflected energy). The changes in ear-canal primary level presumably result in similar changes in stimulus characteristics reaching the cochlea. In regions where the energy reaching the cochlea was increased, efferent effects were apparently enhanced. However, this enhancement may be attributed to a modification of OAE generation due changes in primary magnitude, rather than suppression of the DPOAE.

### **103 Human Sonar Exploration of Enclosed Spaces**

Virginia Flanagan<sup>1</sup>, Sven Schörnich<sup>2</sup>, Michael Schraner<sup>2</sup>, Magnus Wahlberg<sup>3</sup>, Thomas Stephan<sup>1</sup>, **Lutz Wiegrebe**<sup>2</sup>  
<sup>1</sup>Dept. of Neurology, LMU, Munich, <sup>2</sup>Division of Neurobiology, <sup>3</sup>Fjord&Belt Marine Biology Center

While sighted humans have an immediate visual spatial impression of space, blind humans typically rely on tactile information from e.g. the white cane. However, some blind humans have reported to rely on the echoes of self-generated sounds to assess space and even obstacles in space. Here we show in a series of formal psychophysical experiments, accompanied by magnetic-resonance imaging, that, in virtual echo-acoustic space, sighted human subjects can be trained to reliably detect small changes in the size of an ensonified room. The fMRI data show that this psychophysical competence is reflected in a stable activation of the planum temporale of auditory cortex as well as the thalamus and, in some subjects, primary-visual cortex. The current data underpin the efficacy of human echolocation and relate the perceptual performance to cross-modal cortical processing.

### **104 Human Echolocation Vs. Echo Suppression: Influence of the Precedence Effect on the Localization of Reflective Surfaces**

**Ludwig Wallmeier**<sup>1</sup>, Nikodemus Geßele<sup>1</sup>, Sven Schörnich<sup>1,2</sup>, Lutz Wiegrebe<sup>1</sup>

<sup>1</sup>Ludwig-Maximilians University Munich, <sup>2</sup>Bernstein Center of Computational Neuroscience Munich

Psychoacoustic studies have shown that echolocation is an effective perception-action ability of humans, especially used by blind people. However, the precedence effect predicts a conflict of echo analysis and echo suppression: When localizing sound sources, the human auditory system suppresses spatial information of echoes, but this information underlies effective echolocation.

A common approach to investigate the precedence effect is the arrangement of two sound sources that present a direct sound (lead) and a delayed reflection (lag), respectively. Using such a setup, several experiments on lag-discrimination suppression have quantified the deterioration of spatial information of the lag produced by the lead.

This study investigates the interaction of echolocation and precedence effect in terms of discrimination suppression. We trained six sighted subjects to perform two versions of an azimuth-discrimination experiment in a virtual acoustic space: In the first version, the subjects had to discriminate between azimuthal positions of a single sound source, the leading of two sources, and the lagging of two sources, respectively. In the second version, the sound sources were replaced by sound reflectors. Here the task was to discriminate between azimuthal positions of a single reflector, the leading of two reflectors, and the lagging of two reflectors, respectively, by evaluating the echoes generated in real time from self-produced vocalizations.

In both versions the subjects' performance was most accurate when only one sound source or reflector was present: Azimuth-discrimination thresholds for a single sound source were typically below 5°. Echolocation thresholds for a single sound reflector were significantly worse but still around 10°.

However, with leading and lagging sound sources or – reflectors, the ratio of lead- and lag-discrimination performance was significantly smaller in the echolocation experiment. These data show that in an echolocation context, the influence of precedence is weakened.

Supported by Studienstiftung des Deutschen Volkes and Graduate School of Systemic Neurosciences.

### **105 Acoustic Modulation Transfer Functions for Human Listeners in Anechoic and Reverberant Environments**

**Duck O. Kim**<sup>1</sup>, Shigeyuki Kuwada<sup>1</sup>, Brian Bishop<sup>1</sup>, Pavel Zahorik<sup>2</sup>

<sup>1</sup>University of Connecticut Health Center, <sup>2</sup>University of Louisville

Important information is conveyed by the modulating envelope of a sound. Acoustic modulation transfer functions (MTFs) form a basis for predicting speech intelligibility (Houtgast and Steeneken, 1985) and can be derived from impulse responses (Schroeder, 1981). Although binaural room impulse responses (BRIRs) have been reported in the literature for human listeners in different acoustic environments, their corresponding acoustic MTFs have not been described. The goals of this study are: 1) to fill this void; and 2) to facilitate interpretation of human listeners' behavioral sensitivities of envelope detection in different environments.

We measured BRIRs in reverberant environments and its anechoic counterparts at various sound source azimuths ( $\pm 180^\circ$ ) and distances (14 ~ 160 cm). Our basic methods are described in Kim et al. (2010) and Kuwada et al. (2010). For derivation of acoustic MTFs from BRIRs, we used 1-octave wide noise carrier center frequencies (CCFs) of 0.25 ~ 16 kHz, and sinusoidal amplitude modulation frequencies of 2 ~ 512 Hz. Acoustic modulation loss was minimal (0 ~ 8 dB) in anechoic environment. In a highly reverberant environment, modulation loss increased monotonically with modulation frequency whereas its dependence on CCF was complex. At 160 cm and 90° azimuth, modulation loss in the contralateral ear was maximal (reaching ~30 dB) for CCFs  $\geq 2$  kHz while, in the ipsilateral ear, it was maximal (reaching 15 ~ 20 dB) for CCFs  $\leq 2$  kHz. Modulation loss decreased with decreasing distance. At 14 cm and 90° azimuth, modulation loss was > 20 dB for CCFs  $\geq 4$  kHz and modulation frequencies of 8 ~ 512 Hz in the contralateral ear whereas it was < 3 dB in the ipsilateral ear. Comparison of 0° and 90° azimuths indicates that modulation loss was smaller in the ipsilateral ear of the 90° case. Thus, turning the ear towards a sound source may be advantageous.

## **106 Behavioral and Objective Measures of the Precedence Effect**

Federica Bianchi<sup>1</sup>, Sarah Verhulst<sup>1</sup>, Torsten Dau<sup>1</sup>

<sup>1</sup>*Technical University of Denmark*

The precedence effect refers to the dominance of directional information carried by a direct sound (lead) over the spatial information contained in its multiple reflections (lags). Several studies have investigated correlates of the precedence effect at different stages along the auditory pathway, but it is still unclear whether it is dominated by peripheral or central processes.

The present study investigated peripheral correlates of the precedence effect by comparing psychoacoustical data with objective measures of lag-suppression. The psychoacoustical experiments considered three perceptual phenomena related to the precedence effect: fusion, localization dominance and lag-discrimination suppression. The objective measurements of peripheral lag-suppression comprised monaural and binaural click-evoked otoacoustic emissions (CEOAEs). Furthermore, auditory brainstem responses (ABRs) to monaural and binaural stimulation were recorded to investigate the extent of the contribution of peripheral monaural suppression to the neural representation of the precedence effect at the brainstem level.

The psychoacoustical data showed a "precedence window" of 1 to 4 ms for all subjects. In the same time range, peripheral lag-suppression observed in the CEOAE recordings was largest with levels up to 8 dB. The ABRs to monaural stimulation reflected the peripheral lag-suppression while the binaural ABRs did not show any additional contribution to monaural suppression. Thus, the results from the present study suggest that some of the main characteristics of the perceptual precedence effect can be attributed to monaural lag-suppression at the cochlea and brainstem level.

## **107 Evidence for Time-Averaged Statistics in Sound Texture Perception**

Josh McDermott<sup>1,2</sup>, Eero Simoncelli<sup>1,2</sup>

<sup>1</sup>*New York University*, <sup>2</sup>*Howard Hughes Medical Institute*

Sound textures are produced by a superposition of multiple similar acoustic events, and are distinguished from many other natural sounds by their temporal homogeneity. We recently suggested that textures might be represented and recognized with statistics that are time averages of acoustic measurements made in the early auditory system. Support for this hypothesis was obtained by synthesizing textures from statistics measured in real-world recordings (rain, fire, etc.) and demonstrating that they resemble the naturally occurring sounds whose statistics they match (McDermott & Simoncelli, 2011). To further explore the role of such statistics in texture perception, we examined the time-dependence of texture recognition and discrimination. We first assessed the effect of duration on the recognizability of textures – both real-world recordings as well as synthetic versions with matching statistics. Recognition of both sets of textures was poor for short durations (less than 100ms) but improved considerably with duration (up to about 1s). One explanation is that

recognition relies on statistics, which are unreliable given a short sample. We next assessed listeners' ability to discriminate between two exemplars of a particular texture. Each exemplar was generated stochastically, such that the waveforms were distinct despite having the same statistics. Unlike for recognition, performance in this task was good for short sounds but declined with duration, even though the longer sounds contain more information to potentially support discrimination. The results can be explained by supposing that listeners retain time-averaged summary statistics of textures. When these statistics are the same for two sounds, discrimination is difficult even if the waveforms are different. The results indicate that listeners are reliant on such statistics once sounds are of moderate length, producing good categorical recognition, but limiting the ability to discern local temporal detail.

## **108 Experience-Dependent Plasticity Engendered by Classroom FM System Use**

Jane Hornickel<sup>1</sup>, Steven Zecker<sup>1</sup>, Nina Kraus<sup>1</sup>

<sup>1</sup>*Northwestern University*

Auditory neuroplasticity is well documented for both life-long and short-term experience with sound. One factor that may underlie both behavioral and neural changes with training is auditory attention. Classroom FM systems have repeatedly been shown to increase attentive behavior in class for children, however the impact of FM system use on auditory nervous system function and reading ability had not been assessed. Children with reading impairments participated in an extensive testing battery assessing speech-in-noise perception, reading ability, cognitive function, and auditory neurophysiology. One cohort wore a classroom FM system for the school year while another did not and all children returned for testing the following summer. Importantly, all children attended the same school. Children who wore the FM system improved in reading and reading-related skills. These improvements were significantly correlated with improvement in neural consistency and the degree of benefit from stimuli presented in a regular (vs. random) context. The control group showed no relationship between the change in behavioral score and the change in neural function. This suggests that improvements in phonological awareness and reading skills after FM system use may be due to enhanced response stability in the auditory brainstem in the representation of stop-consonants and similar relationships between may be found for cortical auditory evoked responses.

## **109 Human Brain Activity in Response to Diverse Musical Tempos**

Tamara Liberman<sup>1</sup>, Eduardo Medina-Ferret<sup>2</sup>, Ricardo Velluti<sup>2</sup>, Marisa Pedemonte<sup>1</sup>

<sup>1</sup>*CLAHU University*, <sup>2</sup>*Hospital de Clinicas*

The human behaviour involves complex motivations which, albeit not clear from a rational viewpoint, would seem to require satisfaction. Music, an important human motivation, is capable of eliciting emotions and modifying behaviour and physiological functions such as the brain activity. Moreover, the human brain possesses the ability to

decode the music structure, distinguishing different parameters, such as tempo.

Human brain electrical activity typically exhibits rhythms with characteristic amplitudes and frequencies which the brain may use for the organization and processing of novel and stored information. Analyzing the EEG in the frequency domain (Fast Fourier Transform).

In this work it is posed the question if three different versions of the same musical theme, only modified in tempo, may provoke different cerebral cortex electrical activity during EEG controlled wakefulness.

It was observed the electroencephalographic activity (temporal lobes, 10-20 system) of four healthy individuals (aged 20 to 45, both genders) evoked by two musical themes (Cocaine, Cale-Clapton; Oh, Pretty woman, Orbison) in three different tempos: unchanged, slower and faster. No other musical parameters were modified.

When comparing a total of 240 windows (5 sec duration) in the three tempo versions and with a silence control (SC) - recorded prior to music input-, the following findings were observed: a) the theta rhythm was significantly different when comparing music with silence and when comparing the songs in different tempos, for both songs; b) delta rhythm was significantly different when comparing silence with songs, although it did not show to be different when comparing songs in different tempos.

The present results lead us to speculate about a possible different processing of the three tempo variations, and this would be especially true for the theta rhythm, which is in accordance with previous reported findings on the role of such rhythm in the information processing.

### **110 Pushing the Limit of Selective Attention in an Overcrowded Auditory Scene**

Willy Cheung<sup>1</sup>, Ross K Maddox<sup>1</sup>, Adrian KC Lee<sup>1</sup>

<sup>1</sup>*Department of Speech & Hearing Sciences, University of Washington*

It is a well-known phenomenon that as the number of streams in an auditory scene increases, selectively attending just one becomes increasingly difficult. Here we sought to investigate the ability of an individual to focus on one auditory stream in the presence of many, and determine the point (number of streams in the scene) at which selective attention breaks down. We presented listeners with several repeating letter streams. To aid discrimination, each stream had a unique virtualized location and pitch. Furthermore, the letter start times were distributed uniformly within each one-second repetition. In half of the trials, there was an additional primer in which the letters were played sequentially, cueing the subject to the sound configuration. Listeners were instructed visually which letter stream to attend, and to press a button when an oddball "R" occurred instead of the target letter. Oddballs were more frequent in non-target streams than they were in the target stream, meaning that simply reporting every oddball heard was not an effective strategy. Oddball detection was determined as a function of time from the stimulus start, and the results obtained will eventually be useful for optimizing effective transfer bit rate

in brain computer interface designs using an auditory display.

This work was funded by grants NIH T32DC009975 awarded to RKM and R00DC010196 awarded to AKCL.

### **111 The Role of Listener Expectation in the Formation and Maintenance of Auditory Streams**

Gerald Kidd Jr.<sup>1</sup>, Timothy Streeter<sup>1</sup>, Eric Thompson<sup>1,2</sup>, Christine Mason<sup>1</sup>, Virginia Best<sup>1,3</sup>, Gregory Wakefield<sup>4</sup>

<sup>1</sup>*Boston University, Boston, MA*, <sup>2</sup>*Air Force Research Lab, WPAFB, OH*, <sup>3</sup>*National Acoustics Laboratory, NSW, Australia*, <sup>4</sup>*University of Michigan, Ann Arbor, MI*

The present study examined the role of observer expectation, based on learned statistical rules, in the formation and maintenance of auditory streams. The stimuli comprising the test sets varied along the physical dimensions of tone frequency or interaural time difference (ITD), corresponding most closely to variation in the percepts of pitch and apparent location, respectively. Markov chains were used to generate the values of frequency or ITD. Observers were asked to discriminate between sequences drawn from Markov chains with differing transition matrices. In more complex conditions, the stimuli were drawn from previously learned sets of nonspeech auditory patterns. Human performance was compared to that of an Ideal Observer under various forms of interference, including variation along an irrelevant stimulus dimension and the presence of a simultaneous masker. The results suggest that this approach has merit in examining auditory streaming and may provide some insights into the limitations of human listeners in forming and maintaining streams across listening conditions with varying degrees of uncertainty. [Work supported by AFOSR and NIH/NIDCD]

### **112 Cortical Processing of the Enhancement Effect in Passive and Active Listening Conditions**

Yang Zhang<sup>1</sup>, Neal Viemeister<sup>1</sup>

<sup>1</sup>*University of Minnesota*

The enhancement effect in auditory psychophysics refers to the heightened sensitivity or "pop out" phenomenon of a probe signal in a broadband mixture of tones when there is preceding stimulation of the tone mixture without the probe component (Viemeister & Bacon, 1982). Animal work has shown evidence for the adaptation of inhibition in the generation of neural enhancement of the probe at the level of inferior colliculus (Nelson & Young, 2010). This EEG study tested ten normal-hearing human adult listeners to further understand cortical processing of the effect. The stimuli were based on Byrne, Stellmack, Viemeister (2011), which consisted of the target sound (T, with probe, 250 ms in duration), the precursor conditioner (C, without the probe, 250 ms in duration), sound pairs of TT, CC, CT and TC with no intervening interval, and sound pairs with a 200 ms silent interval to test persistence. The interval between pairs was randomized between 1500 and 2000 ms. No consecutive identical stimuli were allowed. The

experiment started with a passive listening condition, which used a movie-watching distraction task. In the active listening condition, the subjects were instructed to respond whether or not the second sound in a stimulus pair involved a noticeable change from the first. Behavioral data confirmed the enhancement effect for CT in each subject. The effect for CT was accompanied by a significant centro-parietal P300 response. The P300 was also consistently observed for the CT stimuli with a 200 ms separation. Minimum norm estimation showed cortical activation for the P300 mainly in temporal and parietal regions. Although the passive listening condition elicited a mismatch-negativity-like response for CT in two subjects, the MMN-like response did not reach statistical significance at the group level. The data provided the first evidence for cortical neural correlates of the enhancement effect and its persistence associated with attentional processing.

### **113 Relating Performance in Speech Intelligibility Tasks with Spatially Separated Maskers to Performance in Basic Binaural Tasks**

**Nathaniel Spencer<sup>1</sup>**, Nathaniel Durlach<sup>1,2</sup>, H. Steven Colburn<sup>1</sup>

<sup>1</sup>*Boston University*, <sup>2</sup>*Massachusetts Institute of Technology*

This work explores how binaural performance in speech processing in complex environments relates to discrimination sensitivity with basic binaural cues. Four normal hearing (NH) listeners and six hearing impaired (HI) listeners (symmetric within 10 dB) were tested. Three HI listeners had moderate hearing losses and three had severe hearing losses. Speech intelligibility (SI) thresholds, corresponding to the signal-to-noise ratio (S/N) for 50% correct, were measured in three virtual-source configurations. In all configurations, the speech target was straight ahead (midline), and two, independent, same-talker maskers were presented. In one configuration (colo), the maskers were co-located with the target. In the second configuration (symm), the maskers were symmetrically placed, each 60 degrees from midline. In the third configuration (asym), the maskers were both placed 60 degrees to the left of the target. Also, binaural just-noticeable differences (JNDs) were measured, in three tasks: interaural-correlation discrimination, interaural-time-difference discrimination, and interaural-level-difference discrimination, using 1/3-octave Gaussian noises centered at 500 Hz and 4 kHz (except that subjects with severe losses were measured at 2 kHz instead of 4 kHz). SI thresholds for the colo case were comparable for NH and HI listeners. In the spatially distributed cases, the NH subjects had significantly lower SI thresholds than the HI subjects. With the exception of one HI subject and with the exception of 4 kHz ITD, the HI subjects performed about as well as the NH subjects in all basic binaural processing measures. Measurements of SI thresholds are also being made for the same virtual stimuli with only one ear stimulated. These data suggest that in cases with high informational masking, SI performance in spatially separated cases can be weak in HI subjects, even when

binaural performance is strong. [Work supported by NIDCD Grant No. 5 R01 DC00100.]

### **114 Spatial Position Related Adaptation in the Inferior Colliculus of Anaesthetised Guinea Pigs**

**Trevor Shackleton<sup>1</sup>**, John Middlebrooks<sup>2</sup>, Alan Palmer<sup>1</sup>  
<sup>1</sup>*MRC Institute of Hearing Research*, <sup>2</sup>*University of California at Irvine*

When a sound alternates between two positions, neurones in cat auditory cortex selectively adapt to respond more to the sound which is closer to the centre of its receptive field. This occurs even at stimulus onset asynchronies (SOAs) of 200 – 400 ms, i.e. presentation rates of 2 – 5 Hz. To determine whether this is an emergent property in the forebrain, or is inherited from lower nuclei, we performed a similar experiment in the inferior colliculus of urethane anaesthetised guinea pigs. Broad band (50 Hz to 20 kHz) 5-ms noise bursts were presented at an average binaural spectrum level of 40 dB/Hz in closed field, so the interaural level difference (ILD) was altered as a surrogate for spatial position. Two trains of noise bursts, "A" and "B" were repeated for 6 s. The SOA between each A pulse varied from 50 ms to 400 ms. B pulses were played symmetrically between successive A pulses. The ILD of the A pulse was varied in 5 dB steps between  $\pm 15$  dB, keeping the average binaural level constant. The ILD of the B pulse was -5, 0, or +5 dB. Within each 6 s stimulus the ILDs of both A and B pulses and SOA were kept constant. There were five repeats of each condition, with 8 s between repeats. The firing rate in the period after each pulse was analysed as a function of both ILD and SOA. Although some neurones showed a tonic adaptation throughout the 6 s duration of the stimulus, many fired consistently throughout. Most neurones fired more after a long SOA, although a few fired most with short SOAs. We found little evidence of stimulus-selective adaptation. Even at the shortest SOA, the ILD of the B pulse had little effect on the ILD function of the responses to the A pulse, and vice versa. Thus, even at rates much faster than those which show selective adaptation in the cortex we showed little effect in the IC. This supports the hypothesis that selective adaptation to spatial position is an emergent property of the forebrain.

### **115 Model of Spike Initiation in the Medial Superior Olive**

**Simon Lehnert<sup>1</sup>**, Christian Leibold<sup>1,2</sup>

<sup>1</sup>*Department Biology II, Ludwig-Maximilians-Universität München*, <sup>2</sup>*Bernstein Center for Computational Neuroscience Munich*

Principal cells of the medial superior olive (MSO) are very fast coincidence detectors in the auditory brainstem that encode low frequency interaural time differences. Their enormously low time constant of only a few hundred microseconds yields from a very low input resistance of about 5M $\Omega$ , at rest, which arises from the expression of low-voltage-activated potassium channels and hyperpolarization-activated unspecific cation channels. Spike initiation is generally assumed to occur in the axon's initial segment (AIS). However, in neurons with very low

input resistance, as in the MSO, this may no longer hold true, because the soma constitutes a huge current sink. Moreover, these cells receive a huge amount of slowly-decaying inhibition, such that their input resistance in vivo is even much smaller than at rest. Hence the question arises: how are these cells able to elicit action potentials?

By using a multi-compartmental model of an MSO cell and its axon, we found that, at rest, the spike initiation segment (SIS) in the model is indeed the AIS, because the electrotonic independence of the AIS from the leaky soma results in an input resistance of the axonal segments that is considerably higher than at the soma. For higher inhibitory conductances, as they are obtained by simulating realistic synaptic activity, the SIS can also be found further distal in the axon. This is because the inhibitory conductance by itself and via opening HCN channels reduces the excitability of the AIS, while more distal axonal regions are much less affected.

We conclude that, although in cases where the AIS itself is not excitable, the axon is, and enables the cell to convey information downstream. We furthermore show that the probability of spike initiation is independent of the SIS, which allows us to provide a reduced MSO model describing the firing rate as a function of only the synaptic current and its derivative.

### **[116] Lateralisation Abilities Utilising Pure Tone Interaural Phase Differences: Making Sense of Space**

**David Greenberg<sup>1</sup>**, David McAlpine<sup>1</sup>, Torsten Marquardt<sup>1</sup>  
<sup>1</sup>*UCL Ear Institute*

Sound source localisation is likely bound by the principal of efficiency of neural coding (Harper and McAlpine, 2004) - the brain employs a strategy that optimises accuracy of performance. From such principles, it seems reasonable to assume that coding and neural representation accuracy of auditory spatial cues is maximised for sounds perceived at 0° azimuth and for those within the range that can be generated by the size of the head. The classic model for the neural representation of spatial cues describes a place code wherein coincidence detector neurons respond maximally when an interaural time difference (ITD) that a neuron is most responsive to is experienced. In contrast, physiological evidence from small mammals suggests peak firing rates of binaural neurons lie largely at ITDs beyond the physiological range (McAlpine et al 2001; Brand et al 2002), maximising the rate of change in firing rate within the physiological range.

To assess the extent to which the representation of azimuthal space in humans might be optimised, we measured just-noticeable-difference (JND) thresholds for interaural phase difference (IPD) as a function of reference IPD for pure tones of 64-1024Hz in normal hearing subjects. Consistent with existing literature the thresholds for 0 azimuth were lowest and as IPD increased, thresholds worsen. With increasing reference IPD the rate of improvement in IPD JND also changes, the sharpest improvement being at small IPDs and becoming more gradual with increasing IPD.

We also found a frequency-dependent change in thresholds consistent with physiological data collected from small mammals. For low frequencies, JNDs increased quickly as a function of increasing reference IPD. As pure tone frequency increased up to 512Hz, IPD JND thresholds worsened at a decreasing rate and to a decreasing degree. It is possible that the range of reference IPDs over which JNDs are low corresponds to those locations along the slopes of ITD functions reported for the guinea pig. There is also no apparent relationship between performance and the range of binaural cues generated by the head-width. The data are consistent with the representation of ITD discrimination being frequency dependent as suggested by Dietz et al, (2009), who reported an apparent over-representation of ITD detectors tuned to 45° IPD in the human brain.

### **[117] GABAB Differentially Regulates Spike Rate in the Medial Superior Olive Depending on Sound Intensity**

**Annette Stange<sup>1</sup>**, Ida Siveke<sup>1</sup>, Michael Pecka<sup>1</sup>, Benedikt Grothe<sup>1</sup>

<sup>1</sup>*Div. of Neurobiology, LMU Munich*

Microsecond differences in the arrival time of a sound at the two ears (interaural time difference, ITD) are the main cues for localizing low-frequency sounds. Neuronally, ITDs are thought to be encoded by coincidence detectors in the medial superior olive (MSO) that integrate binaural excitatory and inhibitory inputs. It has been suggested that gain control of the binaural inputs is crucial for the coincidence detection mechanism to maintain high temporal precision across a wide range of sound intensities (Grothe and Koch 2011 *Hear. Res.* 279:43). Interestingly, it has recently been demonstrated in acute brain slice preparations that the synaptic gain of MSO inputs can be modulated by GABAB-dependent processes (Hassfurth et al., 2010 *J. Neurosci.* 30:9715). However, in the intact brain, the role of GABAB for ITD processing in the MSO is unknown. Here, we combined in vivo extracellular recordings of single MSO neurons with simultaneous pharmacological manipulations to investigate the influence of GABAB signalling for ITD processing. Adult, anesthetized Mongolian Gerbils were presented with pure tone stimulation at different ITDs and at multiple sound intensities while the GABAB receptor agonist baclofen (BAC) or the GABAB receptor antagonist CGP 55845 were applied iontophoretically onto MSO neurons with multibarrelled electrodes. At moderate sound intensity the overall spike rate typically decreased during application of the agonist BAC relative to control conditions. Respectively, applying the antagonist CGP 55845 increased spiking at these intensity levels. Importantly, when the sound intensity was either lowered or increased, GABAB agonist and antagonist application had differential effects on the spike rate of MSO neurons depending on sound intensity. These results suggest a possible role for GABAB in normalizing ITD sensitivity of MSO neurons according to the characteristics of the environment.

## **118 Quantification of Geometrical Parameters of Spherical and Globular Bushy Cell Axons**

**Marc Ford**<sup>1,2</sup>, Olga Alexandrova<sup>1</sup>, Benedikt Grothe<sup>1</sup>

<sup>1</sup>*Department Biologie II, Ludwig-Maximilians-Universität München*, <sup>2</sup>*Graduate School of Systemic Neurosciences GSN-LMU*

Interaural time differences (ITDs) in the order of tens of microseconds comprise the dominant cue for localizing sounds in the horizontal plane. Neuronally, ITDs are first computed in the medial superior olive (MSO) by coincidence detection of excitatory and inhibitory inputs of both the ipsilateral and contralateral ear. While the excitatory inputs from the spherical bushy cells (SBCs) innervate MSO neurons directly, the inhibitory pathways include an additional synapse at which the excitatory input (arising from globular bushy cells, GBCs) is converted into an inhibitory output. Despite the additional synaptic delay, recent experimental and theoretical data indicate similar arrival time of excitatory and inhibitory inputs at the MSO, suggesting the involvement of anatomical factors that influence axonal conduction velocity. Indeed, it is reported that GBC axons represent the largest diameter fibers of the trapezoid body. However, detailed knowledge of the geometrical parameters determining conduction velocity in GBC and SBC axons is lacking. Two of the major determinants of conduction velocity in myelinated axons are (1) fiber diameter and (2) internode length. Using anterograde labelling in combination with immunohistochemical staining of nodal marker proteins, we measured axon diameter and internode length in SBC and GBC axons. We found that the diameter of GBC axons is more than twice the diameter of SBC axons. Accordingly, internode length in GBC axons is larger than that found in SBC axons. Assuming that myelin thickness increases linearly with fiber diameter, these findings indicate that conduction velocity in GBC fibers exceeds that in SBC fibers. Taken together, the differences in geometrical parameters of the two fiber types could compensate for the additional synaptic delay, and thus might be crucial for ITD detection.

## **119 Neural Coding of Interaural Level Differences in the Inferior Colliculus Is Altered in Adult Animals as a Result of Temporary Unilateral Conductive Hearing Loss**

**Jennifer Thornton**<sup>1</sup>, Kanthaiiah Koka<sup>1</sup>, Heath Jones<sup>1</sup>, Dalian Ding<sup>2</sup>, Richard Salvi<sup>2</sup>, Daniel Tollin<sup>1</sup>

<sup>1</sup>*University of Colorado Anschutz Medical Campus*, <sup>2</sup>*Center for Hearing and Deafness, State University of New York at Buffalo*

The interaural level difference (ILD) is a cue used by animals to localize the source of high-frequency sounds. In the presence of a mild-moderate conductive hearing loss (CHL; e.g., ear infection), sound localization abilities in humans can be persistently compromised due to altered ILD cues, especially during “sensitive periods” early in life. However, recent research suggests that via behavioral

training, adult animals are able to adapt to the presence of such altered auditory input, suggesting that plasticity can also occur in the central auditory system of adults. To test the hypothesis that plasticity can occur in the central auditory system of adults, we introduced 6 weeks of unilateral CHL (~15-20 dB) to adult chinchillas (n=6) via foam earplug. Single-unit recordings from inferior colliculus (IC) neurons indicated that after 6 weeks of earplug-induced CHL, there was an effective decrease and an increase in the efficacy of ipsilateral inhibitory afferent inputs to the IC contralateral (n=19 neurons) and ipsilateral (n=12) to the ear that had the CHL, respectively. Across neurons, ILD sensitivity in IC neurons contralateral and ipsilateral to the CHL shifted by ~10 dB and ~7 dB, respectively, relative to normals (n = 109 neurons). In both ICs, the direction of the shift was consistent with a compensation for the altered acoustical ILD cues due to the CHL. Furthermore, control experiments examining cochlear anatomy as well as peripheral auditory system measurements (cochlear microphonic and compound action potential) confirm that the shift in ILD sensitivity in IC neurons does not result from inadvertent damage to the auditory periphery due to earplugging or a residual hearing loss (multi-frequency tympanometry was also performed in some cases). Unilateral CHL-induced shifts of ILD sensitivity suggest that a compensatory form of plasticity has occurred in response to a temporary unilateral CHL by at least the level of the IC.

## **120 Computation of Interaural Time Difference in the Owl's Auditory Coincidence Detector Neuron**

**Kazuo Funabiki**<sup>1,2</sup>, Go Ashida<sup>3</sup>, Masakazu Konishi<sup>2</sup>

<sup>1</sup>*Osaka Bioscience Institute*, <sup>2</sup>*California Institute of Technology*, <sup>3</sup>*University of Maryland*

Both the mammalian and avian auditory systems localize sound sources by computing the interaural time difference (ITD) with submillisecond accuracy. In the avian auditory system, neural circuits for this computation consists of axonal delay lines from the cochlear nucleus magno-cellularis (NM) and coincidence detector neurons in the nucleus laminaris (NL). We designed coaxial glass electrodes that allowed us to obtain in vivo intracellular recordings from NL neurons of the owl. Using this technique, we were able to record the postsynaptic response during sound stimulation and measure their input-output properties. Binaural tonal stimuli induced sustained depolarizations (DC) and oscillating potentials whose waveforms reflected the stimulus. The amplitude of this sound analog potential (SAP) varied with ITD, whereas DC potentials did not. The amplitude of the SAP was correlated with firing rate in a linear fashion. Spike shape, synaptic noise, the amplitude of SAP, and responsiveness to current pulses differed between cells covering different frequencies, suggesting an optimization strategy for sensing sound signals in neurons tuned to different frequencies. Biophysical mechanisms underlying this computation will be discussed with the model simulation.

## **121 A Tonal Gradient of Intrinsic Properties in the Superior Olivary Complex Underlies Efficient Extraction of Sound Localization Cues**

**Michiel Remme**<sup>1,2</sup>, Jason Mikiel-Hunter<sup>2,3</sup>, Roberta Donato<sup>3</sup>, John Rinzel<sup>2</sup>, David McAlpine<sup>3</sup>

<sup>1</sup>Humboldt University Berlin, <sup>2</sup>New York University, <sup>3</sup>University College London

Neurons in the medial superior olive (MSO) and lateral superior olive (LSO) of the auditory brainstem code for sound source location in the horizontal plane by extracting interaural time differences (ITDs) from the stimulus fine structure and interaural level differences (ILDs) from the stimulus envelope, respectively. Both cell types are tuned to frequency and are organized along a tonotopic (frequency) axis. We studied whether the intrinsic properties of MSO and LSO cells are specialized along the tonotopic axis in order to optimize the localization of behaviorally-relevant sounds. The statistics of such sounds vary with frequency, e.g., the signal to noise ratio of combined behaviorally-relevant and background noise stimuli typically decreases with increasing frequency. Also, auditory nerve encoding of sounds changes with increasing frequency, moving from a phase-locking to an envelope coding strategy.

Using *in vitro* whole-cell recordings we characterized the membrane filters of cells in the guinea pig MSO and LSO with ZAP current injections. We demonstrate a systematic gradient in membrane properties across the main tonotopic axis of both nuclei. This gradient is manifest as a systematic change in intrinsic resonant properties, with neurons at the low-frequency end exhibiting the highest resonant frequencies (~400 Hz), and neurons at the high-frequency end exhibiting purely low-pass characteristics. Simulations indicate that sensitivity to temporal cues in natural sounds increases with a neuron's peak resonant frequency, contributing to the efficient extraction of behaviorally-relevant signals in noisy environments. In contrast, sensitivity to sound level cues decreases with resonant frequency. The data suggest a continuum in biophysical properties underlies the transformation in neural coding strategy along the tonotopic axis, from one emphasizing the stimulus fine-structure to one emphasizing the stimulus envelope. The observed gradient provides a coherent explanation for temporal performance limits observed behaviorally.

## **122 Reassessing the Role of Inhibition in the MSO**

**Michael Roberts**<sup>1</sup>, Nace Golding<sup>1</sup>

<sup>1</sup>The University of Texas at Austin

Principal neurons in the medial superior olive (MSO) respond to the source of a sound by comparing the timing of excitatory inputs received from pathways originating at both ears. *In vivo* recordings suggest that inhibitory inputs to the MSO shift the temporal dynamics of interaural time difference (ITD) detection, but the biophysical mechanisms underlying this are not understood. We have investigated these mechanisms using two approaches. First, in

recordings from a novel brain slice preparation that retains the input circuitry to the MSO, we found that direct stimulation of the auditory nerve evoked inhibitory responses in MSO neurons that preceded excitatory responses by up to several hundred microseconds. Second, in conventional brain stem slices we investigated the effects of preceding inhibition on coincidence detection in MSO neurons using two electrode dynamic clamp recordings. ITD response functions were simulated by independently stimulating ipsilateral and contralateral excitatory afferents to evoke EPSPs with relative time differences covering the range of  $\pm 0.6$  ms. The ITD protocol was then repeated using the dynamic clamp to simulate an IPSP preceding the contralateral EPSP by 0.3 ms. In neurons that fired action potentials in response to coincident EPSPs, inhibition decreased the halfwidth and the peak amplitude of the ITD response function without shifting the mean and median mass of the response function with respect to interstimulus timing. Similarly, in neurons where summation remained subthreshold, the halfwidth and peak amplitude of the response function were decreased while the mean and median response timing were unaltered. Together, these results suggest that coincidence detection in the MSO remains remarkably linear in the presence of inhibition. Thus, we propose that inhibition on its own cannot account for the shift in ITD response function timing observed in *in vivo* recordings.

## **123 The Dependence of the Binaural Interaction Component (BIC) of the Auditory Brainstem Response (ABR) on the Binaural Cues to Sound Source Location in the Chinchilla**

**Alexander Ferber**<sup>1,2</sup>, Jennifer Thornton<sup>1,2</sup>, Kanthaiiah Koka<sup>1</sup>, Daniel Tollin<sup>1,3</sup>

<sup>1</sup>Department of Physiology & Biophysics, University of Colorado Medical School, Aurora, CO, USA,

<sup>2</sup>Neuroscience Training Program, University of Colorado Medical School, Aurora, CO, USA, <sup>3</sup>Department of Otolaryngology, University of Colorado Medical School, Aurora, CO, USA

The sound-evoked BIC is the residual ABR remaining after subtracting the binaurally-evoked ABR from the sum of the monaurally-evoked ABRs. The  $\beta$  peak (also referred to as DN1), is the first negative peak in the BIC. Latencies of  $\beta$  in both human and animal studies indicate a brainstem origin for this electrophysiological potential related specifically to binaural processing occurring at the level of the inferior colliculus (IC). The IC is a site of convergence of inputs from all brainstem nuclei, many of which whose neurons are sensitive to the binaural acoustical cues to location such as the interaural time (ITD) and level (ILD) differences. The BIC may be of important diagnostic value – for example, altered latencies and amplitudes of the  $\beta$  peak in children and adults are correlated with and predictive of the long-term behavioral deficits in binaural processing associated with chronic conductive hearing loss. In humans, cats and guinea pigs the  $\beta$  peak amplitude has been shown to depend systematically on the binaural cues to location with maximal amplitudes for

ITDs and ILDs of zero (midline sources) and  $\beta$  can often no longer be detected once the ILDs and/or ITDs exceed the physiological range. In this regard, the BIC is also informative for perception as the changes in latencies and amplitudes of the  $\beta$  peak with changes in stimulus ILDs or ITDs are correlated with psychophysical performance (lateralization, discrimination, binaural masking level differences) in both normal- and hearing-impaired subjects. Here we extend these results to *Chinchilla lanigera*, a precocious species that hears nearly the same frequency and sound pressure range (audiogram) as humans and which we have shown has evoked-potential thresholds and middle ear function that is virtually adult-like already at birth. The characteristics of the BIC and its dependence on ITD and ILD are comparable to those reported in humans and other species. Supported by NIDCD R01-DC011555

### **124 Coupling of the Motion of the Tympanic Membrane to the Manubrium in Human Cadaveric Temporal Bones**

Rachelle Horwitz<sup>1,2</sup>, Jeffrey Tao Cheng<sup>1,3</sup>, Ellery Harrington<sup>4</sup>, Ivo Dobrev<sup>3,4</sup>, J. Mauricio Flores-Moreno<sup>4</sup>, Cosme Furlong<sup>4</sup>, John Rosowski<sup>1,3</sup>

<sup>1</sup>Massachusetts Eye & Ear Infirmary, <sup>2</sup>Massachusetts Institute of Technology, <sup>3</sup>Harvard Medical School,

<sup>4</sup>Worcester Polytechnic Institute

A recent study by Cheng et al. (ARO 2011), using stroboscopic holography, has shown that the lateral surface of the human tympanic membrane (TM) lying along the manubrium moves in a frequency dependent manner with sound stimulation. At low frequencies the TM surface motion is consistent with simple rotation of the manubrium; at frequencies between 1 and 10 kHz they observed motion more consistent with translation and bending of the manubrium. Above 10kHz, the lateral surface of the TM along the manubrium shows a continuation of the wave-like pattern that dominates the motion of the rest of the TM surface. We hypothesize that these wave-like motions lateral to the manubrium are consistent with a decoupling of the flexible TM from a more rigid manubrium. To test this hypothesis, we measured the TM surface motion from the lateral side and the manubrium motion from the medial side of the TM surface in the same preparation. Unidentified cadaveric temporal bones were used with controlled sound stimuli applied to the lateral surface of the TM. Stroboscopic holograms of the TM and manubrium in response to pure tones between 1 and 20kHz were then gathered and used to quantify displacement amplitude and phase angle on the entire TM surface and the manubrium. Preliminary results from two temporal bone measurements show that the TM surface motion lateral to the manubrium at high frequency presents similar wave like motion patterns as seen in the earlier study, while the manubrium motions obtained from the medial side measurement do not exhibit wave-like motions. This result supports the hypothesis that the manubrium and TM are not strongly coupled along the entire lateral surface of the manubrium at higher frequencies.

### **125 Contribution of Different Pathways in Bone Conduction in Chinchilla**

David Cahan<sup>1</sup>, Christof Rösli<sup>2</sup>, John Rosowski<sup>1,2</sup>

<sup>1</sup>Harvard-MIT Health Science and Technology,

<sup>2</sup>Massachusetts Eye and Ear Infirmary

We investigate the significance and frequency dependency of different pathways believed to contribute to hearing by bone conduction (BC) in chinchilla. Suggested major pathways include middle ear ossicular inertia, cochlear fluid inertia, cochlear shell compression, and the fluid pathways into the inner ear. These pathways eventually converge in creating a pressure difference across the partition just as in air conduction. Our BC stimulator was either an audiologic bone vibrator or bone-anchored hearing aid (BAHA) implanted on the chinchilla's skull. We made measurements of the BC produced sound pressure in the ear canal (Pec), cochlear potential (CP), differential stapes velocity ( $\Delta V_{st}$ ), and differential scala sound pressure ( $\Delta P_s$ ), while a) sealing and opening the external ear, b) sealing and opening the posterior middle ear cavity, and c) interrupting the incudo-stapedial joint.

In two experiments occluding the ear canal during BC stimulation resulted in increase in Pec and decreases in CP for frequencies below 1 kHz. However between 1 kHz and 3 kHz, both Pec and CP increased. The latter was consistent with ear canal occlusion effects in which Pec and CP are expected to increase.

In another experiment, sealing the posterior cavity produced higher Pec and CP between 400 Hz and 2.5 kHz. This result suggests an effect of sound produced by compression of the middle ear cavity walls. In other ears, Pec and CP were either unchanged or the changes were highly frequency dependent. Interruption of the incudo-stapedial joint in BC stimulation had little consistent effect on Pec, but seemed to decrease CP by as much 20 dB from 300 Hz to 1 kHz and 1.5 kHz to 3 kHz. The effect of joint interruption on differential stapes motion was highly variable. Differential scala sound pressure in one animal increased at frequency up to 3 kHz and was unchanged at high frequency.

From this study we found that intra-animal changes were consistent and repeatable; however, we saw significant inter-animal variability in these effects.

### **126 A New Estimate of the Middle-Ear Transmission Matrix in Chinchilla**

Mike Ravicz<sup>1</sup>, John Rosowski<sup>1,2</sup>

<sup>1</sup>Eaton-Peabody Lab., Harvard Medical School, <sup>2</sup>Harvard-MIT Division of Health Science and Technology, Massachusetts Institute of Technology

The middle-ear (ME) transmission 2-port matrix describes the transformation between middle-ear input and output state variables (sound pressure and volume velocity) in either direction and is independent of the middle-ear load. We present new element values [A B; C D] in chinchilla computed from measurements of ME input admittance  $Y_{ME}$ , stapes velocity  $V_s$ , and ear-canal and vestibular sound pressures  $P_{TM}$  and  $P_v$ , respectively, in the same animals (Ravicz et al., ARO 2011, #47). These new element values are most reliable between 100 Hz and a

few kHz. The new element values are consistent with the anatomical ME “transformer ratio”, other physical limits (Shera and Zweig, JASA 1992), and measured ME transfer functions with finite loads. The new values show similarities and differences to those from a previous study that used a different method (Songer and Rosowski, JASA 2007). The ME output impedance (seen by the inner ear)  $Z_{MEsrc}$  is more than a factor of 10 lower than previous estimates at low frequencies and is relatively independent of ear-canal loads used experimentally. The new 2-port matrix provides estimates of cochlear input impedance and cochlear vestibule sound pressure in the undisturbed inner ear. Supported by NIDCD.

### **127 Contribution of the Ear Canal to Sound Distribution and Wave Motion on the Tympanic Membrane Surface**

**Jeffrey Cheng**<sup>1</sup>, Michael Ravicz<sup>1</sup>, Ellery Harrington<sup>2</sup>, Cosme Furlong<sup>1,2</sup>, John Rosowski<sup>1,3</sup>

<sup>1</sup>Massachusetts Eye and Ear Infirmary Harvard Medical School, <sup>2</sup>Worcester Polytechnic Institute, <sup>3</sup>MIT-Harvard Division of Health Sciences and Technology

It has been suggested that the tilt of the tympanic membrane (TM) in the ear canal has a significant effect on how sound waves conducted down the ear canal stimulate the TM and generate traveling waves on the TM surface. Others argue that the dimensions of the TM are small compared to the wavelength of most sound stimuli and the differences in sound field down the canal across the TM surface are insignificant. In this study, we test these ideas by comparing sound-induced TM surface displacement measured with stroboscopic holography in human temporal bones after replacement of the bony ear canal with an artificial ear canal whose position can be varied. The new ear canal is made of a straight tube with dimensions similar to the human ear canal, and includes a transparent window that allows laser illumination of the majority of the TM surface for holographic measurements. Like the bony ear canal, the angle between the long axis of the artificial canal and the surface of the TM is about 45 degrees. Therefore plane waves propagating down the canal are first incident on one edge of the TM and then propagate through the air to the opposite edge. Effects of varied sound-delivery directions on TM motion are studied by rotating the bone to change the relative orientation of the TM and the canal. A probe microphone is used to measure the sound field across the TM in the different TM canal configurations. Measurements of wave motions on the TM surface, together with the sound field measurements will determine whether sound waves traveling down the ear canal lead to a spatial separation of the stimulus at the TM, which results in differences in wave motion at different TM locations.

### **128 Estimation of the Orthotropic Elastic Properties of the Rat Pars Tensa Using Indentation Testing and Model-Based Optimization**

Ehsan Salamat<sup>1</sup>, Sumit Agrawal<sup>1,2</sup>, Abbas Samani<sup>1</sup>, Hanif Ladak<sup>1</sup>

<sup>1</sup>The University of Western Ontario, <sup>2</sup>London Health Sciences Centre

Accurate finite-element (FE) models of the eardrum can potentially be used to understand eardrum function and to optimize diagnostic tests and surgical procedures. However, the accuracy of these models depends on the elastic properties specified when constructing them. Although the eardrum is an orthotropic elastic structure, for simplicity, several investigators have measured the eardrum's elastic properties (specifically the Young's modulus) under the assumption of isotropy, thus limiting the applicability of these measurements. A few investigators have attempted to measure the Young's modulus from strips that were cut from the eardrum along two perpendicular directions, specifically the radial and circumferential directions. However, cutting strips can potentially cause damage to soft tissue and has several technical challenges. In this work, an indentation-based method was developed to estimate the orthotropic elastic properties of the eardrum *in situ*, i.e., without cutting strips from the eardrum and while maintaining its natural attachments to the ear canal. A custom-built indentation apparatus was used to perform indentation testing on 3 rat eardrums *ex vivo* after immobilizing the malleus to avoid the confounding effects of the ossicular chain and cochlear load on eardrum response. Testing was done on the pars tensa. The unloaded shape of each eardrum was measured using a Fourier transform profilometer, a non-contacting optical technique. FE models were constructed for each eardrum from corresponding shape measurements in order to simulate the indentation procedure. The orthotropic elastic properties of each specimen were then estimated by numerically optimizing these parameters in each model so that simulation results matched corresponding experimental data for that specimen; a variant of the Nelder-Mead (i.e., Simplex) optimization algorithm was used. The orthotropic elastic parameters of the rat pars tensa were estimated to be  $E_C = 23.4 \pm 1.6$  MPa,  $E_R = 58.7 \pm 4.2$  MPa, and  $G_{CR} = 35.6 \pm 3.3$  MPa where  $E_C$  is the elasticity in the circumferential direction,  $E_R$  is the elasticity in the radial direction and  $G_{CR}$  is the in-plane shear modulus.

### **129 Multiple-Point Vibration Measurements on the Gerbil Tympanic Membrane**

**Nima Maftoon**<sup>1</sup>, Zinan He<sup>1</sup>, W. Robert J. Funnell<sup>1</sup>, Sam J. Daniel<sup>1</sup>

<sup>1</sup>McGill University, Montréal, Canada

The tympanic membrane acts as an interface between the outer and middle ear. Understanding the response of the middle ear to sound stimuli is highly dependent on our knowledge of tympanic-membrane vibrations. This study addresses the issue by presenting *in vivo* vibration

measurements done at multiple points on surgically exposed gerbil tympanic membranes. Glass-coated plastic microspheres are placed on the pars tensa, the pars flaccida and the manubrium in order to increase light reflection. The microspheres also act as well-defined targets for repeated measurements. A laser Doppler vibrometer measures motions of the microspheres while the tympanic membrane is stimulated by audio-frequency sine sweeps in the ear canal. Vibrations of different parts of the tympanic membrane with both open and closed middle-ear cavity are explored and discussed. At low frequencies all points on the pars tensa and manubrium move in phase. At frequencies above about 2.5 kHz the vibration pattern on the pars tensa becomes more complex and different locations show very different responses. In some experimental ears the pars flaccida shows a resonance in the frequency range of 500 to 900 Hz, the effect of which can be seen in the umbo response.

### **130 Three-Dimensional Motion of the Malleus and Incus in the Living and Cadaver Gerbil Ear**

**Willem Decraemer**<sup>1</sup>, Ombeline de La Rochefoucauld<sup>2</sup>, Elisabeth Olson<sup>2</sup>

<sup>1</sup>University of Antwerp, <sup>2</sup>Columbia University, New York, USA

Recently we presented (MOH 2011, Williamstown, USA) some measurements of 3D motion of the gerbil middle ear. The discussion was based on experimental observations of a single specimen. In the present contribution we extend the analysis and discuss similarities and dissimilarities between results from different animals. The location of the immediate rotation axis is not only related to the anatomical suspension of the ossicles but also to the location of the principal axes of the malleus and incus block. In one case experiments were performed on the same ear in the living animal, directly post mortem and one day post mortem showing evolving postmortem effects indicating that it is important in reports on experimental results on middle ear mechanics to specify the condition of the experimental animal. As many experimenters have to deal with limitations of experimental setup or lack of sufficient experimental observation time to perform a fully fledged 3D motion study we explored what simple 1D or 2D experiments can show and formulate some recommendations on how to optimally conduct such experiments.

### **131 Mechanics of Human Tympanic Membrane**

**Jef Aernouts**<sup>1</sup>, Joris Dirckx<sup>1</sup>, Jeffrey Tao Cheng<sup>2</sup>, John Rosowski<sup>2</sup>

<sup>1</sup>University of Antwerp, <sup>2</sup>Eaton-Peabody Laboratory and Harvard Medical School

The biomechanics of the human tympanic membrane yield a very sensitive sound transmission in a broad frequency range. It is known that tympanic membrane motion patterns are complicated in both their spatial and frequency dependence.

In the present work, a finite element model of the tympanic membrane was constructed to simulate acoustic behaviour. A measured tympanic membrane geometry with accurate thickness distribution was imported. Middle ear and cochlear impedance was modelled as a spring, mass, damper system.

First, the model was validated based on recent stroboscopic holography measurements in which full-field displacement patterns in human tympanic membranes for various acoustic frequencies were recorded.

Then, the model was used to formulate answers to questions like: what type of displacement patterns exist for various frequencies and how do they contribute to vibrations of the ossicular chain, what is the role of the conical shape of the membrane and what is the advantage of the angular placement in the ear canal.

### **132 Malleus and Incus: Correlates of Size**

**N Wendell Todd**<sup>1</sup>, Francis Creighton<sup>1</sup>

<sup>1</sup>Emory

**Background:** Wide ranges of dimensions of the malleus and incus are reported for various human populations. Unaddressed, however, are concordance of malleus and incus sizes, bilateral symmetry, whether ossicle size correlates with otitis media, and whether second branchial arch derivatives have more variability than first arch derivatives.

**Objectives/Hypotheses:** To quantitatively describe the malleus and incus in another United States population. **Hypothesis 1:** An ear's malleus and incus sizes are concordant. **Ho 2:** A cranium's malleus and incus sizes have bilateral symmetry. **Ho 3:** Sizes of malleus and incus are unrelated to the mastoid size indicator of childhood otitis media. **Ho 4:** Second branchial arch derivatives have more variability than do first arch derivatives.

**Study Design:** Post-mortem material-analysis.

**Methods:** From 41 adult crania without clinical otitis, the ossicles were quantitatively studied: mass, linear distances, and the angle that of the head of the malleus meets the manubrium.

**Results:** Sizes of clinically normal mallei (e.g., 21.2 to 30.7mg), and incudes (e.g., 24.4 to 37.4mg) were varied. Concordance of malleus and incus mass was found. However, no relation of sizes with mastoid size was found. Variability in first arch derivatives was similar to that of second arch derivatives.

**Conclusions:** Clinically normal mallei and incudes had masses and dimensions that varied, even more than previously reported, from ear to ear. Nevertheless, bilateral symmetry was exhibited, as was concordance of masses.

### **133 Acoustic Oscillation of Guinea Pig Stapes Visualized Through High-Speed Video Camera Analysis**

**Mitsuru Ohashi**<sup>1</sup>, Nozomu Matsumoto<sup>1</sup>, Takashi Kimitsuki<sup>1</sup>, Shizuo Komune<sup>1</sup>

<sup>1</sup>*Department of Otorhinolaryngology, Graduate School of Medical Science, Kyushu University*

<Objective> Fixation of the ossicles with chronic inflammation or sclerotic degeneration leads to hearing loss. In order to improve the level of hearing, fixated part must be repaired surgically. In such cases, it is most important to evaluate the stapes mobility. However, it has not cleared the dynamic behavior of the stapes to date. The aim of this study is quantitative visualization of the stapes motion during acoustic oscillation using the new type of high speed video camera system.

<Methods> Adult albino guinea pigs were used in this study.

The high speed video camera system (VW-5000, Keyence, Osaka, Japan) was used for recording and analysis.

The tympanic bulla was exposed and then opened through submandibular approach. The microscope of the system was placed just above the tympanic bulla, then the incudo-stapedial joint and stapes head were clearly viewed under the monitor of the system.

The tone burst sound waves were used as acoustic stimuli and delivered at a distance 5 to 10mm from tympanic membrane. The stimulus sound of 125, 250, 500 and 1 kHz at different levels of magnitude were generated by the EP/EMG measuring system (Nihon Kohden, Tokyo, Japan).

<Result> We succeeded to record the fine acoustic oscillation of the stapes in absolute value. Images were recorded at the rate of 4000fps (frame per second). Vibration profiles were measured with propriety analysis software. The period of oscillation was in synchronism with the frequency of stimulus sound. The amplitude of oscillation was proportional to the acoustic pressure level.

<Conclusion>

Our new technique is valuable for evaluation of stapes mobility and may provide important information concerning the surgical procedures.

### **134 High-Resolution 3D Surface Model of Bone and Soft Tissue Structures in the Human Middle Ear**

**Johan Aerts**<sup>1</sup>, Joris Dirckx<sup>1</sup>, Manuel Dierick<sup>2</sup>, Luc Van Hoorebeke<sup>3</sup>

<sup>1</sup>*Laboratory of BioMedical Physics, University of Antwerp, Belgium*, <sup>2</sup>*Centre for X-ray Tomography, Ghent University, Belgium*, <sup>3</sup>*Radiation Physics research group, Ghent University, Belgium*

This work aims to provide 3D surface models of the human middle ear with the correct morphology of all functional components: both the bone structures (ossicles) and the soft tissue structures (ligaments, muscle tendons and muscles). Current state-of-the-art human middle ear models already include the bone structures with their exact morphology. This is, however, not so for the soft tissue

structures. In most cases they are only implemented as abstract and simplified elements, which has its influence on the model accuracy. Thus, more precise morphological data of the soft tissue structures are required to get more realistic results from middle ear models.

The most popular techniques to obtain high-resolution morphological data of the middle ear are X-ray microtomography and histological sectioning. Another possibility is the use of magnetic resonance microscopy (MRM) but this technique has limited resolution compared to the aforementioned techniques. With histological sectioning a good distinction can be made between bone and soft tissue structures, but the technique is destructive and time-consuming in the sample preparation. X-ray microtomography has the advantage that it is non-destructive, but a disadvantage is that it is unable to image soft tissue due to low X-ray absorption. However, this problem can be solved by staining the soft tissue using phosphotungstic acid (PTA), which was successfully implemented to the middle ear.

Five 3D-models of the human middle ear are presented. These models were reconstructed from X-ray microtomography scan slices of PTA-stained samples. The morphological parameters are compared with data known from literature.

### **135 GluR2 Receptors at the IHC and OHC Afferent Synapse in the Rat Cochlea**

**Rodrigo Martinez-Monedero**<sup>1</sup>, Catherine Weisz<sup>1,2</sup>, Shilpa Chatlani<sup>1</sup>, Paul Fuchs<sup>1</sup>, Elisabeth Glowatzki<sup>1</sup>

<sup>1</sup>*Johns Hopkins Hospital*, <sup>2</sup>*University of Pittsburgh*

We are studying the expression of the AMPA receptor subunit GluR2 at hair cell synapses in the mammalian cochlea using immunocytochemistry and electrophysiology. The presence of the GluR2 subunit in the AMPA receptor channel is physiologically important, as it converts the ion channel into a calcium impermeable channel. This can have consequences for the vulnerability of the hair cell synapse to sound overexposure.

We examined whole mount preparations of the apex-middle area of the rat cochlea at P8 (before hearing onset) and at ~P22 (after hearing onset). We used two different antibodies against the GluR2 subunit, gaining similar results. Presynaptic ribbons were labeled with an antibody against CTBP2. We focused our analysis on the endings of the type I and type II spiral ganglion afferent fibers that innervate inner and outer hair cells (IHCs and OHCs), respectively.

We observed GluR2 expression on the endings of the type I and type II fibers at both ages, P8 and P22. GluR2 dots were mostly juxtaposed to the synaptic ribbons labeled with CTBP2. The relationship between GluR2 and CTBP2 labeling, the distribution, number and volume of dots differed at P8 compared to P22. For example, at P8, a percentage of GluR2 dots appeared with no juxtaposed presynaptic ribbon dots, whereas at P22, the relationship of GluR2 to CTBP2 dots was ~1. The volumes of CTBP2 and GluR2 dots were larger at P8 compared to P22.

Using whole cell recordings of type II afferent fibers at ~P8, we confirmed that GluR2 is part of the postsynaptic

AMPA receptors: Recordings with intracellularly applied spermine did not affect the rectification index of EPSCs, suggesting that the GluR2 subunit is part of the postsynaptic AMPA receptors. NASPM and Philanthotoxin, both toxins that only affect GluR2 lacking receptors, failed to reduce the EPSC amplitude.

We conclude that both at the IHC and OHC afferent synapse, before and after hearing onset, the postsynaptic AMPA receptors are calcium impermeable.

### **136 A Point Mutation in the Hair Cell Nicotinic Cholinergic Receptor Enhances Hearing-In-Noise Ability**

Paul Allen<sup>1</sup>, Dana Belles<sup>2</sup>, Phillip Cistrone<sup>2</sup>, **Anne Luebke**<sup>1</sup>  
<sup>1</sup>University of Rochester Medical Center, <sup>2</sup>University of Rochester

The medial olivocochlear (MOC) efferent system provides feedback to the cochlea, and has been hypothesized to act as a gain control mechanism whose function may serve to enhance signal-in-noise processing. We have tested this hypothesis directly, by using a genetically-modified mouse model the Chrna9L9'T line of knockin mice with a threonine for leucine change (L9'T) at position 9' of the second transmembrane domain of the  $\alpha 9$  nAChR subunit [Taranda et al., *PLoS*. 2009 20;7] in which the magnitude and duration of efferent cholinergic effects were increased; rendering  $\alpha 9$ -containing receptors that were hypersensitive to ACh, had slower desensitization kinetics, and reduced noise-induced hearing loss. We used the acoustic startle response (ASR) and the ability of prepulses to inhibit the ASR [ie, prepulse inhibition (PPI)] to assess the mouse's ability to detect prepulse signals presented in quiet or embedded in masking noise. The ASR was measured in response to brief 80-130dB SPL noise bursts, delivered in quiet or in the presence of a 60dB SPL background noise, and all animals exhibited a robust startle response to both conditions. We then tested PPI with prepulses presented in quiet, or in the presence of a continuous 60dB SPL broadband masker. We have defined threshold to be that prepulse level which inhibits the ASR by 50%. The knock-in mice (L9'T/L9'T) exhibited an *increase* in their PPI thresholds (delivered in quiet); yet exhibited a *decrease* (improvement) in their PPI thresholds with masked noise. PPI behavioral testing with (L9'T/WT) heterozygous line is planned to determine if there is a dosage effect for this allele. In summary, we have found that the Chrna9L9'T mouse knock-in line shows enhanced hearing-in-noise abilities when assayed with PPI, suggesting that increased MOC efferent feedback can not only ameliorate sound trauma, but may improve signal-in-noise detection.

This work was supported by grants NIDCD R01 (DC003086) and NIDCD P30 (DC005409).

### **137 Thrombospondin 1 Gene Expression Is Involved in Olivocochlear Innervation and Cochlear Physiology, and Is Modulated by Olivocochlear NACHR Alpha9 Activity**

**Douglas Vetter**<sup>1</sup>, Stephane Maison<sup>2</sup>, Sevin Turcan<sup>3</sup>, M. Charles Liberman<sup>2</sup>, Jack Lawler<sup>4</sup>

<sup>1</sup>Univ. Miss. Medical Center, <sup>2</sup>Mass Eye and Ear Infirmary, <sup>3</sup>Memorial Sloan Kettering Cancer Center, <sup>4</sup>Beth Israel Deaconess Medical Center

Mice lacking the alpha9 cholinergic receptor subunit exhibit abnormal development of olivocochlear (OC) synapses. To continue pursuing the mechanisms underlying these changes, we used Affymetrix gene chips to compare global transcript expression levels in wild type vs. alpha9 null mice between P3 and P60. Between P10 and P13, a period spanning the time of maximal synaptic reorganization in the cochlea, significant differences were observed in thrombospondin 1 (Thbs1) and its receptor (Cacn $\alpha 2\delta 1$ ). From P10 to P13, wild type Thbs1 expression decreased ~30%, whereas it increased 10% in alpha9 nulls. Between P10 and P13, wild type expression of Cacn $\alpha 2\delta 1$  decreased slightly, while it increased by ~55% in alpha9 nulls. The Thbs1/Cacn $\alpha 2\delta 1$  signaling system has been implicated in glutamatergic synapse formation in the CNS.

To investigate a role for Thbs1 expression in cochlear synaptogenesis, we assessed the structure and function of the OC system in Thbs1 null mice. In cochlear whole mounts immunostained for synaptophysin, medial OC terminals (under outer hair cells) were disorganized and larger than those of wild types. Lateral OC synapses (under inner hair cells) were larger and fewer in number. The structural phenotype is similar to that we reported for the alpha10 null mice. Thresholds for ABRs and DPOAEs in Thbs1 nulls were elevated 15-25 dB at all frequency regions examined except the highest frequencies tested (32 and 45kHz). Peripheral effects of the medial OC system, assessed by shocking the OC bundle while measuring DPOAEs, were normal in Thbs1 nulls.

Thus, Thbs1 expression appears to be involved in the development and function of cholinergic synapses in the cochlea, and may help explain the synaptic defects observed following loss of alpha9/10 expression.

Research support: R01 DC 006258 (DEV), P30 DC05209 and R01 DC00188 (MCL) and HL49081 (JL).

### **138 Is Mutated Prestin Protein Autoregulated?**

**Mary Ann Cheatham**<sup>1</sup>, Kasuaki Homma<sup>2</sup>, Elyssa Katz<sup>1</sup>, Jing Zheng<sup>2</sup>, Chongwen Duan<sup>2</sup>, Roxanne Edge<sup>1</sup>, Peter Dallos<sup>1</sup>

<sup>1</sup>The Hugh Knowles Center, Northwestern University, Evanston IL, <sup>2</sup>The Hugh Knowles Center, Feinberg School of Medicine, Northwestern University, Chicago IL

Compound action potential thresholds indicated normal sensitivity in heterozygous mice with only one copy of wildtype (WT) prestin (Cheatham et al., 2005). Measurements of outer hair cell (OHC) length and prestin protein expression showed that cells were near-normal in

length and in the amount of protein targeting the plasma membrane, suggesting that prestin protein expression was being autoregulated. In order to obtain a better model to test prestin's functional significance, knockin (KI) mice were developed to overcome the reduced stiffness and length of OHCs in prestin knockout (KO) mice. For C1 KIs (K233Q, K235Q, R236Q; Oliver et al., 2001), the peak of the nonlinear capacitance (NLC) function was shifted in the hyperpolarizing direction but the mice showed no change in sensitivity. In contrast, the 499 KIs (V499G/Y501H; Dallos et al., 2008) showed threshold shift due to the fact that NLC and electromotility were vastly reduced. By mating prestin KO and KI mice, it was possible to compare various combinations of prestin alleles with respect to changes in cochlear anatomy and physiology. In spite of the fact that one of the alleles is effectively a null, we refer to these offspring as compound heterozygotes. For the C1 KI mice crossed with mice lacking prestin, the distortion product otoacoustic emissions were WT-like. In addition, the protein estimated using various methods was near normal suggesting autoregulation. Measurements of NLC were also similar to those obtained in C1 KI mice. For 499 compound heterozygotes, the mice exhibited a threshold shift. Outer hair cells were also longer than if only 50% prestin protein was being expressed. Hence, we confirm our original observation that when only one copy of prestin is available, the amount of protein produced is WT-like, independent of whether the prestin gene is WT or mutated. (Work supported by NIDCD Grant #DC00089).

### **139 The Influence of Supernumerary Rows of Inner Ear Sensory and Support Cells on Frequency Selectivity in Rbl2-Deficient Mice**

**Katyarina Brunette**<sup>1</sup>, JoAnn McGee<sup>1,2</sup>, Ashley Holly<sup>1,2</sup>, David Wright<sup>1,2</sup>, Erin Hegner<sup>1,3</sup>, Sonia Rocha-Sanchez<sup>4</sup>, Sarah Stimmler<sup>1</sup>, Edward Walsh<sup>1,2</sup>

<sup>1</sup>Boys Town National Research Hospital, <sup>2</sup>Creighton University School of Medicine, <sup>3</sup>University of Cincinnati, <sup>4</sup>Creighton University School of Dentistry

The retinoblastoma (Rb) family of proteins commonly known as the pRb pocket proteins, comprise the transcription products of three closely related genes, the Rb susceptibility gene (Rb1), as well as the Rb-like genes, Rb1 and Rbl2. The pRb protein products constitute a well recognized collection of tumor suppression factors that are crucial components of the cell cycle regulatory machinery and influence the G1 phase to S-phase transition and in doing so promote cell quiescence. Consequently, when Rb genes are inactivated, cells reenter the cell cycle, proliferate, undergo mitosis and differentiate. In Rocha-Sanchez et al. (2011), we reported that Rbl2 (p130) null mice are as sensitive, or nearly as sensitive to tone-bursts spanning their responsive frequency range as wild-type control mice, in spite of the presence of well organized supernumerary rows of both inner and outer hair and support cells in the apical half of the cochlea. That finding led us to extend the study to include an analysis of tuning curves generated using a distortion product otoacoustic emission (DPOAE) suppression paradigm. Previously, we reported that tuning curves centered on 8 and 16 kHz and

acquired from Rbl2-deficient mice were indistinguishable from normal control animals. We have since expanded the study to generate tuning curves at other center frequencies, including one centered on 5.7 kHz, which targets the apical cochlea, the location populated by two rows of inner hair cells and 4-5 rows of outer hair cells. Preliminary indications are that frequency selectivity and cochlear amplifier gain may be normal, even under these conditions. If this observation holds, these data challenge one of the staple theories of modern inner ear biology; the idea that cochlear function depends on a highly-structured, rigidly conserved collection of sensory and supporting cells.

Supported in part by NIH NIDCD/5T35DC008757-05.

### **140 On the Morphology of Mouse Deiters Cells**

**Arya Parsa**<sup>1</sup>, Paul Webster<sup>1</sup>, **Federico Kalinec**<sup>1,2</sup>

<sup>1</sup>House Research Institute, <sup>2</sup>University of Southern California

Deiters cells extend from the basilar membrane to the reticular lamina and, together with pillar cells, structurally define the micro-architecture of the organ of Corti. Most of the studies describing Deiters cells morphology were focused on the apical phalangeal process and the middle region that cradles the base of the outer hair cells, whereas the basal pole received relatively little attention. Looking at the mouse organ of Corti, we found that Deiters cells' basal region is not a cylinder as usually depicted but its diameter first decreases progressively from approximately 10  $\mu\text{m}$  to as low as 3  $\mu\text{m}$ , remains constant along a segment of variable length and then increases to about 6  $\mu\text{m}$ , forming a well-defined "lower-limb" —with the corresponding thigh, leg and foot— that anchors the cell to the basilar membrane. This limb, which can be as much as 21  $\mu\text{m}$ -long, wraps little more than the characteristic rope-like cytoskeletal stalk of Deiters cells, and the foot corresponds to the basal cone of microtubules, actin and microfilaments described by earlier morphologists. The length of the limbs and the angle between the limbs and the basilar membrane varies among cochlear regions and within a same region with cell's position, but the feet of the three rows of Deiters cells always localize close to each other in a well-defined  $13.1 \pm 0.4 \mu\text{m}$ -wide stripe running all along the organ of Corti, just next to the feet of the outer pillar cells. The Deiters' feet distribute inside the stripe in a precise arrangement, with a center-to-center distance of  $6.5 \pm 0.2 \mu\text{m}$  and average area of  $25.8 \pm 1.1 \mu\text{m}^2$ . These previously unidentified morphological features of Deiters cells could be important for the mechanical response of the organ of Corti.

Supported by NIH Grant R01 DC10146

## **141 Does Oxidative Stress Generate Distinct Types of Calcium Waves in the Supporting Cells of the Organ of Corti?**

**A. Catalina Vélez-Ortega<sup>1</sup>**, Ruben Stepanyan<sup>1</sup>, Ghanshyam P. Sinha<sup>1</sup>, Gregory I. Frolenkov<sup>1</sup>  
<sup>1</sup>University of Kentucky

Acoustic overstimulation leads to oxidative stress in the cochlea that results in the production of the lipid peroxidation byproduct, 4-hydroxynonenal (4-HNE). Since 4-HNE can activate the transient receptor potential ankyrin 1 (TRPA1) cation channel, we evaluated the presence of this channel in the different cell types within the cochlea. The uptake of the small cationic dye FM1-43 into various cell types was assessed in cultured mouse cochlear explants with disrupted mechanotransduction machinery but stimulated with the TRPA1 agonist cinnamaldehyde. FM1-43 uptake was observed in most cell types of the wild type cochlear epithelium, except in Claudius's cells and it was completely absent in the cochlear epithelium of *Trpa1*-knockout animals (*Trpa1*<sup>-/-</sup>). FM1-43 uptake was not blocked by incubation with the non-specific P2 purinergic antagonist PPADS, ruling out the entry of FM1-43 via P2X channels. FM1-43 uptake was not observed in the absence of TRPA1 stimulation. Live cell ratiometric Ca<sup>2+</sup> imaging revealed robust Ca<sup>2+</sup> responses to the application of 4-HNE in Hensen cells, cells of the Kolliker's organ and epithelial cells near the spiral prominence, but not in Claudius' cells of wild type mice. No Ca<sup>2+</sup> responses to 4-HNE were detected in *Trpa1*<sup>-/-</sup> animals. Interestingly, Ca<sup>2+</sup>-waves generated by extracellular ATP and 4-HNE were somewhat different. While ATP typically resulted in oscillating responses that propagated as a Ca<sup>2+</sup> wave, 4-HNE generated in Hensen's cells sustained Ca<sup>2+</sup> responses that persisted even after removal of 4-HNE. These long-lasting responses did not propagate to the neighboring Claudius' cells. Then, we used local UV stimulation of photo-activatable (caged) Ca<sup>2+</sup> chelators in different cell types in the cochlear epithelium. We found significant cell-specific differences in the ability of different cell types to generate and/or propagate Ca<sup>2+</sup> waves. Supported by NIDCD/NIH (R01 DC009434)

## **142 Inner Ear Gap Junctions Have No Acetylation to Modify Charge Selectivity in Permeability**

**Hong-Bo Zhao<sup>1</sup>**, Yan Zhu<sup>1</sup>, Chun Liang<sup>1</sup>  
<sup>1</sup>University of Kentucky Medical Center

Gap junctional coupling in the cochlea plays an important role in hearing. Dysfunction of gap junctions can induce hearing loss. Connexin 26 (Cx26) and Cx30 are predominant isoforms in the cochlea. Cx26 is permeable to both cationic and anionic molecules, while Cx30 is only permeable to cationic molecules not to anionic molecules. We reported that inner ear gap junctions have strong charge selectivity in permeability; Cx26 is mainly responsible for permeability to anionic molecules in the cochlear gap junctions. This charge selectivity may play an important role in intercellular signaling in the cochlea (Zhao, 2005; Gossman and Zhao, 2008). Recently, it has

been reported that acetylation of connexin N-terminal may be able to modify connexin permeability and charge selectivity. In this study, we investigated whether there is acetylation for post-transcription modification in inner ear gap junctions and whether acetylation modifies inner ear gap junction charge selectivity. Nat-5 is a critical enzyme for acetylation, particularly N-acetylation. We examined the Nat-5 expression in the cochlea. Immunofluorescent staining for Nat-5 shows that there is no apparent Nat-5 expression and activity in the cochlear sensory epithelium. Also, sequence analysis shows that both Cx26 and Cx30 have the same acetylation site in their N-terminals. This is inconsistent with the difference of charge selectivity in Cx26 and Cx30 permeability. These data indicate that there is no acetylation to modify Cx26 and Cx30 charge selectivity in the inner ear. Charge selectivity in inner ear gap junctions is determined by Cx26 and Cx30 intrinsic charge selectivity.

Supported by DC05989

## **143 Supporting Cell Gap Junctions Play an Important Role in Active Cochlear Amplification in Vivo**

**Yan Zhu<sup>1</sup>**, Chun Liang<sup>1</sup>, Liang Zong<sup>1</sup>, **Hong-Bo Zhao<sup>1</sup>**  
<sup>1</sup>University of Kentucky Medical Center

Connexin mutations or dysfunction of gap junctions can induce a high incidence of nonsyndromic hearing loss. However, gap junctions and connexins in the inner ear only exist in supporting cells; hair cells have neither gap junctions nor connexin expression. Here, we report that gap junctions in the cochlear supporting cells can influence active cochlear amplification. Connexin26 (Cx26) and Cx30 are predominant isoforms in the inner ear gap junction. We found that both Cx26 and Cx30 deficiency could reduce active cochlear amplification. Distortion product otoacoustic emission (DPOAE) was reduced. However, DPOAE at low frequency in high intensities remained and appeared as high as those in wild type mice. We further used loxP-Cre technique to selectively delete Cx26 expression in Deiters cells and pillar cells, which support outer hair cells standing on the basilar membrane in vivo. Targeted deletion of Cx26 in DCs and PCs can induce hearing loss. DPOAE was also reduced. The reduction was severe at high frequency range. However, the cochlea had normal development. Hair cells and spiral ganglion neurons also had no apparent degeneration. Patch clamp recording shows that outer hair cell electromotility was left-shifted. These data reveal that Cx26 deficiency can reduce active cochlear amplification to induce hearing loss. Our findings also suggest that connexin deficient mice provide good mouse models to study active cochlear amplification in vivo, given they have no direct genetic modification on prestin and can avoid side-effects of prestin modification on active cochlear mechanics.

Supported by DC05989

## **144 Adherence Junctions in the Organ of Corti and Cochlear Function**

Marcia M Mellado Lagarde<sup>1</sup>, Lingli Zhang<sup>1</sup>, Jian Zuo<sup>1</sup>

<sup>1</sup>St Jude Children's Research Hospital

Auditory hair cells (HCs) are polarized cells with extraordinary machinery at their apexes to transduce sound waves into electrical signals. HCs are inserted into a checkerboard-like epithelium, alternating with different types of supporting cells (SCs). Apical tight junctions between HCs and SCs are important in separating the high K<sup>+</sup> endolymph at the apex and low K<sup>+</sup> perilymph at the base of the HCs that is required for mechano-electrical transduction. Adherence junctions (AJs), basal to the tight junctions, are linked to the actin cytoskeleton and should be responsible for keeping HCs and SCs tightly joined, thus contributing to the mechanical properties of the reticular lamina. We hypothesize that specific deletion of key proteins of the AJ should reduce the rigidity of the reticular lamina and produce changes in hearing. We used the Cre-loxP system in mice to specifically delete beta-catenin, vezatin or spectrin beta-2 from cochlear SC. Mice with one copy of a CreER allele: Fgfr3iCreER or PlpCreER, and two copies of a floxed allele of one of these proteins were injected i.p. with tamoxifen at different postnatal ages between P0 and P30. Littermates with only Cre or floxed alleles, also injected with tamoxifen, were used as controls. Auditory brainstem responses (ABRs) showed similar hearing thresholds at frequencies between 4 and 44 kHz for control and conditional knockout (cKO) mice of any of these proteins. Immuno-histochemical analysis of cochlear whole-mounts showed normal morphology in the cKO mice. Our results suggest that either the half-life of these proteins is very long so that complete deletion from the SC side of AJs is difficult to achieve or that it is compensated by alternative proteins in order to maintain normal properties of the junctions. To effectively disrupt AJs we may need to delete one or more of these proteins at the same time from SCs and HCs. Supported by: Wellcome Trust Fellowship (MML), NIH, ALSAC and Hartwell Foundation.

## **145 Belly Spot and Deafness (Bsd) and Mutanlallemande (Mtl) Are Two New Mutants of Lmx1a Gene with Severe Cochlear and Vestibular Defects**

Beatriz Lorente<sup>1</sup>, Georg Steffes<sup>1</sup>, Selina Pearson<sup>1</sup>, Rachael Brooker<sup>1</sup>, Sarah Spiden<sup>1</sup>, Jean-Louis Guénet<sup>2</sup>, Karen P Steel<sup>1</sup>

<sup>1</sup>Wellcome Trust Sanger Institute, <sup>2</sup>Institute Pasteur

Belly Spot and Deafness (*bsd*) arose as a recessive spontaneous mutation in a 129S5 genetic background. The homozygous mice display head tossing and circling behaviour, an indication of vestibular defects, and they also have short tails and a white belly spot of variable size. A similar phenotype was observed in homozygous mutanlallemande (*mtl*) mice which arose as a spontaneous mutation on a mixed genetic background. The analysis of hearing function by auditory brain stem responses (ABR) revealed that *bsd* mutants are deaf

whereas heterozygote and wildtype littermates have normal hearing. The *bsd* homozygotes showed no defects in the middle ear; however inner ears were smaller than controls and looked severely malformed. Paint-filled ears at E16.5 revealed that *bsd* and *mtl* mutants have abnormal vestibular systems which lack an endolymphatic duct and semicircular canals and have short cochlear ducts.

The original *dreher* mutation (Deol, 1964; Manzanares et al., 2000; Millonig et al., 2000; Nichols et al 2008; Koo et al 2009) is an allele of the *Lmx1a* gene. Both our novel reported alleles show similarities with *dreher*. Complementation tests between *bsd* and *mtl* and between *mtl* and *dreher* strongly suggest that *bsd* and *mtl* are also mutant alleles of the *Lmx1a* gene.

To determine the *Lmx1a* mutation in *bsd* and *mtl* mutant mice we performed PCR followed by sequencing analysis of genomic DNA and cDNA. Our results indicate that the *mtl* phenotype is caused by a single G to A transition affecting the splice site of the 3' end of exon 4 of transcript *Lmx1a-001*. This leads to an extended exon 4 bearing a premature stop codon and hence to the truncation of the transcript. In *bsd* mutants PCR amplification of exons 3 and 7 from genomic DNA resulted in reproducible multiple PCR products instead of the targeted amplicon.

The characterization of these two new alleles of the *Lmx1a* gene will provide new insights into the role of this gene in the development of the cochlea and vestibular system.

## **146 Hearing Impairments and Cochlear Changes in Type1 Diabetes Model Mice**

Takeshi Fujita<sup>1</sup>, Daisuke Yamashita<sup>1</sup>, Sayaka Katsunuma<sup>1</sup>, Hitoshi Tanimoto<sup>1</sup>, Shingo Hasegawa<sup>1</sup>, Ken-ichi Nibu<sup>1</sup>

<sup>1</sup>Kobe University Graduate School of Medicine

Recent several population-based studies suggested the association between diabetes and hearing impairment. But the relationship between diabetes and hearing loss has not been as firmly recognized as the association between diabetes and its known complications affecting the renal, visual, and peripheral nervous systems. The aim of this study was to investigate the pathophysiology underlying diabetes-associated hearing loss through experiments using type1 diabetic mice.

Streptozotocin induced male C57BL/6J diabetic mice were used. Auditory evoked brainstem responses (ABR) were measured to evaluate hearing function at 1, 3 and 5 month after induction of diabetes (n = 10 at each time point). Mild loud noise was exposed to animals (n = 8) 5 months after induction of diabetes and ABRs were undergone before being exposed to noise, 1, 3, 5, 7, and 14 days after noise exposure. Cochlear blood flow was measured by laser doppler flowmeter. Histological changes were observed by hematoxylin and eosin (HE) staining. Vessel wall thickness was measured via CD31 immunostaining. Spiral ganglion cells (SGCs) were counted in each specimen.

Chronologic changes in the ABR threshold shift were not significantly different between the diabetic group and controls throughout the observation period. Vessel walls in the modiollus of the cochleae were thick in diabetic group. Recovery from noise-induced injury was significantly

impaired in diabetic mice. Reduction of cochlea blood flow and SGCs were observed in diabetic mice cochleae after noise exposure.

### **147 Round Window Function Is Required for Normal Cochlear Responses to Super-Threshold Stimuli**

**Qunfeng Cai**<sup>1</sup>, Carolyn Whitcomb<sup>1</sup>, Jessica Eggleston<sup>1</sup>, Richard Salvi<sup>1</sup>, Wei Sun<sup>1</sup>, Bo Hua Hu<sup>1</sup>

<sup>1</sup>*State University of New York at Buffalo*

The round window of the cochlea serves as a vent for release of inner ear pressure generated by stapes vibration during acoustic stimulation. Previous investigations have shown that loss of round window function results in mild hearing loss. However, it is not clear how round window dysfunction affects the cochlear responses to super-threshold stimuli. To address this question, we developed a rat model with surgically-blocked round window, which had an average threshold shift of  $13.1 \pm 9.6$  dB assessed by auditory brainstem responses. With this model, we first examined the input/output function of distortion product otoacoustic emission (DPOAE) and found a reduction in the DPOAE amplitude following round window closure. Interestingly, the slope of the Input/output function became flatter compared with that seen in the contralateral control ears ( $0.26 \pm 0.15$  vs.  $0.64 \pm 0.27$  dB/dB). This slope change is distinct from those seen in sensorineural hearing loss (a steep slope) or conductive loss (a parallel slope). We then examined the input-output function of the amplitudes of acoustic startle reflex evoked by broadband noise bursts and found a marked reduction in the reflex amplitude. Finally, we examined the effect of round window closure on cochlear responses to acoustic overstimulation. Rats were exposed to a broadband noise at 120 dB SPL for 2 h. The ears with round window closure exhibited a temporary threshold shift of  $25.4 \pm 27.8$  dB, which was significantly less than that in the control ears ( $61.9 \pm 19.6$  dB). Moreover, the ears with round window closure showed no permanent threshold shift, whereas the control ears exhibited an average of  $15.3 \pm 13.9$  dB permanent threshold shifts. Taken together, the results suggest that the round window closure affects the magnitude of basilar membrane vibration provoked by super-threshold stimuli. (Supported by NIH R01 DC010154-01A2 to BH Hu; R01DC009091 and R01DC009219 to RS)

### **148 Using the Cochlear Microphonic to Estimate the Location of Missing Outer Hair Cells Along the Cochlear Partition**

**Mark Chertoff**<sup>1</sup>, Brian Earl<sup>1</sup>, Janna Sorensen<sup>1</sup>, Dianne Durham<sup>1</sup>

<sup>1</sup>*University of Kansas Medical Center*

The long term goal of this research is to develop clinical tests that identify the structures in the cochlea that are damaged and cause hearing loss. This is motivated by progress in genetic and tissue transplantation approaches for curing hearing loss, which require more accurate diagnostics than presently available to target treatment

locations. Here we examine if the cochlear microphonic (CM), a physiologic signal that is dominated by outer hair cells (OHCs), can estimate the location of missing OHCs along the cochlear partition. The CM was recorded to a low frequency tone embedded in a series of noise maskers of various bandwidths to progressively unmask the contributions of OHCs to the CM. The purpose of this study was to determine if the function relating the amplitude of the CM to masker cutoff frequency could be used to estimate the location of missing OHCs.

Mongolian gerbils were exposed to high-level tones of various frequencies and durations to create a group of animals that varied in the location and extent of damage along the cochlear partition. After two weeks recovery, the CM was recorded via a round window electrode in response to a 733 Hz tone-burst. The signal was presented at 80 dB SPL in the presence of noise high-passed in third-octave intervals between 0.4 and 45 kHz. Animals were sacrificed and the cochlea fixed, sectioned, and stained with phalloidin. OHCs were imaged using confocal microscopy and counted with ImageJ software.

CM amplitudes were normalized relative to an unmasked condition and plotted as a function of cochlear distance to create a cumulative amplitude function (CAF). In unexposed animals, the CAF was a sigmoidal function that saturated between 10-11 mm from the apex. In exposed animals, the CAFs plateaued at various locations which were related to the position where OHCs were absent. We conclude that the shape of the CAF may be useful in locating regions of missing OHCs along the cochlear partition.

### **149 Listening to Your Neighbor: Matching of Inner Ear Sensitivity and Call Frequency in the Tropical Coqui Frog Along an Altitudinal Gradient**

**Sebastian Meenderink**<sup>1</sup>, Peter Narins<sup>1</sup>

<sup>1</sup>*UCLA*

Males of the Puerto Rican coqui frog (*Eleutherodactylus coqui*) produce a distinct two-syllable call ('Co'-'Qui'), with each of the syllables carrying information for conspecific males and females, respectively. It is known that the spectral content of these calls systematically changes with altitude above sea level. Since acoustic communication involves both the generation and the detection of a signal, we recorded multiple calls of male coqui frogs in the field, and assessed the frequency range over which their inner ears were sensitive. For the latter, distortion product otoacoustic emissions (DPOAEs) were recorded using a small, portable setup that is easily deployed in the field. It is found that both the spectral content of the calls and the inner ear sensitivity change in a similar fashion along an altitudinal gradient. As a result, the call frequencies and the auditory tuning are closely matched at all altitudes. We suggest that the animal's body size determines the frequency particulars of the call apparatus and the inner ear. Moreover, we demonstrate that both the call characteristics and their altitudinal dependence have remained stable over a 20-year period, reinforcing the notion of the call as a reproductive isolating mechanism.

Supported by NIH grant no. DC-00222 and UCLA Academic Senate grant no. 3501 to PMN, and NWO-VENI grant no. 863.08.003 to S.W.F.M..

### **150 Novel Method for Intratympanic Injection of Compounds in Adult Mice**

Naoki Oishi<sup>1</sup>, Fu-Quan Chen<sup>2</sup>, Carlene Brandon<sup>2</sup>, Su-Hua Sha<sup>2</sup>

<sup>1</sup>University of Michigan, <sup>2</sup>Medical University of South Carolina

Local application of drugs into middle ear has the potential to increase efficacy of treatments and reduce systemic side effects. Among the several existing local application methods, the simplest and most frequently used is 'traditional' injection through the tympanic membrane. However, a concern about transtympanic injection is that a hole is made in the tympanic membrane which compromises its integrity. This could potentially influence auditory processing, reflected by changes in auditory brainstem response (ABR) thresholds and in the intensity of hearing loss induced by traumatic noise. In order to elucidate the effects of transtympanic injections on auditory processing, we tested the effects on hearing function by assessment of ABR thresholds and on the magnitude of noise-induced hearing loss. Transtympanic injection itself induced 10-20 dB threshold shifts 3 days after injection of a control solution, and significantly decreased noise-induced permanent threshold shifts (PTS) in mice exposed to noise 3 days after injection compared to mice that did not receive injections. We then designed a new surgical approach for delivery of siRNA or other compounds through the otic bulla into the middle ear. With this new injection method, no threshold shift was observed 3 days post-injection. Furthermore, the levels of PTS hearing loss were identical between mice with or without injections. In addition, fluorescence was observed in hair cells and spiral ganglion cells 6 to 48 h after injection of fluorescently-tagged compounds delivered by this method. This new surgical approach of intratympanic injection should provide an improved method for auditory research in mice, in particular for studies of noise-induced hearing loss.

Supported by grant R01 DC009222 and DC003685 from the National Institute of Health.

### **151 A Specialized Case in Drug Development: Alternative Methods for Preliminary Ototoxicity Screening in Guinea Pigs**

Matthew Abernathy<sup>1,2</sup>, Rachel Tapp<sup>1</sup>, Joshua Yoder<sup>1</sup>, Phaedra Cole<sup>1</sup>, David Gauvin<sup>1</sup>, Theodore Baird<sup>1</sup>

<sup>1</sup>MPI Research, <sup>2</sup>Western Michigan University

When developing drugs for middle ear administration or those with possible middle or inner ear exposure, the FDA indicates that auditory brainstem response (ABR) evaluations and microscopy of relevant otic tissues, including cytochrome c oxidase (COX), should be conducted on all studies. Due to the methods necessary to conduct middle ear microscopy and create CGs, it is not possible to

conduct each assay within the same ear. When administered locally, ototoxic agents can induce varying degrees of toxicity within the same animal. Current approaches are somewhat unsatisfactory, as each ear cannot be thoroughly assessed for all possible effects. Additionally, the methods necessary to create CGs are arduous, and technical errors can result in sample damage, making data interpretation difficult. Another drawback to this approach is that temporal bone processing can lead to extended reporting timelines. The need for a screening method which enables concurrent middle ear and hair cell assessments while maintaining acceptable data reporting timelines is apparent. A rapid histopathologic method was developed to evaluate the conductive structures within the middle ear as well as the auditory hair cells. In addition to thoroughly evaluating possible causes for ABR threshold increases, the method also incorporated evaluations of the middle ear mucosa and Eustachian tube to assess local membrane toxicity. To ascertain method suitability, an experiment was conducted utilizing 10% kanamycin (KM), administered through a middle ear catheter to 7 female guinea pigs for 4 consecutive days. ABR evaluations were conducted pretest, and on days 5 and 8. Using serial sectioning, the hair cells were assessed in midmodiolar regions. Additionally, representative sections were taken to evaluate the middle ear mucosa and middle ear structures. The results of the experiment suggest that this method can adequately detect signs of ototoxicity in a timely manner.

### **152 Evaluation of Cochlear Temporal Acuity by Using Time-Stressed Stimuli**

Lijie Liu<sup>1</sup>, Lijuan Shi<sup>1</sup>, Aixue Fu<sup>1</sup>, Awad Almklass<sup>2</sup>, Steve Aiken<sup>3</sup>, Jian Wang<sup>1,3</sup>

<sup>1</sup>Department of Physiology & Pharmacology, Medical College of Southeast University, Nanjing, China,

<sup>2</sup>Department of Physiology & Biophysics, Dalhousie

University, Halifax, Canada, <sup>3</sup>School of Human Communication Disorders, Dalhousie University, Halifax, Canada

In our recent studies on cochlear damage induced by either noise or hyperbilirubinemia, we identified the need to evaluate potential changes in temporal processing resolution of the cochlea. The methods for such tests must be highly accurate and sensitive because the potential changes may be very small. We developed and compared two methods to meet this challenge by using time-stressed stimuli. The first method measures responses to click pairs with a varied inter-click interval (ICI). With the ICI reduced to 1 ms, the responses (auditory brainstem responses (ABR) and compound action potentials (CAP)) to the second click in the pair are reduced in amplitude and overlapped with responses to the first click. Therefore, peak amplitude measurement may be impossible or difficult at short intervals. We proposed the use of waveform root-mean-square amplitude (RMS) to replace peak amplitude measures. Waveform RMS allows for a precise estimation how the response to the second click attenuates with decreasing ICI despite the overlap in the responses. This approach is especially effective in CAP

testing due to the large signal-to-noise ratio of responses. Using this method, we have been able to see temporal resolution changes in both mice and guinea pigs after a sub-clinical noise exposure that does not cause permanent threshold shift. A deficit in temporal processing has also been demonstrated using this method in neonatal mice in which hyperbilirubinemia is established. Our second method uses a sequence of clicks with ICIs jittered around the target values (e.g., 1, 2, 4 ms, etc). When the ICI is small, the evoked responses are largely overlapped, but continuous loop averaging deconvolution (CLAD) can be used to recover the responses to individual stimuli when the stimulus sequence is non-isochronous (Ozdamar 2006, *J Acoust. Soc. Am.* 119(1): 429-438). We have created a version of this processing method using the OpenEx platform with TDT system III (Tucker-Davis Technology, FL, USA). The data are being collected and analyzed.

### **153 Identification of Adeno-Associate Viral Vectors (AAV) That Target Mammalian Cochlear Cells**

Yilai Shu<sup>1,2</sup>, Na Lu<sup>1,2</sup>, Marco Petrillo<sup>1</sup>, Huawei Li<sup>2</sup>, Zhengming Wang<sup>2</sup>, Guangping Gao<sup>3</sup>, Zheng-Yi Chen<sup>1</sup>  
<sup>1</sup>Eaton-Peabody Laboratory, Massachusetts Eye and Ear Infirmary, Harvard Medical School, <sup>2</sup>Eye Ear Nose and Throat Hospital of Shanghai medical school, Fudan University, <sup>3</sup>Microbiology & Physiology Systems, University of Massachusetts Medical School

Efficient delivery into the cochlea has been a major challenge that hinders the study of gene function in the cochlea and the development of gene therapy for genetic deafness. Inner ear hair cells are particularly refractory to conventional delivery means. Recent work has shown that adenovirus and some adeno-associated virus (AAV) are capable of infecting some cochlear cell subtypes. However the viral vectors that are capable of transduce a wide range of cochlear cell types need to be identified.

We have systematically tested 12 AAV vectors for their capacity to transduce cochlear cell subtypes in neonatal and mature mouse inner ears. AAV vectors were chosen for their characteristics in minimum toxicity, sustained expression, the capacity to infect postmitotic cells, and the efficient viral production. AAV vectors of different serotypes (serotypes 1, 2, 5, 6, 6.2, 7, 8, 9, rh8, rh10, rh39 and rh43) carrying a GFP reporter were delivered into the scala media by cochleostomy.

In neonatal (P1-P4) cochleae injected with AAV, 6 AAV serotypes (1, 2, 5, 6.2, 7 and 8) showed cochlear cell type specific GFP expression 4 weeks after injection. The infected cell types included inner and outer hair cells, Deiters' cells, inner Pillar cells, inner phalangeal cells and inner border cells. The GFP level varied from robust by AAV1 to relatively weak expression by AAV5. By ABR, four out of five AAV serotypes tested (2, 6.2, 7 and 8) resulted in no hearing loss in any frequency; whereas AAV1 induced a slight shift. In the P14 mouse, similar cochlear cell subtype expression patterns were observed by AAV serotypes.

Our study identified new AAV vectors that can be used for a targeted delivery into specific cochlear cell subtypes,

with a sustained expression level over the long term and minimum impairment on hearing. The AAV vectors will be suitable for applications including functional study of cochlear cell type specific genes and correction of genetic deafness by gene therapy.

### **154 Optical Imaging of the Mouse Cochlea Through the Otic Capsule Using Autofluorescence and Endogenous Second Harmonic Generation**

Xin Yang<sup>1</sup>, Chia-Lung Hsieh<sup>1</sup>, Ye Pu<sup>1</sup>, Demetri Psaltis<sup>1</sup>, Konstantina Stankovic<sup>2,3</sup>

<sup>1</sup>Ecole Polytechnique Federale de Lausanne, <sup>2</sup>Harvard Medical School, <sup>3</sup>Massachusetts Eye and Ear Infirmary

For vast majority of people with sensorineural hearing loss – the most common type of hearing loss worldwide - the underlying cause is not known because the inner ear cannot be biopsied today without destroying hearing, and intracochlear cells cannot yet be imaged with sufficient resolution to establish diagnosis. Intracochlear imaging has been technologically challenging primarily because of the limited access due to the surrounding bone, and because of small and narrow cochlear chambers. Three-dimensional cochlear imaging without sectioning has recently been investigated *ex vivo* or *in vivo*, using computed tomography, magnetic resonance imaging, optical coherent tomography, and confocal fluorescence microscopy. Among these methods, confocal microscopy is advantageous for its high resolution and deep penetration depth, yet disadvantageous for the necessity of exogenous labeling. The exogenous dyes or antibodies may result in tissue deformation and artifacts, thus limiting interpretation of the results. We report, for the first time, imaging of the mouse cochlea *ex vivo* through the encasing bone using near infrared femtosecond laser as the excitation, and endogenous autofluorescence and second harmonic generation (SHG) as the contrast mechanisms, without any exogenous labeling. Cochleas from 9 week old mice were fixed using intracardiac and intracochlear perfusion with 4% paraformaldehyde, extracted, and rinsed in PBS 3 times prior to imaging. A subset of mice was exposed to noise, which caused permanent threshold shift, 3 weeks prior to sacrifice. We find that both SHG and autofluorescence exhibit strong contrast allowing cellular, and even subcellular resolution of intracochlear cells, including hair cells and spiral ganglion neurons. Specific, noise-induced pathologic changes in intracochlear cells can be detected. Our results provide the basis for future exploration of autofluorescence and SHG *in vivo*.

### **155 BODIPY Conjugated Xylosides Reveal Repair and Regeneration of the Semicircular Canal Cupula**

Holly A. Holman<sup>1</sup>, Vy M. Tran<sup>1</sup>, Sailaja Arungundram<sup>2</sup>, Kuberan Balagurunathan<sup>2</sup>, Richard D. Rabbitt<sup>3,4</sup>

<sup>1</sup>Dept. Bioengineering, Univ. Utah, Salt Lake City, UT,

<sup>2</sup>Dept. Medicinal Chem., Univ. Utah, Salt Lake City, UT,

<sup>3</sup>Dept. Bioengineering and Dept. of Otolaryngology-Head

Neck Surgery, Univ. Utah, Salt Lake City, UT, <sup>4</sup>Marine Biological Laboratory, Woods Hole, MA

Sensory hair bundles in the cochlea and vestibular organs are covered by acellular connective hydrogel tissues rich in glycosaminoglycans (GAGs). These materials are critical to auditory and vestibular sensation, evidenced by that fact that disruption of the cochlear tectorial membrane or semicircular canal cupula through mechanical damage, protein expression, or disease leads to profound sensory deficits. Despite their importance, the process of repair and regeneration of these key connective tissues remains largely unknown. Xylosides are well-known to prime GAGs in various cellular systems. We have developed a novel compound conjugating boron-dipyrromethene (BODIPY) dyes with xylosides to examine regeneration and repair of the semicircular canal cupula, *in vivo*. When introduced into the extracellular space the compound passively enters the Golgi apparatus rendering new GAGs produced by cells fluorescent. The compound was injected bilaterally into the endolymph and fluorescence was observed over time while recording single unit afferent activity. One semicircular canal cupula was disrupted by a partial compression of the ampulla, while the other ear was observed under control undamaged conditions. Cristae in both ears expressed vigorous fluorescence within 15 minutes. Undamaged control cupulae remained transparent and did not show fluorescence over the 8-hour time course of the experiment. In the damaged ear, local punctate fluorescence was observed within 30 minutes demonstrating local generation of new GAGs within the regenerating cupula. The large distance from the cupula periphery to sites of punctate labeling demonstrates repair was not simply due to cells around the periphery but, instead, must have involved local production. Further observations by confocal microscopy suggest an infiltration of fibroblast-like cells responsible for repair. The process is unusual given the high K<sup>+</sup> concentration in endolymph. BODIPY conjugated xylosides provide a new window to observe the process and may facilitate development of new means to promote repair. [Sponsored by NIH R01 006685 & R01GM075168]

### **156 Purification of Fibroblasts from the Spiral Ganglion**

Annett Anacker<sup>1</sup>, Alice Burghard<sup>1</sup>, Thomas Lenarz<sup>1</sup>, Karl-Heinz Esser<sup>2</sup>, **Gerrit Paasche<sup>1</sup>**

<sup>1</sup>Hannover Medical School, <sup>2</sup>School of Veterinary Medicine Hannover

Cultures of freshly isolated spiral ganglion cells (SGC) are used to investigate the effects of neurotrophic factors *in vitro*. These cultures are well established, but contain more cell types than just SGC. At least fibroblasts and glial cells are also known to be present in the cultures. In the present study we try to isolate and purify fibroblasts from this culture.

The spiral ganglia were dissected from newborn rats (P3) and dissociated enzymatically and mechanically. To isolate fibroblasts from this cell culture, fibroblast specific medium based on DMEM supplemented with fetal calf serum (FCS) and penicillin/streptomycin was used. To separate

fibroblasts and glial cells cell numbers between 100.000 and 500.000 per 25 cm<sup>2</sup> were seeded into culture flasks in order to introduce different times between passages.

The obtained cells were cultured for 48 hours in a 96 well plate at a concentration of 1,5 x 10<sup>4</sup> cells/well and then fixed with 4% paraformaldehyde before immunolabeling with primary antibodies against the 200 kD neurofilament (SGC), vimentin (fibroblasts and glial cells) and the S100 protein (glial cells). The staining was visualized by fluorescent secondary antibodies.

Medium optimized for fibroblasts in combination with dropping the laminin/ ornithin coating as typically used for SGC prevented growth of SGC but not glial cells. Morphologically, the fibroblasts are more flat with larger rounded nuclei whereas glial cells are more spindle shaped with a small cytoplasm. When seeding 100.000 cells/25cm<sup>2</sup> the number of glial cells was strongly reduced after the first passage. Any further passaging had only a minor influence on the numbers of glial cells, but the overall growth rate was reduced with increasing passage number. In contrast, when seeding 400.000 cells/25cm<sup>2</sup> the growth rate was less influenced, but the number of glial cells was not further reduced compared to the lower seeding density.

It is possible to receive fibroblast enriched cell cultures from the spiral ganglion, but until now it is not yet a pure fibroblast preparation.

Funded by: BMBF: FKZ 01EZ1001B

### **157 A Rapid Method for Reducing the Expression of Specific Genes in the Inner Ear by Applying Vivo-Morpholino Oligos Into the Scala Media of the Cochlea in Mice**

qing chang<sup>1</sup>, Xi Lin<sup>1</sup>

<sup>1</sup>Emory University

Mutations in many genes cause deafness. Mouse models are valuable tools for studying the mechanisms of hearing loss caused by genetic mutations. Traditional gene knock out mouse models are powerful tools for investigating underlying deafness mechanisms. However, the process of generating such models is time and money consuming. Here we describe a rapid method to reduce expression of specific genes in the inner ear as an alternative way for obtaining mouse models of specific genetic defect.

Gjb2 is the gene we targeted for a reduced expression in this project. Vivo-morpholino oligos were designed to bind specifically to the first 25bps of Gjb2 CDS. The Cx26 knock down mouse model was generated by injecting vivo-morpholino Gjb2 oligo into the scala media of P0 to P2 mice. Examined by both whole mount immunostaining and Western blot quantification, we found that the expression of Cx26 was markedly reduced in the cochlea. Immunolabeling from cochlear sections demonstrated that the expression of Cx26 was significantly reduced in both sensory epithelium and in the lateral wall of the cochlea. In addition, the ABR test showed that mice after such injections were profoundly deaf across all frequencies tested.

Morphological examination at P21 showed that the organ of Corti in the apical turn retained in the immature state

(e.g., the tunnel of Corti was not opened). The cells in the organ of Corti in the middle and basal turns were degenerated, as well as the corresponding spiral ganglion neurons. These morphological features were similar to the findings observed in the cochlea of conditional Cx26 null mice. Toxicity of the vivo-morpholino oligos was tested using both in vitro and in vivo assays. We found that 80nM of vivo-morpholino produced minimum toxic effect on the growth of organ of Corti tested in vitro. When vivo-morpholino Gjb2 scrambled oligo and a standard control unrelated to Gjb2 were injected (80 nM), we found that these controls produced elevated hearing thresholds at high frequencies ( $\geq 18$  kHz), where injections were made. In contrast, the vivo-morpholino Gjb2 oligo showed hearing loss across the whole frequency range of 4-32 kHz. These findings suggest that injections of vivo-morpholino Gjb2 oligo into the scala media of the cochlea at early postnatal age is a promising approach for knocking down specific protein expressions in the cochlea. Such an approach may yield significant savings in both money and time required for generating mouse models of specific genetic mutations.

### **158 Evaluation of Nanoconjugated Delivery of Cisplatin for Reduction of Ototoxicity in a Murine Model of Head and Neck Squamous Cell Carcinoma**

Nicholas Rockefeller<sup>1</sup>, Stephanie Cohen<sup>1</sup>, Dianne Durham<sup>1</sup>, Mark Cohen<sup>1</sup>, Yelizaveta Shnayder<sup>1</sup>

<sup>1</sup>University of Kansas Medical Center

A nanoconjugated Hyaluronan-cisplatin (HA-cisplatin) is a novel chemotherapy delivery system which is selectively targeted to lymphatics and should decrease systemic side-effects of standard cisplatin therapy such as ototoxicity. This study utilized buccal injection of head and neck squamous cell carcinoma cell line MDA-1986 into athymic nude mice. Following development of a standard tumor burden, mice were given 3 weeks of standard cisplatin chemotherapy (weekly intraperitoneal injection), nanoconjugated HA-cisplatin (subcutaneous peritumoral injection), saline (intraperitoneal injection) or hyaluronan (HA) by subcutaneous peritumoral injection. Mice were sacrificed at the conclusion of therapy (3 weeks) or three weeks after no additional therapy (6 weeks). Drug efficacy was evaluated by cervical lymph node and tumor measurements and histology. Ototoxicity was evaluated by otoacoustic emissions (DPOAE) and cochlear histology. Mice receiving control treatment (saline or HA alone) showed an average increase in tumor size of 196% at 3 weeks and 1261% at 6 weeks. DPOAE measurements were robust in both groups at both survival times. Mice treated with the standard cisplatin formulation showed a 148% increase in tumor size at 3 weeks and 768% increase at 6 weeks. DPOAE measurements were decreased in amplitude at both survival times compared to controls as well as pre-treatment baselines. Mice treated with the HA-cisplatin conjugate showed a 31% increase in tumor size at 3 weeks and a 12% decrease in tumor size at 6 weeks. DPOAE amplitudes were decreased compared to controls and baseline measurements but slightly

increased compared to mice treated with standard cisplatin. Our results show a significantly better outcome for tumor suppression with HA-cisplatin compared to standard cisplatin with a slight reduction in ototoxic side effects as measured by otoacoustic emissions.

### **159 Local Application of Copper Sulfate Protects Cochlear Hair Cells Against Carboplatin in Chinchillas**

Dalian Ding<sup>1</sup>, Haiyan Jiang<sup>1</sup>, Richard Salvi<sup>1</sup>

<sup>1</sup>University at Buffalo

Carboplatin, a second-generation platinum chemotherapeutic drug, selectively damages inner hair cells and type I spiral ganglion neurons in chinchillas. Previous studies including our own indicate that cisplatin and other platinum-based compounds are transported from blood into the cochlea and hair cells via copper transporters. Ctr1 has been identified as a major influx transporter for cisplatin and carboplatin, whereas the sequestration and efflux of these drugs occurs via two P-type ATPases, ATP7A and ATP7B. Studies in cochlear organotypic cultures and other systems have shown that cellular import of cisplatin through Ctr1 is competitively inhibited by extracellular copper. Therefore, we hypothesized that the increase of extracellular copper would down regulate uptake of platinum compounds into the inner ear and hair cells via Ctr1 and protect against ototoxicity. To test this hypothesis, 5 chinchillas were treated with 50 mg/kg (i.p.), a dose that causes significant inner hair cell loss. Just prior to carboplatin treatment; 50  $\mu$ l of copper sulfate (100  $\mu$ M) was placed on the round window membrane of the right cochlea while the quantity of saline was placed on left round window membrane as control. Two weeks after carboplatin treatment, both cochleae from each treated chinchilla were processed to obtain cochleograms showing the proportion of inner hair cell and outer hair cell loss as a function of cochlear location. Inner hair cell loss is typically very similar in both cochleae of carboplatin-treated chinchillas. However, in the current study, inner hair cell loss was greatly reduced in 80% (4 of 5) of the copper sulfate treated cochleae compared to the saline treated cochleae; only one animal had a similar loss of inner hair cells in both cochleae. These results indicate that application of copper sulfate to the round window provides significant protection against carboplatin-induced hair cell loss presumably by reducing the influx of carboplatin into the hair cells via Ctr1.

### **160 Inhibition of P53 Reduces Cisplatin-Induced Ototoxicity**

Julien Menardo<sup>1,2</sup>, Domenico Maiorano<sup>3</sup>, Jean-Luc Puel<sup>1</sup>, Jing Wang<sup>1,2</sup>

<sup>1</sup>INSERM, <sup>2</sup>Université Montpellier 1 & 2, <sup>3</sup>Institut de Génétique Humaine

Background and Aims: Cisplatin is a widely used cancer therapy drug that unfortunately has major side effects in normal tissues, notably ototoxicity in cochlea. Despite intensive research, the mechanism of cisplatin-induced ototoxicity remains unclear, and protective approaches against cisplatin induced ototoxicity are lacking. The aim of

this study was to investigate intracellular pathways involved in cisplatin ototoxicity in the neonatal mouse cochlear explants in vitro and in p53 knockout mice in vivo to develop effective therapeutic strategies to prevent cisplatin-initiated hearing loss.

**Methods:** The cochlear explants from p3 mice were exposed to cisplatin (0 to 20 $\mu$ M) for 5 days. p53 knockout and wild-type mice were exposed to a single dose of cisplatin (16 mg/kg, intraperitoneally). The immune labelling technique and Western blot analysis were used to investigate the molecular mechanisms responsible for cisplatin ototoxicity. The auditory brainstem response and distortion product otoacoustic emissions were recorded to evaluate the auditory functions. Counting of the sensory hair cells was performed using scanning electron microscopy and confocal microscopy.

**Results:** We showed that early phosphorylation of p53 on its serine 15 during cisplatin ototoxicity has a crucial role in cisplatin induced hearing loss and cochlear cell apoptosis. Thus, pharmacological inhibition of p53 in cochlear explants in vitro attenuated cochlear cell apoptosis. In addition, the deletion of p53 in mice prevented cisplatin induced hearing loss and cochlear cell apoptotic cell death. **Conclusion:** Our results demonstrate a critical role of p53 in cisplatin ototoxicity and support targeting p53 as an effective strategy to prevent harmful side effects of cisplatin ototoxicity in patients undergoing chemotherapy.

### **161 Cisplatin-Induced Hair Cell Death Is Inhibited by the Spin Traps OKN-007 and Tempol**

**Alexander Claussen**<sup>1</sup>, Robert Floyd<sup>2</sup>, Carter Van Waes<sup>1</sup>, Lisa Cunningham<sup>1</sup>

<sup>1</sup>National Institute on Deafness and Other Communication Disorders, National Institutes of Health, <sup>2</sup>Experimental Therapeutics, Oklahoma Medical Research Foundation

Cisplatin-induced ototoxicity is mediated in part by generation of reactive oxygen species, and several antioxidants have been shown to inhibit cisplatin ototoxicity. Spin traps serve as antioxidants by reacting with free radicals to form stable free radical products. Tempol is a nitroxide spin trap with superoxide dismutase mimetic activity that has been used as a radioprotectant and neuroprotectant in animal models. OKN-007 (also known as NXY-059) is a nitron spin trap with an excellent safety profile in humans.

OKN-007 (100, 200 and 500  $\mu$ M) and tempol (100, 500 and 1000  $\mu$ M) were each non-toxic to sensory hair cells in whole-organ cultures of adult mouse utricles. Cisplatin was administered for 24 hours followed by 24 hours in cisplatin-free culture media, resulting in significant ( $p < 0.05$ ) loss of hair cells compared to non-treated controls. OKN-007 (200  $\mu$ M) significantly inhibited cisplatin-induced hair cell death at a range of cisplatin doses (30, 35 and 50  $\mu$ g/mL) ( $p < 0.05$ ). Similarly, tempol (500  $\mu$ M) also inhibited cisplatin-induced (30  $\mu$ g/mL) hair cell death ( $p < 0.05$ ).

An important consideration in studies of cisplatin ototoxicity is that the proposed protectant must not inhibit the anti-tumor efficacy of cisplatin. OKN-007 and tempol each have demonstrated anti-tumor activity, and *in-vitro* data indicate

that tempol does not reduce the anti-tumor efficacy of cisplatin. Our data indicate that the spin traps OKN-007 and tempol each inhibit cisplatin-induced hair cell death, and they suggest that spin traps may hold promise as a co-therapy aimed at inhibiting cisplatin-induced hearing loss.

This work was supported by the NIDCD Division of Intramural Research and the NIH Clinical Research Training Program, a public-private partnership supported jointly by the NIH and Pfizer Inc (via a grant to the Foundation for NIH from Pfizer Inc).

### **162 Otoprotective Mechanisms of Dexamethasone, Melatonin and Tacrolimus in Gentamicin-Induced Hair Cell and Hearing Losses: A Pharmacodynamic Study**

**Esperanza Bas Infante**<sup>1,2</sup>, Thomas R Van De Water<sup>1</sup>, Chhavi Gupta<sup>1</sup>, John Dinh<sup>1</sup>, Ly Vu<sup>1</sup>, Fred F Telischi<sup>1</sup>

<sup>1</sup>University of Miami, <sup>2</sup>Hospital Clinico Universitario Research Foundation

**Background and aims:** Exposure to an ototoxic level of an aminoglycoside can result in a hearing loss. This study investigates the otoprotective efficacy of dexamethasone (DXM), melatonin (MLT) and tacrolimus (TCR) treatments in gentamicin (GM) exposed animals and organ of Corti explants.

**Experimental approach:** Adult rats were divided into: 1) controls treated with saline-only (S); 2) exposed to GM-only (GM); and GM-exposed groups treated with either DXM, MLT or TCR, groups 3-5) released from gelfoam applied on the round window membrane and delivered via a mini-osmotic pump to the round window membrane niche in the contralateral ear. Auditory function and cochlear surface preparations were studied. In vitro studies of GM initiated oxidative stress, pro-inflammatory cytokine mRNA levels, the mitogen activated protein kinase (MAPK) pathway and caspase-3 activation were performed in 3-day-old rat organ of Corti explants.

**Key results:** DXM, MLT and TCR decreased levels of reactive oxygen species in GM-exposed explants. The mRNA levels of TNF- $\alpha$ , IL-1 $\beta$  and the receptor TNFRI were significantly reduced in GM+DXM and GM+MLT groups. Phospho-p38 MAPK levels decreased in GM+MLT and GM+TCR groups, while c-Jun-N-terminal kinase phosphorylation was reduced in GM+DXM and GM+MLT groups. Caspase-3 activation decreased in GM+DXM, GM+MLT and GM+TCR groups. These results were consistent with in vivo observations. Local treatment of GM-exposed rat cochleae with either DXM, MLT or TCR protects auditory function and prevents auditory hair cells loss independent of the method of delivery

**Conclusions and implications:** GM-exposed explants exhibit an increase in oxidative stress and initiation of an inflammatory response that leads to the activation of MAPK signaling and apoptosis of affected hair cells. The three compounds tested in this study demonstrate otoprotective properties which could be beneficial in devising treatments to prevent GM ototoxicity-induced hearing loss.

**163 The Hair Cell Death of Mammalian Vestibular Epithelia Induced by Neomycin Is Ameliorated by Using a siRNA Targeting MAPK1 or PLGA Nanoparticles Loaded with the siRNA**

Wei Li<sup>1</sup>, Xiaoping Du<sup>1</sup>, Xinsheng Gao<sup>1</sup>, W. Mark Saltzman<sup>2</sup>, Satish I. Kuriyavar<sup>1</sup>, Richard Kopke<sup>1,3</sup>

<sup>1</sup>Hough Ear Institute, Oklahoma City, OK, <sup>2</sup>Department of Biomedical Engineering, Yale University, New Haven, CT,

<sup>3</sup>Dept. of Physiology and Otolaryngology, University of Oklahoma Health Sciences Center, OKC, OK

It has been shown that MAPK1/3 activation in supporting cells is a common response to damage, acting to promote hair cell death in the mammalian cochlea. Hair cell death was reduced when MAPK1/3 activation was prevented. It is possible MAPK1/3 would also play a role in hair cell death in vestibular epithelia as seen in cochlea. Promising results have been produced by using RNAi in treating infectious diseases, cancers, neurodegenerative diseases, etc. However, there are serious concerns with using lipoplexes, which are the most widely used small-interfering RNA (siRNA) delivery systems, due to their toxicity and immunogenicity. A new method using poly (lactic-co-glycolic acid) (PLGA) nanoparticles densely loaded with siRNA has been shown to lead to efficient and sustained gene silencing. In this study, PLGA nanoparticles loaded with the siRNA targeting MAPK1 (siMAPK1-NPs) as well as siRNA targeting MAPK1 delivered by a commercially available cationic liposome kit (siMAPK1) were employed to prevent hair cell death caused by neomycin in organotypic cultures of mouse saccules. Hair cell loss was induced by administering 4 mM neomycin in organotypic cultures of mouse saccules. Both siMAPK1 and siMAPK1-NPs significantly increased hair cells survival. Similar protective effects were achieved by using either siMAPK1-NPs or siMAPK1. The down-regulation of MAPK1 was confirmed by using qRT-PCR. These results demonstrated that MAPK1 is involved in the death of hair cells of vestibular epithelia and inhibition of MAPK1 gene expression can prevent hair cell death induced by neomycin in mammalian vestibular epithelia. PLGA nanoparticles loaded with siRNA can be used as a useful tool in siRNA knockdown studies of the inner ear.

**164 Dietary Nutrients Attenuate Gentamicin Ototoxicity: Reduced Hearing Loss and Increased Hair Cell Survival in Guinea Pigs Maintained on Supplemented Diet**

Colleen LePrell<sup>1</sup>, Eric Rudnick<sup>1</sup>, Mark Nelson<sup>1</sup>, Diane Prieskorn<sup>2</sup>, Susan DeRemer<sup>2</sup>, Josef Miller<sup>2</sup>

<sup>1</sup>University of Florida, <sup>2</sup>University of Michigan

Gentamicin is an aminoglycoside antibiotic that is toxic to sensory cells in the inner ear, thus inducing hearing loss. Much of the damage to the sensory cells is induced by metabolic stress and related free radical production. Several antioxidant agents that serve to attenuate free radical production and corresponding oxidative stress insult have been shown to attenuate gentamicin ototoxicity. Here, we present data collected in parallel studies in two

different laboratories; the data confirm the potential for protection against gentamicin ototoxicity using a combination of antioxidant nutrients that effectively reduce noise-induced hearing loss (beta-carotene, vitamins C and E, and magnesium). In both studies, we maintained guinea pigs on a nutritionally complete standard laboratory diet (2040 Teklad Global Guinea Pig Diet) or a custom-manufactured version of the 2040 with additional dietary nutrient supplements (TD.08623, manufactured with increased levels of beta-carotene, vitamins C and E, and magnesium). Dietary manipulation was initiated either 10 days (UM), or 28 days (UF), prior to gentamicin insult. Gentamicin was delivered at a dose of 140 mg/kg/day, for 14 days (UF) or 16 days (UM). In both studies, robust, statistically significant protection of the sensory cells was observed. In addition, threshold shifts (measured using auditory brainstem response thresholds) were reduced in animals maintained on the supplemented diet for 28 days pre-gentamicin at 2, 4, and 8 kHz, with less evidence for preserved function at higher frequencies (16 and 24 kHz). Protection at the lower frequencies extended to at least 9 weeks post-gentamicin. ABR assessments were limited to 12 and 32 kHz in the animals maintained on enhanced diet for 10 days pre-gentamicin, and functional protection was not reliably observed. These data confirm the potential for protection of the inner ear against gentamicin ototoxicity using dietary supplements. Additional studies are needed to determine dose-response curves for single and combined agents, as well as to measure the effects of decreasing the pre-gentamicin treatment time.

Supported by University of Florida College of Public Health and Health Professions (CGL) and the Ruth and Lynn Townsend Professor of Communication Disorders (JMM).

**165 Molecular Mechanisms of Glucocorticoid Protection Against Glutamate-Induced Cochlea Damage**

Inna Meltser<sup>1</sup>, Agneta Viberg<sup>1</sup>, Barbara Canlon<sup>1</sup>

<sup>1</sup>Karolinska Institutet

Glucocorticoids protect the cochlea from acoustic damage by activating glucocorticoid receptors (GR) (Tahera et al, 2006) that are located primarily on hair cells and spiral ganglion neurons. The activation of the GRs after acoustic trauma is positively correlated to the activation of the transcription factor NF- $\kappa$ B (Tahera et al, 2006). NF- $\kappa$ B together with Akt/PKB is also involved in glucocorticoid-induced hair cells protection against the inflammatory cytokine TNF $\alpha$  (Haake et al, 2009). Here we studied the molecular mechanisms of the synthetic glucocorticoid dexamethasone (DEX) on early postnatal cochlear explants damaged by glutamate. Glutamatergic excitotoxicity is an established model of acoustic trauma in vitro (Wang and Green, 2011) that results in the deafferentation of sensory inner hair cells (IHC) from spiral ganglion neurons (SGN). By pharmacological inhibition of the downstream GR pathways in control and glutamate treated explants we characterized the effect of DEX on the cochlea recovery after glutamate-induced trauma. The inhibitors of NF- $\kappa$ B (NF- $\kappa$ B activation inhibitor III) and Akt/PKB (SH-6) were used to block NF- $\kappa$ B and Akt/PKB

pathways respectively. NF- $\kappa$ B and Akt/PKB regulate the protein synthesis and the balance between pro- and anti-apoptotic cascades. The effect of the selective NF- $\kappa$ B and Akt/PKB inhibitors on DEX -induced recovery suggests that these pathways are important for synaptogenesis in the cochlea.

Supported by AFA Trygghörsäkringsbolaget, Tysta Skolan and Karolinska Institute

### **166 Laminin 211-Mediated FAK Activation as a Mechanism of Alport Related Strial Pathology in Mice**

**Dominic Cosgrove**<sup>1</sup>, Daniel Meehan<sup>1</sup>, Duane Delimont<sup>1</sup>, Marisa Zallocchi<sup>1</sup>, Linda Cheung<sup>1</sup>, Brianna Johnson<sup>1</sup>, Alexis Varvares<sup>2</sup>, Michael Anne Gratton<sup>2</sup>

<sup>1</sup>Boystown National Research Hospital, <sup>2</sup>Saint Louis University

Alport syndrome, which affects approximately 1 in 5000, is a disease caused by mutations in specific basement membrane type IV collagen genes. The syndrome is characterized by delayed onset and progressive glomerular dysfunction associated with progressive hearing loss. We have discovered that the initiation of glomerular pathology involves the deposition of an uncharacteristic Laminin (Laminin 211) in the glomerular basement membrane (GBM) which directly activates focal adhesion kinase (FAK) signaling. FAK activation leads to downstream activation of pro-inflammatory nuclear factor kappa B (NF $\kappa$ B) responsive genes in glomerular podocytes, which contribute to progressive GBM destruction and glomerulosclerosis. Inner ear pathology in Alport mice is associated with progressive thickening of the strial capillary basement membranes (SCBM) resulting in strial dysfunction and a drop in endocochlear potential culminating in elevated ABR thresholds. We surmised that the mechanism underlying strial dysfunction might be similar to that observed for glomeruli. Laminin 211 was indeed found to be expressed in Alport SCBMs, but not in strain-matched (129 Sv) wild type SCBMs. As observed in Alport glomeruli, the Laminin 211 in the stria was associated with localized activation of FAK (as observed by immunostaining for pFAK397). Strial marginal cells (but not intermediate or basal cells) cultured on Laminin 211 showed activation of NF $\kappa$ B as well as elevated expression of NF $\kappa$ B responsive genes MMP-9 and IL-6 relative to cells cultured on Laminin 521. Although preliminary, collectively these data suggest that the underlying molecular mechanism of strial pathology and glomerular pathology in Alport syndrome may be quite similar. Supported by R01 DC006442 and R01 DK055000.

### **167 Alport Mice Do Not Have Systemic Hypoxia**

**Krysta Gasser**<sup>1</sup>, Alexander Limjuco<sup>1</sup>, Tessa Varvares<sup>1</sup>, Michael Anne Gratton<sup>1</sup>, Flint Boettcher<sup>1</sup>

<sup>1</sup>Saint Louis University

Alport Syndrome is characterized by a mutation in one of the novel isoforms of Type IV collagen that results in glomerulosclerosis and a progressive sensorineural hearing loss. Thickened basement membranes

surrounding capillaries of the stria vascularis are the cause, at least in part, of the hearing loss. Thickened basement membranes in turn produce hypoxia in the cochlea (See Limjuco et al, ARO 2012). A series of studies was conducted to determine if mice modeling the autosomal recessive form of Alport Syndrome have whole-body or systemic hypoxia which would add to the cochlear-based hearing loss. In the first experiment, non-invasive measures of oxygen saturation, heart rate, and perfusion index were made using pulse oximetry. Although the average pulse oxygen saturation (SpO<sub>2</sub>) in the 9 wk old Alport mice was lower than that of the wild-type littermates, the difference was not significant. Moreover, the range of SpO<sub>2</sub> measures in the mutant mice was quite large. Immunohistochemistry was performed on brain sections prepared from these mice. Little to no immunoreactivity for hypoxia-inducible factor 1a (HIF-1a) was noted in the mutant mice and their wild-type littermates. Wild-type littermates exposed to a hypoxic atmosphere (8% O<sub>2</sub>, 4 Hr) showed decreased SpO<sub>2</sub> and reactivity for HIF-1a. A final study employed the auditory brainstem response (ABR) model of gap detection. The latencies to ABR waves 1-5 were compared for noise stimuli separated by a short silent period. As expected, the ABR peak latencies for waves 1-5 shifted for the second noise of a pair compared to the first. However, the latency shifts were similar for the 9 week old wild type and Alport mice. Collectively, these data suggest that Alport mice do not have systemic hypoxia and that the peripheral hearing loss in the Alport mice is not accompanied/compounded by a central auditory effect.

### **168 A Murine Model of Cytomegalovirus-Induced Sensorineural Hearing Loss and the Role of Persistent Cochlear Inflammation**

**Scott Schachte**<sup>1</sup>, Manohar Mutnal<sup>1</sup>, Mark Schleiss<sup>1</sup>, James Lokensgard<sup>1</sup>

<sup>1</sup>University of Minnesota

Congenital cytomegalovirus (CMV) infection is the leading cause of sensorineural hearing loss (SNHL) in children. During murine (M)CMV-induced encephalitis, the immune response controls viral dissemination and facilitates clearance from the brain. While the importance of CMV-induced SNHL has been described, the mechanisms surrounding its pathogenesis and the role of inflammatory responses remain unclear. This study presents a neonatal mouse model of profound SNHL in which MCMV preferentially infected both cochlear perilymphatic epithelial cells and spiral ganglion neurons. Surprisingly, MCMV infection induced cochlear hair cell loss by 21 days postinfection, despite a lack of direct hair cell infection. Flow cytometric, immunohistochemistry, and quantitative PCR analysis of MCMV-infected cochleae revealed a robust and chronic proinflammatory response, including an increase in macrophage reactive oxygen species production. These data support a pivotal role for inflammation during MCMV-induced SNHL.

## 169 Audiovestibular Features in Mice with the GJB2 P.V37I Mutation and Their Modulating Factors

Yin-Hung Lin<sup>1</sup>, Ying-Chang Lu<sup>1</sup>, Chen-Chi Wu<sup>1</sup>, Pei-Jer Chen<sup>2</sup>, Shu-Wha Lin<sup>3</sup>, Yi-Ning Su<sup>4</sup>, Chuan-Jen Hsu<sup>1</sup>

<sup>1</sup>Department of Otolaryngology, National Taiwan University Hospital, Taipei, Taiwan, <sup>2</sup>Graduate Institute of Clinical Medicine, National Taiwan University, Taipei, Taiwan, <sup>3</sup>Transgenic Mouse Models Core (TMMC), National Taiwan University, Taipei, Taiwan, <sup>4</sup>Graduate Institutes of Clinical Genomics, National Taiwan University, Taipei, Taiwan

The GJB2 p.V37I is a common mutation identified in East Asians with sensorineural hearing impairment (SNHI). Despite its clear association with mild-to-moderate SNHI, the pathogenic mechanisms of p.V37I remain elusive, as clinically many homozygous subjects reveal normal hearing. To elucidate its pathogenicity, we generated a knock-in mouse strain homozygous for the Gjb2 p.V37I mutation (i.e. Gjb2<sup>tm1Dontuh/tm1Dontuh</sup> mice). In the present study, we further characterized the audiovestibular phenotypes in this mutant strain, and investigated the gene expression profile in the cochlea of the mutant mice. Gjb2<sup>tm1Dontuh/tm1Dontuh</sup> mice at 4, 8 and 12 weeks were subjected to audiologic assessments using auditory brainstem response (ABR) and a battery of vestibular evaluations. Then we used RNA microarrays to examine differential gene expression between Gjb2<sup>tm1Dontuh/tm1Dontuh</sup> and Gjb2<sup>+/+</sup> mice by comparing inner ear RNA expression. Gjb2<sup>tm1Dontuh/tm1Dontuh</sup> showed elevated hearing thresholds as compared to wild type mice, whereas none of the homozygous mice revealed vestibular deficits. As to RNA expression, genes that presented a fold change higher than 2 were selected for further analysis. There were 111 genes showing significantly different expression between Gjb2<sup>tm1Dontuh/tm1Dontuh</sup> and Gjb2<sup>+/+</sup> mice, including 56 genes up-regulated and 55 genes down-regulated in Gjb2<sup>tm1Dontuh/tm1Dontuh</sup> mice. Based on their ontology and function, many genes with increased expression were related to transmembrane transport, whereas many genes with decreased expression were related to immune system development and bio-mineral formation. These preliminary results provide insight into potential interacting genes affected by the GJB2 p.V37I mutation, which may play a crucial role in modulating the phenotype. In addition, this study also provides a valuable screening tool for differential gene expression in transgenic mouse models.

## 170 Pathogenesis of Hearing Loss in a Mouse Model of Townes-Brock Syndrome

Joseph Rutledge<sup>1</sup>, Krysta Gasser<sup>1</sup>, Susan Kiefer<sup>1</sup>, Michael Rauchman<sup>1,2</sup>, Michael Anne Gratton<sup>1</sup>

<sup>1</sup>Saint Louis University, <sup>2</sup>Saint Louis Veterans Affairs Medical Center

Townes-Brocks Syndrome (TBS) is an autosomal dominant disease specifically associated with mutation of the SALL1 gene. The diagnosis is made based on the clinical triad of congenital defects: imperforate anus, dysplastic ears, and thumb malformations. There is also a

high association of sensorineural hearing loss (90%) and kidney failure (42%) in these patients.

A mutation in the allele, sall1-ΔZn<sup>2-10</sup>, reliably mimics the TBS symptoms in mice. Although the aberrant renal function of this mouse model has been assessed, there has been little investigation into the etiology and extent of hearing dysfunction. Our initial ABR studies of 5-month-old mice have demonstrated severe sensorineural hearing loss in sall1-ΔZn<sup>2-10</sup> heterozygotes, with a significantly greater loss when compared to age-matched littermates. In situ labeling of Sall1 expression in the otic vesicle was demonstrated as early as E10.5 and in the cochlea at E17.5, which corresponds to a critical time in cochlear and hair cell development. Further staining for sall1-ΔZn<sup>2-10</sup> in P18 cochlea reveals a well-circumscribed expression pattern in the spiral ganglion cells and fibers supplying the organ of Corti.

Light microscopy of the 5-month-old heterozygote cochleae reveals varying degrees of pathologic processes in the organ of Corti, with decreased numbers of outer hair cells and a greatly reduced density of spiral ganglion cells when compared to wild type littermates. Ultrastructural analyses of sall1-ΔZn<sup>2-10</sup> heterozygotes elucidated further structural defects in pillar cells, outer hair cells, and supporting cells in the organ of Corti. Any surviving outer hair cells in the heterozygote samples presented with flawed or absent stereocilia.

This study provides the first evidence of the pathogenesis of hearing loss that TBS patients suffer, and offers a new model for studying etiology and treatments for congenital hearing loss syndromes.

## 171 Expression of Ferlins in the Organ of Corti

Danny J. Soares<sup>1</sup>, Neeliyath A. Ramakrishnan<sup>1</sup>, Dennis G. Drescher<sup>1</sup>

<sup>1</sup>Wayne State University School of Medicine

The mammalian ferlin gene family encompasses a total of six different genes (FER1L1-FER1L6) that encode calcium binding proteins of approximately 2 kDa. Each ferlin protein comprises 4-7 sequential C2 domains and a C-terminal transmembrane domain. Ferlin proteins are thought to act as important modulators of calcium-dependent membrane fusion events in a range of tissues, including the inner hair cells of the cochlea. Of the products of six known mammalian ferlin genes, FER1L2 (otoferlin) has been implicated in DFNB9 deafness. Whereas otoferlin has been shown to be necessary for hair-cell neurosecretion, little is known about FER1L4 and FER1L6, which are even-numbered ferlin genes with sequences most homologous to that of FER1L2 (otoferlin). We hypothesized that FER1L4 and FER1L6 proteins may exist as functional components of the inner ear and possibly play a role in hereditary non-syndromic deafness. In the present study, we generated a cDNA library from the rat organ of Corti for use in PCR amplification. Gene-specific primers were synthesized for amplification of rat FER1L4 and FER1L6. Results revealed that FER1L4 was absent from the organ of Corti transcription library, while FER1L6 was present. After complete sequencing of

FER1L6, protein domain analysis was performed through PFAM® and SMART databases. Analysis showed that FER1L6 was similar in sequence to otoferlin, but lacking a C2A domain. FER1L6 also had a C2DE domain characteristic of the dysferlin (odd-numbered) gene family. C2 domain analysis and alignment of FER1L6 C2 domains was achieved through the use of EMBOSS, revealing complete preservation of calcium-binding residues in domains C2E and C2F. The results of this study point to the presence of actively transcribed FER1L6 within the rat organ of Corti, with well-conserved calcium binding residues in the distal C2 domain.

## **172** Hearing Loss in Xeroderma pigmentosum (XP) and Mechanism of Inner Ear Disorder

**Daisuke Yamashita**<sup>1</sup>, Takeshi Fujita<sup>1</sup>, Shingo Hasegawa<sup>1</sup>, Naoki Otsuki<sup>1</sup>, Ken-ichi Nibu<sup>1</sup>

<sup>1</sup>Kobe University Hospital

Xeroderma pigmentosum (XP) is rare disease to produce solar sensitiveness and skin cancer by photosensitivity for autosomal recessive inherited disease. A healing mechanism of the gene DNA (nucleotide) is affected by ultraviolet rays. There are eight cause genes of XP (seven and variant group of A - G with the genetic complementation), and a gene of all is identified. The cause gene of the A group in particular was identified in Japan in 1990, and it was named XPA gene. The cause gene is present on human chromosome 9, and it is thought with a gene of the protein about DNA repair mechanism. It is thought that there are patients with approximately 500 XP now in Japan. The incidence of the skin cancer is considered to be approximately 2,000 times of the healthy subject by a decrease of the DNA reparability by ultraviolet rays and therefore is forced to a severe ultraviolet ray blockades. Also, in addition to skin disease, various neurologic symptoms including an intellectual impairment and the movement disorder develop from progressive neuropathy and hearing impairment, and the medical treatment for the life is required. Though the cause genes are apparent, but it is conditions that the basic therapy is not yet established. About the hearing impairment, the clinical courses of the onset time and degree and progress of hearing loss are various. Therefore we have examined clinical picture in the hearing impairment of the XP patients whom we experienced this time. Also, effects of various kinds of antioxidant are expected by this disorder and contribution of the oxidative stress, but the detailed developmental mechanism and therapy are not yet established. Therefore we investigate the mechanisms of the inner ear disorder using the mouse which knocked out the DNA repair gene, by assessing hearing function and morphological changes in the cochlea.

## **173** Genotype and Phenotype Correlation in GJB2 Mutations (DFNB1) and Structural Analysis of Non-Inactivating Mutations

**Shujiro Minami**<sup>1</sup>, Kazunori Namba<sup>1</sup>, Hideki Mutai<sup>1</sup>, Tatsuo Matsunaga<sup>1</sup>

<sup>1</sup>National Tokyo Medical Center

[Introduction] Mutations in GJB2, encoding a gap junction protein Connexin-26 (Cx26), are the most common cause of non-syndromic autosomal recessive hearing impairment, ranging from mild to profound. The aim of this study was 1) to study genotype/phenotype correlations, 2) to predict alteration of the protein structures by homology modeling, for establishing the guideline for genetic counseling of DFNB1 in Japan. [Method] We analyzed 126 Japanese patients carrying biallelic GJB2 mutations, which was validated by direct sequencing. To obtain deeper understanding of the molecular pathology of the non-inactivating mutations of GJB2, three dimensional structures of the mutants of Cx26 channel were modeled using SWISS-MODEL with the crystal structure of Cx26 (PDB ID: 2ZW3\_A-F chain) as their template. [Result] A total of 16 pathological mutations were identified, which were subclassified as 8 inactivating such as 235delC, and 8 non-inactivating mutations such as R143W. We defined three genotype classes: biallelic inactivating (I/I; 92 persons [73%]), biallelic non-inactivating (NI/NI; 10 persons [8%]), and compound heterozygous inactivating/non-inactivating (I/NI; 24 persons [19%]). In the I/I class, 62% of persons had profound HI, 14% had severe HI, and 22% had moderate HI. In the I/NI class, 58% of persons had profound HI, 21% had severe HI, and 17% had moderate HI. More than 3 quarters (80%) of persons in the NI/NI class had only a moderate or mild degree of HI, and no person in this class had profound HI. R143W was speculated to disrupt oligomerization of the Cx26 subunits through depletion of electrostatic interaction between R143 and P87. [Conclusion] In this study of persons segregating GJB2-related deafness, we found inactivating mutations of GJB2 to be associated with a greater degree of hearing impairment than were non-inactivating mutations. We deduced the impairment mechanism of non-inactivating one with protein structures.

## **174** Cochlear Developmental Disorder Rather Than Hair Cell Loss Causes Congenital Deafness for Connexin26 (GJB2) Deficiency

**Chun Liang**<sup>1,2</sup>, Yan Zhu<sup>1</sup>, Liang Zong<sup>1</sup>, Guang-Jin Lu<sup>1,2</sup>, Hong-Bo Zhao<sup>1</sup>

<sup>1</sup>University of Kentucky Medical Center, USA, <sup>2</sup>Maternal and Children Health Care Hospital of Baoan, Shenzhen, P.R. of China

Connexin 26 (GJB2) mutations are the most common cause of hereditary congenital hearing loss and responsible for 70-80 % of nonsyndromic hearing loss in children. However, the deafness mechanism underlying this common nonsyndromic hearing loss still remains largely undetermined. It has been reported that knockout (KO) of Cx26 in the cochlea can induce deafness. The

cochlea has developmental disorders, severe hair cell loss, and spiral ganglion neuron degeneration. The deafness is considered resulting from hair cell loss or degeneration. In this study, through the fine examination of the deafness occurrence and cell degeneration development in Cx26 KO mice, we found that deafness is not resulted from hair cell loss and cell degeneration. The deafness in Cx26 KO mice was congenital. Auditory brainstem response (ABR) in Cx26 KO mice was not recordable after birth, prior to hair cell loss and spiral ganglion neuron degeneration, which significantly occurred afterward postnatal day 17 (P17). The hearing loss occurred at whole-frequency range. Distortion product otoacoustic emission (DPOAE) was also reduced but recordable before P17. In wild type (WT) mice, clear ABR was detectable at P14 and the ABR threshold reached at the matured level at P16. DPOAE was also recordable at this postnatal developmental stage. These data indicate that Cx26 deficiency induced congenital deafness is not resulted from hair cell loss. KO of Cx26 could induce cochlear development disorders, which may primarily cause hearing loss in Cx26 KO mice. Supported by DC05989

### **175** Reduced Expression of PHEX in the Ear and Neuronal Loss in the Spiral Ganglia of a Mouse Model of Endolymphatic Hydrops

Qing Zheng<sup>1</sup>, Maroun Semaan<sup>1</sup>, Fengchan Han<sup>1</sup>, Yuxi Zheng<sup>1</sup>, Heping Yu<sup>1</sup>, Cliff Megerian<sup>1</sup>

<sup>1</sup>Case Western Reserve University

Hypothesis: Reduced expression of PHEX in the ear causes progressive spiral ganglion neuron (SGN) loss in the *Phex*<sup>Hyp-Duk</sup> mutant mice. Background: The male mouse carrying the *Phex*<sup>Hyp-Duk</sup> gene, a mutant allele of the phosphate-regulating gene *Phex*, exhibits vestibular dysfunction and hearing loss. Histological analysis of the cochlea demonstrated endolymphatic hydrops (EH) by postnatal day (P) 21 and SGN loss by P90. The SGN loss occurred in a consistent topographic pattern with loss beginning at the cochlear apex. Methods: Spiral ganglion cell counts were conducted at P60, P90 and P120 in both control and mutant mice. RT-PCR and immunohistochemical analyses of *Phex* and activated caspases-3, -8 and -9 were performed on cochlear obtained from mutants and controls (+/Y). Terminal deoxynucleotidyl transferase-mediated dUTP-biotin nick-end labeling assay (TUNEL) was carried out on two affected mice and two controls. Results: Compared to mutant mice, the spiral ganglion cell counts in control mice were greater in the apical turn, and both the apical and the middle turn of the cochlea at P90 and P120, respectively ( $P < 0.01$ ). *Phex* gene and protein are expressed in the normal ears but are down-regulated in the mutant ears. *Phex*<sup>Hyp-Duk</sup> /Y mice expressed activated caspases -3, -8 and -9 in cochlear tissues as early as P14. Topographically, at P40 expression of activated caspase was mostly confined to the apex. By P90, the activity gradually decreased in the apex and increased in the basal turn of the cochlea. TUNEL staining demonstrated apoptosis induction at P90 in the apical and basal turns of the mutant cochleae. Conclusion: Immunohistochemical

studies and TUNEL staining demonstrated induction of apoptosis in the *Phex*<sup>Hyp-Duk</sup> male mouse. The pattern observed in this model is reminiscent of the SGN loss seen in human temporal bone specimens of EH. *Phex* mutation and its reduced expression are the original causes. This work was supported a grant from the American Otologic Society (CAM) and by the NIDCD grants R01DC007392, R01DC009246 (QYZ).

### **176** An Investigation Into the Role of Variation in the 12sRNA, TPMT and COMT Genes to the Incidence of Aminoglycoside Ototoxicity in Children with Cystic Fibrosis

Ghada Al-Malky<sup>1</sup>, Ranjan Suri<sup>2,3</sup>, Tony Sirimanna<sup>4</sup>, Sally Dawson<sup>1</sup>

<sup>1</sup>UCL, Ear Institute, London, UK, <sup>2</sup>Department of Paediatric Respiratory Medicine, Great Ormond Street Hospital, London, UK, <sup>3</sup>Portex Unit, Institute of Child Health, UCH, London, UK, <sup>4</sup>Department of Audiology & Audiological Medicine, Great Ormond Street Hospital, London, UK

Aminoglycoside ototoxicity is a complication that children with cystic fibrosis face as they need repeated courses of these antibiotics to control *pseudomonas aeruginosa* chest infections. Ototoxicity leads to progressive high-frequency sensorineural hearing loss which, when affecting speech frequencies, can lead to significant delay in speech and cognitive development and affect quality of life. Longer life expectancy in cystic fibrosis patients means a lifelong hearing deficit is an increasingly important issue for these patients.

Our earlier results using high-frequency audiometry and DPOAEs suggested a clear dichotomy in outcome in a cohort of 52 children with cystic fibrosis treated with aminoglycoside antibiotics. Twelve (23%) children were shown to have ototoxicity of which 11 had history of exposure to  $>10$  (mean $\pm$ SD:21 $\pm$ 11) courses. However, some children had remarkably good hearing despite a similar exposure to aminoglycoside antibiotics. We are therefore investigating a possible genetic contribution to ototoxicity susceptibility in these patients.

Previous work has established that susceptibility to aminoglycoside ototoxicity can have a genetic basis. Fischel-Ghodsian (1993) reported that the maternally inherited A1555G mutation in the mitochondrial 12S rRNA gene is associated with increased susceptibility to aminoglycoside ototoxicity and many reports followed to confirm this finding. More recently, Ross *et al.* (2009) identified genetic variants in SNPs of two drug-metabolism genes that were highly associated with cisplatin-ototoxicity. These are the genes encoding thiopurine S-methyltransferase (TPMT) and catechol O-methyltransferase (COMT). Cisplatin ototoxicity has been shown to follow a similar apoptotic cell death pathway and clinical presentation to aminoglycoside ototoxicity. The aim of this study is to assess the occurrence of these genetic mutations in children with cystic fibrosis and their correlation with ototoxicity.

DNA was extracted from blood or saliva samples and genotyping is being performed for:- the A1555G mutation

in 12sRNA, the rs12201199 variant in TPMT gene and the rs4646316 variant in COMT gene. The frequency of these mutations and an analysis of a possible contribution to aminoglycoside ototoxicity in these patients will be presented at the meeting.

### **177 Human Intraoperative Acoustically Evoked Intracochlear Potential Recordings from the Round Window Pre and Post Cochlear Implantation**

**Baishakhi Choudhury**<sup>1</sup>, Oliver F. Adunka<sup>1</sup>, Craig A. Buchman<sup>1</sup>, Shuman He<sup>1</sup>, Margaret Dillon<sup>1</sup>, Benjamin P. Wei<sup>1</sup>, Douglas C. Fitzpatrick<sup>1</sup>

<sup>1</sup>*University of North Carolina at Chapel Hill*

The indications for cochlear implantation have broadened to include patients with a substantial amount of functional hearing in low frequencies but that have poor speech recognition scores. If this low frequency residual hearing is preserved after cochlear implantation it can be combined with the electric stimulation from the implant, which can help improve hearing outcomes post-surgically. Currently surgeons have no knowledge of the status of residual hearing during cochlear implantation surgery. If hearing status could be monitored intraoperatively, feedback regarding damage or even potential damage could be useful for optimal electrode placement. Previous studies in gerbils with normal hearing and noise-induced hearing loss (NIHL) have shown that reductions in the acoustically evoked cochlear microphonic (CM) and, to a lesser extent, the compound action potential (CAP) are a sensitive measure of trauma to intracochlear structures (e.g., Choudhury et al., *Otol. and Neurotol.* 32:1370-1378, 2011). Based on these results, similar measures were taken from the round window of human cochlear implant patients pre and post implantation. Intraoperative CM response magnitudes to low frequency tone bursts pre-implantation correlated with pre-surgical audiogram thresholds at the same frequencies. In addition to the CM and CAP, a phase locked neural potential to low frequencies was also observed (the "neurophonic"). When residual hearing was present, changes in CM magnitude were detectable post implantation. These results indicate that changes in hair cell and neural potentials due to insertion effects can be detected intraoperatively during a cochlear implantation. Supported by NIDCD T32-DC005360.

### **178 Hemorrhage in the Endolymphatic Sac of Patients with Enlarged Vestibular Aqueduct (EVA)**

**Minbum Kim**<sup>1</sup>, Hee Nam Kim<sup>1,2</sup>, Jaeyoung Choi<sup>2</sup>

<sup>1</sup>*Hana ENT Hospital*, <sup>2</sup>*Yonsei University*

Objective: Most of the patients with enlarged vestibular aqueduct (EVA) experience sudden hearing deterioration, but the exact mechanism is unclear. We analyzed magnetic resonance (MR) images and the cellular components of endolymph obtained from the endolymphatic sac in patients with EVA, in order to demonstrate the cause of sudden hearing loss. Methods: A total of 25 patients (50 ears) with EVA, who had severe to

profound hearing loss, were included in this retrospective clinical study. MR examinations were performed by a 3.0-Tesla MR system using an 8-channel sensitivity-encoding head coil. We analyzed endolymphatic fluid harvested from the endolymphatic sac during cochlear implantations in four patients. Results: The area of low signal intensity in the endolymphatic sac was observed on T2-weighted MR images for 15 of 50 ears. This area was observed more frequently in patients who experienced recent sudden hearing loss (10/12, 83%) than those with stable hearing (5/38, 13%) (Fisher's exact test,  $p < 0.001$ ). In addition, this area showed high signal intensity on fluid attenuated inversion recovery images. Cytologic analysis of the aspirated endolymph from the endolymphatic sac in the patients with this area revealed many erythrocytes. Conclusion: Our updated data suggests that hemorrhage in the endolymphatic sac could be a cause of sudden hearing deterioration in patients with EVA.

### **179 Histopathological Human Temporal Bone Study of Mucopolysaccharidosis Type I / Hurler Syndrome**

**Shin Kariya**<sup>1,2</sup>, Sebahattin Cureoglu<sup>2</sup>, Patricia Schachern<sup>2</sup>, Kazunori Nishizaki<sup>1</sup>, Michael Paparella<sup>3</sup>

<sup>1</sup>*Okayama University*, <sup>2</sup>*University of Minnesota*, <sup>3</sup>*Paparella Ear Head & Neck Institute*

Mucopolysaccharidosis type I / Hurler syndrome is an autosomal recessive disease caused by a deficiency of  $\alpha$ -L-iduronidase activity. Recurrent middle ear infections and hearing loss are common complications in Hurler syndrome. Although sensorineural and conductive components occur, the mechanism of sensorineural hearing loss has not been determined. The purpose of this study is to evaluate the quantitative inner ear histopathology of the temporal bones of patients with Hurler syndrome.

Eleven temporal bones from 6 patients with Hurler syndrome were examined. Age-matched normal control samples consisted of 14 temporal bones from 7 cases. Temporal bones were serially sectioned in the horizontal plane and stained with hematoxylin and eosin. The number of spiral ganglion cells, loss of cochlear hair cells, area of stria vascularis, and cell density of spiral ligament were evaluated by light microscopy.

There was no significant difference between Hurler syndrome and normal controls in the number of spiral ganglion cells, area of stria vascularis, or cell density of spiral ligament. The number of cochlear hair cells in Hurler syndrome was significantly decreased compared with normal controls.

Auditory pathophysiology in the central nerve system in Hurler syndrome remains unknown, however, decreased cochlear hair cells may be one of the important factors for the sensorineural component of hearing loss.

### **180 Prestin in Membranes Is a Tetramer**

**Richard Hallworth**<sup>1</sup>, Michael Nichols<sup>1</sup>

<sup>1</sup>*Creighton University*

The membrane motor protein prestin has been thought to function as an oligomer, but its stoichiometry is unknown.

Evidence from Western blots and an electron density mapping study of purified prestin has variously suggested dimeric and tetrameric configurations. However, both methods require removal of prestin from its lipid environment, which challenges interpretation of the results. Prestin expressed and synthesized in Human Embryonic Kidney (HEK) cells has been shown to be functional, by non-linear capacitance and mechanics measures. Our approach to prestin stoichiometry has been to isolate single prestin molecules, each tagged with a molecule of enhanced Green Fluorescent Protein (eGFP), in membrane fragments of HEK cells. We exposed isolated prestin-eGFP molecules to continuous excitation and detected their fluorescence using a high numerical aperture objective and a high quantum efficiency CCD camera. The fluorescence of each molecule decreased monotonically in quantized steps until it reached background levels. The average number of steps to background was typically in the range 2.5 to 3.0. We hypothesized that the observed single molecules of prestin were tetramers, and that some eGFP molecules did not fluoresce, either because they did not fold correctly or because they were inadvertently bleached in the process of setting up the observation. Consistent with this hypothesis, we performed similar studies using an eGFP-coupled construct of the human Cyclic Nucleotide Gated ion channel, isoform A3, which is an obligate tetramer, and found similar results. Our evidence suggests, therefore, that prestin in HEK cells exists as tetramers. Supported by State of Nebraska LB692.

### **181 Homo- And Hetero-Oligomerization in the Slc26a Family**

Benjamin Currall<sup>1</sup>, Heather Jensen-Smith<sup>1</sup>, Richard Hallworth<sup>1</sup>

<sup>1</sup>Creighton University

The motor-protein prestin is thought to be a homo-oligomer, but it is unclear how prestin-prestin oligomerization occurs or if it is necessary for function. We first used the acceptor-photobleach variant of fluorescence-lifetime (FLIM) based Förster resonance energy transfer (FRET) analysis to demonstrate that homo-oligomerization is not only common to mammalian and non-mammalian prestin orthologs, but also occurs in widely divergent members of the Slc26a family of proteins. We then tested the hypothesis that a similar protein-protein interaction motif was conserved throughout the Slc26a family by measuring FRET between different Slc26a family molecules. Our results show that hetero-oligomerization can occur between family members. These results suggest that homo-oligomerization is a conserved property of the Slc26a family and that a common protein-protein interaction motif exists.

Supported by P20 RR16469 from the National Center for Research Resources (NCRR).

### **182 Microdomains Shift and Rotate in the Plasma Membrane of Cochlear Outer Hair Cells**

Rei Kitani<sup>1</sup>, Federico Kalinec<sup>1</sup>

<sup>1</sup>House Research Institute

Except at its basal region, the lateral plasma membrane of cochlear outer hair cells (OHCs) is literally packed with motor and associated proteins organized in microdomains. Membrane microdomains are connected by hundreds of 25-nm long “pillars” to similar cytoskeletal microdomains composed by long, parallel actin filaments cross-linked by shorter spectrin tetramers. Membrane potential-dependent conformational changes in motor proteins (prestins) result in reversible changes of cell length following cycle-by-cycle electrical stimulation. We labeled the lateral surface of isolated guinea pig OHCs with polystyrene microspheres ( $\varphi=0.5 \mu\text{m}$ ) and, using 1,000 fps high-resolution video recording, investigated their movement simultaneously at the apical, middle and basal region of cells stimulated with a 50 Hz external alternating electrical field. Under electrical stimulation, microspheres attached to non-motile cells or the basal region of OHCs didn't move, whereas those at the middle and apical regions of the OHCs' lateral wall showed robust back and forth displacements. During stimulation the directions of microspheres' trajectories changed from random to parallel to the electrical field with angular speeds of up to 6 rad/s, and were back to random after 5 min without stimulation. Microspheres responses were affected by changes in plasma membrane cholesterol levels and cytoskeleton integrity as well as inhibitors of OHC motor response. We concluded that membrane microdomains are able to shift and rotate in the plane of the lateral plasma membrane of cochlear OHCs, and membrane lipid composition as well as the membrane skeleton regulates their dynamics.

### **183 Voltage Dependent Conformational States of Prestin Measured by FLIM-FRET Techniques**

Chance Mooney<sup>1</sup>, Robert Raphael<sup>1</sup>

<sup>1</sup>Rice University

The transmembrane protein prestin forms an integral part of the mammalian sense of hearing by providing the driving force for the electromotility of the outer hair cell. This provides the cochlea with an ability to amplify mechanical vibrations, allowing for a high degree of sensitivity and selectivity in auditory transduction. This phenomenon, driven by changes in the transmembrane potential, is thought to be the result of conformational changes in self-associating prestin oligomers. We have previously utilized Förster resonance energy transfer (FRET), by acceptor photobleach methods, to detect the changes in these conformational states in response to controlled voltage stimuli. While these methods reported positive results, the standard deviation of the FRET efficiency was not sufficient for determining nanoscale changes in prestin organization. Here we expand upon this work by utilizing fluorescence lifetime imaging (FLIM) detected by time correlated single photon counting

(TCSPC), the most accurate FRET measurement technique available. FLIM techniques measure the characteristic fluorescence decay profiles of reporters; changes in these profiles can be caused by quenching processes such as FRET activity. Human embryonic kidney cells are used to host prestin molecules that are genetically encoded with either teal fluorescent protein (TFP) or the yellow fluorescent protein variant citrine. Individual cells are then voltage-clamped and the intermolecular distance between TFP and citrine is probed via FLIM-FRET methods. This has revealed large changes in detected FRET efficiencies between hyperpolarized cells (~42% efficiency) and depolarized cells (~13% efficiency), implying significant voltage-dependent changes in prestin conformation.

### **184 Non-Steroidal Anti-Inflammatory Agents Alter Prestin Function**

Guillaume Duret<sup>1</sup>, Robert Raphael<sup>1</sup>

<sup>1</sup>Rice University

Prestin (SLC26A5) is a motor protein essential for the electromotility of the outer hair-cells (OHC) and the amplification of sound in the cochlea. Prestin activity can be studied in cell lines that express prestin by measuring the nonlinear capacitance (NLC) using electrophysiological methods. Prestin is a mechano-sensitive protein and prestin function is altered by reagents known to change membrane mechanical properties. The non-steroidal anti-inflammatory drug (NSAID) salicylate has been shown to inhibit the NLC and the electromotility of OHC and prestin-expressing HEK cells. It is thought to compete with anions such as chloride for the anion-binding site on prestin. Other NSAIDs such as ibuprofen, naproxen, piroxicam or diflusalin can trigger side effects related to hearing and even cause tinnitus by an unknown mechanism. Here, we investigate a possible mechanism for these adverse reactions by examining the effects of these drugs on the function of prestin. The prestin-associated NLC is monitored by whole-cell as well as inside-out patches from HEK cells expressing prestin, and recorded before and after the perfusion of NSAIDs. This allows a cell-by-cell comparison of the NLC parameters in the presence and absence of the tested molecule. Ibuprofen and naproxen both showed an effect on the half-maximum voltage ( $V_{1/2}$ ) and the charge density parameters of the NLC. The effect of ibuprofen was particularly pronounced, shifting  $V_{1/2}$  from -70 mV to -52 mV and increasing the maximal charge movement by 30%. Further studies with piroxicam and diflusalin will contribute to our understanding of whether NSAIDs act through alteration of the mechanical properties of the membrane or specifically interfere with prestin function.

### **185 The Chloride-Channel Inhibitor Anthracene-9-Carboxylic Acid Directly Interacting with the Motor Protein Prestin**

Csaba Harasztosi<sup>1</sup>, Anthony W. Gummer<sup>1</sup>

<sup>1</sup>University Tübingen

Anthracene-9-carboxylic acid (9AC) is known as a voltage-gated chloride-channel blocker that also reduces the electrically induced motility of the organ of Corti (Nowotny & Gummer, 2006; Scherer & Gummer, 2004). Previous reports about the axial stiffness of isolated outer hair cells (OHCs; Eckrich et al., 2008 ARO, #517) and nonlinear capacitance (NLC) of OHCs (Harasztosi & Gummer, 2010 ARO, #584) indicate that 9AC directly acts on OHCs.

To decide whether 9AC is directly interacting with prestin, the cytoskeleton or its effect is mediated by chloride channels associated with prestin (Homma et al., 2010), we measured NLC as a signature of motor activity in OHCs isolated from the guinea-pig cochlea and in prestin-transfected human embryonic kidney 293 (HEK293) cells. Data were fitted with the sum of a voltage independent linear component, the first derivative of the two-state Boltzmann function and a sigmoidal function (Santos-Sacchi & Navarrete, 2002).

Extracellular application of 500  $\mu$ M 9AC significantly and reversibly reduced the  $Q_{max}$  parameter in both OHCs and HEK293 cells by  $38 \pm 9 \%$  and  $44 \pm 15 \%$ , respectively. The presence of 500  $\mu$ M 9AC in the intracellular solution did not influence the blocking effect of the extracellular applied drug. Reduction of the chloride concentration in the extracellular and intracellular solutions to 5 mM by replacing chloride with gluconate caused a negative  $K_d$  shift of 0.9 mM of the dose-response curve of the extracellular applied drug.

Reduction of the NLC of both OHCs and prestin transfected HEK293 cells by 9AC suggests that 9AC directly interacts with the motor complex. The ineffectiveness of intracellular applied 9AC suggests that 9AC has probably more extracellular accessibility to prestin. Taken together, the intracellular-chloride sensitivity of the extracellular applied 9AC implies that although both chloride and 9AC change the conformation of the motor protein, they probably act at different binding sites.

### **186 Fluoride Alters Prestin-Associated Charge Movement and Membrane Curvature**

Alex Sweeney<sup>1</sup>, Christian Corbitt<sup>1</sup>, Brenda Farrell<sup>1</sup>, Vera Moiseenkova-Bell<sup>2</sup>, Daniela Burchhardt<sup>1</sup>, Ramya Srinivasan<sup>1</sup>, Amy Manzo<sup>3</sup>, Theodore Wensel<sup>1</sup>, Fred Pereira<sup>1</sup>, William Brownell<sup>1</sup>

<sup>1</sup>Baylor College of Medicine, <sup>2</sup>Case Western Reserve University, <sup>3</sup>Wright State University School of Medicine

Prestin facilitates outer hair cell (OHC) electromotility through voltage-gated conformation changes and the movement of anions, namely chloride, within the cell membrane. This displacement current exhibits a bell-shaped capacitance. Additional observations suggest that both the voltage at which the peak capacitance occurs and the maximum charge movement are modified by different anionic species within the cytoplasm. We specifically examined fluoride's effect on charge movement with

whole-cell patch clamp in a guinea pig model. First, OHCs were harvested from a guinea pig temporal bone preparation and bathed in extracellular fluoride. Subsequently, intracellular fluoride was introduced through a micropipette following the formation of the whole-cell configuration, and the membrane capacitance was measured in response to a voltage ramp. In the presence of fluoride, OHCs exhibit a depolarized voltage at peak capacitance ( $1 \pm 14$  mV) and similar charge density ( $0.08 \pm 0.04$  pC/pF) relative to what is observed in the presence of chloride ( $-58 \pm 25$  mV,  $0.13 \pm 0.01$  pC/pF, respectively). Separately, to examine the effects of fluoride on the structure of a model lipid membrane, unilamellar lipid vesicles were created in solutions containing different anions and their size (curvature) measured with electron microscopy. We found that fluoride produces a significant decrease in size and, correspondingly, a relative increase in membrane curvature. Given fluoride's observed ability to alter membrane curvature in unilamellar lipid vesicles, it is possible that it changes the curvature of the lateral wall membrane and depolarizes the maximum voltage where charge movement occurs without affecting the charge density. The depolarizing voltage shift of prestin-associated charge movement and the increase of membrane curvature resemble the effect of removing cholesterol from the cell membrane. Supported by NIH/R01 DC00354 & DC02775.

### **187 Chloride Flux in Prestin-Expressing Cells**

**Sheng Zhong**<sup>1</sup>, Shumin Bian<sup>1,2</sup>, Dhasakumar Navaratnam<sup>2,3</sup>, Joseph Santos-Sacchi<sup>1,4</sup>  
<sup>1</sup>*Surgery (Otolaryngology), Yale University School of Medicine*, <sup>2</sup>*Neurobiology, Yale University School of Medicine*, <sup>3</sup>*Neurology, Yale University School of Medicine*, <sup>4</sup>*Cellular & Molecular Physiology, Yale University School of Medicine*

In prestin-expressing cells, intracellular Cl<sup>-</sup> ([Cl<sup>-</sup>]<sub>i</sub>) flux plays a preeminent role in promoting prestin activity, especially since the resulting V<sub>n</sub> shift in prestin's state-probability function (inferred from nonlinear capacitance - NLC) along the V<sub>m</sub> axis will effect a motile response. For example, with perforated patch clamp and local perfusion, changing extracellular Cl<sup>-</sup> concentration from 1 mM to 140 mM using prestin's NLC as a measure of intracellular Cl<sup>-</sup> indicates a several mM increase in intracellular Cl<sup>-</sup> concentration. Nevertheless, the mechanism underlying Cl<sup>-</sup> flux in prestin-expressing cells is not clear.

To better define Cl<sup>-</sup> flux, the CFP-YFP-based ratiometric Cl<sup>-</sup> indicator (Cl-sensor, *J. Neurosci. Meth.*, 2008, 170, 67) was modified to reduce pH sensitivity by shifting the pK<sub>a</sub> away from the physiological pH range. Using excitation ratiometric imaging of fluorescence, [Cl<sup>-</sup>]<sub>i</sub> was measured in either induced- or non-induced prestin-expressing HEK cell-lines transfected with our new Cl-sensor construct. Upon changing local extracellular perfusion from 0.2 mM to 140 mM Cl<sup>-</sup> buffer, fluorescence measures indicate a significant difference between induced- and non-induced prestin cell-lines.

We also evaluated [Cl<sup>-</sup>]<sub>i</sub> flux using a Cl-sensor fusion product of prestin at the C-terminal to better gauge flux near prestin's intracellular binding site. Comparison of [Cl<sup>-</sup>]<sub>i</sub> flux in HEK-293T cells transfected with a normal prestin-Cl-sensor or a prestin construct with a C-terminal deletion that eliminated NLC (P709-Cl-sensor) showed no statistical difference in flux. These data suggest that prestin's NLC is separable from Cl<sup>-</sup> movement induced by prestin, as we previously suggested (Bai et al., *Biophys. J.*, 2009, 96, 3179). Further experiments are underway, including voltage dependence of flux by simultaneously monitoring fluorescence ratio signals and NLC using perforated patch.

(Supported by NIDCD DC00273 to JSS and NIDCD DC 008130 to JSS and DN)

### **188 Purification of Prestin for Structural Studies: Preliminary Phase**

**Alberto Rivetta**<sup>1</sup>, Yufeng Zhou<sup>1</sup>, Dhasakumar Navaratnam<sup>2,3</sup>, Clifford Slayman<sup>1</sup>, Joseph Santos-Sacchi<sup>1,3</sup>  
<sup>1</sup>*Department of Cellular and Molecular Physiology*, <sup>2</sup>*Neurology*, <sup>3</sup>*Surgery, Yale University School of Medicine*

Prestin is the molecular motor responsible for the motility of outer hair cells (OHCs) in the organ of Corti. The molecular mechanism of Prestin's action is still unknown, although a general hypothesis is that membrane voltage changes prompt intra-Prestin charge movements, producing conformational changes that transmit to the OHC lateral membrane. Obviously, a high-resolution structure for Prestin would help address the molecular basis for motion in this important membrane protein, and with this aim, we began trials to purify the protein in large amounts and in monodispersity; both features are prerequisites for crystallization. Insect cells were used to express gerbil Prestin, and also to express human SLC26A6 (A6) as a control. [A6 is a non-electromotile membrane protein which shares 40% identity with Prestin]. Both genes were engineered with a TEV-GFP-8xhis tag at the C-terminus. Cell membranes were solubilized with foscholine 14, a phospholipid-like detergent, and both proteins were partially purified by affinity chromatography. Yields were ~0.5 mg of Prestin per liter of culture ( $2 \times 10^6$  cells/ml), and ~2 mg of A6. The partially purified proteins were separated by size exclusion chromatography. Approximately half of the Prestin eluted at a retention volume indicating aggregation, and the other half at a retention volume indicating the molecular mass of a dimer. A6 protein eluted mainly at the dimer retention volume, in a nearly symmetric peak. These results demonstrate that A6 can remain monodisperse in the presence of foscholine 14, but that Prestin is less stable. We are now trying to improve Prestin's stability by purifying it in the presence of salicylate, a functional inhibitor of Prestin. We are also exploring A6 monodispersity, versus susceptibility to aggregation, in other detergents and as a function of protein concentration and storage time.

(Supported by NIH 00273 to JSS and DC 008130 to DN and JSS)

### **189 Simultaneous Real Time Monitoring of Prestin Insertion Into the Plasma Membrane by NLC and Fluorescence**

Shumin Bian<sup>1</sup>, Dhasakumar Navaratnam<sup>2,3</sup>, Joseph Santos-Sacchi<sup>1,4</sup>

<sup>1</sup>Yale School of Medicine, Department of Surgery-Otolaryngology, <sup>2</sup>Yale School of Medicine, Department of Neurology, <sup>3</sup>Yale School of Medicine, Department of Neurobiology, <sup>4</sup>Yale School of Medicine, Department of Cellular and Molecular Physiology

We recently developed a tetracycline-inducible HEK cell line that expresses prestin at levels far above that obtained with transient transfection. Because of the greater signal to noise ratio we were able to observe recapitulation of events occurring during the development OHC electromotility (Abe et al., 2007), showing an early rise in prestin's nonlinear charge density ( $Q_{max}$ ) and a shift in prestin's voltage operating point ( $V_h$ ) to depolarized levels. The cell line also enabled us to observe developmental characteristics that were impossible to measure in developing OHCs, including an abrupt change in the valance (z) of nonlinear charge, and the development of a prestin associated leakage current. We have begun to analyze in real-time the insertion of prestin into the membrane by synchronizing bolus delivery of prestin from the Golgi apparatus, using real time monitoring of membrane capacitance coupled with temperature jump techniques. Additionally, we monitor prestin delivery to the membrane using fluorescence observation of YFP tagged prestin. This approach provides a powerful means to understand not only membrane trafficking of prestin, but also subsequent events following its insertion. (Supported by NIH NIDCD DC000273 to JSS DC008130 to JSS and DN)

### **190 Lizard and Frog Prestin: Evolutionary Insight Into Functional Changes**

Jason Pecka<sup>1</sup>, Jie Tang<sup>1</sup>, Kirk Beisel<sup>1</sup>, David He<sup>1</sup>

<sup>1</sup>Creighton University

Mammalian prestin (SLC26A5) is unique among SLC26A5 orthologs and SLC26A paralogs in its motor properties. Prestin functions in mammalian cochlear outer hair cells with a unique capability to perform direct, rapid, reciprocal electromechanical conversion. During evolution, the ion transport capability, typical of SLC26A members, was replaced by an innovation that is unique to the therian OHCs with a voltage dependent motility. All therian species, including monotremes and marsupials, appear to have derived motility in SLC26A5 peptides. Both amphibian and reptilian lineages represent phylogenetic branches in the evolution of tetrapods (~375 million years ago (MYA) and subsequent amniotes (~320 MYA)). We examined the motor and transport functions of lizard (*Anole carolinensis*) and frog (*Xenopus tropicalis*) prestin to characterize the progression of prestin from a transporter into a motor protein. Their heterogenic expression, membrane-targeting, nonlinear capacitance (NLC), transporter capabilities and membrane movement were examined using transfected HEK 293 cells. Our data showed transporter capabilities similar to chicken prestin;

whereas, the NLC appeared comparable to that of platypus. The ability of lizard and frog prestins to facilitate membrane movement is currently being assessed. These data will provide insights into the acquisition of unique electrophysiological properties in observed in therian prestin.

### **191 A Computational Study on the Elastic Propagating Wave of the Basilar Membrane Agitated by the Outer Hair Cell Motility**

Jong-Hoon Nam<sup>1</sup>

<sup>1</sup>University of Rochester

Acoustic stimuli delivered at the basal end of the cochlear coil create the traveling wave of the basilar membrane (BM) that propagates toward the apex. In response to the vibrating BM, the outer hair cells (OHCs) generate force to amplify the BM vibration. We created a fully deformable 3-D finite element model of the organ of Corti (OC) that faithfully represents the complicated OC geometrical structures (Nam & Fettiplace, 2010). To further investigate the dynamic interaction between the OHCs and their surrounding tissues, we newly added the kinetics of the mechano-transduction channel, K<sup>+</sup> current through membrane and somatic motility. We investigated if the OHCs' interaction with the tectorial membrane (TM) and the BM creates any characteristic vibrating pattern in the OC, the TM or the BM. With newly reported OHC membrane properties (Johnson, Beurg et al., 2011), the OHC somatic force was so large that the cochlear partition became easily unstable. The instability originating from the transduction channel (Nam & Fettiplace, 2008) was relayed by the OHC membrane motor to vibrate the TM and the BM. Interestingly, the vibration of the BM due to the OHC instability propagated from the base toward the apex. The propagating oscillation was observed only when 1) the longitudinal stiffness gradient of the BM is similar to reported values, and 2) when OHC was tilted. The propagating direction is determined by the direction of the BM stiffness gradient not the direction of the OHC tilt. The propagating speed and the wave length were dependent on the stiffness of the BM and the longitudinal coupling strength of the BM. No fluid dynamics was incorporated with the computer model. Therefore, our observed propagating wave of the BM is different from the fluid-induced traveling wave. However, the speed and the wave length (7 m/s and 190  $\mu$ m at 18 kHz location) of our observed elastic propagating wave are comparable to the fluid-induced traveling wave.

### **192 Does Prestin Directly Bind to Cholesterol?**

Chongwen Duan<sup>1</sup>, Kazuaki Homma<sup>1</sup>, Robert Magin<sup>1</sup>, Jessie Chen<sup>1</sup>, Peter Dallos<sup>1</sup>, Jing Zheng<sup>1</sup>

<sup>1</sup>Northwestern University

Prestin is the motor protein of outer hair cells (OHCs), responsible for OHCs' electromotility. It is known that the basolateral membrane of OHCs has exceptionally low cholesterol content in comparison to other cells. Manipulating cholesterol in the plasma membrane can significantly change prestin's function as evidenced by

nonlinear capacitance (NLC) measurements. However, it is not known whether the effects of cholesterol on prestin's function are due to its direct effect on prestin itself, and/or an influence on the properties of the lipid surrounding the prestin molecules. Therefore, we have investigated potential direct interaction between prestin and cholesterol. Several prestin mutants, designed to identify potential cholesterol binding sites, were created. The properties of these modified molecules were characterized, including their membrane targeting capability and NLC. Preliminary data suggest that prestin can bind to cholesterol directly. We are now identifying the cholesterol binding site(s) of prestin. (Work supported by NIH Grants DC010633 and Northwestern URG 75SUMMER111094).

### **193 Transmembrane Potential Distribution Along Isolated Outer Hair Cells to External Electrical Field – Theory and Experiment**

**Sripriya Ramamoorthy<sup>1</sup>, Teresa Wilson<sup>1</sup>, Tao Wu<sup>1</sup>, Alfred L. Nuttall<sup>1</sup>**

<sup>1</sup>*Oregon Health & Science University*

The sensory outer hair cells (OHC) in the inner ear play an important role in active amplification of sound-induced vibrations by virtue of their somatic motility. The OHC forms a crucial part of the path of flow of transduction-current generated by deflection of the hair bundles at their apex. They are also electrically excited during current injection experiments in animals as well as in cochlear implants. The distribution of transmembrane potential along the OHC is therefore important for auditory research. We measure the transmembrane potential induced along the perimeter of isolated OHCs from guinea pigs in response to electrical field at various orientations relative to the OHC axis. The electrical field is set up using a wire-electrode pair. Percentage changes in the fluorescence intensity of the potentiometric dye loading the cell membrane is used to determine the changes in transmembrane potential. The potentiometric sensitivity of the dye is calibrated by applying known voltage-steps (hyper-polarizing as well as de-polarizing) to cells under simultaneous whole cell patch-clamp. The effect of the distribution of conductance along the OHC perimeter, such as the larger conductance at the OHC base vs. apex, on the induced transmembrane potential is investigated theoretically and experimentally. The implications of this study for cochlear mechanics are discussed. Research supported by NIH grant 1R01DC000141 (ALN).

### **194 Cochlear Melanin Does Not Affect the Magnitude of Linear and Non-Linear Capacitance of Outer Hair Cells (OHC) in a Guinea Pig Model**

**Christian Corbitt<sup>1</sup>, Rishi Kumar<sup>1</sup>, William Brownell<sup>1</sup>, Brenda Farrell<sup>1</sup>**

<sup>1</sup>*Bobby R. Alford Department of Otolaryngology/Head and Neck Surgery, Baylor College of Medicine*

Longitudinal studies show that melanin plays a role in protecting the hearing of humans. Hearing thresholds are lowered with increasing deposition of melanin in aged and

environmentally matched populations. Studies of melanin's influence on hearing in animals following noise induced trauma suggest these changes include an effect on OHCs. One study shows the cochlear microphonic of albinos exhibits higher permanent threshold shifts following sustained noise trauma when compared with pigmented animals. Our goal is to establish if the non-linear electrical properties of the OHCs found prior to noise induced trauma are influenced by the presence of melanin in the cochlea at the cellular level. We study the effect of melanin on the OHC with the recognizable phenotype of pigmentation in guinea pigs (i.e., tricolors, tri). We use whole cell voltage clamp and measure the capacitance of isolated OHCs across the cochlea of tricolors and compare the results with age-matched albinos, (alb). Our data show no statistical significant difference between the two groups. The voltage at peak capacitance and charge density for tri (# 40) and alb (# 64) are  $-80 \pm 26$  and  $-58 \pm 25$  mV, and  $0.0011 \pm 0.0002$  and  $0.0013 \pm 0.001$  pC/ $\mu\text{m}^2$ . The linear characteristics of the membrane are also similar. The specific linear capacitance is  $0.008 \pm 0.001$  (alb) and  $0.0090 \pm 0.001$  pF/ $\mu\text{m}^2$ (tri) and the electrical size of the non-lateral wall regions including the cuticular plate are:  $5.0 \pm 1.3$  (tri) and  $6.1 \pm 0.5$  pF (alb) and  $2.33$  (tri) versus  $2.36$  pF (alb). Although a larger tricolor data set is needed to verify our findings, the data currently suggests cochlear melanin, evident by pigmentation in the spiral ligament, does not affect the magnitude of the non-linear or linear capacitance of OHCs across the guinea pig cochlea prior to noise trauma. This suggests OHCs from albino guinea pigs not exposed to noise trauma are a suitable model for OHCs from pigmented animals. Supported by NIH RO1DC00354.

### **195 Sex Affects the Robustness of Outer Hair Cell (OHC) Tonotopic Relationships**

**Federica Farinelli<sup>1</sup>, Christian Corbitt<sup>1</sup>, William Brownell<sup>1</sup>, Brenda Farrell<sup>1</sup>**

<sup>1</sup>*Baylor College of Medicine*

Electrical characteristics of the functional regions (e.g., lateral wall, cuticular plate) of the OHC are obtained from the relationships among the surface area of the membrane, the magnitude of the linear and non-linear capacitance and the total non-linear charge, where the size and capacitance are determined from morphometric and admittance measurements of isolated OHCs under voltage clamp at a controlled pressure ( $2 \pm 1$  mm Hg). Surprisingly, the correlation coefficients of the relationships improve, and the p-values of the slopes, intercepts and roots of the relationships become more significant when data from female guinea pigs are removed from the analysis. The improved robustness of the relationships is not explained by weight of the animals. Because the cochlea possesses estrogen receptors we suggest the ovarian cycle influences the membrane properties of OHCs. We use the relationships compiled with data obtained from male guinea pigs (# 40) to uncover the electrical features. Specifically, the size of the non-lateral wall regions is obtained from the exponential relation between linear capacitance and the total charge ( $6.4 \pm 0.6$

pF). The size of the cuticular plate ( $1.7 \pm 1.0$  pF) is uncovered from the relationship between the linear capacitance and the surface area of the membrane. We find the specific linear capacitance of the lateral wall ( $0.0093 \pm 0.0005$ , pF/ $\mu\text{m}^2$ ) and the peak specific capacitance ( $0.0095 \pm 0.001$  pF/ $\mu\text{m}^2$ ) do not differ significantly across the cochlea. We find the total charge increases linearly with the size of the lateral wall (slope:  $0.0015 \pm 0.0001$  pC/ $\mu\text{m}^2$ ) implying the charge density is constant. This relationship exhibits a non-zero intercept ( $0.88 \pm 0.2$  pC) suggesting there is a region in the lateral wall where the functional charge density is greater than the mean. This approach provides the first experimental evidence albeit subtle for sex differences at the cellular level within the cochlea. Supported by NIH RO1DC00354.

### **196 Cochlear Nonlinearity: Matching the Inner Hair Cell Dynamic Range to the Natural World**

**David Mountain**<sup>1,2</sup>

<sup>1</sup>*Boston University Hearing Research Center*, <sup>2</sup>*Boston University Dept. of Biomedical Engineering*

The receptor-current noise resulting random opening and closing of transduction channels in inner hair cells may be the fundamental constraint on several aspects of auditory performance. A two-state Boltzmann model for the transduction channels predicts that the ratio of the maximum receptor current to the rms value of the noise is only 26 dB. This is a surprisingly small value when we consider that the ratio of the loudest sounds in nature to the weakest sound that we can detect is on the order of 100 dB. I propose that two compressive nonlinearities, one due to the cochlear amplifier and the other due to the nonlinearity in inner hair cell transduction have co-evolved to fit the dynamic range of the natural world to the dynamic range of the inner hair cell.

In this context, modeling results as well as analysis of published experimental data will be presented that suggest that the function of the medial efferent reflex is to convert the sensory organ from a system that is optimized for very low sound levels to one optimized for wide dynamic range. In particular, the medial efferent reflex decreases the cochlear amplifier gain by just the right amount so that the nonlinearity in the basilar membrane response lines up perfectly with the inner hair cell nonlinear transduction process to produce a hair cell receptor potential that is proportional to the logarithm of the sound pressure level. This logarithmic compression is the optimal approach for transmitting information through noisy communication channels such as the auditory nerve when coding signals such as speech that have exponential amplitude distributions.

This work is funded by NIH grant DC 000029

### **197 Flow in the Reticular Lamina-Tectorial Membrane Gap and Forces on the Inner Hair Cell Hair Bundles**

**Yizeng Li**<sup>1</sup>, Karl Grosh<sup>1</sup>

<sup>1</sup>*University of Michigan, Ann Arbor*

Fluid flow stimulates the hair bundles (HB) of the inner hair cells (IHC) of the cochlea, opening the mechano-electric transducer (MET) channels of the IHCs. The resulting current depolarizes the cell body inducing neurotransmitter release and, ultimately, auditory nerve stimulation. The active machinery of the cochlea, driven by motility of outer hair cells (OHC), both tunes the microfluidic excitation of the IHC HBs and provides for nonlinear compression. Two different kinds of flow: (1) shearing of fluid between the reticular lamina (RL) and tectorial membrane (TM) and (2) so-called pulsating flow in the RL-TM gap have been implicated as the dominant source of fluidic stimulation of the IHC HB, but the frequency and spatial dependence of these flows for IHC stimulation is unresolved in vivo (Nowotny and Gummer, PNAS, 103: 2120-2125). Indeed, the relative importance and interaction of the active processes and flow modalities likely varies with tonotopic location. In this work, we build a cross section model of the cochlea which can be incorporated into our previous 3d finite element cochlear model (Ramamoorthy et al., JASA, 121:2758-2773, Meaud and Grosh, JASA, 127:1411-1421). Besides an active electromechanical model of the organ of Corti, the cross section model contains both shear and pulsatile flows in the RL-TM gap. The viscous flow over the IHC HB is explicitly modeled to obtain the forces on the IHC HB and also the deflection of the HB. The difference between the IHC HB and BM responses is compared at the base and the apex of the cochlea. This work also assesses the relative importance of the longitudinal flow in the scala vestibuli, scala tympani, sulcus, and the RL-TM gap.

(The work is supported by NIH NIDCD R01-04084)

### **198 Kinetics of Mechanoelectrical Transduction Affect Hair Cell Tuning**

**Gregg B. Wells**<sup>1</sup>, Anthony J. Ricci<sup>2</sup>

<sup>1</sup>*Texas A&M University System Health Science Center*,

<sup>2</sup>*Stanford University*

**Background:** Mechanoelectrical transduction (MET) in sensory bundles of hair cells is the first major step in translating mechanical energy into electrical energy in the auditory system. Tonotopic variations in activation kinetics and adaptation kinetics of MET have been proposed to function together to form a bandpass filter in this energy conversion. The contribution of this bandpass filtering to hair cell tuning, however, remains poorly characterized in turtle hair cells. These hair cells have intrinsic electrical resonance that produces tuning and amplification in the absence of time dependent mechanotransduction. The goal of this computational study is to investigate how kinetics of MET affect tuning in turtle hair cells.

**Methods:** A Hodgkin-Huxley type computational model of turtle hair cells is developed that incorporates the tonotopically varying properties of voltage dependent  $\text{Ca}^{2+}$  and BK channels that produce electrical resonance. It also

incorporates tonotopically varying properties of the MET channel. The model is parameterized with electrophysiological behaviors of each channel. Kinetics of activation and adaptation of the MET channel are varied to determine how the time-dependence of MET affects the intrinsic tuning and amplification of the electrical resonance under conditions of static and sinusoidally varying displacements of the hair bundle.

Results: Steady-state MET current is responsible for setting resting potential of the hair cell in order to optimize electrical resonance. Adaptation with static displacement of the hair bundle changes the dynamic range of hair cell tuning. Activation and adaptation kinetics of the MET channel apply low pass and high pass filtering, respectively, on the electrical resonance with sinusoidal displacement of the hair bundle.

Conclusion: The kinetics of MET activation and adaptation sharpen tuning around the characteristic frequency of the hair cell.

Supported by NIH/NIDCD 5R01DC003896 to AR.

### **199 Mechanical Loading of Active Hair Bundles**

**Dáibhid Ó Maoiléidigh<sup>1</sup>**, A. J. Hudspeth<sup>1</sup>

<sup>1</sup>*Howard Hughes Medical Institute and Laboratory of Sensory Neuroscience, The Rockefeller University*

As the mechanoreceptive organelles of the auditory, vestibular, and lateral-line systems, hair bundles are specialized for detecting a variety of distinct inputs. The bundles of various receptor organs accordingly differ in their shapes and physiological properties. Moreover, hair bundles are attached to a range of accessory structures that deliver inputs and impose passive mechanical loads. We propose that the elastic, viscous, and inertial loads adjust the operating points of active hair bundles and by that means alter their signal-detection abilities. We use a simple description of active hair-bundle motility to show how the mechanical environment regulates the bundles' behavior and responsiveness.

Depending on its mechanical load, a hair bundle can function as a switch, active oscillator, quiescent resonator, or low-pass filter. A bundle may display either a sharply tuned, nonlinear, and sensitive response or an untuned or weakly tuned, linear, and insensitive response. The resonant frequency of a tuned hair bundle depends upon both the active response of the bundle and the passive properties of the load.

The hair bundles of auditory organs may be loaded to enhance their frequency selectivity, dynamic range, and sensitivity to weak stimuli. As a consequence, experimental observations on hair bundles from which the overlying accessory structures have been removed may not reflect the bundles' responses in an intact organ. For example, our description predicts a significant effect of the tectorial membrane on the hair bundles of outer hair cells in the mammalian cochlea.

Our parsimonious characterization of active hair-bundle motility provides a qualitative explanation of most observations on hair-bundle motion from different receptor organs and organisms. The predictions of this description

are general, do not depend on many of the details included in complex models of hair-bundle motility, and provide a framework for understanding the operation of hair bundles in a variety of contexts.

### **200 Cochlear Model Shows Phase Difference Between the Reticular Lamina and Basilar Membrane Motion**

**Allyn Hubbard<sup>1</sup>**, Duk Joong Kim<sup>1</sup>, David Mountain<sup>1</sup>

<sup>1</sup>*Boston University*

We previously reported (Hubbard *et al* 1999) results from a sandwich model (de Boer 1990) of the cochlea that fit chinchilla basilar membrane (BM/stapes) velocity data (Ruggero 1997). This model produced a 50 degree reticular lamina (RL) velocity phase lead relative to the BM at the characteristic frequency (CF ~ 8 kHz). We have now refined the model's parameters to represent the gerbil cochlea.

In the present model, RL volume velocity phase leads the BM volume velocity phase by 70 degrees at the spatial location of maximum BM motion for 14 kHz. Chen *et al* (2011) measured RL and BM motion, and found that at lowest SPLs, RL phase led BM phase by roughly 80-86 degrees

Apical to that spatial region of the model, the RL and BM become nearly out of phase; although when that happens, the magnitudes are quite small (-35 dB from the peak). Still more apically (~1 mm past the maximum BM location), the model's RL and BM are back in phase. This means that in the region where the model's outer hair cell (OHC) forces produce amplification, the simulated motion of the RL and BM are a combination of two modal responses. One mode is the organ of Corti (OC) moving transversely as a unit, as in a classical model. The other mode is the height change of the OC due to OHCs deforming the entire organ.

Funded by NIH grant DC 000029

### **201 Relationships Between Cochlear Tuning and Delay Probed with a Nonlinear Transmission-Line Model**

**Bastian Epp<sup>1</sup>**, Christopher Bergevin<sup>2</sup>, Christopher A. Shera<sup>3</sup>

<sup>1</sup>*Technical University of Denmark*, <sup>2</sup>*Columbia University*,

<sup>3</sup>*Harvard Medical School*

Otoacoustic emissions have provided both a powerful scientific and clinical tool into cochlear function, though their utility has generally been confined to assaying sensitivity. However, evidence has been emerging that stimulus-frequency emissions (SFOAEs) can also be used as a means to estimate frequency selectivity in populations (Shera *et al.*, 2002 PNAS 99:3318-3323). The basic idea is that delays associated with emission generation reflect build-up times of the cochlear filters: The sharper the tuning, the longer the delay. SFOAE delays vary with frequency, in a fashion consistent with changes in tuning along the length of the cochlea (i.e., broadening from base to apex). Additionally, delays vary considerably across species and appear longest in humans, an observation

that has broad comparative ramifications. Understanding the full implications of these types of variations in SFOAE delay requires answering basic questions about the relationship between tuning and delay in the cochlea. For example, is it possible to disentangle delays associated with propagation as opposed to filter build-up? Can SFOAE delays be used to estimate tuning in individuals? And a question stemming from the pioneering studies of von Békésy: How do differences in the tonotopic map (e.g., number of octaves spanned from base to apex) or morphological properties (e.g., cochlear length) affect tuning and delay estimates? To address these questions, we use a time-domain implementation of a nonlinear computational transmission-line model recently developed for examining connections between cochlear mechanics, OAEs, and psychophysics (Epp et al., 2010, JASA 128:1870-1883). Specifically, we investigate how changes in mechanical and morphological properties affect relationships between delay and tuning.

### **202 3D Numerical Simulation of the Wave Propagation in the Human Cochlea**

**Frank Boehnke<sup>1</sup>, Daniel Koester<sup>2</sup>, Katharina Braun<sup>1</sup>, Thomas Stark<sup>1</sup>**

<sup>1</sup>*Dept. of Otorhinolaryngology, Munich, Germany,* <sup>2</sup>*P+Z Engineering, Munich, Germany*

The aim of this study is the numerical simulation of the wave propagation of travelling waves along the cochlear partition in the human inner ear in three dimensions. Different mathematical discretization techniques (Finite Volume FV, Finite Elements FE) were used and compared. A main problem is the fluid-structure coupling which was handled by a new approach using the FV method. The viscous and compressible fluid (lymph) and an anisotropic solid (cochlear partition) were represented in a similar manner. The allocation is realized by switching a binary variable. Therefore problems with the adaption of differing variables and computing nets in the domains (fluid and solid) were prevented. The results show the characteristic frequency to space distribution of displacements along the cochlear partition and permit further conclusions concerning the acoustic signal processing in the cochlea especially with inserted electrodes used for electrical stimulation of the hearing nerve.

This work was sponsored by MED-EL (Innsbruck, Austria)

### **203 Cochlear Model: 3D Traveling Waves and Organ of Corti Power Amplification**

**Charles Steele<sup>1</sup>, Sunil Puria<sup>1</sup>**

<sup>1</sup>*Stanford University*

In previous work with cochlear models with a flat partition, the three-dimensional (3D) motion of the viscous fluid has been treated with the 'WKB' method, including both slow and fast waves. Results for the passive response show good agreement with experiments for the basilar membrane response and for the pressure in the fluid for high sound levels. The architecture of the organ of Corti leads to a feed-forward/backward approximation for the effect of the active process on the basilar membrane. The results yields favorable comparison with experiments for

low sound levels, including neural thresholds (Yoon et al., 2011). For the actual stimulation of inner hair cells, a detailed model for the entire structure of the organ of Corti has been used. The calculations have been restricted to frequencies below the "best frequency" for the location. These offer an explanation for the phase and peak splitting observed in neural fibers (Steele and Puria, 2005).

The combination of the full wave behavior of the cochlea with the detailed response of the organ of Corti has seemed to be prohibitive from any direct computational or asymptotic approach. However, the new work extends the calculation for the organ of Corti to high frequencies and short wave lengths. Consequently, we now have an iterative approach to the full problem. We compute the stapes to basilar membrane volume integral and power flow using different sections of the cochlea and compare with recent measurements (Ren et al., 2011). The sections of the BM include a full wave, half wave, and single points for varying levels of cochlear amplification. The feed-forward/backward offers a reason for the architecture of the organ of Corti. Another consequence appears to be a substantial focusing of pressure in the subreticular membrane fluid acting on the inner hair cell stereocilia.

### **204 A Theoretical Model of Basilar Membrane of the Hearing Organ**

**Amitava Biswas<sup>1</sup>**

<sup>1</sup>*University of Texas*

The basilar membrane of the hearing organ is often regarded as a paragon of transduction. To understand how the hearing system works, experts have proposed detailed models of its specific aspects – the transfer of acoustic energy from the atmosphere to the tympanic membrane via the external ear; the coupling of the tympanic membrane to the oval window of the cochlea via ossicles; the resultant fluidic oscillations in the cochlear ducts; the formation of traveling waves in the basilar membrane of the cochlea; subsequently the mechanical stimulation of inner hair cells and the consequential transduction of nerve impulses. Experts have also proposed very elaborate models to explain how enhancement of the traveling waves in the basilar membrane may be resulting from synchronized changes in the length of outer hair cells (OHCs). Although it is unrealistic that any OHC would contract in length without expanding in diameter, the models proposed by the experts have so far incorporated the longitudinal contraction of OHCs only, suggesting that the impact of any diametric expansion of OHCs would be relatively trivial. Here we show that the basilar membrane could behave like a Beam-Column system, which may be significantly influenced by the diametric expansion of OHCs.

**[205] Modelling Intracochlear Sound Pressures, 10 to 1000 Hz, Using an Electrical Lumped-Element Analog**

**Torsten Marquardt<sup>1</sup>**

<sup>1</sup>*Ear Institute, University College London*

Although detailed transmission-line models of the cochlea have been successfully applied to simulate intracochlear pressures and impedance measurements, much can still be learned from fitting simpler models to such experimental data in order to describe the basic acoustic principles and estimate species-specific parameters such as the compliances of round window, middle ear and entire basilar membrane, or perilymph inertia and viscous damping within subsections of the cochlea. However, previously proposed lumped-element models were either used to just illustrate the acoustic principles schematically, or, when applied in quantitative analysis, were unable to capture the physiological data in satisfying detail. Building up from these models, our improved circuit requires 14 elements to simulate the frequency-dependence of intracochlear pressure and cochlear impedance measurements, including their changes in response to various surgical manipulations, in surprising detail. The extensive data sets from cat by Nedzelnitsky (1980) and from guinea pig by Franke and Dancer (1982) were chosen to be fitted because the low-frequency characteristics in these two species are distinctly different. Subsequently, the model was adapted to describe available human data. Nedzelnitsky, V. (1980). "Sound pressures in the basal turn of the cat cochlea," *J. Acoust. Soc. Am.* 68, 1676-1689.

Franke, R., and Dancer, A. (1982). "Cochlear mechanisms at low frequencies in the guinea pig," *Arch. Oto-Rhino-Laryngol* 234, 213-218.

**[206] Simulation of Cochlear Traveling Waves and the Medial Olivocochlear Reflex**

**Yi-Wen Liu<sup>1</sup>, Lu-Ming Yu<sup>1</sup>, Kuang-Yi Lin<sup>1</sup>, Kuo-Chieh Chiu<sup>1</sup>**

<sup>1</sup>*National Tsing Hua University*

A computer model for simulation of cochlear traveling-wave inhibition by medial olivocochlear (MOC) reflex is presented. The model consists of a transmission-line model for cochlear traveling waves, piezoelectric outer hair cell (OHC) models that facilitate wave amplification, inner hair cell models that convert hair-bundle motion to auditory-nerve firing, and a probabilistic network that describes the neural circuitry of MOC reflex pathway. In the present model, MOC efferent firing causes OHCs to be hyperpolarized, which lowers prestin-associated capacitance and reduces the gain of cochlear amplification. Simulation shows that reticular-lamina displacement in response to a pure tone can be reduced by more than 30% at 80 dB SPL due to MOC inhibition. This model is potentially useful for testing various hypotheses regarding how MOC efferents affect human perception of complex stimuli, such as speech and music.

**[207] Life Cycle of Distortion Product (DP) Waves**

**Egbert de Boer<sup>1</sup>, Alfred Nuttall<sup>2,3</sup>**

<sup>1</sup>*Academic Medical Center*, <sup>2</sup>*Oregon Health & Science University*, <sup>3</sup>*Kresge Hearing Research Institute*

It is generally assumed that Distortion Product (DP) waves originate in the region where the responses of the two primary tones overlap. With a one-dimensional approximation of cochlear mechanics the "life cycle" of a cochlear DP wave starting from that area can be traced. When the cochlea is 'active', i.e., amplifies waves, the reverse DP wave traveling towards the stapes will undergo amplification on its way. At the stapes the wave is reflected and returns as a (weaker) forward wave. Further on, this wave will undergo amplification again. When reflection and amplification are substantial, the DP wave finally arrives in the region where it originated in the form of a forward wave. This forward wave actually will be dominant over a considerable part of the length of the cochlea, and in this capacity it has been observed experimentally. In that region of dominance the wave is characterized as having an "Inverted Direction of Propagation (IDWP)". Several detailed questions have now been studied in a more realistic three-dimensional model of the cochlea. The role played by short waves has been re-evaluated, and a few necessary corrections, in particular one connected with the load at the stapes, were found and applied. By prescribing a definite non-zero reflection of the DP wave at the stapes, many of the properties of observed DP waves could be simulated. An additional finding was that minor inaccuracies of the "inverse solution method" applied proved unexpectedly important in this context. Accordingly, further research, in which we also touched upon the topic of group delays, was conducted with the greatest care. Supported by NIDCD DC 00141

**[208] Semicircular Canal Dehiscence Effects on Air- And Bone-Conducted Hearing in a 3D Finite-Element Model**

**Namkeun Kim<sup>1</sup>, Charles Steele<sup>1</sup>, Sunil Puria<sup>1</sup>**

<sup>1</sup>*Stanford University*

Semicircular canal dehiscence (SCCD) is a pathological opening in the rigid bony wall of the inner ear. Clinical observations have shown that SCCD simultaneously enhances bone-conduction (BC) sensitivity and decreases air-conduction (AC) sensitivity especially for signals below 1kHz. We used a 3D finite element model of the middle and inner ear derived from  $\mu$ CT scans of a human cadaver temporal bone to simulate the effect of an SCCD on the air-bone gap for the first time. The fluid pressures within the scala vestibuli (SV) and scala tympani (ST) at the basal end of the cochlea, as well as the basilar membrane (BM) velocity along the length of the cochlea, were calculated in response to both AC and BC stimulation, with and without SCCD. The inertial effects of the middle-ear structures and scalae fluids were simulated in the BC case by applying a sinusoidal vibratory displacement to the attachment surfaces between the middle-ear ligaments and the bony walls of the middle ear, as well as to the bone surrounding the inner ear. With AC stimulation an

SCCD decreased the pressure in both the SV and ST by up to 10-20 dB and the differential pressure between the SV and ST by 10-15 dB below 1kHz, consistent with experimental results (Nakajima et al., 2011). With BC stimulation an SCCD increased BM velocity by up to 15-20 dB below 1 kHz, as shown previously (Sohmer et al., 2004; Songer and Rosowski, 2005). Depending on the direction of the applied BC stimulation, preliminary simulation results indicated differences of up to 10 dB above 1 kHz in the resulting BM velocity, which could potentially explain why some SCCD patients do not experience BC hearing loss, but instead only experience vertigo symptoms.

### **209 The Impact of the Endocannabinoid System on Sound Localisation**

**Barbara Trattner<sup>1</sup>, Sarah Berner<sup>1</sup>, Felix Felmy<sup>1</sup>, Benedikt Grothe<sup>1,2</sup>, Lars Kunz<sup>1</sup>**

<sup>1</sup>University of Munich, <sup>2</sup>Bernstein Center for Computational Neuroscience Munich

For sound localisation animals exploit differences in arrival time and amplitude of sound waves at both ears. These cues are initially computed in the auditory brainstem in the medial and lateral superior olive (MSO and LSO), respectively. Despite the required temporal precision, dynamic changes induced by neuromodulators are of great importance in this system. We studied the role of the endocannabinoid system in the MSO of the Mongolian gerbil (*Meriones unguiculatus*) using immunohistochemical stainings and patch-clamp recordings from neurones in acute brain slices. Immunohistochemically, we found a predominantly presynaptic localisation of the cannabinoid receptor CB1 during the period around hearing onset, i.e. P10-P15. This distribution completely reverted in animals older than P20 to almost exclusively postsynaptic localisation of CB1. In addition, a glial subpopulation expresses high amounts of CB1. The endocannabinoid-synthesising enzymes diacylglycerol lipase  $\alpha/\beta$  were localised to the soma of postsynaptic cells at all developmental stages tested. In accordance with presynaptic localisation, depolarisation-induced suppression of inhibition and excitation were successfully elicited between P10-P15. In animals older than P20 physiological evidence for presynaptically located CB1 receptors could not be found, however a CB1-dependent hyperpolarisation by endocannabinoids was measured. Voltage-clamp recordings suggest that an increased  $K^+$  conductance underlies this hyperpolarisation. In addition, we measured that endocannabinoids modulate glycinergic currents. Our results suggest that the endocannabinoid system plays an important role in the physiology of auditory neurones and exhibits rigorous changes during development. In animals aged P10-P15 over-excitation of these neurones might retrogradely suppress inputs via presynaptic CB1, whereas in older animals endocannabinoids might adjust the temporal tuning of these neurones by postsynaptic mechanisms.

### **210 Relationship Between Binaural Characteristic Delay and Phase Is Consistent with Cochlear Disparities**

**Philip Joris<sup>1</sup>, Shotaro Karino<sup>1,2</sup>**

<sup>1</sup>Lab of Auditory Neurophysiology, University of Leuven, Leuven, Belgium, <sup>2</sup>Dept. of Otolaryngology, Faculty of Medicine, University of Tokyo

The sensitivity of low-frequency binaural cells in the inferior colliculus (IC) to interaural time differences (ITDs) was discovered using pure tones (Rose et al., 1966). This first study introduced the concept of characteristic delay (CD) as the ITD of constant relative response amplitude at different stimulus frequencies. This concept was refined and put on a quantitative basis by Yin and Kuwada (1983), who also defined characteristic phase (CP) as the frequency-independent component in the relationship between best interaural phase and frequency. McAlpine et al. (1996) reported a surprising inverse relationship between CD and CP, where large CDs are associated with small, negative CPs and large CPs with small, negative CDs. This observation has not been followed up and its basis is unclear.

We studied the effects of differences in characteristic frequency (CF) on CD and CP with a coincidence analysis. Responses of cat auditory nerve (AN) fibers to tones were obtained for a range of frequencies, as in binaural experiments. We counted coincidences between spiketrains of pairs of fibers with similar but not identical CF, and subjected the resulting trains of coincidences to a CD-CP analysis (Yin and Kuwada, 1983). We compared the outcome with responses to binaural beats recorded in the IC.

In the IC, we find that CD and CP values show an inverse relationship, similar to the result of McAlpine et al. (1996). In the AN, random mismatches in CF of pairs of fibers generate time and phase differences in coincidence patterns. Interestingly, here as well, CD and CP values reveal an inverse relationship.

These results suggest CF mismatches as a plausible mechanism for the generation of CD and CP and their inverse relationship. Mismatches in the CF of inputs to binaural coincidence detectors, combined with a constant time delay resulting from the slightly longer pathlength of contralateral relative to the ipsilateral inputs, may suffice to generate binaural tuning.

Supported by FWO (G.0714.09 and G.0961.11) and BOF (OT-09-50) (Flanders, Belgium).

### **211 Implications of Coincidence Counts in Spike Trains of Convergent Auditory Nerve and Trapezoid Body Fibers on Binaural Temporal Sensitivity**

**Tom Franken<sup>1,2</sup>, Philip Joris<sup>1</sup>**

<sup>1</sup>Lab of Auditory Neurophysiology, University of Leuven, Leuven, Belgium, <sup>2</sup>Department of Neurology, University Hospitals Leuven, Leuven, Belgium

Coincidence detection by medial superior olive cells underlies sensitivity to interaural time difference (ITD) and interaural correlation ( $\rho$ ). The nature of this process is an

unsettled issue: is it akin to a counting of coincident spikes, or rather to a correlation of waveforms?

We analyze spiketrains to broadband noise of auditory nerve (AN) and trapezoid body (TB) fibers by counting coincidences. Effects of ITD are examined by delaying "ipsi-" versus "contralateral" inputs; effects of changes in rho are examined by using responses to different noises. We vary the number of inputs; the length of the coincidence window; the monaural and binaural coincidence threshold (the number of input spikes on one or both sides sufficient to be counted as a coincidence). We examine the resulting patterns of coincidences for rate and for general shape of ITD and rho sensitivity.

We find that multiple inputs are required to obtain a physiologically plausible number of coincidences. However, high numbers of inputs decrease binaural sensitivity due to a high baseline level of monaural coincidences, which can be countered by increasing the threshold for monaural versus binaural coincidences. Second, elevation of the binaural threshold to values larger than 2 causes a drastic decrease in rate and in sensitivity to ITD and rho. Third, lengthening the coincidence window favors monaural coincidences, decreasing binaural sensitivity. Finally, a smaller number of TB than AN fibers is needed to generate physiologically plausible coincidence patterns.

We conclude that the temporal patterns of monaural fibers are such that convergence of multiple inputs is required to achieve physiological spike rates. To obtain coincidence patterns consistent with actual binaural responses, the monaural summation threshold must be higher than the binaural threshold and the binaural threshold must be very low. These findings suggest that the fundamental operation is coincidence counting of single spikes.

Support provided by grants from FWO (G.0714.09 and G.0961.11) and BOF (OT/09/50) (Flanders, Belgium) and an FWO fellowship to TPF.

## **[212] Pharmacological Evidence of a Functionally Segregated ILD Processing Pathway**

**Nathaniel Greene<sup>1</sup>**, Kevin Davis<sup>1</sup>

<sup>1</sup>*University of Rochester*

Interaural level differences (ILDs) are the primary cues that animals use to localize high-frequency sounds in the horizontal plane. Several lines of evidence suggest that a pathway specialized to process this cue is initiated by the lateral superior olive (LSO). The principal target of excitatory LSO projections is the contralateral central nucleus of the inferior colliculus (ICC), wherein three major response types can be distinguished based on the patterns of excitation and inhibition observed in contralateral pure-tone frequency response maps. Type V unit maps show V-shaped excitation and no inhibition; type I maps show I-shaped (level-tolerant) excitation flanked by inhibitory sidebands; and type O maps show an O-shaped island of excitation near best frequency threshold bounded by inhibition at higher levels. When tested with dichotic stimuli, type V units show binaural facilitation, whereas type I and type O units show binaural excitatory/inhibitory

interactions. Based on the close resemblance of their monaural and binaural response properties with those of LSO units, it has been conjectured that type I units receive their dominant excitatory inputs from the LSO. To test directly this hypothesis, the responses of ICC units were compared before and after pharmacological blockade of LSO activity by injection of the non-specific excitatory amino acid antagonist kynurenic acid. During LSO inactivation, many ICC type I units were silenced or showed substantially reduced discharge rates. In contrast, the discharge rates of most type V and O units were unchanged. Taken together, these results suggest that type I units represent the midbrain component of a functionally segregated ascending pathway specialized to process ILDs. Supported by NIH grants R01 DC 05161, P30 DC05409, and T32 DC009974.

## **[213] ATP Modulation of Developing Auditory Brainstem Neurons**

Sasa Jovanovic<sup>1</sup>, Beatrice Dietz<sup>1</sup>, Jana Nerlich<sup>1</sup>, Mandy Sonntag<sup>1</sup>, Christian Keine<sup>1</sup>, Rudolf Rubsamen<sup>1</sup>, **Ivan Milenkovic<sup>1</sup>**

<sup>1</sup>*Institute of Biology, University of Leipzig*

In the developing nervous system, discrete bursts of spontaneous electrical activity arise independent of experience or any environmental input. This bursting activity may play a major role in axonal pathfinding, refinement of topographic maps, dendritic morphogenesis and the segregation of axonal terminal arbours. In the auditory system, such bursting activity is endogenously generated in the cochlea by the ATP-mediated activation of the cochlear inner hair cells, and is thereafter transferred to the central auditory system. Here we show that purinergic signaling is also effective in auditory brainstem neurons. We investigated the physiological effects of P2X receptors on neuronal excitability from prehearing to early stages of auditory signal processing. Our results demonstrate that extracellular ATP can evoke Ca<sup>2+</sup>-dependent bursting in neurons expressing P2X receptors. Further analysis revealed that the expression of P2X receptors in the brainstem is developmentally and topographically regulated. In the cochlear nucleus bushy cells, ATP increases spontaneous and acoustically evoked activity *in vivo*, but these effects diminish with maturity. We found that ATP not only augmented glutamate driven firing, but it also evoked APs in the absence of glutamatergic transmission. During postnatal development, endogenously released ATP contributes to firing activity by facilitating AP generation and prolonging AP duration. Given the enhancing effect of ATP on AP firing and confinement of P2X-R to certain auditory brainstem nuclei, and to distinct neurons within these nuclei, it is conceivable that purinergic signaling plays a specific role in organization of developing neuronal circuits.

## **214** Cross-Fostering Increases Auditory Sensitivity in Developing Rats

Shana Adise<sup>1</sup>, Aminat Saliu<sup>1</sup>, Adrián Rodríguez-Contreras<sup>1,2</sup>

<sup>1</sup>City College of New York (CUNY) Biology Department,

<sup>2</sup>The Graduate Center (CUNY)

Unlike humans, where hearing begins in utero, hearing onset in rats occurs during postnatal development. This indicates that the mechanisms controlling hearing development are under genetic control. However, experience can also play a role. Here, we compared auditory development in Wistar rats reared under standard conditions (naïve pups) to rats that were cross-fostered at postnatal day (P) 5. We used the auditory-evoked brainstem response (ABR) technique to measure hearing responses of P13-P15 pups to broadband clicks (1 to 50 kHz) of varying intensities (0 to 82 dB SPL). We report the % of pups with ABRs and their mean ( $\pm$  sem) ABR threshold. At P13, only one naïve pup had reliable ABRs (72 dB, n=10 pups). Auditory responses of naïve pups increased to 55% at P14 ( $57 \pm 7$  dB, n=9) and to 100% at P15 ( $50 \pm 5$  dB, n=10). In contrast, our preliminary data shows that 100% of pups from cross-fostered litters had ABRs at P13 ( $66 \pm 5$  dB, n=6), and lower thresholds at P14 ( $39 \pm 1$  dB, n=6) and P15 ( $35 \pm 2$  dB, n=6) compared to naïve pups. Next, we hypothesized that the positive effect of cross-fostering on hearing development depends on the duration of cross-fostering experience. Therefore, we cross-fostered a litter of P5 pups with a litter of P12 pups and measured ABRs at P14 and P15. For pups with a short cross-fostering experience (P12 pups cross-fostered to a P5 litter mom), we found that 80% of pups produced reliable ABRs at P14 ( $72 \pm 3$  dB, n=10) and at P15, all pups responded ( $42 \pm 4$  dB, n=10). These results show a positive effect on hearing onset but not on hearing thresholds. Interestingly, in the long cross-fostering condition (P5 pups cross-fostered to a P12 litter mom), 100 % of pups had ABRs at both P14 ( $58 \pm 5$  dB, n=10) and P15 ( $44 \pm 5$  dB, n=5). Overall, our results show a positive effect of cross-fostering on hearing development and suggest that duration and experience of cross-foster mothers are key variables that affect hearing development in Wistar rat pups.

## **215** The Developing Connectome: Growth Dynamics of the Calyx of Held

Dakota Jackson<sup>1</sup>, Marlin Dehoff<sup>1</sup>, Brian Hoffpauir<sup>1</sup>, Jonathan Wu<sup>1</sup>, Tom Deerinck<sup>2</sup>, Mark Ellisman<sup>2</sup>, George Spirou<sup>1</sup>

<sup>1</sup>West Virginia University, <sup>2</sup>University of California San Diego

The calyx of Held, perhaps the largest nerve terminal in the mammalian brain, grows rapidly to establish precise 1:1 innervation of the principal neuron of the medial nucleus of the trapezoid body (MNTB). We used serial block face scanning electron microscopy (SBFSEM) to assay numbers and sizes of inputs innervating individual MNTB cells at P3, P4 and P6, and study of cells at P2 is underway. Cells from the medial MNTB were studied to minimize tonotopic differences in maturation. We have

achieved a large sample size for EM studies of 37 completely sampled cells at P3, 18 cells at P4 and 45 cells at P6, and measure terminal size strictly as the apposed surface area of contact between the nerve terminal and postsynaptic somata and proximal dendrite. These reconstructions revealed cells at each age that were contacted by two large ( $> 30 \mu\text{m}^2$  apposed surface area) inputs, which indicates competition among inputs. At P3, 62% (23/37) of cells had only small synaptic inputs ( $< 35 \mu\text{m}^2$  apposition area), 16% (6/37) had only a single large input ( $> 80 \mu\text{m}^2$  and more than three times the size of the next largest input) and 22% (8/37) had at least two large inputs (largest input  $> 35 \mu\text{m}^2$  and less than three times the size of the next largest input). At P4, only 1/18 (6%) had only small synaptic inputs, 83% (15/18) had a single large input, and 11% (2/18) had competing inputs. We captured a larger sample of 45 cells at P6; 9% (5/46) had only small inputs, but these were larger than at earlier ages, 34/46 (74%) had a single large input, and 17% (8/46) had competing inputs. These data indicate a rapid growth phase between P3-4, and a slower resolution of synaptic competition over the ensuing two days. At P6, one-half of the competing cells were near threshold criteria to identify a winning input, and several cells with only small inputs showed nuclear folding patterns atypical of principal cells. For all inputs, nerve terminal size would be greater except for the presence of thin glial processes that interpose between the nerve terminal and MNTB cell membranes. We are exploring a range of ultrastructural features that distinguish competing inputs across this developmental time frame.

## **216** Development of Auditory Brainstem Centers in $\text{Ca}_v1.3^{\text{flx/flx-Pax2cre}}$ Conditional Knock-Out Mice: Role of Neuronal Activity from the Periphery

Michael Boesen<sup>1</sup>, Jan Hirtz<sup>1</sup>, Marlies Knipper<sup>2</sup>, Marco Rust<sup>1</sup>, Lukas Rüttiger<sup>2</sup>, Eckhard Friauf<sup>1</sup>

<sup>1</sup>Animal Physiology Group, Department of Biology, University of Kaiserslautern, Germany, <sup>2</sup>Department of Otolaryngology, Tübingen Hearing Research Centre, University of Tübingen, Germany

Voltage-gated calcium channels have poorly understood functions in brain development. The  $\text{Ca}_v1.3$  subunit is a predominant isoform in neurons, and  $\text{Ca}_v1.3$  channels are responsible for transmitter release from inner hair cells (IHCs). Genetic knockout of  $\text{Ca}_v1.3$  channels ( $\text{Ca}_v1.3^{-/-}$ ) abolishes transmitter release from IHCs and thus leads to deafness. Systemic  $\text{Ca}_v1.3^{-/-}$  mice exhibit anatomical malformations as well as reduced volumes (up to 58%) and neuron numbers (up to 35%) in the auditory brainstem nuclei (Hirtz et al., J Neurosci, 2011). These defects may be caused by a missing  $\text{Ca}^{2+}$  influx in IHCs or in auditory brainstem neurons. We generated tissue specific conditional  $\text{Ca}_v1.3^{\text{flx/flx-Pax2cre}}$  KO mice to figure this out. As Pax2 is expressed in IHCs, yet virtually absent in auditory brainstem areas (Ohyama and Groves, Genesis, 2004),  $\text{Ca}_v1.3$  channels in the conditional KO mice are selectively impaired in IHCs, beginning in early development. We diagnosed hearing functions in these mice by auditory

brainstem responses (ABR) and otoacoustic emissions (DPOAE). Volumetric brainstem center analysis was performed to elucidate possible dysplasias. Thresholds for click-, noise-, and pure-tone evoked ABRs were greatly impaired. DPOAEs had reduced amplitudes and showed a general impairment of cochlear amplification in conditional KOs. Auditory brainstem nuclei were normally shaped, but exhibited smaller volumes in SOC and CN (LSO 24%, MNTB 28%, DCN 14%, AVCN 18%, PVCN 38%). The IC and SPN showed no volume difference. The cell count in the SOC was reduced only in the LSO and MNTB (each about 36%). Neuron density was unaffected in the SOC. Brain sizes and the volume of the brainstem were not diminished. Refinement in the MNTB-LSO projection was not impaired as single fiber strength and convergence ratio were unaltered in conditional KOs. Our results point to a crucial contribution of peripheral sensory-neuronal activity in the development of functional central auditory circuits.

### **217** Encoding the Pitch of Sounds Using Synchrony Receptive Fields

Jonathan LAUDANSKI<sup>1</sup>, Romain Brette<sup>2</sup>

<sup>1</sup>*Equipe Audition, Ecole Normale Supérieure, Paris,*

<sup>2</sup>*Equipe Audition, Ecole Normale Supérieure, DEC, 75005 Paris*

Pitch constitutes a major dimension of auditory perception along which periodic (or near-periodic) sounds can be organized. Although the role of pitch is essential in the perception of music and important when dealing with source segregation in complex auditory scene, the neural mechanisms underlying pitch perception remain unclear [1]. Many models have been proposed including models relying purely on the rate-based strategy and filters selectivity along the tonotopic axis, or models relying on the accurate timing of spikes [2], as well as intermediate models [3] using both the tonotopic and temporal organization of auditory nerve activity (for a review see [4]).

We propose here a model of pitch perception based on the synchrony produced within groups of peripheral neurons. We first describe how auditory stimuli can induce synchronous output of peripheral neurons. This stimulus-based synchrony is independent of the spiking neuron model and can thus be used to define the synchrony receptive field (SRF) of a group of neurons [5]. We describe two types of SRFs of peripheral auditory neurons and show how they relate to the patterns of synchrony evoked in a neural population by periodic sounds. This allows us to show how one can encode periodicity by hard-wiring these synchronous assemblies onto specific group of coincidence detectors. We use this synchrony-based scheme to compute the pitch of a large variety of sounds, including different voices and musical instruments (RWC music database) independently of sound intensity, or type of source. In order to expose the differences existing between classical correlation-based approach of pitch computation and our use of synchronous spiking population, we describe our model performances in a one parameter discrimination task. We finally highlight the

interest of SRFs with respect to the biological plausibility of the emergence of such synchronous neural assemblies.

#### Acknowledgements

This work was supported by the European Research Council (ERC StG 240132).

#### References

1. Winter I: The Neurophysiology of Pitch in Pitch, (2005) 99-146, [http://dx.doi.org/10.1007/0-387-28958-5\\_4](http://dx.doi.org/10.1007/0-387-28958-5_4).
2. Licklider JCR: A duplex theory of pitch perception, *Experientia* 7 (1951): 128.
3. Loeb GE, White MW, and Merzenich MM: Spatial cross-correlation, *Biol. Cyber.* 47, no. 3 (1983): 149-163.
4. de Cheveigné A: Pitch Perception Models, in *Pitch*, (2005), 169-233, [http://dx.doi.org/10.1007/0-387-28958-5\\_6](http://dx.doi.org/10.1007/0-387-28958-5_6).
- 5 Goodman DF and R Brette (2010). Learning to localise sounds with spiking neural networks, *Adv. in N.I.P.S.* 23, 784-792.

### **218** Evaluation of Pitch Representations Measured Concurrently in Auditory Brainstem and Cortex, and Their Relationship to Behavioral Measures of Pitch Salience

Anathanarayan Krishnan<sup>1</sup>, Christopher Smalt<sup>1</sup>, Gavin Bidelman<sup>2</sup>, Saradha Ananthakrishnan<sup>1</sup>, Jackson Gandour<sup>1</sup>  
<sup>1</sup>*Purdue University,* <sup>2</sup>*Rotman Research Institute*

Studies examining the neural correlates of pitch salience have commonly utilized iterated rippled noise (IRN) in fMRI paradigms. While there is disagreement on whether or not such correlates emerge prior to primary auditory cortex, the use of IRN and previous fMRI results have also been challenged by the suggestion that these purported cortical pitch responses are driven by acoustic attributes of IRN other than pitch (e.g., spectrotemporal flux). Here, we reconcile these inconsistencies by assessing the degree to which pitch-relevant information contained in the concurrently recorded brainstem frequency following response (FFR) and cortical pitch response (CPR) to IRN stimuli are correlated with a listener's perceptual judgments of pitch salience. Individual pitch discrimination thresholds (F0 DLs) served as a perceptual measure of pitch salience. Pitch-specific responses were isolated by preceding IRN stimuli (evoking a pitch response) by a noise precursor (evoking obligatory onset responses). A control condition (IRNo) in which IRN was processed to remove its pitch, but sparing spectrotemporal modulations, was employed to ensure CPRs were driven by pitch instead of other latent acoustic features. Results showed that neural FFR/CPR magnitudes systematically increase, and behavioral F0 DLs improve with increasing stimulus periodicity, indicating more robust encoding for salient pitch. No reliable responses were evoked by IRNo, confirming that pitch rather than other acoustic attributes elicits the CPR to IRN. Correlation analyses revealed close connections between responses at all three levels of processing. We infer that neural correlates of pitch salience emerge in early, pre-attentive stages of brainstem pitch processing; that they are maintained with high fidelity by early cortical processing, and that such representations

may contribute to the formation of perceptual salience of pitch.

### **219 Phase Locking to Envelope and Fine Structure in the FFR: Implications for Spatial Attention**

**Dorea Ruggles**<sup>1,2</sup>, Hari Bharadwaj<sup>1</sup>, Barbara Shinn-Cunningham<sup>1</sup>

<sup>1</sup>*Boston University*, <sup>2</sup>*University of Minnesota*

Neural synchronization in the sub-cortical auditory pathway is reflected in scalp-recorded measurements of responses to periodic acoustic stimuli. The total neural synchrony can be decomposed into both polarity-tolerant “envelope” and polarity-sensitive “carrier” responses. Individual differences in the overall strength of phase locking to periodic stimuli predict differences in the ability to process supra-threshold inputs during complex listening tasks. Here, we tested 22 normal-hearing adults aged 18 – 55 in a series of experiments to test whether differences in brainstem encoding explain differences in perceptual ability, and whether age influences these relationships. FFRs were analyzed by computing the phase locking value (PLV; a measure of phase consistency) separately for carrier and envelope components of the responses. Envelope phase locking was the primary component of low frequency elements (100-300 Hz) of the FFR, while carrier phase locking dominated higher frequencies. In a taxing, spatial selective auditory attention task, the same listeners were asked to report a stream of digits spoken from a source simulated from directly ahead (azimuth 0°) while ignoring competing digit streams 15° to the left and right. In addition, frequency modulation (FM) detection thresholds were measured. For all listeners, FM threshold predicted spatial selective attention ability. Envelope phase locking at the fundamental frequency was correlated with spatial selective attention for younger, but not older listeners. Older listeners had generally weak envelope phase locking; evidence suggests these listeners compensated for weak envelope encoding by depending more heavily on higher frequency carrier phase locking cues. This work illustrates the importance of cue redundancy in everyday listening and demonstrates that both age and listening conditions affect the information available for completing an auditory task. [Funding from NIDCD and an NSSEFF fellowship.]

### **220 Estimation of the Level of the Cubic Difference Tone in the Frequency Following Response (FFR)**

**Hedwig Gockel**<sup>1</sup>, Robert Carlyon<sup>1</sup>, Redwan Farooq<sup>1</sup>, Louwai Muhammed<sup>1</sup>, Christopher Plack<sup>2</sup>

<sup>1</sup>*MRC-Cognition and Brain Sciences Unit*, <sup>2</sup>*University of Manchester*

Studies of the pitch of complex tones often use noise to mask distortion products such as the cubic difference tone (CDT), which, for 2 components  $F_1$  and  $F_2$ , has a frequency of  $2F_1-F_2$ . This is true both for psychophysical studies and for measures of the frequency following response (FFR) - a scalp-recorded measure of phase-

locked brainstem activity that is often assumed to reflect residue pitch. However, whereas audible CDTs probably arise from cochlear processes and are propagated along the basilar membrane, a component at the CDT frequency may also arise in the FFR from nonlinearities in the responses of neurons that are driven by more than one harmonic. To assess this we compared the spectral magnitude of the FFR at the CDT frequency in response to a complex tone, to that in response to a pure tone of identical frequency presented at various levels.

The FFR was measured for six subjects, using 100-ms 75-dB-SPL complex tones containing components 2-4 of a 300-Hz fundamental frequency with all harmonics shifted together up or down from their nominal (harmonic) frequencies by 56 Hz. This frequency-shifted complex allowed independent assessment of the levels of the CDT and the quadratic difference tone at  $F_2-F_1$  (the envelope rate). Stimuli were presented in alternating polarity at a rate of 3.57 Hz. We used a “vertical” montage (+ Fz, - C7, ground=Fpz) for which the FFR is assumed to reflect phase-locked neural activity from rostral generators in the brainstem. FFR waveforms for each polarity were averaged and then either added, to enhance responses related to stimulus envelope, or subtracted, to enhance temporal fine structure responses.

The effective CDT level in the subtraction waveform of the FFR was substantially higher than that commonly estimated in psychophysical experiments, indicating (possibly neural) contributions to the CDT in the FFR beyond that originating from the audible propagated component.

Acknowledgement

Supported by Wellcome Trust Grant 088263.

### **221 Objective Information-Theoretic Algorithm for Detecting Brainstem Evoked Responses to Complex Stimuli**

**Gavin M. Bidelman**<sup>1</sup>

<sup>1</sup>*Rotman Research Institute, Baycrest Centre for Geriatric Care*

The scalp-recorded frequency-following response (FFR), a potential with putative neural generators in the rostral brainstem, can provide a robust representation of the neurophysiological encoding of complex stimuli. The FFR is rapidly becoming a valuable tool for understanding the neural transcription of speech and music, language related processing disorders, and brain plasticity at initial stages of the auditory pathway. Despite its potential clinical and empirical utility, determining the presence of a response is still dependent on the subjective interpretation by an experimenter/clinician. The purpose of the present work was to develop and validate a fully objective procedure for the automatic detection of FFRs elicited by complex stimuli, including speech. Mutual information (MI) was quantified between the spectrographic representation of neural FFRs and their evoking acoustic stimuli. To remove the human subjectivity associated with typical response evaluation, FFRs were first simulated at known signal-to-noise ratios (SNRs) using a computational model of the auditory periphery. The MI at which model FFRs contained

+3dB SNR was taken as the criterion threshold ( $\Theta_{MI}$ ) for a present response.  $\Theta_{MI}$  was then applied as a binary classifier to the MI computed from actual neurophysiological responses from human participants ( $n=35$ ) recorded either with or without the presentation of a stimulus (i.e., evoked response vs. sham recording). Results show high overall accuracy (93%) in the metric's ability to identify true responses from sham recordings. Complementary results were found in the metric's test performance characteristics with a sensitivity and specificity of 97% and 85%, respectively. The present results demonstrate that the mutual information between a complex acoustic stimulus and its corresponding brainstem representation can provide a completely objective and robust method for automated FFR detection.

### **222 A Subtraction Method to Reduce Cochlear Implant Electrical Artifact Contamination of Sustained Auditory Brainstem Responses**

**Christopher J. Smalt<sup>1</sup>**, Ananthanarayan Krishnan<sup>2</sup>, Thomas M. Talavage<sup>1</sup>

<sup>1</sup>*School of Electrical and Computer Engineering, Purdue University, IN, USA*, <sup>2</sup>*Department of Speech, Language and Hearing Sciences, Purdue University, IN, USA*

Auditory evoked potential recordings in cochlear implant (CI) recipients are plagued by an electrical artifact that complicates acquisition of a reliable neurophysiological measurement. This electrical artifact arises from the firing of CI electrodes, and results in an externally measurable amplitude that is a function of current level, but typically around 50  $\mu$ V. Removing the artifact is achievable for a transient measurement such as the Auditory Brainstem Response where the response lags the stimulation artifact with no overlap. However, in a sustained response such as the Frequency Following Response (FFR), the artifact and response coincide and separation becomes more complex. The goal of this research is to model the electrical artifact generated by the CI and compensate for this artifact in the measured EEG, with the simplest approach being a direct subtraction. Our approach exploits the fact that electrical stimulation produces a known electrode firing pattern during each presentation, such that the EEG artifact should be repeatable. To adequately resolve the temporal characteristics of a single electrode firing, a custom National Instruments data acquisition system was used for recordings at a sampling frequency of 250 kHz. A controlled test bed was developed by placing EEG electrodes in a water bath proximal to the CI, and was found to produce an artifact with characteristics similar to that observed in an actual CI user. A simple subtraction approach was found to reduce the amplitude of the artifact 1-2 orders of magnitude. Band-pass filtering the resulting signal preserves the FFR, while further reducing the magnitude of the artifact. Further testing of the approach was conducted by measuring the acoustic FFR in normal hearing participants with a CI positioned near the head to simulate the artifact. Initial results suggest it may be possible to recover the FFR of a normal hearing subject by

this technique, which may then be readily applied to CI users.

### **223 Neural Discrimination of Stop Consonants in Musician and Nonmusician Children**

**Dana Strait<sup>1</sup>**, Samantha O'Connell<sup>1</sup>, Nina Kraus<sup>1</sup>

<sup>1</sup>*Northwestern University*

Deficits in the perception and neural discrimination of closely-related stop consonants characterize auditory-based learning deficiencies such as developmental dyslexia and impaired speech-in-noise perception. Given that musical training hones the perception of minute acoustic differences that distinguish sounds, we asked whether early childhood musical training confers advantages in the subcortical discrimination of the closely-related stop consonants /ba/ and /ga/. These sounds differ only in their high-frequency harmonic spectra over the most spectrotemporally dynamic portion of the stimulus, the formant transition, due to their distinct second formant trajectories. Subcortical responses to /ba/ and /ga/ reflect the tonotopic organization of the auditory system in that consonants with higher frequency second formants elicit earlier neural responses than those with lower frequency second formants. By employing cross-phase analyses to objectively measure the degree to which subcortical response timing differs to these speech syllables in child musicians and nonmusicians, we reveal that musicians demonstrate enhanced subcortical discrimination of stop consonants during pivotal developmental years. Furthermore, the extent of subcortical stop consonant discrimination correlates with auditory attention performance, providing a biological basis for musicians' enhanced auditory cognitive function. Outcomes may be considered by clinicians, educators and scientists concerned with training-induced neuroplasticity, especially as it relates to the neural transcription of speech in children with and without learning impairment.

Supported by NIH F31DC011457-01 and NSF 0921275.

### **224 A Comparison of Medial Olivocochlear Efferent Effects on Auditory Nerve Compound Action Potentials and Stimulus Frequency Otoacoustic Emissions (SFOAEs) in Guinea Pigs**

**Wei Zhao<sup>1</sup>**, Maria Berezina<sup>2,3</sup>, John J. Guinan, Jr.<sup>1,2</sup>

<sup>1</sup>*Eaton-Peabody Laboratories, MEEI; Dept. of Otolaryngology & Laryngology, Harvard Medical School*, <sup>2</sup>*Speech and Hearing Bioscience and Technology, Harvard-MIT Division of Health Sciences and Technology*, <sup>3</sup>*Eaton-Peabody Laboratories, MEEI*

A common method to non-invasively assess the inhibition produced by medial olivocochlear (MOC) efferents in humans has been to measure changes in otoacoustic emissions (OAEs). However, the MOC inhibition that is relevant for neural coding by the cochlea is the inhibition of auditory-nerve (AN) fiber responses. There has only been one previous study directed at determining the correspondence between MOC effects on OAEs and

neural responses (Puria et al. J Acoust Soc Am 99:500). This study used distortion product OAEs (DPOAEs) and found a highly variable relationship between MOC effects on DPOAEs and neural responses. There has not been a study of the relationship between MOC effects on stimulus frequency OAEs (SFOAEs) and neural responses.

We evoked MOC activity in anesthetized guinea pigs using shocks at the floor of the fourth ventricle and monitored their effects on SFOAEs and on AN compound action potentials (CAPs) from tone pips. At each frequency studied, SFOAE and AN CAP level functions at identical levels and frequencies were obtained with and without shock-evoked MOC inhibition. SFOAEs were separated from the probe sounds by a suppressor tone at a nearby frequency and a higher sound level.

Our preliminary results show that there are different patterns of MOC effects on SFOAEs and AN CAPs along a variety of dimensions. The patterns of MOC effects on CAP amplitudes and latencies as well as on SFOAE magnitudes and phases will be quantified along the dimensions of sound level, shock level, and time.

Supported by NIDCD RO1 DC00235, RO1 DC005977, P30 DC005209 & an NSF fellowship

### **225 Capturing Temporal Precision in the Neural Code: Showcasing a 3D Physiological Imaging Technique**

**Erika Skoe<sup>1</sup>, Nina Kraus<sup>1</sup>**

<sup>1</sup>*Auditory Neuroscience Laboratory, Northwestern University ([www.brainvolts.northwestern.edu](http://www.brainvolts.northwestern.edu))*

We have developed a three dimensional imaging technique, the cross-phaseogram, that captures the temporal precision of auditory brainstem processing in a visually-striking, easy to interpret rendering. This technique, which provides a clear picture of neural timing, was developed to supplement methods based on the subjective identification of individual response peaks. In addition to reviewing recent publications that formed the proof of concept for this technique, we will validate the phaseogram by replicating results derived from subjective peak measurements. We will also illustrate how the phaseogram can capture the multi-dimensional nature of auditory expertise and plasticity. Through this showcasing, we will demonstrate the advantages that the phaseogram method has over previous techniques. For example, this technique minimizes human error and subjectivity associated with peak timing measurements and it facilitates the measurement of neural timing under conditions where manual identification of peaks is difficult (e.g. responses collected in background noise). Unlike methods that focus on individual peaks, the phaseogram also provides a more holistic rendering of neural timing, making it an ideal technique for analyzing responses to long-duration, spectrotemporally-complex stimuli like speech. The phaseogram algorithm is also automated and objective, reducing processing time from days to minutes and eliminating the need for a trained peak picker or multiple blind peak raters. In addition, the phaseogram can uncover temporal precision that is imperceptible to the naked eye, including temporal phenomena occurring at

high frequencies where the response is close to the noise floor. By being objective and automated, and by producing results that are interpretable in individual subjects, this imaging technique is positioned to be an invaluable tool for analyzing auditory brainstem responses to complex sounds. [NIH R01-DC010016 and NSF 0842376].

### **226 Brainstem Neural Encoding of Envelope and Temporal Fine Structure of Complex Stimuli in Normal and Impaired Ears**

**Saradha Ananthakrishnan<sup>1</sup>, Ananthanarayan Krishnan<sup>1</sup>, Christopher Smalt<sup>1</sup>, Gavin Bidelman<sup>2</sup>**

<sup>1</sup>*Purdue University*, <sup>2</sup>*Rotman Research Institute, Baycrest Centre for Geriatric Care*

Speech perception deficits in hearing impaired (HI) listeners have been shown to be associated with a reduced ability to use temporal fine structure (TFS) information as compared to normal hearing listeners. A possible reason for this reduced sensitivity may be decreased phase locking ability, although experiments on animals with hearing loss have yielded mixed results. Here we examine whether neural representation, as reflected in the scalp recorded brainstem frequency following response (FFR), of envelope and/or the TFS is degraded in HI listeners, compared to normal hearing listeners. FFRs were recorded from normal hearing and HI listeners with mild to moderate sensorineural hearing loss using iterated rippled noise (IRN) stimuli with positive (IRN[+]) and negative gain (IRN[-]) at delays of 2 and 4 ms. These two conditions produce differences in waveform fine structure but minimal changes in the stimulus' envelope. Also, the pitch of IRN[+] corresponds to 1/d (d = delay in ms) whereas that of IRN[-] is an octave lower, 1/2d. Pitch-related neural periodicity was computed from FFRs by examining response autocorrelation functions. In addition, spectral analysis was performed by computing the harmonic product spectrum to identify the dominant frequency in the responses. Comparisons between responses of the FFR to these stimuli in the normal hearing listeners suggest robust neural phase locking to both envelope and TFS. In contrast, neural phase locking to envelope and TFS were severely degraded in the HI listeners. While the degraded neural phase locking to TFS in HI listeners appears to be consistent with established perceptual data, the degradation in neural phase locking to envelope is not. It is possible that the IRN stimuli used here do not provide adequate temporal periodicity information for the HI listeners.

### **227 Effects of Noise-Induced Permanent Hearing Loss on Bushy Neurons in the AVCN in CBA Mice**

**Chongyu Ren<sup>1</sup>, Yong Wang<sup>1</sup>**

<sup>1</sup>*Otolaryngology/Neuroscience Program, University of Utah*  
Congenital and early onset hearing loss alter neuronal and synaptic properties in the anteroventral cochlear nucleus (AVCN). However, it is not well known how noise induced hearing loss affects principal neurons in the AVCN. In this study, we aim to investigate such effects. CBA/CaJ mice

(p21-28) were exposed for 2 hours to an octave band noise (8- to 16-kHz) at 109 dB sound pressure level to produce a permanent hearing threshold shift (PTS). This noise exposure leads to type I ganglion cell afferent terminal damage, mechanosensory hair cell loss and eventual ganglion cell degeneration. Comparing to effects from the temporary threshold shift (TTS) noise exposure, which does not result in spiral ganglion cell loss, we hypothesize that changes in auditory nerve synapses and neuronal properties in the AVCN may be different in response to PTS noise damage. We examined endbulb synapse and bushy neuron properties 2 weeks (~P40 day) after the PTS noise exposure. Compared to control and TTS groups, 1) Spontaneous mEPSC frequency was significantly decreased in PTS animals; mEPSC decay time appears to be slower in both PTS and TTS groups, but the mEPSC amplitudes are comparable in all groups, 2) The membrane input resistance of the bushy neuron is higher in PTS noise exposed animals, and 3) There is no difference in hyperpolarization activated current, but the low-voltage-activated K conductance may be smaller in PTS animals. Our results suggest that permanent hearing loss have different effects on auditory nerve endbulb synapses on bushy neurons in the VCN. This is likely due to the presence of degeneration of spiral ganglion cells after the PTS noise exposure.

### **[228] Biomarker Expression in the Brain of Rats After Blast Exposure and Effects of an Antioxidant Treatment**

Xiaoping Du<sup>1</sup>, Jianzhong Lu<sup>1</sup>, Don Ewert<sup>1</sup>, Weihua Cheng<sup>1</sup>, Wei Li<sup>1</sup>, Robert Floyd<sup>2</sup>, Richard Kopke<sup>1,3</sup>

<sup>1</sup>Hough Ear Institute, Oklahoma City, OK 73112,

<sup>2</sup>Experimental Therapeutic Research Program, Oklahoma Medical Research Foundation, OKC, OK 73104, <sup>3</sup>Dept. of Physiology & Otolaryngology, University of Oklahoma Health Sciences Center, OKC, OK 73104

Our current study demonstrates that an antioxidant treatment (HPN07 and NAC) can largely protect cochlear hair cells and restore hearing loss after blast exposure (14 psi, 3 blasts). However, blast exposure can also cause brain damage and effects of antioxidant treatment on brain are still unclear. In this study, antibodies against c-fos (an immediate early gene), APP (amyloid precursor protein A4) or GFAP (glial fibrillary acidic protein) were used as biomarkers to study effects of blast and the antioxidant treatment on brain. Rats were exposed to 3 blasts (14 psi). The antioxidants were intraperitoneally injected 1 hour after blast exposure in one group of rats. Rats with or without blast were injected carrier solutions and used as controls. All animals were intracardially perfused with 10% paraformaldehyde 3, 24 hours, 7 and 21 days after blast (6 rats at each time point in each group). Brains were collected and cryosectioned. ABC immunohistochemical staining was conducted. Numerous positive c-fos stained cells were found in cortex, hippocampus and brainstem at all time points. Significantly fewer numbers of c-fos positive neurons were found in the hippocampus and the retrosplenial granular cortex 3 h after blast, as well as in the DCN 24 h after blast in rats treated with the

antioxidants. Positive APP staining was found only in cortex 21 days after blast exposure and the antioxidant treatment significantly inhibited APP expression in cortex. Increased GFAP expression was found in cortex, hippocampus and brainstem after blast exposure. However, less GFAP expression was found only in the DCN after the antioxidant treatment. Results of this study further demonstrate that brain damage caused by blast is very broad, and also provide evidence that early antioxidant treatment for blast trauma may not only protect cochlear hair cells and restore hearing, but also has an impact on central structures as well (Supported by ONR grant #N00014-09-1-0999).

### **[229] Cochlear Lesions Reduce the Proliferation of Glial Cell Precursors During a Sensitive Period in the Rat Auditory Brainstem**

Aminat Saliu<sup>1</sup>, Natalia Maldonado<sup>2</sup>, Vivek Khatri<sup>1</sup>, Shana Adise<sup>1</sup>, Kiran Ramnarine<sup>1</sup>, Luis Cardoso<sup>2</sup>, Adrián Rodríguez-Contreras<sup>1</sup>

<sup>1</sup>Biology, City College of New York, <sup>2</sup>Biomedical Engineering, City College of New York

Deafferentation experiments in the auditory system can result in neuronal loss, re-organization of synaptic connections and alterations in the size of auditory brainstem nuclei. Here, we tested the hypothesis that cochlear lesions lead to a decrease in the proliferation of glial cell precursors in the medial nucleus of the trapezoid body (MNTB), a brainstem nucleus involved in sound localization. To examine cell proliferation in the MNTB, we acutely injected the thymidine analog EdU in rat pups at postnatal day (P) 3, P9 and P21, and examined brainstem sections using multi-fluorescence labeling (n=6 rats). We found that about 40-70% of EdU+ cells were NG2+, a hallmark marker of glial cell progenitors. In addition, the density of proliferating cells changed with age (EdU+ cells/mm<sup>2</sup>: 200 ± 8 at P3; 239 ± 14 at P9; 26 ± 4 at P21), suggesting that cell proliferation is developmentally regulated. Hence, we examined the time course of cell proliferation between the ages of embryonic day (E) 19 and P31 (n=43). We found that the density of EdU+ cells increased from perinatal ages, reached a plateau from about P2-P12, declined sharply between P13-P15 and remained at low levels until P31. Interestingly, maturation of hearing as assessed with micro CT scans and auditory evoked potentials was strongly correlated with the decrease in cell proliferation, suggesting a link between cell proliferation in the MNTB and the maturation of the auditory periphery. To test this idea, we performed bilateral cochlear lesions at P1, P5, P9, P12 and P15, and examined the density of EdU+ cells one day after the lesion. We found that cochlear lesions did not have an effect on cell proliferation at P2 and P6 but the density of EdU+ cells at P10, P13 and P16 (n=10) decreased by 30-60% when compared to sham controls. These results provide evidence for a sensitive period in postnatal development when damaging the cochlea affects proliferation of glial cell precursors in the auditory brainstem.

### **230 Changes in Excitatory Synaptic Transmission to Bushy Cells Following Noise-Induced Hearing Loss**

Ruili Xie<sup>1</sup>, Paul Manis<sup>1</sup>

<sup>1</sup>University of North Carolina at Chapel Hill

Loss of peripheral sensory input can have long-term consequences for central sensory processing. In the auditory system, exposure to an intense noise damages hair cells in the cochlea and presumably reduces synaptic drive onto the principal cells of the cochlear nucleus. We investigated the long-term effects of noise-induced hearing loss (NIHL) on excitatory synaptic transmission onto bushy cells in the anteroventral cochlear nucleus (AVCN). CBA/CaJ mice, P25, were exposed to 8-16 kHz noise of 116dB SPL for 2 hours, to induce a permanent threshold shift. The mice were then raised in a normal vivarium environment for 7 weeks (at about P75) before electrophysiological analysis. Voltage-clamp recordings were made from bushy cells in parasagittal slices of the cochlear nucleus to measure the excitatory postsynaptic currents (EPSC) evoked by auditory nerve stump stimulation. Two major changes in endbulb synaptic transmission were found from mice with NIHL. First, compared to normal hearing CBAs, the paired pulse ratio of the eEPSCs from NIHL mice were significantly increased, suggesting that the release probability at endbulb synapses decreased with NIHL. Second, there were more response failures and increased asynchronous release events near the end of 50-pulse stimulus trains at 100 Hz and 400 Hz in bushy cells from NIHL mice. These observations indicate that the precise and reliable synaptic transmission normally associated with the endbulb synapses is altered following NIHL. In particular, the ability to transmit sustained information at high rates is compromised.

Supported by a DRF Research Grant (R.X.) and NIDCD grant R01DC004551 (P.B.M).

### **231 Effect of Demyelination on Sound Signal Transmission in the Auditory Brainstem**

Sei Eun Kim<sup>1</sup>, Sang Yeon Lee<sup>1</sup>, Jun Hee Kim<sup>1</sup>

<sup>1</sup>University of Texas Health Science Center, San Antonio

Myelinated axons in the mammalian CNS are uniquely designed to support rapid and efficient saltatory impulse propagation. Myelin loss can eventually lead to axonal degeneration and irreversible damage to motor and sensory function. Hearing disorders with a loss of hearing acuity yet normal cochlear function may arise from axonal demyelination in auditory pathways. However, it is not known how the loss of myelin sheaths affects synaptic function at the level of individual synapses in the mammalian auditory nervous system. We have studied changes in synaptic function that result from demyelination at single synapses in the auditory brainstem, using the Long-Evans Shaker (LES) rat, which is the most severe demyelinating mutant and completely lacks myelination in the CNS due to a retroviral genetic lesion that specifically disrupts expression of myelin basic protein (MBP). We examined auditory brainstem responses (ABRs) in normal Long-Evans (LE) and demyelinating LES rats. There was

no significant difference in the ABR threshold between the LE and the LES rats. However, ABRs in normal LE rats displayed distinct waves I-IV, while in LES rats wave II and III were not distinguishable, indicating that wave II and III merged with wave I and IV, respectively. In LES rats, however, ABRs showed a significant prolongation of wave I and IV latencies at 90 dB stimulation. To study the electric pulse propagation, we recorded action potentials at the calyx of Helds auditory nerve terminals in auditory brainstem using whole-cell patch clamp recording. The LES rat lacking MBP and axonal myelination showed significantly prolonged action potential latency and pronounced synaptic timing errors even at nearly three weeks after birth, while in normal LE rats synaptic timing is very precise without presynaptic latency shift. Thus, our preliminary results suggest that myelination is crucial for auditory nerve to carry out sound signals with high timing precision.

### **232 Effects of Unilateral Hearing Loss on the Vulnerability of the Contralateral Normal Hearing Ear in Noise Exposure**

Hyun Woo Lim<sup>1</sup>, Seung Hyo Choi<sup>2</sup>, Jin Kyung Seo<sup>1</sup>, Yoon Suk Ahn<sup>1</sup>, Jong Woo Chung<sup>1</sup>

<sup>1</sup>Asan Medical Center, University of Ulsan College of Medicine, Seoul, <sup>2</sup>Jeju National University College of Medicine, Jeju, Korea

Objective: To investigate the functional and histologic changes of the normal hearing ear following acoustic trauma in the animal model with contralateral unilateral hearing loss.

Materials and Methods: Six-week-old CBA mice were assigned into four different study groups. Single side deafened (SSD group) mice underwent unilateral deafening procedure for the right ear by cochlear destruction. Sham group underwent the sham surgical procedure for the right ear without inner ear destruction. Two different control groups were used; monaural noise exposure group and binaural noise exposure group. All mice were exposed to acoustic trauma inducing transient threshold shift (TTS) at the age of 10 weeks. The change of hearing thresholds of both ears were serially investigated by auditory brainstem response (ABR) and distortion product otoacoustic emissions (DPOAE) for 4 weeks. The pattern of recovery from TTS and cochlear structural change of study groups were compared among study groups.

Results: In terms of ABR threshold shifts in left ears, SSD group mice ended up with permanent threshold shift (PTS) of 10 dB while other control groups showed full recovery from TTS. The DPOAE threshold shifts of left ears show no significant difference among study groups. In histologic evaluation, no definite structural difference was found in H&E and 8-oxo-guanine staining. TUNEL-positive nuclei were, however, found at the proximal area of the organ of Corti, spiral ganglion, and stria vascularis in SSD group compared with other groups without such histologic findings.

Conclusion: We demonstrated the normal hearing ear is more vulnerable to acoustic trauma in the situation of

permanent contralateral hearing loss. The suspected regions of cochlea responsible to the increased vulnerability are mainly located at the proximal portion of the organ of Corti, spiral ganglion and stria vascularis.

### **233 Neural Activity Patterns in Auditory Brain Areas Following Conductive Hearing Loss**

Jaina Negandhi<sup>1,2</sup>, Robert Harrison<sup>1,3</sup>

<sup>1</sup>*Auditory Science Laboratory, Neuroscience and Mental Health, Hospital for Sick Children,* <sup>2</sup>*Physiology Department, University of Toronto,* <sup>3</sup>*Department of Otolaryngology - Head and Neck Surgery, University of Toronto*

**Introduction:** 50% of Canadian children have one ear infection before their third birthday, and 13% of these children have reoccurring ear infections (1). It is possible that during early years, chronic ear infections leading to conductive loss (CHL) can affect speech and language development and more. However, little is known about the activity state of the auditory system during conductive loss. **Hypothesis:** There are high levels of spontaneous activity at the inner hair cell synapse, and literature suggests that CHL has little effect on general auditory activity levels. We hypothesise that CHL may down-regulate glutamate release at the inner hair cell synapse, and lead to significant auditory deprivation.

**Methods:** In mouse models of CHL, we quantified neural activity patterns in cochlear nucleus and inferior colliculus using c-fos immuno-labelling. This experimental group was compared to mice with total cochlear deafferentation, and to normal controls. Conductive loss was induced by blocking ears with dental cement for 3 days. Cochlear deafferentation was achieved by injecting sterile water into the cochlea. Throughout, hearing thresholds were estimated using ABR to tonal stimuli (2kHz -32kHz).

**Results:** Subjects with CHL showed a 50-60dB SPL elevation in hearing threshold. We found a statistically significant reduction in c-fos labelled cells in cochlear nucleus and central nucleus of inferior colliculus compared to controls. This decreased c-fos expression suggests a change in resting neural activity generated at the inner hair cell synapse leading to a reduction in activity levels in the ascending auditory pathways.

**Conclusions:** During CHL, there is little or no cochlear involvement, and no haircell damage. However, this study indicates CHL alters resting neural activity patterns in the auditory periphery. Such changes (reductions) of peripheral auditory activity may have influence on the developing central brain especially during postnatal years when the system is still highly plastic. These results signify the effect of CHL during otitis media on neural activity in the developing brain.

### **234 Somatosensory Projections to the Cochlear Nucleus Are Upregulated After Unilateral Deafness**

Chunhua Zeng<sup>1</sup>, Ziheng Yang<sup>1</sup>, Lauren Shreve<sup>1</sup>, Sanford Bledsoe<sup>1</sup>, Susan Shore<sup>1</sup>

<sup>1</sup>*University of Michigan*

There are distinct synaptic terminal distributions and associated vesicular glutamate transporters (VGLUTs) for auditory nerve and specific somatosensory projections in the cochlear nucleus (CN). Auditory nerve fibers project primarily to the magnocellular regions of the ventral cochlear nucleus (VCNm) and deep layers of dorsal cochlear nucleus (DCN) and predominantly colabel with VGLUT1; whereas the spinal trigeminal nucleus (Sp5) and Cuneate nucleus (Cu) projections terminate primarily in the granule cell domains (GCD) of the CN and predominately colabel with VGLUT2 (Zhou et al., JCN 2007; Zeng et al., Neuroscience, 2011). Cu projections exhibit more prominent distributions in the GCD than Sp5, while Sp5 projections have a greater number of projections in the VCNm and deep DCN. Unilateral cochlear damage results in significant decreases in VGLUT1 in the ipsilateral VCNm, while VGLUT2 is significantly increased in the ipsilateral GCD and VCNm beginning at two (Zeng et al, J. Neurosci 2009), and still apparent at 6 weeks after deafness (Zeng et al., 2010 ARO abstract). In the current study, we examined the distributions of VGLUT2 positive Sp5 and Cu terminals in the CN 3 weeks after unilateral deafness. Both Sp5 and Cu exhibited a greater number of terminals in the CN. In addition to the increased number of terminals, a greater percentage of these terminals was co-labeled with VGLUT2 (50%) compared with control animals (25%) with normal hearing. More VGLUT2-labeled Sp5 endings were located in the VCN, whereas more VGLUT2-labeled Cu terminals were shown in deep DCN after deafness. The increased Sp5 and Cu projections and their stronger association with VGLUT2 suggest that following unilateral cochlear damage, the enhanced VGLUT2-mediated glutamatergic inputs previously shown (Zeng et al., J. Neurosci., 2009) are, at least in part, attributed to a greater number of projections from Sp5 and Cu. These enhanced glutamatergic inputs, in compensation for the reduced VGLUT1 resulting from auditory nerve loss, may contribute to the increased spontaneous rates observed in the CN in tinnitus. The Sp5 and Cu nuclei may play different roles in this process. Supported by NIH P01 DC00078 and R01 DC004825.

### **235 Auditory Nerve Regeneration and Spiral Ganglion Preservation Maintain Connections with the Cochlear Nucleus**

Yehoash Raphael<sup>1</sup>, Seiji Shibata<sup>1</sup>, Chunhua Zeng<sup>1</sup>, Ziheng Yang<sup>1</sup>, Susan Shore<sup>1</sup>

<sup>1</sup>*University of Michigan*

Many individuals with severe hearing loss also suffer from debilitating tinnitus. In ears with extensive hair cell loss, the peripheral nerve processes of the auditory nerve (ANF) degenerate leading to eventual neuronal degeneration. Loss of ANFs following acoustic trauma is a significant

factor in predicting tinnitus (Bauer et al., J. Neurosci Res, 2007; Zeng et al., J. Neurosci., 2009; Schaette and Kempster, Hear. Res., 2009), implicating ANF loss as a major causal factor in tinnitus. Furthermore, we have shown that loss of ANF connections, as signified by vesicular glutamate transporter 1, VGLUT1, to the cochlear nucleus (CN) is an important signal for non-auditory projections from other parts of the brain (signified by VGLUT2) to infiltrate the CN. These non-auditory projections likely play an important role in generating hyperactivity that leads to tinnitus (Zeng et al, J. Neurosci, 2009). Here we test the hypothesis that enhanced ANF regeneration and spiral ganglion preservation in deaf ears result in maintenance of ANF connections with the brain, potentially restoring normal spontaneous activity in CN neurons, which will reduce or eliminate tinnitus in the guinea pig model. Adeno-associated viral vector with an NT-3 gene insert was delivered via scala tympani to guinea pigs two weeks after neomycin-induced unilateral deafness. Fourteen weeks later, following perfusion fixation, the cochleas and CNs were assessed. NT-3 therapy resulted ANF growth within the cochlea and survival of spiral ganglion neurons as well as maintenance of VGLUT1/VGLUT2 ratios in the regions of CN receiving ANF and non-auditory inputs, respectively. Restoring the balance of excitation from ANF and non-auditory projections the CN may provide an important therapeutic avenue for tinnitus reduction in patients with severe hearing loss and ANF degeneration.

This work is supported by The Williams Professorship, and NIH/NIDCD grants T32 DC-005356, and P30 DC-05188.

### **[236] Acoustic Insult Reverses Maturation of Excitatory But Not Inhibitory Synaptic Responses in the Lateral Superior Olive**

**Nadia Pilati**<sup>1</sup>, Cornelia Kopp-Scheinflug<sup>1</sup>, Haresh Selvaskandan<sup>1</sup>, Matthias Hennig<sup>2</sup>, Ian Forsythe<sup>1</sup>  
<sup>1</sup>MRC Toxicology Unit, University of Leicester, <sup>2</sup>Institute for Adaptive and Neural Computation, School of Informatics, University of Edinburgh

Brainstem auditory circuits undergo synaptic reorganization during maturation of hearing, but it is often assumed that the mature auditory brainstem exhibits little synaptic plasticity. The lateral superior olive (LSO) computes interaural level differences (ILD) by summation of ipsilateral excitatory and contralateral inhibitory synaptic inputs which arise from the respective cochlea. Using in vitro whole-cell patch clamp, in vivo auditory brainstem recordings (ABR) and computational modelling, we characterized developmental changes in synaptic inputs to the LSO and correlated these changes with maturation of ABR hearing thresholds and ILD functions. The decay kinetics of both EPSCs and IPSCs greatly accelerated during the development of mature hearing thresholds so that decay times ( $\tau$ ) were matched in mature mice. The relative input strength of excitation and inhibition also converged to similar values on maturation, so that excitation and inhibition achieve an equilibrium which is stable over time (up to P36). Computational modelling shows that ILD functions are mature when this equilibrium

is reached. However following exposure to loud sounds this equilibrium is disrupted. One week after sound trauma the EPSC decay time-constants were significantly slower while IPSC decay times were unchanged. These changes were accompanied by decrease in expression of mRNA in GluA4. Thus exposure to loud sound induces changes in subsynaptic receptor at excitatory inputs the LSO while inhibitory inputs are unchanged. The change in EPSC decay is reversible. We conclude that sound trauma induces central changes in synaptic transmission, distinct from peripheral auditory damage, by induction of glutamate receptor subunits expressed during earlier stages of development

### **[237] Tonotopic Organization of the Hyperpolarization-Activated Current (I<sub>h</sub>) in the Mammalian Medial Superior Olive**

**Veronika Auer**<sup>1</sup>, Simon Lehnert<sup>1</sup>, Christian Leibold<sup>1</sup>, Ursula Koch<sup>1</sup>

<sup>1</sup>Biologie Department II, LMU Muenchen, Germany

Interaural time differences (ITD) of sounds arriving at the two ears are the major auditory cue used to identify the azimuthal location of a low frequency sound source. ITDs are first encoded in neurons in the medial superior olive (MSO). The MSO is tonotopically organized along its dorsal-ventral axis, such that very low frequency sounds are encoded dorsally and higher frequency sounds are represented ventrally. Here we investigated in a gerbil brain slice preparation the biophysical properties of MSO neurons with different best frequencies. For this purpose, the MSO was subdivided into three regions based on its tonotopic map, namely a high frequency (HF), a middle frequency (MF) and a low frequency (LF) region. Patch clamp recordings were performed to compare both intrinsic electrical and synaptic properties of MSO neurons between these regions. The data revealed that the conductance of hyperpolarization-activated cyclic nucleotide-gated (HCN) cation channels, the membrane properties of the neurons and the time course of inhibitory postsynaptic potentials (IPSPs) vary along the dorsal-ventral axis. HCN current density was larger and the steady-state activation curve of I<sub>h</sub> was more positive in neurons in the HF region compared to neurons in the LF region. Consistent with our observation of a dorsal-ventral gradient in HCN current density we also found a dorsal-ventral gradient in the half-width of evoked IPSPs. Simulation results from a single-compartment model suggest that tonotopic organization of HCN current density and IPSP kinetics are functionally related to auditory processing in the different frequency channels: Faster IPSPs and an increased level of HCN in high-frequency neurons reduce the level of temporal summation of inhibitory inputs. Thus, tonotopic specialization may enable these neurons to accurately encode ITDs over a wide range of frequencies.

### **238 Biphasic and Compartment-Specific Changes in Dendritic Kv3.1b of Binaural Auditory Neurons Following Manipulations of Synaptic Inputs**

Yuan Wang<sup>1</sup>, Yong Lu<sup>2</sup>, Maile R. Brown<sup>3</sup>, Leonard K. Kaczmarek<sup>3,4</sup>, Edwin W. Rubel<sup>1</sup>

<sup>1</sup>Virginia Merrill Bloedel Hearing Research Center, Department of Otolaryngology, Uni. of Washington,

<sup>2</sup>Department of Anatomy and Neurobiology, Northeast Ohio Medical University, <sup>3</sup>Departments of Pharmacology, Yale University School of Medicine, <sup>4</sup>Departments of Cellular and Molecular Physiology, Yale University School of Medicine

The high-threshold voltage-gated potassium channel 3.1b (Kv3.1b) facilitates fast spiking and influences the precision of temporal coding. Here we use immunocytochemistry to examine subcellular changes in Kv3.1b protein level in chicken nucleus laminaris (NL) following differential manipulations of synaptic inputs. Dendrites of NL neurons segregate into dorsal and ventral domains, receiving excitatory input from the ipsilateral and contralateral ears, respectively, via nucleus magnocellularis (NM). Without intervention Kv3.1b is distributed largely symmetrically between the two dendritic domains, although slightly higher dorsally. Following unilateral cochlea removal, Kv3.1b level in deprived NL domains (dorsal ipsilaterally and ventral contralaterally) exhibits a biphasic change with transient decrease at 1-6h, recovery at 12h, and increase at 24-96h, as compared to the other domain of the same neurons. The initial decrease is more distinct in the high frequency region while the increase is detected first in the low frequency region and later throughout the whole nucleus. In contrast, transection of NM axons led to decreases in Kv3.1b levels in deprived ventral domains at all time points up to 24h. These data suggest that the initial decrease may result from cessation of action potentials caused by either manipulation while the later increase induced by cochlea removal require the silent presynaptic appositions that largely remain following cochlea removal but are gradually eliminated following axon transection. In addition, we examine the distribution of FMRP (Fragile X Mental Retardation Protein) in NL neurons, an mRNA-binding protein required for activity-regulated Kv3.1b expression. NL neurons express remarkably high level of FMRP in the soma and dendrites. Notably, dendritic FMRP is accumulated at enlarged branch points and terminal endings. The role of FMRP in compartment-specific cellular events such as Kv3.1 regulation is under current investigation.

### **239 The Sound of Silence: Ionic Mechanisms Encoding Sound Termination**

Conny Kopp-Scheinflug<sup>1</sup>, Adam Tozer<sup>1</sup>, Sue Robinson<sup>1</sup>, Bruce Tempel<sup>2</sup>, Matthias Hennig<sup>3</sup>, Ian Forsythe<sup>4</sup>

<sup>1</sup>MRC Toxicology Unit, <sup>2</sup>University of Washington,

<sup>3</sup>University of Edinburgh, <sup>4</sup>University of Leicester

Offset-responses upon termination of a stimulus are crucial for perceptual grouping and gap detection. These gaps are

key features of vocal communication, but an ionic mechanism capable of generating fast offsets from auditory stimuli has proven elusive. Offset-firing arises in the brainstem superior paraolivary nucleus (SPN) which receives powerful inhibition during sound and converts this into precise action potential (AP) firing upon sound termination. Whole-cell patch recording in vitro showed that offset-firing was triggered by IPSPs rather than EPSPs. We show that AP firing can emerge from inhibition through integration of large IPSPs, driven by an extremely negative chloride reversal potential (ECl), combined with a large hyperpolarization-activated non-specific cationic current (IH), with a secondary contribution from a T-type calcium conductance (ITCa). On activation by the IPSP, IH potently accelerates the membrane time constant, so when the sound ceases, a rapid repolarization triggers multiple offset APs which match onset timing-accuracy.

### **240 Faithful Transmission at the Inhibitory MNTB-LSO Synapse and the Role of Glycine Uptake Transporter GlyT2**

Florian Kramer<sup>1</sup>, Désirée Griesemer<sup>1</sup>, Eckhard Friauf<sup>1</sup>

<sup>1</sup>University of Kaiserslautern, Animal Physiology Group

High frequency transmission is crucial for information processing in the mammalian auditory brainstem. Neurons in the medial nucleus of the trapezoid body (MNTB) can faithfully follow glutamate-mediated input rates of up to 800 Hz. Less is known about the glycinergic projection from the MNTB to the lateral superior olive (LSO), which is involved in sound localization. This system is ideally suited to analyze the faithfulness of transmission at inhibitory synapses, which, in contrast to excitatory inputs, has not been investigated so far. We analyzed the MNTB-LSO connection in acute mouse brain slices at P10-12. Focal electrical stimulation in the MNTB was combined with patch-clamp recordings of LSO neurons at 25 or 37°C, and stimulation frequencies ranged from 1 Hz to 100 Hz. IPSCs showed a frequency-dependent decrease in amplitude and an increase in failure rate (94% vs. 64% for 100 Hz at the end of a 40 s trial) for both temperatures. The magnitude was temperature-dependent. These results suggested that the amount of glycine that is continually released upon high frequency stimulation is temperature-dependent and that an enzyme-based mechanism participates in the supply. We hypothesized that the glycine transporter GlyT2 is involved and helps to replenish the transmitter supply. To test our hypothesis, we used GlyT2<sup>-/-</sup> mice. IPSC kinetics and amplitude were not altered, but the success rate of the electrical stimulation was decreased to 15% (n=171; WT: 63%, n=67). The IPSCs of responding GlyT2<sup>-/-</sup> cells declined more rapidly during high frequency stimulation (50 Hz, 60 s, 37°C) than in wild-type and tended to reach significantly lower steady state levels. In summary, our results indicate that the faithfulness of inhibitory transmission in the MNTB-LSO path is lower than in the excitatory transmission to the MNTB. The lack of GlyT2 results in a lower glycine amount in the presynaptic terminals, which becomes crucial only during prolonged high frequency stimulation.

## **[241] Neuronal Size Gradient Discovered in the MNTB Requires Auditory Activity**

Jessica A. Hill<sup>1</sup>, Cornelia Kopp-Scheinflug<sup>2</sup>, Yuan Wang<sup>1</sup>, Ian D. Forsythe<sup>2</sup>, Edwin W Rubel<sup>1</sup>, Bruce L Tempel<sup>1</sup>

<sup>1</sup>University of Washington, <sup>2</sup>University of Leicester  
*dfw*<sup>2J</sup> mutant mice have a null mutation in the plasma membrane calcium ATPase 2 (PMCA2) causing deafness in homozygotes(-/-) and high frequency hearing loss in heterozygotes(+/-). Outer hair cells express PMCA2 and *dfw*<sup>2J</sup> -/- mutants show hair cell loss and abnormalities. Because neurons in the medial nucleus of the trapezoid body (MNTB) also express PMCA2, we postulated these neurons may also be lost or abnormal. To test this hypothesis we used Nissl stained sections to measure MNTB volume, cell number, and cell size for +/+, +/-, and -/-. We found no significant difference in total MNTB volume or cell number between genotypes, but there was a decrease in cell size between +/+ controls and -/-.

The MNTB exhibits a tonotopic gradient with medial cells responding best to high frequencies and lateral cells responding best to low frequencies. To determine if cell size was differentially regulated along the tonotopic axis, observers blind to genotype measured cell sizes along this axis. In +/+ controls the medial cells were significantly smaller than the lateral cells suggesting the presence of a cell size gradient. This size gradient is decreased in +/- and absent in -/-, data which is corroborated by capacitance measurements.

To determine if the absence of the neuronal size gradient in -/- was caused by abnormal inputs from the cochlea, we used DTR mice in which hair cells can be selectively ablated. These mice also show no cell size gradient after hair cells have been ablated suggesting auditory activity is necessary for the maintenance of the gradient. To determine if the gradient could return after activity was reinstated, we treated gerbils with TTX to block action potentials arising in the cochlea. Normal gerbils showed a cell size gradient but the gradient was absent in gerbils treated for 48 hours with TTX. In gerbils allowed to recover for 7 days after TTX treatment, the gradient had recovered suggesting these changes in neuron size are plastic and reversible.

## **[242] Physiology of Unipolar Brush Cells in the Dorsal Cochlear Nucleus**

Carolina Glogowski<sup>1</sup>, Laurence Trussell<sup>1</sup>  
<sup>1</sup>Oregon Health & Science University

The dorsal cochlear nucleus (DCN) integrates auditory input with multisensory signals from various brain regions. Multisensory signals are conveyed by mossy fibers which terminate in the deep layer of the DCN and whose main targets are granule cells. However, a large subset of granule cells also receives multisensory input through a feedforward excitatory pathway mediated by an excitatory interneuron called the unipolar brush cell (UBC). UBCs have a peculiar morphology, with a single short dendrite terminating in a brush-like structure that interdigitates with a single pre-synaptic mossy terminal. UBCs are also prominent in the vestibular cerebellum. One cerebellar

model suggests that the large irregular synapse onto UBCs entraps the transmitter glutamate and slows diffusion. Thus, the prolonged glutamate transient leads to a characteristic slow-decaying post-synaptic current (EPSC) which mediates repetitive firing in UBCs. DCN UBCs share homology with their cerebellar counterparts. Although they are one of the primary targets of mossy fibers carrying multisensory signals, their impact on granule cell activity in either DCN or cerebellum has never been directly investigated. We have made recordings from UBCs in slices from 3-week old mouse DCN, characterizing the basic intrinsic and synaptic properties of these neurons. We find that DCN UBCs exhibit bimodal firing (tonic vs burst mode) dependent on the resting membrane potential. Evoked EPSCs have a striking biphasic decay, with a slow component lasting hundreds of milliseconds. We also observed that EPSC amplitudes show strong synaptic depression and have very low trial-to-trial variability, suggestive of a high probability of transmitter release. These features are consistent with a model in which the large UBC synapse may function to amplify signals from mossy fibers, thereby increasing the salience of a subset of non-auditory signals.

## **[243] Responses of a Spherical Bushy Cell Model to Realistic Inputs**

Thomas Kuenzel<sup>1</sup>

<sup>1</sup>RWTH Aachen University

Low-frequency spherical bushy cells (SBC) of the anteroventral cochlear nucleus receive strong excitation by one or very few auditory nerve fibers. SBC not only maintain the high temporal precision already present in the auditory nerve inputs but even enhance phase-locking. The mechanisms of this enhancement are not fully understood. Among other things convergence with inhibitory inputs was suggested to play a role. In a recent in-vivo study [Kuenzel T et al., 2011] inhibition was found to further increase the dynamic spike threshold of SBC. In that study an SBC model was used to simulate membrane potential responses upon convergence of excitatory and hyperpolarizing inhibitory inputs. The model replicated some key features seen in the in-vivo recordings.

Here I extend these simulations by driving the excitatory input of the SBC model with presynaptic spike arrival times recorded in the cochlear nucleus of the gerbil. The data consist of spontaneous activity of various rates and responses to pure tone stimuli. The first derivative of the simulated membrane potential is analyzed. A hyperpolarizing inhibitory synapse model is added to the SBC model, driven by the same spike-arrival times with a short delay.

Responses of the SBC model without inhibitory inputs support the observation made in the in-vivo study that refractory processes alone do not cause non-monotonic tuning. However the inclusion of the inhibitory synapse does indeed produce non-monotonic responses of the model. Only a weak inhibitory synaptic conductance, which summates during the stimulus due to the long decay time constant, is necessary for this. The influence of delay, decay time constant and maximum conductance of the

inhibitory input on the simulated tuning and temporal precision of the SBC model are explored in more detail.

### **[244] Effects of Glycinergic Inhibition on Spectral and Temporal Coding in the Rat's Ventral Cochlear Nucleus**

**Matthew Roos**<sup>1</sup>, Bradford May<sup>1</sup>

<sup>1</sup>*The Johns Hopkins University*

Anatomical studies of the rat's ventral cochlear nucleus (VCN) have produced a wealth of information on a local inhibitory circuitry with the capacity to refine the spectral and temporal tuning characteristics of inputs from the auditory periphery. To explore the spectral coding properties of this well-defined functional anatomy, physiologically classified neurons were evaluated with the method of random spectral shapes (RSS). Changes in discharge rate during pseudorandom variations of the amplitude spectrum of RSS stimuli reveal the frequency selectivity of a neuron's excitatory and inhibitory inputs. As previously noted in domestic cats, primarylike and chopper units in rats exhibited excitatory receptive fields that were centered on BF, predominately linear, and level tolerant. Chopper units displayed stronger off-BF inhibition than primarylike units, but similar spectral selectivity. To assess temporal coding, the method of random temporal shape (RTS) stimuli was applied. Rate changes during variations in the temporal envelope of RTS stimuli reveal the temporal characteristics of a neuron's excitatory and inhibitory inputs. Preliminary results indicate that temporal coding is better among chopper units than primarylike units, with transient choppers (Ch-T) providing the most selective representation. A potential role for glycinergic inhibition in the enhanced temporal selectivity of Ch-T units was tested with iontophoretic applications of strychnine. The glycine antagonist effectively transformed Ch-T units into less temporally specialized chopper response patterns. These preliminary observations suggest that glycinergic inhibition is an essential element of temporal coding in the VCN.

### **[245] Tonotopic Specialization of Cellular and Synaptic Properties in Nucleus Magnocellularis: Implications for Input Integration**

**Stefan N. Oline**<sup>1</sup>, R. Michael Burger<sup>1</sup>

<sup>1</sup>*Lehigh University*

Neurons in nucleus magnocellularis (NM) receive inputs from auditory nerve fibers, and process temporal information that is then conveyed to binaural neurons in nucleus laminaris. NM is tonotopically organized primarily along a single rostrocaudal axis and shows specialized properties that vary along this axis. These include differences in distribution or density of voltage gated channels as well as synaptic input number, morphology, and strength. These adaptations contribute to the tuning precision of individual neurons that process a narrow range of frequencies. However, how these features cooperate to contribute to NM response properties has not been comprehensively evaluated. To begin to address this

problem, we investigated both pre- and postsynaptic properties that impact the computational efficacy of NM neurons across the tonotopic axis. Specifically, we evaluated the temporal selectivity of NM neurons postsynaptically and short-term plasticity of their synaptic inputs. One measure of NM input selectivity that can provide insight into the temporal integration properties of individual neurons is the voltage slope-threshold of the cell, defined as the minimum rate of depolarization at which the cell will fire an action potential. We used whole cell patch clamp recordings to inject a series of ramped depolarizing currents into the neuron evoking systematically varying rates of depolarization. We found that slope threshold and integration time differs significantly between neurons that process high versus low frequency. To further examine how synaptic input interacts with the tonotopic variation in threshold, we investigated excitatory postsynaptic currents in voltage clamp under different rates of stimulation to measure synaptic depression. High characteristic frequency (CF) neuron inputs were more robust at each stimulation frequency tested, and depressed less than their low CF counterparts. Taken together these data suggest that specialization of these auditory neurons to an input frequency is facilitated by both pre- and postsynaptic properties. This work was supported by NIH/NIDCD R01-DC008989.

### **[246] Innervation of the Ventral Cochlear Nucleus in Mice That Lack Npr2, a Receptor Guanylyl Cyclase**

Xiao-Jie Cao<sup>1</sup>, Cindy Lu<sup>2</sup>, Samantha Wright<sup>1</sup>, Lisa Goodrich<sup>2</sup>, **Donata Oertel**<sup>1</sup>

<sup>1</sup>*University of Wisconsin*, <sup>2</sup>*Harvard Medical School*

Spiral ganglion cells bifurcate as they enter the central nervous system, with the ascending branch innervating the anterior ventral cochlear nucleus (aVCN) and the descending branch innervating the posterior VCN and DCN. The axons of cutaneous sensory neurons also bifurcate as they enter the spinal cord, one branch heading rostralward and the other caudalward. Like cutaneous sensory neurons, spiral ganglion cells in *cn/cn* mice, mice that lack the receptor guanylyl cyclase *Npr2*, fail to bifurcate (Schmidt et al., *J Cell Biol* 179:331, 2007; Lu et al., *J Neurosci* 31:10903, 2011). To understand what the consequences are of the failure to bifurcate on the innervation of the ventral cochlear nucleus, we have made whole-cell patch-clamp recordings in slices. As in *cn/+* and *+/+*, the principal cells in *cn/cn* mice are clearly recognizable. Mutant bushy cells generally fire transiently after the onset of a depolarization but occasionally fire tonically throughout a 200 ms-depolarization. Mutant T stellate cells consistently fire tonically for the duration of a depolarization as in the wild type. Resting potentials and input resistances are not significantly different in *cn/cn*, *cn/+* and *+/+* neurons. Responses to shocks of excitatory inputs to neurons in the VCN are, however, unusual. In *+/+* and *cn/+* mice, responses to trains of shocks consistently show synaptic depression, the first synaptic response being large and succeeding responses becoming

progressively smaller; the degree of depression depends on the cell type and on the rate of shocks. Unlike in *cn/+* mice, numerous synaptic failures were observed in bushy and T stellate cells of *cn/cn* mice over a wide range of shock strengths. The observation that failures were observed in both bushy and T stellate cells in responses to the first of a train of shocks suggests that failures are caused by conduction failure presynaptically. This work was supported by grants from the NIH DC000176 to D.O. and DC009223 to L.V. G..

## **247** Commissural Axons of the Mouse

### **Cochlear Nucleus**

**M. Christian Brown**<sup>1,2</sup>, Marie Drottar<sup>1</sup>, Thane E. Benston<sup>1</sup>, Keith N. Darrow<sup>1,3</sup>

<sup>1</sup>*Massachusetts Eye & Ear Infirmary*, <sup>2</sup>*Harvard Medical School*, <sup>3</sup>*Worcester State University*

Commissural axons connect the cochlear nucleus (CN) on one side with the CN on the opposite side. The terminal arbors of these axons have not been demonstrated. In order to study their terminations, we labeled commissural axons with the anterograde tracer biotinylated dextran amine (BDA), which was injected into the dorsal subdivision of the CN of mice. The number of commissural axons was correlated ( $R=0.97$ ) with the number of labeled radiate multipolar neurons of the ventral subdivision of the CN, suggesting they are the source of most of the axons. Labeled commissural axons averaged 2.1  $\mu\text{m}$  in diameter (10 fibers measured just before entry into the opposite CN). These axons are thicker than auditory-nerve fibers. Commissural axons exited the injected CN via the dorsal acoustic stria and crossed the midline in the dorsal half of the brainstem. On the side opposite from the injection, they entered the CN by various routes (dorsal, intermediate, or ventral acoustic striae). Terminal arbors of individual axons were generally confined to a single CN subdivision (22 out of 24 fibers). The arbors were extensive. Some axons terminated over much of the dorso-ventral extent of the CN. Each axon produced numerous swellings: One formed 576 en passant and 118 terminal swellings. Electron microscopy indicated myelination of the axons and synapses from the labeled swellings onto dendrites and neurons. Our data suggest that individual commissural axons influence wide areas of the CN and thus affect processing for a wide range of characteristic frequencies.

Supported by: NIDCD RO1 DC01089.

## **248** Enwrapping of Perisynaptic Astrocytes Around Endbulb Synapses of the Rat Ventral Cochlear Nucleus

**Cheryl Clarkson**<sup>1</sup>, Maria Rubio<sup>1</sup>

<sup>1</sup>*University of Pittsburgh*

Astrocytes, non-neuronal cells, play a key role in the modulation of synaptic transmission (Di Castro et al., 2011; Oliet et al., 2004) by adjusting the glutamate clearance via glutamate transporters (Huang and Bergles, 2004) and acting as physical barriers restricting glutamate spillover to nearby postsynaptic densities (PSD) (Oliet et al., 2004). Previous studies show that changes in neuronal activity

induce shifts in astrocytes perisynaptic enwrapping. After synaptic potentiation in the hippocampus or sensorial stimulation in the cortex, the glial enwrapping increases in both pre and postsynaptic neuronal compartments (Genoud et al., 2006; Lushnikova et al., 2009). The astrocytic response after neuronal changes is indispensable for coordinating and maintaining normal brain networks (the tripartite synapse, Perea et al., 2009). However, the function of astrocytes in the auditory system of normal and hearing impaired conditions is still poorly understood, and the coverings of perisynaptic astrocytes within auditory synapses remain unexplored. In this study, we investigate the relationship between perisynaptic astrocytes and endbulb synapses in normal hearing (sham) and after 10-days monaural conductive hearing loss (earplugging) rats. To do so, ultrastructural data is volumetrically reconstructed and morphometric features extracted. Our data of normal hearing animals show that the extension of perisynaptic astrocytes enwrapping endbulbs is about 30%, with the extension of enwrapping varying between small (1-2  $\mu\text{m}$ ; 43%) and medium (2-4  $\mu\text{m}$ ; 20%) sized endbulbs. We also find that 88% of the endbulb PSDs have astrocyte processes nearby, suggesting that astrocytes restrict the glutamate spillover between active synaptic zones. Our results suggest that perisynaptic astrocytes around the endbulbs are an important component to preserve or improve the temporal coding of sound information arriving from auditory nerve fibers.

## **249** Synaptic Lights: Localizing Presynaptic Inputs in an Identified LSO Dendritic Tree

**Alan Cooper**<sup>1</sup>, Daniel Case<sup>1</sup>, Deda Gillespie<sup>1</sup>

<sup>1</sup>*McMaster University*

The large principal cells of the lateral superior olive (LSO) compute interaural intensity differences by comparing converging excitatory and inhibitory inputs in what is generally represented as a simple summation. In light of this relatively simple computation the bipolar morphology of these projection neurons, which can span 200  $\mu\text{m}$ , appears unnecessarily complex. In order to better understand how dendritic integration might influence the computation performed by LSO principal cells, we developed a method to map the distribution of phenotypically distinct inputs along these cells. We describe light microscopic methods that are comparatively inexpensive and straightforward and can be used in both neonatal and adult tissue.

We used patch pipettes to label cells with biocytin in acute 300  $\mu\text{m}$  slices from early postnatal rat pups or sharp electrodes to label cells with Lucifer Yellow in fixed tissue slices from adult rats. Slices were resectioned at 60  $\mu\text{m}$  and excitatory and inhibitory presynaptic terminals were labeled using immunofluorescence for vesicular transporters. Tissue sections were cleared by processing through the high refractive index mounting medium 2,2'-thiodiethanol (measured RI=1.515), permitting bright, high resolution images to be acquired throughout the relatively thick tissue sections at the confocal microscope. Serial

optical sections were reconstructed to produce a 3-D representation of the entire cell together with the location of its presumptive presynaptic inputs.

### **[250] Direct Projections from Multiple Nuclei of the Superior Olivary Complex to the Medial Geniculate Body of the Thalamus in the Rat**

**Albert S. Berrebi<sup>1</sup>**, M.- Auxiliadora Aparicio<sup>2</sup>, Yong-Ming Jin<sup>1</sup>, David M. Sloan<sup>1</sup>, Marcelo Gómez-Alvarez<sup>2</sup>, Francisco Javier Bernardo<sup>2</sup>, Enrique Saldaña<sup>2</sup>

<sup>1</sup>*Sensory Neuroscience Research Center, West Virginia Univ. School of Medicine, Morgantown, WV,*

<sup>2</sup>*Neuroscience Institute of Castilla y León (INCYL), Univ. of Salamanca, SPAIN*

It is generally accepted that ascending projections from the superior olivary complex (SOC) do not extend beyond the level of the inferior colliculus (IC). Here we report the existence of direct projections from the SOC of the rat to the medial geniculate body (MGB).

We initially injected the bidirectional tracer biotinylated dextran amine (BDA) into the superior paraolivary nucleus (SPON), which is one of the largest nuclei of the rodent SOC. In addition to the known projections of the SPON (Saldaña et al., *Neurosci* 163:372-387, 2009; Viñuela et al., *Front Neuroanat* 5:1, 2011), in each case we observed a somewhat sparse, but consistent, projection to the ipsilateral MGB. SPON fibers enter the MGB via the brachium of the IC and target preferentially the medial division of the MGB (MGBm), the suprageniculate nucleus, the marginal zone, the posterior intralaminar nucleus and the dorsal region of the dorsal division of the MGB (MGBd); all of these territories are known to send projections to the lateral nucleus of the amygdala (Doron & Ledoux, *J Comp Neurol* 425:257-274, 2000), which is implicated in processing the emotional aspects of auditory information. Scarcer labeled SPON fibers were found in the ventral division of the MGB (MGBv), whereas no labeled fibers were observed in other thalamic nuclei.

To characterize those SPON neurons that innervate the thalamus, we then made large injections of the retrograde tracer FluoroGold into the MGB. As expected, we found abundant labeled neurons throughout the ipsilateral SPON. We also noted abundant labeled neurons in other SOC nuclei, including the ipsilateral MSO and the contralateral LSO, as well as in an ill-defined territory wedged between the medial nucleus of the trapezoid body and the SPON. Our unbiased stereological estimates indicate that approximately 50 % of all MSO and SPON neurons, and 25 % of all LSO neurons innervate the MGB.

Supported by grants FIS PI10/01803 (E.S.) and NIH DC-002266 (A.S.B.).

### **[251] Synaptic Plasticity at Steady-State**

**Hua Yang<sup>1</sup>, Matthew Xu-Friedman<sup>1</sup>**

<sup>1</sup>*University at Buffalo, SUNY*

Auditory nerve fibers commonly show high levels of activity, even in the absence of sound. In vitro studies of auditory nerve synapses in the cochlear nucleus, at so-called endbulbs of Held, show significant depression when driven at these high rates compared to rested synapses.

However, when synapses are driven at physiologically-relevant rates for some time, it is not known whether the deterministic mechanisms of synaptic plasticity, so clear in rested synapses, play much of a role, or whether the stochastic properties of release dominate EPSC amplitude. We investigate this question by delivering extended regular or Poisson-distributed trains and quantifying EPSC amplitude at steady-state. We find that EPSC amplitudes vary in consistent ways from trial to trial, yet the previous interval is a poor predictor of the next EPSC amplitude, which is quite unlike rested synapses. This indicates that EPSC amplitude is influenced by multiple deterministic processes that act over a longer history of activity to either enhance or reduce EPSC amplitude. We investigate the duration of this influence in two ways, by comparing trains in which a single stimulus is skipped, and by a reverse correlation analysis of activity levels preceding EPSCs. Furthermore we find that the stochastic properties of release that ride on these deterministic changes play an important role in the input-output function of the synapse.

### **[252] Stimulus-Timing Dependence of Auditory-Somatosensory Bimodal Plasticity in Dorsal Cochlear Nucleus Neurons**

**Seth Koehler<sup>1</sup>**, Greg Basura<sup>1</sup>, Ishwan Biswas<sup>1</sup>, Susan Shore<sup>1</sup>

<sup>1</sup>*University of Michigan*

Neurons in the dorsal cochlear nucleus (DCN) integrate auditory and somatosensory inputs. Bimodal stimulation with sound and electrical activation of spinal trigeminal nucleus (Sp5) induces long-term enhancement or suppression of subsequent sound-evoked responses in DCN units (Dehmel, ARO 2011). In the present study, we hypothesize that the bimodal plasticity observed in vivo is mediated by synaptic plasticity at parallel fiber synapses, which convey somatosensory input from Sp5 to DCN.

Bimodal plasticity was measured by recording spontaneous and sound-evoked neural activity before and after bimodal stimuli. To test the involvement of spike-timing dependent plasticity (STDP), we altered the order and interval between sound and Sp5 stimuli. Single and multi-unit spikes were recorded using multi-channel extracellular electrode arrays spanning the DCN tonotopic axis.

Bimodal stimulation induced stimulus-timing dependent long-term suppression and enhancement of sound-evoked firing rates. In each unit, bimodal plasticity was most effective at a particular Sp5-sound interval. Timing rules in some units were similar, but broader, than those found for STDP in vitro (Tzounopoulos, 2007). Bimodal stimulation with sound-Sp5 intervals of 20 – 40 ms induced maximal suppression or enhancement, while simultaneous Sp5-sound stimulation induced minimal suppression or enhancement. Reversing the order of the sound and Sp5 stimuli inverted the long-term effect on firing rates. These results suggest that STDP plays a role in the bimodal induction of long-term plasticity in DCN neural activity. The modification of sound-evoked responses by somatosensory context may be a mechanism for the putative role of the DCN in adaptive filtering. It may also

play a role in the development of somatosensory-based tinnitus by contributing to elevated spontaneous firing rates in DCN neurons.

Supported by NIH RO1 DC004825 (SES), P30 DC05188 (SES), R03 DC009893-01 (GB), and T32 DC00011 (SDK).

### **253 Intrinsic Plasticity of MSO Neurons in Vitro Before Hearing Onset**

**Sheree D. Cherry<sup>1</sup>**, Travis A. Babola<sup>1</sup>, Nace L. Golding<sup>1</sup>

<sup>1</sup>*Section of Neurobiology and Center for Learning and Memory, University of Texas at Austin*

In mature gerbils, the intrinsic properties of KCNA1 and HCN channels in the medial superior olive (MSO) play a critical role in setting the fine temporal resolution required for binaural coincidence detection. Previous studies have demonstrated that in mature MSO neurons both of these channel types control the resting membrane potential as well as impart a low input resistance (<10 M $\Omega$ ) and fast membrane time constant (~0.3 ms).

We asked whether changes in ion channel properties might be induced prior to hearing onset either by synaptic and/or firing activity. To address this question, we made whole-cell recordings from MSO neurons in gerbil brainstem slices before hearing onset (P9-P11; 35°C). To induce changes in the properties of voltage-gated ion channels, we generated patterns of synaptic and firing activity in a frequency range that were modeled after spontaneously occurring activity. Synaptic stimuli consisted of a 100 Hz train of 10 stimuli that repeated every 2 seconds for 20 repetitions. Trains of synaptic stimuli that elicited a mixture of action potentials and subthreshold EPSPs decreased the input resistance of MSO neurons by 42% compared to baseline ( $p=0.025$ ), while the membrane time constant decreased by 66% (13.7 ms to 4.6 ms,  $n=5$ ,  $p=0.006$ ). Concurrent with the change in input resistance, the membrane potential hyperpolarized by 5-10 mV. Subsequent experiments explicitly pairing subthreshold (3-8 mV) EPSPs and action potentials (the latter elicited by brief current pulses aligned at the peak of EPSPs) triggered decreases in input resistance and membrane time constant of 47% and 67%, respectively ( $p=0.007$  and  $0.006$ ,  $n=5$ ), suggesting that the number of action potentials during induction stimuli was not a strong determinant of the magnitude of intrinsic plasticity. Taken together, these findings indicate that the maturation of intrinsic membrane properties of MSO neurons is driven by synaptic and firing activity before the onset of hearing.

### **254 Group II mGluR-Mediated LTD of GABAergic Transmission in Avian Cochlear Nucleus Magnocellularis Neurons**

**Zheng-Quan Tang<sup>1</sup>**, William Hamlet<sup>1,2</sup>, Emilie Hoang Dinh<sup>1</sup>, Wei Shi<sup>1,2</sup>, Yong Lu<sup>1,2</sup>

<sup>1</sup>*Northeast Ohio Medical University*, <sup>2</sup>*Ket State University School of Biomedical Sciences*

Long-term plasticity, particularly long-term depression (LTD), a persistent activity-dependent reduction in the efficiency of synaptic transmission, has been extensively studied at glutamatergic synapses, but is poorly

understood at inhibitory synapses. In this study, we show that activation of group II metabotropic glutamate receptors (mGluRs) induces LTD of GABAergic transmission in chicken cochlear nucleus magnocellularis (NM) neurons. Immunohistochemistry and western blot confirmed the expression of group II mGluRs in the NM. Whole-cell recordings from brain slice preparations showed that bath application of group II mGluR agonist DCG-IV (4  $\mu$ M) for 10 minutes induced a strong initial inhibition followed by LTD of evoked IPSCs or IPSPs in NM neurons. The LTD was not abolished by APV (50  $\mu$ M), an antagonist for NMDA receptors. The signaling transduction pathway mediating the LTD appeared to involve adenylyl cyclase and protein kinase A, because the LTD was sensitive to SQ 22536 (50  $\mu$ M) and KT 5720 (1  $\mu$ M), their respective inhibitors. Application of LY 341495 (10 nM), a selective antagonist for group II mGluRs, increased the amplitude of IPSCs evoked by presynaptic stimuli that concurrently activated both the glutamatergic and GABAergic pathways. The enhancement of IPSCs by LY 341495 was not different at stimulus frequencies of 3.3, 100, or 300 Hz. These results suggest that sustained activity of endogenous group II mGluRs may constitutively regulate the basal level of GABA release in vivo.

Supported by NIH Grant DC008984 to YL.

### **255 In Vivo Dynamic Regulation of Afferent Activity on Dendritic Patterning of Binaural Auditory Neurons**

**Yuan Wang<sup>1</sup>**, Edwin W. Rubel<sup>1</sup>

<sup>1</sup>*Virginia Merrill Bloedel Hearing Research Center, Department of Otolaryngology, Uni. of Washington*

Neuronal dendritic structure responds to changes in afferent inputs. Chicken nucleus laminaris (NL) provides a suitable model to study compartment-specific dendritic regulation with a matched intracellular control. Dendrites of NL neurons segregate into dorsal and ventral arborizations, receiving excitatory input from the ipsilateral and contralateral ears, respectively, via nucleus magnocellularis (NM). Transection of NM axons to the contralateral NL leads to rapid retraction of ventral, but not dorsal, dendrites of NL neurons. Blocking action potentials from one ear by either cochlea removal or temporary treatment of tetrodotoxin (TTX), a sodium channel blocker, led to significant retraction of affected NL dendrites within 8h, comparable to that induced by transection of NM axons. More importantly, when the inner ear activity was allowed to recover from TTX treatments, retracted NL dendrites regrew to their normal length within 48h. Analyses of dendritic structure suggest that these structural changes involve selective elimination/addition of terminal dendritic branches. These results indicate that early changes in NL dendrites following alternations in afferent inputs are not cellular events towards degeneration, but activity-dependent dynamic modulation, particularly by action potentials.

To explore whether presence of silent presynaptic appositions contributes to NL dendritic maintenance, we examined changes in NL dendrites at 96h following unilateral cochlear removal. In addition to persistent

cessation of action potentials, cochlea removal decreases the neuronal number of NM, which presumably affects the pattern and/or the total number of presynaptic terminals apposed to NL dendrites. We found that animals with a higher percentage of cell death in the ipsilateral NM tended to have a higher degree of dendritic retraction in NL. This correlation supports a role of presynaptic contacts in postsynaptic dendritic maintenance in the absence of action potentials.

### **256 Training/Career Development Workshop and Early Stage/New Investigator Workshop**

**Janet Cyr<sup>1</sup>**, Christine Livingston<sup>1</sup>, Susan Sullivan<sup>1</sup>, Bracie Watson<sup>1</sup>

<sup>1</sup>NIH/NIDCD

NIDCD will offer two concurrent workshops targeted to specific audiences. One workshop is specifically targeted to individuals interested in Training and Career Development. The second workshop is targeted to Early Stage Investigators and New Investigators.

Workshop #1: Targeted to individuals interested in Training and Career Development.

The *Training and Career Development* workshop will include an overview of research training and career development opportunities appropriate for graduate students, postdoctoral fellows and new clinician investigators. The discussion will include the submission and review of individual NRSA fellowship awards (F30, F31 & F32), as well as the mentored career development awards (K08, K23 & K99/R00) and the NIH Loan Repayment Program. Drs. Janet Cyr and Susan Sullivan will lead the presentation.

Workshop #2: Targeted to Early Stage Investigators (ESI) and New Investigators (NI).

The *Early Stage/New Investigator* workshop will provide practical information on how grant applications are processed within NIH/NIDCD including Institute and study section assignments, pay lines, and the roles of program and review staff. The goal is to provide information to early stage investigators to facilitate their successful transition from trainee to independent investigator. Specific information will be presented regarding funding opportunities for early stage investigators (ESIs), including the NIH Research Program Grant (R01) and the NIDCD Small Grant Award (R03), and recent changes in peer review. Drs. Bracie Watson and Christine Livingston will lead the presentation.

### **257 In Vivo Juxtacellular Recordings of the Gerbil Medial Superior Olive**

**Marcel van der Heijden<sup>1</sup>**, Jeannette Lorteije<sup>1</sup>, J. Gerard G. Borst<sup>1</sup>

<sup>1</sup>Erasmus MC, Rotterdam, The Netherlands

Neurons in the medial superior olive (MSO) receive excitatory information from both ipsi- and contralateral spherical bushy cells of the cochlear nucleus. MSO cells are sensitive to the arrival times of tones at both ears, suggesting that they function as coincidence detectors. However, direct measurements of their synaptic inputs during auditory stimulation have not yet been reported. To

investigate how MSO cells process interaural time differences we made juxtacellular recordings from anesthetized gerbils. In the absence of auditory stimulation, all recorded cells showed small, positive-going events whose durations matched those of EPSPs in slice recordings. Despite the high rate of these events (>400 events/s) the spontaneous firing rate of MSO neurons was typically low (<10 sp/s). During tone stimulation, the subthreshold activity turned more regular owing to phase locking to the stimulus. The largest events triggered spikes, which showed excellent phase locking at low frequencies (vector strength typically >0.8). The correlation between the event size and spike initiation suggests that these events represent extracellularly recorded EPSPs. Remarkably, the response to low-frequency (<300-Hz) tones presented to either ear often consisted of a stereotyped sequence of inputs with preferred delays. During stimulation with binaural beats, neurons were sensitive to phase disparities between the inputs from both ears. The resulting binaural input pattern generally matched the prediction from summation of the two monaural responses well. Our data thus show that in vivo juxtacellular recordings can be used to study the inputs from both ears to MSO neurons.

### **258 Modelling the Future of Spatial Hearing**

**David McAlpine<sup>1</sup>**, Nicol Harper<sup>1,2</sup>

<sup>1</sup>UCL, <sup>2</sup>University of Oxford

Models of binaural processing developed for human listeners in the first half of the 20th century (and supported by psychophysics) were eventually assessed employing in vivo experimental paradigms in a range of small mammals. In particular, a series of reports throughout the 1980's by Yin and colleagues not only revealed many of the basic aspects of the neural coding of binaural hearing but also inspired a subsequent generation to re-examine fundamental aspects of the original models. Exploiting data sets obtained over the last half century, I will demonstrate the importance of these data sets in developing the next generation of models of spatial hearing.

### **259 Long-Term and Short-Term Changes in Synaptic Gain in the Mature ITD Processing Circuit**

**Benedikt Grothe<sup>1</sup>**, Ida Siveke<sup>1</sup>, Michael Pecka<sup>1</sup>, Annette Stange<sup>1</sup>

<sup>1</sup>Ludwig-Maximilians-Universitaet Muenchen

Following the fundamental study by Rose et al. (1966, J Neurophysiol 29:288), which defined the basic physiological properties of interaural time difference (ITD) sensitivity in the mammalian auditory system, Goldberg and Brown (1968, J Neurophysiol 32:613) and Yin and Chan (1990, J Neurophysiol 64:465) established in their seminal studies the medial superior olive (MSO) as the primary ITD detector. Although discussing their data in general support for the model proposed by Jeffress, both studies already emphasized deviations from a rigid version of this model. In particular, both studies found indirect evidence for inhibitory inputs, a fact that stipulated a large portion of the authors' work. Although we now consider the

ITD processing circuit as a more complex system consisting of more functional inputs than originally thought, we only start to appreciate that ITD processing performed by the MSO circuit is not only extraordinarily precise, but also rapidly adaptive and highly dynamic. Rather unexpectedly, our studies recently revealed the presence of neuromodulators like GABA<sub>B</sub> receptors (Hassfurth et al., 2011 J Neurosci 30:9715) and even the cannabinoid receptor CB1 (Trattner, Grothe Kunz, unpublished) in the gerbil MSO. Our ongoing in vivo recordings conducted while simultaneously agonizing or antagonizing GABA<sub>B</sub> receptor action suggest that the synaptic gain of the excitatory and inhibitory inputs are constantly adjusted to the environmental conditions. Moreover, we obtained evidence for modifications of ITD tuning of MSO cells that endure for multiple days after moderate but long-lasting sound exposure (Siveke et al, submitted). Together, our results demonstrate that the MSO is a highly dynamic system that adapts to acoustic stimulation changes at multiple time scales. Supported by SFB870

### **260 Neural Mechanisms for Reverberation Compensation in the Early Auditory System**

**Bertrand Delgutte<sup>1,2</sup>, Michaël Slama<sup>1,3</sup>, Luke Shaheen<sup>1,4</sup>**

<sup>1</sup>Eaton-Peabody Laboratories, Massachusetts Eye & Ear Infirmary, <sup>2</sup>Research Laboratory of Electronics, MIT, <sup>3</sup>Harvard Medical School, <sup>4</sup>Harvard-MIT Division of Health Sciences and Technology

Speech reception depends critically on low-frequency modulations in the amplitude envelope of speech signals. Reverberation attenuates these modulations, yet speech reception remains robust in everyday settings. To assess whether the auditory system possesses mechanisms for reverberation compensation, we measured responses of single units to sinusoidally amplitude modulated (SAM) broadband noise presented in simulated anechoic and reverberant environments. Recordings were made from both auditory-nerve (AN) fibers in anesthetized cat and inferior colliculus (IC) neurons in awake rabbit.

At both sites, reverberation decreased the modulation depth of responses to SAM noise, but the degradation was smaller in the neural response than in the acoustic stimulus. This form of compensation could largely be explained by the compressive shapes of the modulation input-output functions (MIOFs), representing the transformation from input modulation depth to neural modulation depth. Although MIOF compression results in reverberation compensation, it may be a more general mechanism for robust coding of stimuli with low modulation depths, as would also occur in noisy environments.

An additional form of compensation was found in some IC neurons (but not in AN fibers) in that the response modulation depth was greater for reverberant stimuli than for anechoic stimuli having the same average modulation depth at the eardrum. This reverberant advantage was observed in ~40% of IC neurons and was influenced by the binaural properties of the stimuli. The reverberant advantage may result from the sensitivity of binaural neurons to temporal fluctuations in the interaural correlation of the reverberant stimuli.

In summary, there appears to be both peripheral and central mechanisms for reverberation compensation in the auditory system, and the central mechanisms may be dependent on binaural processing.

Supported by NIH Grants R01 DC002258 and P30 DC005209

### **261 Sensitivity to Interaural Level Differences Determines Virtual Acoustic Space Minimum Audible Angles for Lateral Superior Olive Neurons**

**Daniel Tollin<sup>1</sup>**

<sup>1</sup>Department of Physiology & Biophysics, University of Colorado Medical School, Aurora, CO, USA

Because the peripheral receptors of the ear have no mechanism to directly sense sound location on their own (unlike the topographic organization of the retina), location must be computed at central levels. The minimum audible angle (MAA), the smallest angle separating two sound sources that can be reliably discriminated, is a psychophysical measure of auditory spatial acuity. In humans and cats, MAAs for tone and noise stimuli range from 1-5°. For high-frequency (>1.5 kHz) tones the predominant cue for azimuth is the interaural level difference (ILD). Neurophysiologically, ILDs are first encoded in the lateral superior olive (LSO). Here, we examined the ability of LSO neurons in barbiturate-anesthetized cats to signal changes in the azimuth of broadband noise sources. Using measurements of acoustical head related transfer functions, the virtual acoustic space technique was used to manipulate sound source azimuth in the physiological experiments. For each neuron signal detection theory was used to compute the smallest increment in sound source azimuth necessary to discriminate that change based on the neurons' discharge rate and associated response variability. Across neurons, minimum neural MAAs were 2.3° for midline sources (median = 4.5°, n = 32 neurons) and as low as 1.4° (median = 3.2°) for sources away from the midline. The neural MAAs for monaural stimulation were considerably worse than for binaural stimulation, illustrating that binaural interaction at the LSO is required for good neural spatial acuity. The exquisite neural acuity for spatial location will be explained in terms of the changes in the frequency-specific acoustic ILD cue with changes in source location along with the underlying sensitivity of the LSO neurons to the acoustical ILD cue itself. The results demonstrate that individual LSO neurons can signal changes in sound azimuth that match or exceeded behavioral capabilities. Supported by: NIDCD R01-006865

### **262 Frequency-Dependent Interaural Delays in the Medial Superior Olive: Implications for Interaural Cochlear Delays**

**Mitchell Day<sup>1,2</sup>, Malcolm Semple<sup>3</sup>**

<sup>1</sup>Massachusetts Eye and Ear Infirmary, <sup>2</sup>Harvard Medical School, <sup>3</sup>NYU

Neurons in the medial superior olive (MSO) are tuned to the interaural time difference (ITD) of sound arriving at the

two ears. MSO neurons respond most strongly at their best delay (BD), at which the internal delay between bilateral inputs to MSO matches the external ITD. Previous evidence suggests that most MSO neurons have BDs that remain constant across tone frequency. We made single unit recordings in the superior olivary complex of anesthetized gerbils and found most neurons localized to the MSO exhibited BDs that shifted with tone frequency. The relation of best interaural phase difference (BP) to tone frequency revealed nonlinearities in some MSO neurons. Others had linear relations with characteristic phase between 0.4-0.6 cycles. Both cases are examples of frequency-dependent BD. The latter is usually associated with the interaction of ipsilateral excitatory and contralateral inhibitory inputs, as in the lateral superior olive, yet all MSO neurons exhibited evidence of bilateral excitation. In their work on the inferior colliculus, Yin and colleagues speculated that interaural cochlear delay (i.e., a delay resulting from the ipsilateral and contralateral inputs onto a cross-correlator originating from slightly different locations along the basilar membrane) may be one mechanism that creates frequency-dependent BDs. We compared BP-frequency relations to a cross-correlation model of MSO which incorporated interaural cochlear delay and an additional frequency-independent delay component. The model precisely fit the MSO BP-frequency relations that exhibited frequency-dependent BDs, consistent with the presence of interaural cochlear delays.

### **263 On the Role of the Wideband Inhibitor in the Dorsal Cochlear Nucleus of Decerebrate Cats**

Oleg Lomakin<sup>1</sup>, Kevin Davis<sup>1</sup>

<sup>1</sup>University of Rochester

The filtering properties of the cat's pinna add prominent spectral notches to free-field sounds that are presumed to provide cues for vertical sound localization. Principal cells (type IV units) in the dorsal cochlear nucleus (DCN) are uniquely sensitive to (are inhibited by) these notches. The traditional conceptual/computational model of the DCN (Nelken and Young 1994; Hancock and Voigt 1999) suggested that this sensitivity was shaped mainly by inhibitory inputs from wideband inhibitors (WBIs), which received auditory nerve inputs over a wide frequency range and inhibited type IV units over a narrow frequency range (wide-input narrow-output WBI model). Recent physiological results have shown however that WBIs are unresponsive to notch-noise stimuli with wide notches and therefore have narrower input bandwidths than previously assumed (Reiss and Young 2005). An update to the computational model based on this narrow-input narrow-output model of the WBI was unable to account fully for the notch sensitivity of type IV units suggesting the need to add a new component to the DCN circuit. The goal of this study was to test whether making the output bandwidth of the WBIs wide while keeping their input bandwidth narrow could explain the responses of type IV units to notch-noise stimuli. Anatomical evidence supports this model configuration, and the results show that such a model can produce strong inhibition in type IV units for wide notches.

Consistent with this model, cross-correlation analyses reveal that WBIs make functional inhibitory connections with type IV units over a wide frequency range. Taken together, these results suggest that WBIs, in narrow-input wide-output form, are sufficient to account for the notch sensitivity of DCN type IV units. Supported by NIDCD grants R01 DC 05161 and P30 DC 005409.

### **264 What and Where Processing in the Inferior Colliculus**

Shigeyuki Kuwada<sup>1</sup>, Pavel Zahorik<sup>2</sup>, Brian Bishop<sup>1</sup>, Duck O. Kim<sup>1</sup>

<sup>1</sup>University of Connecticut Health Center, <sup>2</sup>University of Louisville

The focus of our research is to elucidate how reverberation affects the processing of envelope and location of monaurally and binaurally presented sounds using neural and behavioral approaches. Thus, the study is couched in a "what" and "where" framework that has been demonstrated in a behavioral study that involved selective deactivation of the auditory cortex of cats (Lomber and Malhotra, 2008). Our preliminary neural observations indicate that some neurons exhibit reverberation resistant azimuth tuning and some neurons exhibit reverberation resistant envelope sensitivity. We also found that azimuth tuning requires binaural stimulation (Kuwada et al., 2011), whereas envelope sensitivity does not necessarily require binaural stimulation. Our human studies found that envelope sensitivity in reverberation can be equivalent under monaural and binaural stimulation. With these findings in mind, we will describe azimuth tuning and envelope sensitivity in inferior colliculus neurons to binaural and monaural stimulation in anechoic and reverberant environments.

### **265 Inhibition of Sox2 Transcription Is Required for Neurogenesis in the Developing Inner Ear**

Lale Evsen<sup>1,2</sup>, Masanori Uchikawa<sup>3</sup>, Satoko Sugahara<sup>3</sup>, Hisato Kondoh<sup>3</sup>, Doris Wu<sup>1</sup>

<sup>1</sup>NIDCD/NIH, <sup>2</sup>University of Maryland, College Park,

<sup>3</sup>Graduate School of Frontier Bioscience, Osaka University, Japan

Sry-related HMG-box 2 (Sox2) is a transcription factor that contains a high-mobility-group (HMG) DNA binding domain. Sox2's role during vertebrate neurogenesis is to maintain a proliferative, progenitor pool akin to its role as an embryonic stem cell factor. In the central nervous system (CNS), Sox2 is thought to inhibit neurogenesis by keeping neuronal progenitors in an undifferentiated state but its action is counteracted by Ngn2 (Neurogenin 2), which promotes neuronal differentiation. The mechanism that mediates this progression from neural proliferation to differentiation is not clear. In the developing inner ear, Sox2 is expressed in the neural-sensory competent domain (NSC) of the otic cup, but its expression is down-regulated in the delaminating neuroblasts that form the cochleo-vestibular ganglion (CVG). This expression pattern suggests that there may be a similar requirement for Sox2 to be down-regulated in the NSC in order for

neurogenesis to proceed, as in the CNS. To investigate the role of Sox2 in neurogenesis of the inner ear, we over-expressed Sox2 in the developing chicken inner ears *in ovo*. Our results indicate that Sox2 readily induces *Neurogenin 1 (Ngn1)* expression, a gene essential for CVG formation. Nevertheless, despite the upregulation of *Ngn1*, neurogenesis fails to proceed based on the lack of *Neurod1* up-regulation and the reduction in the size of CVG. In contrast, over-expression of *Ngn1* or *Neurod1* is sufficient to cause ectopic neuroblast formation. We provide evidence that *Ngn1* and *Neurod1* inhibit Sox2 expression at the transcriptional level. Taken together these results, we propose that Sox2 normally initiates neurogenesis by up-regulating *Ngn1*, which in turn promotes progression of neurogenesis by down-regulating Sox2 and up-regulating *Neurod1*. In specimens over-expressing Sox2, the lack of neurogenesis is due to the inability of *Ngn1* to repress the transcription of exogenous Sox2.

### **266 Phenotypic and Molecular Analyses of Different *vangl2* Mutants Demonstrate Dominant Effects of the *Looptail* Mutation During Hair Cell Development**

Haifeng Yin<sup>1</sup>, Catherine Copley<sup>1</sup>, Lisa Goodrich<sup>2</sup>, Michael Deans<sup>1</sup>

<sup>1</sup>Johns Hopkins University School of Medicine, <sup>2</sup>Harvard Medical School

Experiments utilizing the *Looptail* mutant mouse, which harbors a missense mutation in the *vangl2* gene, have been essential for studies of planar polarity during hair cell development. As the name suggests, heterozygous *Looptail* mice have distinctively curled tails indicating that the *Looptail* mutation has a dominant phenotype. However it is unclear how mutant Vangl2 protein could exert a dominant effect in these mice because the mutant protein is unstable and is not delivered to the cell surface like normal Vangl2. We addressed this by comparing the development of hair cells between *Looptail* mice and *vangl2* knockout mice missing a large portion of the *vangl2* gene, and by assaying molecular interactions between mutant Vangl2 and normal proteins *in vitro* and *in vivo*. Overall the *vangl2* knockout phenotype is milder than the phenotype of compound mutants carrying both the *Looptail* and *vangl2* knockout alleles. In compound mutants, more hair cells are affected and individual hair cells show greater changes in orientation when quantified. We further demonstrate using a heterologous cell system that the protein encoded by the *Looptail* mutation (Vangl2<sup>S464N</sup>) disrupts Vangl1 and Vangl2 delivery to the cell surface because of oligomer formation between Vangl1 and Vangl2<sup>S464N</sup>, or Vangl2 and Vangl2<sup>S464N</sup>, coupled to the intracellular retention of Vangl2<sup>S464N</sup>. As a result, Vangl1 protein is missing from the apical cell surface of vestibular hair cells in *Looptail* mutants, but is retained at the apical cell surface of hair cells in *vangl2* knockouts. Similarly the distribution of Prickle-like2, a putative Vangl2 interacting protein, is differentially affected in the two mutant lines. In summary, we provide evidence for direct physical interaction between Vangl1 and Vangl2 through a

combination of *in vitro* and *in vivo* approaches and propose that this interaction underlies the dominant phenotypic traits associated with *Looptail*.

### **267 Fibroblast Growth Factor 20 Signaling Is an Essential Regulator of Cochlear Outer Hair Cell Development**

Sung-Ho Huh<sup>1</sup>, Jennifer Jones<sup>1</sup>, Mark Warchol<sup>1</sup>, David Ornitz<sup>1</sup>

<sup>1</sup>Washington University School of Medicine

The organ of Corti (OC) is a complex mechanosensory structure that transduces sound vibrations into neuronal signals. The OC contains one row of inner hair cells (IHC) and three rows of outer hair cells (OHCs), separated by pillar cells (PCs). In addition, each sensory hair cell is associated with an underlying supporting cell (SC). The cellular signals that specify the distinct phenotypes of cochlear hair cells are not known. The mechanisms that regulate the formation of OHCs are particularly significant, since the loss of OHCs is a leading cause of sensorineural deafness and age-related hearing loss. Although mouse mutants lacking fibroblast growth factor (FGF) receptor 1 suggest a role for FGF signaling in OHC development, the underlying mechanisms regulating OHC development are not known. To further examine the role of FGF signaling in cochlear development, we have generated *Fgf20* knockout mice by replacing exon 1 with a  $\beta$ -galactosidase gene (*Fgf20* <sup>$\beta$ Gal</sup>). Heterozygous mice (*Fgf20* <sup>$\beta$ Gal<sup>+</sup></sup>) have normal hearing and normal cochlear histology. Analysis of these mice indicates that *Fgf20* is first expressed within the domain of Sox2+ sensory progenitor cells in the developing otic vesicle. Mice that lack a functional *Fgf20* gene (*Fgf20* <sup>$\beta$ Gal/ $\beta$ Gal</sup>) are viable and healthy but are congenitally deaf. Interestingly, *Fgf20* <sup>$\beta$ Gal/ $\beta$ Gal</sup> mice develop normal numbers of IHCs, but are specifically deficient in OHCs and outer supporting cells. Those mice also have patterning defects throughout most of the cochlear sensory epithelium. These studies show that the organ of Corti can be subdivided into developmentally distinct medial (IHCs and inner SCs) and lateral (OHCs and outer SCs) compartments that are under the control of distinct developmental programs. This model posits the existence of distinct progenitor cells that give rise to medial and lateral compartments of the organ of Corti. The viability and hearing loss in *Fgf20* knockout mice suggest that *FGF20* is an excellent candidate for a deafness-associated gene in humans. Funding: Deafness Research Foundation and Action on Hearing Loss Foundation.

### **268 Wnt/ $\beta$ -Catenin Signaling Regulates Prosensory Proliferation and Hair Cell Differentiation**

Bonnie Jacques<sup>1</sup>, Alain Dabdoub<sup>1</sup>

<sup>1</sup>UCSD School of Medicine

Canonical Wnt/ $\beta$ -catenin signaling is known to regulate proliferation and progenitor cell maintenance during development, in addition to regulating otic placode formation. While Wnt/ $\beta$ -catenin signaling has also been shown to be upstream of Sox2, a regulator of the cochlear

prosensory domain, its functional role within the prosensory domain and during hair cell differentiation has not been determined. With a *TCF/Lef:H2B-GFP* reporter mouse we identified high levels of Wnt/ $\beta$ -catenin activity throughout the cochlear duct during the proliferating phase of the prosensory domain, which becomes restricted during organ of Corti differentiation.

To identify the functional role for this pathway, E12 through E16 cochlear cultures were used to inhibit and activate canonical Wnt signaling. Cultures established at E12 (prior to terminal mitosis) when Wnt signaling is high showed a significant reduction in proliferation and hair cell formation when treated with Wnt inhibitors, whereas exposure to Wnt activators at this stage significantly up-regulated proliferation and expanded the Sox2-positive prosensory domain. At E13, pathway inhibition also reversibly blocked the formation of hair cells, while activation caused a significant increase in hair cells. Most interestingly, Wnt activation after the period of terminal mitosis was also able to induce proliferation within a subset of Sox2-positive cells resulting in a mitotic expansion of the Sox2-positive prosensory domain in the lateral region; limited cell cycle re-entry could also be observed at E16. We provide evidence suggesting that this proliferative expansion of the prosensory domain is likely attributed to the up-regulation of the cell cycle regulator CyclinD-1, and demonstrate that these ectopic Sox2-positive cells are competent to differentiate into hair cells. We conclude that Wnt/ $\beta$ -catenin plays a dual function, regulating both hair cell differentiation and the proliferative capacity of the sensory epithelium.

### **269 Planar Cell Polarity Signaling and Cellular Adhesion Act Independently for Hair Cell Polarity and Epithelial Morphogenesis in the Vestibular Organs**

**Dong-Dong Ren<sup>1,2</sup>, Dong Qian<sup>2</sup>, Fang-Lu Chi<sup>1</sup>, Ping Chen<sup>2</sup>**

<sup>1</sup>*Eye and Ear, nose, throat Hospital, Fudan University,*

<sup>2</sup>*Department of Cell Biology, Emory University*

The mammalian vestibular sensory organs consist of alternating arrangement of sensory hair cells and supporting cells. Each hair cell shows distinctively an intrinsic polarity, sporting an asymmetrically positioned primary cilium, the kinocilium, and rows of microvilli-derived stereocilia with graded heights. All of the hair cells are coordinately oriented within each vestibular organ, displaying a tissue polarity that is parallel to the plane of the sensory epithelium and known as planar cell polarity (PCP). In the saccule and the utricle of the vestibule, hair cells are oriented in opposite directions along a line of polarity reversal. During development, the saccule and the utricle show a distinct gradient of cell proliferation, differentiation, and polarity establishment in a continuous epithelium. The first sign of hair cell polarity is observed around the line of polarity reversal and expands from the striolar region of the saccule and utricle, parallel to the birth order of these cells. Membrane-associated PCP proteins, Vang-like 2 (Vangl2) and Frizzled 3 (Fz3), show polar distribution along the PCP axis. The polar distribution

of PCP proteins precedes the formation of hair cell polarity. As reported previously, PCP mutants show normal morphology of maculae but randomly oriented hair cells and the lost of polar distribution of PCP proteins. In contrast, the conditional knockout of a component of cell adhesion, p120-catenin, leads to morphogenesis defects, including significantly reduced size, and an undulated appearance of the epithelium. These morphologic defects, however, are not accompanied by loss of asymmetric partition of PCP protein Fzd3 or PCP defects in the macular organs. Together, these data suggest that p120-dependent cell adhesion is not essential for hair cell polarity while it is required for integrity and morphogenesis of the vestibular epithelia.

### **270 A Tale of Two Motors: Regulation of Auditory Hair Cell Planar Polarity by Microtubule-Mediated Processes**

**Conor Sipe<sup>1</sup>, Xiaowei Lu<sup>1</sup>**

<sup>1</sup>*University of Virginia*

In the mammalian organ of Corti (OC), planar polarity of individual auditory hair cells is defined by their V-shaped hair bundle. At the tissue level, all hair cells display uniform planar polarity across the epithelium. Although it is known that tissue planar polarity of the OC is controlled by non-canonical Wnt/planar cell polarity signaling, the hair cell-intrinsic polarity machinery is poorly understood. Previous work in our lab uncovered a role for the microtubule motor molecule Kif3a in regulating hair cell polarization through both ciliary and non-ciliary mechanisms. Our work suggests that Kif3a coordinates hair bundle orientation with basal body positioning through localized activation of Rac-PAK (p21-activated kinase) signaling at the cortex. Our working model predicts that microtubule capture at the hair cell cortex is required for correct polarization. To understand further how microtubule-dependent processes control hair cell polarization, particularly how microtubule capture is controlled during hair bundle development, we set out to investigate the role of the Lissencephaly 1 (Lis1) gene. Lis1, mutated in the human developmental brain disease lissencephaly, is a major regulator of the cytoplasmic dynein microtubule motor complex. Using a genetic approach, we have identified a requirement of Lis1 for aspects of auditory hair cell polarization and subsequent survival of developing hair cells. In addition to having misoriented hair bundles, Lis1 mutant hair cells display a progressive bundle morphology defect. A majority of hair cells in the Lis1 mutant OC degenerate by postnatal day 7, suggesting that Lis1 also has a pro-survival function. We are currently investigating the molecular and cellular defects underlying the hair bundle morphology and cell death phenotypes. Our study has uncovered previously unappreciated functions of the human disease gene Lis1 and provides further insights into the role of microtubule-mediated processes in hair bundle morphogenesis.

## **271 The Inferior Half of the Chicken Basilar Papilla Undergoes a Partial Phenotypic Conversion to a Superior Fate in Response to Forced Expression of Wnt9a During Embryogenesis**

Donna M. Fekete<sup>1,2</sup>, R. Keith Duncan<sup>3,4</sup>, Kirsten M. Luethy<sup>1</sup>, Deborah J. Biesemeier<sup>1</sup>

<sup>1</sup>*Department of Biological Sciences, Purdue University,*

<sup>2</sup>*Purdue University Center for Cancer Research,*

<sup>3</sup>*Department of Otolaryngology, University of Michigan,*

<sup>4</sup>*Kresge Hearing Research Institute*

Wnt9a transcripts are expressed in non-sensory cells arrayed along the superior edge of the developing basilar papilla (BP) of the chicken at embryonic days (E) 7-10 (Sienknecht and Fekete, 2008). From this location, the secreted ligand could generate a diffusion gradient across the adjacent prosensory domain to regulate patterning and cell fate specification. To test this, we overexpressed Wnt9a throughout the otic ectoderm by injecting the right otocyst with RCAS-Wnt9a retrovirus on E3. On E18, infected BPs were 35% wider than the contralateral controls (n=7), with many additional hair cells (HCs) and supporting cells. Increased cell numbers resulted from greater mitotic indices on the infected sides at E6.5-8 (n=12). On E17-18, the inferior half of Wnt9a-infected BPs resembled the superior half in cell density, HC shapes, abundance of Ribeye+ pre-synaptic foci per HC, innervation density, and thickness of the mesoderm beneath the basilar membrane. Whole-cell voltage-clamp recordings of HCs were taken from the extreme superior and inferior edges of E18-E19 BPs. Steady-state current-voltage relationships were generated for four experimental groups: superior and inferior HCs from Wnt9a-injected and control BPs. In addition, similar curves were generated for the fast, calcium-sensitive components of the current traces to isolate contribution from calcium-activated potassium channels. Although the fast current components, possibly comprised of large-conductance BK-type potassium channels, were significantly greater in superior compared with inferior HCs, the magnitude of this current was unaffected by viral infection. In contrast, steady-state outward currents were significantly larger in Wnt9a-treated inferior HCs than controls from that same region, possibly indicating a role for the ligand in upregulating slow, delayed rectifier potassium currents. We conclude that by E19 the inferior BP is only partially converted into a superior phenotype by Wnt9a.

## **272 Divergent Functions for Netrin1 in Chicken and Mouse Canal Morphogenesis**

Allison Nishitani<sup>1</sup>, Tony Del Rio<sup>1</sup>, Lisa Goodrich<sup>1</sup>

<sup>1</sup>*Harvard Medical School*

Across the animal kingdom, the vestibular apparatus of the inner ear exhibits a characteristic morphology, with three semicircular canals grossly oriented with the three dimensions of space. Canals develop from pouches of epithelium that grow out of the otic vesicle. Subsequently, in a highly restricted area in the center of the pouch, the basement membrane breaks down and the epithelial cells

lose their columnar morphology, allowing the two opposing walls of the pouch to come together and fuse. The cells in this region, called the fusion plate, are then removed, leaving the remaining epithelium on the perimeter to form the canal rim. Hence, the final structure of the canal is determined by when and where fusion occurs.

A critical regulator of fusion in the mouse is the secreted protein Netrin1 (Ntn1). *Ntn1* is expressed in fusion plate cells and in mice mutant for *Ntn1*, the basement membrane remains intact and fusion fails to occur. Conversely, in mice with expanded *Ntn1*, basement membrane breakdown expands and the canal is truncated. We asked whether Ntn1 plays a similar role in chicks as in mice. RCAS viruses producing either a myc-tagged version of Ntn1 or a secreted form of GFP were injected into the chick otic vesicle at E3. Infected cells positive for Ntn1-myc were reliably scattered throughout the epithelium and variably in the mesenchyme. Paintfilling of the inner ear at E7 revealed an unexpected change in canal morphology. In 13/13 embryos, fusion failed to occur fully in at least one canal, resulting in some cases in formation of a cystic vestibular apparatus with no canals. Thus, in chicks, overexpression of Ntn1 has the same morphological effect as the lack of Ntn1 in mice. Moreover, the Ntn1 overexpression phenotype closely mirrors effects of blocking cell death in the chick inner ear (Fekete et al., 1997). Indeed, cell death is thought to play an important role in resorption of the fusion plate in chicks, while the role of cell death in mouse canal formation remains unclear. In other tissues, Ntn1 inhibits cell death by binding to DCC and/or Unc5H dependence receptors. These results suggest that Ntn1 plays distinct roles in canal formation in chicks and mice, and highlight the fact that distinct cellular processes have evolved to sculpt the same complex structure in different species.

## **273 Afferent Synaptogenesis in Vitro by Spiral Ganglion Neurons (SGNs) on Inner Hair Cells (IHCs) with Endogenous NT-3 Replaced by BDNF in the Postnatal Organ of Corti (OC)**

Qiong Wang<sup>1</sup>, Tian Yang<sup>1</sup>, Jennifer Kersigo<sup>1</sup>, Bernd Fritsch<sup>1</sup>, Steven Green<sup>1</sup>

<sup>1</sup>*Department of Biology, University of Iowa*

The neurotrophins BDNF and NT-3 are expressed in the developing OC; the cognate receptors, TrkB and TrkC, are expressed in SGNs. After birth in rodents, BDNF expression declines to an insignificant level, while NT-3 continues to be expressed, mainly in IHCs and adjacent supporting cells. Previous results (Wang & Green, *J Neurosci*, 2011) using neonatal rodent organotypic cochlea explant cultures suggested that endogenous NT-3 in the postnatal organ of Corti has a distinctive role, not mimicked by exogenously added BDNF, in promoting SGN synapse regeneration on IHCs. Here we ask about the equivalence of NT-3 and BDNF by examining innervation and reinnervation of IHCs by SGNs in neonatal explants from NT3kiBDNF mice (NT-3 coding sequence replaced by BDNF). In vivo innervation of the organ of Corti in postnatal day 0 (P0) NT-3kiBDNF mice was disordered

and the base was apparently innervated by two sets of fibers, auditory and vestibular (also see Tessarollo et al., *J Neurosci*, 2004). After 3 days in vitro (DIV), in an organotypic cochlear culture that preserves only SGN to HC connections, we found, remarkably, that cochlear SGNs innervate only IHCs in NT3kiBDNF mice. That is, with BDNF replacing NT-3, outer hair cell innervation was missing. Interestingly, some fibers on IHCs were immunopositive for peripherin, a putative marker of type II SGNs in mature cochleae. Although disorganized, postsynaptic densities were present at afferent terminals on IHCs in NT3kiBDNF mice indicating that synaptogenesis on IHCs can occur with BDNF replacing NT-3. Synaptogenesis also occurs in vitro in co-cultures of isolated HCs from NT3kiBDNF mice and dissociated SGNs. We have shown limited synapse regeneration in vitro following excitotoxic disruption of afferent synapses on IHCs. However, this reinnervation is deficient in NT3kiBDNF mice, especially in the cochlear base. These data indicate that NT-3 and BDNF play overlapping but distinct biological roles in afferent synaptogenesis in the cochlea.

Funded by NIH grants R01 DC009405 (SHG), P30 DC010362

#### **[274] Ca<sub>v</sub>1.3 Regulates Synaptic Ribbon Size and Position in Sensory Hair Cells**

Lavinia Sheets<sup>1,2</sup>, Teresa Nicolson<sup>1,2</sup>

<sup>1</sup>Oregon Hearing Research Center and Vollum Institute, Portland, OR 97239, <sup>2</sup>Howard Hughes Medical Institute, Oregon Health & Science University, Portland, OR 97239

The L-type voltage gated calcium channel Ca<sub>v</sub>1.3 is required for hair-cell neurotransmission and is critical for normal hair cell maturation, yet a specific role for Ca<sub>v</sub>1.3 in hair-cell ribbon synapse development has not previously been described. We therefore examined the unique ribbon synaptic protein Ribeye and postsynaptic density marker MAGUK in two zebrafish *ca<sub>v</sub>1.3a* mutant alleles. In 3-day-old larvae of both alleles we observed significantly enlarged presynaptic Ribeye and postsynaptic MAGUK immunolabeled punctae. Additionally, we saw a disruption of MAGUK localization that appeared progressively worse in 5-day-old compared to 3-day-old larvae.

To test whether the phenotype we observed in *ca<sub>v</sub>1.3a* mutants was due to disruption of channel function we applied L-type Ca<sup>2+</sup> channel blockers to wildtype larvae. Significantly enlarged Ribeye and MAGUK punctae were observed following acute exposure (15 minutes -1 hour) of wildtype 3-day-old, but not 5-day-old, larvae to isradipine or verapamil. Moreover, enlarged Ribeye puncta also occurred when release of intracellular calcium stores was specifically inhibited with cyclopiazonic acid. Using quantitative PCR, we saw increased Ribeye transcript in 3-day-old larvae exposed to either isradipine or cyclopiazonic acid, indicating that intracellular calcium is negatively regulating Ribeye expression in the hair cells of pre-hearing larvae.

These results suggest Ca<sub>v</sub>1.3 plays a key role in regulating Ribeye during hair-cell synapse formation and that it is

required for the maintenance of pre-and postsynaptic juxtaposition.

#### **[275] Reactivation of Herpes Simplex Type 1 in Latently Infected Vestibular and Trigeminal Neurons in Response to Heat**

Shruti Nayak<sup>1</sup>, Vladimir Camarena<sup>2</sup>, Maggie Kuhn<sup>1</sup>, Angus Wilson<sup>1</sup>, Ian Mohr<sup>1</sup>, Moses Chao<sup>1</sup>, Pamela Roehm<sup>3</sup>

<sup>1</sup>New York University School of Medicine, <sup>2</sup>University of Miami, <sup>3</sup>New York University

Herpes simplex type 1 (HSV1) is extremely prevalent, with seropositivity rates of up to 90% in the adult US population. Reactivation of HSV1 occurs in 30% of infected individuals, most recognizably in the form of cold sores resulting from reactivation of HSV1 in trigeminal ganglion neurons (TGNs). HSV1 reactivation has been implicated in vestibular neuritis, which may follow HSV1 re-entering the lytic lifecycle in latently infected vestibular ganglion neurons (VGNs). Bell's palsy and delayed facial palsy after neurotologic surgery are also hypothesized to result from HSV1 reactivation in geniculate ganglion neurons. To further understand the types of neuronal insults that can lead to HSV1 reactivation and production of infectious virus, we have modeled heat injury on cultured latently infected neurons of different types. Although heating cultures to 43°C does not reactivate HSV1 in superior cervical sympathetic ganglion neurons it does lead to viral reactivation in both VGN and TGN cultures. Differences in non-neuronal cellular composition of the cultures and in TRPV signaling account for the majority of the differential sensitivity to heat demonstrated by cultured neurons *in vitro*. Thus both neuron-specific intracellular signaling and cellular microenvironment can affect susceptibility to potential HSV1 reactivation triggers. Knowledge of these factors is critical in understanding HSV1-reactivation related diseases.

#### **[276] Optical and Thermal Responses of Semicircular Canal Afferent Neurons in the Oyster Toadfish**

Rhiannon Johnson<sup>1</sup>, Micah Frerck<sup>1</sup>, Suhrod Rajguru<sup>2,3</sup>, Holly Holman<sup>1</sup>, Stephen Highstein<sup>4</sup>, Richard Rabbitt<sup>1,4</sup>

<sup>1</sup>Department of Bioengineering, University of Utah,

<sup>2</sup>Department of Biomedical Engineering, University of

Miami, <sup>3</sup>Department of Otolaryngology, University of

Miami, <sup>4</sup>Marine Biological Laboratory, Woods Hole

Exquisite temperature sensitivity of the inner ear has been well documented (*Exp Brain Res*. 2010, 200:269-75). The changes in ambient temperature are a particular challenge for cold-blooded animals that must maintain sensory signals over large ranges of body temperature. Presently, we compared responses of semicircular canal afferents to changes in temperature (10-37°C) of the crista ampullaris in the oyster toadfish. The temperature changes were generated by perfusion of temperature-controlled perilymph or application of pulsed laser radiation. The thermal stimuli were applied only to the labyrinth, and the fish body temperature was maintained at ambient using a sea-water bath. We recorded the temperature-dependent

changes in spontaneous discharge rate, regularity, adaptation to step hair bundle displacements and responses to sinusoidal head rotations of single-units. A variety of afferent responses to thermal perfusion alone were observed: some neurons were insensitive to temperature, and some showed an increase while others decreased the discharge rate with temperature. This suggests the presence of temperature compensating mechanisms in the hair-cell/afferent complexes that allow sensitive function over a wide range of temperatures. Further, we compared single unit responses to temperature changes generated by perfusion or by application of 980nm or 1862nm light. Application of laser light revealed a differential time-course of temperature change even when the total  $\Delta$  temperature matched that caused by perfusion. Results are consistent with the hypothesis that inhomogeneous, wavelength specific, absorption underlies differences between the three forms of heat delivery. Organelle and protein specific wavelength sensitivity may be relevant to development of future prosthetic or therapeutic application of infrared neural stimulation. [Supported by DC006685 & DC011481]

### **277** Infra-Red Laser Stimulation Modulates Vestibular Nerve Afferent Responses in the Mammalian Labyrinth

Joong Ho Ahn<sup>1</sup>, David Lasker<sup>1</sup>, Dai Chenkai<sup>1</sup>, Gene Fridman<sup>1</sup>, Charles Della Santina<sup>1</sup>

<sup>1</sup>Johns Hopkins Vestibular NeuroEngineering Lab

Pulsed infrared (IR) laser stimulation of vestibular sensory neuroepithelium has recently been shown effective in eliciting action potentials on vestibular afferents in fish (Rajguru, *et al* 2011), but whether the same is true in mammals is unknown. We sought to determine whether IR irradiation of the nerve or crista evokes phase-locked responses of vestibular afferent fibers in mammals.

Adult wild-type 450-650 g chinchillas were used for this experiment. After the bullae were opened and the superior vestibular nerves were exposed, glass microelectrodes were directed into each superior vestibular nerve to measure single unit afferent activity of the superior vestibular nerve. To stimulate with IR laser, we drilled a hole just above the crista ampullaris of the superior vestibular canal, and an optical fiber was positioned inside the canal aiming directly to the ampulla, approximately 300-500  $\mu$ m above hair cells. Optical stimulation was delivered using a Capella pulsed infrared laser (Lockheed-Martin Aculight, Bothell, WA, USA) operated at 1863 nm, with trains of single pulses at repetition rates between 1 and 200 pps.

Direct IR illumination of the vestibular nerve elicited no measurable activity in any animal. During crista irradiation, most afferents showed apparent caloric/convection responses to indirect optical radiation with various latencies (0.979 – 2.533 sec). However, when the IR laser was directly aimed at the superior canal crista, IR irradiation modulated afferent activity in a tightly phase-locked manner with a latency of 1.5 msec following the onset of each IR pulse up to the highest pulse frequency of

200 pulses/s. Both excitatory and inhibitory effects with slower dynamics were also observed.

Infrared stimulation of ampullary hair cells elicits, excitatory, inhibitory and phase-locked responses in mammalian vestibular nerve afferent fibers.

*Support: The Johns Hopkins Vestibular Neurophysiology Research Fund*

### **278** Addition of Chronic Direct Current Stimulation Improves Vestibular Prosthesis Dynamic Range

Gene Fridman<sup>1</sup>, Charles Della Santina<sup>1</sup>

<sup>1</sup>Johns Hopkins University

The Johns Hopkins Multichannel Vestibular Prosthesis (MVP) is designed to mimic function of the vestibular labyrinth for those suffering from profound bilateral vestibular hypofunction. It detects head motion and modulates the frequency of biphasic current pulses delivered to the vestibular nerve. In the normal chinchilla labyrinth, afferent neurons in each inner ear maintain a spontaneous firing rate (mean 60spike/s) and increase or decrease firing rate about this baseline in response to head motion. The MVP encodes head motion toward the implanted ear up to  $\sim 500^\circ/s$  by increasing stimulus pulse rate above baseline, but pulsatile stimuli cannot force an afferent fiber to fire below its spontaneous baseline rate, so MVP-induced responses during inhibitory head rotations are often limited to  $\sim 40^\circ/s$ .

We hypothesized that MVP stimulation could encode a wider range of head velocities if spontaneous afferent activity were suppressed by low amplitude direct current (DC). MVP would then have full control of an afferent's firing rate. To overcome biological safety concerns with DC stimulation at the metal electrode-tissue interface, we developed a safe DC stimulator. This device delivers alternating current across each electrode's metal-saline interface, but effectively delivers DC to the tissue using pulse-synchronized valves arranged in a bridge circuit. DC current was delivered to chinchillas via thin artificial-perilymph-filled tubes implanted in the labyrinth near the vestibular nerve. To monitor stimulation effectiveness, we used video-oculography to assay vestibulo-ocular reflex eye movements in darkness with and without DC stimulation as we delivered steps in pulse rate via the MVP.

Experiments with 3 animals showed stable responses while stimulated with 120uA DC current for over 40 minutes. Consistent with the hypothesis, responses to inhibitory pulse rate steps increased from  $50\pm 4^\circ/s$  without DC to  $68\pm 8^\circ/s$  with DC.

**279** **Concurrent Modulation of Pulse Frequency and Current with Coordinate Transformation Yields Improved 3D VOR Dynamic Range, Symmetry and Alignment in Monkeys Using a Multichannel Vestibular Prosthesis**

Natan Davidovics<sup>1</sup>, Mehdi Rahman<sup>1</sup>, Chenkai Dai<sup>2</sup>, JoongHo Ahn<sup>2</sup>, Gene Fridman<sup>2</sup>, Charles Della Santina<sup>1,2</sup>

<sup>1</sup>Johns Hopkins University Department of Biomedical Engineering, <sup>2</sup>Johns Hopkins University Department of Otolaryngology – Head & Neck Surgery

An implantable prosthesis that stimulates vestibular nerve branches to restore sensation of head rotation and the 3D vestibular ocular reflex (VOR) could benefit individuals disabled by bilateral loss of vestibular sensation. Our group has developed a vestibular prosthesis that partly restores normal function in animals by delivering biphasic current pulses via electrodes implanted in semicircular canals. This approach has been limited by insufficient velocity of VOR response to head movements in the inhibitory direction (away from the implant), and misalignment between direction of head motion and prosthetically-elicited VOR. We report that significantly larger VOR eye velocities in the inhibitory direction can be elicited by adapting a monkey to an elevated baseline stimulation rate and current prior to stimulus modulation and then concurrently modulating (“co-modulating”) both rate and current below baseline levels to encode inhibitory angular head velocity. Co-modulation of pulse rate and current amplitude above baseline can also elicit larger VOR eye responses in the excitatory direction (head movement toward the implant) than either pulse rate or current modulation alone. We also show that combining these stimulation strategies with a precompensatory 3D coordinate transformation results in improved alignment of VOR eye responses. By demonstrating that a combination of co-modulation and precompensatory transformation strategies achieves a robust VOR with significantly improved symmetry and alignment in an animal model that closely resembles humans with vestibular loss, these findings provide a solid preclinical foundation for application of vestibular stimulation in humans.

Support: NIDCD R01DC9255

**280** **Supporting Cell Deficits Underlie the Rapid Balance Deterioration of the Twister Mice**

Xing Zhao<sup>1</sup>, Yan Zhang<sup>1</sup>, Sherri Jones<sup>2</sup>, Hui Zhang<sup>1</sup>, Yinfang Xu<sup>1</sup>, Yunxia (Yesha) Lundberg<sup>1</sup>

<sup>1</sup>Boys Town National Research Hospital, <sup>2</sup>East Carolina University

Beyond developmental stages, the reliance of hair cells (HC) and synapses on supporting cells (SC) is not fully appreciated. Here we have identified compromised SCs as the cause of age-related deterioration of balance and hearing in the twister mouse, *Otog<sup>tw</sup>/Otog<sup>tw</sup>*, and have used the mouse as a model to understand the extent and mechanism by which SCs support vestibular sensory processing and maintenance at older ages. The

underlying gene *otogelin* is exclusively expressed in SCs in wildtype mice. *Ex vivo*, twister SCs show significantly reduced proliferation potential and adhesion. *In vivo*, mutant SCs become apoptotic at older ages, which leads to increased HC apoptosis as compared to wildtype mice. Mutant mice also have a nearly 50% reduction of Ribeye and GluR puncta at the synapses, and express *erbB3* at a much lower level. As emerging evidence shows that *erbBs* in SCs play a key role in vestibular synaptic formation and maintenance, we postulate that insufficient *erbB* signaling is likely the mechanism for the HC and synaptic degeneration in the twister mice. Although older twister mice also have an easily detachable otoconial membrane during tissue sectioning, such a defect cannot account for the degree or rate of sensory reduction when their linear vestibular evoked potentials are compared with those of other vestibular mutants. Taken together, the data illustrate the vital importance of SCs in optimizing the function and survival of HCs and synapses.

**281** **Functional Cooperation of Two Otoconial Proteins Oc90 and Nox3**

Yinfang Xu<sup>1</sup>, Liping Yang<sup>1</sup>, Sherri Jones<sup>2</sup>, Xing Zhao<sup>1</sup>, Yan Zhang<sup>1</sup>, Yunxia (Yesha) Lundberg<sup>1</sup>

<sup>1</sup>Boys Town National Research Hospital, <sup>2</sup>East Carolina University

Otoconia formation is a series of tightly regulated biochemical events, and requires the finely coordinated involvement of numerous proteins. In this study, we have discovered that Oc90 (otoconin-90), the predominant otoconial constituent, and Nox3 [NAD(P)H oxidase], a non-constituent essential for otoconia formation, are functionally interlinked. Oc90 recruits other component proteins such as *otolin* to form the organic matrix of otoconia, and Nox3 generates reactive oxygen species (ROS). However, the precise role of Nox3 in calcification is still unclear. We have found that single heterozygous mutant mice for Oc90 and Nox3 have very minor otoconia defects and normal balance, whereas double heterozygous mutants show minor otoconia defects but severe imbalance. In addition, double null mice (mutant Nox3 here is functional null) present severe hearing loss at high frequencies, whereas single null mice have normal hearing. Electron microscopy shows that Oc90-Nox3 double null mice have accelerated hair cell degeneration. Protein analysis reveals structural modification of Oc90 by Nox3, and *in vitro* calcification analysis in cells stably expressing these proteins singly and doubly shows more intense calcification in the double transfectants. Oc90 single transfectants readily produce ROS, suggesting that the functional synergy between Oc90 and Nox3 arise from an overlapping signaling mechanism that involves ROS. These data demonstrate that Oc90 and Nox3 augment each other's function, and that a certain level of ROS signaling is necessary for normal sensory function in the inner ear.

## **282 Temporally and Spatially Regulated Expression of Otoconial Genes**

Yinfang Xu<sup>1</sup>, Yunxia (Yesha) Lundberg<sup>1</sup>

<sup>1</sup>Boys Town National Research Hospital

Otoconia are minute bio-crystals composed of proteins and CaCO<sub>3</sub>, and are indispensable for sensory processing in the utricle and saccule. Malformation, dislocation and degeneration of otoconia can lead to various types of human vestibular dysfunction such as dizziness/vertigo and imbalance. Limited by anatomical and methodological constraints, otoconial research lags far behind the study of other biomineralized structures, such as bone and teeth. In order to better understand the mechanism controlling otoconia formation and maintenance, we have examined comprehensively the spatial and temporal expression patterns of critical otoconial genes in the mouse inner ear at developmental, mature and aging stages. We show that the expression levels of all otoconial genes are much higher in the utricle and saccule compared to other inner ear tissues before P0 in C57Bl/6J mice. Particularly, the expression of a few of these genes is restricted to the utricle and saccule. After P7, expression of all otoconial genes in the utricle and saccule is drastically reduced, while a few different sets of genes gain expression advantage in the adult and aging ampulla, canals, and cochlea, indicating a potential for ectopic calcification or ectopic debris formation in these latter tissues at old ages. The data suggest that the expression of otoconial genes is tightly regulated spatially and temporally during developmental stages and can become dys-regulated at adult and aging stages.

## **283 Vestibular Behavioral Analysis and Otolith-Ocular Response in Casp3 Deficient Mice**

Kael Kuster<sup>1</sup>, Patrick Armstrong<sup>1</sup>, Adrian Perachio<sup>1</sup>, Scott Wood<sup>1,2</sup>, Tomoko Makishima<sup>3</sup>

<sup>1</sup>University of Texas Medical Branch, <sup>2</sup>Universities Space Research Association, NASA Johnson Space Center,

<sup>3</sup>University of Texas Medical Branch

Casp3 deficient (Casp3KO) mice show circling behavior suggestive of vestibular dysfunction. Our goal was to characterize vestibular function in Casp3KO mice using a combination of behavioral tests and vestibulo-ocular reflex (VOR) analysis, and to correlate inner ear histology.

Wild-type C57BL6 (WT) and Casp3KO mice, two to seven months of age, were compared. Circling, air-righting, and tail hanging tests were performed to assess vestibular behavior. Lateral canal VOR function was evaluated during sinusoidal rotation about an earth vertical axis. Otolith-ocular function was evaluated using both the synchronized counter-rotation paradigm (CR) and with sustained angular rotation of the main axis independent of the eccentric axis using various angular velocity profiles (pseudo-off vertical axis rotation, pOVAR). Horizontal eye velocity and vertical eye position were evaluated as a function of acceleration. Hair cell numbers in each vestibular sensory patch were assessed using whole mount preparations.

The Casp3KO mice had a tendency of circling counter-clockwise. Air-righting test and tail hanging test were abnormal in most Casp3KO mice.

In WT mice, modulation of slow phase eye velocity and vertical eye position increased proportionally to CR and pOVAR stimulus intensity. In Casp3KO mice, responses to angular stimuli was greatly attenuated but response to CR and pOVAR was similar to WT mice. Hair cell numbers were significantly decreased in the anterior- and lateral cristae in Casp3KO mice (ANOVA, P<0.05). The anterior crista was often fused with the lateral crista. The utricle had decreased number of hair cells, but had normal appearance.

Casp3KO mice have severely impaired lateral canal VOR function, but have normal otolith-ocular function. The behavioral test results and histological studies correlate well. Our preliminary results suggest that Casp3KO mice may provide a model of canal dysfunction with relatively intact otolith responses.

## **284 Characterization of a Hyperpolarization-Activated Current (I<sub>h</sub>) in Vestibular Calyx Terminals**

Frances Meredith<sup>1</sup>, Scott Mann<sup>1</sup>, Katherine Rennie<sup>1</sup>

<sup>1</sup>University of Colorado School of Medicine

Calyx afferent terminals surround the basolateral region of type I hair cells in the vestibular epithelia and express several ionic conductances which may shape postsynaptic events. These include TTX-sensitive inward Na<sup>+</sup> currents, voltage-dependent outward K<sup>+</sup> currents sensitive to 4-aminopyridine, tetraethylammonium and the KCNQ channel blockers linopirdine and XE991 (Dhawan et al. 2010, Hurley et al. 2006, Rennie and Streeter 2006) and a K(Ca) current blocked by apamin and nifedipine (Meredith et al. 2010). Here we describe an inwardly rectifying current in gerbil semicircular canal calyx terminals (postnatal days 3-41) sensitive to voltage and to cyclic AMP (cAMP). Using whole cell patch clamp, we recorded from isolated calyx terminals still attached to their type I hair cells. A slowly activating, non-inactivating current was seen with hyperpolarizing voltage steps negative to -79 mV. The current elicited by a -139 mV, 650 ms voltage step had a mean amplitude of -82.6 ± 11.4 pA (SEM, n = 40). Hyperpolarizing current injections produced a time-dependent depolarizing sag followed by a rebound afterdepolarization or action potential in current clamp. External Cs<sup>+</sup> and ZD 7288 blocked the inward current by 97 and 80% respectively confirming it was I<sub>h</sub>. Mean half-activation voltage was -124 mV (n = 5) which shifted to -115 mV in the presence of cAMP (n = 4). Activation kinetics were well described by a monoexponential fit to the current. Under control conditions, the median tau (τ) was 394 ms (n = 25) during a -139 mV voltage pulse. With intracellular cAMP, τ increased significantly to 228 ms (P = 0.026, n = 6).

Physiological roles of I<sub>h</sub> in other cells include control of resting membrane potential and input resistance. Despite the relatively negative activation range of I<sub>h</sub>, preliminary data suggest that membrane excitability in calyces increases when I<sub>h</sub> is blocked by ZD 7288. Additional

experiments will further investigate the role of  $I_h$  in vestibular calyx terminals. Supported by NIDCD DC008297 to KJR and 5T32NS007083 to FLM.

### **[285] Inhibition of K<sup>+</sup> Currents in Type I Vestibular Hair Cells by Aminoglycosides**

Scott Mann<sup>1</sup>, Hayley Ross<sup>1</sup>, Matthew Johnson<sup>1</sup>, Frances Meredith<sup>1</sup>, Katie Rennie<sup>1</sup>

<sup>1</sup>University of Colorado School of Medicine

Significant ototoxicity limits use of aminoglycoside antibiotics (AG). Several mechanisms may contribute to death of both auditory and vestibular hair cells. AG enter outer hair cells of the cochlea through apical transduction channels (Marcotti et al. 2005) and inhibit the basolateral KCNQ4-mediated current ( $I_{K,n}$ ) by PIP<sub>2</sub> sequestration (Leitner et al. 2011). At birth vestibular hair cells have delayed rectifier K<sup>+</sup> current and by the 3<sup>rd</sup> postnatal week type I hair cells also express a low-voltage activated K<sup>+</sup> current that resembles  $I_{K,n}$  in outer hair cells. Using whole cell patch clamp, we tested the effects of AG and KCNQ channel modulators on K<sup>+</sup> currents ( $I_K$ ) in type I vestibular hair cells isolated from gerbil semicircular canals.

Extracellular neomycin (1 mM) rapidly reduced peak outward  $I_K$  by  $16 \pm 4\%$  ( $n = 9$ ) in mature type I hair cells. Gentamicin (5 mM) reduced peak  $I_K$  by  $16 \pm 3\%$  ( $n = 8$ ). Intracellular neomycin (1 mM in the patch electrode solution) reduced  $I_K$  by  $17 \pm 6\%$  ( $n = 12$ ). KCNQ modulators were used to probe KCNQ channel involvement. XE991 (20  $\mu$ M) did not reduce  $I_K$  in mature type I cells and the neomycin-induced reduction in  $I_K$  was not reversed by the KCNQ agonist flupirtine (10  $\mu$ M). Application of intracellular poly-D-lysine (200 $\mu$ g/ml) to sequester PIP<sub>2</sub> did not reduce  $I_K$ . Extracellular 4-aminopyridine (4-AP, 1mM) blocked a component of  $I_K$ . Application of extracellular AG in the presence of 4-AP gave no further inhibition of  $I_K$ . In immature type I cells (postnatal days 5-8), extracellular neomycin reduced  $I_K$  by  $19 \pm 3\%$  ( $n = 5$ ). Fluorescent imaging confirmed that externally applied Texas Red conjugated gentamicin was rapidly taken up by vestibular hair cells.

We conclude that AG significantly reduce the 4-AP-sensitive  $I_K$  in early postnatal and mature type I cells. K<sup>+</sup> current inhibition differs from that seen in outer hair cells, since it does not involve PIP<sub>2</sub> sequestration or KCNQ channels.

Supported by American Otological Society and NIDCD DC008297 to KJR

### **[286] Spontaneous Synaptic Events in the Vestibular Calyx Terminal**

Stephen Highstein<sup>1</sup>, Mary Ann Mann<sup>1</sup>, Richard D Rabbitt<sup>1,2</sup>

<sup>1</sup>Marine Biological Laboratory, <sup>2</sup>University of Utah

The unique morphological structure of the vestibular calyx suggests that synaptic transmission from type-I hair cells to calyceal nerve chalice might differ from the more commonly studied hair-cell/bouton ribbon synapses. To examine this, we recorded excitatory post-synaptic currents (EPSCs) and potentials (EPSPs) using whole cell

patch clamp of calyceal endings in lagenas and utricles isolated from the turtle, *Trachemys scripta elegans*. Preliminary results are reported here. In voltage clamp mode (VC) at negative holding potentials (e.g., -60mV), miniature excitatory synaptic currents (mEPSCs, avg. size -19pA) were observed with spontaneous rates 11-119 events/s. The mean unitary event size accounting for simultaneous multiquantal release was -12pA/event with a mean depolarizing charge delivered to the calyx of 13fC/event. The mean mEPSC rise and fall times were 0.25 and 0.67ms respectively. In some records, large action-potential inward events (ca. 2-5nA) were also observed indicating that the spike generation site was not always space clamped. The frequency of mEPSCs could be increased >300% by deflecting the hair bundle of the type-I hair cell contained within the recorded calyx. The amplitude of mEPSCs could be reduced by depolarizing the cell. In current clamp mode (CC), action potentials could be evoked by depolarizing the resting potential, and rose directly out of the baseline indicating an axonal origin. Spontaneous mEPSPs were also observed in CC, consistent with mEPSCs observed in VC. Results suggest relatively small unitary quantal size and high vesicle release rates at the hair-cell/calyx synapse. [Supported by DC 00814(SMH) & DC006685 (RDR)]

### **[287] Interaction of Horizontal Translation and Yaw Rotation Signals on Convergent Neurons in the Vestibular Nuclei**

Min Wei<sup>1</sup>, Hongge Luan<sup>1</sup>, Laurel Carney<sup>1</sup>, Shawn Newlands<sup>1</sup>

<sup>1</sup>University of Rochester

Vestibular afferents innervating the utricle that code acceleration in the horizontal plane and afferents innervating the horizontal semicircular canal that code yaw rotation terminate in similar areas of the vestibular nuclei. About 2/3 of central vestibular neurons which carry yaw rotation signals but not eye movement signals (non-eye movement cells) also code horizontal translation. In neurons coding both roll tilt and horizontal translation, Angelaki and colleagues have reported non-linear interactions of the two signals that appear to facilitate the discrimination of tilt from translation. The interaction of translational and rotational signals in the horizontal plane, where orientation relative to gravity does not change, has not been as well studied. In our protocol, using single unit recording techniques in awake, behaving macaques on an apparatus with a turntable mounted on a horizontal sled, convergent neurons were identified that carried both rotational and translational signals. After characterizing their responses to sinusoidal yaw rotation and horizontal translation stimuli individually, we recorded the responses to combined stimuli, usually 2 Hz sinusoidal translation at 0.1 g peak acceleration near the best response vector for the neuron with superimposed 0.5 Hz sinusoidal yaw rotation at a peak velocity of 30°/sec. The resultant response to the combined stimuli was compared to the response to the individual stimuli. A linear addition of the responses to individual stimuli did not predict the combined response well. There is a non-linear interaction of yaw and

translational stimuli such that responses when the animal is moved in the excitatory direction for both stimuli is larger than predicted by linear combination of the responses to the stimuli individually. We hypothesize that these responses could be explained by a coincidence detection mechanism which fires most robustly for combined movements in the excitatory direction.

### **288 Do Visual Motion After Effects (MAE) and Vestibular After Effects (VAE) Interact?**

**Benjamin Crane<sup>1</sup>**

<sup>1</sup>*University of Rochester*

The visual motion after effect (MAE) is the illusion of movement occurring after viewing visual motion such that a static pattern appears to move in the opposite direction. Recently, an analogous vestibular after effect (VAE) has been described: After a suprathreshold motion, perception of subsequent movement is biased, often in the opposite direction. Eleven human subjects, age 21 to 69 (mean 39) participated. Fore-aft motion or optic flow was studied with a central fixation. There was a first interval (adapter) stimulus which consisted of 15 cm of forward or backward motion over 1.5s (peak acceleration 42 cm/s/s, peak velocity 20 cm/s) which could be either visual or vestibular. The visual stimulus simulated motion through a star field which included appropriate binocular disparity at 100% coherence. This was followed by a interstimulus interval (ISI) of 500 ms. The test stimulus (second interval) was 500 ms and included a maximum of 5 cm of motion which was adjusted based on prior responses until the point of subjective equality (PSE) when the motion was equally likely to be identified as forward or backwards was reached. The visual test stimulus had decreased coherence to near 50% depending on the subject's thresholds. Using this protocol there was a significant visual MAE in 9 of 11 subjects in which perception of the test stimulus was always biased in the opposite direction of the adapter. There was a significant VAE in 5 of 11 subjects and in 3 of these subjects it was biased in the opposite direction. Combining a visual adapter stimulus with a vestibular test stimulus did not yield a significant VAE in any subject or in the group as a whole. Combining a vestibular adapter with a visual test stimulus produced a significant effect in a single subject – this subject had a significant VAE and MAE but both were in the opposite direction of the effect seen with the combined condition. We conclude that although VAE and MAE can cause similar effects on perception of future stimuli of the same modality, but one sensory modality does not influence subsequent perception of the other.

### **289 Facing Animal Rights Extremism: A Community Response**

**David Jentsch<sup>1</sup>**

<sup>1</sup>*University of California Los Angeles*

The techniques used by opponents of animal-based biomedical research are evolving and increasingly blend harassment of and attacks on individual researchers with their campaigns against universities and institutions. Additionally, the public component of their activism

involves characterizing research as useless, redundant and/or unethical. This presentation, and the ensuing discussion, will focus on the methods that individual researchers, clinicians and supporters of animal-based biomedical research can use to counteract the impact of the multi-dimensional threats from animal rights activists. From advocacy to education to activism, the role of the community of researchers in defending science is never more apparent.

### **290 Spontaneous Rate Groups in the Cochlear Nerve: Physiological Differences, Structural Basis and Vulnerability to Noise**

**Charles Liberman<sup>1,2</sup>**

<sup>1</sup>*Harvard Medical School*, <sup>2</sup>*Massachusetts Eye and Ear Infirmary*

Each type-I cochlear nerve fiber contacts a single inner hair cell (IHC) by a single terminal swelling forming a single synaptic complex; however, each IHC is contacted by 10 – 30 type-I fibers. We have long known that type-I fibers differ in spontaneous discharge rate (SR), and that SR is highly correlated with threshold sensitivity, maskability by continuous background noise, fiber caliber, mitochondrial content, location of the synaptic contact on the IHC circumference, complexity of the pre-synaptic ribbon and the nature and number of central targets in the cochlear nucleus. This talk will summarize more recent immunohistochemical work showing that high-SR synapses have more AMPA receptors and that low-SR fibers are more vulnerable to the primary neuronal degeneration seen after “temporary” noise-induced hearing loss. The latter observation may help explain why aging ears have more difficulty with speech in noise.

Research supported by NIDCD R01 00188

### **291 Spike Generation in the Spiral Ganglion Neuron - At the Origin of the Auditory Code**

**Mark Rutherford<sup>1</sup>, Nikolai Chapochnikov<sup>1,2</sup>**

<sup>1</sup>*Inner Ear Lab - University of Goettingen Medical School*,

<sup>2</sup>*Bernstein Center for Computational Neuroscience*

In addition to the place and rate code for sound frequency and intensity, the cochlea generates a temporal code for the periodicity of low-frequency tones and for fluctuations of sound amplitude. The significance of envelope modulation for speech comprehension is evident in the performance of cochlear implants, which function despite poor frequency resolution in terms of cochlear place. The behavioral relevance of 10-100  $\mu$ s interaural time differences in mammals and birds indicates the precision of the temporal code underlying sound source localization. Therefore, the first auditory synapse must generate an accurate and reproducible temporal code. Inner hair cell (IHC) neurotransmitter release to spiral ganglion neuron (SGN) spike initiation is the final biophysical transformation between a sound stimulus and the afferent neural code. In the cochlea of mice and rats, this transformation relies upon a 1:1 connection between an IHC ribbon-type pre-synapse and a postsynaptic SGN. We characterized spike generation at this functionally- and anatomically-unique connection, which exhibits generally strong and highly

variable discrete EPSCs. SGNs fired a single short-latency spike in response to sustained currents of sufficient onset speed. When EPSC-like current-clamp stimuli approximated the mean physiological EPSC ( $\approx 300$  pA) - several times larger than rheobase ( $\approx 50$  pA) - spikes were triggered with microsecond latency ( $\approx 500$   $\mu$ s) and precision ( $< 50$   $\mu$ s). Due to a large synaptic conductance, tight anatomical coupling, and phasic excitability, SGN spikes are locked to IHC exocytosis-timing with little distortion. SGNs are able to fire at high rates in response to sound, however, their phasic excitability suggests that a train of discrete synaptic events is required for repetitive firing. This fast, reproducible, and reliable initial encoding of sound is instrumental for a precise auditory temporal code.

### **292 Multivesicular Release and Phase-Locking at Hair Cell Ribbon Synapses**

**Henrique von Gersdorff<sup>1</sup>**, Cole Graydon<sup>2</sup>, Soyoun Cho<sup>1</sup>, Geng-lin Li<sup>1</sup>, Bechara Kachar<sup>2</sup>

<sup>1</sup>*Vollum Institute, OHSU*, <sup>2</sup>*NIDCD*

Recordings from auditory nerve endings in the cochlea and amphibian papilla display large EPSC events. These EPSCs are presumably caused by multivesicular release. Two underlying mechanisms have been proposed: multiple docked vesicles underneath the synaptic ribbon release simultaneously (coordinated fusion), or vesicles tethered to the synaptic ribbon undergo homotypic fusion prior to fusion with the presynaptic membrane (compound fusion). Under coordinated fusion, all fusion-competent vesicles are restricted to the presynaptic membrane, while compound fusion implies fusion-competent vesicles some distance from the presynaptic membrane. We will compare vesicle pool estimates at a bullfrog ribbon synapse using ultrastructural and physiological methods. By manipulating presynaptic calcium microdomains with presynaptic buffers, we find tight congruence between anatomical and functional vesicle pools. Under stronger presynaptic buffering conditions, which restrict Ca rises to a few nanometers above the plasma membrane, we still observed large EPSC events. We thus suggest that multivesicular release is due to a highly synchronous form of coordinated fusion of docked vesicles beneath the synaptic ribbon. The ribbon may function as a booster of the local Ca concentration by restricting the volume available for Ca ions to diffuse at the active zone. Ca nanodomains produced by the opening of a single Ca channel can thus trigger multivesicular release. Furthermore, we will propose that large multiquantal EPSCs produce EPSPs that are better phase-locked to a sinewave stimulus than small EPSPs. Multivesicular release thus enhances the precision of spike phase-locking at the auditory nerve.

### **293 Regulation of Synaptic Release from Ribbon Synapses of Cone Photoreceptors in Light and Dark**

**Wallace Thoreson<sup>1</sup>**

<sup>1</sup>*University of Neb. Med. Center, Omaha, NE*

In darkness, cone photoreceptors have a relatively depolarized membrane potential that stimulates the opening of L-type  $Ca^{2+}$  channels beneath the synaptic ribbon. Light hyperpolarizes cones, causing these channels to close. We studied mechanisms of release from cones by obtaining simultaneous whole cell recordings from cones and second-order neurons in the salamander retina slice preparation. Although fast transient and slow sustained release from cones both involve the synaptic ribbon, the dominant mechanisms regulating release differ in light and dark. When cones are hyperpolarized (e.g., in bright light), release evoked by subsequent depolarization requires the opening of  $<3$   $Ca^{2+}$  channels per vesicle fusion event at the peak of release. This high release efficiency may improve detection of small light decrements. With maintained depolarization (e.g., in darkness), release efficiency diminishes to low levels as the releasable pool of vesicles becomes depleted. Under these conditions, the sustained rate of vesicle release is not determined by individual  $Ca^{2+}$  channel openings but by the rate at which the releasable pool can be replenished. Replenishment is  $Ca^{2+}$ -dependent allowing changes in  $[Ca^{2+}]_i$  driven by changes in cone membrane potential to control the rate of release.  $Ca^{2+}$ -dependent sites involved in replenishment are further from  $Ca^{2+}$  channels ( $>200$  nm) than are release sites ( $<50$ - $100$  nm). This links the sustained rate of release to average  $[Ca^{2+}]_i$  rather than individual channel openings and may help to make sustained release in darkness less noisy by reducing synaptic noise introduced by the stochastic probability of individual channel opening. Combining the clustering of  $Ca^{2+}$  channels at the ribbon with the use of a high  $Ca^{2+}$  affinity release mechanism allows the cone synapse to shift between two signaling modes as the cone moves from bright light to darkness.

### **294 Properties of Synaptic Transmission at Different Hair Cell Ribbon Synapses – a Functional Comparison**

**Elisabeth Glowatzki<sup>1</sup>**

<sup>1</sup>*The Johns Hopkins School of Medicine, Baltimore, MD, USA*

Over the last decade we have accumulated substantial knowledge about the properties of synaptic transmission at hair cell ribbon synapses. The main methods that were used include capacitance recordings from hair cells that monitor exocytosis, optical methods monitoring vesicle fusion or calcium influx at synaptic sites and postsynaptic recordings monitoring excitatory postsynaptic events or action potentials in afferent nerve fibers. Different preparations have been chosen for investigating synaptic transmission, utilizing different species and organs, for example the zebrafish lateral line organ, turtle and frog papilla, frog sacculus, the mammalian cochlea and

vestibular organs. Also, ribbon synapses have been investigated in depth in the retina in different cell types. A number of features at ribbon synapses seem to be found universally, like the association with calcium channels that activate at fairly negative voltages. Other features may only apply to some ribbon synapses. For example, multivesicular release seems to be prominent at several ribbon synapses, but not all. As our knowledge accumulates, it becomes more obvious that ribbon synapses do not just follow a general mechanism by which synaptic transmission occurs. In contrast, individual synapses seem to be quite specialized for their specific tasks in the specific organ they are functioning in. The goal of this presentation is to discuss and compare the properties of individual ribbon synapses. I will compare data that have been recorded in different preparations and I will discuss features of synaptic transmission in the context of the specialization of individual organs that specific ribbon synapses function in.

Supported by NIDCD R01 006476 to EG and the Vestibular Fund, Department of Otolaryngology Head and Neck Surgery, The Johns Hopkins School of Medicine.

### **[295] Synaptotagmins and Otoferlin at the Auditory Hair Cell Ribbon Synapse: Where Are We Now ?**

**Saad Safieddine<sup>1</sup>**, Maryline Beurg<sup>1</sup>, Nicolas Michalski<sup>1</sup>, Didier Dulon<sup>1</sup>, Christine Petit<sup>1</sup>  
<sup>1</sup>*Institut Pasteur*

The first synapse of the auditory system, between inner hair cells (IHCs) and spiral ganglion neurons, has the remarkable property to encode auditory hair cell receptor potentials into patterned trains of neural action potentials. The IHC transmitter release (glutamate) involves voltage-gated Cav1.3 channels that control vesicle fusion (exocytosis) tightly at the ribbon active zone. A key issue raised by this synaptic process concerns the identification of the Ca<sup>2+</sup> sensors that transduce Ca<sup>2+</sup> signals into fast and tightly regulated synaptic vesicle fusion at the IHC ribbon synapses. Remarkably, synaptotagmins 1 and 2, considered as the major Ca<sup>2+</sup> sensors at the CNS synapses, are not detected in mature IHCs, suggesting that the IHC synapses use an as yet unidentified "synaptotagmin-like" calcium sensor. Genetic screening for an hereditary form of human deafness has led to the identification of otoferlin, a six C2 domain protein, which is defective in the recessive form of human deafness DFNB9. The study of the corresponding null mutant mice led us to suggest that otoferlin may be major Ca<sup>2+</sup> sensor at the IHC ribbon synapse. Despite significant data accumulated in the past five years in support of otoferlin being a Ca<sup>2+</sup> sensor, the accurate steps of the vesicle cycle when otoferlin may act continues to be intensely debated. Here, we will discuss new findings and current concepts about the functions of otoferlin and synaptotagmins both at the immature and mature IHC ribbon synapses.

This work was supported the French National Research Agency, ANR-07-Neuroscience (S.S) and Louis-Jeantet for Medicine Foundation (C.P).

### **[296] Active Synaptic Vesicle Trafficking in Turtle Auditory Papilla Hair Cells**

**Anthony Ricci<sup>1</sup>**, Michael Schnee<sup>1</sup>, Manuel Castellano-Munoz<sup>1</sup>, Jee-Hyun Kong<sup>1</sup>, Joseph Santos-Sacchi<sup>2</sup>  
<sup>1</sup>*Stanford University*, <sup>2</sup>*Yale University*

The turtle auditory papilla is tonotopically organized and provides a mature hearing organ in which to investigate presynaptic release mechanisms of hair cells. These hair cells are largely innervated by one afferent fiber with a tonotopically varying number of synapses. Previous data suggested that vesicle release, using the single sine technique to track capacitance, was linear over a large range of calcium influx. This result also indicated that in order to maintain continual release vesicles not within the immediate vicinity of the synaptic region had to be recruited. Identifying distinct pools of releasable vesicles proved to be difficult in turtle papilla hair cells due to their somewhat unique ability for recruiting vesicles. Paired pulse experiments, designed specifically to identify vesicle pools, produced facilitated release as opposed to depletion, again supporting an argument for rapid recruitment of vesicles. In order to better follow vesicle trafficking a dual sine wave techniques was developed that allowed for continual monitoring of membrane capacitance even in the face of conductance changes. This technique led to the identification of two distinct release modes. The first varied linearly with calcium entry, was depletable, and represented all vesicles associated with the synaptic ribbon. The second had an invariant and rapid release rate and required recruitment of vesicles from outside of the synaptic region. Correlating with the second mode a superlinear increase in internal calcium was observed, intimating a role for calcium induced calcium release.

This work was funded by NIDCD Grant DC009913 to AJR, core grant P30 44992 and MCM was funded by the Cajamadrid Foundation

### **[297] Probing Synaptic Transmission at Retinal Ribbon Synapses Using Light**

**David Zenisek<sup>1</sup>**  
<sup>1</sup>*Yale University School of Medicine*

In vision, balance, and hearing, sensory receptor cells translate sensory stimuli into electrical signals whose amplitude is graded with stimulus intensity. The output synapses of these sensory neurons must provide fast signaling to follow rapidly changing stimuli, while also transmitting graded information covering a wide range of stimulus intensity and sustained for long time periods. To meet these demands, specialized machinery for transmitter release—the synaptic ribbon—has evolved at the synaptic outputs of these neurons. This talk will focus on recent results from our laboratory using two complimentary techniques: imaging individual synaptic vesicles in dissociated neurons using total internal reflection fluorescence microscopy (TIRFM) and paired electrophysiological recordings of retinal neurons in slice

before and after being subjected to acute photodamage using a synaptic ribbon-targeted peptide.

## **[298] Using Whole Exome Sequencing to Identify Novel Deafness Genes**

**Marci Lesperance**<sup>1</sup>, Sarah Emery<sup>1</sup>, Margit Burmeister<sup>1</sup>, Ericka King<sup>1</sup>, Karen Majczenko<sup>1</sup>, Jishu Xu<sup>1</sup>, Jun Li<sup>1</sup>

<sup>1</sup>*University of Michigan*

A remarkable number of genes and proteins important in the development and maintenance of hearing have been identified through the study of large families with hereditary deafness. However, genetic heterogeneity makes it difficult to efficiently identify the molecular etiology in families that lack *GJB2* mutations, particularly for most types of dominant hearing loss. We are using next-generation sequencing technologies to identify novel deafness genes in small dominant families. In Family 106, segregating autosomal dominant high-frequency sensorineural hearing loss (SNHL), a genome scan was performed by genotyping 6,000 single nucleotide polymorphisms (SNPs) using HumanLinkage-12 chips (Illumina). Parametric linkage analysis was performed with MERLIN (Abecasis et al. 2002), identifying a 15 Mb linkage region on chromosome 19q13.11-19q13.33, with a multipoint LOD score of 4.01. This locus partially overlaps the DFNA4 locus (Chen et al. 1995), but excludes *MYH14* (Donaudy et al 2004). Mutations in a second DFNA4 gene, *CEACAM16* (Zheng et al 2011), were excluded by DNA sequencing. Whole exome sequencing of an uncle-nephew affected pedigree member pair was performed, using the Nimblegen Whole-Exome SeqCap method for target capture to select for coding exons. Purification and quality assessment was performed (Agilent 2100 Bioanalyzer), with 72-108 base paired-end sequencing (Illumina Genome Analyzer II). Known variants described in db SNP, HapMap, 1000 Genomes, and the University of Washington Exome Variant databases were filtered. 7 novel candidate variants predicted to be damaging were found in both samples within the linkage interval. With this approach, we are identifying candidate variants in additional families with dominant SNHL, recessive SNHL, and otosclerosis. Identifying dominant genes is more difficult, but preliminary linkage information and sequencing two distantly related family members is helpful to reduce the number of candidate variants.

## **[299] Whole Exome Sequencing of Four Members in a Family Segregating High Frequency Hearing Loss in an Autosomal Dominant Manner Identifies a New Genotype-Phenotype Correlation in a Known Deafness Gene**

**Byung Yoon Choi**<sup>1</sup>, Ah Reum Kim<sup>2</sup>, Jin Woong Choi<sup>2</sup>, You Sun Chung<sup>2</sup>, Kyu-Hee Han<sup>2</sup>, Namhiseon Kim<sup>3</sup>, Seung-Ha Oh<sup>2</sup>

<sup>1</sup>*Department of Otorhinolaryngology, Seoul National University Bundang Hospital, Seongnam, South Korea,*

<sup>2</sup>*Department of Otorhinolaryngology, Seoul National University College of Medicine,* <sup>3</sup>*Industrial Biotechnology*

*and Bioenergy Research Center, Korea Research Institute of Bioscience*

Given emerging new technologies such as next generation sequencing, we aimed to make a molecular genetic diagnosis of high frequency hearing loss in a multiplex family. We performed whole exome sequencing of two affected and two unaffected family members of the family segregating high frequency hearing loss in an autosomal dominant manner. Capture was done by NimbleGen SeqCap EZ Human Exome Library v2.0 and the sequencing was performed by HiSeq2000 using paired-end (2x100). Comprehensive bioinformatic analyses of the genome of the four members revealed twenty two possibly pathogenic variants. To further reduce down the number of candidate variants, additional three members were recruited and the twenty two variants were screened by Sanger sequencing from the additional three members. Following this, we were left with only six variants. Among these variants, two variants (one in *TECTA* and the other in *ORC4L*) were detected in the genes that are expressed in the inner ear. Therefore, it is most likely that hearing loss in this family can be attributed to one of these two variants. Interestingly, p.T237I variant in *TECTA* resides in the Entactin (ENT) domain of this protein. This is contrasted with the report in the literature that mutations in this domain cause mid-frequency hearing loss, since our family segregates high frequency hearing loss. Therefore, our result may reveal a new genotype phenotype correlation. We are currently working to see further if one of these two variants is really pathogenic. In conclusion, whole exome sequencing of a trio and an unaffected member in a family enables us to reach a gene list with only a very few candidate genes in a family segregating dominantly inherited high frequency hearing loss, possibly revealing a new genotype –phenotype correlation. This result sheds light upon the important future implication of whole exome sequencing in molecular genetic diagnosis of an autosomal dominant hearing loss in Koreans.

## **[300] Identification of New Deafness Genes Using High Throughput Technologies in Italian and Qatari Populations**

**Giorgia Giroto**<sup>1</sup>, Moza Alkowiari<sup>2</sup>, Khalid Abdulhadi<sup>3</sup>, Flavio Faletra<sup>1</sup>, Diego Vozzi<sup>4</sup>, Danilo Licastro<sup>4</sup>, Emmanouil Athanasakis<sup>1</sup>, Ramin Badii<sup>2</sup>, Paolo Gasparini<sup>1</sup>

<sup>1</sup>*Med Gen, Dep of Repr Sci IRCCS-Burlo Garofolo, Univ of Trieste,* <sup>2</sup>*Molecular Genetics Laboratory, Hamad Medical Corporation, Doha, Qatar,* <sup>3</sup>*ENT Division, Hamad Medical Corporation, Doha, Qatar,* <sup>4</sup>*CBM srl., Basovizza, Trieste, Italy*

Hereditary Hearing loss (HLL) is a common sensory disorder. Most cases (70%) are non-syndromic (NSHLL) with *GJB2* gene mutations, *GJB6* deletion, and A1555G mitochondrial mutation playing a major role worldwide. In particular, *GJB2* mutations, *GJB6* deletion, and A1555G mitochondrial mutation account for approximately 35% of Italian pathogenic alleles and almost no other common genes have been identified. Regarding the Qatari population, a molecular screening for these common genes/mutations on 126 Qatari patients clearly

demonstrates that GJB2, GJB6 deletion and A1555G accounts for a minor proportion of NSHL cases in this population. Thus, these findings strongly suggest that many genes for NSHL await identification and, until recently, linkage analysis was the first step in positional cloning approaches. Now, the availability of Next Generation Sequencing (NGS) technologies opens new perspectives in the search for causative genes. To increase our knowledge on the molecular bases of HHL in the Italian and Qatari populations, an extensive use of high throughput technologies such as High Density SNPs arrays (i.e for linkage data) and Next Generation Sequencing has been planned. Six Italian families (dominant inheritance) and 5 Qatari ones (recessive inheritance), all negatives for the presence of mutations in the most common HHL genes, have been selected. HD SNPs arrays have been utilized to get "sniff" linkage data and define a number of candidate loci to be applied in the NGS filtering phase. NGS protocols have been used to obtain whole exome data. After filtering (dbSNP and in-house database), some candidate genes have been identified in both populations. Results have been validated by Sanger sequencing and should be further investigated at the functional level. They will definitely increase our knowledge of new HHL genes, further confirming the importance of such new technologies for disease gene identification. Data will be presented and discussed.

### **[301] A Massively Parallel Headache - Should Exome Sequencing Play a Role in Small OtoSCOPE®-Negative Families?**

**Eliot Shearer**<sup>1,2</sup>, Michael Hildebrand<sup>1</sup>, Steve Scherer<sup>3</sup>, Richard Smith<sup>1,4</sup>

<sup>1</sup>Dept of Otolaryngology, University of Iowa, <sup>2</sup>Dept of Molecular Physiology & Biophysics, <sup>3</sup>Human Genome Sequencing Center, Baylor College of Medicine, <sup>4</sup>Interdepartmental PhD Program in Genetics, University of Iowa

**Background:** Sensorineural hearing loss is the most common human sensory deficit, affecting one of every 500 newborns. 57 genes have been causally implicated in non-syndromic hearing loss (NSHL). The OtoSCOPE® platform provides simultaneous comprehensive genetic screening of these genes dramatically improving the clinical diagnosis and management of deaf and hard-of-hearing families.

**Methods:** An American family segregating autosomal dominant, non-progressive, downsloping NSHL was studied. Sufficient meioses were unable to unambiguously map a candidate interval and because allele segregation was consistent with disease-causing variants at several known DFNA loci, one affected individual was screened using the OtoSCOPE® platform. An autosomal dominant NSHL variant was not identified. Based on this result, exome sequencing was performed on the same affected individual using SureSelect 50MB exome capture followed by SOLiD sequencing. Reads were mapped using BWA and analyzed using GATK and ANNOVAR.

**Results:** OtoSCOPE® screening identified 35 rare nonsynonymous or indel variations however none segregated with the deafness phenotype. With the SureSelect 50MB exome sequencing, 85% of the exome was covered at a variant-calling threshold of 10X depth of coverage. 54,609 variants were identified, of which 2,946 were rare and heterozygous. Filtering using ANNOVAR and specifically looking at variants within genomic regions defined by allele segregation identified 11 candidate variants which are now being studied.

**Conclusions:** The OtoSCOPE® platform should be used in families segregating deafness if linkage analysis has not been done or if the number of informative meioses precludes identifying a single linked interval. If variants are not found in the genes included on OtoSCOPE®, exome sequencing should be considered. Exome sequencing has been used successfully in many families segregating Mendelian diseases like deafness however there are significant limitations associated with its use. These limitations are discussed and the role of exome sequencing as a complement to the OtoSCOPE® platform is discussed.

### **[302] Genome Wide Association Study Aimed at the Identification of New Candidate Genes for Age-Related Hearing Loss**

**Giorgia Giroto**<sup>1</sup>, Nicola Pirastu<sup>1</sup>, Morag Lewis<sup>2</sup>, Beatriz Lorente<sup>2</sup>, Karen P Steel<sup>2</sup>, Paolo Gasparini<sup>1</sup>

<sup>1</sup>Med Gen, Dep of Repr Sci IRCCS-Burlo Garofolo, Univ of Trieste, <sup>2</sup>Wellcome Trust Sanger Institute, Wellcome Trust Genome Campus, Hinxton, Cambridge CB10 1SA, UK

Age-related hearing loss (ARHL) or presbycusis is a complex disease with multifactorial etiology. Thus, research is still needed to understand the genetic factors underlying ARHL. To reach this goal an integrated strategy, based on two main approaches, has been designed: genetic analysis in human populations and functional studies in animal models. The genetic analysis has been planned as follows: A) a genome-wide association study (GWAS) on qualitative traits, B) a replica phase of the data, and C) whole exome resequencing of some selected patients. Up to now, by meta-analysis of data from 6 isolated populations some significant and suggestive loci/genes (including genes known to be involved in auditory development and function but also genes whose function is still unknown) have been found. The replica phase in additional sample cohorts (approx. 2000 samples coming from Italy, UK and Silk Road countries) is in progress, as well as the validation of data obtained from whole exome resequencing of cases selected from large Italian pedigrees showing segregation of ARHL.

Matching these data with those previously obtained in our quantitative analysis (Giroto et al. JMG 2011), we were able to define a list of strong candidate genes that have been chosen for validation. Briefly, we are investigating the expression of these candidate genes by immunohistochemistry and by confocal microscopy using wildtype mice at 4 and 5 days old. Three of these candidates show striking specific expression at the top of

sensory hair cells in the cochlea, another one is expressed in the marginal cells of the stria vascularis and other six are clearly expressed throughout the cochlea. These findings further confirm the usefulness of combining GWAS population data with expression studies to identify strong candidates for ARHL that may provide new targets for hearing impairment treatment and prevention.

### **303 Identification and Characterization of Mouse Models of Age-Related Hearing Loss**

**Michael Bowl**<sup>1</sup>, Prashanthini Shanthakumar<sup>1</sup>, Joanne Dorning<sup>1</sup>, Susan Morse<sup>1</sup>, Carlos Aguilar<sup>1</sup>, Laura Wisby<sup>1</sup>, Andrew Parker<sup>1</sup>, Sara Wells<sup>2</sup>, Paul Potter<sup>1</sup>, Steve Brown<sup>1</sup>  
<sup>1</sup>*Mammalian Genetics Unit, MRC Harwell, Harwell Oxford, UK*, <sup>2</sup>*Mary Lyon Centre, MRC Harwell, Harwell Oxford, UK*

Age-related hearing loss (Presbycusis) is a significant health and social burden on the population and is one of the four leading chronic health conditions experienced by the elderly. Greater than 25% of adults aged 50 and over have a hearing loss of 30 dB or more (increasing to 70-80% of people aged 75 and over), and with current projections that by 2050 the world's population aged 60 and over will be ~2 billion, this is a major public health problem. At MRC Harwell we are utilizing a large-scale N-ethyl-N-nitrosourea (ENU) mutagenesis screen to identify mouse models of aging. G3 pedigrees, of ~100 mice, are bred and enter a phenotyping pipeline comprising recurrent assessment across a wide range of disease areas including, diabetes and metabolism, neurobehaviour, bone analysis, renal/hepatic function, cardiac disease, clinical chemistry, and sensorineural. The Deafness Model Discovery team is taking advantage of this screen to identify models of presbycusis. We conduct recurrent auditory phenotyping at several timepoints, consisting of Clickbox (20kHz tone, 90dB SPL) at 3, 6, 9 and 12 months of age, and Auditory-Evoked Brainstem Response (click, 8, 16, 32kHz) at 3 and 9 months. As of September 2011, 60 pedigrees have entered the phenotyping pipeline, of which 11 have completed auditory screening. To date 3 pedigrees have confirmed phenotypes with elevated hearing thresholds. One pedigree has a high frequency hearing impairment at 9 months of age, another shows elevated hearing thresholds at all frequencies at 3 months of age, and a third demonstrates early onset deafness coupled with circling behaviour indicative of a vestibular defect. Mapping studies and characterization of these mutant mice is underway. The Harwell Aging Mutant Screen is already producing pedigrees with interesting auditory phenotypes. Investigation of these, and as yet unidentified pedigrees, promises to increase our understanding of the genetics underlying hearing and its age-related decline.

### **304 Identifying Drug Targets for Prevention and Treatment of Hearing Loss**

**Rachel Burt**<sup>1,2</sup>, Marina Carpinelli<sup>1,2</sup>, Michael Manning<sup>1,2</sup>, Anne Cooray<sup>1,2</sup>  
<sup>1</sup>*Walter & Eliza Hall Institute*, <sup>2</sup>*Hearing Co-operative Research Centre*

**Background:** Age-related hearing loss (presbycusis) is a significant public health issue and is predicted to become increasingly so given the aging population. Noise, and drug-induced hearing-loss are also common. The molecular mechanisms resulting in these conditions are poorly understood. However, it is clear that apoptosis of cells within the cochlea is often involved. Through better understanding of the genetics of hearing loss it is hoped that we will identify therapeutic targets for prevention and treatment of presbycusis and environmentally-induced hearing loss.

**Objectives:** To understand the molecular basis of hearing loss so as to identify drug targets for prevention and treatment of deafness.

**Method:** A combination of reverse and forward genetic approaches to studying hearing loss in mouse models, have been used to characterize the genetic and molecular variation underlying hearing loss. Two major streams of work are underway. Firstly, Ethyl Nitrosourea (ENU) mutagenesis screens are being conducted to identify genes involved in progressive forms of hearing loss. Secondly, a panel of engineered mouse strains harboring mutations in apoptotic regulators is being assessed for hearing loss, to better understand the role of cell death in the auditory system.

**Results:** Mutations at particular points of the intrinsic pathway of apoptosis have a profound effect on the auditory system. In addition, genome-wide ENU mutagenesis screens have generated a number of mutant mouse strains with subtle and progressive forms of hearing loss. Several interesting mutations are currently being mapped and characterized.

**Conclusion:** Our work suggests that tightly regulated apoptosis is required for both development and maintenance of hearing. Targeting of apoptotic regulators may prove useful in prevention of cell death and resultant hearing loss in the ear. Future work is planned to test this hypothesis.

### **305 A Dense Gene-Centric Association Study Identifies Common Variation That Is Significantly Associated with Pure Tone Average**

**Nathan Pankratz**<sup>1</sup>, James Pankow<sup>1</sup>, Guan-Hua Huang<sup>2</sup>, Barbara Klein<sup>3</sup>, Ronald Klein<sup>3</sup>, Karen Cruickshanks<sup>3</sup>  
<sup>1</sup>*University of Minnesota*, <sup>2</sup>*National Chiao Tung University*, <sup>3</sup>*University of Wisconsin-Madison*

Age-related hearing loss is a common chronic condition with a complex etiology. While there are well-known environmental risk factors, family and twin studies have consistently shown that genetics plays a significant role in developing the condition. Linkage studies have identified several regions and a few rare genes, but genome-wide

association studies (GWAS) have so far failed to identify common variation associated with hearing loss at genome-wide significance. By using the HumanCVD Genotyping BeadChip, we employed a pathway approach, interrogating 50,000 SNPs distributed across ~2,000 genes/loci previously associated with a range of cardiovascular, metabolic and inflammatory syndromes. Genotyping was performed for 3,627 adults (from 1635 families) ages 45-79 years from the Epidemiology of Hearing Loss Study (EHLS) and the Beaver Dam Offspring Study (BOSS). We focused on a quantitative endophenotype that should have greater statistical power than a dichotomous phenotype to detect subtle effects. Pure tone average (PTA) was computed using 0.5, 1, 2, and 4 KHz data for the better ear. Linear mixed effects models were then used to identify associations with individual SNPs while controlling for familial relationships and age. The most significant association was with SNPs in the GRK5 region on chromosome 10 (minimum  $p=2.2 \times 10^{-8}$ ; rs10886439;  $\beta=-2.0$  for each copy of the C allele). This exceeded both array-wide significance ( $p < 1 \times 10^{-6}$ ) and conventional genome-wide significance ( $p < 5 \times 10^{-8}$ ), and the p-value was several orders of magnitude lower than the region with the next most extreme p-values ( $p=1 \times 10^{-5}$ ). When analyzing the 973 prevalent hearing-loss cases in this cohort using a logistic model, the odds ratio for the less frequent allele (C; allele frequency 15%) was 0.76 ( $p=0.009$ ). This study is the first to identify the GRK5 region as being associated with a hearing phenotype.

### **306 Spns2 Deficiency Causes Deafness and Defects in the Cochlear Lateral Wall in Mice**

Jing Chen<sup>1</sup>, Neil Ingham<sup>1</sup>, Selina Pearson<sup>1</sup>, Johanna Pass<sup>1</sup>, David Goulding<sup>1</sup>, John Kelly<sup>2</sup>, Daniel Jagger<sup>2</sup>, Andrew Forge<sup>2</sup>, Karen Steel<sup>1</sup>

<sup>1</sup>Wellcome Trust Sanger Institute, <sup>2</sup>UCL Ear Institute

Spns2 is thought to act as a sphingolipid transporter based upon a previous zebrafish mutant study. Little is known about its function in mammals. *Spns2*-deficient mice showed highly elevated auditory brainstem response (ABR) thresholds at 14 weeks in a high-throughput targeted mutagenesis programme (the Sanger Institute's Mouse Genetics Project). *Spns2*-deficient mice rapidly lost their hearing from 2 weeks to 3 weeks old. Immunofluorescence analysis of wild type mice showed that Spns2 is expressed in both the organ of Corti and lateral wall. Degeneration of hair cells was revealed by scanning electron microscopy from 4 weeks old only, indicating that this may be a secondary change. A low endocochlear potential (EP) suggested dysfunction of the lateral wall. Morphological changes of marginal cell tight junctions were observed and capillaries in the stria vascularis appeared expanded, but this does not seem to affect their permeability to BSA-FITC. However, the expression of the critical proteins involved in the formation of EP, Kcnj10, Cx26 and Cx30, were found to be decreased in *Spns2*-deficient mice. Disruption of expression of lateral wall proteins may be sufficient to account for the abnormal EP production. Targeted ablation of *Spns2* in the inner ear by using Sox10-Cre gave a

similar phenotype to the original mutation suggesting that Spns2 is required locally in the inner ear rather than systemically for normal hearing. These mutant phenotypes suggest that Spns2 plays a critical role in hearing in mice.

### **307 Pannexin Deficiency Can Induce Hearing Loss**

Yan Zhu<sup>1</sup>, Chun Liang<sup>1</sup>, Liang Zong<sup>1</sup>, Hong-Bo Zhao<sup>1</sup>

<sup>1</sup>University of Kentucky Medical Center

As a new gap junction gene family, pannexins have distinct expression patterns in the mammalian cochlea, suggesting that pannexins also play an important role as connexins in hearing. In this study, we used a loxP-Cre gene knockout (KO) technique to knockout Pannexin 1 (Panx1) expression in the cochlea. We found that KO of Pannexin1 could induce hearing loss. Auditory brainstem response (ABR) in Panx1 KO mice was reduced. The ABR threshold in Panx1 KO mice could be increased about 30 dB SPL in comparison with wild-type (WT) littermates. However, distortion product otoacoustic emission (DPOAE) in Panx1 KO mice was not significantly changed. Cochlear microphonics (CM) also was not significantly reduced. Connexin 26 (Cx26) and Cx30 are two major connexin isoforms expressed in the cochlea. Panx1 KO did not alter and reduce Cx26 and Cx30 expressions. Immunofluorescent staining shows that Cx26 and Cx30 had normal expression in the Panx1 KO mouse cochlea. These data indicate that pannexins can play divergent, rather than redundant, functions in the cochlea and are critical for hearing.

Supported by DC05989

### **308 A Noncoding Point Mutation of Zeb1 Causes Inner Ear Malformation in Twirler Mice**

Kiyoto Kurima<sup>1</sup>, Ronna Hertzano<sup>2</sup>, Oksana Gavrilova<sup>1</sup>, Kelly Monahan<sup>1</sup>, Karl Shpargel<sup>1</sup>, Garani Nadaraja<sup>1</sup>, Yoshiyuki Kawashima<sup>1</sup>, Kyu Yup Lee<sup>1</sup>, Taku Ito<sup>1</sup>, Yujiro Higashi<sup>3</sup>, David Eisenman<sup>2</sup>, Scott Strome<sup>2</sup>, Andrew Griffith<sup>1</sup>  
<sup>1</sup>NIH, <sup>2</sup>University of Maryland, <sup>3</sup>Aichi Human Service Center

Heterozygous Twirler (*Tw*) mice display circling behavior associated with malformations of the inner ear. The purpose of our study was to characterize the Twirler ear phenotype and to identify the causative mutation. *Tw*+/+ inner ears have irregular semicircular canals, abnormal utricular otoconia, a shortened cochlear duct, and hearing loss, whereas *Tw*/*Tw* ears are severely malformed with barely recognizable anatomy. We identified a noncoding nucleotide substitution, c.58+181G>A, in the first intron of the *Tw* allele of *Zeb1* (*Zeb1*<sup>*Tw*</sup>). *Zeb1* is a zinc finger transcription factor that is thought to repress expression of epithelial-specific genes in developing inner ear mesenchyme (See abstract by Hertzano et al.). A knockin mouse model of c.58+181G>A recapitulated the *Tw* phenotype, whereas a wild type knockin control did not, confirming the mutation as pathogenic. We observed increased levels of *Zeb1*<sup>*Tw*</sup> transcript and protein in comparison to wild type *Zeb1*. *Zeb1*-null mouse ears appear to be normal or near-normal, whereas *Tw* ears

have a pathologic disruption of epithelial and mesenchymal cell identities. We conclude that a noncoding point mutation of *Zeb1* acts via a gain-of-function to disrupt regulation of *Zeb1*<sup>Tw</sup> expression and leads to abnormal development of the inner ear in Twirler mice.

### **309** Modifier(S) of Hypothyroidism-Induced Hearing Impairment in *Pou1f1*<sup>dw</sup> Dwarf Mice

**Qing Fang**<sup>1</sup>, Chantal Longo-Guess<sup>2</sup>, Leona Gagnon<sup>2</sup>, Michelle T. Fleming<sup>1</sup>, Thomas J. Jones<sup>1</sup>, Amanda H. Mortensen<sup>1</sup>, David F. Dolan<sup>1</sup>, Kenneth R. Johnson<sup>2</sup>, Sally A. Camper<sup>1</sup>

<sup>1</sup>University of Michigan, <sup>2</sup>The Jackson Laboratory

Modifier(s) of hypothyroidism-induced hearing impairment in *Pou1f1*<sup>dw</sup> dwarf mice

Thyroid hormone has pleiotropic effects on cochlear development, and genomic variation influences the severity of associated hearing deficits. DW/J-*Pou1f1*<sup>dw/dw</sup> mutant mice lack pituitary thyrotropin, which causes severe thyroid hormone deficiency and profound hearing impairment. To assess the genetic complexity of protective effects on hypothyroidism-induced hearing impairment, an F1 intercross was generated between DW/J-*Pou1f1*<sup>dw/+</sup> carriers and an inbred strain with excellent hearing derived from *Mus castaneus*, CAST/EiJ. Approximately 24% of the (DW/J x CAST/EiJ) *Pou1f1*<sup>dw/dw</sup> F2 progeny had normal hearing. A genome scan revealed a locus on Chromosome 2, named modifier of *dw* hearing, *Mdwh*, that rescues hearing despite persistent hypothyroidism. This chromosomal region contains the modifier of tubby hearing 1 (*Moth1*) locus that encodes a protective allele of the microtubule-associated protein MTAP1A. DW/J-*Pou1f1*<sup>dw/+</sup> carriers were crossed with the AKR strain, which also carries a protective allele of *Mtap1a*, and we found that AKR is not protective for hearing in the (DW/J x AKR) *Pou1f1*<sup>dw/dw</sup> F2 progeny. Thus, protective alleles of *Mtap1a* are not sufficient to rescue DW/J-*Pou1f1*<sup>dw/dw</sup> hearing. We carried out a cross between DW/J and 129P2/OlaHsd. 129P2/OlaHsd is another strain with protective alleles of *Mtap1a*. About 15% of the (DW/J x 129P2/OlaHsd) *Pou1f1*<sup>dw/dw</sup> F2 progeny had normal hearing, and there was a broad distribution of hearing acuity, consistent with the idea that multiple loci interact to confer protection. The *Mdwh* locus was the most significant protective locus found in this cross. We expect that identification of protective modifiers will enhance our understanding of the mechanisms of hypothyroidism-induced hearing impairment.

### **310** Digenic Inheritance of Deafness Caused by 8J Allele of Myosin-VIIA and Mutations in the Genes Encoding Scaffolding Molecules Harmonin and Sans

Qing Yin Zheng<sup>1,2</sup>, John Scarborough<sup>3</sup>, Heping Yu<sup>1</sup>, Ye Zheng<sup>1</sup>, Peter Gillespie<sup>3</sup>

<sup>1</sup>Case Western Reserve University, <sup>2</sup>The Jackson Laboratory, <sup>3</sup>Oregon Health & Science University

Deaf mouse lines have contributed substantially to our understanding of inner-ear function. We identified a spontaneously arising mouse line that exhibited profound deafness; complementation experiments showed that it was a *Myo7a* allele, which we refer to as *Myo7a*<sup>sh1-8J</sup>. Genomic characterization indicated that *Myo7a*<sup>sh1-8J</sup> arose from deletion of 6.4 kb of genomic DNA encompassing exons 38-40 and 42-46. *Myo7a*<sup>sh1-8J</sup> mice had no detectable auditory brainstem response, displayed highly disorganized hair-cell stereocilia, and had no detectable *Myo7a* protein. Weak expression of *Myo7a* transgenes did not rescue the inner-ear phenotype. We generated mice that were digenic heterozygotes for *Myo7a*<sup>sh1-8J</sup> and one of each *Cdh23*<sup>v-2J</sup>, *Pcdh15*<sup>av-3J</sup>, or *Ush1g*<sup>js</sup> mutations, or a *Ush1c* null allele. Significant levels of age-related hearing loss were detected in *Myo7a*<sup>sh1-8J/+</sup>:*Ush1g*<sup>js/+</sup> and *Myo7a*<sup>sh1-8J/+</sup>:*Ush1c*<sup>-/+</sup> mice when compared to age-matched single heterozygous animals, indicating a genetic interaction of these molecules. These experiments show the importance of *Myo7a* protein abundance for development and maintenance of hair-bundle structure and function. Moreover, the readily available *Myo7a*<sup>sh1-8J</sup> mice will be useful for dissecting the role of *Myo7a* in the inner ear.

### **311** Cell Type-Specific Transcriptome Analysis Reveals a Major Role for *Zeb1* and miR-200b in Mouse Inner Ear Morphogenesis

**Ronna Hertzano**<sup>1</sup>, Ran Elkon<sup>2</sup>, Kiyoto Kurima<sup>3</sup>, Annie Morrisson<sup>1</sup>, Siaw-Lin Chan<sup>1</sup>, Michelle Sallin<sup>1</sup>, Andrew Biedlingmaier<sup>1</sup>, Douglas Darling<sup>4</sup>, Andrew Griffith<sup>3</sup>, David Eisenman<sup>1</sup>, Scott Strome<sup>1</sup>

<sup>1</sup>University of Maryland, <sup>2</sup>The Netherlands Cancer Institute, <sup>3</sup>NIDCD, NIH, <sup>4</sup>University of Louisville

Cell type-specific transcriptome analysis reveals a major role for *Zeb1* and miR-200b in mouse inner ear morphogenesis

Ronna Hertzano<sup>1</sup>, Ran Elkon<sup>2</sup>, Kiyoto Kurima<sup>3</sup>, Annie Morrisson<sup>1</sup>, Siaw-Lin Chan<sup>1</sup>, Michelle Sallin<sup>1</sup>, Andrew Biedlingmaier<sup>1</sup>, Douglas Darling<sup>4</sup>, Andrew J. Griffith<sup>3</sup>, David J. Eisenman<sup>1</sup>, Scott E. Strome<sup>1</sup>

The mammalian inner ear is a highly complex sensory organ and mutations in over 100 genes underlie hereditary human non-syndromic hearing loss. Nevertheless, little is known about the signaling cascades downstream of deafness genes. Genome-wide expression profiling is an invaluable tool for gaining systems-level understanding of biological processes. We developed and validated a simple and novel protocol to specifically isolate sensory epithelial cells, neurons, blood vessels and mesenchyme

of auditory and vestibular epithelia from newborn wild-type mice. Our protocol is based on flow cytometry to sort and capture cells labeled with commercially available antibodies to endogenously expressed cluster of differentiation (CD) antigens. Transcriptome profiling of the sorted cells identified cell type-specific expression clusters. Computational analysis detected transcription factors and microRNAs that play key roles in determining cell identity in the inner ear. Specifically, our analysis revealed the role of the *Zeb1/miR-200b* pathway in establishing epithelial and mesenchymal identity in the inner ear. Furthermore, we detected a deregulation of Zeb-1 pathway in the inner ear of Twirler mice, which manifest, among other phenotypes, severe auditory and vestibular defects (see abstract by Kurima et al.). Finally, we show the utility of this approach for characterizing compartment-specific genes and protein-protein networks. Adoption of this isolation strategy to study other mouse mutants for hearing and balance could overcome many of the obstacles to understanding the function of deafness genes.

### **312 Epidemiology of Pediatric and Adult Cochlear Implants, United States, 2001-2009**

**Howard J. Hoffman**<sup>1</sup>, Chuan-Ming Li<sup>1</sup>, Claudia A. Steiner<sup>2</sup>  
<sup>1</sup>NIDCD, NIH, <sup>2</sup>CDOM, HCUP, AHRQ

Recent epidemiology studies of cochlear implants (CIs) are based on 1990's data and restricted to pediatric populations. In 2000, we began tracking CIs as a Healthy People 2010 objective to assess rates by age, sex, race/ethnicity, and other factors for preschool ( $\leq 5$  y) and school-aged (6–17 y) children, young (18–44 y), middle-aged (45–64 y), and older (65+ y) adults. CI surgery data are produced by HCUP, an annual, nationally-representative sample of inpatient CIs, in addition to inpatient and outpatient CI data with complete ascertainment in some States: 18 (39.4% of U.S. population) in 2001, increasing to 27 (56.8%) in 2009. CIs were estimated combining the Nationwide Inpatient Sample with the State Ambulatory Surgery Database. The CI-eligible severe-to-profound sensorineural hearing loss (S-P SNHL) population was estimated using the National Health Interview Survey (NHIS) by averaging the reported numbers of “deaf” over 5 years. Other sources of estimates for the CI-eligible population yield similar results. CIs increased from 3,481 in 2001 to 6,717 in 2009. The annual prevalence (rate per 10,000 with S-P SNHL) also increased steadily and was highest for preschool children, 902 per 10,000 (9.0%) in 2001, 13% in 2009. School-aged children were next highest, 103 per 10,000 (1.0%) in 2001, 3% in 2009. The adult prevalence was 39 per 10,000 (0.4%) in 2001, 0.85% in 2009. CIs were slightly more likely for females (odds ratio [OR] = 1.09; 95% confidence interval [CI]: 1.08, 1.11) and, compared to non-Hispanic (NH) whites, much less likely for NH blacks (OR=0.43; CI: 0.42–0.45) and Hispanics (OR=0.11; CI: 0.10–0.12). Yearly CI surgeries nearly doubled in the past decade, with highest rates among children. However, the proportion of preschool-aged children receiving CIs is considerably lower than the 55% suggested recently (Bradham & Jones, 2008), since the authors misinterpreted the cumulative

number of pediatric CIs in an FDA report as an annual number.

### **313 Cochlear Implantation in Children with Congenital Cytomegalovirus Infection**

**Akinori Kashio**<sup>1</sup>, Yusuke Akamatsu<sup>1</sup>, Erika Ogata<sup>1</sup>, Nodoka Adachi<sup>2</sup>, Takuya Yasui<sup>1</sup>, Shotaro Karino<sup>1</sup>, Takashi Sakamoto<sup>1</sup>, Akinobu Kakigi<sup>1</sup>, Shinichi Iwasaki<sup>1</sup>, Tatsuya Yamasoba<sup>1</sup>

<sup>1</sup>University of Tokyo, <sup>2</sup>Saitama Children's Medical Center  
Objective

To assess outcome of cochlear implantation (CI) on Japanese deaf children with congenital cytomegalovirus (CMV) infection.

Materials and Methods

We retrospectively reviewed data from 13 pediatric patients who received CI and who had been tested for and diagnosed with congenital CMV infection. The subjects were divided into 2 groups on the basis of developmental quotient (DQ), i.e., high DQ group (DQ  $\geq 70$  n = 7) and low DQ group (DQ < 70 n = 6). Meaningful auditory integration scale (MAIS) scores and meaningful use of speech scale (MUSS) scores were analyzed before implantation through 30 months after CI. The Wechsler verbal intelligence quotient (VIQ) and monosyllable recognition tests were also administered at the age of entry into school. The results were compared with those for a control group of 30 children who had been found to have a *GJB2* mutation (*GJB2* group).

Results

The mean MAIS score increased to be  $31.8 \pm 5.4$  and  $30.5 \pm 4.9$  by 30 months in high and low DQ groups, respectively. The mean MUSS score also increased up to  $28.6 \pm 6.2$  and  $17.5 \pm 0.7$  in the high and low DQ groups, respectively. The MAIS and MUSS scores at 30 months after surgery were  $28.5 \pm 7.5$  and  $23.5 \pm 10.4$ , respectively in the *GJB2* group. The average VIQ and monosyllable recognition test scores were  $97.8 \pm 4.57$  and  $76.0\% \pm 10.7\%$ , respectively, in the high DQ group and  $87.1 \pm 26.8$  and  $65.3\% \pm 20.8\%$ , respectively, in the *GJB2* group; These scores did not differ significantly between the 2 groups.

Conclusions

The scores in all examinations were equivalent between the high DQ and *GJB2* group. Although the MAIS score in the low DQ group was equivalent to that in other groups, the MUSS scores were lower compared to other groups. These findings indicate that in terms of auditory integration, good performance can be expected after CI in children with congenital CMV infection, although, performance pertaining to speech and language development is influenced by the coexisting disorders.

### **314 Chronic Otitis Media - Quality of Life Measured With Disease-Specific and General Questionnaires**

Ingo Baumann<sup>1</sup>, B Gerendes<sup>1</sup>, Peter K Plinkert<sup>1</sup>, Mark Praetorius<sup>1</sup>

<sup>1</sup>University of Heidelberg Medical Center

Background: Chronic suppurative otitis media (CSOM) is frequently associated with symptoms of inflammation like discharge from the ear or pain. In many cases, patients suffer from hearing loss causing communication problems and social

withdrawal. The objective of this work was to collect prospective audiological data and data on general and disease-specific quality of life with validated quality of life measurement instruments to assess the impact of the disease on health-related quality of life (HR-QOL).

Methods: 121 patients were included in the study. Patients were clinically examined in the hospital before and 6 months after surgery including audiological testing. They filled in the quality of life questionnaires SF-36 and Chronic Otitis Media Outcome Test 15 (COMOT-15) pre-operatively and 6 and 12 months post-operatively, respectively.

Results: Complete data records from 90 patients were available for statistical analysis. Disease-specific HR-QOL in patients with CSOM improved after tympanoplasty in all the scales of the COMOT-15. There was no difference in HR-QOL assessment between patients with mesotympanic respectively epitympanic

CSOM. However, we did find the outcome to be worse in patients who underwent revision surgery compared with those who underwent primary surgery. Audiometric findings correlated very well with the subscale hearing function from the COMOT-15 questionnaire. General HR-QOL measured with the SF-36 was not significantly changed by tympanoplasty.

Conclusions: Tympanoplasty did lead to a significant improvement of disease-specific HR-QOL in patients with CSOM while general HR-QOL did not change. Very well correlations were found between the subscale hearing function from the COMOT-15 questionnaire and audiological findings. Revision surgery seems to be a predictor for a worse outcome.

### **315 Defect of Cochlear Modiolus Area in 3D-CISS Imaging of the Patients with Enlarged Vestibular Aqueduct (EVA) Correlates with Severity of Sensorineural Hearing Loss**

Hyoung-Mi Kim<sup>1</sup>, Jun Ho Lee<sup>2</sup>

<sup>1</sup>CHA University, <sup>2</sup>Seoul National University

Enlarged vestibular aqueduct (EVA) is most commonly observed radiologic abnormality in children with sensorineural hearing loss. Clinically, it associates with fluctuating hearing loss which often progresses toward deafness during childhood. EVA can occur as sole isolated radiologic abnormality or in combination with cochlear malformations. The aim of the study was to determine the relationship between the severity of hearing loss and radiologic abnormality determined by 3D-CISS thin section

MR imaging in patients with isolated EVA. 3D-CISS MR images with 1.0 mm thickness were obtained from 48 ears of 24 patients with profound hearing loss associated with bilateral isolated EVA confirmed by TBCT. The area of cochlear modiolus, volume of enlarged endolymphatic sac and signal intensity of endolymphatic duct and sac were measured by drawing ROI using digital morphometry. Diameter of enlarged endolymphatic duct was determined at midpoint between common crus and its external aperture. These values were compared with audiological data. The audiogram showed profound high-frequency hearing loss. No significant correlation was found between patient age and degree of hearing loss. Degree of cochlear modiolus deficiency consistently correlated with severity of hearing loss. There was no correlation of the degree of enlargement of endolymphatic duct and sac with degree of hearing loss. In addition, variable signal intensities within endolymphatic duct and sac failed to prove a relationship with hearing loss, which suggests structural enlargement of endolymphatic sac is not the direct cause of hearing loss in EVA. In conclusion, these data demonstrate a close relationship between severity of hearing loss and defect of cochlear modiolus area in patients with isolated EVA. These findings are critical toward an understanding of the etiology of deafness during cochlear development, which may be affected by abnormally enlarged endolymphatic sac.

### **316 Intracochlear Drug Delivery with a Programmable Microsystem: On-Board Control of Dosing**

Jason Fiering<sup>1</sup>, Ernest Kim<sup>1</sup>, Erin E Pararas<sup>1</sup>, Mark J Mescher<sup>1</sup>, Erich L Gustenhoven<sup>1</sup>, William F Sewell<sup>2</sup>, Michael J McKenna<sup>2</sup>, Sharon G Kujawa<sup>2</sup>, Jeffrey T Borenstein<sup>1</sup>

<sup>1</sup>Charles Stark Draper Laboratory, <sup>2</sup>Massachusetts Eye and Ear Infirmary and Harvard Medical School

Intracochlear drug delivery, as opposed to transtympanic or systemic drug delivery, may be advantageous in treating hearing and vestibular disorders. Direct infusion through either a cochleostomy or the round window membrane is expected to enable accurate dosing, reduce side effects, and permit the administration of emerging compounds that would otherwise not traverse the blood—cochlea barrier. However, the design and testing of a device to safely and efficaciously perfuse the cochlea presents unique engineering challenges. We have previously described a concept for reciprocating intracochlear drug delivery; a volume of solution is repeatedly infused and then withdrawn, resulting in zero net volume transfer to the scala tympani while allowing transport of drugs by diffusion and mixing with the perilymph. Furthermore, we have demonstrated a microfluidic prototype device, miniaturized and wearable by guinea pigs. We have used this device to perform reciprocating intracochlear drug delivery and have measured delivery of test compounds in vivo.

To advance this prototype toward an implantable device for future therapeutic use in humans, further miniaturization and on-board control of dosing are required. Here we present the addition of a programmable

microfluidic drug reservoir. The reservoir will allow sustained delivery suitable for long-term tests of apical drug distribution while preserving animal mobility. By means of a programmable micropump, the reservoir modulates drug concentration supplied to the reciprocating carrier fluid yet maintains zero net volume transfer. Additionally, we discuss integration of the reservoir with the related microfluidic components and the system level design. We characterize the dosage range and reservoir lifetime in a bench apparatus, and we present preliminary results showing in vivo animal tests of the new functionality in an integrated prototype microsystem.

### **317** Saliva Polymerase Chain Reaction Assay to Screen for Congenital Cytomegalovirus Infection in a Guinea Pig Model

**David Mann**<sup>1</sup>, Albert Park<sup>1</sup>, Matt Firpo<sup>2</sup>, Yong Wang<sup>1</sup>, Kurt Retzlaff<sup>2</sup>, Patti Larabee<sup>2</sup>

<sup>1</sup>*Division of Otolaryngology-HNS, University of Utah,*

<sup>2</sup>*Department of Surgery, University of Utah*

The most common infectious cause of sensorineural hearing loss (SNHL) in newborns is cytomegalovirus (CMV). Current estimates suggest that up to 40% of all non-syndromic SNHL in infants is caused by congenital CMV infection. We have developed a guinea pig model for inducing CMV labyrinthitis via transplacental transmission, using the species-specific guinea pig cytomegalovirus (gpCMV). To demonstrate the utility of the guinea pig as a model for human congenital cytomegalovirus (CMV), we evaluated the effectiveness of detecting congenital CMV infection by real-time polymerase chain reaction (PCR) on blood, urine, and saliva samples. Blood, urine, and saliva samples were collected from guinea pig pups delivered from pregnant dams inoculated with gpCMV. These samples were then evaluated for the presence of gpCMV by real-time PCR. We found that 28 of the 31 pups tested positive for gpCMV by ELISA. The sensitivity and specificity for the real-time PCR assay on saliva samples were 78.6% and 90.9%, respectively. The sensitivity for real-time PCR on blood and urine samples was significantly lower at 32.1% for both. Our data suggest that saliva may be a good biological marker for detecting congenital CMV infection. Moreover, our findings are similar to what has been reported in recent screening studies on human newborns. Thus, the guinea pig provides an excellent model of congenital CMV infection and will be utilized in further studies aimed at developing optimal antiviral therapies to treat CMV-induced sensorineural hearing loss.

### **318** Transcription Factor NFkB Plays a Key Role in Vestibular Schwannoma Tumorigenesis

Martijn Briet<sup>1,2</sup>, **Sonam Dilwali**<sup>3,4</sup>, Michael Platt<sup>1,5</sup>, Konstantina Stankovic<sup>1,4</sup>

<sup>1</sup>*Department of Otolaryngology and Laryngology, Harvard Medical School,* <sup>2</sup>*Department of Otorhinolaryngology, Leiden University Medical Centre,* <sup>3</sup>*Harvard-MIT Program in Speech and Hearing Bioscience and Technology,* <sup>4</sup>*Eaton Peabody Laboratories, Department of Otolaryngology, Mass Eye and Ear Infirmary,* <sup>5</sup>*Department of*

*Otolaryngology-Head and Neck Surgery, Boston University* Sporadic vestibular schwannomas (VS) are the most common tumors of the cerebellopontine angle, and they typically present with sensorineural hearing loss. Hundreds of genes have been implicated in VS growth. To simplify this daunting complexity, we performed the first pathway analysis of all reported genes using Ingenuity Pathway Analysis (IPA) software. Genes discovered through hypothesis-driven and high-throughput molecular studies were identified through a Pubmed literature search and analyzed in IPA. The genes that were most interconnected in a given network were termed "nodal" genes, and assumed to play a key role in VS tumorigenesis. The top 3 most statistically significant nodal genes included 2 genes already implicated in VS tumor growth (i.e. filamentous actin and platelet-derived growth factor), and a gene that had never been reported in association with VS: a pro-inflammatory transcription factor NF-kB. To validate the relevance of NF-kB for VS growth, mRNA expression in VS tumors was compared to mRNA expression in healthy human great auricular nerve using real time quantitative RT-PCR, and 44-fold higher expression in VS ( $p = 0.003$ ) was found. Next, cultured VS tumors were treated with two potent NF-kB inhibitors, 5-aminosalicylic acid and sodium salicylate, and change in proliferation was measured. The proliferation rate decreased substantially, and in a dose dependent manner, for VS cells treated with either compound re VS cells receiving no treatment: 91.8 % in 5 mM and 98.1 % in 10 mM 5-aminosalicylic acid vs. 91.4 % in 5 mM and 96.7 % in 10 mM sodium salicylate. These results substantiate NF-kB as an essential contributor to growth of VS, and point to NF-kB as a promising new target to prevent formation or stop progression of these tumors.

[Supported by NIH grants K08 DC010419 and T32 DC00038]

### **319** Lack of Ototoxicity from Otological Application of FST-200 or FST-201

**Karen Pawlowski**<sup>1,2</sup>, Elena Koulich<sup>1</sup>, Charles G. Wright<sup>1,2</sup>, Peter S. Roland<sup>1</sup>

<sup>1</sup>*UT Southwestern Medical Center at Dallas,* <sup>2</sup>*UT Dallas*

Otitis externa (OE) and acute otitis media (AOM) are two of the most common otologic disorders requiring outpatient antibiotic treatment. There is long standing interest in developing formulations that are easy to administer and that would limit systemic exposure to antibiotics. The preparations used in the present investigation were formulated to allow repeated applications to the external

ear canal to treat OE, or through a tympanostomy tube, to treat AOM, without risk to hearing or equilibrium.

The formulations tested in this study were designed to provide dual therapeutic effects for the treatment of OE and AOM: antimicrobial and anti-inflammatory activities. The formulations contained 0.1% dexamethasone (Dex) and one of two concentrations of povidone iodine (PI): 1% PI (FST-201) or 2% PI (FST-200). Both PI and Dex have long histories of use as topical preparations. Dex, a topical steroid, at a concentration of 0.1% has been proven safe in several otic and ophthalmic products for over four decades. PI is a broad spectrum antiseptic with effectiveness against a variety of bacteria, viruses, and fungi. Iodine and iodine derivatives have been used to treat ophthalmic, otic, oral, dermal and other infections. Some animal studies using PI showed it did not affect vestibular or cochlear function when applied topically to ears with perforated tympanic membranes. Other studies, using a significantly higher concentration of PI and/ or added detergents, have noted some cochleotoxicity after direct administration to the middle ear. However, otic formulations combining Dex and PI have not been tested for ototoxic effects.

In the present study, we performed tympanostomies and inserted ventilation tubes in a rat model and administered the new formulations containing low doses of PI, plus Dex, over a period of 7 days. The animals were monitored for an additional 7 days to determine the safety of these new formulations. Hearing levels were monitored over the duration of the study via auditory brainstem (ABR) testing and the condition of the middle and inner ear tissues was evaluated histologically. Neither of the new PI/Dex formulations tested caused pathologic changes in the ear that significantly affected auditory function.

### **320 Antioxidant Protection of the Human Inner Ear – Does It Really Work? a Randomized Controlled Trial**

Dan Bagger-Sjöbäck<sup>1</sup>, Karin Strömbäck<sup>2</sup>, Georgios Papatziomos<sup>1</sup>, Malou Hultcrantz<sup>1</sup>, Sten Hellström<sup>1</sup>, Christina Larsson<sup>1</sup>, Henrik Smeds<sup>1</sup>, Bo Tideholm<sup>1</sup>, Lars-Olaf Cardell<sup>1</sup>, **Anders Fridberger<sup>3</sup>**

<sup>1</sup>Karolinska University Hospital, <sup>2</sup>Uppsala University, <sup>3</sup>Karolinska Institutet

In animals, antioxidants such as N-Acetylcysteine can protect the inner ear from harmful effects of loud sounds, but there is insufficient data to establish efficacy in humans. We have identified a clinical situation that allows a potential protective effect to be rigorously studied.

Stapedotomy, an operation performed to ameliorate the conductive hearing loss that follows from otosclerosis, involves using microdrills or lasers close to the sensory cells of the cochlea. Although the operation produces a robust improvement in low-frequency hearing, high-frequency hearing often does not improve and ~1% of patients suffer complete sensorineural hearing loss as a result of surgical trauma. In our trial, patients undergoing stapedotomy received N-Acetylcysteine at 150 mg / kg body weight or matching placebo. The study was double-blind, using stratified randomization based on age and

preoperative hearing. The main outcome variable was hearing thresholds at 6 and 8 kHz one year after surgery. Secondary outcome measures included high-frequency hearing at 8 weeks, and the incidence of tinnitus and vertigo. Power calculations showed that 150 patients would give 90% probability of detecting a 10 dB-intergroup difference. The present results are from the first interim analysis based on 80 patients. Overall hearing results were good in both groups, matching or even surpassing previously published materials. However, no significant intergroup difference in hearing thresholds was detected at any frequency. There was a trend for the treated group to have more tinnitus and to rate surgery less effective than the placebo group. Hence, the interim analysis provides no evidence for a protective effect and suggests that N-acetylcysteine may adversely affect hearing after stapedotomy. Evaluation of hearing results after surgical interventions is complex and we propose that air-conduction thresholds should be given greater weight when assessing the effects of stapes surgery.

### **321 Hemispheric Dominance and Cell Phone Use**

Bianca Siegel<sup>1</sup>, Priyanka Shah<sup>2</sup>, Susan Bowyer<sup>3</sup>, **Michael Seidman<sup>4</sup>**

<sup>1</sup>Albert Einstein College of Medicine, Department of Otorhinolaryngology, <sup>2</sup>Wayne State University, Department of Otolaryngology, <sup>3</sup>Henry Ford Health System, Department of Neurology, <sup>4</sup>Henry Ford Health System, Department of Otolaryngology

Objective: To determine if there is an obvious association between sidedness of cell phone use and auditory or language hemispheric dominance (HD). Ninety-six percent of right handed people are left HD. We have observed that most people use their cell phones in their right ear.

Study design: A survey was emailed to over 5,000 individuals using "SurveyMonkey.com".

Methods: A one page survey with modifications of the Edinburgh Handedness protocol was utilized. Sample questions included: hand used to write with, amount of phone usage, right or left ear used to listen to phone conversations, as well as if respondents had had a brain tumor.

Results: 717 surveys were returned. 90% of the respondents were right handed (RH); 9% left handed (LH); 1% ambidextrous (A). 68% of the RH people used the phone in their right ear, 25% in the left and 7% used either ear. 72% of the LH used their left ear, 23% used their right ear and 5% had no preference. Usage averaged 540 min/mo for eight years.

Conclusions: We demonstrated that there is a correlation between hand dominance and laterality of cell phone use (72.8%). Most right handed, left brain dominant people use the phone in their right ear. Similarly, most left handed, right brain dominant people use the phone in their left ear, despite no perceived difference in their hearing in their left or right ear. There has recently been a preponderance of literature regarding the relationship between cell phone use and cancer. The fact that few tumors were identified in

this population does not rule out an association, but does reduce suspicion.

### **322 The Facial Nerve Canal in Patients with Bell's Palsy Investigated by High-Resolution Computed Tomography Using Multiplanar Reconstruction**

Aya Murai<sup>1</sup>, Shin Kariya<sup>2</sup>, Kazunori Nishizaki<sup>2</sup>

<sup>1</sup>Department of Otolaryngology, Kochi Health Sciences Center, <sup>2</sup>Department of Otolaryngology-Head and Neck Surgery, Okayama University Graduate School of Medicine

Bell's palsy is the most common cause of peripheral facial paralysis resulting from acute dysfunction of the cranial nerve VII. The edema and inflammation of the facial nerve in the facial nerve canal lead to both compression and ischemic damage of the nerve. A recent study shows that Bell's palsy usually coincides with narrower facial nerve canal of patient, at least as far as the labyrinthine segment is concerned. However, the controversial reports about the dimension of facial nerve canal in patients with Bell's palsy have been published. These previous studies used high-resolution computed tomography, magnetic resonance imaging or histological temporal bone sections to measure the facial nerve canal. In histological studies, temporal bones are usually cut in horizontal serial sections. The images are normally obtained in axial, coronal and sagittal plane. It may be difficult to critically evaluate on facial nerve canal, because these sections and images may not be perpendicular to the longitudinal axis of facial nerve canal. The image obtained by computer tomography with multiplanar reconstruction (MPR-CT) is perpendicular to the facial nerve canal. The purpose of this study is to show the cross-sectional area of the facial canal using MPR-CT.

Twelve patients with unilateral Bell's palsy were enrolled in this study. The cross-sectional area of facial nerve canal both in affected and unaffected sides was measured at the labyrinthine segment, horizontal segment, and mastoid segment by MPR-CT.

The mean cross-sectional area at the labyrinthine segment of facial nerve canal in the affected temporal bone was significantly smaller than that in the unaffected temporal bone. There were not statistical differences between the affected and unaffected temporal bones in the mean cross-sectional area both in horizontal and mastoid segment.

These findings suggest that the narrow facial nerve canal may be one of the risk factors of Bell's palsy.

### **323 Development of New Factors for Determining the Level of Facial Muscle Relaxation Using Facial Muscle Electromyography**

Yang-Sun Cho<sup>1</sup>, Ga Young Park<sup>1</sup>, Young-Jin Kim<sup>2</sup>, Joung Hwan Mun<sup>2</sup>, HaYoung Byun<sup>1</sup>, Il Joon Moon<sup>1</sup>

<sup>1</sup>Samsung Medical Center, Sungkyunkwan University School of Medicine, <sup>2</sup>Sungkyunkwan University School of Life Science and Biotechnology

Introduction

Using the facial nerve monitoring system in otologic surgeries is helpful for preservation of nerve. To find out this system working, it is necessary to check the level of muscle relaxation. The train-of-four stimulation at ulnar nerve is usually used for measuring the level of neuromuscular blockade during general anesthesia. But each muscles shows different degree of relaxation at the same dosage of neuromuscular relaxant. The aim of this study was evaluating the relationship between facial electromyography and the level of facial muscle relaxation during general anesthesia.

Methods

Six New Zealand white rabbits were anesthetized with intravenous ketamine and 1% isoflurane. The extratemporal facial nerve and sciatic nerve were exposed and 28 gauge monopolar needle electrodes connected to the stimulator were inserted directly to the nerves. Electromyography using wireless system (Noraxon) was recorded from the orbicularis oris and gastrocnemius muscles after electrical stimulation. (0.1-5mA). Also, facial and sciatic electromyographic response was obtained with increasing intravenous infusion of muscle relaxant. Twenty-five factors including Median Frequency(MF) and SPA(Spectrum Area) were obtain from the electromyographic signal. By the method of principal component analysis (PCA), the principle factors were extracted from various factors.

Results

After applying the results to twenty-five factors mainly used in analyzing electromyographic signal, some principal factors related to the depth of muscle relaxation were obtained. The principal factors were MF and SPA. The MF was related to the depth of muscle relaxation according to the dosage of muscle relaxant and decreased with high dose of muscle relaxant. The SPA was related to the current of electrical stimuli within the same depth of muscle relaxation and increased with high current of electrical stimulation.

Conclusion

The level of muscle relaxation can be estimated through extracted principle factors. It will be possible to quantify the electromyographic signal by the depth of muscle relaxation and dose of muscle relaxant. Based on results, it can be possible to expect the level of facial muscle relaxation and the appropriate current of electrical stimuli which is needed in the direct facial nerve monitoring.

### **324 Wireless Laryngeal EMG Recording from Freely Behaving Mice Using Flexible Polyimide-Based Electrodes**

Hananeh Esmailbeigi<sup>1</sup>, S.E. Roian Egnor<sup>1</sup>

<sup>1</sup>Howard Hughes Medical Institute Janelia Farm Research Campus

The purpose of this study is to record the electromyography (EMG) signals from the cricothyroid muscles of mice during vocalization. To date, attempts to record vocalizations from head-fixed mice have been unsuccessful. In this study we take advantage of wireless technology and microfabrication technology to record from vocalizing freely behaving mice.

The miniature telemetry systems developed by Gabbiani et al. 2011 was used to wirelessly transmit two channels of EMG data to a remote digital receiver. The light weight of the transmitter (0.1 g), and its small dimensions (6.5x8x2 mm) allowed for it to be placed subcutaneously on the skull. A battery-powered unit that was controlled using an on/off magnetic switch was implanted intraperitoneally. The power unit weighs 2.8 g and is 13 mm in diameter and 8 mm in height. It enables 55 hours of recording. Custom-designed flexible polyimide-based EMG electrodes were microfabricated at the University of Maryland Nanocenter. The electrodes consist of 300 nm platinum sandwiched between two layers of 5 µm thick polyimide. The two circular contact sites were 10 µm in diameter. The electrode was 60 µm wide at the widest point inside the muscle. The impedance of the electrodes were on average 300 Kohms. The electrode's unique design induced minimal implantation damage to the muscle. The electrode's features enabled it to be secured on both ends of the muscle; allowing the electrode to retain contact with the muscle despite movement due to vocalization and respiration. The light weight of the thin electrode and its flexibility enabled the electrode to move freely with the cricothyroid muscle. In this study we have designed and implemented a miniature subcutaneous wireless EMG recording unit for recording vocalization from freely moving mice.

### **325 Identifying MicroRNAs That Are Involved in Age-Related Hearing Loss**

**Qian Zhang**<sup>1</sup>, Edward Walsh<sup>2</sup>, Joann McGee<sup>2</sup>, Garrett Soukup<sup>1</sup>, David He<sup>1</sup>

<sup>1</sup>Creighton University, <sup>2</sup>Boystown National Research Hospital

Age-related hearing loss (ARHL, presbycusis), a progressive sensorineural hearing loss occurring bilaterally at higher frequencies, is the most common type of human hearing impairment. It is generally believed that the organ of Corti (OC) and stria vascularis (SV) are two main pathological sites that undergo degeneration during presbycusis. Accumulating evidence suggests that dysfunction of miRNA regulatory networks is responsible for some physiological and pathological changes associated with aging. Previous studies have shown that miRNA 96/182/183 family and Let7 family play roles during development and regeneration in the inner ear. We questioned which microRNAs are also involved in the onset and progression of ARHL in the mammalian inner ear. Two different strains of mice, C57BL/6J (which has early onset age-related hearing loss) and CBA/J (which is often used as a control for age-related hearing loss) were used for analysis. The organ of Corti (OC) and stria vascularis (SV) of CBA mice were collected from newborn and 8 month old mice, and microarray analysis was used to identify which miRNAs show significant changes in expression. The differential expression levels of miRNAs were also validated by q-RT-PCR on both strains. Our results show that among 609 mouse miRNA probes, 32 out of 83 miRNAs detected in the OC and 37 out of 84 miRNAs detected in the SV exhibit significant changes >2-

fold ( $p < 0.05$ ) with aging. Some miRNAs that demonstrate upregulation (miRNA29a, miRNA143, let7b) or downregulation (miRNA181a, miRNA17) have previously been shown to be involved in cell death pathways in other systems. Our study suggests that changes in expression of these miRNAs might affect aging-related pathways in OC and SV in the mammalian cochlea. (Supported by NIH grants: R01 DC009025 to GS and R01 DC004696 to DH)

### **326 Age-Related Hearing Loss in MnSOD Heterozygous Knockout Mice**

**Makoto Kinoshita**<sup>1</sup>, Akinori Kashio<sup>1</sup>, Takahiko Shimizu<sup>2</sup>, Tatsuya Yamasoba<sup>1</sup>

<sup>1</sup>Department of Otolaryngology Head and Neck Surgery, University of Tokyo Hospital, Japan, <sup>2</sup>Department of Molecular Gerontology, Tokyo Metropolitan Institute of Gerontology, Japan

Age-related hearing loss (AHL) is an aging process of the inner ear. Oxidative stress has been considered as one of the leading causes, since the resultant mitochondrial DNA (mtDNA) damage, which is commonly present in the aged cochlea, induce apoptosis of the important structures in the cochlea. Manganese superoxide dismutase (MnSOD), the antioxidant enzyme acting within the mitochondria, protects the mtDNA from damage. It is reported, however, that heterozygous null for MnSOD showed no increase in the amount of hearing loss relative to the background strain (LeT and Keithley EM. 2007). Although it is ideal to use MnSOD-null mice, they die within several weeks after birth, which makes it impossible to investigate the pathological consequences of oxidative damage in their adult tissues in vivo. To confirm the findings by Le and Keithley, we obtained MnSOD heterozygous knockout (HET) mice during generation of tissue-specific MnSOD knockout mouse (Ikegami T, et al. 2002). We enrolled HET mice and their littermate wild-type (WT) C57BL/6 mice as controls. Auditory brainstem response (ABR) thresholds were measured at 4 and 16 months of age. After ABR measurements, paraffin-embedded cochlear sections were obtained. The ABR thresholds and spiral ganglion cells (SGCs) density were compared between young and old HET and WT mice. WT and HET mice showed nearly normal ABR thresholds at 4, 8, and 16 kHz and slightly increased thresholds at 32 kHz at 4 months. At 16 months, ABR thresholds of both mice were significantly increased at all frequencies tested. ABR thresholds did not significantly differ between HET and WT mice at either age at any tested frequency. The SGC density also did not significantly differ between HET and WT mice at either age. These findings imply that even half the amount of MnSOD is sufficient to maintain the hearing equivalent to age.

### **327 Down-Regulation of Na-K-Cl Co-Transporter1 (NKCC1) Protein Expression May Be a Mechanism for Age-Related Hearing Loss**

**Bo Ding<sup>1</sup>**, Robert Frisina<sup>1</sup>, XiaoXia Zhu<sup>1</sup>, Joseph Walton<sup>1</sup>  
<sup>1</sup>*Univ. South Florida*

Degeneration of certain cochlear cell types is a hallmark of age-related hearing loss, clinically referred to as presbycusis. Presently, the underlying mechanisms remain to be fully elucidated, however the work by Schmiedt and colleagues points to the stria vascularis as a key contributor to cochlear age-related pathology. In addition, previous data from humans suggests a relationship between low serum aldosterone (ALD) levels and severity of presbycusis {Tadros et al., *Hear. Res.*, 2005, 209(1-2)10-18}. Our initial in vitro data using HT-29 cells in culture showed that ALD increases NKCC1 protein expression, from 2 hours up to 48 hours. These data are the first to suggest that ALD can up-regulate NKCC1 protein expression. Interestingly, we found that there was no increase in NKCC1 mRNA levels. To shed further light, we have extended our investigation to an in vivo mouse model. Hearing thresholds in young adult (n=4, age 2-4 months) and aged (n=4, age 23-24 months) CBA/CaJ mice were tested using auditory brainstem response audiometry (ABR). Subsequently the cochlea were harvested and subjected to mRNA (RT-PCR) and protein extraction for NKCC1. Relative to the young adults, ABR threshold shifts in the aged mice ranged from about 20-30 dB depending on sound frequency, from 3-48 KHz. Protein expression of cochlear NKCC1 was decreased in the aged group compared to young adult mice. Interestingly, we found no age-related change in mRNA expression. Confirmation of equal loading was done via beta-actin controls. In sum, these findings suggest that post-translational regulation of NKCC1 may contribute to age-related hearing loss, and an improved understanding of these mechanisms may lead to new therapeutic approaches for treating presbycusis.

Supported by NIH Grant P01 AG009524

### **328 Age Related Hearing Loss in the Animal Model of Diabetes with Obesity**

**Kazuma Sugahara<sup>1</sup>**, Junko Tsuda<sup>1</sup>, Eiju Kanagawa<sup>1</sup>, Takefumi Mikuriya<sup>1</sup>, Makoto Hashimoto<sup>1</sup>, Hiroaki Shimogori<sup>1</sup>, Hiroshi Yamashita<sup>1</sup>  
<sup>1</sup>*Yamaguchi University*

It is known that the prevalence of hearing loss is high in the patients with diabetes. However, the causes of hearing loss have not been clear. In the present study, we evaluated the hearing function in animal model of diabetes with obesity. TSOD male mice used in study were derived from the Tsumura Research Institute. Age- and sex-matched non-diabetic TSNO mice served as controls. Blood samples were collected from TSOD and TSNO mice at 3, 5, 8 months of age. Blood glucose concentrations of TSOD mice were significantly higher than those of controls. In addition, Body weights of TSOD mice were greater than those of controls. These data were indicated that the model animal showed the symptoms of diabetes

with obesity in our breeding conditions. We evaluated the ABR thresholds of animals in 3, 5, 8, 12 month of age. There was no different in ABR thresholds between TSOD mice and controls in 3 or 5 month of age. However, the elevation of ABR thresholds were observed in 8 month aged TSOD mice. The thresholds of 8 months aged TSOD mice were significantly larger than those in controls. We could not clarify the histological characteristics in the inner ear of 8 months aged TSOD mice. Now, we examine more aged animals to elucidate the cause of hearing loss. TSOD mouse were used as the animal model of obese diabetes showed many symptoms and histological changes in many organs. It was indicated that TSOD mice show the symptom of hearing loss in this study.

### **329 Efferent Synapses Return to Aged Inner Hair Cells**

**Amanda Lauer<sup>1</sup>**, Zayer Minh<sup>1</sup>, Paul Fuchs<sup>1</sup>, David Ryugo<sup>1,2</sup>, Howard Francis<sup>1</sup>

<sup>1</sup>*Johns Hopkins University School of Medicine*, <sup>2</sup>*Garvan Institute*

Efferent innervation of the cochlea undergoes extensive modification early in development, yet changes in this innervation for models of presbycusis are only beginning to be understood. Cumulative alterations in the cochlea affecting information transfer from the auditory periphery to the brain may contribute to age-related hearing deficits. The status of efferent innervation in the vicinity of inner hair cells (IHCs) is a possible source of pathology when comparing young and old C57BL/6 mice. Consequently, we used transmission electron microscopy to analyze serial sections through IHCs and to reveal increased axosomatic efferent innervation in older animals. Axosomatic terminals contained focal accumulations of small vesicles and were sometimes observed opposite postsynaptic cisterns. Synaptic vesicle size and shape were heterogeneous. Inter-receptor synapses (contacting two IHCs) and axodendritic synapses were also evident in older animals. Efferent morphology in older animals was reminiscent of what has been previously found in very young C57 mice (Shnerson A, Devigne C, Pujol R., Age-related changes in the C57BL/6J mouse cochlea. II. Ultrastructural findings. *Dev Brain Res* 2:77-88, 1982). Increased axosomatic innervation was associated with fewer afferent synapses per IHC, an increased proportion of lost outer hair cells, and elevated auditory brainstem response thresholds. Degenerative changes that return the organ of Corti to an immature state, such as low afferent activity, may engage signaling pathways that promote efferent innervation of the IHCs. [Support from NIDCD grants DC00143, DC05909, DC05211, DC00232, DC000023, DC009353, NEI grant EY001765, NHMRC grant 1009482, and grants from the American Hearing Research Foundation, National Organization for Hearing Research, Deafness Research Foundation, Garnett Passe & Rodney Williams Memorial Foundation.]

### **330 Age-Related Neuroplasticity in the Central Auditory System**

**Nikolai Hubert**<sup>1,2</sup>, Moritz Gröschel<sup>1,2</sup>, Sebastian Jansen<sup>1,2</sup>, Susanne Müller<sup>3</sup>, Arneborg Ernst<sup>1</sup>, Dietmar Basta<sup>1,2</sup>

<sup>1</sup>Department of ENT at UKB, Hospital of the University of Berlin, Charité Medical School, Germany, <sup>2</sup>Department of Biology, Humboldt-University of Berlin, Germany,

<sup>3</sup>Neuroscience Research Center, Charité University Medicine Berlin, Germany

Age-related hearing loss (presbycusis) is one of the most common health issues in modern societies. Although traditionally linked to deprivation of inner ear structures, hearing problems of the elderly can not always be explained by mere loss of sensory input. Thus, a deeper understanding of the age-related physiological and morphological changes within the central auditory pathway could be of vital importance for the development of new preventive and therapeutic strategies against presbycusis. Here, we investigated neuroplastic changes in central auditory key structures of aged NMRI-mice with reported moderate age-related hearing loss.

Manganese accumulation as a correlate of calcium-dependent activity was surveyed by magnetic resonance imaging in the central auditory system of 6-week and 13-month old mice 24 hours after injection of MnCl<sub>2</sub>. Additionally, cell densities of the investigated structures were determined in histological preparations. Finally, extracellular recordings were performed in acute brain slices of both age groups in order to monitor spontaneous neuronal activity *in vitro*.

In most of the investigated structures, an increase in manganese accumulation was detected in MRI scans of aged compared to young animals. Activity changes were also surveyed by electrophysiological recordings in acute brain slices. In addition, a significant reduction of cell density was detected in several subcortical nuclei, pointing towards age-related neurodegeneration.

The elevated levels of manganese accumulation found in this study are in tune with propagated reports of increased neuronal activity in the aging auditory pathway, which can be hypothetically viewed as a compensatory effect due to reduced input from the periphery. Furthermore, progressive age-related neurodegeneration could have serious consequences for central processing of auditory information.

### **331 Age-Related Changes in Basement Membrane Anionic Sites in the Cochlea**

**Mitsuya Suzuki**<sup>1</sup>, Takashi Sakamoto<sup>2</sup>, Akinori Kashio<sup>2</sup>, Yoshihiro Ikemiyagi<sup>1</sup>, Tatsuya Yamasoba<sup>2</sup>

<sup>1</sup>Sakura Medical Center, Toho University, <sup>2</sup>University of Tokyo

Basement membrane anionic sites (BMAS) are involved in selective transport of electrically charged macromolecules, such as albumin and globulin, in glomerular or cochlear capillaries. Using cationic polyethyleneimine (PEI), we examined age-related changes in BMAS in the cochlea in C57BL/6 mice. The mice were grouped according to age as follows: 3 days, 4 weeks, 8 weeks, 6 months, and 12 months. They were decapitated, and their bony labyrinths

were removed; these were immersed in a 0.5% PEI solution (M.W. 1800; pH 7.4) for 15 min and were rinsed with 0.1 M cacodylate buffer. Next, they were immersed in 2% phosphotungstic acid and 2.5% glutaraldehyde at 4°C for 3 h to stain the PEI particles and fix the tissue. Each labyrinth was decalcified by immersion in 10% EDTA acid solution. Next, they were postfixed in 2% osmium tetroxide at 4°C for 2 h and were embedded in epoxy resin. Ultrathin sections of the cochlea and ampullar crista were double stained and were examined using a transmission electron microscope. The number and sizes of the PEI particles in the capillary and epithelial BMs of the labyrinths were measured. In all animals, PEI particles were evenly distributed in the capillary BM of the spiral ligament, spiral prominence, and ampullar crista, and in the epithelial BM of Reissner's membrane. In the stria vascularis, PEI particles were evenly distributed in the capillary BM in 3-day-old mice. In 4- and 8-week-old mice, the number of PEI particles did not markedly change; however, PEI particle sizes markedly decreased compared to those observed in 3-day-old mice. In 6- and 12-month-old mice, PEI particles were hardly detected in the strial capillary BM. In the strial capillary BM in these mice, the laminae rarae externa and interna disappeared but the lamina densa extended. We speculated that components of extracellular matrix, such as heparan sulfate proteoglycan, changed in the strial capillary BM with age, thereby BMAS reduced.

### **332 Oxidative Stress, Inflammation and Autophagic Stress as the Key Mechanisms of Premature Age-Related Hearing Loss in SAMP8 Mouse Cochlea**

**Julien Menardo**<sup>1,2</sup>, Yong Tang<sup>1,2</sup>, Sabine Ladrech<sup>1,2</sup>, Marc Lenoir<sup>1,2</sup>, Christophe Michel<sup>1,2</sup>, Jérôme Bourien<sup>1,2</sup>, Guy Rebillard<sup>1,2</sup>, Jean-Luc Puel<sup>1,2</sup>, **Jing Wang**<sup>1</sup>

<sup>1</sup>INSERM, <sup>2</sup>Université Montpellier 1&2

**Aims:** In our aging society, age-related hearing loss (ARHL) or presbycusis is increasingly important. Here, we study the mechanism of ARHL using the senescence-accelerated mouse prone 8 (SAMP8) which is a useful model to probe the effects of aging on biological processes.

**Results:** We found that the SAMP8 strain displays premature hearing loss and cochlear degeneration recapitulating the processes observed in human presbycusis (i.e. strial, sensory and neural degeneration). The molecular mechanisms associated with premature ARHL in SAMP8 mice involve oxidative stress, altered levels of anti-oxidant enzymes and decreased activity of Complexes I, II and IV which in turn lead to chronic inflammation and triggering of apoptotic cell death pathways. In addition, spiral ganglion neurons (SGNs) also undergo autophagic stress and accumulated lipofuscin.

**Conclusion:** Our results provide evidence that targeting oxidative stress, chronic inflammation or apoptotic pathways may have therapeutic potential. Modulation of autophagy may be another strategy. The fact that autophagic stress and protein aggregation occurred

specifically in SGNs also offers promising perspectives for the prevention of neural presbycusis.

### **333 MicroRNA Expression in the Aging Mouse Cochlea**

**Yoshihiro Noguchi<sup>1</sup>, Masatoki Takahashi<sup>1</sup>, Keiji Honda<sup>1</sup>, Ayako Nishio<sup>1</sup>, Ken Kitamura<sup>1</sup>**

<sup>1</sup>*Tokyo Medical and Dental University*

MicroRNAs (miRNAs) are approximately 22 nucleotide, double-stranded, non-coding RNAs, and are shown to regulate the stability and translation of the target RNAs. MiRNA levels change over the life of the individual and are associated with many disorders and aging. Recently mutations in miRNA-96 (miR-96) were shown to cause both autosomal dominant non-syndromic hereditary hearing loss in humans and progressive hearing loss in a mutant mouse, *Dmdo*, suggesting that miRNAs play an important role in hearing. The aim of the present study is to investigate the time-course changes in miRNA expressions in the cochlea of age-related hearing loss mouse. C57BL/6 mouse was used as a mouse model of age-related hearing loss. Auditory brainstem responses (ABRs) and distortion-product otoacoustic emissions (DPOAEs) were carried out to evaluate the auditory functions. ABR thresholds for tone-burst stimuli at 8, 16, and 32 kHz rapidly increased at 10 months of age, and reached undetectable levels by 16 months of age. DPOAE levels gradually decreased to the noise levels by 12 months of age. Thirty-six ears from 18 mice at the age of 1 month, 36 ears from 18 mice at the age of 10 months, and 30 ears from 15 mice at the age of 16 months were used for miRNA expression analyses. Membranous labyrinths were dissected from otic capsules in RNAlater solution (Ambion). Total RNAs including small RNAs were purified by each age group. The quality and quantity of each RNA preparation were determined using a Model 2100 Agilent BioAnalyser. miRCURY LNA microRNA Array (Exiqon) was used for miRNA expression profiles. Several miRNAs were up-regulated or down-regulated with age.

### **334 In Vitro Flavoprotein Imaging to Study Age-Related Changes in Auditory Cortical GABAergic Function**

**Kevin Stebbings<sup>1</sup>, Donald Caspary<sup>2</sup>, Jeremy Turner<sup>2</sup>, Daniel Llano<sup>1</sup>**

<sup>1</sup>*University of Illinois at Urbana-Champaign*, <sup>2</sup>*Southern Illinois University College of Medicine, Springfield*

Despite great strides in the treatment of age-related hearing loss through the use of peripheral hearing aids, older adults often continue to have substantial difficulty in real life, multi-talker, situations. We hypothesize that central mechanisms, including loss of cortical GABAergic function, may be responsible for these complex auditory perception deficits. We have developed a quantitative imaging approach to study the changes in GABAergic activation triggered by stimulation of auditory thalamocortical afferents. Auditory thalamocortical brain slices were cut from young (3-4 months) or old (>20 months) CBA/J mice. Electrical stimulation of thalamocortical fibers was used to activate the auditory

cortex. We imaged cortical activation using flavoprotein autofluorescence (excitation light 450-490 nm/emission 515 nm long-pass). A series of stimulation amplitudes ranging from 5-500  $\mu$ A were used, and a 4-parameter sigmoidal dose-response model was used to fit the data. The width of activation and parameters from the sigmoid model were similar across animals (n=10), all with coefficients of variation that were less than 50%. Cortical activation was diminished by approximately 95% by blockade with 80  $\mu$ M DNQX, by 97% with DNQX + 100  $\mu$ M APV and by 98% with 1  $\mu$ M TTX, suggesting that the cortical signal is predominantly caused by orthodromic synaptic activation of thalamocortical afferents. We also observed that the width of activation was highly sensitive to GABAA blockade with 100 nM Gabazine and that this sensitivity differed between aged and young mice (EC50 ratio Gabazine vs. normal ACSF = 3.24 +/- vs. 1.77 +/-, p<0.05). These data suggest that flavoprotein imaging of thalamocortical slices is a viable approach to the study of age-related changes in cortical GABAergic function, and that feedforward inhibition in the thalamocortical system may diminish with age.

### **335 Prolactin Is Associated with Hearing Loss in Aged Mice**

**Robert Marano<sup>1</sup>, Jennifer Tickner<sup>2</sup>, Rachel Burt<sup>3</sup>, Marina Carpinelli<sup>3</sup>, Anne Cooray<sup>3</sup>, Sharon Redmond<sup>1</sup>**

<sup>1</sup>*Ear Science Institute Australia and the Ear Sciences Centre, The University of Western Australia*, <sup>2</sup>*School of Pathology and Laboratory Medicine, The University of Western Australia*, <sup>3</sup>*Molecular Medicine Division, Walter & Eliza Hall Institute of Medical Research*

Background: Age related hearing loss (ARHL) is so named as it is a condition that worsens with age. Furthermore, the condition may appear prematurely and/or be occurring at an advanced rate in comparison to other organs of the body and singularly may interfere with quality of life. The development of ARHL is considered to be due to a number of factors including environmental and genetic. However, no definitive genetic component has yet been discovered with several genes thought to play an interactive role. Here we describe a study aimed at discovering genes that are differentially expressed in the cochlea of aged mice compared to a younger cohort. We then aimed to correlate the expression of these genes to potential morphological changes of the cochlear and hearing loss. Methods: Microarray analysis was used to determine differential gene expression between pooled samples of 4 wk, 15 wk and 45 wk old mice. To examine a correlation between hearing loss and gene expression a second cohort of mice was used. Hearing ability was measured using ABR with click and pure tone responses measured at 4, 8, 16 and 32 KHz. Gene expression within the cochlea of these mice was determined using quantitative real-time PCR. Results: Microarray analysis revealed a number of genes differentially regulated. However, the most significant change was recorded for prolactin (Prl) at a 108-fold increase. Subsequent analysis on the second cohort of mice indicated that several developed a significant increase in hearing threshold, which was associated with

age and gender. Further analysis using PCR indicated the hearing loss in these animals was also correlated with increased Prl expression. **Conclusion:** Hearing loss in aged mice was gender specific with only the females exhibiting a significant threshold shift. In addition, female mice also demonstrated Prl expression within the cochlea while males of the same age did not. Therefore, Prl may be associated with age related hearing loss in mice.

### **336 Morphological Effects of Dietary Restriction in the Aging Rat Cochlea**

**Paula Mannström<sup>1</sup>**, Mette Kirkegaard<sup>1</sup>, Mats Ulfendahl<sup>1</sup>  
<sup>1</sup>*Karolinska Institutet, Sweden*

Age-related hearing loss is a growing problem in the aging population. Oxidative stress increases with age and one reason is the reduced vascular flow in the body. It has been shown that caloric restriction enhances longevity between 30 to 50% and the proposed theory suggests that this is due to reduced oxidative damage in a delayed aging process. Caloric restriction has also been reported to slow down age-related hearing loss. The aim of the present study was to investigate age-related morphological changes within the cochleas of rats kept on normal diet and subjected to dietary restriction.

Female Sprague Dawley rats, either subjected to a 30% restricted diet or having free access to food were sacrificed at 28-31 months of age. A control group was sacrificed at 2 months of age. Tissue sections from the cochleas were used to estimate the total number of hair cells and spiral ganglion neurons, soma volume of the neurons, and total volume of the stria vascularis using unbiased stereological methods.

Stria vascularis volume decreased with age, more apparent in the animals having free access to food than those on dietary restriction. The number of hair cells was affected by age more than the spiral ganglion neurons, while dietary restriction resulted in no statistical significant effect on either cell type. The some size of the spiral ganglion neurons was slightly increased in the old animals with free access to food.

Aging seems to affect the number of hair cells and stria vascularis volume primarily. Loss of neurons appears to be a secondary effect, and their increased soma size could be explained as an early sign of degeneration. Stria vascularis, which is the vascularized part of the cochlea benefits most from the dietary restriction, probably by maintaining sufficient vascular flow, and thereby reducing the oxidative damage to the tissue.

### **337 Age-Related Gene Expression Changes in the Inferior Colliculus of Het4 Mice**

**Richard Altschuler<sup>1</sup>**, A Genene Holt<sup>2</sup>, Richard Miller<sup>1</sup>, Jochen Schacht<sup>1</sup>, Cathy Martin<sup>1</sup>, Karin Halsey<sup>1</sup>, David Dolan<sup>1</sup>

<sup>1</sup>*University of Michigan*, <sup>2</sup>*Wayne State University*

UM-Het4 mice are a genetically heterogeneous strain from MOLF/Ei, 129S1/SvImJ, C3H/HeJ and FVB/NJ grandparents and do not have the Cdh23753A allele at the Ah11 locus. To study age-related changes in their inferior colliculus (IC), 182 genes were pre-selected based on

roles in synaptic neurotransmission / responses, oxidative and ER stress and/or literature on age-related changes. Gene expression was compared in young adult, moderately aged (22-24 month old) and very aged (27-29 month old) animals. Each mouse was also tested for hearing thresholds, gap detection and pre-pulse inhibition of the acoustic startle reflex. Forty-eight genes showed significant changes in expression in very aged mice compared to young animals, with expression increased in 27 genes and decreased in 21. Genes with increased expression included voltage gated calcium channel subunits, GFAP and caspase4. Genes with decreased expression included BDNF, TASK5, several heat shock proteins, two neuroligins and vesicular glutamate transporters. We found significantly decreased Aquaporin4 expression in moderately aged Het4 mice and significantly increased expression in the very aged as has been previously reported by Christensen et al (2009) in CBA/J mice. We also found this expression pattern of early aging decrease and late aging increase in another 9 genes, including map kinase 1 and the ER stress protein Hmox1. Many genes had significant expression decreases only in the moderately aged mice and no significant change in the very aged mice. This included the alpha1 subunit of the GABA receptor and GAD, both shown to have age-related decreases in the rat IC (Caspary et al, 2008 for review). There was greater incidence of hearing loss and decreases in gap detection in the very old Het4 mice compared to the moderately aged that could provide another influence on levels of gene expression in the IC of very aged Het4 mice.

These studies were supported by NIH grant AG025164 and P30 DC05188

### **338 Multi-Level Analysis of Age Related Declines in Auditory Temporal Processing**

**Aravindakshan Parthasarathy<sup>1</sup>**, Stephanie Gardner<sup>1</sup>, Edward Bartlett<sup>1,2</sup>

<sup>1</sup>*Department of Biological Sciences*, <sup>2</sup>*Weldon School of Biomedical Engineering, Purdue University*

Loss of auditory temporal processing with age can be attributed, in part, to deficits in the central auditory pathway. This could be due to the loss of inhibition observed at various auditory nuclei with age. We have previously demonstrated a loss of temporal processing with age, independent of differences in hearing thresholds, using amplitude modulation following responses (AMFRs). Here an attempt has been made to understand how these evoked potentials correlate with the responses of small neural populations as well as at the level of single neurons in the auditory mid-brain. AMFRs were recorded in young and aged F-344 rats to sinusoidally and asymmetrically amplitude modulated sounds varying in modulation depth and modulation frequency (MF). Local field potentials (LFPs) as well as single unit responses to the sound stimuli were analyzed from the inferior colliculus (IC) of the same animals. Immunohistological analysis of the IC was done to determine how loss of GABAergic markers correlate with age-related loss of temporal processing. Preliminary results suggest a correlation between GAD

65/67 and declines in AMFR responses. Age-related decreases in AMFR amplitudes were observed with decreases in depth and increases in MF. Similar results were observed in the unit responses, with aged animals showing a lower temporal precision to faster MFs, though the maximum responsive MF was lower in both age groups. The most sensitive depth detection thresholds in both young and aged animals were comparable to those measured by AMFRs. The LFPs were low pass in nature with the aged animals showing a greater reduction in response for faster MFs. The LFP cut-off frequency and the depth detection thresholds were more similar to the AMFRs than the unit responses. These results together indicate that the LFPs form a bridge between the AMFRs and the unit responses, and that differences observed at the population level translate to an extent to the level of the single neuron.

### **339 Ghrelin Receptor Deficiency Modulates Hearing in Obese Mice**

Michelle L. Seymour<sup>1</sup>, Yuxiang Sun<sup>1,2</sup>, Fred A. Pereira<sup>1,3</sup>  
<sup>1</sup>Huffington Center on Aging and Department of Molecular and Cellular Biology, <sup>2</sup>Children's Nutrition Research Center, Department of Pediatrics, <sup>3</sup>Bobby R. Alford Department of Otolaryngology-Head and Neck Surgery, Baylor College of Medicine

Hearing loss is the most common sensory impairment, affecting nearly 10% of the adult population and 50% of those over age 75. Presbycusis is the most common cause of hearing loss, involves age-related degeneration of the inner ear function, and results in a sensorineural hearing loss beginning at the high frequencies and progressing to the middle and low frequencies. Several medical conditions associated with advancing age are implicated in presbycusis, including cardiovascular disease, hyperlipidemia, diabetes mellitus and immune function impairment. However, the relationships of these conditions with hearing loss are not well characterized or understood. Mouse models of deficiencies in the appetite-stimulating hormone ghrelin, its receptor (the ghrelin receptor, GHS-R), and the appetite-suppressing hormone leptin have the potential to address some of the issues of presbycusis because these mouse models have alterations in feeding behavior, glucose homeostasis, lipid metabolism, and induction of thymopoiesis. These findings led us to hypothesize that ablation of GHS-R in leptin deficient mice will improve auditory function, reduce cochlear cholesterol levels and minimize age-related degeneration of the cochlea. Indeed, preliminary findings indicate that ablation of the ghrelin receptor in leptin deficient mice improves insulin sensitivity, adiposity and serum lipid profiles. Furthermore, hearing thresholds differ between the genotypes at 5 months of age. We are currently expanding our evaluations of these auditory outcomes with age (young and old), as well as in the context of long-term feeding studies to alter nutritional lipid intake. Collectively, these studies will provide valuable information regarding how common alterations in the metabolic milieu with age affect the cochlear and hearing function and, thus, influence the clinical management of

these conditions to preserve audition. Supported by grants: NIH AG029641, DK079638 and USDA/CRIS ARS 6250-51000-055 to YS, and NIH Training Grant AG00183 to MLS.

### **340 The Effect of Aging on VEGF Expression and Vascular Structure in Swiss Webster and C57BL/6 Mice**

David Clinkard<sup>1,2</sup>, Thileep Kandasamy<sup>1</sup>, Hosam Amoodi<sup>1</sup>, Robert Harrison<sup>1,3</sup>, Joseph Chen<sup>1,4</sup>, Vincent Lin<sup>1,4</sup>  
<sup>1</sup>University of Toronto, <sup>2</sup>Queen's University, <sup>3</sup>Hospital for Sick Children, <sup>4</sup>Sunnybrook Health Sciences Centre

Introduction: Previous work has shown a strong association between alterations in cochlear vasculature, aging and the development of presbycusis. The important role of vascular endothelial growth factor (VEGF) and its receptors Flt-1 and Flk-1 in angiogenesis suggests a potential role for involvement in this process. The aim of this study was to characterize vascular structure and VEGF and its' receptors in young and old C57BL/6 and Swiss Webster Mice.

Methods: Cochlea were characterized with qRT-PCR, immunohistochemistry, and histological quantification of vasculature within the stria vascularis. Auditory evoked potentials were also performed to verify age-related hearing loss in the old C57BL/6 mice.

Results: Old C57BL/6 mice exhibited high frequency hearing loss. Qualitative analysis of protein expression by immunohistochemistry showed decreased VEGF labeling in the basal turn of old C57BL/6 cochlea as compared to apical sections. Old C57BL/6 mice demonstrated significantly decreased blood vessel cross sectional area in the stria vascularis. Aged C57BL/6 mice had a significantly reduced number of blood vessels as compared to young animals, irrespective of basal or apical location. There was no significant difference in VEGF gene expression as measured by qRT-PCR. Swiss Webster mice failed to show any differences in vascular structure, immunohistological staining or VEGF expression in the basal or apical locations as a result of age. As expected, hearing remained stable in both young and old swiss Webster mice.

Conclusion: The marked deafness of aged C57 mice could be associated in part by the decreased VEGF expression in the basal turn altering vascular development and in turn playing a contributory role in presbycusis development. These alterations in gene expression and vascular structure were absent in both young and old Swiss Webster mice, whom all had normal hearing.

### **341 Fucoidan Promotes Mechanosensory Hair Cell Regeneration Following Aminoglycoside-Induced Cell Death**

In Seok Moon<sup>1</sup>, Won-Sang Lee<sup>1</sup>, Se Ra Park<sup>1</sup>, Jae Young Choi<sup>1</sup>

<sup>1</sup>Yonsei University College of Medicine

Objective: Lateral line system of the zebrafish is a useful model for study of hair cell toxicity and regeneration. We found that low molecular weight fucoidan (LMWF)

stimulated the regeneration of mechanosensory hair cells after neomycin-induced cell death in zebrafish lateral line. The aims of this study were to quantify the regenerative effects of LMWF and determine their relationship to the Notch and FGF signaling pathways.

**Methods:** Wild-type zebrafish and three different transgenic zebrafish lines (Pou4f3::GFP, scm1::GFP, and ET20::GFP) were used. At 4.5e6 days post-fertilization, lateral line hair cells of larvae were eliminated using neomycin (500 mM). Larvae were then treated with LMWF. Neuromasts were observed using confocal microscopy. Stereocilia morphology was observed using scanning electron microscopy, and the location and status of regeneration was assessed using 5-bromo-2-deoxyuridine (BrdU) incorporation.

**Results:** Hair cells damaged by neomycin treatment regenerated faster in wild-type and Pou4f3::GFP larvae treated with LMWF (50 mg/ml) than in untreated controls. LMWF also enhanced the regeneration of supporting cells in scm1::GFP and ET20::GFP larvae. Increased numbers of BrdU-labeled cells were found after LMWF treatment in neuromast regions corresponding to internal and peripheral supporting cells. The effect of LMWF was mimicked by the Notch signaling inhibitor N-[N-(3,5-difluorophenacetyl)-1-alanyl]-S-phenylglycine t-butyl ester (DAPT), but the effects of LMWF and DAPT were not additive.

**Conclusion:** LMWF enhances the regeneration of hair cells damaged by neomycin. The mechanism may involve the Notch signaling pathway. LMWF shows promise as a therapeutic agent for hearing and balance disorders.

### **[342] Proliferation of Cochlear Supporting Cells in Juvenile Opossums: A Potential Model for Auditory Hair Cell Regeneration in Mammals?**

**Brad Walters**<sup>1</sup>, John VandeBerg<sup>2,3</sup>, Jian Zuo<sup>1</sup>

<sup>1</sup>St. Jude Children's Research Hospital, <sup>2</sup>Texas Biomedical Research Foundation, <sup>3</sup>Southwest National Primate Research Center

It is currently accepted that auditory hair cells (HCs) are not readily regenerated in mammals while non-mammalian vertebrates are capable of robust HC regeneration via the proliferation and differentiation of supporting cells (SCs). This suggests that the ability to regenerate auditory HCs was lost sometime during the past 300 million years of mammalian evolution. Marsupials diverged from eutherian mammals ~150 million years ago, and therefore may have retained the ability to regenerate auditory HCs. To investigate the proliferative capacity of SCs in a marsupial, cochleae were collected from gray short-tailed opossums (*Monodelphis domestica*) at postnatal days 6 (P6), 14 (P14), 28 (P28), and 60 (P60) and subsequently labeled by immunofluorescence for proliferating cell nuclear antigen (PCNA), myosin VIIa (*Myo7a*) and Sox2. PCNA positive SCs were readily detected in the postnatal opossum cochlea at all ages from P6 - P60. In contrast, SCs did not co-label with PCNA in cochleae from wild type C57BL/6 mice at similar ages. To investigate the proliferative capacity of cochlear SCs after HC loss, P35 opossums

were given an injection of either kanamycin (1500mg/kg) or saline, and subsequently injected once daily for 8 days with the thymidine analog BrdU before being perfused at P44. Kanamycin treatment resulted in a complete loss of OHCs in the middle and basal turns of the cochlea, and a significant loss of OHCs in the apical turn. In both the saline and the kanamycin treated cochleae, Sox2 and BrdU double positive cells were detected in the organ of Corti, suggesting that SCs are proliferative in the opossum cochlea between P35 and P44, and that opossums may have the potential for auditory HC regeneration.

Supported by grants from the Robert J. Kleberg, Jr. and Helen C. Kleberg Foundation, the National Institutes of Health (NIDCD), the Office of Naval Research, and the American Lebanese Syrian Associated Charities (ALSAC) of St. Jude Children's Research Hospital.

### **[343] Hes5 Specific siRNA Increases Hair Cell Regeneration in Aminoglycoside Treated Mouse Utricle**

Jae-Yun Jung<sup>1,2</sup>, Matthew Avenarius<sup>1</sup>, Evgenia Alpert<sup>3</sup>, Elena Feinstein<sup>3</sup>, **Yehoash Raphael**<sup>1</sup>

<sup>1</sup>University of Michigan, <sup>2</sup>Dankook University, <sup>3</sup>Quark Pharmaceuticals Inc

As in most sensory end-organs, sensory cells (hair cells) in the vestibular sensory epithelia (VSE) are thought to degenerate with aging. In some cases, hair cell death occurs following exposure to ototoxic medication, trauma, and/or infection, regardless of biological senescence. Although loss of vestibular function can be managed with medication, rehabilitation exercise and compensation, these strategies are often insufficient, especially for patients with bilateral vestibulopathy or multisensory deficits. Treatment modalities that augment the limited intrinsic hair cell regeneration of the damaged VSE will likely help alleviate vestibulopathy symptoms. To enhance the low-level spontaneous hair cell regeneration, we treated damaged VSE with siRNA designed to block *Hes5*. *Hes5* is known to inhibit *Atoh1* expression of supporting cells during development. We induced a severe lesion in the VSE of mice by injecting streptomycin to the posterior semicircular canal of the left ear. One week later, the ear was treated with *Hes5* siRNA (experimental group) or saline (control group). Two weeks later, a total of three weeks after the ototoxic insult, we compared the number of hair cells between the *Hes5* siRNA treated group and the vehicle treated group and found significantly more hair cells in the *Hes5* siRNA treated mice than in control mice. *Hes5* and *Atoh1* gene expression levels analyzed by qRT-PCR in *Hes5* siRNA treated mice showed decreased *Hes5* gene expression (half fold) and increased *Atoh1* expression level (nine fold), compared to control mice. These results suggest that down regulation of *Hes5*, which is known to suppress supporting cell transdifferentiation into new hair cells, can enhance regeneration in mammalian VSE. Considering the lack of toxicity and ease of delivery, it is likely that siRNA can be further developed into a clinically feasible therapy for enhancing hair cell regeneration in the VSE.

**344 Lgr5+ Supporting Cells Form Replication Foci in Response to Wnt/ $\beta$ -Catenin Overexpression in the Postnatal Mouse Cochlea *in Vivo***

Bryan Kuo<sup>1</sup>, Renjie Chai<sup>2</sup>, Zhiyong Liu<sup>1</sup>, Anping Xia<sup>2</sup>, Makoto Taketo<sup>3</sup>, Alan Cheng<sup>2</sup>, Jian Zuo<sup>1</sup>

<sup>1</sup>*Department of Developmental Neurobiology, St. Jude Children's Research Hospital,* <sup>2</sup>*Department of Otolaryngology-Head and Neck Surgery, Stanford University School of Medicine,* <sup>3</sup>*Department of Pharmacology, Graduate School of Medicine, Kyoto University.*

During the early development of the inner ear, Wnt signaling has been shown to play a role in the formation of the otic placode, and lineage tracing has shown that Wnt-responsive cells are present postnatally in the cochlea and the vestibular sensory organs. However, its role postnatally is unknown. *Lgr5* is a Wnt target gene that is expressed in actively cycling cells of the intestinal crypt and hair follicles of the skin, and lineage tracing shows that *Lgr5*+ cells can self-renew and give rise to the major cell types and derivatives of the aforementioned organs. Thus, *Lgr5* has been proposed to be a marker of stem cells in these organs. *Lgr5* has been recently shown to be expressed in the third Deiters' cells, inner pillar, and inner phalangeal cells of the mouse organ of Corti during the first week of postnatal development. We hypothesize that these *Lgr5*+ supporting cells might represent the progenitor/stem cells of the postnatal mouse inner ear, and that Wnt/ $\beta$ -catenin overexpression in these cells would result in hair cell formation. We therefore characterized the *Lgr5*-EGFP-IRES-CreER;Rosa-floxed-stop- $\beta$ -catenin overexpressor mouse to test this hypothesis. Following the induction at P0-P1, *Lgr5*+ cells medial to the inner hair cells (likely inner phalangeal cells) divided and formed many isolated replication foci throughout the cochlea that persisted up until P21. The Wnt-responsive cells did not express Myosin7a or Calbindin, but expressed Sox2 and *Lgr5*. BrdU incorporation begins at P4, and we are investigating when cell death within the foci occurs. We conclude that the Wnt/ $\beta$ -catenin overexpression in *Lgr5*+ supporting cells leads to their division, but is not sufficient to promote their differentiation into hair cells. Supported in part by NIH DC006471 (J.Z.), NIH DC008800 (J.Z.), NIH DC011043 (A.C), and NIH CA21765, the Office of Naval Research N000140911014 (J.Z.), and ALSAC of SJCRH. J. Z. is a recipient of The Hartwell Individual Biomedical Research Award.

**345 A Quest for P27Kip1 Small Molecule Inhibitors for Hair Cell Regeneration in the Mammalian Cochlea**

Luigi Iconaru<sup>1</sup>, Anang Shelat<sup>1</sup>, Richard Kriwacki<sup>1</sup>, Jian Zuo<sup>1</sup>

<sup>1</sup>*St Jude Children's Research Hospital*

Noise-induced hearing loss (NIHL) is primarily caused by alteration of inner ear hair cells (HCs). Humans and other mammals cannot spontaneously regenerate damaged HCs. However, chicken, fish and amphibians have the

ability to regenerate the damaged sensory HCs by proliferation and transdifferentiation of the neighboring supporting cells (SCs), therefore recovering their hearing. In mice, HC and SC progenitors exit the cell cycle between embryonic days 12 and 14 and do not proliferate thereafter. This stage of development correlates very well with the expression of the cell cycle inhibitor, p27Kip1 (p27), in the organ of Corti, suggesting that p27 plays a role in terminal differentiation in this tissue. This hypothesis is supported by studies in which inactivation of p27 in mouse postnatal SCs or HCs has led to cell proliferation and HC regeneration, revealing the potential of p27 small molecule inhibitors (therapeutic drugs) for regeneration of functional HCs in mammalian vertebrates.

Cyclin-dependent kinases (Cdks), when activated by binding to subunits termed cyclins, are the master regulatory of cell division. Protein p27 is an intrinsically disordered protein (IDP) that inhibits the enzymatic catalytic activity of nuclear Cdk2/cyclin E (and A) complexes, blocking progression from G1 to S phase of the cell cycle and accounting for the ability of p27 to enforce cell cycle arrest.

We hypothesize that small molecules which bind specifically and tightly to p27 will compete for its binding and thus activate Cdk/cyclin complexes. Such small molecules have potential as transient inhibitors of p27-mediated cell cycle arrest and terminal differentiation and may serve to initiate HC regeneration in the organ of Corti. We are using fragment-based drug discovery (FBDD) methods, utilizing NMR spectroscopy as the primary screening technique. After the validation of initial fragment hits we used cheminformatics analysis to identify 2nd generation inhibitors. In the last decade, FBDD has emerged as a successful alternative to more traditional high-throughput screening approaches. However, the technique has received limited application toward IDP targets. We seek to demonstrate that p27, a prototype IDP, is a "druggable" target and that its function can be modulated by small molecules *in vivo*. We will present our initial results toward this goal.

We gratefully acknowledge support from ALSAC; Garwood Research Fellowship (to L. I.); ONR N00014-09-1-1014 and NIH R01DC006471 (to J. Z.); NIH R01CA082491 and R01CA092035 (to R. W. K.); NCI Cancer Center Core Grant P30CA21765 (at St. Jude) and The Hartwell Foundation (to J. Z.).

**346 Reprogramming of Mouse Cochlear Cells by Retroviral Transduction of IPS Factors**

Xiangxin Lou<sup>1</sup>, Takayuki Nakagawa<sup>1</sup>, Koji Nishimura<sup>1</sup>, Juichi Ito<sup>1</sup>

<sup>1</sup>*Department of Otolaryngology-Head and Neck Surgery, Graduate School of Medicine, Kyoto University*

Loss of hair cells in the mammalian cochlea leads to permanent sensorineural hearing loss, because the sensory epithelium of mammalian cochleae has limited capacity for regeneration. In embryonic or neonatal cochleae of mammals, some reports have indicated the existence of stem- or progenitor-cell populations, while

adult cochleae have virtually no such cell population. Hence, reprogramming or partial reprogramming of adult cochlear cells could induce regeneration in adult cochleae. Yamanaka et al. has established the method for reprogramming of somatic cells into induced pluripotent stem (iPS) cells by introduction of four transcription factors, Oct3/4, Sox2, Klf4 and c-Myc. In the present study, we examined whether Yamanaka's four factors can induce reprogramming of cochlear cells, which may result in generation of iPS cells from cochlear cells. We introduced Yamanaka's factors into otospheres derived from postnatal day-1 mouse cochlear epithelia using retrovirus, and analysed alterations in cell characteristics. After transduction of Yamanaka's factors, otospheres generated colonies that displayed embryonic stem cell (ESC)-like morphology and expressed markers of iPS cells. ESC-like colonies derived from otospheres are able to differentiate into three embryonic germ layers. Their transplantation into nude mice resulted in the formation of teratoma. These findings demonstrate that transduction of Yamanaka's factors is capable of inducing reprogramming of otospheres, suggesting that the method for generation of iPS cells might be utilized for full or partial reprogramming of cochlear cells.

### **347 Direct Conversion of Cochlear Non-Sensory Epithelial Cells to Neurons**

Rachel Weichert<sup>1,2</sup>, Alain Dabdoub<sup>1</sup>

<sup>1</sup>UCSD School of Medicine, <sup>2</sup>SDSU Department of Audiology

Spiral ganglion neurons (SGNs) transmit sound information in the form of electrical signals from the mechanosensory hair cells in the inner ear to the brainstem. Once lost, SGNs do not regenerate; therefore, one approach to hearing loss treatment is the use of gene therapy for the induction of endogenous cells. A target cell population for induction is non-sensory epithelial cells (NSECs). Previously studies have demonstrated that the transcription factors Neurog1, Sox2 and NeuroD1 are required for the formation and survival of SGNs. While these factors, at various efficiencies, were sufficient to induce neuronal phenotypes in NSECs primarily at embryonic stages (Puligilla et al., J. Neurosci. 2010), much needs to be accomplished to improve the efficiency of neuron induction at postnatal stages and to closely match the unique morphological and electrophysiological characteristics of SGNs. Here we show that overexpression of the transcription factor Ascl1, a neurogenic bHLH transcription factor, in NSECs generates induced neurons at high efficiency at both embryonic and postnatal stages. Furthermore, the induced neurons resulting from the double overexpression of Ascl1 and NeuroD1 exhibit characteristic neuronal morphology, express neuronal markers, synaptic proteins, fire action potentials and electrophysiologically begin to resemble the endogenous SGN phenotype.

Overall, our results indicate that overexpression of neurogenic transcription factors is sufficient to reprogram non-sensory epithelial cells into functional neurons. These induced neurons could provide a strategy to endogenously

regenerate the spiral ganglion neurons which would have significant impact on research and advancement in cochlear implants as well as in medical treatment of hearing loss and deafness.

### **348 Sensory Epithelial Cells Acquire Features of Prosensory Cells Via Epithelial-To-Mesenchymal Transition**

Lei Zhang<sup>1</sup>, Zhengqing Hu<sup>1</sup>

<sup>1</sup>Wayne State University

Epithelial to mesenchymal transition (EMT) plays a critical role during normal development and in adult tissue repair. It is known that immortalized epithelial cells can undergo an EMT and become cancer stem cells, and that epithelial cells from mouse pancreatic islet and avian inner ear can acquire mesenchymal trait in vitro via EMT. However, it is unclear whether epithelial cells from mammalian sensory system can undergo an EMT and obtain features of stem/progenitor cells. In this study, we used mouse utricle sensory epithelial cells (MUCs) as a mammalian cell model to address this issue. When cultured on two-dimensional substrates, dissociated MUCs gradually lost their columnar shape and started to expand on the substrate with down-regulation of expression of epithelial junction markers and up-regulation of genes and proteins that are widely shown in mesenchymal cells. Moreover, MUCs expressed genes and proteins that are usually presented in prosensory epithelial cells and stem cells. These MUCs showed potential to differentiate into epithelial cells via a reverse EMT when they were forced to suspend in culture medium. Our findings reveal that sensory epithelial cells from mammalian tissue can undergo an EMT to become cells expressing features of stem cells, which can be induced to become epithelial cells via a reverse EMT. The outcomes of this study may provide a novel approach to generate epithelial progenitors for use in cell replacement therapy to treat a number of human diseases, such as hearing loss and vision loss.

### **349 A Cell Line of Multipotent Inner-Ear Progenitor Cells Reveals a Molecular Switch from Proliferation to Differentiation**

Kelvin Y. Kwan<sup>1</sup>, David P. Corey<sup>2,3</sup>

<sup>1</sup>Rutgers University, <sup>2</sup>Harvard Medical School, <sup>3</sup>Howard Hughes Medical Institute

The inner ears of birds and fishes can regenerate sensory hair cells, by division and differentiation of adjacent supporting cells. Mammals have lost this ability. Two of the genes that are upregulated during avian hair cell regeneration are c-Myc and Sox2. To determine whether c-Myc promotes cell division in mammalian inner ears, we isolated mouse E13 cochlear prosensory cells and infected them with a c-Myc retrovirus. Infected cells upregulate self-renewal genes, continuously divide and maintain their multipotent cell identity, expressing early markers of the cochlear prosensory region. Epigenetic alterations are likely responsible for self-renewal since only transient expression of the viral c-Myc is required.

In vitro, the cells divide in response to the growth factor bFGF, but down regulate c-Myc and express the cell-cycle control genes *Rb* and *p27* upon its removal. When cultured as adherent cells, they differentiate into bipolar and pseudo-unipolar neurons similar to those found in spiral ganglia. When cultured as otospheres, they assumed characteristics of prosensory epithelia upon exiting the cell cycle, showing circumferential actin bands and E-cadherin junctions. Engraftment of these mouse progenitor cells into embryonic chicken otocysts provided the final differentiation cues: Identified by mCherry expression, mouse progenitor cells in chicken basilar papilla became supporting cells and functional hair cells. Hair cells had fully developed hair bundles and accumulated AM1-43.

RNA-Seq and ChIP-Seq analysis of progenitor cells revealed that c-Myc and Sox2 co-occupy ~85% of their promoters to control a subset of genes that are responsible for cell division and maintaining prosensory cell fate. Upon differentiation, c-Myc expression is reduced and no longer binds to the promoters. The cell fate decisions to become different cell types are relinquished to Sox2, thus providing a molecular switch from proliferation to differentiation.

### **350 Comparison of Morphology and Phenotype Between in Vitro Cultivated Human Tympanic Membrane Keratinocytes and Epidermal Keratinocytes**

**Peder Aabel**<sup>1</sup>, Helge Rask-Andersen<sup>2</sup>, Magnus von Unge<sup>1</sup>, Marja Boström<sup>2</sup>

<sup>1</sup>Akershus University Hospital, <sup>2</sup>Uppsala University Hospital

Living tissue replacements based on cultured cells are used to treat full thickness skin defects caused by large burns. Likewise, tissue replacement with cultivated cells and living tissue equivalents can become a favorable optional treatment modality for patients with persistent tympanic membrane defects. Several research groups have recently reported cultivation of human tympanic membrane cells on different matrix materials to demonstrate their potential use in otology. Little research has so far been published that seeks to optimize the conditions for cultivation of tympanic membrane cells to make them suitable for cell-based treatment or transplantation.

Our ongoing research aims to investigate the expansion and the behavior of tympanic membrane keratinocytes in culture. The cells from the human tympanic membranes are provided from donors undergoing temporal bone surgery during which the tympanic membrane is sacrificed. The membranes are enzymatically treated and primary cultures are established. They are cultivated under various conditions. After cultivation the cells are analyzed for proliferative capacity, degree of differentiation and other cell phenotype characteristics by immunofluorescence. Viability is examined by the use of Calcein Ethidium assay. Cell morphology is also described.

The cells are currently under analysis and the results will be presented at the conference.

### **351 BMP6 Inhibits Proliferation in Cultured Post-Hatch Chicken Auditory Epithelium**

Sidya Ty<sup>1</sup>, Sean Campbell<sup>1</sup>, Jennifer McCullar<sup>1</sup>, Elizabeth Oesterle<sup>1</sup>

<sup>1</sup>University of Washington

Identifying negative and positive regulators of supporting cell proliferation is important for developing therapies to stimulate hair cell regeneration in mammals. We study the post-hatch chicken inner ear, known for its robust regenerative capacities, to guide our studies attempting to induce hair cell regeneration in mammals.

Members of the powerful transforming growth factor beta (TGF $\beta$ ) superfamily are potent regulators of progenitor and stem cell proliferation in many adult tissues. We cultured post-hatch chicken basilar papilla using organotypic culture techniques and found that adding exogenous BMP6 inhibits supporting cell proliferation in a dose-dependent manner. Blocking the Acvr2B type II receptor with a soluble Acvr2B/Fc receptor chimera significantly increased supporting cell proliferation, suggesting inhibitory signaling occurs via this receptor. Previously, we localized Acvr2B and phosphorylated Smad1/5/8, activated downstream effector molecules, to supporting cells in mature avian sensory epithelium (McCullar et al., 2010 J. Neurosci). Immunocytochemistry using an anti-BMP6 antibody shows strong BMP6 expression in auditory hair cells and in hyaline cells, a non-sensory cell type flanking the inferior edge of the sensory epithelium. ALK3 and ALK6 are type 1 receptors commonly involved in BMP signaling. Blocking these receptors individually, or in combination, with soluble receptor(s) did not significantly effect proliferation. Blocking ALK2, another type 1 receptor often involved in BMP signaling, did alter supporting cell proliferation. In sum, these findings support the idea that hair cells in post-hatch chicken auditory sensory epithelium release BMP6 normally that tonically suppresses supporting cell proliferation.

Work supported by NIH grants R01-DC03944 R01, P30-DC04661, and P30-HD002274.

### **352 Identification of Tympanic Border Cells as Slow-Cycling Cells in the Cochlea**

**Mirei Taniguchi**<sup>1</sup>, Norio Yamamoto<sup>1</sup>, Takayuki Nakagawa<sup>1</sup>, Eriko Ogino<sup>1</sup>, Juichi Ito<sup>1</sup>

<sup>1</sup>Graduate School of Medicine, Kyoto University

Mammalian cochlear sensory epithelial cells have been considered to have little capacity to regenerate because they stop proliferation at later stage of embryogenesis, and never regenerate after birth. This makes sensorineural hearing loss that is mostly caused by impairment of cochlear sensory epithelial cells an intractable disease. Recently, however, mouse inner ear stem cells were identified by dissociating neonatal inner ear organs, suggesting the regenerative capacity of mammalian cochleae. Since dissociation of cells causes loss of information on localization, the localization of inner ear stem cells is unknown so far although it is very important for developing new therapeutic approaches to regenerate inner ear hair cells. Stem cells are normally slowly proliferating in adult organs and so-called slow-cycling

cells, turned out to be stem cells in several organs including brain and skin. In this study, using an exogenous proliferation marker, 5'-bromo-2'-deoxyuridine (BrdU) in combination with an endogenous proliferation marker Ki67, we identified tympanic border cells, which locate beneath the basilar membrane, as slow-cycling cells in the murine cochlea *in vivo*. Immunohistochemistry showed that tympanic border cells were positive for nestin, which is one of the putative stem/progenitor cell markers. These findings indicate that the tympanic border cell is included in candidates for inner ear stem/progenitor cells, and further analyses to characterize this cell population will be beneficial for the development of regenerative medicine for inner ear disorders.

### **353 Induction of Pluripotent Stem Cells in the Utricles of Transgenic Mice**

**Alyssa Huebner<sup>1</sup>, Chandrakala Puligilla<sup>1,2</sup>, Matthew Kelley<sup>1</sup>**

<sup>1</sup>*National Institute on Deafness and Other Communication Disorders, National Institutes of Health,* <sup>2</sup>*Medical University of South Carolina*

Hearing and balance disorders have a significant impact on quality of life, particularly in older individuals. In most cases, the underlying basis for these impairments is the loss of mechanosensory hair cells. In adult mammals, once hair cells are lost they are not replaced. In contrast, studies in embryonic and early postnatal mice have demonstrated a limited ability for hair cell replacement that can be correlated with the presence of a limited population of stem cells. With maturation, these stem cells are rapidly lost, a process that coincides with the absence of hair cell replacement. In contrast with mammals, other vertebrates retain the ability to replace hair cells throughout life, suggesting that stem cells are retained within non-mammalian inner ears. The recent demonstration that pluripotent stem cells can be induced through the expression of four genes (cMyc, Sox2, Oct4, and Klf4; MSOK) suggests the possibility that induction of pluripotency in inner ear sensory epithelia could lead to hair cell regeneration. To investigate this hypothesis, we attempted to induce pluripotent stem (iPS) cells within inner ear sensory epithelia *in vitro*. Utricles from a recently generated transgenic mouse line in which the MSOK genes can be transiently induced with doxycycline were dissected and established as floating cultures. Hair cells were eliminated by treatment with aminoglycosides. Explants were then cultured for 14 days, 20 d, or 30 d with differing concentrations of doxycycline. To determine if the cells within the explants had become iPS cells, qPCR was used to assess the expression of the MSOK genes as well as other indicators of pluripotency, such as Nanog, SSEA-1, Lin28A, and Rex1. In addition, immunohistochemistry was used to examine any potential hair cell regeneration. Initial results indicate limited induction of iPS cells, suggesting that conditions within adult utricular epithelia may be inhibitory for stem cell induction.

### **354 Modeling Otic Placode Induction in Three-Dimensional Culture**

**Karl Koehler<sup>1</sup>, Andrew Mikosz<sup>1</sup>, Eri Hashino<sup>1</sup>**

<sup>1</sup>*Indiana University School of Medicine*

Pluripotent stem cells can be efficiently differentiated into various neuronal subtypes in the nervous systems. However, comparatively few reports exist describing the derivation of neurons identical to those in cranial placode-derived sensory ganglia. Here, we describe a novel method for generating placodal neural progenitor cells using a combination of small molecules to regulate BMP signaling. Studies have shown that the establishment of the preplacodal ectoderm during the late blastula and early gastrula stages is predominantly governed by a low (medial) to high (lateral) concentration gradient of BMP molecules. As gastrulation progresses, inhibition of BMP signaling appears to be necessary for generation of the preplacodal region versus epidermis. We translated this natural mechanism *in vitro* by treating mouse embryonic stem cell-derived embryoid bodies with various doses of BMP molecules and small molecule inhibitors for over 8-10 days. Using qRT-PCR, we observed a dose-dependent upregulation of the preplacodal markers, such as Six1 and Dlx3/5, after 5 days of BMP4 treatment. Subsequent treatment with small molecule inhibitors of BMP signaling for another 3-5 days caused a further upregulation of Dlx3/5 and the preplacodal markers Six1 and Eya1. To monitor morphological changes of embryoid bodies during these treatments, we used time-lapse imaging. Beginning at day 4 of BMP4 treatment, a thin epithelium was detected around the outer edge of the embryoid bodies. By day 7, we observed the formation of vesicle-like structures budding off from the embryoid bodies. Approximately 80% of cells in these vesicle-like structures were Dlx5-positive and gave rise to migrating TUJ1-positive neurons. These results provide evidence that placode formation can be induced from mouse embryonic stem cells in 3D culture. This protocol could be used as a model system to recapitulate formation and differentiation of otic placode-derived cells *in vitro*.

### **355 Reinnervation of Hair Cells and Cochlear Nucleus by Engrafted Neurons Derived from Stem Cells**

**Yasheng Yuan<sup>1,2</sup>, Kunio Mizutani<sup>1,2</sup>, Yenfu Cheng<sup>1,2</sup>, Hainan Lang<sup>3</sup>, Charles Liberman<sup>1,2</sup>, Fuxin Shi<sup>1,2</sup>, Albert Edge<sup>1,2</sup>**

<sup>1</sup>*Department of Otolaryngology, Harvard Medical School,*

<sup>2</sup>*Eaton-Peabody Laboratory, Massachusetts Eye and Ear Infirmary,* <sup>3</sup>*Medical University of South Carolina*

We used mouse embryonic stem cell-derived neural progenitors to replace spiral ganglion neurons in a denervated mouse model. After ouabain was applied to the round window niche, 90% of type I spiral ganglion were removed, resulting in an elevation of ABR threshold above 80 dB. We then injected neural progenitors into the nerve trunk via the cerebello-pontine angle. These cells expressed a tau-GFP fusion protein allowing us to trace their processes *in vivo*. We did a step-wise induction of ES cells into neural progenitors before transplantation, which

gave rise to  $84.9 \pm 10.7\%$   $\beta$ -tubulin III positive neurons and  $13.2 \pm 1.6\%$  GFAP positive glial cells upon differentiation *in vitro*. The surgical approach without cochleostomy minimized the cochlear trauma and preserved cochlear function (DPOAE). Ten days after transplantation, small grafts located in the nerve trunk at the basal turn expressed endogenous GFP and neuron-specific markers. Three months after transplantation, grafted neural progenitors traced by their GFP expression grew extensive neural processes to hair cells at the mid-basal turn and also grew into the cochlear nucleus. Presynaptic marker, CTBP2 and post-synaptic marker, PSD95 were observed at contacts of grafted neural fibers with hair cells. In the cochlear nucleus, presynaptic marker, VGLUT1 was observed at contacts of grafted neural fibers and cochlear nucleus cells. Functional improvement was suggested by a decrease in ABR threshold at 32 kHz ( $6.7 \pm 1.7$  dB,  $n=6$ ). Our studies demonstrate the feasibility of replacement of spiral ganglions with stem cells. Supported by NIH grant DC007174

### **356 High-Resolution MRI of Stem Cell Graftment in the Human Temporal Bone Using Superparamagnetic Iron-Oxide Nanoparticles**

**Cristiano Piron**<sup>1</sup>, Karl Koehler<sup>1</sup>, Akihiro Matsuoka<sup>2</sup>, Michael Fritsch<sup>1</sup>, Eri Hashino<sup>1</sup>

<sup>1</sup>Indiana University School of Medicine, <sup>2</sup>University of California at San Diego

Magnetic resonance imaging (MRI) has recently emerged as one of the predominant imaging modalities for tracking stem cells in live animals in a noninvasive and longitudinal manner. However, little information is available whether MRI can be successfully applied to monitor stem cells in the cochlea, since imaging the cochlea is significantly more difficult than imaging the brain because of the cochlea's complex bony structure. The goal of this study was to acquire high-resolution 3-D MRI data that can be used to quantitatively evaluate the spatio-temporal pattern of stem cell engraftment in the human temporal bone. To increase the resolution of images, superparamagnetic iron-oxide (SPIO) nanoparticles were used as a contrast agent. To determine the optimal labeling condition, undifferentiated mouse embryonic stem (ES) cells were grown *in vitro* with SPIO at various concentrations for 24 to 96 hrs. SPIO at 300  $\mu\text{g}/\text{mL}$  was found to yield the best results with efficient intracellular uptake and no detectable toxic effects. Additionally, uptake efficiency was dramatically increased by treating cells with protamine sulfate. Scanning of human cadaver temporal bones in the presence or absence of labeled ES cells were carried out on a Varian 9.4 T MR system with an actively shielded horizontal bore. Axial T1-weighted images were acquired using a 3D asymmetric spin-echo pulse sequence. Acquired serial images were uploaded into the 3D Slicer software for modeling and quantitative analysis. Our analysis revealed that the measurements of the cochlea (length, height and volume) from our MRI data were comparable with those obtained from serial histological sections. Furthermore, detailed anatomical features, such

as semicircular canals and cochlear turns, could be viewed from any angle in the 3D reconstructions. These results are promising for the potential use of MRI to evaluate the outcome of stem cell transplantation in the inner ear of human patients.

### **357 Decellularized Mouse Ear Tissues: Scaffolds for Inductive Stem Cell Regeneration**

**Peter Santi**<sup>1</sup>, Shane Johnson<sup>1</sup>, Heather Schmitz<sup>1</sup>

<sup>1</sup>University of Minnesota

In order to investigate the connective tissue elements of the ear and to produce extracellular matrix (EM) scaffolds for inductive stem cell regeneration, we chemically removed all of cells of the ear. After decellularization, ear tissues (primarily in the cochlea) were decalcified, dehydrated, cleared to transparency and imaged whole using a scanning thin-sheet laser imaging microscopy (sTSLIM). In addition to the bony labyrinth, there was an abundance of EM that survived the decellularization process, including EM of the spiral ligament, basilar membrane and the spiral limbus. The organ of Corti was absent, while the spiral ganglion neurons appeared as hollow shells surrounded by EM and tube-like extensions of EM along their nerve processes. EM of the basilar membrane was present and Reissner's "membrane" persisted as a thin sheet of basement membrane. EM components of the stria vascularis, including the capillaries and their extensions were present but were often detached from the spiral ligament or were partially attached to the spiral ligament by matrix components of the radiating arterioles. In order to determine the composition of the EM's, whole cochlea immunohistochemistry was performed using antibodies against collagen type IV and laminin. Epitopes for both of these proteins were still present and their reactivity was expressed within the vascular elements and to a lesser degree within the basement membrane. We are currently attempting to seed samples of decellularized ear tissues with stem cells to determine if stem cells will engraft and differentiate using substrate cues present with the EMs of the ear. Successful inductive stem cell regeneration using decellularized ear tissues may prove to be a useful way of repairing damaged ear tissues using autologous donor stem cells. Supported by the NIDCD, the Capita and Lions Foundations.

### **358 Initiation, Progression and Interactions of Neural Correlates of Noise-Induced Tinnitus Along the Auditory Axis**

**Jinsheng Zhang**<sup>1</sup>, Xueguo Zhang<sup>1</sup>, John Moran<sup>2</sup>

<sup>1</sup>Wayne State University, <sup>2</sup>Henry Ford Health System

It has been considered that noise-induced tinnitus results from a cascade of maladaptive plastic changes following acoustic injuries and peripheral deafferentation. These changes are manifested by hyperactivity, increased bursting discharges, hypersynchrony and tonotopic reorganization. It has yet to be determined how neural correlates of the noise-induced tinnitus initiate, progress and interact along the auditory axis. We set out to explore

this by conducting simultaneous recordings in the dorsal cochlear nucleus (DCN), inferior colliculus (IC) and auditory cortex (AC) of rats before, during, and after intense tone exposure.

First, we investigated the relationship between spontaneous activity and sound-driven activity. We found that, following acoustic trauma, response to sound stimulation was decreased in the DCN, IC and AC. Compared to control animals, various changes in spontaneous rate in the DCN, IC and AC were seen. Interestingly, the spontaneous rate in different DCN neurons was inversely correlated to the stimulus-driven activity rate. That is, the spontaneous rate was higher in DCN neurons that had diminished stimulus-driven activity, and vice versa. However, this feature was not seen in IC and AC neurons.

Second, we computed coherence as a measure of neural connectivity and interactions for all recorded channels/sites within and among the DCN, IC and AC. We found that there was significant enhancement of interactions within the DCN and IC as well as between the DCN and IC after both the onset and offset of the intense tone. In contrast, neural connectivity within the AC decreased after tone onset and offset. The interactions of the AC with both the IC and DCN did not increase until 60 to 120 min after the tone offset. That is, the tone exposure enhanced network interactions quickly at the brainstem level but much later at the cortical level.

The data could help explain that transient tinnitus may primarily originate from pathological changes at the brainstem level whereas chronic tinnitus primarily originates at the cortical level following the progression and interactions of neural correlates of tinnitus at higher auditory centers.

### **359 Noise-Induced Reduction of an Apamin-Insensitive Afterhyperpolarization Current Mediates Hyperexcitability in Tinnitus Mice**

Shuang Li<sup>1</sup>, Thanos Tzounopoulos<sup>1</sup>

<sup>1</sup>University of Pittsburgh

Tinnitus has been associated with increased spontaneous activity of auditory nuclei (termed here as hyperexcitability). Hyperexcitability of the Dorsal Cochlear Nucleus (DCN) principal neurons (fusiform cells) is a consistent neural correlate for tinnitus. While previous studies have suggested that part of this hyperexcitability is mediated by decrease in GABAergic inhibition (Middleton et al., 2011), the role of changes in intrinsic properties remains unclear. In mice with behavioral evidence of tinnitus (tinnitus mice), DCN fusiform cells showed increased spontaneous firing rate (SFR) in the presence of blockers for excitatory and inhibitory neural transmission, indicating that intrinsic properties mediate tinnitus-related hyperexcitability. To assess behavioral evidence of tinnitus, we used a reflex-based gap detection method (Turner et al., 2006; Middleton et al., 2011). We compared intrinsic properties of fusiform cells between control mice and tinnitus mice one week after noise induction. No difference was seen on resting membrane potential, input resistance and action potential parameters such as

threshold, amplitude, maximal rise slope, maximal decay slope as well as half-width. However, we observed significant differences in afterhyperpolarization (AHP). To isolate the SK channel-mediated IAHP component, we applied apamin (100nM). No significant difference was observed on the amplitude and kinetics of the apamin-sensitive IAHP between control and tinnitus mice. However, the amplitude of the apamin-insensitive IAHP was significantly decreased in tinnitus mice. Our findings reveal that noise-induced reduction of apamin-insensitive AHP current mediates tinnitus-related hyperexcitability of DCN fusiform cells.

### **360 Linking Auditory Nerve Fibre Deafferentation and Tinnitus-Related Neuronal Hyperactivity in a Mouse Model**

Lara Li Hesse<sup>1</sup>, Lucy Anderson<sup>1</sup>, Kai Jannis Hildebrandt<sup>1</sup>, Gestur Bjorn Christianson<sup>1</sup>, Jennifer Linden<sup>1</sup>, Roland Schaette<sup>1</sup>

<sup>1</sup>UCL Ear Institute

We have recently demonstrated that tinnitus patients with normal audiograms show reduced amplitude of wave I of the auditory brainstem response (Schaette and McAlpine, 2011). A similar reduction of wave I has been found in mice with deafferentation of auditory nerve fibres after temporary hearing loss (Kujawa and Liberman, 2009). Here we have investigated whether such a reduction in the amplitude of wave I after mild acoustic trauma correlates with the development of a neurophysiological correlate of tinnitus. Mice were exposed to an octave-band noise (8-16 kHz) at 96 dB SPL for 2 hours under anaesthesia. ABR recordings were obtained before and 4 weeks after acoustic trauma. For click-evoked ABRs, we found that the amplitude of wave I was significantly reduced after noise exposure, whereas the response thresholds remained unchanged. Electrophysiological recordings from the inferior colliculus were performed 4 weeks after trauma. The mice were anaesthetized with ketamine/medetomidine, and recordings were carried out using Neuronexus silicon probes with 16 electrode contacts. In acoustically traumatised mice, the spontaneous firing rates of IC neurons were significantly higher than in control mice. These results demonstrate a direct link between a reduction in the amplitude of ABR wave I and neuronal hyperactivity in the central auditory system, and therefore support a role for deafferentation of auditory nerve fibres in the development of tinnitus.

References:

Kujawa SG, Liberman MC (2009): J Neurosci 29:14077-14085.

Schaette R, McAlpine D (2011): J Neurosci 31:13452-13457.

Supported by the British Tinnitus Association and Boehringer Ingelheim Fonds.

**361 Acute Effect of Noise Exposure on Spontaneous Activity Suggest the Existence of Activity-Dependent Plasticity (LTP and LTD) in the DCN, in Vivo**

Yuan Gao<sup>1</sup>, Nauman Manzoor<sup>1</sup>, James Kaltenbach<sup>1</sup>  
<sup>1</sup>Cleveland Clinic Foundation

Acute effect of noise exposure on spontaneous activity suggest the existence of activity-dependent plasticity (LTP and LTD) in the DCN, *in vivo*.

Yuan Gao, Nauman Manzoor, James Kaltenbach

Both Hebbian and anti-Hebbian synapses are found in the DCN on fusiform and cartwheel cells, and there is evidence that long-term potentiation (LTP) and long term depression (LTD) can be induced in these cell types by the co-activation of their postsynaptic membranes and inputting parallel fibers (Fujino and Oertel 2003; Tzounopoulos, Kim et al. 2004). However, both forms of plasticity have been demonstrated only *in vitro* using the brain slice preparation. Whether either or both forms of activity-dependent plasticity are inducible *in vivo* remains unknown. Here, we investigated the immediate effect of acute sound exposure on DCN spontaneous activity in anesthetized hamsters. The level and duration of exposure was varied between 85 and 109 dB SPL and from 2 to 10 minutes, respectively. We report that a long-lasting change of DCN activity of putative fusiform cells can be triggered *in vivo* by moderate sound exposure (after a 2 minute exposure to a tone at a level of 109 dB SPL, the corresponding frequency region of the DCN shows a significant increase of spontaneous activity with a ratio=2.25 at 10 minutes after exposure, and ratio=2.75 at 20 minutes after exposure,  $n=5$ ,  $P<0.05$ ). We further report that the induced changes are dependent on both the tonotopic locus and level of stimulation. PSTHs collected from our unit clusters displayed buildup or pauser-buildup patterns, suggesting that our recordings were from fusiform cells. The sustained increases in spontaneous activity that followed within minutes of acute sound exposure suggest that LTP and LTD can be induced in DCN fusiform cells by a short duration of intense sound *in vivo*, but the direction of the change depends on the tonotopic locus of the recording as well as the intensity and duration of the stimulus. In addition, this finding raises the possibility that activity dependent plasticity may play a role in the induction of hyperactivity by moderate levels of sound exposure, which is believed to be a potential factor contributing to tinnitus in noise-exposed animals.

**362 Comparison of Tonotopic Profiles of Noise Induced Hyperactivity in the Inferior Colliculus and Dorsal Cochlear Nucleus**

Nauman Manzoor<sup>1</sup>, James Kaltenbach<sup>1</sup>  
<sup>1</sup>Cleveland Clinic Foundation

Noise exposure causes increased spontaneous activity (hyperactivity) in brainstem auditory system centers including the dorsal and ventral cochlear nuclei (DCN and VCN) and the inferior colliculus (IC). We recently showed that ablation of the DCN results in an immediate loss of hyperactivity in the contralateral IC, suggesting that the

DCN is a likely source of hyperactivity in the IC. In the present study, we sought further verification that the DCN is an important source of hyperactivity in the IC by comparing the tonotopic profiles of hyperactivity at the two levels. Our hypothesis was that if hyperactivity in the IC is independent of hyperactivity in the DCN, the two nuclei should show different tonotopic profiles of activity. Conversely, similar tonotopic profiles would be consistent with the view that the IC inherits its hyperactivity from the DCN. Adult Syrian hamsters were exposed to 115 dB SPL tone at 10kHz for 4 hours for induction of hyperactivity. Activity in the DCN and IC were separately mapped (i.e., in different animals) along the tonotopic axis using multi-unit recordings in both noise exposed and control animals to generate activity profiles. Tone-exposed animals were mapped at different post exposure recovery times to generate three subsets of activity profiles; and their respective activity profiles were compared with maps from their respective control (unexposed) groups. The magnitude of activity measured in the IC was found to be lower than that in the DCN in both the exposed and control groups, suggesting more powerful inhibitory effects on spontaneous activity in the IC than in DCN. However, two important similarities were found. In both DCN and IC, exposed animals initially showed a broad distribution of hyperactivity along the tonotopic axis. With increasing post-exposure recovery time the peak of the activity profile at both levels converged to a more restricted region corresponding to 11-14 kHz. Second, a normalized comparison of activity profiles from the two levels (corrected for differences in absolute levels) revealed very similar shapes in the activity profiles at the two levels, with peaks occurring in corresponding frequency loci. These similarities are consistent with a bottom-up model of hyperactivity transmission, further suggesting that the IC inherits its hyperactivity from the DCN. (This work was supported by NIDCN grant R01 DC009097).

**363 Forward Masking Enhances the Auditory Brainstem Response in Rats Treated with Sodium Salicylate**

Xiao-Peng Liu<sup>1</sup>, Jing-Tian Ni<sup>1</sup>, Lin Chen<sup>1</sup>

<sup>1</sup>Auditory Research Laboratory, School of Life Sciences, University of Science and Technology of China

Forward masking usually suppresses the auditory brainstem response (ABR) evoked by a probe tone. Here, we show that in the rat treated with a high dose (250-300 mg/kg) of sodium salicylate (NaSal), a tinnitus inducer, forward acoustic masker can surprisingly enhance, rather than reduce, the ABR. Prior to NaSal treatment, a forward narrow band noise with a central frequency of 6 kHz, 12 kHz or 16 kHz caused a reduction in the amplitude of the ABR evoked by a tone burst with a frequency same as the central frequency of the masker. However, after NaSal treatment, the forward masker would unexpectedly increase the ABR amplitude. The enhancing effect was most prominent at a higher frequency. The observed effect could be manifested in the normal rat in the presence of artificial tinnitus (a background tone), suggesting an underlying mechanism associated with tinnitus. We

propose that in NaSal-treated rats, the induced tinnitus can internally mask the ABR as an external background sound does, and a forward acoustic masker can temporarily silence tinnitus to result in a rebound of the otherwise masked ABR. Our study suggests a feasibility of using the ABR with a forward masking paradigm as an objective indicator of subjective tinnitus. Supported by the National Basic Research Program of China (Grants 2011CB504506 and 2007CB512306), the National Natural Science Foundation of China (Grants 30970977 and 30730041) and the CAS Knowledge Innovation Project (Grant KSCX1-YW-R-36).

### **364 Local Application of Sodium Salicylate Changes Neural Responses to Sounds in the Dorsal Cortex of the Inferior Colliculus**

Chirag Patel<sup>1</sup>, Huiming Zhang<sup>1</sup>

<sup>1</sup>University of Windsor

Sodium salicylate (SS) is widely used as a treatment for inflammation and chronic pain and it is one of the major tinnitus-inducing drugs. Systemic application of SS can change spontaneous activity and/or sound-driven responses in neurons in the auditory cortex and subcortical structures including the inferior colliculus. *In vitro* experiments have revealed that SS can affect a number of neurotransmitter receptors and ion channels in neurons in the auditory cortex and inferior colliculus, suggesting that the drug can affect the activity of these neurons through local neural mechanisms. While the local effect of SS on cortical auditory activities has been confirmed by *in vivo* neuropharmacological studies, the local effect on collicular auditory activities has yet to be examined. This study was therefore conducted to record evoked local field potentials from the dorsal cortex of the inferior colliculus and to examine whether these potentials can be affected by local microiontophoretic SS application.

A rate-level (field potential amplitude by sound pressure level) function was generated by recording an evoked field potential to a contralaterally presented tone burst at multiple (typically 7) sound pressure levels at the best frequency of a recording site. An iso-intensity curve was generated by recording the potential at multiple (typically 7) frequencies at a fixed sound-pressure level. Three hundred presentations were generated at each stimulus condition (combination of sound pressure level and frequency) and all presentations of sounds (e.g., 7X300) were presented either in 7 repetitive blocks or a completely randomized sequence. Results reveal that local SS application can alter both the rate-level function and the iso-intensity curve. Furthermore, the drug can differently affect a rate-level function (or an iso-intensity curve) generated by using repetitive sound blocks and a function (or a curve) generated by using a randomized sound sequence.

Research supported by NSERC of Canada.

### **365 Intense Noise Exposure Has No Significant Effect on the Rate of Spontaneous Activity in the Inferior Colliculus of the Freely Moving Rat**

Stefanie Kennon-McGill<sup>1,2</sup>, Hongyu Zhang<sup>1</sup>, Dianne Durham<sup>1</sup>, Hinrich Staecker<sup>1</sup>, Thomas Imig<sup>1</sup>

<sup>1</sup>University of Kansas Medical Center, <sup>2</sup>Neuroscience Program, University of Kansas Medical Center

Tinnitus, or ringing in the ears, is the perception of sound when no external sound is present. One explanation of how tinnitus may be generated is that when the peripheral auditory system sustains damage, central auditory structures become deafferented and subsequently display an increase in spontaneous activity perceived as tinnitus. We sought to determine whether changes in spontaneous activity occur in a noise-induced tinnitus model. To do this, we noise exposed Long-Evans rats unilaterally with 118 dB SPL 16 kHz sound for four hours while the rats were anesthetized with isoflurane. The rats showed high frequency hearing loss as determined by elevated auditory brainstem response thresholds measured a minimum of 10 days following noise exposure. The greatest threshold elevation occurred at 16 kHz, with an average threshold shift of 26 dB SPL. A minimum of 8 days after noise exposure, we utilized single unit recording to measure the rate of spontaneous activity from single units in the inferior colliculus of awake, freely moving rats (control group: n= 8 animals, 102 units; damaged group: n= 21 animals, 259 units). We also determined units' responses to tone and noise bursts. We found no significant increase in the overall spontaneous activity of units in damaged rats as compared to control rats. These data contrast with previous studies that report an increase in spontaneous activity after sound damage. A number of factors may be responsible for the two different outcomes, including the use of anesthesia in the previous studies, animal species, parameters of noise exposure, and single unit versus multi-unit response measures.

### **366 Auditory Evoked Potentials Changes in Patients Suffering Tinnitus**

Matías López-Paullier<sup>1</sup>, Eduardo Medina-Ferret<sup>1</sup>, Ricardo Velluti<sup>1</sup>, Marisa Pedemonte<sup>2</sup>

<sup>1</sup>ORL Hospital de Clínicas, <sup>2</sup>Facultad de Medicina CLAEH

Tinnitus is a symptom characterized by the perception of a sound without external stimulation. Mechanisms that underlie tinnitus perception are still not well understood; nevertheless, nowadays it is accepted that interactions between altered cochlear inputs and distorted central auditory processing provoke it. The subjective tinnitus may be the result of the expression of neural plasticity and this pathology may develop because a particular input from the ear decreased. The tinnitus perception may result in a reduction of central inhibition, mediated by the auditory efferent system, at central levels.

Since tinnitus is a perception, many levels of auditory processing could participate in its generation, introducing changes in the evoked responses. Our aim is to explore the brainstem auditory evoked potentials (BAEP, 10 ms)

and the long latency auditory potentials (LLAP, 500ms) shifts in patients suffering tinnitus.

Five patients with unilateral subjective idiopathic tinnitus were studied. Both BAEP and LLAP were recorded with two different sound intensities -high and low- at 70 and 60 dB over the patient specific threshold respectively. Recordings were done during EEG controlled wakefulness. Statistical analyses were applied, comparing right and left responses in the same patient.

Preliminary results showed: 1) both BAEP and LLAP studied in the frequency domain (Fast Fourier Transform) had significant changes in the evoked potentials power spectra; 2) decrement in I to IV wave's amplitude, measured peak to peak, were found in the BAEP contralateral to the tinnitus perception; 3) LLAP exhibited amplitude differences between the sides during low intensity stimulation, the higher amplitude appeared contralateral to the tinnitus perception in two patients and ipsilateral in one of them.

Conclusion. Unilateral tinnitus perception determined changes in the amplitude and power spectra of BEAP and LLAP waves comparing both sides studied during EEG controlled wakefulness.

### **367 Learning and Generalization Following Multiday Practice on the Identification of Rapid Speech**

**Karen Banai<sup>1</sup>**, Yizhar Lavner<sup>2</sup>

<sup>1</sup>University of Haifa, <sup>2</sup>Tel Hai College

Fast speech is harder to comprehend and remember than slower speech, especially for individuals with hearing impairments, the elderly and when listening to speech in a non-native language. Although listeners are known to adapt to rapid speech over the course of as few as 10 trials, whether longer-term practice with rapid speech results in further learning remains unclear. The goal of the present study was to determine whether 5 sessions of practice on a sentence verification task presented in a non-native language (Hebrew) in which speech rate increased gradually, resulted in learning of the trained task and in generalization to untrained materials. Over the course of training, the performance of the majority of trained listeners improved significantly; by the last training session they were able to consistently verify sentences compressed to 25% of their original duration. Compared to untrained listeners, performance of trained listeners improved significantly on the trained condition and learning transferred to conditions in which the trained materials were presented by novel male and female speakers, but not to a condition in which new materials were presented by the speaker used during training. These findings suggest that while multiday training on time compressed speech results in learning even beyond the initial adaptation phase, this longer term learning is specific to the content of the practiced materials. That learning generalized to untrained speakers leads us to conclude that learning may have relied on speech representations that are acoustically invariant. Because learning did not generalize to untrained sentences, these findings are more consistent with the suggestion that learning may have

eased the memory load associated with listening to rapid speech than with an increase in the rate of speech perception or with improved attentional tracking of rapidly changing speech elements.

### **368 Discrimination of Speech Modulation Cues by Infants**

**Laurianne Cabrera<sup>1,2</sup>**, Josiane Bertoincini<sup>1</sup>, Christian Lorenzi<sup>1,2</sup>

<sup>1</sup>Université Paris Descartes, CNRS, <sup>2</sup>Ecole Normale Supérieure

Profoundly deaf children are currently fitted with cochlear implants (CI) at younger and younger ages with reasonable success. However, the underlying auditory mechanisms of speech-perception development are not well known, and information regarding the ability of infants to discriminate the impoverished speech modulation cues delivered by the implants' processors is still lacking. Vocoders simulate the transmission of spectro-temporal speech modulations via CI in normal-hearing (NH) individuals by degrading selectively the amplitude-modulation (AM; slow modulations in amplitude over time) and frequency-modulation (FM; fast oscillations in instantaneous frequency close to the center frequency of the band) cues in a limited number of frequency bands.

The present study assessed the ability of 6-month-old French-learning NH infants to discriminate voicing (/aba/ versus /apa/) for disyllables processed by a tone-excited vocoder. A visual habituation procedure was used to measure discrimination capacities.

The vocoder degraded FM cues within each band. The original AM component was lowpass filtered at either half the bandwidth of normal cochlear filters or at 16 Hz (in order to attenuate fast, F0-related fluctuations, and thus simulate poor temporal resolution). Spectral resolution was either high (32 bands), as for normal ears, or low (8 bands) as shown for most CI users.

Eighty 6-month-old infants were shown to discriminate the voicing contrast in each condition. This suggests that, as for adults, infants do not require fine spectral and temporal modulation cues to discriminate voicing. However, some vocoded speech signals seem to require extra time of habituation to be discriminated, unveiling the importance of training when speech modulation cues are degraded. These findings demonstrate that the impoverished spectral and temporal cues delivered by current implant processors can be used by 6-month-old NH infants to discriminate speech sounds.

### **369 Speech Discrimination and Spatial Release from Masking in Toddlers with Cochlear Implants**

**Christi Hess<sup>1</sup>**, Erica Ehlers<sup>1</sup>, Alyssa Lamers<sup>1</sup>, Jenny Saffran<sup>1</sup>, Ruth Litovsky<sup>1</sup>

<sup>1</sup>University of Wisconsin- Madison

A growing body of research has used standardized tests to demonstrate that school-aged children with cochlear implants (CIs) do not perform as well as their normally hearing (NH) peers on measures of speech perception and discrimination skills. A gap in our knowledge exists

regarding these skills in infants and toddlers. Given the trend towards early implantation during infancy, it is crucial that speech discrimination measures at that age be available. In addition, bilateral cochlear implantation is being provided to a growing number of young children, with little understanding about the difference in performance between toddlers with unilateral cochlear implants (UCI) and toddlers with bilateral cochlear implants (BiCI).

In this study, the ability of toddlers with UCIs and BiCIs (ages 24-36 mo.) to discriminate consonant contrasts that vary in voicing and place of articulation in their native language is being investigated. Testing is conducted using a novel reaching-for-sound methodology. Dependent variables percent correct and latency will help to determine whether unilateral implantation is sufficient for the development of speech discrimination skills and if bilateral implantation facilitates the rate at which these discrimination skills develop. Results from the speech discrimination task will be compared to measures of spatial unmasking in the same toddlers with UCIs and BiCIs. We will evaluate whether early bilateral activation promotes the ability of young children to segregate target speech from background maskers, in particular when target and masker are spatially separated.

### **370 Does Perceptual Learning of Degraded Speech Generalize to a Novel Voice and Accent?**

**Julia Huyck<sup>1</sup>, Rachel Smith<sup>2</sup>, Ingrid Johnsrude<sup>1</sup>**  
<sup>1</sup>Queen's University, <sup>2</sup>University of Glasgow

Despite marked variability in the acoustic realization of speech, perception is robust for most listeners. This robustness is partly due to improvements in the perception of unusual-sounding, accented, or degraded speech with experience. Here we were interested in this perceptual learning and its generalization. In particular, we examined whether learning of spectrally degraded (noise-vocoded; NV) speech is specific to the trained voice and accent. Listeners were asked to report all the words they could understand from 20 training and 20 testing sentences. 12 British and 12 Canadian listeners participated in each of 3 conditions (6 groups): Some listeners were trained with NV speech from a talker with a "foreign" (Canadian or British) accent and tested with sentences from a different talker with a "native" (British or Canadian) accent. Other listeners were trained with native-accented NV speech and tested with sentences from the same talker (and accent), providing an estimate of maximal post-training performance (learning control). The remaining listeners were not trained but were tested with native-accent NV sentences to estimate baseline performance (naïve control). The cross-linguistic design minimized material effects because, across groups, each stimulus counted as both native- and foreign-accented. Regardless of nationality, learning foreign-accented NV speech (in one voice) generalized completely to native-accented NV speech (in a different voice), as indicated during testing by better performance than naïve controls and similar performance to the learning control group. Thus,

perceptual learning of degraded speech is not specific to the voice and accent used during training, suggesting that this learning pertains to abstract, linguistic representations, rather than to representations based on the acoustic features of a particular voice or accent. [This work, and the salary of JJH, was funded by the National Sciences & Engineering Research Council of Canada].

### **371 Is Perceptual Learning of Noise-Vocoded Speech Enhanced by Audiovisual Speech Information?**

**Rachel Wayne<sup>1</sup>, Ingrid Johnsrude<sup>1,2</sup>**

<sup>1</sup>Queen's University, <sup>2</sup>Linköping University

Perceptual learning of spectrally degraded speech occurs more rapidly when listeners are given feedback: the opportunity to map the linguistic content, presented in clear auditory form, onto the degraded auditory utterance (Davis et al, 2005). Here, we investigate whether learning is further enhanced by facial gestural information presented concurrently with either the clear auditory sentence (Experiment I), or with the degraded utterance (Experiment II). Recorded sentences were noise-vocoded (NV; 4 channels; 50- 8000 Hz), a popular (although limited) simulation of speech transduced through a cochlear implant. In Experiment I, each trial began with an auditory-alone presentation of a degraded sentence for report (D), followed by clear auditory feedback or audiovisual (i.e., talking face) feedback and then a degraded sentence repetition. Word report after the initial "D" indexes learning over trials. Performance in the clear audiovisual feedback (DCvD) condition was indistinguishable from that in the auditory-only feedback (DCD) condition, and both were higher than in a control condition without the opportunity to map NV speech sounds onto previously heard clear content (DDC). This finding replicates Davis et al (2005) and indicates no benefit for audiovisual feedback over auditory-only feedback. In Experiment II, two groups saw facial movements concomitantly with the initial "D" sentence presentation (Dv), simulating the natural experience of listening with a cochlear implant. One of these groups received a second degraded auditory-alone presentation (DvD). Despite the lack of clear information at any point, learning in the DvD group was significantly greater than in all other groups, including a DCvD group. These results indicate that perceptual learning mechanisms may capitalize on visual concomitants of speech, although alternative explanations must be considered. The importance of this work in rehabilitative contexts will be discussed. Funding: NSERC Canada.

### **372 Understanding a Target Voice in the Presence of Competing Talkers: Do Listeners Benefit from Continued Experience with a Particular Target or Masker Voice?**

**Fabienne Samson<sup>1</sup>, Ingrid Johnsrude<sup>1</sup>**

<sup>1</sup>Queen's University

When characteristics of a target voice such as spatial location or talker identity are held constant, it is not masked as effectively by competing speech signals. This

suggests that experience with a particular voice over time might facilitate perceptual organization in multi-talker environments. Here, we examine whether listeners benefit from experience with a particular voice only when it is the target, or whether they can also benefit when it is a masker. Twenty normal-hearing participants were asked to follow a target voice presented concurrently with two masker voices, using an adaptation of the Coordinate Response Measure procedure (Bolia et al., 2000). Recordings from 12 male and 12 female talkers were used as stimuli, with target and masker voices being always of the same sex. Four conditions were defined: Target (Target voice identity constant across successive trials), Masker (one masking voice constant across successive trials), Switch (one voice constant, but its role switches from target to masker across successive trials), and Baseline (voices different across successive trials). Target detection was measured at three Target-to-Masker Ratios (TMRs; -3, 0, +3 dB). Repeated-measures ANOVA on accuracy revealed significant main effects of TMR and Condition, and no TMR by Condition interaction. Pairwise comparisons showed significantly better performance in the Target compared to the three other conditions, and a trend towards worse performance in the Masker condition compared to the Baseline condition. Thus, experience with a target voice appears to unmask this target in a three-talker situation compared to when no voice is held constant over trials. Moreover, experience with a voice that is not consistently the target (i.e., is sometimes or always a masker) is not helpful, possibly because the constant voice captures listeners' attention even when it is not the target. Funding: NSERC Canada, FRSQ Quebec.

### **373 The Lack of Effect of Target/masker Continuity on Speech Intelligibility in a Cocktail Party Task**

**Clayton Rothwell<sup>1</sup>, Nandini Iyer<sup>2</sup>, Douglas Brungart<sup>3</sup>, Brian Simpson<sup>2</sup>, Robert Gilkey<sup>1</sup>**

<sup>1</sup>Wright State University, <sup>2</sup>Air Force Research Lab, <sup>3</sup>Walter Reed Army Medical Center

Spatial filters are one way to account for target intelligibility in a cocktail party task. Two previously proposed types of filters are Listener-Max, increased gain at the target location, and Listener-Min, reduced gain at the masker location (Durlach *et al.*, 2003). Recent studies (Best *et al.*, 2008 & 2010) suggest filter establishment takes time and auditory input (so called build-up). In this experiment, speech reception thresholds were measured using the Modified Rhyme Test (MRT) for continuous and discrete targets (at 0° azimuth) in unrelated continuous and discrete speech maskers (flanking, ±18°, or collocated, -18°). For the continuous target, target phrases were presented during the observation intervals and irrelevant same-talker phrases were presented from the target location at all other times. In the discrete target condition, there were only target phrases (no irrelevant phrases outside the observation interval). Likewise, the continuous maskers played at all times (including the observation interval), whereas the discrete maskers only played during the observation interval (never outside of it). Better

performance with a continuous target would suggest Listener-Max filter build-up, whereas better performance with a continuous masker would suggest Listener-Min filter build-up. However, the results showed no evidence of filter build-up of either kind, suggesting that prolonged exposure to an auditory stimulus does not lead to measurable improvements in spatial filtering. An experiment designed to investigate possible filter build-up within the MRT carrier phrase (i.e., within 1-s) is planned. [This work was supported by a grant received from the Air Force Office of Scientific Research (AFOSR)].

### **374 Sensitivity to Temporal Structure in the Human Auditory System**

**Tobias Overath<sup>1,2</sup>, Josh H. McDermott<sup>2</sup>, Jean M. Zarate<sup>2</sup>, David Poeppel<sup>2</sup>**

<sup>1</sup>University College London, <sup>2</sup>New York University

Natural sounds are structured over time, and it remains unclear how this structure is encoded by the auditory system. Inspired by the use of image scrambling to study object recognition (e.g. Grill-Spector & Malach, 1998), we investigated neuronal tuning to acoustic temporal structure by measuring fMRI responses to speech signals scrambled at different timescales. We reasoned that mechanisms for encoding temporal structure might be tuned to the structure in familiar natural sounds, such that the unnatural signals produced by scrambling would evoke a weaker response. Scrambling was accomplished with an algorithm that divided a sound signal into fixed-length segments (30-960 ms) and reordered them pseudo-randomly to create a sound "quilt". To minimize boundary artifacts, a segment order was selected that approximately matched the segment-to-segment envelope changes in the original signal; segments were then appended using pitch-synchronous overlap-add. The resulting signals differed in temporal structure from the original sound to an extent that depended on the segment length.

We used a localizer contrast (960 vs. 30 ms quilts) to define regions of interest (ROIs) sensitive to the temporal structure of speech, and probed their responses to other stimuli. The ROIs were located bilaterally in the STS. Their response increased with segment length up to 480 ms, suggesting sensitivity to syllable-length structure. We found that the effect of scrambling was a) apparently speech-specific (quilts from environmental sounds and control sounds with speech-like modulations each failed to produce an effect of segment length), b) independent of pitch and prosody (quilts from noise-vocoded speech produced an effect), and c) independent of lexical access and syllabic familiarity (quilts from familiar and unfamiliar spoken languages both produced effects). The results reveal sensitivity to complex temporal structure that cannot be explained in terms of amplitude modulation sensitivity.

### **375 Long-Term Stress Influences Speech**

#### **Recognition in Noise**

**Martin Benka Wallén**<sup>1</sup>, Dan Hasson<sup>1</sup>, Töres Theorell<sup>1,2</sup>, Hugo Westerlund<sup>2</sup>, Barbara Canlon<sup>1</sup>

<sup>1</sup>Karolinska Institutet, <sup>2</sup>Stress Research Institute, Stockholm University

While it is established in experimental studies that stress can modulate auditory function, little is known if similar responses occur in humans. In order to determine the possible associations and interactions between *i)* long-term stress, *ii)* acute stress, and *iii)* hearing problems, 348 individuals (140 men; 208 women) ranging in age from 23 to 71 years were studied. The sample was selected based on emotional exhaustion-scores (long-term stress), representing either low, intermediate, or high levels of emotional exhaustion (EE). EE was assessed with five items from the Maslach Burnout Inventory. Pure tone thresholds were assessed at 0.5, 1, 2, 4, and 8 kHz. Speech recognition in noise was assessed with the Hearing in Noise Test (HINT) both before and after an acute stress task comprising an emotional Stroop test combined with a cold pressor test and a social evaluation task. Linear regression analyses were conducted to determine the association between HINT and EE-scores at baseline, after the acute stress, and on the possible interaction between acute stress and EE-scores on the HINT. All analyses were adjusted for age, audiometric hearing loss, and sex. Overall, the results demonstrated that the ability to hear speech in noise decreased with increasing levels of EE. The whole model explained between 5–28 % of the total variance, and associations were stronger for men than for women. HINT-scores improved after the acute stress in both men and women; however there were no significant interactions with EE in this respect. These results indicate that men with higher EE have more difficulties to understand speech in noisy environments. Taken together, the findings highlight, for the first time, that EE is an additional factor that will partially affect the complex nature of speech processing in noise.

#### **Acknowledgements**

MBW is supported by the FAS Centre for Research on Hearing Problems in Working Life, and by Tysta Skolan. DH is supported by a grant from FAS Centre for Research on Hearing Problems in Working Life and Tysta Skolan. BC is supported from the Swedish Research Council, FAS, the Karolinska Institute, and Tysta Skolan. HW partially worked within the FAS Centre Stockholm Stress Center.

### **376 Use of a One-Back Sentence**

#### **Recognition Task to Examine Listening Effort**

**Eric R. Thompson**<sup>1</sup>, Sarah C. Sullivan<sup>1</sup>, Nandini Iyer<sup>2</sup>, Brian D. Simpson<sup>2</sup>, Douglas S. Brungart<sup>3</sup>

<sup>1</sup>Ball Aerospace & Technologies Corp., <sup>2</sup>Air Force Research Lab, <sup>3</sup>Walter Reed National Military Medical Center

Recent results suggest that in some circumstances, noise or distortion in an audio signal has no measurable effect on performance in simple word or sentence recognition

tasks, but has a substantial effect on the listening effort required by the listener to achieve that performance. These listening effort effects are usually examined by having listeners perform unrelated secondary tasks while attending to the primary speech stimulus. This experiment examines an alternate paradigm for manipulating listening effort based on a one-back response task where sentences were presented sequentially and the listener identified words from the sentence presented prior to the most recent sentence rather than from the most recent sentence. The experiment was conducted using a corpus of five-word sentences that are syntactically correct, but semantically ambiguous (e.g., Jill bought six hot cards), and the effects of listening effort were explored by manipulating the listening task (normal or one-back), the masker (none, speech-shaped noise, or unrelated babble), and the gating of the masker (on only during stimulus presentation or on continuously during the stimulus and response periods). Preliminary results show a significant overall drop in performance from 0-back to 1-back conditions, and independent effects of memory and masking. [Supported by AFOSR]

### **377 Lip Reading Ability Is Related to Visual Attention in Normal Hearing Subjects**

**Jeremy Loebach**<sup>1,2</sup>, Nicholas Altieri<sup>2,3</sup>, David Pisoni<sup>2</sup>

<sup>1</sup>St. Olaf College, <sup>2</sup>Indiana University, Bloomington, <sup>3</sup>University of Oklahoma

Lip reading was assessed in a large sample of normal hearing individuals. Significant variability was observed across subjects as to their overall lip reading scores (ranging from 2% to 42% correct). Cluster analysis was used to divide subjects into three groups based on their performance: Low (n=24, M = 7%), Normal (n=27, M=13%) and High performers (n=23, M=19%). These groupings were then used to compare subject performance on a variety of visual attention tasks. The Useful Field of View task assesses the processing speed required to integrate visual information during extremely brief presentations of visual displays (10 msec) and the size of their overall perceptual space. Here, High performing lip readers had significantly faster reaction times than the Low performing lip readers without affecting accuracy, indicating that lip reading proficiency may be related to visual information capture and integration. The Flanker Congruency task assesses distraction from extraneous visual information during a monitoring task, and is manipulated by increasing cognitive loads. Here, High performing lip readers had significantly faster reaction times than Low performing lip readers without affecting accuracy, indicating that lip reading ability may be related to better monitoring of visual information despite distracting flanking information. The Stroop task examines a subject's ability to suppress a dominant task response (reading) in order to shift their attention to visual stimulus features (font color). Subjects in the High performing group had significantly faster reaction times than subjects in the Low performing group, indicating that lip reading ability was related to the speed at which subjects can suppress automatic responses. Taken together, these data suggest that while lip reading is an

ability that exists in the general population, it is quite variable, and appears to be linked with the speed and allocation of visual attention, integration and suppression.

### **378** Sine-Wave Speech Recognition in Tonal Language

Li Xu<sup>1</sup>, Yan-Mei Feng<sup>2</sup>, Ning Zhou<sup>3</sup>, Guang Yang<sup>2</sup>, Shan-Kai Yin<sup>2</sup>

<sup>1</sup>Ohio University, <sup>2</sup>Shanghai Jiao Tong University, <sup>3</sup>University of Michigan

Sine-wave replicas of natural speech have been shown to be highly intelligible in English. In the present study, sine-wave tone and sentence recognition was examined in Mandarin Chinese, a tonal language. Forty-one normal-hearing, native Mandarin-Chinese-speaking listeners participated in the experiments. Results showed that sine-wave tone recognition performance was slightly above chance. However, sine-wave sentence recognition performance was excellent, approximately 90% correct on average. Therefore, the function load of lexical tones on sine-wave speech recognition is limited and the high-level recognition of sine-wave sentences is likely attributed to the perceptual organization that is influenced by a top-down process.

### **379** Customized Dichotic Stimulation Maps Improve Speech Recognition in Noise for Bilateral Implant Users

Ning Zhou<sup>1</sup>, Bryan Pflingst<sup>1</sup>

<sup>1</sup>University of Michigan

The ability to perceive electrical stimulation with cochlear implants varies across stimulation sites probably due to variation in pathology or other conditions near the implanted electrodes. The aim of this study was to optimize speech processor maps for bilateral implant users by identifying and removing sites with poor psychophysical results. For each stimulation site in each ear, psychophysical tests were performed to measure both temporal acuity as assessed by amplitude modulation detection thresholds (MDTs) and channel interaction as assessed by MDT elevation in the presence of a masker. Customized dichotic maps were created on an individual basis using the measure that showed the same across-site-mean ear difference in psychophysical function as the ear difference in speech recognition.

Dichotic stimulation was used for preserving frequency selectivity, because frequencies of the sites that were to be removed could be represented in the other ear. In dichotic Map A, for each of the 22 spectral channels, the ear with better psychophysical performance was stimulated. In dichotic Map B, five different poorly-performing sites from each ear, distributed along the tonotopic axis, were removed. For both maps, each implant transmitted a reduced set of spectral channels complementary to those in the contralateral ear. Two additional experimental maps were tested as controls.

For the majority of the subjects, channel interaction predicted ear differences in speech recognition. Most subjects were able to fuse the complementary channels centrally. As a group, consonant and vowel recognition at

0 dB signal to noise ratio as well as speech reception thresholds for CUNY sentences in amplitude modulated noise significantly improved using Map B compared to the subjects' clinical everyday-use map.

Work supported by NIH-NIDCD grants R01 DC010786, T32 DC00011, and P30 DC05188.

### **380** Comparison of Costs Between Sequential and Simultaneous Bilateral Cochlear Implants

Sang Cheol Kim<sup>1</sup>, Ju Hyun Jeon<sup>1</sup>, Seung Hyun Koh<sup>1</sup>, Jae Young Choi<sup>1</sup>

<sup>1</sup>Yonsei University College of Medicine

It is well known that bilateral cochlear implants (CIs) gives more benefits to deaf patients because it can provide binaural hearing advantages and that the short time interval between both CIs can give better help to establish bilateral auditory brain plasticity. However, there is some controversy over the timing of 2nd CIs, sequential or simultaneous. Therefore, we conducted this study to compare the cost-effectiveness between sequential and simultaneous CIs. Those who underwent bilateral CIs at Yonsei university health system on between December of 2004 and January of 2011 were included and their medical records were retrospectively reviewed. Nine patients (3 males and 6 females) underwent simultaneous bilateral CIs (SiCI) and six patients (5 males and 1 female) did sequential bilateral CIs (SeCI). The time interval between 1st and 2nd CIs in the sequential CI (SeCI) group was 44.7 months (range 9-67 months) The average ages in SeCI group were 28.3±11.2 months on the first CIs and 73.8±20.7 months on the 2nd CIs. The 1st, 2nd and total operation times in SeCI group were 181±76.0, 120±19.4 and 301±90.0 minutes respectively. The 1st, 2nd and total anesthesia times were 212±80.6, 162±36.4 and 373±96.6 minutes respectively. The 1st, 2nd and total hospitalization times were 6.2±2.5, 4.2±1.9 and 9.6±2.6 days. The 1st, 2nd and total hospitalization expenses were 24,082,713±4883,601, 24,158,366±334,618 and 48,176,734±1,134,370 won. In the simultaneous (SiCI) CI group, the average age, operation time, anesthesia time, hospitalization time and expense were 21.6±14.6 months, 246±47.2 minutes, 280±49.5 minutes, 6.2±3.3 days and 46,073,011±1,861,028 won respectively. The anesthesia time in SiCIGs was shorter than the total time in SeCIGs and the hospitalization expense decreased by half. In conclusions bilateral simultaneous CIs was more cost-effective than bilateral sequential CIs.

### **381** Binaural Interactions in the Auditory Cortex of Congenitally Deaf Cats

Jochen Tillein<sup>1,2</sup>, Peter Hubka<sup>3</sup>, Andrej Kral<sup>3</sup>

<sup>1</sup>ENT Department, J.W. Goethe University Frankfurt, Germany, <sup>2</sup>Medel Innsbruck, Austria, <sup>3</sup>Experimental Otolaryngology, ENT Clinics, Medical University Hannover

Congenitally deafness leads to various functional deficits in the auditory cortex such as decrease in binaural sensitivity (Tillein et al., Cereb. Cortex 2010, 20:492). To investigate the effect of congenital auditory deprivation on unit

responses to the ipsilateral and contralateral ear, cortical responses in field A1 of 5 congenitally deaf cats (CDCs) and 5 acutely deafened controls were investigated. All animals were stimulated via binaural cochlear implants with pulse trains (500Hz, 3 pulses). Responses to monaural and binaural stimulation at intensities between 0-12 dB above brainstem response thresholds were recorded using 16-channel microelectrode probes.

According to monaural responses properties cells were classified as contralateral excitatory - ipsilateral excitatory cells (EE), responsive at contralateral ear (EO), ipsilateral ear (OE), predominantly binaural ear (PB) and non responsive cells (OO). Within EE cells, facilitation (binaural response > 120% of the summation of monaural responses) and occlusion (binaural response < 80% of the summation of monaural responses) were tested.

Rate-level functions revealed a highly significant decrease in dynamic range and saturation level of neurons in CDCs (WMW,  $p < 0.001$ ) for both monaural as well as binaural stimulation. Slightly lower unit thresholds in deaf cats were observed for both ipsilateral and contralateral ear (WMW,  $p < 0.05$ ). More ipsilaterally responsive (OE) cells were found in CDCs (WMW;  $p = 0.02$ ). Binaural interactions were also significantly affected by deafness: less facilitation in binaural stimulation was observed (WMW;  $p = 0.02$ ).

The present findings reveal an effect on intensity representation in the deaf auditory cortex, possibly due to homeostatic synaptic scaling in absence of adequate input. Additionally, more ipsilaterally responsive cells were observed, and less binaural facilitation indicating an effect on fundamental binaural convergence and processing.

Supported by DFG (Kr 3370/1-3)

### **382 Unilateral Versus Bilateral Temporal Processing in Bilateral Cochlear Implant Users**

**Tyler Churchill<sup>1</sup>, Antje Ihlefeld<sup>1</sup>, Alan Kan<sup>1</sup>, Robert Carlyon<sup>2</sup>, Ruth Litovsky<sup>1</sup>**

<sup>1</sup>University of Wisconsin, Madison, <sup>2</sup>MRC Cognition & Brain Sciences Unit, Cambridge, U.K.

Cochlear implant (CI) listeners struggle to discriminate both rates and interaural time differences (ITDs) bilaterally for pulse trains faster than about 300 pps (Kong, et. al., J. Acoust. Soc. Am., Vol. 125, No. 3, March 2009, pages 1649–1657; van Hoesel, J. Acoust. Soc. Am., Vol. 124, No. 6, December 2008, pages 3861–3872). However, it is unclear whether temporal processing is limited similarly for rate and ITD processing. No prior study has compared bilateral and unilateral rate limitations within the same CI listeners. One possibility is that temporal processing is limited by peripheral temporal resolution, in which case rate limitations may not be bilaterally symmetric between pitch-matched electrodes, and the worse unilateral temporal rate discrimination limits should predict ITD processing limits. Alternatively, it is possible that temporal limitations for rate and ITD processing originate from separate central auditory processing stages, yielding left/right rate discrimination performances matched to each other, but not necessarily to ITD curves. Yet another possibility is that there is a common central

mechanism for rate and ITD discrimination, resulting in matched performance for all tests at a given electrode.

The current study explored unilateral rate and bilateral ITD discrimination with low-rate pulse trains within the same CI listeners. Three pitch-matched electrode pairs were tested (basal, middle, and apical) at each of 4 base rates (100, 200, 300, and 500 pps). Bilaterally implanted CI listeners were tested in 2AFC tasks a) with a temporal pitch discrimination task in each ear using 100% versus 135% of base rates and b) with a left/right discrimination task using  $\pm 500 \mu\text{s}$  ITDs.

Results show significant correlation of ITD discrimination and rate discrimination in the worse ear across all electrode pairs. Analyses indicate that temporal limitations for rate and ITD discrimination are not separate and arise either from peripheral or common central mechanisms.

Acknowledgments: NIH-NIDCD (DC008083, Litovsky)

### **383 Exploring Mechanisms Involved in Localization Ability in Children Who Use Bilateral Cochlear Implants**

**Yi Zheng<sup>1</sup>, Shelly Godar<sup>1</sup>, Ruth Litovsky<sup>1</sup>**

<sup>1</sup>Binaural Speech and Hearing Laboratory, University of Wisconsin – Madison

Studies of sound localization ability use either a spatial acuity measure (e.g., minimum audible angle, MAA), or an absolute localization task, where sound source location identification ability is quantified. Children who use bilateral cochlear implants (BiCIs) are remarkably adept at right-left discrimination tasks for sources varying in locations about midline, and they do so typically within 12 months after activation of the second implant (Godar and Litovsky, 2010; Litovsky et al., 2006). However, many of the children have difficulty in an absolute localization task (Grieco-Calub and Litovsky, 2010). This study tested the hypothesis that within subjects localization ability is related to discrimination of sources whose locations vary within the same hemifield. We used a pairwise comparison analysis scheme that aims to model how children map acoustic space to a spatially-relevant perceptual representation in an absolute localization identification task. MAAs were used to quantify discrimination abilities either across- or within-hemifield, and were compared with absolute localization. Results suggest that within-hemifield discrimination abilities serve as better predictors of the perceptual mapping observed in absolute localization tasks than discrimination across hemifields. This is presumably because discrimination of the right vs. left hemifields activates different populations of neurons whereas within a hemifield spatial mapping is more finely tuned within a given neural population. Finally, we conducted preliminary studies on sensitivity to interaural time difference (ITD) and interaural level difference (ILD) cues, using direct electrical stimulation. Stimuli were 100 pps, presented to pitch-matched electrodes in the two ears. Preliminary observations suggest poorer ITD than ILD sensitivity. Data are cautiously interpreted with the view that spatial hearing abilities in children who use BiCIs depend on a complex

array of cues, experiences and perhaps cognitive abilities to map cues onto perceptual space.

Work supported by NIH-NIDCD Grant R01 DC008365 (Litovsky)

### **384 Investigating the Effect of Interaural Mismatch and Channel Interactions in Multi-Electrode Stimulation Using a Bilateral Cochlear-Implant Simulator**

Alan Kan<sup>1</sup>, Eric Bostwick<sup>1</sup>, Corey Stoelb<sup>1</sup>, Matthew Goupell<sup>2</sup>, Ruth Litovsky<sup>1</sup>

<sup>1</sup>University of Wisconsin-Madison, <sup>2</sup>University of Maryland - College Park

In bilateral cochlear implants (CIs), interaural mismatch in the place-of-stimulation can occur for electrodes of the same number in the two ears due to difference in the insertion depth and neural survival across the ears. Channel interactions between adjacent electrodes also occur due to current spread along the basilar membrane. The combination of these effects on sound image perception and binaural sensitivity in CI users is largely unknown. One might hypothesize that when there is an interaural mismatch, channel interactions of two closely-spaced electrodes might aid in sound image fusion since the area of interaural frequency match is greater. However, it is unclear what would happen when two remotely-spaced electrodes are stimulated and there is interaural mismatch. One approach in investigating this issue is to use a vocoder simulation of CIs with normal-hearing listeners. We used a Gaussian-enveloped tone (GET) vocoder with 500-ms stimuli that had a 1.5-mm bandwidth. This vocoder simulates an 8-electrode array with 1.5-mm spacing (Greenwood's function) between electrodes and a current spread of about 6.75 dB/mm. A high-interaction pair (1.5-mm spacing) and a low-interaction pair (4.5-mm spacing) were tested with interaural offsets of 0, 1.5, 3, 4.5 and 6-mm. Two experiments were conducted using headphones. In the first experiment, subjects were asked to describe the number (1, 2, 3, or 4), location (left, center, right) and strength of sound sources heard (strong, weak, diffuse). In the second experiment, interaural level and time differences were applied to the sounds and subjects were asked to indicate the number and perceived location(s) of sound sources inside the head. Results will be discussed in the context of how much mismatch can be tolerated before subjects lose the ability to perceived unitary images with high degree of "localization strength."

Work supported by NIH-NIDCD (R01 DC003083 to R. Litovsky; R00 DC010206 to M. Goupell)

### **385 Attending to a Single Ear Using Bilateral Cochlear Implants**

Matthew Goupell<sup>1</sup>, Alan Kan<sup>2</sup>, Ruth Litovsky<sup>2</sup>

<sup>1</sup>University of Maryland - College Park, <sup>2</sup>University of Wisconsin - Madison

Cherry [J. Acoust. Soc. Am., 25, 975-979 (1953)] showed that normal-hearing (NH) listeners who were presented with dichotic speech over headphones could recall words in the attended ear almost perfectly and ignore speech in

the other ear. We studied this effect in people who are deaf and use bilateral cochlear implants (CIs), because it is unclear if they would be able to ignore an ear like NH listeners. Stimuli (sentences with 5 key words) were presented to CI listeners through the direct audio input and to NH listeners over headphones. In each condition there was a female target (T) and a male masker (M). Various target-to-masker ratios (TMRs) were used. There were 5 conditions: T in attended ear only, T in attended ear and M in opposite ear, T and M in attended ear, T and M in both ears, and T in attended ear and M in both ears. NH listeners were tested on these conditions by always attending to the same ear. CI listeners were tested separately for each ear because of likely asymmetries.

Data show that when T and M were in opposite ears, NH listeners had near perfect performance in understanding speech, even at low (poor) TMRs. When T and M were in the same ear (either monaurally or diotically), performance was greatly reduced. Having T in one ear and M in both reduced performance almost as much as the monaural and diotic masking cases, even though binaural masking release was expected. Preliminary data from CI listeners showed that much larger TMRs are needed for performance to be comparable to NH listeners. CI listeners were more affected by M in the unattended ear, showing a faster decline in speech understanding as a function of TMR. Nonetheless, performance was better compared to conditions where T and M were presented in the same ear. The results imply that CI listeners have a difficulty in attending to just one ear, seemingly from some sort of central masking.

Support provided by the NIH Grants R00 DC010206 (MJG) and R01 DC003083 (RYL).

### **386 Localization by Normal Hearing Listeners Using Individualized Head-Related Transfer Function Filtered Speech Stimuli Processed Through a Noise Vocoder**

Heath Jones<sup>1</sup>, Alan Kan<sup>1</sup>, Ruth Litovsky<sup>1</sup>

<sup>1</sup>Waisman Center, University of Wisconsin - Madison

The inability to perceptually localize and discriminate between sound sources originating from different locations can often result in difficulties in hearing speech in noisy environments. Segregation of sound sources relies heavily on sound localization abilities which occur via binaural processing of acoustical cues to sound location. However, for individuals using cochlear implants (CIs), the benefits of binaural interaction is substantially lower than normal hearing (NH) individuals, possibly contributing to the deficits in sound localization performance that is observed in CI users. Of the many factors contributing to this localization deficit, one could be the loss of localization cues in the encoding of acoustic information by the CI speech processors. In order to test the hypothesis that the filtering occurring during CI speech processing disrupts the ability to accurately localize sound sources, the present study investigates the abilities of NH listeners to localize virtual free-field stimuli that has been subjected to similar signal processing used in CI encoding strategies. Speech stimuli are convolved through individualized head-related

transfer functions (HRTFs) and the resulting stimuli are then processed through a noise vocoder in order to simulate CI processing. Performance on a sound localization task using free-field, virtual free-field, and noise-vocoded virtual free-field stimuli, was measured in quiet and in the presence of noise that varied in level using various levels of background noise. Results begin to identify the stage at which sound source localization ability is degraded during the process of converting acoustic signals into electric stimulation for CI users, and investigates how the presence of noise affects listeners' performance. Outcomes of this study have implications for developing CI encoding strategies aimed at enhancing and improving the ability to accurately localize speech signals in a noisy environment.

### **387 Music Training in Cochlear Implant Users**

**John Galvin<sup>1</sup>, Qian-jie Fu<sup>1,2</sup>**

<sup>1</sup>House Research Institute, <sup>2</sup>University of Southern California

Music perception is difficult for cochlear implant (CI) users, especially when more than one instrument is playing at a time. Music training with simple stimuli has been shown to improve CI performance in relative simple listening tasks. It is unclear whether it is better to train with an easy or difficult task to improve performance for challenging listening conditions, such as music perception with multiple instruments. In this study, CI patients were trained to identify melodic contours. Before training was begun, baseline melodic contour identification (MCI) performance was extensively measured, with and without a competing masker. The masker pitch, timbre and timing were varied to see which cues (if any) subjects might use for segregation. Other baseline measures included familiar melody identification (FMI), with and without rhythm cues. After completing baseline measures, subjects were divided into two groups. One group trained with contours presented in isolation. The other group trained with contours presented with a competing masker; only minimal pitch cues were provided (and no timing or timbre cues) for the training. Both groups trained at home for ~half-hour per day, 5 days per week, for one month. Subjects were trained on pitch ranges not used for testing. After training was completed, subjects returned for follow-up measures to see whether any training benefits had been retained. Preliminary results showed that while MCI performance with and without a masker improved for both training groups, there was a greater improvement when training with the masker. Even though the masker did not present any timing or timbre cues, training with the masker appeared to improve CI listeners' use of these cues when segregating the masker and target contour. FMI also improved in both MCI training groups. The results suggest that training with difficult stimuli that are representative of "real-world" conditions may provide a greater benefit than training with simple stimuli.

### **388 The Effects of Spectral Resolution and Channel Interaction on Melodic Contour Identification Using CI Simulations with Musicians and Non-Musicians**

**Joseph Crew<sup>1,2</sup>, John Galvin<sup>1</sup>, Qian-Jie Fu<sup>1,2</sup>**

<sup>1</sup>House Research Institute, <sup>2</sup>University of Southern California, Department of Biomedical Engineering

Cochlear implant (CI) users perform poorly in difficult listening situations (e.g. music, multiple talkers) due to poor spectral resolution (limited number of channels) and channel interaction (spectral overlap). Music experience and/or training may help to offset these limitations. In this study, melodic contour identification (MCI) was measured under different conditions of spectral resolution and channel interaction in musicians and non-musicians. We hypothesized that musicians would likely be less susceptible to reduced spectral resolution and/or increased channel interaction.

Normal hearing (NH) subjects were tested while listening to acoustic CI simulations. Sinewave rather than noiseband carriers were used because in previous pitch related studies, sinewave vocoders more closely reflected actual CI performance. Spectral resolution was varied by changing the number of channels. Channel interaction was simulated by distributing different amounts of the temporal envelope information extracted from each analysis band across channels; this was analogous to changing the carrier band filter slope in a noiseband vocoder.

Preliminary results for both groups showed that MCI performance improved as the spectral resolution increased, and worsened as the channel interaction increased. There was a tradeoff between spectral resolution and channel interaction as performance with 8 fully independent channels was comparable to 16 slightly or moderately smeared channels. Overall performance was better for musicians, and musicians were less susceptible to channel interaction than were non-musicians. The better performance by musicians suggest that music training may help offset the poor spectral resolution and strong channel interaction typically experience by CI users.

### **389 Effect of Low-Pass Filtering on Musical Sound Quality Perception in Cochlear Implant Users**

**Alexis Roy<sup>1</sup>, Patpong Jiradejvong<sup>1</sup>, Courtney Carver<sup>1</sup>, Charles Limb<sup>1,2</sup>**

<sup>1</sup>Johns Hopkins University School of Medicine, <sup>2</sup>Peabody Conservatory of Music

Cochlear implant (CI) users report poor sound quality (SQ) during music listening. In a previous study, we used a novel assessment method (referred to as CI-MUSHRA) to quantify the effect of specific acoustic parameters on SQ judgments in CI users. Using this method, we demonstrated that removal of low frequencies by high-pass filtering had only a limited impact on SQ evaluation by CI users in comparison to normal hearing (NH) controls. The aim of the present study was to examine the effects of high frequency removal by low-pass filtering on SQ

perception. We hypothesized that removal of high frequencies would have a limited impact on SQ ratings by CI users in comparison to NH controls. We used CI-MUSHRA to study comparative SQ ratings for five randomly presented versions of a musical segment (25 segments total with 5 versions each): the original stimulus, 8-, 4-, 2-kHz low-pass filtered stimuli, and a 1 kHz low-pass filtered stimulus with white noise addition (to serve as the anchor). Subjects were required to provide SQ ratings between 0 (very poor) to 100 (excellent) for each version; ratings reflect perceived SQ difference among test stimuli. NH controls (n=9) displayed a significant correlation between SQ ratings and high frequency information ( $p < 0.01$ ) and consistently made SQ discriminations among all versions ( $p < 0.01$ ). CI users (n=4) displayed an insignificant correlation between SQ ratings and test stimuli with greater than 4 kHz of frequency information ( $p > 0.05$ ) and did not rate the original stimulus, 8-, and 4-kHz low-pass filtered stimuli as significantly different ( $p > 0.05$ ). Taken together, these results provide evidence that the addition of high frequency information above 4 kHz has little impact on SQ for CI users, which is indicative of the poor SQ of CI-mediated music perception. In addition, this study further demonstrates the versatility of the CI-MUSHRA to quantify the impact of acoustic parameter manipulation on SQ perception.

### **390 Listening Effort with Cochlear-Implant Simulations**

Carina Pals<sup>1,2</sup>, Anastasios Sarampalis<sup>3</sup>, Deniz Baskent<sup>1,2</sup>  
<sup>1</sup>University Medical Center Groningen, <sup>2</sup>Behavioral and Cognitive Neuroscience, University of Groningen,  
<sup>3</sup>Department of Experimental Psychology, University of Groningen

Research on cochlear implants (CIs) has traditionally focused on improving speech intelligibility. However, there may be additional ways that CI processing strategies can benefit CI users, for example by reducing listening effort. Such improvements are not captured by current clinical or research tests and there is no way to differentiate between two CI programs that provide the same speech intelligibility, but may otherwise differ in their ability to reduce listening effort.

The hypothesis of the present study was that best speech intelligibility and lowest listening effort would be observed at different program settings of CIs. A dual-task paradigm was used to evaluate changes in speech intelligibility and listening effort with CI simulations. In a dual-task paradigm, a primary and a secondary task are performed simultaneously, competing for limited cognitive resources. An increase in effort associated with the primary task then results in decreased performance on the secondary task, providing a measure for effort. More specifically, in the present study, response times on a linguistic (rhyme-judgment) and a non-linguistic (mental-rotation) secondary task reflected changes in effort associated with the primary listening task (intelligibility). Speech stimuli were sentences processed with 2- to 24-channel noise-band vocoders, simulating CI processing. The results showed that increasing the number of channels improved both

intelligibility and listening effort. However, while intelligibility reached a plateau at about 6 channels, response times on the secondary tasks continued to decrease until 8 channels. Such listening effort benefits in CIs would not be observed with intelligibility tests alone. [Work supported by Rosalind Franklin Fellowship and Heinsius Houbolt Foundation; partial support provided by Cochlear Europe Ltd.]

### **391 3D Representation of the Human Cochlea with Standard and FLEX EAS Electrodes**

Katharina Braun<sup>1</sup>, Frank Boehnke<sup>1</sup>, Silke Helbig<sup>2</sup>, Elias Scherer<sup>1</sup>, Thomas Stark<sup>1</sup>

<sup>1</sup>Dept. of Otorhinolaryngology, Munich, Germany, <sup>2</sup>Dept. of Otorhinolaryngology, Goethe-University Frankfurt, Germany

The aim of this study was to create a three-dimensional data set of the cochlea without and with specially prepared (omitted metal) standard (long) and FLEX<sup>EAS</sup> electrodes for later computation of the mechanical wave propagation in the cochlea. Human temporal bones were implanted with standard electrodes and FLEX<sup>EAS</sup> electrodes and scanned with a high-resolution  $\mu$ -computer-tomograph (6 and 12  $\mu$ m). These data were analyzed, segmented and used for 3D reconstruction. In addition all temporal bones underwent fixation methylmethacrylate embedding to allow cutting of the undecalcified bone with the electrode in situ. Histologic results were correlated to the 2D images. The 2D images showed the electrode entering the scala tympani through the round window or a cochleostomy without causing damage to the bone. 3D visualization demonstrated that insertion through a cochleostomy led to a straighter position of the electrode in the scala tympani than the insertion through the round window. Therefore we conclude that the position of the inserted electrode in the scala tympani is influenced by the surgical approach. This 3D model of the cochlea with inserted FLEX<sup>EAS</sup> electrodes will allow the study of the mechanical influence of cochlear implant electrodes on the wave propagation along the cochlear partition.

This work was sponsored by MED-EL (Innsbruck, Austria)

### **392 Residual Hearing in a Guinea Pig Model of Hybrid Cochlear Implants**

Chiemi Tanaka<sup>1</sup>, Anh Nguyen-Huynh<sup>1</sup>, Katie Loera<sup>1</sup>, Lina Reiss<sup>1</sup>

<sup>1</sup>Oregon Health and Science University

Hybrid cochlear implants (CIs) are designed to preserve low-frequency hearing and allow combined acoustic-electric stimulation in the same ear. However, ~30% of these CI patients have >20 dB of threshold shift post-operatively (Gantz et al., 2010). The residual hearing loss (HL) onset spans from immediately after surgery to months after CI activation. We hypothesize that in addition to surgical trauma, electrical stimulation also damages cochlear cells, leading to the residual HL.

Eight 2-month-old normal-hearing guinea pigs were implanted with an 8-ring animal electrode (Cochlear Limited, Australia) in the left cochlea via a cochleostomy.

These animals were divided into two groups: 1) chronic acoustic and electric stimulation (CAES); 2) no stimulation (NS). Two non-implanted animals were chronic acoustic stimulation controls (CAS). Auditory brainstem responses (ABRs) at 1, 2, 6, and 16 kHz and electrically-evoked ABRs (EABRs) were recorded biweekly to monitor changes in acoustic and electric hearing. Elevated ABR thresholds indicated HL at 6 and 16 kHz in three animals after the surgery; two were placed in the CAES group and one in the NS group. Three of five animals with minimum post-operative HL were placed in the CAES group and two in the NS group. In CAES animals, CIs were activated 5 weeks after surgery. Behavioral responses and EABR thresholds were used to program C- and T-levels, respectively. CAES and CAS animals were stimulated 3 hours/day, 5 days/week with modulated white noise delivered via a loudspeaker and a Freedom speech processor as applicable. C-levels were re-programmed weekly to maximize the dynamic range.

After 5 weeks of stimulation, two of five animals in the CAES group had further HL beyond post-operative thresholds. In contrast, none of the animals in the NS or CAS group had progression of HL during the same time frame. Updated thresholds, ABR/EABR input-output functions, and histological analyses after 12 weeks of chronic stimulation will be presented, and relevance to the etiology of residual HL with a CI will be discussed.

Work supported by NIH-NIDCD grant P30DC010755 and NCRN grant KL2RR024141.

### **393** Integration of Vowel Identification Cues in Listeners with a Cochlear Implant and a Hearing Aid

Mario Svirsky<sup>1</sup>, Elad Sagi<sup>1</sup>, Chin-Tuan Tan<sup>1</sup>, Matthew Fitzgerald<sup>1</sup>, Ksenia Prosolovich<sup>1</sup>, Katelyn Glassman<sup>1</sup>, Xiang Zhou<sup>1</sup>, Arlene Neuman<sup>1</sup>

<sup>1</sup>NYU School of Medicine

Clinical practice with cochlear implants is undergoing a quiet, but significant change. Current criteria have yielded a quickly expanding group of "electroacoustic" cochlear implantees who have useful residual acoustic hearing in the contralateral ear. However, the mechanisms listeners use to integrate potentially disparate information from the acoustic and electrical ears are still unclear.

In this study, we used "conflicting cue" vowels to determine whether bimodal listeners identify vowels responding primarily based on acoustic cues, electrical cues, or one out of many possible combinations of both kinds of cues. Stimuli included three synthetic vowels (/i/, /a/, and /u/), as well as all six possible conflicting cue vowels. There were nine possible responses representing the most common monophthongal English vowels.

When presented with conflicting cue vowels, some listeners' responses were largely based on the acoustic input, and other listeners' responses were largely based on the electrical input. There were also some listeners whose response patterns were more complex, e.g. consistently responding /u/ when the acoustic stimulus was /i/ and the electrical stimulus was /a/. This result is analogous to the McGurk effect, obtained when the audio and visual parts of

a stimulus encode different phonemes, except in our case it is the electrical and the acoustic stimuli that encode different vowels. These data will help determine how acoustic and electrical information are integrated by individuals with different amounts of residual hearing, and provide insight into the different cognitive strategies they use for electroacoustic speech perception.

### **394** Predicting Performance with Current Shaping Tasks Using an Estimate of the Electro-Neural Interface

David Landsberger<sup>1</sup>, Arthi Srinivasan<sup>1,2</sup>, Monica Padilla<sup>1</sup>  
<sup>1</sup>House Research Institute, <sup>2</sup>University of Southern California

In previous experiments, we have determined that the effectiveness of current shaping (e.g. reduction in spread of excitation from current focusing or improved place pitch discrimination) is highly variable. We hypothesize that the variability in current shaping effectiveness is dependent on the quality of the "electro-neural interface." In other words, we hypothesize that when the electrodes are close to the stimulating neurons (i.e. not stimulating near a dead region) and when nothing is interfering with current flow to the neurons (e.g. from ossification), current focused stimulation will be more effective and subtler changes in physical stimulation will be detectable.

We measured the thresholds for MP and TP stimulation for 8 different locations per subject to provide an indication of the quality of the electrode-neuron interface. (e.g. Bierer and Faulkner, 2010). Thresholds were measured using an adaptive 2 interval forced-choice task.

A subjective scaling task which has previously been shown to be highly predictive of the reduction in spread of excitation between MP and TP stimulation will also be measured for the same 8 locations per subject. The TP thresholds (representing an estimate of the quality of the electrode-neuron interface) will be correlated with subjective scaling results (representing a reduction in spread of excitation from between MP and TP stimulation.) Furthermore, the thresholds of the TP stimuli will be compared with current shaping data which has been collected with the same subjects. The data will include forward-masked threshold curves, electrode and virtual channel discrimination, and benefits in place pitch discrimination provided by current focusing.

A comparison of thresholds from TP stimulation with the subjective scaling task, virtual channel discrimination, and spread of excitation reduction from current focusing should indicate how dependent current shaping performance is on the electrode-neuron interface.

### **395** Loudness Summation Using Focused and Unfocused Electrical Stimulation

Monica Padilla<sup>1</sup>, Arthi G. Srinivasan<sup>1,2</sup>, David M. Landsberger<sup>1</sup>

<sup>1</sup>House Research Institute, <sup>2</sup>University of Southern California

If current focusing provides a narrower spread of excitation at a fixed loudness level, then presumably the current focusing stimulates a more selective population of

neurons. It is known that when multiple electrodes are stimulated in an interleaved fashion (as in a speech processing strategy), loudness summation occurs. However, it is unknown if current focused stimulation interleaved on multiple channels provides the same degree of loudness summation as monopolar stimulation (MP).

Loudness summation for MP and partial tripolar (pTP) stimulation was tested for 7 Advanced Bionics cochlear implantees. The loudness of individual electrodes 2, 4, 6, 7, 8, 9, 10, 11, 12, and 14 in MP and pTP stimulation mode were balanced to a reference of electrode 8 in pTP mode set to a medium loud level. Two sets of multi-channel stimuli were created with stimulation levels on each electrode set to the loudness-balanced amplitudes previously measured. Multi-channel complex 1 consisted of stimulation on electrodes 6, 7, 8, 9, 10, 11, and 12 and multi-channel complex 2 consisted of stimulation on electrodes 2, 4, 6, 8, 10, 12, and 14. If MP and pTP loudness summation is equivalent, then each multi-channel complex will be equally loud in MP and pTP modes. The loudness of the MP complexes was balanced to the pTP complexes.

The amplitude shift required to maintain equal loudness between the MP and pTP complexes was less than  $\pm 0.5$  dB for all subjects. This suggests that loudness summation is very similar for both MP and pTP stimulation. For multi-channel complex 1 (where adjacent electrodes were used), loudness summation was similar for both MP and pTP stimulation. However, for multi-channel complex 2 (with greater spacing between stimulation sites), MP loudness summation is larger (positive offset) than pTP summation for all but one subject. Regardless of these differences, results show that loudness summation is very similar for both stimulation modes.

### **396 Testing the Phase Prediction of a Nonlinear SFOAE Generation Model**

**Kathleen Dunckley<sup>1</sup>, Jonathan Siegel<sup>1</sup>**

<sup>1</sup>*Hugh Knowles Center, Roxelyn and Richard Pepper Dept. of Comm. Sci. and Disord., Northwestern Univ.*

In an attempt to understand the origins of fine structure in the amplitude of the stimulus frequency otoacoustic emission (SFOAE), Talmadge et al. (2000) created a cochlear model that included distributed roughness and weak nonlinearity. The model demonstrated that nonlinearity can modify the magnitude and phase behavior of the emission fine structure, specifically as a function of the eliciting stimulus level. Schaier et al. (2006) measured SFOAE in adults with normal hearing using probe levels between 40-70 dB SPL and a fixed suppressor level of  $L_{\text{probe}} + 15$  dB. Their results revealed a systematic reduction in SFOAE latency with increasing stimulus level, but phase did not approach zero at the highest probe stimulus levels, as would be expected if a nonlinear mechanism dominated the emission. However, varying both the probe and suppressor level complicates interpretation because the effectiveness of the suppressor varies with its level. Incomplete suppression results in an underestimate of the emission and would be especially problematic for emission generators basal to the place of

the probe. Excessively high suppressor levels can also activate the acoustic reflex, which would be expected to introduce a short-latency contaminant.

Stimulus frequency otoacoustic emissions (SFOAE) were measured in young, normal-hearing participants with fixed suppressor levels below the acoustic reflex threshold (assessed in each subject). Measurements were made over half-octave wide regions centered at 1, 2, 4, and 8 kHz and probe stimulus levels ranging from 7-68 dB FPL. Preliminary results reveal only small changes in the rapidly rotating phase over a range of stimulus levels in which peripheral mechanics and otoacoustic emissions exhibit strong deviations from linear behavior, but present results are not yet available at higher probe and suppressor levels to form definitive conclusions.

Supported by NIDCD grant R01 DC008420 and Northwestern University.

### **397 Evaluating Frequency Selectivity in Humans and Chinchillas with Stimulus-Frequency Otoacoustic Emission Tuning Curves**

**Karolina Charaziak<sup>1</sup>, Jonathan Siegel<sup>1</sup>**

<sup>1</sup>*Northwestern University*

It has been suggested that stimulus-frequency otoacoustic emission suppression tuning curves (SFOAE STCs) have potential for estimating the frequency selectivity of auditory function. Here, we report SFOAE STCs obtained from 10 normal-hearing humans and 8 chinchillas together with corresponding benchmark measures of frequency selectivity. The probe level was fixed at 10 dB SL (16-29 dB SPL) for humans and at either 20 or 30 dB SPL for chinchillas. The probe frequency spanned ranges around 1 and 4 kHz for humans, and 1, 4 and 12 kHz for chinchillas. To construct a tuning curve the suppressor frequency and level was varied until the recorded change in the ear canal sound pressure (i.e., SFOAE "residual") reached a level of -6 dB SPL ( $\pm 1$  dB). For a 1 kHz probe, unlike human STCs, chinchilla's STCs did not demonstrate tuning on the high-side even for suppressor frequencies higher than 2 octaves above the probe tone. Interspecies comparisons at 4 kHz revealed that in both cases STCs were tuned, with higher  $Q_{10}$  observed for the human data. A better agreement between STCs for the two species was reached after applying a correction for the apical-basal transition [Shera et al, JARO, 11(3): 343-365, 2010]. Mean SFOAE residual phase usually varied by less than .25 cycles across suppressor frequencies, except for 1 kHz chinchilla STCs (mean phase change  $\sim 1.6$  cycles), suggesting that lack of STC tuning was caused by contributions from SFOAE sources located basal to the characteristic place of the probe tone. Mean STCs were in good agreement with corresponding mean behavioral or CAP tuning curves indicating that SFOAE carry information about frequency selectivity, when contributions from "basal sources" are not dominant. However, individual SFOAE STCs often demonstrated irregular shapes (e.g., double tips) which may hamper estimation of frequency selectivity of a given ear.

Supported by an AAA Student Investigator Research Grant, NIH Grant DC-00419 and Northwestern University.

### **398 Spatial Distribution of Stimulus-Frequency Otoacoustic Emissions Generators in Humans**

Rachael Baiduc<sup>1</sup>, Karolina Charaziak<sup>1</sup>, Jonathan Siegel<sup>1</sup>  
<sup>1</sup>*Hugh Knowles Center, Roxelyn and Richard Pepper Dept. of Comm. Sci. and Disord, Northwestern Univ.*

Stimulus-frequency otoacoustic emissions (SFOAEs) are usually demonstrated by suppressing them with tones near the frequency of the probe tone that evokes them. However, it has been also shown in animals that SFOAEs can be suppressed by tones more than an octave higher in frequency. The resulting emissions demonstrate relatively shallow phase slopes indicating shorter group delays than for suppressors near the probe frequency [Siegel, ARO Abst. 2006], which could be interpreted as contributions either from sources extending basally from the characteristic place of the probe or from emissions generated via a different mechanism (i.e., nonlinear distortion). Here, we report similar measurements in normally-hearing human subjects. The SFOAEs were evoked with low level probe tones (37 dB FPL) from 0.3 to 5 kHz. The emission was revealed with suppressors either near the probe frequency and/or at fixed ratios of either 1.6 or 2.1 times the probe frequency. The SFOAEs obtained with the higher-frequency suppressors were smaller compared with the near-probe suppressor and showed progressively decreasing phase slope when the ratio was increased from 1.6 to 2.1, consistent with the extended source hypothesis but not with the nonlinear distortion hypothesis. The emission level measured with the simultaneous presentation of the near- and high-frequency suppressors was comparable, but not identical to the emission measured with only the near-probe suppressor. We conclude that SFOAE sources located near the characteristic place of the probe make the greatest contribution in normal-hearing human ears, but that there are measurable contributions from sources extending basal from the place of the probe. These basally-located sources may complicate the interpretation of SFOAE patterns observed in subjects with local OHC lesions.

Supported by NIDCD grant R01 DC008420 and Northwestern University.

### **399 Equivalence of Swept- And Discrete-Tone Stimulus-Frequency Otoacoustic Emissions**

Radha Kalluri<sup>1,2</sup>, Christopher A. Shera<sup>3,4</sup>  
<sup>1</sup>*House Research Institute*, <sup>2</sup>*Keck School of Medicine, University of Southern California*, <sup>3</sup>*Eaton-Peabody Laboratories*, <sup>4</sup>*Harvard Medical School*

At low and moderate stimulus levels, stimulus-frequency otoacoustic emissions (SFOAEs) are thought to arise by a single mechanism and from a localized region near the emission's tonotopic place. Such spatial and mechanistic specificity make SFOAEs easier to interpret than other emission types (e.g., DPOAEs). However, long

measurement times limit the practical utility of SFOAEs, both as a research and a clinical tool. To improve the efficiency of SFOAE measurements, and inspired by previous work on DPOAEs (Long et al., 2008), we developed a fast SFOAE measurement method based on stimulus sweeps. In contrast to standard SFOAE methods in which the emission is measured in the steady state, one tone at a time, the swept-tone method sweeps continuously from one frequency to another. Here, we facilitate the interpretation and utility of swept-tone SFOAEs by demonstrating their equivalence to SFOAEs acquired with the discrete-tone paradigm. Using an interleaved suppression paradigm, we measured SFOAEs at 20 and 40 dB SPL in one ear each of 6 adult subjects using both methods. Probe frequencies were swept from 0.5 to 4 kHz at rates of 2, 4, 8, and 16 Hz/ms. The suppressor was fixed at 50 Hz below the probe frequency and at 60 dB SPL. To minimize drift, measurements with the discrete- and swept-tone paradigms were interleaved. Discrete-tone responses were analyzed using Fourier transforms and swept-tone responses using least-squares estimation. SFOAEs derived using the two methods were nearly equivalent at all 4 sweep rates, but measurement times for the swept-tone paradigm were approximately 8 times faster. In addition, we show that phase-gradient derived estimates of SFOAE delay are equivalent to emission latencies obtained directly in the time domain by least-squares estimation. Our results show that SFOAEs measured using the more efficient swept-tone method are equivalent to those obtained using the standard discrete-tone paradigm.

### **400 Two-Tone Suppression of TBEOAE at Different Latencies**

Sho Otsuka<sup>1</sup>, Makio Kashino<sup>2,3</sup>, Koichi Hirota<sup>1</sup>  
<sup>1</sup>*The University of Tokyo*, <sup>2</sup>*NTT Communication Science Laboratories*, <sup>3</sup>*Tokyo Institute of Technology*

In previous studies, tone-burst-evoked otoacoustic emissions (TBEOAEs) were used to estimate BM delay non-invasively.

In the recorded signal, there appears a number of peaks and dips, each with different levels and latencies. Heuristically, the TBEOAE latency was defined as the time between the stimulus onset and the time when TBEOAEs reach the maximum level. However, the sources of these peaks have not been determined experimentally and the definition of the TBEOAE latency includes much ambiguity. The present study measured the two-tone suppression (2TS) tuning curves of TBEOAEs at different latencies in six audiometrically normal subjects. In 2TS measurements, the suppressor was swept in frequency ( $f_s$ ) at constant level, with the probe kept at a constant level and frequency ( $f_p$ ). The probe and suppressor levels were fixed at 60 dB SPL. 2TS tuning curves were measured at 0.75 - 2 kHz. In the whole frequency region, the best frequency (BF) of the 2TS tuning curve shifted to lower frequency with increasing latency. At 1 kHz, the BF of 2TS tuning curves shifted from 1.2 of  $f_s/f_p$  to 0.9 of  $f_s/f_p$  with increasing latency. At the latency defined as the highest peak position, the BF of 2TS was slightly higher than the probe frequency. 2TS tuning

curves for the other frequencies showed the same tendency as the 1-kHz results. If the 2TS of TBEAEs originates in the overlap region of two traveling waves (evoked by the probe and suppressor tone bursts), this result implies that short-latency peaks originate in the basal region of the cochlear, relative to the sources of long-latency peaks. This result provides a clearer definition of the OAE latency and may lead to a more accurate estimation of cochlear tuning.

#### **401 Attention and the Effect of Active Listening on the Medial Olivocochlear Reflex**

**Peter G. Jacobs<sup>1</sup>**, Eric A. Wan<sup>2</sup>, Frederick J. Gallun<sup>1,3</sup>, Daniel McDermott<sup>1</sup>, Dawn Konrad-Martin<sup>1,3</sup>

<sup>1</sup>VA RR&D National Center For Rehabilitative Auditory Research, Portland VA Medical Center, <sup>2</sup>Oregon Health & Science University, Department of Biomedical Engineering, <sup>3</sup>Oregon Health & Science University, Department of Otolaryngology

The purpose of this study was to investigate the role of the medial olivocochlear (MOC) efferent pathway in active auditory attention. Prior literature suggests that the MOC reflex can change based on input from the auditory and visual cortex. In this paper results are presented from an experiment in which 10 normal hearing subjects performed both an active listening task and a passive listening task while their MOC reflex was measured. The MOC reflex was measured during both the active and passive listening conditions. During the active listening condition, a stimulus frequency otoacoustic emission was evoked in the ipsilateral ear by presenting a constant tone and the MOC was elicited in the contralateral ear using broadband noise as an elicitor. Within the broadband noise, subjects were asked to identify the presence of a tone in a two-alternative forced choice paradigm. A cue was presented to the contralateral ear immediately prior to the target stimuli. The cue was either (1) at the same frequency as the target, (2) at a frequency outside of the target critical band, or (3) not present at all. During the passive listening task, the identical audio stimuli were presented, but the subjects received no instructions other than to sit and watch a silent movie. The purpose of evaluating the three cue types was to investigate whether the subjects' MOC reflex changed relative to the cue frequency since prior work suggests that a subjects' attention bandwidth – the frequency range over which they are searching for a target stimulus – could be dependent on the functionality of the MOC. Results indicate that there was a small but statistically significant increase in the MOC reflex amplitude during active listening as compared with passive listening. There was no significant difference in MOC reflex strength measured under different cue conditions. (Project support came from the Department of Veterans Affairs RR&D C7693M and NIH 1R21 DK079283-01A).

#### **402 Effect of Contralateral Noise on Speech Perception and Transient Otoacoustic Emissions in Adults**

**Mallory Robb<sup>1</sup>**, Lauren Shaffer<sup>1</sup>

<sup>1</sup>Ball State University

Otoacoustic emission (OAE) suppression provides researchers and clinicians with a non-invasive method to evaluate the integrity and function of the efferent auditory pathway. It has been hypothesized that one of the effects of activating this pathway is to aid in the discrimination of speech in the presence of background noise. The purpose of this study was to evaluate the effects of contralateral acoustic stimulation using both behavioral and physiologic measures, and to determine if a correlation exists between them. This was accomplished by measuring the effect of contralateral noise on 1) speech perception scores in the presence and absence of ipsilateral babble noise and 2) transient evoked (TE) OAEs. Ten normal hearing adults were tested with the Quick Speech-in-Noise test (Quick SIN) under six different signal-to-ipsilateral noise ratio test conditions with two different contralateral noise conditions (with and without contralateral noise). Participants' TEOAEs were also tested under two conditions (with and without contralateral noise). Results indicate that while the presence of ipsilateral babble degrades speech in noise performance, when contralateral noise was added in the presence of ipsilateral speech babble, performance improved. When the improvement of the Quick SIN score was correlated with the amount of TEOAE suppression, no statistically significant relationship was found at any TEOAE frequency band. This lack of significant correlation stands in contrast to the work of Kumar and Vanaja (2004), but is consistent with the findings of Mukari and Mamat (2006).

#### **403 The Influence of Spontaneous Otoacoustic Emissions on Threshold Microstructure and Psychophysical Tuning**

**Rachael Baiduc<sup>1</sup>**, Jungmee Lee<sup>1</sup>, Sumitrajit Dhar<sup>1</sup>

<sup>1</sup>Hugh Knowles Center, Roxelyn and Richard Pepper Dept. of Comm. Sci. and Disord, Northwestern Univ.

Comparison of psychophysical behavior from ears with and without spontaneous otoacoustic emissions (SOAEs) may aid understanding of cochlear mechanics in general and SOAE generation in particular. Hearing thresholds exhibit minima and maxima, a pattern known as threshold microstructure. Most reports of threshold microstructure suggest a link to SOAEs. High-frequency SOAEs have often been associated with hearing loss or cochlear pathology, leading to the expectation that threshold microstructure may disappear in their vicinity. Prior comparisons of psychophysical tuning between ears with and without SOAEs have demonstrated sharper tuning in ears with emissions. These reports have not assessed tuning directly at SOAE frequencies, leaving the connection between SOAEs and tuning poorly understood. The relationship between SOAEs, threshold microstructure, and psychophysical tuning was explored here, with special emphasis on high frequencies.

Threshold microstructure and simultaneous-masked psychophysical tuning curves (PTCs) were assessed for SOAEs ranging in frequency from 1273-13942 Hz in 18 subject pairs (matched on age, ear, gender, and thresholds surrounding the SOAE). Data were analyzed according to SOAE status (present or absent) and SOAE frequency (low or high). Results indicate: (1) subjects with SOAEs exhibit threshold microstructure, regardless of emission frequency; (2) subjects with SOAEs do not demonstrate significant quantitative differences in psychophysical tuning compared to subjects without SOAEs; (3) PTCs are influenced by the presence of multiple, adjacent SOAEs, which may produce shifted tuning curve tips, multiple tips, or at times, inverted tuning curves. High-frequency SOAEs may have a greater effect on PTC morphology than low-frequency SOAEs. Results will be discussed in the context of the global resonance model of SOAE generation.

Supported by NIDCD grant DC008420 and Northwestern University.

#### **404 Decay and Persistence of Implicit Memory for Sound: Evidence from Auditory Stream Segregation Context Effects**

**David Weintraub<sup>1</sup>, Christophe Micheyl<sup>2</sup>, Joel Snyder<sup>1</sup>**  
<sup>1</sup>University of Nevada, Las Vegas, <sup>2</sup>University of Minnesota

The purpose of the current study was to determine the extent to which implicit memory effects in the perceptual organization of sound sequences declines over time due to passive decay versus active interference from other stimuli. Toward this aim, we took advantage of two recently discovered context effects in the perception of auditory streaming, the perceptual organization of sequential sounds into distinct streams. These two context effects depend on (1) the acoustic parameters of previous sounds and (2) previous perceptual organization of these sounds, respectively. Accordingly, the experiments measured how listeners' perceptual organization of a tone sequence was influenced by the frequency separation, or the perceptual organization, of the two preceding sequences. The results demonstrated clear evidence for decay of context effects over time, and little evidence for interference. However, they also revealed that context effects can be surprisingly persistent. These findings suggest the existence of two types of memory traces for sound patterns, one that decays rapidly over time and another that does not. The robust effects of decay and persistence were strikingly similar for the two types of context effects, suggesting that the rapidly decaying and persistent memory traces each contain information about both basic stimulus features of sounds (i.e., frequency separation) and the perceptual organization of these sounds. [Work supported by NSF BCS1026023 and NIH DC007657]

#### **405 Attention and Awareness Are Insufficient to Facilitate Buildup of Auditory Stream Segregation**

**Brian Metzger<sup>1,2</sup>, David Weintraub<sup>2</sup>, Joel Snyder<sup>2</sup>**  
<sup>1</sup>University of Illinois, Urbana-Champaign, <sup>2</sup>University of Nevada, Las Vegas

A notable example of central involvement in sound segregation is the influence of attention, which may be necessary for listeners to perceive two segregated streams of low (A) and high (B) tones, after a period of 'buildup' during which listeners perceive one integrated stream of tones. The purpose of the current study was to determine whether buildup can occur in the absence of awareness and conversely whether making sounds accessible to awareness (and attention) is sufficient for buildup to occur. Buildup was measured as the likelihood of a repeated context tone that matched the A or B frequency to increase the likelihood of hearing a subsequent ABA test pattern as segregated. Awareness of the context tones was prevented by embedding them as integer-multiple harmonics in a series of complex periodic tones. Results showed that participants reported more streaming when the context tones were frequency-matched to A or B, compared to when they were mismatched in frequency and/or masked in a harmonic complex. Surprisingly, however, mistuning the context tone relative to the rest of the harmonic did not facilitate buildup, despite the fact that the context tone was accessible to awareness as a pure-tone object separate from the complex tone. Even presenting the context tone in a separate ear from the rest of the harmonic complex did not facilitate buildup, which ruled out peripheral masking of the context tone as the reason for lack of buildup. Finally, presenting the test tones as mistuned harmonics embedded in harmonic complexes, similar to the context tones, eliminated the possibility that timbre changes from context to test reset any buildup that occurred during the context. Together, these results show that while awareness (and attention) may be necessary for buildup of stream segregation, these factors are insufficient by themselves to facilitate the buildup process. [Work supported by NSF grant BCS-1026023]

#### **406 Practice Reduces Informational Masking by Improving Decision Strategy and Reducing Lapse Rates**

**Pete Jones<sup>1</sup>, David Moore<sup>1</sup>, Sygal Amitay<sup>1</sup>**  
<sup>1</sup>MRC Institute of Hearing Research

Detection thresholds for a fixed-frequency tone deteriorate by as much as 20-50 dB in the presence of a spectrally unpredictable multi-tone complex. Here, we examined the extent to which this informational masking can be attenuated by practice. We also examined the mechanisms underlying this perceptual learning by quantifying changes in internal noise, decision efficiency and lapse rates (attention).

We measured detection thresholds for a 1 kHz pure tone in quiet and in a 65 dB (SPL) notched multitone masker (223-4490 Hz) across 5 training sessions (900 trials each). The masker consisted of 30 sinusoids, the amplitudes, phase

and frequencies of which were independently randomised prior to every presentation. Masking level was calculated as the threshold difference between the quiet and masked condition. Decision efficiency was quantified by comparing the observed strategy to the ideal. Decision strategy was the correlation between the difference in level between the target and standard interval, and the listener's response, as measured independently for 11 third-octave spectral bins. Decision weights were used to estimate the decision variable for each trial, under the assumption that listeners responded to the interval containing the greatest sum weighted dB level. Psychometric functions were fitted to each listener's responses as a function of this decision variable, with the slope taken as an index of internal noise and the asymptote an index of lapse rate.

Group (n = 8) mean masking decreased significantly across training sessions. Significant improvements in both decision efficiency and lapse rates were also found, and each was a predictor of learning. However, there was no significant change in internal noise between sessions.

We conclude that practice can substantially improve detection performance in unpredictable noise, and that such learning is subserved by improvements in sustained (lapse rates) and selective (decision efficiency) attention.

#### **407** **Supra-Modal Benefit of Tetris in Auditory Training**

**Yu-Xuan Zhang<sup>1</sup>, David R. Moore<sup>1</sup>, Sygal Amitay<sup>1</sup>**

<sup>1</sup>MRC Institute of Hearing Research

We previously reported that a single session of training on Tetris, a popular computer game that requires fast visual-motor control, improved tone frequency discrimination. One explanation is that playing Tetris provides supra-modal arousal that facilitates contextual or procedural learning. This would be predicted to saturate quickly and afford little practical benefit. Alternatively, playing Tetris may improve attention processes involved in auditory perception, as improved visual attention has been shown following action game training. A third possibility is that playing Tetris produces neurochemical signals (e.g. increased striatal dopamine produced by computer games), that enhance the effects of contiguous auditory experience. To test these hypotheses, we trained three participant groups for four successive daily sessions, either on Tetris alone, FD with a roving standard (FDr), or Tetris alternating with FDr (FDr+Tetris). Before and after training, all participants were tested on FDr, auditory working memory for frequency (WMf), and the visual Attention Network Test (ANT). The Tetris group did not differ from the untrained Control group in any test, indicating that multi-session playing of Tetris alone did not produce learning in auditory perception, WM, or visual attention. The FDr group improved more than Controls on the FDr task, but not on the ANT. FDr learning also transferred to WMf. Critically, improvement on both FDr and WMf was larger in the FDr+Tetris than the FDr group. Thus, playing Tetris enhanced, but did not produce auditory learning, suggesting that motivating and engaging computer games induce neurochemical changes that can augment the effect of training across modalities.

#### **408** **A Simpler Explanation for Detection Thresholds of Stimulus-Pairs as a Function of Stimulus Separation**

**Peter Heil<sup>1</sup>, Jesko Verhey<sup>2</sup>, Benedikt Zoefel<sup>1</sup>**

<sup>1</sup>Leibniz Institute for Neurobiology, Magdeburg, Germany,

<sup>2</sup>Department of Experimental Audiology, Otto-von-Guericke University, Magdeburg, Germany

Detection thresholds for a pair of very brief tone- or noise-bursts are lower than those for a single such burst. Krumbholz and Wiegrebe (Hearing Res 124:155-169, 1998) measured detection thresholds in human listeners for tone- and noise-burst pairs as a function of the temporal separation of the two bursts of each pair. For tone-burst pairs, they found thresholds to increase up to a few milliseconds before reaching a plateau. Further, the time-constant(s) involved appeared to scale inversely with the carrier frequency of the tones. For noise-burst pairs, thresholds were independent of temporal separation down to the shortest value measured (1 ms). The results were convincingly interpreted in terms of temporal overlap of auditory-filter responses elicited by the two successive stimuli. The authors also presented a model to account for the data in a quantitative fashion which, however, and despite its complexity, did not describe the data satisfactorily. Their model consists of a fourth-order gamma-tone filter, followed by a squaring device, a low-pass filter, a spike generator with high spontaneous activity and a compression exponent, and a matched-filter detector with stimulus-dependent weights.

Here, we examine whether a much simpler model, inspired by our LIEFTS model (e.g. Neubauer and Heil, Brain Res. 1220: 208-223, 2008), can satisfactorily account for the data of Wiegrebe and Krumbholz. The LIEFTS model involves leaky integration (i.e. low-pass filtering) of the stimulus, event formation, and temporal summation and was developed to explain detection thresholds for tones of different durations and envelopes as well as spiking properties of auditory-nerve fibers. We find that the combination of a simple first-order gamma-tone filter with the event-forming step and the temporal summation stage of the LIEFTS-model provides a much better description of the thresholds measured by Wiegrebe and Krumbholz than their complex model. This finding provides further support for the LIEFTS model.

Supported by the Deutsche Forschungsgemeinschaft (SFB-TR 31).

#### **409** **Extending Frequency Bandwidth Above 4 KHz Improves Speech Understanding in the Presence of Masking Speech**

**Sunil Puria<sup>1,2</sup>, Suzanne Carr Levy<sup>1</sup>, Daniel J. Freed<sup>1</sup>, Michael Nilsson<sup>1</sup>**

<sup>1</sup>EarLens Corporation, <sup>2</sup>Stanford University

The hypothesis that extending hearing aid frequency bandwidths from 4 to 10 kHz can improve speech understanding in masking speech was tested in normal-hearing and hearing-impaired subjects. Reception thresholds of sentences (RTSs) were measured for two

different target and masker spatial arrangements (simulated using HRTFs and insert earphones): 1) asymmetric, with the target at  $-45^\circ$  and two maskers at  $+45^\circ$ ; and 2) diffuse, with the target in front at  $0^\circ$  and four maskers at  $\pm 45^\circ$  and  $\pm 135^\circ$ . Hearing In Speech Test (HIST) sentences and masking speech materials were presented using low-pass filter (LPF) cut-off frequencies of 4, 6, 8, and 10 kHz. For the mild-moderate sensorineural hearing-impaired subjects, the CAM2 fitting algorithm (Moore et al., 2010) and a multi-band high-frequency compressor were also used.

For normal-hearing subjects ( $n=21$ ), the mean RTS for the asymmetric case was  $-16.2$ ,  $-18.1$ ,  $-18.5$ , and  $-19.7$  dB for the 4, 6, 8, and 10 kHz LPF frequencies respectively, compared to  $-7.7$ ,  $-9.3$ ,  $-9.9$ , and  $-10.3$  dB for the diffuse case. Using pairwise t-tests ( $p<.05$ ), the significant RTS improvements are for all but the 6 to 8 and 8 to 10 kHz pairs for the asymmetric case and for all but the 6 to 8 kHz for diffuse case. For hearing-impaired subjects ( $n=24$ ), the mean RTS for the asymmetric case was  $-10.5$ ,  $-11.0$ ,  $-11.5$ , and  $-11.8$  dB for the respective LPF frequencies, compared to  $-1.7$ ,  $-2.0$ ,  $-2.7$ , and  $-2.3$  dB for the diffuse case. The significant RTS improvements are from 4 to 8 and 4 to 10 kHz for the asymmetric case, and from 4 to 8 kHz for the diffuse case.

The results suggest that acoustic cues above 4 kHz provide an increased ability to understand target speech in masking speech by up to 34% for normal-hearing subjects and 13% for hearing-impaired subjects (using 1dB~10%, Nilsson et al., 1994). CAM2 provides enough gain to give partial audibility for frequencies up to 10 kHz. [Supported in part by R44 DC008499 SBIR and ARRA supplements to SP from the NIDCD of NIH].

#### **410 Does Energetic Masking Limit Performance in Spatialized Speech Mixtures?**

Virginia Best<sup>1</sup>, Eric Thompson<sup>1</sup>, Christine Mason<sup>1</sup>, Gerald Kidd, Jr.<sup>1</sup>

<sup>1</sup>Hearing Research Center, Boston University

This study tested the hypothesis that energetic masking limits the magnitude of spatial release from masking in multiple-talker listening situations, particularly for listeners with sensorineural hearing loss. A speech target was presented simultaneously with two or four speech maskers. The target was always presented diotically, and the maskers were either presented diotically or dichotically. In dichotic configurations, the maskers were symmetrically placed by introducing interaural time differences (ITDs) or infinitely large interaural level differences (ILDs; monaural presentation). Target-to-masker ratios for 50% correct were estimated. Thresholds in all separated conditions were poorer in listeners with hearing loss than listeners with normal hearing. Moreover, for a given listener, thresholds were similar for conditions with the same number of talkers per ear (e.g. ILD with four talkers equivalent to ITD with two talkers) and hence the same signal-to-noise ratio at each ear. The results are consistent with the idea that increased energetic masking, rather than a specific spatial deficit, limits performance in hearing-impaired listeners for spatialized speech mixtures.

#### **411 Visual Benefit in Bimodal Training of Speech Understanding with Highly Distorted Speech Sound**

Mika Sato<sup>1</sup>, Tetsuaki Kawase<sup>1</sup>, Shuichi Sakamoto<sup>2</sup>, Yo-iti Suzuki<sup>2</sup>, Toshimitsu Kobayashi<sup>1</sup>

<sup>1</sup>Tohoku University Graduate School of Medicine,

<sup>2</sup>Research Institute of Electrical Communication, Tohoku University

To improve postoperative rehabilitation programs after artificial auditory device implantation, this study evaluated the effect of bimodal training under seven experimental conditions of extremely distorted speech sound.

Word recognition under the seven conditions of two-band noise-vocoded speech was measured for auditory (A), visual (V), and auditory-visual (AV) modality conditions after a few hours of bimodal (AV) training. The experiment was performed using subjects with normal hearing.

A-only and AV word recognition performances were significantly different under the seven auditory conditions. A-only and AV word recognition, and V-only and AV word recognition were significantly correlated. However, the correlation between A-only and AV word recognition was ambiguous, although V-only word recognition was correlated with AV word recognition under all frequency conditions. V-only word recognition was also well correlated with AV benefit.

The findings suggest the importance of visual cues in AV speech perception under extremely deteriorated auditory conditions, and the possible effectiveness of bimodal training in postoperative rehabilitation for patients with postlingual deafness who have undergone artificial auditory device implantation.

#### **412 A Reduction of Auditory Perceptual Learning by Minimally Masking Noise**

Beverly A. Wright<sup>1</sup>, Nicole Marrone<sup>2</sup>, Helen Han<sup>1</sup>, Eric C. Hoover<sup>1</sup>

<sup>1</sup>Northwestern University, <sup>2</sup>University of Arizona

Perceptual skills improve with practice, providing a method to treat sensory deficits and enhance normal perceptual abilities. However, improvement on most perceptual tasks requires considerable time and effort, because mere exposure to sensory stimuli rarely yields learning. We recently reported that this effort can be markedly reduced simply by alternating performance of the task to be learned with stimulus exposure alone [Wright et al. 2010, J. Neurosci.]. Here we show that the benefit of the additional exposures can be blocked if those exposures are presented simultaneously with minimally masking noise. We trained adults on one of two target tasks (categorization of a non-native phonetic contrast or frequency discrimination) using 6 different training regimens ( $n=8$ /group). Combining periods of performing the target task with periods of additional exposure to the same stimuli yielded more learning than did the same amount of target-task performance without the additional exposures. Thus, the additional exposures enhanced learning. This benefit was lost when the additional exposures were presented with noise designed to produce

minimal masking, whether or not the noise was presented during the periods of task performance, and whether or not a non-target task was performed with the additional exposures. The enhanced learning was partially restored when the noise was presented during the periods of target-task performance and not during the periods of additional exposure. Hence, the additional exposures were only effective when they were presented in quiet. These results demonstrate that the presence of additional stimulus exposures is not sufficient to enhance learning; these exposures require further processing to be useful. That this processing was disrupted by minimally masking noise suggests that listening in noise places processing demands on the auditory system that are sufficient to hijack the resources necessary for learning enhancement. [Supported by NIH]

#### **413 Intensity, Spectral Tilt, and the Intelligibility of Consonants in Noise**

**Christopher Boven<sup>1</sup>, Jont Allen<sup>1</sup>, Robert Wickesberg<sup>1</sup>**

<sup>1</sup>*University of Illinois at Urbana-Champaign*

For certain speech consonants in noise, elevated presentation levels have been found to reduce intelligibility (Hornsby, 2005). One possible explanation is the upward spread of masking in the cochlea. To test this hypothesis, 16 speech consonants in noise at a 0 dB signal-to-noise ratio were played at 65 dBA and 85 dBA to 17 human subjects. At each intensity, a negative or positive spectral tilt filtered the speech alone in order to increase or decrease any effects from the upward spread of masking. For a positive spectral tilt, the speech spectrum was lowered by 6 dB between 0 and 500 Hz, the level was increased at a rate of 6 dB per octave from 500 Hz to 2 kHz, and above 2 kHz the spectrum was amplified by 6 dB. These filter parameters were reversed for the negative spectral tilt. An unfiltered condition was used to replicate previous research. We found that the average intelligibility was the same across all three conditions at 65 dBA. At 85 dBA, intelligibility was reduced for the unfiltered and negative spectral tilt conditions. For the positive spectral tilt condition, however, there was no decrease in intelligibility. The absence of a decrease in intelligibility at 85 dBA with a positive spectral tilt, while the recognizability at 65 dBA was not affected by this filter, suggests that the upward spread of masking may have been responsible for the reduced intelligibility in the unfiltered and negative spectral tilt conditions at 85 dBA.

#### **414 Interrelation Between Sensation Level and Auditory Evoked Potentials Under Conditions of Masking Release**

**Bastian Epp<sup>1</sup>, Ifat Yasin<sup>2</sup>, Jesko L. Verhey<sup>1</sup>**

<sup>1</sup>*Department of Experimental Audiology, University of Magdeburg, Germany,* <sup>2</sup>*Ear Institute, University College London, United Kingdom*

The audibility of important sounds in natural acoustical environments is often hampered due to the presence of other masking sounds. The amount of masking depends on characteristics of the sound sources such as spatial position and spectro-temporal properties of the emitted

signals. The present study investigates the interrelation between auditory evoked potentials and the level above masked threshold. The amount of masking can be reduced due to the presence of certain signal properties which are beneficial for detection. Psychoacoustical experiments showed that both, coherent intensity fluctuations across frequency and interaural phase disparities, result in a masking release (comodulation masking release, CMR, and binaural masking level difference, BMLD) compared to a condition where those properties are not present. The present study investigates if the release from masking is also observed in auditory evoked potentials. The audibility of a masked tone is varied by introducing (i) interaural target phase disparities and (ii) a coherent masker level fluctuations in different frequency regions. The psychoacoustical results of the subjects participating in the present study are in agreement with the finding that the overall release from masking when both signal properties are present is the sum of CMR and BMLD. Late auditory evoked potentials were recorded within these subjects for the stimuli at different signal-to-masker ratios. The data indicate differences in N1 between stimuli with and without interaural disparities, but no difference between present and absent comodulation. However, P2 is not only sensitive to the increase in audibility when the masker level fluctuations in different frequencies regions are changed from uncorrelated to comodulated, but its magnitude is also consistent with the psychoacoustical finding of an addition of the masking releases when both cues are present.

#### **415 A Systematic Survey of the Factors Affecting the Slope of the Psychometric Function for Masked Speech**

**Alexandra Woodfield<sup>1,2</sup>, Michael A. Akeroyd<sup>1</sup>**

<sup>1</sup>*MRC Institute of Hearing Research (Scottish Section),*

<sup>2</sup>*University of Strathclyde*

Many studies have looked at the effects of different maskers on the intelligibility of target speech. Their analyses have often concentrated on changes in threshold, but rarely considered changes in the slope of the psychometric function. This slope quantifies the rate at which intelligibility improves with level. It is, therefore, crucial in determining the degree of perceptual benefit a listener will gain if signal-to-noise ratio (SNR) can be improved, for instance by a hearing aid. Here, psychometric function data from the literature has been systematically reanalysed in order to identify the major factors that affect slope.

Citation searches were undertaken to identify potential studies. To be included, a study needed to report at least one psychometric function that measured speech intelligibility as function of SNR over at least 3 points. The data for each individual function was fitted with a common logistic equation and the maximum slope derived. The stimuli, presentation method, and participant details for each study were also extensively coded. We found 74 studies that met the inclusion criteria, giving 622 individual psychometric functions. Primary factors affecting the slope were found to be, the type of masker (median slope =

4%/dB for speech maskers compared to 8.3%/dB for static noise maskers), the number of speech maskers (median slope = 3.2%/dB for 1 masker compared to 4.7%/dB for 2 maskers), and the predictability of the target speech (median slope = 14%/dB for highly predictable targets compared to 7%/dB for unpredictable targets).

This survey codifies the literature on the slope of psychometric functions for speech, demonstrating that it is affected by both target and masker qualities. The perceptual benefit offered by an improvement in SNR, therefore, depends greatly on listening environment.

#### **416** Effects of Spectral Smearing on Temporal and Spectral Masking Release in Low- And Mid-Frequency Regions

**Agnès C. Léger**<sup>1</sup>, Brian C.J. Moore<sup>2</sup>, Dan Gnansia<sup>3</sup>, Christian Lorenzi<sup>1</sup>

<sup>1</sup>*Ecole Normale Supérieure, Paris, France; Université Paris Descartes, Paris, France; CNRS, France,* <sup>2</sup>*Dept. of Experimental Psychology, University of Cambridge, Cambridge, UK,* <sup>3</sup>*Neurelec, France*

Léger et al (2011) reported deficits in the identification of consonants in noise by hearing-impaired listeners using stimuli filtered into low- or mid-frequency regions, for which audiometric thresholds were normal or near-normal. The deficits could not be fully explained in terms of reduced audibility, temporal-envelope processing or frequency selectivity. However, previous studies indicate that the listeners may have had auditory filters broadened by a factor of about 1.3, despite having normal or near-normal audiometric thresholds in the tested regions. The present study aimed to determine whether the speech-perception deficits could be explained by such a small reduction of frequency selectivity.

Consonant identification was measured for normal-hearing listeners in quiet and in steady, unmodulated and modulated noises using the same method as Léger et al (2011). Various amounts of reduced frequency selectivity were simulated using a spectral-smearing algorithm. Performance was reduced only for spectral-smearing factors greater than 1.7. For all conditions, identification scores for hearing-impaired listeners could not be explained by a mild reduction of frequency selectivity. Therefore, the speech-perception deficits demonstrated by the hearing-impaired listeners cannot be fully explained in terms of reduced frequency selectivity.

References:

Léger A., Moore B. C. J. & Lorenzi C. 2011. Spectral and temporal masking release in the low- and mid-frequency range for normal-hearing and hearing-impaired listeners. *J Assoc Res Otolaryngol*, Abs.: 965.

Acknowledgements:

A. Léger, B.C.J. Moore and C. Lorenzi were supported by a grant from the Royal Society (International Joint Project, 2009R3). A. Léger was supported by a CIFRE grant from ANRT and Neurelec. B.C.J Moore was supported by the MRC (UK).

#### **417** Discrimination of Speaker Sizes Through Speech Sounds: Dependence on Sound Duration

**Chihiro Takeshima**<sup>1</sup>, Minoru Tsuzaki<sup>2</sup>, Toshio Irino<sup>3</sup>  
<sup>1</sup>*J.F. Oberlin University,* <sup>2</sup>*Kyoto City University of Arts,* <sup>3</sup>*Wakayama University*

Several psychophysical studies have demonstrated that the human auditory system has a mechanism to extract information about speaker size from speech sounds. We have shown that the auditory system segregates vowel sequences into two perceptual streams based on speaker size when the size factors between the consecutive vowels were alternated rapidly. It suggests that the auditory system perceives difference in speaker size even from the short-duration vowels. It is, however, unknown how long the vowels should be to satisfy a reasonable discrimination in size. To investigate more specifically the effects of sound duration on the size extraction, the present study measured the discriminability of speaker size as a function of the vowel duration.

The stimuli were synthesized vowels whose spectral envelope (i.e., acoustic factor associated with the length of vocal tract) was scaled to represent the shorter or longer vocal tract. The stimuli were 16, 32, 64, 128, or 256 ms long and were presented against the pink noise. The discriminability for the speaker size was measured with the method of constant stimuli. The two-interval, two-alternative forced-choice paradigm was used, where the subject's task was to select the interval perceived to be uttered by a smaller person. Three source conditions were prepared; (1) 125-Hz pulse trains, (2) 250-Hz pulse trains, and (3) a random noise.

Just-Noticeable Differences (JNDs) in the speaker size were estimated from psychometric functions of *d'* against the scaling value of the spectral envelope. It was observed that the JNDs had similar dependence on vowel duration for all the driving source conditions; JNDs had no significant differences for 32 ms or longer durations, although JNDs rose remarkably when the duration was 16-ms. This indicates that the time constant of the auditory temporal integration might be 32 ms which is consistent with that obtained for the lower limit of the pitch perception.

#### **418** Visual Shadowing of Information in Ongoing Speech; a New Look at the “Cocktail Party”

**Ervin Hafter**<sup>1</sup>, Jing Xia<sup>2</sup>, Sridhar Kalluri<sup>2</sup>

<sup>1</sup>*University of California Berkeley,* <sup>2</sup>*Starkey Hearing Research Center*

The “dichotic listening” paradigm presents independent speech to a subject's (S)'s two ears via headphones. Attention is directed to one ear by having (S) shadow (repeat) the ongoing speech on one side. Tests of recall show that (S) knows little about the unattended stimuli. While the use of independent talkers and messages provides a semi-naturalistic model of auditory interference, it has problems: 1) in addition to listening to the attended ear, S must also prepare for and execute shadowing; 2)

what is more, (S) experiences acoustic interference from his own voice. A quite different approach is exemplified by the “coordinate response measure” or (CRM). There, multiple talkers say a single sentence, “Ready, *name*, go to *color number* now.” (S) is told to attend to the talker who says a specific name and report the color and number spoken by him or her. While CRM offers valuable, well defined measures of performance such as misses and intrusions, it is less natural, with a lock-stepped syntactic and semantic structure across all trials. The present study preserves some of the naturalness of “dichotic listening” albeit without the (S) speaking, while allowing for immediate measures of auditory processing as in the CRM. A set of short stories are read from different azimuths and a stream of questions is presented on a frontal screen. The questions are based on information recently presented in one of the stories. In “visual shadowing,” (S) uses buttons to answer all questions and receives monetary rewards for correct responses. For direction of attention, the visual display also marks the “primary source” from which the majority of questions are taken. This reincarnation of the “cocktail party” allows for study of such effects of shared attention as spatial bandwidths for distraction and inclusion (eavesdropping), reflexive shifts of attention and the speed and ability to switch attention.

#### **419** Bumetanide-Induced Hyperpolarization by IK-Ca Channel Activation Correlates with Aminoglycoside Uptake Enhancement in MDCK Cells

Yueqin Yang<sup>1</sup>, Takatoshi Karasawa<sup>2</sup>, Tian Wang<sup>1</sup>, Qi Wang<sup>1</sup>, Peter Steyger<sup>1</sup>, **Zhi-Gen Jiang<sup>1</sup>**

<sup>1</sup>Oregon Health & Science University,

<sup>2</sup>karasawa@ohsu.edu

Loop diuretics such as bumetanide (BUM) and furosemide (FUR) enhance aminoglycosides ototoxicity when co-administered to patients and animal models. The underlying mechanisms remain poorly understood. We investigated the effect of these diuretics on cellular uptake of aminoglycosides, using Texas Red-tagged gentamicin (GTTR) imaging and intracellular/whole-cell recordings on the MDCK cells. We found that BUM and FUR concentration-dependently enhanced cytoplasmic GTTR fluorescence up to 2-fold. This enhancement was suppressed by non-selective cation channel (NSCC) blocker La<sup>3+</sup> and K<sup>+</sup> channel blockers Ba<sup>2+</sup> and clotrimazole (CLT), but not by tetraethylammonium (TEA), 4-aminopyridine (4-AP) and glipizide, and not by Cl<sup>-</sup> channel blockers diphenylamine-2-carboxylic acid (DPC), niflumic acid (NFA), and CFTR<sub>inh</sub>-172. BUM and FUR hyperpolarized MDCK cells in physiological solutions by ~14 mV, increased whole-cell I/V slope conductance; the BUM-induced net current I/V showed a reversal potential (V<sub>r</sub>) ~-80 mV. BUM-induced hyperpolarization and I/V change was suppressed by Ba<sup>2+</sup> and CLT, but not by apamin, 4-AP, TEA, glipizide, DPC, NFA and CFTR<sub>inh</sub>-172. Ba<sup>2+</sup> and CLT alone depolarized cells by ~18 mV and reduced I/V slope with a net current V<sub>r</sub> near -85 mV, and reduced GTTR uptake by ~20%. La<sup>3+</sup> alone hyperpolarized

the cells by ~-14 mV, reduced the I/V slope with a net current V<sub>r</sub> near -10 mV, and inhibited GTTR uptake by ~40%. In the presence of La<sup>3+</sup>, BUM caused negligible potential or I/V change. BUM failed to cause any current or potential changes in cells recorded with pipettes containing high levels of free Ca<sup>2+</sup> (1 mM). In conclusion, NSCCs constitute a major transmembrane pathway for cationic aminoglycosides; BUM enhances aminoglycoside uptake by hyperpolarizing cells that increases cation influx driving force; the hyperpolarization is caused by IK activation likely via a surge of intracellular Ca<sup>2+</sup>. Funded by NIDCD R01 04716 (ZGJ), R01 04555 (PSS), F32 DC008465, R03 DC009501 (TK).

#### **420** Exploring the Role of GLUT10 in Auditory Physiology Using a Transgenic Mouse Model

**Ying-Chang Lu<sup>1,2</sup>**, Chen-Chi Wu<sup>2</sup>, Yin-Hung Lin<sup>2</sup>, Yi-Ching Lee<sup>3</sup>, Yuan-Tsong Chen<sup>3</sup>, Wenxue Tang<sup>4</sup>, Xi Lin<sup>4</sup>, Jau-Min Wong<sup>1</sup>, Chuan-Jen Hsu<sup>2</sup>

<sup>1</sup>Institute of Biomedical Engineering, National Taiwan University, Taipei, Taiwan, <sup>2</sup>Department of Otolaryngology, National Taiwan University Hospital, Taipei, Taiwan,

<sup>3</sup>Institute of Biomedical Sciences, Academia Sinica, Taipei, Taiwan, <sup>4</sup>Department of Otolaryngology, Emory University School of Medicine, Atlanta, Georgia, USA

Glucose is the main energy source in the cochlea. Glucose transporters (GluTs) are necessary for facilitating entry of glucose into cells. The *SLC2A* gene family encodes 13 members of GluT isoforms that share a common structure and all have been cloned. However, the physiological functions of many of the GluTs have not been fully elucidated. In our previous study, we found that the facilitative glucose transporter 10 (GluT10), encoded by the *SLC2A10* gene, was expressed at significant levels in the normal cochlear cells. In the present study, we further explored the function of GLUT10 in a knock-in mouse model with the *Slc2a10* c.383G>A mutation. This mutant mouse strain was generated using an ENU approach, and has been documented to demonstrate arterial abnormalities (Cardiovasc Res. 2009). Homozygous mice (n=10), heterozygous mice (n=10) and wild-type mice (n=10) were subjected to audiologic assessments using auditory brainstem response (ABR), a battery of vestibular evaluations, and inner ear morphological studies. The expression of *Slc2a10* mRNA in the inner ear were examined by semi-quantitative RT-PCR, and the expression of GluT10 protein was investigated using Western blotting and immunofluorescence methods. Hearing thresholds at P35-P42 in homozygous, heterozygous and wild-type mice were 36.6 ± 4.5, 35.4 ± 4.2 and 37.2 ± 5.2 dB SPL, respectively, showing no difference among the groups (ANOVA, p>0.05). None of the homozygous or heterozygous mice revealed vestibular and inner ear morphology deficits. The expression of *Slc2a10* mRNA and GluT10 protein in the inner ear was not affected in the homozygous and heterozygous mice. Normal or near-normal audiovestibular phenotypes in mice segregating the *Slc2a10* c.383G>A mutation indicate that, despite the abundant expression of GluT10 protein in the

inner ear, its function appeared dispensable. It can be inferred that various GluT members in the inner ear might compensate for each other in function.

#### **421 Loss of Kv1.3 Potassium Channels Impairs Auditory Function**

**Lei Song**<sup>1</sup>, Valeswara-Rao Gazula<sup>2</sup>, Joseph Santos-Sacchi<sup>1</sup>, Leonard Kaczmarek<sup>2</sup>

<sup>1</sup>Department of Surgery, <sup>2</sup>Department of Pharmacology, Yale University School of Medicine

The voltage-dependent potassium channel Kv1.3 regulates a variety of physiological functions including cell volume regulation, proliferation, and insulin signaling. Within the nervous system, deletion of the Kv1.3 gene has been shown to greatly increase the sensitivity of the olfactory system, where it is expressed in mitral cells of the olfactory bulb. It has been demonstrated that Kv1.3 channels are also present in presynaptic terminals within the medial nucleus of the trapezoid body within the auditory brainstem (Gazula et al 2010). The consequences of suppressing Kv1.3 channels in the auditory systems are, however, unknown.

We used the auditory brainstem response (ABR) to measure audition in Kv1.3 *-/-* mice. The Kv1.3*-/-* mice had a near parallel ~20 dB SPL ABR threshold elevation across all frequencies tested (2~32 kHz). Independent of sound levels, the latency of ABR wave I was delayed by ~0.5 ms compared to wild type animals, and is cumulative since the latency of wave II peak was almost ~ 1 ms longer than in controls. Waveform changes were also observed in the Kv1.3 *-/-* mice: 1) peaks were broader and 2) merging of wave III and IV was observed. The ABR changes indicate that the activity of Kv1.3 channels contributes to normal synaptic function and the synchronization of spike generation. Results from a set of measurements in which we stimulated animals repeatedly with an 11.3 kHz level series, and changed the rate of stimulus delivery support our conclusions. At high stimulus rates of up to 60 per sec, wild type controls showed only a slight deterioration of the ABR waveform. In contrast, the waveform observed in Kv1.3 *-/-* mice was strikingly different, even at 40 per sec. Because ABR wave I is affected in the Kv1.3 *-/-* mice, indicating a deficit at an early stage in auditory processing, we are currently investigating the localization of Kv1.3 channels within the cochlea.

(Supported by NIH/NIDCD grants DC01919 to LKK and DC00273 to JSS)

#### **422 In Vitro Analyses of the Cellular Mechanisms of Mutations of Kv7.1 Channels**

**Atefeh M. Nik**<sup>1</sup>, Hyo Joeng Kim<sup>1</sup>, Ebenezer N. Yamoah<sup>1</sup>

<sup>1</sup>Department of Anesthesiology & Pain Medicine University of California, Davis

Although Jervell and Lange-Nielsen (JLN) syndrome constitutes bilateral deafness that affects several families around the globe, the underlying cellular mechanisms remain uncertain. The inner ear is exclusively endowed with a positive endocochlear potential (EP) that serves as the main driving force for the generation of receptor potential in hair cells to confer hearing. Deterioration of EP

leads to hearing loss or deafness. The generation of EP relies on the activity of many ionic channels and transporters to establish active potassium cycling within the inner ear, including Kv7.1 channels. We performed site-directed mutagenesis of the human Kv7.1 channel, to generate known mutations of the channel that have been reported to cause JLN syndrome, namely W248F, T322M, T311I, A336fs, G589D, E543f and Q530X. We show that reconstitution of the pore and C-terminal mutant channels in heterologous expression (CHO and HEK293 cells) results in nonfunctional channels. Moreover, the mutation W248F, which occurs at the S4-S5 linker, produces a functional channel with robust inward rectification compared to the wild type channel. Although JLN syndrome is autosomal recessive, we blended the wildtype with the mutant channels to understand the underlying mechanism for the non-functional mutant channels. We will provide data to demonstrate that the underlying etiology of JLN-mutations in Kv7.1 ensue from direct functional defect as well as dysfunctional protein trafficking. These observations provide insight into the detailed cellular mechanisms of JLN syndrome.

#### **423 Loss of E-Cadherin Impairs Stria Vascularis Integrity and Endocochlear Potential**

**Hannes Maier**<sup>1</sup>, Michaela Schweizer<sup>2</sup>, Mark-Oliver Trowe<sup>1</sup>, Andreas Kispert<sup>1</sup>

<sup>1</sup>Medizinische Hochschule Hannover, Germany,

<sup>2</sup>Universitätsklinikum Hamburg-Eppendorf, Germany

**Introduction** Sensitivity of the cochlea crucially depends on the endocochlear potential (EP) that, in turn, relies on the insulation of the intrastrial compartment by epithelial basal cells. E-cadherin is a key factor in mesenchymal to epithelial transitions needed for the formation of the basal cell layer. Here we demonstrate that E-cadherin is not required for formation, but for late differentiation of basal cells and deletion results in reduction of EP and severe hearing deficits.

**Methods** Experiments were performed in conditional E-cadherin mice Tbx18<sup>cre/+</sup>; Ecadherin<sup>fllox/fllox</sup> (EcadKO), while Tbx18<sup>cre/+</sup>; E-cadherin<sup>fllox/+</sup> and Tbx18<sup>+/+</sup>; E-cadherin<sup>fllox/+</sup> littermates served as controls. Hearing thresholds were determined by auditory evoked brainstem responses (ABR) to alternating clicks and EP was recorded in the 1<sup>st</sup> turn of anesthetized animals.

**Results** In adult mice (4w) E-cadherin was found in the spiral ligament except in type III and IV fibrocytes and in the stria vascularis in basal and marginal cells but not in intermediate cells.

Otic fibrocyte differentiation, condensation and initiation of basal cell differentiation were normal. Gross morphological changes beside hypoplasia were absent. Primarily stria vascularis architecture was affected and the dense infoldings of basal cells were disrupted in EcadKO mice.

ABRs thresholds were significantly increased in EcadKO mice from 58.6.2±5.2 dB peSPL to 86.6±3.7 dB peSPL (MV±SD; n=13/10) at 4 weeks and 59.6±3.8 dB peSPL to 125.9±6.4 dB peSPL (n=8/8) at 12 weeks of age. The EP was significantly decreased from 119.0±6.2 mV to

65.0±9.4 mV (n=7/6, 4w) and 114.9±11.1 mV to 31.0±7.5 mV (n=6/5, 12w).

Discussion We suggest that loss of E-cadherin interferes with the establishment of the EP at two levels: first, by the failure to establish a tight, functional basal cell layer, and second, by the loss of Kir4.1-positive functional intermediate cells.

### **424** Generation of Tension by Cultured Type 3 Spiral Ligament Fibrocytes

John Kelly<sup>1</sup>, Andrew Forge<sup>1</sup>, Daniel Jagger<sup>1</sup>

<sup>1</sup>University College London

The spiral ligament is suggested to play diverse roles in cochlear function, including fluid and ion homeostasis, mediation of inflammatory responses to trauma, and tensioning of the basilar membrane. There are 5 main fibrocyte sub-types, each identified by their location within the ligament and by their expression of key protein markers. In this study we derived a sub-culture from the spiral ligament of the guinea pig cochlea, in which the cells displayed a mechanically active phenotype, and expressed protein markers reported previously for type 3 fibrocytes *in vivo*. These markers included aquaporin-1 (aqp1), vimentin, connexin43 (cx43), and acto-myosin cytoskeletal elements. The cells formed extensive stress fibers, which contained alpha smooth muscle actin, and which were associated with the molecular motor myosin II (myoII). Accordingly, cell-populated collagen lattice gels displayed time-dependent contraction, which could be prevented reversibly by blebbistatin, an inhibitor of myoII. Cx43 immunofluorescence was evident within intercellular gap junctional plaques, and RT-PCR confirmed the expression of cx43 mRNA. Cells were coupled via dye-permeable gap junctions, which were blocked by meclofenamic acid (MFA), an inhibitor of cx43-containing channels. MFA reversibly prevented contraction of cell-populated collagen lattices, suggesting that intercellular coupling may modulate the contractility. The data show that the sub-cultured cells can generate myosin-dependent tension on a collagen-based substrate, and thus suggest that the cells have anatomical and functional properties in common with those predicted for type 3 or "tension" fibrocytes. Consequently, our results support the hypothesis that type 3 fibrocytes regulate tension in the spiral ligament-basilar membrane complex, and so determine high-frequency auditory sensitivity.

### **425** Acid Sensing Ionic Channel Currents in Spiral Ganglion Neurons of the Mouse

Antonia Gonzalez Garrido<sup>1</sup>, Rosario Vega<sup>1</sup>, Enrique Soto<sup>1</sup>

<sup>1</sup>Instituto de Fisiologia-BUAP

Acid-sensing ionic channels (ASICs) are members of the degenerin epithelial sodium channel (DEG/ENaC) superfamily. ASICs are widely distributed in the central and peripheral nervous system. They have been implicated in synaptic transmission, pain perception, and the mechanoreception in peripheral tissues. The role of ASICs in the cochlea has not been determined, so that further information on the subunits expressed in cochlear tissues

is the first step to clarify its role, which may be related to the control of cell excitability, homeostatic processes, and mechanotransduction. In this work we studied the pharmacology of the ASIC currents in spiral ganglion neurons from the C57/BL mouse (P3 - P5). Currents were activated by an extracellular pulse of pH (6.1, 5s) acid solution, typical response was an inward current with very fast activation and desensitization with a  $\tau = 126 \pm 12$  ms. In order to define the ion selectivity of the current, replacing equimolarly sodium chloride by choline chloride in the extracellular solutions (pH 7.4 and 6.1) caused a  $93.5 \pm 1.6\%$  reduction of the proton gated current. Current was sensitive to 100  $\mu$ M amiloride which reduced the current  $72 \pm 2.4\%$ . Moreover, 100  $\mu$ M gadolinium reduced the current  $67 \pm 8.7\%$ , gadolinium ions mainly inhibit ASIC3 subunits, thus suggest that this subunit is part of these channels. The use of 300  $\mu$ M zinc and 10  $\mu$ M TPEN (a zinc chelator) caused a potentiation of  $62 \pm 11\%$  and  $31 \pm 11.8\%$  of the proton gated current, these results represent an evidence of the presence of ASIC2a and ASIC1a subunits. Together, these results show that ASIC channels are functionally expressed in the spiral ganglion neurons and provide us with the information of the ASIC subunits forming these channels.

### **426** Developmental Profile of Murine Spiral Ganglion Neuron Intrinsic Excitability

Robert A. Crozier<sup>1</sup>, Robin L. Davis<sup>1</sup>

<sup>1</sup>Rutgers University

Spiral ganglion neurons (SGN) are the first neural components of the auditory pathway and are responsible for faithfully conveying sound information from the hair cells to the central nervous system. The establishment of the auditory system circuitry begins during embryogenesis and continues to refine postnatally through the onset of hearing.

We have begun to profile the development of SGN intrinsic excitability in mice during each day of the first postnatal week using whole-cell current clamp recordings to assess threshold, accommodation, action potential latency and current excitability. We have previously reported in 1 week old mice that features of intrinsic excitability of spiral ganglion neurons are tonotopically organized such that rapidly accommodating, high threshold neurons are found in the base and slowly accommodating, low threshold neurons in the mid-apical ganglion (Liu & Davis, *J. Neurophysiol.* 2007). We find that base and apex neurons retain this tonotopic profile from postnatal day 7 (P7) down to and including P5. At P3 and P4, the earliest time points for which we have data, base neurons begin to manifest a prominently more immature phenotype such that they display lower thresholds (P7 vs. P4 base:  $-42 \pm 0.9$  mV, n=24 vs.  $-49.7 \pm 1.2$  mV, n=9;  $P < 0.01$ ), slow accommodation (P7 vs. P4 base APmax:  $1.25 \pm 0.13$ , n=24 vs.  $18.8 \pm 3.0$ , n=9;  $P < 0.01$ ) and longer latencies (P7 vs. P4 base:  $7.4 \pm 0.4$  ms, n=24 vs.  $17.3 \pm 0.4$  ms, n=9;  $P < 0.01$ ). In addition, current excitability, defined as the current from holding to threshold, is also significantly reduced with less current required in base neurons to reach threshold (P7 vs.

P4 base: 167.7±11.1 pA, n=24 vs. 67.2±4.4 pA, n=9;  $P < 0.01$ ).

These data indicate that during the first days of postnatal development, SGNs undergo rapid and considerable alterations in their intrinsic excitability that may be important for their appropriate integration into a functional auditory neural circuit. Funded by NIH NIDCD RO1-DC01856.

#### **427 Mice Lacking the $\beta$ -Subunit, KCNE3 Have Altered Functional Phenotype of Spiral Ganglion Neurons**

Wenyang Wang<sup>1</sup>, Choong Ryoul Sihn<sup>1</sup>, Hyo Jeong Kim<sup>1</sup>, Ebenezer Yamoah<sup>1</sup>

<sup>1</sup>University of California Davis

To date, little is known about the underlying cellular and molecular mechanisms of progressive hearing loss (PHL) that affects our aging population. Degeneration of hair cells and spiral ganglia neurons (SGNs) are common phenotypes associated with PHL. KCNQ4 channels have been identified as the target of a form of PHL, DFNA2

Here, we hypothesize that the  $\beta$ -subunit, KCNE3 modulates the activity of KCNQ4 channels in SGNs to regulate the resting membrane potential and their excitability. The KCNEs serve as single-pass subunits of several  $K^+$  channels to dictate specific biochemical and functional changes. The study uses normal (wildtype) and null-mutant KCNE3 mice as the experimental models, and exploits classical techniques such as electrophysiology, and biochemistry to determine the *in vivo* functions of the KCNE3 subunit. The results are as follows: 1) Null deletion of KCNE3, resulted in robust expression of KCNQ channel currents (linopirdine/XE-991-sensitive current) in SGNs. 2) The resulting effects are altered resting membrane potentials, activation threshold of action potentials as well as action potential duration, and their refractory periods. 3) The effects of null deletion of KCNE3 subunits were prominent in basal versus apical SGNs. Finally, we predict that deletion of KCNE3 may be a potential strategy to enhance KCNQ channel currents to control membrane potential of SGNs in excitotoxic conditions, such as glutamate excitotoxicity.

#### **428 Molecular Mechanisms of Calmodulin Regulation of hKCNQ4 Channel Activity**

Choongryoul Sihn<sup>1</sup>, Hyo Jeong Kim<sup>1</sup>, Ebenezer Yamoah<sup>1</sup>  
<sup>1</sup>UC Davis

The KCNQ4 (Kv7.4) gene is expressed in hair cells (HCs) and spiral ganglion neurons to form the voltage-gated potassium channel responsible for  $I_{K,N}$ . The importance of the gene is underpinned by the evidence that mutations in the channel result in progressive hearing loss associated with DFNA2.

Previous studies have demonstrated that KCNQ4 channel currents could be modulated by increased intracellular  $Ca^{2+}$  ( $[Ca^{2+}]_i$ ). Presumably, the calcium binding protein, Calmodulin is constitutively tethered to the C-terminus of KCNQ4 channel, sensing changes in  $[Ca^{2+}]_i$  to modulate the channel activity. Whereas Calmodulin regulation of other ionic channels, such as  $Ca^{2+}$  channels, has been

studied in detail, the underlying molecular mechanism for  $Ca^{2+}$ /Calmodulin regulation of KCNQ4 channels is unclear. Using the whole-cell recording of CHO cells expressing KCNQ4 and CaM-mutants, (dominate negative (CaMDN), N-lobe and C-lobe mutants) we have obtained data that provide detailed molecular mechanisms for the  $Ca^{2+}$ /CaM-dependent reduction of KCNQ4 channel currents. Co-expression of KCNQ4 channels and CaMDN resulted in increased current size and the voltage-dependent activation of the current shifted leftward. By employing the C- and N-lobe mutants, the mechanism of modulation of the current became apparent. Additionally, CaMDN enhanced the open probability of unitary currents. Moreover, the unitary conductance was unchanged compared to the data obtained when the KCNQ4 channel is expressed alone.

Funded by the NIH/NIDCD.

#### **429 Regulation of hKCNQ4 Channel Function by the $\beta$ -Subunit, hKCNE3**

Hyo Jeong Kim<sup>1</sup>, Choong Ryoul Sihn<sup>1</sup>, Ebenezer Yamoah<sup>1</sup>

<sup>1</sup>University of California Davis

The human KCNQ4 (hKCNQ4) gene encodes the voltage-dependent  $K^+$  channel that serves as a major contributor in controlling the resting membrane potential of hair cells and spiral ganglion neurons. Previous reports have shown that genetic alterations of the channel results in progressive hearing loss. In addition to the alpha subunits unit of the channel that constitute the pore, small integral membrane protein KCNEs(1-5) serve as their auxiliary subunits, modulating their functions. Indeed, KCNEs subunits are promiscuous, regulating voltage-dependent  $K^+$  channels in multiple families, such as KCNQs( $K_v7$ ), KCNC4 ( $K_v3$ ), and hERG( $K_v11$ ). Much is known about the association between KCNQ1 and KCNE subunits, however little is known about whether other members of KCNQ family (KCNQ2-5) form functional multimeric complexes as well.

Here, we used heterologous mammalian expression system to determine how hKCNE3 modify hKCNQ4 channel functional activity. Whole cell outward KCNQ4 current traces were elicited with depolarizing voltage steps from a holding potential of -80 mV. The results showed that co-expression of hKCNQ4 channels and hKCNE3 resulted in a decline in the current-density in comparison with expression of hKCNQ4 alone. Additionally, hKCNE3 altered the voltage-dependent activation of the whole-cell current. To determine the underlying mechanisms for the inhibitory effects of hKCNE3, we generated HA- and c-Myc-epitope tagged hKCNQ4 and hKCNE3 to assess potential effects of the auxiliary subunit on the trafficking and plasma membrane expression of the hKCNQ4 channel. Our results indicate that the differences in current-densities and voltage-dependence result from functional regulation of the alpha subunit as opposed to trafficking and membrane expression.

### **430 Localization of Divalent Metal Transporters (DMT1) in the Cochlea**

Haiyan Jiang<sup>1</sup>, Dalian Ding<sup>1</sup>, Jerome Roth<sup>1</sup>, Richard Salvi<sup>1</sup>  
<sup>1</sup>University at Buffalo

Many heavy metals are essential microelements, but at high concentrations they can be toxic (e.g., iron, manganese). Divalent metal transporter 1 (DMT1, also known as DCT1, SLC11A2, Nramp1) is responsible for the transport of a broad range of divalent metal ions. The biotoxicity, ototoxicity, distribution and transport of heavy metals have recently attracted considerable attention. Many heavy metals are transported into cells via DMT1 which maintains homeostatic levels by controlling intestinal and cellular uptake. DMT1, which is located in vesicular membranes, is considered as a key modulator regulating metal levels within the body. DMT1 has four distinct isoforms which differ in C-terminus (termed -IRE and +IRE) and N-terminus (termed exon 1A and 1B or exon 2). Antigen specific antibodies which recognize the -IRE, +IRE, and 1A forms of DMT1 were used to compare differences in their expression and localization in the organ of Corti, stria vascularis, spiral ganglion neurons (SGN), and auditory nerve fibers of the cochlea of adult and newborn (P3) rats. Immunolabeling of the 1A isoform indicated that it was absent from cochlear hair cells and auditory nerve fibers in both adult and newborn rats. However, 1A immunolabeling occurred in the cytoplasm of marginal cells of stria vascularis in P3 rats whereas in adults it was primarily localized at the junction between the marginal cells as well as in basal cells of stria vascularis. The -IRE isoform was also absent in hair cells of both adult and newborn rats; however, -IRE immunolabeling was present in nucleus of SGN in P3 rats whereas in adults, -IRE labeling shifted to the cytoplasm of SGN. In addition, the -IRE isoform was absent in auditory nerve bundles in P3 rats, but was present in the cochlear efferent nerve fibers of adult rats. In stria vascularis, diffuse -IRE labeling was present on the surface of marginal cells of P3 rats whereas intense -IRE labeling was present on the marginal cell surface of adult rats. As with other isoforms, +IRE was absent from hair cells in both adult and newborn rats. However, +IRE labeling was detected at the openings of the habenula perforata in adult rats, the supporting cells surrounding SGN and the cytoplasm of SGN. In auditory nerve, +IRE was observed in supporting cells surrounding the nerve fibers in both adult and P3 rats. The +IRE isoform was expressed on the surface of marginal cells and expression increased from diffuse in P3 rats to intense in adult rats. These results indicate the three DMT1 isoforms are mainly expressed in the marginal cells of stria vascularis, SGN, and afferent nerve fibers; only -IRE is expressed in efferent nerve fibers. The information regarding the distribution of these three DMT1 isoforms in the cochlea may prove helpful in understanding the transport of divalent metal ions into the developing and mature cochlea.

### **431 Hormone-Induced Changes in the Expression of Estrogen Receptors in the Auditory System and Associations with Behavioral Changes**

Konstantina Charitidi<sup>1</sup>, Barbara Canlon<sup>1</sup>

<sup>1</sup>Department of Physiology and Pharmacology, Karolinska Institutet

Previous experimental and clinical studies suggest that estrogens affect the auditory system but there is limited evidence on how estrogen receptors in the auditory system are modulated by hormonal manipulations. In the present study, the expression levels of estrogen receptor alpha and beta (ER $\alpha$  and ER $\beta$ ) were determined in both the peripheral (cochlea) and central auditory structures (inferior colliculus) in ovariectomized (OVX) and 17 $\beta$ -estradiol-supplemented animals. qRT-PCR was used in order to determine the transcription levels of the two types of ERs. We found that ER $\alpha$  was down-regulated after estradiol treatment in ovariectomized animals in both the peripheral and central auditory structures, whereas ER $\beta$  was not affected. Estrogen receptor levels were also analyzed in mice in the different phases of the estrous cycle (proestrous, estrous, metestrous and diestrous) and the analysis showed that both estrogen receptors fluctuate in synchrony with estrogen levels. Behavioral experiments showed that OVX mice supplemented with 17 $\beta$ -estradiol had an increased pre-pulse inhibition (PPI) and latency of the acoustic startle response (ASR) compared to OVX + placebo. Neither the ASR magnitude nor the habituation of the ASR was affected. Regulation of ER levels in these auditory structures and influence of PPI scores by estrogen levels, imply a functional effect of the hormonal status on the auditory system.

<sup>1</sup>Supported from the Swedish Medical Research Council, Karolinska Institutet, Karolinska Funding for Doctoral Studies (KID), Tysta Skolan.

### **432 Slc44a2 (CTL2) Knockout Mouse Generation and Initial Characterization of Its Phenotype**

Pavan Kommareddi<sup>1</sup>, Thankam Nair<sup>1</sup>, Danielle Miller<sup>1</sup>, Maria Galano<sup>1</sup>, Yehoash Raphael<sup>1</sup>, Thom Saunders<sup>1</sup>, Thomas Carey<sup>1</sup>

<sup>1</sup>University of Michigan

Solute carrier 44 (slc44) family of genes (slc44 a1-a5) code for a group of putative transporter proteins. We identified slc44a2 (CTL2-choline transporter-like protein 2) as a target of antibody-mediated hearing loss in mice and guinea pigs. Slc44a2 is also implicated as a target antigen (HNA3a, 3b) in transfusion related acute lung injury (TRALI). To investigate the functional significance of slc44a2, we developed a knockout mouse model system. An overview of the creation of the slc44a2 knockout mice and our early phenotypic characterization is presented here. The murine slc44a2 gene spans 34 Kb on chromosome 9. Exons 3-10 which span the first extracellular loop that is postulated to be important in transporter function were chosen for deletion. After construction and transfection of the targeting vector in ES

cells, only one of 1500 clones was identified with homologous recombination. Subcloning of the positive colony yielded only 5 positive clones out of 100 screened clones. In spite of the rarity of properly targeted ES cells, we successfully generated transgenic mice containing the neo selection cassette and the floxed *slc44a2* exons 3-10. Homozygous transgenic mice (*neo-rCTL2/neo-rCTL2*) express full length mRNA for p1 and p2 *slc44a2* isoforms and have normal hearing. Mice homozygous for deletion of *neo* (*neo-/- rCTL2*) and *neo-/- CTL2-/-* homozygous mice (*slc44a2-/-*) had profound hearing loss (80-90dB). *Neo+/+Slc44a2-/-* mice expressed mRNA spliced from exon 2 to exon 11, resulting in mRNA of 2.5 kb as opposed to 3.3kb in *neo+/+slc44a2+/+* and *wt/wt*. The deletion creates a frame shift resulting in mRNA that codes an 18kDa protein consisting of 150 amino acids, of which the first 29 are identical to *slc44a2* followed by 121 that lack homology to known proteins. Loss of outer hair cells in *neo-/- rCTL2* and *neoCTL2-/-* mice also suggests gene disruption. Our early analysis indicates that *slc44a2* is critical for normal ear development and function.

### **433** IRS2-Deficient Mice Show Sensorineural Hearing Loss That Is Delayed by PTP1B Loss of Function

Silvia Murillo-Cuesta<sup>1,2</sup>, Guadalupe Camarero<sup>1</sup>, Águeda González-Rodríguez<sup>1,3</sup>, Lourdes Rodríguez-de la Rosa<sup>1,2</sup>, Deborah Burks<sup>3,4</sup>, Carlos Avendaño<sup>5,6</sup>, Ángela Valverde<sup>1,3</sup>, Isabel Varela-Nieto<sup>1,2</sup>

<sup>1</sup>Instituto de Investigaciones Biomédicas Alberto Sols CSIC-UAM, <sup>2</sup>Centro de Investigación Biomédica en Red de Enfermedades Raras (CIBERER), <sup>3</sup>Centro de Investigación Biomédica en Red en Diabetes y Enfermedades Metabólicas (CIBERDEM), <sup>4</sup>Centro de Investigación Príncipe Felipe, <sup>5</sup>Dep. Anatomía, Histología y Neurociencia. Facultad de Medicina UAM, <sup>6</sup>Instituto de Investigación Hospital La Paz

The insulin receptor substrate proteins (IRS) are key mediators of insulin and insulin-like growth factor 1 signaling. Protein tyrosine phosphatase 1B dephosphorylates and inactivates both insulin and IGF-1 receptors. IRS2-deficient mice develop type 2-like diabetes. In addition, IRS2 deficiency leads to developmental defects in the nervous system. IGF1 gene mutations cause syndromic sensorineural hearing loss in men and mice. However, the involvement of IRS2 and PTP1B in hearing onset and loss has not been studied. Here we study the hearing function and cochlear morphology of IRS2 null mice and the impact of PTP1B deficiency. We have studied the auditory brainstem responses and the cochlear morphology of systemic *Irs2-/- Ptpn1+/+*, *Irs2+/+Ptpn1-/-* and *Irs2-/-Ptpn1-/-* mice at postnatal ages. The results indicated that *Irs2-/-Ptpn1+/+* mice present a profound congenital sensorineural deafness and altered cochlear morphology with hypoinnervation of the cochlear ganglion and aberrant stria vascularis, compared to wild type mice. Simultaneous PTP1B deficiency in *Irs2-/-Ptpn1-/-* mice delays the onset of deafness. We show for the first time that IRS2 is essential for hearing and that PTP1B inhibition may be

useful for the treatment of deafness associated to hyperglycemia and type 2-diabetes.

### **434** Generation of Mice with Hearing Impairment Induced by Gene Transfer in the Embryonic Inner Ear Utilizing a Connexin30-Targeted ShRNA Expression Vector

Toru Miwa<sup>1</sup>, Ryosei Minoda<sup>1</sup>

<sup>1</sup>Department of Otolaryngology-Head and Neck Surgery, Kumamoto University, Graduate School of Medicine

Mutation in gap junction beta-6 (GJB6), the gene that codes for connexin30 (Cx30), causes hereditary deafness in humans and mice. Short hairpin RNAs (shRNA) that are used for gene silencing by RNA interference (RNAi), are processed into short interfering RNAs (siRNA) that bind to the RNA-induced silencing complex. This complex cut and knockdown target proteins and/or genes. We investigated whether RNAi induced hearing impairment by transferring a shRNA expression vector (shRNA-Cx30), which targeted Cx30 and fused EGFP as a reporter gene, into the otocyst of normal mice using electroporation.

At embryonic day 11.5 (E11.5), shRNA-Cx30 was microinjected through the uterus into the otic vesicle of CD-1 normal mice and electroporated. Electroporated embryos were delivered at E18.5. Some fetuses were removed to prepare frozen sections, and some fetuses were raised by surrogate mothers until functional and morphological assessments on postnatal day 30 (P30). An auditory brainstem response (ABR) and immunostaining was used for the assessments. As a control, a random sense shRNA expression vector (shRNA-scramble) fused EGFP was used.

At E18.5, both shRNA-Cx30 and shRNA-scramble were transferred to the prosensory lesion and lateral wall. At P30, both shRNA-Cx30 and shRNA-scramble were primarily transferred to the inner hair cells, outer hair cells, stria vascularis, and supporting cells, as well as to the spiral ligament and spiral limbus. At P30, there was a significant increase in the hearing thresholds of ABR in the shRNA-Cx30 group compared to the shRNA-scramble group. Immunostaining showed Cx30 in the spiral ligament, spiral limbus, and supporting cells in the shRNA-scramble group, while Cx30 was observed only in part of the spiral ligament and supporting cells in the shRNA-Cx30 group.

These results suggest that the siRNA processed from transferred shRNA suppressed the expression of Cx30, resulting in the development of hearing impairment.

### **435** Spiral Ligament Fibrocytes Up-Regulate Cxcl2 in Response to NTHi Via an ERK2-Dependent Activation of C-Jun

Sejo Oh<sup>1</sup>, Jeong-Im Woo<sup>1</sup>, David J. Lim<sup>1,2</sup>, Sung K. Moon<sup>1</sup>

<sup>1</sup>House Research Institute, <sup>2</sup>University of Southern California

Otitis media (OM), one of the most common pediatric infectious diseases, causes inner ear inflammation resulting in sensorineural hearing loss. It is believed that bacterial molecules in the middle ear cavity enter the inner

ear through the round window membrane. OM-induced inner ear inflammation is characterized by infiltration of inflammatory cells such as monocytes and polymorphonuclear leukocytes (PMNs). Previously, we demonstrated that the spiral ligament fibrocytes (SLFs) up-regulate MCP-1/Ccl2 in response to nontypeable *Haemophilus influenzae* (NTHi), which is a major attractant for cochlear infiltration of monocytes. However, little is known about a chemoattractant involved in OM-induced cochlear infiltration of PMNs. Here we showed that NTHi-induced SLF-derived Cxcl2 contributes to OM-induced inner ear inflammation through Cxcr2-mediated recruitment of PMNs. Unexpectedly, NF- $\kappa$ B-independent signaling appeared to be involved in Cxcl2 induction in response to NTHi. We further demonstrated that activation of c-Jun via a TLR2/MyD88-dependent MEK1/ERK2 signaling pathway is required for NTHi-induced Cxcl2 up-regulation in SLFs. Moreover, we found that NTHi-activated c-Jun strongly binds to the proximal AP-1 binding motif of Cxcl2, whereas the distal AP-1 binding site was not critically involved in NTHi-induced Cxcl2 up-regulation. Our study will bring an insight into the molecular pathogenesis of OM-induced inner ear inflammation and provide a novel strategy for the prevention of inner ear complication secondary to middle ear inflammation. [Supported in part by NIH grants DC008696, DC006272 and DC011862]

#### **436 A Novel Role of a NF- $\kappa$ B Binding Motif Silencing NTHi-Induced Cxcl2 Up-Regulation in Rat Spiral Ligament Fibrocytes**

Sejo Oh<sup>1</sup>, Jeong-Im Woo<sup>1</sup>, David J. Lim<sup>1,2</sup>, Sung K. Moon<sup>1</sup>  
<sup>1</sup>House Research Institute, <sup>2</sup>University of Southern California

Spiral ligament fibrocytes (SLFs) play a pivotal role in inner ear inflammation secondary to otitis media. Since SLFs up-regulate monocyte chemotactic protein-1 (MCP-1/Ccl2) and Chemokine (C-X-C) ligand 2 (Cxcl2) in response to nontypeable *Haemophilus influenzae* (NTHi) via a NF- $\kappa$ B-dependent signaling pathway, we hypothesized that NF- $\kappa$ B-dependent signaling pathway is also involved in NTHi-induced Cxcl2 up-regulation in the SLFs. Unexpectedly, we found that SLFs induce Cxcl2 in response to NTHi via ERK2-dependent c-Jun activation. Moreover, qRT-PCR analysis showed that rat SLFs paradoxically enhance NTHi-induced Cxcl2 up-regulation by the pretreatment with CAPE and JSH, NF- $\kappa$ B inhibitors, which suggests a silencing role of the NF- $\kappa$ B-dependent signaling pathway in NTHi-induced Cxcl2 up-regulation. We found two highly conserved NF- $\kappa$ B binding sites in the 5' flanking region of rat Cxcl2 through the motif analysis. Interestingly, we found that the distal NF- $\kappa$ B binding site exists in rats and bovines, but not in mice and humans. Consistently, the NF- $\kappa$ B inhibitor-mediated enhancement of NTHi-induced Cxcl2 up-regulation was not observed in mice. Through the site-directed mutagenesis of the 5' flanking region of rat Cxcl2, we mutated either NF- $\kappa$ B binding site or both. The proximal NF- $\kappa$ B binding site appeared to be essential for NTHi-induced Cxcl2 up-regulation. In contrast, the distal NF- $\kappa$ B binding site was found to negatively regulate NTHi-

induced Cxcl2 up-regulation, indicating a paradoxical function of the distal NF- $\kappa$ B binding site as a silencer. Further studies are necessary to elucidate the molecular mechanism involved in a silencer function of the distal NF- $\kappa$ B binding motif of rat Cxcl2. [Supported in part by NIH grants DC008696, DC006276 and DC011862].

#### **437 Nitric Oxide Mediates TNF-Induced Apoptosis in Auditory Hair Cells**

Hun Yi Park<sup>1</sup>, Mi Hye Lee<sup>1</sup>, Sung Un Kang<sup>1</sup>, Hye Sook Hwang<sup>1</sup>, Keehyun Park<sup>1</sup>, Yun-Hoon Choung<sup>1</sup>, Chul-Ho Kim<sup>1</sup>

<sup>1</sup>Ajou University School of Medicine

**Objectives/Hypothesis:** The purpose of the present study was to ascertain whether tumor necrosis factor-alpha (TNF- $\alpha$ ) could induce apoptosis in auditory hair cells and to investigate the role of nitric oxide (NO) on TNF- $\alpha$ -induced auditory cell death.

**Methods:** UB-OC1 cells and zebrafish were exposed to TNF- $\alpha$ . Flow cytometry, terminal deoxynucleotidyl transferase (TdT)-mediated dUTP-biotin nick end labeling (TUNEL) assay, assay of mitochondrial membrane potential (MMP) and electron microscopy were used to show that TNF- $\alpha$  could induce apoptosis in auditory hair cells and neuromast cells in zebrafish. For measurement of NO, Greiss assay was performed. Western blot was used to measure inducible NO synthase (iNOS) expression. NO scavenger N-acetylcysteine (NAC) and iNOS blocker NG-methyl-L-arginine (NMA) were used to determine whether NO and iNOS were responsible for TNF- $\alpha$ -induced cell death. Antibodies against phospho-p53 (p-p53), phospho-ERK (p-ERK), phospho-JNK (p-JNK), phospho-p38 (p-p38) and cleaved caspase 3 were used to assess the role of JNKs, ERKs, p38 signaling pathway(s) in iNOS expression in response to TNF- $\alpha$  in UB-OC1 cells.

**Results:** Flow cytometric analysis, TUNEL assay, MMP and electron microscopy all demonstrated that TNF- $\alpha$  could induce apoptosis in UB-OC1 cells. TNF- $\alpha$  significantly increased NO generation and iNOS expression. Pretreatment with NMA attenuated TNF- $\alpha$ -induced cell death and caspase-3 activation. Also, TNF- $\alpha$  treatment increased p-p38 and pretreatment of NMA reduced this increased expression of p-p38.

**Conclusions:** TNF- $\alpha$  can induce apoptosis in auditory hair cells, and NO production in response to TNF- $\alpha$  is essential for hair cell apoptosis. NO-mediated TNF- $\alpha$ -induced apoptosis is associated with activation of the p38 pathway in UB-OC1 cells. These results add to understanding of the role of NO in cytokine-induced apoptosis in hearing loss.

#### **438 Relation Between Formation of Aggregations and Upregulation of Heart Shock Protein in Animal Models**

Takefumi Mikuriya<sup>1</sup>, Kazuma Sugahara<sup>1</sup>, Yoshinobu Hirose<sup>1</sup>, Eijyu Kanagawa<sup>1</sup>, Shuhei yoshida<sup>1</sup>, Hioaki Shimogori<sup>1</sup>, Akira Nakai<sup>1</sup>, Hiroshi Yamashita<sup>1</sup>

<sup>1</sup>Yamaguchi University Graduate School of Medicine

Aggregations, made of damaged protein, misfolding protein and abnormal product cause the cytotoxic activity and cell death when they are formed. Neurodegenerative

diseases example for Alzheimer's disease and systemic amyloidoses, have been recognized to be associated with inappropriate deposition of protein aggregates. Although the mechanism of pathogenic aggregations is not fully understood, several reports targeting at aggregations are reported in animal researches.

In cochlea, we previously demonstrated that some aggregations were increased in spiral ganglion cells during aging. We also demonstrated that aggregations in spiral ganglion cells increased after noise injury as same as aging model. These results suggest that aggregations may be involved in the mechanism of inner ear damage and show a new strategy for diseases in inner ear.

Heat shock response plays a critical role in formation or degradation of aggregation. Heat shock response is characterized by induction of heat shock proteins (HSPs) in response to stresses such as heat shock. HSPs act as molecular chaperone which stabilizes denatured proteins, facilitates their removal or repair, and some HSPs also inhibit apoptotic pathways. HSP inducer, geranylgeranylacetone, can induce HSPs in cochlear cells, which prevent both noise injury and age-related hearing loss. Here, we show that the relation between formation of aggregation and HSP upregulation and demonstrate the possibility that increase of aggregation may a protective role in spiral ganglion cells.

#### **439 Serum Inflammatory Cytokines Potentially Underlie Hearing Loss in Immune Disorders**

**Barbara Larrain<sup>1</sup>, Fran Hausman<sup>1</sup>, Beth Kempton<sup>1</sup>, Carol MacArthur<sup>1</sup>, Dennis Trune<sup>1</sup>**

<sup>1</sup>*Oregon Health & Science University*

The susceptibility of the inner ear to circulating inflammatory factors is often proposed as a mechanism by which hearing loss occurs during systemic infections or immune disease. These may include systemic autoimmune disease, chronic otitis media, acute otitis media, etc. However, little research has been conducted on the assessment of circulating inflammatory cytokines that may play a role in the susceptibility of the inner ear. Previous studies from this laboratory have shown sensorineural hearing loss during experimental acute and chronic otitis media, as well as systemic autoimmune diseases. Occasionally the hearing loss in otitis media is contralateral to the inflamed middle ear, suggesting a mechanism other than simple round window transmission of inflammatory cytokines. Also, although circulating antibodies are occasionally reported in human autoimmune hearing loss, the basic profile of inflammatory cytokines that accompany such disease has not been established. Therefore, the present study was designed to assess by ELISA the expression of serum cytokines as a potential mechanism for inner ear pathology and hearing loss. Serum was collected from a variety of animal models of potential inflammatory sensorineural hearing loss. These included MRL/lpr autoimmune mice before and after systemic disease onset, BALB/c mice inoculated with heat-killed bacteria, C3H/HeJ mice with chronic otitis media, and aging BALB/c mice. Sera from these mice were

analyzed by multiplex ELISA for several inflammatory cytokines (interleukins, TNF $\alpha$ , MIP-1, MIP-2, and KC). All models showed significantly higher levels of circulating serum cytokines during the progression of disease and development of hearing loss. This is interpreted as evidence for a potential vascular route of inflammatory factors underlying immune-based cochlear pathology. Thus, serum analysis of patients with unexplained hearing loss may reveal elevated inflammatory markers to guide diagnosis and therapy.

Supported by NIH-NIDCD R01 DC005593

#### **440 SP600125-A JNK Inhibitor Also Acts as an Antioxidant in TNF $\alpha$ -Challenged Organ of Corti Explants**

**Chhavi Gupta<sup>1</sup>**

<sup>1</sup>*University of Miami*

**Background:** Tumor necrosis factor  $\alpha$  (TNF $\alpha$ ) plays a significant role in hearing loss following acoustic trauma, vibration-trauma, bacterial meningitis, cisplatin exposure, and autoimmune sensorineural hearing loss. SP600125 is an inhibitor of JNK which binds reversibly to the anthrapyrazolone domain of JNK. Fluorescence microscopy of FITC-phalloidin-stained TNF $\alpha$  + SP600125-treated explants show preservation of hair cell density. A gene expression study shows that SP600125 prevents downstream up regulation of Bax while not affect Bcl-2 expression. The present study tests the involvement of oxidative stress in TNF $\alpha$ -induced hair cell loss and the antioxidant ability of SP-600125.

**Methods:** Organ of Corti explants were dissected from anesthetized P-3 rats and transferred into serum-free media. Explants were divided into four groups: 1) non treated controls; 2) TNF $\alpha$  (2 $\mu$ g/ml); 3) TNF- $\alpha$ +SP600125 (10 $\mu$ M) and 4) SP600125 only. To study the oxidative stress pathway, levels of total reactive oxygen species (ROS), superoxide dismutase, catalase, Nitric oxide species (RNS) and 4-Hydroxy-2-noneal (HNE) were recorded after 48hrs of culture. Confocal microscopy was used for detecting levels of reactive oxygen species and HNE. Superoxide dismutase, catalase activities and Nitric oxide species were measured spectrophotometrically.

**Results:** superoxide dismutase and catalase activities were significantly reduced in TNF $\alpha$  treated group compared to the control. Activities of these enzymes in TNF- $\alpha$ +SP600125 treated group and in SP600125 only group was higher compared to TNF $\alpha$  treated group. No difference in RNS level was recorded between groups.

**Conclusion:** TNF $\alpha$  induces oxidative stress through ROS and not through RNS. Treatment with SP600125 leads to decrease in oxidative stress in the TNF  $\alpha$ -challenged explants and therefore is a promising treatment against inflammation-induced oxidative stress.

#### **441 Neurotrophic Support of Spiral Ganglion Neurons (SGNs): A Perspective from Gene Expression Profiling**

**Erin M Bailey**<sup>1</sup>, Ramon Galindo<sup>1</sup>, Steven H Green<sup>1,2</sup>  
<sup>1</sup>Department of Biology, University of Iowa, <sup>2</sup>Department of Otolaryngology, University of Iowa

Following loss of hair cells (HCs), SGNs degenerate and gradually die. In rats, this occurs over ~14 wks (Alam et al., 2007). SGN death may be due directly to loss of HCs and loss of hair cell-derived neurotrophic factors (NTFs). However, previous data from our lab has shown that while NT-3 expression is greatly reduced in the organ of Corti after HC death, expression of other NTFs persists throughout the period during which most SGNs die. NTFs expressed at significant levels in the organ of Corti during this period include CNTF and some GDNF family members. Preliminary data suggest that these can support SGN survival in vitro and we can ask the extent to which they are able to replace NT-3. Thus, HC-derived NTFs are not the sole support of SGN survival, explaining prolonged SGN survival in the absence of HCs. If HC-derived NTFs are not entirely necessary for SGN survival, it is possible that SGN death is an indirect outcome of HC loss, perhaps due to degenerative changes in the cochlea initiated by HC loss. Our inability to distinguish these possibilities implies that we do not yet know enough about neuronal responses to loss of hair cells. We therefore used microarrays to profile gene expression in spiral ganglia from deafened and age-matched control hearing rats. Ganglia were obtained at postnatal day (P) 32, a time at which SGN loss has just become significant and at P60, a time at which ~50% of the SGNs are still alive. Transcriptional differences were observed between deaf and hearing ganglia at P32 and P60 but, remarkably, the greatest transcriptional differences were between P32 and P60 ganglia from control hearing rats, implying considerable change due to maturation. Very few significant differences were observed in expression of apoptotic, NTF, or NTF receptor genes between hearing and deaf ganglia. Thus, at any one time most or all of the SGNs do not appear to behave as NTF-deprived neurons. The direct cause of SGN death may not be NTF deprivation.

#### **442 Hair Cell Tiplink Proteins Mediate Aminoglycoside Entry and Toxicity**

John Kim<sup>1</sup>, Garani Nadaraja<sup>1</sup>, **Markus Huth**<sup>1,2</sup>, Lauren Luk<sup>1</sup>, Renji Chai<sup>1</sup>, Anthony Ricci<sup>1,3</sup>, Alan Cheng<sup>1</sup>  
<sup>1</sup>Dept. of Otolaryngology, Head & Neck Surgery, Stanford University, Stanford, CA, <sup>2</sup>Dept. of Otorhinolaryngology, Head & Neck Surgery, Inselspital, University of Bern, Switzerland, <sup>3</sup>Dept. of Molecular and Cellular Physiology, Stanford University, Stanford, CA

Aminoglycoside (AG) entry into sensory hair cells causes cell death and permanent hearing loss. Previous work showed that open mechanotransducer (MET) channels are required for AG entry and damage. Hair cell tiplink proteins consisting of cadherin23 and protocadherin15 are required for MET channel opening. Here, we test the hypothesis that tiplink integrity is required for AG entry and toxicity via genetic and pharmacologic disruption of tiplinks.

Whole organ three-day-old (P3) mouse cochlea were cultured overnight, and treated with BAPTA (5mMx15min) to break hair cell tiplinks. Next, organs were exposed gentamicin conjugated to Texas Red (GTTR; 3µMx1h), or FM1-43 (10µMx10-15s). Robust GTTR uptake was detected in control hair cells with the most intense GTTR labeling in basal turn hair cells; despite histograms showing that uptake is non-uniform within each region. Uptake of GTTR and FM1-43 was significantly reduced in BAPTA-treated hair cells. No GTTR uptake was observed in cadherin23<sup>-/-</sup> cochleae, whereas robust uptake was noted in cadherin23<sup>+/-</sup> and wildtype cochleae. Data also suggests that GTTR might enter nerve fibers and that this uptake was unaffected by BAPTA treatment. Parallel experiments using gentamicin and detection with anti-gentamicin antibodies yielded similar results. During recovery in aminoglycoside-free media for 48h, hair cells degenerated in gentamicin-treated cochleae and this degeneration was significantly reduced by BAPTA pre-treatment and cadherin23 deficiency. In comparison to immediately after BAPTA treatment, cochleae cultured for an additional 24h demonstrated increased GTTR and FM1-43 uptake, but fluorescent uptake remained significantly less than untreated, cultured cochlea, suggesting partial recovery of tiplinks and MET channel patency. Taken together, these data suggest tiplink integrity is required for AG entry and toxicity in hair cells. (Supported by NIH DC011043, DC003896, DC012183, P30 44992 and SNF PBSKP3\_130635/1)

#### **443 Adult Zebrafish Utricle Sensory Hair Cells Respond to Gentamicin**

**Kevin Wang**<sup>1</sup>, Phillip Uribe<sup>1</sup>, Chien-Wei Chen<sup>1</sup>, Qi Wang<sup>2</sup>, Peter Steyger<sup>2</sup>, Jonathan Matsui<sup>1</sup>  
<sup>1</sup>Department of Neuroscience, Pomona College, <sup>2</sup>Oregon Hearing Research Center, Department of Otolaryngology, Oregon Health & Science University

The sensory hair cells found in the inner ear die when humans are treated with aminoglycoside antibiotics, including gentamicin, leading to permanent hearing loss. Most studies using aminoglycosides in zebrafish (*Danio rerio*) have focused on the hair cells found in the lateral line and not in the inner ear. We characterized the ototoxic effects of gentamicin on hair cells found in the utricle. Adult GFP-Brn3c transgenic zebrafish, whose hair cells express green fluorescent protein, received an IP injection of gentamicin (10-30 mg/kg) and allowed to recover for four hours. Zebrafish were euthanized and the heads were removed and fixed. Utricles were extracted, mounted, imaged using a confocal microscope, and hair cell counts were performed to create a dose-response curve. Increasing concentrations of gentamicin resulted in lower hair cell densities in the striolar but not the extrastriolar regions of the utricle. Fluorescently tagged gentamicin (GTTR) was injected into zebrafish to determine where the gentamicin was exerting its cytotoxic effects and the inner organs were imaged using a confocal microscope. Preliminary data show that there was a two-fold increase in the number of GTTR-labeled cells in the extrastriolar regions when compared to the striolar regions.

Experiments are underway to determine the effects of gentamicin on the hair cells found in the saccule.

#### **444 Subcellular Behavior of Fluorescently Labeled Gentamicin and Neomycin in Zebrafish Lateral Line Hair Cells**

Dale Hailey<sup>1,2</sup>, Robert Esterberg<sup>1,2</sup>, Tor Linbo<sup>1</sup>, Edwin Rubel<sup>1,2</sup>, David Raible<sup>1</sup>

<sup>1</sup>University of Washington, <sup>2</sup>Virginia Merrill Bloedel Hearing Research Center

Aminoglycoside-induced hair cell death causes permanent sensorineural hearing loss. Aminoglycosides are valuable antibiotics for treating systemic bacterial infections, and there is significant interest in mediating their toxicity. One approach is to determine how these drugs enter hair cells, and how they are trafficked and processed. It may then be possible to target mechanisms of their toxicity, or accelerate their metabolism. The fluorophore Texas Red has been used to label gentamicin (Wang & Steyger, JARO, 2009). We labeled gentamicin and neomycin with Texas Red, and designed a system to study entry and trafficking of aminoglycosides in zebrafish lateral line hair cells. These hair cells are present on the surface of larvae, readily acquire labeled aminoglycosides, and are easily co-labeled with vital dyes or fluorescent protein fusions that indicate subcellular organelles. Using fluorescence microscopy, we are studying the behavior of gentamicin and neomycin. As reported previously, aminoglycoside hair cell entry requires mechanotransduction; mechanotransduction mutants (e.g. *mariner/myo7a*) block entry (Ernest S et al, Hum Mol Genet, 2000). In hair cells maintained in conditions that block cold-sensitive endocytic and trafficking processes, neomycin and gentamicin rapidly enter hair cells, and diffusely label the entire cell volume outside the nucleus. This diffuse pool does not freely diffuse through the cytosol; calculated diffusion rates are 5 fold slower than for larger cytosolic molecules. In addition, punctae appear which do not colabel with markers of conventional clathrin-mediated endocytosis (i.e. Rab5-GFP or EEA1-YFP), or mitochondrial markers. Formation of the punctae is inhibited by cold treatment, and the punctae colocalize with dyes that accumulate in low pH environments. These data suggest aminoglycosides accumulate in membrane-bound structures that require trafficking to form. We are currently investigating molecular mechanisms required for punctae formation. Additionally we are evaluating whether disrupting their formation affects aminoglycoside toxicity. Lastly, we are evaluating whether there are discernable differences between the behavior of gentamicin and neomycin that may underlie differences in the toxicity profiles of these aminoglycosides.

#### **445 Assessment of Hearing in Larval Zebrafish: Microphonic Potential Recording**

Zhongmin Lu<sup>1</sup>, Alexandra DeSmidt<sup>1</sup>

<sup>1</sup>University of Miami

Death or malfunction of sensory hair cells in the ear results in hearing loss. Due to a combination of powerful genetics, excellent embryology, and exceptional in vivo

visualization, the zebrafish (*Danio rerio*) has become a valuable vertebrate model for investigating function of human genes that are conserved in the zebrafish. The zebrafish has the simplest vertebrate inner ear having sensory hair cells that are structurally, genetically, and functionally similar to those in other vertebrates including humans. The goal of this project was to develop a physiological method that can quickly and reliably evaluate auditory function of young larval zebrafish, and to standardize it to be used on larvae at different ages. Each zebrafish larva was embedded in agarose, and its right ear was directly stimulated with a glass microprobe that was driven by a calibrated piezoelectric actuator. Extracellular microphonic potentials were recorded from hair cells in the inner ear using a beveled glass micropipette filled with standard fish saline. Robust microphonic responses were obtained from the otic vesicle of larval zebrafish of 2 to 8 days post fertilization in response to vibratory stimulation at 20, 50, 100, and 200 Hz. The results show that microphonic responses increase monotonically with stimulus intensity, stimulus frequency, and age of zebrafish larvae. Key factors affecting microphonic responses were also discussed. In summary, the microphonic recording method can assess hair cell function of wild-type zebrafish as well as hearing mutants/morphants. Combined with the morpholino gene knockdown technique, this method is useful for studying the role of target genes in hearing and balance.

#### **446 The Study of Activation Kinetics in the Mammalian Auditory System**

Anthony Peng<sup>1</sup>, Joey Doll<sup>2</sup>, Anthony Ricci<sup>1</sup>

<sup>1</sup>Stanford University, Otolaryngology-Head & Neck Surgery, <sup>2</sup>Stanford University, Mechanical Engineering

Activation kinetics of the mechanotransduction channel in hair cells contribute to the filtering characteristics of the hair bundle, and possibly contribute to the frequency selectivity of the hair cell. In turtle hair cells, activation kinetics and adaptation kinetics have been measured and shown to vary tonotopically. In mammalian hair cells, adaptation kinetics vary tonotopically for outer hair cells, but not inner hair cells. Activation kinetics in the mammalian auditory system, on the other hand, have been too fast to measure. The goal of this study is to determine the activation kinetics of mammalian hair cells and determine if rates vary tonotopically in inner and outer hair cells. Previously, photodiodes detected motion up to approximately 40kHz, which is much lower than the mammalian hearing limits of >100kHz, and probe stimulus rates were limited by probe resonances. By reducing stray capacitances and modifying circuit topology, we have developed a photodiode to investigate activation kinetics in mammals which are capable of measuring responses up to 230kHz. We have also developed faster probes by testing different piezo actuators and identifying mechanical resonance sources that allows us to measure activation time constants of at least 16 microseconds for inner hair cells.

#### **447** Tonotopic Variation in the Mechanotransducer Channels of Mouse Cochlear Hair Cells

Robert Fettiplace<sup>1</sup>, Kyunghye X. Kim<sup>1</sup>

<sup>1</sup>University of Wisconsin-Madison

The cochlea's tonotopic organization is supported by spatial gradients in a plethora of cellular features, a focal property being the hair cell mechanotransducer (MT) channel. The molecular identity of this channel is currently unknown so we have documented its characteristics to provide constraints on possible candidates. MT currents were recorded in outer hair cells of neonatal (P2 – P10) mice at apical, middle and basal locations. MT currents recorded at the apex with a glass probe driven by a piezoactuator had a maximum amplitude of  $0.71 \pm 0.1$  nA at -84 mV, a working range (10 – 90 per cent) of 0.3  $\mu$ m and fast adaptation (time constant =  $0.16 \pm 0.03$  ms). Although similar properties were seen at other locations, because of the decreased height of the hair bundles, it was difficult to adequately stimulate them. Fluid jet stimulation (Kros et al. 1992) was therefore preferred and gave peak MT amplitudes of 0.9, 1.2 and 1.5 nA at apex, middle and base. Current-displacement relationships were fit by a single Boltzmann with working range well under 0.1  $\mu$ m. The reason for the difference between the two types of stimulation is unclear but it suggests the glass probe method substantially over-estimates the working range. At all positions, current amplitudes increased 1.5 to 2 fold when hair bundles were bathed in low Ca<sup>2+</sup> endolymph and became strongly inwardly rectified with slope conductances at negative potentials of 28, 46 and 60 nS for apex, middle and base. In contrast, the conductance at positive potentials (about 7 nS) changed little with location. The Ca<sup>2+</sup> permeability of the MT channel, PCa/PCs, deduced from reversal potentials, showed a small but significant decrease from apex ( $6.1 \pm 0.7$ ; n=7) to base ( $4.4 \pm 0.5$ ; n=21). Our results are consistent with a change in channel properties (including unitary conductance; Beurg et al. 2006) along the cochlea and suggest multiple channel isoforms varying in their extracellular aspect. Supported by NIDCD grant RO1 DC01362

#### **448** Bifurcation Dynamics of Spontaneously Oscillating Hair Bundles

Dolores Bozovic<sup>1</sup>, Lea Fredrickson-Hemsing<sup>1</sup>, Seung Ji<sup>1</sup>, Robijn Bruinsma<sup>1</sup>

<sup>1</sup>UCLA

We will present experimental and theoretical analysis of the phase-locking response observed in spontaneously oscillating hair bundles of the bullfrog sacculus. Under sinusoidal stimulation, the phase-locked amplitude exhibits an Arnold Tongue, consistent with theoretically predicted dynamical behavior. An offset that steadily increases in time, imposed on the position of the bundle, is observed to progressively suppress spontaneous oscillations. This transition displays strong frequency modulation, with the period diverging at the critical point. We propose that the system is poised near a multi-critical bifurcation, with a mixture of infinite-period and supercritical Andronov-Hopf characteristics.

#### **449** Effects of Prolonged Stimulation on Spontaneous Oscillations of Hair Bundles in the Bullfrog Sacculus

Albert Kao<sup>1</sup>, Dolores Bozovic<sup>1</sup>

<sup>1</sup>UCLA

Spontaneous oscillations are believed to constitute one of the signatures of an active process exhibited by hair bundles under in vitro conditions. We apply large-amplitude stimuli, both as steady-state offsets and as trains of sine waves, in conjunction with variations of the ionic environment surrounding the bundles, thus investigating possible mechanisms of self-tuning. Deflections of the hair bundle larger than the physiological range, on the order of microns, suppressed active mechanical oscillations of the hair bundles, with normal motion gradually resuming after several hundred milliseconds. Our results showed that the duration of the quiescent regime and recovery of active motility show sensitive dependence on the duration of the applied stimulus and on the ionic conditions of the aqueous environment.

#### **450** Detection of Sub-Nanometer Mechanical Signals by Bullfrog Sacculus Hair Bundles

Yuttana Roongthumskul<sup>1</sup>, Albert Kao<sup>1</sup>, Sebastiaan

Meenderink<sup>1</sup>, Dolores Bozovic<sup>1</sup>

<sup>1</sup>UCLA

Bullfrog sacculus has been shown to detect subnanometer-level mechanical signals under in vivo conditions. In this work, we explore whether comparable sensitivity can be exhibited by individual hair bundles in vitro. We study the dynamics of single hair bundles from the Bullfrog sacculus under stimulation near threshold levels. We report on the steady-state, phase-locked response to small sinusoidal stimuli. Time-dependent phase locking of the oscillation over multiple cycles of the stimuli are also examined.

#### **451** Domains of TRIOBP Necessary to Generate the Unusually Dense Actin Bundles of Stereocilia Rootlets

Shin-ichiro Kitajiri<sup>1</sup>, Elizabeth Bielski<sup>2</sup>, Tomoki Iemura<sup>1</sup>, Tatsuya Katsuno<sup>1</sup>, Fumi Ebisu<sup>1</sup>, Sakat Chacroborty<sup>2</sup>, Juichi Ito<sup>1</sup>, Takeshi Sakamoto<sup>2</sup>

<sup>1</sup>Kyoto University, <sup>2</sup>Wayne state University

Mutations of TRIOBP cause of human hereditary nonsyndromic deafness DFNB28. TRIOBP KO mice do not develop stereocilia rootlets thereby causing deafness. Biochemical analyses showed that TRIOBP-4 is a novel F-actin bundling protein. Espin 3A and fimbrin, actin bundling proteins localized in the stereocilia core and cross link actin filaments that have an ~12 nm distance between actin filaments in the bundle. We found that although the molecular weight of TRIOBP-4 (107 kDa) is twice larger than that of Espin 3A/Fimbrin, TRIOBP-4 bundles actin with almost no space between filaments, suggesting TRIOBP-4 might wrap around F-actin bundles. To address the question as to how TRIOBP-4 forms these unusually

dense F-actin bundles, we investigated the F-actin bundling sites of TRIOBP-4 by biochemical /biophysical assay and cell biological assay. TRIOBP-4 has two repeated motifs, referred to as R1 and R2 that were hypothesized to be the binding sites with F-actin. To test this, we purified TRIOBP-4 mutant proteins with either the R1 or R2 domains removed. These deletion mutants of TRIOBP-4 were still able to form F-actin bundles. F-actin bundle dynamics were visualized by TIRF microscopy in real time. Localizations of R1 and R2 in cultured cell line were observed by transfecting GFP-tagged TRIOBP-4 mutants. We found that the repeat sequences, R1 and R2, have different mechanisms for actin bundling formations.

#### **452 Stereociliary Espins and the Forked Proteins of *Drosophila*, Orthologous Actin-Bundling Proteins Required for Auditory Function**

**Dina Beeler**<sup>1</sup>, Lili Zheng<sup>1</sup>, James Bartles<sup>1</sup>

<sup>1</sup>*Northwestern University Feinberg School of Medicine*

Although the forked proteins of *Drosophila* are putative orthologs of the espin actin-bundling proteins of hair cell stereocilia, relatively little is known about their activities. The espin actin-bundling proteins are the target of deafness mutations in mice and humans and are required to increase the diameter and stability of the stereociliary parallel actin bundle. By analogy, the forked proteins are required to assemble large parallel actin bundles in the developing neurosensory bristles of *Drosophila* pupae. Recently, it has been noted that forked mutant flies show auditory dysfunction in the form of reduced sound-evoked potentials measured from their antennae. Here, we uncover some activities of the forked proteins and clarify their relationship to the espins. When expressed in transfected LLC-PK1-CL4 epithelial cells the major forked isoform, forked A, was targeted to the nucleus and assembled large nuclear actin bundles. This unexpected result was also observed in Cos-7 cells and *Drosophila* S2 cells. Untagged forked A also formed nuclear actin bundles. An examination of forked A fragments revealed that the protein is composed of two major functional domains: an N-terminal domain that targets the nucleus, owing to a previously unrecognized nuclear localization signal, and a C-terminal domain that targets microvillar actin bundles (LLC-PK1-CL4) or stress fiber-like actin bundles (Cos-7), by analogy to espins. Accordingly, the purified recombinant C-terminal domain of forked A bound and bundled F-actin *in vitro* similarly to espin constructs. The identification of the forked peptides and amino acids required revealed a degree of homology to espins greater than that appreciated previously. Since certain espin isoforms contain functional nuclear localization signals, we suggest that the forked and espin proteins constitute a family of evolutionarily related actin-bundling proteins that are required for auditory function and can transit between cytoplasmic actin bundle-containing structures and the nucleus (NIH DC004314, JB).

#### **453 The Bundle Proteome of Adult Mouse Vestibular Hair Cells**

**Jocelyn Krey**<sup>1</sup>, Peter Gillespie<sup>1</sup>

<sup>1</sup>*Oregon Health & Science University*

While the study of deafness-linked genes has led to the identification of a number of proteins that are localized to the hair bundle, the complete network of proteins that constitute the bundle remains poorly defined. Our lab has developed and optimized a proteomic approach towards the identification and quantification of hair bundle proteins from developing chicken and rat utricles. Using this approach, we have identified hundreds of bundle proteins over a wide dynamic range (~100,000-fold), many of which have known functions in the bundle or are encoded by known deafness genes (Gillespie & Shin, ARO 2012 Abstract). We have now adapted this proteomic approach towards the analysis of adult (P21-P23) mouse hair bundles. Using nano-scale liquid chromatography and mass spectrometry we have identified and quantified proteins present in purified mouse hair bundles as well as in whole utricular epithelium. This bundle-to-epithelium comparison allowed us to obtain a measure of the degree to which each protein is specifically enriched within the hair bundle as well as to separate authentic bundle proteins from contaminants. We identified many bundle-enriched proteins known to be important for bundle function including FSCN2, RDX, MYO6, MYO7A, PTPRQ, and PMCA2, as well as additional proteins with suspected or unknown functions in hair cells. Comparison of the mouse bundle proteome with our results from developing chick and rat bundles suggests that the major protein constituents of the hair bundle do not vary significantly between species or developmental time-points, although there were some differences in protein abundance between mammalian and avian bundles. These results provide the first determination of the adult mouse bundle proteome. We plan to use these techniques to perform future experiments using genetic mouse models of deafness to globally determine changes in protein expression that occur as a consequence of bundle dysfunction.

#### **454 Hair-Bundle Membrane Domains Compartmentalize Calcium Pumping and Phosphatidylinositol Signaling**

**Hongyu Zhao**<sup>1,2</sup>, Diane Williams<sup>1</sup>, Moritoshi Hirono<sup>3</sup>, Jung-Bum Shin<sup>4</sup>, Britta Brügger<sup>5</sup>, Peter Gillespie<sup>1,2</sup>

<sup>1</sup>*Oregon Hearing Research Center, Oregon Health and Science University*, <sup>2</sup>*Vollum Institute*, <sup>3</sup>*Yamada Research Unit, RIKEN Brain Science Institute*, <sup>4</sup>*Department of Neuroscience, University of Virginia*, <sup>5</sup>*Heidelberg University Biochemistry Center, University of Heidelberg*

Lipids play important functional and structural roles in cells, including modulation of protein function and domain formation. Using quantitative nano-electrospray-ionization tandem mass spectrometry, we characterized the lipid components of vertebrate hair bundle. The headgroup composition of bundle lipids was similar to those of other plasma membranes, with 43% phosphatidylcholine, 28% cholesterol, 15% phosphatidylethanolamine, 6%

phosphatidylserine, 3% phosphatidylinositol, with the remainder from minor species. Acyl chain composition of each lipid species was also similar to that of other plasma membranes. Some of these lipids are spatially segregated; the bundle's membrane is divided into at least two structural and functional domains, with distinct lipid and protein components. One membrane domain, at and above stereocilia basal tapers, is enriched in the lipid phosphatase PTPRQ (protein tyrosine phosphatase Q), the most abundant bundle transmembrane protein, and polysialylated ganglioside glycolipids. By contrast, the shaft membrane domain contains the plasma-membrane  $\text{Ca}^{2+}$ -ATPase PMCA2w/a, the second-most abundant bundle transmembrane protein, and phosphatidylinositol 4,5-bisphosphate (PIP2), concentrated in particular at stereocilia tips. The taper ganglioside domain is not a traditional lipid-raft domain, as it is insensitive to cholesterol extraction with cyclodextrins. Cholesterol extraction does affect distribution of PMCA2 within the shaft domain, however, suggesting that it resides within cholesterol-containing microdomains within stereocilia. These large-scale membrane domains within stereocilia allow compartmentalization of  $\text{Ca}^{2+}$  extrusion, actin dynamics, and transduction regulation.

#### **455 Cochlear Lymphatics**

**Joe Adams**<sup>1</sup>, Saumil Merchant<sup>2</sup>

<sup>1</sup>Massachusetts Eye & Ear Infirmary, <sup>2</sup>Massachusetts Eye & Ear Infirmary

In most tissues interstitial fluid (lymph) leaks from capillaries and returns to vascular circulation via lymphatics. There is little reason to suppose that the inner ear is an exception to this rule but lymphatics have never been described in the cochlea. We present evidence for the existence of lymphatic vessels in the spiral ligament of the mouse cochlea using antibodies that have been shown (in other organs) to mark different parts of lymphatic systems. One of these antibodies, raised against Prox1, stains what appear to be initial lymphatic vessels closely associated with type I fibrocytes. Cochlear blood vessels do not stain for Prox1. Immunostaining with another lymphatic marker, podoplanin, reveals a solitary vessel within the spiral ligament that is considerably larger than those that are Prox1 positive, and which appears only sporadically in sections separated by 80 microns. This appears to be a lymphatic collecting vessel.

The paucity of capillaries near the organ of Corti means that oxygen and glucose are conveyed to the organ of Corti via perilymph and that metabolic wastes are removed by perilymph. This necessitates a high perilymph turnover rate, which implies the presence of lymphatics. There are reports of markers being readily cleared from perilymph and there is a report of KLH being found in the cervical lymph node following KLH injections into perilymph, evidence of lymphatic cochlear drainage. Further, it is well established that leucocytes enter the spiral ligament following acoustic trauma and the established route of return of invasive leucocytes from other tissues is via lymphatics. The presence of cochlear lymphatics has important implications for considerations of drug delivery to

the cochlea, for survival of apical sensory cells in patients with basal cochlear implants, and for immune cell trafficking following cochlear damage.

#### **456 Infusion of Atrial Natriuretic Peptide Improves Hearing Thresholds in Mice**

**Janet Fitzakerley**<sup>1</sup>, Aaron Clarke<sup>1</sup>, George Trachte<sup>1</sup>

<sup>1</sup>University of Minnesota Medical School

Atrial natriuretic peptide (ANP) and its receptor (NPR-A, a guanylyl cyclase) are present in the cochlea, suggesting that natriuretic peptides (NPs) and cyclic guanosine monophosphate (cGMP) influence auditory transduction. Our global hypothesis is that NPs are critical regulators of stria vascularis function, and that dysregulation of the NP pathway contributes to the pathophysiology of Meniere's disease. Recent studies have established that administration of a phosphodiesterase inhibitor improves hearing, while decreased cochlear cGMP concentrations are correlated with age-related hearing loss. Furthermore, NPR-A knockout mice are more likely to be deaf than wild-type mice. The current study was designed to determine whether ANP infusion alters hearing in mice.

Data were obtained from CBA/J and NPR-A knockout mice. 10 minutes of saline infusion served as control, and were followed by continuous intra-arterial infusion of various concentrations of ANP for a maximum of 60 minutes. 12 kHz thresholds were determined at 3 minute intervals using standard auditory brainstem response (ABR) techniques. At the end of the infusion, plasma ANP concentrations were determined, and the cochleae were removed and cochlear cGMP concentrations were measured.

Infusions resulting in plasma concentrations of 0.1 and 0.4 ng/mL ANP lowered thresholds between 5 and 20 dB. These threshold improvements peaked ~10 minutes after the ANP infusion began and returned to control levels after 30-40 minutes. Higher ANP concentrations did not produce threshold improvements. The magnitude of the threshold improvements was dependent upon the hearing status of the animal, with the largest changes being observed in animals that had a mild to moderate hearing loss. Heterozygous NPR-A knockout mice did not exhibit significant threshold improvements in response to ANP infusion. These results represent additional evidence that NPs and cGMP are critical modulators of inner ear function.

#### **457 Basement Membrane Dysfunction Causes a Hypoxic Microenvironment**

**Alexander Limjuco**<sup>1</sup>, Kaveh Karimnejad<sup>1</sup>, Daniel Meehan<sup>2</sup>, Dominic Cosgrove<sup>2</sup>, Michael Anne Gratton<sup>1</sup>

<sup>1</sup>Saint Louis University, <sup>2</sup>BoysTown National Research Hospital

Alport syndrome is caused by mutations in type IV collagen genes, and ultimately leads to renal failure and progressive sensorineural hearing loss. A mutation in the  $\alpha 3(\text{IV})$  type IV collagen gene disrupts basement membrane homeostasis resulting in thickening of stria capillary basement membranes (SCBMs). Our previous studies show a mild high frequency hearing loss,

decreased endocochlear potential and susceptibility to noise-induced hearing loss in the COL4A3 knockout mouse. Recent data showing increased content of heparan sulfate proteoglycan in SCBMs suggests reduced transcapillary movement of metabolic nutrients and waste leading to the hypothesis that changes in SCBM filtration properties create a hypoxic microenvironment in the scala media. This hypothesis is supported by previous data showing upregulated proinflammatory cytokines and matrix metalloproteinases (MMPs) 2 and 9 in the Alport lateral wall. These proteins, known to be upregulated by hypoxia, can function to disrupt basement membrane homeostasis. This study examines gene and protein markers of hypoxia and its targets in cochleae of Alport, wild-type (WT), and WT mice exposed to hypoxia (8% O<sub>2</sub>, 4H). It is postulated that induction of hypoxia inducible factor-1 $\alpha$  (HIF-1 $\alpha$ ) causes upregulation of facilitated glucose transporter-1 (GLUT1) and vascular endothelial growth factor (VEGF) in the WT-hypoxic and Alport cochlear lateral wall, but not the normoxic WT cochlear lateral wall. Gene expression of HIF-1 $\alpha$ , as well as GLUT1, VEGF 165 and two of its receptors, Flk1 and NP1, were upregulated in Alport and WT-hypoxic stria homogenate. Increased HIF-1 $\alpha$  and GLUT1 protein in the Alport and WT-hypoxic cochlea were noted by fluorescence and peroxidase immunohistochemistry and confirmed by Western blots. Outer hair cells and spiral ligament fibrocytes were most reactive for HIF-1 $\alpha$  with less reactivity in stria marginal cells. These data are the first to demonstrate that SCBM thickening results in disruption of SCBM homeostasis. SCBM thickening is seen in presbycusis, Alport syndrome, diabetes and systemic lupus erythematosus can cause a hypoxic microenvironment. Moreover, lower levels of oxygen likely contribute to the decreased endocochlear potential and susceptibility to noise-induced hearing loss noted previously in the Alport mouse.

#### **458 The Developmental Rise in the Endolymphatic K<sup>+</sup> Concentration in the Cochlea and the Endolymphatic Sac Is Delayed in *Slc26a4*<sup>-/-</sup> Mice, a Model for Hearing Loss with Enlarged Vestibular Aqueduct**

Xiangming Li<sup>1</sup>, Philine Wangemann<sup>1</sup>  
<sup>1</sup>Kansas State University

Mutations of *Slc26a4* cause enlargement of the membranous labyrinth and the vestibular aqueduct, delays in the postnatal development of the cochlea, and hearing loss. The enlargement and observed delays in the structural development of stria vascularis raised the question whether the transition of endolymph composition from a Na<sup>+</sup>-rich to a K<sup>+</sup>-rich fluid would be delayed in *Slc26a4*<sup>-/-</sup> (KO) mice compared to *Slc26a4*<sup>+/-</sup> (HET) mice. Here we determined in isolated temporal bones the transepithelial potential (V<sub>t</sub>) and the perilymphatic (K<sub>peri</sub>) and endolymphatic (K<sub>endo</sub>) K<sup>+</sup> concentrations with double-barreled ion selective electrodes. Measurements were made between embryonic day (E) 14.5 and postnatal day (P) 100 in the cochlea and the endolymphatic sac (ES). In

the cochlea, between E14.5 and E17.5, K<sub>endo</sub> was 10 mM and V<sub>t</sub> was 0 mV in HET and KO mice. At P0, K<sub>endo</sub> rose to 73 mM in HET and to 34 mM in KO mice and V<sub>t</sub> rose to +2 mV in HET and KO mice. In adult mice (P38-P100), K<sub>endo</sub> was 146 mM in HET and 135 mM in KO mice and V<sub>t</sub> was -16 mV in HET and -3 mV in KO mice. K<sub>peri</sub> was ~3 mM in HET and KO mice throughout development. In the ES, between E14.5 and E17.5, K<sub>endo</sub> was 15 mM and V<sub>t</sub> was -5 mV in HET and KO mice. At P0, K<sub>endo</sub> rose to 76 mM in HET and to 35 mM in KO mice and V<sub>t</sub> rose to -2 mV in HET and to +1 mV in KO mice. In conclusion, the onset of K<sup>+</sup> secretion appears to be just prior to birth. The delayed establishment of the adult ion composition in KO mice may be a function of the enlarged volume. Lumen formation, growth and enlargement of the inner ear is likely supported by NaCl-driven fluid secretion since endolymph in the embryonic inner ear is low in K<sup>+</sup> and presumably rich in Na<sup>+</sup> and Cl<sup>-</sup>.

Supported by KCALSI and CVM-SMILE.

#### **459 Otoacoustic Emission Through Waves on Reissner's Membrane**

Tobias Reichenbach<sup>1</sup>, Aleksandra Stefanovic<sup>1</sup>, A. J. Hudspeth<sup>1,2</sup>

<sup>1</sup>The Rockefeller University, <sup>2</sup>Howard Hughes Medical Institute

The cochlea not only acts as a detector of sound but can also produce tones itself. These otoacoustic emissions are a striking manifestation of the mechanical active process that sensitizes the cochlea and sharpens its frequency discrimination. It remains uncertain how these mechanical signals propagate back to the middle ear, from which they are emitted as sound. Although reverse propagation might occur through waves on the basilar membrane, experiments suggest the existence of a second component in otoacoustic emissions. We have combined theoretical and experimental studies to show that mechanical signals can also be transmitted by waves on Reissner's membrane, a second elastic structure within the cochlea. We have developed a theoretical description of wave propagation on the parallel Reissner's and basilar membranes and its role in the emission of distortion products. By scanning laser interferometry we have measured traveling waves on Reissner's membrane in the gerbil, guinea pig, and chinchilla. The results accord with the theory and thus support a role for Reissner's membrane in otoacoustic emission.

#### **460 Response Properties of the Otolithic Membrane from the Frog Sacculus**

Sebastian Meenderink<sup>1</sup>, Elliott Strimbu<sup>1</sup>, Asja Radja<sup>1</sup>, Dolores Bozovic<sup>1</sup>

<sup>1</sup>UCLA, Dept. of Physics & Astronomy

The sacculus is one of the end organs in the anuran ear. Its macula supports a few thousand hair cells that are responsible for the transduction of low-frequency vibrations (substrate/air borne) and has served as a model system in which to study the activity of hair cells and their bundles. When mechanically isolated from the overlying otolith membrane (OM), bundles often exhibit spontaneous

oscillations that result from an interplay between channel opening/reclosure and myosin-based adaptation of the transduction complex. The active hair bundle motility may act as the “cochlear amplifier” in non-mammalian species, and perhaps supplements somatic electromotility in the mammalian cochlea. *In vivo*, saccular hair cells are not mechanically isolated—the vast majority of cells are covered by the OM to which the hair bundles are attached. The presence of the OM significantly changes the hair-bundle dynamics: it abolishes spontaneous oscillations, reduces the sharpness of tuning, and linearizes responses. Here we present data on the mechanical response of OM from the frog sacculus, both under natural conditions (*i.e.* on top of the macula) and in isolation. A small glass fiber was partially inserted into the OM and used to deliver sinusoidal stimuli in one direction. In synchrony with the stimulus, high-speed videos were acquired from which the motion of the OM was extracted. Preliminary results on the elastic properties of the OM indicate that it moves in phase with the stimulus. The amplitude of OM movement gradually decreased with distance from the stimulus probe, but at a faster rate in the isolated OM, indicating sensitive dependence on the boundary conditions. Effectively, the coupling of hair bundles to the OM entrains the response of all hair cells in the sacculus to the impinging stimulus. Supported by NIH grant RO1 DC011380-01A1.

#### **461 Ototoxicity of the Cholesterol Chelator Hydroxypropyl- $\beta$ -Cyclodextrin in the Mouse**

Mark Crumling<sup>1</sup>, Li Qian Liu<sup>1</sup>, Paul Thomas<sup>1</sup>, Jennifer Benson<sup>1</sup>, Ariane Kanicki<sup>1</sup>, Karin Halsey<sup>1</sup>, David Dolan<sup>1</sup>, R. Keith Duncan<sup>1</sup>

<sup>1</sup>*Kresge Hearing Research Institute, University of Michigan*  
Cyclodextrins are cyclic oligosaccharides that can efficiently transport cholesterol. This property has been leveraged in several applications, including the use of hydroxypropyl- $\beta$ -cyclodextrin (HPbCD) as a treatment for the lysosomal storage disorder Niemann-Pick Type C disease (NPC). However, two lines of study suggest caution in the widespread use of HPbCD. First, hair cell excitability and cochlear mechanics are sensitive to membrane cholesterol (Brownell et al., 2011; Purcell et al., 2011). Second, wild-type and NPC cats treated with HPbCD exhibit increased auditory thresholds (Ward et al., 2010). To examine auditory system effects further, we studied the impact of HPbCD on auditory function in wild-type mice (FVB/NJ). Single subcutaneous injections of 8,000 mg/kg HPbCD were given to mice ~5 weeks of age. Age-matched controls were injected with saline. Auditory brainstem response (ABR) thresholds, measured one week after injection, were significantly greater in HPbCD treated mice than controls (30 dB greater for 4, 16, and 32 kHz tone bursts). Increases in ABR threshold were accompanied by decreases in DPOAE response, implicating a negative effect on the cochlear amplifier. Histological analysis of treated ears revealed a profound loss of outer hair cells with approximately 20% absent in the apex and up to 100% loss in the mid-cochlea to base. Prestin expression appeared normal in surviving OHCs from treated mice. Inner hair cell counts, spiral ganglion

cell counts, and gross morphology of the cochlear duct and stria vascularis were similar in treated and control ears. Filipin staining indicated that cholesterol levels were similar in treated and control ears one week after injection. Further study is required to identify the time course of cholesterol changes and the mechanisms of hair cell loss following HPbCD treatment. The results may point to approaches that preserve auditory function and thereby expand the potential use of HPbCD as a therapeutic tool.

#### **462 Proteomic Analysis of Luminal Fluid of the Endolymphatic Sac of Meniere's Disease Patients: Pilot Study for the Biomarkers of Meniere's Disease**

Sung Huhn Kim<sup>1</sup>, Jin Young Kim<sup>1</sup>, Se Ra Park<sup>1</sup>, Jae Young Choi<sup>1</sup>

<sup>1</sup>*Yonsei University*

**Objective:** This study was performed to identify unique proteins in luminal fluid of the endolymphatic sac of Meniere's disease patients.

**Materials and Methods:** Luminal fluid of the endolymphatic sac was sampled from control (n=2) and Meniere's disease patients (n=2) during acoustic tumor surgery via translabyrinthine approach and endolymphatic sac surgery, respectively. Protein profiles of each sample were analyzed with liquid chromatography-mass spectrometry (LC-MS/MS) technique followed by 1-DE. Then, proteins which exist only in the Meniere's disease were analyzed.

**Results:** Total 3114 proteins in control and 763 proteins in Meniere's disease were identified after LC-MS/MS. Total 465 out of 763 proteins was identified only in the luminal fluid of Meniere's disease. They can be classified as immunoglobulin variants including autoantibodies, complements, albumin variants, globin variants, protease inhibitor, transferrin variants, cellular structures, and enzymes participate in the various cellular process and functions. Among 465 proteins 26 proteins is likely to be the candidate for the biomarkers which have high protein scores, exist also in the plasma, and involved in the immunologic reactions as autoantibodies and in the fluid regulation as enzymes.

**Conclusion:** This is the first study which analyzed whole protein profile of luminal fluid of endolymphatic sac of Meniere's disease. There were unique proteins only exist in the Meniere's disease which suggests those proteins can be used as biomarker for the diagnosis of Meniere's disease.

#### **463 Mouse Strain Differences in Auditory Discrimination Learning**

Simone Kurt<sup>1</sup>, Günter Ehret<sup>1</sup>

<sup>1</sup>*University of Ulm*

Understanding neural mechanisms of brain plasticity due to motor, auditory and perceptual learning in mammals requires a reliable training and test apparatus, well controlled procedures for measuring learning progress as well as success in an easily accessible animal model. Here, we present a newly developed behavioral learning paradigm for auditory discrimination learning in mice using

a shuttle-box. We test discrimination of auditory stimuli, basic motor activity, the development of sensory-motor learning, reaction times (attention to stimuli and motivation to respond) and the time courses of the acquisition of motor and cognitive skills in genetically different mouse strains. Thus differences in motor performance, motivational backgrounds and in the ability for acquisition of perceptual (auditory) knowledge can be tested in a very efficient way. We show that certain strains are suitable, others unsuitable for this paradigm. Mice of a suitable strain can genetically be manipulated in order to test the specific influences of a certain gene on the mentioned parameters (behavioural phenotyping in the shuttle-box). The data presented will show how the shapes of learning curves express the above mentioned parameters measuring the development of motor and cognitive skills in different mouse strains. They demonstrate that the shuttle-box discrimination learning paradigm opens up a new window to study brain functions in mice via a behavioural approach.

#### **464 Central Auditory Processes, Cognitive Development and Reading in Hearing-Impaired and Deaf Children with Cochlear Implants or Hearing Aids**

Inger Uhlén<sup>1,2</sup>, Björn Lyxell<sup>3</sup>, Birgitta Sahlén<sup>4</sup>, Marianne Ors<sup>5</sup>, Cecilia von Mentzer<sup>3</sup>, Elisabet Engström<sup>1</sup>, Magnus Lindgren<sup>6</sup>, Petter Kallioinen<sup>7</sup>

<sup>1</sup>CLINTEC, Karolinska Institutet, <sup>2</sup>Dpt of Audiology and neurotology, Karolinska University Hospital, Stockholm, <sup>3</sup>Behavioral sciences, Linköping University, <sup>4</sup>Logopedy, phoniatriy and audiology, Lund University,

<sup>5</sup>Neurophysiology, Lund University, <sup>6</sup>Psychology, Lund University, <sup>7</sup>Phoniatrics, Stockholm University

Central auditory processes, cognitive development and reading in hearing-impaired and deaf children with cochlear implants or hearing aids.

Inger Uhlén, MD PhD and Elisabet Engström MD, CLINTEC, Karolinska Institute, Björn Lyxell, prof and Cecilia von Mentzer, Dpt of Behavioral Sciences, Linköping University, Petter Kallioinen, Dpt of Phonetics, Stockholm University, Birgitta Sahlén, PhD, Dpt of Audiology and Phoniatriy, Lund University, Marianne Ors, PhD, Dpt of Neurophysiology, Lund University and Magnus Lindgren, associate prof, Dpt of Psychology, Lund University

The present study will focus on cognitive development and central auditory processes in children with hearing aids and/or cochlear implants (CI). A specific purpose is to examine how an individually designed phonological intervention programme can affect neurophysiological development and development of cognitive and reading skills. The study is a longitudinal design, where the children are followed over a period of three years. Three groups of children are included in the study: children with CI, children with hearing-aids and normal hearing children. The children are between 5 to 7 years old when they enter the study. The phonological intervention is administrated via internet in the children's home and the actual training is

being managed by the parents, supported by a speech pathologist.

Language and cognitive skills have been tested with a protocol developed for children with hearing impairment. Event related potentials comprising MMN and N400 are components of central auditory processes that may correlate to behavioral skills. MMN is elicited by the optimum paradigm with five different deviants, while N400 uses congruent, within or between category violation of a word/picture combination. Preliminary results show that these components can be elicited children of all categories, with significant differences between the groups as well as for the different conditions. Further analysis will reveal the impact of training on central auditory processing.

#### **465 Behavioral Training Strengthens Intracortical Pathways in A1 That Mediate Response to Rewarded Tone**

Fei Guo<sup>1</sup>, Irakli Intskirveli<sup>1</sup>, David T. Blake<sup>2</sup>, Raju Metherate<sup>1</sup>

<sup>1</sup>University of California, Irvine, <sup>2</sup>Georgia Health Sciences University

Auditory behavioral training can alter the organization of primary auditory cortex (A1) in adults. However, the mechanisms underlying experience-dependent plasticity are not well understood. To address this issue, we trained adult rats to detect a 5 kHz tone in order to receive a food reward. After 14 days training, physiological mapping in a terminal experiment under urethane anesthesia confirmed that the 5 kHz characteristic frequency (CF) representation in A1 was expanded relative to naive control rats. We then placed a 16-channel silicon multiprobe in middle- (~10 kHz) and high- (~20 kHz) CF regions and obtained current-source density (CSD) profiles evoked by a range of tone stimuli (CF  $\pm$  1-3 octaves in 0.25 octave steps). Our goal was to determine the laminar profile of changes in the expanded 5 kHz region by determining "CSD receptive fields" (CSD-RFs), and infer changes to thalamocortical and/or intracortical inputs.

Behavioral training altered CSD-RFs at the 10 kHz, but not 20 kHz, site. At the 10 kHz site, current sinks evoked by a 5 kHz tone (the target stimulus) were enhanced in layer 2/3, but not layer 4, and the bandwidth of the layer 2/3 current sink RF was increased (20 dB above threshold); these results imply training-induced plasticity along intracortical pathways. The layer 4 current sink RF was not clearly separable into thalamocortical and intracortical components, but the results implied lesser, if any, changes to thalamocortical inputs. Finally, we related behavioral performance ( $d'$ ) to CSD changes in individual animals, and found a strong correlation between  $d'$  on the final day of training and the amplitude of the 5 kHz-evoked current sink in layer 2/3 ( $r^2 = 0.763$ ). The prediction of behavioral performance by the target stimulus-evoked current sink in layer 2/3 suggests that this intracortical pathway has particular importance for brain plasticity underlying learning.

**466 Representation of Cognitive and Motivational Aspects of Auditory Tasks in the Auditory Cortex of Macaques**

Michael Brosch<sup>1</sup>, Ying Huang<sup>1</sup>, Mikhail Babanin<sup>1</sup>, Elena Selezneva<sup>1</sup>, Henning Scheich<sup>1</sup>

<sup>1</sup>Leibniz Institut für Neurobiologie

More recent findings have demonstrated that auditory cortex also subserves functions other than sound perception and auditory memory. Here we addressed the question how procedural and motivational aspects of an audio-motor task affect neuronal firing in auditory cortex. Two long-tail macaques were trained to perform a simple audiovisual task switching paradigm in which subjects had to report, by bar release, the termination of an audiovisual stimulus. Procedural aspects of the task were singled out by requiring the subjects to attend either to the auditory modality or to the visual modality. Motivational aspects were singled out by having the subjects perform the two tasks with different sizes of rewards. Analysis of multiunit activity from several hundred recording sites in primary and secondary auditory fields revealed that both aspects were most strongly reflected in slow changes (in the order of seconds) of firing rate in auditory cortex. The slow firing changes typically started after onset of the audiovisual stimulus and continued throughout the entire duration of this stimulus. These changes were seen both when the monkeys attended to the auditory and to the visual modality, but were generally stronger and seen in more units in the former condition. Reward expectation was also reflected in the slope of the changes: typically, expectation of a large reward resulted in stronger firing changes than a small reward. Our results support and extend previous accounts of cognitive aspects of auditory cortex function.

**467 Simultaneous But Not Sequential Bilateral Lesion of Gerbil Auditory Cortex Does Not Extinguish Pre-Learned Discrimination Performance of Fast Amplitude Modulated Tones**

Manfred Depner<sup>1</sup>, Holger Schulze<sup>1</sup>

<sup>1</sup>University of Erlangen-Nuremberg

Fast periodic amplitude modulations (AM), which are perceived as "roughness" or virtual pitch, are an important characteristic of mammalian vocalizations like animal communication calls or human speech. In a previous study (Deutscher et al., *Neuroreport* 17, 2006) we demonstrated that bilateral ablation of auditory cortex (AC) eliminates the ability of gerbils to learn to discriminate between such AM differing in modulation frequency (fm). Here we demonstrate that this is not the case if AC hemispheres are ablated sequentially rather than simultaneous. Learning behavior and discrimination performance were studied using an aversive shuttle-box go/no go paradigm. Gerbils were trained for 15 days to discriminate between two AM tones with identical 2kHz carrier frequency and 160Hz or 320Hz fm, respectively. Afterwards animals received sequential ablation of the AC in both hemispheres, either in left-right or right-left order. Each cortical ablation was followed by 15 days of additional

training. Results were compared to sham lesioned control animals.

In contrast to simultaneous bilateral ablation of complete gerbil AC (cf. Deutscher et al., *Neuroreport* 17, 2006), sequential bilateral ablation did not lead to a comparable severe impairment of pre-learned discrimination performance. This was independent of the order of the ablation. Animal subgroups that received cortical ablation of left or right hemisphere first both showed no effect on discrimination performance.

Our results indicate that one AC is sufficient for maintaining learned discrimination performance of fast AM and the consecutive ablation of the second AC reveals a subcortical reorganization process that is triggered by the ablation of the first AC hemisphere and that needs one intact AC to preserve the ability to discriminate fast AM even after lesion of the second AC.

**468 Primary Auditory Cortex Encodes the Strength of Auditory Memory**

Kasia Bieszczad<sup>1</sup>, Norman Weinberger<sup>1</sup>

<sup>1</sup>University of California Irvine; Center for the Neurobiology of Learning and Memory

In addition to its neural code for the features of sound, the auditory cortex is now known to be a substrate for *auditory learning and memory*. Most extensively studied is the representation of tonal frequency in the primary auditory cortex (A1). Frequency-specific representational physiological plasticity develops when both animal and human subjects learn the behavioral relevance of sound-frequency. First discovered in studies of associative learning, local shifts in frequency receptive fields (Bakin & Weinberger, *Br. Res.*, 1990) can transform the global representation of frequency in the tonotopic A1 map to enlarge the representation of a signal tone-frequency. The amount of cortical increase in the signal's representational area is a direct function of the level of its acquired behavioral importance (Rutkowski & Weinberger, *PNAS*, 2005). A possible reason for signal-specific area gains in A1 to be so graded by signal-importance may be to strengthen memory for more important signals. We tested the memory-strength/area-gain hypothesis in groups of rats trained to respond to a signal-tone for water reward. Memory strength was determined by the resistance to behaviorally extinguish responses to the unrewarded signal. Greater gains in A1 area were indeed significantly positively correlated with an increased resistance to extinction, i.e., stronger memory. Furthermore, area gains that survived more extensive extinction training predicted the spontaneous recovery of the extinguished signal-specific behavior. Therefore, the amount of representational area of a signal-frequency in A1 appears to encode memory to link auditory cognition to action. As the amount of area gain can be controlled by training stratagems (Bieszczad & Weinberger, *Neurobiol. Learn. Mem.*, 2010), auditory cortical areal substrates of memory strength could be manipulated in treatments of auditory comprehension disorders and tinnitus.

Supported by NIH(NIDCD): DC-02938 and DC-010013 to NMW & DC-009163 to KMB.

### **469** Rising Vs. Falling Sweeps Categorization Modifies the Functional Properties and the Temporal Precision of Auditory Cortex Neurons

Quentin Gaucher<sup>1</sup>, Victor Adenis<sup>1</sup>, Chloe Huetz<sup>1</sup>, Boris Gourévitch<sup>1</sup>, Jean-Marc Edeline<sup>1</sup>

<sup>1</sup>CNPS, UMR 8195, Orsay, France

Over the last 20 years, many studies have described the receptive field reorganizations of auditory cortex neurons occurring when a particular sound frequency became significant. Surprisingly, not much is known about changes occurring in auditory cortex receptive fields when more complex sounds become significant.

In the present study, rats were trained in a shuttle box to discriminate between rising sweeps (used as CS+) and falling sweeps (used as CS-) in an aversive task (10 CS+ and 10 CS-/session). After achieving an initial discrimination up to 90% of correct responses in 10-20 sessions, rats were trained to generalize to 3 different sets of rising/falling sweeps used as CS+/CS-. When a new pair of CS+/CS- was introduced, the animals performance decreased to 60-70% but came back around 90% of correct responses in two training sessions. Spectro-temporal receptive fields (STRFs) of auditory cortex neurons were tested under urethane anesthesia after completion of behavioral training. In trained animals (n=5), the STRFs were larger both in bandwidth (2.75 vs. 1.95 octaves) and duration (20.23 vs. 11.04ms) than in control animals (n=4) and the response strength within the STRFs was higher (50.9 vs. 28.6 spikes). In trained animals, testing the cortical responses to the rising/falling sweeps used during the task revealed that the firing rate was significantly higher at the rising than at the falling sweeps, a difference not observed in recordings obtained in control animals. Also, the spike-timing reliability observed at the presentation of the rising and falling sweeps was higher in the trained animals than in the control animals. Altogether, these results indicate that a categorization between rising and falling sweeps affects both the basic STRF properties and the spike-timing reliability in responses to complex stimuli.

Supported by CNRS and ANR "Hearing Loss".

### **470** Physiological Mechanisms of Working Memory in the Auditory Cortex of Humans and Nonhuman Primates

Ying Huang<sup>1</sup>, Norman Zacharias<sup>1</sup>, Reinhard König<sup>1</sup>,  
Michael Brosch<sup>1</sup>, Peter Heil<sup>1</sup>

<sup>1</sup>Leibniz Institute for Neurobiology

Working memory refers to the processes used for temporarily storing information and is a fundamental prerequisite for our abilities to perform everyday functions. It involves a broad network of brain areas including sensory cortices. A role of auditory cortex at an early processing stage also appears likely because of the high accuracy of auditory working memory. Our study aims to identify physiological working-memory correlates in the auditory cortex. We use a convergent approach with

humans, where we monitor neural activity by means of magnetoencephalography (MEG), and in monkeys, where we record local field potentials (LFPs) and action potentials (APs).

Human subjects and macaque monkeys listened to sequences of two tones with different or identical frequencies (in humans 1.5 and 1.6 kHz, separated by a silent interval [delay] of 2 s; in macaques 1 and 3 kHz, delay of 800ms. In one condition, the target requiring a GO-response was a pair of low-frequency tones; thus subjects had to memorize the first tone only if its frequency was low, but not if it was high. In the second condition, the target was a pair of high-frequency tones, so subjects had to memorize the first tone only if its frequency was high.

In humans (n=12), the recorded magnetic fields were analyzed using a source model with several regional sources distributed throughout the brain. Two sources, one in each hemisphere, were seeded at the border of Heschl's gyrus and the planum temporale. In each hemisphere, this source was stronger, reflecting increased neural activity, during the delay period between the tones in the memory condition compared to the non-memory condition.

In macaque monkeys (n=2), LFPs and APs were recorded simultaneously from the right auditory cortex during task performance (of one monkey so far). In line with our results in humans, we found LFPs to be more negative during the delay period in the memory than in the non-memory condition. Differential firing in the two conditions and during the delay period was also found in about half of the multi-units.

Our results in both humans and macaques suggest that auditory cortex is involved in auditory working memory and that a potential neural correlate of this memory is sustained activity.

### **471** Lower Spectral Component and Fine Temporal Structure Are Important for Sound Discrimination Behavior of Guinea Pigs

Hisayuki Ojima<sup>1</sup>, Ken-Ichi Tabei<sup>2</sup>, Masato Taira<sup>1</sup>

<sup>1</sup>Graduate School, Tokyo Medical and Dental University,

<sup>2</sup>Division of Applied System Neuroscience, Nihon University School of Medicine

In the previous studies we showed that guinea pigs could be trained to discriminate one target natural sound from other non-target distracter sounds. The target natural sound was a step sound, sounded like a broadband noise (0.15 - 12 kHz), with the primary energy peak at a relatively low spectral position (0.64 kHz). It consisted of 14 similar segments. The training schedule was extremely simple and included the restricted diet and a standard conditioning with food. The conditioning, however, was conducted for 2 or 3 animals together so that animals learned to compete for approaching a reward site earlier than anyone else, like in a "first come, first served" policy.

In the present study, what acoustic parameters are critical for animals to identify the target sound has been examined by modifying acoustically the target sound once they reach the level in which they almost perfectly discriminate the target from the distracters. The modification included low-cut, high-cut, time-reversed, segment order-changed,

minor-segment eliminated, major-segment eliminated, and inter-segment gap expanded versions of the target sound. Of these, animals could dissociate the time-reversed version of the original target sound in almost all cases and low-cut version in most cases. Since, in the initial evaluation of sound identification by animals, the low-cut was made at a relatively higher spectral position (about 1.5 kHz), including the primary energy peak. In the present study, we further examined whether the primary energy peak was critical for animals to identify the target sound, by applying different types of low-cut versions of target, including and excluding the primary energy peak. Besides, since coarse temporal structure, i.e., segment order, was necessarily changed in the time-reverse processing of the target sound in the previous study, we attempted to apply a time-reversed sound in which the component segments were locally time-reversed without changing the overall segment order. Results showed that both new versions of modification could be dissociated from the original target by guinea pigs. It suggests that in our learning procedure, guinea pigs rely on lower spectral components even without the highest energy peak and fine, rather than coarse, temporal structure of sound for their sound identification.

#### **472 Neural Correlates of Pitch Discrimination During Passive and Active Listening**

**Jennifer Bizley**<sup>1</sup>, Kerry Walker<sup>2</sup>, Fernando Nodal<sup>2</sup>, Andrew King<sup>2</sup>, Jan Schnupp<sup>2</sup>

<sup>1</sup>University College London, <sup>2</sup>University of Oxford

We have obtained electrophysiological recordings from the auditory cortex of freely moving ferrets while they perform a pitch discrimination task. Neural data were obtained using microelectrode arrays (Neuralynx, WARP-16 devices), which were chronically implanted into the auditory cortex of ferrets, following methods adapted from those used by Eliades and Wang (2008). Neural signals were recorded from animals while they were tested, in twice-daily sessions, over the course of a year. Over this time period the electrodes were independently advanced through the auditory cortex approximately weekly. Animals were trained in a two-alternative forced choice task that required them to judge whether the second of two artificial vowel sounds (the “target”) was higher or lower in pitch than a preceding “reference” sound (Walker et al 2009). Local field potential (LFP) and spike data were recorded, both during the behavioral task, and immediately before or after, when the animal was passively listening to the same sounds. ROC analysis revealed that high and low pitch targets often differentially modulated the LFP power observed during the target sound. The LFP power was also often predictive of the animal’s behavioral response. In many cases the LFP power discriminated the animal’s judgment with a slightly greater accuracy than it did the pitch of the acoustic stimulus. We examined the timescale over which the LFP power became informative about either the pitch of the sound or the animal’s behavioral response and observed that choice probabilities emerged later in the neural response than stimulus sensitivity, which was

highest at the onset and offsets of the target sound. LFPs recorded in the same animals while they were either awake and passively listening, or asleep, differed considerably in their amplitude, shape and tuning from those recorded when the same animals were actively discriminating the target pitch. ROC analysis applied to responses collected in the passively listening animal frequently revealed these responses to be less informative about the target pitch than those recorded during behavior.

#### **473 Behavioral State Modulates Accuracy of Stimulus Reconstruction from Single-Trial Neural Activity in Auditory Cortex**

**Stephen David**<sup>1</sup>, Bernhard Englitz<sup>1</sup>, Jonathan Fritz<sup>1</sup>, Shihab Shamma<sup>1</sup>

<sup>1</sup>University of Maryland

Sensory behavior requires real-time readout of task-relevant information from the neural population response to a single stimulus presentation. We used linear decoding methods to investigate: (1) how the accuracy of sensory representations is affected by correlated neural noise and (2) how representations change as specific stimulus features become behaviorally relevant.

To study the effects of noise correlations, we recorded the simultaneous activity of groups of neurons (n=66 recordings, 2-10 neurons per experiment) in ferret primary auditory cortex (A1) during passive listening to a bandpass noise stimulus modulated by a naturalistic temporal envelope. We measured the accuracy with which the stimulus envelope could be reconstructed from single-trial responses using a linear decoder and compared this result to one obtained after shuffling responses of individual neurons across trials, thereby removing noise correlations. We found that shuffling systematically improved reconstruction accuracy (mean correlation between actual and reconstructed envelope: r=0.47 non-shuffled, 0.51 shuffled), reflecting an average decrease of about 15% in explained stimulus variance due to noise correlations. A second-order decoder that explicitly accounted for pair-wise correlated activity showed no improvement over the linear decoder, indicating little or no synergistic stimulus information in correlated A1 activity beyond what can be measured with a linear decoder.

To study the effects of behavior on the population code, we measured the activity of neural populations in A1 during a task that required the discrimination of amplitude modulated tones (12 Hz) from unmodulated pure tones, both with random carrier frequency (100 Hz to 8KHz). A linear classifier was used to decode the modulation rate and carrier frequency during behavior and during passive listening to the same sounds. Preliminary data from one animal (n=22 recordings) revealed that during the behavior, modulation rate could be classified with about 8% greater accuracy while carrier frequency could be classified with slightly worse accuracy. These results suggest that task-driven attentional modulation in A1 serves both to enhance the discriminability of task-relevant stimulus features and to diminish the discriminability of task-irrelevant features. Taken together, these findings demonstrate that intrinsic brain activity can influence the

accuracy of representations in A1 in ways that emphasize task relevant features.

#### **474 Robust Representation of Attended Speech in Human Auditory Cortex**

**Nima Mesgarani**<sup>1,2</sup>, Edward Chang<sup>1,2</sup>

<sup>1</sup>University of California San Francisco, <sup>2</sup>Keck Center for Integrative Neuroscience

A unique and defining property of human speech perception is the ability to robustly process speech sounds in the context of noisy and interference-filled acoustic conditions. A common, everyday condition is the multi-speaker environment where selective listening is required for listening, also known as the "cocktail party effect". The mechanism by which the human auditory system carries out sound processing under these conditions is largely unknown. An attractive mechanism for speech encoding in multi-speaker environments is the implementation of dynamic "top-down" modulation of attention towards the intended signal.

In this study, we used high-resolution intracranial direct recordings (electrocorticography) from the superior temporal gyrus (STG) in patients with intractable epilepsy in order to investigate the neural correlates of auditory selective attention. The behavioral paradigm was based upon the Coordinate Response Measure (CRM) corpus which is widely used for multi-speaker communications research. The patients are instructed to report the color and number associated with a call sign (e.g. "Tiger") in a mixture of two speakers, without knowing a priori which speaker will be the target in a given trial. We used stimulus reconstruction method from the high-gamma envelope of neural responses to investigate the encoding of the spectrotemporal features of attended speech.

The reconstructed spectrograms from the same acoustic sound mixture, but in two different attention conditions resembled the spectrogram of the target speaker in isolation, indicating an enhanced neural representation of the attended voice. In addition, using a linear classifier trained on the representation of single speakers, we successfully decoded the spoken words and the identity of the attended speaker from the responses to the mixture. We find that task performance is well predicted by a rapid increase in attention-modulated neural selectivity across both local single-electrode and population-level cortical responses. These findings demonstrate that the temporal lobe cortical representation of speech does not merely reflect the external acoustic environment, but instead correlates to the perceptual aspects relevant for the listener's intended goal.

#### **475 Antioxidants D-Methionine and L-Carnitine Modulate Neuronal Activity Through GABAergic Inhibition**

**Calvin Wu**<sup>1</sup>, Kamakshi Gopal<sup>1</sup>, Bibesh Shrestha<sup>1</sup>, Ernest Moore<sup>1</sup>, Guenter Gross<sup>1</sup>

<sup>1</sup>University of North Texas

We have reported previously that the antioxidants D-methionine (D-Met) and L-Carnitine (L-Car) are protective against cisplatin and pentylenetetrazol induced

neurotoxicity in auditory cortex networks (ACNs) growing in vitro. D-Met, a potential otoprotective agent that is currently in human clinical trial phase, protected ACNs from cisplatin-induced toxicity [1]. L-Car effectively reduced pentylenetetrazol-induced excitatory activity in the networks [2]. The underlying mechanism of action of this protection is still not fully understood. We have used networks derived from dissociated auditory cortices of mouse embryos grown on microelectrode arrays (MEAs) to functionally assay the pharmacological effects of D-Met and L-Car. The IC50 values were  $1.08 \pm 0.05$  mM and  $0.22 \pm 0.01$  mM, respectively, with efficacies of 100%. In the presence of 1.0 to 40  $\mu$ M bicuculline, a GABAA receptor antagonist, the sigmoidal concentration-response curves were shifted to higher values. With 40  $\mu$ M bicuculline, the IC50 of D-Met and L-Car were  $11.22 \pm 0.96$  mM and  $3.57 \pm 0.26$  mM, with no change in efficacy. The dissociation constant (KB) for bicuculline under D-Met titration was 0.92  $\mu$ M. The more than 10-fold increase in IC50 values under bicuculline suggests that D-Met and L-Car modulate neuronal activity through GABAA receptors. The GABAA receptor site may serve as an efficacious drug target for neuroprotective agents to regulate over-excitation.

[1] D-methionine protects against cisplatin-induced neurotoxicity in auditory cortex networks in vitro. Association for Research in Otolaryngology 24th Annual Midwinter Meeting. 2011, February 19-23, pp 151-152, Baltimore, MD.

[2] An in vitro model for testing drugs to treat tinnitus. Eur J Pharmacol (2011) 667:188-94.

#### **476 Hyperacusis: Evidence for Cortical Disinhibition**

Andrew Norris<sup>1</sup>, **Borka Ceranic**<sup>2</sup>, Paul Radomskij<sup>2</sup>, Sudhagar Kuttva<sup>2</sup>

<sup>1</sup>Department of Otolaryngology, St George's Hospital, London, U.K., <sup>2</sup>Department of Audiovestibular Medicine, St George's Hospital, London, U.K.

One possible pathophysiological mechanism underlying hyperacusis is disinhibition at the cortical level that increases the gain of the afferent auditory signal. To investigate this hypothesis, a study was conducted, involving 12 patients and 13 controls, who underwent auditory testing, including recording of transient evoked otoacoustic emissions (TEOAEs) and cortical evoked auditory responses (CERA) potentials. The medial olivocochlear (MOC) suppression test and recording of the stapedial reflexes ascertained the absence of any distal efferent pathology.

CERA: characteristics of the N1-P2 component elicited by binaural presentation of repetitive 1000Hz tone bursts delivered in 3 successive blocks of 40 averaged responses at 40, 50, 60 and 70 dB SL were examined, including N1-P2 amplitudes, change in N1-P2 amplitude between blocks, N1 and P2 latencies, change in N1 and P2 latency between blocks and the N1 and P2 latency/stimulus intensity relationship.

The preliminary results of this study indicated a consistent trend for larger N1-P2 amplitudes in the patients' group at every intensity, with statistical significance for the three-

block global average value at 60dB, with higher values in patients than controls ( $p=0.01$ ). The intra-group analyses showed increased P2 latencies between blocks in patients at 40 dB SL, with marginal significance ( $p=0.05$ ). The inter-group analyses indicated marginally longer P2 latencies in patients in block 1 at 60 dB SL ( $p=0.06$ ), while significantly longer in patients than in controls for the global average at 60 dB SL ( $p=0.04$ ).

TEOAE responses in patients with hyperacusis had a tendency of the larger amplitudes and wider range than in the control group.

These preliminary findings support the hypothesis that hyperacusis is a manifestation of an increased gain in the auditory system, as a result of cortical disinhibition.

#### **477 GABA Shapes SAM Response Properties in Rat Medial Geniculate Body**

Rui Cai<sup>1</sup>, Donald Caspary<sup>1</sup>

<sup>1</sup>*Department of Pharmacology, Southern Illinois University School of Medicine*

Recent studies by Bartlett and Wang (2007, 2011) indicate that in response to amplitude modulated and high-rate click stimuli, medial geniculate body (MGB) neurons display unique, more complex response properties relative to those observed at lower levels of the auditory neuraxis. Responses to modulated stimuli include neurons that display combinations of synchronized and non-synchronized responses often producing unique, "V" or "M" shaped rate modulation transfer functions (rMTFs). The present study used iontophoretic application of the GABA<sub>A</sub> receptor (GABA<sub>A</sub>R) agonists (GABA & gaboxadol) and the antagonist (gabazine) to examine the putative role of GABA inhibition in shaping MGB response properties to modulated stimuli. Tonal and broadband noise sinusoidally amplitude modulated (SAM) stimuli were used to generate rMTF from isolated single neurons and occasional small clusters in MGB. Consistent with previous studies in awake marmoset, three major response types were observed in response to SAM stimuli in the urethane anesthetized rat: synchronized, non-synchronized, and mixed. GABA<sub>A</sub>R blockade or activation of MGB GABA<sub>A</sub>Rs finds that both synchronized and non-synchronized responses could be selectively altered. GABA<sub>A</sub>R blockade selectively enhanced synchronized activity near best modulation frequency especially in neurons with a clear rate-modulation peak. GABA<sub>A</sub>R blockade in neurons showing mixed and non-synchronous responses at high modulation frequencies often exhibited enhanced responses at higher modulation frequencies with little or no change at the rMTF minima. GABA application in this population of neurons suppressed either or both the high asynchronous and/or low synchronous portion of the rMTF. These preliminary data suggest that the major inhibitory inputs to MGB from IC and the thalamic reticular nucleus likely contribute to the generation of the complex responses to SAM stimuli seen in auditory thalamus.

Supported by NIH DC000151.

#### **478 Cortical Projections from Auditory and Visual Cortex to the Superior Colliculus of the Cat**

Nicole Chabot<sup>1</sup>, Ameer J. McMillan<sup>2</sup>, Stephen G. Lomber<sup>3,4</sup>

<sup>1</sup>*University of Western Ontario, Department of Physiology and Pharmacology*, <sup>2</sup>*University of Western Ontario, Department of Anatomy and Cell Biology*, <sup>3</sup>*University of Western Ontario, Department of Physiology and Pharmacology*, <sup>4</sup>*The Center for Brain and Mind*

The superior colliculus (SC) is critical for the accurate guiding of the head and eyes to both visual and acoustic stimuli. This study compared similarities and differences in the origins of the visual and auditory corticotectal projections to the SC. To accomplish this, we unilaterally deposited wheat-germ agglutinin conjugated to horseradish peroxidase (WGA-HRP) into the SC of five mature cats (>6M). Three days later, the animals were perfused with PBS and brains fixed with a solution of 1% glutaraldehyde mixed with 1.5% of paraformaldehyde. Following cryoprotection in 30% sucrose, brains were cut, 60 microns thick, in the coronal plane. One series (every fifth section) was reacted for the presence of the neuronal tracer using TMB. An adjacent series was reacted with DAB. Two other series were reacted to reveal the presence of Nissl bodies and cytochrome oxidase. Labelled cells were plotted using NeuroLucida. In visual cortex, large numbers of labelled neurons were identified in the infragranular layers of area 17, area 18, and the visual areas of the middle suprasylvian sulcus. All of these areas have been identified to contribute to accurate orienting to a visual stimulus. In contrast, auditory cortex possessed no or very few labelled neurons in areas involved in acoustic orienting, namely primary auditory cortex, the dorsal zone of auditory cortex, and the posterior auditory field. The vast majority of the labelled neurons were found in the infragranular layers of the auditory field of the anterior ectosylvian sulcus. Overall, these results show significant differences in the visual and auditory pathways to the SC. In visual cortex, each area that plays a significant role in visual orienting has a direct projection to the SC, while in auditory cortex most areas that play a significant role in acoustic orienting do not have a direct projection to the superior colliculus.

#### **479 Noradrenergic Modulation of Spectrotemporal Receptive Fields (STRF) and Responses to Vocalizations in the Guinea Pig Auditory Cortex**

Quentin Gaucher<sup>1</sup>, Boris Gourévitch<sup>1</sup>, Chloé Huetz<sup>1</sup>, Jean-Marc Edeline<sup>1</sup>

<sup>1</sup>*CNRS, UMR 8195, Univ. Paris-Sud, Orsay, France*

Over the last years, several studies have established that auditory cortex neurons respond to communication sounds by temporal spike patterns displaying a high trial-to-trial reliability. In a previous study, we investigated how spectrotemporal receptive fields and responses to conspecific vocalizations are modulated by cortical inhibitions. A partial blockage of GABA<sub>A</sub> receptors by gabazine application (10 $\mu$ M) expanded the cortical STRFs

in the spectral and temporal domains and, as expected, increased the firing rate to communication sounds. Unexpectedly, it also increased the spike timing reliability of cortical responses during presentation of conspecific and heterospecific vocalizations. These effects were not observed with a partial blockage of GABAB receptors. Here, we evaluated to what extent the noradrenergic system modulate the (i) cortical STRFs and (ii) responses to natural sounds. Phenylephrine (PHE,  $\alpha$ 1 agonist) and Isoproterenol (ISO,  $\beta$  agonist) were topically applied in the primary auditory cortex of urethane anesthetized guinea pigs while recording multiunit activity via 16 channel electrode arrays. PHE reduced for about 30 minutes the cortical STRFs (both in terms of bandwidth and of duration) and decreased the responses evoked by vocalizations. In contrast, ISO expanded the STRFs in the spectral and temporal domains and it increased the responses to vocalizations. Both PHE and ISO decreased the spike timing reliability. These results indicate that  $\alpha$ 1 and  $\beta$  noradrenergic receptors act in opposite directions to control the cortical STRFs and the responses to communication sounds, but in our experimental conditions, they did not increase the temporal precision of neuronal responses at presentation of communication sounds.

#### **480 Functional Connections Between Dopaminergic Midbrain and Auditory Cortex in the Macaque Monkey**

Judith Mylius<sup>1</sup>, Jonathan Lovell<sup>1</sup>, Michael Brosch<sup>1</sup>

<sup>1</sup>Leibniz Institut für Neurobiologie

This study concerns effects of dopaminergic midbrain on neuronal activity in the auditory cortex of primates. It was motivated by recent findings that activation of auditory cortex is related to motivational and cognitive aspects of auditory tasks. Here we tested how electrical stimulation of ventral tegmental area and adjacent midbrain regions affected local slow wave field potentials and discharges in auditory cortex and cortical zones dorsal and ventral thereof. We found that stimulation with 6-ms trains of brief 100- $\mu$ A biphasic pulses resulted in electrically evoked potentials (EEPs) that consisted of several waves within the range of 20 to 500 ms. Similarly shaped EEPs could be observed from different regions in the midbrain, spanning a range of maximally 5 to 7 mm. In some regions the shape of EEP could be grossly and reversibly changed by subcutaneous injection of the D1-receptor antagonist Schering 23390, demonstrating an involvement of the dopaminergic subpopulation in the generation of the EEPs. The shape of the EEPs was similar in parietal and temporal cortex, suggesting that midbrain activation is broadcast into various cortical fields. Since we were also able to evoke action potentials in cortex by electrical stimulation we conclude that midbrain can also provide suprathreshold drive for cortical neurons. Our results suggest functional connections of dopaminergic cells in the ventral tegmental area with auditory cortex, which may contribute to motivational and cognitive functions of cortex.

#### **481 Receptive Field Analysis of Nearby Neurons in Cat Primary Auditory Cortex**

Craig Atencio<sup>1</sup>, Christoph Schreiner<sup>1</sup>

<sup>1</sup>UCSF

Primary auditory cortex (AI) is composed of circuits that are characterized by corticocortical and interlaminar connections. In these circuits, receptive field parameters may vary across layers, though the variability within layers has not been quantified. We addressed this by both presenting a dynamic moving ripple stimulus and recording from single units using a linear sixteen channel probe that was orthogonally oriented to the cortical surface. We then reconstructed spectrotemporal receptive fields (STRFs). From the recordings we identified channels where pairs of single units had been obtained, and then compared the STRF parameters of these pairs. We found that best frequency was highly similar across the population. Likewise, latency was highly similar, though differences in latency became greater in infragranular layers. Sharpness of tuning showed some variability, with the greatest differences in infragranular layers. STRF similarity was moderate for pairs, while firing rate and phase-locking to the ripple stimulus were similar. Best temporal and spectral modulation frequency were similar for pairs, with a similar degree of variability in different layers. Our results show that within short distances, best frequency is relatively preserved within cat AI. Other parameters, however, may be moderately variable, perhaps indicating that once tonotopy is ordered, the demands of other behavioral constraints may shape the connectivity of the cortical circuit.

#### **482 Laminar Organization of Frequency and Intensity Processing in Primary Auditory Cortex and the Influence of Dopaminergic Neuromodulation**

Max F.K. Happel<sup>1,2</sup>, Marcus Jeschke<sup>1</sup>, Frank W. Ohl<sup>1,2</sup>

<sup>1</sup>Leibniz-Institute for Neurobiology, Magdeburg, Germany,

<sup>2</sup>Otto-von-Guericke University, Magdeburg, Germany

We previously showed that within primary auditory cortex (AI) of Mongolian gerbils polysynaptic corticocortical connections mediate excitatory and inhibitory interactions between cortical columns across broad cortical space (Happel et al. 2010, Moeller et al. 2010). This allows a highly precise temporal convergence of thalamocortical and horizontal inputs important for spectral integration (Happel et al., 2010), potentially implying a level-independent mechanism. Within a cortical column, current-source-density (CSD) analysis revealed that purely stimulus-driven aspects of cortical processing in anaesthetized animals mostly involve synaptic activation of granular input layers III/IV and upper layers I/II. However, studies using intracortical microstimulation (ICMS) demonstrated effective modulation of cortical circuits by activity in infragranular layers. Specifically, ICMS combined with cortical silencing suggested a local fast-acting excitatory cortico-thalamocortical loop originating from deeper layers, reentering granular cortical input layers. Activation of this recurrent corticothalamic loop,

measurable by the strength of infragranular sink activity, correlated with behavioral detection learning of ICMS. To further investigate the role of infragranular synaptic circuits in AI, we modulated their responsiveness by systemic application of dopamine agonists, since D1/D5 receptors in gerbil AI are predominantly located on pyramidal cells in layers V/VI. Dopamine facilitated early, intracolumnar input processing by increasing short-latent infragranular sink activity and subsequent prolonged activation of other layers. We propose that dopamine-modulation within primary sensory cortex supports a more salient representation of biologically significant stimuli by a mechanism of learning-induced gain control of corticothalamic interactions.

#### **483 Using PET Imaging and Autoradiography to Link Brain Nicotinic Acetylcholine Receptors to Cognitive Function in Rat**

**Raju Metherate**<sup>1</sup>, Kasia Bieszczad<sup>1</sup>, Ritu Kant<sup>1</sup>, Cristian Constantinescu<sup>1</sup>, Hideki Kawai<sup>1</sup>, Norman Weinberger<sup>1</sup>, Jogeshwar Mukherjee<sup>1</sup>

<sup>1</sup>University of California, Irvine

Nicotinic acetylcholine receptors (nAChRs) in the brain are important for cognitive function; however, their specific role in relevant brain regions remains unclear. In this study we use the novel compound 18F-nifene to examine the distribution of nAChRs in the rat forebrain, and for individual animals relate the results to behavioral performance on an auditory-cognitive task. We first show negligible binding of 18F-nifene in mice lacking the  $\beta 2$  nAChR subunit, consistent with previous findings that 18F-nifene binds to  $\alpha 4\beta 2^*$  nAChRs. We then examined the distribution of 18F-nifene in rat using three methods: in vivo PET, ex vivo PET and autoradiography. Generally, 18F-nifene labeled forebrain regions known to contain nAChRs, and the three methods produced similar relative binding among regions. Importantly, 18F-nifene also labeled some white matter (myelinated axon) tracts, most prominently in the temporal subcortical region that contains the auditory thalamocortical pathway. Finally, we related 18F-nifene binding density in several forebrain regions to each animal's performance on an auditory-cued, active avoidance task. The strongest correlations with performance after 14 days training were found for binding density in the temporal subcortical white matter, subiculum and medial frontal cortex (correlation coefficients,  $r > 0.8$ ). These findings suggest that individual performance is linked to nicotinic functions in specific brain regions, and further support a role for nAChRs in sensory-cognitive function.

#### **484 Hijacking Neural Oscillations to Reveal Control of Auditory Attention**

**Hari Bharadwaj**<sup>1</sup>, Adrian K C Lee<sup>2</sup>, Barbara G Shinn-Cunningham<sup>1</sup>

<sup>1</sup>Department of Biomedical Engineering, Boston University,

<sup>2</sup>Institute for Learning and Brain Sciences (I-LABS), University of Washington

Frequency tagging of sensory inputs (presenting stimuli that fluctuate periodically at rates tracked by cortex) is often used to study attentional modulation of neural responses. In a visual scene, the visual steady-state response (VSSR) at the frequency modulating an attended object is enhanced, while the VSSR to a distracting object is suppressed. However, attention causes less consistent effects on the auditory steady-state response (ASSR). Here, we measure how spatially directed attention modulates the ASSR in different neural regions when listeners hear two competing binaural speech streams, each modulated at a different frequency around 40 Hz. Using a whole brain cortically constrained distributed source localization approach, we find that in contralateral auditory cortex, attention enhances the ASSR power at the frequency of an attended stream. The attended-stream modulation frequency also drives phase-locked responses in left precentral sulcus (IPCS), overlapping with the left Frontal Eye-Fields (FEF) an area known to control eye gaze and spatial attention; importantly, this region shows no phase-locking to the distracting stream. Our results show that auditory cortex communicates with FEF in an attention-specific manner. Moreover, the neural activity pattern helps explain why past auditory studies, most of which used dichotic rather than binaural stimuli and analyzed results in sensor space or using dipoles rather than in source space, produced inconsistent results.

#### **485 Changing Microcircuits in the Subplate of the Developing Auditory Cortex**

**Sarada Viswanathan**<sup>1</sup>, Patrick Kanold<sup>1</sup>

<sup>1</sup>University of Maryland

Changing microcircuits in the subplate of the developing auditory cortex

Subplate neurons (SPNs) are a population of neurons in the mammalian cerebral cortex that exist predominantly in the prenatal and early postnatal period. Loss of SPNs prevents the functional maturation of the cerebral cortex. SPNs receive subcortical input from the thalamus and relay this information to the developing cortical plate and thereby can influence cortical activity in a feed-forward manner. Using transgenic animals we studied the morphology of SPNs and find that subsets of SPNs extend dendrites into the cortical plate. Little is known about potential feedback projections from the cortical plate to SPNs. We thus investigate the spatial distribution of intracortical synaptic inputs to SPNs in vitro in mouse auditory cortex by photostimulation. We find that subclasses of SPNs receive inputs from deep as well as superficial layers including layer 4. We find that superficial cortical inputs to SPNs emerge in the 2nd postnatal week. Our data thus suggests that distinct circuits are present in the subplate and that while SPNs participate in an early

feed-forward circuit they are also involved in a feedback circuit at older ages. Together our results show that SPNs are tightly integrated into the developing thalamocortical and intracortical circuit.

#### **486 Cellular Properties and Microcircuit Architecture of Corticocollicular Neurons**

Jason W. Middleton<sup>1</sup>, Gordon M. G. Shepherd<sup>2</sup>, Thanos Tzounopoulos<sup>1</sup>

<sup>1</sup>Department of Otolaryngology, University of Pittsburgh,

<sup>2</sup>Department of Physiology, Northwestern University

Information processing in the auditory system involves a bidirectional flow of signaling. Acoustic signals that originate in the sensory periphery (i.e., inner ear) travel to the cerebral cortex and form the bottom-up pathway. Moreover, signals originating in the cortex are transmitted in the reverse direction and form the top-down pathway. While many anatomical and functional studies have focused on the bottom up pathway, the cellular properties and synaptic connectivity of the top-down pathway remain largely unknown. Here we characterized the intrinsic properties and microcircuit architecture of auditory cortical neurons that project to the inferior colliculus (IC). Cortical cells projecting to the IC (corticocollicular) were labeled by injecting fluorescent retrograde tracers in the IC. This labeling revealed two distinct projection neurons: one localized in layer 5B (L5B) and one in layer 7 (L7). We used a combination of whole cell recording and laser scanning photostimulation (LSPS) techniques to study the intrinsic properties and the microcircuit organization of corticocollicular neurons. L5B corticocollicular neurons receive excitatory inputs from supragranular layers (L2/3) while L7 corticocollicular neurons receive much weaker local input. However, the intrinsic physiological properties of both cell classes are similar. They both exhibit significant hyperpolarizing-activated inward current (I<sub>h</sub>) and adapt very slowly in response to depolarizing current injection. Our findings reveal the existence of parallel cortical top-down circuits that project to the IC. Elucidating the cellular properties and the functional anatomy of top down auditory circuits will contribute significantly towards the understanding of normal and pathological auditory processing.

#### **487 Matching Spontaneous and Evoked Activity in Auditory Cortex for Natural Stimuli: Evidence for Probabilistic Inference**

Stephen David<sup>1</sup>, Bernhard Englitz<sup>1</sup>, Ralf Haefner<sup>2</sup>, Pietro Berkes<sup>2</sup>, Gergo Orban<sup>2</sup>, Mate Lengyel<sup>3</sup>, Shihab Shamma<sup>1</sup>, Jonathan Fritz<sup>1</sup>, Jozsef Fiser<sup>2</sup>

<sup>1</sup>University of Maryland, <sup>2</sup>Brandeis University, <sup>3</sup>Cambridge University

Neuronal responses in the sensory cortices of awake animals exhibit highly structured variability, both during evoked activity (EA) and spontaneous activity (SA). A previous study of neural activity in V1 showed that neural response variability in EA and SA, rather than a pesky nuisance, may be a hallmark of statistical inference carried out by visual cortex (Berkes et al., 2011), and suggests that variability represents uncertainty about stimuli, and

that cortical activity patterns are samples from an internal, probabilistic model of the environment. EA can be interpreted as representing samples from the posterior probability distribution of possible causes underlying sensory input. In the absence of a stimulus, this probability distribution reduces to the prior expectations assumed by the internal model as reflected by SA. If EA and SA represent samples from the same model of the environment, then the distribution of SA should be identical to that of EA averaged over natural stimuli.

In this study, we test two predictions of this Bayesian framework for sensory cortical responses: (1) results should be valid in auditory as well as visual cortex, (2) the match between evoked and spontaneous activity should be specific to the distribution of neural activity evoked by natural stimuli, but not to that evoked by artificial stimulus ensembles. To test these predictions, we analyzed single-multi-unit data (N=110 over 26 recordings) recorded simultaneously from multiple electrodes in A1 and secondary auditory cortex (tonotopic areas PPF and PSF (Bizley et al., 2005)) of awake ferrets in three stimulus conditions: a natural stimulus (continuous speech), white noise (0-20 kHz) artificial stimulus condition, and a spontaneous activity condition where the animal was listening in silence. We measured dissimilarity between the silence and stimulus condition distributions using Kullback-Leibler divergence. In agreement with predictions, we found that the distribution of speech-evoked activity is consistently more similar to SA than the distribution of noise-evoked activity both for the instantaneous distribution of activity and for transition probability. These results provide new evidence for cortical adaptation to natural stimuli and also provide support for the sampling hypothesis (Fiser, 2010).

#### **488 Sound Frequency Encoding by Small Populations of Auditory Cortical Neurons: An Information Theoretic Analysis**

Martin Pienkowski<sup>1</sup>, Jos Eggermont<sup>1</sup>

<sup>1</sup>University of Calgary

The tuning curve (TC) is a common descriptor of how the sensory neuron response varies with some stimulus parameter. An important issue is which region of the TC is most informative about the stimulus, i.e., which of the possible responses reduces the most uncertainty about the stimulus that was presented. A recent information theoretic analysis (Butts and Goldman, 2006) revealed that when neuronal variability (in response to the same stimulus) is high, only the strongest responses stand out above the "noise", making stimuli at the peak(s) of the TC most distinguishable. As the variability decreases and finer discrimination becomes possible, the steeply-sloping regions of the TC become increasingly informative. When the variability drops sufficiently low, the sloping regions encode stimuli more efficiently than peak regions.

An analysis of sound frequency TCs of individual primary auditory cortical (AI) neurons shows that firing rates are highly variable and maximal information is always conveyed at the tuning curve peaks (Montgomery and Wehr, 2010). However, studies of the representation of

interaural timing differences (Harper and McAlpine, 2004), sound frequency (Han et al., 2007) and sound intensity (Dean et al., 2005) have suggested that neural *populations* represent auditory stimuli most effectively using their tuning curve slopes, not peaks. These analyses, however, were based on sequential recordings and assumed that "noise" spike activity was uncorrelated across neurons. They also employed the Fisher information metric, which breaks down for small neural populations. Here, we analyze the sound frequency information encoded by 1-32 simultaneously recorded auditory cortical neurons, to determine the conditions under which small neural populations transition from best discriminating between stimuli that elicit the maximum response to those that fall at the flanks of the tuning curve.

#### **489** Tonotopic Organization of Posterolateral Superior Temporal Gyrus in Humans: Task Modulation and Implications for Complex Sound Processing

Mitchell Steinschneider<sup>1</sup>, Kirill Nourski<sup>2</sup>, Hiroyuki Oya<sup>2</sup>, Hiroto Kawasaki<sup>2</sup>, Matthew Howard<sup>2</sup>

<sup>1</sup>Albert Einstein College of Medicine, <sup>2</sup>University of Iowa

Intracranial recordings reveal that the posterolateral portion of the superior temporal gyrus (PLST) in humans is responsive to a broad array of sounds, is tonotopically organized (see abstract by Nourski et al.), and may harbor multiple, distinct fields. Here, we sought to: 1) characterize the relationship between patterns based on pure-tone responses and differential sensitivity to more complex stimuli, and 2) investigate modulation of cortical activation patterns by the subject's participation in a behavioral task. Experiments were performed in patients being evaluated for surgical remediation of medically intractable epilepsy. The patients were implanted with high density subdural grid electrodes centered over perisylvian cortex. All procedures were IRB and NIH-approved, and all patients gave informed consent prior to their study participation. Experimental stimuli were pure tones (250-8000 Hz), bandpass noise (BPN) bursts, trains of acoustic clicks, and consonant-vowel (CV) syllables. The stimuli were delivered diotically during passive-listening experiments and in a target detection task. Responses were characterized by the averaged evoked potential and high gamma (75-150 Hz) event-related band power.

Responses to BPN paralleled the patterns defined by pure-tone responses, particularly at higher BPN center frequencies. Click trains elicited responses with a tonotopically-arranged profile, wherein higher click rates engaged sites most responsive to lower frequency tones. Responses to CV syllables that varied along consonant place of articulation exhibited some degree of tonotopically-driven patterns. Tone- and BPN-elicited responses were generally stronger to target than non-target stimuli.

Spectral specificity of tone-evoked responses within PLST is an important factor in determining responses to more complex sounds. Ongoing analyses future experiments will refine the associations observed between PLST activation patterns elicited by simple and complex sounds. Supported

by NIH RO1-DC004290, UL1RR024979, and the Hoover Fund.

#### **490** Context-Dependent Modulation of Auditory Responses in the Mouse Amygdala

Jasmine Grimsley<sup>1</sup>, Sharad Shanbhag<sup>1</sup>, Jeffrey Wenstrup<sup>1</sup>

<sup>1</sup>Northeastern Ohio Medical University

Adult female mice produce the same vocal call during courtship behavior and during fearful situations. We investigated whether amygdalar responses to this call are modulated by the context in which the call is presented. Neurons were recorded wirelessly from awake, freely moving male CBA/CAJ mice that were implanted with bundles of 15 drivable electrodes. We obtained responses to the vocal call (72 ms, 1/s) and noise bursts (30 ms, 1/s) over a range of sound levels. Responses were recorded under a neutral-odor condition and then during the presence of predator odor. Both suppressive and excitatory responses to the acoustic stimuli were common, with many neurons exhibiting excitation that persisted beyond the duration of the stimulus. In many cases, acoustic responses differed with the odor context. In 20 single-unit and 69 multi-unit responses, we used mutual information (MI) to compare the amount of contextual information in the spike trains, analyzed in 50-ms time bins. Units that responded to the vocal call carried significantly more contextual information than units that did not respond to these calls (45/89 responded [14 single units], mean MI = 0.19 bits vs. MI = 0.08 bits;  $F(1, 87) = 16.5$ ,  $p < 0.001$ ). Units that responded to noise also carried more contextual information than noise unresponsive units (45/89 responded [11 single units], mean MI = 0.18 bits vs. MI = 0.09 bits;  $F(1, 87) = 10$ ,  $p = 0.002$ ). Single and multiple unit responses showed the same pattern of modulation. Contextual information in noise responses tended to occur within the onset portion of the response while contextual information in the responses to the vocal call tended to occur within the prolonged portion of the response. Thus, odor-context modulated responses to the social call differently than responses to artificial, neutral stimuli.

Supported by NIDCD grant R01 DC000937

#### **491** Breaking Down the Cortical Representations of Speech in LFP and MUA

Nai Ding<sup>1</sup>, Shihab A. Shamma<sup>1</sup>, Jonathan Z. Simon<sup>1</sup>, Stephen V. David<sup>1</sup>

<sup>1</sup>University of Maryland, College Park

The neural coding of sound in auditory cortex has been investigated extensively using various neural measures, including multi-unit activity (MUA), local field potential (LFP), and magneto-/electroencephalography (MEG/EEG). These measures reflect neural activity at different spatial scales and are available from different experimental populations, e.g. animal models, epileptic patients, and healthy human subjects. Although these neural signals are complementary, their results are difficult to bring together, since the functional relationship between them is still poorly understood. In fact, response properties measured

from these signals, such as latency and the upper frequency limit of phase locking, are often not consistent with each other.

This study characterizes and compares the cortical representation of speech in MUA, high gamma power, and low-frequency phase-locked LFP. Recordings were made using high impedance electrodes in the primary auditory cortex (A1) of awake ferrets. All neural signals were analyzed under the unified framework of the spectrotemporal receptive field (STRF). Several consistent results were found. (1) STRFs estimated from MUA decay within 50 ms, whereas those estimated from phase-locked LFP last more than 100 ms, which may explain the long latency responses found in MEG/EEG studies. (2) STRFs are very similar whether measured by high gamma power or MUA. (3) Phase locking to the fast modulations of speech (70-200 Hz) is strong for LFP measures, but very weak in the corresponding MUA measures. (4) The neural tracking of fast modulations in LFP is largely independent of the neural tracking of slow modulations (<50 Hz).

These results suggest that neural signals in auditory cortex can be attributed to two major processes. The high gamma power is closely related to MUA and spiking within the local region. The phase-locked LFP contains several separated components, probably reflecting contributions from both thalamic and cortical inputs to A1.

#### **492 Sharp LFP Tuning Revealed by Component Analysis in Guinea Pig Auditory Cortex**

**Alain de Cheveigné**<sup>1</sup>, Jean-Marc Edeline<sup>2</sup>, Quentin Gaucher<sup>2</sup>, Boris Gourévitch<sup>2</sup>

<sup>1</sup>CNRS / ENS / Université Paris Descartes, <sup>2</sup>CNRS, UMR 8195, Univ. Paris-Sud, Orsay, France

Local field potentials (LFP) recorded in the auditory cortex of mammals often have spectrotemporal receptive fields (STRFs) that are less selective than unit activity recorded on the same electrode. This may in part reflect the wider "listening sphere" of LFPs relative to spikes due to the greater current spread at low frequencies, suggesting that neural sources underlying LFPs might be more narrowly tuned than usually assumed. We recorded LFPs and spikes from auditory cortex of guinea pigs using 16-channel electrode arrays. LFPs were processed by a component analysis technique known as denoising source separation (DSS), that produces optimally-tuned linear combinations of electrode signals. Linear combinations were found to have sharply tuned responses, closer to spike-related tuning, whereas the LFP signals of individual electrodes had a tuning that was broad and often multimodal. This result is consistent with two distinct hypotheses. The first is that neural sources underlying the LFPs are better tuned than the signals observed at the electrodes, the component analysis analysis having partially succeeded in "demixing" them. The second, more conservative, is that the tuning is latent in the activity sampled by the electrodes, in the sense that a neuron capable of forming a similar linear combination would have access to it. Both hypotheses imply that the neural activity sampled by LFPs may not be as poorly tuned as

the recorded signals suggest. Linear combinations of signals from electrode arrays are useful to reveal latent information carried by these signals, and are justified by the fact that the observations themselves are linear combinations of neural sources.

Supported by ANR grants ANR-06-NEURO-021 and ANR-09-BLAN-0370, Royal Society International Joint Project, and CNRS Neuroinformatique program.

#### **493 Spike Synchrony Within and Across Auditory Cortical Fields of the Cat**

**Andres Carrasco**<sup>1</sup>, Stephen Lomber<sup>1,2</sup>

<sup>1</sup>Department of Physiology and Pharmacology, University of Western Ontario, London, Ontario, Canada, <sup>2</sup>Centre for Brain and Mind, University of Western Ontario, London, Ontario, Canada

Investigations of auditory cortex neuronal activation have shown that neuronal response time can encode acoustic stimulus features. In particular, relationships between stimulus intensity/duration and spike response synchrony between neurons have been examined. In the present study we investigate the prevalence of neuronal spike time coincidences across four fields of cat auditory cortex. Neuronal responses were recorded in primary auditory cortex (A1), second auditory cortex (A2), anterior auditory field (AAF), and posterior auditory field (PAF). Pure tones, noise bursts, upward frequency modulated signals, and con-specific vocalizations were used to evoke activity in auditory cortex of pentobarbital anesthetised animals. Simultaneous recordings across and within cortical lamina were performed with twelve site axial array microelectrodes (150 µm linear spacing), and four channel tungsten matrix microelectrodes. Spike time cross-correlation analyses of neuronal response activity were conducted. Our results revealed that neuronal engagement across A1 laminae showed higher response rates of synchrony as a function of recording and characteristic frequency proximity. Furthermore, spike activity induced by acoustic stimulation follow precise response patterns of activation across auditory cortical fields. Specifically, cross-correlation analyses demonstrated directional patterns of activation between cortical regions: AAF→A1, AAF→A2, AAF→PAF, A1→A2, A1→PAF, and A2→PAF. The present investigation demonstrates that patterns of neuronal spike synchrony across and within various fields of cat auditory cortex are influenced by neuronal proximity as well as spectral response features during simple and complex acoustic stimulation.

#### **494 Dynamic Multiplicative and Additive Modulations in Single Neurons of Monkey Primary Auditory Cortex**

**Roohollah Massoudi**<sup>1</sup>, Marc van Wanrooij<sup>1,2</sup>, Sigrid van Wetter<sup>1</sup>, Huib Versnel<sup>3,4</sup>, John van Opstal<sup>1</sup>

<sup>1</sup>Dept. Biophysics, Donders Institute., Radboud university Nijmegen, The Netherlands, <sup>2</sup>Dept. Otorhinolaryngology, Donders Inst., Radboud University Medical Centre Nijmegen, The Netherlands, <sup>3</sup>Department of Otorhinolaryngology, University Medical Center Utrecht,

*The Netherlands, <sup>4</sup>Rudolf Magnus Institute of Neuroscience, Utrecht, The Netherlands*

Identical acoustical signals can have different meanings and require different actions for different behavioral or mental states. These meanings and actions could already be reflected in neuronal activity along the auditory pathway. Computationally, a useful way of integrating separate information sources is by a multiplicative (gain) modulation,  $r(t, x, y) = f(t, x) g(t, y)$ , signifying a separable representation of acoustic tuning,  $f(t, x)$ , and behavioral task-related aspects,  $g(t, y)$ . Experimentally, gain modulations have been shown to be an important mechanism in integrating information from sensory, efference copy, proprioceptive, and attention signals in cortical and subcortical areas (e.g., parietal cortex, superior and inferior colliculi). Its existence in primary auditory cortex (A1), however, has so far not been studied. In contrast, additive modulations have been suggested in A1 with respect eye position:  $r = f(x) + g(y)$ . Here, we study how top-down factors such as reward expectation modulate acoustic responses in A1.

We recorded single-unit responses from A1 of two trained macaque monkeys exposed to a series of broadband spectral-temporally modulated sounds (ripples) under different behavioral conditions. We observed systematic changes in cell responses when the monkey was actively engaged in an auditory detection task relative to a passive condition. These top-down modulations were independent of the spectrotemporal receptive fields of the cells, but were highly dynamic, changing rapidly during different trial epochs (baseline, sound onset, ripple onset, prediction, and motor response). Our analysis focused on whether these modulations were either additive or multiplicative. Additive components were mostly observed during baseline periods (no sound, no task), while during acoustic epochs gain-modulations dominated. These results show how cognitive and motor-related information are usefully combined with acoustic signals in A1 at a single-neuron level.

#### **495 Sustained Firing of Model Cortical Neurons Yields Richly Structured Spectro-Temporal Receptive Fields**

**Michael Carlin<sup>1</sup>, Mounya Elhilali<sup>1</sup>**

<sup>1</sup>*Johns Hopkins University*

It has been proposed that sustained firing of central auditory neurons is a coding scheme used in thalamo-cortical centers, contributing to an internal representation for processing complex auditory scenes. We propose a framework that explicitly quantifies this notion of neural persistence and varies the shapes of model spectro-temporal receptive fields (STRFs) so as to maximize population response, subject to constraints that minimize redundancy in the learned ensemble. We demonstrate the emergence of STRFs that are bandpass, localized, and reflective of the rich spectro-temporal structure of natural sounds. Furthermore, we explore diversity in the learned ensembles across timescales relevant to natural sounds and speculate on how the proposed framework yields

population responses that align with those based on sparse coding principles.

#### **496 Hearing-Impairment in Adult Ferrets Induces Partial Crossmodal Reorganization and Multisensory Dysfunction in Core Auditory Cortex**

**M. Alex Meredith<sup>1</sup>, Leslie Keniston<sup>1</sup>, Brian Allman<sup>2</sup>**

<sup>1</sup>*Dept of Anatomy and Neurobiology, Virginia*

*Commonwealth University, <sup>2</sup>Center for Hearing and Deafness, State University of New York at Buffalo*

Most experimental studies of crossmodal plasticity have examined subjects that experienced complete sensory loss early in life. However, many adults suffer from partial sensory loss and few crossmodal effects have been reported in this population. Therefore, the present experiment was initiated to measure the extent of crossmodal reorganization that occurs in response to partial hearing loss in adult animals. The core auditory cortices were examined (multichannel single-unit recording) in adult, male ferrets that were ototoxically hearing impaired (avg. 49dB threshold) or age-matched, hearing controls. Computer-controlled somatosensory, visual, and auditory stimuli were presented alone and in combination while responses of neurons in primary auditory (A1) and anterior auditory field (AAF) were recorded. Neurons responding only to acoustic stimulation were reduced in the hearing impaired animals (from 74% to 31%). In contrast, the proportion of neurons activated by more than one sensory modality increased substantially (from 26% to 69%), of which trimodal neurons represented the largest proportion (from 0% to 25%). Because multisensory convergence can lead to dramatic levels of response integration when stimuli from more than one modality are present (and thereby interfere with residual auditory processing), we also compared the integrative capacity of the multisensory neurons in the partially-deaf animals versus hearing controls. Interestingly, although partially deafened cortex revealed an increase in multisensory convergence (~2.5 x), the increased proportions of multisensory neurons did not exhibit commensurate increases in multisensory integration. Instead, fewer instances of multisensory integration were observed as was particularly evident in the reduction of multisensory depression. Such multisensory dysfunction may be attributed to the system-wide excitatory/inhibitory imbalance known to accompany sensorineural hearing loss. Supported by NIH: NS39460 & R03DC011374-01

## **497 Amplified Extrastriate Visual Cortical Projections to Auditory Cortical Regions Following Deafness**

Melanie Kok<sup>1</sup>, Nicole Chabot<sup>2</sup>, Stephen Lomber<sup>2,3</sup>

<sup>1</sup>Graduate Program in Neuroscience, The University of Western Ontario, London, ON, Canada, <sup>2</sup>Department of Physiology and Pharmacology, The University of Western Ontario, London, ON, Canada, <sup>3</sup>Department of Psychology, The University of Western Ontario, London, ON, Canada

The loss of a sensory modality is often accompanied by the expansion or heightened ability of the remaining sensory modalities. Cat auditory cortex is known to undergo cross-modal reorganization following deafness, such that deaf animals are better able to detect visual motion than hearing controls. This adaptive advantage was identified to be dependent on a region within auditory cortex, the dorsal zone (DZ). As such, the purpose of the present investigation was to examine the connectational adaptations that might subserve this cross-modal plasticity. Deafness was induced by co-administration of kanamycin and ethacrynic acid, which produces permanent, rapid and profound bilateral hearing loss via the destruction of cochlear hair cells. We deposited biotinylated dextran amine (BDA) unilaterally into the DZ of hearing and late-deafened (onset >6M) cats in order to reveal cortical afferent projections. Two weeks following the tracer deposit, the animals were perfused with a paraformaldehyde solution, the brain was cryoprotected with 30% sucrose, and cut in 60  $\mu$ m coronal sections. Immunohistochemistry was then performed on the tissue to reveal the tracer. Adjacent sections were stained for Nissl bodies, cytochrome oxidase or SMI-32. Overall, the pattern of cortical projections to DZ was similar in both deaf cats and hearing controls. However, notable differences included an increase in neuronal labeling on the medial bank of the suprasylvian sulcus in deaf cats compared to hearing controls. The medial bank is comprised of the anteromedial lateral suprasylvian visual area (AMLS) and posteromedial lateral suprasylvian visual area (PMLS), both of which play a role in visual motion processing in hearing cats. These observations suggest that amplified cortical projections from visual areas on the medial bank of the suprasylvian sulcus to DZ may underlie the cross-modal reorganization that functionally manifests as superior visual motion detection ability in the deaf animal.

## **498 Lateral Asymmetry in Cortical Potentials from Controls and Unilaterally Deaf**

Yvonne Sininger<sup>1</sup>, Anjali Bhatara<sup>2</sup>, Elias Ballat<sup>3</sup>, Yolín Sung<sup>3</sup>

<sup>1</sup>David Geffen School of Medicine at UCLA, <sup>2</sup>Université Paris Descartes, <sup>3</sup>UCLA

This investigation asks whether the ear of stimulation and/or the type of stimulus influence the hemispheric laterality or quality of cortical auditory system activity. We further ask whether early-onset unilateral deafness and the side of deafness will influence the findings. Methods: Participants included right handed, young adults with

normal hearing in one (n=12) or both (n=22) ears. Acoustic change complexes were recorded from 64 channels using NeuroScan SynAmps2 amplifiers and Neuroscan Electrode Caps. Stimulus change conditions included frequency (50% upward change) level (+ 10 dB change) and silent gap (20 ms). Tones of 500 and 4000 Hz were employed for all tasks and broad-band noise was used for gap and level tasks. All conditions utilized an onset stimulus lasting 700 ms followed by the change condition for a total recording of 1500 ms. Analysis of onset and change responses included latency and amplitude measures for N100. When possible, grand averages were submitted to dipole source modeling assuming two symmetrical dipoles and a 3-shell spherical head model using Neuroscan "Source" software. Results-Controls: Tonal stimuli when presented to the left ear, reveal larger responses from contra-lateral (right side) electrodes while tones to the right ear consistently shows a symmetrical response. The overall effect is for a predominant right hemisphere response for tonal stimuli. This was supported by overall greater dipole strength in the right hemisphere for tonal stimuli. When noise is used both ears demonstrate a larger contra-lateral response. Unilateral- For tonal stimuli the contra-lateral response was greater for both left and right ears but for noise stimuli the response is greater from the right side electrodes regardless of ear. Thus the patterns of laterality based on electrophysiologic recordings show 1) normally occurring changes in laterality of processing based on the ear and stimulus type, 2) differences between controls and unilaterally deaf subjects when comparing like sides (ears) of stimulation and 3) differences in unilaterally deaf subjects based on the side of deafness.

## **499 Cortical and Thalamic Abnormalities in Mice with Gap-Detection Deficits**

Lucy Anderson<sup>1</sup>, Jane Mattley<sup>1</sup>, Jennifer Linden<sup>1,2</sup>

<sup>1</sup>UCL Ear Institute, London UK, <sup>2</sup>UCL Dept. of Neuroscience, Physiology and Pharmacology, London UK

To understand the mechanisms behind auditory temporal processing it may be necessary to investigate how malfunctions of the auditory system lead to auditory temporal processing deficits. Behavioural work has shown ~50% of males in a litter of inbred BXSB/MpJ mice have significantly decreased ability to detect brief gaps in noise; the same mice have "neocortical ectopia" (small nests of neurons in layer I) in the frontal lobe. Similar ectopia have been reported to be associated with developmental disorders in humans.

We have previously shown medial geniculate body (MGB) neurons from ectopic male BXSB/MpJ mice are significantly less likely to respond following brief gaps in noise compared to those recorded from non-ectopic, genetically-identical littermates, although basic response properties and auditory brainstem responses are normal. Here, we asked whether the MGB gap-detection deficits present in ectopic mice correlated with the size of their cortical ectopia. Most ectopic animals had a single ectopia located in the motor cortex, and animals with larger ectopia in motor cortex had larger thalamic deficits in gap-

detection. Thus, physiological abnormalities in the MGB of these mice may be associated with the magnitude of morphological abnormalities in motor cortex.

In other animal models, deficits in auditory temporal processing have been associated with morphological abnormalities in the auditory thalamus. We examined the morphology of the MGB in BXSB/MpJ mice, reconstructing subdivision volumes from brain sections stained for cytochrome oxidase. The volume of the dorsal MGB was significantly smaller in ectopic compared to non-ectopic mice ( $p < 0.001$ , t-test), but there were no significant differences between ectopic and non-ectopic animals in ventral or medial MGB volumes.

Thus, these findings suggest a link between presence and size of ectopia in motor cortex, morphological abnormalities in the dorsal MGB, and neural gap-detection deficits in the auditory thalamus.

### **500 Cortical Thickness Differences in Heschl's Gyrus of Hearing Impaired and Normal Hearing Infants**

Daniel J. Tward<sup>1</sup>, Jianqiao Feng<sup>1</sup>, Kristen Smith<sup>2</sup>, Mekibib Altaye<sup>3</sup>, Ellis Arjmand<sup>3</sup>, Marguerite Care<sup>3</sup>, Jannel Phillips<sup>3</sup>, Sara Robertson<sup>4</sup>, Charlotte Ruder<sup>3</sup>, Scott Holland<sup>3</sup>, J. Tilak Ratnanather<sup>1</sup>

<sup>1</sup>Johns Hopkins University, Baltimore, MD, <sup>2</sup>Georgia State University, Atlanta, GA, <sup>3</sup>Cincinnati Children's Hospital, Cincinnati, OH, <sup>4</sup>Wright State University, Dayton, OH

This study expands the volumetric analysis of the Heschl's gyrus (HG) encompassing the primary auditory cortex via high resolution 3D magnetic resonance image scans of hearing impaired (HI,  $n=16$ ) and normal hearing (NH,  $n=26$ ) infants (age 8-19 months) by Smith et al. (Cereb. Cortex, 21:991-998, 2011) to cortical thickness. Subvolumes of HG previously analysed were mapped to scans in native space, upsampled and contrast filtered to facilitate segmentation of the white matter (WM) mask. The resulting triangulated WM surface was used to delineate the HG cortical surface via dynamic programming of sulcal curves either side of the HG (Ratnanather et al., NeuroImage, 20:359-77, 2003). The WM mask was dilated and edited yielding gray matter (GM) segmentation. Histograms of distances of GM voxels relative to the HG surface yielded Labeled Cortical Distance Maps (LCDMs). Thickness and associated volume were obtained from LCDM while the surface area was obtained from the surface. For NH infants, values of  $1010 \pm 320$  mm<sup>3</sup>,  $306 \pm 83$  mm<sup>2</sup> and  $2.97 \pm 0.43$  mm for the left HG and  $754 \pm 314$  mm<sup>3</sup>,  $225 \pm 99$  mm<sup>2</sup> and  $2.83 \pm 0.45$  mm for the right HG were obtained. Similarly for HI infants,  $950 \pm 428$  mm<sup>3</sup>,  $257 \pm 138$  mm<sup>2</sup> and  $3.34 \pm 0.42$  mm for the left HG and  $798 \pm 450$  mm<sup>3</sup>,  $219 \pm 115$  mm<sup>2</sup> and  $3.06 \pm 0.27$  mm for the right HG were obtained. Hearing status contributed significantly to between group variance only for thickness (Anova) with the HG thicker in the HI group ( $p < 0.002$ , 1-sided t-test). For the 8 HI infants who were implanted, the difference in pre and post- Multiple Frequency Averaged Thresholds was found to decrease with thickness. Thicker HG in HI infants may reflect the dual impact of the auditory degeneration and absence of auditory stimulation. While

additional work is needed to examine other factors and post-implantation measures, preliminary results suggest that HI infants with thicker HG may need a different rehabilitative strategy. (Research supported by NIH R01-DC07186 and P41-RR015241 grants).

### **501 Comparing the Effects of Different Hearing Aids on Sound Processing in Primary Auditory Cortex of Mongolian Gerbils**

Konstantin Tziridis<sup>1</sup>, Sönke Ahlf<sup>1</sup>, Micheal Heiden<sup>1</sup>, Holger Schulze<sup>1</sup>

<sup>1</sup>ENT Hospital Erlangen

Impairment of the peripheral auditory system caused by acoustic trauma, ongoing noise exposure, mechanical injuries or presbycusis leads to hearing deficits in humans that are generally attempted to be compensated by the use of hearing aids (HA) adapting these devices to the individual hearing impairment. Unfortunately, these adjustments often do not lead to "normal" sound and speech perception and the HA is refused by the patient. As perception of sound is determined by its cortical processing and representation we here examine the effects of two different HA – a single (HA1) and a six channel device (HA6) - on sound processing in primary auditory cortex of Mongolian gerbils.

Single and multi-units responses to pure tones were recorded in the left auditory cortex of gerbils with and without commercial HA attached to the contralateral ear. In healthy, normal hearing animals, we found a strong increase in firing rate and a shift in the best frequency (BF) reflecting the spectral characteristics of the HA1 when it was switched on. In contrast, hearing impaired animals (acoustic trauma at 2 kHz, 115 dB SPL, 75 min) unexpectedly showed a different pattern of HA effects, namely no significantly increase firing rate or shift of the BF. Contrary to these results first recordings with the HA6 after the acoustic trauma - in the hearing impaired animals - indicate an increase of spike rate as well as a shift of BF comparable to the results observed in healthy animals.

These results point to a reduced dynamic range of auditory cortical neurons in the hearing impaired animals that cannot be compensated by the HA1 but maybe by the HA6. This may explain the problems reported by many patients with the old-typed single-channel HA; especially the diminished loudness range between hearing threshold and threshold of pain, which in turn may explain the problems with speech intelligibility in noisy environments.

### **502 Tinnitus Related Changes in Auditory Cortex of Mongolian Gerbils**

Soenke Ahlf<sup>1</sup>, Konstantin Tziridis<sup>1</sup>, Holger Schulze<sup>1</sup>

<sup>1</sup>ENT Hospital Erlangen

A perceived sound is the product of sensory information processing using excitatory and inhibitory neuronal interactions along the auditory pathway. Damage to the auditory receptor epithelium of the cochlea may lead to distortion of this auditory information processing through malfunctional synaptic transmission, e.g. lateral inhibition.

This may result in plastic reorganization of the auditory system and finally tinnitus, an erroneous auditory percept that is reflected in the abnormal activity within and plastic reorganization of tonotopic maps.

In this project we use an animal model with noise-trauma (2kHz, 115dB SPL, 75min) induced subjective tinnitus, as behaviorally verified using pre-pulse inhibition of acoustic startle response (gap-noise paradigm). To investigate neuronal mechanisms leading to subjective tinnitus we recorded responses from single and multi units in auditory cortex (AI). Following noise trauma we found a temporal dynamic of tonotopic reorganization: neuronal population's best frequency (BF) distribution first shifted significantly to lower frequencies immediately post trauma (day 0) but to higher frequencies between day 2 and 3 compared to pre-trauma conditions. Interestingly, between day 4 and 7 post trauma the BF distribution reached pre-trauma conditions again, although the tinnitus percept was still behaviorally detectable, at least for 12 weeks post trauma.

Our results demonstrate that tinnitus-related plastic changes within AI must be more subtle than mere changes in tonotopic map organization. Describing these subtle changes may give us the chance for a more detailed model explaining the development of subjective tinnitus and to develop possible new treatment strategies for this disease.

This work was funded by the Interdisciplinary Center for Clinical Research at the University Hospital Erlangen (IZKF).

### **503 Auditory Evoked Potentials in Children with Moderate Deafness and Language Impairment**

**David Bakhos**<sup>1,2</sup>, Sylvie Roux<sup>2</sup>, Emmanuel Lescanne<sup>1,2</sup>, Frédérique Bonnet-Brilhaut<sup>1</sup>, Catherine Barthelemy<sup>1</sup>, Nicole Bruneau<sup>2</sup>

<sup>1</sup>Tours Hospital, University François-Rabelais, <sup>2</sup>INSERM U930

Abstract

Objective: To investigate electrophysiological markers of cortical auditory processing in 2 subgroups of children with moderate deafness treated with hearing aids, dissociated according to their language abilities.

Patients and method: Eleven children aged 8-12 years (mean age: 10,9 years) with bilateral moderate sensorineural hearing loss treated with hearing aids, age-matched with 11 children with normal hearing and language, participate in this study. They were divided in 2 subgroups according to their spoken language and literacy skills assessed via a set of seven standardized computerized language tests from a battery of oral language tests (BILO). Six children were good scorers (L+) while five fell into the fair score category (L-). The stimuli were pure tone (1100 Hz, 50 ms duration, 70 dB SPL) presented with different interstimulus interval (700, 1100, 1500, 3000 ms) via loud speakers. Cortical auditory evoked potentials were recorded from 28 Ag-AgCl cup electrodes referenced to the nose. Peak latency and amplitude of each deflection culminating at fronto-central and temporal sites were analysed.

Results: The L+ and L- children mainly differed on the temporal N1c wave, which was absent in L- and present in L+ although of smaller amplitude than in controls.

Conclusion: These data confirm that the temporal N1c is a good marker of language impairment as previously shown in speech language impairment children.

Further researches are needed to demonstrate if this marker would be used as a predictive index of language performance in order to determine its potential prognostic value to improve the management of these children.

### **504 Descending Auditory Pathway: An ABR Analysis After Cortical Ablations**

**Veronica Lamas**<sup>1</sup>, Juan Carlos Alvarado<sup>2</sup>, Miguel A. Merchán<sup>1</sup>

<sup>1</sup>Institute of Neuroscience of Castilla y León, <sup>2</sup>University of Castilla La Mancha

The aim of this study was to understand the effect of the auditory cortical descending inputs on brainstem electrical evoked potential, at different times following bilateral or unilateral cortical ablation. To do so, auditory brainstem responses (ABR) were performed in Wistar rats before and after cortical removal. Accordingly, animals were classified in four groups: groups 1 and 2, with bilateral cortical ablation that were evaluated at 1 and 7 and 15 and 30 days post lesion, respectively. Groups 3 and 4, with unilateral cortical ablation that were evaluated with the ABR, also at 1 and 7 and 15 and 30 days post lesion, respectively. Lesions were performed following Paxinos and Watson coordinates. Auditory stimuli consisted of 0.1 ms alternating polarity click with a repetition rate of 11 bursts/s, delivered in 10 ascending step from 10 to 90 dB (SPL), and presented through tubal earphone inserted into the external auditory canal. Responses were averaged 1000 times, amplified and filtered (500 – 3000 Hz). ABR threshold was defined as the stimulus level that evoked a peak-to-peak voltage 2SD above the mean background activity. Records performed at 80 dB SPL were used for posterior off line amplitude and latencies analysis. Data showed increases in thresholds at 1 and 7 days post lesion in the bilateral but not the unilateral lesioned group. Decreases in amplitude were observed in all waves in the bilateral and unilateral (after ipsilateral stimulation) cortical ablated groups at 1 day post lesion. A reduction in wave I and in the interpeak I-IV latencies was observed at 15 and 30 days post lesion in the bilateral but not unilateral ablated group. No changes were observed in any parameter of the ABR recordings after contralateral stimulation in the unilateral ablated group. This finding suggests a cortical influence over the electrical properties of the neurons in the auditory brainstem pathway. Financial support from the Spanish MICINN (BFU2009-13754-C02-02).

## **505 Binaural Time-Intensity Interactions in Auditory Cortex of Hearing and Deprived Cats**

**Peter Hubka**<sup>1</sup>, Jochen Tillein<sup>2,3</sup>, Andrej Kral<sup>1</sup>

<sup>1</sup>*Experimental Otolology, ENT Clinics, Medical University Hanover, Germany,* <sup>2</sup>*J.W.Goethe University Frankfurt, Germany,* <sup>3</sup>*MEDEL Innsbruck, Austria*

Integration of interaural time and intensity differences is crucial for the orientation in the auditory space. The impact of congenital deafness on this feature in the auditory cortex has not been described yet. In the present study, we have characterized the effects of interaural time delays (ITD) on the cortical representation of interaural intensity (level) differences (ILD) evoked by intracochlear electrical stimulation. Congenitally deaf cats (CDC,n=5) and hearing controls (HC,n=5) in adult age were stimulated through cochlear implants with charge-balanced biphasic pulses (200µs/phase) in a wide bipolar configuration. Unit activity was recorded in auditory cortical field AI by 16-channel Neuronexus probes. In order to analyze the influence of ITD on ILD functions, ILD functions (under equal average binaural level) were measured at ITDs of  $\pm 200\mu\text{s}$ ,  $\pm 100\mu\text{s}$  and  $0\mu\text{s}$ . In controls, population of all ILD functions showed systematic ipsilateral shift as interaural time differences shifted contralaterally. The rising phase of ILD functions in mean changed from  $1.75\pm 5.6\text{dB}$  for ipsilateral ITD ( $-200\mu\text{s}$ ) to  $0.82\pm 6.6\text{dB}$  for ITD  $0\mu\text{s}$  and  $0.4\pm 5.9\text{dB}$  for contralateral ITD ( $200\mu\text{s}$ ;  $p < 0.035$ ). The shift of ILD functions was observed also in CDCs, however, it was not systematic. The rising phase of ILD functions changed from  $2.13\pm 6.4\text{dB}$  for ipsilateral ITD ( $-200\mu\text{s}$ ) to  $0.80\pm 4.9\text{dB}$  at ITD  $0\mu\text{s}$  and  $1.24\pm 6.0\text{dB}$  at contralateral ITD (ITD  $200\mu\text{s}$ ; NS). Additionally, unit responses to ILDs were different in CDCs with shorter response duration, sharp onset responses and less spikes (for ITDs, comp. Tillein J et al., 2010). The results demonstrate a deficit in integration of ITDs and ILDs in congenitally deaf cats despite their rudimentary sensitivity to binaural cues. Supported by DFG (Kr 3370/1-3).

## **506 Interaural Time Difference Envelope and Carrier Sensitivity in the Auditory Arcopallium of the Barn Owl**

**Philipp Tellers**<sup>1</sup>, Jessica Lehmann<sup>1</sup>, Hartmut Fuehr<sup>1</sup>, Hermann Wagner<sup>1</sup>

<sup>1</sup>*RWTH Aachen University*

Barn owls use interaural time differences (ITD) to determine the azimuthal direction of a sound source. ITDs are processed in two pathways, the midbrain and the forebrain pathways. Frequency-tuning curves in the midbrain nucleus ICx show one broad peak. Sensitivity is restricted mainly to frequencies above 3 kHz. ITD curves in the midbrain are symmetric around the main response peak, and can well be described by across-frequency integration and the existence of a characteristic delay at zero characteristic phase. By contrast, ITD curves of neurons in the forebrain auditory arcopallium (AAR) were asymmetric with peaks at small contralateral ITDs and a higher contralateral shoulder, while frequency tuning

curves exhibited two peaks, one in the low ( $< 3\text{kHz}$ ) and the other in the high ( $> 3\text{kHz}$ ) frequency range (Vonderschen and Wagner, *J Neurophysiol* 101: 2348 (2009)). We hypothesized that the ITD tuning curves of AAR may be composed of a low-frequency envelope and a high-frequency carrier component. To test this we used both correlated and anti-correlated binaural noise stimuli. In anti-correlated noise one of the two stereo channels is inverted. Anticorrelated stimuli should shift carrier-dependent responses by half a period but not affect envelope-dependent responses. Joris et al. (*Hear Res* 216-217: 19 (2006)) developed a metric based on correlation that allowed to judge the contribution of envelope (correlation index 1) and carrier (correlation index -1). We recorded extracellularly from 125 neurons in the AAR, and used a metric similar to that of Joris et al. to judge the contribution of envelope and carrier to the ITD tuning curves. Most of the units had negative correlation coefficients, indicating a stronger influence of the carrier than the envelope. The correlation coefficients in the sample ranged from -0.8 to 0.3 with a mean of -0.24. These data suggest that carrier information dominates in the responses of AAR neurons to varying interaural time differences.

## **507 Effects of Exposure to Moderate-Level, Bandlimited Sounds on the Adult Auditory Cortex: Importance of Steep Cutoff Slopes**

**Martin Pienkowski**<sup>1</sup>, Raymundo Munguia<sup>1</sup>, Jos J. Eggermont<sup>1</sup>

<sup>1</sup>*University of Calgary*

We have been exposing adult cats to moderate-level ( $\sim 70$  dB SPL), behaviorally-irrelevant sounds for several weeks to months. The sounds have consisted of random tone pip ensembles or noise, with various bandwidths and center frequencies, but always sharply bandlimited. Auditory brainstem response thresholds and amplitudes were unaffected by the exposure. However, spike and LFP activity in the region of primary auditory cortex (AI) normally tuned to the exposure band was long-term suppressed while activity in neighboring regions was usually enhanced.

Here, we present the results of similar exposure to two new stimuli. "Factory noise" was comprised of a mix of various power tool and machine sounds. Its long-term spectrum was lowpass with a sharp cutoff at  $\sim 16$  kHz. We found the typical pattern of suppression inside the exposure frequency range and enhancement outside, but only around the 16 kHz edge frequency. No suppression was observed at frequencies more than about an octave below the 16 kHz edge despite the fact that the stimulus energy was dominated by these frequencies. This strongly argues against a frequency-specific, top-down "habituation" to the stimulus.

To determine the importance of steep stimulus cutoff slopes for producing the observed suppression/enhancement profile in AI, we are exposing adult cats to a dense tone pip ensemble with a flat spectrum between 2 and 4 kHz, and shallow cutoff slopes (16 dB/oct) on both sides. The findings will be compared to

those from a previous experiment which used a sharply cutoff 2-4 kHz exposure stimulus of the same intensity, and which resulted in a dramatic suppression of AI activity within and beyond 2-4 kHz, and enhancement at <1 and >16 kHz. We hypothesize that the shallow-sloped exposure will have a significantly weaker effect on neural activity in AI.

### **508 Auditory Response Property of Neurons in the Amygdala and in the Striatum**

**Guang-Di Chen<sup>1</sup>**, Senthilvelan Manohar<sup>1</sup>, Richard Salvi<sup>1</sup>  
<sup>1</sup>*SUNY at Buffalo*

Although the amygdala lies outside of the classical auditory pathway, it has long been known to receive auditory information that contributes to the emotional aspects of sound perception. Likewise, the striatum receives auditory inputs that contribute to vocal learning. Although the basic auditory response properties of the amygdala and striatum have been explored in rat, they are not fully understood. To gain a better understanding of their auditory processing characteristics, we recorded from acoustically responsive neurons in the dorsal division of the lateral amygdala and the overlying striatum. Auditory neurons in the amygdala and striatum of the adult rat responded to all frequencies within its range of hearing. The lowest thresholds at characteristic frequency (CF) of the neurons were in good agreement with the behavioral audiogram indicating that all audible frequencies are represented in these brain regions. Within the amygdala, a "primary-like" region was found in which nearly all neurons: (1) were sharply tuned, (2) tonotopically organized (dorsal, low frequency, ventral-high frequency, and (3) possessed monotonic discharge rate-intensity function. While the neurons in the amygdala had both short-latency (~15 ms) and long-latency responses (>50 ms), the neurons in the striatum had only a short-latency (~10 ms) response component. The short-latency response in the amygdala might be important for the fear-escape reaction and the long-latency response might be related to other emotional reactions. The short-latency and sharp temporal responses of the neurons in the striatum would presumably make these neurons extremely sensitive to the temporal structure of vocal communications and aid in sound imitation. Thus, neurons in the rat amygdala and the striatum respond to acoustical stimulation with short latency, low thresholds, and sharp tuning, acoustic feature processing that may be relevant to auditory fear conditioning, emotional reaction to sounds and vocal learning. Supported by grants from NIH (R01DC009091; R01DC009219)

### **509 Origins of Visual LFPs in Macaque A1**

**Yoshinao Kajikawa<sup>1</sup>**, Charles Schroeder<sup>1,2</sup>  
<sup>1</sup>*Nathan Kline Institute*, <sup>2</sup>*Columbia University, Psychiatry*

Visual inputs contribute to auditory perception under many natural conditions. For example, a visual object pulls the localization of a sound towards itself when its spatial location is incongruent with that of an auditory object (the ventriloquist effect). Similarly, when a syllable with a consonant /b/ is presented while viewing a face vocalizing

a consonant /g/, we often hear a consonant /d/ (the McGurk effect). A1 is a potential candidate region for the audiovisual integration underlying these effects. To investigate this issue, we analyzed cortical responses in A1 to conspecific vocalizations and their modulation in monkeys viewing movies of a vocalizing face. To enforce attention to both modalities, we trained monkeys to perform an audiovisual (AV) oddball task. In each trial, specific auditory, visual, and AV versions of a vocalization were repetitively presented (non-targets), and targets (oddballs) differed from non-targets in either or both modalities. Laminar LFP, current source density (CSD) and multiunit activity (MUA) profiles were recorded using linear array multielectrodes. LFP responses to vocalizations inverted in polarity across cortical layers, with attendant CSD and MUA components, indicative of their local generation in A1. In contrast, though LFP responses to monkey facial gestures were observed, and perhaps modulated within A1, their polarity was constant across A1 layers and their amplitude grew with depth. Thus, while spatiotemporal patterns of auditory LFP could be attributed to local synaptic activity in A1, co-located visual LFPs appeared to receive their largest contributions by volume conduction from regions outside of primary auditory cortex.

### **510 Adaptation of MEG Responses to Pure Tones in the Guinea Pig**

**Gestur Christianson<sup>1</sup>**, Maria Chait<sup>1</sup>, Alain de Cheveigné<sup>2</sup>, Jennifer Linden<sup>1,3</sup>

<sup>1</sup>*UCL Ear Institute, University College London*, <sup>2</sup>*École Normale Supérieure, Paris*, <sup>3</sup>*Department of Neuroscience, Physiology and Pharmacology, University College London*  
Using a newly developed magnetoencephalograph (MEG) for small animals, we have measured cortical responses to onsets and sound transitions in the guinea pig using tone complexes. The small-animal MEG system has 9 magnetometers placed in an 8x8 mm square array. An additional set of 3 magnetometers and one accelerometer are used to measure and suppress environmental noise. Sound is delivered using Etymotics transducers in either closed- or free-field conditions. Auditory onset responses occur with a latency of approximately 50 ms, roughly half that observed in humans, and last 300-400 ms, while offset responses are weak. We have also observed MEG responses consistent with stimulus specific adaptation (SSA). When short pips presented at a regular repetition rate were switched between two frequencies, a greater response was obtained for the first tone following a transition, suggesting that responses to later tones were reduced by adaptation. This effect was significant when the separation between frequencies was greater than an octave. Consistent with previous physiology results, the adaptation was rapid, the response being adapted by the second tone after the transition. The number of tones presented between transitions seems to be a greater determining factor in the adaptation than inter-transition spacing. In the long term, joint MEG and electrophysiology in the same animals will allow us to elucidate the neural basis of the MEG

response, bridging the gap between human brain imaging and invasive animal electrophysiology.

### **511 There Is More Than One Way to Scan a Cat: an Assessment of Two Imaging Techniques for Optimal Auditory Cortex Activation**

**Amee McMillan**<sup>1</sup>, Trecia Brown<sup>2</sup>, Marc Joanisse<sup>3</sup>, Jessica Grahn<sup>3</sup>, Stephen Lomber<sup>2,3</sup>

<sup>1</sup>*Department of Anatomy and Cell Biology, University of Western Ontario,*

<sup>2</sup>*Department of Physiology and Pharmacology, University of Western Ontario,*

<sup>3</sup>*Department of Psychology, University of Western Ontario*

Our long-term goal is to characterize neural representations of acoustic stimuli to better understand organization within auditory cortex. The first step in these studies is to describe the extent of auditory cortex activation in response to acoustic stimulation. We used functional magnetic resonance imaging (fMRI) because it is an effective tool for assessing global brain activation. The purpose of the present investigation was to determine the optimal imaging protocol to maximize sensitivity to activity in cat auditory cortex. Conventional fMRI scanning methods produce loud sounds which present a challenge to investigations of auditory cortex activity utilizing traditional "continuous" scanning methods. To overcome this potential confound, "sparse" scanning methods have been developed, in which stimuli are presented during gaps between acquisitions. In this study, both methods were compared for optimal detection of auditory cortex activation in the cat. Data were acquired from anesthetized cats (ketamine/domitor/isoflurane) in a 7T Varian scanner. A block design was used for sparse scanning trials (TR=8s, TA=3s) in which a four volume block of acoustic data was collected separated by a block of baseline activity where no stimuli were presented. A similar design was used during continuous scans (TR=3s, TA=3s) in which a ten volume block of acoustic data were collected separated by a block of baseline activity. Stimuli consisted of broadband noise bursts and pure tones at 0.5 and 10kHz at 80dB. In a cohort of adult female cats, sparse scanning elicited a considerably larger activation in the inferior colliculi than the continuous method. Conversely, continuous scanning produced notably larger cortical activation and, interestingly, a larger activation of the medial geniculate body (MGB). Results indicate that sparse scanning is optimal for investigations of midbrain activity while continuous scanning is better suited for explorations of thalamocortical activity.

### **512 Effects of Prepulse Inhibition on N1/P2 Complex of the Late-Latency Auditory Evoked Potential; Comparison in Healthy Volunteers**

**Khayria Al-Abduljawad**<sup>1,2</sup>

<sup>1</sup>*King Saud University,* <sup>2</sup>*King Saud University*

The auditory brain stem response (ABR) is considered as the auditory evoked potential (AEP) that is most widely used by audiologists. However, other kinds of AEPs also

provide information not obtainable with the ABR, such as, late-latency auditory evoked potentials (LLAEPs), also known as cortical evoked potentials. These responses occur in the range of 100-300 ms after the stimulus, and overlap with the so-called 'endogenous' or 'cognitive' potentials. The N1 and P2 peaks are affected by the level of behavioral arousal, and are suppressed by sedative drugs, for example benzodiazepines. Prepulse inhibition (PPI) of the loud acoustic response is the suppression of the response that is normally evoked by an intense stimulus. In this study we examined if the N1/P2 complex of the auditory evoked potential is susceptible to PPI, and compared the amplitudes of these responses and their suppression in twenty healthy volunteers, ten males and ten females. Their mean age was 26.5 years. Before entering the study their hearing thresholds at 0.5, 1, 2 and 4 k Hz was measured. None of them were found to have thresholds above 20 dB. The female subjects in this study showed slightly higher auditory evoked potential responses and lower response latencies than the males. The findings are consistent with sex differences that are known to occur in a number of evoked potentials in different modalities; such differences have been attributed to differences in skull dimensions, brain volume and conduction distances. Keywords: late latency auditory evoked potential; N1/P2 complex; prepulse inhibition PPI.

### **513 Characterisation of the BOLD Response in Cat Auditory Cortex**

**Trecia A. Brown**<sup>1</sup>, Marc F. Joanisse<sup>2</sup>, Stephen G. Lomber<sup>1,2</sup>

<sup>1</sup>*Department of Physiology & Pharmacology, University of Western Ontario, London, ON, Canada,* <sup>2</sup>*Centre for Brain and Mind, University of Western Ontario, London, ON, Canada*

Much of what is known about the cortical organization for audition in humans draws from studies of auditory cortex in the cat. However, these data build largely on electrophysiological recordings that are both highly invasive and provide less evidence concerning large-scale patterns of brain activation. Functional magnetic resonance imaging (fMRI) overcomes these limitations by providing a macroscopic perspective of distributed activity across the cortex in a non-invasive manner. The present study used fMRI to characterize stimulus-evoked activity in auditory cortex of the anaesthetized (ketamine/isoflurane) cat, focusing specifically on the blood-oxygen-level-dependent (BOLD) signal time course. Functional images were acquired for adult cats in a 7T MRI scanner. To determine the BOLD signal time course, we used a stroboscopic scanning procedure in which scans were acquired at 15s intervals, with the auditory stimuli presented at randomized delays of 1-12s prior to each scan. This procedure presented 1s broadband noise bursts (85 dB SPL) in between scan acquisitions in a way that was uncorrelated with the gradient noise generated by the scanner; it thus maximized our ability to isolate stimulus-evoked cortical activity. Preliminary results indicate that the BOLD response peaks 2-3s post-stimulus onset in cat auditory cortex, then returns to near-baseline levels 7-8s

post-stimulus onset. The observed peak latency is comparable to that reported in humans and in non-human primates (3-4s). However, the time course of activity in cat auditory cortex occurs on a comparatively shorter scale than in cat visual cortex where the BOLD response peaks at 9-10s after stimulus onset. The results of this study will provide a foundation for the design of future auditory fMRI studies in the cat.

#### **514** Neuronal Responses to Frequency-Modulated Tones in the Right and Left Auditory Cortices in the Rat

Daniel Suta<sup>1</sup>, Kateryna Pysanenko<sup>1</sup>, Josef Syka<sup>1</sup>

<sup>1</sup>*Inst Exp Med ASCR, Prague, Czech Republic*

The left auditory cortex (AC) in humans is involved in the processing of the temporal parameters of acoustical signals, specifically in speech perception, whereas the right AC plays a dominant role in pitch and melody perception. We recently demonstrated the existence of a hemispheric lateralization in acoustical signal processing in rats: inactivation of the right AC impaired the discrimination of the direction of frequency modulation (FM), whereas inactivation of the left AC impaired the temporal discrimination of gap sequences. In this study we characterized the neuronal responses in the left and right ACs of anesthetized rats to upward and downward FM tones. Neuronal activity in the AC was recorded using a multichannel microelectrode in response to acoustical stimulation by FM sweeps with different modulation rates. Neurons frequently showed a stronger response for one direction of the FM; this selectivity for FM direction was observed to be distributed equally in both the left and right hemispheres. In correspondence with the results of behavioural tests, the neuronal response to stimuli of slow FM reflected the sound frequency at the beginning of the FM stimulus rather than the FM itself, and the responses to slow FM stimuli often resembled the responses evoked by pure tones. Neuronal selectivity for the FM direction was found in the case of medium and fast FM sweeps. A difference between the left and right AC was found in responses to fast FM upward vs. downward sweeps starting from the same frequency. In this case, neurons in the right AC displayed greater FM direction selectivity. This observation correlates with the results of our recent behavioural study that showed that discrimination of such FM stimuli in the rat is impaired by a lesion of the right AC. At the present time we are investigating possible neuronal correlates of the lateralization of temporal discrimination in the AC. Supported by GACR 309/07/1336, P303/11/J005, LC554, AV0Z50390512.

#### **515** Tonotopic Organization of Posterolateral Superior Temporal Gyrus in Humans: Basic Response Properties Revealed by Intracranial Recordings

Kirill Nourski<sup>1</sup>, Mitchell Steinschneider<sup>2</sup>, Hiroyuki Oya<sup>1</sup>, Hiroto Kawasaki<sup>1</sup>, Matthew Howard<sup>1</sup>

<sup>1</sup>*The University of Iowa*, <sup>2</sup>*Albert Einstein College of Medicine*

Auditory cortex in humans has been hypothesized to function as a system of core, belt and parabelt fields. The place of cortex on posterolateral superior temporal gyrus (PLST) within this hierarchy and its organization are not clear. Orderly representations of sound frequency provide a criterion for field mapping within auditory cortex. Understanding response patterns elicited by pure tones may help functional characterization of PLST.

Subjects were neurosurgical patients undergoing chronic invasive monitoring for refractory epilepsy. Stimuli were tone bursts (frequency 0.25-8 kHz), delivered diotically via insert earphones in passive-listening experiments. Recordings were made over perisylvian cortex using subdural grids and were characterized by measuring high gamma event-related band power. Activation patterns were analyzed using a sparse logistic regression classification algorithm.

Pure tones elicited robust responses in PLST, centered around the transverse temporal sulcus. Responses from individual recording sites had a frequency selectivity and were typically broadly tuned. In several subjects, mirror-image response patterns around a low-frequency center were observed, while in others, a partial representation of this pattern was seen. Activation expanded with tone intensity, with preservation of tonotopic features. Classification analysis of whole-grid data yielded above-chance accuracy, typically reaching maximum at 100-150 ms after stimulus onset. The accuracy was higher from the right hemisphere.

Results suggest the existence of multiple fields within PLST with spectrally diverse, convergent inputs. Higher tone classification accuracy in the right hemisphere is consistent with the concept of functional asymmetry of human auditory cortex. Ongoing work (see abstract by Steinschneider et al.) is examining relationships between responses to tones and complex sounds, and task-related modulations.

Supported by NIH RO1-DC004290, UL1RR024979, and the Hoover Fund.

#### **516** Binaural Masking Level Differences in Guinea Pig Auditory Cortex

Heather Gilbert<sup>1,2</sup>, Trevor Shackleton<sup>1</sup>, Alan Palmer<sup>1</sup>

<sup>1</sup>*MRC Institute of Hearing Research*, <sup>2</sup>*University of Nottingham*

Binaural masking release is a psychophysical phenomenon whereby the spatial properties of a signal can affect its audibility within a background noise. Against a background of diotic noise (No), a signal that has had its phase inverted in one ear ( $S\pi$ ) is more audible than its diotic counterpart (So). The difference in the thresholds for

these two conditions is known as the binaural masking level difference (BMLD), and is typically around 12-15 dB. It has previously been shown that the responses of low-frequency neurons in the inferior colliculus (IC), that are sensitive to interaural time differences, provide a neural substrate for the BMLD. Here we extend these observations to the auditory cortex.

Neural responses were measured in the primary auditory cortex of urethane anaesthetised guinea pigs. In each stimulus condition, a broadband noise and a 500 Hz signal were either identical at the two ears or the tone or noise was inverted in one ear (NoSo, NoS $\pi$ , N $\pi$ S $\pi$  and N $\pi$ So). The noise and tone were simultaneously gated with a duration of 150 ms. Masked thresholds were computed using signal detection theory taking into account mean firing rates and trial-by-trial variability. As in the IC, individual auditory cortex neurons could signal the presence of the tone in the masking noise by either an increase or a decrease in discharge rate, in a manner generally consistent with their interaural time difference sensitivity. Across the sample of auditory cortex neurons the magnitude of the BMLD was of the order of that shown psychophysically.

### **517 Neural Mechanisms Underlying FM Sweep Rate Selectivity in the Mouse Auditory Cortex**

**Magdalena Carrasco**<sup>1</sup>, Michael Trujillo<sup>1</sup>, Khaleel Razak<sup>1</sup>  
<sup>1</sup>Univ. California, Riverside

Frequency modulated (FM) sweeps are components of vocalizations. In the mouse auditory cortex there is selectivity for a narrow range of FM sweep rates. When tested with rates between 0.1 to 20 kHz/msec, the vast majority of neurons in the primary auditory cortex (A1) are selective for slow rates (<2 kHz/msec). The majority of neurons in the anterior auditory field (AAF) are selective for fast (>3 kHz/msec) or intermediate (1-3 kHz/msec) rates. Here, we focused on the mechanisms underlying such selectivity.

The dominant mechanism shaping selectivity for fast or intermediate rates is sideband inhibition. The majority (23/33) of neurons selective for fast or intermediate sweep rates exhibited a delayed high-frequency sideband inhibition with an average arrival time of ~3 msec and bandwidth of 4 kHz. Exclusion of these sidebands from the sweep eliminated or reduced rate selectivity in most of these neurons. In 5/33 neurons, duration tuning mechanism shaped rate selectivity. These neurons were selective for the duration of the CF tone. Sweeps of different rates spend different durations in the excitatory receptive field. Because of duration tuning to excitatory frequencies, neurons will respond differently to different rates. In these neurons, exclusion of sideband frequencies does not impact rate selectivity. None of the non-selective or slow-rate selective (n=10) neurons exhibit sideband inhibition. These neurons were sensitive to long duration excitatory tones.

We iontophorezed gabazine, a GABA-a receptor antagonist to determine the relative contributions of intracortical inhibition and inheritance from sub-cortical

sites in shaping cortical FM rate selectivity. ~50% of neurons selective for fast or intermediate rates lose rate selectivity in the presence of gabazine. These data suggest that cortically generated sideband inhibition shapes FM rate selectivity in a significant proportion of cortical neurons in the mouse.

### **518 Frequency Characteristics of Auditory Steady-State Response (ASSR): Modulation of Dipole Moment as a Function of Carrier Frequency**

**Asuka Otsuka**<sup>1</sup>, Masato Yumoto<sup>2</sup>, Shinya Kuriki<sup>3</sup>, Seiji Nakagawa<sup>1</sup>

<sup>1</sup>The National Institute of Advanced Industrial Science and Technology (AIST), <sup>2</sup>Graduate School of Medicine, The University of Tokyo, <sup>3</sup>Research Center for Advanced Technologies, Tokyo Denki University

Auditory steady-state response (ASSR) is a sinusoidal neurophysiological signal synchronized to periodic amplitude modulation (AM) of a sound. Neuromagnetically recorded ASSR is originated from the cortex, though ASSR is elicited from every anatomical locus on the auditory afferent pathway. The amplitude of ASSR is modulated as a function of physical parameters of sounds such as intensity (maximum at 70 dB SPL) and AM frequency (maximum at 40 Hz). As for carrier frequency, linear decrease from 250 to 4 kHz has been reported; however, it is yet unclear if such linearity would be consistent for wider frequency range when output of the sound intensity is strictly under control.

This study explored the frequency characteristics (FC) of neuromagnetic ASSR elicited in response to 40-Hz AM chirp tones. The tones were delivered binaurally at equal sound pressure level, as confirmed by recording the output in the ear canal, throughout the carrier frequencies ascended exponentially from 100 to 12.5 kHz, in duration of 5, 15 and 45s. Equivalent current dipole (ECD) was estimated for all time samples of the neuromagnetic signals. The FC curve was computed using the strength of the ECD moment, reflecting the ASSR sensitivity to the carrier frequency swept at each time point.

The ASSR moment started to increase in a few hundred ms after the onset of the tones, reached the peak at 500~700 Hz, diminished over 2~5 kHz, stayed plateaus through 10 kHz with exhibiting a small peak at 8 kHz then finally decreased towards 12.5 kHz. The initial increase and final decrease agreed with the results of auditory threshold measurement, indicating the effect of loudness on the FC curve. Besides, the shift in the sensitivity from lower to higher frequency bands may be associated with the critical band width, functioning to increase the ASSR moment strength when sideband components of the AM chirp tones were detected by the adjacent auditory-filters. These results suggest that certain compensation by FC curve may be necessary when evaluating any auditory function indexed by ASSR.

## **519** Source Localization of Cortical Auditory Evoked Potentials: Evaluation of Methods

Allison Bradley<sup>1</sup>, Jun Yao<sup>1</sup>, Jules Dewald<sup>1</sup>, Claus-Peter Richter<sup>1</sup>

<sup>1</sup>Northwestern University

Cochlear implants (CI) have been successful at restoring some hearing to people with sensorineural hearing loss. Yet, there is still a large variation in patient outcomes, such as speech perception ability, that is unaccounted for by patient or device characteristics. There is growing evidence that differences in cortical activity may explain why some patients do so much better than others. However, options for examining cortical activity in CI patients are limited, as the CI is not compatible with MRI. Electroencephalography (EEG), however, is a convenient method of examining the neural activity of the cortex, and is compatible with cochlear implants.

In our studies we use a high-density array of electrodes (160 contacts) on the scalp and source localization algorithms to gain insight into what parts of the cortex are active in response to sound. For this calculation, a head model is required. To improve the accuracy of the source localization, a subject-specific model based on an MRI scan of the subject's head is usually implemented. However, as CIs are not compatible with MRI this is not possible with CI patients. Therefore, in this study, we examined whether Computed Tomography (CT) scans may be used to create a subject specific head model with sufficient accuracy and resolution.

In this study, head models were created using a CT image and an MRI image of the same patient, in addition to a head model based on an averaged MRI data set. Simulations of scalp EEG, where the location of the cortical source was predetermined, allowed us to quantify the accuracy of the source localization results. The effect of different head models on localization accuracy could thus be determined. Simulations were repeated with different source localization algorithms and different source locations, as both of these factors also affect localization results.

## **520** Cortical Electrophysiology of Vowel Discrimination in Infants

Barbara Cone<sup>1</sup>

<sup>1</sup>University of Arizona

The specific aims of this study were to obtain cortical evoked responses in response to vowel contrasts: /a/, /i/, /o/, /u/ from awake infants, and to compare these results to their perceptual performance on a test of vowel discrimination. The subjects were 28 infants, aged 5-10 months. Stimuli used were synthesized vowel tokens: /a/, /i/, /o/, /u/ presented at 70 dB SPL. Stimuli were presented in an odd-ball paradigm for CAEP tests, in which one token served as the standard, and one as deviant with the probability of deviant=25%. In the "control" condition, the same token was used for the standard and the deviant. CAEP tests were run using both a 1/s and 2/s stimulus rate. For the vowel-discrimination perception test, infants were trained and tested using an observer-based

psychophysical method described in Cone & Garinis (2009), with visual reinforcement.

At the 1/s rate, /i/ and /o/ evoke P1-N1 amplitudes that are significantly larger than those seen in the control condition (or for the /a/-/u/ contrast. At the 2/s rate, all contrasts evoke responses that are more than 2 s.d. larger than the control condition. The results for the N1-P2 component are similar to those for P1-N1, with significantly larger responses observed for all vowel contrasts compared to control conditions at stimulus rates of 2/s.

Perceptual results indicate that, on average, there is a 72% hit-rate for detecting a vowel change, and a 21% false alarm rate. In individual infants, larger ACC difference waves were observed for those contrasts demonstrating better perceptual performance.

The translation of these findings into a clinic metric of speech perception will be discussed.

## **521** Day-By-Day Maturation of Cortical Sound Representations Following the Onset of Hearing

Daniel Polley<sup>1,2</sup>, Tania Rinaldi Barkat<sup>1,3</sup>, Troy Hackett<sup>4</sup>

<sup>1</sup>Eaton-Peabody Laboratory, Massachusetts Eye and Ear Infirmary, <sup>2</sup>Harvard Medical School, <sup>3</sup>Harvard University,

<sup>4</sup>Vanderbilt University School of Medicine

We recently described a critical period in mouse auditory thalamocortical development that begins shortly after hearing onset and ends four days later (Barkat et al., 2011). To understand how auditory representations of increasing complexity 'come online' during early postnatal development, we performed in vivo recordings from the mouse auditory cortex (Actx) at postnatal day (P) 10 to P21. Receptive fields and tonotopic maps were precise and orderly from the earliest age of sound-evoked spiking in the Actx (P10), yet underwent substantial additional elaboration through P18. Maturation of elementary features, such as threshold, latency and bandwidth, overlapped with ostensibly more complex features such as aural dominance and interaural level difference (ILD) tuning. Cortical development could reflect maturation of intrinsic circuitry or could simply report changes at lower levels of the auditory system. We used two approaches to disambiguate these possibilities: First, we compared development of sound representations in Actx to the inferior colliculus and medial geniculate body; second, we characterized the postnatal development of neurochemical markers for excitatory (VGLUT1 and 2) and inhibitory (parvalbumin, PV) synaptic transmission in the Actx directly. Subcortical recordings suggested that maturation of basic responses properties, such as latency and threshold was largely inherited, while aspects of binaural representations could not be explained by subcortical development. Immunohistochemical analysis revealed that the overall amount and laminar organization of excitatory and inhibitory markers were disorganized before the onset of hearing but developed rapidly thereafter, with PV signaling maturing slightly later than VGLUT. Collectively, these data highlight substantial modifications to sound representations in the Actx in the days following

hearing onset, which likely form the basis for early critical periods of experience-dependent plasticity.

### **522 Comparison of Evoked Activity in Supragranular and Granular Layers in the Mouse Primary Auditory Cortex**

**Daniel Winkowski<sup>1</sup>**, Shihab Shamma<sup>1</sup>, Patrick Kanold<sup>1</sup>  
<sup>1</sup>*University of Maryland*

The auditory cortex is a laminated structure that processes sensory information from the external environment. The precise nature of the transformation of sensory information across cortical laminae at the level of cortical networks is unknown. Here, we used in vivo two-photon calcium imaging techniques to measure response properties and functional organization of neurons located in supragranular and thalamorecipient layers of mouse primary auditory cortex (A1). We found that neurons in both laminae responded to sound and that sound evoked responses of a local group of neurons were, on average, more correlated with one another in thalamorecipient layers when compared with responses of neurons in supragranular laminae. This larger fraction of locally correlated activity in populations of neurons leads, on average, to a more homogeneous organization in thalamorecipient laminae as compared with that within supragranular layers. These results suggest that the representation of sensory information is transformed in stages beyond the very first stage of cortical processing in A1. Collectively, these results provide insight into how the representation of sensory information is transformed as it propagates through various stages of cortical processing.

### **523 A Magnetic Resonance Image and Histological Atlas of the Guinea Pig Brain and Brainstem**

**Marie Drottner<sup>1</sup>**, Hernan Jara<sup>1</sup>  
<sup>1</sup>*Boston University School of Medicine*

**Purpose:** The neuronal connectivity of the auditory system is typically characterized using retrograde and anterograde tracers to describe the circuitry. Frequently the guinea pig is a model system in which to study these central auditory pathways and connections. However, there exists no comprehensive paper, digital or 3-dimensional anatomical reference atlas upon which to compare data. High resolution, contrast enhanced magnetic resonance imaging was used to create a 3-dimensional digital data set which will form the basis of a complete reference atlas. **Results:** Using an ex-vivo fixed brain sample, an MRI data set of coronal, axial and sagittal slices was collected. After scanning, the brain was processed and sectioned at 80 um creating an histological companion atlas to the magnetic resonance images.

**Conclusion:** This work shows selected sections of MRI slices with their matching histology. The high resolution magnetic resonance images show an accurate congruence with Nissl stained histological sections. The complete atlas will be annotated and published as an open access digital atlas that can be used as a reference work for guinea pig auditory research.

### **524 Long-Term Modification of Noradrenergic Circuitry Prolongs Auditory Cortical Plasticity**

**Ana Raquel Martins<sup>1,2</sup>**, Robert Froemke<sup>1</sup>

<sup>1</sup>*NYU School of Medicine*, <sup>2</sup>*University of Coimbra, Portugal*  
Neuronal networks of the cerebral cortex are plastic, maintaining the capacity to reorganize throughout life. While neuromodulator release is required for cortical plasticity, it is uncertain how subcortical neuromodulatory systems, such as the noradrenergic locus coeruleus, interact with and refine cortical circuits.

Here we determine the dynamics of cortical receptive field plasticity at the synaptic and spiking levels using in vivo whole-cell recording. Adult rats were anesthetized, stimulation electrodes implanted in the locus coeruleus, and a craniotomy performed over the primary auditory cortex (A1). After mapping A1, whole-cell recordings were made from A1 neurons, and pure tones of varying frequencies and intensities were presented to the animal to characterize tonal receptive fields.

Pairing sensory stimulation (pure tones) with locus coeruleus activation (to release noradrenalin) could dramatically change the tuning properties of A1 neurons. In most cases, pairing induced large increases of tone-evoked synaptic and spiking responses. In some cases, these changes were highly stimulus-specific, while in other cases, stimulus preference was degraded and neuronal tuning was degraded. The degradation of frequency tuning was observed immediately after pairing, while the emergence of new stimulus preference occurred 30+ minutes later. Multiple cell recordings from the same animal for hours after pairing suggested that these changes in A1 tuning could persist for 8+ hours.

Furthermore, some A1 neurons were initially unresponsive to auditory stimuli. During and after locus coeruleus pairing, however, tone-evoked responses could suddenly emerge, persisting for 30+ min. This suggests the involvement of the locus coeruleus arousal system in the integration of 'silent neurons' into a specific auditory memory trace or cortical representation of certain, potentially behaviorally important sensory stimuli.

Finally, the unusually long duration of this form of receptive field plasticity seemed to be linked to changes induced within locus coeruleus directly. After pairing, locus coeruleus neurons developed responses to tonal stimuli, and thus may continue to provide a neuromodulatory signal for hours after pairing. Preventing this sensitization of locus coeruleus limited the duration of cortical plasticity.

We hypothesize that such changes to cortical tuning curves have important implications for the detection and/or discrimination of different sensory inputs. In particular, increased excitability could make it easier for a network or animal to detect the presence of a stimulus, in exchange for reduced discriminative abilities.

## **525 Neuroplasticity After Repeated Noise**

### **Trauma in the Central Auditory Pathway**

**Moritz Gröschel**<sup>1,2</sup>, Annekatrin Coordes<sup>1</sup>, Susanne Müller<sup>3</sup>, Romy Götze<sup>2</sup>, Arne Ernst<sup>1</sup>, Dietmar Basta<sup>1,2</sup>

<sup>1</sup>*Department of ENT at UKB, Hospital of the University of Berlin, Charité Medical School, Germany,* <sup>2</sup>*Department of Biology, Humboldt-University of Berlin, Germany,*

<sup>3</sup>*Neuroscience Research Center, Charité University Medicine Berlin, Germany*

Noise exposure leads beside peripheral damage to profound changes within central auditory structures. Recent studies have shown that a single noise trauma is followed by a dramatic reduction of cell densities and an increased calcium related activity in several structures involved in central auditory processing. This effect occurs within the first hours and days after acoustic overstimulation and is accompanied by a significant hearing loss. It remains unclear to what extent the affected structures are influenced in case of a recurrence of traumatic impact. The present study should thus clarify the effect of a repeated noise exposure on the anatomy and physiology of the central auditory system. Normal hearing mice were exposed once or twice to a broadband noise (5-20 kHz, 115 dB) for 3 hours under anaesthesia. Second trauma was applied one week after the first one. 7 or 14 days later, hearing thresholds were determined by ABR recordings. Calcium-dependent neural activity was measured by 7T-MRI scanning 24 hours after injection of a manganese chloride solution. Signal strengths in several central auditory structures were measured in all treatment groups and compared with those of normal hearing controls. In addition, cell densities were determined in auditory brain areas using histological staining techniques to identify neurodegeneration. The results demonstrate that auditory thresholds are only slightly increased after a second noise exposure. In contrast, the effect of noise on auditory brain areas (i.e. calcium-dependent activity and apoptotic cell loss) is significantly enhanced after repeated exposure. Activity changes also occurred after the application of moderate sound and were strengthened with increasing noise intensity (especially in higher structures). Due to the fact that auditory thresholds do not change in a similar manner it could be hypothesized, that some calcium-dependent neural activity increase is associated with protection from hearing loss.

## **526 Short-Term Plasticity Sharpens Frequency Responses and Results in Level-Independent Tuning in Primary Auditory Cortex of the Mouse**

**K. Jannis Hildebrandt**<sup>1</sup>, Maneesh Sahani<sup>2</sup>, Jennifer F. Linden<sup>1,3</sup>

<sup>1</sup>*Ear Institute,* <sup>2</sup>*Gatsby Computational Neuroscience Unit,*

<sup>3</sup>*Department of Neuroscience, Physiology & Pharmacology, University College London*

The frequency tuning of neurons in primary auditory cortex is not fixed but can change depending on the sensory context in which it is tested. Here, we tested the frequency tuning of auditory cortex neurons using a pseudo-random

sequence of tone pairs; within the sequence each tone was repeated, so that the first tone was preceded by a tone of random frequency and intensity, and the second by exactly the same stimulus. Inter-stimulus intervals between all tones (within or across tone pairs) were 600 ms. We recorded both single- and multi-unit activity in the core auditory cortex of anaesthetised mice and estimated frequency-intensity response areas (FRAs) from either first tones (preceded by random tones) or second tones (preceded by the same stimulus). We then compared characteristic frequency (CF) as well as bandwidth and best frequency (BF) at different levels above threshold between the first-tone and second-tone FRAs. For test stimuli preceded by a random tone (first-tone FRAs), tuning depended on level; BF at 20 dB above threshold was up to 1.5 octaves lower than CF. However, for tones preceded by the same tone (second-tone FRAs), BF at higher levels shifted towards CF, resulting in more level-invariant coding of sound frequency and finer frequency tuning. While the responses to frequencies near and above CF were not different in the two conditions, sensitivity to frequencies below CF was often reduced for tones preceded by the same stimulus. This effect was most prominent in neurons for which BF differed strongly from CF in first-tone FRAs. At these below-CF frequencies, no change of the threshold was observed, but the slope of the level-response function decreased, indicating a reduction in response gain. Our results are in good agreement with models suggesting that tuning in auditory cortex is partly shaped by connections along the tonotopic axis and that short-term plasticity of these connections can alter tuning.

## **527 Effects of Tone Duration and Fundamental Frequency on Stream Segregation by Phase Relation**

**Lena-Vanessa Dolleza**<sup>1</sup>, Naoya Itatani<sup>1</sup>, Stefanie Günther<sup>1</sup>, Georg M. Klump<sup>1</sup>

<sup>1</sup>*Animal Physiology & Behavior Group, IBU, Carl-von-Ossietzky University Oldenburg, Germany*

Auditory stream segregation can be elicited by different phase relations of the components of a harmonic complex (HC, Roberts et al. 2002). Different phase relations are known to elicit different streaming percepts. The present study using the ABA-paradigm (van Noorden, 1975) confirms the results of Roberts et al. (2002). Itatani and Klump (2011) reported neural correlates of streaming by phase relation of HC stimuli in the bird auditory forebrain. Their study, however, did not allow discerning whether the separate representation of HC with different phase relation is represented better by temporal response features or by the neurons' response rate. Here we report data from a combined neurophysiological (bird) and psychophysical (human) study varying the tone duration (TD, 40 or 125 ms), tone repetition time (TRT, 100 or 400 %), fundamental frequency (100 or 400 Hz), low-frequency cutoff of components (ranging from 100 to 5300 Hz in physiology and from 500 to 4500 Hz in psychophysics), and phase relation of components (cosine, alternate or random phase). In the psychophysical study different numbers of ABA- triplets (5 or 30 ABA-cycles) were

presented that encompass the range of cycles analyzed in physiology (20 out of 30 presented ABA-cycles). Analyzing these data with similar statistical measures allows evaluating whether perceptual streaming by phase relation is better represented by the neurons by a temporal or a rate code.

The neurons' spike rate responses matched the psychophysical results more closely than did the temporal responses. There were no significant main effects of TD and TRT both in psychophysics and the rate response (contrary to the temporal responses), all other main effects were significant for all measures. Interactions revealed a comparable pattern. Therefore we conclude that rate responses represent perception better than temporal responses.

Funded by the DFG (SFB/TRR 31) and a Georg-Lichtenberg stipend to L-V. D.

### **528** Passive Sound Exposure Does Not Explain Inhibitory Plasticity for Natural Calls in Adult Mice

Rudolph Mappus<sup>1</sup>, Frank Lin<sup>2</sup>, Alex Dunlap<sup>2</sup>, Tamara Ivanova<sup>1</sup>, Robert Liu<sup>1</sup>

<sup>1</sup>Emory University, <sup>2</sup>Georgia Institute of Technology

The neural plasticity that arises in adult auditory cortex as sounds gain behavioral relevance is of increasing interest. A series of studies have investigated this in the context of a mouse model where the natural ultrasound calls of pups become recognized by mouse mothers (Liu et al, 2006; Liu and Schreiner, 2007; Galindo-Leon et al, 2009). One of the striking findings when recording from awake, head-restrained mice has been longer duration evoked inhibition to ultrasound pup calls in mothers (M) compared to pup-naive virgins (V). This has led to questions about the mechanism for such inhibitory changes. One hypothesis is that exposure to the sounds themselves, irrespective of the social behavioral context of pup rearing, can be responsible for this plasticity. Indeed, recent studies in adult cats (Norena et al, 2006; Pienkowski and Eggermont, 2009) have demonstrated that passive, continuous exposure to moderate level sounds in a specific frequency band can suppress neural activity to those frequencies. In this report, we thus tested whether passive exposure alone to the ultrasounds generated from the maternal context could induce the same inhibitory plasticity observed in M. Using a microphone to pick up ultrasounds from the cage of a mother with pups (P0-P21), we filtered, amplified and fed this signal to an ultrasound speaker that broadcast these sounds to a physically separated cage housing a virgin littermate of the mother. We then performed single unit recordings from the auditory cortex of these passively exposed virgins (PEV) to determine the duration of pup call-evoked inhibition. Preliminary data indicates that such evoked inhibition in PEV is not significantly different from that observed in V, but is different from M. Hence, passive sound exposure in adult mice does not explain M's call-evoked inhibitory changes. Instead, the social interaction with pups and/or hormonal changes associated with motherhood may play a larger role. Funded by NIH DC8343.

### **529** Comparison of Response Properties and Task Related Plasticity in Ferret Primary and Secondary Tonotopic Auditory Cortex

Jonathan Fritz<sup>1</sup>, Serin Atiani<sup>2</sup>, Stephen David<sup>1</sup>, Michael Locastro<sup>1</sup>, Diego Elgueda<sup>1</sup>, Bernhard Englitz<sup>1</sup>, Susanne Radtke-Schuller<sup>3</sup>, Shihab Shamma<sup>1</sup>

<sup>1</sup>University of Maryland, <sup>2</sup>University of Montreal, <sup>3</sup>Ludwig Maximilians University, Munich

To investigate the role of higher cortical areas in acoustic information processing, task-related receptive field and response plasticity, we recorded from two secondary, tonotopically organized cortical areas (PPF and PSF) in the posterior ectosylvian gyrus (PEG) (Bizley et al., 2005) of trained ferrets. We trained six ferrets on a conditioned avoidance auditory task that required them to distinguish a set of rippled noise or band pass noise stimuli (reference stimuli) from pure tones (target stimuli). We physiologically mapped mirror image tonotopic maps, corresponding to A1 and the two tonotopic areas of PEG (confirmed by neuroanatomical studies). We recorded from single units in A1 (165 neurons) and PEG (210 neurons) during two behavioral conditions: while the animals were in a quiescent state of passive listening, and while in an active state during task performance. We found some differences in response properties during passive listening between A1 and PEG, and even more marked differences in active conditions. When we compared rapid task-related receptive field plasticity (Fritz et al., 2003) in A1 and PEG, we found that PEG receptive fields exhibited changes reflecting the target and reference stimuli in a similar manner to A1. However, unlike A1, we also observed robust task-related changes in firing rates and response dynamics in PEG. Specifically, in many cases, responses to behavioral target vs reference stimuli diverged substantially during the active state for PEG neurons, presumably allowing for greater discrimination in these cells between the two classes of acoustic stimuli during active listening vs quiescent (non-task) listening. Such response modulation, observed at a single cell and population level, may be pivotal for categorical encoding of attended auditory objects, previously observed in secondary auditory cortex (Tsunada et al., 2011) and prefrontal cortex (Cohen et al., 2006; Fritz et al., 2010). Insight into the differential types and magnitude of task-related plasticity in secondary auditory cortex may clarify the functional contributions of these higher auditory areas to acoustic representation, and auditory attention and memory.

### **530** Auditory Object Based Cortical Representation During Speech Segregation

Nai Ding<sup>1</sup>, Jonathan Z. Simon<sup>1</sup>

<sup>1</sup>University of Maryland, College Park

The neural mechanism underlying the cocktail party phenomenon is studied in normal-hearing subjects using magnetoencephalography (MEG). The subjects listen to two co-located speakers, one male and one female, each narrating a story. The subjects were instructed to attend to only one speaker. Based on single-trial analysis, we

demonstrate that neural activity in auditory cortex is dominantly synchronized to the slow temporal modulations of the attended speech, and, critically, not to the acoustical modulations of the speech mixture. From this neural activity, the temporal envelope of the attended speech can be accurately reconstructed, even for novel stimuli. The unattended speech is also represented cortically, but more weakly, and with a distinct spatial-temporal response profile. Therefore, the two mixed speech streams have been neurally segregated and are represented by separate and distinct spatial-temporal neural codes.

The dependence of the neural coding mechanism on the relative intensity of the two simultaneous speakers was also investigated. When the relative intensity is changed over a ~10 dB range, the acoustics of the stimulus change dramatically, but the listeners still understand the attended speaker with greater than 50% intelligibility. It is demonstrated that neither neural representation of the two speakers in auditory cortex is affected by the relative intensity of the two speakers. Therefore, it is the perceptual importance, rather than the physical dominance, of a speaker that determines the spatial-temporal neural encoding of the fundamental acoustic features of the segregated stream. Taken together, these results suggest that, in a complex auditory scene, the cortical representation of sound is organized in terms of auditory objects, e.g. speakers, and each auditory object is encoded differently, based on top-down attention.

### **531 Repetition Suppression for Pitch Using fMRI**

**Tobias Overath**<sup>1</sup>, Sukhbinder Kumar<sup>1,2</sup>, Timothy D. Griffiths<sup>2</sup>

<sup>1</sup>University College London, <sup>2</sup>Newcastle University

Despite its ubiquity in speech and music, the cortical origins and neural mechanisms underlying pitch perception are still not well understood. While some researchers have shown cortical correlates of pitch in lateral Heschl's gyrus (HG) (Patterson et al., 2002; Penagos et al., 2005; Puschmann et al., 2010), others argue for a locus in planum temporale (PT) (Hall & Plack, 2009). A more distributed representation of pitch along the HG has also been argued (Griffiths et al., 2010), where different parts of HG have specific functions within a pitch system (Kumar et al., 2011). Similarly, evidence from animal studies is similarly variable in that some studies show a single locus (Bendor and Wang, 2005), while others (Bizley et al., 2009) suggest a distributed representation of pitch.

Previous fMRI studies have generally used sustained sounds of several seconds duration within a sparse temporal sampling acquisition design. This design assesses only the steady-state response to pitch and lacks information about the temporal dynamics of the response. Here, we make use of an adaptation fMRI paradigm (Grill-Spector and Malach, 2001) using roving pitch values (Garrido et al., 2009) and three different pitch types (harmonic complex, clicktrain, regular interval noise) to elucidate areas in human auditory cortex that show repetition suppression (RS) to repeated presentations of a pitch stimulus. The decay of activity with the number of

repetitions was modelled using an exponential decay function  $\exp(-k \cdot n)$ , where  $k$  is the decay constant and  $n$  is the number of repetitions. We determined the value of the decay constant  $k$  for each voxel of the auditory cortex by using a Taylor series expansion around a nominal value of  $k$ . Initial data reveal the fastest decay constants in mid to lateral HG, extending posterior-laterally into Heschl's sulcus. The data provide further support for specific pitch mechanisms in mid to lateral HG.

#### References

- Bendor & Wang (2005) *Nature*, 436: 1161-1165.  
Bizley et al. (2009) *J Neurosci*, 29: 2064-2075.  
Garrido et al. (2009) *Neuroimage*, 48: 269-279.  
Griffiths et al. (2010) *Current Biology*, 20: 1-5.  
Grill-Spector & Malach (2001) *Acta Psychol (Amst)*, 107: 293-321.  
Kumar et al. (2011) *J Cogn Neurosci*, 23: 3084-3094.  
Patterson et al. (2002) *Neuron*, 36: 767-776.  
Penagos et al. (2005) *J Neurosci*, 24: 6810-6815.  
Puschmann et al. (2010) *Neuroimage*, 49: 1641-1649.

### **532 Neural Mechanisms of Rhythmic Masking Release in Monkey Primary Auditory Cortex: Implications for Models of Auditory Scene Analysis**

**Yonatan Fishman**<sup>1</sup>, Christophe Michey<sup>2</sup>, Mitchell Steinschneider<sup>1</sup>

<sup>1</sup>Albert Einstein College of Medicine, <sup>2</sup>University of Minnesota

The ability to detect and track relevant acoustic signals embedded in a background of other sounds is crucial for hearing in complex acoustic environments. This ability is exemplified by a perceptual phenomenon known as 'rhythmic masking release' (RMR). To demonstrate RMR, a sequence of tones forming a target rhythm is intermingled with physically identical 'distracter' sounds that perceptually mask the rhythm. The rhythm can be 'released from masking' by adding 'flanker' tones in adjacent frequency channels that are synchronous with the distracters. RMR represents a special case of auditory stream segregation, whereby the target rhythm is perceptually segregated from the background of identical distracters. The neural basis of this perceptual effect is unknown. Previous studies suggest the involvement of primary auditory cortex (A1) in the perceptual organization of sound patterns. Here, we recorded neural responses to RMR sequences in A1 of awake monkeys in order to identify neural correlates and underlying mechanisms of RMR. We also tested whether current models of stream segregation, when applied to these responses, can account for the perceptual organization of RMR sequences. We find that responses to distracters are suppressed by the simultaneous flankers, leading to target responses that are larger than distracter responses. Resultant neural response patterns thus correlate with the perceptual restoration of the target rhythm in RMR. We also find that predictions of two physiological models of stream segregation parallel psychoacoustic data for RMR in humans. These results provide additional support for the view that important aspects of auditory perceptual

organization may be explained by relatively basic neural mechanisms at the cortical level.

### **533 Modeling of Harmonic Sensitive Neurons in the Primary Auditory Cortex of Marmoset Monkeys**

**Eyal Dekel<sup>1</sup>, Lei Feng<sup>1</sup>, Xiaoqin Wang<sup>1</sup>, Kechen Zhang<sup>1</sup>**

<sup>1</sup>*Johns Hopkins University*

Neurons that are sensitive to harmonic complex tones have been shown to exist in central auditory structures from the inferior colliculus to the auditory cortex. Our goal in this project was to investigate whether a computational model

comprised of excitatory and inhibitory units can account for the high-level complex neural responses to various simple and complex stimuli in the primary auditory cortex, using data recorded from harmonic-sensitive neurons in the auditory

cortex of awake marmosets (*Callithrix jacchus*). The stimuli presented to these neurons included pure tones, two-tone combinations, random harmonic tone stacks and jitter. Three models with increasing level of complexity were designed

to account for the observed cortical responses, representing the neural connections in different stages of the auditory processing hierarchy. All of the models included the combination of inhibitory and excitatory neurons, modified from

previously suggested models of A1. Models 1 and 2 included a simple feed-forward network with three excitatory neurons and two inhibitory neurons, all converging to a final output, with (Model 2) and without (Model 1) lateral connections between them. These two models consider the thalamus as a relay and represent the cortical layers alone.

Model 3 simulates the auditory processing from the IC, through the thalamus and into A1. The recorded data from each neuron was divided to optimization and validation data sets, and the parameters of each model were fitted based on the optimization data set using exhaustive search optimization of the mean square error (MSE) between the measured and predicted responses. The model's predictive capability was measured using the unseen validation data set, and the models were compared using the correlation coefficient ( $r$ ) and the Bayesian information criterion (BIC), which also penalizes for increased model complexity. The fitting results suggest two main points: 1) Complex models (such as Model 3) fit the data better than the simple ones (Models 1 and 2), but their large number of parameters gives them a higher BIC score. Also, for the simple stimuli presented here, these complex models do not generalize as well as the simple ones, probably due to over-fitting of noise. 2) A reoccurring solution to the fitted models suggest that lateral connections between the inhibitory and excitatory units support a co-tuned relationship between their weights (similar mean and variance), forming a subunit that may possibly underlie the observed neural responses to harmonic sound structures.

### **534 Area of Cortical Representation in Detection of Acoustic Signals**

**David Blake<sup>1</sup>, Ezekiel Carpenter-Hyland<sup>1</sup>, Almira Vazdarjanova<sup>1</sup>**

<sup>1</sup>*Georgia Health Sciences University*

The rules governing cortical plasticity that occurs in learning to detect an acoustic signal are three-fold. First, all neurons become more responsive and increase their receptive field sizes. Second, neural responses to the task target are followed by acetylcholine, which naturally reinforces them. Third, neural activity during attended behavioral trials is selectively suppressed. The net effect is a spreading of the cortical signal largely by an increase of the area of the response. Recently, we blocked the expression of an immediate early gene during detection learning in rats. In the session while the block was present, no behavioral differences emerged between controls and gene block groups. One day later, the gene block group performed the task as though its memory for the target was erased, while the control group had no impact. Cortical mapping of the groups one day after the gene block behavioral session revealed that the experimental group had a stronger response to the target than the control group, and a smaller cortical area of response. A model that utilizes a cross correlation measure is sensitive to cortical area of representation and can explain the experimental results. Incorporating these results with prior work on learning-induced plasticity in auditory cortex suggests that mechanisms operate to enhance the cortical area of the response to improve its behavioral salience.

### **535 A Region in Human Auditory Cortex Exhibits Pitch-Selective Responses Across a Wide Range of Natural and Synthetic Sounds**

**Samuel Norman-Haignere<sup>1</sup>, Josh McDermott<sup>2</sup>, Nancy Kanwisher<sup>1</sup>**

<sup>1</sup>*MIT*, <sup>2</sup>*NYU*

Pitch is a salient perceptual feature of many real-world sounds, including music and speech. Despite longstanding interest, evidence for a pitch center in auditory cortex has remained controversial. Using small collections of synthetic stimuli, some groups have observed elevated responses to sounds with pitch in a focal region of auditory cortex (near Heschl's gyrus), while others have observed anatomically distributed responses throughout auditory cortex. Here we use fMRI to search for regions that respond more to pitched than unpitched sounds across a wide range of synthetic and natural sound categories. In experiment 1, subjects were scanned while listening to synthetic sounds that varied in pitch salience, frequency composition, harmonic resolvability, and harmonicity (via spectral jittering). In each subject tested and across 4 independent contrasts, we observed a small, distinct region in the planum polare (anterior to Heschl's gyrus) that responded more strongly to sounds with resolved harmonics compared to both frequency-matched noise and sounds with unresolved harmonics. We also observed a strong response to sounds with frequency components that were resolvable but inharmonic. Resolved harmonics thus appear sufficient to activate this region irrespective of

whether they share a fundamental frequency, as though they engage pitch processing mechanisms even when lacking a clear pitch. In experiment 2, we examined the selectivity of this region by testing its response to several different natural sound categories that varied widely in their low- and high-level features. Despite this variation, we observed a strong response to pitched sound categories (e.g. music, pitched environmental sounds) and a weak response to sound categories with weaker pitch (e.g. drum tracks, unpitched environmental sounds). These results support the existence of a small, distinct region in human auditory cortex that is selectively involved in the processing of pitch.

### **536 Coding Spectral Edges in the Auditory Cortex**

Nicolas Catz<sup>1</sup>, Arnaud Norena<sup>1</sup>

<sup>1</sup>*CNRS laboratory of integrative and adaptive neurobiology*  
Sensory systems have to make sense of the natural environment where relevant signals and background noise are mixed together. They can rely on the fact that relevant signals often present physical properties, such as spectral edges, which may differentiate them from background noise. However, “spectral discontinuities” may also be created in presence of cochlear insults. These “spectral discontinuities” have been found to result in dramatic changes in auditory cortex, such as the reorganization of the tonotopic map.

In this study, we recorded neural activity (multi-unit activity and local field potentials) in the auditory cortex of anesthetized guinea pigs evoked by stimuli presenting a spectral contrast (“notched spectrum”). Three bandwidths (half, one and two octaves), two depths (-30 dB or no stimulation within the notch) and two slopes of the notch were studied. The stimuli lasted 3 mns and were composed of pure tones of different frequencies (all frequencies between 500 Hz and 32 kHz by 1/8 octave step) presented randomly over time. All stimuli used in the study served two purposes simultaneously; they provided a given sensory environment to the animal, and at the same time, they allowed the characterization of the spectro-temporal receptive fields of cortical neurons.

We found that cortical responses evoked by the “notch frequencies” were dramatically decreased, especially for the half-octave notch. On the other hand, the cortical responses evoked by the “edge frequencies” of the notch were dramatically enhanced; this enhancement was sensitive to the depth and the slope of the notch: it was maximal when there was no stimulation within the notch and when the slope of the notch was the steepest.

Overall, these results suggest that the central auditory system enhances the “spectral edges” of acoustic stimuli, while suppressing the frequencies between the edges, especially when the edges are relatively close to each other (1 octave or less).

### **537 Adaptive Mechanisms Underlying the Perceptual Bias of Ambiguous Stimuli in Auditory Cortex**

Bernhard Englitz<sup>1</sup>, Ping-Bo Yin<sup>1</sup>, Sahar Akram<sup>1</sup>, Stephen V. David<sup>1</sup>, Claire Chambers<sup>2</sup>, Daniel Pressnitzer<sup>2</sup>, Jonathan B Fritz<sup>1</sup>, Shihab Shamma<sup>1</sup>

<sup>1</sup>*University of Maryland, College Park*, <sup>2</sup>*Equipe Audition, Ecole Normale Supérieure*

Stimuli are interpreted in the context of the preceding sensory environment. Bistable stimuli provide a substrate for probing the effects of different contexts on the neuronal population response. Shepard tones are complex acoustical stimuli - consisting of an octave-spaced stack of pure tones - which have a tonal character but non-unique pitch. A sequence of two Shepard tones separated in frequency by 6 semitones is bistably perceived as either ascending or descending in frequency, the so-called ‘tritone paradox’. We present tritonal Shepard pairs in different auditory contexts - themselves sequences of Shepard pairs in a more restricted range - and compare the neural responses in both upward and downward contexts. These sequences have been shown to influence perception of the tritone pair in humans (Chambers et al, in prep). Single cell recordings are collected from the auditory cortex of 6 awake, passively listening ferrets.

Neurons respond to Shepard tones with a wide variety of responses based on their basis properties. By applying a range of dimensionality reduction techniques, we obtain a low-dimensional representation of the Shepard tones from the population neuronal responses. Shepard tones with different base pitch, map to a circular structure thus capturing the periodic nature of the Shepard tone stimulus. When mapped to the circle of pitch classes, the tritone Shepard tones appear systematically shifted ( $p < 1e-15$ ,  $\sim 1/4$  tone) from their expected base pitch, depending on the contextual sequence presented before. Using long sequences of Shepard tones we find that neuronal adaptation can explain these shifts. Given that the shifts are systematic they constrain how the activity in A1 leads to perception. Different decoding strategies predict consistent or opposite interpretations of the neural responses when compared to human perception of the same stimuli. We suggest a decoding strategy consistent with both bistable, stable and biased Shepard pairs.

### **538 Next Generation Sequencing in Case Control and Family Studies of Disease**

W. Richard McCombie<sup>1</sup>

<sup>1</sup>*Cold Spring Harbor Laboratory*

The rapid changes in DNA sequencing technology that have occurred over the past several years have revolutionized our ability to understand human genetics. As a result of these changes in technology we are now able to sequence the genomes of hundreds to thousands of individuals and the protein coding regions or exomes of thousands to tens of thousands of individuals. I will explain the various concepts of next generation sequencing and how the change in the technology has changed the way we can do biology and soon change the way medicine is carried out. Both whole genome sequencing and

sequencing the protein coding areas of genes have their place as we look to uncover the variation that leads to a variety of human diseases. In particular I will discuss how we use both exome sequencing and whole genome sequencing on different populations in order to understand the genetic variation that underlies major psychiatric disorders. The exome sequencing approaches let us study large case control populations where we need to look at thousands of individuals to determine the genetic variation that makes them susceptible to psychiatric disorders. In addition we are extensively involved in whole genome sequencing where we query every nucleotide of the genome of multiple members of affected families. These family studies present a unique opportunity because they allow us to more readily filter out variants that do not contribute to the disease phenotype but rather are just part of the normal background of human variation. By sequencing the entire genome of multiple individuals from these families with and without the disorder we hope to uncover the variation that leads to their illness. This is only recently become possible due to advances in sequencing technology. Therefore we can now carry out what previously was called old-fashioned human genetics by looking at traits inherited within families but by looking at the nucleotide level of resolution. As technology continues to advance we will shift more and more towards whole genome sequencing and this will become more and more common in the clinic as a diagnostic approach.

### **539 Using Gene Capture and Massively-Parallel Next Generation Sequencing Technologies to Enhance the Current Universal Newborn Hearing Screening Program**

**Xi Lin<sup>1</sup>**, Wenxue Tang<sup>1</sup>, Shoeb Ahmad<sup>1</sup>, Jingqiao Lu<sup>1</sup>  
<sup>1</sup>*Emory University School of Medicine*

Targeted capture and sequencing of a group of disease-linked human genes by the next-generation sequencing (NGS) method has been used feasibly to screen genetic mutations accurately. One major barrier for epidemiological scale uses of the NGS technology for mutation screening, however, seems to be the high per-sample cost during the gene enrichment step. We have developed a low-cost method for capturing exons of >80 genes known to cause deafness in humans. Results showed that our approach achieved specificity, multiplexicity, uniformity and depth of coverage in exon captures suitable for sequencing applications by the NGS systems. Reliable genotype calls for various homozygous and heterozygous mutations (e.g., single-nucleotide substitution and small insertion/deletion) were achieved. The results were confirmed independently by conventional Sanger sequencing.

The high coverage depth and cost benefits of our new gene capture approach is applied for genetic screening of newborns who fail the first-round universal newborn hearing screening (UNHS) by either DPOAE or ABR. We first built a wild type (WT) SNP database obtained from hundreds of normal hearing adult subjects. Genetic variations obtained from NGS data analysis after filtering

through the WT SNP database were compared with reported deafness mutations stored in database. So far we have entered >3,500 entries into such a database including about 170 genes. If no matching mutations were found, we used a computational approach to predict potential effects of the variants on the protein function by performing the scale-invariant feature transform (SIFT) analysis. Preliminary data obtained from 96 samples found a spectrum of mutations in *GJB2*, *SLC26A4*, *WFS1*, *DFNB59*, *GJB4*, *CDH23*, *KCNE1*, *MYO15A*, *KCNJ10*, *MYO1F*, *GJB3*, and *POU3F4* genes. More findings of the study will be discussed. We will also discuss features of the genetic hearing screening that significantly enhance the current UNHS programs.

### **540 Improving the Clinical Care of Patients Affected by Hearing Loss Using Massively Parallel Sequencing**

**Richard Smith<sup>1</sup>**, Robert Eppsteiner<sup>1</sup>, Jose Gurrola<sup>1</sup>, A. Eliot Shearer<sup>1</sup>

<sup>1</sup>*University of Iowa*

Massively parallel sequencing (MPS) is revolutionizing human genetics and promises to be the harbinger of personalized medicine. In the treatment of deaf and hard-of-hearing persons it has made comprehensive genetic testing possible, changing the clinical evaluation of these persons. The OtoSCOPE platform, which we have developed, uses targeted sequence capture paired with MPS to sequence all exons of all genes involved in hearing loss simultaneously. In a proof-of-principle study, we have shown that OtoSCOPE offers a sensitivity, specificity and reproducibility sufficient for genetic diagnosis of hearing loss in a clinical setting. We have also shown that 12 samples can be barcoded precapture without compromising results thereby reducing the cost of testing. To streamline data analysis, we have developed a bioinformatics platform, which incorporates allele frequencies of deafness gene variations in multiple ethnically different control populations. This comprehensive platform will be integral to personalized gene-and-mutation-specific habilitations options for the treatment of hearing loss.

### **541 Exome Sequencing for Human Genetics**

**Tom Walsh<sup>1</sup>**

<sup>1</sup>*University of Washington*

The very rapid diffusion of genomic technology in the past 18 months has opened possibilities for genetics studies that heretofore geneticists could only dream of. Of the currently widespread genomic sequencing approaches, exome sequencing is perhaps the most broadly applicable and tractable. I will focus on exome-sequencing-based human genetics studies in three overlapping classes: (1) discovery of the genes responsible for Mendelian traits in clinically well-characterized families; (2) identification of causal mutations carried by individual patients in genes already known to influence complex traits; and (3) discovery of novel genes responsible for complex traits, identified in particularly informative individual cases or families; for example the discovery of de novo mutations

responsible for psychiatric illness. All these classes of projects focus on discovery and characterization of genes of major effect on a phenotype, based on a common-disease-multiple-rare-alleles model and an understanding of genetic heterogeneity.

### **542 Next Generation Sequencing in Molecular Epidemiological Studies of Deafness**

Xue Liu<sup>1</sup>

<sup>1</sup>University of Miami

For a genetically heterogeneous disease such as genetic deafness which is determined almost exclusively by single genes or at most pairs of genes at different loci, rather than complex multifactorial interactions, the advent of the "\$1000 genome sequence" will clearly make it possible to determine the genetic cause for a patient's deafness that is "not on the chip", simply by sequencing their genome to identify their "private" mutation. Recent advances in NGS have provided unprecedented opportunities for the large scale screening of DNA variation throughout the genome. The recent technological advances in "target-enrichment" methods and next generation sequencing (NGS) offer a unique opportunity to break through the barriers of limitations imposed by gene arrays (limited number of basepairs) and now allow for the complete analysis of all known deafness-causing genes. It is expected that use of this new technology in our large population-based DNA samples of deaf individuals will result in determination of the molecular epidemiology of NSHL and will result in a new wave of discoveries of the remaining genes for Mendelian disorders. We have collected DNA samples from 600 probands from multiplex families with no mutations in the common deafness genes from three unique cohorts. The three populations under study, China, Turkey and the USA, vary in the genetic epidemiology of deafness. We will determine the overall frequencies of different forms of genetic deafness in each of the three populations and identify ethnic differences in the distribution of genes for HL using target-enrichment/NGS. We will complete mutation screening of all genes causing NSHL using target-enrichment/NGS and perform exome sequencing in patients without a second mutant allele. We will identify new genes for ARSNHL using traditional and innovative technologies in the collected consanguineous families and in the selected probands are the offspring of deaf couples and have extensive family histories of deafness but do not carry mutations in any known deafness gene.

### **543 Identifying and Characterizing Risk Loci for Coronary Artery Disease**

Kelly Frazer<sup>1</sup>

<sup>1</sup>University of California San Diego

Genome-wide association studies have identified single nucleotide polymorphisms (SNPs) in the 9p21 gene desert associated with coronary artery disease (CAD) and type 2 diabetes. Despite evidence for a role of the associated interval in neighbouring gene regulation, the biological underpinnings of these genetic associations with CAD or

type 2 diabetes have not yet been explained. Here we identify 33 enhancers in 9p21; the interval is the second densest gene desert for predicted enhancers and six times denser than the whole genome ( $P < 6.55 \times 10^{-33}$ ). The CAD risk alleles of SNPs rs10811656 and rs10757278 are located in one of these enhancers and disrupt a binding site for STAT1. Lymphoblastoid cell lines homozygous for the CAD risk haplotype show no binding of STAT1, and in lymphoblastoid cell lines homozygous for the CAD non-risk haplotype, binding of STAT1 inhibits *CDKN2BAS* (also known as *CDKN2B-AS1*) expression, which is reversed by short interfering RNA knockdown of *STAT1*. Using a new, open-ended approach to detect long-distance interactions, we find that in human vascular endothelial cells the enhancer interval containing the CAD locus physically interacts with the *CDKN2A/B* locus, the *MTAP* gene and an interval downstream of *IFNA21*. In human vascular endothelial cells, interferon- $\gamma$  activation strongly affects the structure of the chromatin and the transcriptional regulation in the 9p21 locus, including STAT1-binding, long-range enhancer interactions and altered expression of neighbouring genes. Our findings establish a link between CAD genetic susceptibility and the response to inflammatory signalling in a vascular cell type and thus demonstrate the utility of genome-wide association study findings in directing studies to novel genomic loci and biological processes important for disease aetiology.

### **544 Using Massively Parallel Sequencing for Gene Discovery in the Middle Eastern Hearing Impaired Population**

Karen B. Avraham<sup>1</sup>, Moein Kanaan<sup>2</sup>

<sup>1</sup>Dept of Human Molecular Genetics, Sackler Faculty of Medicine, Tel Aviv University, Tel Aviv, Israel, <sup>2</sup>Department of Biological Sciences, Bethlehem University, Bethlehem, Palestinian Authority

Conventional methods to screen for mutations in the hearing impaired population focus primarily on *GJB2*, the most frequent cause of childhood deafness, and previously discovered mutations in other known genes. In the Middle East, each gene has been screened individually, focusing on 9 and 13 genes in the Jewish Israeli and Palestinian Arab populations, respectively. Present screening therefore misses most mutations in other known genes found worldwide and all mutations in genes not yet associated with hearing loss. Our Israeli Jewish-Palestinian Arab cohort is composed of over 500 unrelated individuals with hearing loss. We have developed a method to screen the exons and flanking intron sequences of all known deafness genes simultaneously, using gene capture and massively parallel sequencing (Brownstein, Friedman et al. *Genome Biology* 2011). We incorporated human orthologues of mouse genes responsible for syndromic or non-syndromic hearing loss as well, since many genes for human deafness are responsible for mouse deafness. For new genes, whole exome sequencing is performed, in conjunction with homozygosity mapping for identification of the chromosomal location of the defective gene. This minimizes the region for which variants must be analyzed. This research will pave the way

for identification of most mutations responsible for hereditary hearing loss in these families, as well as for new gene discovery, and subsequently to further understanding of the biological mechanisms involved in hearing loss.

### **545 Scene Analysis in the Natural Environment**

**Michael Lewicki**<sup>1</sup>, Bruno Olshausen<sup>2</sup>, Annemarie Surlykke<sup>3</sup>, Cynthia Moss<sup>4</sup>

<sup>1</sup>Case Western Reserve University, <sup>2</sup>UC Berkeley, <sup>3</sup>Univ. Southern Denmark, <sup>4</sup>Univ. Maryland

Scene analysis is a term currently used in many fields of research -- from psychophysics to animal behavior -- which has come to encompass a broad range of tasks, questions, and experimental approaches. In this talk, I will review recent progress related to scene analysis from a broad perspective that includes behavioral, physiological, and computational aspects. Scene analysis is a universal problem solved by nearly all animals. It is not the end point of perception but an integral part of natural behavior, which depends on the coordination of perception and action.

There are many types of scene analysis problems that occur in different species and different modalities. In this talk, I will discuss many of these and place them in a common framework. I will emphasize several under-appreciated aspects of scene analysis that stand in contrast to the traditional view that emphasizes sequential feature extraction and pattern grouping. First, the information processing in scene analysis can take place at multiple levels and depends upon interactions between these levels in order to identify and resolve ambiguous perceptual patterns. Second, scene analysis requires memory to integrate information across time and modality to perform tasks such as search, segregation and recognition. Third, one of the overriding goals in scene analysis is to form a persistent representation of the three-dimensional scene in order to drive locomotion and navigation. Finally, these processes are not passive but are tightly integrated with actions that select what information to gather to progress toward behavioral goals. Obtaining insight into how scene analysis operates in natural, complex sensory environments, in contrast to simplified laboratory settings, remains a formidable challenge, but recent use of more sophisticated manipulations of both natural stimuli and behavior promise to offer new insights into this complex problem.

### **546 Understanding Real-World Hearing with Sound Analysis and Synthesis**

**Josh McDermott**<sup>1</sup>

<sup>1</sup>New York University

An ultimate goal of hearing research is to understand how the auditory system supports behavior in natural environments, where sound signals have complex structure not reflected in traditional laboratory stimuli. As listeners, we must recognize events and objects from these signals, yet it is typically not obvious how to extract the relevant properties from the acoustic input. Despite the challenging nature of real-world recognition, the auditory system performs remarkably well, far better than the best

computer-based hearing systems. This talk will discuss how clues to our auditory competence can be obtained using sound analysis and synthesis. Analysis of natural sounds reveals a diverse set of statistical properties that the auditory system is potentially attuned to. Synthesis of sounds with these properties provides a strong test of their perceptual importance, and can produce stimuli that have unique experimental applications. I will discuss examples of this approach that provide insight into our ability to recognize and segregate natural sounds, and that illustrate how sound analysis and synthesis can facilitate the study of real-world hearing.

### **547 Transformations in Processing of Naturalistic Sounds from Auditory Midbrain to Cortex**

**Christoph Schreiner**<sup>1</sup>, Jonathan Shih<sup>1</sup>, Craig Atencio<sup>1</sup>  
<sup>1</sup>UCSF

The main goal of computational neuroscience of the auditory system is to quantitatively describe information processing in auditory centers. Successful descriptions will link, and eventually account for, the principles of auditory processing from synaptic, cellular, network, and behavioral perspectives. Since processing is highly nonlinear, it precludes a single approach that can account for all naturally occurring stimulus configurations. By using parametrically characterized sounds with some natural sound features, multi-dimensional linear/nonlinear processing models may reveal significant characteristics of central auditory behavior. We will discuss these models within the framework of spectro-temporal receptive fields and how they may be used to account for transformations in sound processing in the auditory midbrain, thalamus, and cortex. These spectro-temporal receptive field models revealed that the nature of interacting receptive field components and the prevalence of nonlinear stimulus combination responses changed along the lemniscal pathway: compared to the mesencephalon and diencephalon, cortical processing showed significant increases in processing complexity, STRF cooperativity, and nonlinearity. The potential implications of these processing changes for the identification of auditory cortical functions and tasks will be discussed.

### **548 Perceptual Adaptation to Room Acoustics**

**Pavel Zahorik**<sup>1</sup>, Eugene Brandewie<sup>1</sup>, Nirmal Srinivasan<sup>1</sup>  
<sup>1</sup>University of Louisville

Reverberant listening environments pose significant challenges for many real-world listening tasks. Such environments degrade important acoustical cues to spatial location and alter the fundamental acoustical changes in the amplitude envelope of speech signals. Not surprisingly, individuals with hearing loss often report significant difficulty in localizing sounds and understanding speech in such environments, yet the normally functioning auditory system appears to be remarkably robust to the effects of acoustic reflections and reverberation. Emerging evidence suggests that at least some of this apparent insensitivity may result from adaptive processes in the

human auditory system that selectively suppress the acoustical contributions of reflective listening environments. Here we summarize recent work in our laboratory that demonstrates room adaptation effects primarily using speech intelligibility tasks. A key component of this research is the use of virtual auditory space techniques that allow both precise control and realistic simulation of various real-world listening environments. [Work supported by NIH R01DC008168].

### **549** Cortical Processing of Vocal Communication Sounds in Naturally Behaving Primates

Xiaoqin Wang<sup>1</sup>

<sup>1</sup>Johns Hopkins University

One of the most important functions of the hearing is to support vocal communication among conspecifics of a species. During vocal communication, the auditory system must deal with both externally generated (from conspecifics) and self-produced sounds (during speaking or vocalizing). While much attention has been given to studies on how the auditory system processes natural sound statistics, little is known on how the auditory system processes self-produced sounds during natural vocal behaviors. Recent studies have shown that the vocal production system in the brain modulates neural activity of the auditory system such that neural representations of self-produced sounds differ from representations of similar sounds that are externally generated. These observations suggest that in a real-world hearing environment, what one's brain actually hears depends not only on statistics of sounds, but also on how sounds are produced. I will review this line of research and discuss the latest findings using wireless neural recording techniques in naturally vocalizing marmoset monkeys.

### **550** Neuronal Dynamics and Representations Using Naturalistic Stimuli: Moving Beyond Simple Playback

Daniel Margoliash<sup>1</sup>

<sup>1</sup>University of Chicago

European starlings readily learn to discriminate small sets of songs after they have learned the task procedure training on an initial song set. The learning rates for second songs are very rapid, approximating what occurs in nature. Examining the activity of forebrain CMM auditory neurons, we find on the first day of second learning a large increase in the population of neurons responsive to the new songs, which returns to baseline over subsequent days. The rates of neuronal and behavioral changes correlate across individuals. Initial training songs also show a transitory increase even though birds are no longer training on them, suggesting that the increase in neuronal activity is task not stimulus related. At baseline (either before or after learning), known stimuli are represented by small numbers of selective neurons. Thus, auditory learning involves very rapid increases in neuronal representations, which relax as memories become distributed, selective, and sparse.

How are the song stimuli represented at the level of individual neurons? We have adopted models developed by Gabriel Mindlin and colleagues describing the dynamics of the syrinx and upper respiratory tract. We verify these models by recording single units in the motor system for song of sleeping birds while presenting artificial model songs. Good model songs elicit responses comparable to those for playback of the bird's own song. It remains an open question whether the receptive field of CMM neurons can be better approximated by models of the vocal apparatus than by the more commonly used spectro-temporal models. CMM neurons are poorly modeled by STRFs but responses to small segments of song motifs can be added linearly to make accurate predictions of responses to complete motifs. This suggests that the appropriate non-linear decomposition of song can model CMM receptive fields.

Supported by grants from NIH (DC007206) and NSF (CRCNS 0905030).

### **551** Chronic Implantation of a Single Channel Laser Stimulator in Cats

Agnella Matic<sup>1</sup>, Alan Robinson<sup>1</sup>, Suhred Rajguru<sup>2</sup>, Stuart Stock<sup>1</sup>, Claus-Peter Richter<sup>1</sup>

<sup>1</sup>Northwestern University, <sup>2</sup>University of Miami

Infrared neural stimulation (INS) uses pulsed, infrared radiation to depolarize neurons in vivo as an alternative to conventional electrical stimuli. The goal of our work is to develop an INS-based cochlear implant that will have more non-overlapping channels for stimulation than a conventional implant. Recent work in our lab has shown that INS of neurons in the cochlea is feasible and safe in an acute feline model. We have also shown that INS can selectively stimulate the cochlea, on the order of a low sound level tone. This study investigated the long-term safety and efficacy with a chronically implanted optical fiber connected to a miniaturized laser stimulator. Normal hearing cats were chronically implanted with a single-channel laser stimulator. Following implantation, the cats were stimulated for ~ 6 hours/day, for 6 weeks. The laser operated at a center wavelength of 1850 nm, 100  $\mu$ s pulse duration, 200 Hz repetition rate, and 250mW peak power (25  $\mu$ J/pulse). Post-operative auditory brainstem responses (ABRs) show an elevation of acoustic thresholds at high frequencies, in the region of the cochlea where the cochleostomy was created. No further elevation of the acoustically-evoked ABRs occurred during the six week duration of the laser stimulation. Optically-evoked ABRs demonstrate that the portable laser delivers sufficient energy to depolarize the neurons. At the laser turn-on, the cats exhibited a behavioral response to the laser (e.g. if the laser was implanted on the left side, the cat turned its head towards the left). Histology shows some tissue growth in the bulla and scala tympani. There was no histological evidence of thermal tissue damage in the stimulated cochleae. Post-mortem microCT confirmed the placement of the optical fibers, 400-1600 $\mu$ m away from the spiral ganglion neurons. These experiments represent the next step towards our goal of constructing a laser-based cochlear implant.

This work was supported by Lockheed Martin Aculight.

### **552 The Bioelectrical Interface of Cochlear Implants – Oriented Collagen as a Potential Electrode Surface Coating to Direct Neurite Outgrowth**

**Stefan Volkenstein**<sup>1,2</sup>, John E Kirkwood<sup>3</sup>, Edwina Lai<sup>3</sup>, Stefan Dazert<sup>1</sup>, Gerald G Fuller<sup>3</sup>, Stefan Heller<sup>2</sup>

<sup>1</sup>*Department of Otolaryngology – Head & Neck Surgery, Ruhr University Bochum, St. Elisabeth-Hospital,*

<sup>2</sup>*Department of Otolaryngology – Head & Neck Surgery, Stanford University School of Medicine, Stanford,*

<sup>3</sup>*Department of Chemical Engineering, Stanford University, Stanford, CA 94305*

In patients with severe to profound hearing loss, cochlear implants (CIs) are currently the only therapeutic option when the amplification with conventional hearing aids does no longer lead to a useful hearing experience. Despite its great success, there are patients in which benefit from these devices is rather limited. One reason may be a poor neuron-device interaction, where the electric fields generated by the electrode array excite a wide range of tonotopically organized spiral ganglion neurons at the cost of spatial resolution. Coating of CI electrodes to provide a welcoming environment combined with suitable surface chemistry (e.g. with neurotrophic factors) has been suggested to create a closer bioelectrical interface between the electrode array and the target tissue, which might lead to better spatial resolution, better frequency discrimination, and ultimately may improve speech perception in patients.

Here we investigate the use of a collagen surface with a cholesteric banding structure whose orientation can be systematically controlled as a guiding structure for neurite outgrowth. We demonstrate that spiral ganglion neurons survive on collagen-coated surfaces and display a directed neurite growth influenced by the direction of collagen fibril deposition. The majority of neurites grow parallel to the orientation direction of the collagen.

We suggest collagen coating as a possible future option in CI technology to direct neurite outgrowth and improve hearing results for affected patients.

### **553 Effect of Eluded Dexamethasone in Cochlear Implant Array on Insertion Forces**

**Yann Nguyen**<sup>1,2</sup>, Thomas Vauchel<sup>1</sup>, Mathieu Miroir<sup>1</sup>, Guillaume Kazmitcheff<sup>1</sup>, Evelyne Ferrary<sup>1,2</sup>, Olivier Sterkers<sup>1,2</sup>, Alexis Bozorg-Grayeli<sup>1,2</sup>

<sup>1</sup>*Inserm UMR-S 867, F-75018 Paris, France/ Université Paris Diderot, Sorbonne Paris Cité, France,* <sup>2</sup>*AP-HP, Hôpital Beaujon, Service d'Oto-rhino-laryngologie et de Chirurgie cervico-faciale, Clichy, Fr*

Long term dexamethasone (DXM) administration can potentially reduce inflammation and fibrosis after cochlear implantation procedure. Cochlear implant arrays with DXM incorporated in the silicone have been recently developed. The aim of this study was to investigate the putative

alteration of insertion forces compared to current array design.

Four models of arrays have been tested: A standard model (Digisonic SP, n=5) currently used in clinical application, a drug-free prototype (n=5), a prototype with 1% eluded DXM silicone (n=5), and a prototype with 10% eluded DXM silicone (n=5) (Neurelec, Vallauris, France). Via a robotized insertion bench, made up of a linearly action motor, a push rod, and an insertion tube, each array has been inserted into an epoxy scala tympani model. The forces were recorded by a 6-axes force sensor (Nano 17, ATI automation, Apex, NC). Each array was tested 7 times, and a mean insertion curve was calculated for each model.

During the first 10 mm insertion, the mean insertion forces were below 0.011 N, and no difference between the 4 models was observed. From 10 to 24 mm insertion, the standard model presented higher insertion forces than the prototype models, with or without DXM. Friction forces for drug free prototype and DXM eluded arrays were similar on all insertion length. Maximal insertion forces were observed between 20 and 24 mm; their mean values were  $0.16 \pm 0.011$  N the standard array (mean  $\pm$  SEM, n=5),  $0.08 \pm 0.012$  N for the drug-free prototype,  $0.09 \pm 0.019$  N for the 1% DXM prototype, and  $0.07 \pm 0.012$  N for 10% DXM prototype.

Incorporation of DXM in silicone does not change insertion force of the array prototype in an artificial model of cochlea. Therefore, these new prototypes could be used in clinical application.

Grants were funded by Neurelec (Vallauris, France), Fondation de l'Avenir (ETO-568), Fondation des Gueules cassées (25-2010)

### **554 The Potential Benefits of Combining Intracochlear Current Focusing Techniques with Dual Electrode Stimulation: A Computational Study**

**Jeroen Braire**<sup>1</sup>, Randy Kalkman<sup>1</sup>, David Dekker<sup>1</sup>, Johan Frijns<sup>1</sup>

<sup>1</sup>*Leiden University Medical Center*

Current focusing techniques (CFTs) in cochlear implants aim at decreasing spread of excitation. Typically, multiple contacts are used simultaneously to alter the field of a single electrode, e.g. (partial) tripoles ((p)TP) and phased array (PA). In dual electrode stimulation (DES), simultaneous stimulation of two contacts is used in an attempt to excite neurons in the area between two principal excitation areas, rather than to diminish the spread of excitation. The present study investigates the effects of combining CFTs and DES using a realistic computational model of the implanted human cochlea.

Excitation patterns of normal DES, (p)TP and PA channels in lateral and medial electrode arrays were simulated and compared. Pitch percepts, loudness levels and excitation densities (the percentage of fibers excited at a specific location) were predicted as a function of current level. Excitation density plots revealed that focused DES can create a more confined excitation region compared to normal DES. However, this focusing effect was stronger in

lateral insertions than it was in medial insertions. It was found that DES with pTP and PA stimulation produces shifting pitch percepts similar to that of normal DES at the same location. Due to side lobes in their excitation patterns, tripoles induce a non-monotonic shift in pitch when changing the current distribution between the channel. As expected, focused DES requires more current to achieve the same loudness as normal DES, with the difference factor depending on stimulation type, loudness level, array position and cochlear location.

The study indicates that combining DES with CFTs can create intermediate pitch percepts as well as normal DES can, while maintaining a high spatial selectivity. This is achieved at the expense of a higher power consumption and the need for more sophisticated means to control loudness.

This study was financially sponsored by Advanced Bionics and the Heinsius-Houbolt Fund.

### **555** Neurotrophic Effects Elicited by Intracochlear Delivery of Brain-Derived Neurotrophic Factor (BDNF) Persist for Three Months After Cessation in Early-Deafened Cats

Patricia Leake<sup>1</sup>, Olga Stakhovskaya<sup>1</sup>, Alexander Hetherington<sup>1</sup>, Ben Bonham<sup>1</sup>

<sup>1</sup>Epstein Laboratory, Dept. of Otolaryngology-HNS, University of California San Francisco

Postnatal development and survival of cochlear spiral ganglion (SG) neurons depend upon both neurotrophic support and neural activity. Our prior studies in neonatally deafened cats have shown that electrical stimulation (ES) ameliorates SG degeneration, and neurotrophic agents can further improve neural survival. Kittens were deafened as neonates (systemic neomycin) and implanted at ~30 days of age with scala tympani electrodes containing a drug-delivery cannula attached to an osmotic pump. BDNF (94µg/ml; 0.25µl/hr) was infused for 10 weeks.

Immediately after BDNF, SG density was higher (80% of normal vs 64% contralateral), and SG cell somata had normal cross-sectional areas that were ~30% larger than cells on the contralateral side. In a second experiment, 10 week BDNF infusion was combined with ~6 months of ES. Combined BDNF+ES resulted in substantially improved SG density (70% of normal density vs 45%) and larger cell size (88 vs 75%), but both SG survival and cell size were reduced compared to immediately after BDNF. BDNF+ES also resulted in a higher density of myelinated radial nerve fibers in the osseous spiral lamina, sprouting of fibers into the scala tympani, angiogenesis in the SG, thicker fibrosis encapsulating the implant, and improved EABR thresholds relative to initial thresholds on chronically stimulated channels.

Here we asked whether neurotrophic effects would persist after cessation of BDNF infusion, without ES. Again BDNF was infused (10 wks), the BDNF cannula was sealed, and animals were studied at ages similar to the BDNF+ES group (mean age, 26 wks). In this BDNF cessation group, SG density was 76% of normal vs 49% contralateral (n=3), survival values similar to combined BDNF+ES.

Interestingly, SG cell size was 96% of normal (BDNF) vs 68% (contra.), and substantial sprouting of radial nerve fibers again was observed. Thus, the SG survival-promoting effects of BDNF persist for at least 3 months (mean, 11 wks) after cessation of BDNF delivery.

Research supported by the NIH, NIDCD Contract #HHS-N-263-2007-00054-C. BDNF donated by Amgen Inc, Thousand Oaks, CA.

### **556** Neural Excitation Patterns of a Variety of Multipolar Electrode Configurations

Johan Frijns<sup>1</sup>, Randy Kalkman<sup>1</sup>, David Dekker<sup>1</sup>, Dirk Vellinga<sup>1</sup>, Filiep Vanpoucke<sup>2</sup>, Jeroen Briaire<sup>1</sup>

<sup>1</sup>LUMC, <sup>2</sup>Advanced Bionics Europe

Animal and clinical studies indicate that multipolar electrode configurations (bipolar, (partial) tripolar, and phased array) can reduce spread of excitation (SoE) and increase dynamic range. Unfortunately, this coincides with higher sensitivity to deficiencies in neural structure, problems attaining loudness and higher power consumption.

This study combines computational modeling with human psychophysical experiments to estimate thresholds, loudness growth curves, dynamic range and SoE for several multipolar electrode configurations.. A group of 8 postlingually deafened adult users of the HiRes90K implant, with an average duration of deafness of 20 yr, participated in the experiments.

The model predicts that multipoles enable focused stimulation with increased dynamic ranges. Additionally, multipoles are more effective for lateral arrays than for medial ones. The focused currents tend to penetrate deeply into the SG and recruit all nerve fibers in a region, while monopoles show less dense recruitment patterns in a broader region of the SG. Multipoles with less active contacts are more effective in reducing far-field ectopic excitation, but have local irregularities in the excitation density. In contrast, phased array represents the other extreme, with a circumscribed region of excitation, but clear far-field effects.

The psychophysical data are in line with the model predictions, if the model assumes a total loss of peripheral processes.

We conclude that multipoles are especially attractive for lateral arrays. Due to their confined SoE they potentially enable simultaneous, independent stimulation. Based on our results a multipolar set-up with 5 active contacts is promising, also because of the only moderately elevated current consumption relative to e.g., tripolar stimulation.

Research was financially supported by Advanced Bionics Corporation and the Heinsius-Houbolt fund.

## **557 Mechanical Characteristics of Cochlear Implant Electrodes Affect the Incidence of Intracochlear Trauma**

**Stephen Rebscher**<sup>1</sup>, Lawrence Lustig<sup>1</sup>, Olga Stakhovskaya<sup>1</sup>, Patricia Leake<sup>1</sup>

<sup>1</sup>*Department of Otolaryngology-HNS University of California, San Francisco*

Recent advances in the implementation of cochlear implants highlight the importance of intracochlear trauma related to electrode insertion. Specifically, high resolution imaging studies have demonstrated electrode mispositioning in implant recipients and suggested that the resulting trauma negatively affects performance. Further, combined electrical and acoustic stimulation has become an accepted therapy for subjects with residual hearing and by its nature requires maintenance of the physical integrity of the cochlea.

To evaluate how the mechanical characteristics of specific electrode designs affect the occurrence of intracochlear trauma, we measured the vertical and horizontal stiffness of 9 electrodes from 3 manufacturers, including the newly developed Advanced Bionics HiFocus V electrode. Electrodes were inserted in cadaver temporal bones using a realistic surgical approach and the bones were prepared for histological evaluation. Here we report on the HiFocus V electrode and compare results to our previous observations. Electrodes tested previously were the Cochlear Banded, Contour and Contour Advance; the Adv. Bionics Clarion, HiFocus w/Postitioner, 1j, Helix, and HiFocus V; and the Nurobiosys electrode (S. Korea).

Incidence of electrode deviation into the scala vestibuli was specific to device design, ranging from more than 35% to 0%. No severe trauma was observed in the newly tested HiFocus V model. Mean insertion depth of the HiFocus V electrode was 427° from the RW. Mean calculated spiral ganglion frequency location of the apical electrode contact was 675Hz. Comparison of the 9 designs tested indicates that electrodes with greater stiffness in the vertical plane are less likely to elicit trauma during insertion than electrodes with equal or greater stiffness in the horizontal plane.

Research supported by Advanced Bionics LLC, Cochlear Ltd, Nurobiosys Inc, NIH Contract # HHS-N-263-2007-00054-C and a grant from the Deafness Research Foundation to O. Stakhovskaya.

## **558 Using a Cochlear Implant as a Recording Device to Measure Cortical Evoked Potentials**

**Myles Mc Laughlin**<sup>1,2</sup>, Thomas Lu<sup>1</sup>, Fan-Gang Zeng<sup>1</sup>

<sup>1</sup>*University of California Irvine*, <sup>2</sup>*Trinity College Dublin*

As the number of people receiving a cochlear implant (CI) increases, so does the work burden on audiologists who must initially and manually fit each CI and also provide lifelong follow up service. The electric compound action potential (ECAP) is an objective measure of auditory nerve function, which can be recorded using only the CI system. ECAPs can improve the fitting process, particularly in a pediatric population, by providing a quick objective

estimate of threshold and comfortable levels. A number of studies have shown the benefit of electric cortical evoked potentials (ECEP) in optimally fitting the speech processing strategy for improved speech perception. However, recording ECEPs requires a dedicated evoked potential (EP) system, limiting its clinical applicability in terms of availability and subject preparation time. Here we demonstrate the feasibility of using a CI-only method to record ECEPs, comparing the results to those obtained by traditional methods.

We recorded N100s in 3 subjects using the CI for recording and stimulation. We achieved this by using the back telemetry options provided in the clinical software (Custom Sound EP), setting the extra-cochlear electrode (MP2) as a recording electrode, an intra-cochlear electrode as the indifferent electrode and then adjusting the delay of the sampling window to cover the ECEP range (10 to 350ms). For comparison, we recorded N100s in the same subjects using a conventional EP system with scalp electrodes and similar stimulation parameters.

The timing and shape of the ECEPs recorded using scalp electrodes generally matched those of the CI recorded ECEPs, which tended to have larger amplitudes. Currently, a CI-only recording takes a number of hours as the clinical software has not been developed for this purpose, but improvements could substantially reduce this. The new CI-only technique eliminates subject preparation time and extra equipment previously needed, making it a potentially useful clinical tool to improve CI fitting.

## **559 Model-Based Validation Framework for Coding Strategies in Cochlear Implants**

**Michele Nicoletti**<sup>1</sup>, Michael Isik<sup>1</sup>, **Werner Hemmert**<sup>1</sup>

<sup>1</sup>*Technische Universität München*

Although modern cochlear implants (CI) are able to restore speech perception to a high degree there is still a large potential for improvements e.g. in music perception and speech discrimination in noise.

To evaluate and optimize novel coding strategies, we have developed a toolbox which codes sound signals into spike-trains of the auditory nerve. We have previously developed a model of the intact inner ear, which we have complemented with detailed models of a CI speech processor, the channel crosstalk and spiral ganglion neuron models. Here we use a model of spiral ganglion type I neurons with Hodgkin-Huxley type ion channels, which are also found in cochlear nucleus neurons (HPAC,  $K_{ht}$ ,  $K_{lt}$ ). Their large time constants might be responsible to explain adaptation to electrical stimulation (Negem & Bruce 2008). We corrected conductances and time-constants to a body temperature of 37°C and solved the differential equations in the time domain with an exponential Euler rule. Depending on the task, we model the neurons at different levels of detail. The electrode was modeled as an array of 12 current point sources at a distance of 0.5 mm from the spiral ganglion neurons. The coupling between electrode and excitation of the neuron was described by the activation function (second derivative of the extracellular potential with respect to the neuron's path). Cannel cross-talk was implemented by a convolution

of the activation function with a spread function (symmetric, slope: 1dB/mm).

With our toolbox we present qualitative comparisons of neurograms elicited by different coding strategies with the situation in the healthy inner ear. Moreover, we conducted qualitative evaluations using two methods: with the framework of automatic speech recognition we evaluated speech discrimination using a noisy database. With the methods of information theory we are able to quantify the transmitted information coded in neuronal spike trains, which allows us to evaluate especially well how well temporal information is coded. The major advantage of our approach is that we are able to evaluate both spectral- and temporal aspects of novel coding strategies before we conduct long-lasting clinical studies.

Supported by within the Munich Bernstein Center for Computational Neuroscience by the German Federal Ministry of Education and Research (reference number 01GQ1004B) and MED-EL Innsbruck.

### **560 Behavioral Loudness Growth Explained by a Patient-Specific Cochlear Implant Model**

**Julie Bierer<sup>1</sup>**, Steven Bierer<sup>1</sup>, Joshua Goldwyn<sup>2</sup>

<sup>1</sup>University of Washington, <sup>2</sup>New York University

Performance on perceptual tasks varies among cochlear implant (CI) listeners. Previous work from our laboratory suggests that differences from channel-to-channel within individuals may play a role in this inter-subject variability. As manufacturers aim to improve spectral information using current focusing techniques, an understanding of the viability of each channel (i.e., the status of the electrode-neuron interface) and how it relates to the perception of loudness and the transmission of information across those channels will be essential. Behavioral thresholds with focused stimulation were obtained for eight adult CI users to identify the channels with the lowest, median and highest thresholds for further testing. Growth of loudness was then measured on the three test channels using magnitude estimation, with eight levels between threshold and 10% above the most comfortable level. Estimates were measured eight times. The results showed that channels with the highest threshold typically had the steepest loudness growth functions, suggesting poor electrode-neuron interfaces.

A computational model developed in our laboratory has been implemented to estimate two factors most likely to influence single-channel perceptual measures: 1) the radial distance between an electrode and its closest stimutable neurons, and 2) the number of surviving neurons near each electrode. Based only on threshold data, the model can be used to estimate the number of active neurons in response to suprathreshold stimulus levels, resulting in neural response growth functions that can be compared directly to loudness growth functions. This presentation will examine the model parameters that best account for the behavioral loudness data.

### **561 Temporal Pitch and CI: How Much Error and How to Minimize It**

**Richard Penninger<sup>1,2</sup>**, Katrien Vermeire<sup>2</sup>, Ingeborg Dhooge<sup>2</sup>, Marc Leman<sup>1</sup>

<sup>1</sup>University Ghent, <sup>2</sup>University Hospital Ghent

Temporal (rate) pitch is gaining popularity because it increases the amount of perceived frequencies for CI users by stimulation one electrode only.

Temporal (rate) pitch has the advantage of being able to provide a continuum of pitches on a single electrode up to approximately 300 Hz. However, this limit varies greatly between subjects and electrodes within the subject with some star patients in being able to use rate pitch up to at least 1000 Hz. Proper encoding of pitch is crucial for music perception, which is typically an extremely challenging task for CI users. Additionally, pitch perception is important for understanding words in tonal languages and the perception of prosodic information in non-tonal languages. The main problems for pitch perception are current spread and the limited number of electrodes. Furthermore apical locations for low frequencies cannot be reached due to the length of the implant and often there is a mismatch between rate and place.

Six CI subjects were asked to identify the higher tone of two tones generated on a single electrode using sinusoidal amplitude modulation (SAM). The base modulation rates ranged from 130 Hz to 693 Hz; target modulation rates were four semitones (26%) higher. The carrier stimulation rate was 5000 Hz. Using a method of constant stimuli, pitch ranking was measured for six base modulation rates on five different electrodes. Three of the five selected electrodes consisted of a basal, a middle and an apical electrode to determine if there was an effect of cochlear region. Additionally, electrodes with the largest and smallest dynamic range (DR) were tested. This approach allows quantification of the effect of dynamic range and location of the electrodes on temporal pitch performance.

Results demonstrate great variability across subjects, place, and dynamic ranges. Not all electrodes provide equal temporal resolution. If a sound processing strategy were to use only electrodes which provide better temporal coding then possibly temporal pitch will be better perceived by implant users, yielding improved language and music perception.

### **562 Spectral and Temporal Analysis of "holes in Hearing"**

**Gary Jones<sup>1</sup>**, Jong Ho Won<sup>1</sup>, Jay Rubinstein<sup>1</sup>

<sup>1</sup>VM Bloedel Hearing Research Center, University of Washington, Seattle, WA, USA

A cochlear implant (CI) electrode in a cochlear "dead region" will excite neighboring neural populations. In previous research that simulated such "holes in hearing," stimulus information in the spectral hole was either added to the immediately adjacent frequency regions or dropped entirely. There was little difference in understanding of vowels, consonants and sentences between the two conditions. This may imply that there is little benefit of ensuring that stimulus information on an electrode in a suspected "dead region" is transmitted. Alternatively,

performance may be enhanced by a broader frequency redistribution, rather than adding stimuli from the spectral hole to the edges.

In the current experiments spectral holes were introduced by excluding selected CI electrodes or vocoder noisebands. Participants were assessed for speech understanding as well as spectral and temporal resolution as a function of the number of active electrodes. In one set of tests the normal input frequency range of the speech processor was distributed among the active electrodes in bands with approximately logarithmic spacing; in the remaining tests information in inactive electrodes was dropped. CNC word scores increased with the number of active electrodes, independent of the test condition: the "dropped" and "redistributed" conditions had similar scores for 1, 2, 4, 8 and 16 active electrodes. Psychophysical results suggest that the near match in word scores may reflect a tradeoff between spectral and temporal cues: at low numbers of electrodes spectral-ripple discrimination was much poorer in the "redistributed" condition than in the "dropped" condition while performance in a temporal modulation task was much better in the "redistributed" condition; Schroeder-phase discrimination was moderately better in the "redistributed" condition.

[Research supported by NIH-NIDCD Grants F31 DC009755, T32 DC000033, F32 DC011431, R01 DC007525, P30 DC04661 and the Advanced Bionics Corporation.]

### **563 Electrode Pitch Patterns in Hybrid and Long-Electrode Cochlear Implant Users: Changes Over Time and Long-Term Data**

**Lina Reiss**<sup>1,2</sup>, Christopher Turner<sup>2</sup>, Sue Karsten<sup>2</sup>, Rindy Ito<sup>1</sup>, Ann Perreau<sup>2</sup>, Sean McMenomey<sup>1</sup>, Bruce Gantz<sup>2</sup>

<sup>1</sup>Oregon Health & Science University, <sup>2</sup>University of Iowa

Recent experiments show that pitch perceived through a Hybrid short-electrode cochlear implant (CI) can shift over several months of implant experience, by as much as 2 octaves (Reiss et al., JARO 2007). Here we describe updated results in short- and long-electrode CI users recruited to have pitch perception measured longitudinally at several time points from hookup to up to 5 years of CI experience; long-term CI users were also recruited to measure electrode pitch adaptation patterns. Pitch perception was measured by having the subject compare the pitch elicited by stimulation of a single electrode with acoustic tones presented to the non-implanted ear. Acoustic tone frequency was varied across trials in pseudorandom, counterbalanced sequence, and the pitch match was estimated as the 25-75% range of the psychometric function.

As in short-electrode CI users, electric pitch changes were observed in long-electrode CI users over time. For both groups, pitch changes often aligned with the CI frequency-to-electrode allocations, consistent with the hypothesis that the brain adapts pitch perception to minimize perceived mismatches between electrically and acoustically stimulated cochlear place frequencies. This trend was particularly apparent when the frequency allocations were changed in experienced CI users, and the subsequent

pitch changes followed the allocation changes. However, not all subjects showed changes consistent with this trend; a subset of long-electrode CI users exhibited downward pitch shifts over time for all electrodes independent of frequency allocation. The reasons for this variability are not clear, but may include differences in hearing loss patterns, hearing aids, and environmental listening experience. These findings have implications for the role of brain plasticity in auditory prosthesis perception, and suggest that experience-dependent changes may need to be measured and factored into device evaluation and design. Work supported by NIH-NIDCD grants R01DC000377, P50DC00242, and P30DC010755, the Iowa Cochlear Implant Clinical Research Center, and the OHSU Cochlear Implant Program.

### **564 Central Neuronal Masking Effects to Binaural-Bimodal Stimulation in the Gerbil**

**Maïke Vollmer**<sup>1</sup>, Armin Wiegner<sup>1</sup>, Tristan Bremer<sup>1</sup>

<sup>1</sup>Comprehensive Hearing Center, University Hospital Wuerzburg, Wuerzburg, Germany

There is increasing evidence that the combination of electric and contralateral acoustic stimulation (binaural-bimodal stimulation, BBS) can significantly improve speech perception in cochlear implant users. Little is known about the neuronal interactions to such signals. The present study investigates masking effects to BBS on neuronal responses in the inferior colliculus and the dorsal nucleus of the lateral lemniscus.

Normal hearing, adult gerbils (*Meriones unguiculatus*) were unilaterally implanted with a round window electrode that maintained acoustic sensitivity in the implanted ear. Earphones were sealed to both auditory meatus for acoustic stimulation. Single electric pulses and single acoustic clicks were presented using a forward-masking paradigm. The delay between the two modes of stimulation changed between 2-80 ms. Electric and acoustic stimuli served as both probes and maskers and were systematically varied in intensity.

Extracellular single neuron responses were recorded contralateral to the implanted cochlea using tungsten microelectrodes. Masking effects to BBS were compared with those to binaural-acoustic stimulation in the same neurons.

In BBS, electric masking had a weak effect on neuronal response strength to the acoustic probe. In contrast, acoustic masking strongly suppressed electric probe responses and demonstrated longer neuronal recovery time constants than electric masking on acoustic responses. In binaural-acoustic stimulation, contralateral masking was more effective than ipsilateral masking. However, in BBS, contralateral masking was less effective if the masker was electric.

The results indicate a strong dominance of acoustic masking on electric responses in BBS, whereas electric masking is relatively ineffective. The magnitude of binaural masking between electric and acoustic responses in BBS appears opposite to that observed in ipsilateral combined electric-acoustic stimulation (EAS) [1]. Results will be

discussed with respect to different mechanisms for contralateral and ipsilateral masking.

Support provided by Interdisciplinary Center for Clinical Research, Wuerzburg, Germany, and MedEI, Innsbruck, Austria.

[1]Vollmer, M., Hartmann, R., Tillein, J.: Neuronal responses in cat inferior colliculus to combined acoustic and electric stimulation. *Adv Otorhinolaryngol.* 67: 61–69, 2010

### **565** The EarLens Photonic Hearing Aid

**Sunil Puria**<sup>1,2</sup>, Suzanne Carr Levy<sup>1</sup>, Daniel J. Freed<sup>1</sup>, Jonathan P. Fay<sup>1</sup>, Michael Nilsson<sup>1</sup>, Rodney Perkins<sup>1</sup>  
<sup>1</sup>EarLens Corporation, <sup>2</sup>Stanford University

An extended-bandwidth nonsurgical open-canal hearing aid, featuring a solely light-activated micromotor transducer in direct contact with the tympanic membrane, is evaluated for its ability to improve speech understanding in multi-talker environments and sound quality for hearing-impaired subjects. Reception threshold for sentences (RTS) values were measured on hearing-impaired subjects (N=13) with and without the photonic hearing aid, using Hearing in Speech Test (HIST) sentences and masking speech materials played back at 65 dB SPL for two loudspeaker configurations: 1) asymmetric, with the target at -45° and two maskers at +45°; and 2) diffuse, with the target in front at 0° and four maskers at ±45° and ±135°. The photonic system was driven via a prototype behind-the-ear multiband high-frequency hearing aid device programmed using the CAM2 fitting algorithm (Moore et al., 2010).

The RTS values for the asymmetric condition were -9.4 dB unaided vs. -13.4 dB aided, indicating a 40% average improvement ( $p < 1e-5$ , pairwise t-test). For the more difficult four-masker diffuse-field condition, the RTS values were -4.5 dB unaided vs. -5.7 dB aided, indicating a 12% ( $p=0.1$ ) average improvement (using 1dB~10%). Both of these RTS improvement values are approximately two times better than those measured using the subjects' own best-fit acoustic hearing aids. Testimonials and Abbreviated Profile of Hearing Aid Benefit (APHAB) scores indicate that the sound quality of the photonic system is also significantly better.

These results suggest that the photonic system's unprecedented 0.2–10 kHz frequency range, compared to the respective 1–4 kHz and 0.1–5 kHz ranges of open- and closed-canal acoustic hearing aids, enables hearing-impaired subjects to perceive acoustic cues that greatly enhance sound quality and their ability to understand target speech in multi-talker environments. [Work supported in part by R44 DC008499 SBIR and ARRA supplement funds to SP from the NIDCD of the NIH].

### **566** Optimal Integration of Sensory Evidence: A Bayesian Journey Through Our Sixth Sense

**Dora Angelaki**<sup>1</sup>, Greg DeAngelis<sup>2</sup>, Yong Gu<sup>3</sup>

<sup>1</sup>Baylor College of Medicine, <sup>2</sup>University of Rochester,

<sup>3</sup>Washington University

A fundamental aspect of our sensory experience is that information from different modalities is often seamlessly integrated into a unified percept. Recent computational and behavioral studies have shown that humans combine sensory cues according to a statically optimal scheme derived from Bayesian probability theory; they perform better when two sensory cues are combined. We have explored multisensory cue integration for self-motion (heading) perception using both visual (optic flow) and vestibular (linear acceleration) signals. We recorded from single neurons in the dorsal medial superior temporal area (MSTd) of visual cortex during a heading discrimination task where trained monkeys, like humans, behaviorally combine visual and vestibular cues to improve heading perception. Under bimodal stimulation, MSTd neurons combine visual and vestibular cues linearly but sub-additively. Neurons with congruent heading preferences for visual and vestibular stimuli show improved sensitivity and lower neuronal thresholds under cue combination. In contrast, neurons with opposite preferences show diminished sensitivity under cue combination. We further show that MSTd responses are significantly correlated with the monkeys' perceptual decisions in a congruency-dependent manner. Deficits in behavior brought by chemical inactivation of this area provide further support of the hypothesis that extrastriate visual cortex mediates multisensory integration for self-motion perception. These findings provide the first behavioral demonstration of statistically-optimal cue integration in non-human primates and identify a population of neurons that may form its neural basis.

### **567** Perceptual Timing of Vestibular Stimuli During Multisensory Integration

**Michael Barnett-Cowan**<sup>1</sup>

<sup>1</sup>Max Planck Institute for Biological Cybernetics

Multisensory stimuli originating from the same event can be perceived asynchronously due to differential physical and neural delays. Yet while transduction of and physiological responses to vestibular stimulation are extremely fast, here I will present results from a series of psychophysical experiments of my own and of others which indicate that the perceived onset of vestibular stimulation is slow compared to the other senses. In each experiment vestibular stimulation is paired with a stimulus from a different modality presented at various stimulus onset asynchronies and psychometric functions are fit to judgments of temporal order and/or synchronicity. Despite differences in the methods used to stimulate the vestibular system across experiments, vestibular stimulation is always found to have to occur prior to other sensory information in order to be perceived synchronously. I will argue that this perceived latency of vestibular stimulation likely reflects the fact that the vestibular system rarely

works alone and that the brain prioritizes physiological response to vestibular stimulation over perceptual awareness of stimulation onset.

## **568** Directional Asymmetries in Human Vestibular Perception

**Benjamin Crane**<sup>1</sup>

<sup>1</sup>*U of Rochester*

Directional asymmetries in vestibular reflexes have aided the diagnosis of vestibular lesions, however, potential asymmetries in vestibular perception have not been well defined. This investigation sought to measure potential asymmetries in human vestibular perception. Vestibular perception thresholds were measured in 24 healthy human subjects between the ages of 21 and 68 years. Stimuli consisted of a single cycle of sinusoidal acceleration in a single direction lasting 1 or 2s (1 or 0.5 Hz), delivered in sway (left-right), surge (forward-backward), heave (up-down), or yaw rotation. Subject identified self-motion directions were analyzed using a forced choice technique, which permitted thresholds to be independently determined for each direction. Non-motion stimuli were presented to measure possible response bias. A significant directional asymmetry in the dynamic response occurred in 39% of conditions tested within subjects, and in at least one type of motion in 92% of subjects. Directional asymmetries were usually consistent when retested in the same subject but did not occur consistently in one direction across the population with the exception of heave at 0.5 Hz. Responses during null stimuli presentation suggested that asymmetries were not due to biased guessing. Multiple models were applied and compared to determine if sensitivities were direction specific. Using Akaike Information Criterion, it was found that the model with direction specific sensitivities better described the data in 86% of runs when compared with a model that used the same sensitivity for both directions. Mean thresholds for yaw were  $1.3 \pm 0.9^\circ/s$  at 0.5 Hz and  $0.9 \pm 0.7^\circ/s$  at 1 Hz and were independent of age. Thresholds for surge and sway were  $1.7 \pm 0.8$  cm/s at 0.5 Hz and  $0.7 \pm 0.3$  cm/s at 1.0 Hz for subjects <50 and were significantly higher in subjects >50 yo. Heave thresholds were higher and were independent of age.

## **569** Temporal and Spatial Integration of Auditory and Vestibular Cues in the Elderly

**Timothy Hullar**<sup>1</sup>, Nai-Yuan Nicholas Chang<sup>1</sup>

<sup>1</sup>*Washington University*

Quantification of vestibular reflexes forms the mainstay of vestibular evaluation. However, many patients with imbalance have normal or near-normal vestibulo-ocular reflexes and vestibular-evoked myogenic potentials. This has led to an increasing interest in other methods for evaluation of balance function which may offer additional diagnostic potential and, perhaps, insights into pathophysiologic mechanisms and even treatment. Many elderly subjects, for example, have considerable imbalance without evidence of significant peripheral vestibular loss. Difficulties with multisensory integration have been implicated as a cause for imbalance in this

population, but accurate quantification of these difficulties has proven elusive. We used novel psychophysical paradigms to evaluate the ability of young and older people without a history of falls to integrate vestibular and auditory cues both in time and in space. In our temporal experiment, we rotated subjects about an earth-vertical axis at frequencies of 0.5 Hz, peak velocities of 20 deg/sec in the dark. We used a temporal-order-judgment task to align the rotation with a dichotically presented 1.0 Hz auditory stimulus. Older subjects tolerated a significantly wider misalignment before reporting that the stimuli were out of phase. These results suggest that older subjects are not able to perform multisensory temporal integration involving vestibular stimuli as well as younger people. In our spatial experiment, detection thresholds for younger and older subjects were determined for rotations at 0.5 Hz in the dark. Thresholds were determined again in the presence of an external point sound source. Thresholds for younger subjects were somewhat better than for older subjects. The external sound source did not improve thresholds significantly for younger subjects but it did for older subjects. Similar changes in other sensory pairs have been observed in autism and dyslexia and suggest a plausible mechanism for imbalance in the elderly. The results also suggest that elderly subjects are more dependent than younger subjects on multisensory integration for improving the spatial accuracy of vestibular inputs. This finding highlights this process as a point of possible pathology and treatment for imbalance in older people.

## **570** Vestibular Contributions to Tilt Perception in Non-Human Primates

**Richard Lewis**<sup>1,2</sup>, Csilla Haburcakova<sup>1,2</sup>, Wangsong Gong<sup>1,2</sup>, Daniel Lee<sup>1,2</sup>, Daniel Merfeld<sup>1,2</sup>

<sup>1</sup>*Harvard Medical School*, <sup>2</sup>*Massachusetts Eye and Ear Infirmary*

We have studied perceived head orientation relative to gravity in the roll plane in rhesus monkeys using a task derived from the subjective visual vertical (SVV) test commonly used with human subjects. Animals were tested during static and dynamic head tilts in the normal state and after vestibular ablation. They were also tested with the head upright and stationary while one vertical semicircular canal was activated with an implanted electrode.

We found that tilt perception in normal monkeys is relatively accurate and improves at higher frequencies where both canal and otolith cues are robust, compared to very low frequencies where vestibular contributions to tilt perception are primarily provided by the otoliths. Vestibular ablation markedly impaired tilt perception measured with the SVV task, suggesting that vestibular cues provide much of the information about head orientation measured with this task. Finally, isolated activation of a vertical canal produced substantial percepts of tilt, indicating that although the canals do not sense gravity their inputs do affect the perceived orientation of the head in space. Most likely canal rotational cues are integrated by the brain to provide this information, and this

process may be critical to accurately separate the otolith input into its gravitational and inertial components.

### **571 Vestibular Heading Discrimination and Sensitivity to Linear Acceleration in Head and World Coordinates**

**Paul MacNeilage<sup>1</sup>**

<sup>1</sup>*Ludwig Maximilian University Hospital of Munich*

Psychophysical measurements of detection and discrimination thresholds have potential value for clinicians diagnosing vestibular disorders because they provide an objective quantification of sensory efficiency as it relates to perception. For example, measurement of perceptual sensitivity to linear motion may prove useful for assessing otolith function. However, it is currently unclear which psychophysical methods and tasks are best suited for standard clinical use. To address these issues we have measured sensitivity of normal human subjects to linear acceleration using a motion platform and a variety of psychophysical methods and tasks. In one study, performance on three tasks was compared: 1) a heading discrimination task, 2) a coarse direction discrimination task (e.g. discriminating leftward versus rightward movement along the interaural axis), and 3) an amplitude discrimination task. Thresholds in the heading task were well predicted by those from the coarse direction task, suggesting that heading discrimination is limited by low-level sensitivity to linear motion. All measurements were made with subjects oriented both upright and side-down relative to gravity allowing us dissociate effects of movement direction in head and world coordinates. Sensitivity depended on the direction of movement in head coordinates (i.e., relative to the utricle and saccule), and on body orientation, but surprisingly did not depend on movement direction relative to gravity. In a separate study, the task was fixed (coarse direction discrimination) but several psychophysical methods were compared including several adaptive staircase procedures and the method of constant stimuli. The adaptive staircase procedures allowed for the fastest (5-10 minutes) but least precise measurements while the method of constant stimuli allowed for the most precise but slowest measurements (20-30 minutes). Nevertheless, threshold values estimated with the various methods were overall comparable.

### **572 Human Perceptual Direction-Recognition Thresholds as a Function of Frequency**

**Yulia Valko<sup>1</sup>, Koeun Lim<sup>1</sup>, Adrian Priesol<sup>2</sup>, Rick Lewis<sup>2</sup>, Dan Merfeld<sup>2</sup>**

<sup>1</sup>*MEEI, <sup>2</sup>MEEI, Harvard Medical School*

We have previously reported human perceptual yaw rotation thresholds as a function of stimulus frequency (Grabherr et al, 2008). For normal subjects, these thresholds were shown to plateau at frequencies above 0.5 Hz and increase substantially at frequencies below 0.5 Hz. This suggests that high-pass filtering modifies the signals that contribute to perceptual yaw rotation thresholds - with the cut-off frequency well above the canal cut-off

frequency. We have recently measured y-translation, z-translation, roll rotation, and roll tilt thresholds as a function of frequency in normal subjects and vestibular hypofunction patients. We find that the pattern of y-translation, z-translation, and roll rotation thresholds versus frequency suggests the influence of a similar high-pass filtering mechanism, while VOR thresholds do not demonstrate the influence of such filtering. Taken together, these findings suggest that a mechanism in the decision-making process high-pass filters the relevant perceptual signal. For example, one way for perceptual discrimination/detection/recognition processes to manage neural drift in perceptual signals is to high-pass filter the signal, thereby eliminating low-frequency drift.

### **573 Functional Analysis of Clarin-1 in the Mouse Inner Ear**

**Ruishuang Geng<sup>1</sup>, Daniel Chen<sup>1</sup>, Charles Askew<sup>2</sup>, Geoff Horwitz<sup>2</sup>, Tomoko Oshima-Takago<sup>3</sup>, Tobias Moser<sup>3</sup>, Jeffrey Holt<sup>4</sup>, Yoshikazu Imanishi<sup>1</sup>, Kumar Alagramam<sup>1</sup>**  
<sup>1</sup>*Case Western Reserve University, <sup>2</sup>University of Virginia, <sup>3</sup>University of Göttingen School of Medicine, <sup>4</sup>Harvard University*

Usher syndrome III (USHIII) is an autosomal recessive disorder characterized by progressive hearing loss and vision loss. It is known that mutation in the human clarin-1 (CLRN1) gene causes USHIII. We previously demonstrated that mouse clarin-1 (Clrn1) transcript was expressed in hair cells and inner ear ganglion cells. We also showed loss of inner ear function in the homozygous knockout (Clrn1<sup>-/-</sup>) mice. Evoked Brainstem response showed significant loss of function accompanied by delayed peak latencies and reduced peak amplitudes. Scanning electron microscopy revealed defects in hair bundle morphology as early as postnatal day 2 (P2). We hypothesized that mutation in Clrn1 affects hair cell function including the function of the ribbon synapse. To dissect the role of Clrn1 in hair cells, multiple experiments were carried out. For example, electrically evoked brainstem response (eEBR) from P21 Clrn1<sup>-/-</sup> mice confirmed delay in peak I latency, and it showed that latencies of peaks II-IV are only secondarily affected. These results, namely delayed peak I latency and reduced peak amplitudes, suggest that the hair cell phenotype in Clrn1<sup>-/-</sup> mice may be due to a defect in the ribbon synapse apparatus and/or mechanotransduction apparatus. We have initiated a series of experiments. These experiments are currently underway, and results will be presented at the meeting.

### **574 A Possible Role for the Stereociliary Lipid Membrane in Generating the Gating Spring Response in Auditory Sensory Hair Bundles**

**Jichul Kim<sup>1</sup>, Peter Pinsky<sup>1</sup>, Charles Steele<sup>1</sup>, Sunil Puria<sup>1</sup>, Anthony Ricci<sup>1</sup>**

<sup>1</sup>*Stanford University*

The gating spring theory for hair cell mechanoelectric transduction (MET) channel activation was first proposed

based on measurements showing that the hair bundle does not behave as a Hookean spring when stimulated, but rather shows a region where compliance increases. This region is correlated with the opening of MET channels. From this data it was postulated that a gating element is in series with a spring. With displacement, the incorporation of the gating element acts to decrease force. Several molecular components have been implicated as the gating spring including, the tip link and an undefined intracellular elastic component. Regarding the gating compliance, the activation gate of the MET channel and myosin 1c are proposed candidates. Present computational analysis presents an alternative approach, suggesting that both gating spring and gating compliance can be ascribed to lipid membrane tenting. By separating the lipid component into two compartments, where mobility of the larger pool is constrained as compared to the smaller tip compartment and where flexibility of the larger pool is completely constrained but is free in tip compartment, it was possible to reproduce force displacement plots comparable to those measured in hair cell bundles.

The key parameters varied included: the relative size of the tip compartment which was varied between 30 and 200 nm in diameter, to represent the tented region often observed in TEM sections of hair bundles, the stiffness of the passive component of the hair bundles and the time at which the measurement was made, to observe the effects of lipid mobility. Plots were generated with various parameters at different times in order to understand the nonlinear behavior of bundle mechanics. Results support the hypothesis that the lipid membrane may play a significant role in generating the measured gating spring response of hair bundles.

This work was supported by grants DC007910 to CRS and DC003896 to AJR from the NIDCD of NIH.

### **575 Deformation of the Stereocilia Tip Membrane: Implications for the Gating Spring and Mechanotransduction Channel**

Richard Powers<sup>1</sup>, Sitikantha Roy<sup>1</sup>, Erdinc Atilgan<sup>2</sup>, William Brownell<sup>3</sup>, Sean Sun<sup>1</sup>, Peter Gillespie<sup>4</sup>, **Alexander Spector**<sup>1</sup>

<sup>1</sup>Johns Hopkins University, <sup>2</sup>Columbia University, <sup>3</sup>Baylor College of Medicine, <sup>4</sup>Oregon Health&Science University

In hair cells, mechanotransduction channels have been localized to tips of shorter stereocilia of the mechanically-sensitive bundle, but it is still unclear how force is transmitted to the channel. The gating spring concept has successfully been used in the analyses of the channel performance, but the compliant part of the gating spring has not been identified. The recent data on the protein composition of the tip link and its stiffness makes the membrane (either itself or in combination with a tether connecting the channel to the stereocilia actin fibers) a good candidate for the compliant component of the gating spring. We use a biophysical model of the membrane-channel complex to test this hypothesis and further clarify the channel arrangement. We characterize the membrane by a bending modulus and tension, and we model possible

channel-cytoskeleton tether as an elastic spring. We use a finite element method and Monte Carlo simulation to compute the deformed shape of the membrane under the action of the tip link force and estimate the stiffness of the system. We show that depending on gating spring stiffness, either membrane alone or the combination of the membrane with a channel-cytoskeleton tether can serve as the gating spring complaint component. If a bundle is characterized by relatively soft gating spring, such as those in bullfrog sacculus, then the need for membrane reinforcement by the tether depends on membrane parameters. If the gating spring is stiffer, such as those from rat outer hair cells, the channel has to be tethered for all biophysically realistic membrane parameters. The developed approach can provide further elucidation of the arrangement of the mechanotransduction channel in hair cells and its membrane environment, including membrane forces, bending moments, and curvature, and obtained results can help in a better understanding of mechanotransduction in hair cells. Supported by grants R01 DC02775 (WEB and AAS) and DC02368 (PGG) from NIDCD.

### **576 Stereocilia Membrane Is Sensitive to Electrical Stimulation**

**Pierre Hakizimana**<sup>1</sup>, William E. Brownell<sup>2</sup>, Stefan Jacob<sup>1</sup>, Anders Fridberger<sup>1</sup>

<sup>1</sup>Center for Hearing and Communication Research, Karolinska Institutet, Sweden, <sup>2</sup>Head and Neck Surgery, Baylor College of Medicine, TX, USA.

Inner ear hair cell stereocilia bundles convert mechanical stimuli into electrical signals. Each stereocilium has a core of actin filaments surrounded by the cell membrane. In cochlear hair cells, this membrane has been shown to exhibit an unusually high lipid mobility compared to the soma and other types of cochlear cells.

Recently, we found that outer hair cell stereocilia undergo rapid nanometre-scale length changes to regulate sound-evoked deflection. Normal (positive) endocochlear potentials (EP) minimized the amplitude of these length changes and maximized the bundle deflection. A reverse trend was seen at negative EPs. Since the actin core is thought to be compact thanks to the extensive cross-linking of the filaments, our results suggested that the stereocilia length changes could be mediated by the membrane dynamics. To probe the stereocilia membrane dynamics, we performed fluorescence recovery after photobleaching (FRAP) experiments on the bundle during electrical stimulation in temporal bone preparations from guinea pigs. The bundle was stained with a membrane-specific dye RH-795. We found that normal EPs decrease significantly the mobile fraction with respect to negative potentials. We suggest that this decrease in the lipid mobility may reflect a tightening of the membrane around the actin core of the stereocilia. This membrane tightening could contribute to the apparent increase of stereocilia stiffness implied by increased bundle movements measured at normal EPs.

## **577 Novel Tools to Monitor Hair Bundle**

### **Development in Live Zebrafish**

Shih-Wei Chou<sup>1,2</sup>, Brian M. McDermott Jr<sup>1,2</sup>

<sup>1</sup>Department of Otolaryngology-Head and Neck Surgery, Case Western Reserve University, <sup>2</sup>Department of Biology, Case Western Reserve University

In vertebrates, the sensations of hearing and equilibrium are permitted by inner ear hair cells. Hair cells are specialized epithelial cells that transduce mechanical signals. Mechanosensation depends on the precise morphology of the hair bundle. Hair bundles, which protrude from the apical surfaces of hair cells, are composed of actin-based stereocilia. The bevel shaped hair bundle requires a host of actin-binding proteins to properly manage hair bundle genesis.

Defects in numerous genes required for hearing result in abnormal hair bundle morphologies; therefore, a substantial amount of effort is put into understanding the genes, and the cognate signaling circuits, that are important for regulating hair bundle development. In general, the exact point in bundle development at which a mutation affects the hair bundle has not been observed in real time. Current strategies for observing morphological changes largely rely on fixed specimens. Here, we develop new tools to visualize the stereocilia and the kinocilia in live zebrafish. Using a hair cell-specific promoter, which drives expression early in hair cell development, we created stable transgenic lines that express fluorescently tagged cytoskeletal proteins, beta-actin-mCherry or GFP-tubulin alpha 1 for labeling stereocilia or kinocilia, respectively, in maculae, cristae, and neuromasts. In conjunction with confocal laser scanning microscopy, these transgenic strains will allow us to monitor the development of the hair bundle. These tools will assist in the characterization of mutant zebrafish with defects in hair bundle genesis.

## **578 Molecular Architecture of the Vestibular Hair Bundle**

Peter Gillespie<sup>1</sup>, Jocelyn Krey<sup>1</sup>, Jung-Bum Shin<sup>1,2</sup>

<sup>1</sup>Oregon Health & Science University, <sup>2</sup>University of Virginia

Inner-ear hair bundles have a unique structure that underlies their sensitivity to mechanical stimulation. We used protein mass spectrometry to identify and quantify those hair-bundle proteins in chick and rat utricles present at approximately ten to a million copies per stereocilium. Quantitation by mass spectrometry is accurate, albeit with significant protein-to-protein variation, and allows us to determine the major structural constituents of the bundle. Moreover, by examining published literature and protein-interaction databases, we can determine important functional interactions of bundle proteins. In chick, we identified 618 proteins from bundles and 1445 proteins in the utricular sensory epithelium, each with a false-discovery rate of 0.2%. We measured the hair-bundle enrichment of each protein by comparing its abundance in bundles to that in utricle; the density of known "deafness genes" in the list of proteins enriched 5-fold or greater in bundles (61 total proteins) was 30x greater than in the list

of epithelium-enriched and epithelium-only proteins, validating our bundle proteome analysis as a powerful strategy for identifying deafness genes. Comparing our estimated protein abundances to the density of known bundle structural features, we concluded that fascin-2 and plastin-1 account for nearly all actin crossbridging molecules, radixin and annexin A5 are the most prominent membrane-to-cytoskeleton linkers, and capping protein (CAPZ) and twinfilin are the major barbed-end capping molecules. Examining known functional interactions between identified bundle proteins, we identified protein and lipid hubs responsible for high densities of interactions, including actin, PIP2, radixin, NHERF2 (SLC9A3R2), RHOA, and CDC42. Radixin and NHERF2 are binding partners, partially colocalize within stereocilia, and likely form a protein complex capable of interacting with many proteins involved in regulating transduction and the cytoskeleton, suggesting that protein sorting in stereocilia may take place at the radixin-NHERF2 complex.

## **579 Kinocilia Mediate Mechanosensation in Nascent Hair Cells**

Katie Kindt<sup>1</sup>, Gabriel Finch<sup>1</sup>, Teresa Nicolson<sup>1</sup>

<sup>1</sup>Oregon Health and Sciences University

Hair cells are mechanosensory receptors that utilize apical hair bundles to sense sound and movement. Each hair bundle is comprised of a single primary cilium (kinocilium) flanking multiple rows of stereocilia. Tip links interconnect stereocilia and are thought to gate mechanotransduction channels. In cochlear hair cells, kinocilia regress shortly after birth and physical removal of kinocilia from vestibular hair cells does not affect mechanotransduction. Therefore, the function of kinocilia in mechanotransduction in mature hair cells is not evident. By applying in vivo imaging of activity and structure sequentially with scanning electron microscopy, we have uncovered a novel role for kinocilia in mechanosensation during development. We have found that nascent zebrafish hair cells require kinocilia and kinociliary links for mechanosensitivity. Although nascent cells have correct planar polarity, functional polarity is reversed. Later in development, a switch to correctly polarized mechanosensitivity coincides with the formation of tip links and the onset of tip link-dependent mechanotransduction.

## **580 Postnatal Switch in Expression of Transmembrane Channel-Like Genes 1 and 2 Underlies Mechanotransduction in Auditory Hair Cells**

Yoshiyuki Kawashima<sup>1,2</sup>, Gwenaëlle Géléoc<sup>3</sup>, Kiyoto Kurima<sup>1</sup>, Andrea Lelli<sup>4</sup>, Valentina Labay<sup>1</sup>, Yukako Asai<sup>4</sup>, Tomoko Makishima<sup>1</sup>, Charles Askew<sup>4</sup>, Doris Wu<sup>1</sup>, Jeffrey Holt<sup>3</sup>, Andrew Griffith<sup>1</sup>

<sup>1</sup>NIDCD/NIH, <sup>2</sup>Tsuchiura Kyodo General Hospital,

<sup>3</sup>Children's Hospital Boston / Harvard Medical School,

<sup>4</sup>University of Virginia

Mutations of transmembrane channel-like gene 1 (*TMC1*) cause deafness in humans and mice. *Tmc1* is expressed in mouse cochlear hair cells. In this study, we investigated

the function of *Tmc1* and the closely related *Tmc2* gene in the cochlea. *In situ* hybridization detected *Tmc2* mRNA in cochlear hair cells of P1 but not P5 mice. Quantitative RT-PCR showed only transient expression of *Tmc2* mRNA that coincided with the developmental onset of mechanotransduction in cochlear hair cells. *Tmc1* expression rose several days after *Tmc2* expression and remained elevated into adulthood.

We generated *Tmc1*<sup>Δ</sup> and *Tmc2*<sup>Δ</sup> mouse lines segregating targeted deletions of *Tmc1* and *Tmc2*, respectively. Auditory brainstem response (ABR) threshold testing showed that *Tmc1*<sup>Δ/Δ</sup> mice are deaf and *Tmc2*<sup>Δ/Δ</sup> mice have normal hearing. Scanning electron microscopy showed structurally intact hair bundles in *Tmc1*<sup>Δ/Δ</sup>; *Tmc2*<sup>Δ/Δ</sup> cochlear hair cells until P5 (base) to P9 (apex). *Tmc2*<sup>Δ/Δ</sup> outer hair cells excised from the apex at P5-P7 had normal mechanotransduction current amplitudes whereas amplitudes were reduced ~35% in *Tmc1*<sup>Δ/Δ</sup> hair cells. *Tmc1*<sup>Δ/Δ</sup>; *Tmc2*<sup>Δ/Δ</sup> hair cells lacked mechanotransduction currents entirely. We were unable to detect FM1-43 uptake in *Tmc1*<sup>Δ/Δ</sup>; *Tmc2*<sup>Δ/Δ</sup> cochlear hair cells, consistent with the absence of functional mechanotransduction channels. Adenoviral-mediated expression of either TMC1 or TMC2 rescued mechanotransduction and FM1-43 uptake in *Tmc1*<sup>Δ/Δ</sup>; *Tmc2*<sup>Δ/Δ</sup> cochlear hair cells. Exogenously expressed GFP-tagged TMC proteins localized at or near tips of stereocilia of *Tmc1*<sup>Δ/Δ</sup>; *Tmc2*<sup>Δ/Δ</sup> inner and outer hair cells.

We conclude that TMC1 and TMC2 are functionally redundant and necessary for cochlear hair cell mechanotransduction. Our results suggest that *TMC1* mutations cause deafness because TMC2 is not expressed and available to compensate for the loss of TMC1 in mature cochlear hair cells.

### **581** Mechanotransduction in Mouse Vestibular Hair Cells Requires

#### **Transmembrane Channel-Like Genes 1 or 2**

Yoshiyuki Kawashima<sup>1</sup>, Gwenaëlle Géléoc<sup>2</sup>, Kiyoto Kurima<sup>1</sup>, Valentina Labay<sup>1</sup>, Yukako Asai<sup>3</sup>, Geoff Horwitz<sup>3</sup>, Tomoko Makishima<sup>1</sup>, Doris Wu<sup>1</sup>, Charles Della Santina<sup>4</sup>, Andrew Griffith<sup>1</sup>, **Jeffrey Holt**<sup>2</sup>

<sup>1</sup>NIH/NIH, <sup>2</sup>Children's Hospital Boston / Harvard Medical School, <sup>3</sup>University of Virginia, <sup>4</sup>Johns Hopkins University School of Medicine

Mutations of transmembrane channel-like gene 1 (*TMC1*) cause deafness but not vestibular dysfunction in humans and mice, yet mouse *Tmc1* is expressed in auditory and vestibular hair cells. Here we investigated the contributions of *Tmc1* and the closely related *Tmc2* gene to balance function. *In situ* hybridization detected *Tmc2* mRNA in vestibular hair cells of P1 and P5 mice. Quantitative RT-PCR showed a rise in *Tmc2* mRNA that coincided with the developmental onset of mechanotransduction in vestibular hair cells. A rise in *Tmc1* expression lagged *Tmc2* expression by several days but remained elevated into adulthood.

We analyzed *Tmc1*<sup>Δ</sup> and *Tmc2*<sup>Δ</sup> mouse lines segregating deletions of exons encoding the first transmembrane domains of *Tmc1* and *Tmc2*, respectively. *Tmc1*<sup>Δ</sup> mice and

*Tmc2*<sup>Δ</sup> mice had normal motor vestibular behavior but *Tmc1*<sup>Δ/Δ</sup>; *Tmc2*<sup>Δ/Δ</sup> double knockout mice showed severe abnormal vestibular behaviors such as ataxic gait, circling, and head-bobbing. *Tmc1*<sup>Δ</sup> mice and *Tmc2*<sup>Δ</sup> mice had normal vestibulo-ocular reflexes (VORs), whereas *Tmc1*<sup>Δ/Δ</sup>; *Tmc2*<sup>Δ/Δ</sup> mice had absent VORs.

Scanning electron microscopy showed structurally intact hair bundles in *Tmc1*<sup>Δ/Δ</sup>; *Tmc2*<sup>Δ/Δ</sup> vestibular hair cells. Utricle hair cells from *Tmc1*<sup>Δ/Δ</sup> mice at P1-P8 had transduction currents indistinguishable from those of controls whereas *Tmc2*<sup>Δ/Δ</sup> hair cells had currents that were reduced ~80%. *Tmc1*<sup>Δ/Δ</sup>; *Tmc2*<sup>Δ/Δ</sup> hair cells lacked transduction currents entirely. Utricle hair cells from *Tmc1*<sup>Δ/Δ</sup>; *Tmc2*<sup>Δ/Δ</sup> mice at P3 also failed to take up FM1-43, consistent with the absence of functional mechanotransduction channels. Adenoviral-mediated expression of either TMC1 or TMC2 rescued mechanotransduction and FM1-43 uptake in *Tmc1*<sup>Δ/Δ</sup>; *Tmc2*<sup>Δ/Δ</sup> utricle hair cells. Finally, exogenously expressed GFP-tagged TMC proteins localized at or near tips of stereocilia of utricle hair cells.

We conclude that TMC1 and TMC2 are functionally redundant and required for mechanotransduction in mouse vestibular hair cells.

### **582** Whirlin Modulates the Actin-Regulatory Function of Espin

Le Wang<sup>1,2</sup>, Junhuang Zou<sup>1</sup>, Zuolian Shen<sup>1</sup>, **Jun Yang**<sup>1</sup>

<sup>1</sup>Moran Eye Center, University of Utah, <sup>2</sup>1st affiliated hospital, Jilin University

Whirlin mutations cause retinal degeneration and hearing loss in Usher syndrome type II (USH2) and nonsyndromic deafness, DFNB31. Its protein recruits other USH2 causative proteins to form a complex at the periciliary membrane complex (PMC) in photoreceptors and the ankle-link of the stereocilia in hair cells. However, the biological function of this USH2 protein complex is largely unknown. Using a yeast two-hybrid screen, we identified espin, an actin-binding/bundling protein involved in human deafness when defective, as a whirlin-interacting protein. The interaction between these two proteins was confirmed by their coimmunoprecipitation and colocalization in cultured cells. This interaction involves multiple domains of both proteins and only occurs when espin does not bind to actin. Espin was partially colocalized with whirlin in the retina and the inner ear. In whirlin knockout mice, espin expression changed significantly in these two tissues. Further studies found that whirlin increased the motility of espin and actin at the actin bundles cross-linked by espin and, eventually, affected the dimension of these actin bundles. In whirlin knockout mice, the stereocilia were thickened in inner hair cells. We conclude that the interaction between whirlin and espin and the balance between their expressions are required to maintain the actin bundle network in photoreceptors and hair cells. Disruption of this actin bundle network contributes to the pathogenic mechanism of hearing loss and retinal degeneration caused by whirlin and espin mutations.

**583 An Additional F-Actin-Binding Site in Large Isoforms of the Stereociliary Actin-Bundling Protein Espin: Contribution to Targeting and Requirement to Block Actin Treadmilling**

Lili Zheng<sup>1</sup>, Dina Beeler<sup>1</sup>, James Bartles<sup>1</sup>

<sup>1</sup>*Northwestern University Feinberg School of Medicine*

The parallel actin bundle scaffold of hair cell stereocilia is cross-linked by multiple classes of actin-bundling protein, but little is known about what each class contributes. This problem is complicated by fact that the espin class of stereociliary actin-bundling protein comes in multiple isoforms that differ markedly in size owing to alternative transcriptional start sites and splicing. In the mouse, the jerker mutation, which causes total espin deficiency, results in abnormally thin, unstable stereocilia. The jerker mutation and DFNB36 human espin mutations both cause deafness and vestibular dysfunction. While many of the actin-related activities of espins have been attributed to their defining 116-amino acid carboxy-terminal actin-bundling module, the large espin isoforms, espin 1 and espin 2, contain an additional F-actin-binding site that is upstream of the actin-bundling module. This additional F-actin-binding site was required to efficiently target espin 1, a major espin isoform in the inner ear, to the microvilli of transfected epithelial cells. The requirement was especially evident for espin 1 bearing the DFNB36 mutations c.2469delGTCA or c.1988delAGAG, which affect the actin-bundling module. The additional F-actin binding site was also required to block actin treadmilling in espin-elongated microvilli and to form nuclear actin bundles in response to espins bearing the jerker mutation. Both activities suggest a cross-linking role for the additional F-actin-binding site. Scanning alanine mutagenesis was used to delineate the boundaries of the additional F-actin-binding site and identify its key residues. The site spanned 13 amino acids and depended critically on two hydrophobic residues and a lysine. A recombinant peptide corresponding to the additional F-actin-binding site bound actin filaments, but not monomeric actin, *in vitro*. Our results suggest that large espin isoforms contain an additional F-actin-binding site that enhances their ability to bind, cross-link and stabilize actin filaments. (NIH DC004314, JB).

**584 Notch Signaling Regulates Formation and Development of the Stereocilia and Mechanotransduction Apparatus of Cochlear Hair Cells**

David He<sup>1</sup>, Shuping Jia<sup>1</sup>, Qian Zhang<sup>1</sup>, Shiming Yang<sup>2</sup>

<sup>1</sup>*Creighton University*, <sup>2</sup>*Chinese PLA General Hospital*

The Notch pathway is an evolutionary conserved cell-cell signaling mechanism involved in cell fate decisions during development. We examined whether the Notch pathway regulated hair-bundle morphogenesis in the cultured organ of Corti of newborn gerbils. Pharmacological inhibition of the Notch pathway induced ectopic hair cells though conversion of supporting cells. Inhibition also produced supernumerary stereocilia in the existing hair cells. Scanning electron microscopy revealed that the newly

emerged stereocilia have tip links. Deflections of the hair bundles generated mechanoelectrical current, suggesting that the mechanotransduction apparatus is functional. However, the ectopic hair cells in the outer hair cell region did not express prestin and potassium currents normally seen in outer hair cells. Thus, Notch signaling is sufficient to regulate formation and development of the stereocilia and mechanotransduction apparatus. However, it appears that Notch is not involved in regulating the expression of ion channels and prestin motors in the lateral membrane. (Supported by NIH/NIDCD grant R01 DC 004696 to DH)

**585 Two-Step Regeneration of Mechanotransduction and Molecular Composition of the Tip Links in Mammalian Cochlear Inner Hair Cells**

Artur Indzhykilian<sup>1</sup>, Ruben Stepanyan<sup>1</sup>, Gregory Frolenkov<sup>1</sup>

<sup>1</sup>*Dept. Physiology, University of Kentucky*

Hair cell mechanotransduction depends on the integrity of the tip links that interconnect stereocilia of neighboring rows in a hair bundle. Although it is well-known that the tip links could regenerate after disruption in Ca<sup>2+</sup>-free extracellular solution, the molecular details of this process are still obscure. Here we used high resolution scanning electron microscopy (SEM) to study the distribution of two known tip link components, protocadherin 15 (PCDH15) and cadherin 23 (CDH23), at the stereocilia surface and along the length of the tip links in the inner hair cells of young postnatal mice. In these hair cells, Ca<sup>2+</sup>-free BAPTA-buffered medium disrupts most (if not all) links between the stereocilia and, therefore, tip link re-assembly can be studied "from scratch". We also recorded mechano-electrical transduction (MET) in these cells and found that the recovery of the MET machinery progresses in two distinct steps. In the first ~12 hour step, an apparently normal set of stereocilia links re-forms at the tips of stereocilia from the molecular components that remained at the stereocilia surface after BAPTA treatment. In parallel, the normal amplitude of MET responses also recovers. However, the extent of Ca<sup>2+</sup>-dependent decay of MET current (adaptation) is still abnormal and so does the molecular composition of the nascent tip links. It is only after 48 hours of recovery that the extent of MET adaptation becomes completely normal. Concurrently, the tip link filaments acquire their normal composition with CDH23 at the upper end of the filament and PCDH15 at the lower end. Thus, we conclude that the molecular composition of the tip link is likely to be dynamic and is refined to optimize MET responses.

Supported by NIDCD/NIH (R01 DC008861 and ARRA supplement 3R01DC008861-01A2S1).

**586 Blast-Induced Tinnitus and Its Related Traumatic Brain Injury (TBI) in Auditory Structures: A MEMRI Study**

Laura Lepczyk<sup>1</sup>, Jessica Ouyang<sup>1</sup>, Edward Pace<sup>1</sup>, Pamela VandeVord<sup>2</sup>, Jinsheng Zhang<sup>1,3</sup>

<sup>1</sup>Department of Otolaryngology-Head and Neck Surgery, Wayne State University School of Medicine, <sup>2</sup>Department of Biomedical Engineering, Wayne State University College of Engineering, <sup>3</sup>Dept. of Communication Sciences & Disorders, Wayne State Univ. College of Liberal Arts & Sciences

Blast-induced traumatic brain injury (TBI) is associated with tinnitus in military and civilian populations. Accumulative evidence suggests that noise-induced tinnitus can develop as a result of peripheral insult to the auditory system that causes hyperactivity and plastic changes at the central level. The underlying mechanisms of blast-induced tinnitus and its related TBI are an underexplored area. In this study, we used manganese-enhanced magnetic resonance imaging (MEMRI) to study neural activity in auditory structures of rats that were behaviorally tested for tinnitus following blast exposure. We evaluated hearing thresholds using ABR, tested for tinnitus using the gap detection acoustic startle reflex paradigm, and performed MEMRI to investigate auditory structures. Our results demonstrated that blast exposure (10 ms, 14 psi) caused a significant hearing threshold shift, which recovered within five weeks. Immediately following the blast, all 12 exposed rats displayed robust behavioral evidence of tinnitus. 7 developed chronic tinnitus and 5 animals' tinnitus disappeared, which were termed as transient tinnitus. Five weeks following one single blast, our preliminary MEMRI data showed a lower intensity ratio in the left central inferior colliculus (CIC) and a moderate decrease in the left medial geniculate body (MGB) in rats with chronic tinnitus compared to controls (n=5). The single blast exposure did not cause significant changes in intensity ratio between chronic tinnitus and control rats in the dorsal cochlear nucleus, ventral cochlear nucleus (VCN), external cortex of the inferior colliculus, right CIC, right MGB, and auditory cortex. The transient tinnitus group had a slightly lowered intensity ratio in the right VCN compared to the chronic tinnitus group. The data suggest that tinnitus may be caused by acoustic overexposure/trauma to the auditory pathways as well as a blast-induced direct impact to the brain.

**587 Blast Induced Tinnitus and Its Related Traumatic Brain Injury in Non-Auditory Structures: A Combined Behavioral and MEMRI Study**

Jessica Ouyang<sup>1</sup>, Edward Pace<sup>1</sup>, Laura Lepczyk<sup>1</sup>, Pamela VandeVord<sup>1</sup>, Jinsheng Zhang<sup>1</sup>

<sup>1</sup>Wayne State University

Tinnitus and hearing loss are the frequent auditory-related co-morbidities of blast trauma. The development and persistence of tinnitus is also compounded by brain mechanisms associated with cognitive problems such as anxiety, memory, emotion and depression. We set out to

develop a realistic and ecologically valid model to address cognitive status (memory) and psychological state (anxiety and emotion) that are associated with the induced tinnitus and the related TBI. In this study, 17 adult rats were randomly divided into control group (n=5), and blast group (n=12). Blast exposure (14 psi) was carried out to expose the left ears of the 12 rats. Blast-induced tinnitus, changes in anxiety and memory were evaluated using gap detection acoustic startle reflex paradigm, elevated plus maze and Morris water maze, respectively. ABRs were used to monitor blast-induced changes in hearing threshold. To investigate blast-induced neural changes in non-auditory brain structures, we conducted in vivo manganese-enhanced magnetic resonance imaging (MEMRI) following injection of MnCl<sub>2</sub> at 67mg/kg and measured intensity ratio over muscle tissue using MRIcro. Our results showed that blasted animals with tinnitus demonstrated high anxiety level and worsened spatial memory, though blasted animals with tinnitus demonstrated stronger spatial learning compared to blasted animals without tinnitus and control animals. Our preliminary MEMRI data showed that blasted animals with tinnitus had higher intensity ratio in the contralateral cingulate cortices, ipsilateral core nucleus accumbens, but lower intensity ratio in bilateral hippocampus, compared to control animals. There was no difference in hippocampal manganese uptake between blasted animals with or without tinnitus. The data further support the involvement of the hippocampus, nucleus accumbens and cingulate cortices in the psychological sequelae of blast-induced tinnitus and TBI.

**588 Modeling Blast Induced Tinnitus**

Edward Lobarinas<sup>1</sup>, Brian Allman<sup>1</sup>, Richard Salvi<sup>1</sup>

<sup>1</sup>University at Buffalo

Blast exposure is one of the most common types of noise trauma that results in both hearing loss and tinnitus. Blast waves that cause traumatic and permanent hearing loss typically range from 175-200 dB SPL. Here we present updates to our animal model of tinnitus (i.e., the acoustic startle reflex, ASR) designed to model unilateral profound hearing loss induced by blast exposure. In preliminary experiments, we have identified that exposure to repeated blasts can cause both hearing loss and traumatic brain injury; effects that can reduce the reliability of the ASR. Consequently, we have modified the paradigm to include crossmodal stimulation which has allowed us to better assess gap prepulse inhibition following blast induced unilateral hearing loss and tinnitus. Ultimately, by using these modified procedures, we show that animals with poor ASR post blast exposure can still show gap prepulse inhibition in an intensity- and frequency-specific manner.

**589 Tinnitus Suppression by Electrical Stimulation of the Rat Dorsal Cochlear Nucleus**

Hao Luo<sup>1</sup>, Xueguo Zhang<sup>1</sup>, Javan Nation<sup>1</sup>, Edward Pace<sup>1</sup>, Laura Lepczyk<sup>1</sup>, Jinsheng Zhang<sup>1</sup>

<sup>1</sup>Wayne State University

Previous studies by our group and others have demonstrated that the dorsal cochlear nucleus (DCN) may

serves as a generator/modulator of noise-induced tinnitus. This prompts the interest of investigating of whether the DCN may be used as a target for effective neuromodulation and suppression of tinnitus. We set out this investigation by chronically implanting the DCN of rats that were tested behaviorally for tinnitus following intense tone exposure. Using gap detection acoustic startle reflex paradigm, our results demonstrated that electrical stimulation to the DCN suppressed behavioral evidence of tinnitus. The data suggest that the DCN may be used as a target to suppress tinnitus through a bottom-up neuromodulation approach. The underlying mechanisms of DCN-stimulation-induced suppression of tinnitus were discussed by comparing with other stimulation modalities.

### **590** Suppression of Tinnitus by NRG1 Over-Expression in the Mouse Hippocampus

Ambrose Kidd<sup>1</sup>, Debin Lei<sup>1</sup>, Jeremy Turner<sup>2,3</sup>, Donald Caspary<sup>2</sup>, Bao Jianxin<sup>1</sup>

<sup>1</sup>Washington University School of Medicine, <sup>2</sup>Southern Illinois University School of Medicine, <sup>3</sup>Illinois College

Tinnitus is a serious health problem with no drugs for the treatment or prevention, mainly due to the lack of understanding of its cellular and molecular pathology. Our gene-array data from a noise-induced tinnitus animal model suggested that synaptic plasticity in the hippocampus could contribute to tinnitus. Neuregulin-1 (NRG1) is a key molecule important for modulating synaptic plasticity both in the peripheral and central nervous system (PNS and CNS). We have made and characterized mouse lines that conditionally over-express NRG1 in the hippocampus. Using the gap-detection startle reflex, we found that salicylate treatment caused a significant increase of the relative startle response of control mice, an indication of tinnitus after the treatment. Subsequently, we discovered that over-expression of NRG1 in the hippocampus blocks salicylate-induced tinnitus. Specifically, we found strong suppression of salicylate-induced tinnitus five months after NRG1 over-expression in the mouse hippocampus. Because of this observation, we hypothesize that NRG1 signaling in the hippocampus contributes to tinnitus. We are currently pursuing different lines of work to understand the role of NRG1 in tinnitus better. First, we are using microarrays to analyze gene expression changes induced by NRG1 over-expression in the hippocampus. This will provide insights into how NRG1 over-expression inhibits tinnitus. Additionally, we are also testing the ability of NRG1 over-expression to prevent noise-induced tinnitus. In total, our work will reveal NRG1 down-stream molecular pathways underlying tinnitus and identify molecular targets for the development of effective therapies against tinnitus.

### **591** Drug Delivery to the Inner Ear of Rats Using Magnetically Steered Nanoparticles

Didier Depireux<sup>1</sup>, Roger Lee<sup>1</sup>, Azeem Sarwar<sup>1</sup>, Ben Shapiro<sup>1</sup>

<sup>1</sup>U of Md College Park

Following noise trauma, treatment of injury and inflammation of the cochlea is essentially dependent on

the ability to deliver drugs to the inner ear structures. To this end, nanoparticles are a natural candidate because of their biocompatibility, the ability to load them with a variety of drugs, and the promise they can deliver their payloads without causing additional injury or trauma to the inner ear. We have used superparamagnetic nanoparticles with a maghemite core, coated with a starch matrix and loaded with fluorescent proteins for post-mortem visualization. We measured the penetration of the cochlear space by these particles as a function of the particles' diameter, external field strength and duration of exposure to the external magnetic field while the particles are being actively steered by a configuration of magnets, both pulling from the contralateral side of the skull and pushing from the ipsilateral side.

We are testing the effectiveness of magnetically pushed nanoparticles functionalized with prednisolone on preventing the emergence of tinnitus in a rat model of noise-trauma induced tinnitus, and we will report on this new method of drug delivery, how much reduction of tinnitus we obtain, and possible future developments.

### **592** Age Effects on Gap Detection in CBA/CaJ Mice Following Sound Exposure

Ryan Longenecker<sup>1</sup>, Kurt Chonko<sup>2</sup>, Stephen Maricich<sup>2</sup>, Alexander Galazyuk<sup>1</sup>

<sup>1</sup>Northeast Ohio Medical University, <sup>2</sup>Case Western Reserve University

In our previous work we studied the effects of sound exposure on the development of behavioral signs of tinnitus in a group of CBA/CaJ mice. Both the control (unexposed) and sound exposed mice were monitored during a three month period following exposure. The presence of tinnitus was assessed by measuring the reduction in the acoustic startle reflex by a preceding silent gap in an otherwise constant acoustic background presented as narrowband noise centered at different sound frequencies. We found that by three months post exposure, 86% of mice developed behavioral signs of tinnitus predominantly within the frequency range from 20 to 25 kHz, although mice were exposed to 16 kHz. All exposed mice also showed a reduction in magnitude of the acoustic startle reflex. The goal of the present study was to determine how aging affects tinnitus in exposed mice. The same group of mice (control and exposed) were monitored up to one year following exposure. We found that control mice showed no significant changes in their gap detection over the one year period. The exposed mice also showed little change. The vast majority of exposed mice (70%) exhibited deficiency in gap detection at 25 kHz. Similar to our observations at three months after sound exposure, by 12 months, all exposed mice showed a much smaller magnitude of startle responses compared to the control (unexposed) mice. The amplitudes of their auditory brainstem responses were much smaller compared to the controls. Histology of the cochlear in the exposed mice was also affected by sound exposure. Results of this study are discussed in the context of a possible link between tinnitus and permanent hearing loss induced by an acoustic trauma.

Supported by the Research Incentive Grant from NEOMED and Tinnitus Research Consortium Grant.

### **593 Effect of Noise Exposure Duration and Intensity on the Development of Tinnitus**

Keerthana Devarajan<sup>1</sup>, Davina Gassner<sup>2</sup>, Dianne Durham<sup>2</sup>, Hinrich Staecker<sup>1</sup>

<sup>1</sup>University of Kansas, <sup>2</sup>Univeristy of Kansas

The goal of this study was to determine the optimum noise exposure that resulted tinnitus verified by gap detection in an acute sound trauma model. Adult rats were treated with 1-2 hrs of monaural 16 kHz sound at 114, 118 and 123 dB. Prior to noise exposure and at 10 days post noise exposure, gap detection was measured at 12, 16 and 20 kHz. Hearing loss in the sound exposed ear was verified using ABR and DPOAE. Tinnitus, defined as the inability to detect a gap prior to a startle noise was present in 30 percent of animals and was not related to the level of noise exposure or to the amount of hearing loss detected. To produce a population of animals with behaviorally verified tinnitus requires noise exposing and screening a significantly larger population of animals.

### **594 Relationship Between Noise Exposure Stimulus Properties and Tinnitus in Rats: Results of a 12-Month Longitudinal Study**

Jeremy Turner<sup>1,2</sup>, Deb Larsen<sup>1</sup>

<sup>1</sup>SIU School of Medicine, <sup>2</sup>Illinois College

Fischer Brown Norway (FBN) rats (n=167) were unilaterally exposed to a 16 kHz, octave band noise at all combinations of three different intensities (110, 116, and 122 dB SPL) and three different durations (30, 60, and 120 min), while 30 rats served as sham-exposed controls. Rats were behaviorally tested for gap-induced prepulse inhibition of the acoustic startle reflex (GPIAS) and prepulse inhibition (PPI) using 60 dB SPL, 1/3-octave backgrounds (for gap) or prepulse stimuli centered at 10 different frequency bands from 4-32 khz. Behavioral testing for tinnitus was conducted before noise exposure to establish a baseline, then at days 1, 3, 7, 14, 21, 28, and monthly thereafter for 12-months. The longer and more intense stimuli led to greater acute tinnitus measured one day after noise exposure, generally seen at frequencies above the trauma (i.e., 20-32 kHz). Over subsequent months the tinnitus pitch appeared to shift down until at 12-months the GPIAS-measured tinnitus settled around 16 kHz (p=0.005), and sometimes lower. The 12-month tinnitus appeared to be largely independent of which noise exposure condition was received. Indeed, some of the strongest tinnitus at 12-months emerged in groups receiving the least intense (110 dB SPL) and shortest duration exposure (30 and 60 min). Additional analyses by individual animals are presented and the relationship between acute tinnitus and chronic tinnitus at 12-months are explored to determine whether acute tinnitus could be used as a predictor for chronic tinnitus. The results are discussed in the context of the interactions between noise exposure and aging in the production of chronic tinnitus.

Study funded by a grant from the Tinnitus Research Consortium.

Behavioral equipment donated by Kinder Scientific in the memory of SIU graduate Dorothy Jean Kinder (Walker).

### **595 Effects of Background Noise on the Acoustic Startle Response**

David Dolan<sup>1</sup>, Karin Halsey<sup>1</sup>, Peter Ghisleni<sup>1</sup>, Richard Altschuler<sup>1</sup>

<sup>1</sup>KHRI, University of Michigan

The acoustic startle response (ASR) is a reflex used in human and animal studies of disease. Preceding the startle-inducing stimulus with a lower level acoustic stimulus can reduce the amplitude of the ASR. This effect is called pre-pulse inhibition (PPI). PPI is considered to be an indicator of sensorimotor gating and is used in metrics of human disorders such as schizophrenia and autism. In animal models using ASR, some studies acquire the startle response in the presence of a background noise. In this case, the "pre-pulse" is a brief increase in the noise amplitude. Here we describe the effects of nine conditions of background noise and their influence on ASR amplitude input/output functions compared to the ASR acquired in quiet. The noise conditions include broad-band noise, and 2-kHz bandwidth noise centered at various frequencies (mice 12-14 kHz and 24-26 kHz, and rats 8-10 kHz and 16-18 kHz). These responses were measured in rats (Sprague Dawley) and 2 strains of mice (UM-HET4 and CBA/j). In general, the effect of any of the background noise conditions has little or no effect on the ASR amplitude obtained from rats. In contrast, the effect of broad-band noise on the ASR amplitude obtained from mice significantly increases with increases in background noise from 40 to 75 dB SPL. In some cases, mice exhibited ASR reduction in the presence of narrow-band noise. These results suggest that studies using pre-pulse inhibition of the ASR should be aware that the amplitude of the ASR can vary with the acoustic environment and needs to be controlled.

Supported by NIH Grant P30DC05188

### **596 Development of a Novel Hearing-Aid for the Profoundly Deaf Using Bone-Conducted Ultrasonic Perception: Assessments of the Modulation Type with Regard to Intelligibility and Sound Quality**

Seiji Nakagawa<sup>1</sup>, Chika Fujiyuki<sup>1</sup>, Takayuki Kagomiya<sup>1</sup>

<sup>1</sup>National Institute of Advanced Industrial Science and Technology (AIST)

Bone-conducted ultrasound (BCU) is perceived even by the profoundly sensorineural deaf. We have objectively proven the BCU perception by neurophysiological measurements and developed a novel hearing-aid using BCU perception (BCU hearing aid: BCUHA) for the profoundly deaf. In the BCUHA, ultrasound, sinusoids with frequency of about 30 kHz, are amplitude-modulated by speech or environmental sounds and presented to the mastoid or sternocleidomastoid by a vibrator. As a result, two sounds are perceived: one is a high-pitched tone due

to the ultrasonic carrier, with a pitch corresponding to a 10-odd kHz AC sinusoid, and the other is the modulator signal itself; i.e., speech or environmental sound. The double-sideband with transmitted carrier (DSB-TC) has been used for the BCUHA as the method of amplitude modulation (AM), however, the DSB-TC is accompanied by a strong high-pitched tone especially when the modulation depth is low.

In this study, several types of amplitude modulation were evaluated with regard to intelligibility and sound quality. The intelligibilities for four-mora Japanese words were measured by using a BCUHA with various types of AM methods, and the subjective impression of the sound was examined using the semantic differential (SD) with twelve pairs of adjective scales and a *questionnaire for listening by hearing-aids* after each session of the word-intelligibility test. Three AM methods, DSB-TC, Double sideband with suppressed carrier (DSB-SC), and transposed modulation (TM), were employed.

DSB-TC and TM had significantly higher intelligibility scores than DSB-SC, whereas no differences were between DSB-TC and TM. Factor analyses of the adjective scales extracted three factors (metallic factor, esthetic factor, and powerfulness factor). All types of BCU speech had higher metallic factor scores and lower esthetic factor scores than air-conducted speech, and DSB-SC had lower esthetic factor score and TM had higher powerfulness factor score than other BCU stimuli did. Further, in general, the results of the questionnaire showed that DSB-TC speech was less distorted, DSB-SC speech was less clear and more distorted, and TM speech was more pleasant and less shrill than other BCU speech. It is suggested that TM speech is closer than other types of BCU speech to air-conducted speech in terms of sound quality, whereas DSB-TC has the least distorted speech. These results provide useful information for further development of the BCUHA.

### **[597] Cochlear Stimulation Via Third Window Vibroplasty in Chinchilla Lanigera: Effects of Round Window and Oval Window Occlusion**

**J. Eric Lupo<sup>1</sup>, Kanthaiah Koka<sup>2</sup>, Herman Jenkins<sup>1</sup>, Daniel Tollin<sup>2</sup>**

<sup>1</sup>University of Colorado School of Medicine Department of Otolaryngology, <sup>2</sup>University of Colorado School of Medicine Department of Physiology and Biophysics  
Pathological conditions such as advanced tympanosclerosis or otosclerosis can preclude access to the oval (OW) and round window (RW) for normal transmission of sound to the cochlea via the ossicular chain. Alternate routes of cochlear stimulation such as mechanical stimulation of the RW or "third" window vibroplasty have been shown to produce physiological responses similar to acoustic stimulation; however, little is known of the physiological effects of direct mechanical third window stimulation in the pathological setting of OW and RW occlusion. To address this, cochlear microphonic (CM) and laser Doppler vibrometer (LDV) measurements of stapes and RW velocities were performed in 6 ears of 4 chinchillas. Baseline measurements to acoustic sinusoidal

stimuli (0.25-8 kHz) were made. Measurements were repeated with an active middle ear implant (AMEI) stimulating the cochlea at a third window (~.3 mm diameter) to the scala tympani (ST) before and after OW occlusion and also after joint RW and OW occlusion. With AMEI stimulation of the cochlear third window, CM waveforms were morphologically similar to acoustic stimuli across all experimental conditions. CM thresholds with RW and third window stimulation were frequency-dependent ranging from 0.25-10 and 0.5-40 mV (rms input to AMEI), respectively. OW and RW fixation, confirmed by LDV measurements, resulted in a mild frequency dependent decrease in CM thresholds up to 1 to 15 dB. AMEI mechanical stimulation through a surgically created cochlear third window into the ST with occlusion of the OW and RW produces CM responses similar to acoustical stimulation but with decreased CM thresholds.

### **[598] Conditions for Optimum Stimulation of the Round-Window Membrane in Humans**

**Sebastian Schraven<sup>1</sup>, Anthony W. Gummer<sup>2</sup>, Hans-Peter Zenner<sup>2</sup>, Ernst Dalhoff<sup>2</sup>**

<sup>1</sup>ENT-Clinic Wuerzburg, <sup>2</sup>ENT-Clinic Tuebingen

Stimulation of the round window (RW) has gained increasing clinical importance. Clinical, as well as human temporal-bone and in-vivo animal studies show considerable variability regarding the stimulation efficiency. The influence of coupling issues on RW stimulation efficiency remained therefore unclear. Here, we present RW-stimulation experiments in human temporal bones showing that three requirements must be fulfilled in order to achieve highly reproducible and efficient stimulation of the cochlea: (1) control of proper RW membrane pretension, (2) actuator adapted to the geometry of the RW membrane and niche, and, (3) well-controlled and stable implantation technique. If these requirements are fulfilled, the amplitude ratio between stapes and actuator vibration is 0.34 for frequencies up to 1.5 kHz and 0.27 for frequencies up to 20 kHz, with a standard deviation of only 4-6 dB at most frequencies.

### **[599] Chronic Multi-Unit Recording from Cat Auditory Cortex**

**James Fallon<sup>1</sup>, Dexter Irvine<sup>1</sup>, Sam Irving<sup>1</sup>, Robert Shepherd<sup>1</sup>**

<sup>1</sup>Bionics Institute, Melbourne, Australia

We have previously shown that neonatal profound deafness results in a loss of the normal cochleotopic organization of primary auditory cortex (AI), but that environmentally-relevant chronic electrical stimulation (CES) via a multi-channel cochlear implant can restore that organization. To explore the time course of this re-establishment of cochleotopy, we are developing procedures to obtain chronic recordings of multi- and single-unit responses from the AI of cats over extended periods.

We have evaluated the stability of AI recordings over time by recording responses to tonal stimuli in two normal-hearing cats. In each cat, a planar silicon electrode array (Blackrock Microsystems; Salt Lake City, Utah) was

implanted in putative AI under sterile conditions. Initial recordings from the arrays were made approximately 4 weeks post-surgery and subsequent recordings at approximately 2-week intervals, with the cats either gently restrained or anesthetized with Xylazil (2mg/kg, s.c.) and Ketamine (20mg/kg, i.m.). Calibrated tone-burst stimuli were presented via a free-field speaker positioned approximately 10 cm from the ear contralateral to the implanted cortex.

Responses to tonal stimuli were observed on 49 of 90 channels (54%) in the initial recording sessions and on 37 of the 90 channels (41%) in the final recording session (4 and 5 months later in the two cats). At 10 recording sites at which a reliable frequency-intensity response area could be recorded over this period there was no significant difference in either characteristic frequency (paired t-test;  $p = 0.68$ ) or threshold ( $p = 0.70$ ). This stability over time indicates that these recording procedures are appropriate to future studies of the time course of the effects of deafness and CES on cochleotopic organization.

This work was funded by the NIDCD (HHS-N-263-2007-00053-C). Bionics Institute acknowledges the support it receives from the Victorian Government through its Operational Infrastructure Support Program.

### **600 The Slopes of Auditory Nerve Input-Output Functions Decrease as Stimulus Pulse Rate Is Increased – for Spike-Rates Less Than 100 Spikes/second**

**Mark White**<sup>1</sup>, Leon Heffer<sup>2</sup>, James Fallon<sup>2,3</sup>, David Sly<sup>2</sup>, Rob Shepherd<sup>2,3</sup>, Stephen O'Leary<sup>2,3</sup>

<sup>1</sup>unaffiliated, <sup>2</sup>Dept. of Otolaryngology, The University of Melbourne, <sup>3</sup>Bionics Institute, Melbourne, Australia

Measuring the slopes of “static” auditory nerve input-output functions may be useful in understanding the communication of low-frequency envelope intensity information to the CNS.

ANF responses to electrical stimulation were recorded in acutely and chronically deafened guinea pigs. Electrical pulse trains of 100 ms duration were delivered via an acutely implanted scala tympani electrode using a monopolar electrode configuration. Stimuli were presented at rates of 200, 1000, 2000 and 5000 pulses/s. Stimulus current was varied to evoke a range of spike discharge rates between 0 and 250 spikes/s. Each neuron's [1] accommodation (i.e., adaptation due to sub-threshold pulses), [2] refraction, and [3] facilitation (i.e., increased excitability due to prior sub-threshold pulses) was measured. Measures from over 200 fibers indicate that refraction, accommodation, and facilitation vary significantly from fiber to fiber. We have not found evidence for significant correlations among these 3 measures.

We estimated each neuron's stochastic Input-Output (IO) function in the following manner: Because we were trying to estimate approximate steady-state neural response, only discharges that occurred after the first 20 ms of each burst were used. For each stimulus current, the mean of the bursts' spike rates was calculated. Similarly, the standard deviation of the bursts' spike rates was

calculated. These two measures were plotted as a function stimulus current on a log-log scale. On this nonlinear scale, we used a piecewise linear fit to estimate how mean spike rate varied with stimulus current. Likewise, we also obtained a piecewise linear fit of the standard deviation data. In the end, we had 2 piecewise-linear functions for each stimulus pulse rate. Most fibers' IO slopes decreased significantly with increased pulse rate at low-to-moderate neural response levels (i.e., < 100 spikes/sec). Similar behavior was exhibited at still higher response levels with the exception of 200 pps stimuli, whose IO slopes dramatically flattened near 150-200 spike/sec, due to “saturation.” From the IO-slope and variability measures we estimated how readily an amplitude modulated pulse train could be “ideally detected” versus an unmodulated pulse train (i.e., an MDT measure). The level of amplitude modulation required for detection varied with current level and stimulus pulse rate. -- in a manner similar, for the most part, to behavioral MDT measures.

### **601 Effects of Pulse Rate on Slopes of Temporal Integration Functions and Threshold-Vs-Pulserate Functions in CI Users**

**Gail Donaldson**<sup>1</sup>, Julia Hartman<sup>1</sup>, Vuday Nandur<sup>1</sup>

<sup>1</sup>University of South Florida

McKay's loudness model for electrical hearing indicates that loudness grows slowly at low current levels but grows more rapidly at higher current levels (McKay and McDermott, 1998, JASA 104, 1061-74; McKay et al., 2001, JASA 110, 1514-24; McKay et al., 2003, JASA 113, 2054-63). This level-dependent pattern of loudness growth has implications for the effects of pulse rate on behavioral measures that involve temporal integration (TI). Specifically, increases in pulse rate are known to shift the electrical operating range to lower current levels where the model predicts that loudness growth will be more gradual. This should lead to steeper TI functions because the slopes of TI functions are inversely related to the rate of loudness growth. Similar effects are expected for increases in stimulus duration. That is, increasing stimulus duration will shift the operating range to lower current levels where loudness growth should be more gradual, leading to steeper threshold-vs-pulserate (THS-vs-pulserate) functions.

The present study tested the above predictions in four cochlear implant users. Stimuli were trains of biphasic current pulses (32 us/ph, monopolar coupling) presented to an electrode near the middle of the implanted array. Detection thresholds were measured for all possible combinations of five pulse rates (200, 500, 1000, 2000 and 5000 pps) and seven stimulus durations (10, 20, 40, 80, 160, 320 and 640 ms) using an adaptive 3AFC procedure. The resulting threshold data were used to construct TI functions for each pulse rate and THS-vs-pulserate functions for each stimulus duration.

Slopes of THS-vs-pulserate functions showed a strong effect of stimulus duration; slopes became significantly steeper as stimulus duration increased from 10 ms to 160

ms and showed a trend to increase further at 320 and 640 ms. Slopes of TI functions showed a weak trend to become steeper as pulse rate increased, with the 200 pps function being significantly shallower than the higher pulse-rate functions (500-5000 pps). Findings are consistent, at least qualitatively, with the level-dependent changes in loudness growth rate described by McKay's model.

### **602 A Hybrid Channel Selection Algorithm for Dereverberation in Cochlear Implants**

**Stefano Cosentino<sup>1</sup>**, Torsten Marquardt<sup>1</sup>, David McAlpine<sup>1</sup>

<sup>1</sup>*UCL Ear Institute, London, UK*

Reverberation has been shown to be extremely detrimental for speech intelligibility in cochlear implant (CI) stimulation due to temporal envelope smearing, low spectral contrast, and flattening of formant transition. The energy-based N-of-M channel selection (ACE strategy) seems not the optimal strategy under such degraded listening conditions. Kokkinakis et al. (2011) showed that signal de-reverberation can improve word recognition scores of CI users up to 90% compared to 20% (average values) in reverberant conditions ( $RT_{60} = 1s$ ). De-reverberation was based on channel selection depending on the ratio between the dry-signal power and the reverberant power (Speech-to-Reverb Ratio, SRR), as computed using the pre-knowledge about the dry-signal waveform. Within each analysis time frame, channels with SRR below a threshold of -5dB were muted. So far implemented as monolateral 128-channel pre-processor, they suggested an implementation of a SRR-based N-of-M selection strategy directly operating on the electrode channels. We tested the use of interaural coherence as an estimator of SRR in a binaural CI configuration, which would allow real-time signal de-reverberation without pre-knowledge of the dry signal. In addition, we propose a hybrid electrode-channel selection criterion based on a combined weighting of reverberation content and relative energy within the channels. Such selection rule can easily be integrated with conventional ACE, improving speech intelligibility in reverberant environments. Objective and subjective tests were performed to evaluate the proposed algorithm. Vocoder simulations with normal hearing subjects were conducted using BKB sentences that were convolved with room impulse responses ( $RT_{60}$  ranging from anechoic to 1.4 s). Our hybrid de-reverberation algorithm shows speech recognition improvements almost as large as simulations of electrode-channel selection based on the pre-knowledge SRR.

### **603 Action Potential Initiation in Auditory Nerve Fibers Via Cochlear Implant Stimulation Is Dependent on Ion Channel Population and Electrode Location**

**Jason Boulet<sup>1</sup>**, Ian Bruce<sup>1</sup>

<sup>1</sup>*McMaster University*

Numerous findings indicate that auditory nerve fibers (ANFs) of deafened cats presented with high rates of electrical stimulation, given by cochlear implants, undergo

spike-rate adaptation and accommodation. A simulation study by Negm and Bruce (EMBC 2008) reported that low-threshold potassium (KLT) and hyperpolarization-activated cyclic nucleotide-gated cation (HCN) channels are the determining components of this behavior, whereas standard Hodgkin-Huxley-type ANF models, containing fast Nav and delayed-rectifier Kv channels only, cannot explain adaptation.

To investigate the effects of the spatial distribution of multiple ion channels species on the neural response, we carry out a compartmental simulation study of the electrical stimulation of a type I feline ANF. We base our neuron morphology on Woo et al. (JARO 2010) and implement two versions of the model: A) just fast Nav and delayed-rectifier Kv at all nodes of Ranvier and B) with the addition of KLT & HCN channels (Yi et al., J Neurophysiol 2010) at the first peripheral node and on the nodes of Ranvier neighboring the soma. Our results indicate that stimulation of peripheral nodes in model B exhibits a higher threshold current for action potential generation, shorter mean latency and smaller jitter than for model A. This effect is observed even at peripheral nodes in model B that do not themselves have the KLT & HCN channels but are adjacent to nodes that do. In contrast, the statistics of action potential generation are identical between the two model versions for stimulation at central nodes of Ranvier. The properties of refractoriness, spike-rate adaptation and accommodation for the two model versions will be explored and discussed.

### **604 A Peripheral Neural Correlate of Temporal Processing by Cochlear Implant Listeners**

**Robert Carlyon<sup>1</sup>**, John Deeks<sup>1</sup>

<sup>1</sup>*Medical Research Council*

Cochlear implant (CI) manufacturers are increasingly interested in presenting fine temporal information via the CI. Unfortunately, the temporal processing of this information by patients is at best modest, and is usually very poor at rates above 300 pulses per second (pps). It also varies substantially across patients. The neural basis of the poor performance remains a matter of debate. We measured rate discrimination on a single mid electrode in nine users of the Freedom cochlear implant. Standard rates of 100 to 500 pps were compared to signal rates 30% higher using a 2I-2AFC task. Rate discrimination by most listeners was best at low rates, but this pattern varied across listeners. We also measured ECAPs to every pulse in these pulse trains, using identical stimuli to the behavioral experiment. As shown previously, the ECAP to pulse trains were usually modulated, typically showing larger responses to odd-numbered than to even-numbered pulses. The depth of this modulation increased from 2.5 % at 100 pps to 14 % at 400 pps. When both ECAP modulation and rate-discrimination scores were averaged across rates, there was a strong negative between-subject correlation ( $r = -0.87, p < 0.01$ ). Furthermore, the ECAP modulation accounted for a significant proportion of the variation in performance as a function of pulse rate for a

given listener. Our preliminary conclusion is that ECAP modulation depth serves as an indicator of neural survival, which in turn affects rate discrimination performance. Hence although processes central to the auditory nerve (AN) may influence rate discrimination, our results show that differences between patients in the ability to discriminate rate changes can be largely accounted for by the AN response. We will also present preliminary results showing whether ECAP modulation accounts for variations in temporal processing across electrodes within a given subject.

### **605 Effects of High and Low Rate Intra-Cochlear Electrical Stimulation on the Higher Central Auditory Pathway**

**Dietmar Basta**<sup>1</sup>, Sebastian Jansen<sup>1</sup>, Romy Götze<sup>1</sup>, Moritz Gröschel<sup>1</sup>, Patrick Boyle<sup>2</sup>, Arne Ernst<sup>1</sup>

<sup>1</sup>Dept. of ENT at ukb, University of Berlin, <sup>2</sup>Advanced Bionics, European Research Centre

Very high (up to 5000 Imp/s) and low rates (e. g. 275 Imp/s) are in use for the intra-cochlear electrical stimulation in cochlear implantees. Little is known about possible different long term consequences of these very different stimulation strategies for the central auditory system. The present study therefore aims to investigate, for the first time at the cellular level, the micro-structural and neurophysiologic consequences of chronic intra-cochlear high- or low rate electrical stimulation within the ascending auditory pathway.

Normal hearing guinea pigs were single-sided deafened by the implantation of a standard HiRes 90k cochlear implant with a HiFocus1j electrode array. The first 4 or 5 electrode contacts could be used to stimulate the cochlear nerve fibers within the first turn of the cochlea. Four weeks after surgery, the speech processor (Auria) was mounted on the back of the animals and programmed, based on the tNRI-values. The animals of the experimental groups were stimulated with a 5000 Imp/s or 275 Imp/s HiRes coding strategy for 3 months. Experimental groups and controls (implanted but not stimulated) experiencing a similar daily acoustic environment (16 hours-radio play).

Animals of both experimental groups (high- or low rate stimulated) showed a significantly lower average spontaneous activity on the implanted as well as the non-implanted side of the medial geniculate body (MGB) and primary auditory cortex (AC) than the controls (implanted but not stimulated). The neuronal cell density of the MGB and AC was bilaterally significantly higher after high- or low rate electrical stimulation compared to the corresponding side of the implanted but not stimulated controls. A conservation of the neuronal structure upon electrical stimulation was observed.

The present findings indicate a neuronal plasticity on both sides of the higher auditory pathway upon unilateral intra-cochlear electrical stimulation. The large rate differences between the coding strategies induced no specific physiological or anatomical effects in the brain areas under study. Further studies should clarify the impact of the observed reduced spontaneous activity for the performance of higher auditory processing.

### **606 Responses of the Inferior Colliculus to Optical Stimulation of the Cochlear Nucleus**

**Rohit U. Verma**<sup>1,2</sup>, Kenneth E. Hancock<sup>1,3</sup>, Amélie Gueux<sup>1,4</sup>, Nedim Durakovic<sup>1,5</sup>, Hilary Nicholson<sup>1</sup>, Colette M. McKay<sup>2</sup>, M. Christian Brown<sup>1,3</sup>, Daniel J. Lee<sup>1,3</sup>

<sup>1</sup>Eaton-Peabody Laboratory, Massachusetts Eye & Ear Infirmary, Boston, MA, <sup>2</sup>Department of Psychological Sciences, University of Manchester, UK, <sup>3</sup>Department of Otolaryngology, Harvard Medical School, Boston, MA, <sup>4</sup>École Polytechnique Fédérale De Lausanne, Switzerland, <sup>5</sup>Warren Alpert Medical School of Brown University, Providence, RI

Infrared neural stimulation (INS) can be used to stimulate auditory neurons in the cochlea and the cochlear nucleus (CN). Results from experiments in the auditory periphery suggest that INS has high spatial selectivity (Izzo AD et al 2007; Richter CP et al 2011). We tested the spatial selectivity of INS applied to the CN by recording gross neural activity in the contralateral central nucleus of the inferior colliculus (ICCN). In our rodent model (Sprague-Dawley rats), we exposed the CN via posterior craniotomy and aspiration of the overlying cerebellum. Radiant energy was delivered using pulsed INS via an optical fiber placed on the surface of the CN. Near-field recordings were made from the IC using a 16-channel probe (NeuroNexus Technologies, Inc.) oriented roughly orthogonal to the tonotopic axis that exists through the depth of the ICCN. Acoustic responses were first used to determine the tonotopic map of the IC's central nucleus by plotting response magnitudes as a function of depth from the IC surface. Our preliminary results suggest that the IC responses to INS of the CN were large and robust, sometimes even for CN stimulation sites that produced small potentials in the far-field auditory brainstem response. Changing the site of INS stimulation in the CN produced a corresponding change in the depth of peak IC response. Early data generated from two animals suggest that INS stimulation of some sites on CN evoked spatially-tuned responses in IC, indicated by a narrow peak in the response magnitude vs. depth profile. Other CN sites provoked a broader response with activation across most of the IC tonotopic axis. This work strengthens the case for development of an optical ABI that functions through INS. The spatial selectivity indicated by our early experiments could overcome some of the inherent problems associated with electrical stimulation such as current spread. Supported by Helene and Grant Wilson Foundation, Fondation Bertarelli & MED-EL Corporation.

### **607 Laser Parameters for Infrared Neural Stimulation in Acute Cat Experiments**

**Ken Zhao**<sup>1</sup>, Suhred Rajguru<sup>2</sup>, Claus-Peter Richter<sup>1</sup>

<sup>1</sup>Northwestern University, <sup>2</sup>University of Miami

Infrared neural stimulation (INS) is a non-contact mode of spatially selective stimulation and shows promise for future applications in cochlear implants (CIs). It is critical to determine the optimal parameters for pulsed infrared stimulation, because delivery of radiation pulses results in heat deposition. In the present report, we conducted

physiological studies of the stimulus parameters (radiant energy, wavelength, pulse duration, and pulse shape) in cat cochleae. The physiological response of auditory neurons was quantified by measuring evoked compound action potentials (CAPs). The data did not show any significant wavelength dependency in the range tested (1855-1885 nm). The results showed that shorter duration pulses evoked greater responses compared to longer duration pulses delivering the same radiant energy. The response correlated with the peak power applied with every infrared (IR) pulse. Investigations into the effect of pulse shape showed that square waves were the least efficient compared to triangle, ramp-up, and ramp-down waveforms, and the responses were proportional to the peak power. This suggests that short duration pulses of shapes that briefly attained peak power were the most efficient form of INS and should be utilized in the development of CIs based on INS.

This work was supported by a grant from Lockheed Martin Aculight.

### **608 Filter Slopes for Infrared Neural Stimulation**

**Claus-Peter Richter**<sup>1</sup>, Suhrud Rajguru<sup>2</sup>, Agnella Izzo Matic<sup>1</sup>

<sup>1</sup>Northwestern University, <sup>2</sup>University of Miami

Spatial tuning curves were obtained from recordings of neural activity in the central nucleus of the inferior colliculus (ICC) while the cochlea was stimulated with infrared laser pulses. The results show that infrared neural stimulation (INS) in the cochlea produces spatially selective responses. However, it is not clear whether the increased selectivity can lead to more identifiable independent channels and thus an improvement over contemporary cochlear implants. With the present experiments, we examined the channel interaction for INS during cochlear stimulation using a three channel light delivery system (LDS). Two lasers operating at a wavelength 1860 nm, pulse duration of 20-100  $\mu$ s, and pulse repetition rate of 10-200 Hz were used for stimulation. Channel interaction was examined during near simultaneous presentation of two optical stimuli, a masker followed by a probe. By calculating the ratio of the compound action potential (CAP) amplitude evoked by the probe alone and evoked by the probe in the presence of the masker, any interaction between two simultaneous stimuli could be determined. The level of the masker that was required to reduce the response to the probe by 3 dB was determined for different spatial distances between the probe and the masker. Stimulation sources were separated by 0-2 mm. The resultant values were used to determine the interaction between the two stimulation sites. From the masker level and the distance between the two stimuli, the filter shape for INS was determined.

At distances >0.4 mm between the sources, little interaction occurred between the stimuli for low (~4  $\mu$ J/pulse) and medium (~20  $\mu$ J/pulse) stimulus levels. Increasing the stimulus levels resulted in interactions between the electrodes. Calculations of the filter slope

from initial measurements resulted in a slope of approximately 20 dB/mm.

Supported by the NIH, Contract No. HHSN260-2006-00006-C / NIH No. N01-DC-6-0006.

### **609 Damage Threshold for Infrared Neural Stimulation**

**Vinay Goyal**<sup>1</sup>, Suhrud Rajguru<sup>1,2</sup>, Agnella Matic<sup>1</sup>, Claus-Peter Richter<sup>1,2</sup>

<sup>1</sup>Northwestern University Feinberg School of Medicine, Dept. of Otolaryngology, <sup>2</sup>Dept. of Biomedical Engineering, Northwestern University

Pulsed infrared radiation has been shown to effectively stimulate neurons. While pulsed infrared has an advantage of spatial selectivity, each radiation pulse deposits thermal energy in the tissue. At high pulse repetition rates, thermal damage is a concern. It is important to investigate the energy range at higher pulse rates, for which there are no functional or histological changes due to thermal energy deposition in the tissue. In the present study, the damage thresholds were studied in guinea pig model.

Guinea pigs were anesthetized and the cochleae accessed via the bulla. A cochleostomy was performed at the basal turn. A 200  $\mu$ m diameter optical fiber was inserted into scala tympani and the cochlear neurons were stimulated at 250 Hz pulse repetition rate and various dosages of radiant energies. Pulse length was 100  $\mu$ s. Evoked compound action potentials (CAP) were measured in 5 minute intervals to track cochlear function throughout the experiment. A 25% decrease in CAP amplitude was defined as damage. At the conclusion of the recordings the cochleae were processed for histology.

For each radiant energy that resulted in damage, the time for the CAP amplitude to drop by 25% was determined and was plotted versus its corresponding energy. As radiant energy increased, the stimulation time until the cochlea was defined as damaged decreased. For the case that damage was observed, the CAP amplitude initially increased possibly due to a net temperature increase.

Damage threshold was detected between 25-45  $\mu$ J/pulse. At radiation energies higher than 45  $\mu$ J/pulse we observed different levels of loss of cochlear function depending upon energy. Radiant energies below 25  $\mu$ J/pulse resulted in no change in cochlear function up to 4h. In addition the tissue observed under light microscopy, did not reveal signs of thermal damage despite changes in cochlear function.

Supported by the NIH under Contract No. HHSN260-2006-00006-C / NIH No. N01-DC-6-0006 and by Lockheed Martin Aculight.

### **610 Infrared Neural Stimulation Induced by Transient Changes in Membrane Capacitance**

Mikhail Shapiro<sup>1,2</sup>, Kazuaki Homma<sup>3</sup>, Sebastian Villarreal<sup>1</sup>, Claus-Peter Richter<sup>3</sup>, Francisco Bezanilla<sup>1</sup>

<sup>1</sup>The University of Chicago, <sup>2</sup>University of California at Berkeley, <sup>3</sup>Northwestern University

Infrared neural stimulation (INS) is an optical technique to stimulate a variety of neurons without any genetic or chemical pretreatment of target cells, which contrasts sharply with other optical neural stimulation techniques

such as optogenetics. Therefore, it holds promise for potential clinical applications, in addition to being a useful tool in basic neuroscience research. In fact, efforts in prosthetic applications of INS have already been made. However, the molecular mechanism of INS has yet to be clarified, which hinders the wider dissemination of this very powerful and potentially general neural stimulation technique.

In order to elucidate the INS mechanism, we performed infrared laser radiation (IR)-dependent voltage-clamp/current-clamp recordings in *Xenopus laevis* oocytes, HEK293T cells, and artificial lipid bilayers. We found that IR induces a rapid local temperature increment, which results in a membrane capacitance ( $C_m$ ) increase. This  $C_m$  increase induces a current under voltage clamp or a transmembrane voltage change in current clamp that are ion channel/transporter-independent. This unanticipated mechanism is fully reversible, and requires nothing but the cell membrane and surrounding ionic solution. Thus, our finding points to the potential generality of the INS method to control the activity of neurons and other excitable cells.

(Work supported by NIH grants GM030376 and DC011481-01A1)

### **611 A Point Process Framework for Modeling Electrical Stimulation of the Auditory Nerve**

**Joshua Goldwyn**<sup>1,2</sup>, Jay Rubinstein<sup>1</sup>, Eric Shea-Brown<sup>1</sup>  
<sup>1</sup>University of Washington, <sup>2</sup>New York University

Simulation studies of auditory nerve responses to electrical stimulation can provide useful insight into the functioning of cochlear implants. Ideally, these studies can identify limitations in existing sound processing strategies and lead to improved methods for providing sound information to cochlear implant users. To accomplish this, models must accurately describe auditory nerve spiking while avoiding excessive complexity that would preclude large-scale simulations of populations of auditory nerve fibers and obscure insight into the essential dynamical and stochastic mechanisms that influence neural encoding of sound information. In this spirit, we develop a point process model of the auditory nerve that provides a compact and accurate description of neural responses to electric stimulation.

Inspired by the framework of generalized linear models, the model consists of a cascade of linear and nonlinear stages. We show how each of these stages can be associated with biophysical mechanisms and related to more detailed models of neuronal dynamics. Moreover, we derive a semi-analytical procedure that uniquely determines each parameter in the model on the basis of fundamental statistics from recordings of single fiber responses to electric stimulation. These response statistics include threshold, relative spread, jitter, and chronaxie. The model also includes dynamical properties that account for refractory and summation effects that influence the responses of auditory nerve fibers to high pulse rate stimulation. We then illustrate how the model can make predictions that elucidate differences in auditory nerve responses to high and low pulse rate stimulation. We close

by studying the response of the model to sinusoidally amplitude-modulated stimulation. This illustrates the potential utility of this modeling framework for simulations of psychoacoustic experiments.

This work has been supported by NIDCD (F31 DC010306 and R01 DC007525), and the Burroughs Wellcome Fund.

### **612 The Contribution of Vowel/Consonant Boundaries to Speech Recognition in Reverberation by Cochlear Implant Users**

**Oldoos Hazrati**<sup>1</sup>, Jaewook Lee<sup>1</sup>, Philip Loizou<sup>1</sup>

<sup>1</sup>University of Texas-Dallas

The Contribution of Vowel/Consonant Boundaries to Speech Recognition in Reverberation By Cochlear Implant Users

Although most cochlear implant (CI) users are able to achieve open-set speech recognition scores of 80% or higher in quiet and anechoic environments, their performance degrades significantly in the presence of reverberation. Self- and overlap-masking effects of reverberation blur acoustic landmarks, which are critically important for distinguishing syllable and word boundaries and understanding speech in reverberation. The present study maintains the hypothesis that when these landmarks are recovered, substantial intelligibility improvements are to be expected. To that end, in order to overcome the destructive effects of reverberation on speech intelligibility by CI users, a method is proposed for removing reverberation energy from the waveform dips/valleys thus making the vowel/consonant boundaries more clear. This method bandpass filters the reverberant signal into a number of channels and classifies the short-time segments in each channel into two classes: class A containing segments that were originally (prior to reverberation) waveform dips or had low-energy, and Class B containing high-energy voiced segments (e.g., vowels). Segments classified into class A are zeroed out while segments classified into class B are retained. Objective evaluation of the proposed approach suggested improvement in intelligibility. Results with CI users using sentences corrupted with high degree of reverberation will be presented.

Research supported by NIDCD/NIH.

### **613 Stapedius Muscle Electromyogram (EMG) Measured During Cochlear Implant (CI) Stimulation in the Cat**

**Ben Bonham**<sup>1</sup>, Russell Snyder<sup>1,2</sup>, Kinuko Masaki<sup>3</sup>, Leonid Litvak<sup>3</sup>, Charles Finley<sup>3</sup>

<sup>1</sup>Epstein Laboratory, UCSF, <sup>2</sup>Utah State Univ, <sup>3</sup>Advanced Bionics

Studies of children implanted with CIs have demonstrated that better performance is achieved with earlier implantation. Differences in performance between groups of children implanted before and after 2 years of age are substantial, and underscore the importance of providing appropriate stimulation to the auditory system early during development.

Post-surgical fitting of the CI involves setting appropriate levels of electrical stimulation. During fitting, upper stimulating current levels are chosen to lie below a maximum comfort level (MCL). High levels of stimulation that cause discomfort disincite users from using their devices and may in fact be detrimental to the ear and to maintenance of auditory discrimination. In older users maximum settings are determined based upon verbal feedback from the CI user. However, this process cannot be used in infant CI recipients. In normal hearing, the stapedius reflex is thought to protect the inner ear from high-intensity sound by pulling the stapes away from the oval window and thereby decreasing transmission of vibrational energy to the cochlea. This reflex may provide objective identification of electrical stimulation levels that are "too loud". The EMG of the stapedius muscle has been proposed as a means for estimating the MCL.

We present results of studies examining stapedius EMG recorded from anesthetized cats acutely implanted with a CI. The results indicate that response latencies may be several 10s of milliseconds, and that the time required for the stapedius response threshold to return to baseline can be several seconds following reflex activation. Further, the stapedius threshold, latency, and response strength depend upon a variety of factors, including stimulus level, duration, pulse rate, and CI electrode configuration.

Supported by Advanced Bionics and UC Discovery Seed Grant #210888

#### **614 Noise Reduction Strategy Provides Speech Reception Benefits for Cochlear Implant Users**

**Ray Goldsworthy**<sup>1,2</sup>, Lorraine Delhorne<sup>2</sup>, Charlotte Reed<sup>2</sup>, Louis Braida<sup>2</sup>

<sup>1</sup>*Sensimetrics Corporation*, <sup>2</sup>*Massachusetts Institute of Technology*

We will summarize results from an ongoing study of a noise reduction strategy being evaluated with cochlear implant users. The strategy uses phase analysis between two microphones spaced 1 cm apart and placed above one ear to selectively filter sounds arriving from in front of the listener. The evaluation is conducted using adaptive speech in noise measures to determine potential benefits of the strategy in comparison to omni- and dipole-directional receptive fields. The acoustic environment used to evaluate the strategy is generated using head-related transfer functions recorded in a room that measures 7.4 by 4.7 by 3.0 meters and that has a reverberation time, the time for the ambient reverberant energy to decay 60 dB, of 0.4 seconds. The acoustic condition being tested uses target speech at 0° in front of the listener and noise sources at 90, 180, and 270° (all sources are located 1 meter away). The speech reception measures are implemented with vowel and consonant materials and an adaptive procedure that converges to 30, 50, and 70% correct on phoneme identification. Preliminary data indicates that cochlear implant users receive approximately 5 dB of signal-to-noise ratio benefit from the strategy over dipole receptive fields and 10 dB of benefit over omni-directional fields. The results indicate that the

strategy is robust in a realistic noise environment that includes at least 3 noise sources and a moderate level of room reverberation. Discussion will focus on integrating this strategy into cochlear implant and hearing aid systems to provide the hearing impaired with improved speech reception in noisy environments.

#### **615 Relationship Between Intracochlear Electrically Evoked Auditory Brainstem Response and Auditory Performance After Cochlear Implant in the Patients with Auditory Neuropathy Spectrum Disorder**

**Ju Hyun Jeon**<sup>1</sup>, Mee Hyun Song<sup>2</sup>, Won Sun Yang<sup>3</sup>, Sera Park<sup>4</sup>, Jae Young Choi<sup>4</sup>

<sup>1</sup>*Inje University College of medicine*, <sup>2</sup>*Kwandong University College of Medicine*, <sup>3</sup>*Sahmyook Medical center*, <sup>4</sup>*Yonsei University College of Medicine*

Auditory neuropathy spectrum disorder (ANS) is a clinical disease entity characterized by preserved otoacoustic emission (OAE) and/or cochlear microphonic potential (CM), and abnormal or absent auditory brainstem response (ABR). Impairment of synchronous neural activity in the auditory pathway including inner hair cell, synapse, spiral ganglion, axon, myelin sheath, and nerve dendrite causes ANSD. We sought to identify the difference of auditory performance after cochlear implant (CI) by analyzing and comparing the EABR patterns between patients with ANSD and those with SNHL. We included nine patients who were diagnosed with ANSD and performed with intracochlear EABR from 2006 to 2010. The control group consisted of nine patients who received CI due to SNHL and performed intracochlear EABR. During EABR, low-, mid-, and high-frequency electrodes were stimulated for the each cochlear implant device. EABR threshold, wave V latency, and amplitude were measured. The results of EABR were grouped into three categories (good response, variable response, no response). Postoperative performance was assessed by CAP (Categories of Auditory Performance) score. All control patients responded to EABR, but only three (33.3%) of ANSD patients responded to EABR. EABR responders in ANSD patients showed similar level of EABR threshold and amplitude compared with controls, but wave V latency is variable. In the EABR responders, CAP score were rapidly improved after CI, but non-responders showed variable response in pre- and post operative auditory performances. We supposed that EABR responders in ANSD patients had a dysfunction of distal auditory pathway such as inner hair cell or synapse, but non-responders had an abnormality at proximal lesion such as spiral ganglion or axon. We may explain the reason of variable outcome in non-responders that unsynchronized signal induced by electrical stimulation delivers incomplete sound information to the brain cortex.

## **616** Reduced Concentration Gradients in the Murine Cochlea Utilizing Novel Round Window Membrane Drug Application Techniques

XiaoXia Zhu<sup>1</sup>, David Borkholder<sup>2</sup>, Robert Frisina<sup>1</sup>

<sup>1</sup>Univ. South Florida, <sup>2</sup>Rochester Institute of Technology

Delivery of potentially therapeutic compounds to the inner ear via the round window membrane (RWM) has advantages over alternative methods. Specifically, the RWM approach minimizes bleeding, with little impact upon functional hearing measures. However, some previous reports show that significant basal-to-apical concentration gradients occur (Plontke et al. *Laryngoscope* 2007;117:1191-1198). The new surgical approach presented here utilizes polyimide infusion tubing placed onto the niche near the RWM, through a bulla-ostomy. Inclusion of a posterior semicircular canalostomy provides additional opportunities to reduce drug concentration gradients. Methods: Young adult CBA/CaJ mice were divided into two groups: bulla-ostomy approach only (B) and bulla-ostomy + canalostomy (B+C). Cochlear function was evaluated by distortion product otoacoustic emissions (DPOAEs) thresholds and auditory brainstem responses (ABRs) (8-51 kHz). Mice were infused with 50mM salicylate in artificial perilymph at a flow rate of 50nl/min for a total volume of 1000nl (20 min); DPOAEs were measured before and after surgery, and at intervals during the infusion. The mice recovered for 1 week, and re-tested. Results: there was no significant impact on auditory function utilizing the RWM surgical procedure, and DPOAE thresholds were elevated reversibly during the salicylate infusion. Comparing the threshold shifts for both methods, the B+C approach had more of a physiological effect than the B approach, especially at lower frequencies - more apical cochlear locations. Unlike mouse cochleostomies, there was no deleterious auditory functional impact after 1 week recovery from surgery. Regarding the B+C approach, it had more drug efficacy at lower frequencies indicating reduced concentration gradients, underscoring potential benefits for more precise control of delivery of inner ear therapeutic compounds.

Supported by NIH Grants P01 AG009524 and K25 DC008291

## **617** Dexamethasone Pharmacokinetics in the Inner Ear Assessed by Injection and Sampling at the Lateral Semi-Circular Canal

Alec N. Salt<sup>1</sup>, Fabrice Piu<sup>2</sup>, Jared J. Hartsock<sup>1</sup>, Ruth M. Gill<sup>1</sup>, Stefan Plontke<sup>3</sup>

<sup>1</sup>Washington University School of Medicine, St. Louis, MO,

<sup>2</sup>Otonomy Inc. San Diego, CA USA, <sup>3</sup>Dept. of

Otorhinolaryngology, Head and Neck Surgery, University of Halle (Saale), Germany

Perilymph pharmacokinetics was investigated by a novel approach, in which perilymph was exchanged with solution containing drug or marker. Solutions were injected at 1  $\mu$ L/min from a pipette sealed into the lateral semi-circular canal, so that fluid leakage at the injection site could not influence results. After wait times of up to 4 hours, the

pipette was removed and multiple, sequential samples of perilymph were taken from the canal. This method allows the rate of elimination of substances from the inner ear to be more accurately defined than with other delivery methods which fill the ear less uniformly. During the injection procedure used here, the cochlear aqueduct provided the outlet for fluid flow, allowing the entire perilymph contents to be replaced. During sampling, CSF entry into the basal turn of scala tympani through the cochlear aqueduct displaced fluid at the canal so that the sequential fluid samples represented perilymph from different locations in the ear. Results were compared for the markers trimethylphenylammonium (TMPA) and fluorescein, and for the drug dexamethasone (dex). For each substance, the concentration in fluid samples showed a progressive decrease as the delay time between injection and sampling was increased. This is consistent with the elimination of substance from the ear over time. The decline with time was slowest for fluorescein, was faster for TMPA and faster still for dexamethasone. Simulation of the experiments showed that elimination occurred more rapidly from scala tympani (ST) than from scala vestibuli (SV). Elimination half-times from ST averaged 54.1, 24.7 and 22.5 min for fluorescein, TMPA and dex respectively and from SV 1730, 229 and 111 min respectively. The rate of dex elimination from ST was considerably faster than previously appreciated. These important pharmacokinetic parameters increase our understanding of drug treatments of the inner ear. Work supported by NIH grant DC01368.

## **618** Functional Responses to Cochlear Implant Stimulation Following NT-3 Upregulation

Bryan E. Pflugst<sup>1</sup>, Yehoash Raphael<sup>1</sup>, Sara A. Bowling<sup>1</sup>, Cameron L. Budenz<sup>1</sup>, Deborah J. Colesa<sup>1</sup>, Elizabeth C. Hyde<sup>1</sup>, Lisa L. Kabara<sup>1</sup>, Seiji B. Shibata<sup>1,2</sup>, Stefan B. Strahl<sup>3</sup>, Gina L. Su<sup>1</sup>, Melissa M. Watts<sup>1</sup>

<sup>1</sup>University of Michigan, <sup>2</sup>University of Iowa, <sup>3</sup>Med-El GmbH

Most cochlear implant users have partial or complete absence of hair cells and auditory-nerve peripheral processes as well as a partial loss of spiral ganglial cell bodies. While it is often assumed that the quality of cochlear implant function depends on the quantity of these elements, the evidence supporting that assumption is sparse. In previous studies we have shown that preserving hair cells and auditory neurons in the implanted ear has large effects on psychophysical multipulse temporal integration and on electrically-evoked compound action potential (ECAP) growth functions. In the current study, we sought to examine the effects of neural survival and regeneration in the absence of hair cells. Cochleae were infused with neomycin to destroy hair cells prior to implantation and an adeno-associated viral vector carrying the NTF-3 gene (AAV.NTF-3) was administered to the scala tympani to upregulate the secretion of NT-3, which has been shown to support the survival of spiral ganglion cell neurons and induce regrowth of peripheral fibers toward the implant in the organ of Corti. Control ears were

deafened and inoculated with an empty virus (AAV.empty). For the AAV.NTF-3 inoculated ears, ECAP growth functions were much steeper than those for the control ears and only slightly shallower than those in ears implanted with good preserved acoustic hearing. Psychophysical detection thresholds versus pulse rate functions and temporal integration functions were slightly lower than those for the control ears but considerably higher and with a more gradual slope than those for ears with good acoustic hearing preservation. These results suggest that neurotrophin treatment in deaf ears restores some but not all features of cochlear-implant function to levels near those in ears with the least cochlear pathology. Work supported by NIH/NIDCD grants R01 DC010412, R01 DC007634, T32 DC005356 and P30 DC05188 and by a contract from MED-EL Corp.

### **619** Effects of Brain Derived Neurotrophic Factor (BDNF) on the Cochlear Nucleus in Cats Deafened as Neonates

**Cherian Kandathil<sup>1</sup>, Olga Stakhovskaya<sup>1</sup>, Patricia Leake<sup>1</sup>**  
<sup>1</sup>*Epstein Laboratory, Dept. of Otolaryngology-HNS, University of California San Francisco*

This study examined the morphology of the cochlear nucleus (CN) in a group of neonatally deafened cats from a previous study in which intracochlear infusion of BDNF resulted in significant neurotrophic effects promoting improved survival of the cochlear spiral ganglion neurons (BDNF, 80% normal; contralateral 64%). Cats were profoundly deafened by systemic injections of neomycin sulfate. Five cats were implanted unilaterally at ~30 days of age using custom scala tympani electrodes with a drug-delivery cannula attached to an osmotic pump. BDNF (94 µg/ml; 0.25 µl/hr) was delivered for 10 weeks, and animals were studied at 14-15 weeks of age. Total CN volume and individual CN subdivision volumes were measured in 50 µm frozen sections (toluidine blue stain). Cross-sectional areas of spherical cell somata and numerical cell density in the anteroventral CN (AVCN) were measured in 5 µm sections that were osmicated, embedded in epoxy and counter-stained (toluidine blue). Comparisons were made between the BDNF-treated and contralateral sides of deafened animals, and CN volume data were compared to normal adult cats (n=4).

Total CN volumes in the deafened group were markedly smaller than normal (BDNF, 61% of normal; contralateral, 55%). The larger CN volume on the BDNF side compared to contralateral (p=0.016; paired t-test) was consistent with the neurotrophic effects of BDNF on SG survival in these animals. Data from the three major CN subdivisions (DCN, PVCN and AVCN) showed a significant difference only for the AVCN volume (p=0.022; 2-way ANOVA, Tukey test). Spherical cell areas were significantly larger in the AVCN ipsilateral to the implant than on the contralateral side (~400 vs 330 µm<sup>2</sup>). The numerical density of spherical cells in the AVCN was significantly lower ipsilateral to the implant compared to contralateral, consistent with the differences in AVCN volume. Together, findings indicate a significant neurotrophic effect of BDNF on the developing cochlear nucleus.

Supported by the NIH, NIDCD Contract #HHS-N-263-2007-00054-C. BDNF donated by Amgen Inc., Thousand Oaks, CA.

### **620** Drug Elution from Cochlear Implants: Feasibility Based on Drug Levels Estimated for the Human Cochlea

**Alec N. Salt<sup>1</sup>, Christopher Miller<sup>2</sup>, Kristien Verhoeven<sup>3</sup>**

<sup>1</sup>*Washington University School of Medicine, St. Louis, MO,*

<sup>2</sup>*Cochlear Ltd Macquarie University, NSW, 2109, Australia,*

<sup>3</sup>*Cochlear Technology Center Belgium Schalienenhoeverdreef 20-1 2800 Mechelen Belgium*

Animal studies suggest that trauma and hearing loss associated with cochlear implantation can be significantly reduced by administering corticosteroids at the time of implantation. In order to produce more effective and prolonged drug delivery, the possibility of using sustained-release materials in cochlear implants has been considered. One difficulty associated with this approach is the ability to predict what drug levels are achieved in the ear and whether a therapeutic drug level can be maintained in the presence of potentially high rates of drug elimination from the cochlea. In the present study, a new computer model of the fluid and tissue spaces of the human inner ear was utilized to calculate perilymph dexamethasone levels produced by cochlear implants with different configurations and elution characteristics. The model incorporates fluid and tissue space dimensions and inter-compartment communications for the human ear. Kinetic parameters were based on measurements in guinea pigs, but with consideration of available data from humans. Perilymph levels were calculated for drug being contained either in the entire implant, or in specific regions of the implant, and for different rates of drug elution. Calculations demonstrated that therapeutic levels of drug were generated at sites close to the elution site, but concentrations rapidly declined for cochlear locations distant from the elution site. Therapeutic levels could be generated with low rates of elution from the implant, and could therefore be generated for a very long time. Alternatively, an end-point, where the drug level falls below a therapeutic level after a given time, could be implemented. These calculations confirm that the incorporation of drugs that elute from cochlear implants is a feasible approach to minimize cochlear trauma associated with cochlear implantation.

Acknowledgement: This project was supported by NIH/NIDCD grant DC01368 and by Cochlear Corp.

## **621 Antiproliferative Effect and Surface Structure Modification of Cochlear Implant Coatings Using Dexamethasone and Hydrogel**

**Guenter Reuter**<sup>1</sup>, Antonina Wrzeszcz<sup>2</sup>, Pooyan Aliuos<sup>2,3</sup>, B. Ditrach<sup>4</sup>, Daniel Haamann<sup>5</sup>, Ingo Nolte<sup>6</sup>, Thomas Lenarz<sup>7</sup>

<sup>1</sup>ENT Lab MHH, <sup>2</sup>ENT MHH, <sup>3</sup>ENT-MHH, <sup>4</sup>RWTH Aachen, <sup>5</sup>RWTH aachen, <sup>6</sup>TiHo, <sup>7</sup>ENT Clinic MHH

The insertion of cochlear implants into the inner ear often causes inflammation and fibrosis inside the scala tympani and thus growth of connective tissue on the implant. Loss of function occurs in implants by increasing the impedance through the fibrous tissue. The approach is growth inhibition of fibroblasts through the release of the steroid dexamethasone (Dex) and a hydrogel coating *in vivo*.

Sustained Dex release is performed from the base material of the implant (polydimethylsiloxane, PDMS) which is covered with a cell adherence reducing NCO-sP (EO-stat-PO) hydrogel. Dex-loaded, unloaded, coated and uncoated PDMS filaments were analysed using scanning electron microscopy and atomic force microscopy to determine surface topography and nano-roughness. Co-cultivation of filaments *in vitro* with cultures of eGFP-fibroblasts was analysed by light and fluorescent microscopy and quantified by cell counting.

Modification of PDMS with Dex and hydrogel changed the structure of the implant surface and resulted in a significant increase of the nano-roughness (surface irregularities, defined by height) of the surface topography compared to untreated PDMS ( $p < 0.05$ ). Highest roughness as well as microscopic cavities was found in Dex-loaded filaments. This may be due to the enclosed Dex crystals, while the crystals in coated samples are covered with hydrogel, smoothing the surface. Comparing the nano-roughness of the modified samples with each other, there was no significant difference found.

In cell culture, due to the diffusion of the released substance into the medium the number of fibroblasts in wells with Dex-loaded samples decreased by 70% compared to the unloaded. The hydrogel showed no effect on the total cell number in the well, yet about 95% fewer cells grew directly on the samples. In addition to the inhibiting effect of the steroid, the higher surface roughness seemed to affect cell growth on the samples also negatively.

## **622 Comparison of Psychoacoustical Methods Used to Estimate Peripheral Gain and Compression in the Presence and Absence of Efferent Activation**

Ifat Yasin<sup>1</sup>, Vit Drga<sup>1</sup>, **Chris Plack**<sup>2</sup>

<sup>1</sup>University College London, <sup>2</sup>The University of Manchester

Several masking paradigms have been used to estimate cochlear gain and compression, including temporal masking curves (TMCs) which compare masked thresholds for a signal in the presence of on- and off-frequency forward maskers (Nelson et al, 2001) and additivity of forward masking (AFM), which measures the

combined effect of two equally effective forward maskers (e.g., Plack & O'Hanlon, 2003).

Behavioral evidence suggests that the amount of gain applied to the basilar membrane (BM) changes during the time course of acoustic stimulation (Strickland, 2008). Physiological and oto-acoustic emission studies indicate an efferent neural pathway that reduces BM gain over time, with a minimum time period from sound onset to efferent cochlear activation of about 31-43 ms (e.g., James et al, 2002). However, TMC or AFM studies often use combined masker and signal durations greater than 50 ms. In order to use these methods to obtain accurate estimates of BM gain and compression prior to efferent activation, the combined signal and masker durations should be less than about 30 ms.

This study compared previous AFM and TMC methods that typically use long maskers (>100 ms) with a new Fixed Duration Masking Curve (FDMC) method, in which the combined masker and signal duration is fixed at 25 ms. This allows estimates of BM gain and compression that are not confounded by the efferent response. Estimates of gain were similar using FDMC and TMC methods, and negatively correlated with signal absolute threshold. Compression exponents obtained with the FDMC method were generally smaller than those obtained with the TMC method, whilst compression estimates obtained with the AFM method were more variable. Our results suggest that estimates of the BM response function with long maskers are largely unaffected by efferent activity.

Supported by EPSRC (grant EP/H022732/1)

## **623 Estimates of Inner and Outer Hair Loss from Behavioral and Otoacoustic Emission Measures**

**Enrique Lopez-Poveda**<sup>1</sup>, Peter Johannesen<sup>1</sup>

<sup>1</sup>University of Salamanca

Differentiating the relative importance of the various contributors to the audiometric loss (HLTOTAL) of a given hearing impaired listener and frequency region is becoming critical as more specific treatments are being developed. The first aim of this study was to assess the relative contribution of inner (IHC) and outer hair cell (OHC) dysfunction (HLIHC and HLOHC, respectively) to the audiometric loss of patients with mild to moderate cochlear hearing loss using combined behavioral and distortion product otoacoustic emission (DPOAE) methods. It was assumed that  $HLTOTAL = HLOHC + HLIHC$  and that HLOHC may be estimated as the reduction in maximum cochlear gain. It is argued that the latter may be safely estimated from compression threshold shifts of cochlear input/output (I/O) curves relative to normal hearing references. I/O curves were inferred behaviorally using forward masking for 26 test frequencies in 18 hearing impaired listeners. Integrated analysis of behavioral and DPOAE data suggested that 7 of the 26 cases suffered from pure OHC loss, one probably suffered from pure IHC loss, and 17 suffered from combined IHC and OHC loss (one more was uncertain). OHC and IHC loss contributed on average 65% and 35% to the total audiometric loss but

variability was large across listeners. Indeed, in some cases, HLIHC was up to 65% of HLTOTAL even for mild losses (< 30 dB HL). The second aim was to explore if HLOHC and HLIHC could be equally obtained from DPOAE I/O curves, a more useful approach in clinical contexts. Reasonable estimates could be obtained in 12 of the 26 cases only and although their trend was broadly consistent with that of behavioral estimates, correlation between DPOAE and behavioral estimates was low. Further research is necessary to design a clinical procedure for obtaining reliable individual estimates of HLOHC and HLIHC.

#### **624 Perception of Across-Frequency Asynchrony by Listeners with Cochlear Hearing Loss**

**Jordan A. Beim<sup>1</sup>**, Magdalena Wojtczak<sup>1</sup>, Andrew J. Oxenham<sup>1</sup>

<sup>1</sup>*University of Minnesota*

Judgments of the perceived timing between two tones remote in frequency by listeners with normal hearing indicate that differences in cochlear response times across frequency may be compensated at higher processing stages yielding veridical perception of the timing between the stimuli [Wojtczak et al., JASA, Pt. 2, (2011)]. Different cochlear response latencies are a result of the spectral filtering performed in the cochlea. Cochlear hearing loss is accompanied by broadening of the cochlear filters and thus may result in an alteration of the basilar-membrane response latencies across frequency. A question arises as to whether the higher-level compensating mechanism exhibits plasticity, allowing it to adjust to the changes caused by the increased filter bandwidths, or is "hard-wired" and results in an altered perception of across-frequency synchrony. Two experiments were run using listeners with cochlear hearing loss. In one experiment, a method of constant stimuli was used to obtain subjective judgments of synchrony/asynchrony between two tones in a pair. In each run, a tone pair consisted of a 250-Hz tone and a tone that was at least two octaves higher in frequency. Depending on the amount of hearing loss in the high-frequency region, the higher-frequency tone was selected from a subset or a full set of frequencies of 1, 2, 4, and 6 kHz. The tones were 40 ms long and were presented at 85 dB SPL or 20 dB SL, whichever was higher. In the second experiment the same tone pairs were used to measure asynchrony detection and discrimination thresholds using an adaptive three-alternative forced-choice procedure. Some but not all the hearing-impaired listeners showed patterns of results that differed markedly from those observed in listeners with normal hearing, suggesting that an altered perception of across-frequency timing may contribute to the difficulties the hearing-impaired experience. [Supported by NIH grant R01 DC010374].

#### **625 Psychoacoustical Characterization of the Effects of Medial Olivocochlear Reflex Activation on Apical and Basal Cochlear Nonlinearity**

**Enzo Aguilar<sup>1</sup>**, Peter T. Johannesen<sup>1</sup>, Almudena Eustaquio-Martin<sup>1</sup>, Enrique A. Lopez-Poveda<sup>1</sup>

<sup>1</sup>*University of Salamanca*

The aim was to characterize the effects of medial olivocochlear reflex activation on apical and basal cochlear nonlinearity. Cochlear input/output curves (IOCs) were inferred psychoacoustically using the temporal masking curve (TMC) method. Probe frequencies (fp) were 500 and 4000 Hz. Masker frequencies (fm) ranged from 0.4 to 1.25 times the probe frequency. Cochlear IOCs were inferred by plotting the level of the linear reference TMC (fm=1600 Hz, fp=4000 Hz) against the masker levels for any other masker. The MOCR was activated with a 60-dB SPL continuous contralateral broadband noise (CN condition). For some subjects, but not all, different probe detection thresholds were obtained for the CN and control conditions. In any case, probe level was set 10 dB above the probe detection threshold in each condition to achieve a constant internal probe excitation across conditions. The slope of the linear reference TMC was comparable for the control and CN conditions, suggesting that the MOCR did not alter the time course of recovery from forward masking per se. In general, on-frequency IOCs were consistent with the CN reducing cochlear gain for low and moderate input levels but the presence and amount of the effect varied across listeners. Interestingly, some IOCs were consistent with the MOCR increasing cochlear responses for stimulus frequencies above the characteristic frequency and for moderate levels. The present results are analyzed and discussed in relation to previously reported physiological cochlear responses.

#### **626 The Effect of Masker Frequency and Level on Cochlear Gain Reduction and Related Learning Effects**

**Kristina DeRoy<sup>1</sup>**, Elizabeth Strickland<sup>1</sup>

<sup>1</sup>*Purdue University*

Previous psychophysical studies in this laboratory are consistent with the hypothesis that forward masking is driven by two mechanisms, excitatory masking and gain reduction. Excitatory masking has been modeled as operating over approximately 20 ms following a masker, while gain reduction has been modeled as operating over longer delays. A likely physiological basis for gain reduction is the medial olivocochlear reflex (MOCR). By measuring masked thresholds at longer delays, gain reduction may be estimated. In the present experiment, gain reduction for varying masker levels was systematically studied. To measure gain reduction, a 6-ms signal was presented 20 ms after the offset of a 50-ms masker. Gain change was estimated for a range of masker levels by subtracting quiet threshold from the masked threshold. The signal was set at 4 kHz and the masker was either on-frequency (4 kHz) or off-frequency (2.4 kHz). The off-frequency masker should have a linear

response at the signal place, removing the effects of compression and thus revealing the rate of gain reduction with level. Differences in growth of signal threshold with masker level for the on- and off-frequency maskers will be discussed. In addition, learning effects will be examined for tasks where gain change is thought to be occurring and similar tasks where gain change is thought to be absent. Because gain reduction may be under some attentional control, it is hypothesized that more long-term learning effects will be seen in gain reduction conditions.

[Research Supported by a Grant from NIH(NIDCD) R01 DC008327]

### **627 Abnormal Loudness Adaptation in Temperature Sensitive Auditory Neuropathy Implies Otoferlin's Role in Sustained Neurotransmitter Transduction**

Dwight Wynne<sup>1</sup>, Arnold Starr<sup>2</sup>, Fan-Gang Zeng<sup>1</sup>

<sup>1</sup>Department of Biomedical Engineering, University of California, Irvine, <sup>2</sup>Department of Neurology, University of California, Irvine

Auditory neuropathy (AN) encompasses disorders of the inner hair cells, the auditory nerve, and/or the synapse between them. A subpopulation of these AN listeners have a temperature-dependent hearing loss resulting from a mutation in the OTOF gene, which codes for the protein otoferlin. We previously showed that these listeners exhibited abnormal loudness adaptation to three-minute tones presented at a comfortable level. The present study extends these findings. We presented tones at 250 Hz and 8000 Hz, band-passed noise octave-centered at those frequencies, and white noise to three temperature-sensitive listeners at subjectively soft (~5 dB SL), comfortable (~25 dB SL), and loud levels. All stimuli were 185 seconds in length, with listeners asked to estimate the subjective loudness of the stimulus every 30 seconds starting at onset. We found significant adaptation to all stimuli regardless of stimulus type, frequency, or level. However, softer stimuli elicited more rapid adaptation than louder stimuli, and high-frequency stimuli elicited more rapid adaptation than low-frequency stimuli for a given level and stimulus type. These results suggest that the abnormal loudness adaptation we initially observed to tones is reflective of a disorder affecting the sustained release of neurotransmitter, which may be caused by impaired replenishment of the readily releasable pool.

### **628 Perception of Concurrent Melodies and Harmonic Resolvability in Normal and Impaired Hearing**

Christophe Micheyl<sup>1</sup>, Heather Krefl<sup>1</sup>, Claire Ryan<sup>1</sup>, Adam Loper<sup>1</sup>, Andrew Oxenham<sup>1</sup>

<sup>1</sup>University of Minnesota

Hearing-impaired listeners often report that their loss negatively impacts their enjoyment of music. The mechanisms that lead from cochlear damage to reduced music appreciation are not well understood. One hypothesis is that reduced cochlear frequency selectivity leads to poorer pitch perception for complex tones

presented in isolation, concurrently (as in a chord), and/or sequentially (as in a melody). To test this hypothesis, we measured fundamental-frequency (F0) discrimination thresholds for isolated and concurrent harmonic tones in hearing-impaired (HI) and normal-hearing (NH) listeners. We also measured the lowest F0 at which listeners were reliably able to discriminate two target "melodies" (pseudo-random four-note sequences) that were presented either in isolation or concurrently with synchronous masker tones. The masker tones had a constant F0 which, depending on the condition, fell either in the same F0 range as that of the target tones or 7 semitones below or above that range. The target and masker tones were filtered into the same frequency region (800-2200 Hz), so that their spectra overlapped completely, and the masker tones were presented either with the first or second target melody. Pure-tone detection thresholds and measures of frequency selectivity (using notched-noise masking and spectral ripple discrimination paradigms) were obtained in the same listeners. The measures were correlated with the pitch and melody-discrimination performance to determine the extent to which the effect of hearing impairment on listeners' ability to perceive variations in the pitch of isolated or concurrent complex tones is associated with reduced frequency selectivity attributable to cochlear damage. The results indicate that resolvability can explain some, but not all, aspects of hearing-loss-related impairments in the perception of the pitch of single, concurrent, and sequential sounds [Work supported by R01 DC 05216; Starkey USA helped with subject recruitment.]

### **629 Detecting a Phase Shift in a Single Component of a Harmonic Complex**

Astrid Klinge<sup>1</sup>, Timo Parnitzke<sup>1</sup>, Georg Klump<sup>1</sup>

<sup>1</sup>University of Oldenburg

Harmonicity is an important simultaneous grouping cue binding frequency components that are integer multiples of a fundamental frequency and separating them from frequency components that do not belong to the harmonic series. A previous study showed that Mongolian gerbils (*Meriones unguiculatus*) are highly sensitive to frequency shifts in a component of a harmonic complex with mistuning detection thresholds of as low as 0.008% Weber fraction for the 32nd component of a 200 Hz complex (Klinge & Klump, 2010). It was suggested that the phase shift that gradually develops between the mistuned and the remaining components is being used as the cue for detection. In order to investigate if this mechanism may provide an explanation of the observed sensitivity we measured the gerbils' threshold for detecting a constant phase shift in a component of a harmonic complex that is introduced without a frequency shift.

Gerbils were trained in an operant Go/NoGo procedure with food rewards to report the phase shift. We determined detection thresholds for the phase shift of the 2nd and 32nd harmonic of a 200Hz-complex comprised of the first 48 harmonics and stimulus durations of 400, 100, and 50 ms. All components (except the target component) started in sine phase. Gerbils were able to detect a phase shift in both the low and the high frequency component of a

harmonic complex. Detection thresholds were considerably lower for the 32nd harmonic (15-29 deg) than for the 2nd harmonic (62-122 deg) and tended to increase with decreasing stimulus duration (except for the 50 ms condition in the 2nd component). The thresholds for detecting "static" phase shifts were similar to the "gradual" phase shift thresholds calculated for mistuning the 2nd harmonic, but they were considerably lower than the "gradual" phase shift thresholds calculated for the 32nd harmonic. The results suggest that the "gradual" phase shifts may provide the cue for mistuning detection. Supported by the DFG (SFB/TRR 31)

### **630 The Time Course of Auditory Perceptual Organization of Unresolved Complex Tones Changes with Age**

**Graham Raynor**<sup>1</sup>, Ingrid Johnsrude<sup>1,2</sup>, Robert Carlyon<sup>3</sup>  
<sup>1</sup>Queen's University, <sup>2</sup>Linköping University, <sup>3</sup>MRC Cognition & Brain Sciences Unit

It has been reported that stream segregation of repeating ABA\_ triplets, where A and B are pure tones of different frequency, is reduced in older, compared to younger, listeners. This finding has been attributed to decreased frequency selectivity in older people (Grimault et al, 2001). Here, we examine whether age-related differences in stream segregation are still observed when the A and B tones are filtered harmonic complexes (A: F0 = 80Hz, B: F0 = 113Hz; "Small dF0" or 127Hz; "Large dF0") that are unresolved by the peripheral auditory system in both younger (18-25) and older (55+) normally hearing adults. Participants attempted to detect temporal irregularities (at 2, 4, 6, or 8 sec) in 10-sec ABA sequences. This task is easiest when the percept is of a single, integrated stream: accuracy thus objectively measures perception (Thompson, et al, 2011). Sequences were presented either continuously, or with 5-second gaps between trials. Mixed-design ANOVA revealed the predicted effect of dF0, and build-up in stream segregation over time. Performance was better in the Gap than in the Continuous condition, consistent with the gaps causing resetting to an integrated percept (Cusack, et al, 2004). With the large dF0, at the later time points (6s and 8s), younger adults performed poorly in both the Gap and Continuous conditions, whereas the older adults performed better after gaps than during the continuous condition, suggesting a delay in segregation. With the small dF0, older adults performed significantly better in both conditions than did younger adults, consistent with diminished segregation overall. Thus, even when differences in peripheral resolvability are controlled, older adults show less segregation than younger people, at least for small dF0. The influence of age-related changes in attentional control on stream segregation is being explored by adding a 3rd condition involving a distracting auditory task during intervals between trials. Funding: CIHR.

### **631 Complex Pitch Perception at High Frequencies: Is the Whole More Than the Sum of the Parts?**

**Andrew Oxenham**<sup>1</sup>, Christophe Micheyl<sup>1</sup>, Adam Loper<sup>1</sup>  
<sup>1</sup>University of Minnesota

A recent study showed that listeners were able to hear the fundamental frequency (F0) of, and discriminate melodies with, harmonic complex tones that consisted only of components above 6 kHz, even when distortion products were masked and the pitch was not conveyed by temporal envelope cues (Oxenham et al., 2011, Proc. Natl. Acad. Sci. 108, 7629-34). This result leads to an interesting dissociation: pure tones above 6 kHz do not convey melodic pitch information, whereas those same tones, when combined within a harmonic complex tone, do. Here we pursued this finding by measuring frequency difference limens (DLs) for pure tones alone and combined within a complex tone. We compared the DLs of the complex tones with those predicted by an optimal-observer model. Very different findings emerged at low and high frequencies. At low frequencies (< 4 kHz), in line with previous studies, listeners' F0DLs for complex tones were not as good as predicted by an optimal combination of information from the individual components presented in isolation. At high frequencies (> 7 kHz), however, F0DLs for complex tones were often at least as good as predicted by an optimal combination of information from the individual tones. Various interpretations are explored. One is that performance at low frequencies is limited by a "central" noise, occurring after the combination of information from the individual pure tones, whereas performance at high frequencies is limited by peripheral noise. Another is that performance at all frequencies is limited by a central representation of the F0 or pitch of the sound, rather than frequency, and that this representation degrades at high F0s. Overall, the results provide us with further insights into the coding of frequency and F0, and suggest that internal representations of these sensory attributes vary across the tonotopic axis in ways that are not captured by current models and theories of pitch. [Work supported by NIH grant R01 DC 05216.]

### **632 Temporal Fine Structure Sensitivity and Frequency Selectivity: Effect of Sound Level on the Detection of Frequency-Shifted Harmonics**

**Frederic Marmel**<sup>1</sup>, Christopher Plack<sup>1</sup>, Robert Carlyon<sup>2</sup>, Hedwig Gockel<sup>2</sup>, Brian Moore<sup>3</sup>

<sup>1</sup>Human Communication and Deafness Division, The University of Manchester, Manchester M13 9PL, UK, <sup>2</sup>MRC Cognition and Brain Sciences Unit, Cambridge CB2 7EF, UK, <sup>3</sup>Department of Experimental Psychology, University of Cambridge, Cambridge, UK

There is evidence that listeners with cochlear hearing loss (CHL) perform poorly on tasks designed to measure temporal fine structure (TFS) processing. This impairment could be explained by multiple factors ranging from a phase locking deficit to a reduction in frequency selectivity (Moore, 2008). We investigated whether a reduction in

frequency selectivity leads to an impairment on the TFS task of Hopkins and Moore (2007), which requires participants to discriminate a bandpass-filtered harmonic complex tone from one in which all harmonics are shifted upwards by the same amount in Hz. If the harmonics are unresolved, performance should depend on TFS cues.

We exploited the fact that frequency selectivity reduces at high levels and presented complex tones at a constant sensation level in threshold-equalizing noise set to a low (20 dB/ERBN) or a high (60 dB/ERBN) sound level. The complex tones had fundamental frequencies ranging from 60 to 625 Hz and were bandpass filtered around the 11th harmonic. Frequency shifts at threshold increased with level, consistent with performance being influenced by frequency selectivity. Further testing using intermediate sound levels showed that the level effect appeared only at the highest level, which is consistent with the results of Moore and Sek (2009, 2011), who used a lower range of levels and found no level effect. Finally, we measured the level effect on excitation patterns by forward masking a pure tone with the complex tone of the TFS task. Shifting the frequency of the harmonics influenced masking at a low but not at a high level, confirming the reduction in frequency selectivity at the higher level. Our results suggest that a reduction in frequency selectivity may contribute to the impaired performance of CHL listeners on this TFS task. However, it does not seem to be the only factor as performance in the TFS task at the high level was still above chance, despite the lack of evidence for resolved components.

### **633 Perceptual Learning for Temporal Fine Structure of Sounds: Do Pitch Discrimination and Sound Localization Share Common Modules?**

Shiho Washizawa<sup>1</sup>, Shigeto Furukawa<sup>2</sup>, Makio Kashino<sup>1,2</sup>

<sup>1</sup>*Interdisciplinary Graduate School of Science and Engineering, Tokyo Institute of Technology,* <sup>2</sup>*NTT Communication Science Laboratories*

Perceptual learning refers to a form of implicit learning by which repeated sensory experience leads to long-lasting alterations in perception. If different perceptual tasks are performed using common processing modules, training in one task could improve efficiencies of the common modules, thereby improving the performance not only of the trained task, but also of the other task. This study was concerned about hypothetical modules for processing temporal fine structure (TFS) of acoustical signals, which is encoded as the neural phase locking at the auditory periphery. We examined whether training and improvement in pitch discrimination task based on TFS (TFS-pitch task) result in improvement in untrained binaural lateralization task based on interaural time difference (ITD) in TFS (i.e., ongoing ITD; TFS-ITD task). The stimulus was bandpass-filtered harmonic complex (F0 = 100 Hz; 8th to 14th harmonics; Moore and Moore, 2003, JASA). In the TFS-pitch task, the listener was asked to discriminate between the harmonic complex and that with individual components shifted in frequency by a common amount (Hopkins and Moore, 2007, JASA). The TFS-ITD

task was to discriminate the stimuli that differed in ongoing ITD. Additional tasks, such as discrimination of envelope ITD, interaural level difference (ILD), and intensity, were employed as untrained control tasks. After training in TFS-pitch task for 12 days, performance of the task improved significantly. However, we did not observe significant improvement in untrained TFS-ITD and the control tasks. The results imply that the processes for pitch and for localization based on TFS do not share common modules, or that the learning effect do not take place in the common modules, if they exist.

### **634 When and How Monaural Envelope Rate-Limitations Affect Processing of Interaural Temporal Disparities in Binaural Detection and Lateralization**

Leslie Bernstein<sup>1</sup>, Constantine Trahiotis<sup>1</sup>

<sup>1</sup>*UConn Health Center*

The purpose of this presentation is to bring together historical and current findings that reveal the presence, influence, and operation of a certain type of “rate limitation” that constrains the processing of interaural temporal disparities (ITDs) conveyed by high-frequency stimuli. Specifically, there appears to be a monaural process that functionally acts as a low-pass “envelope filter,” the output of which serves as input to more central stages of processing. The low-pass filtering appears to attenuate fluctuations of the envelope above about 150 Hz and is not attributable to the width of initial, peripheral bandpass filtering. We show converging empirical evidence and theoretical analyses that demonstrate and describe when and to what degree the rate-limitation affects the processing of ITDs conveyed by a variety of types of stimuli in experimental contexts concerning binaural detection and lateralization. Included are recent findings concerning a potential neurophysiological correlate of the rate-limitation, how it may vary with the center-frequency of the stimulus, and, perhaps surprisingly, conditions under which listeners may employ a strategy of utilizing information in “off-frequency” filters in order to overcome deleterious effects of the rate-limitation in ITD discrimination and lateralization tasks. [Work supported by research grant NIH DC-04147 from the National Institute on Deafness and Other Communication Disorders, National Institutes of Health]

### **635 Relationships Among Aging and Temporal Sensitivity at Multiple Time Scales**

Frederick J. Gallun<sup>1</sup>, Dawn L. Konrad-Martin<sup>1</sup>, Michelle R. Molis<sup>1</sup>, Serena Dann<sup>1</sup>, Sean D. Kempel<sup>1</sup>, Jay J. Vachhani<sup>1</sup>

<sup>1</sup>*National Center for Rehabilitative Auditory Research, Portland VA Medical Center*

Temporal analysis of auditory information occurs at multiple time scales in the auditory system, from comparisons of interaural differences in time of arrival, which differ by tens to hundreds of microseconds, to burst onset times in speech, which differ by tens of milliseconds. How such sensitivity may become impaired with age is not yet clearly understood, but the impacts are potentially very

serious for the understanding of speech and analysis of the auditory scene. Younger and older subjects with relatively similar audiograms were tested on three measures of temporal sensitivity, each requiring successively longer time differences for similar performance: binaural discrimination of interaural differences in time of onset, monaural detection of gaps between stimuli, and bilateral detection of gaps between stimuli. Each measure was examined using both click stimuli and rising-frequency chirps. Clicks and chirps had similar spectral profiles, but the chirps were designed to produce relatively synchronous patterns of maximum activation across the basilar membrane. Data will be presented showing the degree to which an age-related decline in temporal sensitivity occurred for all three tasks with both stimulus types, and examining whether or not performance on the various measures and stimuli are statistically related. The relative independence of the measures, as well as each of their relationships with aging, addresses the hypothesis that separate mechanisms exist at the various time scales, as well as within and between ears, and that each could be independently impacted by aging. Differential effects of the chirp and click stimuli address the hypothesis that older listeners benefit less from synchronous activity on the auditory nerve than do younger listeners. (Supported by VA RR&D: Merit Award C7450R; CDA C4963W; CDTA C7113N; CDA C6116W)

### **636 Temporal Cues and Modulation Rate Interplay with Attention to Detect a Target Sound Embedded in Background Noise**

Sahar Akram<sup>1</sup>, Jonathan Z. Simon<sup>2</sup>, Mounya Elhilali<sup>3</sup>, Bernhard Englitz<sup>1</sup>, Shihab Shamma<sup>1</sup>

<sup>1</sup>Institute for System Research, University of Maryland, College park, Maryland 20742, <sup>2</sup>Department of Electrical and Computer Eng., University of Maryland, College park, Maryland 20740, <sup>3</sup>Department of Electrical and Computer Eng., Johns Hopkins University, Baltimore, Maryland 21218

Parsing a complex auditory scene into different objects is easily accomplished by humans, but the underlying mechanisms are not well understood. Perceptual cues need to be extracted in an interplay of bottom-up saliency and top-down attentional modulation.

We investigate this problem focusing on temporal cues and modulation rates using human psychophysical and magnetoencephalographic (MEG) data. The participant's attention is drawn to different features of the auditory scene, composed of a rhythmic (7 Hz), regular target buried in a random, irregular background. The investigation is meant to complement an earlier study using a 4 Hz rhythm, given the low-pass sensitivity of neurons to tone repetition rates, and also the different brain rhythm classes for 4 Hz (theta) and 7 Hz (alpha).

The experimental results reveal an increase in the neural response to the attended target compared to unattended task for the 7 Hz rate target, in both power and phase coherence, similar to the previous results obtained for the 4 Hz target. However, the strength of the response was lower compared to the 4 Hz rate, as predicted by the low-

pass Modulation Transfer Functions (MTFs) of auditory neurons. There was no significant neural build-up effect correlated with behavioral detectability of 7 Hz target over time, in contrast to the significant build-up seen in the 4 Hz case, both behaviorally and neurally, but in agreement with earlier work directly comparing 4 Hz and 7 Hz rhythmic streams. Brain activity was not significantly lateralized when comparing attended vs. unattended task for 7 Hz target rate, in contrast to a significant right lateralization was shown in the 4 Hz condition.

The findings illuminate the interaction between attended temporal features and known temporal modulation tuning in auditory cortex and provide some cues for auditory object formation.

### **637 Effect of Timing on Perceptual Continuity of Streams**

Golbarg Mehraei<sup>1</sup>, Adrian KC Lee<sup>2</sup>, Scott Bressler<sup>3</sup>, Barbara Shinn-Cunningham<sup>3,4</sup>

<sup>1</sup>Speech and Hearing Bioscience and Technology program Harvard-MIT, <sup>2</sup>Speech and Hearing Sciences, University of Washington, <sup>3</sup>Hearing Research Center, Boston University, <sup>4</sup>Department of Cognitive and Neural Systems, Boston University

A desired sound stream is typically picked out of a scene by directing attention to a known feature of that stream, such as its location, pitch, or (for speech) talker identity. Past studies show that perceptual continuity of a task-irrelevant feature enhances the ability to selectively attend to a stream of target words; for instance, continuity of speaker identity improves the ability to selectively attend to words from a given direction. The current study manipulated the inter-word delay (IWD) in competing sound streams to test whether the influence of continuity of an irrelevant feature weakens as the IWD increases.

A sequence of three pairs of simultaneous digits (values 1 to 4) was presented. Within each simultaneous digit pair, one digit was spoken by a male talker and one spoken by a female talker, each simulated as being spoken from the left or right of the listener. Listeners were instructed to report the digits based either on location (left or right) or talker gender (male or female). On half the trials, the same talker spoke all digits from one direction, while in the other trials, the middle digit from a particular location switched talker identity (pitting the continuity of the task-relevant feature against the continuity of the task-irrelevant feature). IWDs of 0, 100, and 600ms were tested.

Overall, performance was better when location and identity worked in concert than when they were in opposition (switch condition). While performance on the first and last digits was generally strong, in the switch condition, performance on the middle digit was worse, revealing the influence of the task-irrelevant cue. In addition, performance on switch trials depended on the feature listeners were told to attend; interestingly, which cue lead to better performance varied from subject to subject. Finally, as hypothesized, even a brief IWD (100ms) reduced the effect of the task-irrelevant cue.

### **638 Comparisons Between Young and Elderly Listeners in the Performances of Basic Auditory Tasks That Rely on Temporal Fine Structure Information**

**Atsushi Ochi**<sup>1,2</sup>, Tatsuya Yamasoba<sup>2</sup>, Shigeto Furukawa<sup>1</sup>  
<sup>1</sup>*NTT Communication Sci. Labs*, <sup>2</sup>*Univ. of Tokyo*

Efficiencies of temporal processing are generally known to deteriorate with age. This study focused on processing of temporal fine structure (TFS), and examined the effects of aging on basic auditory abilities that rely on TFS information, which is encoded by the phase locking of the auditory nerve. Three classes of listeners were tested: young (20s to 30s) normal hearing (YNH), elderly (60s) with clinically almost normal hearing (ENH), and elderly with mild hearing loss (EHL). The experiments consisted of seven types of tasks: binaural lateralization based on (1) interaural time difference (ITD task) and on (2) interaural level difference; pitch discrimination using (3) the "frequency-shifted harmonic complexes" [Moore and Moore, *JASA*. 113, 977-85 (2003)], for which TFS is considered to be the reliable cue (TFS-pitch task), (4) 1100 Hz tone, for which both "place" and "temporal" cues are available (Tone-pitch task), and (5) the "Huggins' pitch" stimuli [Cramer and Huggins, *JASA*. 30,413-7 (1958)], for which the interaural difference in phase or TFS is the available cue (Huggins-pitch task); (6) intensity discrimination task; and (7) detection of 1100 Hz tone in the notched noise with varying notch widths [Patterson, *JASA*. 59, 640-654 (1976)], through which auditory filter bandwidth was derived. Of these seven tasks, TFS-pitch and Huggins-pitch tasks showed significantly higher thresholds for ENH and EHL than for YNH, indicating age effects, but showed no significant differences between ENH and EHL, suggesting little or no effect of hearing loss. The other tasks, including ITD and Tone-pitch tasks, showed no significant differences among the listener groups. The two tasks with significant aging effects are common in that the both rely on TFS information and involve pitch judgments. The results could be interpreted as indicating that a mechanism responsible for pitch processing based on TFS is particularly susceptible to aging.

### **639 Gap Detection and Noise Fluctuation in Normal and Impaired Hearing**

**Joseph Hall**<sup>1</sup>, Emily Buss<sup>1</sup>, Erol Ozmeral<sup>1</sup>, John Grose<sup>1</sup>  
<sup>1</sup>*University of North Carolina at Chapel Hill*

This study investigated temporal gap detection in adults with normal hearing and with sensorineural hearing impairment. In addition to providing information about the ability to process the temporal envelope of a sound, the approach was intended to offer insights about how reduced frequency selectivity in hearing-impaired listeners might affect the temporal cues that underlie performance. We measured gap detection for noise carriers having bandwidths of 50, 100, 200, and 400 Hz at a center frequency of 500 Hz and bandwidths of 50 and 400 Hz at a center frequency of 4000 Hz. Carriers were either a Gaussian noise or a low-fluctuation noise having a relatively flat temporal envelope. Whereas performance was expected to improve with increasing bandwidth for Gaussian noise, the expectation was that gap detection would worsen with increasing bandwidth of the low-fluctuation noise. This is because the frequency selective nature of the peripheral auditory system would begin to introduce envelope modulations when the low-fluctuation noise bandwidth approached and exceeded the auditory filter bandwidth. Such modulations were expected to interfere with the ability of the listener to perceive the externally imposed gap. Of interest was whether this effect might be shifted to wider stimulus bandwidths in hearing-impaired listeners, where the auditory filter bandwidth was expected to be relatively wide. Some trends in the data were consistent with this expectation.

### **640 Binaural Speech Localization with Adaptable Gammatone Filters**

**Tom Goeckel**<sup>1</sup>, Michael Wolf<sup>1</sup>, Mohamad Abbas<sup>1</sup>, Hermann Wagner<sup>1</sup>, Gerhard Lakemeyer<sup>1</sup>  
<sup>1</sup>*RWTH Aachen University*

Binaural speech source localization gives a mobile service robot the ability to locate and focus on a single person in an acoustically cluttered environment. We extended our existing sound localization algorithm, which relies on interaural time differences (ITD), with a speech detection algorithm and an adaptable gammatone filterbank specialized on the detection and localization of speech signals. The signal is recorded at two microphones, that are spaced at 20.5cm, and gets subdivided into time frames of 25ms. The signal detector measures the entropy in the spectrum and the signal energy to decide whether it contains a potentially interesting sound source, otherwise the time frame will be ignored. A spectral analysis tries to determine the base frequency and cepstrum of a possible speech signal. If successful, these informations are both used to adapt the filter parameters of the filterbank and to weight the 48 narrow frequency bands during the across-frequency integration of the ITD cues. Other parts of the frequency spectrum are covered by broader filters and are assigned a lower weight. To improve performance, the ITD cues of each of the narrow bands are extracted in parallel on a graphics processing unit using the CUDA API by Nvidia. The localization maps of each frequency band are

weighted and integrated to yield the final map. The local maxima of this map correspond to the position estimates of the current time frame which are interpolated across time to form the output of our system.

The system has been tested with one and two speakers at different positions and with different degrees of background noise.

### **641 Spatial Release from Energetic and Informational Masking Evaluated Using Non-Speech Free-Field Stimuli**

Peter Bremen<sup>1</sup>, John C Middlebrooks<sup>1</sup>

<sup>1</sup>*Department of Otolaryngology, University of California Irvine*

The auditory system creates an internal neuronal representation of the acoustic world based on binaural and spectrotemporal cues present at the listener's ears. This process is especially challenging when multiple sound sources are present. The current study is part of an effort to better understand the neuronal mechanisms governing this process, which has been termed auditory scene analysis. We investigated the influence of spatial, spectral, and temporal cues on detection of a signal in the presence of a masker. Although the present study tested human listeners, we evaluated non-speech stimuli that eventually could be applied to animal psychophysical and physiological procedures.

We measured thresholds for detection of a pure tone signal in the presence of a multi-tone masker complex, using 2-alternative forced choice. Maskers consisted of multiple tone pips and were similar to the multiple burst same (MBS) and multiple burst different (MBD) stimuli used in the informational masking literature (e.g. Kidd et al. 1994). Signal and masker could be gated on synchronously or asynchronously. For so-called energetic maskers, all frequencies were drawn from a band  $\pm 1/3$  of an octave wide centered at the signal frequency and therefore overlapped with the critical band of the auditory filter containing the signal frequency. In contrast, for so-called informational maskers, masker frequencies occupied a broad range that excluded the signal band. We tested several spatial configurations of signal and masker presented in a free field.

In conditions of energetic masking, spatial release from masking was minimal and could be explained by physical acoustics and peripheral filter mechanisms. Informational masking, however, showed spatial release as large as ~50 dB, consistent with previous results using headphone and speech stimuli. We are optimistic that this stimulus paradigm will lend itself to animal studies of the neural substrates of auditory scene analysis.

### **642 Differential Emergence of Sound Localization Abilities in Bilaterally Implanted and Hearing Toddlers**

Erica Ehlers<sup>1</sup>, Christi Hess<sup>1</sup>, Ruth Litovsky<sup>1</sup>

<sup>1</sup>*UW-Madison*

In recent years there has been an increase in the number of children receiving bilateral cochlear implants (BiCI).

Previous findings from our lab suggest that sound localization abilities in children with BiCIs are better when in the bilateral listening mode compared with the unilateral mode. However, children ages 5-14 perform significantly worse than their normal-hearing peers. Additionally in toddlers, head turns and eye gaze were used as measures of perceived location. Some toddlers were able to discriminate left versus right with high accuracy while others were unable to perform the task at all.

The current study was conducted using a novel "Reaching for Sound" (RFS) approach that enabled us to measure discrimination and localization as well as produce reliable results from all tested children. Children were trained to reach for sounding objects hidden behind a curtain. Toddlers with BiCIs, (n=6, 27-42 mo.), were tested in both BiCI mode and unilateral mode. Their data were compared to chronologically age-matched children (n=15) with normal hearing (NH). The testing apparatus was a semi-circular table with nine holes, spaced 15° apart from -60° to 60°. The stimulus consisted of the carrier phrase "When I hide I say" followed by three bursts of white noise. Novel results in 15 NH toddlers showed highly developed localization abilities (average RMS of 15.34). Preliminary results also indicated that toddlers who use BiCIs could discriminate left versus right for locations as small as  $\pm 15^\circ$  when in bilateral mode, but performed significantly worse in the unilateral mode. When localizing, RMS errors for the 15 NH children ranged from 2.89 to 37.5 degrees, while errors for the BiCI group ranged from 37.17 to 52.39 degrees. Results show that the RFS method has proved to be a successful paradigm to test young children. While the NH listeners performed highly on the sound localization task, it appears that this skill is still developing in BiCI toddlers.

Work supported by NIH-NIDCD grant R01 DC 008365 (Litovsky)

### **643 Adaptive Control of the Sonar Beam Pattern by the Echolocating Bat, *Eptesicus Fuscus***

Lakshmi Krishnan<sup>1,2</sup>, Melville Wohlgenuth<sup>1,3</sup>, Cynthia Moss<sup>1,4</sup>

<sup>1</sup>*University of Maryland, College Park*, <sup>2</sup>*Department of Electrical and Computer Engineering, Inst. for Systems Research*, <sup>3</sup>*Inst. for Systems Research*, <sup>4</sup>*Neuroscience and Cognitive Science Program, Inst. for Systems Research*

Echolocating bats face the complex task of decoding information from returning sonar echoes and adjusting subsequent sonar call parameters in response to these echo returns. Previous research has examined how the amplitude, direction and delay of returning echoes influence the spectral-temporal features of sonar calls, but adaptive changes in the sonar beam pattern have not yet been measured in bats tracking multiple objects in space. The purpose of this project is to understand the spatial modulations in the bat's sonar beam pattern that may aid in tracking prey amongst various sources of acoustic interference.

We trained echolocating big brown bats, *Eptesicus fuscus*, to rest on a platform and track a tethered insect approaching at different speeds, in an open environment and in the presence of a distractor. The bat's FM vocalizations were recorded with a 30-channel wideband ultrasonic microphone array (20-100 kHz) that allows for the reconstruction of the sonar beam pattern. Preliminary analysis of single microphone recordings of the bat's sonar calls suggests that it modifies the spectro-temporal parameters of its sonar call structure when a distractor is present. In the presence of a single distractor, the calls are higher in amplitude when the insect is behind the distractor, and weaker when the insect is closer to the bat than the distractor. The slope of the FM signal is also modulated in the presence of a distractor. The microphone array data will yield important information about adaptive spatial modulations in sonar calls, and clarify whether modulations in signal structure in the presence of distractors are due predominantly to changes in the directional characteristics of the sonar beam, fine time and frequency domain changes in the sonar calls, or both. The results of this study will help us understand how the bat shapes the echo information it receives from its environment, and how it may use this information to analyze a complex acoustic scene.

#### **644 Measurement of Controlling Directivity of Echolocation Pulse in Japanese Horseshoe Bats During Intercepting a Fluttering Moth**

Naohiro Matsuta<sup>1</sup>, Shizuko Hiryu<sup>2,3</sup>, Hiroshi Riquimaroux<sup>2,3</sup>, Yoshiaki Watanabe<sup>2,3</sup>

<sup>1</sup>Graduate School of Engineering, Doshisha University,

<sup>2</sup>Faculty of Life and Medical Sciences, Doshisha University, <sup>3</sup>Neurosensing and Bionavigation Research Center

If direction of echolocation pulse is defined as the direction of bat's attention, beam width can be considered as the spatial window that the bat can perceive environmental information. By using 31 ch microphone array system (17 ch: horizontal plane, 17 ch: vertical plane, 3 ch: both planes), we measured both direction and beam width of pulses emitted by CF-FM bats (*Rhinolophus ferrumequinum Nippon*, CF2 frequency: approximately 70 kHz) during aerial approaching to a fluttering moth in a chamber (8 m × 3 m × 2 m). Echolocation pulses were also precisely recorded by an onboard telemetry microphone (Telemike) mounted on the flying bat, which was synchronously monitored with measurement of bat's flight path by using high-speed video camera. When the bat approached the moth within approximately 1 m (terminal phase), the bat was found to expand beam width (half-amplitude angle) of FM component of echolocation pulse from approximately ± 20 - 30° up to ± 45° horizontally, and from approximately ± 10 - 20° up to ± 40° vertically. The bandwidth of the FM component with broaden beam width was 13 ± 3 kHz, which was not different from that of pulses emitted during approach phase (12 ± 3 kHz). Although we need further investigation to clarify how the bat expanded beam width, our findings suggest that the bat may not

change beam width by broadening bandwidth of sound, but employs some mechanisms to modify beam width, such as changing structure of noseleaf. When the bat approached the moth within approximately 1 m, some of moths exhibited evasive flight maneuver. Our results demonstrated that measured beam width was always larger than angle  $\Delta\theta$  between target and pulse directions, where  $\Delta\theta$  was considered to increase with decrement of distance between bat and moth. We suggest that the bats adjusted beam width to retain moving target in spatial window of echolocation at final stage of capturing. [Research supported by JSPS and ONR grant]

#### **645 The Effects of Masking Noise on Open and Closed Loop Sound Localization Performance in Cope's Gray Treefrog (*Hyla Chrysoscelis*)**

Michael Caldwell<sup>1</sup>, Mark Bee<sup>1</sup>

<sup>1</sup>University of Minnesota

At breeding choruses, female frogs must assess and locate a calling mate among a background of competing sounds from other signalers and abiotic sources. In many ways, this task is analogous to the human 'cocktail party problem', where a partygoer struggles to follow the speech of a single interlocutor among many noisy guests. In masking noise, many animals show increased response thresholds and poorer performance in sound discrimination tasks, which potentially result in increased exposure to predators, increased energy expenditure, and selection of low-quality mates. It is often suggested that these effects are due, in part, to impaired sound localization in noise. While studies of human subjects demonstrate clear effects of masking noise on sound localization abilities, we know much less about how noise affects source localization in non-human (specifically, non-mammalian) animal models. Here, we report results from a study of source localization in frogs. In contrast to mammals, most frogs have ears that are coupled through wide and permanently open Eustachian tubes, making them inherently directional pressure-difference receivers. Using behavioral phonotaxis tests, we investigated the effects of masking noise on the localization of male mating calls by female gray treefrogs in both open loop and closed loop listening conditions. Open loop conditions assessed localization acuity; closed loop conditions examined the frog's ability to use behavioral tactics to hone in on a sound source or to improve localization by integrating information over time. By studying constraints faced by frogs localizing sounds in a complex acoustic environment, as well as adaptations for overcoming these challenges, we hope to uncover biologically diverse solutions to common problems of acoustic communication in noisy environments. [This work is supported by NIDCD R01 5R01DC009582.]

## **646 Front/Back Confusion and the Masking Effects of Noises with Illusory Locations**

W. Owen Brimijoin<sup>1</sup>, William Whitmer<sup>1</sup>, Michael Akeroyd<sup>1</sup>  
<sup>1</sup>MRC Institute of Hearing Research

A listener's acoustic world is in constant motion because of head movements, however small they might be. This motion gives useable information: head turns have been shown to contribute to resolving the location of an auditory signal, especially in disambiguating front/back confusions. By turning the head and processing the resulting dynamic changes in location cues, one can determine whether it is coming from the front or the back.

Head movements can also be used to *create* front/back confusion. We used high-speed motion capture to synchronously and smoothly move a sound source as a function of head movement. Presenting a sound from behind a listener but moving it in the direction it would have moved if it had been located in the front resulted in the compelling percept of the sound *being* in front. The contrariwise effect occurred if the sound was presented from the front but moved as if it were behind the listener. Experiments showed that the strength of the illusion was dependent on the spectral content of the sound: the salience of the illusion was strongest for a sound that was low-pass filtered at 512 Hz and was reduced as a function of increasing cut-off frequency.

We used this front/back illusion to investigate the masking of speech and tones by low-pass noises with real or illusory positions. For a signal located in front of a listener, a noise in the back that moved so as to create the percept of a noise from the front was as effective a masker as a noise *actually* located in the front. We found, however, an asymmetry in masking patterns: for a signal and a noise co-located in front of a listener, moving the noise so as to create the percept of a noise from behind did not result in any spatial release from masking. This masking demonstrates a functional consequence of the relationship between head movements and the resulting rotation of the acoustic world, showing that that listeners use head movements to help establish spatial channels of information.

## **647 A Behavioral Study of the Precedence Effect in Cats Under Head-Free Conditions with Speakers Aligned in Horizontal, Vertical, and Diagonal Conditions**

Yan Gai<sup>1</sup>, Janet Ruhland<sup>1</sup>, Tom Yin<sup>1</sup>  
<sup>1</sup>University of Wisconsin-Madison

The precedence effect (PE) is an auditory illusion that occurs during localization of sounds coming from different spatial locations with time delays. In the past, it has been mostly studied with head-fixed animals in the horizontal plane, where binaural timing and level cues are abundant. Both summing localization (i.e., the perception of an illusory sound in a position between the two targets) and localization dominance (i.e., the localization of only the leading sound) have been observed in the horizontal plane. In contrast, there is evidence showing that only localization dominance exists in the vertical plane in head-

fixed cats (Tollin and Yin, J Neurophysiol. 90:2149-62, 2003) as well as head-fixed human subjects (Dizon and Litovsky, JASA 115:3142-55, 2004). Here we describe results using stimuli mimicking the PE in three cats under head-free conditions for a variety of paired-sound conditions along the horizontal, vertical, and diagonal axes in the frontal hemifield. We monitored gaze and head positions using a scleral search coil technique. The animals were given trials with a standard saccade task that required them to make gaze shifts from a central fixation LED to the perceived source of paired acoustic targets simulating the PE. Since the PE is an illusion, only a small percentage of the trials were PE stimuli; the majority were simple single source saccade targets that served as control trials. We observed both summing localization and localization dominance in all three dimensions, although the localization performance in elevation with the short noise pips was relatively inaccurate for both double-source (PE) and single-source (control) conditions. In addition, simulations of the auditory periphery were performed to explain the observed PE in elevation based on spectrum cues. Supported by NIH/NIDCD- DC07177.

## **648 The Precedence Effect in Sound Localization: Distinct Roles for Interaural Time and Level Differences Suggested by Behavioral, Modeling, and Acoustic Data**

Andrew D. Brown<sup>1</sup>, G. Christopher Stecker<sup>1</sup>  
<sup>1</sup>University of Washington

Normal-hearing listeners effectively localize sound in echoic environments by responding to early-arriving spatial cues carried by the direct signal rather than spurious later-arriving cues carried by reflections. The temporal extent of this "precedence effect" strongly depends on the recent stimulus history. We conducted a series of investigations to measure "fusion" and "lateralization dominance" aspects of the precedence effect for "lead-lag" click pairs and slow trains of such click pairs (4/s) lateralized by interaural time differences (ITD) or interaural level differences (ILD). Fusion echo thresholds and lateralization responses were measured simultaneously in four conditions: (1) Baseline trials consisted of a single "source-echo" click pair, (2) Buildup trials consisted of 12 "conditioner" source-echo click pairs and a final test pair identical to the conditioner pairs, (3) Breakdown trials consisted of 12 conditioner pairs and a "switched" test pair in which the interaural cues were swapped between the "source" and "echo" clicks, and 4) Re-buildup trials consisted of 11 conditioner pairs, an intervening switched pair, and a final test pair identical to the 11 conditioner pairs. Results suggested (1) that the precedence effect is more robust for ITD than for ILD in terms of both lead-lag fusion and lateralization dominance of the lead and (2) that fusion and lateralization dominance are separate phenomena, particularly evident under "buildup" conditions. Binaural modeling and acoustic recordings can be used to understand the consequences of these behavioral data in a variety of natural listening environments.

## **649** Spatial Variation of Individual Differences in Sound Localization

Guillaume Andeol<sup>1</sup>, Sophie Savel<sup>2</sup>, Lionel Pellieux<sup>1</sup>, Anne Guillaume<sup>3</sup>

<sup>1</sup>IRBA, <sup>2</sup>LMA/CNRS, <sup>3</sup>LAB

Studies of sound-localization often show substantial differences in performance across participants. The origin of such inter-individual differences is still not well understood. In this study, 25 young (<35 years old) normal-hearing listeners performed an absolute-sound-localization task with individualized head-related transfer functions (HRTFs). The task involved localizing 119 targets distributed uniformly on the surface of a 1.40 m virtual sphere. Participants gave their responses by pointing on a smaller-scale replica of the virtual sphere (GELP technique). To reduce procedural-learning effects, participants received procedural training prior to the localization tests. Unsigned left/right and up/down errors, and front/back and up/down reversals, were measured. Large inter-individual differences were observed for each of these measured variables. For left/right errors, individual differences appeared to depend on the lateral/medial location of the targets. For up/down errors, front/back reversals and up/down reversals, individual differences appeared to depend mainly on the up/down location of the target. We propose an explanation for the effect of target location on individual performance in terms of three factors: a low-level perceptual factor (related to the extraction of acoustic sound-localization cues), a high-level perceptual factor (related to spatial cognition), and a factor related to perceptual preferences between different types of acoustic sound-localization cues.

## **650** Localization of Two Concurrent Sound Sources Using a Neural Decoder

Mitchell Day<sup>1,2</sup>, Bertrand Delgutte<sup>1,3</sup>

<sup>1</sup>Massachusetts Eye and Ear Infirmary, <sup>2</sup>Harvard Medical School, <sup>3</sup>MIT

Recent studies in mammals suggest that the azimuth of a sound source in the horizontal plane can be accurately identified by a neural decoding model which compares the summed activity between all the neurons in the inferior colliculi (IC) of each hemisphere. This “two-channel” representation is effective for single sound source ITDs in anechoic space. Here we tested two neural decoding models on the more difficult task of identifying the azimuths of two concurrent sounds. Single unit recordings were made in the IC of unanesthetized rabbits to stimuli presented in virtual acoustic space. Rate responses were measured for two concurrent, uncorrelated broadband noises presented at every spatial combination in the frontal azimuthal plane, in 30 deg increments. A rate probability distribution was created for every spatial combination assuming that either the pattern of average individual neural activity across the population was “known” to the decoder (“labeled-line” decoder) or that firing rates were summed over each hemisphere (“two-channel” decoder). For both decoders, the rate on each stimulus trial was classified to the spatial combination with the greatest probability (maximum likelihood). The labeled-line decoder

was able to localize every spatial combination of sources, with somewhat decreased accuracy at lateral locations. This ability was preserved when the decoder only used data from neurons with either low (<1.5 kHz) or high (>2.5 kHz) best frequencies (BFs). The two-channel decoder localized most combinations with moderate accuracy, although some spatial combination classifications differed widely between low and high BFs. For two sources located symmetrically about the midline, the two-channel decoder often misclassified the combination as a single source located in the center. These differences in decoder performance make contrasting, testable predictions regarding psychophysical performance.

Supported by NIH grants R01 DC02258 and P30 DC05209.

## **651** Loss of Sensitivity to Dynamic Sound Localization Cues in Listeners with Impaired Low-Frequency Hearing

Ewan Macpherson<sup>1</sup>, M. Alasdair Cumming<sup>1</sup>

<sup>1</sup>University of Western Ontario

Information about front/rear sound source location is available in the relationship between a listener's rotation of their head and the resulting changes in interaural time and level differences. This information is likely particularly valuable to listeners with hearing impairment who might lack access to the high-frequency spectral cues for front/rear location provided by the pinna. In normally hearing listeners, a minimum head movement angle (MHMA) of 5-10 degrees is sufficient for accurate front/rear localization of low-frequency (0.5-1 kHz) noise-band targets [Macpherson 2009, JASA 125:2691(A)]. Listeners with near-normal low-frequency thresholds but precipitous high-frequency hearing loss benefit similarly from dynamic localization cues [Macpherson et al 2011, JASA 129:2486(A)]. In the present study, we measured MHMAs for clearly audible low-frequency and wideband (0.5-16 kHz) targets in listeners with moderate hearing impairment (45-60 dB HL) at low-frequencies (250-1000 Hz) and gently sloping losses at higher frequencies. Neither stimulus could be localized accurately by these listeners without head movement. Localization accuracy improved relative to a static-head condition for large (40-deg) head movements at low head-turn velocity (50 deg/s), but MHMAs were at least four times larger than those for normally hearing and precipitous-loss listeners. Unlike those groups, the group with low-frequency impairment showed little benefit of head motion at a higher velocity (200 deg/s). An additional subject with mild (20-30 dB HL) low-frequency loss showed intermediate MHMA elevation. The results suggest that low-frequency hearing loss impairs the effective processing of dynamic sound localization cues and support the hypothesis that low-frequency interaural time-difference is the primary dynamic cue.

## **652** Eccentric Eye Position Shifts Azimuth Estimates of Interaural Time Differences in the Direction of Ocular Fixation

Laura Junig<sup>1</sup>, Christina Cloninger<sup>1</sup>, Paul Allen<sup>1</sup>, Emily Clark<sup>1</sup>, William O'Neill<sup>1</sup>, Gary Paige<sup>1</sup>

<sup>1</sup>*Dept. of Neurobiology & Anatomy, U. of Rochester School of Medicine and Dentistry*

Visual space is encoded in eye-centered coordinates, whereas auditory space is encoded in head-centered coordinates. The eyes move frequently during natural behavior, and the spatial maps of these two modalities are dynamically integrated to support navigation and object identification. However, we demonstrated that during *prolonged* changes in eye position, free-field auditory spatial perception shifts in the direction of eye position (by ~40% and with a time constant of ~1 minute). In the present study we examined the effect of eye position on sound lateralization using a range of interaural timing difference (ITD) cues presented using headphones.

In Experiment 1, head-fixed subjects continuously fixated a central or eccentric ( $\pm 20^\circ$  left or right) target. After two minutes, localization trials began in which continuous auditory targets (150ms noise bursts [200-1000 Hz], at 5Hz) were presented within an ITD range of  $\pm 450 \mu\text{s}$ . A joystick-guided laser pointer was aimed at the perceived azimuth associated with the lateral perception of the target. In Experiment 2, the target and pointer modalities were reversed. The joystick now guided an auditory pointer by dynamically adjusting ITD, which subjects aligned with LED visual targets presented in the range  $\pm 40^\circ$  azimuth.

Both experiments demonstrated robust effects of eccentric eye position. Response azimuths for visual pointing to sound targets (ITDs), and for auditory (ITD) pointing to visual targets were biased toward the direction of ocular fixation. Additionally, there was substantial individual variation in the azimuth-ITD gain functions. Many subjects dramatically overestimated the location of auditory cues beyond the predictions of the spherical head model.

These findings extend the previously-reported eye position effect on free-field sound localization to also include headphone presentation of ITD-dependent lateralization. Classic models of neural processing of ITD spatial cues lack a mechanism to explain the dependence on eye position. The influence of eye position on auditory spatial perception is a fundamental property of auditory spatial perception, likely requiring a stage of central processing beyond the initial coding of ITDs.

*Supported by the Schmitt Foundation and NIH P30-DC05409 (Center for Navigation & Communication Sciences)*

## **653** Minimum Audible Angle in the European Starling (*Sturnus Vulgaris*)

Arne Feinkohl<sup>1</sup>, Georg Klump<sup>1</sup>

<sup>1</sup>*Carl von Ossietzky University Oldenburg*

Sound localization is not a trivial task for birds having small heads in relation to the wavelength of sounds they use for communication. Theoretical considerations about sound source localization and physical measurements of binaural cues in the auditory system of a songbird, the European

starling (*Sturnus vulgaris*), suggested that in the hearing range of the starling the maximum interaural level differences (ILD) are about 10 dB and the maximum interaural time differences (ITD) are about 100 $\mu\text{s}$  (Klump & Larsen 1992). In this psychoacoustic study we investigate the acuity of starling sound localization using operant conditioning techniques to determine the minimum audible angle (MAA).

For measuring the MAA four individuals were trained to detect a switch in azimuth sound source location after being presented with repeated stimuli from a fixed location (reference). The stimuli (overall roving level 63  $\pm$  3 dB) were pulses of broadband noise (0.5-6 kHz) or tones (1, 2 or 4 kHz) with a duration of 1000 ms. Additionally, broadband noise and 2-kHz tones with a duration of 100 ms were presented. The azimuth angle used for switching ranged from 11 $^\circ$  to 90 $^\circ$ . The resulting psychometric functions were analyzed using signal detection theory (threshold criterion  $d' = 1.0$ ).

The starlings' smallest MAA of approximately 18 $^\circ$  was measured for broadband noise and 4-kHz tones indicating a best sound localization acuity being comparable to the absolute localization accuracy of other songbirds. The starlings' MAA is improved at the longer stimulus duration and with an increase in frequency from 1 to 4 kHz. Based on the geometry of the head, the MAA at 4 kHz corresponds to an ILD of about 1 dB and an ITD of about 21  $\mu\text{s}$  (Duda & Martens 1998, Kuhn 1977). The probability of detecting the switch increased with an increasing number of repetitions of the reference suggesting that a template of the reference is formed in the starlings' brain that improves with each repetition.

Supported by a Georg Lichtenberg stipend to A.F.

## **654** Effects of Interaural Level and Time Differences on the Externalization of Sound

Torsten Dau<sup>1</sup>, Jasmina Catic<sup>1</sup>, Sebastien Santurette<sup>1</sup>, Jörg Buchholz<sup>2</sup>

<sup>1</sup>*Technical University of Denmark*, <sup>2</sup>*National Acoustic Laboratories, Australia*

Distant sound sources in our environment are perceived as externalized and are thus properly localized in both direction and distance. This is due to the acoustic filtering by the head, torso, and external ears, which provides frequency dependent shaping of binaural cues, such as interaural level differences (ILDs) and interaural time differences (ITDs). Further, the binaural cues provided by reverberation in an enclosed space may also contribute to externalization. While these spatial cues are available in their natural form when listening to real-world sound sources, hearing-aid signal processing - such as wide dynamic range compression - affects the ILDs and thereby potentially reduces the perceived degree of externalization. In the present study, the effect of room reverberation on the spectro-temporal behavior of ILDs was investigated. This was done by analyzing speech played at different distances and recorded on a head-and-torso simulator in a standard IEC 268-13 listening room. Next, the effect of ILD fluctuations on the degree of externalization was investigated in a listening experiment

with normal-hearing listeners. The experiment was performed in the same standard listening room and a distant speech source was simulated via headphones using individual binaural impulse responses. The speech signal was then processed such that the naturally occurring ILD fluctuations were compressed. This manipulation reduced the perceived degree of externalization in the listening experiment, which is consistent with the physical analysis that showed that a decreased distance to the sound source also reduced the fluctuations in ILDs.

### **655 Absolute and Relative Localization Strategies in Expectation of a Distractor Sound**

**Beata Tomorivova<sup>1</sup>**, Lubos Hladek<sup>2</sup>, Norbert Kopco<sup>1</sup>  
<sup>1</sup>TU Kosice, Slovakia, <sup>2</sup>UPJS Kosice, Slovakia

A series of studies of horizontal sound localization with a preceding distractor showed that localization responses can be biased away from the distractor location by up to 10°, even on the interleaved baseline trials on which the target was preceded by no distractor [Kopco et al., JASA, 121, 420-432, 2007; Tomorivova et al., ARO Abstract #1019, 2009; Proc. Forum Acusticum 2697-2702; 2011].

Here performance obtained in several experiments was analyzed with the goal of examining whether the observed biases might be related to a change in listener's localization strategy. In the experiments, subjects localized 2-ms frozen noise bursts presented either in the left (-11° to -79°) or the right (11° to 79°) hemifield of the frontal horizontal plane. A distractor preceded the target by 25 to 400 ms on some trials. Distractor's location was fixed throughout a run, either ahead or on the side of the listener, and its frequency of occurrence was parametrically varied.

Since the distractor always came from a known location, the listeners could use it as an anchor for computing a relative position of the following target. Therefore, the observed biases might be a consequence of listeners' switching between an absolute localization strategy, used when no distractor is presented, and a relative strategy, used when the distractor information can be used. To assess this hypothesis, three response measures were analyzed, separately for the responses in the runs with and without the distractors: standard deviations, correlation coefficients, and temporal drifts in response biases. Improvements in some of the measures were observed on the distractor runs. This result suggests that the distractor can provide additional relative information for target localization, and that listeners change their strategies to benefit from this information.

[Supported by the European Commission and KEGA #3/7300/09]

### **656 Visual Capture of Auditory Stimuli Differs in Azimuth and Elevation**

**Adam Bosen<sup>1,2</sup>**, William O'Neill<sup>1,2</sup>, Paul Allen<sup>1,2</sup>, Gary Paige<sup>1,2</sup>

<sup>1</sup>Department of Neurobiology & Anatomy, <sup>2</sup>University of Rochester School of Medicine and Dentistry

When an auditory target is simultaneously presented in close proximity to a spatially well-defined visual target, the perceived location of the sound is typically attracted towards the visual image. This effect, called visual capture, has been extensively studied in azimuth, but has received surprisingly little attention in elevation. Because sound localization in elevation is generally less precise and accurate than in azimuth, we expected that visual capture of auditory targets would be stronger in elevation than in azimuth. However, observations from various experiments in our laboratory (not specifically directed at this question) suggested otherwise.

This experiment re-evaluated visual capture with the specific goal of addressing elevation in comparison with azimuth. Young normal-hearing adults localized broadband noise targets using manual laser pointing, both with and without the presentation of a central visual fixation reference. Visual capture was quantified as the change (with vs. without the visual reference) in mean accuracy and precision (std. dev. of accuracy) of sound localization. Results generally demonstrated robust visual capture in azimuth in the region around the visual reference. Interestingly, visual capture of the same set of targets proved less robust in elevation, with some subjects showing negligible effects despite lower performance in elevation than in azimuth. This finding runs counter to the commonly held notion that visual spatial capture is radially symmetrical, and to earlier cognitive studies of the ventriloquism effect.

Supported by the Schmitt Foundation and NIH P30-DC05409 (Center for Navigation & Communication Sciences)

### **657 Oculomotor Adaptation of Sound Localization Depends Upon the Temporal Relationship Between Targets and Eye Movements**

**Emily Clark<sup>1</sup>**, William O'Neill<sup>1</sup>, Gary Paige<sup>1</sup>

<sup>1</sup>Dept. of Neurobiology & Anatomy, U. of Rochester School of Medicine and Dentistry

We previously described a unique oculomotor adaptation by which prolonged changes in eye position shift the perception of auditory space in the same direction as ocular deflection (averaging ~40%, with a mean time constant of ~1 min.). One consequence is that localization of ongoing sounds overshoots target azimuth when the head is fixed but the eyes are free to move during laser pointing. The overshoot is reduced or eliminated when the eyes are fixed. However, this distinction disappears when transient targets are presented, whether or not the eyes are fixed or free to guide localization from memory. A parsimonious explanation is that adaptation is determined by eye position at the time targets are presented. Note that

ongoing targets provide a continuous sampling during and after eye movements, but transient targets may register at any moment with respect to any eye movement.

To test this concept, subjects (N=6, age <30) localized transient targets (5Hz noise bursts) while fixating a visual reference. Each trial began with center (0°) fixation, followed by eccentric (either 20° left or right) fixation. Subjects waited 10 seconds after the ocular deflection before localizing the target, while maintaining eccentric fixation. Targets were presented during one of three different times in the trial: A) immediately before eccentric fixation while the eyes were still fixated centrally, B) immediately after eyes were shifted eccentrically, or C) after 10 seconds of eccentric fixation. These conditions were compared to a baseline condition with only center fixation and no 10 second delay between target presentation and subject response. The key variable is the time between the attainment of a new eye position and target presentation. Results for condition A were indistinguishable from baseline. In contrast, a small response overshoot arose in condition B, when targets were presented shortly after fixating eccentrically. Overshoot was largest for condition C, when targets were presented after 10 seconds of eccentric fixation. We conclude that oculomotor adaptation of auditory spatial perception depends upon eye position at the time of target presentation, and not on subsequent changes in eye position, including those that occur during localization itself.

*Supported by the Schmitt Foundation and NIH P30-DC05409 (Center for Navigation & Communication Sciences)*

### **658 The Role of Pinna Features in Vertical Plane Localization**

**Robert Baudo<sup>1</sup>**, Alan Musicant<sup>1</sup>

<sup>1</sup>*Psychology, Mid. Tenn. St. Univ.*

The pinna plays a major role in vertical plane localization of sounds, but how much of a role does each individual feature contribute? We sought to replicate the Gardner & Gardner (1973) study, and, by making use of the pinna model information from Shaw (1982), to more clearly explicate the role of individual parts of the pinna. We followed the previous protocol with progressive filling of pinna cavities. However, we expanded the vertical range (in the median sagittal plane) from the original +/- 18° to a more expansive region of +/- 45°. The contribution of the individual features of the scapha, fossa and upper and lower concha has been examined by using smaller molds than those utilized in the original study. This has allowed us to observe the effect of each feature, rather than using the subtraction method of Gardner & Gardner. We have observed major changes in the distribution pattern of median sagittal plane responses, an aspect of the original experiment that was not reported, and perhaps not observed, due to the limited range of loudspeaker placement. The error index utilized by Gardner & Gardner did not allow for a determination of changes to patterns of responding. Our analysis of the data, from four of an expected ten subjects, demonstrates that errors in

identifying broad band noise stimuli occur for higher placed (degree) loudspeakers when the fossa is occluded and even more so when the upper, lower, and complete concha are occluded. Occlusion of the scapha and upper concha has led to increased error with loudspeakers located below 0°. Occlusion of the upper, lower, and complete concha results in compression of perceived location, as subjects identified the origin of the stimulus as originating closer to the 0° position. This compression is observed for the upper most loudspeaker locations and to a lesser extent, the lower most locations.

### **659 Hearing Through New Ears: Adaptation in Sound Localization in Cats Following Ear Canal Perturbation**

**Amy Hong<sup>1</sup>**, Janet Ruhland<sup>2</sup>, Yan Gai<sup>1</sup>, Tom Yin<sup>3</sup>

<sup>1</sup>*Univ. Wisconsin*, <sup>2</sup>*Univ. Wisconsin*, <sup>3</sup>*Univ. of Wisconsin*

Hearing through new ears: adaptation in sound localization in cats following ear canal perturbation

Accurate sound localization relies on neuronal processing of acoustic stimuli. Along the horizontal plane, or azimuth, the auditory system relies on two binaural acoustic inputs, interaural disparities in time of arrival and level of sound at the ears. In contrast, localizing sounds in elevation relies on broadband spectral shape of the head-related transfer function (HRTF) which is a product of the direction-dependent filtering properties of the head and pinnae. Perturbation of spectral cues by pinna occlusion in humans, bats, and ferrets dramatically diminishes localization performance, which in humans can recover with time. Here, we studied the adaptation to new spectral cues, or altered HRTFs, in cats via bilateral application of excavated ear molds. The cats localized noise targets along the horizontal and vertical plane with head unrestrained gaze shifts. The horizontal and vertical components of saccadic gaze shifts were accurate for all cats prior to wearing ear molds but localization accuracy declined appreciably immediately following ear mold application, especially for the vertical components of both the horizontal and vertical targets. Accuracy is summarized by the slope, or gain, of the linear regression relating the localization responses to corresponding noise targets. Cats were able to adapt to new spectral cues in some cases spontaneously through wearing the ear molds continuously and in other cats only after "retraining" them through the use of bimodal stimuli during localization training. Longer latencies exhibited after ear mold application suggested a greater difficulty in localizing sounds in elevation. Also, the cats appeared to retain their original spatial cues allowing them to quickly revert back to their normal localization behavior once the ear molds were removed. Supported by NIH grant DC07177.

### **660 The Reference Frame of Sounds**

**Marc van Wanrooij<sup>1,2</sup>**, Tom van Grootel<sup>1</sup>, Denise van Barneveld<sup>1</sup>, Ad Snik<sup>2</sup>, John van Opstal<sup>1</sup>

<sup>1</sup>*Dept. Biophysics, Donders Institute, Radboud University Nijmegen, The Netherlands*, <sup>2</sup>*Dept. Otorhinolaryngology*,

*Donders Inst, Radboud University Medical Centre  
Nijmegen, The Netherlands*

The human auditory system represents sound-source directions initially with respect to the head-fixed ears. To orient gaze, and/or to determine whether a light occurred at the same location as the sound, the orientation of eyes and head should be incorporated to specify the target location relative to the eyes.

Here we test (1) whether this transformation involves a stage in which sounds are represented in a supramodal (e.g. world-centered) reference frame, and (2) whether acoustic spatial updating occurs at a topographically organized motor level representing gaze shifts, or within the tonotopically organized auditory system.

Human listeners generated head-unrestrained gaze shifts from a large range of initial eye and head positions toward a) tones at different center frequencies, b) broadband sounds only, and c) broadband sounds with simultaneous and spatially-unaligned visual stimuli, presented in the midsagittal plane. Tones were heard at a fixed illusory elevation, regardless of their actual location, that depended in an idiosyncratic way on initial head and eye position, as well as on the tone's frequency. Gaze shifts to broadband-sounds were accurate, even though they were biased by vision (ventriloquist effect) when a light was simultaneously presented. Still, initial eye and head positions were fully incorporated.

The results support the at-first-sight paradoxical hypothesis that the auditory system represents sounds in a supramodal (non-auditory) reference frame, by incorporating eye and head orientation at a tonotopic (auditory) stage.

### **[661] Inner Ear Transcriptome Analysis of Transgenic MicroRNA Misexpression Reveals the Downregulation of Hundreds of MiR-96 MiR-182 and MiR-183 Target Genes**

**Michael D Weston<sup>1</sup>, Songila Doi<sup>1</sup>**

<sup>1</sup>*Oral Biology Department, Creighton University*

MicroRNAs (miRNAs) are negative post-transcriptional regulators of gene expression. Mutations in members of the miR-183 family (miR-96) cause hearing loss in DFNA50 and in the Dimenuendo mouse. In silico, thousands of genes are predicted to be regulated by miR-183 family. Transgenic mice (Tg[GFAP-miR-183/miR-96/miR182]) that misexpress neurosensory specific miR-183 family miRNAs in organ of Corti supporting cells were developed as a model system to discover relevant miRNA/target gene interactions of this miRNA family. We had previously characterized a progressive and complete loss of auditory hair cells (HCs) in this model, validating a potent negative effect of miR-183 family microRNAs as predicted by the mutual exclusion hypothesis of miRNA-target gene expression. Morphologically, the model also implicated microRNA mediated effects on cell proliferation, differentiation and survival. Triplicate Affymetrix MoGene 1.0 ST and miRNA 2.0 array data were collected from P18 WT and Tg littermates; an age when functional and morphologic changes in the organ of Corti are readily apparent. Microarray analysis revealed 40% of genes

downregulated in Tg mice (t-test,  $p < 0.05$ , avg ratio  $\geq 1.25$ ) had at least one predicted miR-96, miR-182 or miR-183 target site (bonferroni  $p < 1 \times 10^{-11}$ , MiRanda database). Similar significance was found using Targetscan and PicTar databases ( $p < 1 \times 10^{-5} - 1 \times 10^{-18}$ ). Gene Set Enrichment Analysis (Broad Institute) revealed 59/201 miRNA target gene sets were overrepresented in Tg downregulated genes at or below  $p = 0.001$  (FWER statistic), but most have significant overlap with genes targeted by the miR-183 family. While no miRNA targets were found to be increased in Tg versus WT inner ears, KEGG pathway and Gene Ontology analyses uncovered 42 upregulated ribosomal protein mRNAs which are consistent with Tg mediated effects on proliferation. These and other findings reveal much that will be useful in elucidating the specific targets and biologic pathways influenced by of the miR-183 family and may have general applicability to refine miRNA target prediction. Supported by NIH/NCRR P20RR018788.

### **[662] Transcriptome Analysis and Genetic Engineering to Develop Highly Specific Reporters of Otic Sensory Progenitor Cell Types for Embryonic Stem Cell Guidance Studies**

**Byron Hartman<sup>1,2</sup>, Roman Laske<sup>1,2</sup>, Saku Sinkkonen<sup>1,2</sup>, Robert Durruthy-Durruthy<sup>1,2</sup>, Kazuo Oshima<sup>1,2</sup>, Stefan Heller<sup>1,2</sup>**

<sup>1</sup>*Department of Otolaryngology, Stanford University School of Medicine, Stanford CA 94305, USA,* <sup>2</sup>*Department of Molecular & Cellular Physiology, Stanford University School of Medicine, Stanford CA*

Inner ear sensory cells are derived from otic sensory progenitors (OSPs) established during early development. Our long term goal is to define the fundamental development programs of OSPs and their derivatives, the hair cells and supporting cells of the cochlea and the vestibular apparatus. We previously have utilized signaling principles of early development to guide embryonic stem (ES) cells in a stepwise manner toward otic fate and promote formation of hair cell-like cells. ES cell guidance offers distinct advantages for investigating developmental mechanisms of the inner ear in a highly controlled and isolated system. However this system still has a number of limitations, including ambiguity and heterogeneity of derived cells. There is a need for development and validation of highly specific markers and selection tools to identify, purify, and manipulate OSPs, hair cells, and supporting cells. We have employed quantitative expression profiling of cell populations from the developing mouse ear and other tissues to identify robust specific markers of OSPs and developing hair cells and supporting cells. Profiled samples include micro-dissected early mouse otic vesicles as well as flow-sorted neonatal hair cells and supporting cells, and several other non-otic cell populations for determining otic specificity. Genes were ranked and clustered based on relative expression in selected populations and several classes of specific makers were identified. We found that many otic markers identified have published expression patterns and/or

phenotypes in the ear highly consistent with our array data. We have selected the most robust markers to construct fluorescent promoter reporter plasmids to use as tools for evaluating and targeting OSPs and hair cells and supporting cells derived from ES cells. Development of highly specific reporters of cellular identity is an important step in efforts to understand and recapitulate the fundamental programs of development of otic sensory epithelial cells.

### **663 Genetic Profiling Along the Longitudinal Axis of Mouse Cochlea During Neonatal Development**

**Eun Jin Son**<sup>1</sup>, Ling Wu<sup>2</sup>, Heejei Yoon<sup>2</sup>, Sunny Kim<sup>2</sup>, Jae Young Choi<sup>1</sup>, Jinwoong Bok<sup>2</sup>

<sup>1</sup>*Department of Otorhinolaryngology, Yonsei University College of Medicine,* <sup>2</sup>*Department of Anatomy, Yonsei University College of Medicine*

The cochlear map is characterized by tonotopic organization along its longitudinal axis, such that the base of the cochlear duct is more sensitive to high frequency sounds and the apical cochlea to low frequency sounds. In effort to elucidate the mechanism by which the tonotopic organization is established, we first attempted to identify genes that are differentially expressed along the tonotopic axis during neonatal development. Cochlear tissues containing the organ of Corti and lateral wall were dissected from P0 and P8 C57BL/6 mice, and divided them into three pieces representing base, middle and apex. Total RNAs were purified from each pool and the gene expression profiles were analyzed using the Affymetrix GeneChip® Mouse Gene 1.0 ST Array. Microarray results of differential gene expression were validated by performing qRT-PCR on selected genes. Gene expression patterns were classified into 9 groups according to two variables: 1) we first identified genes showing an increasing, decreasing or no gradient from base to apex, and 2) then compared the expression patterns between P0 and P8. Genes classified into the 9 groups were subjected to GSEA (gene set enrichment analyses) to interpret the data focusing on specific biological processes categorized by gene ontology (GO) terms. We also analyzed expression domains of a few selected genes by *in situ* hybridization. Our data should provide basic information for further investigation regarding the acquisition of tonotopic map during mammalian cochlear development.

### **664 In Vivo Proteomics: Imaging of Single Protein Molecules in the Developing Inner Ear Reveals Heterogeneities in Protein Kinetics**

**Andres Collazo**<sup>1,2</sup>, Le Trinh<sup>3</sup>, Joseph Huff<sup>4</sup>

<sup>1</sup>*House Research Institute,* <sup>2</sup>*University of Southern California,* <sup>3</sup>*California Institute of Technology,* <sup>4</sup>*Carl Zeiss MicroImaging, LLC*

Fluorescence correlation spectroscopy (FCS) provides quantitative data on the dynamics of single protein molecules in living cells. Most FCS studies have been

limited to analyzing fluorescently tagged exogenous proteins. We have previously developed a gene trap approach in zebrafish that fluorescently labels endogenous proteins and offers a unique opportunity to analyze the properties of single proteins during organogenesis as well as identify new molecular candidates for auditory and vestibular disorders. Here, FCS is used to analyze the mobility of multiple proteins during the development of the inner ear. Strikingly, the diffusion coefficients calculated vary greatly for the proteins analyzed, with some proteins having significantly different values not only across different cell types and regions of the developing inner ear but also at different times during development. One protein (Ctnna) even had significantly different values between apical versus lateral cell membranes of hair cells. The eight proteins studied have a broad range of expression with most being restricted to specific cell types or regions of the inner ear. For example, two of the proteins (Gnb2 and Rab3A) are only expressed in hair cells within the inner ear and appear as these cells differentiate. In terms of sub-cellular compartments, there were proteins restricted to the nucleus, cell membrane or cytoplasm. All but one of the proteins studied (Ctnna) have not had their inner ear expression described before. This is the first study to use FCS *in vivo* to analyze the dynamics of endogenous proteins in vertebrates. Our comparative FCS approach provides unprecedented analyses of the proteome during organogenesis in living embryos. (Supported by NIH, NIDCD and the Ahmanson Foundation)

### **665 The Link Between Notch and FGF Pathways in Sensory Cell Specification in the Mammalian Cochlea**

**Vidhya Munnamalai**<sup>1</sup>, Toshinori Hayashi<sup>1</sup>, Olivia Bermingham-McDonogh<sup>1</sup>

<sup>1</sup>*Department of Biological Structure, University of Washington*

The loss of mechanosensory hair cells in the cochlea is one of the leading causes of hearing loss. During development, FGFs have been shown to be important for the development of the inner ear and the specification of the sensory cells of the cochlea. Pharmacological inhibition of fibroblast growth factor receptors reduced hair cell formation. Recent studies suggest that FGF20 interacts with Fgfr1 to regulate sensory cell formation. FGF20 is expressed between E13.5 and E15.5 in the cochlea in a base to apical sweep along the cochlear duct just prior to hair cell differentiation. Based on these studies, we postulated that perhaps exogenous FGF20 could increase hair cell formation in the developing cochlea. However it was difficult to assess any increases in hair cells numbers upon addition of FGF20 to cochlear explants.

When explants were treated with the notch inhibitor, DAPT we found that FGF20 was down regulated suggesting that FGF20 could be regulated by Notch signaling. Previously we showed that Notch inhibition with DAPT inhibited prosensory formation in E12 explants. Addition of FGF20 in the presence of DAPT showed a partial rescue of hair cells but a broader rescue of Sox2 in our explant studies.

Given its temporal expression and regulation by Notch it is possible that the Notch prosensory effect is mediated by FGF20.

### **666 Expression of Neurog1 Instead of Atoh1 Can Partially Rescue Organ of Corti Cell Survival**

Israt Jahan<sup>1</sup>, Ning Pan<sup>1</sup>, Jennifer Kersigo<sup>1</sup>, Lilian E. Calisto<sup>2</sup>, Ken A Morris<sup>2</sup>, Benjamin Kopecky<sup>1</sup>, Jeremy S. Duncan<sup>1</sup>, Kirk W. Beisel<sup>2</sup>, Bernd Fritzschn<sup>1</sup>

<sup>1</sup>University of Iowa, Department of Biology, Iowa city, IA,  
<sup>2</sup>Creighton University, Department of Biomedical Sciences, Omaha, NE

Abstract:

In the mammalian inner ear neurosensory cell fate depends on three closely related transcription factors, *Atoh1* for hair cells and *Neurog1* and *Neurod1* for neurons. We have previously shown that neuronal cell fate can be altered towards hair cell fate by eliminating *Neurod1* mediated repression of *Atoh1* expression. To test whether a similar plasticity is present in hair cell fate commitment, we have generated a knockin (KI) mouse line (*Atoh1*<sup>KI*Neurog1*</sup>) in which *Atoh1* is replaced by *Neurog1*. Expression of *Neurog1* under *Atoh1* promoter control alters the cellular gene expression pattern, differentiation and survival of hair cell precursors in both heterozygous KI mice (*Atoh1*<sup>+/*KI**Neurog1*</sup>) and homozygous KI mice (*Atoh1*<sup>KI*Neurog1*/KI*Neurog1*</sup>). Homozygous mice develop patches of organ of Corti precursor cells that express *Neurog1*, *Neurod1*, several prosensory genes and neurotrophins. In addition, these patches of cells receive afferent and efferent processes. Some cells among these patches form multiple microvilli but not stereocilia. Importantly, *Neurog1* expressing mutants differ from *Atoh1* null mutants, as they have intermittent formation of organ of Corti cells, as opposed to complete 'flat epithelia' in the absence of *Atoh1*. Co-expression of *Atoh1* and *Neurog1* in heterozygous KI mice results in anomalous hair cell polarity, extra outer hair cell formation and disruption or fusion of stereocilia in later stages of development. Heterozygous KI mice show a hair cell phenotype that differs from haploinsufficiency of *Atoh1* (*Pax2cre*: *Atoh1*<sup>+/*f*</sup>) indicating some function of *Neurog1* expression in developing hair cells. Our data suggest that *Atoh1*<sup>KI*Neurog1*</sup> can provide some degree of functional support for survival of organ of Corti cells by attracting nerve fibers. In contrast to the apparent fate plasticity of neurons, hair cell precursors can, at the time of upregulation of *Atoh1*, be maintained for a limited time by *Neurog1* but do not transdifferentiate as neurons.

### **667 Conditional Deletion of Atoh1 in the Hoxb1 Lineage Causes Degeneration of Auditory Hair Cells Following Specification, Suggesting a Role for Atoh1 in Hair Cell Maturation**

Kurt Chonko<sup>1</sup>, Bernd Fritzschn<sup>2</sup>, Stephen Maricich<sup>3</sup>

<sup>1</sup>Department of Biology, Case Western Reserve University,  
<sup>2</sup>Department of Biology, University of Iowa, <sup>3</sup>Department of Pediatrics and Neurosciences, Case Western Reserve University

The basic helix-loop-helix transcription factor *Atoh1* (*Math1*) is necessary for the production of inner ear hair cells and several neuronal subtypes in the cochlear nucleus (CN). Previous work from our laboratory demonstrated that conditional deletion (CKO) of *Atoh1* using a *Hoxb1*<sup>Cre</sup> driver line resulted in loss of neurons in the posteroventral and dorsal CN. Surprisingly, we also found that *Hoxb1*<sup>Cre</sup>; *Atoh1*<sup>CKO</sup> mice had absent distortion product otoacoustic emissions, suggesting profound deficits in hair cell function. We therefore sought to characterize various measures of cochlear morphology in *Hoxb1*<sup>Cre</sup>; *Atoh1*<sup>CKO</sup> mice. The cochlea of *Hoxb1*<sup>Cre</sup>; *Atoh1*<sup>CKO</sup> mice are normal in size but exhibit progressive degeneration of hair cells beginning embryonically, with the majority of loss occurring between E16.5 and P0. Outer hair cell loss is more severe than inner hair cell loss. Interestingly, hair cell loss is regionally variable, being most severe in the mid-apical turns of the cochlea and ultimately leading to the formation of gaps within the hair cell line. Furthermore, *Hoxb1*<sup>Cre</sup>; *Atoh1*<sup>CKO</sup> mice experience a significant loss of spiral ganglion neurons after birth, the timing of which is discordant with the loss of hair cells. We used fate mapping and other techniques to demonstrate that *Hoxb1* is expressed in a regionally-variable manner in the developing sensory epithelium from embryonic through postnatal ages. Taken together, this data suggests that *Atoh1* is required for hair cell maturation and/or survival, and that loss of *Atoh1* expression following hair cell specification results in degeneration of the sensory epithelium.

### **668 Design of Viral Vectors for Dual Expression of Atoh1 and MicroRNAs to Promote Hair Cell Fates**

Michelle L. Stoller<sup>1</sup>, Kyle A. Patton<sup>1</sup>, Donna M. Fekete<sup>1</sup>

<sup>1</sup>Purdue University

Although the transcription factor, *Atoh1*, is an essential component for hair cell (HC) development and differentiation, other factors such as microRNAs (miRNAs) are also important for HC generation and maintenance. For example, the miR-183 family affects HC number and distribution in zebrafish embryos. One of its members, miR-96, is crucial for proper HC maturation, and mutations in its seed region underlie deafness in mice and humans. We hypothesize that this highly-conserved miRNA family may facilitate *Atoh1*-mediated HC induction in gene-therapy approaches. To test this in the embryonic chicken otocyst, we created a series of RCAS viral vectors. Vectors were designed with a bifunctional cassette containing a

900bp intron carrying the genomic sequences for miR-182, -96 and -183, followed by the Atoh1 gene fused to sequences for a hemagglutinin (HA) flu tag. We confirmed that this cassette produces both functional miRNAs and the Atoh1-HA fusion protein in vitro before producing RCAS viruses carrying the same cassette. As a control, we generated RCAS encoding Atoh1-HA that lacks the miRNA intron but retains its associated splice donor and acceptor sites upstream of Atoh1-HA. Viral stocks were titered using antibodies against the retroviral gag protein (3C2) or the HA tag (HA.11). Unfortunately, both RCAS vectors yield 100-fold reduced titers of the Atoh1 fusion protein as compared to the 3C2 epitope. In vivo injections show a similar disparity in protein expression. These findings suggest that the additional splice sites flanking the miRNA intron reduced the efficiency of generating the Atoh1-HA-encoding splice variant. In an attempt to improve the vector design, we are currently inactivating the splice donor site associated with the miRNA intron, a manipulation that should not prevent processing of the miRNAs. Our long-term goal is to use these vectors to explore the possibility that miRNAs may enhance Atoh1's ability to promote HC development and regeneration.

### **669** Dual Role of Sox2 in Specification of Sensory Competence and Regulation of Atoh1 Expression

Chandrakala Puligilla<sup>1</sup>, Matthew Kelley<sup>2</sup>

<sup>1</sup>Department of Pathology and Laboratory Medicine, Medical University of South Carolina, Charleston, <sup>2</sup>NIDCD, NIH, Bethesda, MD

The HMG transcription factor Sox2 is the earliest marker of the prosensory domain within the developing inner ear and deletion of Sox2 leads to a complete absence of prosensory cells. Similarly, the bHLH transcription factor Atoh1 is the earliest known marker for hair cells and is normally expressed in a subset of the Sox2-positive prosensory cells. Consistent with these developmental roles, expression of Atoh1 is lost in Sox2 mutants. However, our previous study has also demonstrated that Sox2 is down-regulated in developing Atoh1-positive hair cells and that the two factors are mutually antagonistic. To further elucidate the nature of the interactions between the Sox2 and Atoh1, Sox2 was transiently activated in GER cells. In contrast with continuous expression, transient activation of Sox2 leads to ectopic hair cell formation, suggesting a direct role for Sox2 in the induction of Atoh1, a conclusion that was confirmed by Chromatin Immunoprecipitation (ChIP) analysis. To determine whether Sox2 also influences the competence of inner ear cells to respond to Atoh1, cochlear cells from Sox2-mutants were transfected with Atoh1. Surprisingly, Atoh1-expressing cells failed to develop as hair cells, demonstrating an additional role for Sox2 and suggesting that induction of prosensory identity is necessary for hair cell formation. To test this hypothesis, Sox2 expression was examined in GER cells that had been transfected with Atoh1. Results indicated that prior to hair cell formation, Atoh1-transfected cells are transiently positive for Sox2 suggesting that these cells go through a "prosensory cell"

phase prior to hair cell differentiation. Overall, these results demonstrate dual roles for Sox2 in the developing inner ear, first in the specification of sensory competence and subsequently in the regulation of Atoh1 expression.

### **670** SOX2 Can Mediate the Effects of Notch Signaling by Specifying the Sensory Progenitors in the Mammalian Inner Ear

Wei Pan<sup>1</sup>, Ying Jin<sup>2</sup>, Robbert Rottier<sup>3</sup>, Amy Kiernan<sup>1,2</sup>

<sup>1</sup>Dept. of Biomedical Genetics, University of Rochester Medical Center, <sup>2</sup>Dept of Ophthalmology, University of Rochester Medical Center, <sup>3</sup>Dept of Cell Biology, Erasmus Medical Center

There are six sensory regions in the inner ear required for transducing sound and balance information. Each organ is comprised of hair cells and supporting cells that arise from a common sensory progenitor. Previously (Pan *et al.*, PNAS. 2010; 107: 15798), we showed that transient induction of Notch signaling using a combination Cre/Tet-on system results in the production of ectopic sensory progenitors in the nonsensory regions of the inner ear, which can subsequently differentiate into hair cells and supporting cells. These results demonstrate that Notch activation is sufficient to re-specify cochlear and vestibular otic progenitors to adopt a sensory fate. However, several questions remained, including the time window in which Notch can act and the downstream mediators of Notch activity. To determine the temporal window, we induced Notch activation in the otocyst at different time points. We determined that ectopic hair cells and supporting cells could be induced by Notch signaling between embryonic day (E)9.5 and E12.5, but not after E14.5, indicating that otic progenitors are competent to respond to Notch within a specific time window. The transcription factor SOX2 is a sensory progenitor marker required for the generation of all six sensory regions in the inner ear. We found that SOX2 expression can be induced by Notch activation, suggesting it is an important downstream target. To test this, we induced SOX2 transiently in the inner ear using the Cre/Tet-on system. We found that SOX2 could induce sensory progenitors similar to the Notch activation experiments. Interestingly, we found the ectopic sensory regions induced by SOX2 were much smaller than those induced by Notch activation, suggesting Notch has some SOX2-independent functions. These results identify SOX2 as a potential Notch effector and define the time window in which Notch can specify sensory progenitors. [Supported by NIDCD 1R01 DC009250 to AEK]

### **671** Dose Sensitivity of Tbx1 in Inner Ear Morphogenesis

Takahisa Watabe<sup>1</sup>, Sho Kanzaki<sup>1</sup>, Takayuki Yamagishi<sup>2</sup>, Takatoshi Tsuchihashi<sup>2</sup>, Masato Fujioka<sup>1,3</sup>, Kaoru Ogawa<sup>1</sup>

<sup>1</sup>Department of Otolaryngology, School of Medicine, Keio University, <sup>2</sup>Department of Pediatrics, School of Medicine, Keio University, <sup>3</sup>Department of Otolaryngology, Keiyu Hospital

Tbx1 is thought to be a responsible gene of DiGeorge syndrome (DGS) of which the clinical phenotype includes craniofacial abnormalities, congenital heart disease, thymic

and parathyroid defects. Hearing impairment occurs in from 44 to 77% of DGS cases. There are reports of sensorineural hearing impairment by inner ear abnormalities in 10% of cases of hearing impairment. So Tbx1 is thought to be required for inner ear morphogenesis. It was supported by Vitelli et al. that Tbx1<sup>-/-</sup> embryos had the inner ear abnormalities at E.9.5. About Tbx1 gene, it was showed by Tonghuan Hu et al. that it shows the dose dependent manner in the morphogenesis of cardiovascular system. It is assumed that the dose sensitivity to Tbx1 gene may underlie in the mechanisms of the inner ear morphogenesis.

The dose sensitivity of Tbx1 in inner ear morphogenesis was evaluated by using the mouse model of which Tbx1 expression level gradually decreased from wild type(Tbx1<sup>+/+</sup>) to null mouse(Tbx1<sup>-/-</sup>) such that Tbx1 mRNA dosage in Tbx1(NEO/NEO) was 0.25% as much as in Tbx1(+/+) by inserting the Frt-flanked neomycin resistant gene (NEO) driven by the PGK promoter in an intron between exon 3 and exon 4 of Tbx1.

The inner ear structure at E.14.5, when the membranous labyrinth of inner ear was formed mostly was compared among Tbx1(+/+), Tbx1(NEO/+), and Tbx1(NEO/NEO) in H.E. stained section.

As compared to Tbx1(+/+), Tbx1(NEO/+) showed the small size in cochlear. Tbx1(NEO/NEO) showed the common cavity and small size in cochlear. This result means that Tbx1 gene may show the dose dependent manner in cochlear morphogenesis, too. This may explain the variable permeability and expressivity of hearing impairment in DGS.

## **672 Morphogens Promote Neurite Outgrowth and Survival of Chick Otic Ganglion Neurons**

Kristen Fantetti<sup>1</sup>, Donna Fekete<sup>1</sup>

<sup>1</sup>Purdue University

Mechanosensory hair cells of the chicken inner ear are innervated by the peripheral processes of statoacoustic ganglion (SAG) neurons. Based on their expression patterns within and surrounding the chick inner ear, we hypothesize that morphogens may function to guide axons towards their peripheral sensory targets or may function as trophic factors for neurons once axons have reached their targets. To test these possibilities, three-dimensional collagen cultures were used to grow E4 chick SAG explants in the presence of either purified proteins or beads soaked in proteins. Explants were cultured under serum-free conditions for 24-40 hours, immunostained for  $\beta$ -tubulin and imaged with a confocal microscope. Neurite outgrowth was quantified by length and density measurements. SAG neurons were unresponsive to Wnts -1, -4, -5a, -6 and -7b presented *in vitro* and Wnts -4 and -5a delivered *in vivo* via retroviral vectors. Wnt bioactivity was confirmed using E6 chick spinal cord explants grown under comparable culture conditions. SAG neurons were unresponsive to FGF2. FGF2 reactivity with chicken cells was confirmed with a fibroblast survival assay conducted in collagen gel cultures. Purified Shh appeared to be toxic to SAG neurons when presented at high concentrations.

Conversely, explants displayed enhanced neurite outgrowth in the presence of a low concentration of Shh, as well as purified BMP4, BMP7, FGF8, FGF10 or FGF19. Cultures with increased neurite outgrowth also contained significantly fewer apoptotic cells, with no effect on cell proliferation, based on TUNEL and anti-phospho-histone-H3 labeling, respectively. When presented as point sources in a bead assay, all growth-promoting molecules but BMP7 enhanced outgrowth on the side of the explants facing the beads. These results suggest that members of the BMP, Shh and FGF morphogen families may influence SAG neurons both trophically and tropically *in vivo*. This work is supported by NIDCD.

## **673 The Level and Duration of Atoh1 Expression Controls Viability and Degree of Differentiation of Hair Cells in Mouse Inner Ear**

Ning Pan<sup>1</sup>, Israt Jahan<sup>1</sup>, Jennifer Kersigo<sup>1</sup>, Jeremy Duncan<sup>1</sup>, Benjamin Kopecky<sup>1</sup>, Bernd Fritzschn<sup>1</sup>

<sup>1</sup>University of Iowa

The organ of Corti is a highly ordered structure containing two different types of hair cells (inner hair cells and outer hair cells) surrounded by seven different types of supporting cells. The molecular mechanism regulating the topologically restricted cell type differentiation remains largely unknown. We recently showed that deletion of a bHLH gene *Neurod1* results in transformation of some outer hair cells in the apex into inner hair cell-like cells. This transformation appears due to premature expression of *Atoh1* gene, which is known to be essential for all hair cell differentiation. To directly test how the level and duration of *Atoh1* expression affect hair cell type differentiation, we generated an *Atoh1* conditional knockout (CKO) mouse line using *Tg(Atoh1-cre)*, in which the *cre* expression is driven by an *Atoh1* enhancer element. The mutant mice show transient limited expression of *Atoh1* in all hair cells. In the organ of Corti, there is progressive loss of all the inner hair cells and the majority of the outer hair cells. The remaining hair cells express hair cell marker *Myo7a*, attract nerve fibers, but do not differentiate normal stereocilia bundles. Some *Myo7a* positive cells persist into adult stages in the position of outer hair cells. Our data suggest that variable *Atoh1* expression levels and duration may control mechanotransduction development, viability, and maintenance of inner vs. outer hair cells. By comparing the list of *Atoh1* target genes in the cerebellum with the list of genes differentially regulated in the inner ear, we identified about 100 potential *Atoh1* target genes in the inner ear. Future directions: Using the genetically engineered *Atoh1* CKO mice, we can identify and quantify the expression levels of genes necessary for differentiation and long-term viability of different hair cell types. This will provide crucial information for regenerating specific hair cell types and reconstituting the organ of Corti.

## **674 The Expression of Fbxo45 in the Developing Inner Ear**

Mayumi Sakuraba<sup>1</sup>, Junko Murata<sup>1</sup>, Hirobumi Tada<sup>2</sup>, Shinsuke Shibata<sup>3</sup>, Kazusaku Kamiya<sup>1</sup>, Hideyuki Okano<sup>3</sup>, Katsuhisa Ikeda<sup>1</sup>

<sup>1</sup>Department of Otorhinolaryngology, Juntendo University School of Medicine, <sup>2</sup>Department of Physiology, Yokohama City University School of Medicine, <sup>3</sup>Department of Physiology, Keio University School of Medicine

Fbxo45 was recently identified as one of the RING finger-type E3s (ubiquitin-protein ligases) that functions at synapses and selectively expressed in the nervous system. Fbxo45 is thought to play an important role in the regulation of neurotransmission by modulating Munc 13-1 at the synapse from the results of Fbxo45 knockdown experiments in primary cultured mouse hippocampal neurons (Tada H et al., 2009). *Fbxo45*<sup>-/-</sup> mouse embryos, which die soon after birth according to respiratory distress, show abnormal innervation of the diaphragm and impaired synapse formation at neuromuscular junction (Saiga T et al., 2009).

We supposed, from the preceding papers described above, that Fbxo45 might be essential both in the neuronal innervation in the developing organ of Corti, and the neurotransmission at the synapse between hair cells and spiral ganglion neurons in adult mammals. As the first step to confirm this, we performed immunostaining of the developing cochlea by using the rabbit polyclonal anti-Fbxo45 antibody. The immunoreactivity (IR) of Fbxo45 was found weakly in the spiral ganglion region and not in the cochlear epithelium at the embryonic day 13.5 (E13.5). At E15.5, Fbxo45-IR was observed in the area including the prosensory region of the cochlear epithelium besides the spiral ganglion neurons. The IR of Fbxo45 became restricted in hair cells and innervating neurons at E17.5. The results may implicate the possible indispensable role of Fbxo45 in the hair cell innervation during mammalian inner ear development.

## **675 Regulation of POU4F3 Gene Expression by Binding of ATOH1 to a Conserved Distal Enhancer**

Masatsugu Masuda<sup>1,2</sup>, Didier Dulon<sup>3</sup>, Kwang Pak<sup>1,2</sup>, Lina Mullen<sup>1,2</sup>, Linda Erkman<sup>4</sup>, Allen Ryan<sup>1,2</sup>

<sup>1</sup>University of California San Diego, <sup>2</sup>VA Medical Center, <sup>3</sup>University of Bordeaux, <sup>4</sup>GeNeuro

The POU-domain transcription factor (TF) POU4F3 is expressed in the hair cells (HCs) of the inner ear, beginning shortly after commitment to the HC fate and continuing throughout life. It is required for terminal HC differentiation and survival. We generated transgenic mice in which eGFP expression was driven by 8.5 kb of *Pou4f3* genomic DNA 5' to the translation start site (*Pou4f3*-8.5-eGFP mice). eGFP was observed in developing Merkel cells and olfactory neurons as well as adult cochlear and vestibular HCs, mimicking the normal expression pattern of POU4F3 protein with the exception of adult outer HCs and ectopic expression in embryonic inner ear neurons. In outer HCs, eGFP expression was noted through the first

three postnatal weeks, but was absent by six weeks. The result suggests the existence of separate enhancers for different HC types. To identify critical gene regulatory elements for *Pou4f3* expression, we compared *Pou4f3* 5' genomic sequence between mammalian species separated by a substantial period (60-100 million years) of evolutionary time; mouse, human, dog, and cow. Bioinformatic analysis revealed three highly-conserved regions within the transgene: 400 bp immediately 5' to the *Pou4f3* ATG, a short sequence at -1.3 kb, and a longer region at -8.2 to -8.5 kb. The latter region contained E-box motifs that bind bHLH TFs, including motifs that can be activated by ATOH1. Co-transfection of HEK293 or VOT-E36 cells with human ATOH1 (hAtoh1) and the transgene as a reporter enhanced eGFP expression when compared to the transgene alone. Chromatin immunoprecipitation (ChIP) following transfection of VOT-E36 cells with hAtoh1-myc/flg showed a much more intense band for the -8.2-8.5 region than was observed with unselected DNA. ChIP enrichment was not observed for the two other highly-conserved 5' regions. The results are consistent with regulation of *Pou4f3* in HCs by ATOH1 binding at a distal enhancer.

(Supported by the research service of the VA and by NIH grant DC00139.)

## **676 Protein Transduction Into the Mouse Otocyst Using Arginine-Rich Cell-Penetrating Peptides**

Ryosei Minoda<sup>1</sup>, Tory Miwa<sup>2</sup>, Momoko Ise<sup>2</sup>

<sup>1</sup>Department of Otolaryngology-Head and Neck Surgery, Kumamoto University, Graduate School of Medicine, <sup>2</sup>Kumamoto University, Graduate School of Medicine

Manipulation of the developing inner ear is an attractive experimental strategy for investigating treatment modalities for inner ear diseases as well as for studying the course of inner ear development. The otocyst, which is formed by invagination of the otic placode on each side of the head at the level of the hindbrain at E9.5 in mice, may be the best target for this because it is a closed and isolated epithelial vesicle and the origin of the anatomical structure of the adult inner ear. The HIV type 1 TAT protein can enter cells when added to culture media. The protein transduction domain of the TAT protein, which contains a high proportion of arginine and lysine residues, has been identified as being responsible for its ability to penetrate the plasma membrane. Short peptide sequences such as the protein transduction domain of TAT are referred to as cell-penetrating peptides (CPPs). The CPPs comprise a class of short cationic peptides with the ability to traverse the cell membrane of many different types of mammalian cells. A wide variety of macromolecules have been attached to these peptides and subsequently internalized. Among the different CPPs, the arginine-rich CPPs have been the most widely studied. Simple poly-arginine peptides with an optimal length of 9-11 residues induce significantly higher cell penetration rates than TAT.

We achieved trans-uterine delivery (TUMI method) of enhanced green fluorescent protein (EGFP) fused to a nine-arginine peptide (EGFP-9R) into E11.5 mouse

embryonic otocysts. The EGFP signal was detected both in the lining cells of the otocysts and in their vicinity at 18 h post-injection. Mice injected with EGFP-9R had normal auditory and vestibular functions. These data suggest that protein transduction using poly-arginine may be a useful alternative strategy to commonly used gene delivery methods for delivering therapeutically relevant molecules to the developing inner ear.

The major application of CPPs is the transduction of proteins and peptides, as described above. Another application is CPP-mediated oligonucleotide delivery for the purpose of RNA-based gene silencing, which interrupts or suppresses gene expression.

### **677 Fate Map of Mouse Otic Cup Closure Reveals a Putative Lineage Boundary Along the Anterior/Posterior Axis of the Endolymphatic Duct**

Lingyan Wang<sup>1</sup>, Han Jiang<sup>1</sup>, Sonja Nowotschin<sup>2</sup>, Anna-Katerina Hadjantonakis<sup>2</sup>, John Brigande<sup>1</sup>

<sup>1</sup>Oregon Hearing Research Center, Oregon Health & Science University, <sup>2</sup>Developmental Biology Program, Sloan-Kettering Institute

A fate map describes what precursors in an organ will give rise to during development. Correlation of a fate map with known domains of gene expression provides insight into the genetic regulation of morphogenesis and cell fate specification. The inaccessibility of the mouse inner ear in utero has precluded construction of a fate map for this organ. We fate mapped the rim of the mouse otic cup using 2 methods: photoconversion of fluorescent protein followed by whole embryo culture (WEC), and microinjection of fluorescent tracers followed by open yolk sac culture (OYS). The Kikume Green-Red mouse exhibits widespread expression of KikGR, a photomodulatable green fluorescent protein that completely and irreversibly converts to red fluorescence upon exposure to short wavelength light. WEC supports otic development from the otic cup to the nascent vesicle stage, and OYS supports growth of the nascent vesicle to the endolymphatic duct (ED) outgrowth stage. The rim of the otic cup was subdivided into 12, 30-degree quadrants with positions 12 dorsal and 3 anterior. Precursors in a 50 $\mu$ m patch of otic epithelium in each of the 12 rim positions were photoconverted by a 350msec exposure to a 250 $\mu$ Watt pulse of 405nm light. Embryos were cultured for 24hr by WEC to the nascent otocyst stage and the distribution of red fluorescent precursors was documented by confocal microscopy. Otic epithelial precursors in the rim of the cup gave rise to daughters that form the ED, the anterior and posterior poles of the otocyst, and the otocyst lateral wall in a highly stereotyped fashion. Dil and DiO-labeled precursors in the nascent otocyst, which arose from positions 10-11 and 1-2 in the rim, gave rise to the ED after 24hr of OYS and appear to respect a boundary along the anterior/posterior axis of the ED. We discuss how this putative lineage boundary may be involved in specifying ED formation and the need for an in vivo fate map of the mouse otocyst.

(Support: NIH R01DC008595 and ARRA 03S2)

### **678 Lineage Analysis of the Embryonic Day 11.5 Mouse Inner Ear**

Han Jiang<sup>1</sup>, Kevin Beier<sup>2</sup>, Lingyan Wang<sup>1</sup>, Constance Cepko<sup>2</sup>, Donna Fekete<sup>3</sup>, John Brigande<sup>1</sup>

<sup>1</sup>Oregon Hearing Research Center, Oregon Health & Science University, <sup>2</sup>Department of Genetics, Harvard Medical School, <sup>3</sup>Department of Biological Sciences, Purdue University

Lineage analysis identifies which cell types arise from a common precursor. Assignment of lineally related cells to known domains of gene expression provides insight into the genetic regulation of patterning and cell fate. In mammals, otic precursors are born during the 2nd week of embryogenesis. We initiated lineage analysis of the embryonic day 11.5 mouse otocyst by transuterine microinjection of a retrovirus encoding the lineage label, human placental alkaline phosphatase (AP), and a variable 24-bp oligonucleotide tag. Serial, 14 $\mu$ m cryostat sections of perfusion-fixed, decalcified, postnatal day 6 inner ears were heat inactivated and AP+ cells were imaged to validate cell type. AP+ cells were microdissected and subjected to nested PCR to amplify the 24-bp tag. AP+ cells sharing the same tag were identified as clonally related. 508 AP+ cells were picked from 6 inner ears and 211 sequences were identified, of which, 145 were unique. 115 of those 145 sequences were from unrelated cells and 30 sequences were shared by cells lineally related. On average, there were five clones/ear (range: 2-10) and 3.2 cells/clone (range: 2-12 cells). Inner hair cells were related to one another and their supporting cells. Vestibular hair cells in the crista were related to one another, their supporting cells, and the nonsensory epithelium lining the ampulla. Hair cell/supporting cell clones were tightly clustered. By contrast, interdental cells, Cladius' cells, and spiral ganglion neurons were related to themselves and were dispersed over hundreds of microns. The large number of unrelated single cells and the small clone size suggest that most otic precursors were near their terminal mitoses at the time of viral integration. Lineage analysis at earlier embryonic stages will further increase clone size and composition to provide a full understanding of the types of cell fate choices otic precursors make and the timing.

(Support: NIH R01DC008595 and ARRA 03S2 [JB] and 2R01DC002756 [DF])

### **679 Wnt/ $\beta$ -Catenin Activity and Function in the Developing Chick Basilar Papilla**

Bonnie Jacques<sup>1</sup>, Alain Dabdoub<sup>1</sup>

<sup>1</sup>UCSD School of Medicine

Canonical Wnt/ $\beta$ -catenin signaling has been implicated in multiple developmental events including the regulation of proliferation, cell fate, and differentiation. Activation of the pathway leads to the down-regulation of GSK3 $\beta$ , which normally targets  $\beta$ -catenin for ubiquitin-dependent proteolysis, and the accumulation of  $\beta$ -catenin in the cytoplasm. This results in nuclear migration of  $\beta$ -catenin where it associates with the TCF/Lef transcription factors, and affects transcription of Wnt target genes.

In the avian basilar papilla (BP), Wnt/ $\beta$ -catenin signaling has been suggested to regulate hair cell formation and recent studies have implicated it in hair cell regeneration. Here we show that  $\beta$ -catenin is expressed throughout the developing sensory epithelium, and transfection of the epithelium with Wnt/ $\beta$ -catenin reporter constructs positively identified canonical Wnt activity throughout the BP. To begin to characterize its function in the developing BP, we performed *in vitro* gain-of-function experiments. Activation of the Wnt/ $\beta$ -catenin pathway between E5 and E7, a period representing the onset of cellular differentiation in the BP, resulted in a significant increase in the number of hair cells and an expansion in the overall size of the hair cell field. BrdU incorporation analysis suggested that this increase may be partly due to an up-regulation in proliferation within the Sox2-positive cells of the prosensory domain. Attempts at inhibiting this pathway are in progress. The robust induction of hair cells indicates a role for this cascade in sensory epithelium development. This data suggests that the Wnt/ $\beta$ -catenin pathway may regulate the size of the prosensory domain and hair cell formation.

### **680 Relationships Between Neuronal and Sensory Fates During Inner Ear Neurogenesis**

Xiaohong Deng<sup>1</sup>, Doris Wu<sup>1</sup>

<sup>1</sup>NIDCD/NIH

Neurons of the auditory and vestibular ganglia are derived from cells delaminating from the neurogenic domain of the otic epithelium at early stages of inner ear development. After neuroblast delamination, this neurogenic region is thought to split and eventually give rise to various sensory organs. Previous fate mapping studies suggest that vestibular and auditory neurogenic fates may be segregated early before neuroblast delamination from the otic epithelium, with auditory and vestibular neuroblasts exiting from the medial and lateral side of the neurogenic domain, respectively. Notably, this medial-lateral relationship also seems to apply to the location of the utricle and saccule that develop subsequently. Therefore, we investigated whether specification of a particular neuronal fate during neurogenesis also obligates the type of sensory organ that forms later. We determined the timing of vestibular neurogenic fate specification in the developing chicken inner ear, and then examined how this timing relates to the establishment of the utricular macula fate in normal and inner ears that have undergone a medial-lateral axial inversion at 19 somite stage *in ovo*, based on expression patterns of regional-specific genes such as *Pax2*, *Crabp-1*, *Gata3*, and *Synaptophysin*, as well as distribution of lipophilic dyes that were focally injected before surgery. Our preliminary results indicate that at 19 somite stage, when neuroblasts are actively delaminating from the otic epithelium, many aspects of the vestibular neurons and macula of the utricle appear to be specified and are resilient to our surgical translocations.

### **681 R-Spondin2 Is Required for Refinement of Patterning in the Sensory Epithelium of the Mouse Cochlea**

Joanna Mulvaney<sup>1</sup>, Andrew Yatteau<sup>1</sup>, Keiyo Takubo<sup>2</sup>, Alain Dabdoub<sup>1</sup>

<sup>1</sup>University of California San Diego, <sup>2</sup>KEIO University School of Medicine, Tokyo, Japan

R-spondins (RSPO) are secreted ligands, thought to play a role in the Wnt signaling pathways and have been shown to facilitate both canonical and non-canonical Wnt signaling. RSPOs potentiate canonical signaling by inhibiting action of the antagonist DKK and promoting phosphorylation of the Wnt coreceptor LRP6. They are thought to facilitate non-canonical Wnt signaling by interaction with Clatherin to promote endocytosis of the Wnt-Frizzled complex. Amongst other developmental processes, RSPOs have been implicated in limb, lung, vascular and craniofacial development, sex determination and myogenesis. Of the four members of the RSPO family, RSPO1, 2, 3 and 4, RT-PCR shows that at E15.5, a time of hair cell differentiation, only RSPO2 is expressed in the cochlea.

To localize and begin to determine its role, we show by *in situ* hybridization that in the mouse cochlea, concurrent with mechanosensory hair cell development, RSPO2 is highly dynamically expressed in the greater epithelial ridge. Expression of RSPO2 initiates between E13.5 and E14.5 and is rapidly upregulated but even more rapidly down regulated. Intriguingly, given the spatial separation between the domain of RSPO2 expression and the developing outer hair cells, examination of E18.5 mice homozygous null for RSPO2, reveals a consistent phenotype of one extra row of outer hair cells beginning in the midbase running to the apex. In addition to supernumerary outer hair cells, we observe an ectopic row of supporting cells. Measurements of the length of the cochlea and observations of stereociliary bundle planar polarity in the mutant are not significantly different to wild type animals allowing us to tentatively rule out a noncanonical Wnt signaling phenotype. Furthermore, data from our lab also suggests that RSPO2 does not mediate canonical Wnt signaling in the cochlea. We are currently investigating alternative potential signaling partners.

### **682 Regulation of P27<sup>Kip1</sup> by Sox2 Is Required to Maintain Quiescence of Neonatal and Juvenile Inner Pillar Cells in the Mouse Auditory Sensory Epithelium**

Zhiyong Liu<sup>1,2</sup>, Brandon Walters<sup>1</sup>, Thomas Owen<sup>1,3</sup>, Katherine Steigelman<sup>1</sup>, LingLi Zhang<sup>1</sup>, Marcia Mellado Lagarde<sup>1</sup>, Marc Valentine<sup>1</sup>, Yiling Yu<sup>1,4</sup>, Brandon Cox<sup>1</sup>, Jian Zuo<sup>1</sup>

<sup>1</sup>St. Jude Children's Research Hospital, <sup>2</sup>University of Tennessee Health Science Center, <sup>3</sup>University of Bath,

<sup>4</sup>Shanghai Medical School

Sox2 plays a critical role in cell fate specification during development and in stem cell formation. However, its role in post-mitotic cells is largely unknown. Sox2 is highly

expressed in supporting cells (SCs) of the postnatal mammalian auditory sensory epithelium, which, unlike non-mammalian vertebrate, remain quiescent, even after sensory hair cell damage. Here we acutely ablated Sox2 specifically in neonatal and juvenile SCs within the postnatal mouse auditory epithelium. We found that Sox2-deficient inner pillar cells (IPCs), a subtype of SCs, re-entered the cell cycle and proliferated. Interestingly, expression of p27<sup>Kip1</sup>, a cell cycle inhibitor, was repressed in Sox2-deficient IPCs. Furthermore, we also observed proliferation of IPCs when p27<sup>Kip1</sup> was acutely deleted, but p27<sup>Kip1</sup>-deficient IPCs still retained Sox2 expression. Moreover, the necessity of Sox2 and p27<sup>Kip1</sup> in maintaining IPC's quiescence declines with maturation. Finally, chromatin immunoprecipitation with Sox2 antibodies and luciferase reporter assays with the p27<sup>Kip1</sup> promoter support a mechanism by which Sox2 directly activates p27<sup>Kip1</sup> transcription in postmitotic IPCs. Together, our data demonstrate that Sox2 plays a novel role as a key upstream regulator of p27<sup>Kip1</sup> in the maintenance of the quiescence state of postmitotic IPCs. Our studies suggest that manipulating functions of Sox2 or p27<sup>Kip1</sup> is an effective approach for proliferation of auditory SCs, an initial but necessary step towards hearing restoration in mammals.

Grants: National Institutes of Health: DC06471 (J. Zuo), DC05168 (J. Zuo), DC008800 (J. Zuo), 1F31DC009393 (K. Steigelman); 1F32DC010310 (B. Cox); and CA21765; Office of Naval Research: N000140911014 (J. Zuo); the American Lebanese Syrian Associated Charities (ALSAC) of St. Jude Children's Research Hospital; and Travel Awards from Academic Programs of St. Jude Children's Research Hospital, University of Tennessee Health Science Center and Society of Developmental Biology (Z. Liu). Sir Henry Wellcome Fellowship (M. Mellado-Lagarde); J. Zuo is a recipient of The Hartwell Individual Biomedical Research Award.

### **683** Altered Otx, Netrin and Bmp Signaling Contributes to Semicircular Canal Defects in Chd7 Deficient Mice

Elizabeth Hurd<sup>1</sup>, Joseph Micucci<sup>1</sup>, Elyse Reamer<sup>1</sup>, Donna Martin<sup>1,2</sup>

<sup>1</sup>The University of Michigan Department of Pediatrics,

<sup>2</sup>Department of Human Genetics

Semicircular canal formation is a complex developmental process involving proliferation, epithelial-to-mesenchymal transition, and fusion of epithelial plates. Disruption of genes encoding transcription factors (*Dlx5*, *Otx1*, and *Gbx2*) or morphogenetic signaling proteins (*Bmps*, *Shh* and *Fgfs*) leads to malformations in semicircular canals. Chromatin remodeling enzymes have also been implicated in cell fate specification during embryonic developmental processes, including mesenchymal cell differentiation. Cell fate decisions are associated with various epigenetic modifications including histone acetylation and methylation. Despite advances in mouse genetics and chromatin biology, our understanding of epigenetic regulation in inner ear and semicircular canal development is incomplete. CHD7 is a chromatin remodeling protein

that is highly expressed in the developing ear and is required for semicircular canal development in both humans and mice. Here we report that mice with heterozygous loss of *Chd7* function (*Chd7*<sup>Gt/+</sup>) exhibit delayed canal genesis, delayed *Netrin1* expression throughout the inner ear and absent *Bmp2* expression in the lateral canal epithelium. *Bmp4* expression is variably absent from the presumptive posterior cristae in *Chd7*<sup>Gt/+</sup> embryos, and is completely absent from both *Chd7* conditional-null (*Foxg1-Cre;Chd7*<sup>Gt/lox</sup>) and germline-null (*Chd7*<sup>Gt/Gt</sup>) mutant embryos. *Otx1* and *Sox2* expression are also absent from *Chd7*<sup>Gt/Gt</sup> otocysts but reduced (*Otx1*) or preserved (*Sox2*) in *Chd7* conditional null embryos. Expression of the dorsal patterning genes *Lmx1a*, *Dlx5*, *Gbx2*, *Pax2* and *Jag1* is unaffected in *Chd7*<sup>Gt/+</sup> and *Chd7*<sup>Gt/Gt</sup> embryonic otocysts. We conclude that *Chd7* regulates expression of genes essential for semicircular canal development. Detailed analysis of the epigenetic modifications underlying these gene expression changes should provide insights into semicircular canal development and potential therapies for individuals with inner ear malformations.

### **684** Regulation of Neuron Content in Statoacoustic Ganglia by Insm1, a Zinc Finger Transcription Factor Expressed in Delaminating Otocyst Progenitors and Nascent Ganglion Neurons

Sarah Lorenzen<sup>1</sup>, Anne Duggan<sup>1</sup>, Jaime Garcia-Anoveros<sup>1,2</sup>

<sup>1</sup>Northwestern University, <sup>2</sup>Hugh Knowles Center for Clinical and Basic Science in Hearing and Its Disorders

*Insm1* is zinc finger type of transcription factor that is transiently expressed throughout the developing nervous system in late (not early) progenitors and nascent (not mature) neurons. In embryonic olfactory epithelium, *Insm1* promotes the transition of progenitors from apical, proliferative and uncommitted (neural stem cells) to basal, terminally-dividing and neuron-producing. Mice lacking the *Insm1* gene contain more apical progenitors and fewer olfactory receptor neurons. In addition, other types of nascent neurons require *Insm1* for proper differentiation or survival. As in the nose, the neuroepithelium of the otic placode contains progenitors that undergo mitosis apically to produce more progenitors, some of which remain apical to eventually produce epithelial cells (sustentacular in the nose and hair plus supporting cells in the inner ear). A different set of apically-generated progenitors migrate basally to produce primary sensory neurons (olfactory receptor neurons in the nose and spiral plus vestibular ganglion neurons in the inner ear). One notable difference is that, while in the nose the basally-migrating progenitors and soma of their neuronal progeny remain within the epithelium, in the ear the equivalent progenitors delaminate from the neuroepithelium and the resulting neurons reside in separate ganglia. We now find that delaminating progenitors from the otocyst and nascent neurons of statoacoustic ganglia express *Insm1*. Furthermore, mice lacking *Insm1* have fewer neurons in spiral and vestibular ganglia. Based on the similarities in

Insm1 expression pattern and Insm1 KO phenotype between embryonic olfactory epithelium and inner ear, we suspect that Insm1 promotes the delamination of progenitors from the otocyst. Based on the role of Insm1 in other types of neurons and of orthologous genes in flies and worms we suspect that Insm1 may also regulate the differentiation, survival and connectivity of nascent spiral and vestibular neurons.

### **685 Ryk, a Transmembrane Wnt Receptor, Plays a Role in Planar Cell Polarity in the Organ of Corti**

Willy Sun<sup>1</sup>, Bonnie Jacques<sup>1</sup>, Alain Dabdoub<sup>1</sup>

<sup>1</sup>UCSD School of Medicine

Planar cell polarity (PCP) refers to the uniform polarization of cells or cellular structures within the plane of an epithelium. The uniform orientation of the stereociliary bundles on the apex of cochlear mechanosensory hair cells is a distinctive example of PCP in a vertebrate organ system. This polarization is essential for accurate perception of sound as stereociliary bundles are only sensitive to vibrations in a single plane, thus hair cell transduction is dependent on the precise development of PCP. While the non-canonical Wnt/PCP signaling cascade has been shown to be responsible for the coordinated orientation of the stereociliary bundles; the underlying mechanism that regulates vertebrate PCP signaling remains to be fully elucidated.

Ryk, a 'related to tyrosine kinase' Wnt receptor, has been shown to play important roles in neurogenesis, axon guidance and synaptogenesis. Here we demonstrate that Ryk is expressed in the cochlea during hair cell differentiation. *Ryk* knockout mice have misorientation in the stereociliary bundles in mechanosensory hair cells demonstrating a role for Ryk in the non-canonical Wnt/PCP signaling pathway. Furthermore, our data indicate that Ryk genetically interacts with Vang-like 2 (*Vangl2*), a core component in PCP, to regulate uniform orientation of the stereociliary bundles. Polarization defects in mice that are heterozygote for both *Ryk* and *Vangl2* are more severe than either heterozygote demonstrating a genetic interaction between these two components in the regulation of PCP in the mammalian cochlea. Taken together, these findings indicate that Ryk is a component of the non-canonical Wnt pathway that functions in PCP regulation in the mouse cochlea.

### **686 Genetic Rescue of Hearing Loss in a Mouse Model of Muenke Syndrome**

Suzanne Mansour<sup>1</sup>, Chaoying Li<sup>1</sup>, Lisa Urness<sup>1</sup>

<sup>1</sup>University of Utah

FGF signaling plays dosage-sensitive roles at multiple stages of inner ear development. Loss-of-function genetic studies show that differentiation of cochlear pillar cells requires inner hair cell-expressed FGF8 signaling to support cell-expressed FGFR3. We studied auditory function in a mouse model of Muenke syndrome (FGFR3P250R). This mutation affects a residue in the extracellular, ligand-binding IgIII-like domain that is common to both the "b" and "c" FGFR3 isoforms, leading

to increased ligand-dependent receptor activation. Heterozygous Muenke model mice have hearing loss (HL) that shows relative sparing of the high frequencies, similar to, but more extreme than the HL of Muenke syndrome subjects. The basis for Muenke model HL is a cochlear supporting cell fate transformation from Deiters' to pillar cells, similar to, but more extreme than that seen in mice lacking the negative feedback regulator of FGF signaling, Sprouty2. Unlike in *Spry2*<sup>-/-</sup> mice, however, HL in Muenke model mice is not rescued by removing one copy of *Fgf8*. Therefore, we tested other cochlear *Fgf* genes, but removing one copy of *Fgf9*, *Fgf8* and *Fgf9*, *Fgf20*, or *Fgf3* also did not restore Muenke model hearing. Surprisingly, we found that removal of one copy of *Fgf10* effected highly efficient functional and structural rescue of the Muenke model inner ear phenotypes. Since neither *Fgfr1* nor *Fgfr2* expression was altered in Muenke model mice, and published studies show that FGF10 does not interact with wild type or Muenke mutant versions of FGFR3c, we hypothesize that Muenke model HL is caused by inappropriate activation of mutant FGFR3b by FGF10, which is strongly expressed in the developing Kolliker's organ, immediately adjacent to the inner hair cell. Progress in testing this hypothesis and determining the normal function of cochlear *Fgf10* will be presented.

### **687 Carbonic Anhydrase 3 Is Downregulated in the Cochlea of Pou3f4-Deficient Mice, a Model for Human DFN3 Deafness**

Ling Wu<sup>1</sup>, Borum Sagong<sup>2</sup>, Jae Young Choi<sup>1</sup>, Un-Kyung Kim<sup>2</sup>, Jinwoong Bok<sup>1</sup>

<sup>1</sup>Yonsei University college of medicine, <sup>2</sup>Kyungpook National University

X-linked deafness type 3 (DFN3), the most prevalent X-linked hereditary deafness, is caused by mutations in the POU3F4 gene, which encodes a member of the POU family transcription factors. We have previously shown that mutations identified in DFN3 patients abolish the transcriptional activity of POU3F4 protein. Thus, the hearing loss in DFN3 is most likely due to mis-regulation of genes important for cochlear development or function. However, downstream targets of POU3F4 in the cochlea remain unknown. As an effort to identify the genes regulated by POU3F4 in the cochlea, we performed microarray analysis using inner ears isolated from neonatal wild type and *Pou3f4*<sup>del-J</sup> mutant mice, a model for DFN3. Among the genes downregulated in the *Pou3f4*-deficient cochlea, Carbonic anhydrase 3 (*Car3*) is of particular interest. *Car3* encodes a cytoplasmic isozyme of carbonic anhydrase family, which has an activity for CO<sub>2</sub> hydration and also functions as an oxyradical scavenger. To better understand the possible role of *Car3* in inner ear development, we examined expression levels and domains of *Car3* in developing cochlea along with other carbonic anhydrase family genes by quantitative real-time PCR and in-situ hybridization. Each carbonic anhydrase gene is expressed in specific regions of the cochlea, but only *Car3* expression domain is closely associated with that of *Pou3f4*. Both *Car3* and *Pou3f4* are strongly expressed in developing otic fibrocytes in the cochlear lateral wall, which

is shown to be severely affected in Pou3f4-deficient cochlea. Furthermore, we found a consensus sequence for POU protein binding in the upstream promoter region of Car3 gene. These results suggest that Car3 may be a direct downstream target of Pou3f4 in the cochlea. We are currently investigating whether Pou3f4 regulates Car3 expression by directly binding to the consensus sequence using an in vitro assay system.

Supported by the Brain Korea 21 Project for Medical Science, Yonsei University

### **688 Cochlear Neurosensory Specification and Competence: You Gata Have Gata**

**Jeremy Duncan<sup>1</sup>, Bernd Fritzsche<sup>1</sup>**

<sup>1</sup>*Department of Biology, University of Iowa*

Early prosensory specification to develop competence in the otic epithelium is disrupted by mutations of *Eya1*, *Pax2*, *Sox2*, *Jag1*, and *Gata3*. How they contribute to the genetic network of the ear and organ of Corti development is unknown. These genes also interact with other factors expressed adjacent to or within the developing organ of Corti and provide the topographical information to respond to *Atoh1* expression and differentiate as orderly distributed inner and outer hair cells. We showed recently that *Gata3* coordinates all cochlear neurosensory development (Duncan et al., 2011 Int J. Dev Bio 55: 297).

*Gata3* is expressed throughout the early placode. As ear development continues *Gata3* is restricted to all prosensory areas except the saccule. It is transiently expressed in vestibular and permanently in spiral ganglion neuroblasts. *Gata3* is expressed in all cells of the organ of Corti through adult. Haploinsufficiency of *Gata3* causes the human disorder Hypoparathyroidism, Deafness, and Renal dysplasia syndrome, and has been linked in mice to early hair cell death. We investigated the role of *Gata3* in cochlear neurosensory specification utilizing a conditionally deleted *Gata3* line and two cre driver lines (*Foxg1<sup>cre</sup>* and *Pax2<sup>cre</sup>*). Although both cre lines are early on expressed in the inner ear, there are major phenotypic differences. While the *Foxg1<sup>cre</sup>·Gata3<sup>ff</sup>* deletion resulted in an ear closely matching that of the null mutant with a cochlear duct devoid of neurosensory cells, the *Pax2<sup>cre</sup>·Gata3<sup>ff</sup>* cochlear duct contained patches of partially differentiated hair cells flanked by *Sox2* positive cells lateral to outer hair cells. qRT-PCR and in situ hybridization of both mutants revealed how *Gata3* interacts with other prosensory genes to upregulate downstream genes. In particular, *Atoh1*, was reduced but not absent with the loss of *Gata3*, indicating that *Gata3* is one of a set of factors necessary for proper *Atoh1* level of expression.

### **689 Human Vestibular Sensory Epithelia: Defining the Environment**

**Ruth Taylor<sup>1</sup>, Shakeel Saeed<sup>1</sup>, Andrew Forge<sup>1</sup>**

<sup>1</sup>*University College London*

Explant human vestibular cultures are the only means to perform experimental studies upon human inner ear tissue. We have access to human sensory tissues from the vestibular system, obtained from patients undergoing surgery for acoustic neuromas (vestibular schwannomas).

In our preliminary studies of human tissue, we have examined the distribution of specific proteins within the utricle in particular those associated with supporting cell communication such as connexin 26 and 30. Interestingly, connexin 30 was found mainly to be present towards the basal region of the sensory epithelium in the body of the supporting cells close to the basement membrane whilst most connexin 26 expression was found in the underlying mesenchyme and not within the epithelium. Expression patterns for connexin 30 following hair cell loss are being examined. As with the mammalian organ of Corti, vestibular supporting cells are specialised for the uptake of glutamate via the glutamate-aspartate transporter (GLAST) localised to supporting cell membranes. In this study we show the presence of GLAST in human utricular tissue. Additionally we have successfully developed procedures to maintain human vestibular tissue for up to 23 days in culture. Quantification of hair cell loss, following exposure of explants to gentamicin for 48 hours, showed a continual decrease in hair cell number throughout the duration of culturing (21 days post-treatment), whilst untreated explant hair cell numbers were maintained over the same time period. Our studies will allow us to assess human vestibular explants with respect to known results from mouse experiments in order to compare the human vestibular sensory epithelia with similar tissue from other mammals.

### **690 A Comparison of the Effects of BDNF and NT-3 in the Deafened Guinea Pig Inner Ear**

**Cameron L. Budenz<sup>1</sup>, Hiu Tung Wong<sup>1</sup>, Bryan E. Pflugst<sup>1</sup>, Yehoash Raphael<sup>1</sup>**

<sup>1</sup>*University of Michigan, Department of Otolaryngology, Kresge Hearing Research Institute*

Auditory rehabilitation in the form of cochlear implantation (CI) requires at least a partially intact auditory neural pathway for proper functioning. Following deafness, there is a variable degree of spiral ganglion neuron (SGN) loss and peripheral auditory fiber (PAF) regression from the basilar membrane area (BMA). While CI is beneficial even in individuals with few remaining SGNs, CI outcomes may be enhanced with optimization of SGN survival and PAF presence. Prior work has demonstrated that administration of neurotrophins into the deafened cochlea increases the survival of SGNs and induces re-growth of PAFs into the BMA. Both BDNF and NT-3 are active in the development and maintenance of inner ear innervation. Here we compare the effects of BDNF and NT-3 delivered to the adult guinea pig inner ear via adeno-associated viral vectors one week following a neomycin-deafening procedure. We find that both BDNF and NT-3 induce robust re-growth of PAFs into the BMA; however, administration of BDNF is associated with a greater degree of fibrous tissue formation, which has the potential to significantly affect CI outcomes and complicate any revision surgery. Related work in the Pflugst lab, which will be reported separately, is underway to examine the effects of NT-3 on cochlear implant function in the adult guinea pig. Future work will be directed toward

determining whether there are differential effects of each neurotrophin on neural regeneration in the cochlear base versus the apex in deafened mature guinea pigs.

This work is supported by The Williams Professorship, and NIH/NIDCD grants DC-010412, DC-007634, T32 DC-005356, and P30 DC-05188.

### **691 Ad. BDNF Induces Nerve Fiber Regeneration Into the Auditory Epithelium of *Pou4f3* Mutant Mice**

**Hideto Fukui<sup>1</sup>, Hiu Tung Wong<sup>1</sup>, Lisa Beyer<sup>1</sup>, Yehoash Raphael<sup>1</sup>**

<sup>1</sup>*Kresge Hearing Research Institute, University of Michigan*

The regeneration of auditory nerve fibers is important for enhancing cochlear implant therapy outcomes and for restoring hearing function in conjunction with hair cell regeneration or stem cell transplantation. Many cases of hereditary hearing loss are aided by cochlear implant prostheses and would likely benefit from auditory nerve regeneration. *Pou4f3* mutant mice are known to lack hair cells and hearing, and thus serve as a model for nerve regeneration in ears with hereditary deafness. We analyzed inner ears of six week old *Pou4f3* mutant mice and determined that they have a flat epithelium with no hair cells and that few or no nerve fibers extend into this epithelium. We inoculated adenoviral vectors with a brain-derived neurotrophic factor gene insert (Ad.BDNF) into the scala media of one month old *Pou4f3* mice and sacrificed the animals two weeks later to assess nerve survival and fiber growth. Some ears were stained for F-actin, myosin VIIa and neurofilament and analyzed as whole-mounts. Other ears were prepared as plastic sections to assess the density and qualitative morphology of surviving spiral ganglion neurons. Our results show that two weeks after endolymph inoculation of Ad.BDNF, the diameter and number of nerve fibers in the auditory epithelium were increased compared to non-treated ears. Spiral ganglion cell density in Rosenthal's canal also was increased. These results show that virus-mediated overexpression of BDNF induced nerve fiber growth into the auditory epithelium of *Pou4f3* mutant mice. The data suggest that nerve fiber regeneration treatment may augment cochlear implant therapy for humans with hereditary hearing loss involving absence of hair cells due to *POU4f3* or other mutations.

Supported by The Williams Professorship and NIH/NIDCD grants DC-005356, DC-007634, DC-001634 and DC-05188.

### **692 Role of Notch Signaling in Hair Cell Regeneration of Mammalian Cochlea**

**Soumya Korrapati<sup>1</sup>, Angelika Doetzlhofer<sup>1</sup>**

<sup>1</sup>*Johns Hopkins University, School of Medicine, Center for Sensory Biology, Dept of Neuroscience*

Unlike in birds, humans and other mammalian species generate hair cells and the surrounding supporting cells only during embryonic development. In birds, following injury, supporting cells function as hair cell progenitors and replace lost hair cells by either cell division or direct trans-differentiation. One of the best candidate pathways for limiting supporting cell plasticity and inhibiting hair cell

regeneration in the mammalian cochlea is the Notch signaling pathway. Notch signaling negatively regulates hair cell differentiation in the developing cochlea. In addition, recent studies have shown that Notch signaling is still active in the terminally differentiated cochlea and that loss of Notch signaling results in a conversion of supporting cells into hair cells. To test if Notch limits hair cell regeneration in the differentiated cochlea, we developed a hair cell ablation/ hair cell regeneration assay using an organotypic cochlea culture system. Brief exposure of early postnatal cochlea cultures to the ototoxic drug gentamicin results in a rapid loss of hair cells without significantly damaging surrounding supporting cells. Addition of  $\gamma$ -secretase inhibitor, known to inhibit Notch signaling, results in robust hair cell regeneration in the hair cell damaged cultures. The newly formed hair cells express hair cell specific markers such as myosin VI and parvalbumin and display actin rich stereocilia on their apical surface. Using an inducible Cre line specifically expressed in supporting cells, we show these newly generated hair cells originate from surrounding supporting cells. Moreover, we will present evidence that Jagged1, a supporting cell specific Notch ligand, is a critical component of Notch signaling in the hair cell damaged cochlea. In summary, our findings suggest that Notch signaling functions in supporting cell maintenance in the hair cell damaged cochlea and release of Notch inhibition is sufficient to allow for supporting cells trans-differentiation into hair cells.

### **693 Relationship Between Vector Dose and Hair Cell Regeneration in the Mouse Vestibular System**

**Paul Enns<sup>1</sup>, Douglas E. Brough<sup>2</sup>, Jennifer Brantley<sup>3</sup>, Hinrich Staecker<sup>1</sup>**

<sup>1</sup>*University of Kansas*, <sup>2</sup>*GenVec Inc.*, <sup>3</sup>*Univeristy of Kansas*  
Atoh1 gene therapy has been demonstrated to induce generation of auditory and vestibular hair cells in a variety of injury models. Most studies have delivered the maximum volume dose of concentrated atoh1 containing vector to achieve a biologically relevant outcome. In this study adult C57Bl/6 mice were fed IDPN, a toxic nitrile compound that results in vestibular hair cell death. Efficacy of IDPN treatment was confirmed by rotarod testing. Ten days post IDPN feeding mice were injected with an Ad28 vector containing atoh1 driven by the glial fibrillary acidic protein promoter (Ad28.gfap.atoh1). Three different doses of vector were administered to mice ranging from 106 to 107 particle units (pu) of vector via the posterior semicircular canal. One to four months post treatment hair cell counts were determined by stereologic estimates of hair cell density. Analysis of type I and II hair cells, and supporting cells were carried out in the saccule and utricle. The contralateral untreated ear served as a control. Prior to analysis animals gross balance function was measured via rotarod testing. All test groups showed a statistically significant recovery in rotarod times. There was a dose related recovery in hair cell number. Untreated control animals that did not receive vector or

received IDPN and a sham vector showed no recovery of rotarod times and no recover of hair cell number.

Supported by NIDCD R01DC008424

### **694 Age-Dependent in Vivo Conversion of Mouse Cochlear Pillar and Deiters' Cells to Immature Hair Cells by Atoh1 Ectopic Expression**

**ZHIYONG LIU**<sup>1,2</sup>, Jennifer Dearman<sup>1</sup>, Brandon Cox<sup>1</sup>, Brandon Walters<sup>1</sup>, Lingli Zhang<sup>1</sup>, Olivier Ayrault<sup>1</sup>, Frederique Zindy<sup>1</sup>, Lin Gan<sup>3</sup>, Martine Rousset<sup>1</sup>, Jian Zuo<sup>1</sup>  
<sup>1</sup>St. Jude Children's Research Hospital, <sup>2</sup>University of Tennessee Health Science Center, <sup>3</sup>University of Rochester

Unlike non-mammalian vertebrates, mammals cannot convert inner ear cochlear supporting cells (SCs) into sensory hair cells (HCs) after damage, thus causing permanent deafness. Here, we achieved in vivo conversion of two SC subtypes, pillar cells (PCs) and Deiters' cells (DCs), into HCs by inducing targeted expression of Atoh1 at neonatal and juvenile ages in novel mouse models. The conversion only occurred in ~10% of PCs and DCs with ectopic Atoh1 expression and started with reactivation of endogenous Atoh1, followed by expression of multiple HC markers; a process that takes at least 3 weeks in vivo. These new HCs resided in the outer HC region, formed stereocilia, could take up FM4-64FX dye, and survived for more than 2 months in vivo; however, they surprisingly lacked prestin expression and mature HC morphology. In contrast, adult PCs and DCs no longer responded to ectopic Atoh1 expression, even after outer HC damage. Finally, permanent Atoh1 expression in endogenous HCs did not affect prestin expression, but caused loss of mature HCs. Together our results demonstrate that in vivo conversion of PCs and DCs into immature HCs by Atoh1 is age-dependent, and resembles initial normal HC development. Therefore combined expression of Atoh1 with additional factors holds therapeutic promise to convert PCs and DCs into functional HCs in vivo for regenerative purposes.

This work was supported by National Institutes of Health: DC06471 (JZ), DC05168 (JZ), DC008800 (JZ), DC010310 (BCC), CA096832 (MFR) and the Core Grant CA21765; the Office of Naval Research N000140911014 (JZ); the American Lebanese Syrian Associated Charities (ALSAC) of St. Jude Children's Research Hospital; travel awards from Academic Programs of St. Jude Children's Research Hospital, University of Tennessee Health Science Center, Society of Developmental Biology, and Howard Hughes Medical Institute Janelia Farm campus (ZL). JZ is a recipient of The Hartwell Individual Biomedical Research Award.

### **695 Death and Regeneration of Vestibular Hair Cells in the Pou4f3-Diphtheria Toxin Receptor Mouse Model**

**Justin Golub**<sup>1</sup>, Tot Nguyen<sup>1</sup>, Richard Palmiter<sup>1</sup>, Clifford Hume<sup>1</sup>, Ling Tong<sup>1</sup>, Edwin Rubel<sup>1</sup>, Jennifer Stone<sup>1</sup>  
<sup>1</sup>University of Washington

We describe a new method to efficiently kill vestibular hair cells (HCs) in adult mice engineered to express the diphtheria toxin (DT) receptor under control of the *Pou4f3* promoter. In utricles, DT injection caused 96% loss of HCs within 14 d. At 40 d post-DT, 17% of HCs were replaced, primarily in striolar and peristriolar regions. The lack of bromodeoxyuridine labeling in replacement HCs and the reduction in supporting cell (SC) numbers suggest HCs were regenerated via direct transdifferentiation. Using a reporter virus delivered only to SCs, we show that *Atoh1* transcriptional activity was upregulated in SCs and detected in HCs by 21 d post-DT, demonstrating that SCs directly transdifferentiated into HCs. FM1-43 was rapidly taken up into replacement HCs, indicating they had active mechanotransduction channels. Following DT injection in neonates, there was near-complete loss of utricular HCs, but HC numbers did not increase over time like in adults. Examination of lateral ampullae post-DT revealed no significant HC replacement in neonates but substantial (11-20%) HC replacement in adults. These observations demonstrated that adult mice have the capacity for some spontaneous regeneration of vestibular HCs, but this capacity, at least in our transgenic mouse model, is lacking in younger mice.

### **696 Lack of the Retinoblastoma Like-1 (P107) Gene Affects Organ of Corti Proliferation, Maturation and Homeostasis**

Laura Scheetz<sup>1</sup>, Taylor Mighell<sup>1</sup>, Lynette Smith<sup>2</sup>, Edward Walsh<sup>3</sup>, Joann McGee<sup>3</sup>, **Sonia Rocha-Sanchez**<sup>1</sup>  
<sup>1</sup>Creighton University, <sup>2</sup>University of Nebraska Medical Center, <sup>3</sup>Boys Town National Research Hospital

The Retinoblastoma (pRB) family of pocket proteins, namely Rb1, Rbl1 (p107) and Rbl2 (p130), are crucial components of a molecular pathway that mediates cellular responses to a variety of signals by controlling the activity of E2F transcription factors and the expression of their target genes during cell cycle progression. In normal conditions, pRB family members are inhibited by cyclin-dependent kinase complexes in response to growth factors. Studies carried on by our group and elsewhere suggest that inhibition of pRB family members (directly, or indirectly via modification of upstream genes) reduce their ability to regulate E2F transcription factors and can trigger unscheduled cell proliferation and generation of supernumerary hair cells (HCs) and supporting cells (SCs) in the mouse organ of Corti (OC). Expression of both Rb1 and p130 in the mouse OC has been previously described. Likewise, the roles of these two genes in HC and SC postmitotic quiescence have been established. Nevertheless, in spite of p107 well known roles in development and tumor suppression, its function in the inner ear and potential importance in HC regeneration

remains unclear. We have gathered histological, molecular and functional evidences suggesting specific roles for p107 in HC and SC proliferation, as well as OC early maturation, and functional homeostasis. As determined by microarray analyses comparing p107<sup>-/-</sup> and WT mouse OC, genes characterizing the p107 null state include a substantial number of genes encoding cell growth, maturation, and differentiation markers. Microarray also suggested upregulation of inhibitors of HC differentiation and SC markers, as well as downregulation of bona fide HC differentiation regulators. Correspondingly, RT-QPCR analyses confirmed microarray results and provided the base for understanding the potential molecular mechanisms underlying p107 function in the mouse OC.

### **697 Hair Cell Transdifferentiation in the Cristae of the Postnatal to Adult Mouse**

**Amber Slowik<sup>1</sup>**, Olivia Bermingham-McDonogh<sup>1</sup>, Byron Hartman<sup>1</sup>

<sup>1</sup>*Department of Biological Structure, University of Washington*

Balance disorders and vertigo are a significant health problem in the United States, with no current effective treatment for the loss of hair cells from the vestibular sensory organs. In non-mammalian vertebrates, hair cell regeneration occurs through transdifferentiation and/or proliferation of support cells. Previous evidence has shown that transdifferentiation of support cells into hair cells is possible in the developing mouse organ of Corti, but this capacity is lost shortly after birth. The loss of transdifferentiation potential in the early postnatal mouse cochlea is concomitant with down-regulation of activated Notch and its effectors, the Hes/Hey family of transcription factors. Analysis of Hes5 expression with in-situ hybridization and Hes5-GFP reporter mice suggests that Notch signaling may still be active in the adult cristae. In other systems where Notch signaling is maintained in the adult, including the subventricular zone and the hippocampal progenitor zone, adult neurogenesis is possible. This suggests that if Notch signaling is active, then the cristae of the adult mouse may retain the ability to generate new hair cells. In this study, we characterize the expression of Notch signaling components in the cristae of early postnatal to adult mice using quantitative real-time PCR. In addition, we describe the capacity for transdifferentiation in response to pharmacological inhibition of Notch as a function of age. Preliminary results suggest that Notch signaling is active in the postnatal and adult cristae and that it continues to maintain hair cell and supporting cell identities through lateral inhibition at P6, past the age where transdifferentiation of hair cells has been shown to last occur in the cochlea.

### **698 Resident Macrophages Are Not Required for Normal Hair Cell Regeneration in the Avian Cochlea**

**Mark Warchol<sup>1</sup>**, Keiko Hirose<sup>1</sup>

<sup>1</sup>*Washington University School of Medicine*

The avian cochlea contains a resident population of macrophages, but the precise function of those cells has

not been determined. Most cochlear macrophages reside in the hyaline cell region, immediately outside of the sensory epithelium. They become activated in response to ototoxic injury and migrate across the inferior border into the sensory region. The avian inner ear can also regenerate hair cells after some forms of ototoxic injury, and it has been speculated that macrophages may play a stimulatory role in this process. In order to determine whether macrophages contribute to regeneration, we examined regenerative proliferation and hair cell recovery in chick cochleae after eliminating most resident macrophages. Cochleae were placed in organotypic culture and treated for 24 hr with liposomally-encapsulated clodronate, which killed >90% of resident macrophages. Following macrophage depletion, hair cells were killed by treatment for 24 hr with 1 mM streptomycin. Control cochleae were cultured in parallel, but did not receive clodronate and contained normal numbers of macrophages. Examination of specimens at two days following ototoxic injury revealed no deficits in hair cell clearance. In all cases, hair cells were extruded from the lumenal surface of the sensory epithelium, and we observed no increase in hair cell debris in the macrophage-depleted specimens. In other specimens, proliferating cells were labeled by addition of BrdU to the culture medium. We found that macrophage depletion did not reduce the proliferation of supporting cells. However, the basilar membranes of macrophage-depleted cochleae contained fewer proliferative mesothelial cells, when compared with untreated controls. Finally, we quantified the numbers of new hair cells after seven days recovery, and observed no differences in regeneration between normal and macrophage-depleted cultures. Ongoing studies are using similar methods to assess the role of macrophages in the regenerating utricle.

### **699 Hearing Improvement by Gene Therapy in a Mouse Model Created by a Conditional Knockout of Gjb2 Gene, Preliminary Study**

**Takashi Iizuka<sup>1</sup>**, Hideki Mochizuki<sup>2</sup>, Tomoko Nihira<sup>2</sup>, Takeshi Nara<sup>3</sup>, Ayako Inoshita<sup>1</sup>, Akira Minekawa<sup>1</sup>, Misato Kasai<sup>1</sup>, Hiroko Okada<sup>1</sup>, Hiromi Kasagi<sup>1</sup>, Kazusaku Kamiya<sup>1</sup>, Osamu Minowa<sup>4</sup>, Tetsuo Noda<sup>5</sup>, Katsuhisa Ikeda<sup>1</sup>

<sup>1</sup>*Department of Otorhinolaryngology, Juntendo University Faculty of Medicine*, <sup>2</sup>*Department of Neurology, School of Allied Health Sciences, Kitasato University*, <sup>3</sup>*Department of Molecular and Cellular Parasitology, Juntendo University Faculty of Medicine*, <sup>4</sup>*Mouse Functional Genomics Research Group, Riken*, <sup>5</sup>*Department of Molecular Biology, Cancer Institute*

Hereditary deafness affects about 1 in 2,000 children and mutations in the *GJB2* gene, coding the gap junction, are the major causes in various ethnic groups, which require normal gene transfer in the early developmental stage to prevent deafness. Mice present an ideal model for inner ear gene therapy because their genome is being rapidly sequenced and their generation time is short. In order to establish the fundamental therapy of congenital deafness, we generated targeted disruption of mouse *Gjb2* gene

using Cre recombinase controlled by P0. Using this animal model, we examined the potential of gene therapy in the inner ear, using the homozygous mutant mice and the heterozygous mutant mice.

Adeno-associated virus vectors (AAV) carrying *Gjb2* gene were injected into the scala tympani through the round window of the cochlea of the homozygous mutant adult and neonatal mice. In the adult mice, the expression of Cx26 was observed in the fibrocytes of the spiral ligament and spiral limbus, but was not seen in the supporting cells and failed to improve the hearing ability. However, in the neonatal mice, the expression of Cx26 was seen in the supporting cells and the hearing ability was improved. We are going to assess the histology of the cochlea in detail. The present paper will present the preliminary data regarding introduction of the virus vector into the *Gjb2* knockout mouse at the neonatal stage.

### **700 Auditory Hair Cell Induction from Human Amniotic Membrane**

**Kyoung Ho Park<sup>1</sup>, Sang Won Yeo<sup>1</sup>**

<sup>1</sup>*Catholic University, College of Medicine*

We tried to demonstrate the differentiation into the auditory hair cells and neurons from stem cells of human amniotic membrane.

This result may raise the possibility of treating the intractable sensorineural hearing loss with amniotic membrane, which is regeneration of inner ear hair cells and neurons.

We isolated the stem cells from the human amniotic membrane and the isolated stem cells were confirmed with the FACS. We used culture medium with EGF and bFGF for neurosphere differentiation, and another culture medium with GDNF, BDNF and NT-3 for hair cell and neuronal differentiation from stem cells. Then, we have done immunofluorescence staining and RT-PCR for characterization of neurosphere and differentiated cells on 7th and 14th culture days.

We could isolate SCs from amniotic membrane, confirmed with FACS with MSC markers, and we demonstrated that MSCs could be differentiated into neural progenitor cells, neurons, and hair cells in a different composition of growth factors within the culture medium. MSCs of amniotic membrane can be differentiated into specific cells in the inner ear, which are auditory hair cells and neurons.

So it can be used in cell therapy for the regeneration of hair cells and neurons in cochlea.

### **701 Transplantation of Human Induced Pluripotent Stem Cell-Derived Neural Progenitors for Regeneration of Spiral Ganglion Neurons**

**Koji Nishimura<sup>1</sup>, Takayuki Nakagawa<sup>1</sup>, Kiyomi Hamaguchi<sup>1</sup>, Juichi Ito<sup>1</sup>**

<sup>1</sup>*Department of Otolaryngology, Head and Neck Surgery, Graduate School of Medicine, Kyoto University*

Several studies have identified embryonic stem (ES) cells as the most promising candidate to replace spiral ganglion neurons (SGNs). Nevertheless, ES-cell based therapy is

complicated by immune rejection and ethical problems. In this context, a method for the reprogramming of somatic cells into pluripotent state was established (Takahashi and Yamanaka, 2006). Previously, we investigated the potential of murine induced pluripotent stem (iPS) cells for use as a source of transplants for the restoration of SGNs and found that they compared favorably with ES cells. (Nishimura et al., 2009). This study aimed to investigate the potential of human iPS cell-derived neural progenitors as transplants for regeneration of SGNs. Human iPS cells generated by retroviral transfection of four reprogramming factors (kindly donated by RIKEN, Japan) were differentiated towards neural fate under conditions of stromal (PA6) cell co-culture with a combination of small-molecule inhibitors of bone morphogenic protein and activin/nodal signals (Morizane et al., 2011). Immunocytochemical and RT-PCR analyses demonstrated that the expression level of pluripotent markers decreased and that of neural markers increased during a course of the neural induction. As transplants, human iPS cell-derived cells under the neural induction protocol for 21 days were used. As recipient animals that exhibited degeneration of SGNs, we generated the following animal models: ten 4-week-old Hartley guinea pigs treated by local application of ouabain via the round window and ten 8-week-old C57BL/6 mice receiving local injection of 3-nitropropionic acid into posterior semicircular canal. And then, human iPS cell-derived neural progenitors ( $4.0 \times 10^5$  cells) were transplanted into the modiolus of the basal portion of the cochlea. Histological analysis performed four weeks after transplantation is presented at the meeting.

### **702 Progression of Neuron-Like Phenotype in Cochlear Non-Sensory Epithelial Cells Induced by Overexpression of Transcription Factor Combinations**

**Wenke Liu<sup>1</sup>, Rachel M. Weichert<sup>2</sup>, Alain Dabdoub<sup>2</sup>, Robin L. Davis<sup>1</sup>**

<sup>1</sup>*Rutgers University*, <sup>2</sup>*University of California San Diego*

Emerging therapeutic approaches for age-related and noise-induced hearing loss target cell replacement of damaged or missing neurons in the cochlea. It is known that during development, non-sensory epithelial cells in the cochlea can be redirected to a neuronal identity (Puligilla et al. *J. Neurosci.* 2010), suggesting that cochlear epithelial cells could serve as an abundant local source of induced neurons.

Here we report that overexpressing transcription factor *Ascl1* (Viebuch et al. *Nature.* 2010) by electroporation induces neuron-like membrane responses in embryonic cochlear non-sensory support cells. 77% of *Ascl1* overexpressing cells (n=22) exhibited inward inactivating current with an average peak amplitude of  $-0.24 \pm 0.04$  nA at a step potential of  $-10$  mV from  $-80$  mV holding potential. Action potentials in the same cells appeared immature due to their relatively long latency ( $42.6 \pm 7.46$  ms, n=4) and small amplitude ( $60.36 \pm 9.58$  mV, n=4) at threshold level. Cells transfected with control vector (n=13) showed no inward currents. The neuron-like phenotype was further refined by co-transfection of *Ascl1* with *NeuroD1*. 50% of

the double-transfected cells (n=10) showed inward currents with larger average amplitude ( $-0.35 \pm 0.14$  nA, n=5). To date, our data is consistent with the idea that action potentials recorded from the double-transfected cells have shorter latency ( $26.65 \pm 7.55$  ms, n=2) and higher amplitude ( $65.78 \pm 15.41$  mV, n=2) action potentials at threshold. The inward currents induced by Ascl1 and NeuroD1 overexpression were completely abolished by 1  $\mu$ M tetrodotoxin.

Our results determined that transfections with multiple transcription factors aid in reprogramming non-sensory epithelial cells to acquire enhanced neuron-like functions. Future studies will focus on identifying additional factors that give rise to neuronal phenotypes that more closely resemble those specific to spiral ganglion neurons.

### **703 Growing Very Hairy Spheres: An in Vitro Model to Study the Biology of Cilia**

Rebecca Bieber<sup>1</sup>, Fuxin Shi<sup>2</sup>, Mark Parker<sup>2,3</sup>

<sup>1</sup>Emerson College, <sup>2</sup>Massachusetts Eye & Ear Infirmary,

<sup>3</sup>St. Elizabeth's Medical Center

One challenge in stem cell biology is to create a model in which cochlear stem cells can differentiate into hair cells in vitro. Several studies have shown that individual cells in a cochlear-sphere can express the hair cell marker myosin 7a, but few studies have demonstrated that these spheres can also express ciliated cells in enough quantity to be useful for in vitro analysis. Here we present simple in vitro method of stimulating immortomouse organ of Corti cells to sprout prodigious microvilli and a single primary cilium. House Ear Institute organ of Corti-1 (OC1) cells isolated from the adult immortomouse organ of Corti were cultured for 3 days either as plated cells or floating spheres on low adherent culture wells in both proliferating (33 °C) and differentiating conditions (39 °C). Cells were then processed for scanning electron microscopy (SEM), RT-PCR, or immunohistochemistry. The results show that after 3 days in culture, OC1 cells grown as floating aggregates in proliferating conditions exhibit significantly more microvilli (mean=576; s.d.=173 microvilli per cell) than plated cells grown in proliferating conditions (mean=256; s.d.=34 microvilli per cell) or cells grown as floating spheres (mean=41; s.d.=46 microvilli per cell) or plated (mean=61; s.d.=19 microvilli per cell) in differentiating conditions. In proliferating conditions, the microvilli were readily apparent in low power light microscopy and many cilium were connected by cross-links observed in SEM. Additionally, each cell exhibited a single primary cilium that labeled with alpha-actin. Individual proliferating cells expressed supporting cell markers such as GFAP, TAK1 and prox1. OC1 cells cultured in differentiating conditions expressed significantly fewer microvilli per cell and lost their primary cilium. These results indicate that OC1 cells cultured as floating aggregates in proliferating conditions may be a useful in vitro tool for the study of primary cilium biology, ciliary development, or function of cross linking proteins.

### **704 Response of Cochlear Blood Flow in Mice Challenged by Inhaled Oxygen Level Measured by Optical Microangiography**

Suzan Dziennis<sup>1</sup>, Roberto Reif<sup>1</sup>, Zhongwei Zhi<sup>1</sup>, Xiaorui Shi<sup>2</sup>, Alfred L. Nuttall<sup>2</sup>, Ruikang Wang<sup>1</sup>

<sup>1</sup>University of Washington, <sup>2</sup>Oregon Health & Science University

Proper cochlear blood flow is important to avoid ischemic damage which may contribute to hearing loss. Measuring cochlear blood flow in response to various physiological stresses has remained challenging, due to the lack of a sensitive detection method and the difficulty in accessing the organ. Optical microangiography (OMAG) is a label free, non-invasive imaging technique capable of measuring slow blood flow velocities such as those found in the blood vessel networks of the cochlea. In this study we used OMAG to measure the *in vivo* changes in cochlear blood flow in mice under different inhaled oxygen concentrations. Measurements were recorded at 1 minute intervals throughout a 20 minute procedure. The relative changes in blood flow were determined, and the heart rate (HR) and arterial blood oxygen saturation (SpO<sub>2</sub>) were measured simultaneously by using a pulse oximeter. The changes in cochlear blood flow and HR were directly correlated to the changes in inhaled oxygen, while the changes in SpO<sub>2</sub> were inversely correlated. In conclusion, we use the OMAG method for the first time to demonstrate a physiologically induced change in cochlear vessel blood flow. That flow is highly sensitive to changes in inhaled oxygen concentrations, which is most likely a compensatory response. This study also demonstrates the feasibility of using OMAG as a non-invasive method for determining changes in cochlear vessel blood flow.\* SD and RR contributed equally to the work. Supported by NIH grants NIDCD DC 000105 (AN), DC 010844 (XS), NIDCD DC 010201 (RW) and NIBIB EB009682 (RW).

### **705 Effects of Sudden Unilateral Deafness on Bilateral Spiral Ganglion Cell Density**

Sebastian Jansen<sup>1</sup>, Moritz Gröschel<sup>1,2</sup>, Jan Wagner<sup>2</sup>, Nikolai Hubert<sup>1</sup>, Arneborg Ernst<sup>2</sup>, Dietmar Basta<sup>1,2</sup>

<sup>1</sup>Humboldt University of Berlin Department of Biology,

<sup>2</sup>Dept. of ENT at UKB, University of Berlin, Charité Medical School

Recently we were able to show a contralateral hearing loss in unilateral deafened guinea pigs. This effect is possibly a result of contralateral hair cell or spiral ganglion cell loss. The aim of this study was therefore to evaluate the effect of mechanical unilateral deafening in normal hearing guinea pigs on unilateral cochlear hair cell and bilateral spiral ganglion cell density. Normally hearing guinea pigs were unilaterally deafened by the destruction of intra-cochlear structures in the first turn of the cochlea (wide cochleostomy, insertion of a filled silicon tube filling the whole diameter of the cochlea). Deafened animals and normal hearing controls were exposed to a standardized acoustic environment with a level of up to 65dB for 90 days. After this stimulation ABR measurements were performed on both

groups and the cochleae were harvested for further exploration. Cochleograms of the basilar membranes were created and hair cell counts performed for the frequencies between 400 Hz and 25 kHz. The modiolus was cut, stained and the spiral ganglion cell density was determined. Hair cell counts showed no significant loss of contralateral outer hair cells in the deafened animals compared to the controls. The evaluation of the spiral ganglion cell density showed significant effects only on the deafened side. As no outer hair cell damage on the contralateral cochlea was detected, the decreased ABR thresholds seem to be due to plastic changes in the spiral ganglion cells and possibly in the central auditory pathway. The present results show clearly the impact of interaural interaction in unilateral deafness.

### **706 Hydrogen Peroxide-Induced Cell Death in Mouse Vestibular Hair Cells**

**Jerneja Stare<sup>1</sup>, Giselle Boukhaled<sup>1</sup>, Melissa Vollrath<sup>1</sup>**  
<sup>1</sup>*McGill University*

Ototoxic insults, including noise exposure, aminoglycoside antibiotics, and cisplatin, are thought to induce hair cell death through a common pathway mediated by the production of reactive oxygen species (ROS). A number of studies have taken advantage of this by using the ROS hydrogen peroxide (H<sub>2</sub>O<sub>2</sub>) to probe the mechanisms and morphological changes associated with hair cell death. These have given insight into cell death pathways and otoprotective mechanisms in guinea pig sensory epithelia and HEI-OCI cells. However, very few studies have investigated the effects of H<sub>2</sub>O<sub>2</sub> application on intact sensory epithelia, and none have attempted to standardize an assay for the mouse model.

We are developing a H<sub>2</sub>O<sub>2</sub> assay to study hair cell death in the mouse utricle. We are treating *in vitro* utricle cultures with low (0.1mM) to high (1mM) concentrations of H<sub>2</sub>O<sub>2</sub> for three hours. In immunology literature, low H<sub>2</sub>O<sub>2</sub> concentrations have been shown to promote cell viability, whereas intermediate and high concentrations have been shown to induce apoptosis and necrosis, respectively. Using FM1-43 as a marker of healthy hair cells, and the nuclear marker propidium iodide to identify dying cells, we are able to use fluorescent microscopy techniques to correlate cell viability with changes in H<sub>2</sub>O<sub>2</sub> concentration. To test the effectiveness of this assay, we are measuring changes in gene expression of common pro-apoptotic, pro-survival, and antioxidant genes.

This assay will enhance our understanding of the effects of ROS on mouse hair cells and support future studies on the molecular mechanisms of hair cell death and otoprotection.

### **707 Differences Between Cochlear Fibrocyte Culture Cells from CD/1 Mice Grown on Different Collagen Substrates**

**David Furness<sup>1</sup>, Ahmad Sheikh<sup>1</sup>, James Randle<sup>1</sup>, Shanthini Mahendrasingam<sup>1</sup>**  
<sup>1</sup>*Keele University, Staffordshire, UK*

Degeneration of fibrocytes in the spiral ligament (SL) is evident in models of presbycusis. Fibrocyte replacement is one possible way to arrest this process. Cultured

fibrocytes are a potential source of replacement cells, but culture cells, typically grown on collagen I, are larger and flatter than native fibrocytes. In SL, the extracellular matrix contains little collagen I. We therefore immunolabelled sections of native CD/1 mouse ligament for several different collagens, to establish which were present, and then grew cultures on different appropriate collagen substrates to see whether cell morphology and expression of proteins was affected. Cells derived from frozen stocks or grown as primary cultures on type I collagen were harvested, seeded onto coverslips coated with collagen I, II, V or IX and grown for several days. They were fixed and labelled with antibodies to various marker proteins such as S-100, aquaporin 1, Na,K-ATPase, caldesmon, tubulin or the actin stain phalloidin, visualised by appropriate secondary antibodies conjugated to fluorescent dyes, and examined by confocal microscopy. Some cultures were prepared for scanning electron microscopy. Cells grown on all collagens appeared similar to each other and there were both large flattened cells, and small spindle shaped cells. However, the cells from the large population on collagen II, V and IX were smaller than those on collagen I. All markers were expressed, but the labelling intensity in a selection of cells was frequently more intense, especially for caldesmon, on collagens II, V and IX. These data suggest that substrate influences the growth of the fibrocytes in culture, affecting morphology and expression patterns of characteristic proteins. Selection of an appropriate substrate, or substrate combination, may be used to modify culture cell phenotype. This will be important in developing cultures best suited for transplantation to repair the SL.

Supported by the Grand Charity and DRUK.

### **708 Survival Signalling in Auditory Hair Cells**

**Daniel Bodmer<sup>1</sup>**  
<sup>1</sup>*University Basel*

Auditory hair cells exist in a finely tuned balance between survival and cell death: exposure to cellular stress disrupts this balance and if the stress is severe, apoptosis-promoting pathways predominate and the cells die.

Lately, survival pathways which operate in hair cells have been defined. A goal of our laboratory is to characterize these signalling pathways in normal inner ears and inner ears exposed to a variety of different forms of stress, such as ototoxic substances and noise overexposure.

Using different approaches such as proteomics with sensitive reverse protein microarrays which allow generating of high fidelity data for protein expression profiling of low levels or transient states of protein abundance as well as knock-out mice with defined lesions in genes coding for proteins involved in intracellular signalling we were able to characterize survival signalling pathways in auditory hair cells.

A molecular biology approach is able to define signalling pathways involved in survival signalling of auditory hair cells. The understanding of molecular events involved in hair cell survival signalling might be of importance in future

prophylactic or therapeutic approaches to prevent/treat hearing loss.

### **709 AICAR Induced Mitochondrial Biogenesis in the Inner Ear**

**Teresa M. Wilson<sup>1</sup>, Irina Omelchenko<sup>1</sup>, Xiaorui Shi<sup>1</sup>, Alfred L. Nuttall<sup>1</sup>**

<sup>1</sup>*Oregon Health & Science University*

Mitochondrial defects are the underlying cause for a variety of hearing-related impairments including noise-induced hearing loss, presbycusis, and several inherited forms of hearing disorders. Currently, the importance of mitochondrial biogenesis to hair cell physiology or that of the non-sensory cells in the cochlea is poorly understood. The transcriptional co-activator, peroxisome proliferator-activated receptor- $\gamma$  coactivator-1 $\alpha$  (PGC-1 $\alpha$ ), is the key regulator of mitochondrial function increasing both mitochondrial energy metabolism and biogenesis. Numerous studies have demonstrated that activation of 5' AMP activated protein kinase (AMPK), either in response to exercise or to pharmacological agents such as 5-aminoimidazole-4-carboxamide-1- $\beta$ -D-ribofuranoside (AICAR) or metformin, leads to significantly increased expression and activity of PGC-1 $\alpha$  and, consequently, the up-regulation of factors involved in mitochondrial biogenesis and respiratory function. At the same time, AMPK activation in endothelial cells results in increased antioxidant expression and reduced reactive oxygen species generation. In this study, we examined whether AICAR could: 1. Affect mitochondrial biogenesis in the inner ear; and 2. Protect against noise-induced hearing loss. We found that AICAR treatment led to increased levels of phosphorylated AMPK $\alpha$  as well as PGC-1 $\alpha$  transcript levels in the cochlea. Higher amounts of the mitochondrial fission protein, FIS1, were detected in both auditory hair cells and marginal cells of the stria vascularis following extended AICAR treatment. Auditory brainstem response analysis following noise exposure demonstrated that AICAR treatment accelerated recovery from acoustic trauma. These results demonstrate that mitochondria in auditory hair cells and cells of the stria vascularis have the capacity to be dynamically regulated with increasing energy demands. Supported by grants 5R01DC000105 (ALN), 1R01DC010844 (XS), and P30DC005983.

### **710 Calcitonin Gene-Related Peptide (CGRP) Exacerbates Excitotoxic Trauma at Inner Hair Cell (IHC) -Spiral Ganglion Neuron (SGN) Synapses in Organotypic Cochlear Explant Cultures**

**Qiong Wang<sup>1</sup>, Dylan Todd<sup>1</sup>, Andrew F Russo<sup>2</sup>, Steven H Green<sup>1</sup>**

<sup>1</sup>*Department of Biology, University of Iowa*, <sup>2</sup>*Department of Molecular Physiology & Biophysics, University of Iowa*

Calcitonin gene-related peptide (CGRP) is one of the neurotransmitters of the efferent innervation of the cochlea. SGNs express all three members of the CGRP receptor complex and CGRP likely participates in lateral olivocochlear regulation of type I SGN responses to IHCs.

Efferent pathways are generally protective against acoustic trauma, with acetylcholine being important for this effect. CGRP negatively regulates cholinergic responses at the neuromuscular junction so we hypothesized that CGRP may exacerbate trauma to IHC-SGN synapses. We tested this directly using an organotypic cochlear culture that preserves synaptic interactions between hair cells and SGNs. We found that CGRP at concentrations up to 10 nM alone does not reduce the number of afferent terminals on IHCs. Exposure to 0.5 mM kainic acid (KA) in these cultures causes rapid degeneration of type 1 SGN synapses on IHCs resulting in complete loss of synapses in 2 h (Wang & Green, *J Neurosci*, 2011). A partial loss occurs with 0.1 mM KA. CGRP exacerbates excitotoxic trauma: inclusion of CGRP (0.1-10 nM) with 0.1 mM KA results in near complete loss of synapses. Cyclic AMP-dependent protein kinase (PKA) is a downstream effector of CGRP and we show that inhibition of PKA is protective against excitotoxic trauma. Our data suggest that the underlying mechanism is a PKA-dependent increase in surface expression of AMPA-type glutamate receptors. This implies a role for CGRP in normally increasing sensitivity of SGNs to glutamate at the IHC-SGN synapse. Under pathological conditions, this can result in increased synaptic damage in excitotoxicity and, possibly, acoustic trauma.

### **711 Effect of Aspiration of Perilymph During Stapes Surgery on the Endocochlear Potential of Guinea Pig**

**ryoukichi ikeda<sup>1</sup>, kazuhiko nakaya<sup>1</sup>, hidetoshi oshima<sup>1</sup>, takeshi oshima<sup>1</sup>, tetsuaki kawase<sup>1</sup>, toshimitsu kobayashi<sup>1</sup>**  
<sup>1</sup>*tohoku university*

Background: Sensorineural hearing loss (SNHL) is one of the most dreaded complications of stapes surgery, which is often performed if the footplate of the stapes is fixed in the oval window (otosclerosis), and is one of the most delicate otologic procedures requiring very fine manipulation of instruments in a narrow area. Suction applied to the vestibule through the oval window during stapes surgery is considered a primary risk for postoperative sensorineural hearing impairment. This study investigated the mechanism of acute phase change in cochlear function caused by aspiration of the opened oval window.

Methods: Guinea pigs were divided into three groups: Stapes footplate removed without suctioning (6 animals), with indirect suctioning (5 animals), and with direct suctioning of the vestibular perilymph (6 animals). Endocochlear potentials (EPs) were measured at the second turn of the cochlea, and temporal bones were examined histologically.

Results: Removal of the stapes footplate without suctioning caused little change in the EP (original value, 80.12  $\pm$  3.52 mV), indirect suctioning caused minor decline of the EP of 9.14  $\pm$  1.84 mV, and partial recovery ensued, whereas direct but gentle suctioning, resulting in dry vestibule, caused reduction in the EP of 16.38  $\pm$  6.63 mV, and recovery was not observed or incomplete. No animals showed profound decrease in the EP.

Conclusion: Gentle suctioning and removal of the vestibular perilymph can cause mild decrease in the EP even without damaging the inner ear structures. Therefore, suctioning of the perilymph should be avoided during stapes surgery because acute hearing loss can result even without damaging the inner ear structures. However, hearing loss may not be profound, if suctioning is not vigorous enough to cause damage to the inner ear structures.

## **712 Auditory Brainstem Response Thresholds and the Tissue Response to Cochlear Implantation in Hearing Guinea Pigs**

**Stephen O'Leary<sup>1</sup>**, Peter Monksfield<sup>2</sup>, Hayden Eastwood<sup>1</sup>, Timothy Connolly<sup>3</sup>, Melanie Souter<sup>4</sup>, Andrew Chang<sup>5</sup>, Gordana Kel<sup>1</sup>

<sup>1</sup>University of Melbourne, <sup>2</sup>University Hospitals Birmingham, <sup>3</sup>Geelong Hospital, <sup>4</sup>Canterbury Hospital, New Zealand, <sup>5</sup>Royal Brisbane Hospital

**Aim:** To determine whether the tissue response to cochlear implantation (CI) influences residual hearing. Specifically, we assessed whether the extent of intracochlear foreign body response (FBR) one month after CI surgery influences post-operative hearing by correlating these factors in 76 guinea pigs from four hearing-preservation CI experiments conducted in our laboratories.

**Methods:** All guinea pigs had normal hearing prior to implantation and underwent cochlear implantation with a silastic/platinum dummy electrode. Pure tone auditory brainstem response (ABR) thresholds were estimated from the implanted ear in response to tone-pips prior to surgery, and at 1 and 4 weeks postoperatively. The cochleae were then fixed in paraformaldehyde, decalcified, paraffin embedded, and mid-modiolar sections were prepared. The treatment groups studied included 2 mg/ml systemic dexamethasone administered 1 hour before implantation, either 2% local dexamethasone or 200 µg n-acetyl cysteine applied to the round window for 30 minutes prior to CI, animals inoculated against keyhole-limpet hemocyanin (KLH), or controls.

**Results:** ABR thresholds (pure tone average 8-32 kHz) were elevated at one week post implantation and then either recovered substantially, remained elevated or progressively deteriorated. A more extensive FBR was associated with a greater threshold shift (i.e. poorer hearing) 4 weeks after surgery, but large post-operative threshold shifts were sometimes observed even when there was a minimal FBR. There was a significant correlation between the percentage of scala tympani (ST) occupied by the FBR and ABR threshold shifts between 1 and 4 weeks after surgery; threshold recovery was associated with minimal FBR only.

**Conclusions:** Hearing following CI is associated with the extent of the FBR within ST. These results support the theory that following CI surgery cochlear mechanics may be dampened by the presence of fibrosis within ST.

## **713 Identifying Cochlear Trauma During a Simulated Cochlear Implantation in Gerbils with a Sloping Noise-Induced Hearing Loss**

**John M. Pike<sup>1</sup>**, Baishakhi Choudhury<sup>1</sup>, Omar Awan<sup>1</sup>, Faisal I. Ahmad<sup>1</sup>, Christine E. DeMason<sup>1</sup>, Kristine Falk<sup>1</sup>, Hira Hasnain<sup>1</sup>, Oliver F. Adunka<sup>1</sup>, Douglas C. Fitzpatrick<sup>1</sup>  
<sup>1</sup>University of North Carolina at Chapel Hill

Cochlear implants are increasingly being provided to patients that have some residual hearing but poor speech understanding. An emerging goal in such patients is to preserve the residual hearing during the cochlear implant procedure and use electroacoustic stimulation (EAS) to improve post-surgical outcomes. However, intracochlear damage during cochlear implantation can reduce the preservation of residual hearing. Such trauma could potentially be identified and avoided if the surgeon could monitor the status of hearing preservation during the surgical procedure. To achieve this capability, we have developed a gerbil model of cochlear implantation and determined that reductions in the cochlear microphonic (CM), and to a lesser degree the compound action potential (CAP), can be used as sensitive markers of intracochlear trauma (e.g., Campbell et al., 2010, *Otol. and Neurotol.* 31:1391-1398). Previous experiments have been done in animals with normal hearing to provide the most sensitive preparation and with a rigid electrode to cause controlled amounts of damage. However, the more clinically relevant condition is with a flexible electrode and a sloping hearing loss with no high frequency hearing but relatively well preserved sensitivity to low frequencies. Here, we report results of simulated implantation using a flexible electrode in a noise-induced hearing loss (NIHL) gerbil model with a sloping hearing loss and anatomical pattern of hair cell loss similar to that of EAS patients. Interestingly, damage to the basal cochlea, which was as far as the electrode could reach, produced CM reductions derived from apically-located hair cells. Reductions were present if a breach in the BM occurred, but were also present in cases with an intact BM after histological inspection. These results indicate that reductions in the CM can be used as a physiological marker for interaction of an implant electrode with cochlear structures located in deaf regions of the cochlea.

Supported by NIDCD T32-DC005360 and the MED-EL Corporation.

**714 Silicone Electrode Arrays Eluting Dexamethasone Protect Against Electrode Insertion Trauma (EIT)-Induced Elevations in Hearing Thresholds and Hair Cell Damage: A Dose Response Study**

Thomas Van De Water<sup>1</sup>, Jorge Bohorquez<sup>2</sup>, Esperanza Bas<sup>1</sup>, Enrique Perez<sup>1</sup>, Isabel Bueno<sup>1</sup>, Chhavi Gupta<sup>1</sup>, Adrien Eshraghi<sup>1</sup>, Soeren Schilp<sup>3</sup>, Carolyn Garnham<sup>3</sup>, Fred Telischi<sup>1</sup>

<sup>1</sup>Univ. of Miami Ear Institute, Department of Otolaryngology, Univ. of Miami Miller School of Medicine, <sup>2</sup>Department of Biomedical Engineering, University of Miami, <sup>3</sup>MED-EL, Innsbruck, Austria

Background: Micronized DXMb released from silicone-electrodes protects the organ of Corti against EIT-induced hearing loss in a guinea pig model of EIT-induced hearing loss.

Material and Methods: Experimental animals were adult pigmented guinea pigs; hearing thresholds were obtained by recording auditory evoked brain stem responses (ABRs) via a dura contacting screw electrode in response to 0.5, 1, 4, 16 kHz pure tone stimuli. Thresholds were determined by a deconvolution program developed by JB. Electrodes of 4 types: 1) silicone; 2) silicone + 10% DXMb; silicone + 1% DXMb; and silicone + 0.1% DXMb were inserted purposefully with additional moderate trauma to a depth of 5 mm into the scala tympani via a cochleostomy. At the end of the 3 mo. period of hearing evaluation cochleae were fixed, organ of Corti whole mounts dissected and stained for the presence of hair cells, nerve fibers and synaptic proteins.

Results: Cochleae implanted with silicone electrodes experienced > 30 dB SPL increase in ABR thresholds for all 4 frequencies and a significant loss ( $p < .05$ ) of hair cells from all turns at 3 mo. post-electrode insertion trauma (EIT), in contrast the ABR threshold increase at 3 mo. post-EIT in the silicone/10%DXMb electrode ears was < 5 dB SPL for all frequencies and there was no significant loss ( $p > .05$ ) of hair cells from any of the cochlear turns. The 1% and 0.1% silicone electrodes also protected hearing against EIT-induced losses but in a dose dependent manner with initial ABR threshold elevations taking a longer period of time post-EIT to return to base line levels. All groups of animals had similar patterns of an initial elevation of ABR thresholds for all frequencies but only the silicone electrode arrays containing dexamethasone regained normal pre-trauma ABR threshold levels.

Conclusion: There was a highly significant level of protection of hearing thresholds against permanent EIT-induced losses in the cochleae receiving the DXMb-eluting electrodes.

**715 Local Pre-Treatment of the Cochlea with AM-111 Prevents Electrode Trauma-Induced Hearing and Cell Loss in an Animal Model of Cochlear Implantation**

Adrien Eshraghi<sup>1</sup>, Chavi Gupta<sup>1</sup>, Thomas Van De Water<sup>1</sup>, Jorge Bohorquez<sup>1</sup>, Carolyn Granham<sup>2</sup>, Esperanza Bas Infante<sup>1</sup>, Maria Victoria Talamo<sup>1</sup>

<sup>1</sup>University of Miami Miller School of Medicine, <sup>2</sup>Medel corporation

Background: Electrode insertion during cochlear implantation causes both acute and delayed hearing loss. AM-111 is an inhibitor of JNK activation of c-Jun, Our earlier work showed that using an osmotic pump, AM-111 can prevent electrode insertion trauma induced hearing loss. The objective of the present study is to test the otoprotective effect of AM-111 placed with Hylumed gel at round window and to better understand the molecular mechanisms involved in AM-111 protection

Methods:Hearing tests (ABR) post electrode insertion trauma (EIT) were performed at days 1, 3, 7,14, 30, 60 and 90 in three treatment groups: 1- EIT; 2- pre-treated with hyaluronate gel ½ hr before EIT. 3- pre-treated with hyaluronate gel with AM-111 ½ hr before EIT. Contralateral ears were controls. FITC-Phalloidin staining performed for hair cells counts to compare IHC and OHC viability at 90 days. Immunostaining for HNE, activated Caspase-3 and phospho-c-Jun performed at 24 hrs post-trauma for: EIT, EIT pre-treated with hyaluronate/AM-111 and contralateral control ears.

Results: There was a progressive increase in ABR thresholds post-EIT in the cochleae of EIT/untreated and EIT/hyaluronate-only treated animals. There was no significant increase in hearing thresholds in cochleae from either EIT/AM-111 treated or unoperated, control ears. Post-EIT immunostaining of both HCs and support cells (SCs) demonstrated the presence of HNE, but activation of Caspase-3 was present only in SCs while p-c-Jun was present only in HCs of the EIT only cochlear specimens. There was no immunostaining for either HNE, Caspase-3 or p-c-Jun in the AM-111 cochlear specimens.

Conclusions: Local delivery of AM-111 ½ hr before CI prevented EIT-induced hearing loss. This result was stable at 3 months. AM-111 prevented the programmed cell death of both HCs and SCs.

**716 Hydrogen Can Protect Outer Hair Cell Loss and Hearing Loss from Noise Exposure Through the Stabilization of PH Values**

Ning Yu<sup>1</sup>, Yan Lu<sup>1</sup>, Shiming Yang<sup>1</sup>, Weiyan Yang<sup>1</sup>, Suoqiang Zhai<sup>1</sup>

<sup>1</sup>Institute of Otolaryngology, The Chinese PLA General Hospital

Noise is a common environmental factor to cause hearing loss. Many studies have been performed on protection and treatment of the noise-induced hearing loss. However, its deafness mechanisms still remain largely undetermined and it also lacks effective methods of protection and treatment. In this study, we investigated the protective effect of hydrogen on noise-induced hearing loss. Guinea

pigs were used and exposed by impulse noise (157 dB SPL at peak level, 100 times). Animals were administered intraperitoneally at 1 hr before noise exposure by saturated hydrogen saline (1 ml/100g weight). The control animals were given by the same amount of normal saline or no injection. Auditory brainstem response (ABR) and blood gas (pH values) were measured immediately after noise exposure and on post-exposure day 1, 2, 4, and 8. Immediately after noise exposure, pH values of saturated hydrogen saline group were stable and maintained around 7.4, while pH values in saline control group and no treatment group were significantly decreased to 7.19 ( $P < 0.05$ ). ABR thresholds in saturated hydrogen saline treated animals were increased by 85 dB SPL. However, the increase was less than that in the non-treated animals ( $p < 0.05$ ). We also examined outer hair cell morphology and succinate dehydrogenase (SDH) activity at post-exposure day 8. The saturated hydrogen saline treated animals had deep SDH staining with more regular cellular arrangement in comparison with other two groups. The surviving outer hair cells were  $116.50 \pm 2.38$ ,  $44.50 \pm 10.02$ , and  $45.17 \pm 12.15$  in saturated hydrogen saline group, normal saline group, and non-treated group, respectively. The hydrogen group had significantly more surviving cells ( $P < 0.05$ ). Our findings suggest that intraperitoneal injection of saturated hydrogen saline can stabilize pH values, which may lead to protection of hair cells from noise-induced damage and hearing loss.

#### **[717] Inhaled Hydrogen Gas Therapy for Prevention of Noise-Induced Hearing Loss (NIHL)**

**Takeshi Matsunobu**<sup>1</sup>, Takaomi Kurioka<sup>1</sup>, Akihiro Shiotani<sup>1</sup>  
<sup>1</sup>*Dept. of Otolaryngology, National Defense Medical College of Japan*

It is widely accepted that reactive oxygen species (ROS) formed in the inner ear in response to high-intensity noise play an important role in noise-induced hearing loss (NIHL). Recent studies have revealed that molecular hydrogen (H<sub>2</sub>) has great potential for selectively reducing cytotoxic ROS, such as hydroxyl radicals (.OH).

This study examined the potential of hydrogen gas to protect NIHL and auditory hair cells from ROS-induced damage, using guinea pigs. We tested this hypothesis with inhaled 1.45% H<sub>2</sub> in air for 5 hours a day in five days continuation after exposed to 121 dB SPL 4-kHz octave band noise for 5 hours. Animals in each group underwent measurements for auditory brainstem response (ABR) before and immediately after the noise exposure, and then at 2, 4 and 7 days after the noise exposure. ABR measurement revealed that there was a better improvement in the threshold shift for the H<sub>2</sub>-treated group as compared to that of non-treated group at 4, 7 days after noise exposure. Furthermore outer hair cells (OHCs) loss of cochlea were examined using phalloidin-stained surface preparation specimens at 7 days after noise exposure. A significant higher survival rates of OHCs were observed of the H<sub>2</sub>-treated group as compared to that of non-treated group in the basal and middle turns. Immunohistochemical analyses for 8-hydroxy-2-

deoxyguanosine (8-OHdG) were performed to examine the amount of oxidative DNA damage that occurred in guinea pig cochlea. Strong immunoreactivities against 8-OHdG were observed in the inner ear tissues of the non-treated group, but in the H<sub>2</sub>-treated group the 8-OHdG signals decreased.

In conclusion, these findings strongly suggest that inhaled hydrogen gas treatment protects against DNA damages by NIHL in organ of Corti and might possibly have therapeutic effects for acute sensorineural hearing loss, including NIHL.

#### **[718] Brain-Derived Neurotrophic Factor Deletion Prevents Noise-Induced Damage in the Mammalian Cochlea**

**Annalisa Zuccotti**<sup>1</sup>, **Wibke Singer**<sup>1</sup>, **Lukas Rüttiger**<sup>1,3</sup>, **Christoph Franz**<sup>1</sup>, **Dietmar Hecker**<sup>2</sup>, **Stephanie Kuhn**<sup>3</sup>, **Hyun-Soon Geisler**<sup>1</sup>, **Iris Köpschall**<sup>1</sup>, **Karin Rohbock**<sup>1</sup>, **Katja Gutsche**<sup>4</sup>, **Julia Dlugaiczyk**<sup>2</sup>, **Walter Marcotti**<sup>3</sup>, **Bernhard Schick**<sup>2</sup>, **Thomas Schimmang**<sup>4</sup>, **Marlies Knipper**<sup>1</sup>  
<sup>1</sup>*University of Tübingen*, <sup>2</sup>*Universitätsklinikum des Saarlandes*, <sup>3</sup>*University of Sheffield*, <sup>4</sup>*Universidad de Valladolid*

Brain derived neurotrophic factor (BDNF), is a secretory neurotrophin known to regulate neurotransmitter release, synaptic proteins, inhibitory circuits and plasticity. Due to early postnatal lethality of BDNF null mutants the function of BDNF for maturation of balanced circuits in the adult auditory system is not understood. We generated a conditional BDNF knockout (KO) leading to viable animals lacking BDNF in the auditory system (BDNF<sup>Pax2</sup> KO). Hearing thresholds in BDNF<sup>Pax2</sup> KO were determined and correlated with outer hair cell (OHC) and inner hair cell (IHC) function. IHCs' Ca<sup>2+</sup>-dependent membrane capacitance, the synaptic vesicle secondary releasable pool size, and ribbon numbers were studied, particularly in high frequency cochlear turns. The results could be linked to a reduced wave I amplitude size at the level of the auditory brainstem responses (ABRs). Hair cell related damage following noise exposure was completely prevented in BDNF<sup>Pax2</sup> KOs. We suggest that the failure of BDNF up-regulation in these mutants led to protection from acoustic trauma, likely caused by enhanced efferent GABAergic input, and maintenance of immature axo-somatic synaptic contacts.

#### **[719] Alpha Lipoic Acid and Noise Induced Hearing Loss: A Prevention and Treatment Trial**

**Cherylea Browne**<sup>1</sup>, **Mayryl Ratanapongleka**<sup>1</sup>, **Gerald Muench**<sup>1</sup>, **Carl Parsons**<sup>1</sup>, **John Morley**<sup>1</sup>  
<sup>1</sup>*The University of Western Sydney*

There are currently no effective treatments for Noise-Induced Hearing Loss (NIHL), however, recent studies have shown that certain antioxidants can, to some extent, protect against NIHL. There is some evidence to suggest a link between NIHL and oxidative stress, and antioxidants may play a role in reducing the damaging effects of reactive oxygen species within the peripheral auditory

system. Our study measured changes in hearing thresholds following acoustic trauma in animals given Alpha Lipoic Acid (ALA), a potent antioxidant, either before or after the acoustic trauma. Male Long Evans rats (n = 16) were separated into 4 experimental groups; (1) pre-ALA (n = 5); 1 week of daily ALA s.c. injections (100mg/kg) + saline followed by acoustic trauma, (2) pre-saline (n = 5); 1 week of daily saline s.c. injections followed by acoustic trauma, (3) post-ALA (n = 3); acoustic trauma followed by 2 weeks of daily ALA s.c. injections (100mg/kg) + saline and (4) post-saline (n = 3); acoustic trauma followed by 2 weeks of daily saline s.c. injections. The acoustic trauma consisted of a 16 kHz bandpass (1/10th octave noise (112 dB SPL)) for 1-hour. The hearing thresholds of the rats in each group were assessed by recording Auditory Brainstem Responses at 0, 4, 8, 16 or 32 days following the acoustic trauma. The experimental procedures were approved by the Animal Ethics Committee of UWS (#A9201). Our hypotheses were that animals treated with ALA would exhibit less hearing loss than controls (saline treated), and the animals pre-treated with ALA would have a reduced hearing loss compared to animals post-treated with ALA. We found that hearing thresholds in rats pre-treated with ALA recovered faster than control (pre-saline treated) rats, while the post treatment with ALA had no effect on threshold recovery rates compared to control (post-saline treated) rats. Our results suggest that antioxidants taken prior to acoustic trauma may assist in the rate of recovery of hearing thresholds.

#### **720 Long-Term Effectiveness of HPN-07 in Treatment of Noise-Induced Hearing Loss**

**Ning Hu<sup>1</sup>**, Richard Kopke<sup>1,2</sup>, Don Nakmalia<sup>1</sup>, Xiaoping Du<sup>1</sup>, Wei Li<sup>1</sup>, Robert Floyd<sup>3</sup>

<sup>1</sup>Hough Ear Institute, Oklahoma City, OK, <sup>2</sup>Oklahoma Medical Research Foundation, Departments of Physiology and Otolaryngology, OUHSC, <sup>3</sup>Oklahoma Medical Research Foundation, Oklahoma City, OK

HPN-07 is a nitron-based free radical trap, which appears to suppress oxidative stress in a variety of disorders and biological models. We have reported that early intraperitoneal administration of HPN-07 can attenuate hearing threshold shift induced by acute acoustic trauma (AAT). Since continuous free radical formation and oxidative damage lasts for a period up to two weeks after the noise exposure, early intervention with antioxidant drugs, such as HPN-07, not only can rescue the damaged cells and tissues, but also may block continuous free radical formation and prevent the on-going oxidative damage. The present study was conducted to test this hypothesis. A chinchilla AAT model was used by exposing animals for 6 hours to 4 kHz OBN at 105 dB SPL. HPN-07 was intraperitoneally administered to animals for 3 days starting at 4 hours after AAT. ABR and DPOAE were measured on 3, 10, 21 and 180 days after AAT. At the terminal stage of 180 days, compound action potential (CAP), cochlear microphonics (CM) and endocochlear potential (EP) were measured. The results showed that, EPs of both HPN-07 treated and untreated groups were

close to the normal range, suggesting that the function of the stria vascularis recovered to normal. ABR threshold shifts of both groups were gradually and significantly attenuated over time, the degree of threshold recovery of the treated group was significantly greater. DPOAE amplitude and threshold shifts of the treated group were also significantly attenuated over time; by contrast, those of the untreated were almost flat across time. CAP and CM results confirmed the significant hearing recovery of the treated group. These findings support early intervention with HPN-07 to rescue AAT-induced hearing loss provides long-term effects in improving hearing recovery. The mechanism may involve interrupting continuous free radical formation in hair cells and/or retro-cochlear tissues. (Work supported by ONR Grant #N00014-09-1-0998)

#### **721 Melatonin Prevents Noise Induced Hearing Threshold Shift and Hair Cell Loss in Rat**

**Sungdo Jung<sup>1</sup>**, Myung-Whan Suh<sup>1</sup>, Chung-Ku Rhee<sup>1</sup>, Kye Hoon Park<sup>2</sup>, Jae-Yun Jung<sup>1</sup>

<sup>1</sup>Dankook University, <sup>2</sup>Soonchunhyang University Cheonan Hospital

Noise causes damage of the auditory system leading to hearing loss. The aim of this study was to investigate preventive role of melatonin, which is known to have anti-apoptotic effect, for noise induced hearing loss (NIHL) in rat. Forty-four adult Sprague-Dawley rats were randomly divided into six groups. Narrow band noise(16kHz) at 120dB for 6 hours was used to induce NIHL. We used two different dose (0.4mg/kg for low dose group, 4mg/kg for high dose group) of melatonin, which were all injected intraperitoneally (IP) four times. IP injection was given one day before, immediately before first and second noise exposure and one time between first and second noise exposure (total four times). Group C was not exposed to noise and treated with vehicle. Group LM and HM were not exposed to noise and treated either with low dose or high dose melatonin. Group NO was exposed to noise and treated with vehicle. Group NL and NH was exposed to noise and treated with either low dose or high dose melatonin.

The hearing thresholds at 4, 8, 12, 16 and 32 kHz were measured by auditory brainstem response (ABR) before the noise exposure and also at 1st, 7th, 14th and 21th day after exposure. Morphological assessment for hair cell damage was performed using the scanning electron microscope (SEM). Apoptosis activity was also compared using Western blotting of caspase-3 in each group. We observed consistent threshold increase (centered at 12 kHz) up to 90 dB SPL until 3weeks after noise exposure. Rats treated with melatonin before and during noise exposure showed significantly less hearing loss. However, there was no difference between the two different dose groups (NH, NL). Hair cell loss was significantly attenuated by administration of melatonin when observed with SEM. Melatonin treatment also reduced caspase-3 activity in the noise exposed cochleae. Preventive treatment with melatonin attenuates hearing threshold shift by reducing

outer hair cell damage. This protective effect is assumed to be related with inhibiting caspase-3 mediated apoptosis. We could not find dose-dependent protective effects in this study.

### **722 Bioconversion of *Scutellaria Baicalensis* Enhances Otoprotective Effect Against Noise Induced Hearing Loss in Mouse**

**Bin Na Hong<sup>1,2</sup>, Keun Ha Park<sup>1</sup>, Ha Na Hong<sup>1</sup>, Tong Ho Kang<sup>1</sup>**

<sup>1</sup>*Kyung Hee University,* <sup>2</sup>*Nambu University*

Noise induced hearing loss (NIHL) has been thought to mainly damage the sensory hair cells of the cochlea through mechanical and metabolic mechanisms. Several pharmacological approaches have been attempted to preventing or treating hair cell damage and hearing loss caused by NIHL. This investigation examines bioconversion of *Scutellaria baicalensis*(SB) which is a natural product contains various flavonoides enhances otoprotective effect against NIHL in mouse. Mouse received orally treatment with SB, bioconversion SB (BSB), baicalin, baicalein, and N-acetyl cysteine beginning 30 min. prior to noise exposure and continuing through this study. All subjects were exposed to 4-kHz pure tone noise at 120-dB SPL for 3h. Hearing threshold shift was assessed by auditory brainstem response (ABR) with tone bursts and clicks, respectively, following noise exposure. Central auditory function was evaluated by auditory middle latency responses (AMLR). Cochlear function was determined based on transient evoked otoacoustic emissions (TEOAEs). Additionally, cochlear hair cell morphology was investigated after noise exposure. The bioconversion has increased baicalein level in the SB through enzymatic hydrolysis of ¥â-D-glucuronide. The BSB efficacies in ABR, TEOAE, and morphologic results were better than SB efficacy. These findings suggest that baicalein is an active constituent in the SB, and bioconversion of SB potentially enhances auditory function from noise-induced hearing loss.

### **723 Transplatin Attenuates Noise Induced Hearing Loss by Inhibiting a TRPV1 and NOX3 Dependent Inflammatory Response**

**Debashree Mukherjea<sup>1,2</sup>, Kelly Sheehan<sup>1</sup>, Tejbeer Kaur<sup>2</sup>, Sarvesh Jajoo<sup>2</sup>, Leonard P Rybak<sup>1,2</sup>, Vickram Ramkumar<sup>2</sup>**  
<sup>1</sup>*Southern Illinois University School of Medicine, Dept. of Surgery, Springfield, Illinois,* <sup>2</sup>*Southern Illinois University School of Medicine, Dept. of Pharmacology, Springfield, Illinois*

Noise induced hearing loss (NIHL) is a significant problem in the United States. Chronic noise exposure leads to irreversible damage to inner ear structures and hearing loss. There are no known treatments available for NIHL. Recent data from our laboratory, as well as others, have led to the hypothesis that NIHL is initiated by the generation of reactive oxygen species (ROS) in the cochlea which promote inflammation, leading to damage or death of cells in the inner ear. Mediators of this inflammatory response include the cochlear specific

NADPH oxidase, NOX3 (a primary source of ROS generation) and transient receptor potential V1 (TRPV1), a nonspecific cation channel, which is induced by ROS and participates in the cochlear inflammation. Increased expression of stress response genes, such as NOX3 and TRPV1, as well as inflammatory genes, such as TNF- $\alpha$ , COX2 and iNOS, were elevated within 48 h of noise exposure and persisted even at 21 days post noise exposure. Thus, targeting NOX3 and/or TRPV1 for inhibition could constitute a viable treatment option for NIHL. We have identified a novel agent, transplatin, which inhibits TRPV1 and NOX3 expression and provides otoprotection against NIHL. Our data indicate that a single systemic or local (transtympanic) administration of transplatin ameliorates NIHL evaluated at 21 days after noise exposure (122 dB SPL OBN at 8 kHz for 1 h) in Wistar rats. Transplatin administered immediately prior to or 48 h prior to noise trauma inhibits up regulation of stress-response and inflammatory genes in the rat cochlea at 48 h and 21 days post noise exposure. Interestingly, transplatin administration also regulated microRNA expression related to inflammatory gene expression in the NIHL model. This is evidenced by data from microarray analysis. These data provide support for using transplatin in the amelioration of NIHL. (Supported by NIH grants R01DC02396 to LPR, R15DC011412 to VR, 1F32DC009950 to DM and funds from SIU SOM)

### **724 Foxo3-Mediated Hair Cell Protection in Noise-Induced Hearing Loss**

**Felicia Gileles<sup>1</sup>, Irfan Rahmen<sup>1</sup>, Patricia White<sup>1</sup>**

<sup>1</sup>*University of Rochester Medical Center*

Hearing loss occurs when the mechanoreceptors of the cochlea are damaged and can be a consequence of prolonged noise exposure, ototoxic agents, and aging. Understanding natural mechanisms that promote hair cell survival might enable construction of a therapeutic to protect human hearing. We have focused our studies on the FOXO transcription factor family. FOXO family activation as a protective response to mechanical trauma has been conserved through evolution and is seen in worms, flies, and mammals. We hypothesize that members of this family play a pro-survival role in the noise-damaged mouse cochlea. We show that Foxo3 is present in the sensory region of the mouse cochlea from birth to adulthood. To determine the function of Foxo3 in the cochlea, we tested auditory function of Foxo3 knockouts and wild-type littermates at two and four months of age. Foxo3 knockouts have normal hearing at two months, but experience mild age related hearing loss compared to normal littermates. In response to a 105 dB noise exposure, Foxo3 knockouts have a significantly larger threshold shifts and concomitant hair cell loss than their wildtype counterparts. Foxo3-dependent protection may be specific to apoptotic cell death, as no significant difference in hair cell loss was observed when neonatal Foxo3 knockout, heterozygous, and wild-type cochleae were cultured in cisplatin. Analysis of mRNA by RT-PCR hours after deafening enables the identification of apoptosis factors and potential Foxo3 targets. Future research will

involve the characterization of these apoptosis factors in hopes that understanding the mechanism of hair cell death will provide critical information necessary to preventing its occurrence.

### **725 Free Radical Scavengers to Mitigate Noise-Induced Hearing Loss: Is There a Role for Red Bull?**

Ragwinder Sahota<sup>1</sup>, Alex Borecki<sup>1</sup>, Joshua Allen<sup>1</sup>, Kyle Hoehn<sup>2</sup>, Henry Pau<sup>3</sup>, Sharon Oleskevich<sup>1,4</sup>

<sup>1</sup>Garvan Institute, <sup>2</sup>University of Virginia, <sup>3</sup>University of Leicester, <sup>4</sup>University of New South Wales

Exposure to acoustic trauma causes an increase in metabolic activity in the inner ear, resulting in free radical production. Free radicals such as nitric oxide (NO•) can cause cellular damage by attacking proteins, lipids, and DNA, which in turn can cause apoptosis and necrosis. For this study, we tested the effect of taurine, a potent NO• scavenger, to mitigate noise-induced hearing loss (NIHL) and the dose response relationship of its effect. Male CBA mice aged 4-10 weeks were randomised into six groups treated with 0.9% saline (control) or taurine (50, 100, 200, 300 or 400 mg/kg) via daily IP injections over 14 days (7 days before and after acoustic trauma). Acoustic trauma was 8-24 kHz banded noise at 110 dB SPL for 2 hrs. Auditory brainstem responses (ABR) were tested at 8, 16 and 24 kHz, and collected one week before, one week after, and one month after acoustic trauma to represent pretreatment thresholds, temporary threshold shifts (TTS), and permanent threshold shifts (PTS), respectively. Our results show that taurine significantly attenuated the effects of noise trauma as shown by ABR threshold shifts when compared to saline controls in all groups ( $P < 0.05$  at 8, 16 kHz for TTS and 8, 16, 24 kHz for PTS). Thresholds shifts were on average 13.2 dB better in all taurine treated mice compared to the saline control group. A taurine dose of 200 mg/kg yielded the greatest effect in mitigating against NIHL compared to saline controls ( $P < 0.05$  at 8, 16, 24 kHz for TTS and PTS). Experiments are underway to analyse the effect of taurine on hair cell survival with cytochrome c histochemistry. Taurine is a safe anti-oxidant, and a common element in normal diets and commercial energy drinks. Our future studies will investigate taurine as a potential therapeutic agent to prevent and/or treat NIHL.

### **726 Antioxidant Treatment Reduces Blast-Induced Cochlear Damage and Hearing Loss**

Jianzhong Lu<sup>1</sup>, Donald Ewert<sup>1</sup>, Wei Li<sup>1</sup>, Xiaoping Du<sup>1</sup>, Ning Hu<sup>1</sup>, Charles Stewart<sup>2</sup>, Robert Floyd<sup>2</sup>, Richard Kopke<sup>1,2</sup>

<sup>1</sup>Hough Ear Institute, Oklahoma City, OK, <sup>2</sup>Oklahoma Medical Research Foundation, Oklahoma City, OK

Unprotected ears, air-filled organs which are susceptible to blast overpressure (BOP) result in the auditory system being vulnerable to primary blast injury. The injury to the auditory system includes damage to the sensory structures on the basilar membrane leading to temporary and permanent hearing loss. Protecting against BOP is limited by the inability to anticipate the timing of exposures.

Therefore therapeutic intervention that might mitigate cochlear damage is desirable. Oxidative stress has been identified as a pivotal pathway of cochlear damage caused by acute acoustic trauma. This study was aimed to determine if administration of a combination of antioxidants 2,4-disulfonyl -phenyl tertiary butyl nitron (HPN-07) and N-acetylcysteine (NAC) beginning 1 h after blast exposure could reduce both temporary and permanent hearing loss. Under animal experimental conditions with free-field exposures to 3 consecutive blast waves at 14 psi, all exposed rats had permanent hearing loss as determined 21 d post exposure by ABR and DPOAE measures, as well as outer hair cell counts. The temporary component of hearing loss in the control group showed a time course after exposure which included an initial ABR threshold shift of 63 dB across 2-16 kHz followed by a recovery period of 7 d during which threshold partially return and stabilized at 30 dB in shift which represented a permanent hearing loss. When compared to controls, animals treated with HPN-07 plus NAC after exposure showed a clear improvement in the recovery of ABR threshold, i.e., a significant reduction in threshold shift at each time point, with an approximately 20 dB reduction being evident at 21 d. Also significantly reduced permanent DPOAE level shift and outer hair cell loss were noted. These findings provide the first evidence that a combination of HPN-07 and NAC when administered shortly after the traumatic event can reduce cochlear damage caused by BOP (Supported by ONR grant #N00014-09-1-0999).

### **727 D-Methionine in Preventing Noise Induced Hearing Loss**

Mariola Sliwinska-Kowalska<sup>1</sup>, Anna Rewerska<sup>1</sup>, Elzbieta Rajkowska<sup>1</sup>, Piotr Politanski<sup>1</sup>

<sup>1</sup>Nofer Institute of Occupational Medicine

Free radical formation appears to be a primary mechanism in developing noise-induced hearing loss. Thus, the intervention with the use of antioxidants has been proposed as an effective rescue method of hair cell survival and associated hearing loss. The purpose of this study was to examine the mechanisms underlying the noise-induced increase in reactive oxygen species (ROS) in the inner ear and to assess the role of an antioxidant D-methionine (D-met) in preventing the noise-induced oxidative stress and hearing loss.

The changes in superoxide dismutase (SOD), catalase, lipid peroxidation (LPO) and the auditory brainstem responses (ABR) were measured in the cochlea 1, 7 and 14 days after noise exposure (4 kHz octave band at the intensity of 118 dB SPL for 8 hours) in C57BL/6 mice. D-met in three doses (100, 200 and 400 mg/kg) was administered 1 h before and 1 h after noise exposure, and up to 3 days following exposure.

The time-dependent alterations in scavenging enzymes facilitating the increase in catalase level were observed in animals exposed to noise. Such changes were attenuated by D-met in the doses 200 mg/kg and 400 mg/kg, and were dose-dependent. In addition D-met in the dose 400 mg/kg promoted the increase in SOD level 7 and 14 days after noise exposure. Audiometric threshold shifts at 4 kHz

and 8 kHz were significantly smaller in animals injected with D-met comparing with the noise-exposed group. These differences were observed independently of drug dose one day after exposure. However, long-lasting (up to 14 days after exposure) protective hearing effect was seen only for D-met in the dose 400 mg/kg.

We conclude that D-met can be an effective drug in attenuating the noise-induced oxidative stress and associated functional loss in mice cochlea.

Acknowledgments. This study was supported by the Ministry of Science and Higher Education of Poland (Grant no. 0445/B/P01/2009/36).

### **728 D-Methionine(D-Met) Pre-Loading Prior to Noise Exposure Significantly Reduces Temporary and Permanent Noise-Induced Hearing Loss (NIHL) in Chinchillas**

**Kathleen Campbell<sup>1</sup>, Cathy Yu<sup>1</sup>, Robert Meech<sup>1</sup>, Daniel Fox<sup>1</sup>, Steven Verhulst<sup>1</sup>**

<sup>1</sup>SIU School of Medicine

D-methionine (D-met) protects against drug- (cisplatin and aminoglycoside) induced and noise-induced hearing loss (NIHL) in animal studies. D-met also significantly protected against radiation-induced oral mucositis and cisplatin-induced hearing loss in small scale Phase 2 clinical trials. In previous studies, D-met protected against NIHL if started 2 days prior to and continued just before and after noise exposure and provided significant NIHL rescue when first administered up to 7 hours after noise exposure. This experiment investigated whether D-met could reduce NIHL when started 2.0 or 2.5 days prior to noise exposure without concomitant or post-administration.

We used 3 groups of 5 male *Chinchillas laniger*. Two groups were injected with 5 intraperitoneal doses of D-met (200mg/kg/dose) in 12 hour intervals starting 2.0 or 2.5 days prior to a 6 hour 105 dB SPL narrow band of noise centered at 4 kHz. The third group (noise-exposed) received equivalent saline as per the 2.5 group.

Auditory brainstem responses (ABRs) were tested at baseline, 1 day post-noise exposure, and 21 days post-noise exposure for tone-burst stimulus frequencies centered at 2, 4, 6, and 8 kHz. After the 21 day ABR testing, animals were sacrificed. Cochleae were harvested for scanning electron microscopy analysis of remaining outer hair cells (OHC) at the specific cochlear regions corresponding to the ABR frequencies.

ABR results demonstrated significant threshold protection both 1 day (4 kHz  $p \leq .01$ ) and 21 days (4 and 8 kHz  $p \leq .05$ ) after noise exposure for the 2.0 day D-met pre-loading paradigm. For the 2.5 day pre-loading paradigm, significant protection was only obtained at 21 days after noise exposure (4 kHz  $p \leq .05$ ). Significant otoprotection with only 5 animals per group is encouraging, but further research will be needed to confirm and expand these findings. OHC data are being analyzed to confirm anatomical protection at specific frequency regions.

### **729 Pulmonary Drug Delivery for Cochlear Protection Against NIHL in a Chinchilla Model**

**Ron Jackson<sup>1</sup>, Rick Rogers<sup>2</sup>, Elizabeth Harper<sup>1</sup>, David Bastiansen<sup>1</sup>, Kejian Chen<sup>1</sup>, Jianzhong Liu<sup>1</sup>, Royce Clifford<sup>1</sup>, John Coleman<sup>1</sup>**

<sup>1</sup>Naval Medical Center San Diego, <sup>2</sup>Harvard School Public Health, Harvard University

The aim of this project was to test whether inhaled antioxidants in a chinchilla animal model exposed to continuous (CN) and impulse noise (ImpN) ameliorated both noise-induced hearing loss (NIHL) and auditory hair cell (HC) loss. Animals were given the low dose antioxidant combination (AC) of N-acetylcysteine (50 mg/kg), D-Methionine (50 mg/kg) and acetyl-L-carnitine (30 mg/kg) via intra-tracheal route for 5 instillations prior to and 5 after the noise exposure (NE). NEs consisted of either 6 hours of 105 dB SPL OBN or 75 paired-impulses at 155 dB SPL peak intensity. Antioxidant efficacy was assessed by auditory brainstem response (ABR) and auditory outer hair cell (OHC) counts compared to noise-exposed, saline instilled animals. The effect of the AC was seen within one week, and at 21 days post-NE threshold shifts (TSs) for AC treated animals were significantly lower than the saline control animals in both types of NEs. Low dose AC showed significant efficacy to reduce NIHL from 6 hrs of CN demonstrating lower TSs from baseline measures as early as one week post noise (3-way ANOVA;  $p < 0.05$ ). The average difference at one week was significant for all four ABR test frequencies. The improvement in hearing continued for both NE saline controls and AC treated animals; however the AC treated animals showed significantly better hearing again in all ABR test frequencies compared to saline controls at 3 weeks post NE. The range of differences between saline and AC was 10 dB SPL lower at the 2 kHz to 12 dB lower at 4, 6 and 8 kHz test frequencies. The AC group significantly protected the OHCs and correlated with the TS data with significantly lower percentage missing OHCs in the combination treated animals. For continuous noise-exposed, saline controls showed from 32 to 65% missing OHCs compared to 8 to 22% missing OHCs for the AC treated group (2-Way ANOVA,  $p < 0.01$  for the four ABR threshold shift frequency regions).

Funded by the Office of Naval Research

### **730 Use of Low Dose Antioxidants in Combination for Prevention of Hearing Loss from Loud Sound of Different Durations and Levels in a Chinchilla Model**

**John Coleman<sup>1</sup>, Jianzhong Liu<sup>1</sup>, Kejian Chen<sup>1</sup>, David Bastiansen<sup>1</sup>, Elizabeth Harper<sup>1</sup>, Ron Jackson<sup>1</sup>**

<sup>1</sup>Naval Medical Center San Diego

Our lab studied the efficacy of a low dose antioxidant combination (AC) consisting of D-Methionine (50mg/kg), N-acetylcysteine (50mg/kg), and acetyl-L-carnitine (30mg/kg) to attenuate hearing loss (HL) after continuous noise (CN). Animals were injected (IP) with the low dose AC or saline 5 times pre- and 5 times post-noise exposure (NE). The NEs were 6 hours of 105 dB SPL and 12 hrs of

101 dB SPL (both centered at 4 kHz OBN). AC efficacy was assessed by auditory brainstem response (ABR) and outer hair cell (OHC) counts. The low dose AC showed significantly reduced threshold shifts (TSs) from baseline measures for 6 hrs of CN as early as 1 week post-NE. The average TS reduction for AC was 11.9 dB SPL across all ABR frequencies. Hearing levels continued to improve for saline controls and AC animals, however the AC showed significantly better hearing vs. controls at 3 weeks post-NE ( $p < 0.05$ ; all freqs). Differences between saline and AC ranged 8 dB SPL lower at 2 kHz to 29 dB lower at 4 kHz (an average 17.6 dB reduction for all freqs). For the 12 Hr NE the AC group trended lower for 1 and 3-weeks post NE time across all ABR frequencies but only showed significance at 3 weeks for the 2 kHz. The average improvement in hearing at 3 weeks post NE from the saline controls was about 5.5 dB SPL for the AC group at 12 hrs of CN. The percent missing OHC data correlated with the TS data for both NE profiles. Although OHC loss was somewhat reduced for the 12-hr AC animals, based on the limited data (additional samples are being processed), the overall treatment effect was not significant. However, %missing OHCs for the 2 kHz test point region was significantly lower for the AC versus saline controls. These data add support that this AC and many antioxidants in general have the property of being oto-protective. For prolonged NEs that may result in reduced antioxidant capacity with time, a sustained release strategy may be required.

Funded by the Office of Naval Research

### **731 Effectiveness of Delayed Oral Administration of a Combination 4-OHPBN and NAC in Treating Noise-Induced Hearing Loss**

**Ning Hu**<sup>1</sup>, Richard Kopke<sup>1,2</sup>, Charles Stewart<sup>3</sup>, Don Nakmalia<sup>1</sup>, Robert Floyd<sup>3</sup>

<sup>1</sup>Hough Ear Institute, Oklahoma City, OK, <sup>2</sup>Oklahoma Medical Research Foundation, Departments of Physiology and Otolaryngology, OUHSC, <sup>3</sup>Oklahoma Medical Research Foundation, Oklahoma City, OK

Oxidative stress by overproduction of free radicals has been recognized as playing an important role in noise-induced hearing loss (NIHL). Several kinds of antioxidants, including 4-hydroxy-phenyl N-tert butyl nitron (4-OHPBN), a nitron-based free radical trap, and N-acetyl-L-cysteine (NAC), have been effective in reducing NIHL. We have reported that a combination of 4-OHPBN with NAC delivered at 4 hours after acute acoustic trauma (AAT) can significantly reduce NIHL, and the extent of hearing threshold shift is less than either of these two drugs used alone. In order to translate to clinical use and apply to real military situations (e.g., battle field), the effectiveness of oral administration at delayed delivery time windows was tested. A chinchilla AAT model was used by exposing animals for 6 hours to 4 kHz OBN at 105 dB SPL. A mixture of 4-OHPBN and NAC dissolved in sucrose was fed to chinchilla for 3 days starting at 8 or 24 hours after AAT. Hearing levels were assessed by using ABR and DPOAE before and 21 days after AAT, respectively. It was

found that the average ABR threshold shift of the 8-hour-delayed intervention group was about 20 dB lower than that of the untreated group. This difference was statistically significant. For the 24-hour-delayed intervention group, the ABR threshold shift still showed about 10 dB lower than that of the untreated group. DPOAE amplitude shift and threshold shift only showed a slight deduction in the 8-hour-delayed group. These results suggest, for carefully selected antioxidant drugs or combinations, NIHL can be rescued by delaying administration up to 8 hours after AAT. The differences in recovery between ABR and DPOAE may be due to limitations of DPOAE sensitivity range, or may suggest that a delayed intervention with a combination of 4-OHPBN and NAC acts on tissues other than outer hair cells. (Work supported by ONR Grant # N00014-08-1-0484)

### **732 Effect of Transplantation of Human Neural Stem Cells on Hearing Recovery in a Guinea Pig Model of Noise-Induced Hearing Loss**

**Hyungchae Yang**<sup>1</sup>, Ponkaj Kumar Banik<sup>1</sup>, Yongbum Cho<sup>1</sup>, Hyungho Cho<sup>1</sup>, Siyoung Cho<sup>1</sup>, Hansung Jeong<sup>2</sup>

<sup>1</sup>Chonnam national university, Department of otolaryngology-head & neck surgery, <sup>2</sup>Chonnam national university, Department of physiology

#### **Objective**

To investigate the replacement and trophic actions of neural stem cells after transplantation into the hearing impaired guinea pig by acoustic trauma.

#### **Methods**

Acoustic trauma was induced by a continuous white noise at 120 dB SPL for 4 h/day for 3 consecutive days. Two days after noise injury human neural stem cells (HB1.F3) were transplanted into the scala tympani of the basal turn. Phalloidin staining and scanning electron microscopy were carried out to detect the status of hair cells of the organ of Corti. Immunohistochemistry with specific antibodies was used to demonstrate the spiral ganglia neurons. Hearing ability was assessed by auditory brain stem response (ABR) evaluation. Neurotrophic factors (Glial cell-derived neurotrophic factor, and angiopoietin-3, Neurotrophin-3) were analyzed by western blot analyses.

#### **Results**

We found the loss of hair cells within the organ of Corti and degeneration of spiral ganglion neurons after noise injury. Thresholds of click evoked ABR and 8 kHz tone burst ABR were increased to 60-75 and 60-80 dB, respectively. After stem cell engraft, the number of cochlear hair cells was increased in the 2nd and 3rd turns of cochlea compared with control group under phalloidin staining and SEM. The number of neuronal cells in the spiral ganglia was also increased in transplanted group. In addition, fluorescent immunohistochemistry with human specific antibody (hNuclei) revealed that implanted human neural stem cells migrated and survived within the spiral ganglia. Furthermore, after transplantation of neural stem cells significant increase in the expression of neurotrophic proteins such as GDNF, NT3 and angiopoietin-3 was observed in cochlea. ABR results showed the hearing

recovery after transplantation. Thresholds of click evoked ABR and 8 kHz tone burst ABR were decreased to 25-40 dB and 35-45 dB, respectively.

Conclusion

Present study has demonstrated that neural stem cells are capable to replace the damaged spiral ganglion cells and to preserve hair cells in noise-induced hearing loss model, and stem cell transplantation also promotes hearing recovery.

### **733 Synaptic Mechanisms Underlying a Combination Therapy for Noise-Induced Hearing Loss**

Jianxin Bao<sup>1</sup>, Debin Lei<sup>2</sup>

<sup>1</sup>Washington University in St. Louis, <sup>2</sup>Washington University

Noise is the most common occupational and environmental hazard. Noise-induced hearing loss (NIHL) is the second most common form of sensorineural hearing deficit, after age-related hearing loss (presbycusis). Although there are promising approaches for reducing NIHL, currently there are no effective medications to prevent NIHL. Development of an efficacious treatment has been hampered by the complex array of cellular and molecular pathways involved in NIHL. We have turned this problem into an advantage by asking whether NIHL can be effectively prevented by a combination therapy targeting multiple signaling pathways. We recently found that antiepileptic drugs that block T-type calcium channels have both prophylactic and therapeutic effects for NIHL. NIHL can also be prevented by an up-regulation of glucocorticoid (GC) signaling pathways. Based on this finding, we have tested a combination therapy for NIHL that includes zonisamide, and anticonvulsant, and methylprednisolone, a synthetic GC drug, in one mouse NIHL condition [white noise, 110 dB sound pressure level (SPL) for 30 minutes], which has dramatic changes for permanent threshold shifts (PTS). We first determined the dose-effect for PTS amelioration by administering each drug two hours before the noise exposure. We determined the median effective dose (ED50) against NIHL for each drug. We have subsequently identified one combination with the strongest synergy against NIHL based on the combination index (CI) method. Currently, we examine whether this prophylactic effect is due to the protection of synaptic connections between inner hair cells and spiral ganglion neurons, between outer hair cells and medial olivocochlear innervation, or both. Thus, this study has not only shown the feasibility of efforts to discover effective drug combinations that act synergistically to prevent permanent NIHL, but also will further our knowledge of how these drugs protect against NIHL.

### **734 Restricted Time Window for Successful Treatment with Dexamethasone After Acute Noise Trauma**

Marcus Mueller<sup>1</sup>, Hubert Loewenheim<sup>1</sup>

<sup>1</sup>University Tuebingen

Noise exposure, despite protection measures, leads to an acute threshold shift and quite frequently to a permanent threshold shift (PTS). Treatments to limit the PTS show that corticosteroids may provide an effective medication. Here we investigated the use of corticosteroids in a guinea pig model of acute noise trauma. Exposure to impact noise led to a permanent hearing loss in the entire frequency range. Hair cell loss was observed in the middle and apical region of the cochlea. For treatment osmotic pumps were subcutaneously implanted immediately, 1, 3, or 7 days after the noise exposure. A catheter was used to apply Dexamethasone (4 mg/ml) to the round window of the cochlea, the pumps (0.5 µl/h) lasted for 14 days, and then PTS was determined. The success of treatment with corticosteroids showed a dependence on the initiation of treatment. When treatment started immediately or one day after noise exposure the PTS was the lowest. When treatment started 3 days after the exposure a reduced effectiveness of rescue in the high frequency range was observed. When treatment started 7 days after noise exposure, effectiveness was reduced further, at most frequencies thresholds were in the range of untreated controls. Conclusion: Permanent hearing loss and hair cell loss was reduced using 4 mg/ml Dexamethasone applied at the round window of the cochlea. The results show a protective effect for treatment with Dexamethasone of at least up to 3 days after the noise insult.

### **735 Extracellular Chloride Regulation of Kv2.1, Contributor to the Major Outward Kv Current in Mammalian Outer Hair Cells**

Xiantao Li<sup>1</sup>, Alexei Surguchev<sup>1</sup>, Shumin Bian<sup>1</sup>,

Dhasakumar Navaratnam<sup>1</sup>, Joseph Santos-Sacchi<sup>1</sup>

<sup>1</sup>Otolaryngology, Neurobiology, Neurology, Cellular and Molecular Physiology Yale University

Outer hair cells (OHC) function as both receptors and effectors in providing a boost to auditory reception. Amplification is driven by the motor protein prestin, which is under anionic control. Interestingly, we now find that the major, 4-AP sensitive, outward K current of the OHC (IK) is also sensitive to chloride, though, in contrast to prestin, extracellularly. IK is inhibited by reducing extracellular Cl<sup>-</sup> levels, with a linear dependence of 0.4%/mM. Other Kv channel conductances in supporting cells, such as Hensen and Deiters' cells, are not affected by reduced extracellular chloride. To elucidate the molecular basis of this Cl<sup>-</sup>-sensitive IK, we looked at potential molecular candidates based on chloride sensitivity and/or similarities in kinetics. For IK, we identified three different Ca<sup>2+</sup>-independent components of IK based on time constant of inactivation: a fast, transient outward current (I<sub>to</sub>), a rapidly activating, slowly inactivating current (I<sub>k1</sub>) and a slowly inactivating current (I<sub>k2</sub>). Extracellular Cl<sup>-</sup> differentially affects these components. Because the inactivation time constant of I<sub>k1</sub>

and *Ik2* are similar to those of *Kv1.5* and *Kv2.1*, we transiently transfected these constructs into CHO cells and found that low extracellular  $Cl^-$  inhibited both channels with linear current reductions of 0.38%/mM and 0.49%/mM, respectively. We also tested heterologously expressed Slick and Slack conductances, two intracellularly  $Cl^-$ -sensitive  $K^+$  channels, but found no extracellular chloride sensitivity. The chloride sensitivity of *Kv2.1* and its robust expression within OHCs verified by single cell RT-PCR indicate that these channels underlie the OHC's extracellular  $Cl^-$  sensitivity.

(Supported by NIH/NIDCD DC00273 to JSS)

### **736 Hair Cell BK Channel Surface Expression Is Affected by PKC**

Alexei Surguchev<sup>1</sup>, Junping Bai<sup>1</sup>, Dhasakumar Navaratnam<sup>1</sup>

<sup>1</sup>*Yale University*

Large conductance potassium channels (BK) channels regulated by both membrane voltage and intracellular  $Ca^{2+}$  represent the major element of electrical tuning in hair cells in non-mammalian vertebrates. This mechanism allows for frequency selectivity. BK channels show faster kinetics and increasing surface expression along the tonotopic axis.

In seeking to identify the molecular mechanisms that underlie these two related phenomena, we used a yeast two-hybrid screen and identified Rack1 (receptor for activated protein kinase C) a WD40 adapter protein as a binding partner of cSLO. Slo and rack 1 are co-localized in hair cells. Moreover, used FRET to confirm the Rack1-Slo interaction in living cells, while reciprocal co-immunoprecipitation confirmed interaction in-vitro. Further, we investigated how increased PKC activity related to Slo surface expression. Using HEK cells stably expressing FLAG-cSlo-YFP we showed that the PKC activator PMA increased Slo surface expression. This effect was inhibited by BIM-1 and the cell permeable  $Ca^{2+}$  chelator BAPTA-AM confirming that the effect was likely mediated by conventional PKC isoforms. In membrane recycling assays we determined that some of this effect was due to increased recycling of Slo to the surface of the cell. Finally we confirmed the physiological relevance of PKC activity in hair cells, where the addition of PMA or monensin both increased cSLO surface expression and the clustering of the channel.

### **737 Cholinergic Activation of Calcium-Gated Potassium Channels in Avian and Mammalian Auditory Hair Cells**

Gijung Im<sup>1,2</sup>, Paul Fuchs<sup>1</sup>

<sup>1</sup>*Otolaryngology-HNS, Johns Hopkins University School of Medicine*, <sup>2</sup>*Otolaryngology-HNS, Korea University College of Medicine*

Efferent neurons release acetylcholine (ACh) to inhibit sensory hair cells of the inner ear. As implied by their voltage-dependence, calcium entry through the ionotropic ACh receptor (AChR) triggers calcium-dependent potassium current to hyperpolarize hair cells. If hair cells are first polarized positive to +20 mV, ACh no longer

activates SK channels, consistent with reduced driving force on calcium entry (Martin and Fuchs 1992, Proc. Roy. Soc. 250:71). At the same time, a ubiquitous post-synaptic cistern and some experimental evidence (Sridhar et al 1997 J. Neurosci. 17:428; Lioudyno et al. 2004 J Neurosci 24:11160) suggest that intracellular stores might contribute additional calcium. Recent evidence has shown that mammalian and avian hair cell AChRs differ approximately 4:1 in their respective calcium permeability (Im et al., ARO 2011). Here we examine the relative contribution of calcium influx to activation of SK channels in chicken and rat auditory hair cells by measuring the decay after a voltage step to +40 mV during prolonged ACh application (2-4 second long outward current at -40 mV). Both cell types were studied in identical ionic conditions (room temp., 5 mM EGTA internal). Chicken short (outer-like) hair cells fell into two categories, those with exponentially decaying SK currents at +40 mV (average time constant  $108 \pm 40$  ms, SD  $n = 7$ ), and others with prolonged, complex waveforms; half-amplitude duration  $728 \pm 323$  ms ( $n = 9$ ) at +40 mV. These extended SK currents may reflect contributions from internal calcium stores to supplement influx through the AChR. In a limited number ( $n = 5$ ) of neonatal rat inner hair cells (P7-10) the ACh-evoked SK current had a decay time constant of  $56 \pm 14$  ms upon a step to +40 mV. Supported by NIDCD R01DC001508 and the National Research Foundation of Korea Grant funded by the Korean Government MEST, Basic Research Promotion Fund (NRF-2010-013-E00015).

### **738 Distinct Roles of Molecular Chaperones in Biogenesis and Degradation of KCNQ4 Channels**

Yanhong Gao<sup>1</sup>, Kirk W Beisel<sup>2</sup>, Liping Nie<sup>1</sup>

<sup>1</sup>*University of California, Davis*, <sup>2</sup>*Creighton University*

The past two decades have witnessed a period of breathtaking discoveries of mutations in KCNQ channels associated with various inherited diseases. The KCNQ family of voltage-gated potassium channels comprises five members (KCNQ1-5) that play important roles in a wide range of biological processes. KCNQ1 proteins assemble with KCNE beta chains to generate  $K^+$  currents in heart, ear, and kidney and functional deficiency in either subunit lead to cardiac arrhythmia and congenital bilateral deafness as seen in Jervell and Lange-Nielsen Syndrome (JLNS). Homo- or hetero- assemblies of KCNQ2 and KCNQ3 subunits elicit the neural M currents, mutations in these channels cause benign familial neonatal convulsions (BFNC), a dominantly inherited epilepsy of the newborn that may or may not followed by myokimia later in life. KCNQ4 are known to be expressed exclusively to the inner ear and central auditory pathways. Dominant-negative mutations of the channel result in progressive hearing loss in DFNA2 patients. Despite the importance of biogenesis and surface expression in KCNQ channels function, little is known about how these processes are controlled at molecular level. In this study, we investigated the molecular pathways underlying biogenesis and degradation of the KCNQ4 channel. A proteomics approach was used to identify chaperone proteins

associated with KCNQ4 channels. We found that heat-shock protein (HSP)40 and HSP70 are associated with the channel. Inhibition of HSP40 and HSP70 expression by siRNA reduces cell surface expression of wild-type KCNQ4 channels, whereas overexpression of these chaperone proteins augments KCNQ4 channels on the cell membrane. In addition, our data indicated that the KCNQ4 channels physically interact with HSP90 paralogs. HSP90 alpha promotes the degradation of the KCNQ4 channel, while HSP90 beta facilitates its surface expression. Finally, we found that the biogenesis or degradation of KCNQ4 channels is mediated by distinct co-chaperones of HSP90. Our findings provide insight into the distinct roles of molecular chaperones in biosynthesis of KCNQ4 and surface expression. Modulation of cell surface expression of normal and defective KCNQ4 channels may offer a potential therapeutic strategy for the treatment of DFNA2 and perhaps can be extended to other membrane protein-associated diseases with trafficking deficiency.

This work was supported by National Institutes of Health National Institute on Deafness and Other Communication Disorders Grant DC008649 and a research award from the American Hearing Research Foundation to L.N.

### **739** Functional Characterisation of Developing Human Hair Cells

Rebecca Lim<sup>1,2</sup>, Aaron Camp<sup>3</sup>, Melissa Tadros<sup>1,2</sup>, Hannah Drury<sup>1,2</sup>, Robert Callister<sup>1,2</sup>, Alan Brichta<sup>1,2</sup>

<sup>1</sup>The University of Newcastle, <sup>2</sup>Hunter Medical Research Institute, <sup>3</sup>The University of Sydney

Background:

The vast majority of studies investigating the maturation of peripheral vestibular function have focused on animal models. Here we report a timeline of the functional development in human vestibular hair cells and calyceal terminals during a period of intense change when whole cell conductances begin to resemble those seen in adults. This basic information is important if we are to establish models of human development using wildtype and genetically modified mice that adequately represent normal and abnormal peripheral vestibular development and function.

Methods:

Human tissue was collected and prepared according to State legislation and regulatory requirements of the University of Newcastle Human Research Ethics Committee. Inner ears from electively terminated human fetuses (11 to 18 weeks gestation; WG) were isolated and semicircular canal cristae excised in ice-cold glycerol-based Ringers' solution. Cristae preparations were then transferred to a recording chamber perfused with oxygenated L15 cell culture media. Whole-cell patch-clamp recordings using potassium fluoride internal solution were made from hair cells and calyx afferent terminals that were embedded within the semi-intact cristae.

Results:

We have successfully recorded and labeled human vestibular hair cells that display a variety of inward and outward rectifying conductances, between 11 and 18 WG. During early fetal gestation, some hair cells show evidence

of sodium conductances similar to those seen in immature rodent hair cells. In subsequent weeks, hair cells begin to express conductances similar to those seen in adult type II and type I hair cells. The earliest expression of the type I hair cell characteristic conductance  $g_{k,l}$  was observed at 14 WG. This appears to approximately coincide with our first recordings from calyceal primary terminals at 15 WG. Our data show human hair cells aged 11-13 WG are still functionally immature but then undergo distinct changes between 14 and 16 WG.

### **740** Light Activation of Channelrhodopsin2 Elicited a Non-Selective Cation Current (NSCC) in Mouse Outer Hair Cells and an Auditory Cell Line (HEI-OC1)

Tao Wu<sup>1</sup>, Teresa M. Wilson<sup>1</sup>, Irina Omelchenko<sup>1</sup>, Michael Bateschell<sup>1</sup>, Lingyan Wang<sup>1</sup>, John Brigande<sup>1</sup>, Zhi-Gen Jiang<sup>1</sup>, Alfred L. Nuttall<sup>1</sup>

<sup>1</sup>Oregon Health & Science University

Channelrhodopsin2 (ChR2) is a light-gated channel. It has been used as a tool to investigate the function of excitable cells and as a treatment intervention in a variety of animal models including the cochlea (ARO 2011 abstract refs). However, to our knowledge, channelrhodopsins have not yet been used in any hair cell study. In mammalian cochlea, outer hair cells (OHCs) amplify sound stimulus by increasing both the amplitude and frequency selectivity of basilar membrane vibration. In this study, we expressed ChR2-mCherry in the auditory cell line (HEI-OC1) expressing prestin and ChR2-tdTomato in mouse OHCs. Through patch clamp recordings, we showed that 100 ms light pulse (473 nm, 1 mW/mm<sup>2</sup>) elicited a typical ChR2 current in ChR2 (+) HEI-OC1 cells; an inward current with a rapid rising peak (e.g.  $-15.9 \pm 2.1$  pA/pF at -60 mV) and a subsequent relaxation at a negative holding potential (Vh) in the solutions blocking K conductances. I-V plots showed the reverse potential (Vr) near 0 mV. In physiological solutions, similar ChR2 currents were elicited with the Vr at  $\sim 0$  mV. In I-clamp mode, the light pulse transiently depolarized ChR2 (+) HEI-OC1 by 11.7 mV. In comparison, no significant change in current and resting potential (RP) was elicited in ChR2 (-) HEI-OC1. In mouse ChR2 (+) OHCs, classical ChR2 currents were elicited with  $-4.0$  pA/pF at -60 mV in the solutions blocking K conductances. I-V plots showed the Vr at  $\sim 0$  mV. In comparison, no significant ChR2 current was elicited in the ChR2 (-) OHCs. This is the first demonstration that ChR2 was successfully expressed in mouse OHCs and HEI-OC1 cells and presented a typical light-sensitive NSCC and depolarization of RP. The data suggests a novel approach to modulate OHC RP, the driving force of transduction current and the somatic motility, and a potential clinical intervention of the cochlear amplification in a non-invasive way. Supported by NIDCD R01DC00105 and R01DC00141.

### **741 Clustering of Cav1.3 Channels and Ca<sup>2+</sup> Microdomains in Mouse Inner Hair Cells During Postnatal Cochlear Development**

Thibaud Parpaite<sup>1</sup>, Yohan Bouleau<sup>1</sup>, Didier Dulon<sup>1</sup>  
<sup>1</sup>Inserm U587 & University of Bordeaux

Using confocal microscopy, we explored the distribution of Cav1.3 channels and CtBP2 (B-domain of ribeye, a marker of synaptic ribbons) in mouse inner hair cells (IHCs) during postnatal development. Freshly dissected mouse cochleae were rapidly fixed with 100% methanol solution at -20°C for 30 min. Immunoreactions were performed using a rabbit polyclonal anti-Cav1.3 at 1/200 dilution (epitope 859-875) and goat polyclonal anti-ctBP2 at 1/200 dilution. We found a progressive increase in co-localisation of Cav1.3 channels and CtBP2 during maturation. At the upper turn of the cochlea (low frequency), co-localisation of the Cav1.3-spots and CtBP2-spots increased from 20 % at P2 to 60 % at P5-P8 and up to 95 % at the post-hearing mature stage P19. Immature P2 IHCs showed a widespread distribution of Cav1.3-spots (evenly distributed above or below the cell nucleus) as compared to P19 IHCs where all Cav1.3-spots were exclusively localized below the cell nucleus. Remarkably, the mean surface area of the Cav1.3 spots, co-localized with CtBP2, also increased during development from 0.075 µm<sup>2</sup> at P2 to 0.15 µm<sup>2</sup> at P5 and up to 0.35 µm<sup>2</sup> at P19. In agreement with these results, by combining whole-cell patch clamp recordings ( $\Delta C_m$  and  $I_{Ca}$ ) and Ca<sup>2+</sup> imaging, we found that the Ca<sup>2+</sup> signals evoked during brief voltage-steps depolarization were more widespread all over the cell surface in immature P5-P7 IHCs as compared to mature P21 IHCs where transient Ca<sup>2+</sup> hot spots (microdomains) could be individually identified. These results confirm that a spatial re-organization and clustering of Cav1.3 channels occur at the IHC ribbons during postnatal maturation, a process that is likely essential to ensure rapid and high exocytosis efficiency.

### **742 The GTPase Rab11b Recycles the Large Conductance Calcium-Activated Potassium Channel**

Sophia Sokolowski<sup>1</sup>, Yoshihisa Sakai<sup>1</sup>, Margaret Harvey<sup>1</sup>, Amy Jordan<sup>1</sup>, Bernd Sokolowski<sup>1</sup>

<sup>1</sup>University of South Florida, College of Medicine, Tampa, FL 33612

The large conductance calcium-activated potassium channel underlies hearing sensitivity in the cochlea of vertebrates. Previously, we used a high-throughput screening method that included LC-MS/MS to determine putative partners that interact with the BK channel (Kathiresan et al., 2009). These studies revealed a potential partner in the small GTPase, Rab11b. Rabs are master regulators of endosomal trafficking, involved in: protein transport to the cell membrane (early endosome), recycling from and to the membrane (recycling endosomes), and protein transport for degradation (late endosomes) in the lysosome. Previous studies show that among the many Rab proteins, Rab11b is involved with either late or recycling endosomes, depending on the

protein. For example, Rab11b limits Cav1.2 channel expression (Best et al., 2011), whereas hERG and anion channels are recycled back to the plasmalemma (Schieff et al., 2000; Delisle et al., 2009). We found Rab11b ubiquitously expressed in hair cells of the mouse. Using reciprocal coimmunoprecipitation and yeast two-hybrid assays, we show that this GTPase interacts with the BK channel. The *Rab11b* gene, cloned from mouse cochlea, is highly homologous, showing a similarity greater than 97% to *Rab11b* from human, cow, mouse, rat, and goat. Using CHO and MDCK cells as heterologous expression systems, we used siRNAs that target endogenous Rab11b, to determine the effects on transfected hemagglutinin-tagged BK expression. Knockdown of Rab11b resulted in a significant decrease in BK expression, whereas overexpression of Rab11b resulted in an increase. These results suggest that Rab11b recycles the BK channel back to the membrane as opposed to leading BK to a degradation pathway. Of interest will be to determine the role of this GTPase in regulating BK under different conditions of auditory stimulation, such as in noise-induced hearing loss.

Supported by NIDCD grant R01DC004295 to BS.

### **743 CDK5 Interacts with Slo and Affects Its Surface Expression and Kinetics Through Direct Phosphorylation**

Jun-Ping Bai<sup>1</sup>, Alexei Surguchev<sup>1</sup>, Dhasakumar Navaratnam<sup>2</sup>

<sup>1</sup>Yale Medical School Dept. of Neurology, <sup>2</sup>Yale Medical School Dept. of Neurology and Neurobiology

Large conductance calcium activated potassium (BK) channels are ubiquitous and play an important role in a number of diseases. In hair cells of the ear they play a critical role in electrical tuning, a mechanism of frequency discrimination. These channels show variable kinetics and expression along the tonotopic axis. Although the molecular underpinnings to its function in hair cells are poorly understood it is established that BK channels consist of a pore forming alpha subunit (Slo) and a number of accessory subunits. Here we identify CDK5, a member of the cyclin dependent kinase family as an interacting partner of Slo. We show CDK5 to be present in hair cells, and expressed in high concentrations in the cuticular plate and in the circumferential zone. In HEK cells we show that CDK5 inhibits surface expression of Slo by direct phosphorylation of Slo. Similarly, we note that CDK5 affects Slo voltage activation and deactivation kinetics, by a direct phosphorylation of T847. Taken together with its increasing expression along the tonotopic axis, these data suggest that CDK5 likely plays a critical role in electrical tuning and surface expression of Slo in hair cells.

This study is supported by National Institute on Deafness and Other Communication Disorders Grant R01-DC-007894.

#### **744** Effects of elevated cGMP levels on BK currents in mature mouse inner hair cells

Barbara Disteldorf<sup>1</sup>, Niels Brandt<sup>1</sup>, Stefan Münkner<sup>1</sup>, Jutta Engel<sup>1</sup>

<sup>1</sup>Saarland University

The NO-cGMP signaling pathway has recently been found to protect inner hair cells (IHCs) from noise trauma (Jaumann et al., submitted). These authors found an otoprotective role for processes mediated by the cGMP-dependent protein kinase type I (cGKI). So far, the targets of cGKI in IHCs are largely unknown.

In various types of smooth muscle cells, elevated cGMP levels activate cGKI, which phosphorylates and activates big conductance, voltage and Ca<sup>2+</sup>-activated K<sup>+</sup> (BK) channels, thereby counteracting cellular depolarization. We therefore analyzed whether cGMP affects BK currents of IHCs, the most important K<sup>+</sup> channels for IHC repolarization.

Whole-cell BK currents of mature IHCs (age: 20±3 days) were recorded upon application of the non-hydrolyzable analogue of cGMP, 8-bromo-cGMP, via the patch pipette. The effect of 3 μM 8-bromo-cGMP was tested at two different Ca<sup>2+</sup> buffering conditions - at a calculated intracellular free Ca<sup>2+</sup> concentration ([Ca<sup>2+</sup>]<sub>i</sub>) of 1.8 nM and of 22 nM.

Surprisingly, 8-bromo-cGMP had opposing effects on BK current densities at -10 mV: it caused an increase by 44% at low [Ca<sup>2+</sup>]<sub>i</sub> (from 0.45 ± 0.04 nA/pF [mean ± SEM, n=9] to 0.65 ± 0.07 nA/pF [n=12]), whereas it reduced BK current density by 36% at 22 nM [Ca<sup>2+</sup>]<sub>i</sub> (from 0.60 ± 0.08 nA/pF [n = 9] to 0.38 ± 0.04 nA/pF [n = 12]). 8-bromo-cGMP selectively affected biophysical properties obtained from I-V fits in the two buffering conditions: it increased V<sub>half</sub> at 22 nM [Ca<sup>2+</sup>]<sub>i</sub> but not at lower [Ca<sup>2+</sup>]<sub>i</sub>. Conversely, 8-bromo-cGMP reduced the slope factor at lower ([Ca<sup>2+</sup>]<sub>i</sub>), but not at the higher ([Ca<sup>2+</sup>]<sub>i</sub>).

Taken together, 3 μM 8-bromo-cGMP had differential effects on BK current density and biophysical parameters as a function of [Ca<sup>2+</sup>]<sub>i</sub>. Depending on local cGMP and [Ca<sup>2+</sup>]<sub>i</sub> concentrations, BK currents may be increased or reduced by the cGMP-cGKI pathway.

#### **745** Functional Alterations Concerning Signal-To-Noise Discriminations in GlyRα3 -/- Mice

Stefanie Buerbank<sup>1</sup>, Konstantin Tziridis<sup>1</sup>, Holger Schulze<sup>1</sup>

<sup>1</sup>University Hospital Erlangen

One of the functional roles of the efferent innervation of the mammalian inner ear is its participation in unmasking of sounds close to background level, thereby contributing to signal-to-noise (S/N) discrimination. Recently the participation of glycine receptors (GlyR) in efferent innervation of the murine cochlea has been demonstrated, with GlyRα3 being the dominating ligand binding subunit in adult animals.

Here we present first evidence that the absence of GlyRα3 alters S/N discrimination in C57/Bl6 mice.

Dissection of inner ear tissue from GlyRα3 +/+ and -/- mice was followed by preparation of RNA, cDNA and qRT-PCR to characterize efferent receptors. Acoustic startle

response in quiet and white background noise at 40 dB SPL, combined with tonal prepulses of sound intensities ranging from 40 to 60 dB SPL was used to assess S/N discrimination. Auditory brainstem responses (ABR) were used to exclude hearing impairment of experimental animals.

On RNA level, we found that other ligand binding GlyR subunits in cochleae from adult GlyRα3 -/- mice remained unchanged. Previously characterized components of efferent innervation were either upregulated or did not show significant alterations. Nevertheless, we could observe differences in prepulse inhibition between GlyRα3 +/+ and -/- mice when combining our stimuli with constant white noise. These differences hint to impaired S/N discrimination in -/- animals. ABR did not reveal significant differences of hearing in -/- compared to +/+ mice.

Our results suggest a participation of GlyRs in efferent innervation of the inner ear that is used for unmasking of sounds. This task is not transferred to other efferent receptors when GlyRα3 is missing. Possible other functions of efferent innervation need to be tested. A participation of auditory brainstem circuits, where GlyRα3 subunits can also be found, still has to be discerned from inner ear effects by local modulation of GlyRs.

This work was funded by the IZKF Erlangen

#### **746** Evidence for Glutamate Spillover in the Synapse Between Type I Hair Cell and Calyx of the Vestibular Nerve Afferents

Soroush Sadeghi<sup>1</sup>, Sonja Pyott<sup>2</sup>, Elisabeth Glowatzki<sup>1</sup>

<sup>1</sup>Department of Otolaryngology-Head and Neck Surgery, Johns Hopkins School of Medicine, Baltimore, MD,

<sup>2</sup>Department of Biology and Marine Biology, University of North Carolina Wilmington, Wilmington, NC

Calyx endings of vestibular afferents are stimulated by glutamate released from type I vestibular hair cells (reviewed in Songer and Eatock 2011). We investigated the properties of this specialized synapse in response to synaptic release of glutamate from the hair cell. We used excised preparations of the horizontal and anterior cristae from 2-4 weeks old rats. We performed whole cell patch clamp recordings from the basal region of the calyces using glass pipettes with resistances of ~7 Mohm. The mean resting membrane potential of calyces was ~-60 mV and about half of the calyces exhibited synaptic activity in the absence of stimulation at room temperature. EPSCs had mean amplitudes of ~55 pA (at a holding potential of -94 mV) and were blocked by the AMPA receptor blocker NBQX (20 μM). Kinetics of EPSCs showed a wide range. Some EPSCs had fast kinetics with time constants of decay (τ<sub>decay</sub>) <1 ms, comparable to those in prehearing auditory afferents of inner hair cells (Grant et al. 2010). Other EPSCs were slower and had τ<sub>decay</sub> values of >40 ms. We hypothesized that such slow kinetics were due to spillover of glutamate. To test this hypothesis, we first increased the glutamate concentration in the synaptic cleft by either hair cell depolarization or application of a general glutamate transporter blocker (200 μM TBOA). Under these conditions, τ<sub>decay</sub> increased by 40%. We then applied a competitive blocker of glutamate receptors (0.25 mM

kynurenic acid) to block the spillover effect, which resulted in a decrease of 60% in  $\tau_{\text{decay}}$ . Furthermore, in immunofluorescence examination of cristae, unlike in the cochlea, presynaptic ribbons and postsynaptic densities were often not juxtaposed. Together, our findings support the presence of spillover of glutamate to AMPA receptors further away from the release sites. We propose that summation of slower EPSCs due to spillover may play a role in signal transmission at the type I hair cell/calyx synapse.

This work was supported by Vestibular Research Fund at Johns Hopkins and National Institute on Deafness and Other Communication Disorders DC006476 to EG.

### **747 Pinball Wizard Is Essential for Transduction, Synaptic Transmission, and Processing Tail-Anchored Membrane Proteins in Hair Cells**

**Shuh-Yow Lin<sup>1</sup>, Jun Shen<sup>2</sup>, David Corey<sup>2</sup>**  
<sup>1</sup>UCSD, <sup>2</sup>Harvard Medical School

Previously we found that pinball wizard (pinball) zebrafish mutants exhibit severe mechanotransduction and synaptic transmission defects in hair cells, and synaptic transmission defects in photoreceptors. In addition, the defects in hair cells were accompanied with mis-expression of Otoferlin. Using immunocytochemistry, we now demonstrate that VAMP2 and syntaxin, but not SV2 and Rab3, are also mis-expressed in the mutant photoreceptors. These results indicate that pinball is critical for the expression of a subset of synaptic proteins in hair cells and photoreceptors. Recently, the mouse pinball ortholog Wrb was found to be the receptor for the tail-anchored (TA) protein processing at the ER membrane. TA proteins belong to a unique class of proteins attached or anchored to cellular membranes through the only transmembrane domain near the end of the protein C-terminal. Consistent with this finding, Otoferlin, VAMP2 and syntaxin, not SV2 and Rab3, are mis-expressed and are TA proteins. It is most likely that the phenotypes of the mutant are caused by membrane anchoring failure of the pinball-dependent TA proteins. To further understand the function of pinball in hair cells and to identify novel essential hair cell TA proteins, we compared a hair cell expression database with a human TA protein database. We found 35 TA proteins that are highly expressed in hair cells. Understanding the role of these proteins could provide important insights in hair cell transduction and transmission.

### **748 A Zebrafish Model for Uncovering the Molecular Mechanisms of Hair Cell Ribbon Synaptic Transmission**

**Sara Mangosing<sup>1</sup>, Elena Cardenas<sup>1</sup>, Lily Liu<sup>1</sup>, Shuh-Yow Lin<sup>1</sup>**  
<sup>1</sup>UCSD

The hair cell ribbon synapse is the first synapse in the auditory and vestibular pathway, and is critical in shaping and preserving sensory responses perceived by the brain. It is different than conventional synapses in the nervous

system with its ability to initiate fast and maintain long-lasting neurotransmitter release. In addition to the specialized synaptic ribbons, this synapse also lacks several common molecules in the neuronal SNARE fusion complex. However, the molecular mechanisms underlying vesicle trafficking, priming/docking and fusion are mostly unknown.

In our laboratory, we have developed several methods that harness the imaging and genetic power of larval zebrafish to identify the essential synaptic molecules and elucidate the functional aspects of the ribbon synapse. (1) We are able to monitor the location and dynamics of synaptic ribbons under various experimental conditions utilizing fluorescent protein tagged ribbon-binding peptides. (2) For tracking synaptic vesicle transportation, targeting and docking, we are able to simultaneously express fluorescent vesicle and ribbon markers in hair cells by transgenesis. (3) We are able to detect postsynaptic activity using a transgenic fish line that expresses genetically encoded Ca<sup>2+</sup> reporter in the afferent neuron. Taken together, these tools will greatly facilitate identification of new players essential for vesicle cycling and fusion in the hair cell ribbon synapse. We are now beginning to assess the potential function of several putative ribbon synaptic proteins by over-expression and dominant-negative mutations. The implications of the result in vesicle trafficking and priming /docking processes in the hair cell ribbon synapse will be discussed.

### **749 Neurotrophin-3 from Supporting Cells Modulates Synapse Number and Auditory Function in the Postnatal Cochlea**

**Guoqiang Wan<sup>1</sup>, Maria Eugenia Gomez-Casati<sup>1</sup>, M. Charles Liberman<sup>2</sup>, Gabriel Corfas<sup>1</sup>**

<sup>1</sup>Children's Hospital Boston, <sup>2</sup>Massachusetts Eye and Ear Infirmary

Neurotrophin-3 (NT-3) in the developing inner ear is critical for survival of spiral ganglion neurons, but its roles in the postnatal cochlea remain unclear. In the adult, NT-3 is expressed by both inner hair cells (IHCs) and their associated supporting cells, in an apex > base gradient. To explore the postnatal roles of supporting-cell derived NT-3, we generated supporting cell-specific NT-3 knockout and overexpression mice using proteolipid protein (PLP)-dependent expression of CreER(t) recombinase. Recombination of the conditional alleles was induced by tamoxifen at early postnatal ages (P1-P7).

Knockout of NT-3 in supporting cells resulted in a 10–20 dB elevation of ABR thresholds at high frequencies (22–45 kHz), without any change in DPOAE thresholds. Immunostaining cochlear whole mounts for ribeye protein revealed a reduction of > 50% in the number of IHC synaptic ribbons in the basal half of the cochlea. Conversely, overexpression of NT-3 by supporting cells resulted in a 10–15 dB decrease in ABR thresholds at high frequencies and a parallel reduction in DPOAE thresholds. Correspondingly, cochlear immunostaining showed a 50% increase in the number of IHC synaptic ribbons in the basal turn.

These results show that supporting cell-derived NT-3 is critical for synapse formation/maintenance in the postnatal cochlea and that its effects are greatest in the basal turn, where endogenous NT-3 expression is lowest.

### **750 Characterization of Nicotinic Acetylcholine Receptor Knockouts**

**Barbara Morley<sup>1</sup>**, Dwayne Simmons<sup>2</sup>

<sup>1</sup>Boys Town National Research Hospital, <sup>2</sup>University of California, Los Angeles

Efferent synaptogenesis and the maturation of efferent-mediated cochlear responses are watershed events during the development of auditory function. The olivocochlear (OC) efferent system plays a major role in the regulation of outer hair cell (OHC) function and is thus a significant contributor to the processing of auditory signals. Cholinergic OC axons modulate OHC motility by inhibiting the Ca<sup>2+</sup>-sensitive motility found in these cells. This efferent inhibition of OHCs is mediated by nicotinic acetylcholine receptors (nAChRs) containing  $\alpha 9$  (Chr $\alpha 9$ ) and  $\alpha 10$  (Chr $\alpha 10$ ) subunits. Activation of OHC nAChRs by the release of ACh from efferent terminals induces Ca<sup>2+</sup> influx. To study the roles of  $\alpha 9$  and  $\alpha 10$  subunits in the development of OC efferent innervation, we engineered both constitutive and conditional mouse strains that have null mutations in the Chr $\alpha 9$  and Chr $\alpha 10$  genes. In the targeting construct, exons 1 and 2 and their flanking intronic sequences were replaced by a loxp-frt-neo-frt-loxp cassette, which effectively eliminates translation of any truncated form of the gene. The strains were backcrossed to the C57BL/6J train to facilitate crossing with the existing alpha7 knockout mouse to produce double and triple knockouts. Here we report the preliminary characterization of the mouse strains. None of the strains have an obvious external phenotype. PCR array studies using custom (Qiagen) arrays showed that several other nAChRs are expressed in the cochlea, as we had previously reported, but that none were up or down-regulated at either PN10 or PN30 in constitutive knockout mice. Preliminary observations of efferent innervation during development were done using choline acetyltransferase (ChAT) to label efferent axons and terminals. In constitutive mutants after birth, efferent axons and terminals innervate inner hair cells (IHCs) followed by innervation of OHCs as found in wild type mice. However during the period immediately following transient innervation of IHCs, there is a significant increase in ChAT immunoreactivity below IHCs and a decrease in ChAT immunoreactivity below OHCs compared to wild-type littermates. We conclude that the constitutive deletion of hair cell nAChRs leads to a failure of efferent terminals to withdraw from the IHC area rather than the retraction of efferent terminals from the OHC area.

This research was supported, in part, by the Deafness Research Foundation (BJM), the American Hearing Foundation (BJM), the State of Nebraska (BJM) and NIH grant DC004086 (DDS).

### **751 Efferent Synapses Activate SK and BK Channels in Cochlear Outer Hair Cells**

Eric Wersinger<sup>1</sup>, Sonja Pyott<sup>2</sup>, Jeremy Braude<sup>2</sup>, **Paul Fuchs<sup>1</sup>**

<sup>1</sup>Johns Hopkins University School of Medicine, <sup>2</sup>University of North Carolina Wilmington

Cholinergic neurons of the brainstem olivary complex project to and inhibit outer hair cells, reducing acoustic sensitivity of the mammalian cochlea. Cholinergic inhibition of cochlear hair cells results from the combined action of ionotropic acetylcholine (ACh) receptors and associated calcium-activated potassium channels. Until recently this process was thought to involve only small conductance, SK potassium channels. However, in contrast to apical outer hair cells (OHCs), ACh-evoked currents in high frequency (basal) OHCs were found to be sensitive to the specific BK channel blocker iberiotoxin (Wersinger et al 2010, PLoSone 5:e13836). Also, immunolabeling showed that BK channels are colocalized with SK channels at the synaptic pole of mid- and basal turn OHCs. BK channels usually have much lower affinity for calcium than do SK channels. Thus, these findings raise the question of whether synaptic release of ACh with limited influx of calcium through postsynaptic ACh receptors can activate both channel types. Here we show that the average waveform of stochastic inhibitory postsynaptic currents (sIPSCs –occurring randomly in time during bath application of high K<sup>+</sup> to activate efferent ACh release) in high frequency outer hair cells was altered by blockade of either SK channels (by apamin) or BK channels (by iberiotoxin). BK channels supported briefer synaptic sIPSCs and SK channels supported prolonged sIPSCs. Consistent with the effects of blockers, sIPSCs recorded from high frequency outer hair cells (that express SK and BK channels) were briefer than sIPSCs recorded from low frequency (apical) outer hair cells that express only SK channels. Likewise, relatively prolonged sIPSCs were recorded from immature high frequency outer hair cells before the developmental onset of BK channel expression (as documented by immunohistology). Supported by NIDCD R01 DC001508 (PAF), P30 DC005211, and a Deafness Research Foundation grant to S.J.P.

### **752 Synaptic Integration by Type II Cochlear Afferents**

**Catherine Weisz<sup>1,2</sup>**, Elisabeth Glowatzki<sup>1</sup>, Paul Fuchs<sup>1</sup>

<sup>1</sup>Johns Hopkins University School of Medicine, <sup>2</sup>University of Pittsburgh School of Medicine

The afferent innervation of the mammalian cochlea is provided by type I and type II spiral ganglion neurons. Myelinated type I neurons encode acoustic frequency, intensity and timing by transmission from single inner hair cells (IHCs). In contrast, the relatively rare (5% of total) type II neurons are thin and unmyelinated, and receive inputs from many outer hair cells (OHCs) along a dendritic field spanning hundreds of microns. Despite this more extensive pool of presynaptic hair cells, type II afferents are thought to be acoustically insensitive (Robertson 1984). Excitatory post-synaptic potentials (EPSPs)

measured during intracellular recordings averaged  $3.8 \pm 2.0$  mV in amplitude (Weisz *et al.*, 2009), indicating a requirement for summation to exceed action potential threshold ( $\sim 25$  mV positive to rest). To evaluate the likelihood of effective synaptic summation, dual intracellular recordings at distances of  $\sim 100$  microns were made from the peripheral process of individual type II fibers as they extend beneath OHCs. Steady-state length constants averaged  $1189.6 \pm 1011.4$  ( $n = 5$  fibers). To locate the action potential initiation zone, supra-threshold current was injected at either electrode and the latency to action potential peak was measured. Regardless of which electrode injected current, the action potential always arrived first at the proximal electrode, and was smaller and broader at the distal electrode, indicating that the action potential was generated closer to the cell body, and then spread peripherally. Focal application of tetrodotoxin confirmed a central location for spike initiation. Supported by NIDCD grants R01 DC000276 and R01 DC006476, P30 DC005211, F31DC010948, T32 DC000023 and a grant from the Blaustein Pain Foundation of Johns Hopkins.

### **753 Adenomatous Polyposis Coli Protein (APC) Is Essential for Normal Ribbon Synapse Assembly and Hearing in the Postnatal Mouse**

**Tyler Hickman<sup>1</sup>**, M. Charles Liberman<sup>2,3</sup>, Michele Jacob<sup>1</sup>  
<sup>1</sup>Graduate Program in Neuroscience, Sackler School of Graduate Biomedical Sciences, Tufts University, <sup>2</sup>Eaton-Peabody Laboratory, Massachusetts Eye & Ear Infirmary, Boston, MA, <sup>3</sup>Program in Speech and Hearing Bioscience and Technology, Harvard-MIT, Cambridge, MA

Normal afferent function in the mammalian cochlea requires coordinated maturation of presynaptic ribbons in inner hair cells (IHCs) and postsynaptic AMPA receptor clusters in spiral ganglion (SG) neurons- the primary auditory neurons that signal sound reception to the brain. Noise damage leads to degradation of ribbon synapses and loss of low spontaneous rate (SR) SG neurons, greatly reducing the dynamic hearing range in noise-exposed animals. Recent studies have demonstrated differences in the size and polarized distribution of ribbon synapses that correlate with the SR of afferent fibers, suggesting that two distinct ribbon synapse types are required for hearing in low and high noise environs. Despite the requisite of functional ribbon synapse assembly and maintenance for hearing sensitivity, the underlying molecular mechanisms are poorly defined. We propose that the adenomatous polyposis coli protein (APC) plays a key synapse-organizing role in the cochlea.

APC is a ubiquitously expressed, large, multi-functional scaffold protein; it regulates the canonical Wnt signaling pathway, cell polarity, microtubule and actin cytoskeleton dynamics, as well as neuronal axon outgrowth and maturation of presynaptic and postsynaptic specializations. Further, APC is concentrated at nicotinic and glutamatergic postsynaptic sites in neurons. We predict that APC directs functional synapse assembly in the mammalian cochlea. To test our model, we have generated a new transgenic

mouse with conditional deletion of APC in postnatal excitatory neurons (APC-cKO) by crossing mice expressing APC flanked by LoxP with mice expressing CamKII-promoter-driven Cre recombinase.

APC-cKO mice, compared with control littermates, exhibit altered afferent ribbon synapse function, as indicated by reduced auditory brainstem response (ABR) thresholds. In addition, we find alterations in both ribbon synapse structure (shift to larger ribbon sizes only) and spatial distribution (loss of polarized localization) within IHCs, based on immunofluorescent confocal microscopic analyses. Our findings identify APC as a critical molecule for proper assembly of afferent synapses and normal hearing. The APC cKO mouse is a useful model for elucidating the specific role of ribbon size and spatial distribution in directing functional output of afferent synapses in the mammalian cochlea.

This work is supported by NIH grants NIDCD R01DC008802 (to MHJ), NINDS P30 NS047243 and NINDS T32 NS061764 (to TTH).

### **754 Developmental Maturation of Vesicle Trafficking at Mammalian Hair Cell Ribbon Synapses**

**Jee-Hyun Kong<sup>1</sup>**, Anthony Ricci<sup>1,2</sup>

<sup>1</sup>Department of Otolaryngology, <sup>2</sup>Department of Molecular and Cellular Physiology, Stanford University

Auditory primary afferent neurons fire continuously in response to sound stimulation with little fatigue. As afferent firing is driven by hair cell synaptic vesicle release, the hair cell must release vesicles at high rates for long periods of time. In order for hair cells to be capable of exocytosing vesicles continuously, a rapid vesicle replenishment mechanism must be in place. The recent development of a two sine wave technology that allows for continuous monitoring of capacitance (used as an indicator of synaptic vesicle fusion) reveals two distinct release components. The first component varied linearly with calcium influx, was depletable and represents all vesicles within the synaptic region. The second, superlinear component had an invariant rate and requires vesicle recruitment from outside the synaptic zone. To distinguish between release components, we undertook a developmental analysis of inner hair cell synaptic release to better understand when and how each component matured. We compared  $Ca^{2+}$  currents and release properties from DW/C3H/He mice and Sprague-Dawley rats between postnatal day (P) P2 and P24.  $Ca^{2+}$  currents peaked at P4 in mice and P7 in rats then decreased to between 30 and 50% of maximum with further development. The half activating voltage shifted hyperpolarized for mice but did not significantly change for rats. In mice, a 3 second depolarization to the peak  $Ca^{2+}$  current resulted in an initial release component that increased during maturation from  $\sim 10$  fF up to  $\sim 40$  fF. The second component remained  $\sim 200$  fF during the postnatal first week. During the second week of development, vesicle trafficking increased dramatically and continued to increase even up to P24. However, both release components showed developmental plateaus starting around P7 in the rat. Data suggests the time

course of maturation varies between species as well as between release components. This work was funded by NIDCD Grant DC009913 to AJR, core grant P30 44992.

### **755 Is Calcium-Induced Calcium Release Promoting Synaptic Vesicle Recruitment in Auditory Hair Cells?**

**Manuel Castellano-Munoz**<sup>1</sup>, Michael E. Schnee<sup>1</sup>, Jee-Hyun Kong<sup>1</sup>, Anthony J. Ricci<sup>1,2</sup>

<sup>1</sup>*Department of Otolaryngology, Stanford University,*

<sup>2</sup>*Department of Molecular and Cellular Physiology, Stanford University.*

Auditory hair cells release synaptic vesicles in an indefatigable manner during prolonged stimulation. However, the distinct mechanism by which reserve pools of vesicles are not depleted is not well understood. Real-time capacitance measurements have shown the existence of a superlinear release component comprising vesicles recruited from a large reserve pool during sustained release. High-speed calcium imaging demonstrated that cytoplasmic calcium levels correlate with capacitance results along with the activation of calcium-dependent SK channels, suggesting that calcium released from intracellular stores might drive recruitment of vesicles. We tested the potential role for calcium stored in the endoplasmic reticulum (ER) in the recruitment of vesicles using the two-sine capacitance technique and swept-field confocal calcium imaging. Pharmacological modulation of ER calcium levels and ryanodine receptors did not change release properties after single stimulation but did reveal modest effects in the superlinear component of release after repeated stimulation.

Supported by NIDCD, Stanford Dean's Postdoctoral Fellowship and Fundacion Caja Madrid Fellowship.

### **756 Characterization of Spontaneous EPSCs in Primary Afferent Fibers in the Turtle Auditory Papilla**

**michael schnee**<sup>1</sup>, anthony ricci<sup>1,2</sup>

<sup>1</sup>*Stanford University,* <sup>2</sup>*Molecular and Cellular Physiology*

The turtle papilla is a mature hearing organ that provides a robust preparation for the investigation of synaptic transmission at an auditory ribbon synapse. Whole cell afferent nerve recordings of spontaneous release reveal a relatively broad amplitude distribution of EPSCs (50 to 300 pA mean 138±61 pA SD N=14). The amplitude data suggests that 1 to 6 vesicles are released for each EPSC assuming a unitary event of 50 pA as previously determined for the frog<sup>1</sup>. The majority of EPSCs were monophasic although every cell had a small fraction of multiphasic events. The spontaneous release rate varied from 0.5 to 39 Hz with a mean of 9.4 ±9.3 Hz N=14. EPSCs were blocked by Ca<sup>2+</sup> channels blockers and the AMPA/kainate antagonist CNQX. Rise times ranged from 205 to 319 μs (mean 289 ± 29 μs N=14). Decay times were more variable with values ranging from 257 to 1060 μs (mean 649 ± 237 μs). No correlation was observed between kinetics and EPSC amplitude; however distinct populations of events could be found, for example EPSC's

with both slow rise and decay times. The tight distribution of EPSC rise and decay times both within and between cells is suggestive of highly synchronous release.

This work was funded by NIDCD Grant DC009913 and core grant P30 44992.

References

Geng-Lin Li, Erica Keen, Daniel Andor-Ardo, A. J. Hudspeth, and Henrique von Gersdorff 2009 J. Neuroscience 29(23):7558–7568

### **757 Bassoon as an Organizer of Inner Hair Cell Presynaptic Structure**

**Zhizi Jing**<sup>1</sup>, Mark Rutherford<sup>1</sup>, Thomas Frank<sup>1</sup>, Moser Tobias<sup>1</sup>, Nicola Strenzke<sup>1</sup>

<sup>1</sup>*InnerEarLab, University of Göttingen, Germany*

Inner hair cells (IHC) of mice lacking the central portion of presynaptic scaffold protein Bassoon (BSN<sup>ΔEx4/5</sup>) were previously shown to mostly lack synaptic ribbons and to have a smaller readily releasable pool of synaptic vesicles and reduced exocytosis, resulting in lower firing rates of auditory nerve fibers. Here, we attempted to distinguish better between the effects of the Bassoon mutation and those of the loss of the synaptic ribbon. We thus compared the BSN<sup>ΔEx4/5</sup> phenotype with that of a newly generated gene trap mutant BSN<sup>gt</sup>, which showed less severe ribbon loss and a higher fraction of ribbon occupied active zones. The mean distance between the remaining ribbons and the active zone was greater in BSN<sup>gt</sup> than in wildtype and the synaptic calcium channel clusters had reduced immunostaining reactivity. The BSN<sup>gt</sup> IHCs showed a slightly less severe reduction of peak Ca<sup>2+</sup> currents and sustained exocytosis compared to BSN<sup>ΔEx4/5</sup>. However, IHC fast exocytosis and single unit responses of auditory nerve fibers showed almost identical response properties between the two mutants. These data suggest that it is not the physical presence or absence of a synaptic ribbon but rather the disruption of presynaptic ultrastructure (e.g. abnormal calcium channel clustering, looser ribbon anchorage) that mainly determines the synaptic phenotype of Bassoon mutants.

### **758 Functional Development of the Medial Olivocochlear Efferent Innervation Before the Onset of Hearing**

Javier Zorrilla de San Martín<sup>1</sup>, Facundo Alvarez Heduan<sup>1</sup>, Ana Belén Elgoyhen<sup>1,2</sup>, **Eleonora Katz**<sup>1,3</sup>

<sup>1</sup>*Instituto de Investigaciones en Ingeniería Genética y Biología Molecular (INGEBI-CONICET),* <sup>2</sup>*Tercera Cátedra de Farmacología, FMED, Universidad de Buenos Aires,* <sup>3</sup>*DFBMC, FCEN, Universidad de Buenos Aires*

Before the onset of hearing (postnatal day (P) 12 in mice), inner hair cells (IHCs) are innervated by medial olivocochlear (MOC) fibers. At P9-11 transmitter release is supported by both P/Q and N-type voltage-gated Ca<sup>2+</sup> channels (VGCC) and negatively regulated by L-type VGCC, functionally coupled to the activation of BK channels (Zorrilla de San Martín et al., 2010). In previous work we showed that the quantal content (m) of transmitter release significantly increased between P5-7 and P9-11 (0.5 and 1.7, respectively) and that this increment was

accompanied by dramatic changes in the short term plasticity (STP) properties of this synapse.

Our present goal is to determine the basis for these developmental changes in synaptic transmission. Postsynaptic responses were monitored in whole-cell voltage-clamped IHCs while electrically stimulating the efferent fibers in isolated mouse organs of Corti. At P5-7,  $\gamma$ -Agatoxin IVA reduced  $m$  to  $37 \pm 6\%$  of control ( $p < 0.01$ ;  $n = 5$  cells) whereas  $1 \mu\text{M}$   $\gamma$ -Conotoxin GVIA failed to block transmitter release ( $n = 5$  cells), revealing that P/Q- but not N-type VGCC partially support transmitter release at the MOC-IHC synapse at this stage. To test whether BK channels modulate transmitter release, P5-7 cochleas were incubated with 100 nM Iberiotoxin, a specific BK channel antagonist. As reported for P9-11,  $m$  increased to  $192 \pm 11\%$  of control ( $p < 0.005$ ,  $n = 5$  cells). In addition, we estimated the readily releasable pool (RRP) size by repetitive stimulation protocols applied to the MOC fibers. The RRP size of the MOC-IHC synapse significantly increased from  $4.7 \pm 1.0$  vesicles at P5-7 to  $10.7 \pm 2.3$  vesicles at P9-11 ( $n = 7$  and  $n = 10$  cells, respectively;  $p < 0.01$ ). Our results suggest that both differences in the subtypes of VGCC that support transmitter release as well as differences in the RRP size, underlie the observed developmental changes in synaptic transmission.

Supported by CONICET, UBA and ANPCyT to ABE, EK; HHMI to ABE, NIHRO1 to PAF, ABE, EK.

### **[759] Short-Term Synaptic Plasticity at the Medial Olivocochlear Hair Cell Synapse in $\alpha 9\alpha 10$ Knock-In Mice**

Jimena Ballester<sup>1</sup>, Facundo Alvarez Heduan<sup>1</sup>, Paul Fuchs<sup>2</sup>, Eleonora Katz<sup>1,3</sup>, Ana Belén Elgoyhen<sup>1</sup>

<sup>1</sup>Instituto de Investigaciones en Ingeniería Genética y Biología Molecular (INGEBI-CONICET), <sup>2</sup>Center for Hearing and Balance, Dept. Otolaryngol-Head and Neck Surgery, Johns Hopkins Univ, <sup>3</sup>Dept. Physiology, Molecular and Cellular Biology, FCEN, University of Buenos Aires

Cochlear amplification is regulated by the central nervous system through medial olivocochlear (MOC) neurons that project from the brainstem and synapse onto outer hair cells (OHCs). The OHCs inhibitory postsynaptic currents (IPSCs) in the OHCs are mediated by the activation of  $\alpha 9\alpha 10$  nicotinic receptors (nAChRs) and SK2 calcium-activated potassium channels. We have generated a mouse with a point mutation (L9'T) in the  $\alpha 9\alpha 10$  nAChR that produces longer-lasting inhibitory postsynaptic currents and changes the magnitude and the dynamics of the efferent-mediated inhibition of cochlear responses (Taranda et al. Plos Biology, 2009). Our goal is now to determine if there is a consequent change in the short-term plasticity (STP) properties of the MOC-hair cell synapse. In order to do so we used the transient MOC-inner hair cells (IHCs) synapse as a model. Synaptic activity was recorded in voltage-clamped IHCs from excised apical turns of wild-type (wt) or  $\alpha 9\alpha 10$  knock-in (kin) mouse cochlea (9-11 postnatal days) during electrical stimulation of the MOC fibers. As was previously shown for spontaneous IPSCs, electrically evoked IPSCs in kin mice

presented longer decay times ( $\tau_{\text{decay}}$  wt:  $46 \pm 3$  ms; kin:  $267 \pm 35$  ms) and smaller peak amplitudes ( $I_{\text{peak}}$  wt:  $-39 \pm 8$  pA; kin:  $-20 \pm 3$  pA) compared to those of wt IHCs. The mean quantum content of the MOC-IHC synapse showed no significant differences between wt ( $1.0 \pm 0.3$ ) and kin ( $0.7 \pm 0.2$ ) mice, indicating no alterations in basal synaptic efficacy. In wt IHCs, prolonged high frequency stimulation produced an increase in the postsynaptic response during the 1st second, followed by depression that produced  $\sim 80\%$  decay in the response. In kin mice, peak responses were reached after  $\sim 3$  sec of stimulation and then decayed to  $\sim 50\%$ . These results show that changes in the dynamics of the nAChR induce dramatic changes in the MOC-hair cell synapse STP properties.

### **[760] Spontaneous Activity of Hair Cells in the Developing Cochlea Is Triggered by Potassium Release from Supporting Cells**

Han Chin Wang<sup>1</sup>, Dwight Bergles<sup>1</sup>

<sup>1</sup>Dept. of Neuroscience, Johns Hopkins School of Medicine  
Before hearing onset, inner hair cells (IHCs) exhibit periodic depolarizations, which results in calcium action potentials, glutamate release at inner hair cell-afferent synapses, and ultimately bursts of action potentials in spiral ganglion neurons. These discrete bursts of activity are thought to promote the survival, maturation, and refinement of auditory circuits in the brain. Previous studies have shown that this activity is initiated by the spontaneous release of ATP by supporting cells within Kölliker's organ. Activation of purinergic receptors in supporting cells also induces a transient crenation. However, the functional significance of these changes in cell shape, and the relationship between this phenomenon and spontaneous electrical activity in the developing cochlea, are not well understood. Here, we report that depolarization of hair cells is primarily induced through the release of  $\text{K}^+$  from supporting cells following crenation, rather than through activation of purinergic receptors in these cells. In support of this hypothesis, crenation events and spontaneous currents in IHCs appear concurrently during development, and both spontaneous and ATP-evoked currents in IHCs were significantly reduced when  $\text{K}^+$  channels were blocked intracellularly. Moreover, recordings from IHCs in  $\text{Ca}^{2+}$  and  $\text{Na}^+$  channel blockers revealed that application of ATP caused a depolarizing shift in EK. These local elevations of  $\text{K}^+$  also increased the frequency of spontaneous efferent synaptic currents in IHCs, the waveforms of which shifted in voltage-clamp recordings from biphasic (inward-outward) to monophasic (inward only) during ATP-induced events, as predicted for a positive shift in EK. These results suggest that supporting cell crenation is intimately linked to spontaneous activity in the developing auditory system, and reveal that supporting cells also modulate release from efferent terminals during this crucial period of development.

## **761 Differential DNA Damage Response Among Auditory Sensory Neurons Following Ototrauma**

O'neil Guthrie<sup>1,2</sup>, Terry Fleck<sup>2</sup>, Helen Xu<sup>2</sup>

<sup>1</sup>Loma Linda Veterans Hospital, <sup>2</sup>Otolaryngology and Head & Neck Surgery, School of Medicine, Loma Linda University

Noise exposure has been shown to precipitate free radical induced DNA damage products in the cochlea. Free radical DNA damage can result in mutated gene fragments that alter cellular functions and/or induce progressive cell death. The nucleotide excision repair (NER) pathway is particularly adapted to protecting both active and inactive genes through genetically distinct subpathways that require a Cockayne syndrome-A (CSA) E3-ubiquitin ligase complex and the xeroderma pigmentosum-C (XPC/nHR23B/centrin2) heterotrimeric preincision complex. The rate limiting factor in both pathways is the zinc-finger scaffolding protein XPA, which positions and activates nucleases for excision of damaged gene fragments. Noise is known to induce progressive degeneration of spiral ganglion neurons, however a subpopulation of neurons consistently remain viable. This difference in viability might be mediated through NER. Therefore, it was posited that noise exposure would induce differential DNA damage responses among spiral ganglion neurons. Male Long-Evans rats were exposed to an 8 kHz octave band of noise at 105 dB SPL for 4 hours. Distortion product otoacoustic emissions were recorded before and after noise exposure and the animals were sacrificed via transcardial perfusion for temporal bone harvesting, immunohistochemistry and quantification of intracellular protein distribution. The results revealed that the majority (~60%) of spiral ganglion neurons do not express NER protein complexes as a defense against noise exposure which may help to explain selective neurodegeneration. However, under normal conditions a cohort of neurons (~40%) exhibited either cytoplasmic or nuclear localization of NER factors. After noise exposure there was a significant ( $p < 0.01$ ) increase in the number of these neurons which indicates that a fraction of the constitutively inactive neurons became active. The translocation of NER factors from the cytoplasm to the nucleus was dependent on the location of neurons along the cochlear spiral. For instance, neurons at the apical coil exhibited significant ( $p < 0.01$ ) nuclear translocation of the CSA complex while neurons at the basal coil revealed significant ( $p < 0.05$ ) nuclear translocation of the XPC complex. This spacial difference in nuclear translocation between CSA and XPC complexes suggests a difference in genome defense repertoire between apical and basal spiral ganglion neurons. Furthermore, noise exposure depleted XPA from the nucleus regardless of location along the cochlear spiral. These findings provide a novel mechanism for interpreting noise induced primary neuropathy and provide a basis for noise induced mutagenesis.

## **762 Alignment of Neurites and Schwann Cells from the Spiral Ganglion to Micropatterned Substrates Involves $Ca^{2+}$ and Cyclic Nucleotide Second Messenger Systems and Rho-Associated Kinase (ROCK)**

Shufeng Li<sup>1</sup>, Bradley Tuff<sup>2</sup>, Joseph Clarke<sup>1</sup>, Linjing Xu<sup>1</sup>, Allan Guymon<sup>2</sup>, Marlan Hansen<sup>1</sup>

<sup>1</sup>Departments of Otolaryngology-Head and Neck Surgery, University of Iowa, <sup>2</sup>Chemical Engineering, University of Iowa

We recently demonstrated that microchannels induced by photopolymerization in methacrylate polymers guide SGN neurite and spiral ganglion Schwann cell (SGSC) growth. While the signaling mechanisms activated by chemotactic molecules (e.g. semaphorins) to direct neurite growth have been widely explored, the mechanisms by which neurons and glia sense and transduce changes in the physical environment into directed growth remain largely unknown. Here we explored the contribution of  $Ca^{2+}$  and cyclic nucleotide second messenger systems and the downstream effector kinase, ROCK, to neurite and glial alignment to micropatterned substrates. We increased  $[Ca^{2+}]_i$  by depolarizing the cultures with elevated (25 mM and 50mM) extracellular  $K^+$  (25K and 50K) or by treating the cultures with the L-type channel agonist, Bay K8466. Both significantly reduced neurite alignment suggesting that chronically elevated  $[Ca^{2+}]_i$  prevents neurite alignment. Treatment with cpt-cAMP, a cyclic AMP analog, significantly reduced SGN neurite and SGSC alignment while 8-bromo-GMP, a cyclic GMP analog, increased neurite alignment suggesting reciprocal antagonism between these cyclic nucleotides. To determine the extent to which micropatterns induce ROCK activity, we quantified ROCK phosphorylation (pROCK) based on immunofluorescence intensity with a phospho-specific ROCK antibody in SGNs. pROCK immunolabeling was significant greater in SGN neurites aligned to micropatterns compared to neurites on unpatterned polymers indicating ROCK activation by micropatterns. Further, treatment with the ROCK inhibitors H1152 or Y27632 significantly reduced SGN neurite and SGSC, but not AC, alignment in a dose-dependent manner. These results suggest that  $Ca^{2+}$ , cyclic nucleotides, and ROCK are key mediators of SGN neurite and SGSC alignment to microchannels.

## **763 The Ability of Micropatterned Methacrylate Polymers to Direct Neurite Growth from Spiral Ganglion Neurons Depends on Pattern Amplitude and Periodicity**

Linjing Xu<sup>1</sup>, Bradley Tuff<sup>2</sup>, Joseph Clarke<sup>1</sup>, Shufeng Li<sup>1</sup>, Allan Guymon<sup>2</sup>, Marlan Hansen<sup>1</sup>

<sup>1</sup>Departments of Otolaryngology-Head and Neck Surgery, University of Iowa, <sup>2</sup>Chemical Engineering, University of Iowa

Both biochemical and physical features in the environment guide the growth of developing neurites and both biochemical and physical micropatterning have been used

to direct the growth of regenerating neurites. We recently demonstrated that line-space grating micropatterns in methacrylate (MA) polymers systems direct neurite growth from ganglion neurons (SGNs). To characterize the aspects of physical features critical for neurite alignment, we used photopolymerization to generate micropatterns of varying amplitudes and periodicities. Varying the photoinitiator concentration and the total radiation dosage received at the sample surface resulted in excellent control of feature depth (Fig. 1). Specifically, ridge-groove amplitude was shown to be readily tunable from 1-10  $\mu\text{m}$ . Feature frequency was controlled by decreasing the spacing or periodicity of the photomask from 10-100  $\mu\text{m}$ . We found that increasing feature amplitude or decreasing periodicity each independently enhanced SGN neurite alignment. To compare the extent to which other neurons and glia align to micropatterns, we prepared cultures from several different neuronal and glial populations, including trigeminal ganglion neurons (TGNs), dorsal root ganglion neurons (DRGs), cerebellar granular neurons (CGNs), astrocytes (ACs), and SG Schwann cells (SGSCs). We found that neurites from SGNs, TGNs, DRGs and CGNs aligned to microchannels. SGN neurites tended to align better than neurites from TGNs and DRGs. In CGNs, Tau-positive neurites (axonal) and MAP2-positive neurites (dendritic) both demonstrated robust alignment. Astrocytes (ACs), like SGSCs, aligned to the pattern. These results indicated that microchannels generally induce neuron and glial alignment although there are differences in the extent of alignment. SGN neurite alignment depends on both microchannels amplitude and periodicity.

#### **764 Elevated P75<sup>NTR</sup> Expression in Vestibular Schwannoma Cells Results from Merlin Inactivation and Contributes to Enhanced Cell Survival**

**Iram N. Ahmad**<sup>1</sup>, Wei Ying Yue<sup>1</sup>, Augusta Fernando<sup>1</sup>, J. Jason Clark<sup>1</sup>, Ryan Beardsley<sup>2</sup>, Ryan L. Deets<sup>1</sup>, Marlan Hansen<sup>1</sup>

<sup>1</sup>University of Iowa, <sup>2</sup>Brigham Young University

We are interested in the differences of vestibular schwannoma (VS) cells compared with normal Schwann cells (SCs) that allow VS cells to survive in the absence of axonal contact. Following loss of axonal contact, normal SCs upregulate p75<sup>NTR</sup> expression ultimately leading to apoptosis. Quantitative RT-PCR and western blots demonstrate that, like denervated SCs, VSs express higher levels of p75<sup>NTR</sup> compared with normal nerves. Replacement of functional merlin into cultured VS cells reduces p75<sup>NTR</sup> expression. Further, p75<sup>NTR</sup> expression is elevated in the sciatic nerves of mice harboring a SC-specific dominant negative merlin mutation (POS<sup>SC6</sup> -121) compared to nerves from wild-type mice. These results imply that the increased p75<sup>NTR</sup> expression in VS cells results from lack of functional merlin expression. ProNGF, a high affinity ligand for p75<sup>NTR</sup>, induces apoptosis in normal SCs, likely by increasing c-Jun N-terminal kinase (JNK) phosphorylation. By contrast, VS cells treated with proNGF fail to die in spite of proNGF-mediated JNK activation. Similarly, we found decreased

apoptosis in sciatic nerve SCs in POS<sup>SC6</sup> -121 mice compared to wild-type mice following axotomy, demonstrating enhanced survival of SCs lacking functional merlin despite elevated p75<sup>NTR</sup> expression. Further, proNGF rescued VS cells from apoptosis due to kinase inhibitors. This pro-survival response was associated with NF $\kappa$ B activation and eliminated by transduction with a dominant negative NF $\kappa$ B isoform. Taken together these results suggest that merlin status determines the extent of p75<sup>NTR</sup> expression and that p75<sup>NTR</sup> signaling promotes survival of SCs lacking functional merlin, such as VS cells. This pro-survival response is due, at least in part, to NF $\kappa$ B activation. Thus, p75<sup>NTR</sup> signaling likely contributes to the persistent survival of VS cells in the absence of axonal contact, in contrast its pro-apoptotic effect in normal SCs.

#### **765 The Tumor Suppression Gene Product, Merlin, Inhibits Neurite Growth from Spiral Ganglion Neurons**

**Joshua Tokita**<sup>1</sup>, Bethany Harpole<sup>1</sup>, Hetel Shah<sup>2</sup>, Marlan R Hansen<sup>1</sup>

<sup>1</sup>University of Iowa Hospitals and Clinics, <sup>2</sup>University of Iowa College of Medicine

Merlin, the product of the NF2 tumor suppression gene, inhibits several intracellular signaling cascades implicated in neuritogenesis and neurite growth such as Ras, Rac, phosphatidylinositol-3 kinase/Akt, extracellular regulated kinase, and c-Jun N-terminal kinase. We find that merlin is expressed in spiral ganglion neurons (SGNs) raising the possibility that merlin regulates SGN neurite growth in addition to its well-known role in Schwann cell tumorigenesis. Using a tamoxifen-inducible Cre-mediated recombination system to conditionally knock out merlin, we demonstrate that reduction of merlin expression increases both the number and length of neurites in SGNs and trigeminal ganglion neurons (TGNs). Treatment with tamoxifen, leading to diminished merlin expression, increased neurite length from 365 $\pm$ 125  $\mu\text{m}$  (mean $\pm$ SE) to 522 $\pm$ 165  $\mu\text{m}$  in cultured neonatal SGNs and from 372 $\pm$ 31  $\mu\text{m}$  to 510 $\pm$ 113  $\mu\text{m}$  in TGNs. Current studies examine the merlin-sensitive signaling pathways that contribute to SGN neurite growth and the influence of merlin status on synaptogenesis. These results raise the possibility that merlin regulates neural development and/or regeneration, in addition to its recognized role in suppressing tumor growth.

#### **766 Characterization of Structural Proteins Within the Spiral Ganglion Neuronal Soma and Initial Processes**

**Felicia L Smith**<sup>1</sup>, Zachary Q Wismer<sup>1</sup>, Robin L Davis<sup>1</sup>

<sup>1</sup>Rutgers University

Spiral ganglion neurons have distinct structural features that vary with cochlear location such as cell body area, axon diameter, and internodal distance. These features are important for neuronal coding in the peripheral auditory system because they can have a direct impact on the timing and filtering of transmitted electrical signals. Furthermore, the spiral ganglion somata are surrounded by

loose myelin and flanked by nodes of Ranvier to ensure safe and efficient action potential propagation.

Our aim is to determine the tonotopically distributed molecular specializations that affect signal transmission through the spiral ganglion. We found that the dendritic marker, microtubule associated protein 2 (MAP2), was distributed in neuronal somata and extended for limited distances along both central and peripheral initial processes. Furthermore, anti-MAP2 antibody-labeled regions within the initial processes were flanked by ankyrin G (AnkG). This molecular configuration, thus, defined the nodes immediately surrounding the soma. Similar to observations *in vivo* (Robertson, *Brain Res* 1976), we found that these nodal distances were not uniform, but varied from cell to cell. Interestingly, our quantitative analysis from *in vitro* preparations showed that these variations were correlated to tonotopic location. Anti-MAP2 antibody labeling distance measured from the center of the soma to the region of AnkG labeling was  $30 \pm 2 \mu\text{m}$  for apical neurons ( $n=8$ ) and  $25 \pm 1 \mu\text{m}$  for basal neurons ( $n=8$ ); a difference that was significant ( $p<0.05$ ). The absolute values were similar to those measured *in vivo*, which ranged from 40 to 25  $\mu\text{m}$ .

In summary, the electrophysiological significance of the cell body is highlighted by the unique intracellular distribution of MAP2 in the spiral ganglion. Moreover, our observations of MAP2 distribution and nodal distance reveal a level of precision associated with tonotopic location. Supported by NIH NIDCD R01 DC-01856

### **[767] Dynamics of TrkB and TrkC Motion in Spiral Ganglion Neurites**

**Kathryn Parker**<sup>1</sup>, Shruti Nayak<sup>1</sup>, Katrin Deinhardt<sup>1</sup>, Yixin Fang<sup>1</sup>, Moses Chao<sup>1</sup>, Pamela Roehm<sup>1</sup>

<sup>1</sup>New York University School of Medicine

Brain-derived neurotrophic factor (BDNF) and neurotrophin-3 (NT3) have an integral and dynamic role in the cochlea. Spiral ganglion neurons (SGNs) require neurotrophins (NTFs) for development, survival and neurite outgrowth, and express TrkB and TrkC receptors which bind to BDNF and NT3 respectively. These NTFs are expressed at different concentrations in a gradient from the apex to the base of the cochlea in a developmentally-specific fashion. Exposure of SGNs to the NTF found at higher concentrations in the opposite ends of the cochlea leads to diametric changes in their firing patterns (Adamson, 2002). To cause these profoundly different effects in SGNs, NTFs are first internalized and then they or their effectors are transported to the site of action. Using live imaging supplemented by images of timed fixed cultures, we have studied the dynamics of BDNF/TrkB and NT3/TrkC receptor trafficking in SGNs. These basic trafficking events underlie appropriate signaling of BDNF and NT3 in SGNs. In cultured SGNs, both TrkB and TrkC are rapidly internalized into vesicles. In apical neurons, TrkC mobility is significantly more rapid than in basal SGNs ( $p = 0.0027$ ) while in basal neurons TrkB is transported more rapidly ( $p = 0.002$ ). Strategies utilizing BDNF and NT3 to improve SGN survival and neurite outgrowth depend upon proper uptake and

localization of NTF/receptor complexes with SGNs. Thus, better understanding of the dynamics of these transport events will allow more rational use of neurotrophins.

### **[768] Stimulation of Spiral Ganglion Neurite Growth by Rho Kinase Inhibitors**

**Donna S. Whitlon**<sup>1,2</sup>, Abraham J. Rozental<sup>1</sup>, Mary Grover<sup>1</sup>

<sup>1</sup>Department of Otolaryngology, Feinberg School of Medicine, Northwestern University, <sup>2</sup>Hugh Knowles Center, Northwestern University

Growth of spiral ganglion neurites *in vitro* is stimulated by exposure to the Rho kinase inhibitor H-1152, as determined by hand measurements and Cellomics software (Lie et al., 2010). To determine the extent to which the automated results are dependent on the inhibitor tested or the software used for analysis, we compared the effects of H-1152 across two commercial (Cellomics and HCA Vision) and one custom written neurite quantification computer programs. All three computerized measurements demonstrated increased neurite length response to H-1152. We further compared the lengths of neurites after 5 days of culture exposed to medium containing: H-1152, two additional Rho Kinase inhibitors, an irrelevant inhibitor (stat 3 inhibitor peptide, 500 $\mu\text{M}$ ), water or no additions, using the HCA Vision program. Cumulative percent histograms of the longest neurite lengths per neuron were generated. Two sets of overlapping graphs resulted. The first set represented wells exposed to water, no additions or an irrelevant inhibitor. The second set, indicating wells with longer neurites, represented cultures exposed to the three Rho Kinase inhibitors, and had median neurite lengths approximately 50% longer than those of the controls. These data emphasize the regulatory effect of Rho kinase on spiral ganglion neurite growth, the reproducibility and robustness of the effects of Rho kinase inhibitors and demonstrate the utility of automated neurite measurements in screening growth inducing factors on spiral ganglion neurons. Supported by the Hugh Knowles Leadership Fund and the Department of Otolaryngology, Northwestern University.

### **[769] Time-Line for Spiral Ganglion Survival After Transtympanic Infusion of Neomycin Sulfate in Albino Guinea Pigs**

**Anette Fransson**<sup>1</sup>, Mats Ulfendahl<sup>1</sup>

<sup>1</sup>Karolinska Institutet, Sweden

The function of a cochlear implant depends in part on survival and responsiveness of the spiral ganglion neurons (SGN). The purpose of this study was to investigate the time-line of SGN survival after transtympanic infusion of the ototoxic agent neomycin sulfate in guinea pigs. Three animals (6 cochleae) in each group were sacrificed at different time points (week 1, 4, 7, 10, 12 and 18) after deafening. A group of three non-deafened animals served as control. Click-ABRs were measured in all animals prior to the infusion of neomycin and every second week thereafter. Before sacrificing the animals frequency specific ABRs were obtained. The total amount of remaining SGN was calculated by using a stereology. In some groups also measures of the volumes of the soma

and nucleus were obtained. The ABR results verified that all animals were profoundly deaf following neomycin infusion. Stereology results showed a rapid degeneration of SGN during the first seven weeks. During the following weeks and until the eighteenth week the progression of degeneration of SGN slowed down significantly.

## **770 Effects of Sex and Reproductive Status on the Frequency-Temporal Resolution Trade-Off**

**Megan Gall<sup>1</sup>**, Jeffrey Lucas<sup>1</sup>

<sup>1</sup>*Purdue University*

Many organisms, including humans, experience changes in hormone profiles related to reproductive status. Songbirds have pronounced sex-specific changes in hormone profiles between the breeding and non-breeding season and therefore make a particularly good model system for exploring the relationship hormone profiles and auditory performance. Increases in steroid hormone profile during the breeding season are accompanied by dramatic sex-specific changes in vocal output. It has been hypothesized that seasonal changes in auditory performance could be related to these seasonal changes in vocalizations and vocalization-based mate selection. Indeed, previous work has shown that frequency sensitivity changes seasonally in several species of songbirds, with up-regulation of sensitivity in the breeding season. Here we explored the effects of sex and season on the trade-off between frequency resolution and temporal resolution in the house sparrow (*Passer domesticus*) using auditory evoked potentials. To the best of our knowledge this is the first study to investigate seasonal changes both in frequency and temporal resolution in songbirds. We used notched-noise masking to determine auditory filter bandwidth at 2, 3, and 4 kHz and a paired-click paradigm to evaluate temporal resolution. We found that individuals with broader filters had better temporal resolution than individuals with narrower auditory filters and that this pattern varied across sexes and seasons. We discuss the potential role of steroid hormones in hair cell tuning and the frequency-temporal resolution trade-off. We also discuss and the potential impact of this trade-off on the processing of song by males and females.

## **771 Synaptic Inputs Coding of Interaural Level Differences in Inferior Colliculus (IC) of Mouse**

**Munenori Ono<sup>1</sup>**, Douglas Oliver<sup>1</sup>

<sup>1</sup>*University of Connecticut Health Center*

Interaural level difference (ILD) is an important cue used to localize a sound source. The IC receives and integrates ILD information from possibly more than one source in the brainstem. However, the synaptic basis for this integration in the IC is unclear. Here, we used in vivo whole-cell voltage clamp recordings to study the synaptic responses of IC neurons to ILD stimuli presented in a closed sound field with minimal crosstalk.

We see 3 types of extracellular responses to ILD stimuli by IC neurons using a constant average binaural intensity

(ABI): contra-preferred (48%), U-shape (22%), and center-preferred (30%). The contra-preferred neurons responded to the maximum negative ILD when the contralateral sound level was highest. U-shape neurons responded to either the maximum negative or positive ILD when either the contralateral or the ipsilateral sound level was highest. The center-preferred neurons showed the peak response at around 0 ILD. Most neurons (69%) showed no response or inhibition to ipsilateral stimuli.

In contrast, 80% of cells (44/55) showed EPSCs in whole-cell recordings in response to ipsilateral and contralateral stimuli. IPSCs to monaural ipsilateral stimuli were seen in 76.5 % of cells. With ABI stimuli, most IC neurons showed the strongest synaptic currents at ILDs favoring the contralateral side. Their EPSCs and IPSCs were well balanced and their response patterns to ILD changes were highly correlated. In other cells, the EPSC was largest around 0 ILD, and the EPSCs and IPSCs were poorly correlated. Recordings of both extracellular and intracellular responses from the same neuron suggest that the synaptic input patterns predict the spike responses.

These results showed that synaptic processing in the IC is more complex than expected from the extracellular responses and suggested that the integration and balance of the excitatory and inhibitory conductances are important in shaping the ILD sensitivity of IC neurons.

NIH grant R01-DC000189 (DLO)

## **772 In-Vivo Whole Cell Recordings Revealed Binaural Mechanism for the Facilitated Response in EI/F Neurons**

**George Pollak<sup>1</sup>**, Na Li<sup>1</sup>

<sup>1</sup>*University of Texas at Austin*

Cells that receive excitation from one ear and inhibition from the other (EI cells) process interaural intensity disparities (IIDs), the cues for localizing high frequencies. EI cells in the inferior colliculus (IC) fire to contralateral stimulation, while ipsilateral stimulation at progressively higher intensities suppresses the spikes evoked by contralateral stimulation. Facilitated EI cells (EI/f) are a variation of EI cells in that facilitated spike-counts, higher than those evoked by the contralateral signal, are evoked with binaural signals having low ipsilateral intensities. To evaluate the binaural mechanism underlying the facilitated binaural response, we made whole cell patch-clamp recordings in 11 EI/f cells in the IC of awake Mexican free-tailed bats. Both spikes and postsynaptic potentials (PSPs) evoked by contralateral, ipsilateral and binaural signal were recorded. Moreover, excitatory and inhibitory synaptic conductances were derived from each response recorded in one cell. Based on both the PSPs and conductances, we propose the inputs that innervate these EI/f cells and show that the basic EI property was produced by innervation from a lower binaural nucleus, presumably the LSO. We then show that these cells also received an ipsilaterally evoked inhibition and an ipsilaterally evoked subthreshold excitation. The facilitation resulted from two features; 1) the ipsilaterally evoked excitation; and 2) a reduction in the ipsilaterally evoked inhibition due to contralateral stimulation. Thus, at

small IIDs, with weak ipsilateral signals, the reduced inhibition allows the combined contralateral and ipsilateral excitatory inputs to generate a larger EPSP than would be evoked by the contralateral excitation alone, thereby generating the facilitated response. Supported by NIH grant DC007856.

### **773 Temporal Nonlinearities for Amplitude Modulation Coding in the Unanesthetized Rabbit Inferior Colliculus**

**Monty Escabi<sup>1</sup>**, Peter Boutros<sup>1</sup>, Duck Kim<sup>2</sup>, Shigeyuki Kuwada<sup>2</sup>

<sup>1</sup>*University of Connecticut*, <sup>2</sup>*University of Connecticut Health Center*

Amplitude modulations (AM) are key acoustic elements in behaviorally relevant sounds. Neurons in the inferior colliculus (IC) respond selectively to AMs where clear evidence for modulation tuning has been described. Yet only a few studies have addressed how nonlinear encoding mechanisms contribute to AM sensitivity in the IC and all these were performed in anesthetized mammals. We thus examine how temporal nonlinearities contribute to AM sensitivity in the unanesthetized rabbit. Spike-triggered average and covariance methods were used to measure 1st and 2nd order Wiener kernels in response to randomly modulated sounds. The nonlinear 2nd order kernels were decomposed into a set of orthogonal modulation filters following Yamada and Lewis (1999). A linear-nonlinear model was devised that included a quadratic nonlinearity, output nonlinearity that incorporates the effects of saturation and rectification (Atencio et al 2008), and a spike generating compartment that includes temporal nonlinearities associated with the spike generating mechanism (Escabi et al 2005). The predictive power of the model was then assessed for random modulated stimuli and sinusoidal AM (SAM). Although the linear filter model alone could predict some aspects of synchronized activity it often failed to predict unsynchronized responses. For instance, the nonlinear model was capable of predicting unsynchronized responses in the neurons rate modulation transfer function that were often observed at high modulation frequencies. In addition the composite nonlinear model was capable of predicting nonlinear phenomena including interactions between modulation frequency channels, nonlinear responses to envelopes of envelopes, and period doubling in the response. Thus the composite nonlinear model explains a number of processing mechanisms that are operative in the IC of the unanesthetized rabbit and which cannot be accounted by conventional linear models.

### **774 Neural Coding of Envelopes in the Inferior Colliculus: Effect of Environment, Location and Binaurality**

**Shigeyuki Kuwada<sup>1</sup>**, Brian Bishop<sup>1</sup>, Duck O. Kim<sup>1</sup>

<sup>1</sup>*University of Connecticut Health Center*

Little is known about neural processing of envelopes in different environments and sound source locations. The virtual auditory space (VAS) method is an efficient way to

produce such sounds. We measured head related and binaural room transfer functions (HRTFs and BRTFs, respectively) in rabbits in anechoic and reverberant environments and generated VAS stimuli by filtering stimuli with the rabbits' own HRTFs and BRTFs. The VAS stimuli were delivered through earphones coupled to custom-fitted ear molds. Neural recordings were made with tungsten-in-glass microelectrodes from neurons in the inferior colliculus of a restrained, unanesthetized rabbit. We determined the neuron's best frequency (BF) and used this information to choose the center of a 1-octave wide noise band. We tested the neuron's responses to modulated VAS sounds at different modulation frequencies (2 - 512 Hz), different azimuths ( $\pm 150^\circ$ ), different distances (10 - 160 cm), and in different environments. In all cases, the sounds were delivered both binaurally and to the contralateral ear alone.

In the anechoic environment, there was dissociation between rate and synchrony to envelopes in some neurons. For example, a neuron shows strong binaural facilitation in rate and yet its synchrony to binaural stimulation is weaker than to that to monaural. In reverberation, some neurons exhibit reverberation resistance in envelope sensitivity, and/or azimuth tuning while others are highly susceptible in both types of processing. Azimuth tuning generally requires binaural stimulation in all environments. Envelope sensitivity is more diverse in that reverb resistance is seen under monaural stimulation in some neurons and under binaural stimulation in others. Synchrony in reverberation generally increases with decreasing distance, whereas in the anechoic environment it is generally constant across distance.

### **775 Modeling IC Responses to Envelope Interaural Time Differences in SAM Stimuli**

**Le Wang<sup>1</sup>**, H. Steven Colburn<sup>1</sup>

<sup>1</sup>*Boston University*

In a subset of cells in the inferior colliculus (IC) with high characteristic frequencies (CF), the firing rate can be modulated by the envelope interaural time difference (ITD). In response to binaural sinusoidally-amplitude-modulated (SAM) tones, many of these envelope-ITD-sensitive IC cells fire maximally at the same ITD at all modulation frequencies (peak-type neurons), whereas many others are maximally suppressed at the same ITD (trough-type neurons). In addition to these peak-type cells and trough-type cells, it has been found that a third category of ITD-sensitive IC cells can exhibit more than one type of envelope ITD sensitivity, depending on the stimulus. Some neurons in the third category show peak-type response at modulation frequencies lower than 150 Hz and trough-type response at modulation frequencies higher than 250 Hz, and other neurons in the same category show the opposite. The behavior of multiple types of envelope ITD sensitivity in single cells has not been observed in lower auditory nuclei (e.g., superior olive), and is thus unlikely to be directly inherited from a single input to the IC. Similar to the dual-type envelope ITD sensitivity in high-CF IC cells, a nonlinear best-phase-versus-frequency function (phase

plot) in response to pure tones was observed in some low-CF IC neurons. A previously developed IC model showed that convergent inputs from the medial and lateral superior olive (MSO and LSO) could largely account for the nonlinear phase plot if the CFs of the MSO input and the LSO input were different (Shackleton et al., *Hearing Research*, 2000). We hypothesize that such a model might also explain the multiple types of envelope ITD sensitivity for high-CF IC cells. To test this hypothesis, we built an IC model with similar convergent inputs from the MSO and LSO. When the CFs of the two inputs are set to be different and the carrier frequency of the SAM tone stimulus is equal to the CF of the LSO input, the dual-type envelope ITD sensitivity can be shown by the model. This result is consistent with the hypothesis that the convergent inputs from MSO and LSO underlie the responses to ITD for both low-CF and high-CF IC neurons.

### **776 Temporal Emphasis in the Binaural System: Lateralization of Amplitude Modulated Binaural Beats**

**Mathias Dietz<sup>1</sup>, Torsten Marquardt<sup>1</sup>, David McAlpine<sup>1</sup>**  
<sup>1</sup>*UCL Ear Institute*

Two tones with slightly different frequencies, one presented to the left and the other to the right ear, result in an oscillating intracranial lateralization, called binaural beat. A noticeable motion can be only perceived with beat frequencies below 5 Hz, even though binaural sensitivity of neurons in the midbrain follows much higher beat frequencies. We examined the lateralization of binaurally-beating tones, which were in addition amplitude modulated (AM) at the same frequency as the binaural beat. The AM was binaurally in phase and emphasizes a certain range of IPD during the beat cycle, so that a clear lateralization of the stimulus can occur, depending on relation between beat and AM phase. The common frequency for both AM and beat was varied between conditions from 4 to 32 Hz. For a beat in which the interaural phase difference (IPD) is zero at either the modulation trough or peak, traditional binaural models predict leading and lagging IPDs to cancel, resulting in no overall lateralization. Despite this, however, listeners clearly lateralized the stimulus at all beat/AM frequencies. The instantaneous IPD just following the onset of each AM cycle correlates much stronger with the perceived lateralization than the IPD at modulation maximum. Single-neuron recordings in the inferior colliculus of guinea pigs were performed with the same stimuli. For static IPDs primary-like neurons responded maximally at the modulation maximum. However, onset-type neurons respond maximally just after the modulation trough and are thus critical to account for the behavioral data: In the conditions with beating IPDs they respond maximally if their respective best IPD coincided with the AM onset. Thus, binaurally-sensitive onset-type neurons may be important for binaural phenomena such as the precedence effect. The data will be compared against models and theories of binaural processing. [M.D. was supported by the Alexander von Humboldt Foundation with a Feodor Lynen Fellowship.]

### **777 Electrode Interactions in Neural ITD**

#### **Coding with Bilateral Cochlear Implants**

**Kenneth Hancock<sup>1,2</sup>, Yoojin Chung<sup>1,2</sup>, Bertrand Delgutte<sup>1,3</sup>**  
<sup>1</sup>*Massachusetts Eye & Ear Infirmary*, <sup>2</sup>*Harvard Medical School*, <sup>3</sup>*Massachusetts Institute of Technology*

Bilateral cochlear implant users make poor use of interaural time difference (ITD) cues in everyday situations. Such environments often include multiple sound sources and acoustic reflections, so that different ITDs occur on different electrode channels. In contrast, previous studies of neural ITD coding have been limited to stimulation of a single channel in each ear. To begin examining how multi-electrode interactions affect neural ITD sensitivity, we recorded from inferior colliculus (IC) neurons in acutely-deafened, anesthetized cats with bilateral cochlear implants.

Each 8-contact intracochlear electrode array was divided into two channels comprising bipolar stimulation between the middle of the array and either its apical or basal end. A "target" pulse train was presented on the channel producing greatest ITD sensitivity. An "interferer" pulse train was presented on the other channel and fixed at zero ITD. Target and interferer were low-rate (20 pps) pulse trains interleaved in time. Rate responses were measured as a function of target ITD for interleave delays systematically varied over one interpulse period.

Most neurons (65%) were sensitive to ITD only for the target, even though robust spiking was often evoked by the interferer. This suggests that although our stimulation channels are rather broad, they still selectively activate different sets of inputs to individual IC neurons. For 75% of IC neurons, the interferer decreased sensitivity to target ITD compared to target stimulation alone. Interestingly, the largest degradation typically occurred for interleave delays of 2-5 ms. For the remaining neurons, ITD sensitivity to the target *increased* in the presence of the interferer. This enhancement most often occurred for very short interleave delays (<1ms). The results suggest that perceptual ITD sensitivity with multi-channel stimulation is likely to depend critically on interleave delay.

Supported by NIH Grants R01 DC005775 and P30 DC005209.

### **778 Linear and Nonlinear Spectral Processing Underlying Auditory Spatial Tuning in Nontotopic Regions of the Inferior Colliculus**

**Sean Slee<sup>1</sup>, Eric Young<sup>1</sup>**  
<sup>1</sup>*Johns Hopkins University*

In this study we measured the spectral processing underlying auditory spatial tuning in nontotopic regions of the inferior colliculus (IC) in unanesthetized marmoset monkeys. We attempted to target the nucleus of the brachium of the IC (BIN), which provides a major auditory projection to the superior colliculus and has been implicated in the formation of the auditory space map present there. We measured sound localization cues in each monkey and used them to filter broadband noise in order to create virtual space stimuli. We also synthesized

binaural random spectral shape (RSS) stimuli, which had random and independent levels between each  $\frac{1}{4}$  octave frequency bin and each ear. We presented both stimuli as well as pure tones in closed field while recording single unit spike responses in the IC. Results can be summarized as follows: 1) Neurons in nontopic IC were usually broadly tuned in frequency with onset, sustained, or no responses to tones. 2) Spatial receptive fields were usually tuned to the contralateral hemifield. Some neurons were broadly tuned while others showed relatively sharp tuning in both azimuth and elevation. 3) We used responses to binaural RSS stimuli to constrain models that transform the binaural stimulus spectrum into discharge rate using a combination of first- and second-order weighting of the spectrum. First-order (linear) weights were often broad, excitatory in the contralateral ear, inhibitory in the ipsilateral ear, and asymmetric across ears. We compared model responses to virtual space stimuli with the neural responses. In some cases the first order RSS model accurately predicted the measured receptive fields while in other cases second-order weighting functions led to significant improvements. Finally, we found a significant correlation between the degree of binaural weight asymmetry and the best azimuth. The results suggest that both linear and nonlinear spectral processing underlies spatial tuning in nontopic regions of the IC.

### **779 Is Neural Sensitivity to Interaural Delay Determined by the Dynamical Instability of the Spike Generator?**

David E. O'Gorman<sup>1</sup>, H. Steven Colburn<sup>1</sup>  
<sup>1</sup>*Boston University*

In both mammalian and avian hearing, the interaural time delay (ITD) is an important cue for sound-source location in the horizontal plane. ITD-sensitive neurons in the brainstem have been shown to function like cross-correlators, which fire when the excitatory signals originating from each ear coincide, these excitations taking the form of overlapping excitatory post-synaptic currents (EPSCs). We are attempting to develop a general state-space description of this process, using the fewest dimensions and the fewest parameters possible. The purpose of this poster is to computationally investigate the hypothesis that a single parameter of the state space, the dynamical instability parameter, largely determines the sensitivity of the spike generator to the inter-EPSC delay. The dynamical instability is quantified by the largest eigenvalue of the stability matrix. Preliminary data from the simple FitzHugh-Nagumo model of spike generation show that, for subthreshold and near-threshold EPSC amplitudes, the inter-EPSC-delay sensitivity of the peak voltage correlates with the amount of dynamical instability. Ongoing work tests the generality of the finding in the context of more detailed biophysical models. Work supported by NIDCD 5 R01 DC005775.

### **780 The Collicular Commissure Modulates Frequency Tuning and Binaural Responses in the Inferior Colliculus**

Llwyd Orton<sup>1</sup>, Adrian Rees<sup>1</sup>  
<sup>1</sup>*Newcastle University*

The commissure of the inferior colliculi (CoIC) reciprocally innervates the midbrain nuclei of the mammalian auditory system, the inferior colliculi (IC). Tracing studies have described a point-to-point connectivity through the CoIC, connecting the frequency-band laminae in each IC. We investigated the functional role of these projections by reversibly deactivating one IC via cryoloop cooling. Experiments were performed in an acute guinea pig preparation, anaesthetised with urethane and Hypnorm.

A thermocouple determined that cooling was restricted to the cooled IC. Single and multi-unit recordings revealed a gradient of deactivation across the IC. A polynomial function fitted the data and indicated that deactivation was maximal in low frequency neurons and negligible above 20 kHz, reaching a 50% deactivation at around 8 kHz. Averaged local field potentials, recorded to clicks, show that amplitude of the afferent volley was unchanged by cooling, suggesting that lower auditory nuclei were unaffected by the paradigm.

The frequency response areas of most single units in the IC contralateral to cooling were modulated by deactivation. The majority of V-shaped monotonic units narrowed in tuning width and fired fewer stimulus driven spikes. Non-V-shaped neurons tended to increase in tuning width and fired more stimulus evoked spikes. Interaural phase difference (IPD) functions to tones were collected for neurons with a low best frequency. IPD functions for around half of these neurons shifted up or down in firing rate. A smaller percentage showed changes in slope over some portion of their function.

We show that cryoloop cooling is a focal, reversible deactivation technique that can be used on subcortical structures in the guinea pig. Recordings contralateral to deactivation indicate that projections via the CoIC can modulate the encoding of both spectral and binaural cues in IC neurons. These results suggest that the CoIC plays a key role in the analysis of sounds.

### **781 Early Age Hearing Loss Induces Audiogenic Seizure and Hyperacusis Behavior**

Wei Sun<sup>1</sup>, Qiang Fu<sup>1</sup>, Senthivelan Manohar<sup>1</sup>, Anand Kumaraguru<sup>1</sup>, Aditi Jayaram<sup>1</sup>, Yuguang Niu<sup>1</sup>, Brian Allman<sup>1</sup>, Ji Li<sup>1</sup>

<sup>1</sup>*State University of New York at Buffalo*

Recent clinical studies suggest that the recurrent otitis media in children may be related with hyperacusis, a marked intolerance to an otherwise ordinary environmental sound. However, it is unclear whether the hearing loss caused by otitis media in early age will affect the sound tolerance later in life and how the central auditory system is affected by early age sound deprivation. In this experiment, we studied the effects of tympanic membrane (TM) damage at postnatal 16 days on sound perception

and GABA receptor expression development in rats. Two weeks after the TM perforation, more than 85% of the rats (n = 23) developed audiogenic seizure (AGS) when exposed to loud sound (120 dB SPL white noise, < 1 minute). The susceptibility of AGS lasted at least sixteen weeks after the TM damage (the hearing loss recovered). The TM damaged rats also showed significantly enhanced acoustic startle responses compared to the rats without TM damage. These results suggest that the early age conductive hearing loss may cause an impaired sound tolerance during development. A strong c-Fos staining has been found in the inferior colliculus (IC) in the TM damaged rats after exposed to loud sound, not in the control rats. These results suggest that the hyper-excitability in the IC was induced by the noise exposure in the TM damaged rats which may trigger AGS. Using gene arrays and Western blotting, we identified a significant reduction of the mRNA and protein level of GABA-A receptor  $\alpha$  and  $\beta$  subunits in the IC in the TM damage rats compared to the control rats. These results indicate that early age conductive hearing loss impairs sound tolerance by reducing the GABA inhibition in the IC. Supported by the Action on Hearing Loss (G42)

### **782 Changes in Somatosensory-Auditory Integration in Inferior Colliculus Accompany Noise Induced Tinnitus**

Malav Parikh<sup>1</sup>, Susanne Dehmel<sup>1</sup>, Sanford Bledsoe<sup>1</sup>, Susan Shore<sup>1</sup>

<sup>1</sup>University of Michigan

The inferior colliculus (IC) receives ascending projections from auditory as well as somatosensory nuclei. Ascending projections from the spinal trigeminal nucleus (Sp5) and the cochlear nucleus converge in the guinea pig IC. Pairing electrical stimulation of the Sp5 with auditory stimulation suppresses, and sometimes increases, neural activity in the external nucleus of the IC (ICx) [Jain and Shore, *Neuroscience Letters* (2006)]. In this study we investigated the effects of noise induced hearing loss on neural activity in both the ICx and the central nucleus of the IC (ICc). Gap detection testing determined the presence of tinnitus. We investigated the strength and prevalence of pathways from the Sp5 to the ICx and ICc by examining unit responses before, during, and 15 to 30 minutes after bimodal Sp5-sound stimulation.

The results indicate suppressive and enhancing bimodal integration in ICx and ICc in normal control animals. After noise-exposure ICx units showed primarily bimodal suppression, especially in animals with tinnitus while ICc units showed primarily bimodal enhancement. Long term effects of bimodal stimulation in control animals were suppression and enhancement in both ICx and ICc units. However, noise-exposed animals with tinnitus showed more enhancement in ICx units than controls.

The long-term bimodal enhancement shown here for ICx units is consistent with previous findings of long-term bimodal enhancement in dorsal cochlear nucleus units of animals with tinnitus (Dehmel et al, ARO 2011). The enhancement seen in ICx units could be a reflection of that seen in dorsal cochlear nucleus units but could also reflect

further bimodal integration due to direct somatosensory inputs to the IC (Zhou and Shore, JCN, 2007).

Supported by National Institutes of Health Grant R01 DC DC004825 and Core Center Grant P30 DC-05188 and the Tinnitus Research Consortium

### **783 Dissecting the Corticofugal Pathways of the Central Auditory System: The Effect of Cortical Stimulation on Neural Firing in the Inferior Colliculus**

Craig D. Markovitz<sup>1</sup>, Hubert H. Lim<sup>1</sup>

<sup>1</sup>University of Minnesota

Corticofugal projections are hypothesized to be involved in central auditory plasticity. For example, central auditory stimulation (acoustic; electrical) paired with a reinforcement signal (leg shock; nucleus basalis stimulation) can produce centripetal best frequency (BF) shifts of neurons within auditory nuclei. Corticocollicular projections have proven to be necessary to elicit these fine BF shifts within the central nucleus of the inferior colliculus (ICC). However, it is unclear how these shifts actually occur in the ICC as past studies have suggested a lack of direct projections from primary auditory cortex (A1) to the ICC. Therefore, we investigated the functional arrangement of projections from A1 to locations across the frequency and isofrequency laminae of the inferior colliculus (IC).

We positioned multi-site electrode arrays into A1 and the IC of anesthetized guinea pigs. After characterizing the acoustic-driven responses on each site to confirm its location (i.e., frequency region and sub-nuclei of A1 or IC), we electrically stimulated different layers of A1 and recorded the corresponding changes in spontaneous and acoustic-driven responses throughout the IC.

Stimulation of A1 output layers elicited excitatory responses within BF-matched regions of the ICC, though these projections were spatially sparse across isofrequency laminae. These excitatory projections are classified into two groups: strict frequency-specific, with connections only to ICC BF-matched neurons; and broad frequency-specific, with connections to neurons with BFs within approximately a 1/2 octave of the stimulated A1 site. The ICC also exhibited suppression of acoustic-driven activity to A1 stimulation. Outer IC regions, though, showed massive and broad excitation to A1 stimulation. In conjunction with previous studies, these results suggest A1 finely innervates BF-matched ICC regions while projections to the non-tonotopic outer IC may provide a reinforcement signal for ICC plasticity.

## **784** Electrical Stimulation of the Inferior Colliculus Reveals an Interval Coding Mechanism Across Neurons for Eliciting Enhanced Activity in Superficial Layers of the Auditory Cortex

**Malgorzata Straka**<sup>1</sup>, Rekha Narayanan<sup>1</sup>, Dillon Schendel<sup>1</sup>, Hubert Lim<sup>1</sup>

<sup>1</sup>*University of Minnesota*

It is unclear how neurons within the central nucleus of the inferior colliculus (ICC) code and transmit fast temporal information (> 100 Hz) to higher auditory centers. We hypothesize that neurons across an ICC isofrequency lamina fire at varying time intervals of less than 10 ms to modulate activity within the primary auditory cortex (A1).

Multi-site electrode arrays were used to stimulate the ICC and record neural activity in best frequency matched regions in A1 of ketamine-anesthetized guinea pigs. Two stimulation paradigms delivered two electrical pulses at intervals less than 10 ms apart. The first paradigm sent two pulses to one site, and the second sent one pulse to two sites in the same ICC lamina. Local field potential areas (LFPs) and spike rates (SR) recorded across different A1 layers were analyzed and compared to responses from single pulse stimuli.

Across cortical layers, stimulation of a single site with two pulses did not elicit activity much larger than the response to one pulse for different intervals, likely due to refractory effects. However, stimulation of two sites or clusters of ICC neurons resulted in enhanced LFP and SR activity (i.e., exceeding the linear sum of activity to the individual stimuli). Generally, the activity peaked at 0 ms and decreased for longer intervals. The pattern for the activity versus stimulus interval curves depended on stimulation location within a lamina as well as the cortical layer. Interestingly, layer II exhibited significantly greater activity than the main input layers III/IV and its enhanced activity resembled psychophysical curves for short-term temporal integration.

Neurons along an ICC lamina may use a spiking interval pattern that is transmitted to and integrated within superficial layers of A1 to code for fast temporal features. Understanding the spatial coding pattern across an ICC lamina and its link to temporal processing can improve stimulation strategies for an ICC-based auditory prosthesis.

## **785** GABAergic Projections from Midbrain Auditory Nuclei to the Superior Colliculus

**Jeffrey Mellott**<sup>1</sup>, Brett Schofield<sup>1</sup>

<sup>1</sup>*Northeast Ohio Medical University*

The external cortex of the inferior colliculus (ICx) and the nucleus of the brachium of the IC (nBIC) are the predominant sources of auditory input to the superior colliculus (SC). Appel and Behan (1990) showed that GABAergic cells in ICx project to the SC in cats, but this has not been confirmed in other species nor has anyone reported GABAergic projections from nBIC. We injected fluorescent tracers into the SC in guinea pigs to label cells in the ICx and nBIC. Injections were large and involved

most or all SC laminae. We then stained the tissue with anti-glutamic acid decarboxylase (GAD) to identify GABAergic cells. We quantified tracer- and immuno-labeled cells in the ICx and nBIC. The nBIC contained more than twice as many cells as the ICx. For each nucleus, most labeled cells were ipsilateral (ICx: 91%; nBIC: 81%). GAD-immunoreactive (GAD+) cells made up ~9% of the tracer-labeled cells in the ipsilateral ICx and ~4% in the contralateral ICx. In both ipsi- and contralateral nBIC, ~11-13% of tracer labeled cells were GAD+.

Our findings show a GABAergic projection from ICx to SC that is primarily ipsilateral, similar to that in cats. We describe for the first time a significant GABAergic projection to the SC from the nBIC. This projection is larger than that from the ICx, and includes ipsilateral and contralateral GABAergic cells. GABAergic projections from the substantia nigra to the SC are considered initiators of saccades; a drop in their high resting firing rate leads to disinhibition of SC cells and a subsequent saccade. Projections from the nBIC and ICx terminate in the deep SC layers, overlapping the nigral projections. Whether nBIC or ICx projections could also initiate a saccade awaits information on their firing properties and the particular SC cells that they target. We conclude that the nBIC is a substantial contributor of inhibition to the SC and possibly the largest source of inhibition from an auditory nucleus. Supported by NIH DC04391.

## **786** Applying Optimal Experimental Design for Studying the Neural Architecture of the Inferior Colliculus of Common Marmosets

**William Tam**<sup>1</sup>, Eyal Dekel<sup>1</sup>, Eric Young<sup>1</sup>, Kechen Zhang<sup>1</sup>

<sup>1</sup>*Johns Hopkins University*

Central Nucleus of Inferior Colliculus (CNIC) neurons have traditionally been classified from their responses to basic auditory stimuli, such as response maps or spectro-temporal receptive fields. However, due to the nonlinearity of many CNIC neurons, it is beneficial to classify neurons based on neural networks, which are universal function approximators. In this study, we present a family of neural networks and use an Optimal Experimental Design (OED) algorithm to optimize these networks online in order to better account for nonlinear properties of Marmoset CNIC units. This family of feed-forward networks contains an auditory nerve (AN) model at its front-end to mimic the auditory periphery. The outputs from the AN model enters a layer of one, two or three inhibitory neurons that inhibits the eventual principle CNIC unit. Results from in-vivo experiments show that the OED algorithm can capture parameters of proposed CNIC neural architectures that can accurately predict responses to validation stimuli as well as simple tone response maps and rate-level functions ordinarily used to characterize such neurons. In addition, when provided with multiple neural models, the OED paradigm quantifies and validates which model fits the neuron best using various excitatory and inhibitory stimuli that take advantage of the neuron's maximum sensitivity towards the provided models. These experiments show that the optimal design algorithm can recover parameters of the neural architecture with fewer

than 300 stimuli; moreover, these parameter values can account for various stimuli and may help answer different physiological function of CNIC neurons. (Supported by NIH-NIDCD DC00115)

### **787 Functional Organization of Projections from the Lateral Lemniscal Nuclei to the Inferior Colliculus in the Pallid Bat (*Antrozous pallidus*)**

Dori Pitynski<sup>1</sup>, Anthony Williams<sup>1</sup>, Zoltan Fuzessery<sup>1</sup>  
<sup>1</sup>*University of Wyoming*

The nuclei of the lateral lemniscus (NLL) send dense projections up to the inferior colliculus (IC); the IC may inherit selectivity from this lower level. The NLL, particularly the intermediate nucleus, are hypertrophied in echolocators, both cetaceans and bats, indicative of its importance in echolocation. The cat, rat, and bat show complex tonotopic organization in the NLL. Retrograde fluorescent tracers were injected into 3 different frequency regions, and data will be used to construct a 3-D model of tonotopy. Results will be used to compare and contrast currently known frequency maps, specifically with the big brown bat. Within the ventral NLL there is a further anatomical subdivision found only in bat species, the columnar region (cVNLL), which varies in location. The columnar region is typified by orderly rows of cells, and response properties include broad tuning and a constant-latency which corresponds to the onset of sound. This implicates its importance in analysis of the temporal properties of sound. The cVNLL is found ventrally in the mustached bat, but dorsally in the big brown bat. The cVNLL in the pallid bat, a novel find, is located dorsally. Gleaners use echolocation to navigate their environment, but passive sound localization to locate insects creating two functionally different systems of localization. The pallid bat's IC show two discrete areas: one that responds to echolocation, and one that responds to low-frequency noise used in passive sound localization. To further our knowledge of the potential roles of the cVNLL, fluorescent retrograde tracers were injected into the echolocation and passive hearing areas of the IC. This approach will show whether the cVNLL is solely involved in echolocation processing, or if it may also play a role in noise localization as well, two biologically relevant behaviors in the pallid bat.

### **788 Dopamine Alters Neuronal Responses in the Inferior Colliculus of Awake Mice**

Joshua Gittelman<sup>1</sup>, Zachary Mayko<sup>1</sup>, David Perkel<sup>2</sup>, Christine Portfors<sup>1</sup>

<sup>1</sup>*Washington State University*, <sup>2</sup>*University of Washington*

Developmental experience, behavioral state and context affect auditory processing. These factors alter selective response properties of neurons in the inferior colliculus (IC), but the mechanisms underlying this dynamic processing are largely unknown. Dopamine (DA) is implicated in context dependent learning and behavior in other brain areas, and DA receptors are present in the IC. Direct application of DA affects neuronal excitability and can also change spike temporal patterns. Whether DA

increases or decreases excitability depends in part on neuron type, and also on which of two receptor classes is activated: D1-like (D1, D5); or D2-like (D2, D3, D4). Evidence suggests that the IC expresses both receptor classes, but to date it is unclear how DA affects individual IC neurons. We recorded from single units in the IC of awake mice before and after iontophoretic application of DA while presenting tones, broadband noise and/or mouse vocalizations. DA affected firing rates in 15/20 neurons. Consistent with both D1-like and D2-like receptor activity, sound-evoked firing rates decreased in some cells (8/15) and increased in others (7/15). In 7/15 cells, spontaneous firing changed in the same direction as sound-evoked firing. DA also affected multiple aspects of temporal firing patterns in 6/20 cells. First, in 2 cells, the variance of first spike latency (jitter) decreased following DA, whereas in 2 cells the jitter increased. Second, in 3 cells, DA application changed the sound-evoked spike patterns to include spike bursts in addition to single or multiple spikes. These diverse changes in firing rate and timing due to DA are similar to what has been observed in other brain areas such as the basal ganglia and cortex. Overall, our data are consistent with the activity of both the D1- and D2-like DA receptors in IC. We suggest that how DA modulates auditory responses in the IC depends on behavioral context.

### **789 Ephrin-B2 Reverse Signaling Is Not Required for the Formation of Layered and Modular Lateral Superior Olivary Inputs to the Inferior Colliculus in the Developing Mouse**

Matthew Wallace<sup>1</sup>, Sarah Kavianpour<sup>2</sup>, Mark Gabriele<sup>1</sup>  
<sup>1</sup>*James Madison University*, <sup>2</sup>*Johns Hopkins Bloomberg School of Public Health*

Graded and modular expressions of Eph-ephrins are known to provide positional information for the formation of topographic maps and patterning in the developing nervous system. Utilizing immunocytochemistry in control animals and X-Gal staining approaches in *lacZ* mutants we have shown that ephrin-B2 expression patterns exhibit a continuous gradient across the tonotopic axis of the central nucleus of the inferior colliculus (CNIC), whereas patterns are discontinuous and modular in the lateral cortex of the IC (LCIC). As converging layered and modular inputs target specific domains within the developing CNIC and LCIC respectively, ephrin-B2 patterns are distinct prior to their downregulation as experience ensues (functional onset of hearing in mouse, P11/12). The present study explores the involvement of ephrin-B2 signaling in the development of projections to the CNIC and LCIC arising from the lateral superior olivary nuclei (LSO). Fluorescent tracing methods in early postnatal fixed tissue preparations were used to compare axonal targeting and establishment of LSO layers/modules in wild-type and ephrin-B2<sup>lacZ/+</sup> mice (ephrin-B2<sup>lacZ/+</sup> incapable of reverse signaling; ephrin-B2<sup>lacZ/lacZ</sup> perinatally lethal). While axonal trajectories of pioneer LSO fibers in ephrin-B2 mutants are somewhat aberrant at birth, both the ipsilateral and contralateral projections form discernible layers and modules in the

developing CNIC and LCIC. Ongoing anterograde and retrograde studies utilizing more focal dye placements aim to determine if ephrin-B2 signaling is necessary for accurate topographic mapping of connections between the LSO and the IC.

### **790 Nonlinear Spectral Interactions Underlying “extraclassical” Receptive Fields in the Central Nucleus of the Inferior Colliculus**

**Nishant Zachariah<sup>1</sup>, Sean Slee<sup>1</sup>, Eric Young<sup>1</sup>**

<sup>1</sup>*Johns Hopkins University*

Auditory neurons have a receptive field usually defined with tones of varying level and frequency or with a method based on broadband stimuli, like the STRF. These define a “classical” receptive field (crf) that shows the effects of a single frequency on the neuron. Here we define the “extraclassical” receptive field (erf) as showing the interactions of simultaneous presentation of two frequencies (see also Schneider and Woolley, *J. Neurosci.* 31:11867, 2011). The erf is likely to be important in processing broadband natural stimuli in which correlated activity is contained across a broad frequency range. The crf and erf were determined for neurons in the central nucleus of the inferior colliculus (ICC) in unanesthetized marmoset monkeys. We used random spectral shape (RSS) stimuli, consisting of a large number (~400) of noises with spectral shapes varying in 1/8 octave frequency bins. Most neuron models derived from the RSS responses had significant erfs (responses to simultaneous pairs of frequencies) which we divide into a central portion with weights over the same frequency range as the crf and an exterior portion, extending over a wider frequency range than the crf. The frequency range of a receptive field is the range over which the model is accurate in predicting responses to stimuli other than those used to compute the model. Inclusion of the erf in the model on average reduced the mean square error for prediction by 45%. erfs were significant in all three major electrophysiological cell types of the ICC. Decomposition of erfs into a series of equivalent filters (eigenspace) revealed the excitatory and inhibitory input patterns of the nonlinearity. Finally, we found that erfs adapt dynamically to both the spectral variance and sound pressure level. This study demonstrates significant nonlinear processing at the level of the ICC that is not captured by linear spectro-temporal receptive field (STRF) models. Supported by NIDCD grants DC00115 and DC005211.

### **791 Spectro-Temporal Interaction in Coding Tone-Tone Pairs in the Mouse Inferior Colliculus**

**Günter Ehret<sup>1</sup>, Thomas Niesner<sup>1</sup>**

<sup>1</sup>*Institute of Neurobiology, University of Ulm, Germany*

Many communication sounds of mammals and birds are vocalized in series of calls or syllables as humans produce series of syllables/words in speech. The question is how the auditory system below the cortical level deals with such

sound series which are perceived as a stream of auditory objects occurring with a certain rhythm.

We recorded extracellularly from 124 single neurons in the adult mouse central nucleus of the inferior colliculus (CNIC) to combinations of two tones, the first one at the characteristic frequency (CF) or 1/2 or 1 octave below or 1/4 octave above CF, the second always at CF. The inter-tone interval was varied in 16 steps between 0 – 500 ms. The whole stimulation was done 10 dB above the threshold at CF. In addition, excitatory and inhibitory receptive fields (see Egorova et al. 2001, *EBR* 140: 145-161) and the tone-response types of the neurons were measured. Major results: Preceding CF-tones generally suppressed the response to the second CF-tone for inter-tone intervals shorter than about 50 ms. This suppression faded away in most neurons for inter-tone intervals longer than about 400 ms. Preceding non-CF tones had a suppression effect in only about 1/3 of the neurons, largely independent of the inter-tone interval duration. In about 10% of the neurons, preceding non-CF tones had strong facilitatory effects on the response to the following CF-tone, however only for inter-tone intervals of 100 ms and longer. These suppression or facilitation effects were independent of the neuron’s shape of receptive fields, tone-response type and location in the CNIC. Facilitation of responses to tones by preceding, spectrally rich sounds could be the “glue” for coding sound sequences for the perception of rhythms. Such a coding is present in a number of neurons at the auditory midbrain level. The study was supported by the DFG.

### **792 Multiple Mechanisms Interact to Shape Rate Selectivity for Downward FM Sweeps in the Pallid Bat IC**

**Anthony Williams<sup>1</sup>, Bethany Chagnon<sup>1</sup>, Dori Pitynski<sup>1</sup>, Zoltan Fuzessery<sup>1</sup>**

<sup>1</sup>*University of Wyoming*

Auditory neurons in the pallid bat have strong rate selective responses to downward FM sweeps attributable to the spectrotemporal pattern of their echolocation call (a brief FM pulse). Here we explore how three distinct mechanisms acting alone or in combination shape FM rate selectivity: 1) duration tuning, 2) high-frequency inhibition (HFI), and 3) two tone facilitation (TTF). In tone-responsive neurons, rate selectivity is largely driven by duration tuning while in FM specialists (non-responsive to tones) FM rate selectivity is largely driven by TTF. HFI also contributes to rate selectivity, regardless of tone response, and can be eliminated by narrowing the bandwidth of the FM sweep to exclude the high-frequency region. However, in cases where more than one mechanism is present, elimination of HFI is not sufficient to eliminate FM rate selectivity if the other mechanisms remain intact. Differential effects of iontophoretic blockade of either glycine or GABA receptors on FM rate selectivity were also observed based on the mechanisms present. Blocking glycine receptors was effective at eliminating HFI while blockade of either GABA or glycine could eliminate duration tuning. In contrast, blockade of glycine receptors eliminated all auditory responses in FM specialists

expressing TTF indicating mechanisms likely related to an excitatory rebound from inhibition. It is unknown why the auditory system utilizes such a diverse array of mechanisms, all capable of shaping FM rate selectivity, and may merely represent distinct but convergent modes of neural signaling all directed at shaping response selectivity for important biologically relevant sounds.

### **793 Populations of Neurons Across Isofrequency Laminae of the Inferior Colliculus Encode Spectro-Temporal Features of Complex Speech Stimuli**

**Thilo Rode**<sup>1</sup>, Taja Hartmann<sup>1</sup>, Roger Calixto<sup>1</sup>, Mino Lenarz<sup>1</sup>, Andrej Kral<sup>1</sup>, Thomas Lenarz<sup>1</sup>, Hubert H. Lim<sup>2</sup>  
<sup>1</sup>Otolaryngology Dept., Hannover Medical University, Hannover, Germany, <sup>2</sup>Biomedical Engineering Dept., University of Minnesota, Minneapolis, USA

The inferior colliculus central nucleus (ICC) has a well-defined tonotopic organization consisting of isofrequency laminae. However, not much is known about how neurons in different locations along an ICC lamina interact to represent sound information. Therefore, we simultaneously recorded temporal firing patterns of neurons across the ICC laminae in response to natural vocalizations in guinea pigs.

Data were obtained from 11 ketamine-anesthetized animals. Eight different vocalizations (30-70 dB SPL, 10 dB steps) were presented through calibrated speakers and the corresponding multi-unit activity was recorded across the ICC. Multi-shank electrode arrays (NeuroNexus Technologies) were positioned into 6-12 different locations across an isofrequency ICC lamina in each animal. We reconstructed the location of each site based on frequency response maps and histology (arrays were stained with a red dye). These reconstructions allowed us to pool data across animals. Post-stimulus time histograms were cross-correlated with the envelope for the frequency band of the vocalization that matched the frequency tuning of the neurons (envelope extracted using the DRNL filter generously provided by Drs. Ray Meddis and Chris Sumner).

We observed that firing patterns of neurons within a specific frequency lamina strongly correlate with the temporal structure of the frequency matched DRNL envelope. Although neurons across an ICC lamina generally follow the envelope shape of the stimulus, different neurons appear to code for different temporal features of the envelope in a complementary pattern. The neurons also exhibit a large variability in firing pattern across trials. Based on these findings, it appears that populations of neurons along an ICC lamina may code for the temporal structure of the stimulus in a complementary yet stochastic pattern on a trial-by-trial basis.

Supported by German Ministry of Research and Education (Grant01GQ0816), Cochlear Ltd. and SFB 599.

### **794 A Recurrent Network Model for Stimulus Specific Adaptation Dynamics**

Zitian Yu<sup>1</sup>, Li Shen<sup>1</sup>, Bo Hong<sup>1</sup>, **John Rinzel**<sup>2,3</sup>

<sup>1</sup>Department of Biomedical Engineering, School of Medicine, Tsinghua University, <sup>2</sup>Center for Neural Science and Courant Institute for Mathematical Sciences, New York University, <sup>3</sup>Center of Neural and Cognitive Computation, TNList, Tsinghua University

Neuronal response decreases when the same stimulus repeats, but recovers when a different stimulus is presented. This phenomenon is called stimulus specific adaptation (SSA). SSA is thought to underlie novelty detection and to contribute to auditory sensory memory. Recently, Mill et al. (2011) used a feed-forward network model of spiking units to explain SSA in the oddball paradigm, which successfully reproduced several neurophysiological aspects of SSA, such as the effect of frequency separation. Here, we present a firing-rate-based recurrent network model which is biologically plausible and reflects the abundance of recurrent connections in cortex as well as in inferior colliculus. The model includes excitatory and inhibitory subpopulations distributed along the tonotopic axis. We introduced both synaptic depression and adaptation, and fitted various aspects of the adapted time courses of neuronal firing rates as well as the dynamics of adaptation and dependence on the oddball's probability. We also simulated the local and global history effects that are reported in previous SSA studies. Our results support the view that neuronal adaptation in a locally recurrent network might be a significant mechanistic contributor to SSA and more generally to auditory memory function.

### **795 Stimulus-Specific Adaptation in the Inferior Colliculus of the Awake Gerbil in Response to Markov Chain Tone Sequences**

**Simon Jones**<sup>1</sup>, Robert Mill<sup>2</sup>, Susan Denham<sup>2</sup>, Georg Klump<sup>1</sup>

<sup>1</sup>Universitat Oldenburg, <sup>2</sup>University of Plymouth

Stimulus-specific adaptation (SSA) occurs when a neuron responds with fewer spikes on average to tones that appear often in a long sequence (standards) than to tones that appear rarely (deviants). SSA has typically been studied using oddball sequences, in which consecutive tones are statistically independent. By using a Markov chain to generate the sequence, the probability of switching from a standard to a deviant or vice versa (psw) and the probability of a tone being a deviant (pdev) can be manipulated separately. A computational model that we recently developed(1), which accounts for SSA in terms of adaptation in narrowly-tuned tonotopic inputs, predicts that SSA will decrease as pdev increases, and increase as psw increases.

In order to test this model, adult Mongolian gerbils (*Meriones unguiculatus*) were chronically implanted with electrodes in the Inferior Colliculus (IC) under isoflurane anaesthesia, allowed to recover, and then placed on a floating platform in a sound attenuating chamber for recording. Recordings were made with a 16-channel Plexon MAP system and sorted offline using Plexon

software. Stimuli were presented from an overhead loudspeaker. These stimuli were blocks of 1000 100ms pure tones generated by two-state first-order Markov chains with varying pdev and psw. Tone pairs were selected to be half an octave apart and centered around the best frequency of the neuron. Each sequence was presented twice; in the second presentation the deviant and standard frequencies were exchanged and SSA calculated.

Our present population of awake IC neurons do not exhibit statistically significant SSA and consequently do not show a relationship between psw or pdev and SSA. Comparison will be made to recordings under anaesthesia to examine its contribution to SSA.

Ref:

1) Mill R, Coath M, Wennekers T, Denham SL, 2011 A Neurocomputational Model of Stimulus-Specific Adaptation to Oddball and Markov Sequences. PLoS Comput Biol 7(8): e1002117

### **796 The Upper Limit of Temporal Coding of Electric Pulse Trains in the Inferior Colliculus of Awake Animals Wearing Cochlear Implants**

**Yoojin Chung**<sup>1,2</sup>, Kenneth Hancock<sup>1,2</sup>, Sung-Il Nam<sup>1,3</sup>, Bertrand Delgutte<sup>1,4</sup>

<sup>1</sup>Eaton-Peabody Laboratories, Massachusetts Eye & Ear Infirmary, <sup>2</sup>Department of Otology and Laryngology, Harvard Medical School, <sup>3</sup>Keimyung University, <sup>4</sup>Research Laboratory of Electronics, MIT

Temporal processing of periodic pulse trains by cochlear implant (CI) listeners is limited to low stimulation rates. CI listeners are able to discriminate the pitch of pulse trains and detect interaural time differences (ITD) at low pulse rates but their performance degrades with increasing rate. Neural responses to electric pulse trains in anesthetized animals also show rate-limitations, but the observed limit of pulse rate following is lower than the behavioral limit. In addition, human CI listeners perceive continuous stimulation even at very high rates but the neurons in the inferior colliculus (IC) show sustained responses only up to a few hundred pulses per second (pps). We hypothesize that neural limits of both temporal following and sustained responses have previously been underestimated due to the effect of anesthesia.

We developed a chronic, awake rabbit preparation for recording single neuron responses to electric stimulation through CI without the possible confound of anesthesia. Adult Dutch-belted rabbits received chronic cochlear implants and were trained to sit still with head fixed for 2-3 hours/day. Responses of single IC neurons to trains of biphasic pulses were measured in daily recording sessions.

Different response patterns were observed in awake rabbits compared to anesthetized cats. On average, units from awake rabbits show higher firing rates and more spontaneous firing. The maximum pulse rates that elicited sustained firing and phase-locked responses were 2-3 times higher in the IC of awake rabbits than in anesthetized cats. Moreover, about 15% of IC neurons in awake rabbit showed sustained (but not phase-locked)

responses to periodic pulse trains at much higher pulse rates (> 1000 pps) than observed in anesthetized animals. In general, the pulse rate following limits of IC neurons in awake animals are more consistent with the perceptual rate limits in human CI subjects.

Supported by NIH Grants R01 DC005775 and P30 DC005209

### **797 Neural Correlates of the Tone Detection in the Inferior Colliculus of Nonhuman Primates**

**Margit Dylla**<sup>1</sup>, Peter Bohlen<sup>1</sup>, Andrew Hrnicek<sup>1</sup>, Ramnarayan Ramachandran<sup>1</sup>

<sup>1</sup>Wake Forest School of Medicine

Detection of sounds is the fundamental function of the auditory system. Our previous studies showed that thresholds to detect a tone displayed a U-shaped relationship with frequency: thresholds were lowest between 1 kHz and 10 kHz, and increased as frequencies deviated from that range. Reaction times to detect tones decreased as the tone sound pressure levels increased beyond threshold. Our goal is to uncover the neuronal antecedents of detection. To that end, we simultaneously measured behavioral and neuronal responses in the inferior colliculus (IC), and examined the roles of neurons showing different response types in detection.

Two nonhuman primates (*Macaca mulatta*) were trained in a reaction time lever release task to report the detection of tones. Appropriate catch trials were interleaved to make sure the monkeys were actually reporting tone detection. Single units were simultaneously recorded from the IC (n=84). The characteristic frequency of these units ranged up to 26 kHz. Most of the units were classified as type V or type I, based on the distribution of excitation and inhibition in frequency response maps. Signal detection theory and Receiver Operating Characteristic (ROC) analyses were used to create psychometric (behavioral), and neurometric functions. Neurometric functions reveal the probability of correct response based on the number of spikes fired by the IC neuron during the stimulus intervals on tone trials and catch trials. On the average, neuronal thresholds matched behavioral thresholds across unit types. However, the slopes of the psychometric functions and the neurometric functions were only weakly correlated. On a trial-by-trial basis, the behavioral choice could be predicted with a probability significantly higher than chance based on the responses of individual IC units. These results suggest that the behavioral responses are strongly related to IC neuronal responses.

### **798 Auditory Filter Widths in the Inferior Colliculus of the Guinea-Pig Determined Using Simultaneous and Forward Notched-Noise Maskers**

**Toby Wells**<sup>1</sup>, Chris Sumner<sup>1</sup>

<sup>1</sup>MRC Institute of Hearing Research

Frequency selectivity is a fundamental and extensively studied property of the auditory system. However, the relationship between psychophysical and physiological

measurements, and whether central mechanisms contribute to perceptual frequency selectivity, remains unclear. Part of the problem stems from making comparisons between measurements made using fundamentally different methods. Psychophysical estimates are made using masking paradigms, whilst many physiological measurements were made using pure tone responses. Also, psychophysics measures detection thresholds, which are not necessarily comparable to mean spike rates. Finally, psychophysical techniques have been refined over time. Modern methods show that perceptual auditory filters exhibit non-linear characteristics presumably reflecting cochlear filtering. For example, cochlear suppression results in wider auditory filters for simultaneous maskers.

We measured frequency selectivity in single units in the Inferior Colliculus of guinea-pigs using simultaneous and forward notched noise masking paradigms, as well as from pure tone response areas. We derived neural detection thresholds using Signal Detection Theory, and neural auditory filter widths using roex functions.

In units that produced clean 'neurometric functions', auditory filter widths were relatively homogenous and increased with characteristic frequency (CF). Bandwidths agreed well with both peripheral measurements using pure tones, and psychophysical measurements in guinea-pigs using notched-noise masking. Furthermore, in high-CF units, auditory filter widths were wider in the simultaneous masking than in the forward masking condition. In low-CF units bandwidths tended not to differ between forward and simultaneous masking. These results suggest that frequency selectivity in Inferior Colliculus reflects peripheral pure tone tuning and perceptual estimates of bandwidths, and that these different methods produce comparable measurements.

### **799 Molecular Mechanics of the Transduction Apparatus in Hair Cells**

**David P. Corey<sup>1</sup>**

<sup>1</sup>*Harvard Medical School and HHMI*

One of the great challenges in auditory neuroscience is to understand the molecular apparatus in hair cells that converts the mechanical stimuli of sound or head movements into neural signals—what von Bekesy called "the final mechanical transformer." With a still-unidentified force-gated channel at its center, this complex may contain a dozen or more proteins that both convey tension to the channel and mediate a continuous adaptation to maintained stimuli. Ultimately, we would like to identify all these proteins, to know how they are bound to each other, and how they respond to tension. It will not be easy.

The study of inherited deafness such as the Usher syndromes has revealed several members of the complex; especially important are two proteins of the tip link, cadherin-23 and protocadherin-15. To begin to understand their behavior under tension, we synthesized the N-terminus of each and solved their atomic structures with X-ray crystallography. Like those of other cadherins, these EC domains have a Greek-key fold of seven beta strands. In three stereotyped locations, Ca<sup>2+</sup> ions bridge

acidic residues to hold together loops both within and between EC domains. A number of deafness-causing mutations alter Ca<sup>2+</sup>-binding residues to weaken the proteins. To understand their mechanics, the cadherins' structures were modeled with steered molecular dynamics calculations in which we could pull on the structure. These showed that the tip link is very stiff—much stiffer than the hypothesized gating spring element—so that it probably does not stretch much when pulling on the channel. The structure of the two N-termini bound to each other reveals an extended handshake arrangement with substantial overlap of both EC domains. Removing Ca<sup>2+</sup> allows increased flexure at the EC1-EC2 hinge, indirectly disrupting the binding to break the tip link.

To begin to identify other members of the complex, we determined the complete transcriptome of hair cells in mouse. In collaboration with Zheng-Yi Chen's laboratory at MEEI, we dissociated and FACS-purified hair cells expressing EGFP, from cochlea and utricle, at developmental stages from E16 to P16. Hair-cell and surrounding-cell fractions were each >99% pure. Deep sequencing of transcripts revealed which genes are preferentially expressed in hair cells and which genes are upregulated as cells gained mechanosensitivity. Many of a select group are candidates for unidentified deafness genes. The data, together with similar data from other laboratories, will be made publically available on a searchable website.

### **800 Nonlinear Spectral Processing by Neurons in the Dorsal Cochlear Nucleus**

**Kevin Davis<sup>1</sup>**

<sup>1</sup>*University of Rochester*

The dorsal cochlear nucleus (DCN) is part of the first auditory structure in the brainstem. It receives ascending input from the auditory nerve and, in turn, projects to the contralateral inferior colliculus. The DCN is notable for its wide variety of cell types, intricate neural circuitry and complex physiology. In particular, most DCN neurons show responses to sound that are dominated by inhibitory effects and exhibit nonlinear spectral integration. This talk will describe the spectral integration properties of two major DCN response types, the current conceptual (and computational) model of the DCN and the role of the DCN in audition. When tested with pure tones, DCN principal cells (fusiform and giant cells) in cats exhibit so-called type IV unit response properties. Type IV units are excited by low-level tones at their best frequency (BF) but are inhibited by high-level tones at nearly all frequencies. Despite the predominance of inhibitory responses to tones, type IV units are excited by broadband noise at all suprathreshold levels. Inhibition is restored by removing energy from (adding a notch to) the broadband spectrum at BF. The current model of the DCN suggests that type IV unit responses to sound are shaped by inputs from two inhibitory interneurons: type II units and wideband inhibitors (WBIs). Type II units (thought to be DCN vertical cells) respond strongly to tones but weakly to noise, and inhibit type IV units to narrowband stimuli. Conversely, WBIs (D-stellate cells in the ventral cochlear nucleus)

respond weakly to tones but strongly to noise, and inhibit type IV (and type II) units to wideband stimuli. The nonlinear integration of spectral energy by type IV units creates an unusual sensitivity to the presence of narrowband peaks and notches in acoustic spectra, of the kind added to sounds in a direction-dependent manner by the external ear. It has thus been speculated that the DCN initiates a pathway specialized to process head-related (monaural) sound localization cues.

### **801 Glycinergic Mechanisms Create Spectro-Temporal Integration in the Auditory Brainstem and Midbrain**

**Jeffrey Wenstrup<sup>1</sup>**

<sup>1</sup>*Northeast Ohio Medical University*

Analysis of complex vocalizations requires integration across the frequency-time structure of these signals. One form of auditory spectro-temporal integration is performed by "combination-sensitive" neurons, which respond to specific, properly timed combinations of spectral elements in vocal signals. Combination-sensitive neurons occur in the auditory forebrain of several species. In the mustached bat, a species in which much of the mechanistic work has been performed, these neurons form orderly arrays in auditory cortex that represent features of sonar targets. This talk describes principal findings concerning the mechanisms and circuitry underlying these combination-sensitive responses: 1. *Combination-sensitive responses are created in several stages within the auditory brainstem and midbrain.* These responses involve facilitation, inhibition, or both, when activated by distinct spectral elements in complex sounds. Mechanistic studies show that combination-sensitive inhibition and facilitation arise in distinct nuclei of the auditory brainstem and midbrain. 2. *Spectral integration underlying combination-sensitive responses requires a non-tonotopic input tuned at least one octave below a neuron's characteristic frequency (CF).* Low-CF neurons in the auditory brainstem project to high-CF regions in brainstem or midbrain auditory centers to create combination sensitivity. 3. *Both facilitatory and inhibitory spectral interactions depend on glycinergic inputs.* Both forms of combination-sensitivity are eliminated by glycine receptor blockade. Surprisingly, facilitatory interactions depend exclusively on glycinergic inputs and are independent of glutamatergic and GABAergic inputs. Facilitation likely results from post-inhibitory rebound activated by the combination of low-CF and high-CF glycinergic inputs. Overall, these studies identify several mechanisms underlying spectral integration and point to important roles played in spectral integration by auditory brainstem and midbrain nuclei. Supported by NIDCD R01 DC00937.

### **802 Spectral Integration Through Thalamocortical and Corticocortical Projections**

**Max Happel<sup>1</sup>, Marcus Jeschke<sup>1</sup>, Frank Ohl<sup>1</sup>**

<sup>1</sup>*Leibniz Institute for Neurobiology, Magdeburg, Germany*

Primary auditory cortex integrates spectral information about acoustic stimuli from afferent feedforward thalamocortical projection systems and convergent intracortical microcircuits. Dissociation of the contributions of both systems is possible by a combination of pharmacological silencing of cortical activity and analysis of the so-called residual current source density. With this approach we found a temporally highly precise integration of both types of inputs when the stimulation frequency was in close spectral neighborhood of the best frequency of the measurement site, in which the overlap between both inputs is maximal. Local intracortical connections provide both directly feedforward excitatory and modulatory input from adjacent cortical sites, which determine how concurrent afferent inputs are integrated. Through separate excitatory horizontal projections, terminating in cortical layers II/III, information about stimulus energy in greater spectral distance is provided even over long cortical distances. These projections effectively broaden spectral tuning width. Based on these data, we suggest a mechanism of spectral integration in primary auditory cortex that is based on temporally precise interactions of afferent thalamocortical inputs and different short- and long-range intracortical networks.

### **803 Responses to Social Vocalizations Across All Areas of Guinea Pig Auditory Cortex**

**Jasmine Grimsley<sup>1,2</sup>, Alan Palmer<sup>1</sup>, Mark Wallace<sup>1</sup>**

<sup>1</sup>*MRC Institute of Hearing Research, Nottingham, UK,*

<sup>2</sup>*Northeastern Ohio Medical University*

Guinea pigs are highly vocal animals that have both low frequency vocalizations, with energy entirely within the frequency range of human speech, and high frequency vocalizations. This makes them an interesting model for studying the neural coding of communication calls across different frequency domains. We postulated that different cortical areas may use different mechanisms for processing social vocalizations. We presented exemplars from all ten of the main adult vocalizations to urethane anesthetized animals while recording from each of the eight areas of the auditory cortex. The ventrorostral belt (VRB) was most responsive to vocalizations and better at discriminating among vocalizations using a rate code than any other area. Furthermore, 10% of VRB cells respond to communication calls, but not to synthetic stimuli such as clicks, noise or pure tones. Area S units are highly selective among vocalizations and provide excellent temporal representations. Area T responded well to some vocalizations, providing reasonably good temporal representations. The primary area AI responded better to vocalizations than the adjacent dorsocaudal core, despite units in both areas having similar tuning properties. The caudal and dorsorostral belts were comparatively

unresponsive to vocalizations; when they did respond it was mainly with a weak response at the onset of a call. The firing rates in response to vocalizations were correlated with how well the spectral characteristics of the call matched the unit's spectral receptive field (SRF) in areas S, T, and for subpopulations of units in VRB and AI. The temporal fidelity of responses were also associated with how well the spectral characteristics of the call matched the unit's SRF for subpopulations of units in VRB and AI. These data suggest that different areas represent vocalizations using different coding strategies and that the SRF is predictive of responsiveness in only some regions.

### **804 Development and Plasticity in Spectrotemporal Integration in Rat Primary Auditory Cortex (AI)**

**Shaowen Bao<sup>1</sup>**

<sup>1</sup>*University of California-Berkeley*

1) Development. Spectrotemporal integration in cortical neurons, as measured by their bandwidth of the excitatory and inhibitory receptive fields, temporal response rate and FM sweep selectivity, undergoes a progressive, multi-staged maturation process. Inhibitor receptive field broadly flanks the excitatory receptive field early in development, and becomes progressively narrower and weaker after postnatal day 35 (P35). By contrast, excitatory receptive field rapidly becomes broader between P16 to P18. Temporal response rate of AI neurons also increases gradually from P14 to P35. FM sweep selectivity does not change over the same developmental period. However, the response magnitude to FM sweeps increased rapidly between P24 and P26. 2) Plasticity. Sensory experience shapes AI representations of these spectrotemporal features in a series of sensitive periods. Exposure to a tone or a FM sweep from P8 to P15 alters the cortical characteristic frequency map. Exposure to broadband stimuli such as FM sweeps or pulsed noise from P16 to P23 results in broadened frequency tuning. Exposure to FM sweeps between P24 and P39 shifts FM sweep direction and rate selectivity. Exposure to pulsed noise during the same period abolishes CF dependence of FM direction selectivity. These sensitive periods coincide with corresponding developmental events: emergence of the CF map, broadening of tuning bandwidth and increase of FM sweep responses. 3) Functions. In developing auditory cortex, spectral integration depends on temporal interactions. Spectrotemporal integration enables statistical learning on sound streams in the environment. The same sound ensemble, when played in different sequences, results in completely different forms of acoustic representations. This form of sequence-dependent learning may be involved in representations of conspecific vocalizations.

### **805 Development of FM Sweep Selectivity in Inferior Colliculus and Auditory Cortex**

**Zoltan Fuzessery<sup>1</sup>**

<sup>1</sup>*University of Wyoming*

The development of neuronal selectivity for species-typical vocalizations has been typically examined at single levels

of the auditory system. Less is known of the developmental trajectories at multiple system levels. This talk will make several points regarding the creation and maturation of selectivity for complex sounds, based on parallel, longitudinal studies of the development of response selectivity in the inferior colliculus and auditory cortex. The subject of these studies, the pallid bat, is well suited because regions of its auditory system supporting echolocation contain an unusually high percentage of neurons that are highly selective for the sweep direction and rate of its echolocation pulse. Such selectivity provides a marker amenable to the assessment of auditory system maturation. Some general trends emerged that may be broadly applicable to sensory processing. A given form of selectivity for a relevant signal may be shaped by multiple mechanisms, at multiple levels. Response selectivity and the underlying mechanisms may be a combination of de novo creation and inheritance from lower levels of the system. Though two levels of the system may express very similar forms of response selectivity, this does not preclude the possibility that the higher level creates its selectivity de novo. Specifically, the inferior colliculus and auditory cortex exhibit very similar selectivity for FM sweeps, but the blockade of intracortical inhibitory circuits can eliminate selectivity, suggesting that the cortex is recreating or refining response selectivity. Finally, some forms of response selectivity appear to mature faster in auditory cortex than the midbrain. Maturation of FM sweep rate selectivity in the inferior colliculus lags by three weeks, suggesting that the top-down corticofugal instruction seen in adults may also play a role in development, and/or that auditory cortex may mature independently of the auditory midbrain.

### **806 New Insights on Vestibular Neuropharmacology: From Bench to Bedside**

**Christian Chabbert<sup>1</sup>**

<sup>1</sup>*INSERM U1051 Montpellier*

Recent epidemiological investigations have highlighted the high prevalence of vestibular dysfunctions in the adult population and its association with aging. Despite a large and unmet medical need, the pharmaceutical options of targeted and efficient drugs to reduce the symptoms associated with vestibular deficits remains largely insufficient. This session intends 1. to emphasize the current state of the medical need for potent pharmacological treatments of vestibular deficits while highlighting questions regarding the molecular targets, therapeutic window and role of pharmacological treatment versus physiotherapy; 2. to give an overview of the fundamental mechanisms of the vestibular system function and the mechanism of action of the drugs currently used in the treatment of vestibular disorders and 3. to present recent discoveries in basic research, that may lead to future drug identification to efficiently alleviate the vertigo crisis and protect the vestibule upon selective impairments. This theme should target a broad audience ranging from ENT clinicians to scientists, including pharmacologists.

## **807 Prevalence of Vestibular Dysfunction and Need for Effective Treatment Modalities**

Lloyd Minor<sup>1</sup>, Yuri Agrawal<sup>1</sup>, Bryan Ward<sup>1</sup>

<sup>1</sup>Johns Hopkins University

Our recent analysis of data from the 2001-2004 National Health and Nutrition Surveys showed that 35% of US adults age 40 years and older have evidence of vestibular dysfunction as measured by a postural metric (Agrawal et al. Arch Int Med 2009 169:938-44). Odds of vestibular dysfunction increased significantly with age and were 70% higher among people with diabetes mellitus. Participants in the surveys with vestibular dysfunction who were clinically symptomatic (ie, reported dizziness) had a 12-fold increase in the odds of falling.

Treatments for vestibular disorders with a clearly defined anatomical and pathophysiological basis (eg, benign paroxysmal positional vertigo and superior canal dehiscence syndrome) are often effective at correcting the disorder and alleviating symptoms. Patients with other disorders for which the etiology is less clearly defined (eg, Meniere's disease) may derive symptomatic relief from empirically-based or ablative therapies. Few treatments currently exist for unilateral or bilateral vestibular loss as well as for vestibular dysfunction with less clearly established etiology. The consequences of vestibular dysfunction on overall health and well being and the risks associated with vestibular disorders support the urgent need for more effective treatment modalities.

## **808 Neuropharmacology of Vestibular System Disorders**

Enrique Soto<sup>1</sup>

<sup>1</sup>Universidad Autónoma de Puebla, México.

Vertigo, dizziness, gaze alterations and imbalance are the main symptoms of vestibular disorders. Vestibular malfunctioning can lead to physical consequences such as reduced postural control and falls and to psychological and psychiatric consequences such as depression, anxiety, panic, agoraphobia, and cognitive defects, especially in the elderly. The goal of the treatment of vestibular disorders should be to control symptoms, reduce functional disability and improve the quality of life of the patients. The otolaryngologists are confronted with a rapidly changing field in which advances in the knowledge of ion channel functions and synaptic transmission mechanisms have led to the development of new scientific models for the understanding of vestibular dysfunction and its management. Also a question about the central or peripheral action of many drugs, but particularly histamine antagonists, has been raised and will be dealt with. In this presentation, drugs acting on vestibular system have been grouped into two main categories according to their primary mechanisms of action: those with effects on neurotransmitters and neuromodulator receptors and those that act on voltage-gated ion channels. Particular attention is given to drugs that may provide additional insight into the pathophysiology of vestibular diseases. A critical review of the pharmacology and highlights of the major advances are discussed in each case. This presentation reviews the neuropharmacology of vestibular disorders

with an emphasis on the mechanism of action of drugs commonly used in the treatment of such disorders and on drugs and targets that may be of potential interest. Drugs that by their systemic effect could secondarily affect vestibular function will not be considered.

## **809 Betahistine Improvement of Vestibular Compensation: Myth or Reality ?**

Michel Lacour<sup>1</sup>

<sup>1</sup>UMR 6149 CNRS/Université de Provence

The effects of histamine derivatives in the treatment of vertigo have led to an extensive literature for a couple of decades, and both agonists and antagonists of the histamine receptors are used as antivertigo medication. Among them betahistine is the most used in Europe but its effect on vestibular compensation remains poorly documented in vestibular patients.

We show here results from animal models demonstrating that betahistine strongly accelerates the behavioral recovery process, and we describe the main mechanisms implicated at the CNS level. We demonstrate also dose- and duration-dependent effects that could explain the placebo-like effect of betahistine reported in previous clinical studies. Indeed, with higher doses than those currently used by the past, given on the long term, we demonstrated a similar acceleration of the recovery process in Menière's patients under betahistine treatment.

Conclusion: 1) Chronic *versus* acute treatment, low dose *versus* high dose are crucial factors in the betahistine treatment of vestibular loss patients; 2) the drug acts more on the time constant of the recovery process than on the vertigo crisis *per se*.

## **810 Specific Histamine H4 Receptor Antagonists Act as Potent Modulators of Mammal Vestibular Function**

Eric Wersinger<sup>1</sup>, Gilles Desmadryl<sup>2</sup>, Sophie Gaboyard-Niay<sup>1</sup>, Aurore Brugeaud<sup>1</sup>, Jonas Dyhrfeld-Johnsen<sup>2</sup>, Christian Chabbert<sup>2</sup>

<sup>1</sup>SENSORION pharmaceuticals, <sup>2</sup>INSERM 1051, Institute for Neurosciences of Montpellier, Montpellier, France

Histamine is a naturally occurring biological amine that exerts a range of effects on many physiological processes through the activation of four different G protein-coupled histamine receptors (H1R-H4R). In addition to their localization in various cells of the immune system, H1-H4 receptors are also found in the central and/or peripheral nervous system. For instance, recent work has shown that H3R is expressed in mammalian vestibular neurons. In addition, H3R antagonist, betahistine, routinely used in the treatment of vertigo can act peripherally by inhibiting the afferent discharge recorded from the vestibular nerve in lower vertebrates.

We aimed to further explore the expression and role of H1R-H4R in afferent neurons from Scarpa's ganglion using a multidisciplinary approach. By combining single cell RT-PCR and immunohistochemical experiments we confirm the expression of H1 and H3 receptors and further demonstrate the localization of the H4R in rat primary vestibular neuron somata. In vitro, whole cell patch-clamp

recordings from P4-P7 cultured rat vestibular neurons revealed strong and reversible inhibitory effects on evoked action potential firing by H4R antagonists with an IC50 in the micromolar range. In vivo, the effect of H4R antagonists on experimentally induced severe vestibular deficits were evaluated in an animal model using a rating system based on multiple criteria: circling, head bobbing and head tilt, tail hanging and air righting reflexes. Each H4R antagonist significantly alleviated the induced vestibular deficits by 20-30%. By contrast, neither of the H3 receptor antagonists (betahistine and thioperamide) tested as reference compounds had significant effects. The present study demonstrates the role of H4R antagonists in modulating vestibular function and suggests that they are strong candidates for a novel, highly efficient treatment of vertigo crisis caused by peripheral vestibular dysfunction.

### **811 Mixed Modulation: Cholinergic Efferents Differentially Excite and Inhibit Vestibular Targets Through Distinct Receptor Subtypes** **Joseph Holt<sup>1</sup>**

<sup>1</sup>University of Rochester

More than one-third of the adult US population has experienced bouts of dizziness or an impaired sense of balance. Of those conditions that directly affect peripheral vestibular organs, it's not surprising that changes in hair cell or afferent function can lead to vestibular problems. But, there is a hesitancy to consider vestibular efferents despite their anatomical prevalence. The importance of an efferent innervation has been underestimated, in part, because its functional role is not well understood. It is clear that when efferent neurons are electrically stimulated under experimental conditions, they can profoundly modify vestibular afferent discharge. Such effects, if they occur under a more physiological setting, would undoubtedly impact vestibular information traveling to the CNS. It then follows that any disruption in efferent physiology could contribute to vestibular dysfunction. Thus, targeting the vestibular efferent system pharmacologically could be of significant clinical utility.

But pharmacological intervention requires an understanding of efferent signaling schemes in the vestibular periphery. Although the cellular and pharmacological bases for efferent actions in mammals are largely unknown, efferent synaptic mechanisms in other vertebrate models have provided some insight. Vestibular efferent neurons are predominantly cholinergic and the effects of efferent stimulation on vestibular afferent discharge can be ascribed to three distinct signaling pathways: (1)  $\alpha 9/\alpha 10$ -nicotinic AChRs and SK-potassium channels in type II hair cells; (2)  $\alpha 4\beta 2$ -containing nicotinic AChRs on calyx and bouton afferents; and (3) muscarinic AChRs and KCNQ potassium channels in calyceal terminals. Interestingly, many of the current drugs commonly used in the treatment of vestibular disorders have prominent anticholinergic effects, some of which could be targeting efferent mechanisms, including the above pathways. Implications for efferent actions in

mammals will be discussed (Supported by NIH DC008981).

### **812 Voltage-Gated Ion Channels in Mammalian Vestibular Organs: Possible Pharmacological Targets in Hair Cells and Primary Afferents**

**Ruth Anne Eatock<sup>1,2</sup>**, Xiao-Ping Liu<sup>2,3</sup>, Gang Li<sup>1,2</sup>, Jocelyn Songer<sup>1,2</sup>, Anna Lysakowski<sup>4</sup>

<sup>1</sup>Harvard Medical School, <sup>2</sup>Massachusetts Eye and Ear Infirmary, <sup>3</sup>MIT, <sup>4</sup>University of Illinois, Chicago

Vestibular pathologies of inner ear origin, such as vestibular neuritis or Ménière's disease, give rise to aberrant afferent signaling which can be so disabling as to require labyrinthectomy. The neural signals reflect the coordinated activities of diverse voltage-gated ion channels expressed by hair cells and primary afferents, including channels selective for K<sup>+</sup> ions (K<sub>V</sub>) and Na<sup>+</sup> (Na<sub>V</sub>). Systematic differences in the complements of K<sub>V</sub> and Na<sub>V</sub> channels are likely to contribute to the major physiological differences between central and peripheral zones of vestibular epithelia. Central-zone afferents have the most irregular spike timing and phasic response dynamics and appear to be more sensitive to toxic insult and aging. Zonal differences in ion channel expression suggest the possibility of manipulating ion channel activity in one afferent population – in order to silence aberrant signals or restore normal excitability – without affecting the other population. Voltage-gated ion channels may also be critical for activity-dependent development and repair.

Low-voltage-activated (LV) K<sub>V</sub> channels from the K<sub>V</sub>1 and K<sub>V</sub>7 families feature prominently in both hair cells and primary afferents of the striola (central zone of maculae) and are implicated in its broad frequency range and irregularity. Activation of LV K<sub>V</sub> channels reduces excitability (the tendency to spike), suggesting an approach to aberrant vestibular signaling. Na<sub>V</sub> channels in hair cells and afferents also differ between zones. Striolar channels include Na<sub>V</sub>1.5 channels which have relatively negative voltage ranges of inactivation and activation. Hair cells tend to express Na<sub>V</sub> channels early in development when synapses are forming. Brugeaud et al. (*J Neurosci* 27:3503, 2007) further showed that the non-Na<sub>V</sub>1.5 channels of immature extrastriolar type II hair cells tend to re-express following denervation of mature tissue. This expression pattern suggests a possible link between Na<sub>V</sub> channel expression in hair cells and the formation of afferent synapses. In that event, pharmacological activation of Na<sub>V</sub> channels might stimulate replacement of damaged afferent synapses.

Supported by DC02290.

### **813 Ondansetron Reduces Vertigo Associated Functional Deficits by Protecting Vestibular Primary Neurons from Excitotoxic Insult in Vivo**

Jonas Dyhrfeld-Johnsen<sup>1,2</sup>

<sup>1</sup>INSERM U1051 - Institute of Neurosciences Montpellier,

<sup>2</sup>Sensorion Pharmaceuticals

Excitotoxic insult of primary vestibular neurons is thought to play a key role in the induction of permanent deficits in vestibular pathologies like ischemia, Meniere's disease and vestibular neuritis. In a recent pilot study, the anti-emetic ondansetron reduced lasting vestibular deficits in a patient population diagnosed with vestibular neuritis. We evaluated the neuroprotective potential of ondansetron in a rodent model of peripheral vestibular excitotoxic insult using behavioral testing, videonystagmography and histological methods.

Adult female Long-Evans rats received repeated transtympanic injections of kainate in physiological serum and either ondansetron or saline (sham) treatment under double-blind, randomized conditions. Spontaneous nystagmus was recorded using infrared video-oculography up to 7h post-insult and behavioral vestibular deficits assessed up to 72h post insult using 5 criteria, each scored on a scale from 0-4: Circling, head-bobbing, tail-hanging and air-righting reflexes and degree of lateral head-tilt. A number of rats were transcardially perfused for histology.

Ondansetron treated rats showed significantly decreased vestibular deficits after the peak kainate-induced vertigo crisis compared to sham-treated rats along with a significant reduction of spontaneous nystagmus. The reduced deficits persisted at 24h, suggesting a lasting protective effect of ondansetron treatment. Electron microscopic histological analysis of vestibular tissue samples showed an accelerated endogenous reparative re-afferentation consistent with reduced initial excitotoxic injury.

We conclude that systemic ondansetron treatment functionally protects the peripheral vestibular endorgans from excitotoxic insult as presently demonstrated using criteria including behavioral deficits, spontaneous nystagmus and tissue damage. As such, ondansetron is a strong candidate for the first neuroprotective treatment in vestibular pathologies leading to permanent deficits.

### **814 Lack of Prostaglandin E Receptor EP4 Causes Hearing Impairment and Aggravates Noise Induced Hearing Loss in Mice**

Kiyomi Hamaguchi<sup>1</sup>, Takayuki Nakagawa<sup>1</sup>, Norio Yamamoto<sup>1</sup>, Juichi Ito<sup>1</sup>

<sup>1</sup>Graduate School of Medicine, Kyoto University

Prostaglandins (PGs) are short-lived chemical mediators in the mammalian body. Among PGs, prostaglandin E2 (PGE2) is most widely produced in the body, most widely found in animal species and has been described as a regulator of numerous physiological functions. Physiological actions of PGE2 are mediated via prostaglandin E receptor subtypes that have been named

EP1, EP2, EP3 and EP4. Among these receptor subtypes, PGE signaling through EP4 is reported to have various functions, such as anti-apoptotic, anti-inflammatory and vasodilative effects.

In our previous study, we reported that EP4 was expressed in the mouse cochlea and its agonist may have protective effect against noise induced hearing loss in guinea pigs.

In this study, to confirm the role of PGE-EP4 signaling in the cochlea, we investigated the auditory system of EP4 deficient mice in the physiological and pathophysiological conditions. The result demonstrated that EP4 deficient mice exhibited modest hearing loss and were susceptible to noise trauma. Histological analysis revealed that surviving outer hair cells (OHCs) of EP4 deficient mice were decreased after noise trauma.

And we also demonstrated that pharmacological inhibition of EP4 amplified the loss of both hearing ability and OHCs induced by noise trauma as observed in EP4 deficient mice, whereas pharmacological activation of EP4 attenuated these loss.

These findings suggest that EP4 signaling is necessary for the maintenance of cochlear physiological function and for cochlear protection against noise-induced damage, in particular OHCs. EP4 might therefore be an effective target for cochlear disease therapeutics.

### **815 Imbalance of Matrix Metalloproteinases Affects Normal Cochlear Function and Potentiates Noise-Induced Cochlear Dysfunction**

Bo Hua Hu<sup>1</sup>, Qunfeng Cai<sup>1</sup>, Donald Coling<sup>1</sup>

<sup>1</sup>State University of New York at Buffalo

Homeostasis of extracellular matrix relies on the balanced functions of matrix metalloproteinases (MMPs) and their intrinsic inhibitors, the tissue inhibitors of metalloproteinases (TIMPs). The current study was designed to investigate the roles of MMP-related genes in the maintenance of normal cochlear function and regulation of cochlear responses to acoustic overexposure. In the sensory epithelium of the normal rat cochlea, we detected the expression of 13 MMPs (MMPs-1, -2, -3, -4, -5, -6, -8, -9, -10, -11, -12, -13, and -14), three TIMPs (Timp-1, -2 and -3) and four Adamts (Adamts-1, -2, -5 and -8). We also found strong enzymatic activity of MMPs that was comparable to the activity level of these enzymes in kidney tissues, and significantly higher than that in the brain tissues. Inhibition of MMP activity using doxycycline, a broad spectrum inhibitor of MMPs, resulted in a mild flat hearing loss, without causing sensory cell death. Interestingly, the hearing loss was partially recoverable after the termination of the drug application. These observations suggest that MMP-related genes contribute to the maintenance of normal cochlear function. In rats exposed to a broadband noise at 120 dB SPL for 2 h, we found time-dependent expression changes in MMP-related genes at 2 h, 1 day and 28 days post-noise exposure. These expression changes were site-specific with more genes altered in their expression levels in the basal partition of the cochlea, consistent with the finding of

greater sensory cell damage in the basal part of the cochlea. Inhibition of MMP activity with doxycycline potentiated noise-induced hearing loss. Taken together, these results suggest that MMP-related genes contribute to normal cochlear function and to regulate cochlear responses to acoustic overstimulation. Manipulation of MMP activity may serve as a novel target for therapeutic intervention of noise-induced cochlear damage. (Supported by NIH R01 DC010154-01A2 to BH Hu)

**816 Insulin-Like Growth Factor1 Promotes Hensen' and Claudius' Cell Proliferation to Regenerate Outer Hair Cells Through the Mitogen-Activated Protein Kinase Kinase/extracellular Signal-Regulated Kinase Pathway**

**Yushi Hayashi<sup>1</sup>, Norio Yamamoto<sup>1</sup>, Takayuki Nakagawa<sup>1</sup>, Juichi Ito<sup>1</sup>**  
<sup>1</sup>*Kyoto University*

In the last year ARO midwinter meeting, we reported that insulin-like growth factor1 (IGF-1) protects cochlear hair cells of neonatal mice *ex vivo* against aminoglycoside through both the phosphatidylinositol 3-kinase (PI3K)/Akt pathway and the mitogen-activated protein kinase kinase/extracellular signal-regulated kinase (MEK/ERK) pathway. We also reported that this effect is through inhibiting apoptosis of cochlear hair cells. In order to investigate where each signal is activated among the cochlear sensory epithelium, we performed immunohistochemistry of phospho-Akt (p-Akt) and phospho-ERK (p-ERK), which show the activation of each pathway, after administration of neomycin with or without IGF-1. When treated with IGF-1, p-Akt was positive in only inner hair cells (IHCs), and p-ERK was positive in Hensen' and Claudius' cells, which indicated that PI3K/Akt and MEK/ERK are activated in IHCs and Hensen' and Claudius' cells by IGF-1 treatment respectively. Next, in order to exclude the possibility of involvement of other mechanisms than inhibition of apoptosis, we tested proliferation status of the explants after IGF-1 treatment using BrdU. Treatment with IGF-1 caused BrdU uptake in Hensen' and Claudius' cells, suggesting that Hensen' and Claudius' cells proliferate to regenerate outer hair cells (OHCs). In order to confirm this, we inhibited proliferation using aphidicolin at concentration where BrdU uptake disappears in Hensen' and Claudius' cells. In this condition, OHC protection by IGF-1 against neomycin attenuated. We concluded that Hensen' and Claudius' cells proliferate to regenerate OHCs by IGF-1 treatment through the MEK/ERK pathway. This proliferation effect as well as inhibition of apoptosis contributes to the protection of cochlear hair cells with IGF-1 at least in neonatal mice.

**817 S-Nitrosylation of Cochlear Proteins and Their Biological Significance in Cisplatin Mediated Ototoxicity**

**Samson Jamesdaniel<sup>1</sup>, Sneha Hinduja<sup>2</sup>, Dalian Ding<sup>2</sup>**  
<sup>1</sup>*The State University of New York, Buffalo, NY*, <sup>2</sup>*The State University of New York, Buffalo*

S-nitrosylation is a redox sensitive protein modification, which is highly specific but reversible mechanism that regulates several signal transduction cascades. Oxidative stress is considered to play a causal role in the ototoxic effects of anti-neoplastic drug, cisplatin. Despite emerging evidences implicating nitroxidative stress as a critical factor in cisplatin toxicity, the significance of cochlear protein S-nitrosylation in cisplatin ototoxicity is poorly understood. In the present study, 16 mg/kg dose of cisplatin decreased distortion product amplitudes and induced massive loss of outer hair cells (OHC) at basal turn of the cochlea, in Wistar rats, 3 days post treatment. These ototoxic effects were accompanied by significant increases in the cochlear expression of at least three S-nitrosylated proteins. The cisplatin-induced increases in S-nitrosylated proteins were immuno-localized in organ of Corti, stria vascularis and spiral ganglions, known cochlear targets of cisplatin toxicity. In addition, cisplatin-induced modulation of cochlear mRNA levels of *Egr1*, *Cdkn1a*, *Rprm*, *Fos*, *Irgm* and *Mpo*, suggested the potential significance of nitric oxide (NO) signaling mechanism in cisplatin ototoxicity. Biological importance of nitrosative stress in cisplatin ototoxicity was indicated by the attenuation of cisplatin-induced S-nitrosylation of cochlear proteins and prevention of associated hearing loss, after co-treatment with Trolox, an inhibitor of peroxynitrite. Thus, cisplatin-induced protein S-nitrosylation, their sensitive cochlear localization and associated up/down regulation of NO signaling genes in cochlea suggests a crucial role of S-nitrosylation in mediating cisplatin ototoxicity. (Funded by NIH/NIDCD: R03DC010225, SJ)

**818 Reduction of Neomycin Dosage Increases Survival of Supporting Cells and Reveals Neurotoxicity of the Aminoglycoside**

**Donald L. Swiderski<sup>1</sup>, Ilaaf Darrat<sup>2</sup>, Hiu Tung Wong<sup>1</sup>, Cameron L. Budenz<sup>1,2</sup>, Yehoash Raphael<sup>1</sup>**  
<sup>1</sup>*Kresge Hearing Research Institute, University of Michigan*, <sup>2</sup>*Department of Otolaryngology - Head and Neck Surgery, University of Michigan*

High dose neomycin treatment induces loss of both sensory hair cells and spiral ganglion cells (SGC) in guinea pigs, which contrasts with the survival of SGC in many profoundly deaf human patients. Because SGC are the targets of cochlear implant stimulation, and their survival has implications for the potential efficacy of any future hair cell regeneration strategy, we investigated whether lower doses of neomycin in the guinea pig model would better simulate the condition of these patients. We also tested whether SGC survival is correlated with the degree of degeneration in the organ of Corti (OC), or the survival of particular cell types (e.g., inner hair cells or pillar cells). Young adult guinea pigs were given 10  $\mu$ l neomycin (1%,

5%, or 10%) by basal turn cochleostomy and were sacrificed at 1 or 3 weeks to evaluate changes in cell number and composition in the OC and Rosenthal's canal. By 1 week, all doses produced a flat epithelium devoid of differentiated cell types in the basal turn and extending toward the apex in a dosage dependent manner. Loss of SGC at 1 week was detected in the basal turn of some specimens, but average differences from control ears were not significant. At 3 weeks, all ears that received 5% neomycin had significant SGC loss but no apical-basal gradient or change in SGC density correlated with loss of a particular OC cell type. This result contrasts with observations that survival of pillar cells or other supporting cells is associated with greater retention of peripheral processes in the deafened OC. Furthermore, the lack of association between SGC loss and OC degeneration is indirect evidence that some SGC loss is primary to neomycin toxicity, not secondary to loss of other cell types. In addition, the change in SGC depletion from 1 to 3 weeks may reveal a window of opportunity for therapies to preserve SGC, such as neurotrophin replacement.

This work is supported by The Williams Professorship, and NIH/NIDCD grants DC-010412, DC-007634, T32-DC-005356, and P30 DC-05188.

### **819** Activation of Cochlear A<sub>1</sub> Adenosine Receptor (A<sub>1</sub>AR) Protects Against Cisplatin Ototoxicity by Suppressing Inflammation

**Tejbeer Kaur**<sup>1</sup>, Debashree Mukherjea<sup>2</sup>, Kelly Sheehan<sup>2</sup>, Sarvesh Jajoo<sup>1</sup>, Leonard P Rybak<sup>1,2</sup>, Vickram Ramkumar<sup>1</sup>  
<sup>1</sup>*Southern Illinois University School of Medicine, Dept. of Pharmacology, Springfield, Illinois,* <sup>2</sup>*Southern Illinois University School of Medicine, Dept. of Surgery, Springfield, Illinois*

Ototoxicity and nephrotoxicity are dose-limiting side effects of cisplatin, a widely used anticancer drug. Recent data from our laboratory have implicated STAT1 in cisplatin-induced hearing loss and have shown that inhibition of STAT1 provides otoprotection. Adenosine (A<sub>1</sub>) receptor (A<sub>1</sub>AR) is expressed in the rat cochlea and provides protection against cisplatin ototoxicity. However, the mechanism underlying this protective action has not been clearly defined. In this study, we test the hypothesis that Adenosine (A<sub>1</sub>) receptor agonist, R-PIA, protects against cisplatin ototoxicity by inhibiting STAT1 activation and function. Pretreatment of immortalized mouse organ of Corti cells, UB/OC-1, with R-PIA (1 $\mu$ M) reduced cisplatin-mediated NOX3 expression and activity. This was associated with reduced Ser<sup>727</sup> phosphorylation of STAT1 and reduced STAT1 luciferase activity, which was reversed by an A<sub>1</sub>AR antagonist, DPCPX. Cisplatin exposure (2.5 $\mu$ M) for 24 h augmented the expression of STAT1 target genes, namely iNOS (~2.5 fold), COX2 (~4.5 fold) and TNF- $\alpha$  (~2.2 fold). Pretreatment with R-PIA, decreased the expression and immunoreactivity of these inflammatory genes in both UB/OC-1 cells, as well as the cochlea. Importantly, trans-tympanic administration of R-PIA in Wistar rats inhibited cisplatin-induced ototoxicity, as measured by auditory brainstem responses (ABRs) and scanning electron microscopy (SEM). These data support

the contention that activation of the A<sub>1</sub>AR protects against cisplatin ototoxicity by inhibiting NOX3 expression, STAT1 activation and the expression of genes involved in inflammation and cell death. We suggest that local (and possibly systemic) administration of A<sub>1</sub>AR agonists to the cochlea could protect against cisplatin ototoxicity in cancer patients. (Supported by NIH grants R01DC02396 and R15DC011412 and funds from SIU SOM).

### **820** Attenuation of Aminoglycoside-Induced Cellular Oxidative Stress with Transplatin

**Michael Brenner**<sup>1</sup>, Debashree Mukherjea<sup>1,2</sup>, Tejbeer Kaur<sup>2</sup>, Kelly Sheehan<sup>2</sup>, Vickram Ramkumar<sup>2</sup>, Leonard Rybak<sup>1,2</sup>

<sup>1</sup>*Dept. of Surgery, Southern Illinois University School of Medicine,* <sup>2</sup>*Dept. of Pharmacology, Southern Illinois University School of Medicine*

Ototoxicity is a common and usually irreversible side effect of aminoglycoside antibiotic therapy. Several studies have implicated reactive oxygen species (ROS) in the pathogenesis of this complication. ROS generation leads to activation of signal transducer and activator of transcription 1 (STAT1). The phosphorylation of STAT1 is an early step in p53-mediated killing in cisplatin-treated utricular hair cell cultures. We hypothesized that STAT1 activation was also involved in development of aminoglycoside-induced ototoxicity and that transplatin, an inactive isomer of cisplatin that abrogates cisplatin ototoxicity in rats, could inhibit STAT1 activation. In gentamicin-treated UB/OC-1 cells, we demonstrated increased STAT1 Ser<sup>727</sup> phosphorylation (pSTAT1) and increased prevalence of pSTAT1-responsive gene products associated with elevated ROS and increased activity of NADPH oxidase isoform 3 (NOX3). Transplatin administration attenuated gentamicin-induced cellular oxidative stress and inflammation with normalization of NOX3, pSTAT1, and TNF alpha levels. The transient receptor potential vanilloid 1 (TRPV1) channel, which may permit aminoglycoside entry into cells, was also upregulated by gentamicin and suppressed by transplatin, suggesting another putative target for otoprotection. Ongoing work investigates transplatin therapy for gentamicin-induced ototoxicity *in vivo*. Transplatin therefore suppresses gentamicin-induced ROS and attenuates activation of STAT1 and its downstream pathways.

Supported by EAM SIUSOM(MJB); 1F32DC009950(DM); R15CA135494(VR) and R01DC02396(LPR).

## **821 Simvastatin Protects Auditory Hair Cells from Gentamicin-Induced Toxicity and Activates Akt Signaling in Vitro**

**Yves Brand**<sup>1,2</sup>, Cristian Setz<sup>1</sup>, Soledad Levano<sup>1</sup>, Alwin Listyo<sup>1</sup>, Eduardo Chavez<sup>2</sup>, Kwang Pak<sup>3</sup>, Allen Ryan<sup>2,3</sup>, Daniel Bodmer<sup>1</sup>

<sup>1</sup>*Clinic of Otolaryngology, Head and Neck Surgery, University Hospital Basel, Switzerland,*

<sup>2</sup>*Surgery/Otolaryngology, UCSD School of Medicine, 9500 Gilman Drive, La Jolla, CA 92093-0666,* <sup>3</sup>*San Diego VA Medical Center, 3350 La Jolla Village Drive, La Jolla, CA 92037*

Inhibitors of 3-hydroxy-3-methylglutaryl-coenzyme A reductase, known as statins, are commonly used as cholesterol-lowering drugs. During the past decade, evidence has emerged that statins can also have neuroprotective effects. Simvastatin, a commonly used statin, increases Akt phosphorylation in the retina *in vivo*, indicating that the PI3K/Akt pathway contributes to the protective effects achieved. However, the effects of statins on the inner ear are largely unknown.

We evaluated whether 3-hydroxy-3-methylglutaryl-coenzyme A reductase is present within the rat cochlea and whether simvastatin is able to protect auditory hair cells from gentamicin-induced apoptotic cell death in an *in vitro* mouse model. We further determined whether simvastatin increases Akt phosphorylation in the organ of Corti.

3-hydroxy-3-methylglutaryl-coenzyme A reductase mRNA was detected in the organ of Corti, spiral ganglion, and stria vascularis by RT-PCR. Moreover, simvastatin produced a dose-dependent reduction of hair cell loss in organs of Corti due to gentamicin, as compared to samples treated with gentamicin alone. The protective effect of simvastatin was reversed by addition of mevalonate, a downstream metabolite blocked by simvastatin, demonstrating the specificity of protection to this pathway. Finally, Western blotting revealed an increase in organ of Corti Akt phosphorylation after simvastatin treatment *in vitro*.

The results support a neuroprotective effect of statins in the inner ear, mediated by reduced 3-hydroxy-3-methylglutaryl-coenzyme A reductase metabolism and Akt activation.

## **822 Targeted Deletion of Oncomodulin Results in Early Progressive Hearing Loss**

**Dwayne D. Simmons**<sup>1,2</sup>, Kevin S. Choi<sup>1</sup>, Aubrey Hornak<sup>1</sup>, Kevin K. Ohlemiller<sup>3</sup>

<sup>1</sup>*UCLA,* <sup>2</sup>*UCLA Brain Research Institute,* <sup>3</sup>*Washington University*

The tight regulation of Ca<sup>2+</sup> is essential for cochlear function, and yet the role of Ca<sup>2+</sup> binding proteins in hair cells remains elusive. While most Ca<sup>2+</sup> binding proteins are found extensively throughout the nervous system, oncomodulin (Ocm), a member of the parvalbumin family, has a restricted expression pattern and in the cochlea is found in the basolateral membrane and hair bundle of outer hair cells (OHCs). To study the role of Ocm in the cochlea, we generated a conditional Cre-lox knockout line

with Cre-recombinase driven by the  $\beta$ -actin promoter. The absence of Ocm expression was confirmed by RT-PCR and immunocytochemistry. Preliminary analysis of  $\beta$ -actin<sup>Cre</sup>;Ocm<sup>-/-</sup> mice reveals no obvious phenotypic abnormalities compared with controls.

Cochlear function was tested in mutant and wild-type littermates from 4 to 12 weeks. At 4 weeks, Ocm<sup>-/-</sup> mutants had normal auditory brainstem responses (ABRs). However by 8 - 10 weeks, Ocm<sup>-/-</sup> mutants have ABR threshold shifts of as much as 60 dB in frequencies above 10 kHz. Hair cell loss was analyzed in Ocm<sup>-/-</sup> mutants from postnatal day 10 through 12 weeks. There was no significant hair cell loss prior to 8 weeks. However after 8 weeks, hair cell loss was pronounced. Basal turn regions of the cochlea demonstrated significant OHC loss, particularly in the first OHC row. Inner hair cell loss was much less pronounced. The pattern of OHC loss was also sporadic with stretches of normal appearing OHCs and stretches where there was a complete absence of row 1 OHCs.

These results suggest that expression of Ocm is essential to cochlear function and may play a protective role in OHCs.

## **823 Jun and Gene Expression in the Spiral Ganglion After Deafening**

**Catherine Kane**<sup>1</sup>, Erin Bailey<sup>1</sup>, Zarin Rehman<sup>1</sup>, Steven Green<sup>1</sup>

<sup>1</sup>*University of Iowa*

Following loss of hair cells (HCs), spiral ganglion neurons (SGNs) gradually die over a period of ~14 wks in rats (Alam et al., 2007). In all these experiments, rats are deafened by daily kanamycin injection from postnatal day 8 (P8) to P16. Alam et al. also showed increased phosphorylation of the transcription factor Jun, known to be associated with proapoptotic gene expression, in SGNs by P32 in deafened rats. While Jun phosphorylation is a typical consequence of neurotrophic factor withdrawal in neurons, its appearance in SGNs is not entirely predictable because at the time increased Jun phosphorylation becomes evident, only NT-3 levels have declined in the organ of Corti and expression of several other neurotrophic factors (NTFs) remains. Either NT-3 has a distinctive role among NTFs in suppressing Jun phosphorylation or Jun phosphorylation is induced by other post-deafening changes. Is Jun phosphorylation necessary for SGN death postdeafening? We used both I-JIP, a peptide inhibitor of JNK activation, and SP600125, a JNK inhibitor. These were infused from a minipump into scala tympani of deafened rats from P32 to P60 via a cannula and cochleostomy. The rats were euthanized at P60 for cell counts using an optical disector method in 50  $\mu$ m cryostat sections. We used phosphoJun immunofluorescence (IF) to confirm inhibition of Jun phosphorylation but a change in the availability of satisfactory anti-phosphoJun antibodies have limited this method. We modified preexisting protocols to minimize technical problems with attachment of cannulae and solubility of SP600125. Cannulae used polyurethane tubing for greater flexibility with a short

polyimide extension inserted into the cochleostomy. Attached nylon and dacron mesh patches were glued to the bone to support the seal between the tubing and the cochlea. Preliminary data from cochleae in which we could verify that infusion was successful show an ~28% increase in SGN survival in the basal turn in I-JIP-treated rats.

### **824 ERK1/2 Activation Is Localised to Supporting Cells in Neonatal and Adult Mouse Utricular Organ Explants Following Hair Cell Damage**

**Gregory Ball<sup>1</sup>, Jonathan Gale<sup>1,2</sup>**

<sup>1</sup>*UCL Ear Institute, 332 Gray's Inn Road, London, WC1X 8EE, UK,* <sup>2</sup>*Department of Cell and Developmental Biology, UCL, London, WC1E 6BT, UK*

Extracellular regulated kinases 1 and 2 (ERK 1/2) have been shown to be important in both cochlear hair cell death and survival. In neonatal cochlea, short term inhibition (8hr) of ERK1/2 activation following aminoglycoside exposure, via the MEK1/2 inhibitor U0126, protects inner hair cells (Lahne & Gale, 2008), whilst long term inhibition (24hr) increases hair cell death (Battaglia et al 2004). Here we further investigate the action of ERK1/2 in hair cell epithelia.

We have used a multiphoton laser to terminally damage individual hair cells in both neonatal cochlear and adult utricular organ explants from mice. Immunolabelling for phosphoERK1/2 in samples fixed post ablation revealed ERK1/2 activation in supporting cells surrounding the damage site. Modification of the damage paradigm allowed targeted damage to supporting cells and again, ERK1/2 activation was localised in supporting cells neighbouring the damage site. These results are consistent with the release of a signalling molecule that has its action predominantly on supporting cells.

Next, we tested whether there were any differences in damage-induced activation of ERK1/2 in immature and adult hair cell epithelia. A cluster of six cells were terminally laser-damaged and the pattern of ERK1/2 activation arising from this lesion examined post fixation by phosphoERK1/2 immunohistochemistry. Damage-induced activation was localised to supporting cells and spread out from the lesion in the minutes following damage, as seen in the neonatal cochlea. However, both the spread and duration of activation was reduced in the adult system. We are investigating whether the different response in adults arises from a reduced capacity to respond, or reduced damage signal release.

Finally, we used the adult utricle model to investigate the role of ERK1/2 signalling during neomycin-induced hair-cell death. Following 24 hours of neomycin, ERK1/2 activity appears localised to supporting cells often in clusters. Inhibiting MEK1/2 for the whole 24 hour period of neomycin-treatment prevented this ERK activation but the improvement in hair cell survival was not statistically-significant. We suggest that manipulating ERK activation in specific cell types is critical.

GJB is funded by an Action on Hearing Loss Studentship.

### **825 The Pou4f3 Regulatory Target Caprin-1 Is Recruited to Stress Granules in Cochlear Hair Cells in Response to Aminoglycoside Damage, Heat Shock and Oxidative Stress**

**Emily Towers<sup>1</sup>, John Kelly<sup>1</sup>, Sally Dawson<sup>1</sup>, Jonathan Gale<sup>1</sup>**

<sup>1</sup>*UCL Ear Institute, University College London, UK*

Under certain types of stress, cells assemble stress granules as a defence mechanism. Stress granules are cytoplasmic ribonucleoprotein aggregates that recruit specific mRNAs for translation silencing leaving a restricted pool of mRNAs free for translation. The importance of stress granule assembly has not long been established and its contribution in vivo and in disease is yet to be characterised. Some key components of stress granule assembly have been identified including T-cell internal antigen 1 (TIA-1) and Caprin-1 the over-expression of which in cell lines is sufficient in itself to cause stress granule assembly.

We undertook a screen to identify the regulatory targets of the transcription factor and DFNA15 gene product Pou4f3. This screen identified the stress-granule-associated protein Caprin-1 as being down-regulated by Pou4f3 as a result of direct interaction with the Caprin-1 promoter. We detected Caprin-1 mRNA and protein in mammalian supporting cells and, at lower levels, in hair cells. As Caprin-1 has been implicated in stress granule formation we examined changes in its expression and cellular localisation in cochlear cultures after heat shock, arsenite and aminoglycoside treatment. All three treatments triggered the formation of TIA-1 and Caprin-1-positive stress granules in hair cells. Single cell qPCR assays established that there was an increase in hair cell Caprin-1 transcription in response to aminoglycoside treatment consistent with a role for Caprin-1 in triggering stress granule assembly. Our results suggest stress granule formation is a common response to cochlear stress and ototoxic damage.

### **826 Gene Therapy After Hearing Loss for Long-Term Neural Protection**

**Patrick Atkinson<sup>1,2</sup>, Andrew Wise<sup>1</sup>, Brianna Flynn<sup>1</sup>, Bryony Nayagam<sup>2</sup>, Clifford Hume<sup>3</sup>, Robert Shepherd<sup>1,2</sup>, Stephen O'Leary<sup>2</sup>, Rachael Richardson<sup>1</sup>**

<sup>1</sup>*Bionics Institute,* <sup>2</sup>*The University of Melbourne,* <sup>3</sup>*The University of Washington*

The administration of exogenous neurotrophins (NTs) to the deafened cochlea via mini-osmotic pumps can promote spiral ganglion neuron (SGN) survival and peripheral fibre regrowth. However, the duration of exogenous NT delivery using such a technique is finite and this protective effect has not been shown beyond two weeks after cessation of NT administration, indicating that long-term NT treatment is required for sustained benefits. Using gene therapy techniques, we aim to provide a sustained source of NT to the deafened cochlea localised to the organ of Corti for long-term SGN survival. Adenoviral-based NT-gene therapy vectors were injected into the lower basal turn scala media of ototoxically-deafened guinea pigs. The

resulting gene expression profiles, effects on SGN survival and peripheral neurite outgrowth were analyzed after seven and eleven weeks of treatment. Adenoviral vectors injected into the scala media remained localized within this small region, limiting an immunogenic response and allowing for more extended expression than is possible with adenoviral gene therapy in other tissues. After a single NT-gene therapy inoculation there was a significant increase in SGN survival in the basal turn of the cochlea (proximal to the injection site) at both seven weeks (1.3-fold increase) and eleven weeks (1.5-fold increase) post inoculation. These increases were statistically different in comparison to contralateral, non-injected cochleae ( $p < 0.05$ ). This result supports the conclusion that gene therapy can enable sustained SGN protection after deafness, following a single injection of adenoviral vectors into the scala media.

### **827 Correction of Deafness and Vestibular Defects in Usher Syndrome Using Antisense Oligonucleotides**

**Jennifer Lentz**<sup>1</sup>, Francine Jodelka<sup>2</sup>, Anthony Hinrich<sup>2</sup>, Kate McCaffrey<sup>2</sup>, Hamilton Farris<sup>1</sup>, Nicolas Bazan<sup>1</sup>, Dominik Duelli<sup>2</sup>, Frank Rigo<sup>3</sup>, Michelle Hastings<sup>2</sup>

<sup>1</sup>LSU HSC, <sup>2</sup>Rosalind Franklin University of Medicine and Science, <sup>3</sup>Isis Pharmaceuticals

Usher syndrome (Usher) is the leading genetic cause of combined deafness and blindness. It is characterized by sensorineural hearing impairment combined with retinitis pigmentosa, and in some cases, vestibular dysfunction. The only treatment for Usher is the use of prosthetics, such as hearing aids and cochlear implants, and the feasibility of curing deafness at the cellular level is uncertain. A mouse model for Usher has been developed based on the Acadian Usher mutation, in which the USH1C.216G>A mutation (216A) has been knocked into the mouse Ush1c gene. The 216AA mice have profound deafness, vestibular dysfunction and develop retinal degeneration characteristic of Usher patients. The 216A mutation creates a cryptic splice site that is used preferentially over the authentic site and produces a truncated mRNA and protein product. We hypothesize that blocking the cryptic splice site with antisense oligonucleotides (ASOs) will activate the authentic site, rescue protein expression and be therapeutic for mice and ultimately Usher patients. ASO activity was optimized using a cell-free splicing system, an ASO-tiling screen and cell lines isolated from the 216AA mice and an Usher patient with the 216AA mutation. 216AA mice were injected with ASOs and correction of splicing and protein expression was quantitated by rt-pcr and western blot, respectively. Hearing was evaluated by auditory-evoked brainstem response (ABR) analysis. A single systemic treatment of ASOs to neonate 216AA mice corrected splicing and protein expression in the cochlea. ASO-treated mice had no circling behavior characteristic of the 216AA untreated mice and normal auditory-evoked brain stem responses at most frequencies, indicating that they can hear. Our results show that ASOs can effectively block cryptic splicing of the 216A transcript in vivo. These results

suggest the therapeutic potential of ASOs in Usher syndrome and other diseases caused by mutations that disrupt splicing.

### **828 Transtympanically Delivered Steroids Impact Thousands of Inner Ear Genes Over Conventional Systemic Delivery**

**Dennis Trune**<sup>1</sup>, Katherine Delaney<sup>1</sup>, Fran Hausman<sup>1</sup>, Beth Kempton<sup>1</sup>, Carol MacArthur<sup>1</sup>, Dongseok Choi<sup>1</sup>

<sup>1</sup>Oregon Health & Science University

Glucocorticoids are given for sensorineural hearing loss, but little is known of their molecular impact on the inner ear. Although hearing recovery is attributed to their immune suppressive functions, they also affect mineralocorticoid driven processes of ion and water homeostasis. Furthermore, in spite of claims of improved hearing recovery with transtympanic delivery of steroids, no studies have actually documented the inner ear molecular functions enhanced with this delivery method. Therefore, to assess steroid driven processes in the inner ear, gene chip analyses were conducted on mice treated systemically with the glucocorticoids prednisolone (oral) or dexamethasone (subQ), or the mineralocorticoid aldosterone (oral). Other mice were given the same steroids transtympanically. Inner ears were harvested at 6 hours, RNA extracted, and 7-8 samples for each treatment processed on the Affymetrix 430 2.0 Gene Chip for expression of its 34,000 genes. Results were statistically analyzed for up or down expression of each gene against control (untreated) mice. Results showed approximately 17,500 genes are normally expressed in the inner ear and steroids alter expression of 55-82% of these. Dexamethasone changed expression of 9,351 inner ear genes following subQ injection, but 14,285 genes (82%) if given transtympanically. A similar pattern was seen with prednisolone, as 7,718 genes were impacted by oral delivery and 10,279 genes when given transtympanically. The mineralocorticoid aldosterone changed expression of only 261 inner ear genes if given orally, but this increased to 9,580 genes if injected transtympanically. These studies show thousands of inner ear genes are affected by steroids, and this number increases significantly if steroids are delivered transtympanically. Thus, ascribing the efficacy of steroids simply to immunosuppression does not appear to be warranted.

Supported by NIH-NIDCD R01 DC005593 and ARRA Supplement DC005593-S1

### **829 Interactive Workshop on 3D Reconstruction of the Ear**

**Peter Santi**<sup>1</sup>

<sup>1</sup>University of Minnesota

As described in a 2011 Science article (331:712) 3D image acquisition, visualization and analysis are becoming increasingly important in science, medicine and engineering. Its rapid growth is due to recent advancements in 3D instrumentation including optical and magnetic based microscopes that produce a well-aligned z-stack of images. However, this "scientific revolution" as some describe it, is still nascent in spite of the increasing

amounts of volumetric data that are being collected. The purpose of this workshop is to provide the audience with interactive tutorials in tissue processing, z-stack image collection, 3D reconstruction, analysis, and to show specific examples of how volumetric data of the middle and inner ear provide important new information that could not be obtained from 2D data sets. Dr. Bartsch is the keynote speaker and he will provide interactive tutorials showing how to use software tools in an imaging pipeline to prepare and analyze 3D reconstructions of inner ear structures. Shane Johnson will also provide details on tissue processing, structure segmentation, and how to compute length, area, number, and volume of cochlear structures. Dr. Jan Buytaert will show how 3D reconstructions of the middle ear can be used to model functional data using finiteelement analysis. Abderrahmane Hedjoudje will describe development and application of a finite element and neuromorphic computational model of vestibular nerve activation using a vestibular prosthesis. Dr. Alec Salt will show how 3D reconstructions of the guinea pig and human can be used to model drug distribution in the ear. Dr. Benjamin Kopecky will show how genetic defects in mice are qualitatively and quantitatively characterized using 3D reconstructions of cochlear structures. Our goal is to have attendees leave the workshop with a good working knowledge of hardware and software tools necessary to produce 3D reconstructions and the time, capabilities and limitations to produce and analyze volumetric data. Interactive materials will be available for attendees to download before attending the workshop at the following hypertext link:  
<http://www.aro.org/mwm/3dworkshop.html>

### **830 Volumetric Image Processing, Quantitative Analysis, and Visualization of Structures in the Inner Ear**

**Hauke Bartsch<sup>1</sup>**

<sup>1</sup>*UC San Diego, Radiology*

The amount of data produced by imaging has steadily increased over the years. Imaging techniques have moved from 2D microscopy to high resolution volumetric acquisitions with an unprecedented level of detail and minute structural information covering whole organs. In order to extract relevant information and to access the information contained in these scans a 3D processing pipeline is presented that corrects for imaging artifacts, is able to reconstruct complex three dimensional structures, and provides quantitative information about morphology. During an interactive tutorial we will start with a general overview on 3D reconstruction and the technical problems posed by the amount of data to be processed. We will outline some effective visualization techniques including multi-planar reconstructions, volume rendering, and projection views on regions of interest. The presented processing stream includes registrations of serial cross-sections, multi-modal 3D elastic registration, reformatting of volumes based on organ specific curvilinear axis, automatic and manual segmentation, surface

reconstruction, smoothing and the generation of pictures and movies for presentations.

Participants should expect to follow the presentation on their own machines using software such as ImageJ and Amira (Visage Imaging Inc.).

### **831 How to Produce 3D Reconstructions of Cochlear Structures**

**Shane Johnson<sup>1</sup>, Heather Schmitz<sup>1</sup>, Peter Santi<sup>1</sup>**

<sup>1</sup>*University of Minnesota*

How to produce 3D reconstructions of cochlear structures (30 min)

Shane Johnson, Heather Schmitz, and Peter Santi, Department of Otolaryngology, University of Minnesota.

Since the cochlea forms complex spiral shapes with graded, lengthwise function, it is beneficial to visualize its 3D anatomy. One can separate and compare individual structures from/to one another to reveal their shape and quantitative differences. Cellular distributions along their length can be visualized with a color map to reveal differences that were not readily apparent due to their complex 3D geometry. In order to produce 3D reconstructions of the cochlea there are a number of steps that must be followed. I will describe the key elements of those procedures that we have developed for mouse cochleas. The histological steps required for TSLIM imaging are: fixation, decalcification, dehydration, and clearing to transparency. Fluorescent labeling can be performed at any point after decalcification depending on the method used. Fixation quality depends on both the type of fixative and route of administration. Aortic perfusion, followed by perilymphatic perfusion and whole-cochlea immersion fixation produces optimal morphology. Paraformaldehyde produces good fixation with little autofluorescence. A combination fixative of paraformaldehyde and glutaraldehyde produces excellent fixation quality and a high level of autofluorescence, which may be suitable for TSLIM imaging, but hinders the use of some immunohistochemical labeling. In order to isolate cochlear structures, a process called segmentation is used. Segmentation requires the color outlining of each cochlear structure in every section. Software tools will be described that make this process less labor intensive and more accurate. After segmentation, 3D isosurface reconstructions are smoothed and their morphometry is determined by the Amira program. The length of segmented structures can be estimated by determining the centroid of a structure and fitting a B-spline curve to it. Using the centroid, the structure can then be virtually resectioned to produce true, cross-sectional area measurements along its length. Segmented structures can be isolated by a simple masking process that allows one to volume render and computationally estimate cell number/density within structures such as Rosenthal's Canal and the organ of Corti. Specific labeling of certain cell types (e.g., outer hair cells with an anti-prestin antibody) and organelles (e.g., nuclei with a DNA label) allow one to automatically determine their number and location within a cochlea.

### **832 Detailed Anatomy of the Inner Ear as the Basis for Modeling Drug Distribution in Guinea Pigs and Humans**

Alec N. Salt<sup>1</sup>, Ruth M. Gill<sup>1</sup>

<sup>1</sup>Washington University School of Medicine

Our interest in the 3D anatomy of the inner ear has been driven by a desire to understand how cochlear fluids are maintained and how applied drugs and other substances are distributed in the ear. Even though the ear is an anatomically tiny structure, applied drugs spread extremely slowly because spread is dominated by passive diffusion. This can result in large concentration gradients between different parts of the ear. Interpretations of drug measurement data therefore typically require some form of computer simulation. Previous simulations have been based on the dimensions of the cochlear scalae, incorporating changes in scala cross section with distance along the cochlea. However, drugs do not remain confined to the fluid filled scalae of the ear but also have access to tissue-filled spaces such as the spiral ligament and spiral ganglion. For this reason, we have reconstructed in 3D all the major fluid and tissue compartments of the cochlea and of the vestibular system. This was performed using Amira software to analyze OPFOS image sets of guinea pig and human ears. Analysis of these compartments showed, for example, that the spiral ligament has a volume considerably larger than expected based on radial histologic sections. This is because the spiral ligament follows a wider spiral than the cochlea fluids and is therefore substantially longer. Spiral ligament volume derived from 3D reconstructions was 3.2  $\mu$ L in guinea pigs and 15.4  $\mu$ L in the human, which corresponds to 54% and 39% of the scala tympani volume respectively. These anatomical data have been incorporated into a simulation program (available for download at <http://oto.wustl.edu/cochlea>). Our current understanding of inner ear fluid physiology is now increasingly based on detailed, 3D anatomic studies of the ear.

This work supported by NIH Grant DC01368

### **833 How to Use 3D Models for Functional Analysis Using the Finite-Element Method**

Jan Buytaert<sup>1</sup>, Johan Aerts<sup>1</sup>, Joris Dirckx<sup>1</sup>

<sup>1</sup>University of Antwerp - Laboratory of BioMedical Physics

Techniques like HROPFOS, TSLIM or  $\mu$ CT generate data stacks of registered serial sections. After segmentation and triangulation using the Amira software package, 3D surface models of the relevant structures are obtained.

Finite-element computer modeling (FEM) has become an established numerical technique to simulate and understand middle ear mechanics. FEM calculations require 3D computer models consisting of a finite number of volume elements, for instance tetrahedrons or hexahedrons, as input.

Step-by-step we will demonstrate how to generate 3D volume models from Amira surface models. The resulting volume models have to fulfill certain conditions and pass several quality checks before they can be used in FEM. Finally, a finite element analysis on a simple middle ear

system using freeware software will be shown to illustrate the useful application of 3D modeling in the functional analysis of middle ear mechanics.

### **834 Virtual Labyrinth Model Accurately Predicts Responses to Stimulation Using a Multichannel Vestibular Prosthesis in Rhesus Monkeys**

Abderrahmane Hedjoudje<sup>1</sup>, Russell Hayden<sup>2</sup>, Chenkai Dai<sup>1</sup>, JoongHo Ahn<sup>1</sup>, Mehdi A. Rahman<sup>2</sup>, Manu Ben Johny<sup>2</sup>, Kevin Olds<sup>2</sup>, Susumu Mori<sup>3</sup>, Charles Della Santina<sup>1,2</sup>

<sup>1</sup>Department of Otolaryngology - Head & Neck Surgery, Johns Hopkins School of Medicine, <sup>2</sup>Department of Biomedical Engineering, Johns Hopkins School of Medicine, <sup>3</sup>Department of Radiology, Johns Hopkins School of Medicine

To facilitate design of multichannel vestibular prostheses that can restore sensation to individuals without vestibular hair cell function, we created a Virtual Labyrinth model of the rhesus labyrinth. Because the geometry and electrical properties of the implanted ear are complex, accurately modeling effects of prosthetic stimuli on vestibular afferent activity requires a detailed representation of labyrinthine anatomy. Model geometry was generated through 3-dimensional (3D) reconstruction of a normal rhesus microMRI acquired with 48  $\mu$ m voxels. Virtual electrodes were positioned within this geometry based on anatomic landmarks and CT scans of implanted animals, and the extracellular potential field during a current pulse was computed using finite element methods. Potential fields then served as inputs to stochastic, nonlinear dynamic models for each of 2415 vestibular afferent axons with spiking dynamics based on a modified Smith and Goldberg model incorporating parameters that varied with fiber location in the neuroepithelium. A well-validated model of myelinated fibers implemented action potential propagation.

We tested the model by comparing predicted and actual 3D angular vestibulo-ocular reflex axes of eye rotation elicited by prosthetic stimuli. Actual responses were measured using 3D scleral coil oculography. The model was individualized for each animal by placing virtual electrodes based on CT localization of real implanted electrodes. 3D eye rotation axes were predicted from the relative proportion of model axons excited within each of the three ampullary nerves.

Multiple features measured empirically were observed as emergent properties of the model, including effects of active and return electrode position, stimulus amplitude and pulse waveform shape on target fiber recruitment and stimulation selectivity. Extension of the model to human anatomy should facilitate optimal design of electrode arrays for clinical application.

Supported by NIDCD R01DC9255

### **835 Genetic Defects Influence Three Dimensional Development of the Inner Ear**

**Benjamin Kopecky<sup>1</sup>, Peter Santi<sup>2</sup>, Shane Johnson<sup>2</sup>, Heather Schmitz<sup>2</sup>, Bernd Fritsch<sup>1</sup>**

<sup>1</sup>University of Iowa, <sup>2</sup>University of Minnesota

The inner ear begins as a flat epithelia that undergoes a highly complex morphogenesis driven by a cornucopia of genes to form a functional three dimensional (3D) organ consisting of six distinct sensory epithelia each in its own unique recess. When a given gene is manipulated, the change can result in the disruption of ear development which can be analyzed to gain insights into the importance of this gene and the specific mechanism through which it acts. Until recently, the analyses of genetic defects were restricted to two dimensions. With the advent of the 3D age, imaging, reconstruction, and analysis are proving not only accessible and inexpensive, but are yielding new insights about ear development of mutations through more precise size quantification and 3D visualization. Imaging of mutants using advanced 3D techniques show the influence of the genetic defect on the 3D development of the inner ear including aberrant histologic differentiation. We will discuss the use of TSLIM in analyzing both normal ears during development as well as a number of unique adult mutants including Pax2-Cre::N-Myc<sup>ff</sup> and Pax2-Cre::Atoh1 <sup>ff</sup> mice illustrating the technical advances of modern 3D imaging for the complete histologic and morphologic analysis of ears in unprecedented detail.

### **836 Current Theories About the Generation of Otoacoustic Emissions and the Clinical Implications**

**Brenda Lonsbury-Martin<sup>1,2</sup>, M. Patrick Feeney<sup>3,4</sup>**

<sup>1</sup>Department of Otolaryngology--Head & Neck Surgery Loma Linda University Medical Center, <sup>2</sup>Division of Research Service VA Loma Linda Healthcare System Loma Linda CA, <sup>3</sup>VA RR&D National Center for Rehabilitative Auditory Research, Portland, OR, <sup>4</sup>Oregon Health and Science University, Portland, OR

The study of otoacoustic emissions (OAEs) has shown that they represent powerful experimental indices of outer hair cell activity as well as useful clinical measures of the intactness of cochlear function. Although OAEs, and particularly transient-evoked OAEs (TEOAEs), have become an important screening method for identifying newborn hearing impairment, one disappointment in their clinical application has been the failure of either TEOAEs or distortion-product OAEs (DPOAEs) to accurately predict the configuration of the clinical audiogram. Since their discovery, an important research interest has been in determining how emissions are generated within the organ of Corti. Early investigators introduced the original notion that OAEs consist of a combination of two emission sources in the form of the generator or distortion constituent and the reflection component. The prevailing view today is consistent with a two-source model with OAEs arising from two locations along the basilar membrane that are associated with distinct mechanisms of generation. According to this reasoning, for DPOAEs, for example, the distortion component arises from the

nonlinear interactions between the f1 and f2 primary tones, while the reflection element originates from the DPOAE frequency place. However, the possibility of DPOAE components arising across a broader region more basal to the primary tones, i.e., significantly above f2, has not typically been addressed in this established formulation. The presentations of this session review our current knowledge about the origins of OAEs and address how a better understanding of these sources may lead to improved estimates of clinical hearing using emissions. Symposium attendees who should benefit from these timely views include researchers in the emissions and cochlear modeling fields, along with practitioners interested in the diagnosis and habilitation of hearing problems.

### **837 Thirty-Plus Years of Uncertainty About OAE Generation. How Weird Is That?**

**David Kemp<sup>1</sup>**

<sup>1</sup>UCL Ear Institute

When in 1970 an extreme case of what we now call spontaneous otoacoustic emission was investigated clinically the source seemed obvious - it could only be a whistling of turbulent blood flow in the stapedial artery! When in 1978 sound evoked OAEs were confirmed other 'obvious' sources were proposed such as middle ear muscle oscillations and nerve-to-mechanical transduction. It was the careful analysis of the detailed biophysical properties of OAEs that constrained speculative hypotheses and pointed to a then-unknown source intimately associated with cochlear function. The discovery of fast outer hair cell motility in 1983 appeared to explain the biological source of OAEs but it left us with a more challenging question- 'What is the function of OHC motility?'- a question which remains topical.

But it wasn't just the cochlear driving force of OAEs that needed explaining. The physical mechanism of sound energy transmission back to the ear canal posed serious problems for cochlear theorists. How could forces generated inside OHCs get back to the ear canal? There was no shortage of ideas about ways it could happen. The problem was and is that the data we have isn't sufficient to be sure which route or mechanism dominates where and when. Does that matter? Yes, because it challenges our understanding of the intricacies of the coupling between outer hair cells, the organ of Corti, tectorial and basilar membranes, the cochlear fluid, and the middle ear, i.e. the very operation of the cochlea.

The reason questions about OAE generation have persisted for more than 30 years is that OAEs originate in the subtlest features of cochlear biophysics and physiology some of which are yet to be discovered or understood. Will a better understanding of OAEs answer current problems in cochlear biophysics and physiology? Will it advance diagnostic audiology? There's a chance it will, and for that reason we must continue to scrutinise and debate all of the evidence in minute detail.

### **838 Mechanisms of OAE Generation: FAQs and Fancy**

**Christopher A. Shera**<sup>1,2</sup>

<sup>1</sup>*Eaton-Peabody Laboratories*, <sup>2</sup>*Harvard Medical School*

Otoacoustic emissions (OAEs) are thought to be mixtures arising from at least two fundamentally different mechanisms within the cochlea. This presentation reviews current understanding of OAE source mechanisms. Questions to be addressed include: What is the evidence for different source types? What are the properties of the different sources? Where are they located? What is the evidence for mixing? How do reverse waves propagate in the cochlea? What determines OAE delay? Do OAE source types differ between the basal and apical regions of the cochlea? Do source types differ across species? When current knowledge appears fuzzy or unclear, the discussion may deviate from the factual.

### **839 Distributed Sources of Otoacoustic Emissions**

**Stephen Neely**<sup>1</sup>

<sup>1</sup>*Boys Town Natl. Res. Hosp.*

Some observations of otoacoustic emissions (OAE) are difficult to reconcile with prevailing models that attribute OAE generation to distinct locations within the cochlea. For example, inverse Fourier-transforms of distortion-product OAEs show several distinct peaks with latencies that are relatively invariant with stimulus level. One model of stimulus-frequency OAEs based on coherent reflection showed best agreement with measurements when contributions include locations both near and far from the characteristic place for the stimulus frequency. Such observations suggest that sources of OAEs may sometimes originate from widely distributed locations within the cochlea.

### **840 An Inconvenient Truth: Significant DPOAE Components Are Generated Basal to F<sub>2</sub>**

**Barden Stagner**<sup>1</sup>, **Brenda Lonsbury-Martin**<sup>1,2</sup>, **Glen Martin**<sup>1,2</sup>

<sup>1</sup>*VA Loma Linda Healthcare System*, <sup>2</sup>*Dept of Otolaryngology, Loma Linda University Medical Center*

Earlier studies in our laboratory described suppression of DPOAEs by a third or interference tone (IT) in a variety of species including rabbits and humans. Unexpectedly, we found suppression and/or enhancement of measured DPOAE levels, when ITs were presented up to several octaves above the  $f_2$  frequency. Previous attempts at explaining these phenomena involved harmonics of the primaries interacting with either  $f_1$  or  $f_2$ , or the IT itself producing components via a complex 'catalyst' route that mixed with the measured DPOAE. Our more recent work has discounted these two notions in favor of a distributed components hypothesis whereby many DPOAE components are generated in amounts roughly proportional to the amount of overlap of the  $f_1$  and  $f_2$  traveling wave tails basal to the  $f_2$  primary frequency place. Supporting evidence for substantial basally-distributed

components will be presented. The properties of these basal components contradict the common assumption that DPOAEs associated with steep or shallow phase slopes are unique signatures for reflection emissions arising from the DPOAE frequency place or distortion emissions generated near  $f_2$ , respectively. Finally, an 'augmented' DP-gram procedure which uses an IT to remove these basally-distributed components will be described that promises to greatly improve both the signal-to-noise ratio and frequency specificity of the DP-gram.

### **841 DPOAE Source Knowledge and Its Impact on Clinical Utility**

**Sumitrajit Dhar**<sup>1</sup>, **Jonathan Siegel**<sup>1</sup>, **Jungmee Lee**<sup>1</sup>, **Gayla Poling**<sup>1</sup>, **Jungwha Lee**<sup>1</sup>

<sup>1</sup>*Northwestern University*

Distortion product otoacoustic emissions (DPOAEs) recorded in the ear canal are composites of multiple components arising from different parts of the cochlea. Differences in phase behavior between these components have been modeled to represent differences in the mechanical basis of their generation. The presence of multiple components in the ear canal recording, along with the differences in their source location and behavior, complicate the clinic utility and interpretation of DPOAEs. For example, the interaction between components with differing phase characteristics often results in a pattern of semi-periodic peaks and valleys in DPOAE level and phase, known as fine structure. The presentation will review evidence examining the influence of DPOAE fine structure and DPOAE source knowledge in both laboratory-oriented and clinic-oriented studies from the literature. Results from recent experiments probing the influence of DPOAE components and fine structure on their utility as a clinical tool, sensitive to small changes in cochlear function, will be reported. [Supported by the NIDCD and Northwestern University]

### **842 Usefulness of Source Knowledge for Detecting Ototoxicity Using DPOAEs**

**Dawn Konrad-Martin**<sup>1,2</sup>, **Peter Jacobs**<sup>1</sup>, **Garnett Mcmillan**<sup>1</sup>, **Kelly Reavis**<sup>1</sup>, **Marilyn Dille**<sup>1,2</sup>

<sup>1</sup>*Portland VA Medical Center, VA RR&D National Center for Rehabilitative Auditory Research*, <sup>2</sup>*Oregon Health & Science University, Department of Otolaryngology/Head & Neck Surgery*

Cisplatin is an effective chemotherapeutic agent that is dose-limited by ototoxic hearing loss. Monitoring changes in distortion-product otoacoustic emissions (DPOAEs) is an important clinical option for cisplatin ototoxicity screening because patients are often too ill to complete a reliable behavioral hearing test. However, DPOAEs sometimes fail to accurately reflect changes in the audiogram from cisplatin, presumably in part because they are mixtures of multiple source components. This presentation will describe results from recent experiments in which we investigate fine-frequency-resolution DPOAE level measurements for total and un-mixed DPOAEs obtained before, during and after cisplatin administration. [Supported by the VA RR&D Service.]

### **843 Analysis of Click-Evoked Auditory Brainstem Responses Using Time Domain Cross-Correlations Between Interleaved Responses**

**Erik Berninger**<sup>1</sup>, Åke Olofsson<sup>2</sup>, Arne Leijon<sup>3</sup>

<sup>1</sup>Dept of Audiology, Karolinska University Hospital, Karolinska Institutet, Stockholm, Sweden, <sup>2</sup>Technical and Experimental Audiology, Department of CLINTEC, Karolinska Institutet, <sup>3</sup>School of Electrical Engineering, Sound and Image Processing Lab, KTH Royal Institute of Technology

Click-evoked auditory brainstem responses (ABRs) were recorded in a wide range of stimulus levels in order to study various forms of signal analysis, e.g., time domain cross-correlation analysis of interleaved responses. Fourteen healthy normal hearing subjects (18-35 yrs, 50% females) without any history of noise exposure participated in this study. They all had pure-tone thresholds better than 20 dB HL (125-8,000 Hz). ABRs were recorded in both ears using 100 µs rarefaction clicks in 10 dB steps, from 71.5 dB nHL down to -18.5 dB nHL (ISO 389-6), at a stimulus repetition rate of 39 Hz (analysis time window, 15 ms). All the responses were band-pass filtered between 30 and 8,000 Hz. The number of sweeps increased with decreasing stimulus level, from 2,000 sweeps at 71.5 dB nHL, up to 30,000 sweeps at -18.5 dB nHL. Each sweep was stored in a database for off-line analysis. Cross-correlation analysis between two sub-averages was performed in the time domain for non-filtered and digitally band-pass filtered (300-1500 Hz) responses for the entire signal and analysis time windows of 1-11 ms and 5-11 ms. Psychoacoustical click thresholds (PCTs) were measured using a Békésy technique with the same insert phone and stimulus as used for the ABR-recordings (repetition rate, 20 Hz). Results revealed mean cross-correlation coefficients exceeding 0.90 in both ears at stimulus levels  $\geq 11.5$  dB nHL for the entire non-filtered ABR. At 1.5 dB nHL, the corresponding mean(SD) cross-correlation coefficient was 0.53(0.32) and 0.44(0.40) for left and right ears, respectively (n=14). In comparison, mean(SD) PCT was -1.9(2.9) and -2.5(3.2) dB nHL for left and right ears, respectively (n=14). Numerically, the cross-correlation coefficient decreased with decreasing analysis time, and use of band-pass filtering. In conclusion, time domain cross-correlation analysis of ABR might form the basis for automatic response identification and future threshold seeking procedures.

### **844 Accuracy of the Auditory Brainstem Response as a Measure of Conductive Hearing Loss**

**Evan Hill**<sup>1</sup>, Gimseong Koay<sup>1</sup>, Henry Heffner<sup>1</sup>

<sup>1</sup>University of Toledo

The purpose of this study was to determine how closely the auditory brainstem response (ABR) can estimate the behavioral threshold shift caused by an obstruction of the external auditory canal (i.e., a conductive hearing loss). Behavioral and ABR thresholds were obtained within a few

minutes of each other in five human observers for clicks and tones (0.5, 2, and 8 kHz) to determine the threshold shift caused by an earplug. The results showed that the tonal ABR estimated the pure-tone behavioral threshold shift to within  $\pm 5$  dB 53% of the time, and no errors were larger than 15 dB. On the other hand, the click ABR always estimated the behavioral threshold shift for clicks to within  $\pm 5$  dB. Interestingly, the ABR was able to estimate the average threshold shift of the five subjects for each stimulus to within 5 dB indicating that it may be a reliable measure of group results. With regard to absolute thresholds, the ABR was surprisingly accurate in estimating the behavioral thresholds for the broad-spectrum click train, although not for the pure tones.

### **845 Relationship Between Hearing Threshold and Status of Tympanic Membrane**

**II-WOO LEE**<sup>1</sup>, Duk-Gyu Lee<sup>1</sup>, Soo-Keun Kong<sup>2</sup>, Sung-Hwan Park<sup>2</sup>

<sup>1</sup>Pusan National University Yangsan Hospital, <sup>2</sup>Pusan National University Hospital

Backgrounds and objectives: Status of tympanic membrane(TM) other than perforation can affect the hearing threshold. Such status may be tympanosclerosis, aging of the TM, simple thickening of the TM. The purpose of this study is to evaluate the effect of intact TM to the hearing threshold according to the frequency.

Materials and Methods: We choose the subjects from the outpatient clinic at random. Exclusion criteria were the TM with perforation and definite evidence of ossicular abnormality. We analyzed the endoscopic findings of the TM with Image J program. Gray scales of TM at cone of light, pars flaccida, pars tensa and where there is tympanosclerotic plaque. The numeric data from the Image J program were compared and analysed with the hearing threshold of pure tone audiogram and distortion production otoacoustic emissions according to the frequency.

Results: The hearing threshold increased as the numeric value of gray scale increases, which means the sclerotic TM could affect the hearing threshold minutely.

Conclusions: Delicate changes of TM might be a cause of hearing loss. Further study may be necessary on the objective method to detect this change which could be a useful diagnostic tool

### **846 Quick Gap Detection Test**

**Robert Chambers**<sup>1</sup>, Isaac Maro<sup>2</sup>, Benjamin Jastrzembski<sup>3</sup>, Stephanie Nagle<sup>4</sup>, Ndeserua Moshi<sup>2</sup>, Odile Clavier<sup>1</sup>, Robert Kline-Schoder<sup>1</sup>, Frank Musiek<sup>5</sup>, **Jay Buckley**<sup>6</sup>

<sup>1</sup>Creare, Inc., <sup>2</sup>Muhimbili University of Health and Allied Sciences, <sup>3</sup>Harvard Medical School, <sup>4</sup>Towson University, <sup>5</sup>University of Connecticut, <sup>6</sup>Dartmouth Medical School

We are currently investigating the nature of the hearing loss associated with HIV infection in a large cohort of HIV positive individuals in Dar es Salaam Tanzania. Part of this assessment includes a measure of central processing using a gap detection test. Performing a gap detection test in this setting is challenging, since it must be short and training time is limited. Initially, we used an adaptive dual-staircase gap detection algorithm. Experience in the field

showed that this test produced unreliable results, and that some subjects could not complete the test despite multiple attempts. Based on our experience, we developed a shorter adaptive single-staircase algorithm. The test presents a 4.5 second burst of white noise, with a gap placed randomly within the middle 2.5 seconds of the presentation. The random gap placement eliminates the need for no-gap presentations, which were present in the previous version to verify that subjects were performing the test correctly. For training, subjects are presented sample gap presentations and trained to press a button when they hear the gap. They are also instructed that they may not hear a gap. The test starts at gap durations of 20 msec. The reductions in gap duration become smaller as the gaps get shorter. Once the test reaches the subject's threshold, the test continues until 10 reversals are recorded. We compared the average gap duration in 139 mostly HIV+ subjects who used both gap detection approaches. The average gap detection threshold with the new gap test was 6.2 msec, compared to 12.4 msec for the previous test ( $p < 0.0001$ ). Time to complete the test fell from 6.1 to 4.9 minutes. The single-staircase uses 31% fewer presentations. The measured gap detection thresholds have roughly 50% the dispersion as the double-staircase test. Test-retest data are being collected. This test shows promise for collecting data on central processing in a challenging environment, although further validation is needed.

#### **847 Auditory Steady State Response in Pediatric Patients with Functional Hearing Loss**

**Kikuko Naka**<sup>1</sup>, Shin Kariya<sup>2</sup>, Haruka Hirai<sup>2</sup>, Aya Murai<sup>2</sup>, Kazunori Nishizaki<sup>2</sup>

<sup>1</sup>*Fukuyama City Hospital*, <sup>2</sup>*Okayama University*

Functional hearing loss is a common condition especially in children that is found in an audiometric evaluation but unexplained by an organic disorder. The term "functional hearing loss" is synonymous with non-organic hearing loss and pseudohypacusis. Results of clinical or audiometric examination are not consistent in functional hearing loss. Several examinations including speech audiometry and auditory brainstem response have been reported to detect functional hearing loss. Because auditory steady state responses has the ability to confirm the frequency-specific and ear-specific hearing thresholds in a short examination time, auditory steady state responses is an useful tool in the assessment of hearing thresholds in children of all ages. This study was conducted to evaluate the clinical utility of high-frequency auditory steady state responses to multiple simultaneous stimuli for hearing evaluation in children with functional hearing loss.

Sixteen patients (24 ears) with functional hearing loss (mean age, 9.9 years) and 17 patients (24 ears) with sensorineural hearing loss (mean age, 9.5 years) were examined by pure-tone audiometry and auditory steady state responses.

In patients with functional hearing loss, pure-tone audiometry thresholds and auditory steady state responses thresholds differed significantly, and were not

significantly correlated at all carrier frequencies. In contrast, patients with sensorineural hearing loss showed no statistically significant difference between pure-tone audiometry thresholds and auditory steady state responses thresholds. Auditory steady state responses thresholds were significantly correlated with pure-tone audiometry thresholds at all carrier frequencies in sensorineural hearing loss.

These results suggest that auditory steady state responses may have an important role in the assessment of auditory function, particularly at low frequencies in patients with functional hearing loss.

#### **848 Results and Analysis of Newborn Hearing Screening Tests in South Korea**

**Su-Kyoung Park**<sup>1</sup>

<sup>1</sup>*Kangnam Sacred Heart Hospital Hallym university College of medicine*

**Background:** In South Korea, newborn hearing screening (NHS) began at private women's hospitals since mid-90's. Since 2006, nationwide survey and sample study were started. The aim of this study is to investigate the results and effectiveness of NHS in the national pilot projects, from 2007 to 2011.

**Methods:** In order to launch a nationwide program, a step wise approach was performed. First, we investigate the incidence of newborn hearing loss (HL) via a nationwide sample survey in 2006 year. In 2007 to 2008, the 1st and 2nd national exhibition NHS project was implemented. The 3rd national NHS project for low income babies have been conducted in all area from 2009 through 2011 year. From 2009, we adopted a coupon system to solve these problems. A free coupon is issued to pregnant women at the public health centers. The coupon consists of two parts, screening test and confirming test with same ID number. Collected coupons from each institute were sent to the Ministry of Health and Welfare to get reimbursement. By analyzing coupons, a tracking of baby will be possible.

**Results:** Regarding the screening method, 77% of all institute used AABR and 23% used (A)OAE. The refer rate was 2.8% in 2007, 2.4% in 2008, 1.3% in 2009 and 1.2% in 2010. The incidence of hearing loss (HL) including unilateral HL over 40dB was 0.18% in 2007, 0.65% in 2008, 0.27% in 2009 and 0.40% in 2010.

**Conclusion:** For the past 4 years, overall refer rate was 1.7% and average HL rate of newborns was 0.51%, which was corrected by ABR performing rate of the refer babies. We organized expert group for NHS, produced clinical guideline of NHS and hand out education materials for screening staffs and parents on related hospitals and public health centers.

## **849** Auditory Training and Mechanisms of Benefit: Identification of Appropriate Outcome Measures

Helen Henshaw<sup>1</sup>, Melanie Ferguson<sup>1</sup>, Daniel Clark<sup>1</sup>, Holly Thomas<sup>1</sup>, David Moore<sup>1</sup>

<sup>1</sup>NIHR National Biomedical Research Unit in Hearing

When designing a complex intervention it is important that the outcome measures adopted are both appropriate for, and sensitive to, the effects of that intervention. If auditory training (AT) in people with hearing loss (PHL) is to be an effective clinical intervention, any task-specific learning needs to transfer to functional benefits in real-world listening situations.

A randomised controlled trial (RCT) of 44 adults with mild sensorineural hearing loss (SNHL) trained on a phoneme in quiet discrimination task. Participants showed significant post-training improvements in hearing disability, with the largest improvement in the most challenging listening situation. There were no significant improvements for speech intelligibility in modulated noise, nor for simple cognitive tasks. There were significant post-training improvements identified for complex measures of cognition (divided attention and visual working memory), in the trained group but not for the control group, although between-group differences just missed statistical significance. These findings suggest that the outcome measures to assess AT benefits need to be appropriately challenging and sensitive to the effects of training. Furthermore, the development of cognitive skills may be as important as the development of sensory processing.

A follow-up study aims to identify optimal outcomes to assess benefits of AT for in people with mild-moderate SNHL. Hearing aid users trained on a phoneme in noise discrimination task, thereby increasing both task difficulty and content validity. Complex cognitive measures of divided and sustained attention, working memory and listening effort were assessed pre and post-training. Functional benefit of everyday listening was examined using an adaptive two-competing speaker task, which requires greater cognitive effort than speech intelligibility in modulated noise. Findings from this study will inform appropriate outcomes to assess benefit for PHL in future training RCTs.

## **850** Interrelationship Between Physiological and Behavioral Measures of Auditory Function

Jungmee Lee<sup>1</sup>, Sumitrajit Dhar<sup>1</sup>, Jungwha Lee<sup>1</sup>, Steve Zecker<sup>1</sup>, Jonathan Siegel<sup>1</sup>

<sup>1</sup>Northwestern Univ.

Attempts to quantify the relationships between various physiological and behavioral measures of auditory function abound in the literature. The absence of strong relationships in these attempts is often blamed on inaccuracies inherent in the underlying measures. Recent advances in calibration techniques have allowed significant improvements in estimating sound pressure levels delivered to the eardrum. Hearing thresholds and DPOAEs were measured in 352 human subjects (10–65 yrs) using

depth-compensated ear simulator calibration. Hearing thresholds between 0.25 and 20 kHz were measured using a modified Békésy procedure. DPOAEs between 0.75 and 20 kHz (f2 frequency range) were recorded using a stimulus-frequency ratio (f2/f1) of 1.22, and stimulus-level combinations of 55/40, 65/55, and 75/75 dB SPL. Subjects also completed standard self-report questionnaires [Hearing Handicap Inventory for Adults (HHIA) and Self Assessment of Communication (SAC)], speech in noise tests [Quick Speech in Noise (QuickSIN) and Hearing in Noise Test (HINT)], and a custom questionnaire where subjects reported their difficulty hearing and hearing in noise on a 10-point scale. Principal component analyses (PCA) with oblique rotation were performed to explore (i) the dimensions of the behavioral hearing thresholds and DPOAEs at different frequencies and stimulus levels, and (ii) the dimensions of the self-report questionnaires and speech-in-noise tests. The factors extracted from the questionnaires and speech in noise tests were regressed against those extracted from DPOAEs and hearing thresholds. The goal was to find the optimal predictive model for one of the measures when all other measures were used as predictor variables. The results of these detailed statistical models will be reported. The outcome of the modeling exercise will further our knowledge about the physiological variables driving auditory behavior. [Research supported by NIDCD R01 DC008420 and Northwestern University]

## **851** Electrophysiological Assessment of Auditory Temporal Processing in CI Listeners

See Youn Kwon<sup>1,2</sup>, Il Joon Moon<sup>3</sup>, Ha-Young Byun<sup>1</sup>, Hee Sung Park<sup>1,2</sup>, Eun Yeon Kim<sup>1</sup>, Sun Hwa Jin<sup>2,4</sup>, Won-Ho Chung<sup>1</sup>, Yang-Sun Cho<sup>1</sup>, Sung Hwa Hong<sup>1</sup>

<sup>1</sup>Department of Otorhinolaryngology, Sungkyunkwan University School of Medicine, Samsung Medical Center,

<sup>2</sup>Hearing Laboratory, Department of Otorhinolaryngology, Samsung Medical Center, Seoul, KOREA, <sup>3</sup>Samsung Medical Center, Sungkyunkwan University, School of Medicine, <sup>4</sup>Department of Clinical Trial Center, Samsung Medical Center, Seoul, KOREA

The ability to detect temporal gap in noise is a one of the well-known method in psychoacoustics for measuring auditory temporal processes (Moore et al., 1997 & Phillips et al., 1999). Previous our study (Moon et al, 2011 ARO midwinter meeting) has shown that electrophysiological change response was recorded with temporal gap stimuli in normal young adults. The present study has two purposes: 1) to determine whether electrophysiological change responses could be elicited by ongoing temporal gap in CI listener, 2) to investigate temporal gap detection ability in CI listener was how correlate with speech performance. 7 CI subjects participated in this study. Broadband-white gap noises were 2 sec in duration and a various temporal gaps were produced after 1 sec for electrophysiologic test. The ability to behaviorally detect temporal gap was measured using a 3-interval, 3-alternative forced-choice paradigm. Cortical P1-N1-P2 responses were recorded using Neuroscan(Biologic) to stimulus onset (onset P1-N1-P2) and temporal gap

(changed P1-N1-P2). Results showed: 1) changed P1-N1-P2 response was increased as a function of gap duration and good agreement with behavioral gap detection threshold, and 2) gap detection ability in CI listener was significant correlated with speech performance (phoneme identification,  $r=-0.98$ ,  $p=0.004$ ; sentence repetition,  $r=-0.86$ ,  $p=0.02$ ). The electrophysiological method provides useful objective measures for studying auditory cortical temporal processing in CI listeners. The electrophysiological test procedure has potential clinical applications not only to determine the auditory temporal resolution in CI user who have difficulty in behavioral response but also to predictive of their future speech perception and localization. [Work supported by a grand 10031764 from STDP of MKE, a grant of Seoul R&D Program (SS100022), part of this study was presented at APSCI 2011]

### **852** Hearing in Women Following Menopause

**Johan Svedbrant**<sup>1</sup>, Rusana Simonoska<sup>2</sup>, Christina Hederstierna<sup>3</sup>, Malou Hultcrantz<sup>2</sup>

<sup>1</sup>Clintec, Dept ENT, Karolinska Univ Hosp, and Skövde Hospital, Sweden, <sup>2</sup>Clintec, Dept ENT, Karolinska Univ Hosp, Sweden, <sup>3</sup>Clintec, Dept Hearing and Balance, Karolinska Univ Hosp, Sweden

#### BACKGROUND:

Epidemiological studies have shown that women have better high-frequency hearing thresholds than men and that age-related hearing loss do not start until after the age of 50 in women, but already after 30 in men. This coincides with the menopausal transition in most women, thus leading us to hypothesize that the menopause triggers auditory deterioration. This can possibly be due to reduced levels of endogenous estrogens, which are known to have protective effects on neurons.

#### METHODS:

Seventy women with a mean age of 51 years at baseline, were tested with blood samples (cortisol, cholesterol and sex hormone levels) together with deep interviews and final menstrual period (FMP). Pure tone audiometry was tested measuring pure tones for frequencies 125-8000Hz with air and bone conduction, and a questionnaire concerning hearing was filled out by all women individually. The same tests were performed at 2 and 7 years follow up. The present study report the 10 year follow up. Hearing decline at each frequency was calculated after 10 years and compared to baseline.

#### RESULTS:

Hearing decline during the menopause period is reported and after 10 years all women had all passed the FMP. Hearing decline longitudinally will be discussed and results will be reported in relation to answers from questionnaires and blood samples.

### **853** Does Estrogen Substitution Affect the Hearing in Girls with Turner Syndrome?

**Asa Bonnard**<sup>1,2</sup>, Malou Hultcrantz<sup>1,2</sup>, Rusana Simonoska<sup>1,2</sup>

<sup>1</sup>CLINTEC, Karolinska Institutet, <sup>2</sup>ENT-clinic, Karolinska University Hospital

Objective: Women hear better than men of the same age but the difference diminish during menopause simultaneously with the change of estrogen levels. Hormone replacement therapy has shown a tendency to sustain a better hearing in postmenopausal women. In Turner syndrome (TS), where the women are biologically estrogen deficient due to lack of or non producing ovaries, there are two different types of hearing problems, the genetic "dip" around 1,5 kHz and the early presbycusis. The presbycusis will appear as early as 25-30 years of age and the need of hearing aid is common. Since the early 80's young girls with TS in Sweden has been treated with Growth hormone to enhance their length and Estrogen to induce puberty. The question is if the estrogen treatment may also improve their hearing?

Materials and methods: 25 women with Turner syndrome between the ages of 25-35 years treated with estrogen since the age of 13 has been selected and age matched with now older women of a cohort of Turner females who were not estrogen substituted. Their medical ear history was obtained from the medical charts as was their karyotypes. The younger cohort were tested with actual audiograms, air and bone conduction with frequencies ranging from 0,25 to 8 kHz. These have been compared statistically with the audiograms from the older cohort at the same age.

Results: No statistical difference has been shown. Further results will be discussed.

Conclusion: The early presbycusis is probably a result of multiple factors where the lack of estrogen is one. Compared to girls with normal estrogen producing ovaries, i.e. an estrogen production already in the preadolescence period, the Turner girls might have their estrogen substitution too late for a good hearing result.

### **854** High Levels of Emotional Exhaustion Induce Hyperacusis After Acute Stress

**Dan Hasson**<sup>1,2</sup>, Martin Benka Wallén<sup>1</sup>, Töres Theorell<sup>2</sup>, Barbara Canlon<sup>1</sup>

<sup>1</sup>Karolinska Institutet, <sup>2</sup>Stress Research Institute at Stockholm University

There is a well-established relationship between stress and hearing problems yet despite increasing evidence, causality is not well-established. Acute stress seems to be protective in experimental animal studies, but has not yet been directly demonstrated in humans. The present study used subjective and objective measures of hearing (PTA and ULL uncomfortable loudness), as well as subjective ratings of emotional exhaustion (EE) using the Oldenburg burnout inventory before and after an acute stress (Emotional Stroop, modified Trier and cold pressor). The sample was drawn from the Swedish Longitudinal Occupational Survey of Health (SLOSH). There were no baseline differences in mean ULL levels between the three

EE groups (one-way ANOVA). After the acute stress exposure there were significant differences in mean levels of ULL ( $p < 0.01$ ) between the EE-groups. Post-hoc analyses showed that the differences in mean ULLs were between those with high vs. low EE. Mean differences between the lowest and highest EE quartile showed a range between 5.5 and 6.5 dB. Those with low levels of EE became more tolerant to higher levels of stimulation after acute stress. When the analyses were stratified for sex there were no differences in mean ULLs for men in different EE-groups, neither pre- nor post-stress. Women, however, displayed a post-stress difference in mean ULLs. The results demonstrate that women, but not men, who show symptoms of long-term stress display hyperacusis after acute stress. The odds of having hyperacusis were 2.5 (2 kHz, right ear; left ns) and 2.2 (4 kHz, right ear; left ns) times higher among those with high EE compared to those with low levels. The salient finding of the present study was that women with high levels of emotional exhaustion become more sensitive to sound after an acute stress task. This novel finding highlights the importance of including EE in the diagnosis and treatment of hearing problems.

### **855 Sound Exposures in Recreational Environments**

**Markus Huth**<sup>1,2</sup>, Gerald Popelka<sup>1</sup>, Nikolas Blevins<sup>1</sup>

<sup>1</sup>*Dept. of Otolaryngology, Head & Neck Surgery, Stanford University, Stanford, CA,* <sup>2</sup>*Dept. of Otorhinolaryngology, Head & Neck Surgery, Inselspital, University of Bern, Switzerland*

Exposure to loud sound is the most preventable cause of permanent sensorineural hearing loss that affects an estimated 300 million people worldwide. Damaging sound exposures (SE) are well characterized and require measures of both level and duration. Occupational SEs are measured easily because the source of the sound is known, the level and duration can be determined with recording sound level meters and are often well regulated. Recreational SEs are much more difficult to measure because the sources and environments are highly variable and the sound levels and durations may not be under the direct control of the user (concert halls, music clubs). Our knowledge of recreational SEs is very limited and needs to be expanded to allow for effective prevention. Cinemas represent a recreational sound source with subjectively increasing sound levels, limited information, with all of the measurement problems mentioned above and not amenable to accurate measurement with conventional sound measurement equipment. The purpose of this study was to accurately determine the SEs in cinemas. A calibrated blinded measurement system was developed that allowed multiple measures during a single presentation. Three movies of different genres (action, comedy, and children's) were measured multiple times at ten different venues in the San Francisco Bay area. SEs ( $L_{eq}$ ) and maximum peak sound levels were determined for each of the conditions. There were no differences in  $L_{eq}$  or peak levels among venues or time of presentation (daytime or day of the week) or among the first, middle or

last rows of seats within a theater. Both  $L_{eq}$  and peak levels were significantly higher for action movies compared to comedies or children's movies. Because the user cannot control the sound level, cinemas should consider reducing the sound levels of action movies or otherwise provide hearing protection devices. This measurement approach is ideal for blinded measurement of many recreational sound sources.

### **856 Ameliorative Effect of 1/3 Octave Sound Stimulation on Pure-Tone Hearing Thresholds in the People with Sensorineural Hearing Loss**

**Eunyee Kwak**<sup>1</sup>, Sangyeop Kwak<sup>2</sup>, Seog-Kyun Mun<sup>3</sup>

<sup>1</sup>*Earlogic Auditory Research Institute,* <sup>2</sup>*Earlogic Corporation,* <sup>3</sup>*Chung-Ang University College of Medicine*

Sound stimulation using a non-traumatic, moderate-level acoustic signal is a well-known method to protect from age-related or noise-induced hearing loss in animals. Several studies reported that sound stimulation can delay hearing loss in DBA/2J and C57BL/6J mice and Fischer 344/NHsd rats, which exhibit progressive sensorineural hearing loss. Pre-sound stimulation (i.e., exposure to a non-traumatic level sound before traumatic noise exposure) reduces noise-induced hearing loss. This protective effect of the sound stimulation has been observed in a number of different species including humans. Post-sound stimulation (i.e., exposure to a non-traumatic level sound after traumatic noise exposure) was also reported to reduce noise-induced hearing loss in animals. In this study, we investigated the effect of sound stimulation on sensorineural hearing loss in 22 participants who had various types of audiogram. Pure-tone hearing threshold changes with or without 2 weeks of sound stimulation were compared. Of 22 participants, 14 participants showed a  $\geq 10$  of hearing threshold decrease at least at one frequency. Two participants showed a  $\geq 10$  of hearing threshold decrease at 5 frequencies. Totally, 26 samples showed a  $\geq 10$  of hearing threshold decrease after the sound stimulation period.

### **857 A DFNA5 Mutation in Two Japanese Families with Autosomal Dominant Hereditary Hearing Loss**

**Ayako Nishio**<sup>1</sup>, Yoshihiro Noguchi<sup>1</sup>, Ken Kitamura<sup>1</sup>

<sup>1</sup>*Tokyo Medical and Dental University*

Genetic analysis has been applied to improve understanding of non-syndromic hereditary hearing loss (NSHL) and is useful for genetic counseling purposes. However, the identifying rate of a causative gene is not necessarily high. DFNA5 was mapped to chromosome 7p15 and the causative gene, *DFNA5*, was identified in a large Dutch family. To date, four different mutations have been detected to cause hearing loss (HL) in two Dutch

families and three East Asian families. Two (c.991-15\_991-13del and c.1183+4A>G) of the mutations were found in Chinese and Korean families and may show a founder effect among East Asians.

We screened for the two mutations in *DFNA5* in a total of 96 unrelated Japanese patients with autosomal dominant NSHL. DNA was extracted from peripheral blood lymphocytes using standard methods after obtaining written informed consent from the donor. The relevant segment of DNA was amplified by polymerase chain reaction (PCR). The PCR products were purified and directly sequenced to identify the mutations. Whenever the mutation was detected, amplification and sequencing were conducted for all coding regions and exon-intron boundaries of *DFNA5*.

Two (2%) of the 96 patients carried the c.991-15\_991-13del mutation, while no patients had c.1183+4A>G mutation. No c.991-15\_991-13del mutation was detected in 90 Japanese normal controls. No other variants in *DFNA5* were detected in the two patients with the 3-bp deletion. In affected individuals in the two families, HL started at high frequencies in the second or third decade, and progressed with age. These findings are consistent with those in Chinese and Korean families with the same mutation. Genetic screening of the c.991-15\_991-13del mutation in *DFNA5* is worthwhile for East Asians with autosomal dominant NSHL.

### **858** LifeGene, a Basis for Epidemiological Hearing Research

**Pernilla Videhult Pierre**<sup>1</sup>, Anders Fridberger<sup>1</sup>, Ann-Christin Johnson<sup>1</sup>, Nancy L Pedersen<sup>1</sup>

<sup>1</sup>*Karolinska Institutet*

Many epidemiologic questions on hearing are incompletely investigated. Among these are:

- Do antioxidant intake and physical activity correlate with a reduced risk of hearing problems?
- What is the correlation between self-reported and audiometrically assessed hearing loss?
- What are the genetic influences on the susceptibility to exogenous hearing loss?

Our research group addresses such questions by using data collected in LifeGene, a project designed to build up a resource for research on the relationships among heredity, environment, and lifestyle. LifeGene aims to recruit 500,000 Swedes and follow them longitudinally for 20 years. At baseline and every 5 years thereafter, physical measurements, including audiometry, and an extensive web-based questionnaire on socio-demographics, lifestyle, personality, work and leisure-time exposures, health history, and occupation are administered. A brief web-based follow-up is administered each year in order to document changes in household composition, changes in symptoms, injuries, and pregnancies. Blood and urine samples are collected at 5 year intervals and stored in a manner that facilitates proteomic, metabolomic, genomic, and epigenomic analyses. Questions and sampling schemes are tailored to the participants' age and life events. Furthermore, the design of LifeGene is expected to allow detection of a gene-environment interaction for a

moderately rare disease (annual incidence of 50 to 100 cases per 100,000) with an odds-ratio of 2.5-3 with 80% probability ( $\alpha=0.0001$ ).

So far, LifeGene has generated audiometric and questionnaire data from 15,000 individuals and the analyses have just begun. Preliminary results show a good correlation between self-reported and audiometrically assessed hearing problems. International cooperate initiatives are welcomed.

### **859** Using Notched or Unnotched Acoustic Stimulation to Treat Tinnitus

**Ming Zhang**<sup>1,2</sup>

<sup>1</sup>*University of Alberta: Rehab Med/Speech Path &*

*Audiology; Medicine/Surg-Otolaryngology, <sup>2</sup>Alberta Health Services: Glenrose Rehab Hosp/Audiology*

Whether notched or unnotched acoustic stimulation is superior in treating tinnitus is a yet unknown but very interesting question. There are millions of tinnitus sufferers in the world, but it is well known that tinnitus is a difficult-to-treat condition. Because the treatment is difficult, many types of treatments have been proposed. One of them is to use acoustic stimulation, which includes music therapy and sound therapy. Music therapy may also be considered as a type of sound therapy. Many types of sound therapies have been proposed and established. Each type has certain merits and has played very important roles in helping tinnitus sufferers. Although many in number, almost all sound therapies can be classified into two large categories: ones that contain tinnitus frequencies and ones that do not. These two categories can also be termed as notched and unnotched, respectively. Which one is superior, notched or unnotched? There seems to be no clear answer yet. It also seems too early for investigators and for us to derive a concrete conclusion. However, as the first step in challenging this question, we completed a literature review. Therefore, in this report, we will describe the results of this literature review. We found that, in the literature, reports which included the use of notched stimulation as a treatment method were fewer than those which included the use of unnotched stimulation. Although fewer in number, the results of the reports which included the use of notched stimulation all indicated that the therapy reduced tinnitus. Interestingly, in certain conditions, the notched stimulation was shown to be more effective than the unnotched stimulation in the reduction of tinnitus. As for the mechanism underlying the treatment of using notched acoustic signals, based on the data reported by Eggermont's group and other groups, we consider that the mechanism behind the notched stimulation tinnitus treatment is more closely related to lateral inhibition of neural hyperactivity and to the remapping of the auditory cortex. Based on such a consideration, we have designed a notch stimulation for the treatment of tinnitus, which was documented in the Tinnitus Research Initiative in 2007. In that design, based on psychoacoustic results, we aim to derive a notched stimulation containing a set of side bands that is expected to maximize the lateral inhibition. Interestingly, a recent report in 2010 supports our design because the spectral range of the stimulation in that design

is similar to ours and their results showed that the tinnitus was reduced. Further details regarding our literature review will be discussed.

### **860** Concurrent Sound Segregation Is Impaired in Schizophrenia

Erin Ramage<sup>1</sup>, Amanda Flores<sup>1</sup>, Griffin Sutton<sup>1</sup>, Sally Barney<sup>1</sup>, Erik Ringdahl<sup>1</sup>, Daniel Allen<sup>1</sup>, Joel Snyder<sup>1</sup>

<sup>1</sup>University of Nevada, Las Vegas

Auditory processing deficits in schizophrenia (SZ) may contribute to impaired real-world functioning by interfering with the segregation of multiple sound sources, such as in the ability to hear speech apart from background noise. Therefore, this study evaluated whether concurrent sound segregation was impaired in SZ and if this was related to impairments on a more ecologically valid speech segregation task. SZ patients and control participants listened to 200 ms complex harmonic sounds consisting of a fundamental frequency and several integer-multiple harmonics, with the second harmonic mistuned by 0, 2, 8, or 16% in relation to the fundamental. Larger mistuning typically elicits perception of a second sound source akin to a pure-tone sound along with a complex buzzing sound. Participants indicated their perception by pressing one of two buttons, one when they heard a single buzzing sound and another when they heard a buzzing sound plus a segregated pure-tone sound. There was a significant mistuning by group interaction on the proportion of pure-tone sounds reported as segregated from the complex because the SZ group did not benefit as much from greater mistuning as compared to the control group. A standardized sentence-perception-in-noise task (QuickSIN) was also administered, which required participants to repeat all the words in a target sentence spoken by a female speaker while ignoring background sentences spoken by other speakers. The SZ group performed significantly poorer on the QuickSIN task as compared to the control group, and lower performance on this task across all subjects was associated with decreased mistuning segregation. The results suggest that impaired concurrent sound segregation in SZ patients may contribute to the difficulties SZ patients have in complex real-world situations such as hearing speech in noisy environments. [Work supported by NIH R21MH079987]

### **861** The Sweep-Frequency Procedure for Clinically Estimating the Middle-Ear Resonant Frequency: Data from Ears with Negative Middle-Ear Pressure and Implications

Xiao-Ming Sun<sup>1</sup>, Kayla R. Eldridge<sup>1</sup>

<sup>1</sup>Wichita State University

A sweep-frequency procedure has been used for estimating the middle-ear resonant frequency (RF) in clinical tympanometry systems. It measures the acoustic susceptance for probe frequencies from 250 to 2000 Hz at a 200-daPa ear canal pressure and the tympanogram peak pressure and then calculates the difference ( $\Delta B$ ). RF is defined as the frequency corresponding to the 0

crossing of the  $\Delta B$  vs. frequency function. A number of studies have suggested that RF has the potential of differentiating between stiffness- and mass-related middle-ear disorders. We tested the RF in 26 normal adult ears and in the same ears with a self-induced negative middle-ear pressure (MEP) between  $-50$  and  $-245$  daPa, using a modified test procedure. Results show that negative MEP causes an increase of RF by approximate 300 Hz on average. However, a correlation analysis displayed that the RF decreased as MEP became more negative, which is incongruent with the effect of increased stiffness on a system. Inspection of individual data exhibited unusual phenomena: (1) No RF was determined in eight ears (30%) because of no 0 crossing for the  $\Delta B$  frequency function, which may be projected to occur at a frequency above 2000 Hz; and (2) There were multiple crossings for the function in ten ears (38%) so that the crossing for the lowest frequency was always determined as the RF, which alludes to an underestimated RF. When data was grouped along with three MEP ranges, only the RF in ears of the low negative MEP group was significantly higher than that in normal ears. The RF in ears of the high negative MEP group tended to be lower than that of normal ears. The number of ears with unidentified RF increased with increasing negative MEP. These results denote limitations of the sweep-frequency procedure in estimating the RF of a stiffened middle ear. The present study also implies that acoustic resonance of the middle ear becomes broader with multiple RFs or RF ranges as the system is distorted by air pressure.

### **862** Identification of Conductive Hearing Loss in Transgenic Mouse Models of Hearing Loss Using Implantable Hearing Aid Stimulation of Round Window Membrane

Wesley M Chin<sup>1</sup>, Omar Akil<sup>1</sup>, Lawrence R Lustig<sup>1</sup>

<sup>1</sup>University of California, San Francisco

Traditional methods of measuring the degree of hearing loss in mouse models utilize testing with auditory brainstem response (ABR) thresholds, but these tests cannot distinguish conductive hearing loss (CHL) from sensorineural hearing loss, a critical and clinically useful distinction. This project aims to establish a method to identify and measure the degree of CHL in mouse models, based upon prior work in the guinea pig by Lupo et al. An implantable hearing aid called a Middle-Ear Transducer (MET, Otologics LLC) has been modified to directly stimulate the round-window membrane of the cochlea, thereby bypassing the ossicular chain and outer ear, to produce a signal that can be measured by ABR. In normal hearing mice, ABR thresholds from round window MET stimulated signals (ave=40.93 dB, n=7) were calibrated to be equivalent to ABR thresholds from normal acoustic signals (ave=38.33 dB, n=15). To demonstrate proof of principle, a maximum CHL was created via removal of the tympanic membrane and partial disarticulation of the ossicular chain in normal hearing mice. While the acoustic ABR thresholds increased due to this induced hearing loss, MET induced signals retained their baseline ABR thresholds (ave=40.86 dB; n=7), thereby demonstrating a

pure CHL. Lastly, we used a transgenic mouse model of hearing loss, Runx2, which contains a mutation in the TGFB pathway of bone metabolism, to elucidate whether the hearing loss previously identified was conductive or sensorineural. Acoustic ABR thresholds demonstrated hearing loss (ave=68.75 dB, n=4), while the MET stimulated signals produced ABR thresholds equivalent to baseline (ave=38.00 dB, n=7). This equates to a 30 dB conductive hearing loss in Runx2 mice. These studies suggest that MET stimulation of the round window membrane is an effective method for identifying conductive hearing loss in mice, and can be useful in measuring the nature and degree of hearing loss in transgenic mouse models.

### **863 Effects of Superior Semicircular Canal Dehiscence on Ear-Canal Reflectance and Ossicular Motion in a Temporal Bone Preparation**

**Gabrielle R. Merchant**<sup>1,2</sup>, Saumil N. Merchant<sup>2,3</sup>, John J. Rosowski<sup>2,3</sup>, Hideko H. Nakajima<sup>2,3</sup>

<sup>1</sup>*Speech and Hearing Bioscience and Technology, Harvard-MIT Division of Health Sciences and Technology,* <sup>2</sup>*Eaton-Peabody Laboratory, Massachusetts Eye and Ear Infirmary,* <sup>3</sup>*Department of Otology & Laryngology, Harvard Medical School*

Superior semicircular canal dehiscence (SCD) is a pathological opening in the superior semicircular canal of the inner ear that can result in various auditory and vestibular symptoms. A quick, inexpensive, and simple non-invasive auditory measurement to aid in the diagnosis of SCD would be of value because it would (1) help select patients who should be referred for further testing such as a high resolution CT scan and (2) demonstrate a functional abnormality in the auditory system resulting from SCD. This project aims to explore two multi-frequency measures that may aid in the diagnosis of SCD. In a temporal bone preparation, a dehiscence was created in the superior semicircular canal and then subsequently patched to explore the effect of SCD. Both ossicular velocity measurements at the stapes and at the umbo, as well as a measure of absorbance of sound energy by the middle and inner ear called ear-canal reflectance (ECR) were measured. Preliminary data suggests that while the dehiscence creates only small changes in the umbo and stapes velocity measurements, its' effects on ECR are more substantial, with a characteristic decrease in ECR creating a notch between 750 and 1100 Hz. A similar pattern was also seen in ECR and umbo velocity data collected on patients with SCD (Nakajima et al., *Ear & Hear*, 2011). These temporal bone results will be compared with this patient data.

### **864 Effects of Various Ototoxic Drugs on New Bone Formation in the Middle Ear Cavity of the Guinea Pig Evaluated with a Micro-CT Scanner**

**Takafumi Yamano**<sup>1,2</sup>, Hitomi Higuchi<sup>1</sup>, Mayumi Sugamura<sup>1</sup>, Hisamitsu Takase<sup>1</sup>, Takashi Nakagawa<sup>1</sup>, Tetsuo Morizono<sup>3</sup>

<sup>1</sup>*Department of Otolaryngology, Fukuoka University School of Medicine,* <sup>2</sup>*Department of Otolaryngology, Fukuoka University Chikushi Hospital,* <sup>3</sup>*Nishi-Fukuoka Hospital*

**Objective :** To visualize and quantify the degree of new bone formation in the middle ear cavity in the guinea pig after topical usage of antiseptics.

**Methods:** Hartley adult guinea pigs were used. Three different antiseptics, methylrosaniline chloride (Gentian Violet), povidone-iodine (Isodine), and Burow's solution were studied.

The temporal bones of the animal were scanned using in-vivo microtomography at the following time points: before, two weeks and four weeks after filling one of the middle ear cavities with the above antiseptics. The SKYSCAN 1178 (SkyScan, Kotich Belgium), is capable of investigate internal microstructures of small animals non-invasively and repeatedly. For the entire head of a guinea pig, a scanning and reconstruction cycle can be performed in less than two minutes. After the measurements were completed, the temporal bones were harvested for histopathologic study. Celloidin embedded specimens were cut into 20 micronthick slices, and were compared with the results of Micro-CT scan.

**Results:** Both the treated and untreated sides were compared and analyzed by Students paired t-test. All three antiseptics that we studied caused massive new bone formation. Isodine (N=5) caused a difference at 2 weeks (P<0.05) and at 4 weeks (p<0.01). Gentian Violet (N=4) caused a difference at 2 weeks (p<0.01) and at 4 weeks (p<0.01). Burow's solution (N=7) caused a difference at 2 weeks (p<0.01) and at 4 weeks (p<0.01). The degree of new bone formation was the most pronounced in Gentian Violet followed by Burow's solution and by Isodine.

**Conclusion:** The SKYSCAN 1178 allows us to make repeated 3-D observations of the temporal bone in the guinea pig. The results were in good agreement with histopathologic study. However, the thickness of the sections obtained with this Micro-CT equipment were 80 microm, and we were unable to analyze the detailed micro structure of the cochlea with CT.

### **865 Variability in RT-PCR Housekeeping Gene Quantification Is Reduced by Improved RNA Extraction**

**Fran Hausman**<sup>1</sup>, Teresa Wilson<sup>1</sup>, Beth Kempton<sup>1</sup>, Carol MacArthur<sup>1</sup>, Dennis Trune<sup>1</sup>

<sup>1</sup>*Oregon Health & Science University*

The extraction of high quality RNA from the ear is necessary for RT-PCR, Affymetrix Gene Arrays, etc., but often yields are reduced due to small tissue amounts, prolonged dissection times for tissue isolation, etc. Furthermore, some experimental treatments may alter

RNA transcription of housekeeping genes and mask treatment effects. Thus, maximizing RNA extraction is critical, particularly for quantitative comparisons between experimental groups. Initial handling of tissues can significantly impact the quality and quantity of the isolated RNA. Therefore, alternative methods of tissue dissection and storage were examined to a) improve yield, b) improve quality, c) provide consistent yield in spite of experimental treatments, d) provide retention of quality with long term storage. We employed steroid treatment of mice prior to tissue collection, which we have determined to alter housekeeping gene yield and raise concerns about statistical comparisons. BALB/c mice were injected transtympanically with either PBS or dexamethasone, middle ear tissues harvested at 6 hours, and RNA extracted by two different techniques. The first was dissection of tissues in cold phosphate buffer with storage in RNAlater at -20 degrees. The second technique was to dissect tissues in RNAlater, blot off any excess RNAlater, then flash freeze in liquid nitrogen and store at -80 degrees. Subsequent RT-PCR of the housekeeping gene GAPDH showed the latter method was far superior. 1) We obtained a higher yield of RNA. 2) The 260/230 ratio was better, indicating less salt contamination in the final sample. 3) The housekeeping gene values had similar crossover values, implying no treatment effects on their expression. 4) The -80 degree freezing provided longer storage without degradation. Adaptation of these steps should provide improved yields of inner ear RNA for the numerous techniques and experimental manipulations currently used.

Supported by NIH-NIDCD R01 DC005593

### **866 A Novel Chitosan Patch Releasing Epithelial Growth Factor (EGF) for Treatment of Chronic Tympanic Membrane Perforations**

**Seung Won Kim**<sup>1</sup>, Hoon Seonwoo<sup>2</sup>, Jong Bin Lee<sup>3</sup>, Eun Jung Kim<sup>1</sup>, Chunjie Tian<sup>1</sup>, Yeon Joo Kim<sup>1</sup>, Seong Jun Choi<sup>3</sup>, Kihyun Kim<sup>1</sup>, Inkyung Sohn<sup>1</sup>, Hun Yi Park<sup>1</sup>, Jong Hoon Chung<sup>2</sup>, Yun-Hoon Choung<sup>1</sup>

<sup>1</sup>Ajou University School of Medicine, <sup>2</sup>Seoul National University, <sup>3</sup>Konyang University

**Background and Objectives:** Most of chronic tympanic membrane (TM) perforations require surgical interventions such as tympanoplasty because it is impossible to heal spontaneously unlike the cases with acute perforations. The purpose of the study was to develop novel therapeutic techniques and scaffolds releasing growth factors to be able to treat chronic TM perforations.

**Materials and Methods;** We evaluated proliferation effects of EGF and FGF on in vitro culture of TM cells using MTT assay. We developed EFG releasing-chitosan patch (EGF patch) based on previous studies (Tissue Eng Part A 2010, J Biomed Mater Res A 2009). We analyzed the characteristics of EGF patch including toxicity, strength, drug releasing, and a scanning electron microscope (SEM) findings. In vivo study (35 rats), we prepared animal models (47 ears) with chronic TM perforations which maintained perforation over 8 weeks using Choungj's COM model 1 (Tissue Eng Regen Med, 2011). The EGF

group (23 ears) was treated with EGF patch, while the control group (24 ears) did not receive any treatment. TM perforations were evaluated with endoscope every week for 10 weeks and then transmission electron microscope (TEM) was done.

**Results;** The proliferation of TM cells was similar between EGF-treated culture and FGF in MTT assay. We decided to use EGF because of cost-effectiveness. Mechanical characteristics were better in the patches composed of 3% chitosan and 3.5% glycerol than other concentrations. EGF was released from the patch until 42days in In vitro system. Animal study showed the healing effect of 56.5% (13/23) in the EGF group and 20.8% (4/24) in the control group (p=0.04). TEM findings of regenerated eardrums in the EGF group showed much more preserved histologic features and thinner eardrums than spontaneously healed TMs.

**Conclusion;** This novel EGF chitosan patch can be used as a nonsurgical intervention technique for treatment of chronic TM perforations.

### **867 Morphometric Study of the Eustachian Tube in Sheep as a Model for Eustachian Tube Disorders in Human**

Felicitas Ullrich<sup>1</sup>, Rolf Salcher<sup>1</sup>, Verena Scheper<sup>1</sup>, Thomas Rau<sup>1</sup>, Thomas Lenarz<sup>1</sup>, **Gerrit Paasche**<sup>1</sup>

<sup>1</sup>Hannover Medical School

Eustachian tube disorders can lead to middle ear infections, which can contribute to hearing problems. Despite several approaches for treatment there is still no effective therapy. To develop and test new treatments, an adequate experimental animal model would be necessary. As the tube of a sheep is considered to be comparable in size to a human tube, we investigated the properties of the Eustachian tube in sheep (Heidschnucke) as a possibility for an appropriate model.

The Eustachian tube and middle ear of 13 half heads of sheep were filled with silicone, blended with barium sulfate to induce x-ray visibility. Three-dimensional images of the half heads were then taken by digital volume tomography. Using this method the silicone filled tubes became clearly visible. Images were analyzed by the software iPlan and a three-dimensional model of every Eustachian tube was made by segmentation. The length, diameters at different positions and three-dimensional shapes were measured.

The average length of the Eustachian tube in Heidschnucke was determined to be 26.5±1.7 mm. The diameter at the isthmus is about 1±0.2 mm and at the pharyngeal part it depends on the dilatation of the tissue. If strongly widened, it can go up to about 8.5x8.8 mm.

The comparison with data of the human Eustachian tube shows, that the tube length in Heidschnucke is slightly smaller than the reported 33 to 38 mm for the length of a human Eustachian tube. Nevertheless, the distance from the pharyngeal opening to the isthmus is with approximately 21 mm comparable in both species.

Supported by: BMBF „Spitzenförderung in den neuen Ländern“ REMEDIS C3

## 868 Pseudomonas Aeruginosa Virulence Factors in Infected Cholesteatomas

Richare Chole<sup>1</sup>, Patricia Gagnon<sup>1</sup>, Joseph Vogel<sup>1</sup>

<sup>1</sup>Washington University in St. Louis

Aural cholesteatomas develop in some ears with chronic otitis media resulting in destruction of bony structures, hearing loss and often chronic bacterial infection. Additionally, infections within cholesteatomas are often highly resistant to eradication with antibiotics and host defenses. We hypothesize that the biofilm phenotype of *Pseudomonas aeruginosa* (PA) within infected cholesteatomas is a virulence factor which renders these bacteria impervious to antibiotics and host defenses.

Three genes known to be responsible for biofilm formation in PA were deleted from PA01, a well characterized isolate: *algD*, *pilA*, and *galU*. Biofilm generation *in vitro* was studied using a crystal violet assay.

The virulence of these strains was studied *in vivo* using the gerbil model of induced cholesteatomas. Five groups of gerbils and one group of controls were used. Six week old gerbils underwent ear cholesteatoma induction by canal ligation. Ears were inoculated with vehicle or 10<sup>6</sup> bacteria. The strains used were PA01 wt, PA01 *algD*-, PA01 *galU*- and PA01 *pilA*-. After eight weeks, animals were double fluorochrome labeled with xylenol orange and calcein to later measure apposition rate. After sacrifice and fixation, heads underwent microCT scanning. After scanning, the bullae were embedded and sectioned for fluorophore measurement of bone apposition rate. The scans were analyzed in a blinded manner with the following measures: tissue density within the bulla, erosion of the external auditory canal, demineralization of the malleus and thickening of the dorsal bulla bone.

Cholesteatomas infected with PA exhibited more enlargement and bone remodeling than uninfected controls. Deletion of biofilm forming genes in PA modified these destructive processes indicating that the biofilm phenotype may be a virulence factor in infected cholesteatomas.

Supported by a grant from the NIDCD R01 DC0000263-24(RAC) and P30 DC004665-11(RAC)

## 869 Transmembrane Protein 16A Is an Intrinsic Ca<sup>2+</sup>-Activated Cl<sup>-</sup> Channel in Human Middle Ear Epithelia

Hyun Jae Lee<sup>1</sup>, Jae Young Choi<sup>1</sup>

<sup>1</sup>Yonsei University

Chloride (Cl<sup>-</sup>) secretion through apical anion channel plays important physiological roles in middle ear mucosa. According to our previous reports, Ca<sup>2+</sup>- activated Cl<sup>-</sup> channel (CaCC). CaCC is dominant anion channel in middle ear epithelia. However, the molecular identity of endogenous CaCC in middle ear epithelia is still unknown. Here, we showed that transmembrane protein 16A (TMEM16A) mediates Cl<sup>-</sup> secretion in response to UTP in human middle ear epithelial cells.

Cl<sup>-</sup> currents were recorded using the whole-cell configuration of the patch clamp technique. Cl<sup>-</sup> currents were isolated by using Cl<sup>-</sup> as the only permeant ion in the pipette and bath solutions. Pipette and bath solutions

contained 140mM N-methyl D-glucamine (NMDG)-Cl, which permitted Cl<sup>-</sup> to be used as the main charge carrier. RT-PCT and immunohistochemical staining for TMEM16A were performed.

Application of 100uM UTP to cultured human middle ear epithelial (HMEE) cells evoked robust inward currents when the membrane potential was held at -60mV. In more details, UTP induced inward current has fast and sustained current. The fast component showed a linear I/V relationship. In contrast, the sustained components showed outward-rectifying I/V relationship. The UTP-induced current was inhibited by CaCC blocker, niflumic acid (50uM). We further confirmed the expression of TMEM16A mRNA and protein in cultured human middle ear epithelial cells.

The biophysical properties Ca<sup>2+</sup>- activated Cl<sup>-</sup> currents induced by UTP is in full agreement with TMEM16A. Further researches about the physiologic role of TMEM16A provide a fundamental step in understanding the mechanism of middle ear disease such as otitis media.

## 870 Measuring Thickness of Middle Ear Mucosa Using MRI, CT and Histology

Mary Ann Nyc<sup>1</sup>, Sang Gyoon Kim<sup>1</sup>, Timothy Jung<sup>1</sup>

<sup>1</sup>Loma Linda University; Jerry L. Pettis VAMC Loma Linda

Abstract

**Objective:** Inflammation of the middle and inner ear is associated with otitis media (OM) and consists of increased middle ear effusion as well as mucous covering the middle ear tissue. The purpose of this study was to evaluate OM by measuring mucosal thickness (MT) using two radiographic methods: magnetic resonance imaging (MRI) and computed tomography (CT). Imaging results were then confirmed by histology.

**Methods:** 28 chinchillas were divided into three groups consisting of a vehicle control group and two glucocorticoid groups. Of the 28 chinchillas: 6 underwent treatment by vehicle control, 10 were treated with ciprofloxacin 0.3%/dexamethasone 0.1% (Ciprodex), and 10 received ciprofloxacin 0.2%/hydrocortisone 1% (Cipro HC). After 96 hrs post LPS inoculation into the superior bullae, chinchillas were euthanized and their temporal bones were removed for imaging and histopathological examination. MRI was conducted on 18 full chinchilla temporal bones, whereas micro CT was performed on 14 single inferior bullae of each chinchilla middle ear cavity. Histology confirmation was completed for all 28 chinchilla specimen.

**Results:** MRI scans produced statistically significant difference in MT measurements among treatment groups (F=146.0861, p-value<0.0001). CT imaging did not produce significant MT measurements across treatment groups using both bone to mucosal thickness ratios ( $\chi^2=1.2404$ , p-value=0.5378) and total average calculated mucosal volume ( $\chi^2=0.9762$ , p-value=0.6138). Histology did produce significant measurements of MT difference among treatment groups ( $\chi^2=40.5267$ , p-value<0.0001). Tukey's post-hoc testing on MRI and histology data revealed that DEX-treated chinchillas exhibited significantly smaller MT values compared to the HC and control groups.

*Conclusion:* Imaging MT seems to be an effective method determining severity of inflammation due to OM. In this study, MRI provided more information about internal, soft tissue structures and was easier to interpret compared to CT imaging. In a clinical setting, imaging by MRI could be used as a non-invasive, and radiation-free method for diagnosing severe or chronic middle ear OM and could be used to track treatment progression of severe cases in an efficient way.

### **871 Regulation of ENaC-Mediated Sodium Transport by Glucocorticoids in Human Middle Ear Epithelial Cell**

**Koh seunghyun<sup>1</sup>, kim sunghuhn<sup>1</sup>, kim jinyung<sup>1</sup>, kim bokyung<sup>1</sup>, Choi jaeyung<sup>1</sup>**

<sup>1</sup>*yonsei university college of medicine*

Regulation of ENaC-mediated sodium transport by glucocorticoids in human middle ear epithelial cell

The middle ear epithelium functions to maintain a fluid-free middle ear cavity. Dysfunction of the middle ear epithelial ion and fluid transport is implicated in the pathogenesis of otitis media with effusion. Most water transport followed Na<sup>+</sup> transport and middle ear mucosa was known to have Na<sup>+</sup> transport channels. The effect of synthetic steroid on Na<sup>+</sup> transport still remains controversial. This study was conducted to 1) identify candidate genes involved in the Na<sup>+</sup> transport pathway, 2) determine whether their level of expression was regulated by the synthetic glucocorticoid dexamethasone. We used the human middle ear epithelia cell line (HMEEC) to determine the level of expression was regulated by corticosteroid. The difference of transcription levels of Na<sup>+</sup> transport regulatory genes and protein expressions of ENaC between control and dexamethasone-treated group were analyzed by quantitative real-time RT-PCR (qRT-PCR) and Western blot.

Transcripts were present for  $\alpha$ -,  $\beta$ -,  $\gamma$ -subunits of epithelial Na<sup>+</sup> channel (ENaC); glucocorticoid receptor (GR); corticosteroid activator 11 $\beta$ -HSD1; glucocorticoid activated Na<sup>+</sup> transport regulators (SGK1, Nedd4-2, and WNK4). Dexamethasone upregulated transcripts for  $\alpha$ - and  $\beta$ -subunits of ENaC, 11 $\beta$ -HSD1, SGK1, and Nedd4-2. Dexamethasone-stimulated gene expression was reduced by mifepristone, but not spironolactone, which means increase in ENaC transcript expression was GR dependent pathway. These observations are consistent with Na<sup>+</sup> absorption by HMEEC, which is mediated by apical ENaC and is under control of glucocorticoids.

We demonstrated Na<sup>+</sup> absorption by HMEEC that is mediated by ENaC and is under control of the synthetic glucocorticoid dexamethasone and glucocorticoid regulatory genes such as 11 $\beta$ -HSD1, SGK1, and Nedd4-2. These results provide an understanding and molecular definition of an important transport function of human middle ear epithelium in the pathogenesis and treatment of otitis media with effusion.

### **872 inner Ear Inflammation Ipsilateral to Clear Middle Ears Suggests Sensorineural Hearing Loss in Chronic Otitis Media May Also Result from Circulating Immune Factors**

**Beth Kempton<sup>1</sup>, Fran Hausman<sup>1</sup>, Barbara Larrain<sup>1</sup>, Carol MacArthur<sup>1</sup>, Dennis Trune<sup>1</sup>**

<sup>1</sup>*Oregon Health & Science University*

The C3H/HeJ mouse has a defect in TLR4 that predisposes it to systemic gram-negative infections and a high incidence of middle ear disease. This mouse serves as a model for the inflammatory mechanisms of chronic otitis media (COM) and the resultant sensorineural hearing loss. However, it has been observed in this mouse that inner ear inflammation and hearing loss occur ipsilateral to a clear middle ear. This raised the question of whether the hearing loss in COM in some cases may be the result of circulating immune factors and not their migration across the round window membrane. To assess this possibility, C3H mice with unilateral and bilateral COM were identified by visual inspection. Sera were collected for Multiplex ELISA of key inflammatory cytokines. Middle ears and inner ears were harvested for qRT-PCR of inflammatory cytokine genes and ion homeostasis genes. Serum cytokine evaluations showed significantly higher levels of some inflammatory cytokines (KC, MIP-2) compared to BALB/c mice. Infected middle ears showed increased expression of all inflammatory cytokine genes, while the uninfected middle ears showed no elevation of any inflammatory genes, implying no active infection. Inner ears ipsilateral to a clear middle ear showed elevated inflammatory cytokine genes, as well as altered expression of several genes related to ion and water homeostasis. Inner ears ipsilateral to infected middle ears showed similar expression levels of these same genes. Thus, the inner ear inflammatory changes were quite similar, regardless of whether they were ipsilateral to an infected or clear middle ear. This inner ear inflammation without concomitant middle ear inflammation suggests circulating inflammatory factors may be acting directly on the inner ear to cause sensorineural hearing loss. This implies that sensorineural hearing loss in chronic OM may not always be due to movement of infection or cytokines across the round window.

Supported by NIH-NIDCD R01 DC005593

### **873 Control of Middle Ear Inflammatory and Ion Homeostasis Genes by Trans-Tympanic Steroid Treatment After Inoculation with Heat-Killed Haemophilus Influenza**

**Jessyka Lighthall<sup>1</sup>, Beth Kempton<sup>1</sup>, Fran Hausman<sup>1</sup>, Carol MacArthur<sup>1</sup>, Dennis Trune<sup>1</sup>**

<sup>1</sup>*Oregon Health & Science University*

The middle ear responds to a bacterial challenge with early alteration in inflammatory and ion homeostasis genes. Previous studies have shown that systemic steroid treatment of mice with acute otitis media leads to a decrease in inflammation and improved fluid clearance. The goals of this study were to evaluate the efficacy of trans-tympanic steroid delivery on middle ear ion

homeostasis and inflammatory gene expression, as well as histologic parameters of inflammation. Balb/C mice received trans-tympanic inoculation with heat-killed *Haemophilus influenzae*, then trans-tympanic treatment with the glucocorticoid prednisolone or the mineralocorticoid aldosterone. Untreated mice were used as controls. Four hours after treatment the middle ears were harvested and mRNA extracted for qRT-PCR. Additional mice were collected after 24 hours for middle ear histologic assessment of the number of inflammatory cells, fluid area, and tympanic membrane thickness. Prednisolone caused significant down-regulation of inflammatory cytokine genes and a few ion homeostasis genes. Aldosterone induced down-regulation of several inflammatory cytokines genes and up-regulation of many ion and fluid transport genes. Aldosterone treatment also caused a decrease in fluid area, number of inflammatory cells, and tympanic membrane thickness, whereas only fluid area and tympanic membrane thickness were decreased with prednisolone. Although some improvement in middle ear inflammation was noted with prednisolone, treatment with aldosterone showed greater fluid clearance and a decrease in inflammatory cells. This reduction of fluid and inflammation by aldosterone is presumably due to its impact on ion and water transport channels. These findings suggest that trans-tympanic steroid administration may be beneficial in the treatment of otitis media though further research is necessary.

Supported by NIH-NIDCD R01 DC009455 and DC005593 (DRT)

#### **874** Epithelial Recognition of Cytoplasmic Nontypeable *Haemophilus influenzae* Through a NOD2-Dependent Signaling Pathway

Sung K. Moon<sup>1</sup>, Jeong-Im Woo<sup>1</sup>, Paul Webster<sup>1</sup>, Sejo Oh<sup>1</sup>, David Lim<sup>1,2</sup>

<sup>1</sup>House Research Institute, <sup>2</sup>University of Southern California

Nontypeable *Haemophilus influenzae* (NTHi), a common pathogen causing otitis media, selectively adheres and internalizes to mucosal epithelium in the middle ear. Although *Listeria monocytogenes* is known to escape from the phagosome to the cytoplasm, it is unclear if internalized NTHi can exist freely in the cytoplasm of host cells. Transmission electron microscopy demonstrated that NTHi can exist either surrounded by an enclosing membrane or freely in the cytoplasm after rupturing the enclosing membrane. Thus, we aimed to further determine which cytoplasmic pathogen recognition receptor is critically involved in recognition of NTHi and its molecules in the cytoplasm of host cells, resulting in up-regulation of DEFB4A, an inducible cationic antimicrobial peptide in response to pro-inflammatory cytokines and bacterial molecules. Silencing of nucleotide-binding oligomerization domain containing-2 (NOD2), a cytoplasmic pathogen recognition receptor, was found to inhibit NTHi-induced DEFB4A up-regulation in the human middle ear epithelial cells. NTHi-induced DEFB4A up-regulation was enhanced by silencing of Card12, an inhibitor of NOD2 by structural

competition, but was inhibited by silencing of RICK, CARD-containing serine/threonine kinase Rip2, downstream of NOD2 signaling. Bacterial internalization assays and endocytosis assays showed that NTHi internalization is inhibited by cytochalasin D, an inhibitor of actin polymerization, but is enhanced by hemolysin, a pore-forming toxin. Consistently, we found that NTHi-induced DEFB4A up-regulation is inhibited by cytochalasin D, but is enhanced by hemolysin. Moreover, silencing of NOD2 appeared to inhibit hemolysin-mediated enhancement of NTHi-induced DEFB4A up-regulation. Taken together, NOD2 signaling is suggested to be required for the recognition of cytoplasmic NTHi in the human middle ear epithelial cells, resulting in DEFB4A up-regulation. [Supported by DC5025 and DC6276]

#### **875** Expression of Toll-Like Receptor 4 in Chronic Otitis Media

Haruka Hirai<sup>1</sup>, Shin Kariya<sup>1</sup>, Mitsuhiro Okano<sup>1</sup>, Tazuko Fujiwara<sup>1</sup>, Yuko Kataoka<sup>1</sup>, Kunihiro Fukushima<sup>1</sup>, Kazunori Nishizaki<sup>1</sup>

<sup>1</sup>Okayama University

Otitis media is one of the most common infectious diseases especially in young children. Multiple factors affect the onset or development of otitis media. The toll-like receptor recognizes pathogen-associated patterns, and has the critical role in the innate immune mechanisms. The toll-like receptor-mediated signaling is considered to be the important factor for clearance of infection and resolution of inflammation in otitis media. The purpose of the present study is to evaluate the histological expression of toll-like receptor 4 (TLR4) that recognizes lipopolysaccharide (LPS) on Gram negative bacteria in tissue samples from patients with chronic otitis media and from controls. Middle ear tissue samples from chronic otitis media were obtained during tympanoplasty. As a control tissue, we used middle ear mucosa that was collected from patients undergoing otologic surgery for cochlear implant. Patients with middle ear inflammation were excluded from the controls. The tissue samples were fixed, decalcified, and embedded in paraffin blocks. The expression of TLR4 in middle ear tissues from patients with chronic otitis media and normal controls were studied by immunohistochemistry. The expression of TLR4 was detected in middle ear samples in patients with chronic otitis media. In contrast, histologic examination of the samples from controls disclosed that a relatively weak expression of TLR4 was found in middle ear mucosa without inflammation. Local expression of TLR4 in middle ear tissues may contribute to both physiological and pathological processes in chronic otitis media. Our data suggest that TLR4 may play a significant role specifically in the pathophysiology of chronic otitis media.

## **876 Effect of PspA and Pneumolysin on the Viability and Virulence of Streptococcus Pneumoniae in the Chinchilla Model of Otitis Media**

Patricia Schachern<sup>1</sup>, Vladimir Tsuprun<sup>1</sup>, Sarah Goetz<sup>1</sup>, Sebahatin Cureoglu<sup>1</sup>, Steven Juhn<sup>1</sup>, David Briles<sup>2</sup>, Michael Paparella<sup>1,3</sup>, Patricia Ferrieri<sup>1</sup>

<sup>1</sup>University of Minnesota, <sup>2</sup>University of Alabama,

<sup>3</sup>Paparella Ear Head and Neck Institute

Pneumococcal proteins are potential strategies for the prevention and treatment of otitis media. We compared the viability and virulence of mutants deficient in pneumococcal surface protein A (PspA) and pneumolysin (Ply) with their wild-type parent strain, D39 type 2.

Chinchilla middle ears were inoculated with 0.5 cc of bacteria: 7 chinchillas with  $1 \times 10^6$  CFU/ml wild-type; 6 with  $6.6 \times 10^5$  CFU/ml Ply; and 6 with  $3.5 \times 10^6$  CFU/ml PspA. Animals were killed at 48 hours. Middle ear effusions (MEEs) were aspirated for culture. Bullae were embedded in epoxy resin, sectioned at a thickness of  $1 \mu\text{m}$ , and stained with toluidine blue. Histopathology of the round window membranes was compared among the 3 groups. Based on these results, we studied the viability of PspA in 30 chinchillas inoculated with  $2.7 \times 10^6$  CFU/ml PspA. Animals were killed at 6, 12, 18, 24, 30 and 36 hours after inoculation, for bacterial counts of MEEs. Bacterial counts were also done at 0, 2, 24, 30 and 43 hours on PspA grown in Todd Hewitt broth (THB).

At 48 hours after inoculation, CFUs in MEEs were significantly lower for the Ply and PspA mutants compared to the wild-type. Counts of the wild-type strain increased; counts of the Ply group remained near the initial inoculum level; there were no viable bacteria in the PspA group. Histopathology in both mutant groups was significantly less than in the wild-type. In the experiment with PspA over time, the majority of MEEs had no viable bacteria 30 hours after inoculation. In contrast, PspA remained viable in THB with an increase of about 2 logs at 43 hours.

Our findings revealed that the mutant deficient in PspA protein was less viable and virulent than the wild-type or Ply strains in chinchilla ears. The PspA strain appeared more vulnerable to host defenses. PspA protein plays a role in complement-mediated opsonization, and can prevent pneumococcal killing by binding host apolactoferrin.

Supported by NIH/NIDCD, R01 DC006452 and NIH/NIAID, R01 A1021458

## **877 Effect of Diesel Exhaust Particles on Human Middle Ear Epithelial Cells**

Sung Woon Kim<sup>1</sup>, Jae-Jun Song<sup>2</sup>, Jone Dae Lee<sup>1</sup>, Sung Won Chae<sup>3</sup>, June Choi<sup>3</sup>, Moo Kyun Park<sup>1</sup>

<sup>1</sup>Soonchunhyang University College of Medicine, Korea,

<sup>2</sup>Dongguk University Ilsan hospital, Ilsan, Korea, <sup>3</sup>Korea University College of Medicine, Korea

Objective: There are many epidemiologic studies that show the association of traffic-related air pollutants and otitis media. In addition, diesel exhaust particles (DEP)

cause inflammatory and allergic response in the airway. In this study, we investigate whether DEP has the cytotoxicity and can induce the inflammation or increase the expression of mucin in immortalized human middle ear epithelial cell lines (HMEECs).

Methods: After treatment of DEP on HMEECs, cell ability was measured by MTT assay. And then we observed the expression of inflammatory cytokines (TNF- $\alpha$ , COX-2) and mucin gene (MUC5AC, MUC5B) by quantitative real-time reverse transcriptase-polymerase chain reaction (RT-PCR) and western blotting.

Results: Cell viability test showed the exposure to more than  $80 \mu\text{g}/\text{mL}$  decreased cell viability. Increased inflammatory cytokines (TNF- $\alpha$ , COX-2) after DEP exposure were analyzed by means of RT-PCR and western blotting. DEP exposure increased the expression of MUC5AC, however it did not induce the expression of MUC5B in HMEECs by means of RT-PCR.

Conclusions: DEP decreased the cell viability and induce the inflammatory response and mucin gene expression in HMEECs. These findings add weight to the hypothesis that environmental diesel exposure is a risk factor of otitis media.

## **878 Effect of Vasopressin on Aquaporin and Inflammatory Gene Expression in Otitis Media**

Carol MacArthur<sup>1</sup>, Fran Hausman<sup>1</sup>, Beth Kempton<sup>1</sup>, Dennis Trune<sup>1</sup>

<sup>1</sup>OHSU

Effect of vasopressin on aquaporin and inflammatory gene expression in otitis media

Ion homeostasis genes are responsible for movement of ions and water in the various spaces in the inner ear and epithelium of the middle ear. Water homeostasis in the kidney and inner ear is regulated by the vasopressin-aquaporin 2 system, but little is known of the role of this regulatory system in the middle ear. Therefore, vasopressin regulation of ion homeostasis in the middle ear during acute otitis media was studied. Balb/c mice, aged 2 months, were trans-tympanically injected with heat-killed *Hemophilus influenzae* at a concentration of  $10^9$  cfu/ml. Four hours later they were trans-tympanically treated with  $5 \mu\text{l}$  of either PBS (controls) or vasopressin ( $50 \mu\text{g}/\text{kg}$ ). The middle ear tissues were harvested at 1, 6, 24 and 72 hours later and total RNA isolated. A separate group of *H. flu* inoculated mice were given vasopressin or PBS by intraperitoneal injection four hours after bacterial exposure and middle ears harvested one hour later. A total of 24 ion homeostasis genes were analyzed for expression with quantitative RT-PCR from the following gene families: aquaporins,  $\text{Na}^+, \text{K}^+$ -ATPase, tight junction claudins,  $\text{K}^+$  transport channels, epithelial  $\text{Na}^+$  channels, and gap junctions. Inflammatory genes were also analyzed. At one hour, aquaporins 2, 3, 4, were upregulated. Aquaporin 1 was downregulated at 6 hours. Aquaporin 3 was upregulated by vasopressin at 24 hours and then downregulated at 72 hours ( $p < 0.05$ ). Slc12a2 (a  $\text{Na}^+, \text{K}^+, \text{Cl}^-$  transporter) was upregulated at 24 hours. No other ion homeostasis genes showed significant changes. Cytokines

were downregulated by vasopressin exposure at one and 6 hour time points. The data suggest that there is a significant interaction between vasopressin and the aquaporin genes in the middle ear that may function in fluid regulation in the setting of otitis media. The downregulation of inflammatory genes may be the direct effect of vasopressin on gene expression or an indirect effect from the clearing of middle ear fluid.

[Research supported by NIH-NIDCD R01 DC009455]

### **879** Changes of Middle Ear Function and Auditory Brainstem Response in Otitis Media Model of Chinchilla - Measurement and Modeling

Rong Gan<sup>1</sup>, Xiyang Guan<sup>1</sup>, Xiangming Zhang<sup>1</sup>

<sup>1</sup>*School of Aerospace & Mechanical Engineering and Bioengineering Center, University of Oklahoma*

This study is to investigate the mechanism for acute otitis media (AOM) induced conductive hearing loss through experimental measurement on AOM model of chinchillas and 3-dimensional modeling of the chinchilla ear. Our hypothesis is that middle ear pressure, middle ear effusion and mechanical changes of soft tissues in the middle ear are three main factors which contribute to the hearing loss with AOM. The AOM was created in chinchillas by transbullar injection of Haemophilus influenzae strain 86-028NP. Three days post inoculation the wideband tympanometry, auditory brainstem response (ABR), and vibration of tympanic membrane (TM) were measured at three experimental stages: intact middle ear cavity (OM-1), middle ear pressure release (OM-2), and effusion drained (OM-3). The changes of middle ear admittance, ABR threshold, and TM displacement were observed in AOM ears in comparison with controls. A 3D finite element (FE) model of the chinchilla ear was created based on a set of micro-CT images of a chinchilla bulla with the resolution of 10  $\mu\text{m}$  in Amira software. Nonlinear material properties were employed for the middle ear soft tissues. The acoustic-structure-fluid coupled analysis was conducted in the FE model over the frequency range of 0.2-10 kHz in ANSYS. OM-3 ear was simulated by changing the thickness of the TM and round window membrane and the mechanical properties of soft tissues in FE model. OM-2 ear was simulated by adding various levels of viscous fluid in the middle ear cavity. OM-1 ear was further simulated by adding static pressure in the middle ear cavity based on OM-2 ear. The results obtained from experimental measurements and FE analysis confirm the hypothesis that middle ear pressure, effusion, and mechanical property changes of soft tissues are three main factors contributing to conductive hearing loss in AOM ears at different frequency ranges. (Supported by NIH R01DC011585)

### **880** A Physiological Function for the Candidate Tumor Suppressor Gene Ecr4 in Regulating Mucosal Hyperplasia During Otitis Media

Allen F. Ryan<sup>1,2</sup>, Arwa Kurabi<sup>1,3</sup>, Kwang Pak<sup>1,2</sup>, Andrew Baird<sup>3</sup>

<sup>1</sup>*Surgery/ENT, UCSD*, <sup>2</sup>*Research Service, San Diego VAMC*, <sup>3</sup>*Surgery/Trauma, UCSD*

Otitis media (OM) is characterized by intense proliferation and differentiation of mucosal epithelial cells that line the middle ear (ME) cavity after ME infection. We used whole-genome gene arrays on cDNAs prepared from tissues harvested prior to bacterial OM, as well as during the onset, progression and resolution phases, to identify differentially expressed candidate regulators of ME tissue proliferation. One gene with expression kinetics inversely proportional to those of mucosal proliferation was Ecr4, a newly recognized candidate tumor suppressor gene of no known physiological function. Encoded in the human genome by C2orf40, Ecr4 expression was normally present in the ME but strongly down-regulated during OM, just prior to the onset of mucosal hyperplasia. Ecr4 gene expression then recovered as hyperplasia ceased in the resolution phase of infection. A physiological function for the Ecr4 gene in regulating the ME response to infection was demonstrated in vitro by transducing Ecr4 into hyperproliferative mucosa harvested from the ME during OM and demonstrating that proliferation and migration was reduced compared to normal ME mucosa. Similarly, transduction of middle ear epithelial cells with the Ecr4 gene in vivo prior to infection prevented the natural decrease in endogenous Ecr4 gene expression and attenuated the mucosal response to infection. Together these data suggest a previously unrecognized physiological function for endogenous Ecr4 gene expression in ME biology and suggest that its down-regulation is a determinant of mucosal hyperplasia. If so, processes including the epigenetic methylation of its promoter that can regulate intrinsic Ecr4 gene expression may also influence the responsiveness of the ME to infection.

### **881** Innate Immunity in a Mouse Model for Otitis Media

Bin Yang<sup>1,2</sup>, Qihong Huang<sup>1</sup>, Feng-chan Han<sup>1,2</sup>, Yan Zhang<sup>1</sup>, Yiqing Zheng<sup>3</sup>, Linda Le<sup>1</sup>, Heping Yu<sup>1</sup>, Qing Zheng<sup>1</sup>

<sup>1</sup>*Case Western Reserve University*, <sup>2</sup>*Binzhou Medical University*, <sup>3</sup>*Sun Yat-Sen University*

We described a recessive mutation in the *Sh3pxd2b* gene (*Sh3pxd2b<sup>nee</sup>*) causing chronic otitis media and hearing impairment at various developmental stages (PLoS One. 2011;6(7):e22622). We found that all mice that had the *Sh3pxd2b<sup>nee</sup>* mutation went on to develop craniofacial dysmorphologies and subsequently otitis media, by as early as 11 days of age. We found noteworthy changes in cilia and goblet cells of the middle ear mucosa in *Sh3pxd2b<sup>nee</sup>* mutant mice using scanning electronic microscopy. By measuring craniofacial dimensions, we

determined for the first time in an animal model that this mouse has altered eustachian tube morphology consistent with a more horizontal position of the eustachian tube. All mutants were found to have hearing impairment. Expression of TNF- $\alpha$  and TLR2, which correlates with inflammation in otitis media, was up-regulated in the ears of mutant mice when examined by immunohistochemistry and semi-quantitative RT-PCR. We will measure motility of immune cells in the *Sh3pxd2b<sup>nee</sup>* mice and report to this meeting. The mouse model with a mutation in the *Sh3pxd2b* gene (*Sh3pxd2b<sup>nee</sup>*) mirrors craniofacial dysmorphology and otitis media in humans. This work was supported by the NIDCD grants R01DC007392, R01DC009246 (QYZ).

### **882 Tissue Remodeling Gene Expression in a Murine Model of Chronic Rhinosinusitis**

**Nathan Sautter<sup>1</sup>**, Dennis Trune<sup>2</sup>, Katherine Delaney<sup>2</sup>, Frances Hausman<sup>2</sup>

<sup>1</sup>*Oregon Health and Science University*, <sup>2</sup>*Oregon Hearing Research Center*

**Objective/Hypothesis:** The Matrix Metalloproteinase (MMP), Fibroblast Growth Factor (FGF) and Bone Morphogenetic Protein (BMP) families regulate tissue remodeling in many normal and pathophysiologic processes. We hypothesize that induction of chronic sinonasal inflammation will be associated with changes in regulation of these tissue remodeling cytokines.

**Methods:** Balb/c mice aged 8-12 weeks were sensitized and treated with intranasal *Aspergillus fumigatis* (AF) three times per week for 1 week, 3 weeks, 2 months and 3 months (n=8 each time point). Sinonasal tissues were evaluated for changes in MMP, FGF and BMP regulation using standard RT-PCR techniques. Additional snouts were processed for histology and immunohistochemistry. Untreated mouse snouts of identical age were used as controls.

**Results:** Significant upregulation of MMP8 was observed at 2 months, and MMP1a, MMP7, MMP8 and MMP12 were all significantly upregulated at 3 months. FGF3 was significantly upregulated at 3 weeks and 3 months, and FGF5, FGF6 and FGF8 were all significantly upregulated at 3 months. BMP8b and BMP9 were significantly upregulated at 3 months. Histologic analysis revealed mucosal, stromal and mucin gland hypertrophy, increased mucin production, and metaplasia with loss of cilia. Antibody staining was strongly positive in the AF treated group.

**Conclusion:** Induction of CRS is associated with time-dependent changes in tissue remodeling cytokine expression occurring in conjunction with inflammatory tissue changes in the mouse model. Antibody staining for upregulated cytokines suggests local production within the sinonasal mucosa. Further study is required to better understand the association between BMP, FGF and MMP regulation and tissue remodeling changes resulting from chronic inflammation.

### **883 Transcutaneous Vagus Nerve Stimulation Enhances Auditory Cortical Responsiveness in Tinnitus Patients**

Santeri Yrttiaho<sup>1,2</sup>, Mikael Bergholm<sup>1</sup>, Kari Malkavaara<sup>1</sup>, Jarmo Lehtimäki<sup>1</sup>, **Jukka Ylikoski<sup>1</sup>**

<sup>1</sup>*Tinnoff Inc.*, <sup>2</sup>*Biomag Laboratory*

**Background:** A recent animal study suggested that a combination of sound and vagus nerve stimulation (VNS) may reverse maladaptive neural plasticity related to tinnitus. Tracking changes in the human CNS in relation to electrical stimulation is, however, challenging due to substantial distortion in electro- or magnetoencephalography (EEG or MEG). We examined the effects of transcutaneous VNS (tVNS) on auditory cortical activation of patients with chronic tinnitus from artifact-corrected MEG data.

**Methods:** N1m responses around of 100 ms after the onset of probe stimuli were registered in the presence/absence of tVNS. tVNS was either applied continuously at 25 Hz to patients' left tragus (current above sensory threshold) or no electrical stimulation was applied. The auditory probe stimuli at a tinnitus frequency and of a comfortable loudness were presented with an MEG-compatible loudspeaker (Panphonics). The tVNS-related artifact was removed with a spatiotemporal signal space separation (tSSS) algorithm from the MEG data. Equivalent current dipoles (ECD) were then fitted to the auditory N1m responses. The N1m wave was analyzed in terms of source level amplitude and latency.

**Results:** Prominent auditory N1m responses were observed in both the 'tVNS on' and the 'tVNS off' condition. The ECD modeling results indicated a source location for these responses in the temporal lobe regions of both cortical hemispheres. The amplitude and the latency of the N1m increased (up to 41%) and decreased (up to 31 ms) with the application of the tVNS, respectively.

**Conclusions:** Auditory cortical activation was modulated by the application of tVNS, suggesting a link between the auditory system and the vagus nerve. In particular, cortical responsiveness to auditory stimuli, as reflected in the N1m response, was increased by tVNS. Thus, tVNS may have the potential of reducing aberrant activity in the auditory tract that is thought to be associated with tinnitus.

### **884 Simultaneous RTMS on the Auditory Cortex & Prefrontal Cortex in Patients with Tinnitus and Depression**

**Sera Park<sup>1</sup>**, Ju Hyun Jeon<sup>1</sup>, Seunghyun Koh<sup>1</sup>, Jae Young Choi<sup>1</sup>, Sang Cheol Kim<sup>1</sup>, Inseok Moon<sup>1</sup>

<sup>1</sup>*Yonsei University College of Medicine*

The objective was to determine whether low-frequency repetitive TMS improves tinnitus and the utility of PET for targeting treatment, and introduce the method and benefit of neuronavigational system for image-guided-TMS.

We tested the hypothesis that tinnitus loudness can be attenuated by low-frequency repetitive transcranial magnetic stimulation (rTMS) individually navigated to cortical areas with excessive tinnitus-related activity as assessed by [15O]H<sub>2</sub>O positron-emission tomography

(PET). Eleven patients with chronic tinnitus and depression underwent this combined functional imaging and rTMS-study. Group analysis of the PET data showed tinnitus-related increases of regional cerebral blood flow. Repetitive TMS was performed at 1 Hz and 90% of the motor threshold for navigated to the individual maximum of tinnitus-related cortical hyperactivity. The tinnitus score was improved after each 5 days of active rTMS, but the degree of depression using self-questionnaire score was negatively correlated.

These data show the feasibility and effectiveness of rTMS guided by individual functional imaging to induce attenuation of tinnitus.

### **885 Electrical Stimulation of the Amygdala to Modulate Noise-Induced Tinnitus and Changes in Cognition and Anxiety**

**Edward Pace**<sup>1</sup>, Xueguo Zhang<sup>1</sup>, Laura Lepczyk<sup>1</sup>, Pamela VandeVord<sup>2</sup>, Jinsheng Zhang<sup>1,3</sup>

<sup>1</sup>Department of Otolaryngology-Head and Neck Surgery, Wayne State University School of Medicine, <sup>2</sup>Department of Biomedical Engineering, Wayne State University College of Engineering, <sup>3</sup>Dept. of Communication Sciences & Disorders, Wayne State Univ. College of Liberal Arts & Sciences

The amygdala (AMG) is believed to be a pivotal limbic structure linking tinnitus to stress, emotion, and anxiety. This may be mediated by abundant connections between the AMG and the auditory and autonomic nervous systems. However, it remains to be determined how the induced tinnitus is associated with changes in limbic functions, and how the AMG modulates tinnitus and tinnitus-associated limbic functions. To answer this question, adult rats were tone-exposed (10 kHz, 3 hours, 90 or 116 dB, SPL). The induced tinnitus, spatial cognition and anxiety were evaluated using gap-detection acoustic startle reflex paradigm, the Morris water maze (MWM) and elevated plus maze (EPM), respectively. Animals' hearing was monitored using ABR and prepulse inhibition testing. Viable rats were then chronically implanted with electrodes in the AMG for electrical stimulation. Our results showed that both the 90- and 116 dB-exposed groups developed tinnitus, which appeared to strengthen over time. ABR data revealed that 116 dB-exposed rats were the only ones to sustain threshold shifts. MWM and EPM results suggested compromised spatial learning and memory and elevated anxiety levels in tinnitus(+) rats. Electrical stimulation of the AMG, including all and selected channel stimulation, yielded moderate suppressive effects on tinnitus both during and immediately after stimulation. In summary, our results suggest that limbic-related functioning may be compromised by strong, long-term tinnitus, and that electrically stimulating the AMG may modulate that tinnitus to some extent.

### **886 Molecular Basis of a Relation of Tinnitus and Stress**

**Marlies Knipper**<sup>1</sup>, Wibke Singer<sup>1</sup>, Annalisa Zuccotti<sup>1</sup>, Mirko Jaumann<sup>1</sup>, Christoph Franz<sup>1</sup>, Hao Xiong<sup>1</sup>, Rama Panford-Walsh<sup>1</sup>, Lukas Rüttiger<sup>1</sup>

<sup>1</sup>Hearing Research Centre Tuebingen

Tinnitus is a non-curable stress-related brain disorder, that is mostly noise-induced and whose origin is unknown. We have addressed the molecular and physiological basis of this disease using a combined approach that included behaviorally tested tinnitus (Rüttiger et al., Knipper, *Hear Res* 2003), hearing measurements (including DPOAEs, ABRs and ABR wave analysis) and markers that trace network activity (Arc/Arg3.1). We also included stress priming in animal models. Data analysed the first time equally hearing impaired animals that were behaviourally distinguished in hearing impaired animals with and without tinnitus. We compared animals between the periphery of the cochlea up to the auditory cortex, including the limbic system. We unraveled a tinnitus specific trait that may explain the relation of tinnitus and stress. The findings are discussed in the context of the role of stress for tinnitus and other mood-related disorders

### **887 Relationship of Tinnitus Pitch and Audiogram Shape in Patients with Chronic Tinnitus**

**Tobias Kleinjung**<sup>1,2</sup>, Berthold Langguth<sup>3</sup>, Peter Kreuzer<sup>3</sup>, Michael Landgrebe<sup>3</sup>, Veronika Vielsmeier<sup>2</sup>, Martin Schecklmann<sup>3</sup>

<sup>1</sup>University of Zurich, Department of Otorhinolaryngology,

<sup>2</sup>University of Regensburg, Department of Otorhinolaryngology, <sup>3</sup>University of Regensburg, Department of Psychiatry and Psychotherapy

Introduction

It still remains unclear, whether the main responsible mechanism for tinnitus generation is reduced lateral inhibition or homeostatic plasticity. On a perceptual level these different mechanisms should be reflected by the relation between the individual hearing curve and the perceived tinnitus pitch. Whereas some studies found the tinnitus spectrum corresponding to the maximum hearing loss, others stressed the relevance of the edge frequency. This study investigates the relationship between tinnitus pitch and audiometric slope in a large sample.

Subjects and methods

A dataset of 105 patients including pure tone audiometry, high frequency audiometry and tinnitus pitch matching was analyzed. The tinnitus frequency was compared with the frequency of maximum hearing loss and the edge of the audiogram (steepest hearing loss) by t-tests and correlation coefficients. These analyses were performed for the whole group and for certain sub-groups (pure tone tinnitus vs. narrow bandnoise like tinnitus; unilateral vs. bilateral tinnitus).

Results

Tinnitus pitch correlated significantly with frequency of maximum hearing loss, but not with the edge frequency and also differed from the edge frequency. Sub-group analyses (uni- and bilateral, tinnitus character, slope

steepness) revealed identical results except for the subgroup with low audiometric slope which revealed no association of pitch neither with edge nor with maximum hearing loss.

#### Conclusion

Results of our study confirm a relationship between tinnitus pitch and maximal hearing loss as compared to the edge frequency, suggesting that tinnitus is rather a fill-in-phenomenon resulting from homeostatic mechanisms, than the result of deficient lateral inhibition. The study further underlines the value of high-frequency audiometry as an important detail in the exploration of a tinnitus patient.

### **888** Hyperacusis Is Associated with Personality Traits

Karin Villaume<sup>1</sup>, Barbara Canlon<sup>1</sup>, Dan Hasson<sup>1,2</sup>  
<sup>1</sup>Karolinska Institutet, <sup>2</sup>Stress Research Institute at Stockholm University

Hyperacusis is a public health disorder that causes distress and disability, but the etiology is not yet known. It is feasible that personality traits may influence hyperacusis, but no one has investigated this at present. Thus, the aim of this study is to explore possible associations between personality traits and hyperacusis.

Hyperacusis was assessed with the Hyperacusis Questionnaire (HQ) by Khalfa et al. (2002), and with uncomfortable loudness levels (ULL's) using pure tones. Personality was measured with the HP51 inventory (Gustavsson et al., 2003). The sample consisted of 348 individuals (140 men and 208 women; aged 23 -71 years). Moderate correlations were found between the personality trait negative affectivity (a facet of neuroticism) and dimensions of the HQ (Spearman's rho,  $r$  range = 0.35 — 0.48,  $p < 0.0001$ ). Weak correlations were found between ULL's on left and right ear 0.5-4 kHz ( $-0.15$  —  $-0.23$ ,  $p < 0.01$ ). Hedonic capacity (a facet of extraversion) was significantly correlated with the HQ ( $r$  range =  $-0.04$  —  $-0.12$ ,  $p < 0.05$ ) but not with the ULL's (ns). Impulsivity was correlated with both the HQ ( $r$  range =  $0.11$  —  $0.21$ ,  $p < 0.05$ ) and the ULL's ( $-0.10$  —  $-0.13$ ,  $p < 0.05$ ; 0.5 kHz, 1 kHz left and 2 kHz left = ns).

These results indicate that there is a relationship between personality traits and the severity of hyperacusis. In conclusion, these findings imply that personality traits need to be considered in the diagnosis and treatment of hyperacusis.

### **889** The Auditory Steady State Response Evoked by 40-Hz Amplitude Modulated Sounds Is Frequency Dependent in Tinnitus But N1 Is Not

Larry E. Roberts<sup>1</sup>, Daniel J. Bosnyak<sup>1</sup>, Ian C. Bruce<sup>1</sup>  
<sup>1</sup>McMaster University

Sound frequencies comprising the tinnitus spectrum track the region of auditory threshold shift (the tinnitus frequency region or TFR), and residual inhibition (RI) produced by band pass noise maskers is maximal when their center frequencies (CFs) are in the same region (Roberts et al.,

JARO 2008, 9:417-435). We investigated whether neural correlates of tinnitus reveal a similar frequency dependence. Neural representations were probed in subjects with chronic tinnitus ( $n = 30$ ) using 40-Hz AM sounds with carrier frequencies either in the TFR (5.0 kHz) or below it (0.5 kHz). Tones were presented following silence when tinnitus subjects experienced their tinnitus (no-masking condition) or following a band pass noise masker (CF 5 kHz) that produced tinnitus suppression (RI). Probe tones and maskers were matched in loudness to a 1 kHz pure tone at 65 dB SL to control for loudness recruitment. The 40-Hz auditory steady-state response (ASSR, localizing to primary auditory cortex) and the N1 transient response (localizing to secondary cortex) were extracted from 128 channel EEG. Age-matched controls without tinnitus ( $n=29$ ) were identically studied.

N1 amplitude was larger in the tinnitus group compared to controls at each probe frequency in both masking conditions ( $p = 0.023$ , no frequency dependence). Masking decreased N1 in all conditions ( $p = 0.000$ ). In contrast, ASSR amplitude was larger in tinnitus subjects than in controls when neural representations were probed below the TFR without masking (probe frequency 0.5 kHz,  $p = 0.034$ ), but the reverse was true for probes in the TFR (5.0 kHz,  $p = 0.045$ ) revealing frequency dependence in this measure. Masking increased ASSR amplitude in tinnitus subjects in the TFR ( $p = 0.005$ ), returning it toward control levels in this frequency region. Variability in sound thresholds and levels did not correlate with these changes. Possible roles for auditory attention and synchronous neural activity in the TFR are considered.

### **890** The Effects of Tinnitus on Sound Localization Ability and Gaps-In-Noise Performance

Hyun joon Shim<sup>1</sup>, Yong-Hwi An<sup>1</sup>, So Young Jin<sup>1</sup>  
<sup>1</sup>Department of Otolaryngology, Eulji Medical Center, Eulji University, Seoul, Korea

Objectives: 1) To investigate whether tinnitus affects sound localization ability.

2) To investigate whether tinnitus affects Gaps-In-Noise (GIN) Performance.

Methods: 1) We performed a sound localization test (SLT) with seven speakers positioned in a semicircle on the horizontal plane at a distance of 1 m from the subject, at 30° intervals. Subjects (40 tinnitus patients (36.7±14.3 years; <20 dB HL), and 40 controls (39.3±12.9 years; <20 dB HL)) were asked to identify the stimulus-presenting speaker, through a forced-choice procedure. The error score was calculated by scoring 1 point for each 30° of difference between the stimulus-presenting speaker and the speaker identified by the subject. 2) GIN test were performed in 120 ears of 60 subjects (43.6±17.6 years) with unilateral tinnitus who showed symmetric hearing ability within 10 dB HL difference at 0.25, 0.5, 1, 2, 3, 4 and 8 kHz (tinnitus side, 14.6±11.2 dB HL; non-tinnitus side 15.1±11.5 dB HL). Comparisons were made between the results of GIN test of tinnitus side and non-tinnitus side.

Results: 1) The mean SLT total error score of the tinnitus group (18.8±9.2) was significantly higher than that of the control group (13.1± 7.5) ( $p < 0.05$ ). Regarding SLT responses for stimulation from speakers located at each side of the listener, mean total error score in patients with tinnitus on the same side as the speaker was higher than that in patients with opposite side or bilateral tinnitus. Age showed a positive correlation with total error score in the tinnitus ( $r = 0.44$ ,  $p < 0.05$ ) and control groups ( $r = 0.35$ ,  $p < 0.05$ ). 2) The average percentage of correct answers in tinnitus ear (67.3±5.5%) was slightly less than that in non-tinnitus ear (70.0±5.5%) ( $<0.05$ ). However, the average of GIN thresholds in tinnitus ear and non-tinnitus ear were not significantly different (5.2±0.6 ms vs. 5.0±0.6 ms). Neither the GIN threshold nor percentage of correct answer in tinnitus ear has correlation to pure tone average, SRT, SDS, frequency of tinnitus, loudness of tinnitus and THI score ( $>0.05$ ).

Conclusions: We consider that tinnitus interferes with sound localization ability and that interference is worse for sound originating from the same side as the tinnitus. However, we found no evidence which supported the influence of unilateral tinnitus on auditory temporal processing.

### **891 Correlation Between Head Shaking After Nystagmus Testing and Affected Side in Horizontal Canal Benign Paroxysmal Positional Vertigo**

Munetaka Ushio<sup>1</sup>, Naoya Egami<sup>1</sup>, Shinichi Iwasaki<sup>1</sup>, Tatsuya Yamasoba<sup>1</sup>  
<sup>1</sup>University of Tokyo

For horizontal canal benign paroxysmal positional vertigo (BPPV), Lempert's otolith repositioning maneuver is usually performed in a clinic. However, the affected side of horizontal canal BPPV sometimes difficult to estimate in comparison with posterior canal BPPV. Mild canal paresis is seen in approximately half of horizontal canal BPPV patients, suggesting the blockage of endolymphatic flow in the semicircular canal or transient changes in the vestibular nuclei. Head shaking after nystagmus (HSN) is mainly exhibited in patients showing canal paresis. We hypothesized that the affected side in horizontal canal BPPV can be estimated using a HSN test.

Thirteen patients were diagnosed as having horizontal canal BPPV between June 2009 and August 2011, based on history, physical examinations and findings of nystagmus. Underlying pathology in these 13 patients was idiopathic canalithiasis in 8, canalithiasis with preceding inner ear disorders in 2, idiopathic cupulolithiasis in 2 and cupulolithiasis with preceding inner ear disorders in 1. Under electronystagmography, eye movements during the positional nystagmus test, HSN test and the caloric test were recorded. In canalithiasis, the side showing larger geotrophic nystagmus was considered as the affected side. In cupulolithiasis, the side showing smaller apogeotrophic nystagmus was considered as the affected side.

In 7 of the 8 patients with idiopathic canalithiasis, the affected side was determined based on nystagmus

findings. Among them, 6 patients (including 3 patients with canal paresis in the affected side) showed unaffected side-beating HSN. One showed no HSN. In the 2 patients with idiopathic cupulolithiasis, the affected side was determined and no canal paresis was seen. Both exhibited affected side-beating HSN. No tendency was seen in patients with preceding inner ear disorders.

Our results suggest that the HSN test can contribute to estimating the affected side in cases of horizontal canal BPPV.

### **892 Optimizing Ocular Vestibular Evoked Myogenic Potential Testing for Superior Semicircular Canal Dehiscence Syndrome: Electrode Placement**

M. Geraldine Zuniga<sup>1,2</sup>, Marcela Davalos-Bichara<sup>1,2</sup>, John P. Carey<sup>1</sup>, Michael C. Schubert<sup>1</sup>, Kristen L. Janky<sup>1,3</sup>

<sup>1</sup>Johns Hopkins University, Otolaryngology – Head and Neck Surgery, Baltimore, MD, <sup>2</sup>Escuela de Medicina Ignacio A. Santos del Tecnológico de Monterrey, Mexico, <sup>3</sup>Boys Town National Research Hospital, Omaha, NE

Purpose: To compare the standard montage for ocular vestibular evoked myogenic potentials (oVEMP) with a montage using a reference electrode on the chin in order to segregate patients with superior semicircular canal dehiscence syndrome (SCDS) from controls.

Subjects: Nine healthy volunteers with no prior history of neurotological complaints and eight patients with a diagnosis of SCDS based on clinical presentation, audiometry and CT imaging

Methods: OVEMPs were recorded in response to 500 Hz tone bursts using 2 different electrode montages. Montage 1 (standard) consisted of an active electrode placed approximately 3 mm below each eye, a reference electrode centered 2 cm below each active electrode and a ground electrode over the sternum. Montage 2 consisted of an active electrode placed approximately 3 mm below each eye, a single reference electrode placed on the chin and a ground electrode over the sternum. For either montage, subjects maintained 30 degree upgaze during testing. Outcome parameters: N10 amplitudes and peak-to-peak amplitudes from both control ears and from the SCDS ears.

Results: For either montage, the separation between oVEMP amplitudes in SCDS patients and controls was significant ( $p < 0.001$ ), but the separation was greater for N10 than for peak-to-peak measures. Recordings with montage 1 revealed an overlap between the range of N10 amplitudes of control (1.8-14.25 microV) and SCDS ears (11.4-36.3 microV). Montage 2, with the chin reference electrode, eliminated overlap in the range of N10 amplitudes between control (5.4-17.8 microV) and SCDS ears (19.3-55.1 microV).

Conclusion: Our findings suggest optimal segregation between control and SCDS ears can be achieved using the reference electrode on the chin and analyzing the n10 amplitudes.

**893 Frequency Tuning Analysis of Vestibular-Evoked Myogenic Potentials Recorded from Multiple Sites of the Sternocleidomastoid Muscles (CVEMP) in Normal Human Subjects**

Wei Wei<sup>1</sup>, Ben Jeffcoat<sup>1</sup>, William Mustain<sup>1</sup>, Yougou Xu<sup>1</sup>, Hong Zhu<sup>1</sup>, Thomas Eby<sup>1</sup>, **Wu Zhou**<sup>1,2</sup>

<sup>1</sup>*Dept Otolaryngology and Communicative Sciences, University of Mississippi Medical Center Jackson MS,*  
<sup>2</sup>*Department of Neurology, Department of Neurobiology and Anatomical Sciences*

Tone burst-evoked myogenic potentials recorded from sternocleidomastoid muscles (cervical VEMP or cVEMP) are widely used clinically to assess vestibular function (for a review, Rosengren et al., 2010). Studies have shown that cVEMP frequency tuning is a useful tool to assess progress of vestibular disorders (for a review, Rauch, 2006). In the present study, we extended frequency tuning analysis of the cVEMPs by constructing detailed tuning curves and characterizing their dependence on three factors including SCM tonic level, sound intensity and recording site along the SCM in normal human subjects. Here we report two main findings. First, we found that tuning curves constructed with more tone frequencies exhibited two distinct peaks, which could not be modeled by a single mass spring system (Todd, 2000). Instead, they were better modeled as linear summation of two mass spring systems, which resonate at ~300Hz and ~1000Hz, respectively. While cVEMP tuning peak frequency was not affected by SCM tonic level, sound intensity and location of recording site on the SCM, cVEMP tuning sharpness was increased at lower sound intensities. Second, we found that polarity of the cVEMP responses at the lower quarter of the SCM was opposite to that at the two upper sites. While the typical positive-negative cVEMP responses at the upper sites reflect inhibition of SCM motoneurons by ipsilateral sound stimulation, the negative-positive cVEMP responses at the lower quarter may reflect excitation of SCM motoneurons by the same stimulation, which support the hypothesis of compartmentation of nerve innervation of the SCM. These results suggest that there are multiple types of cVEMP responses that are generated by separate generators with different resonance frequencies and are also mediated by different vestibular-colic reflex pathways. Future studies are to investigate the implications of these results on development of more specific VEMP tests.

**894 Influences of Altered Neck Muscles and Low Extremities Information on Head Tilt Response Test**

**Alejo Suarez**<sup>1</sup>, Dario Geisinger<sup>1</sup>, Enrique Ferreira<sup>1,2</sup>, Cecilia San Roman<sup>1</sup>, Gonzalo Sotta<sup>1</sup>, Hamlet Suarez<sup>1</sup>  
<sup>1</sup>*Laboratorio de Otoneurología. Facultad de Medicina, CLAEH, Uruguay.,* <sup>2</sup>*Depto. de Ingeniería Eléctrica. Universidad Católica del Uruguay.*

Perception of earth (gravitational)-vertical is determined by the correct central fusion of information arriving from the retina, vestibular end organs and different somatosensory sensors. Different conditions may lead to an altered

perception and estimation of verticality, although there are some controversies about its interpretation and correlation with a specific disfunction. Previous communications, showed changes in the perception of gravitational vertical when vibration is applied to the neck muscles.

We presented earlier a dynamic test to evaluate subject's perception of verticality, named Head Tilt Response (HTR) (J Vestib Res. 2010;20(5):381-9).

5 parameters are evaluated to characterized to analyze the HTT response: Steady state error: Steady state angle error between the bar position and head position. Rise time: Time (in seconds) it takes for the subject to move its head from 5% to 95% of the bar step. Overshoot: Some subjects may overreact to a bar angle change and tilt their heads a larger angle than necessary before coming down to the right value. The value of this maximum head tilt as a percentage of the right angle needed is usually called overshoot. Settling time: Time (in seconds) to reach its steady state angle within 2%. Delay time: Time it takes for the subject to react to a step in the bar angle.

In the present work we look at the influence of a disturbance in the information from 2 different somatosensory cues, in perception of verticality through the HTR: muscular neck afference and an altered base of support. The test was performed in 4 different conditions, while the subject is in a standing position: with no external perturbation, with a foam as the base of support, applying vibration in subjects' neck, and with the last two conditions applied together. 2 different population are studied, a normal control group and a group of patients with unilateral peripheral vestibular loss, clinically compensated. We will present data showing some differences in the HTR response according to the condition analyzed. Also, differences between normal subjects and those with a compensated unilateral peripheral vestibular deficit in HTR response will be discussed.

**895 Ocular Vestibular Evoked Myogenic Potentials in Response to Midline Skull Taps: Input-Output Function of a Utricular Reflex**

**M. Geraldine Zuniga**<sup>1,2</sup>, Kimanh Nguyen<sup>1,3</sup>, Miriam Welgampola<sup>4</sup>, John P. Carey<sup>1</sup>

<sup>1</sup>*Johns Hopkins University, Otolaryngology – Head and Neck Surgery, Baltimore, MD,* <sup>2</sup>*Escuela de Medicina Ignacio A. Santos del Tecnológico de Monterrey, Mexico,* <sup>3</sup>*University of California, Los Angeles, Head and Neck Surgery, Los Angeles, CA,* <sup>4</sup>*Institute of Clinical Neurosciences, Royal Prince Alfred Hospital, Sydney University, Australia*

Background: Previous works suggest that the ocular vestibular evoked myogenic potentials (oVEMP) in response to midline skull taps elicits a utriculo-ocular reflex. The Mini-Shaker has been proposed to deliver a repeatable stimulus for this test.

Objectives: (1) To analyze the effects of intensity (force level) of the Mini-Shaker on oVEMP n10 and peak-to-peak amplitudes. (2) To determine if there is an optimal intensity for oVEMP testing.

Methods: Six healthy volunteers (age range 25-46 y) with no prior history of neurotological complaints underwent

oVEMP testing with midline taps with a repetition rate of 5 pulses per second. Stimuli were delivered by a Brüel & Kjaer Mini-Shaker Type 4810. Intensities at the skull were measured with a Brüel & Kjaer force transducer type 8230-001 and ranged from 0.6-8 Newtons (N).

Results: Response grew linearly with stimulus intensity in this range ( $r = 0.87$ ,  $p < 0.001$ ). OVEMP responses were absent in all ears at 0.6 N, and present in all ears at 2 N and above. Greatest mean ( $\pm$  SD) amplitudes were recorded at 6 N (n10: 6.3 microV  $\pm$  2.6; peak-to-peak: 14.1 microV  $\pm$  4.7) and 8 N (n10: 8.6 microV  $\pm$  3.1; peak-to-peak: 19.6 microV  $\pm$  7.2). Signal-to-noise ratio (SNR) ranged from 1.0-3.0 and was best for 6 N.

Conclusion: Greater stimulus intensity delivered by the Mini-shaker produces greater oVEMP amplitude, but also more variability between subjects. When measuring suprathreshold responses across groups, 6 N may be the stimulus intensity with the best SNR for testing this utricular reflex.

### **[896] Gait Analysis of Peripheral Vestibular Loss Patients**

**Mi Joo Kim**<sup>1</sup>, TaeWoo Kim<sup>1</sup>, SeoJin Jang<sup>1</sup>, Ah Ram Yu<sup>1</sup>, Eun Ji Lee<sup>1</sup>, Gyu Cheol Han<sup>1</sup>, Soo-Chan Kim<sup>2</sup>  
<sup>1</sup>Gachon University, <sup>2</sup>Hankyong National University

Objective:

Out of all the outpatients complaining dizziness, more than half of them showed negative diagnosis according to nystagmus and position change. As such patients increase, developing a device that monitors vestibular function in long term is needed for accurate diagnosis. This study focuses on developing diagnostic and monitoring device that is inexpensive and portable, and has high test sensitivity. The intention of the device is to perform objective, fast, and manageable test that patients can record by themselves. In addition, various sensors would be added to operate the device in remote clinic condition.

Methodology:

Participated patients were a total 80, of 40 patients had acute peripheral vestibular loss, and of 40 were normal. We used four pieces, 3-axis MotionNode system each of sensors were attached to central forehead, center of waist, center of both shin in front. All the information from sensors were lively recorded to mobile mini computer (W2, Cowon, Seoul, Korea) with windows 7 which attached in waist. The protocol was 40m rectilinear walking test for 2 times with open-eyes. Raw data from gyro sensors and accelerometers were analyzed in both legs by swing & stance phase of gait cycle.

Result:

All patients had more than 2 dominant frequencies which were distinctive in pitch(z-axis) rotation. Those dominant frequencies showed unclear boundary between them regardless of the position of sensors. The patients with peripheral vestibular loss had relatively bigger roll motion compared to the normal group. In addition to that, the patients showed swing phase prolongation in lesion side and irregularity of gait cycle in 40m walking test as well.

Conclusion:

We think it would be remarkable parameter of vestibular screening test using MotionNode system in accordance with gait cycle and frequency analysis which reflects localization of disease even taking into account age differences and each individual gait characteristics.

### **[897] Latency of the Long Latency Vestibular Electrical Evoked Potential in Control Human Subjects Shows Stimulus Strength Dependency**

**Benn Smith**<sup>1</sup>, Michael Cevette<sup>1</sup>, Jan Stepanek<sup>1</sup>, Daniela Cocco<sup>1</sup>, Gaurav Pradhan<sup>1</sup>, Kenneth Brookler<sup>1</sup>, David Zappala<sup>2</sup>, Mark Ross<sup>1</sup>

<sup>1</sup>Mayo Clinic in Arizona, <sup>2</sup>Mayo Clinic in Florida

Introduction: A technique for obtaining a human vestibular electrical evoked potential (VEEP) has recently been reported.

Objective: To describe characteristics of the human VEEP long latency waveform including the novel property of dependency of latency on electrical stimulus strength.

Methods: Adult control subjects (23 ears) were studied with transcutaneous bipolar electrical stimulation of the mastoid region. Evoked potentials were recorded over Cz-A1/2 using standard signal averaging techniques. Late responses were produced at 2.5 mA and, for 5 of these subjects, at a range of current strengths from 1 to 25 mA.

Results: In control subjects, mastoid stimulation at 2.5 mA yielded Cz-A1/2 late responses of median amplitude 61 microvolts (range 1.6-104; SD 25) and of median latency of 10.2 ms (range 6.0-13.3; SD 4.9). This response progressively increased in latency from 8.6 to 22.6 ms (mean latency increase of 1.3 ms/mA) as current strength was raised in 10 incremental steps from threshold current level in all 5 subjects studied in this way.

Conclusions: (1) In neurologically normal adult control subjects reproducible long latency VEEP responses can be obtained reliably, (2) the VEEP late response latency increases incrementally with increasing current strength as previously reported in animal experiments, (3) the current strength-response pattern of the VEEP late response in human control subjects may be a reflection of increasing inhibition mediated by vestibular efferent pathways, and (4) future studies are needed to define further the nature and origin of the VEEP late response in health and disease.

### **[898] Is There a Relationship Between Gait Scores (Speed, Functional Gait Assessment, Dynamic Gait Index) and Balance Accelerometry Measure (BAM) Scores in Persons with and Without Vestibular Disorders?**

**Susan Whitney**<sup>1</sup>, Gregory Marchetti<sup>1,2</sup>, Chia-Cheng Lin<sup>1</sup>, Jennica Roche<sup>1</sup>, Gabriel Furman<sup>1</sup>, Mark Musolino<sup>3</sup>, Mark Redfern<sup>1</sup>

<sup>1</sup>University of Pittsburgh, <sup>2</sup>Duquesne University,

<sup>3</sup>Crossroads Consulting LLC

The purpose of the project was to determine if there was a relationship between BAM scores and gait in persons with and without vestibular dysfunction. Gait consisted of a

timed 6 m walk, the functional gait assessment (FGA) and the Dynamic Gait Index (DGI). The BAM, developed as part of the NIH Toolbox project, measures standing balance. Eighty-four healthy subjects and 18 subjects with peripheral vestibular disorders were tested. Subjects stood in Romberg eyes open (EO) and eyes closed (EC), on foam (EO/EC), and in tandem Romberg (EO/EC). The BAM accelerometer captured mediolateral and anteroposterior accelerations of sway, quantified using path length (mGs) for the 40 s trials. The healthy group had significantly faster gait speeds and better DGI and FGA scores (all  $p < 0.02$ ) than subjects with vestibular disorders. Mean path length sway was significantly greater in the group with vestibular disorders only on EC/foam compared with healthy subjects ( $p < 0.03$ ). Total FGA score was significantly associated with sway in the EC/firm surface ( $r = 0.38$ ,  $p < 0.01$ ), EO/foam surface ( $r = 0.33$ ,  $p < 0.01$ ), EC/foam surface ( $r = 0.41$ ,  $p < 0.01$ ), and the EO/tandem stance condition ( $r = 0.33$ ,  $p < 0.01$ ) in all subjects. Total DGI score was weakly correlated with sway under the EC/firm, EO/foam, EC/foam and EO/tandem condition (all  $p < 0.02$ ) among all subjects. Gait speed was weakly but significantly correlated with sway under EC/firm surface and EO/foam surface conditions ( $r = 0.20-0.21$ ,  $p < 0.04$ ) in all subjects. There were weak to moderate associations between gait and BAM scores. These relationships are for a cross-sectional evaluation of patients with chronic symptoms. A prospective study of persons with acute symptoms is planned. Standing postural control and functional gait are associated in patients with chronic peripheral vestibular disorders.

Funded by the Blueprint for Neuroscience Research, National Institutes of Health, under contract HHS-N-260-2006 00007-C.

### **899** Variability of Advanced Analytic Measurements by Posturography in Normal Subjects

Michel Toupet<sup>1</sup>, Alexis Bozorg Grayeli<sup>2</sup>

<sup>1</sup>Centre d'Explorations Fonctionnelles Otoneurologiques & IRON, Paris, France, <sup>2</sup>Otolaryngology Department, Beaujon Hospital, Inserm UMRS867, Paris Diderot University, Paris, France

Introduction: Balance is the result of a dynamic process involving multiple sensory inputs and several types of strategies. The aim of this study was to evaluate the intra- and inter individual variability of several posturography parameters in normal subjects.

Materials and Methods: Twenty-one adult subjects (15 females and 6 males, mean age: 42 years) with no balance disorders and no history of neurological or vestibular disorders were included in this prospective study. Posturography was carried out twice at 15 min. of interval (test-retest), in the morning (9:00 a.m.), at noon and in the evening (7:00 p.m.), on 3 consecutive days in a week period. Posturography was performed by a conventional plate bearing 3 pressure sensors (Balance Quest, Micromedical Technologies, Chatham, Ma). Tests were conducted in 3 conditions on stable and unstable

plate: Eyes open, closed, and standardized optokinetic stimulation (in an increasing difficulty order). Each trial (6 conditions) lasted 30 seconds. The sampling rate was set at 50 Hz. The following parameters were recorded: Total displacement length (mm), confidence ellipse surface containing 90% of all recorded positions (mm<sup>2</sup>), Length/Surface (mm<sup>-1</sup>). The score of energy consumption was assessed in 3 frequency bands via postural stability index (PSI), postural control index (PCI) and postural instability index (PII) (Posturopro® Software, Inserm, Marseilles, France). Moreover, fractal (% of Hausdorff points) and diffusion analysis (critical time and amplitude) were conducted. Finally, sensory preference and visual dependency indexes were calculated based on surface measurements.

Results: Relative standard deviation (RSD) representing variability increased with difficulty of the conditions for length and surface measurements. RSD also increased for PSI and PCI in high frequency (1.5-10 Hz). Repeatability as evaluated by test-retest correlation also decreased in difficult conditions for length, surface, and PII. Test and retest were not correlated for sensory preference and visual dependency indexes. Significant intra individual variability was observed for the length, and sensory preferences as a function of the test schedule.

Conclusion: Posturography parameters in normal individuals showed significant inter- and intra individual variability. This variability is probably due to different postural strategies adopted during the test, the patient's learning curve, and his (or her) general condition at the time of the test. These results suggest that several trials are necessary to define the postural performance in a patient especially during rehabilitation.

### **900** Simple Screening Tests of Balance Function for Epidemiological Studies

Helen Cohen<sup>1</sup>, Ajitkumar P Mulavara<sup>2</sup>, Brian T Peters<sup>3</sup>, Christopher Miller<sup>3</sup>, Haleh Sangi-Haghpeykar<sup>1</sup>, Jacob J Bloomberg<sup>4</sup>

<sup>1</sup>Baylor College of Medicine, <sup>2</sup>Universities Space Research Association, <sup>3</sup>Wyle Laboratories, <sup>4</sup>NASA/Johnson Space Center

Computerized dynamic posturography (CDP) system has been used as a gold standard for assessing vestibular contributions to postural control to delineate normals from clinical populations, however, CDP is not useful for population-scale epidemiological studies and for other remote locations such as landing sites after space flight where limited test facilities are available. Therefore simple but well validated screening tests of balance control are needed. We compared the postural control performance on standing balance tests using pitch sway referencing with that on a compliant foam surface with eyes open and closed without and with head movements at 0.33 Hz in the pitch and yaw planes. Kinematic measures were obtained from inertial motion sensors attached to the head and torso during the performance of these tests. Fifteen normal subjects with no history of vestibular or other neurologic disorders showed significant differences between the tests when comparing their trunk angular velocities and

accelerations in all planes of motion especially on the pitch sway referenced/compliant surface and eyes closed conditions. This finding supports other studies in the literature that using a foam support surface provides multidirectional sway than pitch ankle-sway referencing testing does on the CDP. We then tested 45 patients with unilateral caloric weakness or post-acoustic neuroma resection, and 60 normals aged 21 to 79 yrs, using the compliant foam tests. Preliminary analysis of the trunk accelerations and angular velocities between patients and normals show plane specific differences depending on the direction of head movements. Comparing the normal and clinical populations, dynamic head movement in the pitch plane during testing was the more sensitive and specific. This finding supports other studies in the literature that dynamic head movement while standing on foam may improve sensitivity of the tests for balance control. Further, results of a small-scale epidemiologic study will also be presented.

Supported by NIH grant R01DC009031 and DC009031-02S1 to HSC and in part by a grant from the National Space Biomedical Research Institute through NASA NCC 9-58 (SA02001) to APM.

### **901 Backward Locomotion as a Predictor of Falls**

**Marcelo Davalos-Bichara**<sup>1,2</sup>, M. Geraldine Zuniga<sup>1,2</sup>, Yuri Agrawal<sup>1</sup>, John P. Carey<sup>1</sup>, Michael C. Schubert<sup>1</sup>

<sup>1</sup>Otolaryngology – Head and Neck Surgery. The Johns Hopkins School of Medicine. Baltimore, MD., <sup>2</sup>Escuela de Medicina Ignacio A. Santos del Tecnológico de Monterrey. Monterrey, Mexico

**Background:** The vestibular system plays an important role in locomotion. Patients with vestibular pathology have an increase in fall frequency. This study has two phases: 1) investigate the characteristics of backward walking in two groups of patients with complaints of dizziness and imbalance and controls; 2) identify gait parameters from forward and backward walking that may predict fall risk.

**Methods:** We measured backward and forward walking in three groups: n=16 healthy volunteers (mean 45 yrs, range 24-81), n=14 patients with a peripheral vestibular lesion (mean 69 yrs, range 43-94), and n=15 patients with non-vestibular dizziness (mean 72 yrs, range 36-89). Subjects performed 2 forward and 2 backward walks over the GAITRite walkway at their preferred gait speed looking straight ahead. Participants are being followed up over a one year period to track fall incidence.

**Results:** Age significantly differed among groups with controls being younger than patients (p<0.001). Backward walking was always slower than forward walking in all 3 groups (p<0.001). When controlling for age, the mean difference in gait speed or cadence across groups for backward and forward walking followed a trend towards significance. Subjects with vestibular pathology used a wider base of support during backward walking (p=0.030), but not during forward walking (p > 0.05). No other GAITRite variables were significant between forward or backward walking among groups. We have collected fall frequency data for 69% of patients over a period of 1-12

months. Twenty percent of patients reported falls, with a mean falls ratio (number of falls/number of months at follow up) of 0.21 ranging from 0-5 total falls per subject.

**Conclusion:** Our preliminary data suggest age is the primary variable contributing to gait speed and cadence, regardless of symptoms or diagnosis. We are continuing to collect data on forward and backward gait to determine the value of these measures as a fall risk assessment tool.

### **902 Analysis of Eye Movement by Original Video-Oculography, HI-VOG**

**Makoto Hashimoto**<sup>1</sup>, Takuo Ikeda<sup>1</sup>, Kazuma Sugahara<sup>1</sup>, Hironori Fuji<sup>1</sup>, Hiroaki Shimogori<sup>1</sup>, Hiroshi Yamashita<sup>1</sup>  
<sup>1</sup>Yamaguchi University

It is essential for investigating vestibular disturbances to use an infrared CCD camera for recording eye. We devised an original video-oculography (HI-VOG) using an infrared CCD camera, a personal computer and public domain software. The analysis was performed using the publish domain software ImageJ program (developed by the U.S. National Institutes of Health). The video image from an infrared CCD camera was captured at 30 frames per second in 320\*240. For analysis of the horizontal and vertical components, the X-Y center of the pupil was automatically calculated using the original macro. For analysis of torsional components, the whole iris pattern, which was rotated each 0.1 degrees, was overlaid with the same area of the next iris pattern, and the angle at which both iris patterns showed the greatest match was calculated. For quantitative analysis, slow phase velocity of each nystagmus, average of slow phase velocity, the visual suppression value, were analyzed automatically. Using HI-VOG, it is possible to inexpensively perform nystagmus analysis from video images recorded by infrared CCD cameras.

### **903 Association of Size and Location of Superior Canal Dehiscence with Clinical Presentation, Audiometric and Vestibular Testing**

**Marlien Niesten**<sup>1,2</sup>, Leena Hamberg<sup>3</sup>, Joshua Silverman<sup>2,4</sup>, Kristina Lou<sup>5</sup>, Andrew McCall<sup>2,4</sup>, Alanna Windsor<sup>2,4</sup>, Hugh Curtin<sup>3,4</sup>, Barbara Herrmann<sup>2,6</sup>, Wilko Grolman<sup>1,7</sup>, Hideko Nakajima<sup>4,8</sup>, Daniel Lee<sup>2,4</sup>

<sup>1</sup>Department of Otorhinolaryngology - Head and Neck Surgery, University Medical Center, Utrecht, <sup>2</sup>Department of Otolaryngology, Massachusetts Eye and Ear Infirmary, Boston, MA, <sup>3</sup>Department of Radiology, Massachusetts Eye and Ear Infirmary, Boston, MA, <sup>4</sup>Department of Otolaryngology, Harvard Medical School, Boston, MA, <sup>5</sup>Tufts Medical Center and Tufts University School of Medicine, Boston, MA, <sup>6</sup>Department of Audiology, Massachusetts Eye and Ear Infirmary, Boston, MA, <sup>7</sup>Rudolf Magnus Institute of Neuroscience, Utrecht, <sup>8</sup>Eaton-Peabody Laboratory, Massachusetts Eye and Ear Infirmary, Boston, MA

The clinical presentation of patients with superior canal dehiscence (SCD) syndrome varies widely and may depend on the radiologic features of the bony defect. To

test this hypothesis, we prospectively analyzed the association between clinical signs, symptoms, audiometric and vestibular testing in SCD patients with the size and location of the dehiscence. From a database of 146 patients with anatomic SCD at our institution, we identified 104 patients with SCD syndrome who had high resolution temporal bone computed tomography (HR-CT) data available on our PACS system for analysis. Voxar 3D (Toshiba) was used to view oblique multiplanar reformatted CT images while making a curved planar reconstruction of the superior semicircular canal (SSC). Using this reconstruction, cross sectional images with a thickness of 0.2 mm were made. The radiodensity of the SSC bone was analyzed with Image J (NIH) software. We defined <300 Hounsfield units (HU) as an absence of bone. In this manner, we determined the length and location of the SCD with respect to the ampulla. Our measurements in 104 patients (147 ears) show that patients with subjective auditory symptoms (with or without vestibular symptoms) have a significantly larger mean size ( $p = 0.03$ ) of the dehiscence located closer to the ampulla ( $p = 0.004$ ) as compared to patients with vestibular symptoms only, as measured with a Mann-Whitney test. Linear regression analysis of the size and location of the SCD suggests a significant influence of dehiscence size on the air-bone gap (ABG) in the low frequencies ( $p = 0.000$ ,  $0.007$  and  $0.039$  at 250, 500 and 1000Hz respectively) and a significant role of both the size ( $p = 0.026$ ) and the location ( $p = 0.003$ ) of the SCD on the cVEMP thresholds at 250Hz. Our study is the largest patient series to date examining SCD size and location and indicates that a larger SCD located closer to the ampulla is associated with 1) auditory symptoms, 2) a larger ABG, and 3) lowered cVEMP thresholds.

#### **904 Electrocochleography SP/AP Ratio Is Associated with Superior Canal Dehiscence Length**

**Bryan K Ward**<sup>1</sup>, Eva K Ritzl<sup>1</sup>, Sergio Gutierrez-Hernandez<sup>1</sup>, Charley C Della Santina<sup>1</sup>, Lloyd B Minor<sup>1</sup>, John P Carey<sup>1</sup>

<sup>1</sup>*Department of Otolaryngology-Head and Neck Surgery, Johns Hopkins University School of Medicine*

**Background:** Recent findings have suggested a relationship between elevated summing potential (SP) to action potential (AP) ratio as measured by electrocochleography (ECoChG) and the presence of superior canal dehiscence (SCD). Additionally this elevated ratio can normalize following operative plugging of the dehiscent semicircular canal. The objectives of this study were to determine (a) the reproducibility of intraoperative ECoChG findings by Arts et al and (b) if there is a relationship between the size of the dehiscence and the pre-plugging SP/AP ratio.

**Methods:** ECoChG was performed intraoperatively on 44 consecutive surgical repairs of SCD by the middle fossa approach between July 2009 and June 2011. When ECoChG could be measured, pre-plugging and post-plugging SP/AP ratios were recorded for all affected and

unaffected ears. Dehiscence length was measured intraoperatively by direct observation.

**Results:** SP/AP ratios were reliably obtained in 18 of the 44 affected ears before and after plugging and 20 of 44 unaffected ears. Mean pre-plugging ratios were 0.54 (SD 0.19) and 0.43 (SD 0.18) in the affected and unaffected ears respectively ( $p < 0.05$ ). Mean post-plugging ratio of the affected ear was 0.41 (SD 0.30). There was a trend toward correcting of the SP/AP ratio ( $p = 0.07$ ). Mean dehiscence length was 3.4 mm (SD 2.1). There was a linear relationship between dehiscence size and pre-plugging SP ( $p < 0.05$ ) and SP/AP ratio ( $R\text{-sq} = 0.22$ ,  $p < 0.05$ ).

**Conclusion:** This study has confirmed the presence of increased SP/AP ratio in ears affected by SCD. In addition, the relationship between dehiscence size and pre-plugging ratio suggests a mechanical influence on the summing potential in patients with SCD.

#### **905 Astrocyte-Secreted Factors Modulate a Gradient of Primary Dendritic Arbors in Nucleus Laminaris**

**Matthew Korn**<sup>1</sup>, Scott Koppel<sup>1</sup>, Karina Cramer<sup>1</sup>

<sup>1</sup>*University of California, Irvine*

Neurons in nucleus laminaris (NL) receive binaural, tonotopically matched input from nucleus magnocellularis (NM) onto bitufted dendrites that display a gradient of dendritic arbor size. These features facilitate the computation of interaural time differences, which are used to determine the locations of sound sources. The dendritic gradient emerges following a period of significant reorganization that coincides with the emergence of astrocytes that express glial fibrillary acidic protein (GFAP) in the auditory brainstem. We examined several properties of NL neurons, first at an immature stage (E13) and then several days later (E17) after the emergence of the dendritic arbor gradient. Major changes included a loss of total dendritic length, a systematic loss of primary dendrites along the tonotopic axis, and lengthening of primary dendrites on caudolateral NL neurons. Next we tested whether astrocyte-derived molecules contribute to these changes. Individual dye-filled NL neurons were imaged repeatedly in organotypic slices. We found that there was a decrease in the number of primary dendrites on neurons treated with astrocyte-conditioned medium, but not control medium. The decrease in the number primary dendrites varied along the tonotopic axis in a gradient similar to that seen in normal development. These results suggest that astrocyte-secreted molecules are able to modulate the number of primary dendrites and that GFAP-positive astrocytes contribute to dendritic maturation during the development of the auditory brainstem.

## **906 Conditional Deletion of En1 in Developing SOC Neurons Disrupts Superior Olivary Complex Development**

Walid Jalabi<sup>1</sup>, Stephen M. Maricich<sup>1</sup>

<sup>1</sup>Case Western Reserve University, Department of Pediatrics, Cleveland, OH

Genetic pathways that control neuronal specification and differentiation in the superior olivary complex (SOC) are poorly understood. We discovered that the homeobox transcription factor En1, which plays an essential role in the establishment and maintenance of the midbrain/hindbrain region during development, is expressed by neurons of the lateral (LNTB), medial (MNTB), and ventral (VNTB) nuclei of the trapezoid body and by a subset of neurons in the lateral superior olive (LSO). To determine the role of En1 in specification and maintenance of these neurons, we conditionally deleted the gene in the developing SOC using the Egr2Cre driver line. Marker analysis revealed that MNTB neurons are completely absent in Egr2Cre; En1CKO mice, while populations of LNTB and VNTB neurons are also missing. In addition, glycine transporter 2 (GlyT2) immunoreactivity in the LSO, which is thought to arise predominantly from projections from the MNTB, is decreased but still present. We did not find any obvious morphological abnormalities of other auditory structures such as the cochlea, cochlear nuclei, nuclei of the lateral lemniscus or inferior colliculus. Genetic fate mapping revealed that En1 is expressed by developing SOC neurons from at least E13.5; we are currently examining earlier ages as well. Finally, auditory brainstem responses from adult Egr2Cre; En1CKO mice showed abnormally short latency and altered morphology of waves II-V. Our findings reveal the importance of En1 in the specification and development of SOC neurons. Supported by NIDCD F32DC011982.

## **907 Developmental Changes in Neurotransmitter Release in the MNTB-LSO Pathway**

Javier Alamilla<sup>1</sup>, Deda Gillespie<sup>1</sup>

<sup>1</sup>McMaster University

The lateral superior olive LSO of auditory brainstem computes interaural intensity differences used for localizing high frequency sounds along the azimuth. Comparator cells of the LSO effectively sum excitatory inputs arising from the ipsilateral ear with inhibitory inputs arising from the contralateral ear and conveyed via glycinergic cells of the medial nucleus of the trapezoid body (MNTB). This comparison requires precise tonotopic organization, and major synaptic refinement of the immature inhibitory MNTB-LSO pathway occurs before hearing onset. Development of neurotransmitter release properties in this circuit is less well-understood, though regulation of the calcium sensors synaptotagmin 1 and 2 during the first three postnatal weeks in auditory brainstem suggests that calcium-dependent neurotransmitter release may undergo significant maturation during the first few weeks.

We made whole-cell patch clamp recordings from principal neurons of the LSO in response to electrical stimulation in the MNTB and obtained measures of release probability, using paired pulse ratio (PPR) and % of failures, for different postnatal ages, stimulation frequencies and external calcium concentrations. Consistent with previous results, we found that PPRs for the youngest slices (before postnatal day 5, or P5) were significantly different from those more than a week old for higher stimulation frequencies (50 and 100Hz) in "normal" (2mM, P=0.0067, Kruskal Wallis) and high (4mM, P=0.0021, KW) calcium external concentrations. Despite the fact that young slices had higher release probabilities as indicated by higher paired pulse depression, younger (P1-2) slices were also more likely than older slices to fail to respond to the first stimulus in the train (P=0.0083, KW). These results point to maturation of release during development in the MNTB-LSO pathway, possibly resulting from changes in calcium-dependent release machinery. Funded by CIHR (DG) and CONACyT (JA)

## **908 Does the Absence of Norepinephrine Affect Auditory Cortical Development?**

Kathryn Shepard<sup>1</sup>, Robert Liu<sup>1</sup>

<sup>1</sup>Emory University

The sensory experience an animal receives during a developmental sensitive period biases neural responses in sensory cortex into adulthood. Though the sensitive period in auditory cortex has been well studied, little research has focused on the molecular mechanisms that enable plasticity during this time. Research in visual cortex has indicated that the neuromodulator norepinephrine (NE) may be critical to permitting sensitive period plasticity, though this finding has been contested. Here, we attempt to resolve whether NE is required for developmental plasticity in auditory cortex through the use of a mutant mouse that is NE-deficient from birth. In this preliminary study, we use multi-unit recordings to map tone responses across auditory cortex in mice lacking the gene for dopamine beta-hydroxylase, the enzyme that produces NE, and mice with normal NE activity. We find that map organization in NE-deficient and NE-competent mice is largely similar, indicating that in an ordinary acoustic environment, auditory cortical development proceeds even in the absence of this major neuromodulator. While this result implies that the absence of NE does not affect cortical map development, it does not rule out the possibility that compensatory mechanisms intervene over the course of development to guide cortical organization in NE-deficient mice. Hence, to more explicitly test whether auditory cortical *plasticity* during development requires NE, future studies will investigate whether exposing NE-deficient and NE-competent animals to an acoustically manipulated environment during development drives differential cortical map plasticity.

Funded by Emory's PRISM fellowship (NSF GK-12 DGE0536941) (K.S.), NIH F31DC011987 (K.S.), and NIH R01DC008343 (R.L.).

## **909 Are Mice Vocal Learners? Effects of Early Deafening on Adult Mouse Courtship Vocalizations**

Elena Mahrt<sup>1</sup>, David Perkel<sup>2</sup>, Ling Tong<sup>2</sup>, Richard Palmiter<sup>2</sup>, Edwin Rubel<sup>2</sup>, Christine Portfors<sup>1</sup>

<sup>1</sup>Washington State University, <sup>2</sup>University of Washington

Auditory experience during development is necessary for normal language acquisition in humans. Although songbirds, some cetaceans, and maybe bats are also vocal learners, vocal learning has yet to be well established for a small laboratory mammal. Mice are one potential model, as male mice sing ultrasonic courtship songs (USVs). Whether acoustic experience is necessary for mice to develop these USVs, however, is not known. To test for vocal learning in mice, we compared USVs emitted by deaf and normal hearing males. Deafness was induced in 21 CBA/CaJ *Pou4f3*<sup>DTR+/-</sup> male mice expressing diphtheria toxin receptors in hair cells by systemic injection of diphtheria toxin (DT) at postnatal day (P) 2. We confirmed deafness by demonstrating an absence of cochlear hair cells at P10 and P20 and by showing no auditory brainstem responses at P20 and P65. Twelve *Pou4f3*<sup>+/+</sup> littermates, also treated with DT at P2, maintained normal hearing and therefore served as controls. USVs were elicited by pairing a single adult (P60-70) male with a normal hearing CBA/CaJ female for 15 to 25 min. Each male was randomly paired with a novel female 5 times over a 10-day period. USVs were recorded using Avisoft Bioacoustics equipment. Behaviors were videotaped to ensure deaf and hearing males interacted with the females. Seventeen out of 21 deaf males and 12/12 hearing males emitted USVs. Vocalizations from 2 of the recording days were categorized into syllable types, and the relative distribution of syllable types was compared between deaf and hearing animals. This analysis revealed that deaf male mice emit the same types of syllables and have a similar distribution of syllables in each syllable category as normal hearing males ( $p > 0.05$ , MANOVA). While additional detailed analysis of vocalization acoustic parameters may reveal subtle effects of deafening, pattern and rate of these male mouse vocalizations are independent of acoustic experience.

## **910 The Layout of the Otic Capsule in Relation to the Endolymphatic Duct and Sac in Man and Macaque: Its Development, Structure and Role in the Pathogenesis of Ménière's Disease**

Leslie Michaels<sup>1</sup>, Sava Soucek<sup>2</sup>

<sup>1</sup>University College London, <sup>2</sup>Imperial College London

In the early embryo the cartilaginous otic capsule grows outward from the vestibular and cochlear portions of the auditory vesicle. Near the endolymphatic appendage of the vesicle there is no primary cartilage developed (Streeter G.L., *Carn. Contrib. Embryol.* 1918; 7: 5-54). We have surmised from later stages that the otic capsule cartilage surrounds and become closely applied to the appendage surface. Thus the outer perichondrium and later its

derivatives of periosteum and membranous bone grow near the epithelium of the endolymphatic duct and sac.

Until about 16w there is a prominent layer of blood vessels at the interface between duct/sac epithelium and perichondrium. The cartilage begins to ossify, blood vessels are diminished and the periosteum, which, by 20w is very cellular, shows marked apoptosis. At about 23w woven bone develops from the periosteal osteoblasts and small and minute Volkmann's canals appear, some in close proximity to epithelium. This tissue is most marked near the opening of the endolymphatic duct into the vestibule (vestibular arch). In the mature periosteum here osteoblasts, bony canals and apoptotic bodies are numerous.

In the mature macaque (Rhesus) monkey the endolymphatic duct is similarly surrounded by a periosteal layer with woven bone. Near its vestibular entrance the periosteal connective tissue shows a marked eosinophilic staining and has numerous canal-like structures and evidence of apoptosis.

Patients with Ménière's disease show widespread apoptotic death of osteoblasts here. It seems likely that the development of periosteum with osteoblasts in continuous proliferation and apoptosis near to the endolymphatic duct and sac in primates serves a homeostatic function, perhaps by production of potassium ions from dead nuclei. Ménière's disease may result from an overreaction of this function. The macaque may be useful for experimental studies of the basis of that disease.

## **911 Connexin 30 Plays a Role in Development of the Stria Vascularis**

John Kelly<sup>1</sup>, Daniel Jagger<sup>1</sup>, Andrew Forge<sup>1</sup>

<sup>1</sup>UCL

Mice lacking connexin (Cx)30 fail to generate endocochlear potential (EP). The stria vascularis (SV) of Cx30<sup>-/-</sup> animals has been examined at times when EP would be expected to be at adult levels, to identify abnormalities potentially associated with lack of EP. The SV of Cx30<sup>-/-</sup> animals was significantly thinner (luminal surface to spiral ligament) than in wild type (WT) littermates. Marginal cells expressed NKCC1 (an ion co-transporter) and Na-K-ATPase at levels comparable with WT mice as judged by immunolabeling, but their nuclei were rounded similar to those in the developing tissue, rather than oblate as seen in mature cells of WT. The basal cell layer was sometimes thicker than normal, a feature seen in immature tissue, but the complexity of tight junctional strands across the plasma membranes, observed by freeze-fracture, was similar in Cx30<sup>-/-</sup> and WT animals, and immunolabeling revealed claudin 11 expression at the basal cells in the Cx30<sup>-/-</sup> animals. Amongst intermediate cells, the intensity of immunolabeling for Kir4.1, a potassium channel intimately associated with EP generation, was noticeably lower in Cx30<sup>-/-</sup> mice and real-time quantitative PCR of SV revealed significantly lower levels of Kir4.1 mRNA in Cx30<sup>-/-</sup> animals in comparison with WT. It has been suggested that loss of Cx30<sup>-/-</sup> results in breakdown of the permeability barriers around SV capillaries, thereby

leading to dissipation of EP (Cohen-Salmon et. al, PNAS 2007). However, injection of animals with the loop diuretic bumetanide, led to the development of oedema in the SV of Cx30<sup>-/-</sup> animals just as in WT animals, indicating intact permeability barriers. Similarly, following tail vein injection of fluorescently tagged albumen, no leakage of fluorescence out of SV capillaries could be detected. The results are consistent with loss of Cx30 retarding maturation of SV and this may be a factor underlying the inability to generate EP.

### **912 PC3 Expression Pattern in Rat Cochleae**

**Momoko Ise<sup>1</sup>, Ryosei Minoda<sup>1</sup>**

<sup>1</sup>*Department of otolaryngology-head and neck surgery, Kumamoto university, graduate school of medicine*

PC3, which is a member of the BTG/TOB family of antiproliferative genes, has a variety of roles, such as a transcriptional co-regulator, pan-cell cycle regulator, differentiation and antiapoptotic factor in neurogenesis, and tumor suppressor gene. Moreover, PC3 is thought to be a specific marker of neurogenerating neuroepithelial cells. These observations suggest that PC3 is involved in the process of neurogenesis and inducing neuronal differentiation. We investigated the expression pattern of PC3 in the normal rat cochlea by immunohistochemistry to assess its possible involvement in the neurogenesis of spiral ganglion cells (SGCs).

PC3 protein was expressed in SGCs at embryonic days 16 (E16) and E20, and postnatal days 4 (P4) and P7. PC3 expression was observed in the cytoplasm of SGCs at E16 and E20, and in both the nucleus and cytoplasm at P4 and P7. The expression of Ki-67, a nuclear antigen that is a marker of dividing cells, was detected in SGCs at E16 and E20, but not detected at P4 or P7. During the period from E16 to P4: this corresponds to the period of neurogenesis and differentiation of SGCs, the subcellular translocation of PC3 protein occurred. It is known that the subcellular localization of a protein is very important for its functional activity. Taken together, it is suggested that PC3 is involved in the neurogenesis and differentiation of SGCs in the rat cochlea.

### **913 A New Microtubule-Binding Protein in the Organ of Corti**

**Jing Zheng<sup>1</sup>, Roxanne Edge<sup>1</sup>, Chongwen Duan<sup>1</sup>, Jessie Chen<sup>1</sup>, Peter Dallos<sup>1</sup>, MaryAnn Cheatham<sup>1</sup>**

<sup>1</sup>*Northwestern University*

The organ of Corti (OC) develops from simple epithelial cells into a complex group of highly polarized hair cells (HCs) and their surrounding supporting cells (SCs). Inner and outer hair cells display diffuse microtubule (MT) networks, while supporting cells such as Deiters' cells, and both outer/inner pillar cells, contain dense bundles composed of thousands of individual MT filaments. The latter allow SCs to provide the basic architectural structure of the OC, and to convey mechanical signals to hair cells. Currently, little is known about how MT bundles/networks develop in the OC. We identified a new MT minus-end binding protein from cochleae, which is capable of dramatically changing cytoskeletal networks, or marshaling

the appearance of other proteins; hence, the name marshalin (Zheng et al., 2008). Since marshalin can also induce MT-bundle formation in cells transfected with marshalin cDNA, we investigated the distribution of marshalin in the OC during the development. Our results show that marshalin protein is strongly expressed in cells that eventually develop into HCs, Deiters' and pillar cells and that its distribution closely correlates with the appearance and organization of MTs in these cells. We also identified several marshalin isoforms with different protein-binding motifs that likely contribute to variations in MT distribution patterns in HCs and SCs. The properties of these isoforms were further investigated in vitro. Primary data suggest that coiled-coil domains and proline-rich regions of the marshalin protein very likely contribute to the bundling of individual MT filaments, thereby influencing MT bundle formation. In addition, the C-terminus directly binds to MT minus ends, thereby preventing MT disassembly. Because of the stylized arrangement of MTs in the OC, the latter provides an ideal environment in which to study this important cytoskeletal protein (Work supported by NIH Grants DC00089, DC010633 and the Knowles Center).

### **914 Septin Protein Expression in the Embryonic and Neonatal Mouse Cochlea**

**Norio Yamamoto<sup>1</sup>, Atsuhiro Yoshida<sup>1</sup>, Hiroko Torii<sup>1</sup>, Takayuki Nakagawa<sup>1</sup>, Juichi Ito<sup>1</sup>**

<sup>1</sup>*Dep. Otolaryngology, Head and Neck Surgery, Graduate School of Medicine, Kyoto University*

Septin proteins are evolutionally well-conserved GTP binding proteins that constitute non-canonical cytoskeleton. Their functions include the lateral compartmentalization of membranes, the cortical rigidity and the regulation of membrane trafficking by associating with membrane lipids, actins and microtubules. Lateral compartmentalization of membranes contributes to the formation of polarity of cells and roles of regulating membrane trafficking include the formation of presynaptic vesicles in neurons. Considering that the cochlea contains many cells that have a strong polarity and receives innervations from auditory nerve, we assumed that Septin proteins had important roles in the cochlea.

To elucidate the functions of Septin proteins in the cochlea, we decided to determine the distribution of Septin proteins in embryonic and neonatal mouse cochleae using immunohistochemistry. In this study we chose three Septin proteins, Septin 4 (Sept4), Septin 5 (Sept5), and Septin 7 (Sept7) that are abundantly expressed in brain tissues. Especially, Sept7 is a core component of most multimeric Septin complexes, indicating that the expression pattern of Sept7 can cover the whole localization of Septin proteins.

Sept4 and Sept5 were undetectable in the cochlea from embryonic days 13 (E13) to postnatal days 3 (P3). Sept4 started its expression in hair cells, outer pillar cells, and Deiters' cells at P7. Sept5 started its expression in outer pillar cells and presynaptic vesicles of efferent nerve terminals also at P7. In contrast, Sept7 started its expression in most cochlear epithelial cells at E13. The expression of Sept7 in cochlear epithelial cells became limited to pillar cells, Deiters' cells, Hensen's cells, and

Claudius cells at P1. Sept7 became strongly expressed in pillar cells and Deiters' cells by P7.

These results suggested that Sept7 contributed to the development of whole cochlear epithelia and maturation of supporting cells was dependent on Sept4, 5, and 7.

### **915 The C1q Protein Family in Zebrafish and Otolith Formation**

Mauricio Miura<sup>1,2</sup>, Olipriya Das<sup>1</sup>, Young-Jin Kang<sup>3</sup>, Richard Kollmar<sup>1</sup>

<sup>1</sup>SUNY Downstate Medical Center, <sup>2</sup>Universidade Federal de Ciencias da Saude de Porto Alegre, <sup>3</sup>University of Illinois at Urbana-Champaign

The protein precerebellin-like has previously been isolated biochemically in the trout as a constituent of the otoliths that are essential for the detection of linear accelerations. Despite its characteristic C1q domain, it has been difficult to identify unambiguously a zebrafish ortholog of precerebellin-like for embryological and functional studies: the zebrafish genome encodes a large number of homologous C1q proteins with similar and low degrees of sequence identity. To clarify the relationship between the trout otolith protein and its zebrafish homologs, we have now conducted a detailed bioinformatics and expression study of the vertebrate C1q family. Zebrafish proteins that contain a C1q domain were identified by an exhaustive search of sequence databases with a profile hidden Markov model (HMMER). The relationship between the C1q proteins was established by building sequence alignments and phylogenetic trees. The expression of select C1q proteins in larval and adult zebrafish was determined by using reverse transcription coupled with polymerase-chain reactions (RT-PCR). Our results demonstrate that a) the size of the C1q protein family in ray-finned fishes is larger than previously known; b) certain clades of C1q proteins contain far more members in ray-finned fish than in other vertebrates; and c) only a small subset of the C1q proteins that are most closely related to trout precerebellin-like is expressed in the adult zebrafish ear. Our results suggest that the C1q family plays an important role in actinopterygian physiology and form the basis for detailed functional studies of specific C1q proteins during otolith morphogenesis.

### **916 The Role of Zic1 and Zic2 in Cell Fate Specification During Inner Ear Development**

Andrew Chervenak<sup>1</sup>, Ibrahim Hakim<sup>2</sup>, Lisa Gerlach-Bank<sup>2</sup>, Kate Barald<sup>1,2</sup>

<sup>1</sup>Cellular and Molecular Biology Graduate Program, <sup>2</sup>Department of Cell and Developmental Biology, University of Michigan, Ann Arbor, MI 48109

Although the inner ear has been the focus of developmental studies for almost 100 years, we have only a rudimentary knowledge of the basic morphological and cellular changes that occur during organogenesis of this key sensory system in vertebrates [reviewed in (1)]. One of the most basic questions is what genes are responsible for the initially uncommitted cells in the otocyst to become neuroblasts that form the statoacoustic ganglion (SAG), prosensory cells that differentiate into hair cells (HC) and

supporting cells (SC), or non-sensory cells that form the other structures within the inner ear. The *Zic* genes, especially *Zic1* and *Zic2*, are involved in many different phases of development, most notably as part of regulatory networks during neural development<sup>2-4</sup>. However, involvement of these genes during development of the inner ear has only been described at the level of gene expression<sup>4</sup>, so functional studies are critically needed. A previous study showed that *Zic2* expression was upregulated in the sensory epithelium of the chick following noise trauma, indicating that *Zic2* may be involved in regeneration of HCs<sup>5</sup>. More recent work from our lab demonstrated that *Zic1* and *Zic2* are both expressed in regions of the developing inner ear, including in the sensory epithelium<sup>4</sup>. Work from the Aruga lab suggests that *Zic1* and *Zic2* may specify either neuronal or sensory tissue, but, depending on the species, there is no consistency in which gene specifies which cell type<sup>2</sup>. Therefore, the experiments in this project examine the role of *Zic1* and *Zic2* in cell fate specification during development of the inner ear and will test the hypothesis that *Zic1* helps specify a neuronal fate and *Zic2* a sensory cell fate in the inner ear.

<sup>1</sup>Barald, K.F. and Kelley, M.W. 2004. *Development*. 131: 4119-4130

<sup>2</sup>Aruga, J. 2004. *Mol. Cell. Neurosci*. 26: 205-221

<sup>3</sup>Merzdorf, C.S. 2007. *Dev. Dyn*. 236: 922-940

<sup>4</sup>Warner, S.J., et al. 2003. *Dev. Dyn*. 226: 702-712

<sup>5</sup>Gong, T.W., et al. 1996. *Hear. Res*. 96: 20-32

### **917 Regulation of Planar Cell Polarity in the Auditory Sensory Epithelium by Ptk7**

Jianyi Lee<sup>1</sup>, Xiaowei Lu<sup>1</sup>

<sup>1</sup>Department of Cell Biology, University of Virginia

Planar cell polarity (PCP) in the auditory sensory epithelium is manifested by the uniform orientation of stereociliary bundles and is regulated by an evolutionarily conserved PCP/tissue polarity pathway. Protein tyrosine kinase 7 (Ptk7) was previously identified in a mouse gene-trap screen as a novel regulator of PCP. Ptk7 mutants displayed neural tube defects, a shortened cochlea and hair bundle misorientation, similar to classic PCP mutants. To elucidate the mechanisms by which Ptk7 regulates PCP in the inner ear, we first performed epistasis analysis between Ptk7 and Fz3/Fz6, two Frizzled (Fz) receptors that act in the core PCP pathway in the inner ear. Surprisingly, we found that hair bundle misorientation observed in Ptk7 mutants was suppressed in Fz3/Ptk7 and Fz6/Ptk7 double mutants, suggesting that Ptk7 normally antagonizes the activity of Fz receptors. Moreover, Fz3/Fz6/Ptk7 triple mutants displayed additive defects in hair bundle orientation compared to either Fz3/Fz6 or Ptk7 mutants. Importantly, Fz3/Fz6, but not Ptk7, were required for membrane recruitment and asymmetric localization of Dishevelled2, a key signaling component in the core PCP pathway. Together, these results suggest that Ptk7 and the core PCP pathway act in parallel to regulate hair cell PCP. To determine the site of action of Ptk7 in the auditory sensory epithelium, we performed genetic mosaic analysis of Ptk7. By inactivating Ptk7 in a mosaic pattern using a

conditional allele of Ptk7, we identified a requirement of Ptk7 in neighboring supporting cells to regulate hair bundle orientation. Currently we are studying the precise function of Ptk7 in supporting cells and how supporting cell-hair cell interactions influence hair bundle orientation. We have identified cytoskeletal defects in the supporting cells of Ptk7 mutants around the onset of hair bundle orientation. Our results suggest that Ptk7 regulates mechanical properties of the auditory sensory epithelium to modulate PCP signaling.

### **[918] Hedgehog Signaling Is Needed for Development and Maintenance of the Cochlear Sensory Epithelium**

**Tomoko Tateya**<sup>1</sup>, Itaru Imayoshi<sup>1</sup>, Ichiro Tateya<sup>2</sup>, Kiyomi Hamaguchi<sup>2</sup>, Makoto Ishibashi<sup>3</sup>, Juichi Ito<sup>2</sup>, Ryoichiro Kageyama<sup>1</sup>

<sup>1</sup>*Institute for Virus Research, Kyoto University,*

<sup>2</sup>*Department of Otolaryngology, Graduate School of Medicine, Kyoto University,* <sup>3</sup>*Human Health Science, Graduate School of Medicine, Kyoto University*

Mechanosensory hair cells and supporting cells develop from a prosensory domain in the developing auditory sensory epithelium. What induces prosensory cell differentiation into hair cells and supporting cells has been poorly understood. Hedgehog (Hh) signaling is one of the candidates that are related to the initiation of prosensory cells into sensory cells because sonic hedgehog (Shh) in the cochlea has been reported to be down-regulated when the differentiation of sensory cells proceeds, and to inhibit hair cell formation in vitro.

Both down-regulation and up-regulation of Hh signaling in vivo have been achieved by genetic inactivation and activation of Smoothed (Smo) specifically in the cochlear epithelium after the prosensory domain begins to be formed. We examined the cochleae of Smo conditional knock-out (Smo cKO) mice. In the mutant cochleae, the differentiation of hair cells was accelerated and accomplished earlier. We also examined the cochleae expressing a constitutively active allele of Smo (Smo-M2). They showed only one row of inner hair cells and no outer hair cells. Prosensory cell markers were expressed in the cells that were supposed to be outer hair cells and adjacent supporting cells, but markers indicating more differentiation such as Atoh1 and Hes5 were down-regulated, suggesting that Hh signaling maintains the property of prosensory cells. These results indicate that withdrawal of Hh signaling is involved in the temporal regulation of the prosensory cell differentiation and maturity.

Smo cKO mice survived after birth and exhibited progressive hearing loss. Hair cell loss was observed in Smo cKO cochleae. These results suggest that Hh signaling is needed not only for development but also for maintenance of the cochlear sensory epithelium.

### **[919] Regulated Bi-Directional Vesicular Trafficking of Specific PCDH15 and VLGR1 Isoforms in Auditory Hair Cells**

**Marisa Zallochi**<sup>1</sup>, Duane Delimont<sup>1</sup>, Dan Meehan<sup>1</sup>, Dominic Cosgrove<sup>1,2</sup>

<sup>1</sup>*Boys Town National Research Hospital,* <sup>2</sup>*University of Nebraska Medical Center*

Mutations within the Usher genes lead to an autosomal recessive disorder called Usher syndrome characterized by congenital deafness and progressive retinitis pigmentosa. The presence of the Usher proteins at the apical (stereocilia) and basal (synapses) aspects of the hair cells suggests a regulated bi-directional trafficking inferring a specific recognition/association pathway for different vesicular sub-pools. Using antibody preparations to PCDH15 (protocadherin 15) and VLGR1 (very large G protein-coupled receptor 1), we examined the distribution of specific isoforms at opposite poles of immature cochlear hair cells. We identified distinct vesicle pools differentially trafficked that contains specific PCDH15 and VLGR1 isoforms. The basally trafficked pool is defined by its association with adaptor protein-1-positive post-transGolgi vesicles and its co-localization with SNAP25. The second pool associates with ADP-ribosylation factor 1-positive vesicles, co-localizes with rab5 and is trafficked to the apical aspect of cochlear hair cells.

These newly found associations to distinct vesicle markers links for the first time a differential trafficking for the Usher proteins, in which the basolaterally trafficked isoforms may be involved in docking/fusion functions while the apically trafficked isoforms may play a role in the endosomal recycling pathway.

NIH grant R01 DC004844

### **[920] Role for Usher Proteins in Hair Cell Synaptic Maturation**

**Marisa Zallochi**<sup>1</sup>, Dan Meehan<sup>1</sup>, Duane Delimont<sup>1</sup>, Dominic Cosgrove<sup>1,2</sup>

<sup>1</sup>*Boys Town National Research Hospital,* <sup>2</sup>*University of Nebraska Medical Center, Omaha NE USA*

The molecular mechanisms underlying hair cell synaptic maturation are not well understood. Protocadherin-15 (PCDH15) has been implicated in the maturation of cochlear hair cell stereocilia, while clarin-1 has been suggested to play a role in both stereocilia development and synaptogenesis. Mutations in these genes cause Usher syndrome, characterized by congenital deafness, vestibular dysfunction and retinitis pigmentosa. Here we show developmental expression of these Usher proteins at opposite poles of isolated hair cells. At P1 they are present at the stereocilia and basal aspects of cochlear hair cells, while at P30 only the apical expression is observed. This very defined pattern of expression at the base of the hair cells suggests they may be indeed playing a role in synaptic development. To establish the in vivo relevance, we performed morphological and quantitative analysis of the synapses in the *Clrn1*<sup>-/-</sup> and Ames waltzerav3J mutant mice. These mice showed a delay in synaptic maturation by immunostaining with the pre- and post-synaptic markers, ribeye and glutamate receptor subunits 2/3

respectively. Collectively, these results show that, in addition to the well documented role for Usher proteins in stereocilia development, specific Usher protein isoforms likely function in synaptic maturation as well.  
NIH grants R01 DC004844

### **921 Roles of Hepatocyte Growth Factor/MET Signaling in the Developing Mouse Inner Ear**

Shumei Shibata<sup>1</sup>, Julie Wu<sup>2</sup>, Pat Levitt<sup>2</sup>, Takahiro Ohyama<sup>1</sup>

<sup>1</sup>*Division of Cell Biology and Genetics, House Research Institute,* <sup>2</sup>*Department of Cell and Neurobiology, Keck School of Medicine, University of Southern California*

Development of inner ear follows the process which can be separated into different stages that are induced by a distinct combination of genes. A number of gene products have been found to be crucial for inner ear development and mutations in some of these genes are known to cause hearing disorders in human.

Schultz and colleagues have revealed that DFNB39, nonsyndromic hearing loss, is caused by several mutations in the Hepatocyte growth factor (HGF) gene and mouse models of HGF dysregulation showed hearing disorders (Schultz et al., 2009). These results strongly suggest that HGF plays an important role on auditory functions. HGF is known to play diverse biological roles in development, proliferation, branching morphogenesis, and cell survival. The c-Met receptor tyrosine kinase (MET) is the only known cell-surface receptor for the HGF-mediated signaling pathway. Although the HGF/MET signaling pathway has been studied in diverse organs and cell types, roles of HGF/MET on inner ear development remain to be elucidated.

Here, we characterized the expression patterns of HGF and MET in the developing mouse inner ear by using *in situ* hybridization and immunohistochemistry. Both HGF and MET are expressed in the cochlear duct at E15.5 and P0, but the expression patterns of both genes do not completely overlap.

To determine the roles of HGF/MET signaling in the developing inner ear, we generated inner ear-specific HGF and MET conditional knockout (CKO) mice by the Pax2-Cre BAC transgenic mice because both HGF and MET homozygous null mutant mice present embryonic lethal phenotype.

We present the physiological and morphological analyses of HGF-CKO and MET-CKO mice and discuss the roles of HGF/MET in the developing inner ear.

### **922 The Role of the Lin28b/let-7 MiRNA Pathway in Cochlea Differentiation**

Erin Golden<sup>1</sup>, Angelika Doetzlhofer<sup>1</sup>

<sup>1</sup>*Johns Hopkins University*

The development of the mammalian auditory sensory epithelium, the organ of Corti, is a carefully orchestrated process that results in the generation of several highly specialized cell types from a single progenitor cell pool. These include the mechanosensory hair cells and their supporting cells. The molecular mechanisms regulating the differentiation of these different cell types are largely

unknown. Using microarray analyses we identified multiple components of the Lin28b/let-7 miRNA pathway expressed within the undifferentiated cochlear sensory progenitor cell pool. Studies in *C. elegans* and vertebrates have shown that the evolutionarily conserved Lin28b/let-7 miRNA pathway plays an important role in the timing of differentiation and the progression of cell fates. Lin28b is an RNA-binding protein that acts to maintain cells in a pluripotent state by repressing the terminal differentiation-associated let-7 family of miRNAs. Using qRT-PCR and *in situ* hybridization analyses we observed that Lin28b is highly expressed in the undifferentiated cochlea sensory progenitor cells and that this expression significantly decreases during sensory epithelium differentiation. Conversely, we observed an increase in let-7 miRNA expression with progressive sensory epithelium differentiation. Based on these findings we hypothesize that the Lin28b/let-7 miRNA pathway is playing an important role in the transition of cochlear progenitor cells to a differentiated state. In order to investigate the role of this pathway in driving cochlea epithelium differentiation we have developed an organotypic cochlea culture system that utilizes lentiviral infection to overexpress or knockdown Lin28b expression prior to or during progenitor cell differentiation. Using GFP transgenic mice we are able to track the effects of Lin28b manipulation on hair cell (Math1/GFP mice) or supporting cell (Lnf1/GFP mice) differentiation in real time. Results of these functional manipulations on cochlea epithelium differentiation will be presented.

### **923 Overexpression of Isl1 Produces Changes in the Inner Ear in Mice**

Gabriela Pavlinkova<sup>1</sup>, Tetyana Chumak<sup>2</sup>, Lada Kuthanova<sup>1</sup>, Romana Bohuslavova<sup>1</sup>, Daniela Buckiova<sup>2</sup>, Josef Syka<sup>2</sup>

<sup>1</sup>*Inst. Biotechnology,* <sup>2</sup>*Inst. Experimental Medicine, Prague, Czech Republic*

Expression studies show that the transcription factor ISLET 1 (Isl1) is present early in the otocyst in the regions that give rise to both sensory and neuronal lineages in the inner ear. We hypothesize that ISL1 specifies neurosensory precursors. To test our hypothesis, we generated transgenic mice overexpressing Isl1 under Pax2 promoter control. Two founders of Pax2-Isl1 transgenic mice with different levels of transgene expression (F1-lower and F2-higher) were further tested. Some of the mutant mice had evident vestibular abnormality manifested as circling behavior. This finding was accompanied by evident pathological changes in the structure of the vestibular part of the inner ear. For example, most calyx endings, which could be selectively labeled by calretinin, were missing. Hearing function was also affected by the Isl1 transgenic expression as demonstrated by altered auditory brainstem responses (ABRs) and distortion product oto-acoustic emissions (DPOAE). The hearing thresholds of F1 mutants increased faster starting from the age of 7 months. The thresholds of 14-15-month-old mutant mice were higher over the whole frequency range in comparison with controls. A significant elevation of the

hearing thresholds of F2 mutants was detected already at the age of 6 months as compared to controls. Fifteen-month-old F2 mice were completely deaf at 1, 2, 32 and 40 kHz, having an 80 to 92 dB SPL hearing threshold at the middle frequencies, while controls showed only a negligible threshold shift with aging. DPOAE changes were comparable with the ABR changes. Furthermore, we detected an evident loss of hair cells, a 50% loss of spiral ganglion cells and a high level of apoptosis in cerebellar neurons in aged mutant mice. Our results show that transgenic Pax2-*Isl1* mice have abnormalities in the central and peripheral parts of the auditory and vestibular pathways. Supported by AVOZ50390512, GACR 309/07/1336, LC 554, AVOZ50520701.

### **924 Hair Cell MicroRNAs Effect Downregulation of Factors That Promote Supporting Cell Differentiation**

**Garrett Soukup<sup>1</sup>**, Timothy Hallman<sup>1</sup>, Jodi Monahan<sup>1</sup>, Christopher Carlson<sup>1</sup>, Zachariah Holmes<sup>1</sup>, Katie Del Vecchio<sup>1</sup>

<sup>1</sup>*Creighton University*

Hair cell loss caused by environmental and genetic factors is exacerbated by the inability of mammalian auditory hair cells to spontaneously regenerate. Recent studies demonstrate that mechanosensitive hair cells can be derived from embryonic or induced pluripotent stem cells, and that *Atoh1* can induce ectopic hair cells in the embryonic mouse inner ear. These studies suggest important guidance strategies for regenerating hair cells that might be used in non-immunogenic therapies, but the efficacy of other factors in effecting hair cell fate remains to be elucidated. We have previously shown the conservation and specific expression of microRNA-183 family members amongst vertebrate hair cells, and that microRNAs are necessary for the differentiation and maintenance of hair cell in the mouse inner ear. We have investigated the ability of hair cell microRNAs in conjunction with *Atoh1* to influence gene expression profiles in presumptive prosensory precursor cells derived from the embryonic mouse otocyst. Microarray analyses of cells transfected with plasmids expressing *Atoh1* and/or hair cell microRNAs exhibit mild changes in gene expression consistent with the function of microRNAs. Nevertheless, results indicate that the miR-183 family effects the downregulation of certain genes associated with supporting cell differentiation and upregulation of certain genes associated with hair cell differentiation. We have validated that miR-183 family members directly target *Notch1* and the *Atoh1* antagonists *Sox2* and *Hes1*. The data indicate that the miR-183 family reinforces hair cell differentiation by regulating key factors involved in lineage specification in the inner ear and suggest that microRNAs might be useful factors in guidance strategies for hair cell regeneration.

This work was supported by NIH-NIDCD:R01DC009025; Nebraska State LB606.

### **925 Expression Profiling of Facs-Sorted Hair Cells with Deep Sequencing**

**Deborah Scheffer<sup>1,2</sup>**, Jun Shen<sup>1</sup>, Mingqian Huang<sup>2</sup>, David Corey<sup>1</sup>, Zheng-Yi Chen<sup>2</sup>

<sup>1</sup>*Howard Hughes Medical Institute and Department of Neurobiology, Harvard Medical School, Boston, MA,*

<sup>2</sup>*Eaton-Peabody Laboratory - Massachusetts Eye and Ear Infirmary, Boston, MA 02114, USA*

To identify genes important for the development and function of hair cells, it would be useful to know the complete transcriptome of hair cells at various times during their differentiation and maturation. Previous efforts at such expression profiling have been compromised by the low sensitivity of oligonucleotide arrays, the difficulty in separating hair cells from the surrounding sensory epithelia, and the inability to identify new genes. We have previously used mutant animals lacking hair cells (*Atoh1*), or mutants with hair cells but no bundles (*Pou4f3*) to approach a hair-cell transcriptome (Scheffer *et al.*, 2007a; 2007b), but these are not perfect models and cannot be used for later developmental stages.

We have now developed a new model for expression profiling in hair cells. We generated a mouse expressing green fluorescent protein (GFP) under the *Pou4f3* promoter, and used fluorescence-activated cell sorting (FACS) to purify dissociated hair cells and non-hair cells. Cells were purified from cochlear and utricular epithelia, at E16, P0, P4, P7 and P16. To increase sensitivity, we used Illumina high-throughput sequencing of cDNAs at a depth of 20-50 million reads per sample.

FACS-sorted hair cells are apparently very pure: more than 50 hair cell genes (such as *Gfi1*, *oncomodulin*, *otofelin*, *Ptprq*, *Atoh1*, *Grxcr1* and *Tmc*) are represented highly in the GFP<sup>+</sup> sample but at least 100-fold less in GFP<sup>-</sup> cells. We have confirmed the expression of new hair-cell specific genes by *in situ* hybridization and immunostaining.

Expression data were assembled into a sortable database that includes additional annotation, such as domain architecture and chromosomal location relative to deafness loci. By one sort criterion, for instance, a third of all known deafness genes occur in the top 3% of the 20,000 genes represented. This database will help to identify genes important in hair-cell transduction and synaptic transmission, in cell-fate determination, and in control of cell cycle, as well as to identifying additional deafness genes. Similar approaches might be used for identifying genes expressed in subsets of hair cells, for instance outer-hair-cell-specific genes that might participate in electromotility.

### **926 Melanoblasts Are Missing from the Stria Vascularis of Lmx1a Mutant Mice by Embryonic Day 16**

**David Nichols<sup>1</sup>**, Judith Bouma<sup>1</sup>, Kirk Beisel<sup>1</sup>, Bernd Fritsch<sup>2</sup>

<sup>1</sup>*Creighton Univ. School of Medicine,* <sup>2</sup>*Univ. of Iowa*

The stria vascularis of the mammalian inner ear is a composite epithelial-mesenchymal structure that includes an intermediate layer of neural crest derived melanocytes.

In the absence of these melanocytes the stria is unable to maintain the ionic composition of the endolymph and the animal is congenitally deaf. *Lmx1a* is a LIM homeodomain transcription factor expressed in the abneural wall of the cochlear duct in embryonic mice. In *Lmx1a* mutants (*Dreher*, Jackson Lab) the stria fails to assemble. Here we use a whole mount *in situ* hybridization stain for dopachrome tautomerase (DCT) to establish the fate of strial melanocyte precursors (melanoblasts) in mutants. At embryonic day (E)12.5 melanoblasts are present in both wildtype and mutant ears. Some are adjacent to the inner ear epithelium while others are scattered in the periotic mesenchyme. In the E14.5 wildtype (+/+ or +/-) cochlear duct most melanoblasts localize to a clearly defined band associated with the abneural wall of the duct (Karen Steel *et al.*, *Development* 115:1111, 1992). This is the first known morphological manifestation of stria vascularis assembly. In E14.5 mutants, melanoblasts are sparse basally and less common than wildtype apically. Most still associate with the stria. By E16.5, melanoblasts are all but absent from the entire mutant ear. This result suggests that melanoblasts are dying or dedifferentiating as they home to the mutant strial epithelium. In either case the absence of *Lmx1a* expression in the abneural wall of the cochlear duct might result in failure to secrete a factor capable of attracting, proliferating and sustaining melanoblasts. Candidate factors include Steel (stem cell) factor (A.K.A. Kit ligand) and/or endothelin 3.

### **927** ephrin B2 Is Required for Proper Development of Otoconia, the Endolymphatic Duct/Sac, and Cochlea

Steven Raft<sup>1</sup>, Leonardo Rodrigues De Andrade<sup>2</sup>, Doris Wu<sup>1</sup>

<sup>1</sup>Section on Sensory Cell Regeneration and Development, NIDCD, NIH, <sup>2</sup>Section on Structural Cell Biology, NIDCD, NIH

Inner ear function requires homeostatic control over the ionic composition of endolymph, a unique extracellular fluid that bathes sensory organ apical surfaces. Recent work indicates that regulation of endolymph composition by discrete transport and absorptive epithelia also influences ear development. For example, null homozygous mutation of *Slc26a4*, homologue of a human deafness gene encoding the anion exchanger PENDRIN, causes acidification of embryonic endolymph, distention of the membranous labyrinth, absent or abnormal otoconia, and deafness in the mouse. A previous study of mice haploinsufficient for the cytoplasmic domain of *ephrin B2* (*Efnb2*), encoding a transmembrane ligand for Eph receptor tyrosine kinases, revealed partially penetrant vestibular dysfunction associated with reduced utricular potassium concentration and a presumed decrease in endolymph volume. To more fully characterize the roles of *Efnb2* in ear development, we used the Cre-lox system to generate conditional null homozygote (cko) mice. Gross inner ear morphology in the embryonic day 19 *Efnb2* cko is comparable to controls. However, the endolymphatic duct/sac is malformed, resembling in its entirety an expanded endolymphatic sac that joins directly (without a

duct) to the sacculus. This structure shows strong up-regulation of *Slc26a4* versus controls. Variably large to giant otoconia, each conforming to one of a small set of unconventional morphologies, are found at the maculae of *Efnb2* cko mice. The *Efnb2* cko cochlea contains all sensory and supporting cell types and is well-patterned but 20% shorter on average than that of *Cre*;*-flox*+/+ controls. Hair cell number scales linearly with basilar membrane length across the genotypic series obtained from our genetic cross. How *Efnb2* controls *Slc26a4* (pendrin) expression and other aspects of ear development is currently under investigation.

### **928** A Massively Parallel Sequencing Study Leads to the Identification of Four Mutations in TMC1 as the Principal Cause of Deafness Among Moroccan Jews

Zippora Brownstein<sup>1</sup>, Lilach M. Friedman<sup>1</sup>, Varda Oron-Karni<sup>2</sup>, Nitzan Kol<sup>2</sup>, Thomas Parzefall<sup>1</sup>, Stavit Shalev<sup>3,4</sup>, Bella Davidov<sup>5</sup>, Mordechai Shohat<sup>1,5</sup>, Dorit Lev<sup>6</sup>, Moshe Frydman<sup>1,7</sup>, Noam Shomron<sup>2,8</sup>, Karen B. Avraham<sup>1</sup>

<sup>1</sup>Department of Human Molecular Genetics and Biochemistry, Tel Aviv University, Israel, <sup>2</sup>Genome High-Throughput Sequencing Laboratory, Tel Aviv University, Israel, <sup>3</sup>Genetics Institute, Ha'Emek Medical Center, Israel, <sup>4</sup>Rappaport Faculty of Medicine, Technion-Israel Institute of Technology, Israel, <sup>5</sup>Department of Medical Genetics, Rabin Medical Center, Beilinson Campus, Israel, <sup>6</sup>Institute of Medical Genetics, Wolfson Medical Center, Israel, <sup>7</sup>Danek Gartner Institute of Human Genetics, Sheba Medical Center, Tel Hashomer, Israel, <sup>8</sup>Department of Cell and Developmental Biology, Tel Aviv University, Israel

The genetic consequences of endogamy in small populations are increased homozygosity and compound heterozygosity for alleles responsible for recessive traits. These demographic features explain the genetics of inherited hearing loss in the Moroccan Jewish population. This population, now numbering ~ 1 million in Israel, has two principal historic origins: Jewish migration to North Africa during the Second Temple period (530 BCE - 70 CE), and migration to North Africa from the Iberian peninsula immediately preceding the Alhambra Decree in 1492. Over the following five centuries, the Jewish population in Morocco grew to ~250,000 and was highly endogamous. After 1948, nearly all Moroccan Jews emigrated to Israel. In our series of Moroccan Jewish families with hearing loss, 10/56 probands (18%) were homozygous for *GJB2* 35delG. Other genes responsible for hearing loss in this population remained elusive, due to the lack of large families for linkage analysis and high cost of Sanger sequencing the many other known deafness genes. We resolved this problem by combining targeted capture and massively parallel sequencing of 246 genes responsible for human and mouse deafness (Brownstein, Friedman *et al.* *Genome Biol.* 2011). In a Moroccan Jewish family, we identified two mutations in *TMC1* (transmembrane channel-like 1, DFNB7/11). Upon Sanger sequencing *TMC1* in other Moroccan Jewish probands, we identified two additional *TMC1* mutations. Collectively, these four *TMC1* alleles explain hearing loss in 43% of the

Moroccan Jewish population. The four mutations are TMC1 R604X and R389X (previously identified) and S647P and W404R (newly identified). None of the 4 *TMC1* mutations was found in 120 deaf probands of other Jewish origins, nor in 138 hearing controls of other Jewish origins. We suggest that the role of 4 *TMC1* mutations in hearing loss in this population is the consequence of founder effects and endogamy among the Jews who lived in Morocco for many generations.

## **929** DFNA54: Candidate Gene Analysis Through Sequence Capture and Next-Generation-Sequencing

Nicolas Gürtler<sup>1</sup>, Benno Röthlisberger<sup>2</sup>, Katia Ludin<sup>2</sup>

<sup>1</sup>Department of Otolaryngology, Cantonal Hospital, Aarau, Switzerland, <sup>2</sup>Genetic Laboratory, Cantonal Hospital, Aarau, Switzerland

### Introduction

Hereditary hearing loss is characterized by a high heterogeneity. Over 100 loci and 50 genes have meanwhile been discovered and identified. A Swiss family with low-frequency hearing loss has been linked to chromosome 5 and published as DFNA54. The search for mutations in a few candidate genes by classic sequencing method, which is time- and labour intensive, was without results. New methods based on higher through-put and array technology offer a much higher yield.

Objective: Mutation mapping in DFNA54 by targeted genome capture in combination with next-generation sequencing

### Methods:

First, a possible larger pathogenic deletion is investigated with an exon focused high-density Roche NimbleGen CGH array. Second, if no deletion is found, a custom Sequence Capture 385K Human Array is designed and manufactured by Roche NimbleGen. One array with a total of 385,000 unique, overlapping probes 60–90 nucleotides in length can be designed covering all exons within the DFNA54 target region. After capturing the targeted regions the DNA is eluted, amplified and then sequenced on a Roche GS Junior instrument. Variants are detected with the SEQNext Software (JSI Medical Systems) and possible pathogenic mutations (nonsense and missense) will be verified by Sanger Sequencing in the patient and further family members.

### Results:

The results of the molecular-genetic analysis are presented.

### Conclusions:

The search for genes in hereditary hearing loss can be facilitated by novel methods such as targeted genome capture in combination with next-generation sequencing.

## **930** Application of Next Generation Sequencing to Genetic Diagnosis in Multiplex Families with Idiopathic Sensorineural Hearing Impairment

Chen-Chi Wu<sup>1,2</sup>, Ying-Chang Lu<sup>3</sup>, Chuan-Jen Hsu<sup>1</sup>, Pei-Lung Chen<sup>2</sup>

<sup>1</sup>Department of Otolaryngology, National Taiwan University Hospital, <sup>2</sup>Department of Medical Genetics, National Taiwan University Hospital, <sup>3</sup>Institute of Biomedical Engineering, National Taiwan University

Despite the clinical utility of genetic diagnosis in addressing idiopathic sensorineural hearing impairment (SNHI), current strategy of mutation screening using Sanger sequencing suffers from the limitation that only a limited number of DNA fragments associated with common deafness mutations can be genotyped. Consequently, definite genetic diagnosis cannot be achieved in many families with obvious family history. In the present study, we applied the next generation sequencing (NGS) technique to 6 multiplex families (i.e. families with multiple affected members) with idiopathic SNHI. NimbleGen sequence capture array was designed to target all exons and 100 bp of flanking sequence from 79 common deafness-associated genes. NGS by HiSeq2000 using paired-end (2x100) protocol was performed to get a greater than 30-fold coverage across the targeted regions. We applied bowtie, samtools, GATK, Picard and IGV for the bioinformatics analyses. After variant calling, sequence variants identified were filtered as follows: allele frequency < 2% on dbSNP130, predicted as deleterious on both PolyPhen2 and SIFT, not excluded by segregation analysis in the pedigrees, and finally confirmed by Sanger sequencing. At the step of variant calling, about 1-3 indel (insertion/deletion) variants and 53-72 non-synonymous missense variants were identified in each of the 6 multiplex families. After variant filtering, we identified the p.P655R (c.1937C>G) variant of the DIAPH1 gene as the pathogenic mutation in a family with autosomal dominant inheritance, and the c.1157\_1160deltagg variant of the DFNA5 gene as the pathogenic mutation in another family with autosomal dominant inheritance. Both are novel mutations in the literature. In conclusion, NGS enables a precise genetic diagnosis in certain multiplex families with idiopathic SNHI by identifying mutations in relatively uncommon deafness genes.

## **931** Mitochondrial Haplogroup Analysis in Patients with Hereditary Hearing Loss

Tomofumi Kato<sup>1</sup>, Yoshihiro Noguchi<sup>2</sup>, Noriyuki Fuku<sup>3</sup>, Haruka Murakami<sup>4</sup>, Motohiko Miyachi<sup>4</sup>, Masashi Tanaka<sup>3</sup>, Ken Kitamura<sup>2</sup>

<sup>1</sup>Tokyo Metropolitan Geriatric Hospital, <sup>2</sup>Tokyo Medical and Dental University, <sup>3</sup>Tokyo Metropolitan Institute of Gerontology, <sup>4</sup>National Institute of Health and Nutrition

Hearing loss (HL) is one of the most common disorders in patients with mitochondrial disease. Many mutations of mitochondrial DNA have been reported to cause HL. Additionally, many modifiers including environmental factors and genetic polymorphisms are involved in HL. The

primary function of mitochondria is to provide energy substrates (such as ATP), and cochleas require many mitochondria. It is indicated that HL is strongly dependent on mitochondrial function. The present study investigated the association between suspected hereditary HL and 12 major mtDNA haplogroups. The subjects comprised 373 unrelated Japanese patients with suspected hereditary HL and 480 controls. 20 out of 373 patients were excluded in the reason that they had been detected to carry the m.1555A>G or the m.3243A>G mutation. The haplotypes were classified into 12 major Japanese haplogroups (i.e., F, B, A, N9a, N9b, M7a, M7b, G1, G2, D4a, D4b and D5). The frequencies of each haplogroup in patients were compared to controls using Pearson *Chi-square* test. The results showed that the frequency of the patients carrying the mitochondrial haplogroup D4b was significantly higher than that of the controls (37/353 (10.5%) vs. 31/480 (6.5%), OR 1.70 [95% CI 1.03-2.79], *P*=0.036). The enhanced evidence was found in subhaplogroup D4b2 (32/353 (9.1%) vs. 24/480 (5%), OR 1.89 [95% CI 1.09-3.28], *P*=0.021), which is characterized by the m.514delCA, m.8020A>C, m.1382A>C, m.8964C.T, and m.9824T>A. No statistically significant difference between groups was found in subhaplogroup D4b1. The m.1382A>C is located in 12S rRNA and is possibly affecting the secondary structure of 12S rRNA. Thus, haplogroup D4b might be associated with the phenotypic expression of hereditary HL.

### **932 Postnatal Onset of Deafness in a Child Heterozygous for GJB2 35delG and DFNB1 Upstream Deletion**

Ellen Wilch<sup>1</sup>, Rachel Fisher<sup>1</sup>, Paul Mark<sup>2</sup>, Karen Friderici<sup>1</sup>  
<sup>1</sup>Michigan State University, <sup>2</sup>Spectrum Health Systems

The incidence of congenital hearing loss varies across populations and over time, but newborn hearing screening programs commonly detect hearing loss in >1 in 1000 newborns. Early therapeutic intervention in children with prelingual hearing loss (HL) is associated with better language development and educational outcomes. With the application of audiologic techniques that make it possible to reliably assess hearing status in very young children and infants, it is now abundantly apparent that some proportion of prelingual HL is not detected at birth.

We report here on a case of a profoundly deaf three-year-old boy, who passed hearing screens by DP-OAE testing within a few days of birth (full-term) and again at 6 months of age. Parental concerns beginning at 12 months of age precipitated a referral for additional audiometry at 21 months. Profound HL was confirmed at 22 months by ABR testing. MRI was normal. The child has since received bilateral cochlear implants and is doing well.

This child is compound heterozygous for the common 35delG mutation of GJB2 and an additional DFNB1 allele identified in the Michigan German-American kindred to which both of his parents belong. This allele bears a 131 kb deletion well upstream of the transcriptional start sites of GJB2 and GJB6 and results in down-regulation of GJB2 and GJB6 transcription. Four other kindred members with this genotype are profoundly deaf.

Postnatal onset of hearing loss has been documented in children with both GJB2- and SLC26A4-related hearing loss. Mutations in these two genes account for perhaps half of prelingual HL with genetic etiology; HL with either etiology commonly presents with no family history. If GJB2 and SLC26A4 testing should become routine in order to identify the majority of infants who are at risk for postnatal onset of HL, interpretation of genetic testing will benefit by development of robust age-of-onset genotype-phenotype correlations.

### **933 Middle-Ear Anomalies and Cochlear Function in Elastic-Fiber Disorders**

Jeffrey A. Marler<sup>1</sup>, Shawn S. Goodman<sup>2</sup>, Zsolt Urban<sup>3</sup>

<sup>1</sup>The Ohio State University, <sup>2</sup>University of Iowa, <sup>3</sup>University of Pittsburgh

Elastic fibers are abundant in resilient tissues such as skin and ligaments. They endow these tissues with structural integrity and elastic recoil. Elastic fibers are found in middle-ear (ME) structures, but it is unclear if they are necessary for normal auditory function. Cutis laxa (CL) is a rare inherited disorder of the elastic tissue. Both congenital and acquired forms exist. Congenital forms are commonly inherited, with 8 known CL genes known to date. In contrast, acquired forms are often caused by inflammatory destruction of the elastic fibers. The goal of this research was to study auditory function in different forms of cutis laxa.

We obtained single and multifrequency (MF) tympanometry, wideband absorbance, audiometric thresholds, and distortion product otoacoustic emissions (DPOAEs) in adolescent and adult male and female subjects (ages 17-67) with acquired CL (n=4) and congenital CL (n=7). Three of 7 subjects with congenital CL had ELN mutations and 1 had an ATP6V0A2 mutation. In the acquired CL group, 1 had normal hearing, 3 had mild, mild-to-moderate SNHL. In the congenital CL group, 5 had normal hearing, 1 had mild mixed HL and 1 (ATP6V0A2) had moderate SNHL. Mann-Whitney U tests showed no significant Peak Ytm 226-Hz or MF tympanometry group differences (U=14, p=0.93; U=9.0, p=0.55); however, wideband absorbance measured at ambient pressure was significantly higher (U=27, p=0.01; U=27, p=0.01) at .25 and .5 kHz in the congenital CL group (Median =0.402, 0.538) while the acquired CL group was within normal limits (Median=0.144, 0.307). Other ME measures were normal. DPOAE levels were within normal limits for all subjects in the congenital CL group except for the ATP6VA2 subject (nonELN mutation). We conclude that elastic fiber dysfunction in congenital CL causes ME anomalies with relatively preserved inner ear function and hearing thresholds.

**934 A Novel COCH Mutation, P.F527C, Associated with Autosomal Dominant Nonsyndromic Hearing Loss, Disrupts the Structural Stability of the VWFA2 Domain**

Hyun-Ju Cho<sup>1</sup>, Hong-Joon Park<sup>2</sup>, Maria Trexler<sup>3</sup>, Hanka Venselaar<sup>4</sup>, Kyu Yup Lee<sup>5</sup>, Nahid G. Robertson<sup>6</sup>, Jeong-In Baek<sup>1</sup>, Beom Sik Kang<sup>7</sup>, Cynthia C. Morton<sup>6,8</sup>, Gert Vriend<sup>4</sup>, Laszlo Patthy<sup>3</sup>, Un-Kyung Kim<sup>1</sup>

<sup>1</sup>Department of Biology, College of Natural Sciences, Kyungpook National University, South Korea, <sup>2</sup>Soree Ear Clinics, Seoul, South Korea, <sup>3</sup>Institute of Enzymology, Biological Research Center, Hungarian Academy of Sciences, Hungary, <sup>4</sup>Radboud University Nijmegen Medical Centre, Nijmegen, The Netherlands, <sup>5</sup>College of Medicine, Kyungpook National University, Daegu, South Korea, <sup>6</sup>Department of Obstetrics, Gynecology and Reproductive Biology, Harvard Medical School, Boston, USA, <sup>7</sup>School of Life Science and Biotechnology, Kyungpook National University, Daegu, South Korea, <sup>8</sup>Department of Pathology, Brigham & Women's Hospital, Harvard Medical School, Boston, Ma, USA

Mutations in COCH have been associated with autosomal dominant nonsyndromic hearing loss (DFNA9) and are frequently accompanied by vestibular hypofunction. Here, we report identification of a novel missense mutation, p.F527C, located in the vWFA2 domain in members of a Korean family with late-onset and progressive hearing loss. To assess the molecular characteristics of this cochlin mutant, we constructed both wild-type and mutant cochlin constructs and transfected these into mammalian cell lines. Results of immunocytochemistry analysis demonstrated localization of the cochlin mutant in the ER/Golgi complex, whereas western blot analyses of cell lysates revealed that the mutant cochlin tends to form covalent complexes that are retained in the cell. Biochemical analyses of recombinant vWFA2 domain of cochlin carrying the p.F527C mutation revealed that the mutation increases propensity of the protein to form covalent disulfide-bonded dimers and affects the structural stability but not the collagen-affinity of the vWFA2 domain. We suggest that the instability of mutant cochlin is the major driving force for cochlin aggregation in the inner ear in DFNA9 patients carrying the COCH p.F527C mutation.

**935 Genetic Mutation and Adult Cochlear Implant Performance**

Robert Eppsteiner<sup>1,2</sup>, A. Eliot Shearer<sup>1,2</sup>, Michael Hildebrand<sup>1,2</sup>, Steve Scherer<sup>3</sup>, Marlen Hansen<sup>1</sup>, Bruce Gantz<sup>1</sup>, Richard Smith<sup>1,2</sup>

<sup>1</sup>University of Iowa Hospitals and Clinics, <sup>2</sup>Molecular Otolaryngology and Renal Research Laboratory, <sup>3</sup>Human Sequencing Center, Baylor College of Medicine

Genetic Mutation and Adult Cochlear Implant Performance Background: Although the vast majority of patients who receive cochlear implants perform well, there is a subset of patients with severe-to-profound hearing loss who do not benefit from cochlear implantation (3-6%). The effect of genetic mutation on cochlear implant performance has been established for very few hearing loss genes (e.g.

those with *GJB2* mutation perform well and those with *DDP1* mutation perform poorly). Given the high surgical and maintenance costs of cochlear implantation, we hypothesize that pre-operative genetic screening can be used to improve patient selection and reduce instances of non-beneficial implantation.

Methods: DNA samples from 28 adult cochlear implant patients with unknown causes of severe-to-profound hearing loss were obtained. Solution-based sequence capture and massively parallel sequencing was performed on all exons and flanking sequence of all known non-syndromic hearing loss genes (66) using the OtoSCOPE® platform. Variants were prioritized and evaluated for pathogenicity using our custom variant-calling and annotation pipeline. Validated mutations were correlated with audiometric data to determine the impact of specific hearing loss mutations on cochlear implant performance.

Results: We completed solution-based sequence capture on 28 cochlear implant patients. There were an average of 65 million reads per sample, with 85% of reads mapping to the reference sequence (hg19), and 52% of reads on target. The average depth of coverage per targeted base was 3,506 reads with 96% of targeted bases having 40X coverage. Initial analysis shows that of the first five patients one known deafness-causing missense mutation was identified and several deafness candidates were identified in the other individuals. Variant analysis is ongoing.

Conclusions: The results from this study may lay the groundwork for improved patient selection with respect to cochlear implantation, thereby improving outcomes and decreasing costs.

**936 The  $\alpha$ -Helical Coiled-Coil Tail of Nonmuscle Myosin-II Mediate Interactions with the Nucleus**

O'neil Guthrie<sup>1,2</sup>, Terry Fleck<sup>3</sup>, Helen Xu<sup>4</sup>

<sup>1</sup>Research Service-151, Loma Linda Veterans Affairs Hospital, Loma Linda CA 92357, USA., <sup>2</sup>Department of Biology, Developmental, Cell and Molecular Biology Group, Duke University, French Fam, <sup>3</sup>Loma Linda Medical Center, CA, <sup>4</sup>Department of Otolaryngology and Head & Neck Surgery, School of Medicine, Loma Linda University Med

Human genetic mutations (MYH9 and MYH14 related diseases) that affect the nonmuscle myosin-II (MyoII) molecular motor result in syndromic and nonsyndromic forms of sensorineural hearing loss but the underlying mechanisms are unresolved. We posit that one potential mechanism to account for MYH9/14 related diseases (e.g., hereditary macrothrombocytopenias) might be the interaction between MyoII and the cell nucleus. As a first approximation, we conducted genetic/transgenic conditional expression experiments to determine whether or not MyoII associates with the nucleus of cells in metazoan tissue. The giant cells within salivary gland organs from 3rd instar *Drosophila melanogaster* larvae were evaluated in living and fixed preparations. A UAS-Gal4 conditional expression system was used to drive gene expression of MyoII specifically within salivary gland

organs. A GFP-MyoII protein trap line, which uses the endogenous MyoII promoter to control expression of full-length GFP-MyoII was also employed. Additionally, epitope immunoreactivity was used to localize endogenous MyoII proteins. The combined results demonstrate that the MyoII molecule may interact with the nucleus. For instance, the molecule formed oligomerized (filament-like) conformations on the cytoplasmic side of the nuclear lamin. The  $\alpha$ -helical coiled-coil tail of the MyoII molecule was necessary and sufficient to mediate all nuclear interactions including perinuclear localization and oligomerization. These interactions affected the morphology of the nucleus and the nuclear associations of filamentous actin and actin-binding proteins. The data provide direct evidence for a nuclear association of MyoII within metazoan tissue and suggest that the interaction between MyoII and the nucleus might contribute to MYH9/14 related diseases.

### **937 Headbobber: A Combined Morphogenetic and Cochleosaccular Mouse Model to Study 10qter Deletions in Human Deafness**

**Annalisa Buniello**<sup>1</sup>, Rachel Hardisty<sup>2</sup>, Richard Smith<sup>2</sup>, Karen P. Steel<sup>1</sup>

<sup>1</sup>Wellcome Trust Sanger Institute, <sup>2</sup>MRC Institute of Hearing Research

The recessive mouse mutant *headbobber* (*hb*) displays the characteristic behavioural traits associated with vestibular defects including headbobbing, circling and deafness. This mutation was identified in a line carrying an integrated transgene and the phenotype mapped to distal chromosome 7. We show that the inner ear of *hb/hb* mutants lacks semicircular canals and cristae, and the saccule and utricle are fused together in a single utriculosaccular sac. Moreover, we detect severe abnormalities of their cochlear sensory cells, stria vascularis looks severely disorganised, Reissner's membrane is collapsed and no endocochlear potential was detected. *Myo7a* and *Kcnj10* expression analysis showed a lack of intermediate cells in *hb/hb* stria vascularis, which explains the absence of endocochlear potential. We used *Trp2* as a marker of melanoblasts migrating from the neural crest at E12.5 and showed that they do not interdigitate into the developing strial epithelium, associated with abnormal persistence of the basal lamina in the *hb/hb* cochlea. After having performed array CGH as well as an extensive expression analysis of candidate genes in the *headbobber* region on *hb/hb* and littermate controls, we can conclude that the *headbobber* combined morphogenetic and cochleosaccular phenotype is caused by an addition of different effects: 1) effect of a 600kb deletion on distal Chr7, with the loss of a few protein coding genes with interesting expression patterns and unknown function in the inner ear; 2) indirect, long range effect of the deletion on the expression of neighboring genes on Chr7, associated with downregulation of *Hmx* genes. Interestingly, deletions of the homologous region in humans have been reported in a number of patients with common features including sensorineural hearing loss and

vestibular problems. Therefore, we propose that *headbobber* is a useful model to gain insight into the mechanisms underlying deafness in human 10qter deletions.

### **938 Progressive and Severe Hearing Loss in the Stonedeaf Mouse Mutant**

**Neil Ingham**<sup>1</sup>, Francesca Carlisle<sup>1</sup>, Selina Pearson<sup>1</sup>, Jing Chen<sup>1</sup>, Morag Lewis<sup>1</sup>, Karen P. Steel<sup>1</sup>

<sup>1</sup>Wellcome Trust Sanger Institute

Hearing sensitivity of mutant mice generated in the Sanger Institute Mouse Genetics Project is assessed at 14 weeks old using the auditory brainstem response (ABR). Some mice had a profound and severe hearing impairment that appeared to be unrelated to a targeted mutation. ABR recordings identified further affected mice which were used to establish a colony for this putative 'stonedeaf' mutation. Hearing sensitivity of stonedeaf mice was tested at 4, 8 and 14 weeks old. Many young mice had some degree of hearing. At 4 weeks, some mice had no measurable ABR and the remaining mice demonstrated a range of click-evoked ABR thresholds from 20 to >90dB. By 8 weeks old, there was a bimodal distribution of click thresholds, where unaffected mice had thresholds below 40dB and affected mice had thresholds above 40dB. By 14 weeks old, hearing loss in affected mice had progressed further; most had no measurable ABR whereas all unaffected mice had normal hearing sensitivity.

Affected mice had normal middle ears and normal inner ear gross morphology. Scanning electron microscopy of the organ of Corti of affected mice aged 5 weeks showed no obvious defect. Degenerative changes and hair cell loss were seen at 9 weeks. Mice with elevated ABR thresholds had an abnormally low endocochlear potential (2–84mV) compared to unaffected mice (92–131mV). Phalloidin staining of the stria vascularis indicated morphological changes in marginal cell tight junctions of affected mice.

The stonedeaf phenotype was inherited as an autosomal recessive trait. Stonedeaf mutants (maintained on a C57BL/6 genetic background) were outcrossed to C3H mice. F1 offspring were backcrossed to homozygous stonedeaf mice to generate mice for linkage analysis. Mapping with microsatellite markers, whole-exome resequencing and comparative genome hybridization is ongoing, but early results suggest a region on chromosome 9 may contain the causative mutation for this progressive and severe hearing loss phenotype.

### **939 Auditory Characterization of a Mouse Model of Fibrous Dysplasia**

**Jolie Chang**<sup>1</sup>, Omar Akil<sup>1</sup>, Edward Hsiao<sup>1</sup>, Tamara Alliston<sup>1</sup>, Lawrence Lustig<sup>1</sup>

<sup>1</sup>University of California, San Francisco

Several developmental bone disorders are associated with hearing loss such as osteogenesis imperfecta, skeletal dysplasias, craniosynostoses and fibrous dysplasia. However, the pathogenesis of these bone diseases in the cochlea and their affect on hearing loss is poorly understood. Fibrous dysplasia is a bone disorder in which localized areas of bone are replaced by abnormal fibrous

tissue. Dysplastic lesions in the temporal bone can be variable in severity and location and can cause both conductive and sensorineural forms of hearing loss. Using the Rs1/Col1 mouse model of fibrous dysplasia with increased Gs activity in bone, we examined the auditory function and described the associated anatomic and histologic changes within the temporal bone. Rs1/Col1 mice have significantly elevated but highly variable auditory brainstem response thresholds. Loss of DPOAE responses suggest a component of conductive hearing loss. Dissection and histologic analysis revealed bony lesions with overgrowth affecting the outer cortex of the otic capsule while the ossicles, modiolar bone, and neural structures are spared. We provide the first description of hearing function and cochlear changes in a mouse model of fibrous dysplasia. Understanding the mechanisms controlling otic capsule bone growth and turnover will direct the development of targeted therapies that can halt the progression of dysplastic bony lesions.

#### **940 Characterization of Auditory and Vestibular Defects in Targeted Mutations of Mouse *Grxcr2***

Matthew Avenarius<sup>1,2</sup>, Jae-Yun Jung<sup>1</sup>, Charles Askew<sup>3,4</sup>, Sherri Jones<sup>5</sup>, Gwenaelle Geleoc<sup>3,4</sup>, David Dolan<sup>1</sup>, Yehoash Raphael<sup>1</sup>, David Kohrman<sup>1,2</sup>

<sup>1</sup>University of Michigan Medical School, Department of Otolaryngology, <sup>2</sup>University of Michigan Medical School, Department of Human Genetics, <sup>3</sup>University of Virginia, Department of Neuroscience, <sup>4</sup>Children's Hospital Boston, Harvard Medical School, <sup>5</sup>East Carolina University, Department Of Communication Sciences and Disorders

We have previously reported on a targeted mutation of mouse *Grxcr2*, which encodes a glutaredoxin-like cysteine-rich protein that is expressed in hair cells in the cochlea and in vestibular organs and is localized to stereocilia. Homozygote *Grxcr2* mutants exhibit significant hearing loss by 3 weeks of age that is associated with defects in bundle maturation. We now report on further characterization of the auditory and vestibular defects in *Grxcr2* mutants: (1) stereocilia bundles exhibit quantitative defects in orientation at early postnatal ages; (2) despite these orientation defects, as well as progressive bundle disorganization, the transduction apparatus assembles in relatively normal fashion as determined by whole cell electrophysiological evaluation of transduction and FM1-43 uptake; and (3) hearing loss and associated stereocilia maturation defects are observed in *Grxcr2* mutants in both *FVB* and *C56BL/6J* genetic backgrounds. We have also demonstrated that reduced *Grxcr2* expression in hypomorphic mutants is associated with progressive hearing loss and stereocilia bundle defects. Finally, evaluation of vestibular evoked potentials demonstrated that *Grxcr2* mutants exhibit higher thresholds and longer peak latencies than control mice in response to linear accelerations, indicating vestibular dysfunction despite relatively normal behavior.

Supported by NIH-NIDCD grants DC003049 (DCK), DC05188 (DCK and YR), DC006443 (SMJ), DC008853 (GSG), and DC000011 (MRA).

#### **941 Generation of a Novel Transgenic Mouse to Drive Inducible, Hair-Cell Specific Expression**

Yukako Asai<sup>1,2</sup>, Varadamurthy Srinivasan<sup>2,3</sup>, Heidi Scrable<sup>4</sup>, Gwenaelle Geleoc<sup>2,5</sup>

<sup>1</sup>Institut Pasteur, <sup>2</sup>University of Virginia, <sup>3</sup>Paraxel International, <sup>4</sup>Mayo Clinic, <sup>5</sup>Children's Hospital Boston, Harvard Medical School

We are working to develop a novel transgenic mouse to allow tight, reversible control of gene expression in hair cells. Our strategy adapts the *lac* operator/repressor (*LacO/LacI*) system (Cronin et al., 2001) for use with the hair cell promoter for Myosin 7A (*Myo7A*). The human *Myo7a* promoter was modified to include two *lac* operator sequences rendering it inducible, yet preserving its activity. The construct was incorporated into adenoviral vectors and validated *in vitro* in tissue from transgenic mice that express *LacI* (Cronin et al., 2001). By adding IPTG to the culture media, we were able to activate gene expression in transfected hair cells. We have recently generated transgenic mice that carry the regulatable Myosin-7a (*MYO7A<sup>lacO</sup>*) promoter to drive expression of  $\beta$ -*actin::eGFP*. We have opted to use this construct for two reasons: (1)  $\beta$ -*actin::eGFP* is a robust fluorescent reporter which will facilitate expression and repression studies; (2) we can study formation and regulation of stereocilia by assessing  $\beta$ -actin incorporation in hair bundles. Four *MYO7A<sup>lacO</sup>- $\beta$ -actin::eGFP* transgenic lines were generated. Three lines demonstrated strong GFP fluorescence. Two were selected for characterization. Both transgenic lines showed robust and specific  $\beta$ -actin::eGFP expression in auditory and vestibular hair cells.  $\beta$ -actin::eGFP expression was localized to stereocilia and was present through adulthood. The mice did not display abnormal phenotypes and hair cell transduction was normal. To obtain double transgenic mice, the founders were crossed with *LacI* mice. Offspring had reduced GFP expression as assessed by quantitative PCR. However, GFP fluorescence was observed in the stereocilia of double transgenic mice, indicating the need for further optimization to obtain tighter control *in vivo*. We are exploring various strategies for improving regulation of expression. Regulatable hair cell expression will be a valuable tool to study gene function during development and age-related hearing loss. (NIDCD Grant #DC008853; #DC008853s)

#### **942 Eliminating Catalase Paradoxically Reduces Age- And Noise-Associated Threshold Elevation in C57BL/6 Mice**

Erin A. Rellinger<sup>1</sup>, Patricia M. Gagnon<sup>2</sup>, Kevin K. Ohlemiller<sup>1,2</sup>

<sup>1</sup>Program in Audiology and Communication Sciences, Washington University, <sup>2</sup>Dept. Otolaryngology, Washington Univ. School Med.

Reducing intrinsic antioxidant capacity can promote both noise- and age-related threshold elevation, as demonstrated in SOD1 and GPx1 knockout (KO) mice. We

examined the effects of unconditionally eliminating the antioxidant enzyme catalase (CAT) in C57BL/6 (B6) inbred mice. Since CAT helps remove peroxide, we posited that CAT KO mice would show increased noise-induced permanent threshold shifts (NIPTS) and accelerated threshold elevation tied to the *Cdh23ahl* allele. Breeders and genotyping protocols were kindly provided by Y.-S. Ho. Liver typing for CAT activity was used to verify genotyping in a subset of mice. Experimental subjects were generated from Het x Het and KO x Het matings. ABR thresholds were tested at 2-4 mos, 6 mos, and 9-10 mos in a total 33 WT, 18 Het, and 41 KO mice in three separate mixed-gender cohorts. 11 WT and 13 KO mice were exposed at 3.5 mos to 30 min of intense noise (4-45 kHz, 110 dB SPL), then retested 2 wks post-exposure.

B6 CAT KO mice show no outward health complications or reduced life span (Ho et al. JBC 2004). Thresholds by genotype were similar at 2-4 mos. However, by 6 mos ABR thresholds above 20 kHz were 20-50 dB higher in WT mice than in KOs. By 9-10 mos, thresholds in WTs were significantly elevated versus KOs at 10-40 kHz. Thresholds in Hets were similar to those in KOs at 6 mos, and intermediate between WTs and KOs at 9 mos. Following noise exposure, KOs again fared significantly better than WTs by about 20 dB for frequencies above 20 kHz.

B6 CAT KO mice show paradoxical protection from the effects of age and noise compared to WT mice. This result is counter to our expectation, and to genetic evidence that CAT deficiency may promote NIPTS in humans (Konings et al. HMG 2007). We posit that CAT elimination leads to up-regulation of other stress responses. This effect could be tied to the B6 background, and specific to known hearing loss alleles in B6.

Supported by P30 DC004665 (R. Chole), T35 DC008765 (W. Clark), R01 DC08321 (KKO)

### **943 Interaction Between VEGF and HGF Signaling in Sporadic Vestibular Schwannomas and Cultured Human Schwann Cells: Hearing Implications**

**Daniel Roberts<sup>1</sup>, Sonam Dilwali<sup>1</sup>, Shyan-Yuan Kao<sup>1</sup>, Konstantina Stankovic<sup>1</sup>**

<sup>1</sup>*Massachusetts Eye and Ear Infirmary/Harvard Medical School*

Vestibular schwannoma (VS) is the most common tumor of the cerebellopontine angle, which typically presents with hearing loss. Mechanisms of this hearing loss are poorly understood; tumor-secreted factors have been implicated. We have explored a specific secreted factor, hepatocyte growth factor (HGF), because mutations in HGF lead to an autosomal-recessive, nonsyndromic hearing loss in humans. HGF is known to interact with vascular endothelial growth factor-A (VEGF-A) in endothelial cells and VEGF-A is thought to play a key role in VS tumorigenesis. Modulation of VEGF-A signaling with bevacizumab leads to tumor shrinkage and improved speech perception in some patients with neurofibromatosis type 2 associated VS. Mechanisms of this hearing improvement have not been understood. We investigated whether HGF levels are elevated in sporadic VS compared

to normal Schwann cells, and whether VEGF and HGF signaling pathways control each other in both VS and normal Schwann cells. When comparing VS to normal Schwann cells, we found substantially higher expression of VEGF, HGF, and HGF receptor cMET mRNA, and elevated secretion of VEGF and HGF. To determine whether VEGF and HGF interact in Schwann cells, we generated a cell culture system using peripheral human Schwann cells. This novel primary cell culture system is 80% pure and readily transfectable with small interfering RNAs (siRNA). siRNAs targeting cMET decreased both cMET and VEGF protein levels, targeting VEGF reduced cMET expression, and targeting VEGF-A receptor VEGFR-2 reduced VEGF and cMET expression. Taken together with our finding that cMET is abundantly expressed in the cochlea, our data suggest that specific targeting of the HGF/cMET pathway, in addition to indirect modulation of HGF via VEGF pathway, may ameliorate or prevent hearing loss associated with VS.

### **944 Robust Functions of Kir and Gap Junction Channels in Pericytes of Spiral Ligament Suggest a Key Role of These Cells In**

**Yuqin Yang<sup>1</sup>, Alfred Nuttall<sup>1</sup>, Zhi-Gen Jiang<sup>1</sup>**

<sup>1</sup>*Oregon Health & Science University*

Pericytes (PC) are smooth muscle-like cells densely populated on microvessels in spiral ligament (SL) and stria vascularis (SV), like in retina, but the functional studies of these cells in the cochlea are scarce. Using acutely isolated capillary segments and whole-cell recording techniques, we revealed the following PC properties that are particularly relevant to precise control of the blood flow in cochlear lateral wall, the critical structure for homeostasis of endolymph potential and K<sup>+</sup> recycling. 1) With physiological internal and external solutions, SL PCs, but not the endothelial cells (EC), showed a robust inward rectification in I/V negative domain, which was enhanced by higher [K<sup>+</sup>]<sub>o</sub> and completely abolished by 100 μM Ba<sup>2+</sup>. [K<sup>+</sup>]<sub>o</sub> 20 mM induced a ~15 mV hyperpolarization and increased slope conductance at -90 mV by ~1 nS. 2) PCs mostly showed an 18β-glycyrrhetic acid-sensitive electrical coupling with up to 18 neighboring ECs, estimated by measurements of input conductance and capacitance. 3) ATP activated a P2X-antagonist PPADS-sensitive transient current in PCs as well as ECs with an I/V reversal potential near +5 mV. 4) Pinacidil 100 μM activates a glipizide-sensitive current with a reversal potential at ~-80 mV. 5) Acetylcholine, norepinephrine, nitrendipine, prazosin, PPADS and glipizide caused no significant change in I/Vs or membrane potentials in SV-PCs in normal solutions. We conclude that local physiological and pathological [K<sup>+</sup>]<sub>o</sub> fluctuation can act on Kir and regulates PC's membrane potential and thus its motor tone. By this mechanism and assisted with gap junction coupling, the PCs may regulate the lateral wall blood flow in correlated with the level of hair cell signal transduction activity via K<sup>+</sup> recycling. Little role is expected for cholinergic and adrenergic neuro factors in this microcirculation but local NO and purinergic signaling may

involve in certain conditions. Supported by NIH grants DC004716 (ZGJ) and DC00105 (ALN).

### **945 A Novel Technique for Culturing Pericytes, Perivascular Resident Macrophages, and Endothelial Cells from Mouse Cochlea**

Lingling Neng<sup>1,2</sup>, Wenjing Zhang<sup>1,2</sup>, Xiaorui Shi<sup>1</sup>  
<sup>1</sup>Oregon Health & Science University, <sup>2</sup>Zhengzhou University

Pericytes (PCs), perivascular resident macrophages (PVMs), and endothelial cells (ECs) are critical components of the blood-labyrinth barrier in the stria vascularis. While the barrier is essential for maintaining inner ear homeostasis, study of the specific roles of these cell types is hindered by the lack of a method for isolating and culturing them. Here we describe a "media-dependant" method for obtaining PC, PVM, or EC primary cultured cell lines directly from explanted mouse stria vascularis tissue. The stria vascularis was harvested under sterile conditions from the lateral wall of 10 - 15 day old C57BL/6J mice, placed in ice-cold perilymph solution, and minced into small pieces (about 1 mm<sup>3</sup>) in culture medium with ophthalmic tweezers. The explanted mixed population of strial cell types was grown in specific culture media to selectively support growth of specific phenotypes. Unwanted phenotypes did not survive the several passages. To obtain ECs, culture medium containing 1% endothelial cell growth factor limited non-EC cell growth and proliferation. To obtain PVMs, 1% human melanocyte growth factor enhanced proliferation of PVMs. Cochlear PCs were grown in a media of DMEM with a low concentration of glucose (1 g/ L) similar to that used to culture PCs from skeletal muscle. Purity of the cultures was on the order of 90% for ECs, 95 % for PCs. Further purification of the primary cultured ECs, PCs, and PVMs was obtained using magnetic bead separation in combination with fluorescence-activated cell sorting (FACS). The purified ECs, PCs, and PVMs were subsequently used to establish three-dimensional (3-D) *in vitro* culture models, including a mono-cell, co-culture, and triple culture system. The different culture models offer a unique opportunity to study the intercellular interactions of ECs, PVMs, and PCs and assess the role each phenotype plays in blood-labyrinth barrier integrity. This work was supported by National Institutes of Health grants NIH NIDCD DC008888 (XS), NIH NIDCD DC008888S1 (XS), NIH NIDCD R01-DC010844 (XS), NIHP30-DC005983.

### **946 Perivascular Resident Macrophages in the Inner Ear Are Essential for Blood-Labyrinth-Barrier Integrity**

Wenjing Zhang<sup>1</sup>, Min Dai<sup>2</sup>, Wenxuan He<sup>2</sup>, Jackie DeGagne<sup>2</sup>, Tianyin Ren<sup>2</sup>, Alfred L. Nuttall<sup>2</sup>, Dennis Trune<sup>2</sup>, Guy Perkins<sup>3</sup>, Xiaorui Shi<sup>2</sup>

<sup>1</sup>Zhengzhou University, <sup>2</sup>Oregon Health & Science University, <sup>3</sup>National Center for Microscopy and Imaging Research

The inner ear has an endothelial blood-tissue barrier in the stria vascularis that is as tight as the blood brain barrier. However, the mechanisms that control stria vascularis endothelial blood-barrier permeability remain largely unknown. In this study, we provide the first evidence that signaling between perivascular resident macrophages (PVMs) and endothelial cells modulates blood-labyrinth barrier (BLB) permeability. Morphological study of these cells with transmission electron microscopy showed a rich network of PVMs' processes contacted capillary by an electron dense basal lamina. Their end-feet of the processes were strikingly rich in mitochondria and were heterogenous in size and shape. The ending of processes of PVMs also surprisingly contained numerous vesicles. The functional study for PVMs *in vitro* and *in vivo* showed that PVMs are critical cellular component for blood-labyrinth integrity as ablation of PVMs in a transgenic mouse model utilizing targeted diphtheria receptor method caused vascular leakage by affecting the formation of tight junctions mediated by pigment epithelial-derived factor. This work was supported by National Institutes of Health grants NIH NIDCD-DC008888 (XS), NIH NIDCD DC008888S1 (XS), NIH NIDCD-DC010844 (XS), NIDCD R01DC00105 (ALN), NIHP30-DC005983.

### **947 Perivascular Resident Macrophages Are Highly Responsive Melanocyte-Like Cells**

Wenjing Zhang<sup>1,2</sup>, Min Dai<sup>1</sup>, Lingling Neng<sup>1</sup>, Xiaorui Shi<sup>1</sup>

<sup>1</sup>Oregon Health & Science University, <sup>2</sup>Zhengzhou University

The blood-labyrinth barrier in the stria vascularis of the adult cochlea is surrounded by a large population of perivascular cells. The cells are identified as perivascular resident macrophages (PVMs), since they are positive for several macrophage surface molecules, including F4/80, CD68, and CD11b. In this study, the PVMs were further characterized as melanocyte-like macrophages. We also investigated shifts in the population of PVMs under conditions such as aging, LPS-initiated inflammation, and noise exposure. The PVMs were found to contain granules of melanin pigment in the cytoplasm and express several melanocyte markers, including cytosolic glutathione S-transferases (GST), glutathione S-transferase alpha 4 (GSTA4). RT-PCR analysis of isolated and purified PVMs from mouse cochlea also detected mRNA for *Gst*, *Gsta4*, and F4/80. Consistent with the RT-PCR results *in vivo*, mRNA for *Gst*, *Gsta4*, and *Gpf480* were detected in newly established mouse primary cultured PVMs. The primary cultured PVMs were positive for both melanocyte marker proteins and F4/80, suggesting the PVMs are pigment-

producing cells. While the PVMs contained an abundant amount of melanin, they were distinguishable from the intermediate cells (also referred to as melanocytes) because the PVMs did not express Kir 4.1, the fiduciary marker of intermediate cells. The PVMs responded strongly to different conditions. The PVM population gradually decreased with age as well as with noise exposure (117 dB SPL for 3 hours on consecutive 2 days). In contrast, the population of PVMs in LPS-treated mouse cochlea were dramatically increased at day 3. The data indicate the PVMs in the vascular wall of the blood-labyrinth barrier may have a role similar to that of astrocytes in blood-brain-barrier and glial cells in the blood-retina-barrier. The role is essential for maintaining tissue hemostasis, including regulation of tissue blood barrier integrity, immunosurveillance, and scavenging of free radicals. This work was supported by National Institutes of Health grants NIH NIDCD DC008888 (XS), NIH NIDCD DC008888S1 (XS), NIH NIDCD R01-DC010844 (XS), NIHP30-DC005983.

#### **948 Calcium Sparks, BK and SK Channels Regulate Myogenic Tone in the Gerbil Spiral Modiolar Artery**

**Gayathri Krishnamoorthy<sup>1</sup>, Katrin Reimann<sup>1,2</sup>, Philine Wangemann<sup>1</sup>**

<sup>1</sup>Kansas State University, <sup>2</sup>Department of Otolaryngology, Head and Neck Surgery, University of Tübingen, Germany  
Ca<sup>2+</sup> sparks and large-conductance Ca<sup>2+</sup>- and voltage-dependent K<sup>+</sup> (BK) channels form a negative feedback mechanism that hyperpolarizes and relaxes vascular smooth muscle cells leading to vasodilation. In this study, we elucidate the role of ryanodine-receptor mediated Ca<sup>2+</sup> sparks and BK channels in regulating vascular tone of the gerbil spiral modiolar artery (SMA). Ca<sup>2+</sup> sparks occurred in pressurized (60 cmH<sub>2</sub>O) SMA with a frequency of 0.9 ± 0.1 Hz. Spark frequency was unchanged between 20 and 60 cmH<sub>2</sub>O, but increased two-fold when pressure was increased from 60 to 80 cmH<sub>2</sub>O. Ryanodine (10 μM) abolished Ca<sup>2+</sup> sparks and increased global cytosolic Ca<sup>2+</sup> at both 40 and 60 cmH<sub>2</sub>O. The effect of ryanodine on vascular diameter was pressure-dependent. Consistent with the principle that Ca<sup>2+</sup> sparks inhibit vasoconstriction, abolishing Ca<sup>2+</sup> sparks with ryanodine caused a robust constriction of arteries pressurized at 40 cmH<sub>2</sub>O. In contrast, ryanodine had negligible effect on diameter of arteries at 60 or 80 cmH<sub>2</sub>O, where spark frequency was highest. However, when arteries at 60 cmH<sub>2</sub>O were first exposed for 1 min to endothelin-1 (1 nM), an agent that increases the Ca<sup>2+</sup> sensitivity of the smooth muscle cells of the SMA, ryanodine caused a vasoconstriction. Iberiotoxin (100 nM), an inhibitor of BK channels, had no effect on vascular diameter, but elicited a robust constriction in the presence of apamin (100 nM), a blocker of Ca<sup>2+</sup>-activated small conductance K<sup>+</sup> (SK) channels. The results indicate that the diameter of the SMA is regulated by Ca<sup>2+</sup> sparks, BK and SK channels as well as the Ca<sup>2+</sup>-sensitivity of the smooth muscle cells of the spiral modiolar artery. This study was funded by NIH R01-DC04280 to PW.

#### **949 Gender Differences in Myogenic Regulation Along the Vascular Tree of the Gerbil Cochlea**

**Katrin Reimann<sup>1,2</sup>, Gayathri Krishnamoorthy<sup>1</sup>, Philine Wangemann<sup>1</sup>**

<sup>1</sup>Department of Anatomy and Physiology, Kansas State University, <sup>2</sup>Department of Otolaryngology, Head and Neck Surgery, University of Tübingen, Germany

Cochlear blood supply originates at the basilar artery, followed by the anterior inferior cerebellar artery, the spiral modiolar artery (SMA) and the radiating arterioles (RA) that feed the capillary beds of the cochlea. Regulation of blood flow is critical for hearing due to the vulnerability of the cochlea to ischemia and oxidative stress. Here, we investigated gender differences in the magnitude of pressure-dependent vascular tone and Ca<sup>2+</sup> sensitivity of smooth muscle cells and the role of endogenous nitric oxide in mediating vascular relaxation. We also estimated the capacity of the cochlear blood vessels to increase blood flow on demand. Vascular diameter and cytosolic Ca<sup>2+</sup> were measured by confocal microfluorometry in pressurized vessel segments obtained from male and female gerbils. In the presence of nitric oxide synthase inhibitor L-NNA (10 μM), increase in pressure increased the pressure-dependent tone in male and female RA and in male, but not in female, SMA. L-NNA caused a larger increase in the Ca<sup>2+</sup> sensitivity in male than in female SMA. In male SMA, this increase in Ca<sup>2+</sup> sensitivity was abolished by the Rho-kinase inhibitor Y27632. The L-NNA induced tone in the SMA of both genders was reduced to ~50% by the Ca<sup>2+</sup> channel blocker nifedipine and to ~85% by the combined presence of nifedipine and the Rho-kinase inhibitor Y27632. The maximal increase in cochlear blood flow achievable by vascular relaxation was estimated to be 2.4 - 3.6-fold, which is less than the dynamic range of current generation and possible metabolic rates in the stria vascularis. This suggests that ischemia is a relevant pathobiological mechanism. The results demonstrate quantitative gender differences in the control mechanisms of cochlear blood flow. The greater magnitude of L-NNA induced tone in male SMA predicts greater restrictions of cochlear blood flow under conditions of impaired endothelial cell function. This finding is consistent with animal experiments and clinical outcomes, which suggest that males are more susceptible to age related hearing loss.

Supported by NIH R01-DC04280.

#### **950 Strial Capillary Endothelial Cells of Guinea Pig Cochlea Exhibit Unique Low K<sup>+</sup> Channels Conductance**

**Zhi-Gen Jiang<sup>1</sup>, Ketao Ma<sup>1,2</sup>, Yuqin Yang<sup>1</sup>**

<sup>1</sup>Oregon Health & Science University, <sup>2</sup>Shihezi University Medical College, PRC

Strial vascularis (SV) capillaries play a critical role in blood-labyrinth-barrier including separating a >100 mV potential gradient between the intrastrial space and blood stream while maintaining necessary metabolites exchanges. The mechanisms required to fulfill these functions remain poorly understood. Using whole-cell and single channel

recording techniques, we explored the channel mechanisms in the capillary endothelial cells (ECs) and pericytes (PCs) in acutely isolated SV capillary segments and in fully dispersed state. Results showed that 1) with physiological internal and external solutions, SV ECs had a membrane potential  $\sim -29$  mV, a  $C_{\text{input}} \sim 29$  pF and a  $R_{\text{input}} \sim 480$  M $\Omega$  ( $\sim 9.4$  pF and  $\sim 1.8$  G $\Omega$  from isolated single cells). The I/V curve of ECs mostly exhibited a mild outward rectification at voltages positive to  $-40$  mV, was slightly flattened by 1 mM  $\text{Ba}^{2+}$  but not significantly changed by 1 mM TEA, 4-AP or 20 mM  $\text{K}^+$ . 2) In contrast, PCs had a membrane potential  $\sim -54$  mV, a  $C_{\text{input}} \sim 85$  pF and a  $R_{\text{input}} \sim 306$  M $\Omega$  ( $\sim 10$  pF and  $\sim 450$  M $\Omega$  for isolated single cells). The PC I/V relation showed a prominent inward rectification at potentials negative than  $-60$  mV, which was enhanced by elevations of  $[\text{K}]_o$  and completely suppressed by 100  $\mu\text{M}$   $\text{Ba}^{2+}$ . 3) Both cell types showed extensive electro-coupling with neighbor cells, which was completely blocked by 30  $\mu\text{M}$  18 $\beta$ -glycyrrhetic acid. Nitrendipine, apamin and glipizide (blockers for IK, SK and  $\text{K}_{\text{ATP}}$  respectively) caused no significant current or voltage responses in both cells. 4) Cell-attached and outside-out patch recordings from ECs occasionally detected activities of 59 pS  $\text{K}^+$ -channels with very low open probability. We conclude that SV ECs normally express little active channels, especially  $\text{K}_{\text{ir}}$ ,  $\text{K}_{\text{Ca}}$  and  $\text{K}_{\text{V}}$  channels, resulting in high membrane resistance thus to economically preserve the highly positive endocochlear potential, whereas SV PCs appear as a regulatory element. Supported by NIH grants DC004716 (ZGJ).

### **951** Intravital Microscopy Imaging of Cochlear Lateral Wall in Live Mice Through a Thinned Otic Capsule

Min Dai<sup>1</sup>, Zachary Urdang<sup>1</sup>, Alfred L. Nuttall<sup>1</sup>, Xiaorui Shi<sup>1</sup>  
<sup>1</sup>Oregon Health & Science University

Direct measurement of cochlear blood flow (CBF) and lateral wall cells is difficult, with many techniques for assessing it still under development. Various techniques have been used to evaluate cochlear blood flow, including laser-doppler flowmetry, fluorescence intravital microscopy, microendoscopy, magnetic resonance imaging as well as approaches based on injection of radioactive or labeled microspheres into the bloodstream. Of these methods, intravital fluorescent microscopy, combined with a "vessel-window" in the cochlear otic wall of the guinea pig, has seen the most success for investigation of capillary diameter and velocity under different conditions. Here we report a new approach using a "thinned otic capsule window" method in combination with intravital microscopy for studying cochlear blood flow and pathophysiology of various lateral wall cell types in a mouse model. Although surgery on mouse cochlea is difficult due to its small size, the benefit of this newly established method is high-resolution imaging of fluorescent-labeled vessels and cells. It provides a way to investigate the cell biology of fibrocytes, pericytes, perivascular resident macrophages, and endothelial cells in different mouse models. Most significantly, imaging through a thinned capsule provides an intact lateral wall

minimizing the disruption of the delicate homeostatic balance. Perforation of the cochlear otic capsule often causes change in cochlear pressure and loss of perilymphatic fluid. This new method is a minimally invasive approach for studying structural and functional changes in cochlear blood flow and lateral wall biology under normal and pathological conditions. This work was supported by National Institutes of Health grants NIH NIDCD-DC008888 (XS), NIH NIDCD DC008888S1 (XS), NIH NIDCD-DC010844 (XS), NIDCD R01 DC000105 (ALN), NIH P30-DC005983.

### **952** Morphological Analysis of Adult Common Marmoset (*Callithrix Jacchus*) Cochlea

Masato Fujioka<sup>1,2</sup>, Keigo Hikishima<sup>3,4</sup>, Hiroataka James Okano<sup>4,5</sup>, Ken-ichiro Wakabayashi<sup>6</sup>, Mitsuhiro Kawaura<sup>2</sup>, Toshio Ito<sup>3</sup>, Kaoru Ogawa<sup>1</sup>, Hideyuki Okano<sup>4</sup>  
<sup>1</sup>Dpt of Otolaryngology, School of Medicine, Keio University, Tokyo, Japan, <sup>2</sup>Dpt of Otorhinolaryngology, Keiyu Hospital, Kanagawa, Japan, <sup>3</sup>Central Institute for Experimental Animals, Kanagawa, Japan, <sup>4</sup>Dpt of Physiology, School of Medicine, Keio University, Tokyo, Japan, <sup>5</sup>Division of Regenerative Medicine, Jikei University School of Medicine, Tokyo, Japan, <sup>6</sup>Dpt of Otorhinolaryngology, Kitasato Institute Hospital, Tokyo, Japan

Model organism is an indispensable tool for biomedical researches and, for translational researches to clinical applications, we have been using a biotechnologically established small non-human primate, Common Marmoset (*Callithrix jacchus*). The animal is used for psychological or behavioral analyses due to its verbal communication, and, in the auditory field, for investigating central pathway including A1 cortex. Here we examined anatomy of peripheral auditory system of Common Marmoset. Four fixed temporal bones were evaluated with CT, MRI and paraffin-embedded sections. Generally, the cochlea is relatively larger in contrast to its smaller skull. It has similar structures in its attics and tympanic cavity to those in human (*Homo sapience*), but in contrast, its mastoid and protympanum differ: Instead of the pneumatic mastoid, there is a common cavity at the corresponding area, which resembles rather to the bulla structure in the lower mammals such as guinea pig. In its protympanum, bony part was abundantly pneumatized and the air-cells were highly developed. With fiber tractography using ultra high-resolution diffusion tensor images obtained by a 7-tesla MRI and cryogenic MRI probe, we successfully distinguished apical fibers from basal fibers. Interestingly, apical-basal tonotopic gradient was preserved even in the twisted auditory nerve. Collectively, feasibility of this primate for basic research of peripheral auditory system was demonstrated. Its cochlea size can be suitable for surgical models; bulla-like structure of mastoid can be applied for the implant of micropump; auditory or facial nerves can be utilized for cranial nerve disease models with repetitive MR neuro imaging that provides time-dependent changes of individual samples without sacrifice. Combined with traditional electrophysiology of A1 cortex

and recently established genetic modification, the species would be a powerful tool for highly-integrated translational researches of auditory diseases/disorders.

### **953 The Evolution of the Mammalian Cochlea**

**Geoffrey Manley<sup>1</sup>**

<sup>1</sup>*Carl von Ossietzky University*

The evolution of high-frequency hearing (> 20 kHz) in mammals has been a controversial issue for many years. Recent advances in paleontological techniques, especially the use of Micro-CT scans, now provide important new insights that are here reviewed.

True mammals arose more than 200MY ago. One identifying feature was, of course, the presence of three middle-ear ossicles, but these ossicles were not necessarily freely-suspended as in modern mammals. The earliest mammalian cochleae were about 2mm long and thus like those of their ancestors. In the multituberculate - monotreme mammalian lineages, the cochlea remained relatively short and did not coil, even in modern representatives. The second main lineage, leading to modern therians, did not develop cochlear coiling for at least 60 MY. Even late Jurassic mammals show only a 270° cochlear coil and a cochlear canal length of only 3 mm. Comparisons to modern organisms and mammalian ancestors and the state of the middle ear strongly suggest that high-frequency hearing was not realized for the first 60 - 100MY of mammalian evolution.

It is likely that mammals developed high-frequency hearing during the early Cretaceous (~125 MY). At that time, eutherian ("placental") mammals arose and possessed a fully coiled cochlea with an ossified spiral ganglion canal. The evolution of modern features of the middle ear and cochlea was, however, a mosaic and different features arose at different times. Ultrasonic hearing developed even later - even the earliest bat cochleae (~ 60 MY) show none of the features characteristic of ultrasonically-sensitive modern bats.

### **954 Effects of Postmortem Time and Fixative on Morphology and Immunostaining of the Cochlea**

**Jennifer O'Malley<sup>1</sup>**, Saumil Merchant<sup>1,2</sup>, Molly Curran<sup>1</sup>, Joe Adams<sup>1,2</sup>

<sup>1</sup>*Massachusetts Eye and Ear Infirmary*, <sup>2</sup>*Harvard Medical School*

While it is known that progressive postmortem (PM) autolysis results in worsening morphology, the extent to which immunostaining is degraded has not been systematically studied. We studied the latter, using mouse cochleae wherein pertinent variables can be controlled.

We previously reported that 4% formaldehyde+1% acetic acid (FA) or 4% formaldehyde+1% acetic acid+0.1% glutaraldehyde (FGA) with celloidin embedding provides the best morphology while not inhibiting immunostaining in perfused tissue. In this study, we used the same six antibodies [prostaglandin D synthase (PGDS), aquaporin 1 (Aqp1), connective tissue growth factor (CTGF), 200 kD neurofilament (NF), tubulin and Na<sup>+</sup>,K<sup>+</sup>-ATPase] to study

changes in morphology and immunostaining with increasing PM times and three fixatives. CBA/CaJ mice were studied with four PM times (½ hr, 1hr, 2hr and 4hr) and three fixes, 4% formaldehyde (F), FA, and FGA. After euthanization, temporal bones were removed, immersed in fix, decalcified in EDTA and embedded in celloidin. The morphology at four PM times corresponded to that seen in human specimens as follows: ½ hr–excellent, 1 hr–good; 2 hr–fair; 4 hr–poor.

NF, tubulin, and Na<sup>+</sup>K<sup>+</sup>ATPase antibodies stained with all three fixes at all PM times. The PGDS antibody stained well with the FA and FGA at all PM times, but was weak with F at long PM times. The Aqp1 antibody stained best with FA. At 4hr PM, with F only, Aqp1 staining was substandard. The CTGF antibody stained best with FGA and failed beyond 1hr PM with all fixes.

Before immunostaining human specimens, it is worthwhile to determine protocols using animal tissue. Although it is impossible to precisely correlate PM time in human tissue with PM times in mice, it is possible to make general predictions for successful immunostaining in human specimens. Except for CTGF, these results predict that these antibodies should work with human temporal bone sections that demonstrate excellent, good and in some cases fair preservation.

Supported by NIDCD

### **955 Different Cells in the Organ of Corti Follow Distinct Death Pathways After Noise Damage**

**Barbara A. Bohne<sup>1</sup>**, Gary W. Harding<sup>1</sup>

<sup>1</sup>*Washington University School of Medicine*

Lack of knowledge about mechanisms of damage hinders identification of pharmacological agents that may ameliorate hearing loss & cochlear damage from noise exposure. To determine cell death pathways in the OC, microscopic examination of plastic-embedded flat preparations from 126 chinchilla cochleae was conducted. These ears were exposed to a 4- or a 0.5-kHz OBN at a moderate SPL (i.e., 72-95 dB) or a high SPL (i.e., 108 or 120 dB). Post-exposure recovery times varied from 1 hr to 14 days. Death pathways must be determined when cells are in the process of degenerating. Depending on exposure SPL, OC cells begin dying during or as long as 1-2 wks after exposure termination. Thus, cochleae must be examined at both short & long recovery times. Cells following the oncotic death pathway swell & eventually develop gaps in their plasma membrane. Their cytoplasmic contents leak into the surrounding tissue. To identify these dying cells microscopically, it is necessary to embed the tissue in a rigid supporting medium before dissection or sectioning. Performing a 'wet-dissection' on an OC containing much cellular debris risks washing away the cells that one is trying to identify. OHC death pathways that were found include: apoptosis (uncommon in our studies), oncosis & a pathway that is neither apoptosis nor oncosis. After intense noise, the most common OHC death pathway is oncosis. A variable number of oncotic OHCs are found in ears fixed 1 hr after exposure to a 4- or a 0.5-kHz OBN at 108 or 120 dB SPL. These dying cells

generally occur in clusters in variable length regions of the OC. OHCs dying by the pathway that is neither apoptosis nor oncosis are scattered among normal-appearing cells. This death pathway is primarily found after exposure to either a 4- or a 0.5-kHz OBN at 72-95 dB SPL. OHCs begin to degenerate during or shortly after termination of the exposure. IHCs and supporting cells die in smaller percentages of their total number than OHCs & their deaths usually do not occur in moderate numbers until several days post-exposure. IHC death pathways that have been identified include: apoptosis; oncosis; and ejection into the endolymphatic space. Supporting cell death pathways that have been identified include apoptosis and oncosis. Many IHCs & supporting cells disappear without leaving any clearly identifiable traces behind.

### **956 Cochlear De-Efferentation Exacerbates Primary Neural Degeneration from Moderate Noise Exposure**

Hajime Usubuchi<sup>1</sup>, Stéphane F. Maison<sup>1</sup>, M. Charles Liberman<sup>1</sup>

<sup>1</sup>*Dept. of Otology & Laryngology, Harvard Medical School*  
Olivocochlear (OC) efferents can reduce noise-induced threshold shifts, but the functional significance has been questioned given that natural environments do not contain sound levels as high as those used in laboratories (Kirk and Smith, 2003). However, recent work shows that threshold recovery after noise can hide massive noise-induced neural degeneration (Kujawa and Liberman, 2009). Here, we ask 1) whether similar neural degeneration occurs after long-duration exposures at "non-traumatic" (84 dB SPL) levels, and 2) whether the OC has a protective role in this arguably more natural context.

The OC system in 6-8 wk CBA/CaJ mice was lesioned unilaterally via stereotaxic injections of melittin into the LSO, where the lateral [L]OC fibers originate, and/or the VNTB, where medial [M]OC fibers originate. 3 wks later, lesioned and control mice were put in cages with small speakers generating 8-16 kHz noise at 84 dB SPL for 1 wk. ABRs and DPOAEs were measured in both ears before, 1 day after, and 1 wk week after trauma. Lesions were assessed by staining brainstem sections for acetylcholinesterase. Neurodegeneration was assessed by immunostaining cochlear whole mounts for synaptic ribbons (CtBP2) and cochlear-nerve terminals (Neurofilaments).

In control mice, the exposure caused ~20% loss of ribbons across the entire cochlea despite a mild temporary (< 20 dB), and no permanent, threshold shift. In mice with partial or complete de-efferentation, permanent threshold shifts were seen (10- 20 dB at high frequencies) and synaptic loss was significantly worse (by as much as 50% in some cochlear regions).

Thus, the OC system protects the ear from permanent damage even at moderate noise levels. Further investigation will better define the contributions of MOC vs. LOC systems.

Research supported by a grant from the NIDCD: R01 DC0188

### **957 Changes in Efferent Nerve Endings and Alpha-Synuclein Within the Mice Cochleae After Noise Exposure**

Shi-Nae Park<sup>1</sup>, Sang A Back<sup>1</sup>, Hong Lim Kim<sup>2</sup>, Kyoung Ho Park<sup>1</sup>, Omar Akil<sup>3</sup>, Laurence Lustig<sup>3</sup>, Sang Won Yeo<sup>1</sup>

<sup>1</sup>*Department of Otolaryngology-HNS, The Catholic University of Korea, College of Medicine, Seoul, Korea,*  
<sup>2</sup>*Laboratory of Electron Microscopy, The Catholic University of Korea, College of Medicine, Seoul, Korea,*  
<sup>3</sup>*Department of Otolaryngology-Head & Neck Surgery, University of California San Francisco, USA*

**Objectives:** It has been known that efferent nerves under the outer hair cells (OHCs) play a role in the protection of these cells from noise. Previously, we showed the localization of  $\alpha$ -synuclein protein within the efferent auditory synapses at the base of the OHCs and its possible relationship with early-onset hearing loss. To further understand the role of the efferent nerves and its relation with  $\alpha$ -synuclein, we compared the morphology of efferent nerve endings and the expression of  $\alpha$ -synuclein within the cochleae in C57 mice before and after noise exposure.

**Methods:** Mice were exposed to white noise at 110-dB sound-pressure level for 15 minutes (15-min noise group) or 60 minutes (60-min noise group) at the age of 1 month. Auditory brainstem responses and distortion product otoacoustic emissions (DPOAE) were recorded. Cochlear morphology with efferent nerve ending was compared. Western blotting was used to examine  $\alpha$ -synuclein expression in the cochlea. **Results:** Compared with mice of 15-min noise group, mice of 60-min noise group showed more severe hearing loss and decreased function in OHCs, especially within high-frequency regions. Sixty-min noise group demonstrated more severe pathologic changes within the cochlea, particularly within the basal turn, than 15-min noise group. Weaker  $\alpha$ -synuclein expression in the efferent nerve endings and cochlear homogenates in 60-min noise group was observed. **Conclusions:** In this study, morphological changes in the efferent nerve endings and decreased expression of  $\alpha$ -synuclein after the noise exposure were firstly observed in mice. Further studies at the cellular and functional levels will be necessary to verify our results.

### **958 Endoplasmic Reticulum Stress Induced by Noise Exposure Is Not Causally Related to Hearing Loss**

Naoki Oishi<sup>1</sup>, Su-Hua Sha<sup>2</sup>

<sup>1</sup>*University of Michigan,* <sup>2</sup>*Medical University of South Carolina*

We investigated the contribution of endoplasmic reticulum (ER) stress to noise-induced hearing loss (NIHL). Twelve-week old CBA/J mice were exposed to 108 dB broadband noise (BBN) at 2-20 kHz for 2 h resulting in permanent threshold shifts (PTS) ranging from 25 to 50 dB at frequencies from 6 to 32 kHz. Loss of outer hair cells (OHCs) occurred initially in the basal turn and spread apically with time after exposure. Levels of phospho-eIF2 $\alpha$

(p-eIF2 $\alpha$ ), a potential marker of ER stress, increased in the inner ear after traumatic noise. However, tauroursodeoxycholic acid (TUDCA), a chemical chaperone and protectant against ER stress, did not attenuate NIHL. Likewise, heterozygous X-box binding protein-1 (XBP1)-deficient mice had the same magnitude of hearing loss after noise exposure as wild type mice, despite the expectation that damage would be exacerbated if ER stress played a causative role. Additionally, other specific ER stress markers such as glucose-regulated protein of 78 kDa (GRP78) and C/EBP homologous protein (CHOP) were not up-regulated, and caspase-12 remained inactive after noise exposure. These results suggest that noise exposure can initiate transient ER stress signals but that NIHL and noise trauma-induced OHC death are not associated with ER stress.

Supported by grant R01 DC009222, DC003685 and core grant P30 DC05188 from the National Institute of Health.

### **959 Asymptotic Threshold Shift in Rats Induced by Long-Duration Continuous Noise**

Brandon Decker<sup>1</sup>, Guang-Di Chen<sup>1</sup>, Edward Lobarinas<sup>1</sup>, Richard Salvi<sup>1</sup>

<sup>1</sup>University at Buffalo

Rats have been extensively used in studies of noise-induced hearing loss and tinnitus to understand the underlying mechanisms of damage and protection. However, a major obstacle encountered in these studies is the large degree of intersubject variability. Previous reports have found that noise-induced hearing loss initially increases during the first 18-24 hours of exposure and then reaches an asymptotic threshold shift (ATS) with relatively little variability across subjects during ATS. The relationship between the noise level and ATS has been extensively investigated in humans and chinchillas (Carder and Miller, 1971; Mills et al., 1979; Gilbert et al., 1979). Above a critical exposure level, ATS increases with noise exposure intensity at the rate 1.6 dB/dB in chinchillas versus 1.7 dB/dB in humans. The critical exposure level is frequency dependent and is on the order of 45-65 dB SPL in chinchillas and 74-82 dB SPL in humans. Since the ATS phenomenon is poorly understood in rats, we investigated the relationship between noise level and ATS by measuring the auditory brainstem response (ABR) threshold. Rats (n=6) were exposed during the 1st week to a narrow-band noise (16-20 kHz) of 78 dB SPL; on the 2nd, 3rd, 4th and 5th week, the noise exposure level was increased to 84, 90, 96 and 102 dB SPL respectively. During each week of the exposure, ABR thresholds were measured on the 3rd and 6th day of each week. The ATS from the 102-dB exposure was approximately 50-55 dB near the exposure frequency and 15-30 dB at frequencies below the octave band noise. ATS increased with noise exposure level at the rate of 1.7-1.8 dB/dB and the critical noise exposure level was approximately 75 dB SPL; these values are similar to those reported for humans, but slightly higher than those for chinchilla. The threshold shifts at low frequencies recovered completely after the exposure, but high frequency thresholds only partially recovered with permanent threshold shifts (PTS) ranging

from 25 to 40 dB. (Supported by NIH grants R01DC009091 and R01DC009219)

### **960 The Functional and Morphological Changes by Noise Without Causing Hearing Loss: A Comparison Between Mice and Guinea Pigs**

Awad Almuklass<sup>1</sup>, Steve Aiken<sup>2</sup>, Jian Wang<sup>1,2</sup>

<sup>1</sup>Department of Physiology and Biophysics, Dalhousie University, <sup>2</sup>School of Human Communication Disorders, Dalhousie University

Noise exposure is the most common cause for sensorineural hearing loss. Recent studies in animals have demonstrated sub-clinical damage to cochlear afferent innervation by noise that did not cause measurable changes in auditory sensitivity. This damage was found in both mice and guinea pigs and was initiated at the ribbon synapses between hair cells and spiral ganglion neurons (SGNs), although there was much less loss of SGNs in guinea pigs than in mice. Since the hearing sensitivity had not changed, standard audiological sensitivity tests could not detect this damage. Given that the ribbon synapse is critical for the temporal resolution of neural transduction in the cochlea, subclinical damage to the synapse is likely to be revealed by testing temporal processing. In the present study, we determined whether the temporal precision of cochlear-neural transduction deteriorated after exposure to noise levels that should produce sub-clinical deficits, and if the functional changes were different between mice and guinea pigs. We also measured ribbon synapse changes following noise exposure in both species. Temporal resolution was evaluated by measuring the electrophysiological responses (the auditory brainstem response and auditory nerve compound action potential) to paired clicks as a function of inter-click interval. Animals were exposed to a broad band noise at 100 dB SPL for 2 hrs. Tests were conducted prior to, and 1, 7, and 35 days following, the noise exposure. As the inter-click interval changed from 30 to 1 ms, response amplitude decreased more for the second click than the first click following noise exposure, although the noise caused no permanent threshold shift. In addition, a deterioration in temporal resolution was indicated by an increase in response latency. Quantitative differences between mice and guinea pigs were seen, corresponding to differences in morphology (data are under processing).

### **961 Noise-Induced Changes Forward Masking Growth Functions of the Rat Auditory Brainstem Response (ABR)**

Eric Bielefeld<sup>1</sup>, Evelyn Hoglund<sup>1</sup>, Lawrence Feth<sup>1</sup>

<sup>1</sup>The Ohio State University

With a long-term goal of assessing techniques for early detection of noise-induced hearing loss, the current study investigated changes in forward masking growth functions of the auditory brainstem response (ABR) in the Sprague-Dawley rat. Off-frequency forward masking growth functions have been shown in humans to be non-linear, while On-frequency functions behave linearly. The non-

linear nature of the Off-frequency functions is attributable to active processing from the outer hair cells. Changes to the Off-frequency forward masking growth function may be an early event in noise-induced hearing loss, and therefore be a sensitive indicator of noise-induced cochlear damage. Seventeen Sprague-Dawley rats' ABRs were recorded with and without forward maskers. The masker threshold was defined as the masker level required to reduce the ABR P1 wave by 50% from the unmasked condition. The first group of rats was then exposed to noise to induce permanent threshold shift. After the noise exposure, the forward masking growth functions were measured, and results showed that the noise rendered the Off-frequency forward masking growth functions more linear. The ABR forward masking growth functions before and after noise exposure for the rat displayed patterns consistent with human behavioral functions. The second group was exposed to a milder noise for 6 hours/day, 4 days per week for several weeks. Off-frequency forward masking growth functions were measured weekly to assess their sensitivity to mild cochlear damage from noise to assess the effectiveness of the approach as a tool for detecting noise-induced cochlear damage. Research was supported by a grant from the Office of Naval Research #N000140911.

### **962** Loss of Directional Sensitivity in the Mouse Cochlear Inner Hair Cells After Intense Mechanical Stimulation

**Ruben Stepanyan**<sup>1</sup>, Artur Indzhukulian<sup>1</sup>, Julie McLean<sup>1</sup>, Gregory Frolenkov<sup>1</sup>

<sup>1</sup>*Department of Physiology, University of Kentucky*

When hair cell stereocilia are deflected by intense acoustical stimulation, the mechanotransduction apparatus is the first to be exposed to excessive mechanical forces. Yet, potential changes of the mechano-electrical transduction (MET) after overstimulation are largely ignored. Here we examined MET responses in cochlear inner hair cells of young postnatal mice before and after intense overstimulation with a fluid-jet. Similar to the previous reports, large deflections of the hair bundle toward the positive (excitatory) direction did not affect MET responses. However, large biphasic (positive and negative) deflections resulted in several changes of MET responses: 1) the amplitude of MET current decreased; 2) MET responses acquired characteristic "tail" currents; and 3) most interestingly, both positive and negative stereocilia deflections began to evoke MET responses. All these MET changes occurred without substantial decrease of the bundle's pivotal stiffness, i.e. presumably before disruption of the actin filaments at the taper of stereocilia. Despite a considerable reduction of the maximum MET current, the adaptation of MET responses was not affected by overstimulation. Likewise, ratiometric calcium imaging revealed complete clearance of intracellular  $Ca^{2+}$  after the end of damaging stimuli. High resolution scanning electron microscopy revealed apparently normal morphology of the stereocilia bundles in the damaged hair cells with only minor overall loss of the tip links. However, close examination of tip link morphology revealed changes in the

angle of their oblique orientation, resulting in a statistically significant decrease of the distance from the tip of the shorter stereocilium to the end of the tip link at the neighboring taller stereocilium. We concluded that the upper end of the tip links is likely to "slide down" after mechanical overstimulation resulting in abnormal directional sensitivity of the MET machinery. Supported by NIDCD/NIH (R01 DC008861)

### **963** Acoustic Analysis of Noise by Titanium Head Golf Driver and Effect of Impulse and Continuous Noise on Mouse Cochlea

**Yong-Ho Park**<sup>1</sup>, Young Chul Kim<sup>2</sup>, Young Ho Kim<sup>3</sup>

<sup>1</sup>*Chungnam National University*, <sup>2</sup>*Chungbuk National University*, <sup>3</sup>*Seoul National University Boramae Medical Center*

Various types of noises can lead to hearing threshold shift. Noise-induced hearing loss (NIHL) by impulse noise has been made with gunshot noise before. The present study was performed to investigate the effect of noise of titanium head golf driver on mouse cochlea and we also compared the effect of impulse noise and continuous noise. A total thirty-one balb/C mice (20 – 22 g) with normal hearing were used in this study. Among these animals, 26 mice were exposed to noise and remaining 5 animals without exposure to noise served as normal control. For the noise exposure, impulse noise (titanium head golf driver's hitting noise) centered around 4.5 kHz with 120.5 dB SPL for 2 hrs (1440 repetitions; 1/5 sec) was used. And continuous noise at the same Hz with same dB SPL was exposed for 288 seconds. Auditory brainstem response (ABR) was measured before noise exposure, day 7, and day 14 after noise exposure. And histopathological examinations were done on day 14 after noise exposure. ABR showed PTS at 4, 8, 16, 32 kHz, and click after exposure of noise and threshold shifts at immediate, 1 week, 2 weeks after noise exposure were statistically significant compared to baseline in impulse noise group. And the threshold shifts were greater than in impulse noise group compared in continuous noise group. Two weeks after noise exposure, histopathologic findings were well correlated with auditory functions. This indicates that repeated long time impulse noise can cause greater damage to the cochlea than short time continuous noise.

### **964** Blast Wave Impact on Auditory Pathway: A Cadaveric Temporal Bone Study

**Kanthaiah Koka**<sup>1</sup>, Travis Pfannenstiel<sup>2</sup>, Xianxi Ge<sup>2</sup>, Jianzhong Liu<sup>2</sup>, Ronald Jackson<sup>2</sup>, Gregory Capra<sup>2</sup>, Vikrant Palan<sup>3</sup>, Mario Pineda<sup>3</sup>, Ben Balough<sup>2</sup>, James Easter<sup>1</sup>

<sup>1</sup>*Otologics LLC, Boulder, CO, USA*, <sup>2</sup>*Navy Medical Center San Diego, San Diego, CA, USA*, <sup>3</sup>*Polytec Inc., Irvine, CA, USA*

The objective of the current study is to examine ossicular motion in response to simulated blast wave and harmonic stimuli in a temporal bone model. Seven human cadaveric temporal bones were prepared by mastoidectomy and extended facial recess exposing the malleus head (M), incus body (I), incus long process (ILP), stapes superstructure (S) and round window membrane (RWM). A

custom built speaker and condensing tube were used to present harmonic stimuli from 100 Hz to 6000 Hz and a simulated blast overpressure waveform. Calibrated stimuli were presented from 85 dB SPL (0.000051 psi) to 135 dB SPL (0.0163). A scanning LDV was used to obtain simultaneous real-time images of the ossicles and round window membrane during harmonic and blast wave stimulation. Ossicular displacement was analyzed in the frequency domain. The peak displacements were averaged across bones; mean and standard errors are presented. The phase difference between stapes and round window was observed to be approximately 180°. The observed out-of-plane peak displacements for harmonic stimuli at 110 Hz and above, and the variation of displacement with frequency, were similar to those reported in the literature. For a single impulse with over- and under-pressure simulating the Friedlander waveform characteristic of blast, the peak ossicular displacements were seen to be significantly (paired t-test,  $p < 0.01$ ) higher than for harmonic stimuli with equivalent peak pressure, and greater than predicted by a widely used acoustic damage model. These results suggest that the response of the auditory system to high intensity, long-duration impulse may not be fully captured by existing models. The displacements and phase relationships observed under these conditions will be used to refine models of acoustic trauma from blast.

### **965 Noise-Induced Expression Changes in MicroRNAs Are Time- And Site-Specific in the Rat Cochlear Sensory Epithelium**

Minal Patel<sup>1</sup>, Bo Hua Hu<sup>1</sup>

<sup>1</sup>State University of New York at Buffalo

Exposure to intense noise causes permanent damage to sensory cells in the cochlea. To develop effective treatments, it is essential to understand the molecular mechanisms associated with cochlear damage. We recently identified the presence of microRNAs (miRNAs) in normal rat cochlea and studied their expression changes after acoustic trauma. To further study whether expression changes in miRNAs are site-specific, we examined expression changes in five miRNAs (miRs 184, 200-b, 224, let-7g and 96) in the apical and the basal sections of the sensory epithelium of the rat cochleae following exposure to a broadband noise at 120dB (SPL) for 2 h, which caused an average threshold shift of 47±4 dB, 32±6 dB and 18±3 dB, measured at 2 h, 1 day and 7 days post-exposure, respectively. In the apical region, significant relative expression changes were detected for miRs 184, 200b, let-7g and 96 at 2 h and 1 day and miRs 184, let-7g and 96 at 7 day post-exposure. However, in the basal region, significant relative expression changes were detected for miR-200b and let-7g at 2 h, for miR-200b at 1 day and for miRs 224 and 96 at 7-day post-exposure. We also examined the spatial distribution of miR-200b using an in situ-hybridization technique and found miR-200b to be localized in both the sensory and supporting cells of the cochlea. Additionally, target predictions for miR-96 and 200b using TargetScan and DAVID bioinformatic software revealed apoptosis-related targets including Taok1, Xiap,

and Map3k2. Further assessment of expression changes in these genes revealed significant upregulation of Taok1 and Xiap and downregulation of Map3k2 after acoustic overstimulation, suggesting that these apoptosis-related genes are associated with miRNA regulation. In conclusion, these results indicate that acoustic trauma induces spatial and temporal expression of miRNAs in the cochlea and may influence the target regulation of apoptosis-related genes.

(Supported by NIH R01 DC010154-01A2 to BH Hu).

### **966 Gene Expression of Apoptosis in Cochlea from Noise-Exposed CBA Mice**

Yun Suk An<sup>1</sup>, SeungHyo Choi<sup>2</sup>, Jin Kyung Seo<sup>1</sup>, Hyun Ja Kwon<sup>1</sup>, Hong Ju Park<sup>1</sup>, Jong Woo Chung<sup>1</sup>

<sup>1</sup>Asan Medical Center, University of Ulsan College of Medicine, <sup>2</sup>Jeju National University College of Medicine

**Background and Objectives:** Exposure to intense noise induces morphologic destruction of the hair cell in the cochlear and apoptosis of the hair cell in the cochlear through metabolic change. To identify the molecular changes associated with noise-induced apoptosis, we used quantitative real-time PCR to evaluate the changes in 84 apoptosis related genes in cochlear samples from Organ of Corti. **Materials and Method:** Four-week-old CBA mice with normal hearing levels-proven with ABR, DPOAE and Prayer's reflexes were used in this study. Noise group mice were exposed to 110 dB SPL white noise for 3 hours per day for 3 consecutive days and control group mice were not exposed to noise in soundproof booth for 3days. The hearing loss documented before and after noise exposure and 1day following noise exposure by ABR and DPOAE. Organ of Cortiin cochlear in each group was obtained immediately 1 day after the noise exposure. Total RNA was extracted using an RNA extraction kit (RNeasy Mini Kit, Qiagen) as per manufacturer's protocols. First strand cDNAs synthesized using oligodTprimed reverse transcription supplied with the RT2First Strand Kit(SABiosciences). The cDNA solution was mixed SuperArray RT qPCR Master Mix and the loaded on to 96-well array. QRT-PCR was performed using the thermal cycler(ABI7000HT, AppliedBiosystems, Foster City, California)**Results:**Real time PCR array revealed that 35genes were up-regulated or down-regulated twofold or more in the CBA mice cochlea. Among these genes, 15 genes were up-regulated tenfold or more ( $p$ -value  $< 0.05$ ). Among 15 genes, three (Bag3, Bnip3l, Mcl1) belonged to Bcl-2 family, three (Casp2, 3, 7) belonged to Caspase family, three(Tnfrsf11b, Tnfrsf1a, Cd70) belonged to TNF ligand and receptor family, two (Bcl10, Card6) belonged to CARD family, four (Traf3, Birc2, Trp53inp1, Trp73) belonged to miscellaneous. **Conclusion:** This study demonstrated differential apoptosis-related gene expression profile in permanent noise-exposed CBA mice. This study may also provide basic information on candidate genes hearing loss after noise induced cochlear dysfunction.

**967 The Role of Septin4 in the Cochlear Supporting Cells During Acoustic Trauma**

Atsuhiko Yoshida<sup>1</sup>, Norio Yamamoto<sup>1</sup>, Takayuki Nakagawa<sup>1</sup>, Juichi Ito<sup>1</sup>

<sup>1</sup>Graduate School of Medicine, Kyoto University

The organ of Corti includes hair cells and supporting cells. The supporting cells, including inner and outer pillar cells and Deiter's cells, form rigid scaffolding with organized bundles of microtubules. These contribute to roles of supporting cells such as withstanding mechanical stress, maintaining the integrity of reticular lamina, transmitting motion of the basilar membrane to the reticular lamina, and transmitting motion of the hair cells between the reticular lamina and the basilar membrane (Slepecky, 1996). However, little is known about molecular mechanisms of these roles of supporting cells. Septins are a family of GTP binding proteins that are well conserved in eukaryotic species except plants. Septins contribute to the lateral compartmentalization of membranes and the cortical rigidity by associating with membrane lipids, actins and microtubules. Because supporting cells in the cochlea are rich in actins and microtubules, we assumed septins have important roles in maintaining the structure of supporting cells by acting with these typical cytoskeleton proteins. Among septin subtypes, we chose septin4 (sept4) that is abundantly expressed in the adult mouse brain.

As a first step to elucidate the function of sept4 in the cochlea, we examined the distribution of Sept4 in the wild-type mouse cochlea and auditory function of Sept4 null mice using auditory brain stem response (ABR). Sept4 was expressed in pillar cells and Deiters' cells, but no differences were seen in the ABR thresholds between sept4 null mice and wild type mice. We also examined auditory functions of them after noise exposure that usually cause temporary threshold shift. The ABR thresholds of sept4 null mice did not recover 2 weeks after the noise exposure, whereas those of wild type mice recovered to the level before the noise exposure as expected. These results suggest that sept4 is involved in the mechanisms of protection or recovery of cochlea from noise induced temporal hearing loss.

**968 Activation and Role of STAT3 in the Noise-Induced Stress Response in the Inner Ear**

Teresa M. Wilson<sup>1</sup>, Irina Omelchenko<sup>1</sup>, Yue Yang<sup>2</sup>, Min Dai<sup>1</sup>, Xiaorui Shi<sup>1</sup>, Alfred L. Nuttall<sup>1</sup>

<sup>1</sup>Oregon Health & Science University, <sup>2</sup>University of Washington

Signal transducers and activators of transcription 3 (STAT3) is a stress responsive transcription factor that relays signals from ligand-bound cytokine and growth factor receptors in the plasma membrane to the nucleus. Many of its target genes, such as VEGF, MnSOD, HIF-1 $\alpha$ , and Survivin, are involved in the regulation of pro-survival and cellular proliferation functions. STAT3 plays a protective role against cerebral and myocardial ischemia/reperfusion injury. Upon ischemic insult, STAT3 is activated through phosphorylation leading to dimer

formation, nuclear translocation and transcriptional activation. Additionally, at least part of the protective capacity of STAT3 occurs independently of its transcriptional activity and has been attributed to the ability of STAT3 to directly regulate mitochondrial complex I activity and respiration and, possibly, to inhibit mitochondrial permeability transition pore opening. In our studies on noise-induced stress responses in the inner ear, we observed that acoustic trauma increased STAT3 protein levels in the capillaries of the stria vascularis. Further examination revealed that noise exposure also induced phosphorylation and nuclear translocation of STAT3 in many cell types in the inner ear including the marginal cells of the stria vascularis, type II fibrocytes, inner hair cells, and in the supporting cells in the organ of Corti. That STAT3 has a possible role in protecting against noise-induced damage to the inner ear was explored through the use of specific STAT3 inhibitors. The findings of these studies will be discussed. Supported by grants 5R01DC000105 (ALN), 1R01DC010844 (XS), and P30DC005983.

**969 Traumatic Noise Activates Rho-Family GTPases Through Transient ATP-Depletion**

Fu-Quan Chen<sup>1</sup>, Su-Hua Sha<sup>1</sup>

<sup>1</sup>Medical University of South Carolina

As molecular switches, small GTPases act as major mediators in transmembrane signaling and as key regulators of the actin cytoskeleton in all eukaryotic cells. In this study, we first characterized the auditory pathology in adult CBA/J mice exposed to broadband noise at 2-20 kHz with an intensity of 106 dB for 2 h. The exposure initially disturbed the actin arrangement of the stereocilia, and resulted in permanent threshold shifts of 35, 60, and 65 dB at 8, 16, and 32 kHz with corresponding hair cell loss two weeks after the noise exposure. No hair cell loss was observed immediately after noise, but losses appeared after 1 h in the basal turn and increased with time following noise exposure and spread apically. The mitochondrial-mediated caspase-independent cell death marker, endonuclease G, was translocated to the nuclei of dying OHC at 1 and 3 h after the noise exposure. We then measured ATP concentrations and investigated small GTPase-linked signaling pathways in the inner ear following noise exposure. The concentration of ATP in cochlear tissue dropped immediately following noise exposure and reached a minimum around 1 h post noise exposure. Noise trauma increased levels of active Rac1, decreased those of active RhoA, and promoted the formation of a RhoA-p140mDia complex indicating activation of the Rho GTPase pathways. In order to test the hypothesis that energy depletion may lead to activation of Rho GTPase pathways and mitochondrial-mediated cell death, we treated the inner ear OC1 cell line with the energy-depleting agent oligomycin. ATP depletion enhanced Rac1 activity and promoted cell death and the rearrangement of the actin cytoskeleton.

Our results suggest that noise trauma induces transient ATP depletion and activates Rho GTPase signaling

pathways that regulate the actin cytoskeleton, leading to structural disruptions of hair cells in the inner ear. Supported by grant R01 DC009222 from the National Institute of Health.

### **970 Elevated Hearing Thresholds and Noise Protection in a Mouse Over-Expressing Alpha Synuclein**

Omar Akil<sup>1</sup>, Jolie Chang<sup>1</sup>, Lawrence Lustig<sup>1</sup>

<sup>1</sup>UCSF Department of Otolaryngology-HNS

Synucleins (Syn) are a family of 3 small, soluble and highly conserved proteins ( $\alpha$ ,  $\beta$  and  $\gamma$ ) expressed in the synaptic region of the central nervous system. While it is known that the protein  $\alpha$  Syn accumulates in the brain of patients with sporadic Parkinson's disease (PD) and increased gene dosage causes a severe dominantly inherited form of PD, little is known about how  $\alpha$  Syn is related to that neurodegeneration.

Previously we demonstrated that  $\alpha$  Syn is expressed in the cochlea and localized predominantly to the efferent auditory synapse at the base of the outer hair cells (OHC) (Akil et al., 2008). Prior studies in  $\alpha$  syn KO mice have also shown that this mutation has little, if any, effect on the synaptic transmission centrally (Abeliovich et al., 2000; Cabin et al., 2004), and within the auditory system, there is no effect on hearing at least through P21 (Park et al., 2009). However, studies have found that in a mouse over-expressing  $\alpha$  syn, neurotransmitter release in the brain is inhibited (Venu et al., 2009).

In this study, we sought to investigate the auditory effects of  $\alpha$  Syn over-expression, and whether hearing is affected as a result of this inhibition of neurotransmitter release. Auditory brainstem response (ABR) recording demonstrated that the mutant mice present an elevated ABR threshold (between 10-20dB) in click, 8, 16 and 32 KHz stimulus when compared to the wild-type (WT) ABR thresholds. This ABR threshold elevation was detected at P21 and persisted in older mice through at least P7months. The compound action potential thresholds between WT and over-expressing mice did not significantly differ. Further, significant differences between WT and over-expressors were not seen in distortion product otoacoustic emissions (DPOAE) nor in the contralateral suppression of DPOAEs at P30 and P90, suggesting that OHC function is intact in the mutant. In contrast, following noise exposure, WT mice demonstrate an ABR threshold shift of 10-20dB greater than the mutant mice (measured 26 days post noise exposure) suggesting a protective effect of  $\alpha$  Syn over-expression against noise-induced hearing loss. On light microscopy, no cochlear abnormalities were identified in the over-expressor mice. Immunofluorescence using anti- $\alpha$  syn antibody revealed strong labeling only in the base of the OHC as expected in the WT cochlea, while  $\alpha$  Syn over-expression resulted in staining in cells throughout the organ of Corti.

Together, these studies suggest that the mild hearing loss and protective effect against noise damage seen in the  $\alpha$  Syn over-expressor mice may be due to the inhibition of neurotransmitter release at one of a number of possible locations in the organ of Corti. Electron microscopy and

electrophysiology will be necessary to further localize and elucidate the nature of these abnormalities.

### **971 Involvement of the Neural Cell Adhesion Molecule (NCAM) in Noise Related Hearing**

#### **Loss as Assessed in NCAM Null Mutant Mice**

Sara Euteneuer<sup>1,2</sup>, Igor Jakovcevski<sup>2</sup>, Melitta Schachner<sup>2</sup>

<sup>1</sup>University Hospital Heidelberg, <sup>2</sup>Zentrum fuer Molekulare Neurobiologie Hamburg

Introduction: Noise induced hearing loss is one of the most frequently recognized occupational diseases. Thus the identification of distinct genetic risk factors, indicating possible starting points for future therapeutic approaches, is highly desirable. The neural cell adhesion molecule (NCAM) has been identified as modulator of glutamatergic synapse strength. Here we tested the hypothesis that genetic ablation of NCAM, which is expressed at the afferent inner ear's synapse, predisposes for development of noise induced hearing loss.

Methods: Frequency specific auditory evoked brain stem responses (ABRs) and distortion product otoacoustic emissions (DPOAEs) were measured before and up to 10 days after noise challenge (90 dB broad band noise, 8-16kHz, for 30min) in NCAM null mutant (KO, n = 5) and matched wild type (WT, n = 6) littermate male and female mice at 8 to 9 weeks of age. Inner ears of animals immediately after noise exposure, as well 4 weeks after noise exposure, were processed for evaluation of the inner ear's afferent innervations pattern.

Results: Hearing thresholds, assessed by ABRs, as well as hair cell function, assessed by DPOAEs, were comparable between NCAM KO and WT mice before noise challenge. Directly after noise exposure, thresholds increased more in the NCAM KO than in WT mice. In the NCAM KO mice, increased ABR thresholds were accompanied by increased DPOAE thresholds, while the latter were unaffected in WT mice. Ten days after noise trauma threshold increases were still evident in the KO mice, while thresholds in WT mice had fully recovered.

Discussion: Our data suggest that ablation of NCAM leads to development of noise-induced hearing loss in this mouse model. The observed phenotype may be not only due to alterations at the afferent inner ear's synapse, but also to widespread changes in the inner ear as observed by persistently increased DPOAE-thresholds.

Supported by the University of Luebeck, School of Medicine, grant E28-2009 (to SE).

### **972 Molecular Pathway Analysis of Noise-Induced Hearing Loss Identifies Hepatocyte Nuclear Factor 4alpha as a Central Player**

Jane B. Jensen<sup>1,2</sup>, Martijn C. Briet<sup>1,2</sup>, Eleni P. Asimacopoulos<sup>1,2</sup>, Konstantina M. Stankovic<sup>1,2</sup>

<sup>1</sup>Department of Otolaryngology, Harvard Medical School, Boston, MA, <sup>2</sup>Eaton Peabody Laboratory, Department of Otolaryngology, Massachusetts Eye and Ear Infirmary, Boston

Noise-induced hearing loss (NIHL) is a problem of profound clinical significance, growing magnitude, and

major societal impact, yet curative therapies do not yet exist. Many genes have been implicated in the cochlear response to noise, and they vary depending on noise parameters. To prioritize functional significance of these genes, we have analyzed them collectively using Ingenuity Pathway Analysis software. Genes reported through hypothesis-driven or high throughput studies in rodents were grouped into 3 categories: (1) genes associated with temporary threshold shift (TTS), (2) genes associated with acute permanent threshold shift (PTS), defined as occurring within 24 hours of noise exposure, and (3) genes associated with subacute PTS, defined as occurring 2 weeks post exposure. For each group, “nodal” genes – i.e. the most interconnected genes in a given network – were ranked according to the statistical significance. The most significant nodal genes included not only genes already known to be associated with the cochlear response to noise, but also genes that have not been described in the cochlea. We have focused on validation of these novel genes in mice. Six 6 week old CBA/CaJ mice were exposed to 8-16 kHz band filtered noise for 2 hours at 97 dB and sacrificed 2 weeks later (TTS group), or at 100 dB and sacrificed 24 hours (acute PPS) or 2 weeks (subacute PPS) later. Age-matched unexposed mice served as controls. We report noise-induced changes in expression of a novel transcription factor, hepatocyte nuclear factor 4 $\alpha$  (HNF4 $\alpha$ ), in the cochlea using immunohistochemistry. While HNF4 $\alpha$  was localized to inner and outer hair cells in all groups, additional specific staining was identified within type 1 fibrocytes of the spiral ligament in acute PTS and TTS groups, or both type 1 and 2 fibrocytes in the subacute PTS group. Our data point to HNF4 $\alpha$  as a novel therapeutic target for NIHL.

[Supported by NIH grant K08 DC010419 and Massachusetts Life Sciences Center]

### **973 Action of Substance P on the Recovery from the Acoustic Trauma**

**Eiju Kanagawa<sup>1</sup>, Kazuma Sugahara<sup>1</sup>, Hideki Toyota<sup>1</sup>, Takefumi Mikuriya<sup>1</sup>, Hiroaki Simogoori<sup>1</sup>, Hiroshi Yamashita<sup>1</sup>**

<sup>1</sup>*Yamaguchi University*

Substance P is a polypeptide composed of 11 amino acids, and it is known as a perception neurotransmitter. We have already reported that the VOR gain increased after the administration of substance P into the inner ear. In addition, the nystagmus after the vestibular disorder was suppressed. In the last meeting, we have reported the role of substance P and NK1 receptor on the recovery from the temporary threshold shift after the intense noise exposure. In the present study, we administered substance P to the inner ear after TTS, and evaluated the synaptic ribbon beneath the inner hair cells.

Hartley male guinea pigs (350 - 400 g) with the normal tympanic membranes and the normal Preyer reflexes were used in this study. Animals were divided into 4 groups (Control group, Substance P group, TTS group, Substance P+TTS group). After the post-auricular incision, mastoid bulla was opened with the drill. Gelatin sponge which

included substance P (10-2 M) (the substance P group and Substance P + TTS group) or saline (the control group and TTS group) was placed on round window membrane. The mastoid bulla was closed with the dental cement. The ABR threshold was measured immediately after this operation to confirm that the hearing function did not change. The animals were exposed to the intense band noise (110 dB SPL for three hours as the TTS model). Twenty four hours later, the temporal bone was removed to evaluate the synaptic ribbon count.

To reveal the synaptic ribbon, the immunohistochemistry was performed using the anti-Neurofilament antibody and anti-CtBP2 antibody. These sample were observed with the fluorescence microscope.

In the TTS group, the density of signals for synaptic ribbon significantly larger than those in the other 3 groups. There is no significant difference in the count number of a synaptic ribbon in the other three groups.

We have reported the effect of substance P in the hearing functional restoration after the intense noise exposure. However, the mechanism of the protective effect of substance P is unclear. The previous reports assumed that substance P has amplified the cochlea nerve compound action potential and that substance P protected the spiral ganglion. In the present study, we showed that the administration of substance P inhibited the change of synaptic ribbon after the intense noise exposure. The result suggests that the polypeptide promotes the recovery of the cochlear function after noise trauma.

### **974 ER stress in aminoglycoside ototoxicity**

**Naoki Oishi<sup>1</sup>, Jing Xie<sup>1</sup>, Jochen Schacht<sup>1</sup>**

<sup>1</sup>*University of Michigan, Kresge Hearing Research Institute*

Under severe or prolonged endoplasmic reticulum stress (ER stress), specific stress-associated apoptotic pathways are activated. We tested whether ER stress plays a role in aminoglycoside ototoxicity. For in-vivo experiments, we used heterozygous knockout mice of X-box binding protein-1 (XBP-1), one of the key components in protective pathways against ER stress. XBP-1 knockout mice showed higher sensitivity to locally injected gentamicin than wild type mice. Systemic co-injection of tauroursodeoxycholic acid (TUDCA), a chemical chaperone that can reduce ER stress, rescued gentamicin ototoxicity in XBP-1 heterozygous knockout mice, suggesting a relationship between ER stress and gentamicin ototoxicity. Interestingly, however, hair cell counts did not show any difference between gentamicin-treated wild type and heterozygous mice. In an organotypic culture of postnatal day 2-3 pups of CBA/J mice, gentamicin treatment did not induce ER stress-related markers in the cochlear neuroepithelium throughout the entire time course towards hair cell death. In contrast, the specific ER stressor tunicamycin induced a specific ER stress-associated apoptosis marker, C/EBP homologous protein (CHOP), in outer hair cells and led to their death. These results indicate that ER stress may play some role in aminoglycoside ototoxicity but may not be associated directly with hair cell pathology. We will discuss the

possible contribution of ER stress to aminoglycoside ototoxicity.

(Supported by research grant DC-003685 and core grant P30 DC-05188 from NIH-NIDOD)

### **975 Calreticulin Binds to Gentamicin and Reduces Drug-Induced Cytotoxicity**

Takatoshi Karasawa<sup>1</sup>, Qi Wang<sup>1</sup>, Larry David<sup>1</sup>, Peter Steyger<sup>1</sup>

<sup>1</sup>Oregon Health & Science University

Aminoglycosides like gentamicin are among the most commonly used antibiotics in clinical practice, and are essential for treating life-threatening tuberculosis and Gram-negative bacterial infections. However, aminoglycosides are also nephrotoxic and ototoxic. Although a number of mechanisms have been proposed, it is still unclear how aminoglycosides induce cell death in auditory sensory epithelia and subsequent deafness. Aminoglycosides bind to various intracellular molecules, such as RNA and phosphoinositides. We hypothesized that aminoglycosides, based on their tissue-specific susceptibility, also bind to intracellular proteins that play a role in drug-induced ototoxicity. By conjugating an aminoglycoside, gentamicin, to agarose beads and conducting a gentamicin-agarose pull-down assay, we have isolated gentamicin-binding proteins (GBPs) from immortalized cells of mouse organ of Corti, HEI-OC1. Mass spectrometry identified calreticulin (CRT) as a GBP. Immunofluorescence revealed that CRT expression is concentrated in strial marginal cells and hair cell stereocilia, primary locations of drug uptake and cytotoxicity in the cochlea. In HEI-OC1 cells treated with gentamicin, reduction of CRT expression using siRNA reduced intracellular drug levels. CRT-deficient mouse embryonic fibroblast (MEF) cells as well as CRT siRNA-transfected wild-type MEFs also had reduced cell viability after gentamicin treatment. A pull-down assay using deletion mutants of CRT determined that the carboxyl C-domain of CRT binds to gentamicin. HeLa cells transfected with CRT C-domain deletion mutant construct were more susceptible to gentamicin-induced cytotoxicity compared to cells transfected with full-length CRT or other deletion mutants. Therefore, we conclude that CRT binding to gentamicin is protective against gentamicin-induced cytotoxicity.

Supported by NIH NIDCD grant R03 DC009501 (T.K.), R01 DC04555 (P.S.S.), and P30 grants DC05983, EY10572, and CA069533

### **976 Gentamicin Uptake in Acoustically Traumatized Cochleae**

Hongzhe Li<sup>1</sup>, Peter Steyger<sup>1</sup>

<sup>1</sup>Oregon Health & Science University

Exposure to intense sound or high doses of aminoglycoside antibiotics can increase hearing thresholds, induce cochlear dysfunction, disrupt hair cell morphology and promote hair cell death, leading to permanent hearing loss. When the two insults are combined, synergistic ototoxicity is evident both physiologically and morphologically. The underlying

mechanism of this synergism remains unknown. One hypothesis is that sound exposure enhances hair cell uptake of cationic aminoglycosides, such as gentamicin. We found that prolonged sound exposure increased gentamicin uptake by murine hair cells. To preclude pathological changes induced by acoustic trauma, we examined whether acute concurrent narrow-band sound exposure increased gentamicin uptake over short periods. We observed negligible changes in hair cell uptake of gentamicin, implying that concurrent moderate-to-intense sound exposure does not directly increase gentamicin uptake. Additional experiments with prolonged sound exposure revealed increased gentamicin permeation across the strial blood-labyrinth barrier, suggesting that changes in strial physiology and/or integrity can lead to increased hair cell uptake of gentamicin, and thus may represent one mechanism of synergistic ototoxicity due to acoustic trauma followed by drug exposure. Therefore, the site of ototoxic synergy could reside in the stria vascularis, in the sensory epithelium, or in both locations.

### **977 Protective Role of Nrf2 in Age-Related Hearing Loss and Gentamicin Ototoxicity**

Keiji Tabuchi<sup>1</sup>, Tomofumi Hoshino<sup>1</sup>, Masahiro Nakayama<sup>1</sup>, Akira Hara<sup>1</sup>

<sup>1</sup>University of Tsukuba

The antioxidant responsive element (ARE) is a cis-acting regulatory element, through which NF-E2-related factor (Nrf2) regulates transcription of genes encoding phase II detoxification enzymes, antioxidants, and other factors essential for cell survival. Under normal conditions, Nrf2 is anchored in the cytoplasm through interaction with Kelch-like ECH-associated protein 1 (Keap1) and subsequently proteolyzed by proteasomes. In contrast, under oxidative stress conditions, Keap1-censored electrophiles inhibit the proteolysis of Nrf2. Having thus escaped Keap1-mediated proteolysis, Nrf2 accumulates in the nucleus and activates ARE-mediated gene transcription. To date, many genes driven by Nrf2, including heme oxygenase 1 (HO1), NAD(P)H:quinone oxidoreductase 1 (NQO1), NHR:quinone oxidoreductase 2 (NQO2), glutathione peroxidase (GPx), superoxide dismutase 1 (SOD1), and peroxiredoxin I (PrxI), have been reported to be involved in the antioxidant defense system. Reactive oxygen species contribute to the formation of several types of cochlear injuries, including age-related hearing loss and gentamicin ototoxicity. In this study, we examined the roles of Nrf2 in age-related hearing loss and gentamicin ototoxicity by measuring auditory brainstem response thresholds in Nrf2-knockout mice. Although Nrf2-knockout mice maintained normal auditory thresholds at 3 months of age, their hearing ability was significantly more impaired than that of age-matched wild-type mice at 6 and 11 months of age. Additionally, the numbers of hair cells and spiral ganglion cells were remarkably reduced in Nrf2-knockout mice at 11 months of age. To examine the importance of Nrf2 in protecting against gentamicin-induced ototoxicity, 3-day-old mouse organ of Corti explants were cultured with gentamicin. Hair cell loss caused by gentamicin treatment was enhanced in the Nrf2-deficient tissues. Furthermore,

the expressions of some Nrf2-target genes were activated by gentamicin treatment in wild-type mice but not in Nrf2-knockout mice. The present findings indicate that Nrf2 protects the inner ear against age-related hearing injuries and gentamicin ototoxicity by up-regulating antioxidant enzymes and detoxifying proteins.

### **978 The Influence of Sphingosine 1-Phosphate Receptor 2 Antagonist on Gentamycin-Induced Hair Cell Loss of the Rat Cochlea**

Masahiro Nakayama<sup>1</sup>, Keiji Tabuchi<sup>1</sup>, Tomohumi Hoshino<sup>1</sup>, Isao Uemaetomari<sup>1</sup>, Akira Hara<sup>1</sup>

<sup>1</sup>University of Tsukuba

Sphingosine 1-Phosphate is a bioactive lysolipid known to regulate many critical biological processes, such as cell proliferation, survival, migration, and angiogenesis. The ligand S1P is produced through the phosphorylation of sphingosine by sphingosine kinases 1 and 2. S1P exerts its function either as a ligand for a family of five specific G-protein coupled receptors (S1P1-S1P5) or as an intracellular second messenger. S1P1, S1P2, and S1P3 are expressed widely in cells and tissues, whereas S1P4, S1P5 are largely confined to cells of the immune and central nervous systems. Aminoglycosides antibiotics including gentamicin induce inner ear hair cell loss and sensorineural hearing loss. Apoptotic cell death is considered to play a key role in this injury. S1P reportedly acted as a cochlear protectant to gentamicin ototoxicity [Nishimura et al, 2010]. The present study was designed to investigate the role of S1P receptors in hair cell death due to gentamicin, by using S1P1-3 receptor antagonists. The cochlear, including organ of Corti, spiral ganglion, was dissected from Sprague-Dawley rats on postnatal days 3 to 5. Expression of S1P1-3 was confirmed in organ of Corti, spiral ganglion by reverse transcription-PCR. Basal turn organ of Corti explants were exposed to 35 µM gentamicin for 48 hours. Specific antagonists of each S1P1-3 were added to the culture medium. Of these, JTE-013, a S1P2 antagonist, significantly increased hair cell loss as compared with the control group exposed to gentamicin alone. This finding suggests that S1P acts as a cochlear protectant against gentamicin ototoxicity via activation of S1P2.

### **979 Cadmium-Induced Neurotoxicity and Ototoxicity in Cochlear Organotypic Cultures**

Hong Liu<sup>1,2</sup>, Hong Sun<sup>3</sup>, Dalian Ding<sup>2,3</sup>, Xuewen Wu<sup>1,2</sup>, Haiyan Jiang<sup>2</sup>, Richard Salvi<sup>2</sup>

<sup>1</sup>The Third XiangYa hospital of Central South University,

<sup>2</sup>Center for hearing and deafness, <sup>3</sup>XiangYa hospital of Central South University

Cadmium (Cd), a kind of heavy metal, was widely used in industry. It was indicated that acute poisoning of Cd, which mainly interferes with respiratory tract, chronic poisoning can respectively lead to renal dysfunction, immune suppression, bone disorder, neurological disorders, hearing loss and so on. To evaluate the ototoxicity and neurotoxicity of Cd in the inner ear, which is increasingly

bothering human life currently, we treated cochlear organotypic culture system of postnatal rat with Cd for 24h and 48h with doses ranging from 10µM to 1000µM. Interestingly, concentrations of Cd exceeding 500µM for 24h and 100µM for 48h resulted in significant damage or loss of cochlear hair cells, while treatment of 1000µM Cd for 48h caused almost all the hair cells missing. Auditory nerve fibers and spiral ganglion neurons were also degenerated with Cd doses exceeded 100µM for 24h and 10µM for 48h. Cd successfully caused severe degeneration of auditory nerve fibers and spiral ganglion neurons, loss of Cochlear hair cells, in dose and time dependence manner. These results may indicate that Cd have neurotoxic and ototoxic effects on cochlea in vitro.

### **980 Ototoxicity of Paclitaxel in Rat Cochlear Organotypic Cultures**

Yang Dong<sup>1,2</sup>, Dalian Ding<sup>1</sup>, Richard Salvi<sup>1</sup>

<sup>1</sup>Center for Hearing & Deafness, University at Buffalo,

<sup>2</sup>Experimental Teaching Center, Shanghai University of Traditional Chinese Medicine

Paclitaxel (taxol) is a widely used antineoplastic drug that is employed alone or in combination to treat many forms of cancer. Paclitaxel blocks microtubule depolymerization stabilizing microtubules and suppressing cell proliferation and other cellular processes. Microtubule proteins are localized to different regions of inner ear; during postnatal development they first appear in the hair cells and later in pillar and Deiters cells. Previous reports indicate that paclitaxel can cause mild to moderate sensorineural hearing loss and histopathologic changes in the mouse cochlea resembling those seen after salicylate or interferon alpha 2a ototoxicity. However, the ototoxic effects of paclitaxel in the developing cochlea in vitro are poorly understood. To evaluate the ototoxicity of paclitaxel in vitro, we treated cochlear organotypic cultures of postnatal day 3-4 rats with paclitaxel for 24, 48 or 72 h with doses ranging from 0.5 to 30 µM. After 24 h treatment, no obvious histopathologies were observed with any of the doses of paclitaxel. After 48 or 72 h, paclitaxel damaged cochlear hair cells in a dose-dependent manner. The initial changes consisted of morphological damage to the stereocilia; this was subsequently accompanied by destruction of the hair cell cuticular plate. Damage increased significantly between 48 and 72 h. Despite damage to the stereocilia and cuticular plate, hair cell nuclei labeled with TOPRO3 appeared normal with little evidence of nuclear condensation or fragmentation, suggesting that hair cell death might occur by necrosis rather than apoptosis. Paclitaxel had little effect spiral ganglion neurons and auditory nerve fibers. These results suggest that paclitaxel is mainly toxic to hair cells in cochlear cultures and may interfere with the postnatal development of the stereocilia and cuticular plate.

### **981 Activation of Apoptotic Pathways in the Absence of Cell Death in an Inner-Ear Immortomouse Cell Line**

Kayla Hill<sup>1</sup>, Fu-Quan Chen<sup>1</sup>, Jochen Schacht<sup>2</sup>, Su-Hua Sha<sup>1</sup>

<sup>1</sup>Medical University of South Carolina, <sup>2</sup>University of Michigan

Aminoglycoside antibiotics and cisplatin (CDDP) are the major ototoxic drugs of clinical medicine due to their capacity to cause significant and permanent hearing loss, as they target the mammalian sensory cells which lack the ability to regenerate. Understanding the pathogenesis of damage is the first step in designing effective treatments and prevention of drug-induced hearing loss. In-vitro systems greatly enhance the efficiency of biochemical and molecular investigations through ease of access and manipulation. HEI-OC1, an inner ear cell line derived from the immortomouse, expresses markers for auditory sensory cells and, therefore, is a potential tool to study the ototoxic mechanisms of drugs like aminoglycoside antibiotics and CDDP. We are currently investigating aminoglycoside-induced signaling pathways and cell death using HEI-OC1 cells. Both HEI-OC1 and HeLa cells efficiently took up fluorescently tagged gentamicin. HEI-OC1 cells responded with changes in a variety of cell death and survival signaling pathways. Within hours, the C-jun N-terminal kinase pathway and the transcription factor AP-1 were activated. At later times, the "executioner caspase", caspase-3 was also activated. These responses were robust and elicited by gentamicin. However, despite the initiation of apoptotic pathways and transient changes in nuclear morphology, cell death was not observed by aminoglycoside treatment, while administration of CDDP lead to significant cell death as determined by flow cytometric measurements. Furthermore, beta-galactosidase analysis ruled out senescence in gentamicin-treated cells. The ability to withstand treatment with aminoglycosides but not with CDDP suggests that this cell line may be helpful in providing some insight into the differential actions of the two ototoxic drugs and possibly into mechanisms of intrinsic repair capabilities after aminoglycoside insult. Supported by grant R01 DC009222 and DC003685 from the National Institute of Health.

### **982 Lipopolysaccharide Priming Initiates Cochlear Inflammation and Accelerates Ototoxicity**

Song-Zhe Li<sup>1</sup>, Kevin Ohlemiller<sup>1</sup>, Keiko Hirose<sup>1</sup>

<sup>1</sup>Washington University

Various forms of preconditioning have been shown to be protective in noise-induced hearing loss while effects of preconditioning have been explored very little in ototoxicity. Systemic low-dose lipopolysaccharide (LPS) is a well-established method of preconditioning that mimics sepsis and causes a sterile inflammatory response that reaches the inner ear through the cochlear vessels. We exposed C57Bl/6J mice (7-9 weeks of age) to low dose LPS (0.5mg/kg-day IP for two consecutive days) as a

preconditioning strategy before a single dose of kanamycin (1000mg/kg) and furosemide (180mg/kg) and expected to find a protective effect of LPS priming in ototoxicity. Surprisingly, we found that mice demonstrate an increase in threshold shift and acceleration of hair cell loss with LPS priming before exposure to ototoxic agents. Robust inflammatory cell recruitment was observed in all mice that were treated with LPS alone, kanamycin/furosemide, or a combination of LPS/kanamycin/furosemide. Numbers of inflammatory cells in the membranous labyrinth were highest in mice exposed to the combination of LPS and ototoxic agents. We postulated that threshold shift would be negatively influenced by the entry of inflammatory cells into the lateral wall, heightening the loss of endocochlear potential (EP) or limiting its recovery after exposure to combination aminoglycoside/loop diuretic. Reduction in EP was observed in both treatment groups (kanamycin/furosemide and LPS/kanamycin/furosemide).

### **983 Ototoxicity of Methylrosaniline Chloride (Gentian Violet): A Longitudinal Study of the Change of CAP and Histopathology in the Guinea Pig**

Hitomi Higuchi<sup>1</sup>, Takafumi Yamano<sup>1</sup>, Mayumi Sugamura<sup>1</sup>, Takashi Nakagawa<sup>1</sup>, Tetsuo Morizono<sup>2</sup>

<sup>1</sup>Fukuoka University, <sup>2</sup>Nishi-Fukuoka Hospital

Purpose:

The purpose of this report is to present data on the ototoxic effect of GV applied in the middle ear cavity in the guinea pig for 5 minutes, 30 minutes, 1 hour, 2 hours, and 24 hours. Two different concentrations, 0.5% and 0.13% were studied.

Material and Methods:

Using Hartley adult guinea pigs, ototoxicity was evaluated by measuring the eighth nerve compound action potentials (CAP) from an electrode placed on the round window membrane. The stimulus sound consisted of click sounds and tone bursts of 4 and 8 kHz. After the initial CAP measurement, the middle ear cavities of the animals were filled with GV solution, with concentrations of 0.5% or 0.13%. After an interval of 5 minutes, 30 minutes, 1 hour, 2 hours, and 24 hours, the middle ear was washed with saline, carefully wicked dry and the reduction in CAP was measured.

After all the measurements were completed, the temporal bones were harvested for histopathologic study. Celloidin embedded specimens were cut into 20 micron thick slices and were examined by light microscopy.

Results:

Mild ototoxicity was detected at 30 minutes when using a 0.5% solution, with progressively decreasing CAP at 60 minutes and a complete abolishment of CAP at 24 hours. An 0.13% solution caused reduction in CAP at 2 hours and severe reduction in CAP was seen at 6 hours. Thus, the GV treatment results in a concentration dependent reduction in CAP. Histopathologic study revealed massive new bone formation in the middle ear cavity and concentration dependent damage of the Organ of Corti.

Conclusions:

Even when a more diluted 0.13% solution was applied on the round window for only 5 minutes and washed with saline, a severe reduction in CAP was still seen at 24 hours. Although GV has excellent antibacterial and antifungal activities, the use of GV should be limited to the external ear canal. The use of this drug in the middle ear cavity is not recommended.

#### **984 Reproductive Ototoxicity of TBBPA in Rat Offsprings**

**Bin Na Hong**<sup>1,2</sup>, Keun Ha Park<sup>1</sup>, Ha Na Hong<sup>1</sup>, Tong Ho Kang<sup>1</sup>

<sup>1</sup>*Kyung Hee University*, <sup>2</sup>*Nambu University*

Tetrabromobisphenol-A (TBBPA) is one of many brominated compounds widely used as flame retardants in consumer products. Although toxicity and teratogenicity of TBBPA in experimental in vivo studies appeared to be low, concern has been expressed recently for the potential endocrine disruptive action of brominated flame retardants. In the present study, we have evaluated the auditory functions of offspring from one-generation reproduction in rats in order to examine the ototoxicity of TBBPA. Exposure to TBBPA started 1 day after mating in females for 2 weeks and 3 dose levels were treated with 0, 100, 300, and 600 mg/kg/day, respectively. The ototoxicity of TBBPA to the offspring was evaluated by auditory brainstem responses (ABRs), auditory middle latency responses (AMLRs), and otoacoustic emissions (OAEs) at 4 and 8 weeks of postnatal age, respectively. Hearing thresholds of ABR and signal to noise responses of OAE were not shown the significantly difference. However, Pa response of AMLRs was disappeared in the 50% of offsprings with 300 mg/kg TBBPA treated group. And the others decreased the Pa amplitude or increased the Pa latency. These results indicated that the exposure to TBBPA in maternal females could damage the central auditory development in offsprings.

#### **985 Hearing Rescue of Connexin30 (Cx30) Knock-Out Mice by AAV1-Mediated Expression of Mouse Cx30 or Cx26 in the Mouse Cochlea**

**Jianjun Wang**<sup>1</sup>, Yunfeng Wang<sup>2</sup>, Shoeb Ahmad<sup>1</sup>, Qing Chang<sup>1</sup>, Wenxue Tang<sup>1</sup>, Binfei Zhou<sup>1</sup>, Huawei Li<sup>2</sup>, Xi Lin<sup>1</sup>  
<sup>1</sup>*Dept of Otolaryngology, Emory University School of Medicine, Atlanta, GA 30322*, <sup>2</sup>*Shanghai Eye & ENT hospital, Fudan University, Shanghai, China*

Non-sensory cells in the cochlea are connected extensively by gap junctions (GJs) that facilitate intercellular ionic and biochemical coupling. Mutations in the genes coding for Cx26 and Cx30 are the most common causes of human nonsyndromic hereditary deafness that affect millions of patients. No mechanism-based therapy is available for treatment. Results of our previous studies suggested that a gene therapy approach to treat deafness in cCx26 and Cx30 null mice at the adult stage is unlikely to be successful. We therefore performed gene-therapy studies using the early postnatal Cx30 null mice. We tagged Cx26 and Cx30 with green fluorescence

protein (GFP), and inserted them into an Adeno-associated virus vector, respectively. The expression of fusion proteins in HeLa cells two days after transfection was confirmed by western blotting showing protein bands of 57 kDa, 53 kDa, and 27 kDa, corresponding to Cx30-GFP, Cx26-GFP and GFP alone, respectively. All detectable GFP fluorescence was colocalized to connexins labeled with specific antibodies in immunostained HeLa cells transfected with Cx30-GFP or Cx26-GFP. Green fluorescent puncta and lines between cells were observed under fluorescence microscope. The normal function of these gap junctions was confirmed by performing dye transfer assay of propidium iodide. Preliminary studies injecting a control viral vector at P0 into the scala media resulted in extensive expression of GFP signal. Importantly, no hearing loss was observed in these mice at adult stage. We are now packaging the AAV vectors into AAV1 recombinant viruses. Based on our previous data, we will inject the recombinant viruses into the scala media of Cx30 null mice at P0 to P1 to find out if the viral-mediated expressions of Cx30 or Cx26 in mouse cochlea can correct deafness in these mutant mouse models of human deafness.

#### **986 Engineered Adipose Stem Cells as Vehicles for Inner Ear Neurotrophin Therapy**

**David Sultemeier**<sup>1</sup>, Patricia Zuk<sup>1</sup>, Ivan Lopez<sup>1</sup>, Larry Hoffman<sup>1</sup>

<sup>1</sup>*University of California, Los Angeles*

Recent studies have shown that mammalian vestibular sensory epithelia exhibit poor intrinsic capabilities for rehabilitation and repair. These capabilities may include reinnervation of existing hair cells by afferents that have lost their calyx following exposure to certain ototoxins. Therefore, it is possible that peripheral vestibular repair may require adjuvant therapies, perhaps over long periods of time, to promote the restoration of afferent innervation and establishment of new synapses. In the present study we have explored the use of adult genetically engineered adipose-derived stem cells (ASCs) as cellular biopumps that could provide neurotrophins following transplantation into the perilymph. Adipose tissue was removed from the interscapular pad in anesthetized chinchillas, and ASCs were harvested and cultured using established procedures. Cells were transduced using a lentiviral vector encoding a multicistronic mRNA that contains genes for *egfp*, human *bdnf*, and *pac* (confers puromycin resistance). We found that transduced ASCs can be induced into either a osteogenic or adipogenic lineage, and therefore continue to exhibit multipotency. BDNF levels from sampled culture media were measured by ELISA to verify supranormal expression of transgenic neurotrophin. Data gleaned from ELISA (BDNF expression) and fluorescence microscopy (EGFP expression) demonstrate that transduced ASCs stably express transgenes *in vitro* for over two months. In addition, cells selected for puromycin resistance were transplanted into the vestibular labyrinth. Results from the ongoing interperilymphatic transplantation experiments suggest that transduced ASCs integrate and express transgenes for over a month after

transplantation. Current studies using cultured explants of mouse Scarpa's ganglion neurons aim to examine whether the recombinant human BDNF exhibits biological activity.

### **987 Screening for Protective Effect in Supplement Drugs Using the Zebrafish Lateral Line**

**Yoshinobu Hirose<sup>1</sup>, Kazuma Sugahara<sup>1</sup>, Hiroshi Yamashita<sup>1</sup>**

<sup>1</sup>*Yamaguchi University Graduate School of Medicine*

The zebrafish lateral line provides a powerful system for studying hair cells and hair cell death. Hair cells can be easily labeled and imaged in vivo with fluorescence microscopy. I have previously described a screening system to rapidly assess drugs for possible ototoxic effects in anti-cancer drugs (Hirose et al., 2011). Also it is possible to screen for protective effects against some ototoxicity drugs.

There are many kinds of supplements in the USA, Europe, Japan, etc. Some of them have an anti-oxidant effect (e.g., Vitamin A, C, E, beta-carotene) or other. Supplements can also be used as a prophylactic treatment, especially against age-related hearing loss. Some countries have trouble with medical expenses, so this type of approach can be useful in such countries.

We have now screened supplement drugs for protective effects against aminoglycoside. 5-7 dpf Zebrafish (*Danio rerio*) embryos of the AB wild type strain were used in this study. Zebrafish larvae were exposed to supplement drugs (0, 10, 50, 100, 200, 400uM), and aminoglycoside. After that, they were fixed in 4% paraformaldehyde, incubated with anti-parvalbumin, and hair cell damage was assessed using a fluorescent microscope. We made a dose-response curve to evaluate protective effects against aminoglycoside.

### **988 AVE7688 (Ilepatril) and Losartan Attenuate Inner Ear Dysfunction in Zucker Diabetic Fatty Rats, a Model for Diabetes Type 2**

**Angela Maria Meyer zum Gottesberge<sup>1</sup>, Stefan Hansen<sup>1</sup>, Thomas Massing<sup>2</sup>, Anja Sasse<sup>1</sup>, Stefan Schaefer<sup>3</sup>**

<sup>1</sup>*University of Duesseldorf, Research Laboratory Department of Otorhinolaryngology*, <sup>2</sup>*University of Duesseldorf, Division of Phoniatrics and Pediatric Audiology*, <sup>3</sup>*DG Cardiovascular Diseases, Aventis Pharma Germany*

AVE7688 (Ilepatril) and Losartan attenuate inner ear dysfunction in Zucker diabetic fatty rats, a model for diabetes type 2.

Meyer zum Gottesberge AM., Massing T., Sasse A., Palma S., Hansen S., Schäfer S

The homozygous (*fa/fa*) Zucker Diabetic Fatty (ZDF) rat was used as an animal model of type 2 diabetes. We investigated whether (i) in diabetes the hearing ability is impaired and structural alterations of the inner ear occur and (ii) whether an inhibitor of neutral endopeptidase and angiotensin converting enzyme (AVE7688 [AVE]) and an angiotensin II receptor blocker (losartan [Los]) could

protect from diabetic otopathy. Treatment was initiated at age of 12 weeks with Los (5 mg/kg/day), or AVE (30mg/kg/day) and continued until age of 42 weeks. Untreated heterozygous animals served as non-diabetic controls.

At age 42 weeks, ZDF rats (n=7) had developed overt diabetes mellitus (HbA1c >10 % after age 15 weeks) and progressive albuminuria (24.4±4.9 mg/h/kg), whereas homozygous, non-diabetic littermates (n=9) remained normoglycaemic and did not develop albuminuria. The hearing threshold was increased in the diabetic animals (placebo) to 45.0±2.1 dB, compared to 34.7±4 in non-diabetic rats (p<0.05). Histopathological changes of the inner ear were confined to the stria vascularis and revealed marked swelling of the melanocytes-like intermediate cells and widening of intercellular spaces in diabetic compared to non-diabetic animals. These alterations were associated with decreased expression of the  $\beta_1$ ,  $\beta_2$ -Na<sup>+</sup>/K<sup>+</sup>-ATPase and KCNJ10 ion channel. In both, the Losartan and AVE7688 groups, hearing threshold was practically normalized (36.1±7.4 dB, n=7 for Los and 35.9±3.3 dB, n=8 for AVE, p<0.05 vs. Placebo), the histopathological changes were almost absent and the expression of the  $\beta_1$ ,  $\beta_2$ -Na<sup>+</sup>/K<sup>+</sup>-ATPase and KCNJ10 ion channel improved.

In conclusion, we describe a "diabetic otopathy" in type 2 diabetic rats, which is characterized by hearing loss and structural alterations of the stria vascularis in the inner ear. Blockade of the Angiotensin II receptor and dual inhibition of neutral endopeptidase and ACE with Ilepatril can prevent this diabetic otopathy.

### **989 Protective Effect of Korean Red Ginseng in 3-NP-Induced Cochlear Damage Animal Model**

**Tian Chunjie<sup>1</sup>, Young Ho Kim<sup>1</sup>, Eun Jung Kim<sup>1</sup>, Youn Ju Kim<sup>1</sup>, Seung Won Kim<sup>1</sup>, Sung Jun Choi<sup>2</sup>, Ki hyun Kim<sup>1</sup>, Hun Yi Park<sup>1</sup>, Yun-Hoon Choung<sup>1</sup>**

<sup>1</sup>*Ajou university*, <sup>2</sup>*Konyang university*

Previous our study has demonstrated that geranylgeranylacetone ameliorated acute cochlear damage induced by administration of 3-nitropropionic acid (3-NP), mitochondrial toxin, in guinea pigs. Korean red ginseng (KRG) is known to have protective effects on hearing loss induced by cisplatin, gentamicin, and noise. Aims of this study are to establish the animal model with hearing loss and vestibular dysfunction using 3-NP and to observe the protection of cochlear function and structures after the administration of KRG.

Male BALB/c mice (6 weeks, 25-30g) were used in this study. To investigate the 3-NP dose-dependent toxic effects on hearing and balance function, 15 mice were randomly assigned to 5 groups and for each group (n=3), left ear was treated with 3-NP in concentration of 300 mM, 500 mM, 800 mM, 1000 mM, and 5000 mM intratympanically and right ear was remained as control. Before and after (on post 1 day, 1 week, and 1 month) 3-NP administration, the mice were observed for any behavioral abnormalities and then, inner ear organs were harvested for morphological evaluation. For investigation

of the protective effect of KRG, animals consisted of 3-NP group (n=12) and 3-NP+KRG group (n=11). For 3-NP/KRG group, mice were pretreated with KRG (300 mg/kg; 0.8 ml/mouse; once a day; PO) for 7 days before 3-NP administration. After administration of KRG, 3-NP (500 mM; 20  $\mu$ l/left ear; intratympanic injection) was administered in both groups and the contralateral ears were used as control. The function of hearing was evaluated on pre2 day, post1 day, 1 week, and 1 month, and then, cochleae were harvested for morphological evaluation.

In the 800 mM, 1000 mM, and 5000 mM 3-NP groups, ABR thresholds exceeded the maximum recording limit at both 16 and 32 kHz one day after 3-NP administration, and there was no recovery of hearing in 1000 mM and 5000 mM 3-NP groups with outer hair cells (OHCs) loss and vestibular dysfunction. In 1000 mM 3-NP group, shortened, clumped, unevenly distributed, and reduced vestibular hair cells' stereocilia was observed.

ABR threshold in KRG-treated group was significantly lower than that in 500mM 3-NP group at both 16 and 32 kHz from post3-NP 1 day to 30 day. There was some OHCs' loss in 3-NP group, whereas all hair cells were intact in control ears and 3-NP+KRG group.

#### **990 7,8,3-Trihydroxyflavone, a Small Molecule TrkB Receptor Agonist, Protects Spiral Ganglion Neurons from Degeneration in Vitro and in Vivo**

Qing Yu<sup>1</sup>, Qing Chang<sup>1</sup>, Keqiang Ye<sup>2</sup>, Xi Lin<sup>1,3</sup>

<sup>1</sup>Department of Otolaryngology, <sup>2</sup>Department of Pathology, <sup>3</sup>Department of Cell Biology, Emory University School of Medicine

Most sensorineural hearing loss cases are caused by loss of cochlear hair cells. The loss of neurotrophic support from hair cells causes secondary degeneration of spiral ganglion neurons (SGNs). The survival of SGNs is critical for successful outcomes of the cochlear implant, which is the only effective treatment so far for patients suffering from severe sensorineural hearing loss. Past efforts to save SGNs from degeneration have found that direct application of neurotrophins (e.g., brain derived neurotrophic factor (BDNF)) into the cochlea is effective in reducing SGN degeneration after hair cell loss in multiple animal models. However, BDNF has a poor *in vivo* pharmacokinetic profile, which is a major limiting factor for its therapeutic applications.

We have identified a number of high-potency small molecules that mimic the neurotrophic effect of BDNF. Here we report 7,8,3-Trihydroxyflavone (7,8,3-THF), one of the most potent compounds found so far, as a high-affinity Tyrosine receptor kinase B (TrkB) agonist that promotes the survival of SGNs both in cochlear cultures and in a conditional connexin 26 knockout mouse model. After killing hair cells by supplementing culture media with 1mM of gentamicin, 7,8,3-THF exerted dramatic protective effects on SGNs maintained in organotypic cochlear cultures for three days. In contrast, the protective effect disappeared when the cochleae obtained from a conditional TrkB-null mice were used, indicating that 7,8,3-THF exerted its effect in a TrkB dependent manner.

Western blots directly demonstrated that 7,8,3-THF activated TrkB in the cochlear cultures. When applied together, co-application of 7,8,3-THF and Neurotrophin 3, but not 7,8,3-THF and BDNF, produced additive protective effects. We also examined the *in vivo* effect of 7,8,3-THF in the conditional connexin 26 (Cx26) null mouse model. When examined two months after mice were born, we found that most SGNs survived after application of 7,8,3-THF into the middle ear by using a gelfoam sterile sponge soaked with the compound. Whereas, about 80% of SGNs degenerated without treatment in the contralateral ear. Our findings suggested that 7,8,3-THF is a promising therapeutic tool for protection of SGN from degeneration both *in vitro* and *in vivo* due to its small molecule structure.

#### **991 WITHDRAWN**

#### **992 Dynamic Uptake of Lipid Nanocapsules in Cochlear Cells After in Vitro and in Vivo Administration**

Florence François<sup>1,2</sup>, Thomas Perrier<sup>3</sup>, Patrick Saulnier<sup>3</sup>, Benjamin Chaix<sup>1,2</sup>, Jing Wang<sup>1,2</sup>, Jean-Luc Puel<sup>1,2</sup>

<sup>1</sup>INSERM, <sup>2</sup>Université Montpellier 1 & 2, <sup>3</sup>Université d'Angers

Background and Aims: Hearing deficits are often caused by loss of sensory, neuronal and stria cells due to a variety of factors (e.g. noise, ototoxic drugs, and aging). Unfortunately, there is currently no effective treatment of hearing deficits. A first step would thus be the design of an effective delivery system able to bring therapeutic agents into cochlear cells. The purpose of this study was to evaluate the ability of nanoparticles to deliver payload loaded siRNA or drugs into cochlear cells.

Methods: Nile Red was encapsulated inside the lipid core nanocapsules (LCNs) to assess the integrity of the LNCs to penetrate into the cochlear cells. A siRNA against p27, a protein expressed in cochlear supporting cells was incorporated within LCNs to evaluate the efficiency of LCNs in delivering therapeutic agents into cochlear cells. Two *in vitro* models (cochlear explant and slice) were used in this study. In addition, the adult C57/BL6J mice were used to evaluate the capability of LNCs to pass through the round window membrane and the distribution of the LNCs inside the inner ear.

Results: Incubation of cochlear explants with LCNs encapsulated Nile red resulted red fluorescence in almost all cochlear cells. The cochlear explants treated with LCNs loaded with siRNA against p27 induced a significant decrease of p27 expression. In addition, our *in vivo* results showed that small LCNs can reach the cochlear cells through the intact round window membrane.

Conclusion: These results are very promising in term of clinical use of LCNS as vehicles to bring into cochlear cells drugs and siRNA for curing hearing deficits.

### **993 Development of a Sustained Release Glucocorticoids Formulation for Intracochlear Delivery**

**Wanwan Yang**<sup>1</sup>, Erik Pierstorff<sup>1</sup>, Yen-Jung Angel Chen<sup>2</sup>, Maria Paola Chaparro<sup>2</sup>, Federico Kalinec<sup>2</sup>, William Slattery<sup>1</sup>

<sup>1</sup>O-Ray Pharma, <sup>2</sup>Section on Cell Structure & Function, Division of Cell Biology & Genetics, House Research Institute

Glucocorticoids (GC) are a class of steroid hormones that are part of the feedback mechanism in the immune system that turns down the immune activity (inflammation). Therefore, they are used to treat diseases caused by an overactive immune system, such as allergies, asthma, autoimmune diseases and sepsis. In otology, GCs are routinely used to treat sudden hearing loss, Meniere's disease, autoimmune inner ear diseases, and certain vestibular disorders. Despite their widespread use, high dose GCs cause serious side effects, including Cushing syndrome, high blood pressure, diabetes, and an increased susceptibility to infection. Therefore, a localized sustained release formulation of GCs is expected to be more effective and safer for cochlear drug delivery. We have developed extended release GC formulations in various dose-ranges utilizing a sustained release polymer formulation. In vitro dissolution studies demonstrated pseudo-zero order drug release profiles which could be tuned for a desired duration of therapeutic delivery. In vivo studies showed no ototoxicity when implanted into guinea pig ears. Pre- and post- treatment otoacoustic emissions and ABRs were performed and good hearing preservation was observed. Pharmacokinetic studies demonstrated GC presence for three months in the cochlea. The ultimate goal of this study is to develop a tunable system for the delivery glucocorticoids to the ear for the treatment of myriad diseases of the inner ear.

### **994 Administration of Superparamagnetic Nanoparticles to the Inner Ear: Safety Tests and Internalization in Endolymph Secreting Cells**

**Celierier Charlotte**<sup>1,2</sup>, Julien Clavier<sup>3</sup>, Yann Nguyen<sup>1,2</sup>, Olivier Sterkers<sup>1,2</sup>, Alexis Bozorg-Grayeli<sup>1,2</sup>, Evelyne Ferrary<sup>1,2</sup>

<sup>1</sup>Inserm UMR-S 867, F-75018 Paris, France/ Université Paris Diderot, Sorbonne Paris Cité, France, <sup>2</sup>AP-HP, Hôpital Beaujon, Service d'Oto-rhino-laryngologie et de Chirurgie cervico-faciale, Clichy, Fr, <sup>3</sup>Inserm UMR-S 699, F-75018 Paris, France/ Université Paris Diderot, Sorbonne Paris Cité, France

Due to the presence of the blood-perilymph barrier, the inner ear is not easily reachable by therapeutics, and new tools have to be developed to overcome this constraint. The superparamagnetic nanoparticles (SNP) could be a solution to this demand. We studied in vitro the mobilization of SNP and their internalization in endolymph secreting cell line (EC5v, Teixeira et al, 2006).

In vitro, three sizes of SNP (100, 200, 500 nm) were mobilized in three solvents (NaCl, glucose, water) through

a magnetic field produced by solenoids. We managed to drive SNP in a catheter mimicking a cochlear implant (polyethylene, 0.3 mm diameter) with four solenoids on a 3 cm curvilinear path, mimicking the shape of the cochlea.

After 48h incubation in presence of 500 nm SNP ( $7.10^6$ ,  $7.10^7$ ,  $7.10^8$  SNP/ml), or 100 nm SNP ( $3.10^3$ ,  $3.10^6$ ,  $3.10^9$ ,  $3.10^9$ ,  $3.10^{10}$  SNP/ml), cellular survival (flow cytometry), and cell internalization (confocal microscopy) were studied. Whereas clear SNP internalization was observed in the EC5v, no toxicity has been found with the 100 nm or the 500 nm SNP compared to control cells without SNP. The SNP were found in lysosomes (LAMP markers).

In conclusion, EC5v cultures with internalized SNP showed no alteration of cell survival. Therefore we can propose SNP as potential vector for inner ear treatment that could be driven along the cochlea to targeted area.

### **995 Novel in Vivo Imaging Analysis of Inner Ear Drug Delivery System: Comparison of Inner Ear Drug Concentrations Over Time After Transtympanic and Systemic Injections**

**Sho Kanzaki**<sup>1</sup>, Masato Fujioka<sup>1</sup>, Akimasa Yasuda<sup>2</sup>, Shinsuke Shibata<sup>3</sup>, Masaya Nakamura<sup>2</sup>, Hirotaka Okano<sup>3</sup>, Kaoru Ogawa<sup>1</sup>, Hideyuki Okano<sup>3</sup>

<sup>1</sup>Department of Otolaryngology Head and Neck Surgery, Keio University, School of Medicine, <sup>2</sup>Department of Orthopedics, Keio University, School of Medicine, <sup>3</sup>Department of Physiology, Keio University, School of Medicine

Purpose: Systemic steroid injections are used to treat idiopathic sudden-onset sensorineural hearing loss (ISSHL) and some inner ear disorders. Recent studies showed that transtympanic (TT) steroid injections are also effective for treating ISSHL. As in vivo monitoring of drug delivery dynamics is lacking, the time course of inner ear drug delivery in live animals is unknown. Here, we used a new in vivo imaging system to monitor drug delivery in live mice and to compare drug concentration over time after TT and systemic injections.

Methods: Transgenic GFAP-Luc mice were purchased from Xenogen Co.Ltd containing a firefly luciferase gene expression cassette that is regulated by a 12 kb of the murine GFAP promoter and the human beta-globin intron 2. Luciferin delivered into the inner ear of these mice reacts with luciferase, and resulting signals are detected in GFAP-expressing cells in the spiral ganglion.

We examined how long these signals persist in the inner ear after TT or systemic injections of luciferin. We used Bioluminescence imaging system (IVIS®) to observe signals in live mice and compared the drug dynamics of luciferin injected via TT and intraperitoneal (IP) injections.

Results: TT and IP injections significantly differed. Signals were detected 5 minutes after TT injection, peaking at ~20 minutes. By contrast, signals were first detected 30 minutes after IP injection.

Discussion: TT and IP drug delivery time differed. In TT mice, signals occurred and disappeared earlier than in IP mice. Delivery time also varied in TT mice. We speculate that the drug might enter the eustachian tube from the

middle ear. We conclude that inner-ear drug concentration can be maintained longer if the two injections are combined. As the size of luciferase differs from that of therapeutics like dexamethasone, combining drugs with luciferase may help us understand in vivo drug delivery dynamics.

### **996 Comparison of Systemic Versus Local Delivery of Fluorescein-Conjugated**

### **Bisphosphonate in the Guinea Pig Cochlea**

Alicia Quesnel<sup>1</sup>, Shuting Sun<sup>2</sup>, Arthur Kristiansen<sup>1</sup>, Harrison Lin<sup>1</sup>, Katherine Belzner<sup>1</sup>, Charles McKenna<sup>2</sup>, William Sewell<sup>1</sup>, Michael McKenna<sup>1</sup>

<sup>1</sup>Massachusetts Eye and Ear Infirmary/ Harvard Medical School, <sup>2</sup>University of Southern California

Bisphosphonates, which have a high affinity for bone and are powerful inhibitors of bone remodeling, offer a potential medical treatment for hearing loss due to otosclerosis. Abnormal bone remodeling in the normally quiescent otic capsule bone is the hallmark of otosclerosis, a disease that leads to conductive and sensorineural hearing loss in humans. There are several rare, but serious, side effects of systemic administration of bisphosphonates that have led to the goal of developing a method for local delivery of these drugs to the inner ear. We evaluated distribution of zoledronate, a third generation bisphosphonate, in the Guinea pig cochlea using systemic (i.p.) delivery and two local delivery methods: a) an osmotic pump via a cochleostomy or b) alginate beads loaded with drug placed on the round window membrane. Fluorescein-conjugated zoledronate was utilized so that the distribution of zoledronate could be examined and quantified by fluorescence microscopy. The animals were sacrificed between 1 to 7 days later. Systemic delivery produced dose-related deposition of zoledronate in the bone of the inner ear with deposition concentrations similar to that observed in the femur. Both local delivery methods led to similar distribution patterns within the cochlea. A significant gradient of fluorescent zoledronate was seen within the cochlea, with high levels of fluorescence at the site of delivery in the basal turn to low levels in the apex. We hypothesize that the gradient of drug deposition with local delivery is accentuated by the extremely high affinity of zoledronate to the bone of the cochlea. Thus strategies to protect bisphosphonates during the early phases of local delivery might enhance distribution throughout the cochlea.

### **997 Mass Spectrometric Analysis of Antioxidants in Cochlear Fluids After Four Differing Routes of Systemic Administration**

Douglas Cotanche<sup>1</sup>, Brian La Brecque<sup>1</sup>, Scott Forsberg<sup>1</sup>, Larisa Altshul<sup>1</sup>, Otto Manneberg<sup>1</sup>, Ramon Molina<sup>1</sup>, Humberto Treviño-Villareal<sup>1</sup>, Rosalinda Sepulveda<sup>1</sup>, Royce Clifford<sup>1,2</sup>, Joseph Brain<sup>1</sup>, Ronald Jackson<sup>2</sup>, Rick Rogers<sup>1</sup>

<sup>1</sup>Harvard School of Public Health, <sup>2</sup>Naval Medical Center

Animal studies have demonstrated that antioxidants delivered systemically by intravenous (IV) administration can effectively protect cochlear hair cells from noise damage. We designed a series of experiments in rats to

administer antioxidants by four different routes and determine the timing and level of their appearance in the cochlear fluids by liquid chromatography/mass spectrometry (LC/MS). Rats were given a dose of either N-acetyl-L-cysteine (NAC), D-methionine (DMET), acetyl-L-carnitine (ALCAR), or a mix of all three which were administered by either IV, IG, intratracheal microspray (IT) or intranasal (IN) routes at appropriate concentrations. Cochlear fluids were extracted at 1h, 4h, and 8h after administration, flash frozen in liquid nitrogen and then analyzed for the presence of the three antioxidants using a Thermo Exactive Orbitrap LC/MS.

Our results indicated that IT administration was the most effective route, as the antioxidants reached high levels in the cochlear fluids within one hour. IV administration was nearly as effective as IT, but the IG and IN routes were much less efficient. A mix of all three antioxidants given together provided the best increase in levels of all three in the cochlear fluids. ALCAR and DMET given alone showed increases in not only their own levels, but also modest increases in the other two in the cochlear fluids. NAC administration when given alone was the least effective, showing barely any increases in NAC in the cochlear fluids and no effects upon DMET or ALCAR levels. These experiments suggested that a mix of all three antioxidants administered by the IT route would be the most effective in preventing cochlear hair cell damage. Indeed, an experiment with chinchillas given the mix by the IT route showed effective protection from both impulse and continuous noise exposure. These studies suggest that a cocktail of antioxidants administered by the pulmonary route may be efficacious in preventing noise damage in human subjects.

Funded by Office of Naval Research Grant # N00014-09-1-1104

### **998 Sustained Release Dexamethasone as a Preferred Treatment Against Various Forms of Hearing Loss**

Anne Harrop<sup>1</sup>, Xiaobo Wang<sup>1</sup>, Rayne Fernandez<sup>1</sup>, Luis Dellamary<sup>1</sup>, Carl LeBel<sup>1</sup>, Fabrice Piu<sup>1</sup>

<sup>1</sup>Otonomy Inc.

Hypothesis / Background: In the US alone, it is estimated that about 30 million individuals suffer from hearing loss. Causes of the debilitating condition are many, including noise induced hearing loss (NIHL) and exposure to ototoxicants (aminoglycosides, chemotherapeutic agents,...). At the cellular level, inflammatory and apoptotic processes are responsible for permanent hearing loss. The therapeutic potential of the corticosteroid dexamethasone, a potent anti-inflammatory, and of the JNK inhibitor SP600125, an anti-apoptotic agent, were compared in various paradigms of hearing loss.

Methods: Both therapeutic agents were formulated in a poloxamer-based hydrogel. Dexamethasone (delivered as OTO-104, a clinical stage product currently being developed for the treatment of Meniere's disease) and SP600125 were administered to guinea pigs intratympanically, and their activity evaluated in models of

acoustic trauma, cisplatin ototoxicity and gentamicin-induced hearing loss.

Results: OTO-104 protected against hearing loss induced by all three forms of trauma (noise exposure, cisplatin and gentamicin). In contrast, SP600125 was effective only against acoustic trauma and cisplatin ototoxicity. Furthermore, in the NIHL setting, OTO-104 provided effective protection when administered before and after noise exposure, while the JNK inhibitor SP600125 had to be given before acoustic trauma to be useful. Studies with the glucocorticoid GR and mineralocorticoid MR receptor antagonist mifepristone demonstrated that the therapeutic benefits of OTO-104 rely primarily on activation of the classical nuclear receptor pathways.

Conclusions: Intratympanic administration of sustained release dexamethasone offers effective protection against hearing loss induced by various insults. In contrast to an anti-apoptotic JNK inhibitor, OTO-104 has a much broader therapeutic potential, and the flexibility to be administered before or after the trauma.

### **999 Intravital Imaging of Auditory Hair Cells and Neurites in the Functional Mammalian Cochlea**

Shelley Batts<sup>1</sup>, Eunice Cheung<sup>1</sup>, Nikolas Blevins<sup>1</sup>, Gerald Popelka<sup>1</sup>, Joan Savall<sup>1</sup>, Mark Schnitzer<sup>1</sup>

<sup>1</sup>Stanford University

Hearing loss afflicts hundreds of millions of people and often results from death of the cochlear hair cells. These cells normally never regenerate, are sensitive to infections and insults, and decline in number during aging. Despite the importance of studying causes and treatments of hair cell loss, the cochlea is one of the last anatomic areas to resist imaging in live mammals due to its small size, fragility, and deep location within the temporal bone. To solve this longstanding challenge in otology, here we introduce minimally invasive surgical and microendoscopy techniques for intravital imaging of hair cells and other cochlear elements while preserving hearing. The resulting three-dimensional images reveal individual hair cell nuclei, hair bundles, and spiral ganglion neurites. Post hoc hair cell counts and immunohistochemical analyses indicate that cochlear microendoscopy does not prompt hair cell loss. Thus, direct observation of functional cochlear microanatomy is now feasible in living mammals and will be a potent tool for examining mechanisms of cochlear damage and informing interventions for hearing restoration.

### **1000 Examining Pathways Regulated in Zebrafish Auditory Hair Cell Regeneration Using Next Generation Sequencing**

Gopinath Rajadinakaran<sup>1</sup>, Huifang Sun<sup>1</sup>, Eric Rouchka<sup>2</sup>, Michael Smith<sup>1</sup>

<sup>1</sup>Western Kentucky University, <sup>2</sup>University of Louisville

In order to develop treatments or preventive measures for auditory hair cell loss, a thorough understanding of the process of auditory hair cell regeneration, which is possible in fish and birds but not in mammals, must be established.

Our previous microarray analysis showed that growth hormone (GH) was significantly upregulated during zebrafish auditory hair cell regeneration, coupled with cell proliferation. We further tested the effects of GH on zebrafish auditory hair cell regeneration after sound exposure and our results showed that GH can efficiently promote post-trauma auditory hair cell regeneration, which may be achieved through stimulating proliferation and suppressing apoptosis. In the current study, we used Next Generation Sequencing (NGS) to examine the possible GH pathways involved in zebrafish auditory hair cell regeneration. Groups of 20 zebrafish were exposed to a 150 Hz tone at 179 dB re 1  $\mu$ Pa RMS for 40 h. Following acoustic exposure, the fish were injected with either zebrafish GH, salmon GH, phosphate buffer, or a zebrafish GH antagonist. In addition, one baseline group received no acoustic stimulus or injection. RNA was extracted from the tissues (both ear and liver) and cDNA was synthesized for NGS. Data was generated using the Illumina Pipeline version SCS 2.8.0 and sequence alignment was done using TopHat. The aligned reads were then annotated using Cufflink and the differential expression of transcripts was performed by Cuffdiff. Only the statistically significant reads were used in further analysis and pathway networks were examined using Ingenuity Pathway Analysis (IPA). Genes with significant regulation were sorted by functional category. Genes associated with cellular growth and proliferation, cell cycle, cell death, cancer, tissue development, and neurological disease were highly regulated in our data sets comparing baseline to buffer-injected fish, buffer-injected to antagonist-injected fish, and buffer-injected to GH-injected fish.

### **1001 SHIELD: An Integrated Gene Expression Database for Inner Ear Research**

Jun Shen<sup>1</sup>, Deborah Scheffer<sup>1,2</sup>, Kelvin Kwan<sup>3</sup>, Cindy Lu<sup>1</sup>, Mingqian Huang<sup>2</sup>, Peter Gillespie<sup>4</sup>, Lisa Goodrich<sup>1</sup>, Zheng-Yi Chen<sup>2</sup>, David Corey<sup>1,5</sup>

<sup>1</sup>Harvard Medical School, <sup>2</sup>Massachusetts Eye and Ear Infirmary, <sup>3</sup>Rutgers University, <sup>4</sup>Oregon Health & Science University, <sup>5</sup>Howard Hughes Medical Institute

The molecular components of mechanotransduction, the genetic causes of many inherited hearing impairments, and the molecular biology of inner ear development remain largely unknown. Our laboratories have recently generated extensive sets of gene expression data for different cell types in the inner ear, which will help illuminate each of these areas. To facilitate the study of genes in the inner ear by efficient mining of the accumulated data, we have developed the Shared Harvard Inner-Ear Laboratory Database (SHIELD), an integrated resource that seeks to compile, organize and analyze our collective knowledge of the inner ear.

Four datasets form the initial components of the SHIELD: One is based on FACS sorting of hair cells and non-hair cells from E16.5 to P16 mouse cochlea and utricle, and deep sequencing of the cDNAs (Scheffer et al., this meeting). A second is derived from a continuous cell line of cochlear progenitor cells and changes in gene expression under differentiating conditions (Kwan et al., this meeting).

The third is microarray data from E12 to P15 mouse spiral and vestibular ganglia (Lu et al., 2011). Finally, we incorporate chicken stereocilia proteins identified by mass spectroscopy (Shin et al., 2007). The annotations were derived from public databases and literatures. We expect that user feedback will continuously tune the accuracy of the annotations and their relevance to the inner ear.

These datasets are combined in a relational database that integrates experimental data and annotations relevant to the inner ear. The SHIELD has a searchable web interface with two data retrieval options: viewing the gene pages online or downloading gene lists with selected fields as an Excel spreadsheet. Each retrieved gene page shows the gene expression data and links to other databases online. Downloaded spreadsheets are suitable for more convenient offline data analysis. The web site will be online in March 2012.

### **1002 Distinct Energy Metabolism of Auditory and Vestibular Sensory Epithelia Revealed by Quantitative Mass Spectrometry and Microarrays**

**Kateri Spinelli**<sup>1,2</sup>, Peter Gillespie<sup>1,2</sup>

<sup>1</sup>Oregon Health & Science University, <sup>2</sup>Oregon Hearing Research Center

Classic biochemical studies in the inner ear suggested that glycolysis is more robust in the mammalian auditory system than in the vestibular system. Applying quantitative mass spectrometry experiments with MS2 intensities to quantify proteins in chick auditory and vestibular sensory epithelia, we find that glycolytic enzymes are enriched three-fold in cochlea, while enzymes responsible for oxidative phosphorylation are elevated at least four-fold in utricle. Directly measuring glycolysis with [3H]glucose, we find that cochlear sensory epithelium carries out glycolysis at a 4-fold higher rate than utricle. Affymetrix microarray analysis demonstrated that while glycolysis transcripts are elevated in cochlea, those for oxidative phosphorylation enzymes are not, suggesting a post-transcriptional mitochondrial regulation in cochlea. This striking difference in relative utilization of the two ATP-production pathways likely reflects the isolation of the auditory epithelium from its blood supply, necessary to prevent heartbeat-induced mechanical disruptions. Indeed, transcripts for five distinct anti-angiogenesis factors are elevated at least 40-fold in cochlea, suggesting mechanisms by which blood-vessel infiltration is prevented. The global view of protein expression afforded by label-free quantitation with a wide dynamic range reveals molecular specialization at a tissue or cellular level.

### **1003 Analysis of the Vestibular Hair and Supporting Cells' Proteome**

**Meike Sofia Herget**<sup>1</sup>, Zhaohua Guo<sup>1</sup>, Taha Jan<sup>1</sup>, Chris Adams<sup>2</sup>, Stefan Heller<sup>1</sup>

<sup>1</sup>Department of Otolaryngology, Stanford University, California, <sup>2</sup>Department of Chemistry, Stanford University, California

The sensory epithelia of the inner ear consists of sensory hair cells and supporting cells. Both cell types have been studied extensively in terms of hair cell function and regenerative capacity. However, isolation of single hair and supporting cells in large numbers for quantitative transcriptome or proteome analyses remains a challenging task. Here, we describe a protocol for a large-scale isolation of pure populations of chicken vestibular hair- and supporting cells. Purification of hair and supporting cells with flow cytometry enabled us to analyze both the hair- and supporting cell's molecular makeup by high resolution mass spectrometry.

To obtain large quantities of isolated vestibular hair- and supporting cells, chicken utricles were dissected at embryonal day 18 and briefly exposed to the styryl dye AM1-43. We screened different enzymatic and mechanical treatments for quick and efficient hair- and supporting cell isolation protocols that preserve cellular morphology. A mild enzymatic cocktail of accumax and low-concentration trypsin combined with mild trituration gave the best results, defined by cell numbers, the extent of cell separation, and the degree of preservation of hair cell morphology. Upon flow cytometry, we were able to separate populations of fluorescent AM1-43-positive hair cells from low fluorescent supporting cells with average numbers of approx. 150,000 hair and 220,000 supporting cells per 120 utricles. Re-sorts confirmed purity of the populations at >95%. Proteomic analysis was carried out for each cell type via 2 dimensional liquid chromatography-mass spectrometry (2D-LC-MS) and revealed a total set of 635 proteins at >95% peptide and 99.9% protein confidence level accounting for two unique peptides. Analysis of proteins exclusively expressed in either population identified 64 proteins that were expressed only in hair versus supporting cells. Vice versa, we found 104 proteins only detectable in supporting cells, but not in hair cells.

### **1004 Yeast Two-Hybrid Analysis of Protein-Protein Interactions for Dopamine D1A and D2L Receptors in Saccular Hair Cells**

**Nathan A. Deckard**<sup>1</sup>, Dakshnamurthy Selvakumar<sup>1</sup>, Marian J. Drescher<sup>1</sup>, Dennis G. Drescher<sup>1</sup>

<sup>1</sup>Wayne State University School of Medicine

Previously, an adenylyl cyclase signaling pathway in a teleost saccular hair cell preparation predicted dopamine signal transduction and dopamine receptor expression by vestibular hair cells (Drescher et al., Neuroscience 171: 1054-1074, 2010). Transcript for dopamine D1A4 and five forms of dopamine D2 was subsequently identified in the teleost hair cell preparation and dopamine D1A and D2L receptor protein was immunolocalized to hair cells in mammalian otolithic vestibular end organs. Yeast two-

hybrid mating protocols have now been employed to identify protein-protein interactions (PPI) mediating a response of vestibular hair cells to the (efferent) neurotransmitter dopamine. For bait constructs, we utilized cDNA for the third intracellular loops of hair cell dopamine D1A4 and dopamine D2L receptors ligated into the GAL4 DNA binding domain of pGBKT7 bait vectors. A saccular hair cell cDNA library in pGADT7 vector was used for prey. Following interaction between bait and prey, the yeast was grown on minimal media activating reporter genes and cDNA from prey in yeast clones was sequenced. The yeast two-hybrid protocol for D1A4 led to the identification of phosphoribosyl pyrophosphate synthetase-associated protein 1 (PRPS1) (96% identity). Mutations in PRPS1 are linked to sensorineural deafness DFN2 and PRPS1 transcript is found in vestibular hair cells. Dopamine D1A4 was found to bind to SNARE-associated protein snapin, suggesting a role for dopamine as an (efferent) neurotransmitter acting at dopamine D1A4 receptors in directing release of hair cell transmitter. Several protein-protein interactions (PPI) for dopamine D1A4 involve mitochondrial proteins including probable mitochondrial import receptor subunit TOM7 homolog of a translocase of the outer membrane with 99% identity for aa 1-55, the entire sequence. Dopamine D2L has been found to interact with Purkinje cell protein 4, a small calmodulin-binding protein, thought to regulate CaMKII activity.

#### **1005 Identification of the Porosome Complex in the Hair Cell**

**Dennis G. Drescher<sup>1</sup>, Won J. Cho<sup>1</sup>, Marian J. Drescher<sup>1</sup>**  
<sup>1</sup>Wayne State University School of Medicine

Porosomes are lipoprotein structures recently proposed to be the universal secretory machinery of the cell plasma membrane, to which synaptic vesicles transiently fuse before secretion. The porosome was first discovered in pancreatic acinar cells (Schneider et al., *Proc Natl Acad Sci USA* 94: 316–321, 1997), and since then identified in many secretory cells. In neurons, porosomes are presynaptic cup-shaped structures, 12-17 nm in diameter, possessing a central plug. The porosome is proposed to form a stable docking assembly which allows the synaptic vesicle to attach, release contents to the extracellular space, and then break off to return to the cytoplasmic compartment. In contrast, the prevailing view of synaptic secretion in hair cells is that vesicles undergo exocytosis according to the classic hypothesis, with the vesicle membrane re-cycled through the plasma membrane and recovered by endocytosis. In the present study, saccular maculae from rainbow trout were dissected and transferred to Trump's fixative. Tissues were post-fixed in 1% osmium tetroxide, dehydrated, and embedded in Embed 812 (EM Sciences). Sections 65-70 nm thick were placed on 200-mesh copper grids, post-stained with aqueous uranyl acetate and Reynolds lead citrate, examined with a Zeiss EM10-CA transmission electron microscope, and photographed. EM photos representing a magnification of 200,000x actual size were analyzed. Results showed clear evidence for the presence of porosome-like structures in the teleost vestibular hair cells. Porosomes appeared

many times in the photos we examined, both for afferent and efferent synapses. Thus we provide, for the first time, evidence that porosome structures indeed exist in the hair cell, a sensory receptor cell. These results suggest a mechanism of hair-cell transmitter secretion different from the conventional exocytotic process currently proposed.

#### **1006 Small GTPase Rac1 Conditional Knockout in Cochlear Hair Cells Does Not Cause Hearing Defects**

**Jie Fang<sup>1</sup>, Jennifer Dearman<sup>1</sup>, Lingli zhang<sup>1</sup>, Jian Zuo<sup>1</sup>**

<sup>1</sup>St. Jude Children's Research Hospital

Rac1, a small GTPase, plays important roles in hair cell development, outer hair cell function and hair cell protection against noise induced hearing loss. Conventional knockout of Rac1 is embryonic lethal around embryonic day 8 (E8). To investigate Rac1's role in hair cells, we used Cre-loxp system to conditionally knockout (cKO) Rac1 specifically in cochlear hair cells. We crossed Rac1 floxed mice with two different hair cell specific Cre mice lines, Gfi1-Cre and Prestin-CreER<sup>T2</sup>, to generate two different Rac1 cKO models. Both models did not show any defects in ABR tests at various frequencies, or morphology of the organ of Corti. These data suggest Rac1 cKO in cochlear hair cells is not sufficient to affect hair cell development and function.

This work was supported by grants from DC006471 (J.Z.), DC008800 (J.Z.), and CA21765), the Office of Naval Research N000140911014 (J.Z.), the National Organization for Hearing Research Foundation (J.F.) and the American Lebanese Syrian Associated Charities (ALSAC) of St. Jude Children's Research Hospital. J. Zuo is a recipient of The Hartwell Individual Biomedical Research Award.

#### **1007 Nesprin4 Knock-Out Mice Suffer from Progressive Hearing Loss Due to Outer Hair Cell Degeneration**

**Danielle R. Lenz<sup>1</sup>, Henning F. Horn<sup>2</sup>, Amiel A. Dror<sup>1</sup>, Zippora Brownstein<sup>1</sup>, Shaked Shivatzi<sup>1</sup>, Kyle J. Roux<sup>3</sup>, Serguei Kozlov<sup>4</sup>, Brian Burke<sup>2</sup>, Colin L. Stewart<sup>2</sup>, Karen B. Avraham<sup>1</sup>**

<sup>1</sup>Dept of Human Molecular Genetics, Sackler Faculty of Medicine, Tel Aviv University, Tel Aviv, Israel, <sup>2</sup>Institute of Medical Biology, A\*STAR, Singapore, <sup>3</sup>Department of Anatomy and Cell Biology, University of Florida, Gainesville, FL, USA, <sup>4</sup>National Cancer Institute, Frederick MD, USA

We are hereby reporting the expression of Nesprin4 (Nesp4) for the first time in the cochlea, with the prediction that Nesp4 plays a role in the maintenance of outer hair cells (OHCs). First identified in secretory epithelial cells (Roux et al. *Proc. Natl. Acad. Sci. USA* 2009), Nesp4 is a KASH-domain protein that resides in the outer nuclear membrane as part of the nuclear envelope-associated LINC (Linker of Nucleoskeleton and Cytoskeleton) complexes. These complexes include KASH domain proteins in the outer nuclear membrane and SUN domain proteins in the inner nuclear membrane, which together

enable the interaction between the nuclear machinery and the cytoskeleton. Nesp4 was also shown to interact with the microtubule motor-protein Kinesin-1 and its inappropriate expression in cultured cells led to mislocalization of the nucleus relative to the centrosome.

Nesp4 is expressed in the mouse inner ear, localizing mainly to the outer nuclear envelope of OHCs. More importantly, upon elimination of Nesp4 expression in a knock-out (KO) mouse model, OHCs are formed, but begin to degenerate rapidly as hearing matures, leading to progressive hearing loss. By P60 all KO mice are completely deaf as determined by auditory brainstem response (ABR) measurements. Despite Nesp4 expression in other tissues, including the sensory organs of the vestibular system, no additional abnormalities could be detected, possibly due to compensation of the remaining three nesprin genes, Nesprin1-3, which share similar expression patterns. Our findings mark Nesp4 as an essential protein for OHCs maintenance and hearing, potentially due to its role in the preservation of polarization in the sensory epithelia.

### **1008** Noise Exposure Induced Nitrotyrosine Increase and Hair Cell Apoptosis in the Guinea Pig Cochlea

Weiju Han<sup>1</sup>, Xingrui Chen<sup>1</sup>, Xiaorui Shi<sup>2</sup>, Alfred L. Nuttall<sup>2</sup>  
<sup>1</sup>The Chinese PLA General Hospital, <sup>2</sup>Oregon Health & Science University

Noise-induced inner ear damage is a significant source of hearing loss for people in industrialized societies. The important cochlear pathologies that occur as a result of noise exposure are increased levels of reactive nitrogen species (RNS) and reactive oxygen species (ROS) that play a significant role in noise-induced hair cell death. The current study was designed to examine noise exposure induced nitrotyrosine change, DNA damage and hair cell apoptosis in the guinea pig cochlea. The distribution of nitrotyrosine (NT) in the organ of Corti and the cochlear lateral wall tissue from the guinea pig was examined using the fluorescence immunohistochemistry method. The single strand DNA (ssDNA) in noise exposure induced apoptotic outer hair cells (OHCs) of guinea pigs was examined by immunohistology method. The immunoactivity of NT in the normal guinea pig was compared with animals exposed to 122dBA broadband noise, 4 h/day, for 2 consecutive days. In the normal animals, NT immunoreactivity was found in the OHCs, inner hair cells (IHCs) and stria vascularis in the lateral wall. Sound exposure increased the NT signal in hair cells and stria vascularis. A quantitative analysis of the NT change in OHCs and stria vascularis showed that the immunolabeling increase was significant ( $P < 0.01$ ,  $n = 16$ ) in the noise exposure induced group compared with that of the control group. Anti-NT antibody and propidium iodide double labeling shows significant increase of nitrotyrosine in the apoptotic OHC. The ssDNA was observed in noise exposure induced apoptotic OHCs, but not in the normal OHCs. These results suggest that noise exposure induced nitrotyrosine increase and ssDNA production are associated with OHCs apoptosis following noise exposure.

This work was supported by Chinese National Natural Science Foundation No. 30973305 and No. 81170908 and NIDCD R01DC000105

### **1009** Small RNA Depletion in Hair Cells Leads to Progressive Stereocilia Defects, Cell Death and Hearing Loss

Marsha Pierce<sup>1</sup>, Heather Jensen-Smith<sup>1</sup>, Edward Walsh<sup>1,2</sup>, JoAnn McGee<sup>1,2</sup>, Megan Korte<sup>2</sup>, Bernd Fritschsch<sup>3</sup>, Garrett Soukup<sup>1</sup>

<sup>1</sup>Creighton University, <sup>2</sup>Boys Town National Research Hospital, <sup>3</sup>University of Iowa

Small regulatory RNAs, such as miRNA and siRNAs, play important roles in cell proliferation, differentiation, and genomic stability. Both pre-miRNAs and siRNAs require Dicer1 cleavage to enter the RNA-Induced-Silencing-Complex (RISC), in which miRNAs reduce target mRNA translation and/or stability. Conditional knockout (CKO) of *Dicer1* in the otic placode using *Pax2-Cre* or in the otocyst using *Foxg1-Cre* has been shown to cause severe defects in sensory epithelial morphohistogenesis, neurogenesis and innervation. Moreover, the extent of hair cell (HC) morphohistological development was shown to correlate with residual miRNA expression in the *Pax2-Cre* model. Similarly, *Dicer1* CKO in sensory epithelia using *Pou4f3-Cre* has been shown to cause profound hearing loss by P38, and HCs appear morphohistologically similar to *Pax2-Cre Dicer1* CKO. To examine the specific effects of small RNA function in HCs, we generated HC-specific *Dicer1* CKO using *Atoh1-Cre*. In this model, HC miRNA depletion is apparent by P18 with no substantial HC loss or hearing deficit. At P6, HC development and maturation appears normal in CKO mice relative to controls. At P16, CKO mice show aberrant inner hair cell (IHC) and outer hair cell (OHC) stereocilia with negligible HC loss. By P28, stereocilia aberrations persist and are substantially increased for apical IHCs. Furthermore, there is considerable HC loss increasing from apex to base. Consistent with these results, audiometric analyses of CKO mice from P21 to P35 demonstrate a progressive hearing loss and diminished DPOAE responses, where CKO mice are profoundly deaf by P35. Strikingly, the model exhibits less severe consequences than germline mutation of a single HC miRNA (miR-96) in the *Diminuendo* mouse. These data demonstrate that small RNAs are not only critical in the development of HCs, but are necessary for HC maintenance and survival.

This work was supported by NIH-NIDCD:R01DC009025; NIH-NCRR:P20RR018788; Nebraska State LB692.

### **1010** Postnatal Assembly of the Striated Organelle in Rodent Inner Ear Vestibular Hair Cells

Robstein Chidavaenzi<sup>1</sup>, Anna Lysakowski<sup>1</sup>

<sup>1</sup>University of Illinois at Chicago

The striated organelle (SO) is a cytoskeletal structure that has been consistently observed sitting just below the cuticular plate in normal, as well as diseased, vertebrate vestibular type I and II hair cells, and cochlear inner hair

cells. Although only a putative structural function has been attributed to it, our intermediate voltage electron microscopy (IVEM) studies point to a precise three-dimensional morphological assembly that suggests the overall design and location of the SO is not random. To further understand the structure and function, we have focused on identifying the organelle's major proteins and determining when the organelle appears during development in rats. Using confocal and light microscopic immunohistochemical methods, prior studies have identified some proteins comprising the SO, but we have verified the presence of  $\alpha$ -2 spectrin (brain fodrin) in EM immunogold experiments. Employing  $\alpha$ -2 spectrin as bait, we pulled down interacting partners in vestibular end-organ tissue using co-immunoprecipitation and identified some of these proteins using liquid chromatography mass spectroscopy. As pertains to its appearance, in contrast to the presence of the SO as early as 10 weeks gestational age in human fetuses (Sans, 1989), we present evidence that in rats and mice that it is absent in newborn pups and is only assembled post-natally. It initially appears on the second postnatal day (P2) and it is fully formed by P6. At later stages, coinciding with certain developmental milestones, such as P8, (auditory brainstem response (ABR) first detected), P12 (the onset of hearing), and P15 (eye opening occurs), no discernible differences were observed beyond those noted at P6. We discuss the implications of its development and protein composition on probable function.

Supported by NIH R01 DC-02521.

### **1011 Characterizing the Cochlea's Electromechanical Operation Via Simultaneous Intracochlear Pressure and Extracellular Voltage Measurements**

**Wei Dong**<sup>1</sup>, Elizabeth Olson<sup>1</sup>

<sup>1</sup>*Columbia University*

The coupling between mechanical vibration and hair cell activity is electromechanical and this coupling is central to the operation of the cochlear amplifier. To characterize the electromechanical process at the micro-cochlear-mechanical level, a hybrid sensor was recently developed composed of our lab's standard micro-pressure sensor (OD 125 microns) with a 28 micron diameter, isonell-insulated platinum electrode adhered to its side. Using the sensor, tone-evoked intracochlear pressure and extracellular voltage were simultaneously mapped very close to and at a series of distances from the basilar membrane (BM), in scala tympani of the first turn of active cochleae of anesthetized gerbils. The cochlear condition was monitored with compound action potential thresholds at different experimental stages. From the spatial variation of pressure and extracellular voltage, the BM velocity and extracellular current density can be derived. Our results showed that the pressure and extracellular voltage were tuned to the local best frequency when they were measured at a location close to the BM. Their amplitudes decreased when they were measured farther away from the BM. Pressure, velocity, extracellular voltage and extracellular current density all showed tuning, nonlinearity

and traveling wave phase accumulation. Modern theories of cochlear amplification include predictions about the relationship between these quantities and are constrained and guided by these measurements.

### **1012 Basilar Membrane Responses to Tone Complexes: Frequency Selectivity and Nonlinear Effects of Stimulus Intensity**

**Corstiaan P.C. Versteegh**<sup>1</sup>, Marcel van der Heijden<sup>1</sup>

<sup>1</sup>*Erasmus MC, Rotterdam, Netherlands*

We measured basilar membrane (BM) responses to irregularly spaced tone complexes in Mongolian gerbil using a laser vibrometer. Tone complexes have several advantages over white noise: single recordings yield the spectral transfer of the BM over a wide (5-25 kHz) frequency range; linear and nonlinear portions of the response are readily disentangled; and the noise floor can be accurately estimated. We found that the effects of overall stimulus intensity of our wideband stimuli were similar to the nonlinear effects found with single-tone stimulation. Compressive growth was restricted to a narrow region near the best frequency (BF) of the recording site. The strongest third-order distortion products occurred just above BF and were sometimes only ~10 dB below the linear responses in the same frequency region. In a second series of experiments, we varied the spectral profile of the stimulus by elevating the intensity of one or several components of the tone complex. Elevating a restricted subset of components has a similar effect on the spectral transfer function as a uniform intensity increment of all components. However, we found that elevating different spectral components had different effects on the spectral transfer function. We analyzed this finding in terms of the "nonlinear history" of the traveling wave on its way to the recording site.

Supported by NWO grants 818.02.007 and 834.10.005 (ALW).

### **1013 Basilar Membrane Response to Laser-Pulse Stimulation in the Sensitive Living Cochlea**

**Tianying Ren**<sup>1</sup>, Wenxuan He<sup>1</sup>, Anders Fridberger<sup>2</sup>

<sup>1</sup>*Oregon Health and Science University*, <sup>2</sup>*Karolinska Institute*

Although a local resonance on the basilar membrane is commonly thought to be important for cochlear mechanics, it has not been demonstrated experimentally in the sensitive living cochlea due to technical difficulties. We stimulated the basilar membrane directly by focusing laser pulses on the cochlear partition, and measured the evoked vibrations using a heterodyne laser interferometer at a longitudinal location ~2.5 mm from the base in sensitive gerbil cochleae. When laser pulses were focused on the same location as for the vibration measurement, the basilar membrane displaced and returned to its equilibrium position almost instantaneously following laser pulses. After this initial brief response, a periodic vibration occurred with a gradual onset and offset. When the laser was focused on a location away from the measured

location, the initial brief response disappeared, but the ringing response remained. Each episode of ringing responses lasted ~1 ms and recurred multiple times in sensitive cochleae. The instantaneous frequency of the first episode of ringing responses increased with time while the following responses vibrated at an approximately constant frequency. The ringing response could not be detected from insensitive cochleae. Laser pulse-induced mechanical, acoustical, and electrical responses were compared to those induced by acoustical clicks. The current results indicate that the basilar membrane does not resonate effectively to a local stimulus and the resonators of other structures inside the cochlear partition likely contribute to responses observed under the sensitive condition.

Supported by NIH-NIDCD.

#### **1014 Visualization of Vibrations Inside the Cochlear Partition in the Sensitive Living Cochlea**

**Tianying Ren<sup>1</sup>, Wenxuan He<sup>1</sup>, Edward Porsov<sup>1</sup>**

<sup>1</sup>*Oregon Health & Science University*

Understanding mechanisms of cochlear amplification and excitation of sensory hair cells requires knowledge of mechanical transformation of the transverse basilar membrane vibration to the radial movement between the tectorial membrane and reticular lamina. By developing a scanning low-coherence heterodyne interferometer we measured sound-induced sub-nanometer vibrations as a function of the radial and transverse locations of the cochlear partition. The magnitude and phase of vibrations were measured at different frequencies and sound levels and presented on the across-sectional view of the cochlear partition. The two-dimensional vibration images show that, at the low and intermediate sound pressure levels, the structures inside the organ of Corti vibrated at a magnitude greater than that of the basilar membrane, and the basilar membrane vibration became more significantly at high sound levels. The vibration inside the organ of Corti saturated at a sound pressure level much lower than the saturation level of the basilar membrane vibration. These data provide a new insight into the micromechanical mechanisms of active hearing.

Supported by NIH-NIDCD.

#### **1015 Verification of the Phase Lead of Reticular Lamina (RL) Vibration to That of Basilar Membrane (BM) at Multiple Longitudinal Locations Along the Cochlea**

**Fangyi Chen<sup>1</sup>, Dingjun Zha<sup>1</sup>, Alfred L. Nuttall<sup>1</sup>**

<sup>1</sup>*Oregon Health & Science University*

Recent development of low coherence interferometry technique allows measuring vibration within the organ of Corti *in vivo*. The reticular lamina (RL) vibration is phase-lead to the basilar membrane (BM) (Chen et al., 2011). This phase lead could be important to the cochlear amplification, a closed-loop feedback system. The phase lead of the motion of the stereocilia relative to the BM vibration is believed to be an important factor in the

cochlear amplification. RL, as one end the stereocilia can initiate the bending motion. In this study, we show the measurement on RL and BM at multiple longitudinal locations along the cochlear partition. This longitudinal pattern verifies our previous result on single point measurement. Results on this study will also provide experimental data to understand the timing of the cochlear amplification. This work was supported by NIDCD grant DC000141 and DC010399.

#### **1016 Two Modes of Wave Propagation in the Organ of Corti**

**Laura Rupprecht<sup>1,2</sup>, Aleks Zosuls<sup>1,2</sup>, David Mountain<sup>1,2</sup>**

<sup>1</sup>*Boston University Department of Biomedical Engineering,*

<sup>2</sup>*Boston University Hearing Research Center*

The complex three dimensional anatomy of the Organ of Corti (OC) suggests the possibility of multiple modes of energy propagation from base to apex. It has been hypothesized that at least two modes are required to achieve sharp tuning at a particular place. Here we present evidence for two modes of wave propagation in the gerbil cochlea.

A small vibrating probe was brought into contact with the underside of the basilar membrane in an excised cochlear preparation. Motion of structures in the OC from both the first and second turn was captured via stroboscopic imaging for stimuli ranging from 10 Hz to 40 kHz. Regions of Interest from images taken at eight different phases of the stimulus were then analyzed using a cross-correlation method to quantify displacement magnitude and phase. Magnitude and phase of the motion were measured as a function of distance from the probe for each of the stimulus frequencies.

Two modes of wave propagation were observed. The first mode was observed in the radial motion of the IHC stereocilia. This mode is thought to reflect the transverse motion of the basilar membrane. A second mode of wave propagation was observed in the motion of the tunnel crossing fibers that is thought to be the response to longitudinal fluid flow. The first mode was slower than the second and the estimated velocity in the basal turn was similar to the velocities measured with acoustic stimulation *in situ* (Ren, 2001). The second mode had a much higher velocity, and propagated in both directions away from the probe. This provides experimental evidence for dual modes of cochlear wave propagation occurring simultaneously in the same experimental preparation.

**1017 Dual-Beam Absolute Nano-Vibrometer Based on Spectral-Domain Phase-Sensitive Optical Coherence Microscopy to Investigate the Cochlear Micromechanics at the Apex of the Guinea-Pig Cochlea**

Hrebesh M. Subhash<sup>1</sup>, Niloy Choudhury<sup>2</sup>, Ruikang Wang<sup>3</sup>, Steven L. Jacques<sup>1</sup>, Fangyi Chen<sup>1</sup>, Yuan Zhang<sup>1</sup>, Dingjun Zha<sup>1</sup>, Anders Fridberger<sup>4</sup>, Alfred L. Nuttall<sup>1</sup>

<sup>1</sup>Oregon Health & Science University, <sup>2</sup>Michigan Technological University, <sup>3</sup>University of Washington, <sup>4</sup>Karolinska Institutet

In the field of cochlear mechanics, there is a great interest in studying the acoustic induced vibrations of various membranes in the complex structure of mammalian cochlea, which is essential for understanding the cochlear mechanics and how the travelling wave of the basilar membrane couples its energy to the mechanosensory receptor cells in the organ of Corti (OC). Most optical measurement of vibration only provides the projection of vibration along the optical axis, making in plane vibration measurements impossible. One of the difficulties this leads to is the impossibility of measuring vibration from basilar membrane and tectorial membrane at the same time as their planes of vibration are thought to be perpendicular to each other. We have developed a dual-beam spectral-domain phase-sensitive optical coherence microscopy system to image absolute vibration parameters from different locations within the apex of the mammalian organ of Corti. A dual angle delay-encoded sample beam was implemented to obtain two imaging beams with a fixed angular separation, which allow absolute measurement of vibration from various structures of the cochlea, such as, basilar membrane (BM), reticular lamina, outer hair cells and tectorial membrane (TM). The system has the potential to provide depth resolved absolute vibration measurement of tissue microstructures from each of the delay-encoded vibration images with a noise floor of ~5nm at 200Hz to 1000Hz. This work was supported by research grants from the National Institute of Deafness and other Communication Disorders Grants R01DC010399 and R01DC000141.

**1018 Mechanical Excitation of IHC Stereocilia: A New Hypothesis That Fits Together Diverse Evidence**

John GUINAN<sup>1,2</sup>

<sup>1</sup>Eaton Peabody Lab, Mass. Eye & Ear Infirmary, Harvard Medical School, <sup>2</sup>Speech and Hearing Bioscience and Technology Program, Harvard-MIT HST

The bending of inner-hair-cell (IHC) stereocilia controls cochlear output, but the mechanisms that produce this bending are poorly understood. Relevant evidence comes from measurements of cochlear motion in in-vitro and live preparations, and inferences about cochlear motions from auditory-nerve (AN) fiber responses. The common conception that IHC excitation is due only to shearing between the reticular lamina (RL) and the tectorial membrane (TM) does not explain the data. A new hypothesis of how IHCs are excited fits many of the

observations into a coherent picture. The key new concept is that the RL-TM gap can vary at acoustic frequencies, at least for low-frequency sounds, and this varying gap produces fluid flow within the gap that bends the IHC stereocilia. Such RL-TM gap changes were reported by Nowotny and Gummer (2006, PNAS 103:2120). Variations in the RL-TM gap may come about because the outer-hair-cell (OHC) stereocilia that connect the RL and TM are not rigid, they may dimple the TM, and, if OHC stereocilia are not perpendicular to the RL and TM, through geometric nonlinearity. Three paths by which IHC stereocilia may be bent are: classical RL-TM shear, changes in the RL-TM gap from passive forces, and changes in the RL-TM gap from OHC contractions. For the first half-cycle of the response to a rarefaction click, these bend IHC stereocilia in the excitatory, inhibitory, and excitatory directions, respectively. The mix of these factors depends on frequency, level and time after click onset. Variations in this mix can explain many previously mysterious observations such as efferent inhibition of the AN initial peak (ANIP) response, and phase reversals across sound levels in both click and tone responses. OHC-induced changes in the RL-TM gap provide a mechanism by which OHC active processes can bend IHC stereocilia and enhance cochlear output without a corresponding change in basilar-membrane motion.

Supported by NIDCD RO1DC00235, P30DC005209

**1019 Measurement of *in Vivo* Outer Hair Cell Length Change**

Dingjun Zha<sup>1,2</sup>, Fangyi Chen<sup>1</sup>, Sripriya Ramamoorthy<sup>1</sup>, Anders Fridberger<sup>1,3</sup>, Alfred L. Nuttall<sup>1,4</sup>

<sup>1</sup>Oregon Health & Science University, <sup>2</sup>Xijing Hospital, Fourth Military Medical University, <sup>3</sup>Karolinska Institutet, <sup>4</sup>Kresge Hearing Research Institute, University of Michigan

In the mammalian cochlea, the normal hearing is refined by amplification of the motion of basilar membrane. It is widely accepted that the amplification of basilar membrane is based on the outer hair cell (OHC) electro-motility, which can change the length of OHC. OHC length change induced by OHC electro-motility force has been studied extensively *in vitro* and *in situ*, but the OHC length change have not been demonstrated *in vivo*, so far. In this study, using *in vivo* optical coherence tomography, we demonstrate that OHC length changes exist in the sensitive cochlea and the timing of length changes depends on the stimulus level. The unexpected timing and magnitude of OHC length changes is very important for explaining how the vibration of basilar membrane is amplified. This work was supported by NIH grants R01DC000141 and R01DC010399.

**1020 Low-Frequency Modulated Quadratic and Cubic Otoacoustic Emissions in Humans**

Markus Drexl<sup>1</sup>, Robert Gürkov<sup>1</sup>, Eike Krause<sup>1</sup>

<sup>1</sup>Centre for Research and Treatment of Vertigo, Balance and Ocular Motor Disorders, LMU Munich

Previous studies have used low-frequency tones to modulate cubic distortion product otoacoustic emissions (CDPOAEs). The CDPOAE is mostly chosen because

amplitudes sufficient for modulation can be evoked with moderate primary tone levels. Quadratic DPOAEs (QDPOAE), however, are more sensitive to minute changes of the cochlear operating point (OP) and are potentially better suited to assess changes of the cochlear OP.

Here, we compare the properties of low-frequency (30 Hz, 80-120 dB SPL) modulated CDPOAEs and QDPOAEs, evoked with F2=2 kHz and 5 kHz in human subjects with normal hearing. The modulation depth is quantified with the modulation index (MI), a measure which considers both amplitude and phase.

Modulated CDPOAEs evoked with F2=2 kHz have amplitude maxima at the zero crossings and amplitude minima at the extremes of the bias tone which correlate positively with the bias tone level. CDPOAEs evoked with F2=5 kHz show very little modulation, even at the highest bias tone level used (120 dB SPL). With QDPOAEs, not only the depth, but also the shape of the modulation pattern is correlated with the bias tone level. At moderate bias tone levels (about 90-110 dB SPL), QDPOAEs evoked with F2=5 kHz show one notch around the zero crossing of the positive going flank of the bias tone (a single modulation pattern). From a bias tone level of about 110 dB SPL, the pattern reverses and shows a double modulation pattern. At the highest bias tone level used (120 dB SPL), quadratic MIs greatly exceed cubic MIs ( $2.0 \pm 0.5$  and  $0.97 \pm 0.06$  (mean  $\pm$  sem), respectively).

Low-frequency modulated QDPOAEs in humans are similar to QDPOAE modulation seen in animal studies and behave as predicted by mathematical models. Human low-frequency modulated QDPOAEs are ideally suited to estimate cochlear OP shifts because of their higher OP shift sensitivity.

Supported by the German Federal Ministry of Education and Research (IFB<sup>LMU</sup> TR-F9)

### **1021 Spectral and Temporal Moments of Click-Evoked Otoacoustic Emissions to Assess Cochlear Tuning in Individual Human Ears: Instantaneous Frequency, Instantaneous Bandwidth, Group Delay, and Group Spread**

**Douglas Keefe<sup>1</sup>**

<sup>1</sup>*Boys Town National Research Hospital*

A click-evoked otoacoustic emission (CEOAE) was analyzed as an analytic signal to calculate its signal-processing moments. As time-smoothed functions over a set of logarithmically-spaced time intervals, a CEOAE has an instantaneous frequency (IF) and instantaneous bandwidth (IB) as its first- and second-order spectral moments. As frequency-smoothed functions over a set of logarithmically-spaced frequencies, a CEOAE has a group delay (GD) and group spread (GS) in delay as its first- and second-order temporal moments. Data were analyzed using a database of CEOAEs recorded in human ears over a 1-16 kHz bandwidth and 0.25-19 ms duration. A basic goal was to evaluate whether CEOAE moments provide insight into cochlear function, especially cochlear tuning. A

clinical goal was to interpret CEOAE moments in each ear, rather than over a group of ears, to enhance the diagnostic value of a CEOAE test. Contrasted with calculating GD as the gradient of an unwrapped phase in frequency (or IF in time), all moments were calculated using the rectangular rather than the polar representation of the analytic CEOAE signal (i.e., no unwrapping). IB is a measure of the cochlear bandwidth along a time axis at a particular IF, which may be analyzed in relation to a reflection site associated with a particular tonotopic place on the basilar membrane. GS is a measure of the spread in GDs at a particular frequency, and may be related to a spatial spread of generation sites on the basilar membrane contributing to a frequency-specific CEOAE. Multiple internal reflections of CEOAEs within the cochlea must also be considered. Moments were classified as valid in each ear based on a combined use of signal-to-noise ratio and phase coherence measures. CEOAE moments reveal the degree of joint scaling properties in frequency and time in normal ears, and show transitions at frequencies separating regions of normal hearing and sensorineural hearing loss. [Research support by the NIH]

### **1022 Contribution of Complex Stapes Motion to Cochlea Activation**

**Jae Hoon Sim<sup>1</sup>, Albrecht Eiber<sup>2</sup>, Michael Lauxmann<sup>2</sup>, Michail Chatzimichalis<sup>1</sup>, Alexander Huber<sup>1</sup>**

<sup>1</sup>*University Hospital Zurich*, <sup>2</sup>*University of Stuttgart*

#### **Introduction**

Classic theories of hearing have considered only a translational component (piston-like component) of the stapes motion as being the effective stimulus for cochlea activation and thus the sensation of hearing. Our previous study (Huber et al. 2008) qualitatively showed that rotational components around the long and short axes of the footplate (rocking-like components) lead to cochlear activation as well.

#### **Aim of the study**

Contribution of the piston-like and rocking-like components of the stapes motion to cochlea activation was quantitatively investigated with measurements in live guinea pigs and a related mathematical description.

#### **Methods**

The isolated stapes in anesthetized guinea pigs was stimulated by a three-axis piezoelectric actuator, and 3-D motions of the stapes and compound action potential (CAP) of the cochlea were measured simultaneously. The measured values were used to fit a hypothesis of the CAP as a linear combination of the logarithms of the piston-like and rocking-like components.

#### **Results**

Both the piston-like and rocking-like components activate cochlear responses when they exceed certain thresholds. These thresholds as well as the relation between CAP and intensity of the motion component were different for piston-like and rocking-like components. The threshold was found to be higher and the sensitivity lower for the rocking-like component than the corresponding values for the piston-like component.

## **1023 Forward and Reverse Impedances of the Human Middle and Inner Ear**

**Hideko Nakajima**<sup>1,2</sup>

<sup>1</sup>*Department of Otolaryngology, Harvard Medical School,* <sup>2</sup>*Eaton Peabody Laboratory, Massachusetts Eye & Ear Infirmary*

Detailed measurements of middle and inner ear transfer functions in the forward and reverse direction of acoustic stimulation are valuable to understand human middle and inner ear acoustics, clinical measurements such as otoacoustic emissions and middle-ear prosthetic devices. For each human temporal bone, we simultaneously measure ear-canal pressure, stapes velocity, and intracochlear pressures in scala vestibuli and scala tympani, while stimulating the ear in the forward and reverse direction. For forward stimulation, sound is presented to the ear canal, and for reverse stimulation, mechanical stimulation is introduced to the round window. To characterize the middle ear, we are able to calculate the forward and reverse pressure gain ( $G_{me\_f}$  &  $G_{me\_r}$ ) and middle-ear impedance ( $Z_{me\_f}$  &  $Z_{me\_r}$ ). In the inner ear, we calculate the forward and reverse impedances by referencing pressures at the scala vestibuli and scala tympani with respect to the stapes volume velocity ( $Z_{sv\_f}$  &  $Z_{sv\_r}$  and  $Z_{st\_f}$  &  $Z_{st\_r}$ ). We are also able to obtain the differential pressure across the partition, the input to the cochlea. Thus, we can characterize the forward and reverse differential impedance ( $Z_{diff\_f}$  &  $Z_{diff\_r}$ ) by taking the ratio between the differential pressure and stapes volume velocity. Gain for the differential pressure can also be calculated by referencing to pressure in scala vestibuli for forward stimulation ( $G_{diff\_f}$ ), and to pressure in scala tympani for reverse stimulation ( $G_{diff\_r}$ ). An assumption made is that volume velocities of the oval and round windows are equivalent in these normal ears during forward and reverse stimulation. Puria (JASA 113:2773-89, 2003) made measurements similar to a subset of our measurements utilizing a different technique, resulting in similar results. Depending on the transfer function, we find similarities and differences between the forward and reverse stimulation.

## **1024 Measurements of Wide-Band Cochlear Reflectance in Humans**

**Daniel Rasetshwane**<sup>1</sup>, Stephen Neely<sup>1</sup>

<sup>1</sup>*Boys Town National Research Hospital*

The total sound pressure measured in the ear canal is composed of a forward-propagating component and a reflected component. Most the energy of the reflected component is due to reflection at the eardrum. However, a measurable contribution to the reflected component comes from the cochlea. Otoacoustic emissions (OAEs) are associated with this reflected component and have been shown to be important noninvasive probes of cochlear function. Ear-canal reflectance is the transfer function between forward and reflected components measured in the ear canal. Cochlear reflectance is the inner-ear contribution to ear-canal reflectance. We describe methods for measuring cochlear reflectance with a wide-band noise stimulus and demonstrate that it has features similar to

those of OAEs (frequency- and level-dependent latency). Measured cochlear reflectance has features similar to results of a model in which mechanical roughness generates linear coherent reflection. Measurements of cochlear reflectance have the potential to infer cochlear function and status, similar to OAE measurements.

## **1025 Developing a Low-Frequency Auditory Threshold Estimation Technique**

**Jeffery Lichtenhan**<sup>1,2</sup>, Nigel Cooper<sup>3</sup>, John Guinan<sup>1,2</sup>

<sup>1</sup>*Harvard Medical School,* <sup>2</sup>*Eaton-Peabody Laboratory of Auditory Physiology,* <sup>3</sup>*Keele University*

Non-behavioral estimates of auditory thresholds are important for managing some forms of clinical hearing loss. Presently there are no true cochlear physiologic responses that can be used as non-behavioral estimates of low-frequency auditory thresholds. Here we illustrate our novel use of round window recorded potentials to objectively estimate neural thresholds for 0.3-1 kHz tones.

At near-threshold sound levels, low characteristic frequency single auditory-nerve fibers preferentially fire at one phase of low-frequency tones. Gross electrode recordings of responses to low-frequency tone bursts, sometimes called the "auditory nerve neurophonic," contain phase-locked compound action potentials (CAPs) and cochlear microphonics (CM). If the same tone burst is presented again, but with the opposite polarity, the CM reverses polarity, but the position of the CAP waveform shifts in time by  $\frac{1}{2}$  cycle. Averaging responses from tones presented separately with opposite polarities yields a waveform in which the CM is cancelled and the CAP appears twice each tone cycle. The result is a neural signal at the tone's second harmonic – the "Auditory Nerve Overlapped Second Harmonic" (ANOSH). Varying the stimulus level in 10 dB steps allows threshold estimation from the ANOSH response. Threshold was defined as the signal level where the interpolated ANOSH response equaled the highest noise measure.

From cats we measured ANOSH thresholds to 0.3-1 kHz tones, traditional tone-pip CAP thresholds from 2-47 kHz, and single-fiber threshold tuning curves. Our results show that both ANOSH thresholds and tone-pip CAP thresholds were about 20 dB higher (i.e., worse) than the most sensitive single-fiber thresholds. Although further experiments are needed to optimize the ANOSH-based threshold estimation, these promising results suggest that this technique could be used clinically in humans. Supported by NIDCD grants F32 DC010112, RO1 DC00235, RO1 DC03687, and P30 DC005209

## **1026 Calretinin Distribution Reveals a Complexity Within the Spiral Ganglion Superimposed on Neuron Sensitivity**

**Wenke Liu**<sup>1</sup>, Robin L. Davis<sup>1</sup>

<sup>1</sup>*Rutgers University*

In the spiral ganglion kinetic parameters of the neurons are graded tonotopically (Adamson et al. *J Comp Neurol.* 2002) whereas neuronal excitability is heterogeneous and the mid-apical region has the greatest average sensitivity (Liu and Davis. *J Neurophysiol.* 2007). Yet, superimposed

upon the distributions of these features is a substantial level of heterogeneity that could indicate additional intrinsic coding mechanisms within the ganglion.

Our previous results showed that the calcium binding protein calretinin had a heterogeneous distribution and greater staining level in the mid-cochlear region (Liu and Davis, *Abstracts of the Association of Research for Otolaryngology*, 34:662. 2011). To determine whether the non-monotonic neuronal excitability is correlated with calretinin protein levels we compared calretinin staining luminance to the electrophysiological assessment of voltage threshold and resting membrane potential of spiral ganglion neurons *in vitro*. We found that while the neuron population reiterated the non-monotonic excitability pattern (voltage threshold: base  $-41.10 \pm 0.67$  mV, middle  $-45.48 \pm 0.62$  mV, apex  $-45.11 \pm 0.99$  mV, resting membrane potential: base  $-66.68 \pm 0.40$  mV, middle  $-64.77 \pm 0.31$  mV, apex  $-64.91 \pm 0.45$  mV), calretinin staining patterns were not correlated with each of these features (voltage threshold and calretinin staining luminance  $R^2=0.05$ , resting membrane potential and calretinin staining luminance  $R^2=0.04$ ), thus indicating a more complex organization than revealed by excitability parameters.

Although not associated with intrinsic neuronal sensitivity, the unique distribution of calretinin may relate to other electrophysiological features, such as the distribution of voltage-gated calcium channels and calcium-activated ion channels, or synaptic transmission. Since hair cells are innervated by multiple nerve fibers, a role for calretinin in these complex neurons may be involved in higher-order parallel processing. Supported by NIH NIDCD R01 DC-01856.

### **1027** Neurotrophins Can Differentially Alter the Soma Area and Survival of Apical and Basal Spiral Ganglion Neurons in Vitro

Felicia L Smith<sup>1</sup>, Robin L Davis<sup>1</sup>

<sup>1</sup>Rutgers University

Spiral ganglion neuronal somata are localized within the action potential conduction pathway and as a consequence can impose limits on firing frequency and timing. It is known that neurons in the apical region are smaller than those within the basal region, thus cell size can have distinct effects on electrical transmission. However, the factors regulating this morphological parameter are still unknown. Our aim is to examine whether the same factors that regulate the electrophysiological phenotype can also alter soma size.

We focused on neurotrophin-3 (NT-3) because it can convert basal neurons into a more apical neuronal phenotype evaluated by levels of voltage-gated  $K^+$  channels (Adamson et al., *J. Neurosci.* 2002), synaptic protein distribution (Flores-Otero et al., *J. Neurosci.* 2007), and firing patterns (Zhou et al., *J. Neurosci.* 2005). Since NT-3 is abundant in apical hair cells and satellite cells (Sugawara et al., *J Comp Neurol.* 2007) we hypothesized that NT-3 might be responsible for the reduced soma area in the apex. Consistent with our hypothesis we found that NT-3 at different concentrations (0.25, 0.5, 1, 5, 10, 50,

100ng/ml) significantly reduced the soma size of apical neurons (control:  $211 \pm 4 \mu\text{m}^2$ ,  $n=5$ ; vs. 10ng/ml NT-3:  $190 \pm 5 \mu\text{m}^2$ ,  $n=5$ ,  $p<0.05$ ), while enhancing survival (control:  $85 \pm 7$ ,  $n=5$ ; vs. 10ng/ml NT-3:  $362 \pm 55$ ,  $n=5$ ,  $p<0.01$ ). However, only apical neuronal area was reduced at the concentrations evaluated and basal neuronal soma area remained unchanged (control:  $269 \pm 7 \mu\text{m}^2$ ,  $n=5$ ; vs. 10ng/ml NT-3:  $286 \pm 18 \mu\text{m}^2$ ,  $n=5$ ), despite their enhanced survival (control:  $153 \pm 22$ ,  $n=5$ ; vs. 10ng/ml NT-3:  $289 \pm 51$ ,  $n=5$ ,  $p<0.05$ ).

In summary, while NT-3 can regulate the electrophysiological phenotype of both apical and basal neurons, its effects on soma area are limited to apical neurons alone. These results indicate that complex regulatory mechanisms are in place to differentially alter phenotypes within the spiral ganglion. Supported by NIH NIDCD R01 DC- 01856.

### **1028** Neural Tuning Measured with Compound Action Potentials in Normal Hearing Human Volunteers

Eric Verschooten<sup>1</sup>, Christian Desloovere<sup>2</sup>, Philip Joris<sup>1</sup>

<sup>1</sup>Lab. of Auditory Neurophysiology, Leuven, Belgium, <sup>2</sup>Dept of Otorhinolaryngology, Head and Neck Surgery, Leuven, Belgium

Frequency selectivity is a fundamental cochlear property. Recent otoacoustic and behavioral measurements suggest that it is higher in humans than in laboratory animals (Shera et al., 2002), but this is disputed based on comparisons of behavioral and electrophysiological measurements across species (Ruggero and Temchin, 2005). There are no direct neural recordings from human single auditory nerve fibers. Here we investigate the use of mass potentials to electrophysiologically quantify tuning in humans.

We combined the forward masking paradigm of Oxenham and Shera (2003) with the recording of compound action potentials (CAP) in human. Forward masking is more suitable to study frequency selectivity than simultaneous masking, because it is less confounded by cochlear nonlinearities. A minimally invasive transtympanic protocol was developed to record CAPs from the cochlear promontory or the niche of the round window of normal hearing volunteers. This involved a custom made ear mold with openings for the transtympanic needle electrode and for acoustic stimulation (ER-2 earphone, calibrated in-situ with an ER-7 microphone).

Brief probe tones were presented at levels of max. 75 dB SPL and a reference masking level causing a criterion reduction (33%) in CAP amplitude was determined. By increasing the reference masker level with 10 dB and varying the notch-width, Q10 values (reciprocal of the relative notch-width) were obtained for different probe frequencies. The human results were compared with Q10s obtained previously with the same paradigm in cats and chinchillas (Verschooten et al., 2010). For the probe frequencies studied, between 2 and 6 kHz, we found that Q10 values in human are  $\sim 1.6$ x higher than for cat or chinchilla.

We conclude that frequency selectivity estimated from CAPs is higher in humans than in cat and chinchilla, consistent with previous reports (Shera et al., 2002; Oxenham and Shera, 2003). Supported by grants from FWO and BOF (Flanders, Belgium).

### **1029** Temporal Response Properties of the Electrically Stimulated Auditory Nerve in the Deafened Guinea Pig

Dyan Ramekers<sup>1,2</sup>, Huib Versnel<sup>1,2</sup>, Stefan Strahl<sup>3</sup>, Wilko Grolman<sup>1,2</sup>, Sjaak Klis<sup>1,2</sup>

<sup>1</sup>University Medical Center Utrecht, <sup>2</sup>Rudolf Magnus Institute of Neuroscience, <sup>3</sup>MED-EL GmbH, R&D

After severe hair cell loss, secondary degeneration of spiral ganglion cells (SGCs) is observed – a gradual process that spans years in humans but only takes weeks in guinea pigs. Being the target for cochlear implants, both the number and the physiological state of the SGCs are important determinants for the effectiveness of a cochlear implant. Until now focus has been on the number of cells and the nerve's response threshold. Our goal is to add to this a characterization of the temporal response properties of the SGCs, which reflect their physiological condition.

Guinea pigs were deafened by co-administration of kanamycin (400 mg/kg) and furosemide (100 mg/kg) two or six weeks before acute experiments. We used a MED-EL Pulsar cochlear implant to electrically evoke and record compound action potentials (eCAPs). Stimuli consisted of biphasic current pulses. The following parameters were varied: phase duration, inter-phase gap, current level, inter-pulse interval and pulse train duration. The eCAP was quantitatively evaluated with respect to amplitude, threshold, dynamic range and refractoriness. Immediately after the electrophysiological data were gathered, the animals were sacrificed for histological analysis.

The eCAP amplitude increased with phase duration and with current level. The threshold and the dynamic range decreased with increasing inter-phase gap. Preliminary data indicate this effect was more pronounced in deafened animals. The dynamic range and the refractory period (both absolute and relative) were larger in deafened than in normal-hearing animals. The potential of these electrophysiological measures towards assessment of the condition of the auditory nerve can be of great benefit to clinical diagnostics.

### **1030** Mapping and Contribution of Spiral Ganglion Neurons to Sound-Evoked Auditory Nerve Response

Yong Tang<sup>1,2</sup>, Jérôme Bourien<sup>1,2</sup>, Marc Lenoir<sup>1,2</sup>, Charlene Batrel<sup>1,2</sup>, Sabine Ladrech<sup>1,2</sup>, Jean-Luc Puel<sup>1,2</sup>, Jing Wang<sup>1,2</sup>

<sup>1</sup>INSERM, <sup>2</sup>Université Montpellier 1 & 2

Degeneration of SGNs without associated loss of hair cells has been shown to occur in animal models and human as the result of aging, noise, ototoxic drugs, or genetic factors. Application of ouabain onto the round window

membrane of gerbil resulted in a selective loss of SGNs (Schmiedt et al., JARO., 2002). Here, we used increasing concentration to fine-tune the loss of SGN ribbon synapses. When correlated with synaptic losses, CAP threshold and amplitude measurements delineated clearly three SGN populations: i) a high ouabain-sensitive population which do not significantly contributes to CAP amplitude and threshold, ii) an intermediate ouabain-sensitive population which participates to CAP amplitude, but not to threshold and iii) a low ouabain-sensitive population which contributes both the CAP amplitude and the threshold. This classification revealed by the ouabain-sensitivity fits accurately with the classification of Schmiedt (Schmiedt, Hear Res., 1989) based on the spontaneous spike rate of auditory nerve fibers; i.e. low (LSR), medium (MSR), and high spontaneous rate (HSR). Ouabain affects preferentially the LSR neurons (i.e. neurons having high threshold) then the MSR neurons, and finally the HSR neurons (i.e. neurons having low threshold). In addition to demonstrate that ouabain constitutes a powerful tool to map the different populations of SGNs and their respective contribution to sound-evoked auditory nerve potentials in gerbil, our results provide a predictive tools to estimate the losses of ribbon synapses in pathological conditions where sensory hair cells are no affected. Altogether, these results may have clinical impacts to set up relevant clinical tests to probe the function state of SGN in human presenting discordance between auditory threshold and decline intelligibility in noisy environments.

The first two authors contributed equally

### **1031** Does the Cochlear Amplifier Play a Role in Dynamic Range Adaptation in the Auditory Nerve?

Bo Wen<sup>1,2</sup>, Bertrand Delgutte<sup>1,3</sup>

<sup>1</sup>Eaton-Peabody Laboratory, Massachusetts Eye and Ear Infirmary, Boston, MA 02114, <sup>2</sup>Department of Otolaryngology and Laryngology, Harvard Medical School, Cambridge, MA 02115, <sup>3</sup>Research Laboratory of Electronics, Massachusetts Institute of Technology, Cambridge, MA 02139

The dynamic range of auditory neurons shifts toward the most probable sound levels in a continuous, dynamic stimulus, thereby improving the coding precision of the prevailing sound levels. Such “dynamic range adaptation” is already observed in the auditory nerve (AN) (Wen et al., J. Neurosci. 29:13797), posing the question of whether the cochlear amplifier contributes to this form of adaptation.

To evaluate the role of the cochlear amplifier in dynamic range adaptation, we recorded from single AN fibers in anesthetized cats and compared the dynamic range shifts produced by tones at the characteristic frequency (CF) vs. tones well below ( $> 1/2$  octave) the CF. Because the basilar membrane motion is only amplified over a narrow region just basal to the characteristic place, the contribution of the cochlear amplifier is assumed to be minimal in the below-CF condition. For both on-CF and below-CF conditions, tone bursts are presented continuously and updated every 50 ms. 80% of the tones are “adaptors” that are either at or well below the CF, with

levels drawn at random from a 12-dB wide distribution. The other 20% are "probes" that are always at CF with levels drawn from a 75-dB wide distribution. The mean levels of the on-CF and below-CF adaptors were chosen to evoke similar firing rates.

For all fibers tested, the dynamic range shift of the probe tone was greater with below-CF adaptors than with on-CF adaptors, with a median difference of 7.6 dB. Further, although the gain of the cochlear amplifier differs between basal and apical regions of the cochlea, there was no obvious effect of CF on the shift difference between the two conditions. These results suggest that the cochlear amplifier does not play a major role in dynamic range adaptation, thereby narrowing down the search for the mechanisms underlying dynamic range adaptation.

Supported by NIH grants RO3 DC011156, RO1 DC002258, and P30 DC005209.

### **1032 Responses of Auditory Nerve Fibers to Tones in Wideband Noise: Within- And Across-Channel Cues for Signal Detection**

Jolet Smans<sup>1</sup>, Corstiaen P.C. Versteegh<sup>1</sup>, Marcel van der Heijden<sup>1</sup>

<sup>1</sup>*Erasmus MC, Rotterdam, Netherlands*

Behavioral data for detecting single tones in wideband noise show a nearly linear growth of threshold with noise intensity over a large (>80-dB) dynamic range. This linearity is difficult to understand in terms of rate coding. On increasing the noise intensity, more and more nerve fibers will be saturated by the noise alone, preventing them from contributing to detecting the tone. Temporal cues such as phase locking are more robust in this respect: vector strength to the tone frequency is primarily determined by S/N ratio and is relatively insensitive to overall intensity. Determining vector strength, however, requires a priori knowledge of the tone frequency and the ability to determine widely separated spike times with respect to the phase of the tone. Moreover, its use is restricted to low-frequency (<4-kHz) tones. Vector strength, however, is not the only way to characterize temporal coding. Other, more heuristic, metrics of temporal coding may well play a role in detecting tones in noise. We recorded the responses to noise and tone combinations of single auditory nerve fibers in anesthetised Mongolian gerbils. The tone was presented at the fiber's characteristic frequency (CF) at different S/N ratios. We then time-compressed and expanded the noise-plus-tone waveforms in order to mimic the responses to the original stimulus of neighboring fibers having different CFs. The responses were analyzed using a number of metrics including spike rate, vector strength, and the peaks and shapes of auto- and cross-correlograms. For low-frequency fibers, vector strength was the most sensitive and robust metric. For most fibers, the temporal metrics derived from correlograms were more sensitive than spike rate. Across-CF processing reduces the need for long "internal delays", but it also leads to reduced sensitivity.

Supported by NWO grant 818.02.007 (ALW).

### **1033 Peripheral Mechanisms for Compensation of Envelope Degradation by Reverberation**

Luke Shaheen<sup>1,2</sup>, Michaël Slama<sup>2,3</sup>, Bertrand Delgutte<sup>1,4</sup>

<sup>1</sup>*Eaton-Peabody Laboratories, Massachusetts Eye & Ear Infirmary*, <sup>2</sup>*Harvard-MIT Division of Health Sciences and Technology*, <sup>3</sup>*Harvard Medical School*, <sup>4</sup>*Research Laboratory of Electronics, MIT*

Information in speech is largely conveyed by temporal modulations in the amplitude envelope. In everyday listening environments reverberation decreases the depth of these modulations, yet speech reception is relatively robust. In order to determine whether the peripheral auditory system possesses mechanisms that compensate for the effect of reverberation, we measured responses of auditory nerve (AN) fibers in barbiturate anesthetized cat to sinusoidally amplitude-modulated (SAM) broadband noise stimuli presented in simulated anechoic and reverberant environments. The modulation frequencies ranged from 4 to 64 Hz and stimulus levels were 10-20 dB above noise threshold.

Reverberation decreased the modulation depth of neural responses to 100% modulated SAM noise, but in most fibers the degradation was smaller than that in the acoustic stimulus. To determine the specific attributes of reverberation that produce this acoustic-to-neural compensation (ANC), we compared the responses to reverberant stimuli with those to anechoic stimuli having the same modulation depth in the ear canal. The response modulation depths were the same for the two stimuli once cochlear filtering was taken into account. This implies the ANC is determined by the modulation input-output function (MIOF), the nonlinear transformation from input modulation depth to response modulation depth. The MIOFs were well fit by a power function; 83% of the exponents were less than 1 dB/dB (median 0.8), indicating a compressive shape resulting in ANC. The exponents did not depend on characteristic frequency or spontaneous discharge rate.

The ANC of the AN is significantly smaller than that of the inferior colliculus (IC) neurons in awake rabbit (Slama & Delgutte, ARO Abstr. #279, 2010). These results suggest that the periphery contributes a compensatory mechanism through MIOF compression, but further compensation occurs between the AN and the IC.

Supported by NIH Grants R01 DC002258 and P30 DC005209

### **1034 BDNF and NT-3 Affect the Excitability and KCNQ Expression of Neurogenin-Induced Neurons**

Amy Yang<sup>1</sup>, Liqian Liu<sup>1</sup>, J. Matthew Velkey<sup>2</sup>, Marti Morales<sup>3</sup>, R. Keith Duncan<sup>1</sup>, Erin Purcell<sup>1</sup>

<sup>1</sup>*University of Michigan*, <sup>2</sup>*Duke University*, <sup>3</sup>*Adrian College*  
Glutamatergic, bipolar neurons may be efficiently derived from embryonic stem cells (ESCs) through doxycycline (dox)-induced overexpression of the transcription factor Neurogenin 1 (Ngn1) (1). These cells are potential candidates for auditory nerve regeneration and yield insight into the development of sensory neurons originating

from the Ngn1-pathway. We are investigating control of the excitability and the expression of voltage-gated potassium channels of Ngn1-induced neurons by the neurotrophins naturally present in the inner ear: brain-derived neurotrophic factor (BDNF) and neurotrophin-3 (NT-3). ESCs were cultured on coverslips in the presence of dox, subsequently treated with neurotrophins, and then assessed with patch clamp electrophysiology, quantitative PCR and immunohistochemistry. We found that BDNF decreased the resting potential (-51 mV, n=19) in comparison to NT-3 (-43, n=13) and control cells (-39 mV, n=15) ( $p < 0.05$ ), indicating an effect of neurotrophin exposure on ion channel expression. We investigated the effects of BDNF and NT-3 on Kv7 (KCNQ) gene expression, as this potassium channel family is known to play a role in setting resting membrane potentials in the ear. BDNF significantly and specifically increased expression of the KCNQ4 potassium channel subtype in comparison to control and NT-3 treated cells (9-fold for BDNF versus 1.6-fold for NT-3,  $p < 0.001$ , ANOVA). KCNQ4 is a Kv7 channel which plays a preeminent role in the auditory system and is implicated in progressive high frequency hearing loss. The other KCNQ subtypes probed (KCNQ2, 3, and 5) were relatively unaffected by neurotrophin treatment, with minor but statistically significant increases in KCNQ2 and KCNQ5 expression. These increases were less than 3-fold in magnitude. Immunohistochemistry revealed increased expression of the KCNQ4 subtype in induced neurons at the protein level. We are currently using patch clamp electrophysiology to explore effects of neurotrophins on firing features and patterns in these cells. Our studies illustrate the potential to combine induced gene expression with extrinsic soluble cues in order to direct cell fate and excitability. The results provide insight into the development of excitability in Ngn1 sensory neurons and the dependence on context cues for determination of phenotypic fate. The specific upregulation of the auditory Kv7.4 subtype by BDNF suggests a role for BDNF in high frequency hearing loss.

1. Reyes JH et al, 2008, *J Neurosci*. 28:12622-31.

### **1035 Spike Encoding of Neurotransmitter Release Timing by Spiral Ganglion Neurons of the Cochlea**

**Mark Rutherford**<sup>1</sup>, Nikolai Chapochnikov<sup>1,2</sup>, Tobias Moser<sup>1,3</sup>

<sup>1</sup>Inner Ear Lab - University of Goettingen, <sup>2</sup>Bernstein Center for Computational Neuroscience, <sup>3</sup>Collaborative Research Center 889

Accurate and reproducible action potential generation in type I spiral ganglion neurons (SGNs) is essential for encoding the temporal structure of sound with precision. At the origin of the auditory code in the cochlea, spike triggering in each SGN relies upon input from a single ribbon-type active zone of a presynaptic inner hair cell (IHC). Using patch-clamp recordings from rat SGN postsynaptic boutons, we studied spike generation in the context of synaptic input. SGNs responded as high-pass filters, firing a single short-latency spike in response to

sustained currents of sufficient onset speed. Most IHC neurotransmission events produced discrete EPSPs that were sufficient to elicit a spike in current-clamp. SGN spike-timing was influenced by variability of EPSC size and kinetics, possibly disadvantageous to temporal-code precision. However, EPSC-like current-clamp stimuli approximating the mean physiological EPSC ( $\approx 300$  pA) - several times larger than rheobase ( $\approx 50$  pA) - triggered spikes with microsecond latency ( $\approx 500$   $\mu$ s) and precision ( $< 50$   $\mu$ s). With increasing EPSC size, differences in EPSC shape and SGN baseline potential had less influence on spike-timing. Increasing EPSC size beyond the physiological mean resulted in less charge-efficient spike generation. Spike latencies were well predicted by a two-compartment exponential integrate-and-fire model. SGN threshold potential shifted to partially compensate for changes in baseline potential. Due to a large synaptic conductance, tight anatomical coupling, and phasic excitability, SGN spikes are locked to IHC exocytosis-timing with little distortion. This fast and reliable initial encoding of sound is instrumental for a precise auditory temporal code.

### **1036 Heterogeneous Distribution of $I_h$ and HCN Channels in Murine Spiral Ganglion Neurons**

**Qing Liu**<sup>1</sup>, Paul Manis<sup>2</sup>, Robin Davis<sup>1</sup>

<sup>1</sup>Rutgers University, <sup>2</sup>The University of North Carolina at Chapel Hill

Spiral ganglion neurons (SGNs) have two distinct patterns of intrinsic membrane properties. In one, the onset time constant at threshold firing increases from base to apex, along the tonotopic axis (Liu and Davis, *J Neurophysiol*. 2007). In the second, the resting membrane potential (RMP) and hyperpolarizing sag magnitude contributed by  $I_h$  are both elevated in the mid-apex region. Because the RMP shows the widest heterogeneity in the base, while  $I_h$  sag magnitude shows the widest range in the middle, we asked whether variations in  $I_h$  and its regulation of the RMP are sufficient to explain the tonotopic difference in heterogeneity. We performed whole cell patch clamp recordings and immunocytochemistry of murine SGNs to evaluate the distribution of  $I_h$  and the underlying ion channel (HCN) subunits.

Consistent with our earlier studies (Mo and Davis, *J Neurophysiol*. 1997b),  $I_h$  current displayed a broad range of maximal conductance from 4 to 16 nS and  $V_{1/2}$  from -105 to -85 mV, while the voltage dependence of the activation time constant ranged from  $\sim 40$  ms at -140 mV to  $\sim 150$  ms at -85 mV. Preliminary data suggest  $I_h$  current magnitude is more heterogeneous in the middle compared to the base, consistent with the heterogeneity in sag magnitude observed in the middle ganglion. This also suggests other ionic currents open at rest contribute to the wide RMP range found in the base. HCN1 labeling was most heterogeneous among cells, and revealed strongest staining surrounding the cell soma. In contrast, HCN4 antibodies labeled only a small fraction of cell bodies, but showed robust axonal staining. Ongoing studies are examining the tonotopic distribution and colocalization of

HCN isoforms. Because the current is cyclic nucleotide gated, associated with neurotransmitter and  $\text{Ca}^{2+}$  regulation, characterizing the precise distribution of each subunit would aid in the understanding of the kinetics and dynamic regulation of  $I_h$  on RMP and firing properties. Supported by NIH NIDCD RO1 DC01856.

### **1037 Predicted Effects of Hearing Loss and Sound Level on Pitch Coding in the Auditory Nerve for Reverberant Conditions**

**Ananthakrishna Chintanpalli<sup>1</sup>**, Michael G. Heinz<sup>1</sup>

<sup>1</sup>*Purdue University*

The neural basis for robust speech perception by normal-hearing (NH) listeners in the presence of competing talkers and/or reverberation is still unknown. The present study used computational modeling to compare the relative effects of hearing loss and sound level on acoustic and neural representations of the periodicity of single and concurrent harmonic tone complexes (HTCs) in reverberation.

Reverberant conditions were simulated by convolving the original stimuli with reverberant impulse responses. Pooled auto-correlation functions were computed from a computational auditory-nerve model, and a periodic sieve template analysis was used to estimate neural pitch and its salience.

For single HTCs, neural pitch was estimated correctly in dry and reverberant conditions. Pitch salience was degraded in reverberation relative to dry, but much less so in the neural representation than in the acoustic. Similar results were obtained for concurrent HTCs. For both fundamental frequencies (F0s), neural pitch salience was degraded in reverberation relative to dry; however, this degradation in neural pitch salience was less than for the acoustic representation, particularly for large F0 differences. Thus, comparisons between acoustic and neural analyses suggest that the cochlea may be the first stage in the auditory system that partially compensates for the acoustic degradation due to reverberation. Predictions for hearing loss due to outer-hair-cell dysfunction indicated that reverberation resulted in a larger degradation of salience relative to dry than for normal hearing. These results suggest that nonlinearity associated with outer hair cells may contribute to the observed cochlear compensation for reverberation. These results provide physiological insight that may be useful towards the development of new signal-processing strategies to improve hearing aids and cochlear implants in multiple-talker environments.

Research supported by NIH Grant R01DC009838.

### **1038 Temporal Fine Structure Coding at High Frequencies Following Noise-Induced Hearing Loss**

**Sushrut Kale<sup>1</sup>**, Michael Heinz<sup>2</sup>

<sup>1</sup>*University of California-Irvine*, <sup>2</sup>*Purdue University*

Recent perceptual studies have suggested that normal-hearing listeners can use temporal fine structure (TFS) information up to frequencies as high as 8 kHz. However,

the general consensus from auditory-nerve (AN) data is that phase locking to TFS disappears above 4-5 kHz in cats and at even lower frequencies in rodents. Furthermore, recent perceptual studies have shown that hearing-impaired listeners have a reduced ability to use TFS cues, which is a deficit that might be associated with reduced precision in phase locking; however, the effects of sensorineural hearing loss (SNHL) on phase locking ability of AN fibers are not well understood.

The present study quantified phase locking to pure tones ranging in frequency from 0.3 to 7 kHz in normal-hearing and hearing-impaired chinchilla AN fibers. SNHL was induced by acoustic overexposure. Pure tones were presented at the characteristic frequency (CF) of AN fibers either at 10-20 dB sensation level or at multiple sound levels ranging from near fiber threshold to high sound levels. For high-CF units (CF > 3 kHz), at least 100,000 or more stimulus driven spikes were obtained to compute the vector-strength metric and to estimate its noise floor.

Results suggest that phase locking to pure tones does not disappear completely at 4-5 kHz, but rather that vector strength continues to roll-off beyond 5 kHz along a low-pass filter function with a ~100 dB/decade high-frequency roll-off. At CFs above 5 kHz, vector strength values were above the estimated noise floor suggesting that significant timing information is available at high frequencies. Furthermore, the fundamental ability of AN fibers to phase lock to TFS at low or high CFs was not affected by SNHL. These neurophysiological results have important implications for understanding perceptual studies of the use of TFS information by listeners with normal and impaired hearing.

Research supported by NIH-NIDCD Grant R01DC009838.

### **1039 Degraded Temporal Coding in Auditory-Nerve Fibers Following Noise-Induced Hearing Loss: A Wiener-Kernel Analysis**

**Kenneth Henry<sup>1</sup>**, Sushrut Kale<sup>1</sup>, Michael Heinz<sup>1</sup>

<sup>1</sup>*Purdue University*

People with hearing loss have great difficulty understanding speech in noise, even with amplification from a hearing aid. Perceptual studies suggest that a deficit in processing of temporal fine structure (TFS) rather than processing of slower envelope (ENV) modulations may be responsible. However, neurophysiological studies in animals have found little degradation in the strength of temporal coding. In the present study, we used Wiener-kernel analyses of auditory-nerve fiber responses to white noise to quantify temporal coding of TFS and ENV in anesthetized chinchillas. The amplitude (normalized spikes/s) and frequency tuning of TFS coding and ENV coding were compared between animals with noise-induced hearing loss and animals with normal hearing. For characteristic frequencies (CFs) greater than 2.5 kHz, TFS coding in impaired fibers increased markedly in amplitude compared to control fibers, which exhibited fairly weak TFS coding in this CF range. Furthermore, TFS coding was broadly tuned to low frequencies (0.5-1 kHz) rather than to CF. ENV coding in these impaired fibers was relatively

high in amplitude, similar to controls. In contrast to TFS coding, ENV coding remained broadly tuned to CF in cases of mild to moderate hearing impairment but generally shifted to broad low frequency tuning with severe impairment. For CFs less than 2.5 kHz, both TFS coding and ENV coding in impaired fibers were similar in amplitude to controls and exhibited increases in the bandwidth of frequency tuning with increasing hearing impairment. These results demonstrate that significant disruptions in temporal coding occur in cases of noise-induced hearing loss. Furthermore, degradation of TFS coding appears to be more pronounced than degradation of ENV coding in cases of mild to moderate hearing loss. The implications of these findings to speech perception in hearing impaired human listeners will be discussed. This research was supported by NIH Grant# R01-DC009838.

**1040 Two Tone Suppression Reveals That the Responses of Single Auditory-Nerve Fibers Receive Amplification from Outer Hair Cells Over a Greater Cochlear Length Than Is Generally Appreciated**

Maira A. Berezina<sup>1,2</sup>, John J. Guinan<sup>1,3</sup>

<sup>1</sup>Speech and Hearing Bioscience and Technology Program, Harvard-MIT HST, <sup>2</sup>Eaton-Peabody Laboratories, Mass. Eye & Ear Infirmary, <sup>3</sup>Eaton-Peabody Laboratories, Mass. Eye & Ear Infirmary, Harvard Medical School

Two-tone suppression (2TS) is a phenomenon in which the response of an auditory nerve (AN) fiber to a probe tone is reduced when a second suppressor tone is present. 2TS arises from the suppressor nearly saturating outer hair cell (OHC) stereocilia transduction current thereby reducing probe-tone cochlear amplifier (CA) gain. Thus, 2TS reveals CA involvement in AN responses. 2TS has been extensively studied for probe tones at the characteristic frequency (CF). However, there are only limited data on 2TS of AN responses for probe tones at frequencies other than CF, i.e. at off-CF frequencies.

In anesthetized cats, AN fiber rate-level functions for probe tones at CF and off-CF frequencies were collected with and without an 80 dB SPL non-excitatory suppressor tone placed outside the high-frequency edge of the tuning curve. Suppression was quantified by the suppressor-induced shift to higher sound levels of rate-level functions. We found that: (1) in individual fibers, 2TS generally increased with increases in probe frequency, but some fibers showed an increase in 2TS followed by a decrease when the probe tone was near the upper edge of the tuning curve. (2) Across fibers, for probe tones at and above CF, the suppression tended to increase as CF increased. (3) Suppression was found throughout the tuning-curve tip so that for fibers with low CFs, suppression was present over a broad range of probe frequencies.

Overall, the data support the hypothesis that as probe-tone frequency increases above CF, the region along the cochlea where OHCs contribute CA to the response moves basally, so that these OHCs are suppressed more by the fixed, high-side (i.e. basal) suppressor tone. Thus,

for an AN fiber, the OHCs that provide cochlear amplification for a CF tone are not the only OHCs that amplify responses of that fiber. For tones above CF, OHCs are involved that are basal to the CF-amplifier OHCs. Supported by NIDCD RO1 DC00235, P30 DC005209 & an NSF fellowship

**1041 A Sensory/behavioral Study of the Contribution of the HCN1 Gene to Auditory Processing in Genetically Engineered C57/129S Hybrid Mice**

James Ison<sup>1</sup>, Paul Allen<sup>2</sup>, Donata Oertel<sup>3</sup>

<sup>1</sup>BCS, University of Rochester, <sup>2</sup>NBA, University of Rochester Medical Center, <sup>3</sup>Dept Neuroscience, University of Wisconsin

Two conductances contribute to the low input resistances of auditory neurons that encode timing. A hyperpolarization-activated, mixed cation conductance (gh) mediated through ion channels that contain HCN1 subunits balances a low-voltage-activated potassium conductance (gKL) at the resting potential. Bushy and octopus cells in null mutant mice that lack HCN1 have smaller gh and gKL and longer time constants (Cao & Oertel, 2011), and *-/-* SPN cells share similar features (Kopp-Scheinflug et al. 2011). The ability of auditory neurons in the brain stem to encode timing with precision is thought to depend on the low input resistance of neurons near rest that gives them a short time constant (Oertel, 1983), but the implication of this idea for auditory temporal processing has not been tested behaviorally. Here we compared hybrid HCN1 *+/+* and *-/-* mice (from JAX, Nolan et al. 2003) using ABR and reflex modification audiometry (as in Allen & Ison, 2010). ABR thresholds showed little variation between any of the mice up to 16 kHz but showed high variability in *+/+* mice at higher frequencies, while mean thresholds were similar in *+/+* (n=6) and *-/-* mice (n=4). Startle (ASR) amplitudes to noise bursts were more variable in *+/+* and less variable but smaller in *-/-* mice. ASR inhibition by abrupt and ramped noise offsets was equal, as was inhibition by gaps in noise, with normal thresholds of 2 - 3 ms. ASR inhibition by a 45 deg. shift in sound location in *-/-* mice was measured at 6 and 11 weeks, and began as equal to *+/+* mice, but degraded to chance levels at 11 weeks. Our ABR data reveal that both groups express to a variable degree the age-related hearing loss of the C57 parent, making any additional effect of gene deletion difficult to determine. However, the relatively normal performance of the young *-/-* mice on gap detection and spatial localization indicates that any real differences must be small, and this suggests the need for larger groups and more refined test stimuli.

**1042 Increased Heart Rate Corresponds to the Level of Aggression Indicated by Emitted Vocalizations in the Big Brown Bat**

Marie Gadziola<sup>1,2</sup>, Rachel Anderson<sup>1,3</sup>, Jeffrey Wenstrup<sup>1,2</sup>  
<sup>1</sup>Northeast Ohio Medical University, <sup>2</sup>Kent State University, <sup>3</sup>University of Pennsylvania

Our previous work found that big brown bats (*Eptesicus fuscus*) possess a diverse repertoire of social vocalizations and that emotion-related acoustic cues are evident in the call structure (Gadziola et al., 2011). That is, different levels of aggression observed in behavioral displays were associated with different temporal structure of call sequences (low and medium aggression) or different syllable composition (high aggression). This study sought to relate these overt behaviors to an animal's internal state, assessed by heart rate. By delivering an irritating stimulus (light poking with a cotton swab), we designed an experimental paradigm that could predictably alter the behavioral state of the animal, confirmed by analyzing emitted vocalizations. We recorded the electrocardiogram (ECG) concurrently with vocalizations and video recordings of behavior. An external heart rate monitor was attached to freely behaving animals and ECG signals were transmitted wirelessly (Triangle Biosystems Inc.). After an acclimation period for the recording of baseline data, instantaneous heart rate was measured over 15-min trials, in which bats received either a short-duration (15 s) or a long-duration (60 s) irritating stimulus. In response to a short irritating stimulus, bats emitted vocalizations indicating a low or medium aggression state on 71% of the trials, whereas the long irritating stimulus evoked high aggression vocalizations on 65% of trials. Further, heart rate remained elevated for significantly longer duration ( $p < 0.001$ ) when trials evoked high aggression states ( $574 \pm 206$ s) than low aggression states ( $227 \pm 246$ s) or no vocalization ( $50 \pm 47$ s). These results confirm the behavioral state classifications assessed by vocalizations and behavioral displays, and provide an objective measure of the animal's internal state. Supported by NIDCD grant R01 DC000937.

**1043 Sensitivity to Voice Onset Time in Rabbits**

Omar Awan<sup>1</sup>, Baishakhi Choudhury<sup>1</sup>, John M. Pike<sup>1</sup>, Douglas C. Fitzpatrick<sup>1</sup>  
<sup>1</sup>Univ. of North Carolina at Chapel Hill

Voice-onset time (VOT) is a critical cue for defining the phonetic boundary between stop consonants such as /ba/ and /pa/. The cue has often been described as categorical, in that there is a sharp distinction between the phonetic boundaries over a narrow range of VOTs, while within a phonetic category VOT differences are less salient. Because animals show a similar categorical distinction to that of humans, the phonetic boundary is thought to occur using an auditory distinction that is common to animals and humans (e.g., Kuhl, P., 1981, J. Acoust. Soc. Amer. 70:340-349). An alternative view has questioned whether VOT perception is truly categorical by measuring within category discrimination thresholds without requiring phonetic distinctions. The results indicate that

discrimination is possible for any standard VOT, although discrimination is best near the phonetic boundary (Carney et al., 1977, J. Acoust. Soc. Amer. 62:961-970). Because the animal studies have been done in few species, the question of whether there is indeed a common acoustic boundary across species is also not clear. For these reasons, we are currently studying VOT discrimination in rabbits. Rabbits were trained to differentiate between /ba/ (0ms VOT) and /pa/ (80ms VOT) using a food reward paradigm. Once responses >80% correct were consistently achieved to the endpoints, stimuli of varying VOT from 10 to 70ms with 10 ms increments were introduced in 20% of trials. The thresholds for detecting a difference was 10 ms rather than 40 ms, i.e., quite different from chinchillas under similar conditions. Human listeners in the same paradigm also had 10 ms thresholds. We interpret these results as reporting thresholds discrimination of VOTs rather than categorical boundaries. Supported by NIDCD R21-DC009475 and T32-DC005360.

**1044 Auditory Stream Segregation of Conspecific and Heterospecific Sounds in Budgerigars (*Melopsittacus Undulatus*) and Zebra Finches (*Taeniopygia Guttata*)**

Mary Flaherty<sup>1</sup>, Erikson Neilans<sup>1</sup>, Kristen Garcia<sup>1</sup>, Micheal Dent<sup>1</sup>

<sup>1</sup>University at Buffalo, SUNY

An animal's ability to accurately separate sounds from multiple sources in the environment is crucial for its survival. However, relatively little work has been done analyzing an animal's ability to segregate sound sources and even less is known about what acoustic cues are important for auditory scene analysis. To date, these few studies have used acoustically simple stimuli. It would be useful to know how different auditory cues present in conspecific and heterospecific sounds are perceived by animals and what information facilitates acoustic segregation versus fusion. The current study utilizes an operant-conditioning classification paradigm to determine how conspecific and heterospecific information affects streaming in budgerigars (*Melopsittacus undulatus*) and zebra finches (*Taeniopygia guttata*). Both species were trained to differentially peck keys in response to either a synthetic zebra finch song consisting of five syllables ("whole song") or to the same song with one syllable omitted ("broken song"). Probe trials consisting of (1) a budgerigar contact call, (2) a budgerigar warble element, (3) a zebra finch contact call, and (4) a zebra finch syllable not found in the original training song were placed into the empty syllable position. If the birds responded as hearing a whole song, it suggested that the altered content was perceptually fused with the rest of the syllables to form one auditory stream. Preliminary results suggest similar findings to human speech segregation research, where similarity in spectro-temporal cues facilitates auditory streaming.

**1045** **Detection Thresholds for Amplitude Modulations of Tones in Budgerigar**

Laurel H. Carney<sup>1</sup>, Angela D. Ketterer<sup>1</sup>, Kristina S. Abrams<sup>1</sup>, Kelly-Jo Koch<sup>1</sup>, Douglas M. Schwarz<sup>1</sup>, Fabio Idrobo<sup>2</sup>

<sup>1</sup>University of Rochester, <sup>2</sup>Boston University

Amplitude modulations in sounds carry information that is relevant for speech, music, and detection of signals in noise. Processing of low-frequency modulations is of particular interest because these frequencies dominate the amplitude-modulation spectrum of speech sounds. Identification of an animal model that is sensitive to amplitude modulations is important for pursuing neural studies of temporal information processing. Previous studies in our lab have shown that rabbits are significantly less sensitive than humans for detection of amplitude-modulated tones and noise and particularly insensitive to low-frequency modulations of tone carriers. Recently, rhesus macaques have been reported to be less sensitive than humans to low-frequency modulations of wideband noise [O'Conner et al., 2011, *Hear. Res.*, 277:37]; rats and chinchilla also have higher thresholds than humans for amplitude modulations of noise [Kelly et al., 2006, *J. Comp. Psych.* 2:98]. The budgerigar was selected for further study of AM detection because this member of the parrot family is a lifelong, non-seasonal auditory learner that has been used successfully in previous behavioral studies. In particular, thresholds for AM detection of wideband noise similar to those of human listeners have been reported in the budgerigar at low modulation frequencies [Dooling and Searcy, 1981, *J. Comp. Phys. A*, 43:383]. We used an operant conditioning procedure to test the hypothesis that budgerigars would have sensitive detection for amplitude modulations of 4-kHz, 50 dB SPL tone carriers at low modulation frequencies (4 to 20 Hz). Thresholds of budgerigars for modulation detection were comparable to those of human listeners in a similar one-interval two-alternative choice task. [Supported by NIDCD-R01-001641]

**1046** **Effects of Spectral and Spatial Proximity on Sequential Auditory Grouping in Cope's Gray Treefrog**

Katrina Schrode<sup>1</sup>, Mark Bee<sup>1</sup>

<sup>1</sup>University of Minnesota

Perceiving vocal signals in large social aggregations requires listeners to perceptually group sequential signal elements by source (e.g., syllables composing words). Humans appear to use commonality in a relatively small number of cues to perform auditory grouping. We know much less about auditory grouping and its role in vocal communication in nonhuman animals. Here, we tested the hypothesis that females of Cope's gray treefrog (*Hyla chrysoscelis*) use spectral and spatial proximity to group the sequential sound elements (pulses) of a communication signal. Female treefrogs select mates based on assessment of mating calls composed of a sequence of pulses. In the laboratory, females exhibit robust phonotaxis toward sequences of 35 artificial pulses simulating a mating call, but discriminate strongly against

similar sequences with missing pulses. In this study, we presented females with spectrally and spatially incoherent sequences of 35 pulses in which alternating groups of 5 pulses had different frequencies ( $\Delta F$ ) and came from different locations ( $\Delta\theta$ ). We tested subjects using two baseline carrier frequencies (1.3 kHz or 2.6 kHz), each of which is present in the natural bimodal spectrum of mating calls, and encoded by a distinct sensory papilla. Subject responses generally indicated greater perceptual integration at smaller values of  $\Delta F$  and  $\Delta\theta$ , though under some conditions subjects showed a surprising willingness to integrate pulses despite large  $\Delta F$ s. The effects of  $\Delta\theta$  were more pronounced for the higher carrier frequency, suggesting potentially independent roles for the amphibian and basilar papillae in spatial grouping. In line with previous studies of frogs, female *Hyla chrysoscelis* are generally more permissive of irregularities in signal frequency and spatial origin than has been shown in humans and other animals thus far, suggesting potential differences in the underlying mechanisms of auditory grouping across taxa. [Supported by NIDCD R01 5R01DC009582.]

**1047** **Behavioral Discrimination of Fine-Scale Information Within Mongolian Gerbil**

**Vocalizations**

Jennifer Gay<sup>1</sup>, Krupa Solanki<sup>1</sup>, Merri Rosen<sup>1</sup>

<sup>1</sup>Northeast Ohio Medical University

The Mongolian gerbil has a repertoire of vocalizations which are emitted in different behavioral contexts. These consist generally of harmonic stacks containing frequency fluctuations over multiple time scales (Ter-Mikaelian, Yapa and Rubsamen, unpublished). Detection of fine frequency fluctuations is presumably important for distinguishing amongst gerbil vocalizations. Discrimination may be aided by the spectral complexity of the vocalizations, as gerbils are better able to detect frequency variations in harmonic stacks than in pure tones (Klinge & Klump '09). Here we used reversals of sound segments as an assay to determine the temporal integration window necessary for detecting frequency fluctuations in a complex signal. A recorded gerbil call was perturbed by subdividing the vocalization into segments of equal durations and reversing each segment. Gerbils were trained using an aversive go/nogo paradigm to discriminate each reversed version from its matched unreversed version. Reversal durations ranged from 5ms to 600ms in order to assess the temporal integration window that contributed to discrimination of this signal. Animals were able to discriminate these versions using temporal integration windows as short as 15ms. This indicates that gerbils can detect fine-scale changes within vocalizations at modulation rates at least up to 66Hz. The cross-frequency information in these vocalizations provides temporal and spectral cues that are likely to decrease the integration window compared to that for pure tones. Support: NEOMED Research Incentive Grant.

## **1048** Development of a Closed-Loop

### **Auditory Perceptual Learning Task for Mice**

Jonathon Whitton<sup>1,2</sup>, Kenneth Hancock<sup>1,3</sup>, Daniel Polley<sup>1,3</sup>

<sup>1</sup>Eaton-Peabody Laboratory, Massachusetts Eye & Ear Infirmary, <sup>2</sup>Harvard-MIT Division of Health, Sciences and Technology, <sup>3</sup>Dept Otolaryngology, Harvard Medical School

Mice are a powerful model system for studies of neural circuit function and plasticity but, due to the difficulties associated with training them to discriminate stimuli using a roving standard and their general reluctance to remain still, are difficult to train in conventional auditory discrimination tasks. Given the importance of linking perceptual changes to the development and plasticity of the auditory system, we have tailored a “closed-loop” auditory discrimination task to the mouse, which we believe is better suited to their cognitive and motoric proclivities. Preliminary auditory learning studies were made in two cohorts of adult mice. Both tasks required mice to use continuous auditory feedback to locate a randomly placed virtual target in a training arena. In order to provide these cues, stimulus features were coupled to changes in position within the behavioral arena in real time. In this way, mice were essentially performing a “hot-cold” task, where closer proximity to the target elicited stimulus features similar to the target and greater distance from the target translated to larger deviations from the target stimulus features. In the first task, mice were trained to discriminate signal-to-noise ratio by modulating the signal amplitude in a fixed noise background according to the mouse’s Euclidian distance from the target. In the second task, mice were simultaneously trained to discriminate changes in frequency and intensity by modulating tone frequency according to position on the y coordinate and intensity on the x coordinate. Mice learned the procedure within 15 daily training sessions. Over approximately 35 additional sessions, mice improved their percentage of successful trials from approximately chance to nearly 100% correct, while reducing the time needed to reach the target by approximately 25%. Ongoing studies in our lab seek to characterize the neurophysiologic correlates of improved performance in these closed-loop learning paradigms.

## **1049** Congenital Amusia Produces Abnormal Perception of Dissonance Despite Normal Perception of Beating: New Evidence for the Role of Harmonicity in Consonance Perception

Marion Cousineau<sup>1</sup>, Josh H. McDermott<sup>2</sup>, Isabelle Peretz<sup>1</sup>  
<sup>1</sup>BRAMS, Université de Montréal, <sup>2</sup>Center for Neural Science, New York University

Western listeners usually prefer consonant chords to dissonant chords, the contrast of which plays a central role in Western music. Classically, dissonance was widely believed to be the product of beating between frequency components. However, inharmonicity has also been proposed as an acoustic correlate, with recent support coming from individual differences (McDermott et al.

Current Biology, 2010). To gain further insight into consonance and its relation to pitch, harmonicity and beating, we explored their perception in amusic listeners. Amusia is a congenital disorder characterized by a failure to acquire musical aptitude in individuals who are otherwise normal, and is ascribed to impaired pitch perception. We used stimuli from McDermott et al. (2010) to assess amusic preferences for musical chords as well as for the isolated acoustic properties of beating and inharmonicity. Amusic and control subjects rated the pleasantness of stimuli on a 9-step scale. Control subjects’ ratings were consistent with previous results, with conventionally dissonant chords such as the minor second consistently rated as unpleasant, and conventionally consonant chords such as the major third consistently rated as pleasant. In contrast, amusic listeners provided inconsistent ratings that showed little resemblance to the pattern found in normal listeners. Despite the absence of preferences for consonant over dissonant chords, amusics showed the normally observed preference for stimuli without beating over matched stimuli containing beats. They did not, however, exhibit the preference observed in normal listeners for harmonic over inharmonic tones. Overall, the results show that the perception of isolated chords and of harmonicity is abnormal in amusic listeners, whereas the perception of beating is spared. The dissociation between beating preferences and consonance preferences provides novel evidence for a strong contribution of harmonicity to consonance and dissonance.

## **1050** Effects of Noise Reduction on AM and FM Reception

David Ives<sup>1,2</sup>, Axelle Calcus<sup>1</sup>, Sridhar Kalluri<sup>3</sup>, Olaf Strelcyk<sup>3</sup>, Christian Lorenzi<sup>1,2</sup>

<sup>1</sup>Ecole normale supérieure, <sup>2</sup>Université Paris Descartes, <sup>3</sup>Starkey Hearing Research Center

The goal of noise-reduction (NR) algorithms in digital hearing-aid devices is to reduce the background noise whilst preserving the original signal. These algorithms may increase the signal-to-noise ratio (SNR) in an ideal case, but they generally fail to improve speech intelligibility. However, due to the complex nature of speech, it is difficult to disentangle the numerous effects of noise reduction which may underlie the lack of speech benefits.

The goal of the present study was to assess the effects of NR algorithms on the ability to discriminate two basic acoustic features known to be crucial for speech identification, namely amplitude modulation (AM) and frequency modulation (FM). Discrimination of complex AM and FM patterns was measured for normal-hearing listeners using a same-different discrimination task. The stimuli were generated by modulating 1-kHz pure tones by either a two-component AM or FM modulator, with modulation rates centered around 3 Hz.

Discrimination of AM or FM patterns was measured in quiet and in the presence of a Gaussian white noise which had been passed through a gammatone auditory filter centered on 1 kHz. The noise was presented at SNRs ranging from -6 to +12 dB. Stimuli were left as such or

processed via a NR algorithm based on the spectral subtraction method.

Noise reduction was found to yield small improvements in discrimination at the higher SNRs of the AM conditions but had little effect, if any, on FM discrimination. The results suggest that the absence of benefit from noise reduction on speech perception does not result from a counterbalancing effect between AM and FM transmission (for narrow band stimuli). In addition, the stimuli were processed with a model of early auditory processing to quantify the fidelity of AM and FM transmission. Predictions from the model compared favorably with the perceptual data.

### **1051 Neuronal Adaptation and Non-Linear Amplitude-Modulation Processing in a Perception Model**

**Stephan D. Ewert<sup>1</sup>**, Carolin Iben<sup>1</sup>, Angela Josupeit<sup>1</sup>

<sup>1</sup>*Medizinische Physik, Universität Oldenburg, Germany*

This study focuses on adaptation and amplitude-modulation processing in an extended version of the computational auditory signal processing and perception model (CASP) by Jepsen *et al.* [J. Acoust. Soc. Am. 124, 422 (2008)]. While CASP successfully accounts for many aspects of simultaneous and non-simultaneous masking in human listeners, the model required changes to the modulation processing stage in order to account amplitude-modulation depth discrimination based on Ewert and Dau [J. Acoust. Soc. Am. 116, 478 (2004)]. Further analysis additionally revealed an undesired interaction of the existing adaptation stage and the non-linear auditory filterbank. Here, an extended version of the CASP model is suggested, incorporating alternative adaptation stages. The goal was to allow for (a) the inclusion of a binaural stage after fast adaptation with a short time constant, and to (b) address the so-called “dynamic range problem” by adaptation to the stimulus statistics [Dean *et al.*, Nat. Neurosci. 8, 1684 (2005)]. A further goal was to investigate the models behaviour without stimulus-specific selection of frequency ranges in the auditory and modulation filterbank. Such a generalization is particularly important if the model is used as front-end in, e.g., quality assessment of hearing aid algorithms. A test battery of psychoacoustic experiments was established and the modified model versions were tested and compared to the data.

### **1052 Auditory Enhancement of Increases in Spectral Amplitude: Evidence for Two Mechanisms**

**Samuele Carcagno<sup>1</sup>**, Catherine Semal<sup>1</sup>, Laurent Demany<sup>1</sup>

<sup>1</sup>*Université de Bordeaux, INCIA, CNRS*

A component of a test sound consisting of a sum of simultaneous tone bursts perceptually “pops out” if the test sound is preceded by a copy of itself with that component attenuated in level. Although this “enhancement” effect is stronger when the test sound and the precursor sound are presented to the same ear, it is also observable when the two sounds are presented to opposite ears. For an

ipsilateral precursor, the effect is known to decay as a function of the time interval (ISI) between the precursor and test sounds. We assessed the magnitude of enhancement at three ISIs (10, 100 and 600 ms) for both ipsilateral and contralateral precursors. The test sound, randomly transposed in frequency from trial to trial, was followed by a probe tone, either matched or mismatched in frequency to the test sound component which was the target of enhancement. Listeners' ability to discriminate matched probes from mismatched probes was taken as an index of enhancement magnitude. The results showed that enhancement decays more rapidly for ipsilateral precursors than for contralateral precursors. This difference in time course suggests that ipsilateral enhancement and contralateral enhancement rely, at least partly, on different mechanisms. It could be hypothesized that, in the experimental task, contralateral precursors were effective only because they provided decision cues about the frequency of the task-relevant test sound component. We tested this hypothesis in an additional experiment by presenting the probe tone before the precursor sound rather than after the test sound. Although the probe tone was then cuing the task-relevant test sound component, contralateral precursors were again found to produce enhancement. This indicates that contralateral enhancement cannot be explained by cuing alone and is a genuine sensory phenomenon.

### **1053 Sensitivity to Phase Spectra of Head-Related Transfer Functions When Perceiving Natural Sounds**

**Nicol S. Harper<sup>1</sup>**, Richard P. W. Watson<sup>1</sup>, Jan W. Schnupp<sup>1</sup>, Andrew J. King<sup>1</sup>

<sup>1</sup>*Department of Physiology, Anatomy and Genetics, University of Oxford*

The head and outer ear produce a direction-dependent filtering of incoming sound, which is described by the head-related transfer function (HRTF). Two HRTF-features important for sound localization are 1) the power spectrum of the HRTF at each ear, and their difference 2) the overall interaural time difference (ITD) of the sound. Various approximations of HRTFs maintain these features, but discard the remainder - the phase spectra (timing details) of HRTFs beyond the overall ITD - replacing it with minimum phase or zero phase. These approximations have been found to be perceptually largely indistinguishable from actual HRTFs, when examined using broadband noise, for most people, at most positions tested. This suggests that the frequency-dependent timing information in HRTFs is of little relevance. However, broadband noise, in contrast to many natural sounds, is notable in having a disordered and unfamiliar phase structure. Here we tested whether minimum-phase HRTF approximations can be distinguished from actual HRTFs when the HRTF-filtered sound is a natural sound - a spoken word. We used binaural HRTFs from the CIPIC database, and a two-alternative forced-choice method at 8 spatial directions. A proportion of subjects could distinguish above chance minimum-phase HRTFs from actual HRTFs for most directions tested. This is in contrast

with a control using broadband noise (with the same spectrum and envelope as the word) – in this case minimum-phase HRTFs and actual HRTFs could rarely be distinguished above chance. Other subjects were mostly at or near chance in both conditions. To examine many more spatial directions, an additional set of forced-choice experiments were done where HRTF direction moved in a stochastic manner, depending on the subjects' responses, towards the directions where minimum-phase HRTFs were most distinguishable. The sensitive proportion of subjects had strongest phase-spectra saliency for lateral directions.

**1054 Hearing in the Classical World: 500 BCE – 200 CE Acoustics, Psychoacoustics, Anatomy and Physiology**  
**Robert Ruben<sup>1</sup>**

<sup>1</sup>*Albert Einstein College of Medicine*

Hearing in the Classical World: 500 BCE – 200 CE

Acoustics, Psychoacoustics, Anatomy and Physiology

The classical world had knowledge of the anatomy of the ear which evolved from the Hippocratic corpus, the 5<sup>th</sup> century BCE acoustical concepts of Empedocles to the anatomical observations of Galen. He perceived the external ear as ornamental and noted the torturous course of the external auditory canal and middle ear cleft but did not recognize the tympanic membrane or the ossicles. He describes the labyrinth, names the cochlear and hypothesizes that it and the other inner ear structures served only as a passive acoustic conduit. Aristotle appears to have recognized the tympanic membrane for this is noted in his theory hearing, which was based on the concept of the vibration of air. This is a basic tenet of the theory of hearing in the classical world which described how sounds enter the head and made their presence felt. The mind had only a passive role as it received direct impression from the outside world and that objects were perceived as they truly existed. This is evidenced by the concept that perception was a mirroring of the external world - that 'like is perceived by like'. There was a basic understanding of acoustics as evidenced by Pythagoras who, for example, determined that plucking a string gave a tone related to the length of the string and that harmony was a mathematical proportion. Aristotle, more than a century, later recognized the time properties of tone but did not relate it to physical phenomena. These observations and speculations became the cannon for the next 1500 years.

**1055 Dynamics of Multisensory Tracking**

Johahn Leung<sup>1</sup>, Vincent Wei<sup>1</sup>, **Simon Carlile<sup>1</sup>**

<sup>1</sup>*University of Sydney*

The ability to perceive and track dynamic moving stimulus is a fundamental behavior that is essential in our daily interactions. These experiments examined the ability to track a moving target using head motion under various stimulus conditions and stimulus modalities. Previous studies have examined smooth pursuit eye tracking and auditory motion localization separately. Here, we combined dynamically updated virtual auditory space (VAS) with a

high speed LED array to generate veridical multimodal moving stimulus. This allows us to derive behavioral norms for head tracking, compare differences in tracking ability across the modalities, and determine if cross modal facilitation occurs.

Three experiments were conducted using auditory, visual and auditory-visual stimuli moving in a 100° arc around the subjects with velocities ranging from  $\pm 20^\circ/\text{s}$  to  $\pm 110^\circ/\text{s}$ . The moving auditory stimulus was rendered with individualized head related transfer functions recorded at 1° separation. Unlike previous work [1], this VAS rendering further integrates near-realtime updates of the subject's head position to ensure the correct external frame of reference is maintained. Apparent visual motion was created with a LED array of density 1.8° with a timing resolution  $\sim 0.1\text{ms}$ . The multimodal stimulus was synchronized temporally then spatially to ensure perceptual unity.

Preliminary results show that subjects were better able to track a visual and bimodal target than an auditory one, as evident in the smaller average RMS error (visual = 4°, bimodal = 4.6°, auditory = 7°) and shorter lag (visual = 5.5°, bimodal = 5.9° and, auditory = 8.9°). Furthermore, tracking ability was influenced by stimulus speed, especially in the unimodal auditory situation where a significant increase in both RMS error and lag for speeds  $> 80^\circ/\text{s}$  was observed.

1. Carlile, S. & Best, V. Discrimination of sound source velocity in human listeners. *J. Acoust. Soc. Am.* 111, 1026–1035 (2002).

**1056 Spectral Ripple Inversion Detection in Normal Hearing Infants**

**David Horn<sup>1,2</sup>**, Lynne Werner<sup>3</sup>, Jay Rubinstein<sup>1,4</sup>, Jong Ho Won<sup>4</sup>, Gary Jones<sup>4</sup>

<sup>1</sup>*University of Washington School of Medicine*, <sup>2</sup>*Seattle Children's Hospital*, <sup>3</sup>*University of Washington, Department of Speech and Hearing Sciences*, <sup>4</sup>*Virginia Merrill Bloedel Hearing Research Institute, Seattle WA*

Spectral ripple inversion detection (SRD) is a relatively quick way to measure a subject's sensitivity to spectral change across a broad frequency range. Thus, there has been recent interest in SRD as a clinical, non-linguistic predictor of speech understanding with a hearing aid or cochlear implant. However, infants' SRD thresholds have not been investigated. The objective of this study was to develop a behavioral method determining SRD threshold in individual infants and to compare infant and adult performance.

Normal-hearing 7 and 9-month-old infants and young adults participated. SRD stimuli had a spectral envelope with logarithmically spaced peaks applied to a broadband noise carrier. SRD thresholds were measured in the sound-field using the observer-based procedure. Ripple density (peaks per octave) was varied to establish threshold with ripple depth (in dB) held constant. Subjects heard 2s spectral ripple stimuli, half of which contained an inversion of the envelope peaks at 1s. Ripple depths of 4, 7, 10, 13 dB, and 30dB were tested to define a spectral modulation transfer function for each age group. Infants

were tested in 3 visits at one ripple depth, whereas adults were tested at several depths.

SRD thresholds were obtained in the majority of infants who returned for 3 visits. Infants showed significantly poorer SRD thresholds than adults. However, threshold improved with increasing ripple depth in the same way for infants and adults.

Thus, testing of SRD threshold in normal hearing infants is feasible. Preliminary results suggest that infants are less efficient at reliably demonstrating SRD at a given ripple depth. However, the similarity between transfer functions of infants and adults is consistent with the hypothesis that spectral resolution is adult-like in 7-9-month-old normal-hearing infants. Further testing of participants at different ages and at other ripple depths, as well as testing of hearing-impaired infants and toddlers is planned.

### **1057** Perceptual Dimensions of Tinnitus-Like Sounds

Jennifer Lentz<sup>1</sup>

<sup>1</sup>Indiana University

Characterization of the tinnitus percept generally involves patients using a questionnaire to label the quality of their tinnitus with terms that are descriptive of environmental sounds. Yet, some of the terms used may be ambiguous and could potentially characterize a wide variety of perceptual experiences. To begin to establish whether these terms appropriately characterize the tinnitus percept, the present study applied a free-classification task to ascertain the perceptual dimensions of tinnitus-like sounds in normally hearing listeners. The stimuli consisted of 60 different sounds that were either recorded from the environment or were digitally generated. Sounds were selected to be representative of the sounds that are used when describing tinnitus (e.g., ringing, tonal, noisy, pulsing, and clicking sounds). Listeners were instructed to place icons associated with each sound on a grid and to place sounds with similar percepts in clusters. In separate conditions, the same listeners were presented with low-level, continuous background sounds to artificially mimic the conditions of tinnitus. In these conditions, listeners were asked to cluster the sounds that were perceived as being similar to the artificial tinnitus near a tinnitus icon already placed on the grid. Multi-dimensional scaling then was conducted on the classification data. The results establish two main perceptual dimensions of tinnitus-like sounds: a noisy versus tonal dimension and a dimension related to the envelope of the stimulus (choppy versus smooth). This method also was able to establish the quality of the tinnitus in the artificial tinnitus conditions. These results suggest that a similar procedure could be used in patients with tinnitus to home in on the quality of the tinnitus.

### **1058** Comodulation Is a Stronger Binding Cue Than the Common Fate of Frequency Swept Components

Jesko L. Verhey<sup>1</sup>, Ian M. Winter<sup>2</sup>, Bastian Epp<sup>1</sup>

<sup>1</sup>Department of Experimental Audiology, University of Magdeburg, Germany, <sup>2</sup>Centre for the Neural Basis of Hearing, University of Cambridge, United Kingdom

Many natural sounds including speech show coherent level fluctuations in different frequency regions. A psychoacoustical effect showing our ability to use this comodulation as a source of information is comodulation masking release (CMR). A common CMR paradigm is the flanking band experiment where a sinusoidal signal is masked by a narrow band masker centred at the signal frequency and one or more remote masker components, commonly referred to as flanking bands (FBs). In this paradigm, CMR describes the effect that the threshold of a sinusoidal signal masked by comodulated masker components is lower than that in the uncorrelated condition where the envelope of the masker components are uncorrelated (CMR(U-C)) or the thresholds in the presence of the on-frequency masker only (CMR(R-C)). The present study investigates if CMR is also observed for a sinusoidal signal embedded in the on-frequency masker, when the centre frequencies of the FBs are swept over time with a sweep rate of one or two octaves per second. The psychoacoustical results show for both, CMR(U-C) and CMR(R-C), that a masking release is also observed with sweeping components. The magnitude of CMR decreases as the sweep rate is increased. CMR is not affected by the direction of the sweeps, i.e., the same CMR is found for all FBs sweeping in one direction and the condition where the FBs with centre frequencies below the signal frequency sweep down in frequency and the FB with centre frequencies above the signal frequency sweep in the opposite direction. The data indicate that comodulation is a more powerful cue than a common change in frequency over time for the binding of frequency components. The results support the hypothesis of wideband inhibition as the physiological mechanism underlying CMR.

### **1059** Consonance Preferences Are Not Universal

Josh McDermott<sup>1</sup>, Alan Schultz<sup>2</sup>, Eduardo Undurraga<sup>3</sup>, Ricardo Godoy<sup>3</sup>

<sup>1</sup>New York University, <sup>2</sup>University of Florida, <sup>3</sup>Brandeis University

In Western culture, some combinations of musical notes are consonant (pleasant) and others are dissonant (unpleasant), a distinction central to Western music. Although the origins of this aesthetic contrast have been debated for centuries, cross-cultural studies of consonance are rare. The possibility thus remains that consonance preferences arise from exposure to Western music, and could be weak or absent in humans lacking such exposure. Here we report experiments on populations in Bolivia with varied exposure to Western music. Participants were asked to rate the pleasantness of a large set of sounds, including isolated chords, pieces of Western

music, scrambled versions of Western pieces with randomized pitch and timing, emotional vocalizations (laughing, crying, etc.), and environmental sounds expected to have positive or negative valence (vomiting, birdsong, etc.). We first tested the Tsimane', an indigenous foraging/farming society residing in remote areas of the Amazon rainforest. They exhibited Western-like responses to vocalizations and some environmental sounds (preferring sounds with positive associations), and gave higher ratings to intact than to scrambled music, indicating some sensitivity to musical structure. Unlike Westerners, however, Tsimane' ratings for consonant and dissonant chords were indistinguishable. This was true both for chords composed of synthetic tones and chords with notes sung by a vocalist. A second population of more Westernized Bolivians from a small Amazonian town also exhibited Western-like responses to vocalizations, environmental sounds, and music scrambling. Additionally, they showed a modest overall preference for consonance over dissonance, although the pattern of ratings for specific chords deviated notably from that observed in Western listeners. We conclude that preferences for consonance vary across cultures, perhaps determined by the degree of exposure to Western music.

### **1060 Sound Localization by the Hearing-Impaired**

**Martijn Agterberg**<sup>1,2</sup>, Marc Van Wanrooij<sup>1</sup>, Myrthe Hol<sup>2</sup>, John Van Opstal<sup>1</sup>, Ad Snik<sup>2</sup>

<sup>1</sup>*Donders Institute for Brain, Cognition and Behaviour,*

<sup>2</sup>*Department of Otorhinolaryngology*

The unimpaired auditory system relies on implicit acoustic cues to extract sound-source directions from spectral-temporal representations: interaural time and level differences determine directions within the horizontal plane (azimuth), and pinna-related spectral-shape cues in the vertical plane (elevation). A controversy in the literature exists for chronic hearing-impaired humans: in many studies these listeners localize sounds surprisingly well, even though the sound-localization cues are impoverished or abolished. Here, we suggest that surprisingly-accurate spatial hearing in monaural listeners arises from the use of experimental set-ups with low variation in sound location, spectrum and level of the acoustic stimuli.

We measured sound localization performance by recording natural head-orienting movements of human listeners with no hearing impairments (n=40), single sided deafness (n=20), unilateral congenital conductive hearing loss (n=20) and unilateral acquired conductive hearing loss (n=12) under various experimental conditions. Sound location, spectrum and level were varied extensively, and in certain cases the spatial cues were perturbed by molding or plugging the ears.

All listeners judged the task to orient their head towards a perceived sound as easy. Nevertheless, our results and analyses indicate that hearing impairments cause serious problems in sound localization under naturalistic conditions when acoustic (location, spectrum, level) uncertainty is large. Surprisingly, hearing-impaired listeners rapidly adjust their behavior to accommodate for other spatial

cues, such as the coarse head-shadow effect and the finely-detailed azimuth-dependent spectral pinna cues. Since these cues are actually ambiguous or poor, healthy listeners rightfully ignore them. Yet, in experimental conditions with low variation in sound location, spectrum and level these ambiguous cues do benefit the hearing-impaired.

### **1061 Missing Fundamental Pitch Perception with Low Frequency Masking Noise in 2- And 3-Month-Old Infants**

**Bonnie K. Lau**<sup>1</sup>, Lynne A. Werner<sup>1</sup>

<sup>1</sup>*University of Washington*

Complex pitch perception plays an important role in many auditory tasks including sound source segregation, speech, and music perception. The ability to perceive the pitch of a harmonic complex with a missing fundamental is a classic phenomenon in complex pitch perception. Although electrophysiological cortical responses to missing fundamental pitch changes have been reported to emerge only between 3 and 4 months, previous psychophysical studies from this laboratory have shown that infants as young as 2 months of age were able to discriminate missing fundamental pitch changes in quiet. This study investigated the ability of 2- and 3-month-old infants to perceive the pitch of missing fundamental complexes with a noise band in the range of the missing fundamental frequency to eliminate the possibility that infants were responding on the basis of combination tone distortion. Infants were tested in an observer-based procedure. Harmonic complexes based on a fundamental of 160 Hz or 200 Hz were presented at 70 dB SPL. To demonstrate missing fundamental pitch discrimination, infants were required to ignore spectral changes in complexes with different harmonics but the same fundamental and respond only when the fundamental changed. After demonstrating the ability to categorize complexes by missing fundamental pitch, infants were required to perform the task with complexes presented with a noise band ranging from 60 to 260 Hz. Noise levels of 50, 60, and 70 dB SPL were tested. Nearly every infant tested was able to complete the missing fundamental categorization task with noise in the range of the missing fundamental, suggesting adultlike perception of the missing fundamental at 2 and 3 months.

### **1062 Technological Regeneration of the Cochlea: Piezoelectric Device at Technology-Biology Interface Can Mimic Function of the Cochlear Sensory Epithelium**

**Takayuki Nakagawa**<sup>1</sup>, Takatoshi Inaoka<sup>1</sup>, Hirofumi Shintaku<sup>2</sup>, Satoyuki Kawano<sup>2</sup>, Shinji Hamanishi<sup>3</sup>, Hiroshi Wada<sup>4</sup>, Tatsunori Sakamoto<sup>1</sup>, Juichi Ito<sup>1</sup>

<sup>1</sup>*Kyoto University,* <sup>2</sup>*Osaka University,* <sup>3</sup>*Sendai National College of Technology,* <sup>4</sup>*Tohoku University*

Cochlear hair cells convert sound vibration into electrical potential, and loss of these cells diminishes auditory function. Therefore, hair cell regeneration has been a central issue in the field of inner ear biology. Previously,

the potential of gene and/or cell therapy for hair cell regeneration has been demonstrated in basic experiments. However, their practical applications are still far from the clinical setting. In the present study, we aimed to regenerate the function of the cochlear sensory epithelium by integration of technology and biology. In response to mechanical stimuli, piezoelectric materials generate electricity, suggesting that they could be used in place of hair cells to create an artificial cochlear epithelium. We have fabricated a life-sized piezoelectric device, which was implantable in the basal turn of the guinea pig cochlea. The piezoelectric device was capable to generate electrical potentials in response to sound stimuli in vitro, indicating its capacity to mimic basilar-membrane and inner-hair-cell function. To show the feasibility of the device, we examined sound transduction from the external ear canal to the piezoelectric membrane after implantation into a guinea pig cochlea, and the generation of electrical output from an implanted device in response to sound stimulation. Laser Doppler assessments revealed that sound stimuli were transmitted through the external auditory canal to a piezoelectric membrane implanted in the guinea pig cochlea, inducing it to vibrate. In addition, the application of sound to the middle ear ossicle induced voltage output from the implanted piezoelectric membrane. These findings establish the fundamental principles for the development of novel hearing devices using piezoelectric materials, although there are many problems to be overcome before practical application.

### **1063 Rho GTPases Regulate the Formation of Apical Junctional Domains of Cochlear Supporting Cells**

Tommi Anttonen<sup>1</sup>, Anna Kirjavainen<sup>1</sup>, Maarja Laos<sup>1</sup>, Ulla Pirvola<sup>1</sup>

<sup>1</sup>*Institute of Biotechnology, University of Helsinki, Finland*  
Rho GTPases are intracellular signaling molecules involved in diverse cellular processes, including cell motility, division and morphogenesis. They have well-established roles in the regulation of actin dynamics. Further, by stabilizing filamentous actin close to the plasma membrane, Rho GTPases have been shown to promote the assembly of cadherin-based adherens junctions. They can also control apical-basal polarity during epithelial morphogenesis. In this study, we have investigated the role of Rho GTPases in supporting cells of the organ of Corti. Cochlear supporting cells have distinct morphological features that likely depend on their elaborate actin and microtubule cytoskeletons. We hypothesized the involvement of Rho GTPases in the establishment and maintenance of these structural specializations. We found that one of the classical GTPases, Cdc42, is expressed in the organ of Corti. We inactivated Cdc42 selectively and efficiently in postnatal mouse cochlear supporting cells applying tamoxifen-inducible Cre-ERT2 approach in vivo. We found that the structural features typical to the various types of supporting cells were largely maintained, except for the apical domains of these cells. Specifically, Cdc42 inactivation impaired postnatal development of the apical F-actin belts.

In addition, the associated adherens junctions were defected and showed signs of abnormal membrane protein trafficking. Understanding the signaling pathways that regulate the architecture and integrity of the apical domains of supporting cells has implications for tissue remodeling events, such as trauma-induced extrusion of dying hair cells and supporting cell scar formation. Further, as recent data suggest that the properties of F-actin belts and adherens junctions may underlie the restrictions in proliferation and phenotypic conversion of mammalian supporting cells, it is of interest to reveal the regulatory role of Rho GTPases on these cellular domains.

### **1064 The Role of P16lnk4a in Mammalian Hair Cell Regeneration**

Brandon C. Cox<sup>1</sup>, Jennifer A. Dearman<sup>1</sup>, Samantha Papal<sup>1,2</sup>, Katherine A. Steigelman<sup>1,3</sup>, Marcus B. Valentine<sup>1</sup>, Jian Zuo<sup>1</sup>

<sup>1</sup>*St. Jude Children's Research Hospital*, <sup>2</sup>*Universite Paris-Diderot*, <sup>3</sup>*University of Tennessee Health Science Center*  
Auditory hair cell (HC) damage is permanent in humans and other mammals; however, non-mammalian vertebrates can regenerate damaged HCs, by proliferation and transdifferentiation of neighboring supporting cells (SC). Interestingly, the cyclin-dependent kinase inhibitor, p16lnk4a, is absent in non-mammalian vertebrates and in mammals, it acts as a tumor suppressor keeping cells in a quiescent state. p16lnk4a expression is induced by age and mitogenic signaling thus, deletion of this protein is attractive as it may allow mammalian SCs to respond to signals released by damaged HCs. Here, we hypothesize that induction of p16lnk4a after HC damage is the physiologically relevant event that prevents HC regeneration and investigate this hypothesis using p16lnk4a-null mice and noise-induced hearing loss (NIHL). We found that p16lnk4a-null mice have normal hearing and normal HC morphology. After NIHL at postnatal day 30 followed by BrdU in the drinking water for 2 weeks, we detected a significant increase in BrdU+ cells within the organ of Corti of p16lnk4a-null mice compared to wild-type controls, all on a mixed background. BrdU+ cells do not co-label with the immune cell marker, CD45, thus are not immune cells. Interestingly, most BrdU+ cells are close to inner HCs and could be inner pillar cells or inner phalangeal cells. We are currently using lineage tracing experiments to confirm that BrdU+ cells are indeed proliferating SCs, as well as measuring changes in p16lnk4a expression after NIHL in wild-type mice. These results provide evidence that p16lnk4a plays a critical role in mammalian HC regeneration after NIHL.

This work was supported in part by grants from the NIH: DC010310 (B.C.C.), DC009393 (K.A.S.), DC006471 (J.Z.), DC008800 (J.Z.), and CA21765, the Office of Naval Research N000140911014 (J.Z.) and the American Lebanese Syrian Associated Charities (ALSAC) of St. Jude Children's Research Hospital. J. Zuo is a recipient of The Hartwell Individual Biomedical Research Award.

**1065 Inhibition of Gamma-Secretase Stimulates Cell Cycle Entry and Hair Cell Differentiation in the Mature Avian Utricle**

**Matthew Barton<sup>1</sup>, Jeffrey Ku<sup>1</sup>, Michael Lovett<sup>1</sup>, Jennifer Stone<sup>2</sup>, Mark Warchol<sup>1</sup>**

<sup>1</sup>Washington University School of Medicine, <sup>2</sup>University of Washington School of Medicine

Hair cell differentiation during otic development is regulated by the Notch pathway. Progression of Notch signaling requires proteolysis by  $\gamma$ -secretase, and treatment with small molecule inhibitors of  $\gamma$ -secretase can block the Notch pathway leading to increased numbers of hair cells. We have examined the effects of interfering with Notch signaling in the mature chick utricle, which has a very robust ability to regenerate hair cells after ototoxic injury. We first treated normal (unlesioned) utricles and cultures of isolated utricular sensory epithelia for 24 hr with 10  $\mu$ M DAPT. Quantification of BrdU uptake revealed extensive cell proliferation in response to DAPT treatment. We also used Next Gen Illumina sequencing to profile DAPT-evoked changes in gene expression, and obtained quantitative data on the expression of over 14,000 genes. Within this data set, the most strongly down-regulated gene was HES5. Expression of several related Notch targets (e.g., HEY1, HEY2, HEYL) was also reduced. These findings are consistent with Notch inactivation. We also observed reduced expression of the CKIs p21 and p27, and a large increase in the expression of cyclin D3. These expression changes are likely to be permissive for cell cycle entry. In other experiments, we examined the effects of long-term Notch inhibition in regenerating utricles. Specimens were treated for 24 hr with streptomycin and then received DAPT for seven days. DAPT treatment resulted in increased numbers of regenerated hair cells, particularly in the striolar region. The striolar region of the normal avian utricle contains numerous type I hair cells, but striolar hair cells that were produced by DAPT treatment all possessed type II immunomarkers. Also, labeling with the styryl dye FM4-64 indicated that many of these new hair cells did not possess functional transduction channels.

**1066 In Vivo Hair Cell Regeneration in the Neonatal Mouse Cochlea**

**Brandon C. Cox<sup>1</sup>, Anne Lenoir<sup>1,2</sup>, LingLi Zhang<sup>1</sup>, Katherine A. Steigelman<sup>1,3</sup>, Jie Fang<sup>1</sup>, Jian Zuo<sup>1</sup>**

<sup>1</sup>St. Jude Children's Research Hospital, <sup>2</sup>Universite Paris-Diderot, <sup>3</sup>University of Tennessee Health Science Center

Damage to hair cells (HCs) in the mammalian cochlea is currently believed to be permanent, resulting in hearing impairment which affects more than 10% of the human population. However, the absence of HC regeneration in the mammalian cochlea has only been confirmed in adults. Although postmitotic, the neonatal murine cochlea is still developing; thus, it may be more plastic and preserve some ability to regenerate. Here, we developed a novel method to damage neonatal, mouse cochlear HCs in vivo. We observed a subsequent increase in HC number and mitotic HC regeneration in the less mature, apical turn of

the cochlea, while no HC regeneration was observed in the more mature, basal turn, or when HCs were damaged a week after birth. Regenerated HCs expressed several HC markers including prestin, a terminal differentiation marker specific for outer HCs, and had immature stereocilia bundles, similar to those of HCs derived from embryonic or induced pluripotent stem cells. We further defined the mechanism of HC regeneration with evidence that neighboring supporting cells changed cell fate, expressing early HC markers, followed by cell division and expression of mature HC markers. Our findings demonstrate that, in contrast to common belief, the neonatal murine cochlea does have the capacity to regenerate HCs after damage and further understanding of this process may lead to therapeutics for the treatment of hearing loss.

This work was supported in part by grants from the National Institute of Health DC010310 (B.C.C.), DC009393 (K.A.S.), DC006471 (J.Z.), DC008800 (J.Z.), and CA21765, the Office of Naval Research N000140911014 (J.Z.), the National Organization for Hearing Research Foundation (J.F.) and the American Lebanese Syrian Associated Charities (ALSAC) of St. Jude Children's Research Hospital. J. Zuo is a recipient of The Hartwell Individual Biomedical Research Award.

**1067 Characterization of the Wnt Signaling in the Postnatal Mouse Utricles**

**Tian Wang<sup>1</sup>, Renjie Chai<sup>1</sup>, Eric Liaw<sup>1</sup>, Anping Xia<sup>1</sup>, Alan G. Cheng<sup>1</sup>**

<sup>1</sup>Department of Otolaryngology-Head and Neck Surgery, Stanford University School of Medicine

Previous studies have suggested that the postnatal mouse utricles have the innate ability to generate new hair cells in normal and diseased states. At present, these hair cell precursors are presumed supporting cells, yet we lack the knowledge of their exact identity and regulatory mechanisms. Canonical Wnt signaling has been particularly implicated to regulate somatic stem cells in several organ systems. Likewise, we hypothesize that active Wnt signals mark progenitor cells in the mouse utricles.

Axin2 is considered a universal Wnt target gene. Using the Axin2LacZ/+ reporter mice, we found robust LacZ expression in stromal cells beneath the sensory epithelium in both the postnatal 3- (P3) and 30-day old (P30) utricles. These stromal cells expressed the mesenchymal markers vimentin and fibronectin, and not the sensory epithelium markers Sox2 and Myosin7a. ELISA showed that LacZ expression decreased with age, and correlated with RT-PCR for Axin2 expression. ELISA and quantitative RT-PCR of organotypic cultures of p3 utricles found that Axin2 expression significantly increased and decreased with Wnt agonist and antagonist, respectively, thus validating Axin2 as a Wnt target.

Lgr5 is another putative Wnt target gene. Using the Lgr5EGFP/+ reporter mice, we found EGFP expression in hair cells and supporting cells in the E15.5 and 18.5 utricles, but completely disappeared at P0, thus contrasted Axin2 expression. In cultured P3 Lgr5EGFP/+ utricles, treatment with 1.0 mM neomycin led to hair cell loss and

EGFP upregulation in a subset of supporting cells in the striolar region, whereas 4.0 mM neomycin extended both into the extrastriolar region. Upon damage, EGFP re-expressed as early as 12hr and persisted at least 6 days. 99.4% Lgr5-EGFP+ve cells were sox2-negative, but 100% Plp1-positive, suggesting heterogeneity among utricular supporting cells. Ongoing fate-mapping studies are performed to probe the behavior of these Wnt-responsive cells. (Supported by NIH DC011043).

### **1068** Wnt Signaling Regulates Cell Fate of Lgr5+ve Hair Cell Precursors in the Postnatal Mouse Cochlea

**Renjie Chai**<sup>1</sup>, Bryan Kuo<sup>2</sup>, Taha Jan<sup>1</sup>, Eric Liaw<sup>1</sup>, Tian Wang<sup>1</sup>, Anping Xia<sup>1</sup>, Roel Nusse<sup>3,4</sup>, Jian Zuo<sup>2</sup>, Alan Cheng<sup>1</sup>

<sup>1</sup>Departments of Otolaryngology-Head and Neck Surgery, Stanford University School of Medicine, <sup>2</sup>Department of Developmental Neurobiology, St. Jude Children's Research Hospital, <sup>3</sup>Developmental Biology, Stanford University, <sup>4</sup>Howard Hughes Medical Institute, Stanford University School of Medicine

The Wnt signaling pathway is critical in regulating cell fate and tissue homeostasis during development. Yet its roles in inner ear development are incompletely understood. Previous studies described isolated cochlear supporting cells display regenerative and ability to form hair cell-like cells. We recently reported that a subset of these supporting cells (the third Deiters cells, inner pillar cells, and inner phalangeal cells) expresses Lgr5, a Wnt target gene expressed in somatic stem cells in rapidly proliferating organs. We hypothesize that Lgr5+ve cells are Wnt-regulated progenitor cells in the cochlea.

Lgr5+ve cells were isolated from dissociated P0-3 Lgr5EGFP/+ cochleae via flow cytometry. When cultured in serum-free media, Lgr5+ve cells formed clonal colonies. Hes5 is expressed in most cochlear supporting cells, and isolated Hes5-GFP+ve generated 49 colonies and 197 Myo7a+ve cells. At identical cell density, Lgr5+ve cells generated 51 colonies and 389 Myo7a+ve cells, suggesting they serve as an enriched precursor cell population to sensory hair cells. 71% Myo7a+ve cells developed stereocilia-like structures expressing phalloidin and espin and 77% expressed prestin. Among these differentiated Lgr5+ve cells, 79% Myo7a+ve cells were outside colonies, 98% of which were EDU-ve. DNA polymerase inhibitor or Wnt antagonist reduced colony formation, EdU uptake and Myo7a+ve cells within colonies, but not the total Myo7a+ve cells, supporting direct differentiation as the main mechanism of hair cell formation. Conversely, Wnt agonist increased mitotic formation of Myo7a+ve cells within colonies. Lineage tracing using P0-3 Lgr5-EGFP/CreRT/+; Rosa26LacZflox/+ or Rosa26TdTomatoflox/+ transgenic mice showed that progenies of Lgr5+ve supporting cells included new hair cells and other supporting cells. Taken together, we conclude that Lgr5+ve cells are Wnt-regulated hair cell precursors in the postnatal mouse cochlea. (Supported by NIH DC011043).

### **1069** Regenerative Capacity of Adult Auditory Nerve After Injury: Observations from an Acute Auditory Neuropathy Model in Vivo and in Vitro

**Hainan Lang**<sup>1</sup>, Devadoss Samuel<sup>1</sup>, Yazhi Xing<sup>1</sup>, Juhong Zhu<sup>1</sup>, Edward Krug<sup>1</sup>, W. Scott Agraves<sup>1</sup>, Jeremy Barth<sup>1</sup>  
<sup>1</sup>Medical University of SC

Spiral ganglion neurons (SGNs) are primary auditory afferent neurons that convey signals from the inner ear to the brainstem. Loss of SGNs occurs with exposure to ototoxic drugs and noise, genetic mutations and age, resulting in permanent sensorineural hearing loss. Recent studies have shown that cochlear stem/progenitor cells can be isolated from auditory sensory epithelium and spiral ganglion of the developing inner ear. However, it is unclear whether neural stem/progenitor cells are present in the adult auditory nerve. The goal of this study is to evaluate the regenerative potential of auditory nerve in adult mouse inner ear. We have established a mouse model of acute SGN degeneration by applying ouabain to inner ear (Lang et al., JARO 2011). In addition to selectively removing type I SGNs, ouabain injury causes hyperplasia and hypertrophy of glia-like cells in the auditory nerves. Transcriptomic analysis revealed an upregulation of Sox2 transcription and altered transcription of a majority of established Sox2-dependent genes (196 of 294) in the auditory nerve shortly after ouabain treatment. The transcription factor Sox2 is predominantly expressed in undifferentiated neural precursors during adult neurogenesis in the central nervous system and is also highly expressed in the developing auditory nerve. A subset of Sox2-positive glial cells dedifferentiated shortly after SGN degeneration suggesting that glial cells may be a source for neurogenesis after acute SGN injury in the adult mouse inner ear. Moreover, we examined the capability of neurogenesis in adult auditory nerve using an in vitro approach established recently in our laboratory. This approach, which employs culturing adult auditory nerves to produce cellular spheres, showed that more proliferative spheres were produced from ouabain-injured auditory nerve than from untreated auditory nerve. The majority of cells in these spheres stained positively for Ki67, BrdU and nestin. Under a strict culture condition for neural differentiation, sphere-derived cells differentiated into cells that express neuronal class III  $\beta$  tubulin and several glial lineage markers including Sox10, S100, p75 and GFAP. Together, our data suggest that 1) neurogenesis and/ or gliogenesis occur in the adult inner ear and the acute SGN degeneration enhances this capability, and 2) Sox2 and its associated regulatory network may play a critical role in the regulation of neural plasticity and repair in adult auditory nerve.

Supported by NIDCD P50DC00422, NIDCD R01DC00713, NCRRL UL1RR029882, NCRRL P20RR16461, and NCRRL P20RR16434.

## **1070** Decision Processes in Cued Informational Masking Experiments

Virginia Richards<sup>1</sup>, Eva Carreira<sup>1</sup>

<sup>1</sup>University of California, Irvine

When a target sinusoid is masked by a random multitone informational masker, thresholds are lower when a preview of the masker precedes the detection interval than when a signal-plus-masker preview precedes the detection interval. In this experiment the decision processes associated with these two types of “cues” were examined. Using a yes/no procedure, the task was to detect a 1000-Hz tone presented concurrently with an informational masker. For the cue and detection interval the number of tones that comprised the masker was independently drawn at random to be 6, 7, or 8. Then, for the cue interval, the frequencies of the masker components were randomly chosen. If the number of components was the same for the masker in the cue and detection interval, the same frequencies were used; if not, the interval with the larger number of masker components used the same components presented in the other interval, plus any additional components with newly chosen random frequencies. The analyses of the data from a two-down, one-up tracking procedure was analyzed to determine the degree to which extra masker tones altered decision strategies. The results indicated that (a) when a masker cue was tested, extra masker components in the cue interval had little effect on responses, but for the detection interval extra components in the region of the signal frequency tended to be associated with “signal” responses; and (b) when a signal-plus-masker cue was tested, extra masker components in the cue interval were associated with “no-signal” responses, and extra components in the detection interval had no measurable impact on responses. These results are not consistent with a model in which decision variables from the cue and detection intervals are compared, and also indicate that listeners adopt different strategies depending on the type of cue tested.

## **1071** Source Separation Model for Multi-Source Environments with Speech Signals

Elias Thorp<sup>1</sup>, H. Steven Colburn<sup>1</sup>

<sup>1</sup>Boston University

Identifying target speech in a multi-speech-source environment is challenging for individuals with hearing impairments. Here, a model for extracting a target sentence from two masking sentences (without prior knowledge of the content of the maskers) is evaluated by measuring speech-intelligibility (SI) performance of listeners who receive only the single-channel output waveform from a modified EC model. Basically, the model receives two binaural inputs, which are the sums of targets and maskers at each ear, and finds the optimal Equalization and Cancellation (EC) parameters for 18 one-third-octave frequency bands in 20-ms time slices, similar to the Short-Time EC model introduced by Rui Wan (Boston University, Biomed. Eng. Dissertation 2011). More specifically, the EC parameters estimated from the inputs are compared to the EC parameters corresponding to each

of the binaural impulse responses at the masker locations (assumed known). The EC parameters of the impulse response that are the closest to the EC parameters for the input are chosen as the final cancellation parameters. In the intelligibility experiment, four normal-hearing listeners were presented with the output of the model, diotically (with the same signal presented to both ears) and asked to write down what words they heard. All speech tokens were taken from the Harvard IEEE corpus (IEEE 1969) and are consistent with Hawley et al (JASA 1999). The percent of key words identified incorrectly was observed for different source and masker locations. Results of this intelligibility test of listening to the output of the short-time EC model coincide well with previously reported data (Hawley et al., JASA 1999) obtained from normal subjects listening to binaural stimuli in a virtual environment and suggest that this model provides an accurate representation of multi-source processing. [Supported by NIH/NIDCD Grant No. 5 R01 DC 00100.]

## **1072** A Simple Test of Auditory Attention Predicts Basic Perceptual Skills

Yu-Xuan Zhang<sup>1</sup>, Cara L. Croft<sup>2</sup>, Sygal Amitay<sup>1</sup>, David R. Moore<sup>1</sup>, Johanna G. Barry<sup>1</sup>

<sup>1</sup>MRC Institute of Hearing Research, <sup>2</sup>University of Manchester

Attention is often cited as a modulator of auditory perception. Despite this, there are currently no robust, easy-to-administer tests of auditory attention. Moreover, few studies have attempted to relate measures of attention to basic psychoacoustic performance. Here we present a simple paradigm that yields significant attention measures and predicts basic hearing abilities.

On each trial, two clearly audible tones were presented sequentially, either at the same or different ears. The frequency of the tones was either the same or differed by at least two filter widths (ERBs). When the task was a same/different frequency judgment, presentation at the same ear provided a mean reaction time (RT) gain of 65 ms ( $p < .001$ ). Decision making was thus facilitated by attention oriented along the task-irrelevant dimension. When judgments in the two stimulus dimensions were congruent (same-frequency same-ear, or different-frequency different-ear), RT was faster by 62 ms ( $p < .001$ ) than when they were incongruent (same-frequency different-ear, or different-frequency same-ear), suggesting the involvement of executive control to resolve conflicts. Both attention effects were replicated when the same/different judgment was based on ear rather than frequency. Mean RT for the frequency task was significantly correlated ( $r = .60$ ;  $p = .009$ ) with spectral resolution (measured with notched noise masking). Further, the congruency gain in RT was correlated with frequency discrimination ( $r = .63$ ;  $p = .004$ ) and backward masking ( $r = .66$ ,  $p = .002$ ). In summary, the new test produced robust measures of selective attention and executive control, and these attention measures accounted for significant individual variances in a range of psychoacoustic tasks.

## **1073 Behavioral Assessment of Perceptual Segregation During a Profile Analysis Task Under Simultaneous Masking**

Yi Shen<sup>1</sup>

<sup>1</sup>University of California, Irvine

This study concerns the segregation of two concurrent harmonic sounds. Unlike many previous studies, segregation is assessed by modeling listening strategies in addition to measurements of task performance. Sensitivity to changes in spectral envelopes (or spectral profiles) was measured for a target harmonic complex in a competing masker complex. Each of the two complexes contained a single formant in the spectral profile at 1 kHz, varying in its peakiness (or profile strength). In a 2-alternative, forced choice design, the target had low profile strength in one interval and high profile strength in the other interval; while the masker had low profile strength in the both intervals. Small perturbations were applied to the profile strength of the two complexes independently in each interval, from which relative decision weights for each of the two sounds were estimated. Listeners were instructed to select the interval with larger target profile strength. Performance thresholds as well as relative weights were measured as functions of fundamental frequency difference (0 – 6 semitones) and relative intensity (-10, 0, and 10 dB SNR) between the target and masker. Results from 6 normal-hearing listeners indicated that both of these two acoustic features assisted segregation. The effect of fundamental frequency difference was not measurable unless the target-to-masker intensity ratio was low.

## **1074 Distribution of Working Memory Resources Across Pitch Sequences**

Sabine Joseph<sup>1</sup>, Sukhbinder Kumar<sup>2,3</sup>, Ben Pearson<sup>1</sup>, Sundeep Teki<sup>2</sup>, Timothy Griffiths<sup>2,3</sup>, Masud Husain<sup>1</sup>

<sup>1</sup>Institute of Cognitive Neuroscience, University College London, UK, <sup>2</sup>Wellcome Trust Centre for Neuroimaging, University College London, UK, <sup>3</sup>Institute of Neuroscience, Medical School, Newcastle University, UK

Working memory tests are used in both patients and healthy subjects to estimate short-term recall. Often such tests involve remembering sequences of letters or numbers, where performance is tested in a purely categorical fashion assuming that each item is either perfectly stored or completely forgotten. Based on these measures, a long-standing model for working memory proposes that working memory capacity is limited to a set number of memory slots that store information with a fixed fidelity (e.g. Luck & Vogel, 1997). However, shared resource models of working memory have challenged this account and suggest that the more items that are held in memory, the less precisely each item can be recalled. This new dynamic framework of working memory has been shown to account for several features of visual working memory such as location, orientation and colour (Bays & Husain, 2008; Bays et al., 2009). The present study aimed to test the validity of this shared resource model for auditory working memory, specifically working memory for pitch.

In a novel pitch matching paradigm, subjects listened to a test sequence of 1, 2 or 4 pure tones where the frequencies were randomly selected from a range of 500-1000 Hz. A randomly selected probe tone drawn from the same frequency pool was then played, whose pitch subjects adjusted to match one of the test tones by rotating a dial. The precision of working memory for pitch for each tone was calculated as the inverse of the standard deviation of pitch matching responses. This pitch matching paradigm provides a measure of the variability of a memory representation around its true value. In this case, the precision of memory for pitch varied with the memory load (number of items in the sequence) as well as on the item's position in the sequence. Our results support the shared resource model for working memory for pitch and show that measuring precision as an index of working memory provides new insights into the dynamic nature of memory allocation in auditory working memory representations.

References:

- Bays P.M. Catalo R.F.G. & Husain M. 2009. The precision of visual working memory is set by allocation of a shared resource. *Journal of Vision*, 9(10):7, 1-11.
- Bays P.M. & Husain M. 2008. Dynamic shifts of limited working memory resources in human vision. *Science*, 321, 851-854.
- Luck, S.J., & Vogel, E.K. 1997. The capacity of visual working memory for features and conjunctions. *Nature*, 390, 279-281.

## **1075 Auditory Figure-Ground Segregation Using a Complex Stochastic Stimulus**

Sundeep Teki<sup>1</sup>, Maria Chait<sup>2</sup>, Deborah Williams<sup>3</sup>, Aiysha Siddiq<sup>2</sup>, Nicolas Barascud<sup>2</sup>, Sukhbinder Kumar<sup>3</sup>, Shihab Shamma<sup>4</sup>, Timothy Griffiths<sup>1,3</sup>

<sup>1</sup>Wellcome Trust Centre for Neuroimaging, University College London, <sup>2</sup>UCL Ear Institute, University College London, <sup>3</sup>Institute of Neuroscience, Newcastle University, <sup>4</sup>Institute of Systems Research, University of Maryland, College Park

In contrast to the disordered acoustic environment, most studies of auditory segregation have used relatively simple signals. We developed a new stimulus – “stochastic figure-ground” (SFG stimulus; Teki et al., 2011) that incorporates stochastic variation in frequency-time space that is not a feature of the predictable sequences used previously. Stimuli consist of a sequence of 50 ms chords containing a random number of pure-tone components. Occasionally, a subset of tonal components repeat in frequency over several consecutive chords, resulting in a spontaneous percept of a “figure” popping out of a background of varying chords. Our behavioral results demonstrate that human listeners are remarkably sensitive to the emergence of such figures (Experiment 1).

To characterize the brain mechanisms that underlie segregation in such a stochastic stimulus, we investigated the degree to which behavior is affected by systematic stimulus manipulations. In Experiment 2, we demonstrate that figure-detection is unaffected when the duration of each chord is reduced to 25 ms, suggesting that detection

depends on the number of repeating chords and not the absolute duration of the figure. In experiment 3, performance was unchanged when white noise (50 ms) was inserted between successive chords. In experiment 4, figures were “ramped” (successive figure components were not repeating but increasing in frequency in steps of  $2^*1$  or  $5^*1$ , where  $1 = 1/24$ th of an octave is the resolution of our frequency-bank). Results show decreased sensitivity, although, remarkably, listeners could still perform the task. Experiment 5 tested figure-detection by removing the “background-only” chords, which preceded and followed the figure and results show no significant effect on performance.

Overall, the notable sensitivity exhibited by listeners cannot be explained by prevailing adaptation-based models of segregation. Using computational modeling, we show that the behavioral data are consistent with the temporal coherence model of auditory scene analysis (Shamma et al., 2010).

References:

Teki, S., Chait, M., Kumar, S., von Kriegstein, K., and Griffiths, T. D. (2011). Brain bases for auditory stimulus-driven figure-ground segregation. *J. Neurosci* 31, 164-171.  
Shamma, S. A., Elhilali, M., and Micheyl, C. (2010). Temporal coherence and attention in auditory scene analysis. *Trends Neurosci*.

### **1076** Role of Auditory Attention, Stream Segregation and Localization for Speech Perception in Spatialized Noise in Children

Imran Dhamani<sup>1,2</sup>, Mridula Sharma<sup>1,2</sup>, Johahn Leung<sup>3</sup>, Simon Carlile<sup>3</sup>, Suzanne Purdy<sup>2,4</sup>

<sup>1</sup>Macquarie University, <sup>2</sup>HEARING Cooperative Research Centre, <sup>3</sup>University of Sydney, <sup>4</sup>University of Auckland

The aim of the current study is to investigate the influence of auditory stream segregation, localization and attention when listening in noise for children with listening concerns. The study assessed the role of auditory attention in four domains namely sustained, divided and selective attention as well as attention switching. Twenty children and teenagers (10-17 years) with and without parental concerns for listening participated in the study. All participants were initially assessed for peripheral hearing sensitivity and basic auditory processing skills. The Listening in Spatialized Noise (LiSN-S) test was used to assess speech perception in noise (Cameron and Dillon, 2007). Sustained attention was assessed using the auditory continuous performance test (Keith, 1994), divided attention using dichotic listening task and selective attention using principles of the Posner cueing paradigm (Posner, 1980) and multi-probe signal method (Dai et al., 1991). The temporal re-orientation time within the selective attention test was used as a measure of attention switching time. Localization was assessed using speech localization in noise test and measured in terms of the mean lateral and polar angle errors. ASA was assessed using a sequential stream segregation task with pure tones using the ABA\_ paradigm (Van Noorden, 1975). The participants with listening concerns showed poorer auditory processing abilities. There were significant

correlations between listening in noise and stream segregation as well as selective attention measures. The results indicate a statistically significant difference between measures of selective attention and attention switching time for the two groups where the participants with the listening concerns had longer temporal reorientation time. The results indicate the importance of auditory attention and stream segregation abilities in evaluating speech perception in noise especially in individuals with auditory processing difficulties.

### **1077** Does Recovering Sound Sources from Embedded Repetition Require Directed Attention?

Keiko Masutomi<sup>1</sup>, Tobias Overath<sup>2</sup>, Makio Kashino<sup>1,3</sup>, Josh H. McDermott<sup>4</sup>, Maria Chait<sup>2</sup>

<sup>1</sup>Tokyo Institute of Technology, <sup>2</sup>UCL Ear Institute, <sup>3</sup>NTT Communication Science Laboratories, <sup>4</sup>Center for Neural Science, New York University

McDermott et al. (ref.) demonstrated that listeners can identify novel “target” sounds from mixtures if they are presented multiple times across different distractors, even in conditions where single mixtures were impossible to segregate. Their results indicate that the auditory system can recover sound sources from mixtures by detecting repeating spectro-temporal structure embedded in the acoustic input.

In the present series of experiments we aim to investigate whether this repetition-based sound segregation requires selective attention to sounds or whether it can occur partially outside the focus of attention. The latter possibility would provide support for its role as an automatic, bottom-up process.

We adapted the protocol of McDermott et al. to a dual task design. Trials consisted of fifteen sound mixtures, each composed of a repeating target and a distractor that changed from mixture to mixture. Participants judged whether a subsequently presented probe appeared in the mixtures. Participants concurrently watched a rapid sequence of serially presented visual stimuli (digits in different colors). One group of participants was required to detect the appearance of a specific digit (‘low load’). Another group of listeners was required to memorize a subset of the digits (e.g. those colored blue) and subsequently report the order (‘high load’). The high load task requires significant attentional and echoic memory resources and thus served to focus processing resources away from the auditory modality.

This study is ongoing. Pilot experiments (N = 10) demonstrated that the average performance on the auditory task ( $d' = 1.35$ ) was significantly better than chance ( $P < 0.0001$ ) even when listeners perform the high load visual task, suggesting that listeners can segregate novel sounds from mixtures when attention is directed elsewhere. Full results including appropriate controls will be presented.

(ref.) McDermott, et al. PNAS. 2011;108(3):1188-93.

## **1078** An Octave Effect in Auditory Attention

Tobias Borra<sup>1,2</sup>, Huib Versnel<sup>2,3</sup>, Chantal Kemner<sup>2,3</sup>, John Van Opstal<sup>4,5</sup>, Raymond Van Ee<sup>1,2</sup>

<sup>1</sup>University Utrecht, <sup>2</sup>Neuroscience Cognition Utrecht,

<sup>3</sup>University Medical Center Utrecht, <sup>4</sup>Radboud University

Nijmegen, <sup>5</sup>Donders Institute for Brain, Cognition and

Behaviour

Attention to a certain frequency, for instance triggered by a cue tone or by imagination, enhances sensitivity for tones around that frequency and reduces sensitivity for distant frequencies (Dai et al., *J. Acoust. Soc. Am.* 89:2937-42, 1991; Hafter et al., *J. Acoust. Soc. Am.* 94:743-7, 1993). This frequency dependence has been described as a single band pass filter, referred to as attention filter. However, this attention filter has primarily been studied over a narrow range of frequencies (<1 octave) while it is not straightforward that reduction of sensitivity would persist over a wide range. For instance, inhibition bands in auditory cortex are typically narrow (<1 octave). In three psychophysical experiments we studied the attention filter over several octaves.

Tones were presented to the right ear in a background of continuous broadband white noise. Detection performance was measured using a two-alternative forced choice design. Tones appeared in one of two 250-ms intervals, separated by 200 ms. The signal-to-noise ratio was set at 75% detection level. Experiment 1: audible cue tones of 1 kHz were presented 1250 ms before the first interval. Experiment 2: cue tones were missing fundamental complexes with an f0 of 0.5 kHz. Experiment 3: subjects were instructed to imagine a musical interval of a "perfect fourth" above a presented tone of 1 kHz (i.e., 1.33 kHz).

In all three experiments we found multiple detection peaks that are not only centered on the attended tone (as previously shown in literature), but also around multiple octaves above and below the attended frequency. These findings challenge the current views of a single-band attention filter. Auditory attention is apparently drawn not to an absolute stimulus property such as the frequency, but rather to a more general class of the tone, "tone chroma". Neural interactions that combine octave-related frequencies, likely located in non-primary auditory cortex, may underlie the octave effect.

## **1079** Effects of the Correlation Between the Fundamental Frequencies and Resonance Scales as a Cue for the Auditory Stream Segregation

Minoru Tsuzaki<sup>1</sup>, Toshio Irino<sup>2</sup>, Chihiro Takeshima<sup>3</sup>, Toshie Matui<sup>4</sup>

<sup>1</sup>Kyoto City University of Arts, <sup>2</sup>Wakayama University,

<sup>3</sup>Oberlin University, <sup>4</sup>Nara Medical University

One of the important functions of our auditory system is to extract the source information which can be utilized in segregating acoustic mixtures into concurrent auditory streams. In case of vocal stimuli, such as speech, the acoustic signal from one source conveys the information about the size of the vocal tract, i.e., the resonance scale (RS), as well as the period of the driving glottal pulse trains, i.e., the fundamental frequency (F0). By applying the

vocoding technique, these two properties can be modified independently. Several psychophysical experiments using such vocoded speech stimuli have shown that we are very sensitive to the change of these two properties, and that both can become an effective cue for the auditory stream segregation.

Although the RS and F0 can be manipulated independently in the framework of the source-filter theory, these properties are not completely independent in the natural environment. Persons which have longer vocal tracts tend to have bigger larynges. The purpose of this study is to investigate whether our auditory perceptual process behaves differently depending on the correlation between the changes in RS and those in F0. To address this question, a paradigm of the auditory stream segregation with the "galloping" rhythm patterns was adopted.

When two different sounds, A and B, are alternated with an "ABA-ABA-" pattern, the degree of auditory streaming is affected by the perceptual distance between A and B. Thus, one can estimate the perceptual distance by looking at the degree of streaming. In the experiment, two types of combinations between RS and F0 were compared. The first was the combination with a positive correlation, and the second was that with a negative combination. The results showed that the negative combination induced a significantly greater degree of segregation than the positive combination. This suggested that our perceptual system is more tolerant to the changes that could happen in the natural environment.

## **1080** Why Would Musical Training Benefit the Neural Encoding of Speech? a New Hypothesis

Aniruddh Patel<sup>1</sup>

<sup>1</sup>The Neurosciences Institute

Mounting evidence suggests that musical training benefits the neural encoding of speech. This paper offers a hypothesis specifying why such benefits occur. The "OPERA" hypothesis proposes that such benefits are driven by adaptive plasticity in speech-processing networks, and that this plasticity occurs when five conditions are met. These are: (1) Overlap: there is anatomical overlap in the brain networks that process an acoustic feature used in both music and speech (e.g., waveform periodicity, amplitude envelope), (2) Precision: music places higher demands on these shared networks than does speech, in terms of the precision of processing, (3) Emotion: the musical activities that engage this network elicit strong positive emotion, (4) Repetition: the musical activities that engage this network are frequently repeated, and (5) Attention: the musical activities that engage this network are associated with focused attention. According to the OPERA hypothesis, when these conditions are met neural plasticity drives the networks in question to function with higher precision than needed for ordinary speech communication. Yet since speech shares these networks with music, speech processing benefits. The OPERA hypothesis is used to account for the observed superior subcortical encoding of speech in musically trained

individuals, and to make specific predictions that can guide future research.

### **1081 Internet Delivery of Speech-In-Noise Testing for High Frequency Hearing Loss**

Marcel Vlaming<sup>1,2</sup>, Robert MacKinnon<sup>1</sup>, Marije Jansen<sup>1</sup>, David Moore<sup>1,3</sup>

<sup>1</sup>National Biomedical Research Unit in Hearing, <sup>2</sup>VU Medical Centre, Amsterdam, <sup>3</sup>MRC Institute of Hearing Research

Assessment of hearing loss is well suited to internet-based delivery since test sounds may be easily formatted on- or off-line, require only moderate bandwidth, and may be presented via headphones or other speaker systems. Calibration of sound level is an issue unless standard hardware is available (e.g. iPhone), but the tolerance of speech-in-noise (SiN) testing to variable overall sound level has made this ecologically important form of assessment practical and popular. The most well-studied and commonly used test is the Digit Triplets Test (DTT), developed for several languages under the European HearCom project ([www.hearcom.org](http://www.hearcom.org)). The digits (0-9) are redundant speech tokens easily identified by people >4 years old. They are presented as triplets against masking noise that is normally a steady wide-band masker. To test for high frequency hearing loss (HFHL), we developed a low-pass filtered noise (LPN) and compared standard audiometry with normal DTT, LPN-DTT, and LPN Consonant-Vowel-Consonant (LPN-CVC) test. Laboratory-based testing via the internet ([www.researchmyhearing.org](http://www.researchmyhearing.org)) compared headphone and loudspeaker sound delivery in adult listeners (n = 40) with hearing along a continuum from normal to severe-HFHL. Results showed a significant linear relationship between audiometric HFHL (3, 4, 6, 8 kHz average) and SiN threshold for all tests. For the normal DTT test, the gradient of the linear fit (0.10) was less than half that of the LPN-DTT (0.21) or the LPN CVC (0.21). Both tests using LPN masking also had better linear fits to the data than the normal DTT. LPN masking thus offers more sensitive prediction of HFHL than the normal DTT. For research, these methods will be used in large-scale studies of hearing that take a 'whole body' approach (e.g. [www.lolipopstudy.org](http://www.lolipopstudy.org), [www.ukbiobank.ac.uk](http://www.ukbiobank.ac.uk)). Clinically, the methods will be available to all and will enhance existing screening, leading to increased detection, advice and intervention.

## Author Index (Indexed by abstract number)

- Aabel, Peder, 350  
 Abbas, Mohamad, 640  
 Abdala, Carolina, 99  
 Abdulhadi, Khalid, 300  
 Abernathy, Matthew, 151  
 Abrams, Kristina S., 1045  
 Adachi, Nodoka, 313  
 Adams, Chris, 1003  
 Adams, Joe, 455, 954  
 Adenis, Victor, 469  
 Adise, Shana, 214, 229  
 Adunka, Oliver F., 177, 713  
 Aernouts, Jef, 131  
 Aerts, Johan, 134, 833  
 Agravas, W. Scott, 1069  
 Agrawal, Sumit, 128  
 Agrawal, Yuri, 807, 901  
 Agterberg, Martijn, 1060  
 Aguilar, Carlos, 303  
 Aguilar, Enzo, 625  
 Ahlf, Sönke, 501, 502  
 Ahmad, Faisal I., 713  
 Ahmad, Iram N., 764  
 Ahmad, Shoeb, 539, 985  
 Ahn, Joong Ho, 55, 56, 57, 58, 59, 277, 279, 834  
 Ahn, Seong-Ki, 47  
 Ahn, Yoon Suk, 232  
 Aiken, Steve, 152, 960  
 Akamatsu, Yusuke, 313  
 Akeroyd, Michael, 415, 646  
 Akil, Omar, 862, 939, 957, 970  
 Akram, Sahar, 537, 636  
 Al-Abduljawad, Khayria, 512  
 Alagramam, Kumar, 573  
 Alamilla, Javier, 907  
 Alessandrini, Marco, 70  
 Alexandrova, Olga, 118  
 Aliuos, Pooyan, 621  
 Alkowiari, Moza, 300  
 Allen, Daniel, 860  
 Allen, Jont, 413  
 Allen, Joshua, 725  
 Allen, Paul, 136, 652, 656, 1041  
 Alliston, Tamara, 939  
 Allman, Brian, 496, 588, 781  
 Al-Malky, Ghada, 176  
 AlmuKlass, Awad, 152, 960  
 Alpert, Evgenia, 343  
 Altaye, Mekibib, 500  
 Altieri, Nicholas, 377  
 Altschuler, Richard, 337, 595  
 Altshul, Larisa, 997  
 Alvarado, Juan Carlos, 504  
 Alvarez Heduan, Facundo, 758, 759  
 Amitay, Sygal, 406, 407, 1072  
 Amoodi, Hosam, 340  
 An, Yong-Hwi, 890  
 An, Yun Suk, 966  
 Anacker, Annett, 156  
 Ananthakrishnan, Saradha, 218, 226  
 Andeol, Guillaume, 649  
 Anderson, Lucy, 360, 499  
 Anderson, Rachel, 1042  
 Anderson, Samira, 72, 76  
 Angelaki, Dora, 566  
 Anttonen, Tommi, 1063  
 Aparicio, M.- Auxiliadora, 250  
 Arjmand, Ellis, 500  
 Armstrong, Patrick, 283  
 Arungundram, Sailaja, 155  
 Asai, Yukako, 580, 581, 941  
 Ashida, Go, 120  
 Ashmore, Krista, 12  
 Asimacopoulos, Eleni P., 972  
 Askew, Charles, 573, 580, 940  
 Atencio, Craig, 481, 547  
 Athanasakis, Emmanouil, 300  
 Atiani, Serin, 529  
 Atilgan, Erdinc, 575  
 Atkinson, Patrick, 826  
 Auer, Veronika, 237  
 Avenarius, Matthew, 343, 940  
 Avendaño, Carlos, 433  
 Avraham, Karen B., 544, 928, 1007  
 Awan, Omar, 713, 1043  
 Ayraut, Olivier, 694  
 Babanin, Mikhail, 466  
 Babola, Travis A., 253  
 Back, Sang A, 957  
 Badii, Ramin, 300  
 Baek, Jeong-In, 934  
 Bagger-Sjöbäck, Dan, 320  
 Bai, Jun-Ping, 736, 743  
 Baiduc, Rachael, 398, 403  
 Bailey, Erin, 441, 823  
 Baird, Andrew, 880  
 Baird, Theodore, 151  
 Bakhos, David, 503  
 Balaban, Carey, 47, 61  
 Balagurunathan, Kuberan, 155  
 Ball, Gregory, 824  
 Ballat, Elias, 498  
 Ballesterio, Jimena, 759  
 Balogová, Zuzana, 78  
 Balough, Ben, 964  
 Banai, Karen, 367  
 Banik, Ponkaj Kumar, 732  
 Bao, Jianxin, 733  
 Bao, Shaowen, 85, 804  
 Barald, Kate, 916  
 Barascud, Nicolas, 1075  
 Barnett-Cowan, Michael, 567  
 Barney, Sally, 860  
 Barry, Johanna G., 1072  
 Barth, Jeremy, 1069  
 Barthelemy, Catherine, 503  
 Bartles, James, 452, 583  
 Bartlett, Edward, 338  
 Barton, Matthew, 1065  
 Bartsch, Hauke, 830  
 Bas Infante, Esperanza, 162, 715  
 Bas, Esperanza, 714  
 Baskent, Deniz, 390  
 Basta, Dietmar, 330, 525, 605, 705  
 Bastiansen, David, 729, 730  
 Basura, Gregory, 86, 252  
 Bateschell, Michael, 740  
 Batrel, Charliène, 1030  
 Batts, Shelley, 999  
 Baudo, Robert, 658  
 Baumann, Ingo, 314  
 Bazan, Nicolas, 827  
 Beardsley, Ryan, 764  
 Bee, Mark, 645, 1046  
 Beeler, Dina, 452, 583  
 Behroozmand, Roozbeh, 94  
 Beier, Kevin, 678  
 Beim, Jordan A., 624  
 Beisel, Kirk W., 190, 666, 738, 926  
 Belles, Dana, 136  
 Belzner, Katherine, 996  
 Benka Wallén, Martin, 375, 854  
 Benovitski, Yuri, 17  
 Benson, Jennifer, 461  
 Benston, Thane E., 247  
 Berezina, Maira A., 1040  
 Berezina, Maria, 224  
 Bergevin, Christopher, 29, 201  
 Bergholm, Mikael, 883  
 Bergles, Dwight, 760  
 Berkes, Pietro, 487  
 Bermingham-McDonogh, Olivia, 665, 697  
 Bernardo, Francisco Javier, 250  
 Berner, Sarah, 209  
 Berninger, Benedikt, 8  
 Berninger, Erik, 843  
 Bernstein, Leslie, 634  
 Berrebi, Albert S., 250  
 Bertoncini, Josiane, 368  
 Best, Virginia, 111, 410  
 Betka, Jan, 78  
 Beurg, Maryline, 295  
 Beyer, Lisa, 691  
 Bezanilla, Francisco, 610  
 Bharadwaj, Hari, 219, 484  
 Bhatara, Anjali, 498  
 Bian, Shumin, 187, 189, 735  
 Bianchi, Federica, 106  
 Bidelman, Gavin, 218, 221, 226  
 Bieber, Rebecca, 703  
 Biedlingmaier, Andrew, 311  
 Bailey, Erin, 441, 823  
 Bielski, Elizabeth, 451  
 Bierer, Julie, 560  
 Bierer, Steven, 560  
 Biesemeier, Deborah J., 271  
 Bieszczad, Kasia, 468, 483  
 Birkholz, Cori, 95  
 Bishop, Brian, 105, 264, 774  
 Biswas, Amitava, 204  
 Biswas, Ishan, 86  
 Biswas, Ishwan, 252  
 Bizley, Jennifer, 472  
 Blake, David, 465, 534  
 Blamey, Peter, 17  
 Blatt, Melissa, 67  
 Bledsoe, Sanford, 234, 782  
 Blevins, Nikolai, 855, 999  
 Bloomberg, Jacob J., 900  
 Blomer, Daniel, 708, 821  
 Boehnke, Frank, 202, 391  
 Boesen, Michael, 216  
 Boettcher, Flint, 167  
 Bohlen, Peter, 797  
 Bohne, Barbara A., 955  
 Bohorquez, Jorge, 714, 715  
 Bohuslavova, Romana, 923  
 Bok, Jinwoong, 663, 687  
 Bokyoung, Kim, 871  
 Bonham, Ben, 555, 613  
 Bonnard, Åsa, 853  
 Bonnet-Brihault, Frédérique, 503  
 Borecki, Alex, 725  
 Borenstein, Jeffrey T., 316  
 Borkholder, David, 616  
 Borra, Tobias, 1078  
 Borst, J. Gerard G., 257  
 Bosen, Adam, 656  
 Bosnyak, Daniel J., 889  
 Bostrom, Marja, 350  
 Bostwick, Eric, 384  
 Boukhaled, Giselle, 706  
 Bouleau, Yohan, 741  
 Boulet, Jason, 603  
 Bourma, Judith, 926  
 Bourien, Jérôme, 332, 1030  
 Boutros, Peter, 773  
 Boven, Christopher, 413  
 Bowl, Michael, 303  
 Bowling, Sara A., 618  
 Bowyer, Susan, 321  
 Boyen, Kristiana, 82  
 Boyle, Patrick, 605  
 Bozorg-Grayeli, Alexis, 553, 899, 994  
 Bozovic, Dolores, 448, 449, 450, 460  
 Bradley, Allison, 519  
 Braid, Louis, 614  
 Brain, Joseph, 997  
 Brand, Yves, 821  
 Brandewie, Eugene, 548  
 Brandon, Carlene, 150  
 Brandt, Niels, 744  
 Brantley, Jennifer, 693  
 Braude, Jeremy, 751  
 Braun, Katharina, 202, 391  
 Bremen, Peter, 641  
 Bremer, Tristan, 564  
 Brenner, Jessica, 21  
 Brenner, Michael, 820  
 Bressler, Scott, 637  
 Brette, Romain, 217  
 Briare, Jeroen, 554, 556  
 Brichta, Alan, 48, 739  
 Bharadwaj, Hari, 219, 484  
 Brigande, John, 677, 678, 740  
 Briles, David, 876  
 Brimjoin, W. Owen, 646  
 Brooker, Rachael, 145  
 Brookler, Kenneth, 897  
 Brosch, Michael, 466, 470, 480  
 Brough, Douglas E., 693  
 Broussy, Audrey, 40  
 Brown, Andrew D., 648  
 Brown, David, 37  
 Brown, M. Christian, 247, 606  
 Brown, Maile R., 238  
 Brown, Steve, 303  
 Brown, Trecia, 511, 513  
 Browne, Cherylea, 719  
 Brownell, William, 186, 194, 195, 575, 576  
 Brownstein, Zippora, 928, 1007  
 Bruce, Ian, 603, 889  
 Brugeaud, Aurore, 40, 810  
 Brügger, Britta, 454  
 Bledsoe, Sanford, 234, 782  
 Bruneau, Nicole, 503  
 Brunette, Katyarina, 139  
 Brungart, Douglas, 373, 376  
 Bruno, Ernesto, 70  
 Buchholz, Jörg, 654  
 Buchman, Craig A., 177  
 Buckley, Jay, 846  
 Buckiova, Daniela, 923  
 Budenz, Cameron L., 618, 690, 818  
 Bueno, Isabel, 714  
 Buerbank, Stefanie, 745  
 Buniello, Annalisa, 937  
 Burchardt, Daniela, 186  
 Burger, R. Michael, 245  
 Burghard, Alice, 156  
 Burke, Brian, 1007  
 Burks, Deborah, 433  
 Burmeister, Margit, 298  
 Burt, Rachel, 304, 335  
 Buss, Emily, 639  
 Buytaert, Jan, 833  
 Byun, Ha-Young, 323, 851  
 Cabrera, Laurianne, 368  
 Cai, Hongxue, 25  
 Cai, Qunfeng, 147, 815  
 Cai, Rui, 477  
 Calcus, Axelle, 1050  
 Caldwell, Michael, 645  
 Calisto, Lilian E., 666  
 Calixto, Roger, 793  
 Callister, Robert, 48, 739  
 Camarena, Vladimir, 275  
 Camarero, Guadalupe, 433  
 Camp, Aaron, 739  
 Campbell, Kathleen, 728  
 Campbell, Sean, 351  
 Camper, Sally A., 309  
 Canlon, Barbara, 165, 375, 431, 854, 888  
 Cao, Xiao-Jie, 246  
 Capra, Gregory, 964  
 Carcagno, Samuele, 1052  
 Cardell, Lars-Olaf, 320  
 Cardenas, Elena, 748  
 Cardoso, Luis, 229  
 Care, Marguerite, 500  
 Carey, John P., 73, 892, 895, 901, 904  
 Carey, Thomas, 432  
 Carlile, Simon, 1055, 1076  
 Carlin, Michael, 495  
 Carlisle, Francesca, 938  
 Carlson, Christopher, 924  
 Carlyon, Robert, 80, 220, 382, 604, 630, 632  
 Carney, Laurel H., 287, 1045  
 Carpenter-Hyland, Ezekiel, 534  
 Carpinelli, Marina, 304, 335  
 Carrasco, Andres, 493  
 Carrasco, Magdalena, 517  
 Carreira, Eva, 1070  
 Carver, Courtney, 389  
 Case, Daniel, 249  
 Casparly, Donald, 334, 477, 590  
 Castellano-Munoz, Manuel, 296, 755  
 Catic, Jasmina, 654  
 Catz, Nicolas, 536  
 Cepko, Constance, 678  
 Ceranic, Borka, 476  
 Cevette, Michael, 897  
 Chabbert, Christian, 40, 806, 810  
 Chabot, Nicole, 478, 497  
 Chacroborty, Sakat, 451  
 Chae, Sung Won, 877  
 Chagnon, Bethany, 89, 792  
 Chai, Renjie, 344, 1067, 1068, 442  
 Chait, Maria, 510, 1075, 1077  
 Chaix, Benjamin, 992  
 Chambers, Claire, 537  
 Chambers, Robert, 846  
 Chan, Siaw-Lin, 311  
 Chang, Andrew, 712  
 Chang, Edward, 474  
 Chang, Ging, 157  
 Chang, Jolie, 939, 970  
 Chang, Nai-Yuan Nicholas, 569  
 Chang, Qing, 985, 990  
 Chang, Sun O, 27  
 Chao, Moses, 275, 767  
 Chaparro, Maria Paola, 993  
 Chapochnikov, Nikolai, 291, 1035  
 Charaziak, Karolina, 32, 397, 398  
 Charitidi, Konstantina, 431  
 Charlebois, Mathieu, 26  
 Charlotte, Celerier, 994  
 Chatlani, Shilpa, 38, 135  
 Chatzimichalis, Michail, 1022  
 Chavez, Eduardo, 821  
 Cheatham, Mary Ann, 138, 913  
 Chen, Chien-Wei, 443  
 Chen, Daniel, 573  
 Chen, Fangyi, 1015, 1017, 1019  
 Chen, Fu-Quan, 150, 969, 981  
 Chen, Guang-Di, 508, 959  
 Chen, Jessie, 192, 913  
 Chen, Jing, 306, 938  
 Chen, Joseph, 340  
 Chen, Kejian, 729, 730  
 Chen, Lin, 363  
 Chen, Pei-Jer, 169  
 Chen, Pei-Lung, 930  
 Chen, Ping, 269  
 Chen, Po-Yin, 65  
 Chen, Xingrui, 1008  
 Chen, Yen-Jung Angel, 993  
 Chen, Yuan-Tsong, 420  
 Chen, Zheng-Yi, 153, 925, 1001  
 Cheng, Alan, 344, 442, 1067, 1068  
 Cheng, Jeffrey, 124, 127, 131  
 Cheng, Weihua, 228  
 Cheng, Yenfu, 355

- Chenkai, Dai, 56, 277  
 Cherry, Sheree D., 253  
 Chertoff, Mark, 148  
 Chervenak, Andrew, 196  
 Cheung, Eunice, 999  
 Cheung, Linda, 166  
 Cheung, Willy, 110  
 Chhan, David, 28, 125  
 Chi, Fang-Lu, 269  
 Chiaravalloti, Agostino, 70  
 Chidavaenzi, Robstein, 1010  
 Chien, Wade, 73  
 Chin, Wesley M., 862  
 Chintanpalli, Ananthakrishna, 1037  
 Chiu, Kuo-Chieh, 206  
 Cho, Hyungho, 732  
 Cho, Hyun-Ju, 934  
 Cho, Siyoung, 732  
 Cho, Soyoun, 292  
 Cho, Won J., 1005  
 Cho, Yang-Sun, 323, 851  
 Cho, Yongbum, 732  
 Choi, Byung Yoon, 299  
 Choi, Dongseok, 828  
 Choi, Hee Jae, 76  
 Choi, Hoseok, 71  
 Choi, Jae Young, 178, 341, 380, 462, 615, 663, 687, 869, 884  
 Choi, Jin Woong, 299  
 Choi, June, 877  
 Choi, Kevin S., 822  
 Choi, Seong Jun, 866  
 Choi, Seung Hyo, 232, 966  
 Choi, Sung Jun, 989  
 Chole, Richare, 868  
 Chonko, Kurt, 592, 667  
 Chou, Shih-Wei, 577  
 Choudhury, Baishakhi, 177, 713, 1043  
 Choudhury, Niloy, 1017  
 Choung, Yun-Hoon, 437, 866, 989  
 Christianson, Gestur, 360, 510  
 Chumak, Tetyana, 923  
 Chung, Jong Hoon, 866  
 Chung, Jong Woo, 232, 966  
 Chung, Juyong, 27  
 Chung, Won-Ho, 851  
 Chung, Yoojin, 777, 796  
 Chung, You Sun, 299  
 Chunjie, Tian, 989  
 Churchill, Tyler, 382  
 Cistrone, Phillip, 136  
 Clark, Daniel, 849  
 Clark, Emily, 652, 657  
 Clark, J. Jason, 764  
 Clarke, Aaron, 456  
 Clarke, Andrew, 63  
 Clarke, Joseph, 762, 763  
 Clarkson, Cheryl, 248  
 Claussen, Alexander, 161  
 Clavier, Julien, 994  
 Clavier, Odile, 846  
 Clifford, Royce, 729, 997  
 Clinkard, David, 340  
 Cloninger, Christina, 652  
 Cocco, Daniela, 897  
 Cohen, Bernard, 50, 51, 52  
 Cohen, Helen, 900  
 Cohen, Mark, 158  
 Cohen, Stephanie, 158  
 Cohn, Edward, 62  
 Colburn, H. Steven, 113, 775, 779, 1071  
 Cole, Phaedra, 151  
 Coleman, John, 729, 730  
 Colesa, Deborah J., 618  
 Coling, Donald, 83, 815  
 Collazo, Andres, 664  
 Cone, Barbara, 520  
 Connolly, Timothy, 712  
 Constantinescu, Cristian, 483  
 Contini, Donatella, 43  
 Cooper, Alan, 249  
 Cooper, Nigel, 1025  
 Cooray, Anne, 304, 335  
 Coordes, Annkatrin, 325  
 Copley, Catherine, 266  
 Corbitt, Christian, 186, 194, 195  
 Corey, David P., 349, 747, 799, 925, 1001  
 Corfas, Gabriel, 749  
 Cosentino, Stefano, 602  
 Cosgrove, Dominic, 166, 457, 919, 920  
 Cotanche, Douglas, 997  
 Cousineau, Marion, 1049  
 Covey, Ellen, 90  
 Cox, Brandon, 682, 694, 1064, 1066  
 Cramer, Karina, 905  
 Crane, Benjamin, 288, 568  
 Creighton, Francis, 132  
 Crew, Joseph, 388  
 Croft, Cara L., 1072  
 Crozier, Robert A., 426  
 Cruickshanks, Karen, 305  
 Crumling, Mark, 461  
 Cumming, M. Alasdair, 651  
 Cunningham, Lisa, 161  
 Cureoglu, Sebahatin, 179, 876  
 Currall, Benjamin, 181  
 Curran, Molly, 954  
 Curtin, Hugh, 903  
 Cyr, Janet, 256  
 Dabdoub, Alain, 6, 268, 347, 679, 681, 685, 702  
 Dai, Chenkai, 55, 57, 58, 59, 279, 834  
 Dai, Min, 946, 947, 951, 968  
 Dalhoff, Ernst, 598  
 Dallos, Peter, 138, 192, 913  
 Daniel, Sam J., 26, 129  
 Dann, Serena, 635  
 Darling, Douglas, 311  
 Darrat, Ilaaf, 818  
 Darrow, Keith N., 247  
 Das, Olipriya, 915  
 Dau, Torsten, 106, 654  
 Davalos-Bichara, Marcela, 892, 901  
 David, Larry, 975  
 David, Stephen, 473, 487, 491, 529, 537  
 Davidov, Bella, 928  
 Davidovics, Natan, 279  
 Davis, Kevin, 212, 263, 800  
 Davis, Robin, 6, 10, 426, 702, 766, 1026, 1027, 1036  
 Dawson, Sally, 176, 825  
 Day, Mitchell, 262, 650  
 Dazert, Stefan, 552  
 de Boer, Egbert, 207  
 de Cheveigné, Alain, 492, 510  
 de Kleine, Emile, 82, 87  
 de La Rochefoucauld, Ombeline, 130  
 DeAngelis, Greg, 566  
 Deans, Michael, 266  
 Dearman, Jennifer, 694, 1006, 1064  
 Deckard, Nathan A., 1004  
 Decker, Brandon, 959  
 Decraemer, Willem, 130  
 Deeks, John, 604  
 Deerinck, Tom, 215  
 Deets, Ryan L., 764  
 DeGagne, Jackie, 946  
 Deguine, Olivier, 18  
 Dehmel, Susanne, 782  
 Dehoff, Marlin, 215  
 Deinhardt, Katrin, 767  
 Dekel, Eyal, 533, 786  
 Dekker, David, 554, 556  
 Del Rio, Tony, 272  
 Del Vecchio, Katie, 924  
 Delaney, Katherine, 828, 882  
 Delgutte, Bertrand, 260, 650, 777, 796, 1031, 1033  
 Delhome, Lorraine, 614  
 Delimont, Duane, 166, 919, 920  
 Della Santina, Charles C., 55, 56, 57, 58, 59, 277, 278, 279, 581, 834, 904  
 Dellamary, Luis, 998  
 Demany, Laurent, 1052  
 DeMason, Christine E., 713  
 Deng, Xiaohong, 680  
 Denham, Susan, 795  
 Dent, Micheal, 1044  
 Depireux, Didier, 591  
 Depner, Manfred, 467  
 DeRemer, Susan, 164  
 DeRoy, Kristina, 626  
 Deshpande, Aniruddha, 20  
 Desloovere, Christian, 1028  
 Desmadryl, Gilles, 810  
 DeSmidt, Alexandra, 445  
 Devarajan, Keerthana, 593  
 Dewald, Jules, 519  
 Dezortova, Monika, 78  
 Dhamani, Imran, 1076  
 Dhar, Sumitrajit, 99, 100, 403, 841, 850  
 Dhooge, Ingeborg, 561  
 Di Pietro, Barbara, 70  
 Dierick, Manuel, 134  
 Dietz, Beatrice, 213  
 Dietz, Mathias, 776  
 Dille, Marilyn, 36, 842  
 Dillon, Margaree, 177  
 Dilwali, Sonam, 318, 943  
 Ding, Bo, 327  
 Ding, Dalian, 119, 159, 430, 817, 979, 980  
 Ding, Nai, 491, 530  
 Dinh, John, 162  
 Dirckx, Joris, 131, 134, 833  
 Disteldorf, Barbara, 744  
 Dittrich, B., 621  
 Dlugaiczyk, Julia, 718  
 Dobrev, Ivo, 124  
 Doetzlhofer, Angelika, 692, 922  
 Doi, Songila, 661  
 Dolan, David, 309, 337, 461, 595, 940  
 Doll, Joey, 446  
 Dollezal, Lena-Vanessa, 527  
 Donaldson, Gail, 601  
 Donato, Roberta, 121  
 Dong, Wei, 1011  
 Dong, Yang, 74, 980  
 Dorman, Michael, 5  
 Dorning, Joanne, 303  
 Drennan, Ward R., 23  
 Drescher, Dennis G., 171, 1004, 1005  
 Drescher, Marian J., 1004, 1005  
 Drexl, Markus, 1020  
 Drga, Vit, 622  
 Dror, Amiel A., 1007  
 Drottler, Marie, 247, 523  
 Drury, Hannah, 48, 739  
 du Lac, Sascha, 49  
 Du, Xiaoping, 163, 228, 720, 726  
 Duan, Chongwen, 138, 192, 913  
 Duelli, Dominik, 827  
 Duggan, Anne, 684  
 Dulon, Didier, 295, 675, 741  
 Duncan, Jeremy, 9, 666, 673, 688  
 Duncan, R. Keith, 271, 461, 1034  
 Duncley, Kathleen, 396  
 Dunlap, Alex, 528  
 Durakovic, Nedim, 606  
 Duret, Guillaume, 184  
 Durham, Dianne, 148, 158, 365, 593  
 Durlach, Nathaniel, 113  
 Durrant, John, 69  
 Durruthy-Durruthy, Robert, 662  
 Dyhrfeld-Johnsen, Jonas, 810, 813  
 Dylla, Margit, 797  
 Dziennis, Suzan, 704  
 Earl, Brian, 148  
 Easter, James, 964  
 Eastwood, Hayden, 712  
 Eatock, Ruth Anne, 812  
 Ebisu, Fumi, 451  
 Eby, Thomas, 893  
 Edeline, Jean-Marc, 469, 479, 492  
 Edge, Albert, 11, 355  
 Edge, Roxanne, 138, 913  
 Egami, Naoya, 891  
 Eggermont, Jos J., 488, 507  
 Eggleston, Jessica, 147  
 Egnor, S.E. Roian, 324  
 Ehlers, Erica, 369, 642  
 Ehret, Günter, 463, 791  
 Eiber, Albrecht, 1022  
 Eisenman, David, 308, 311  
 Eldridge, Kayla R., 861  
 Elgoyhen, Ana Belén, 758, 759  
 Elgueda, Diego, 529  
 Elhilali, Mounya, 495, 636  
 Elkon, Ran, 311  
 Ellisman, Mark, 215  
 Emery, Sarah, 298  
 Engel, Jutta, 744  
 Englitz, Bernhard, 473, 487, 529, 537, 636  
 Engström, Elisabet, 464  
 Enns, Paul, 693  
 Epp, Bastian, 201, 414, 1058  
 Eppsteiner, Robert, 540, 935  
 Erkmann, Linda, 675  
 Ernst, Arne, 525, 605  
 Ernst, Arneborg, 330, 705  
 Escabi, Monty, 773  
 Eshraghi, Adrian, 714, 715  
 Esmailbeigi, Hananeh, 324  
 Esser, Karl-Heinz, 22, 156  
 Esterberg, Robert, 444  
 Eustaquio-Martin, Almudena, 625  
 Euteneuer, Sara, 971  
 Eysen, Lale, 265  
 Ewert, Donald, 228, 726  
 Ewert, Stephan D., 1051  
 Faletta, Flavio, 300  
 Falk, Kristine, 713  
 Fallon, James, 2, 17, 599, 600  
 Falvo, Michael, 67  
 Fang, Jie, 1006, 1066  
 Fang, Qing, 309  
 Fang, Yixin, 767  
 Fantetti, Kristen, 672  
 Farinelli, Federica, 195  
 Farooq, Redwan, 220  
 Farrell, Brenda, 186, 194, 195  
 Farris, Hamilton, 827  
 Faulstich, Michael, 49  
 Fay, Jonathan P., 565  
 Feeney, Patrick, 37, 836  
 Feinkohl, Arne, 653  
 Feinstein, Elena, 343  
 Fekete, Donna M., 271, 668, 672, 678  
 Felmy, Felix, 209  
 Feng, Jianqiao, 500  
 Feng, Lei, 533  
 Feng, Yan-Mei, 378  
 Ferber, Alexander, 123  
 Ferguson, Melanie, 849  
 Fernandez, Rayne, 998  
 Fernando, Augusta, 764  
 Ferrary, Evelyne, 553, 994  
 Ferreira, Enrique, 894  
 Ferrieri, Patricia, 876  
 Ferrucci, Luigi, 73  
 Feth, Lawrence, 961  
 Fettiplace, Robert, 447  
 Fettes, Margaret, 44  
 Fiering, Jason, 316  
 Finch, Gabriel, 579  
 Finley, Charles, 613  
 Firpo, Matt, 317  
 Fiser, Jozsef, 487  
 Fisher, Rachel, 932  
 Fishman, Yonatan, 532  
 Fitzakerley, Janet, 456  
 Fitzgerald, Matthew, 13, 393  
 Fitzpatrick, Denis, 37  
 Fitzpatrick, Douglas C., 177, 713, 1043  
 Flaherty, Mary, 1044  
 Flanagan, Virginia, 103  
 Fleck, Terry, 761, 936  
 Fleming, Michelle T., 309  
 Flores, Amanda, 860  
 Flores-Moreno, J. Mauricio, 124  
 Floyd, Robert, 161, 228, 720, 726, 731  
 Flynn, Brianna, 826  
 Ford, Marc, 118  
 Forge, Andrew, 306, 424, 689, 911  
 Forsberg, Scott, 997  
 Forsythe, Ian D., 236, 239, 241  
 Fox, Daniel, 728  
 Francis, Howard, 329  
 François, Florence, 992  
 Frank, Thomas, 757  
 Franken, Tom, 211  
 Fransson, Anette, 769  
 Franz, Christoph, 718, 886  
 Fraysse, Bernard, 18  
 Frazer, Kelly, 543  
 Fredrickson-Hemling, Lea, 448  
 Freed, Daniel J., 409, 565  
 Frerck, Micah, 276  
 Friauf, Eckhard, 216, 240  
 Fridberger, Anders, 320, 576, 858, 1013, 1017, 1019  
 Friderici, Karen, 932  
 Fridman, Gene Y., 55, 57, 58, 59, 277, 278, 279  
 Friedman, Lilach M., 928  
 Friedrich Jr., Victor L., 51  
 Frijns, Johan, 554, 556  
 Frisina, Robert, 327, 616  
 Fritsch, Michael, 356  
 Fritz, Jonathan B., 473, 487, 529, 537  
 Fritzsche, Bernd, 9, 273, 666, 667, 673, 688, 835, 926, 1009  
 Froemke, Robert, 524  
 Frolenkov, Gregory I., 141, 585, 962  
 Frydman, Moshe, 928  
 Fu, Aixue, 152  
 Fu, Qiang, 781  
 Fu, Qian-Jie, 387, 388  
 Fuchs, Paul, 135, 329, 737, 751, 752, 759  
 Fuehr, Hartmut, 506  
 Fuente, Adrian, 81  
 Fuhrman, Susan, 69  
 Fuji, Hironori, 902  
 Fujioka, Masato, 671, 952, 995  
 Fujita, Takeshi, 146, 172  
 Fujiwara, Tazuko, 875  
 Fujiyuki, Chika, 596  
 Fuku, Noriyuki, 931  
 Fukui, Hideto, 691  
 Fukushima, Kunihiko, 875  
 Fuller, Gerald G., 552  
 Fullgrabe, Christian, 75  
 Funabiki, Kazuo, 120  
 Funnell, W. Robert J., 26, 129  
 Furlong, Cosme, 124, 127  
 Furman, Gabriel, 898  
 Furman, Joseph, 69  
 Furness, David, 707  
 Furukawa, Shigeto, 633, 638  
 Fuzessery, Zoltan, 89, 787, 792, 805  
 Gaboyard-Niay, Sophie, 40, 810  
 Gabriele, Mark, 789  
 Gadziola, Marie, 1042

- Gagnon, Leona, 309  
Gagnon, Patricia M., 868, 942  
Gai, Yan, 647, 659  
Galano, Maria, 432  
Galazyuk, Alexander, 592  
Gale, Jonathan, 824, 825  
Galindo, Ramon, 441  
Gall, Megan, 770  
Gallun, Frederick J., 401, 635  
Galvin, John, 387, 388  
Gan, Lin, 694  
Gan, Rong Z., 31, 33, 879  
Gandour, Jackson, 218  
Gantz, Bruce, 1, 563, 935  
Gao, Guangping, 153  
Gao, Wei, 61  
Gao, Xinheng, 163  
Gao, Yanhong, 738  
Gao, Yuan, 361  
Garcia, Kristen, 1044  
Garcia-Anoveros, Jaime, 684  
Gardner, Stephanie, 338  
Garnham, Carolyn, 714  
Gasparini, Paolo, 300, 302  
Gasser, Krysta, 167, 170  
Gassner, Davina, 593  
Gaucher, Quentin, 469, 479, 492  
Gauvin, David, 151  
Gavrilova, Oksana, 308  
Gay, Jennifer, 1047  
Gazula, Valeswara-Rao, 421  
Ge, Xianxi, 964  
Geisinger, Dario, 894  
Geisler, Hyun-Soon, 718  
Géléoc, Gwenaëlle, 580, 581, 940, 941  
Geng, Ruishuang, 573  
Gerendes, B, 314  
Gerlach-Bank, Lisa, 916  
Geßele, Nikodemus, 104  
Gfeller, Kate, 1  
Ghisleni, Peter, 595  
Gilbert, Heather, 516  
Gileles, Felicia, 724  
Gilkey, Robert, 373  
Gill, Ruth M., 617, 832  
Gillespie, Deda, 249, 907  
Gillespie, Peter, 310, 453, 454, 575, 578, 1001, 1002  
Giroto, Giorgia, 300, 302  
Gittelman, Joshua, 788  
Glasberg, Brian, 75  
Glassman, Katelyn, 13, 393  
Glogowski, Carolina, 242  
Glowatzki, Elisabeth, 135, 294, 746, 752  
Gnansia, Dan, 416  
Gockel, Hedwig, 80, 220, 632  
Godar, Shelly, 383  
Godoy, Ricardo, 1059  
Goeckel, Tom, 640  
Goetz, Sarah, 876  
Goldberg, Jay M., 38  
Golden, Erin, 922  
Golding, Nace L., 122, 253  
Goldsworthy, Ray, 614  
Goldwyn, Joshua, 560, 611  
Golub, Justin, 695  
Gómez-Alvarez, Marcelo, 250  
Gomez-Casati, Maria Eugenia, 749  
Gong, Wangsong, 570  
Gonzalez Garrido, Antonia, 425  
González-Rodríguez, Águeda, 433  
Goodman, Shawn S., 933  
Goodrich, Lisa, 246, 266, 272, 1001  
Gopal, Kamakshi, 475  
Görga, Michael, 95  
Gotta, Romy, 525, 605  
Goulding, David, 306  
Goupell, Matthew, 384, 385  
Gourévitch, Boris, 469, 479, 492  
Goyal, Vinay, 609  
Grahn, Jessica, 511  
Graham, Carolyn, 715  
Gratton, Michael Anne, 166, 167, 170, 457  
Graydon, Cole, 292  
Green, Steven H, 273, 441, 710, 823  
Greenberg, David, 116  
Greene, Nathaniel, 212  
Greger, Bradley, 19  
Griesemer, Désirée, 240  
Griffith, Andrew, 308, 311, 580, 581  
Griffiths, Timothy D., 531, 1074, 1075  
Grimley, Jasmine, 490, 803  
Grolman, Wilko, 903, 1029  
Gröschel, Moritz, 330, 525, 605, 705  
Grose, John, 639  
Grosh, Karl, 197  
Gross, Guenter, 475  
Grothe, Benedikt, 117, 118, 209, 259  
Grounds, John, 64  
Grover, Mary, 768  
Gruhlke, Alyson, 95  
Gu, Yong, 566  
Guan, Xiyang, 33, 879  
Guénet, Jean-Louis, 145  
Guerrero, Shiloh, 49  
Guex, Amélie, 606  
Guillaume, Anne, 649  
Guinan, John J., 224, 1018, 1025, 1040  
Gummer, Anthony W., 185, 598  
Günther, Stefanie, 527  
Guo, Fei, 465  
Guo, Zhaohua, 1003  
Gupta, Chhavi, 162, 440, 714, 715  
Gürkov, Robert, 1020  
Gurrola, Jose, 540  
Gürtler, Nicolas, 929  
Gustenhoven, Erich L, 316  
Guthrie, O'neil, 761, 936  
Gutierrez-Hernandez, Sergio, 904  
Gutsche, Katja, 718  
Guymon, Allan, 762, 763  
Haamann, Daniel, 621  
Haburcakova, Csilla, 570  
Hackett, Troy, 521  
Hadjantonakis, Anna-Katerina, 677  
Haefner, Ralf, 487  
Hafer, Ervin, 418  
Hah, Young-Sool, 47  
Hailey, Dale, 444  
Hajek, Milan, 78  
Hakim, Ibrahim, 916  
Hakizimana, Pierre, 576  
Hall, Joseph, 639  
Hallman, Timothy, 924  
Hallworth, Richard, 180, 181  
Halpin, Chris, 28  
Halsey, Karin, 337, 461, 595  
Hamaguchi, Kiyomi, 701, 814, 918  
Hamanishi, Shinji, 1062  
Hamberg, Leena, 903  
Hamlet, William, 254  
Han, Changduk, 71  
Han, Feng-chan, 175, 881  
Han, Gyu Cheol, 896  
Han, Helen, 412  
Han, Kyu-Hee, 299  
Han, Weiju, 1008  
Hancock, Kenneth E., 606, 777, 796, 1048  
Hansen, Marlan R, 762, 763, 764, 765  
Hansen, Marlen, 935  
Hansen, Stefan, 988  
Happel, Max F.K., 482, 802  
Hara, Akira, 977, 978  
Harada, Tatsuhiko, 35  
Harasztosi, Csaba, 185  
Harding, Gary W., 955  
Hardisty, Rachel, 937  
Harper, Elizabeth, 729, 730  
Harper, Nicol S., 258, 1053  
Harpole, Bethany, 765  
Harrington, Ellery, 124, 127  
Harrison, Robert, 233, 340  
Harrop, Anne, 998  
Hartman, Byron, 662, 697  
Hartman, Julia, 601  
Hartmann, Taja, 793  
Hartssock, Jared J., 617  
Harvey, Margaret, 742  
Hasegawa, Shingo, 146, 172  
Hashimoto, Makoto, 328, 902  
Hashino, Eri, 354, 356  
Hasnain, Hira, 713  
Hasson, Dan, 375, 854, 888  
Hastings, Michelle, 827  
Hausman, Fran, 439, 828, 865, 872, 873, 878  
Hausman, Frances, 882  
Hayashi, Toshinori, 665  
Hayashi, Yushi, 816  
Hayden, Russell, 834  
Hazrati, Oldooz, 612  
He, David, 79, 190, 325, 584  
He, Shuman, 177  
He, Wenxuan, 946, 1013, 1014  
He, Zinan, 129  
Hecker, Dietmar, 718  
Hedderstierna, Christina, 852  
Hedjoudje, Abderrahmane, 834  
Heffer, Leon, 600  
Heffner, Henry, 844  
Hegner, Erin, 139  
Heiden, Micheal, 501  
Heil, Peter, 408, 470  
Heinz, Michael G., 1037, 1038, 1039  
Helbig, Silke, 391  
Heller, Stefan, 552, 662, 1003  
Hellström, Sten, 320  
Hemmert, Werner, 559  
Henin, Simon, 102  
Hennig, Matthias, 236, 239  
Henry, Kenneth, 1039  
Henshaw, Helen, 849  
Hergert, Meike Sofia, 1003  
Herrmann, Barbara, 903  
Hertzano, Ronna, 308, 311  
Hess, Christi, 369, 642  
Hesse, Lara Li, 360  
Hessler, Roland, 22  
Hetherington, Alexander, 555  
Hickman, Tyler, 753  
Hickson, Louise, 81  
Higashi, Yujiro, 308  
Highstein, Stephen, 276, 286  
Highstein, Steve, 46  
Hight, A. Edward, 45  
Higuchi, Hitomi, 864, 983  
Hikishima, Keigo, 952  
Hildebrand, Michael, 301, 935  
Hildebrandt, K. Jannis, 360, 526  
Hill, Evan, 844  
Hill, Jessica A., 241  
Hill, Kayla, 981  
Hinduja, Sneha, 817  
Hinrich, Anthony, 827  
Hirai, Haruka, 847, 875  
Hirono, Moritoshi, 454  
Hirose, Keiko, 698, 982  
Hirose, Yoshinobu, 438, 987  
Hirota, Koichi, 400  
Hirtz, Jan, 216  
Hiryu, Shizuko, 644  
Hittner, Emily, 72  
Hladek, Lubos, 655  
Hoang Dinh, Emilie, 254  
Hoehn, Kyle, 725  
Hoffman, Howard J., 312  
Hoffman, Larry, 39, 986  
Hoffpauir, Brian, 215  
Hoglund, Evelyn, 961  
Hol, Myrthe, 1060  
Holland, Scott, 500  
Holly, Ashley, 139  
Holman, Holly A., 155, 276  
Holmes, Zachariah, 924  
Holstein, Gay R., 50, 51  
Holt, A Genene, 337  
Holt, Jeffrey, 573, 580, 581  
Holt, Joseph, 43, 44, 811  
Homma, Kasuaki, 138  
Homma, Kazuaki, 192, 610  
Honda, Keiji, 333  
Hong, Amy, 659  
Hong, Bin Na, 722, 984  
Hong, Bo, 794  
Hong, Ha Na, 722, 984  
Hong, Sung Hwa, 851  
Hoover, Eric C., 412  
Hopkins, Kathryn, 75  
Horn, David, 1056  
Horn, Henning F., 1007  
Hornak, Aubrey, 822  
Hornickel, Jane, 108  
Horwitz, Geoff, 573, 581  
Horwitz, Rachelle, 124  
Hoshino, Tomofumi, 977  
Hoshino, Tomohumi, 978  
Howard, Matthew, 489, 515  
Hrnicek, Andrew, 797  
Hsiao, Edward, 939  
Hsieh, Chia-Lung, 154  
Hsu, Chuan-Jen, 169, 420, 930  
Hu, Bo Hua, 147, 815, 965  
Hu, Ning, 720, 726, 731  
Hu, Zhengqing, 348  
Huang, Guan-Hua, 305  
Huang, Mingqian, 925, 1001  
Huang, Qihong, 881  
Huang, Ying, 466, 470  
Hubbard, Allyn, 200  
Huber, Alexander, 1022  
Hubert, Nikolai, 330, 705  
Hubka, Peter, 24, 381, 505  
Hudspeth, A. J., 199, 459  
Huebner, Alyssa, 353  
Huetz, Chloé, 469, 479  
Huff, Joseph, 664  
Huh, Sung-Ho, 267  
Hullar, Timothy, 569  
Hultcrantz, Malou, 320, 852, 853  
Hume, Clifford, 695, 826  
Hunter, Lisa, 37  
Hur, Dong Gu, 47  
Hurd, Elizabeth, 683  
Husain, Masud, 1074  
Huth, Markus, 442, 855  
Hütten, Mareike, 22  
Huyc, Julia, 370  
Hwang, Hye Sook, 437  
Hyde, Elizabeth C., 618  
Iben, Carolin, 1051  
Ibrahim, Nadine, 94  
Iconaru, Luigi, 345  
Idrobo, Fabio, 1045  
Imamura, Tomoki, 451  
Ihlefeld, Antje, 382  
Iizuka, Takashi, 699  
Ikeda, Katsuhisa, 674, 699  
Ikeda, Ryoukichi, 711  
Ikeda, Takuo, 902  
Ikemiyagi, Yoshihiro, 331  
Im, Gijung, 737  
Imanishi, Yoshikazu, 573  
Imayoshi, Itaru, 918  
Imig, Thomas, 365  
Inaoka, Takatoshi, 1062  
Indzhuklian, Artur, 585, 962  
Ingham, Neil, 306, 938  
Inoshita, Ayako, 699  
Inskirveli, Irakli, 465  
Irina, Toshio, 417, 1079  
Irvine, Dexter, 2, 599  
Irving, Sam, 599  
Ise, Momoko, 676, 912  
Ishibashi, Makoto, 918  
Isik, Michael, 559  
Ison, James, 1041  
Itatani, Naoya, 527  
Ito, Juichi, 346, 352, 451, 701, 814, 816, 914, 918, 967, 1062  
Ito, Rindy, 563  
Ito, Taku, 308  
Ito, Toshio, 952  
Ivanova, Tamara, 528  
Ives, D. Timothy, 23  
Ives, David, 1050  
Iwasaki, Shinichi, 313, 891  
Iyer, Nandini, 373, 376  
Jackson, Dakota, 215  
Jackson, Ronald, 729, 730, 964, 997  
Jackson, Ryan, 25  
Jackson, Wesley, 85  
Jacob, Michele, 753  
Jacob, Stefan, 576  
Jacobs, Peter G., 36, 401, 842  
Jacques, Bonnie, 268, 679, 685  
Jacques, Steven L., 30, 1017  
Jaeyung, Choi, 871  
Jagger, Daniel, 306, 424, 911  
Jahan, Israt, 9, 666, 673  
Jajoo, Sarvesh, 723, 819  
Jakovcevski, Igor, 971  
Jalabi, Walid, 906  
James, Chris, 18  
Jamesdaniel, Samson, 83, 817  
Jameyson, Elyse M., 23  
Jan, Taha, 1003, 1068  
Jang, SeoJin, 896  
Janky, Kristen L., 62, 892  
Jansen, Marjie, 1081  
Jansen, Sebastian, 330, 605, 705  
Jara, Hernan, 523  
Jasien, Jessica, 67  
Jastrzembski, Benjamin, 846  
Jaumann, Mirko, 886  
Jayaram, Aditi, 781  
Jeffcoat, Ben, 893  
Jenkins, Herman, 597  
Jennings, J. Richard, 69  
Jensen, Jane B., 972  
Jensen-Smith, Heather, 181, 1009  
Jentsch, David, 289  
Jeon, Ju Hyun, 380, 615, 884  
Jeong, Hansung, 732  
Jeschke, Marcus, 482, 802  
Jesteadt, Walt, 95  
Ji, Seung, 448  
Jia, Shuping, 584  
Jiang, Haiyan, 159, 430, 979  
Jiang, Han, 677, 678  
Jiang, Zhi-Gen, 419, 740, 944, 950  
Jianxin, Bao, 590  
Jin, So Young, 890  
Jin, Sun Hwa, 851  
Jin, Yaojing, 79  
Jin, Ying, 670  
Jin, Yong-Ming, 250  
Jing, Zhizi, 757  
Jinyung, Kim, 871  
Jiradejvong, Patpong, 93, 389  
Joanisse, Marc, 511  
Joanisse, Marc F., 513  
Jodelka, Francine, 827  
Joeng Kim, Hyo, 422  
Johannesen, Peter, 623, 625  
Johnson, Ann-Christin, 858  
Johnson, Brianna, 166  
Johnson, Kenneth R., 309  
Johnson, Matthew, 285  
Johnson, Rhiannon, 276  
Johnson, Shane, 357, 831, 835  
Johnsrude, Ingrid, 370, 371, 372, 630  
Johny, Manu Ben, 834  
Jones, Gary, 562, 1056  
Jones, Heath, 119, 386  
Jones, Jennifer, 267  
Jones, Pete, 406

- Jones, Sherri, 280, 281, 940  
 Jones, Simon, 795  
 Jones, Thomas J., 309  
 Jordan, Amy, 742  
 Jordan, Paivi, 44  
 Joris, Phillip, 210, 211, 1028  
 Joseph, Sabine, 1074  
 Josupeit, Angela, 1051  
 Jovanovic, Sasa, 213  
 Ju, Y., Sungtaek, 39  
 Juhn, Steven, 876  
 Jung, Jae-Yun, 343, 721, 940  
 Jung, Sungdo, 721  
 Jung, Timothy, 870  
 Junig, Laura, 652  
 Kabara, Lisa L., 618  
 Kachar, Bechara, 292  
 Kaczmarek, Leonard, 238, 421  
 Kageyama, Ryoichiro, 918  
 Kagomiya, Takayuki, 596  
 Kajikawa, Yoshinao, 509  
 Kakigi, Akinobu, 313  
 Kale, Sushrut, 1038, 1039  
 Kalinec, Federico, 140, 182, 993  
 Kalkman, Randy, 554, 556  
 Kallioinen, Petter, 464  
 Kalluri, Radha, 45, 399  
 Kalluri, Sridhar, 418, 1050  
 Kals, Mathias, 14  
 Kaltenbach, James, 361, 362  
 Kamiya, Kazusaku, 674, 699  
 Kappel, Sean D., 635  
 Kan, Alan, 382, 384, 385, 386  
 Kanaan, Moein, 544  
 Kanagawa, Eiju, 328, 973  
 Kanagawa, Eijyu, 438  
 Kandasamy, Thileep, 340  
 Kandathil, Cherian, 619  
 Kane, Catherine, 823  
 Kang, Beom Sik, 934  
 Kang, Hung-Soo, 47  
 Kang, Sung Un, 437  
 Kang, Tong Ho, 722, 984  
 Kang, Young-Jin, 915  
 Kanicki, Ariane, 461  
 Kanold, Patrick, 485, 522  
 Kant, Ritu, 483  
 Kanwisher, Nancy, 535  
 Kanzaki, Sho, 671, 995  
 Kao, Albert, 449, 450  
 Kao, Chugn-Lan, 65  
 Kao, Shyan-Yuan, 943  
 Karasawa, Takatoshi, 419, 975  
 Karimnejad, Kaveh, 457  
 Karino, Shotaro, 210, 313  
 Kariya, Shin, 179, 322, 847, 875  
 Karsten, Sue, 563  
 Kasagi, Hiromi, 699  
 Kasai, Misato, 699  
 Kashino, Makio, 400, 633, 1077  
 Kashio, Akinori, 313, 326, 331  
 Kataoka, Yuko, 875  
 Kato, Tomofumi, 931  
 Katsuno, Tatsuya, 451  
 Katsunuma, Sayaka, 146  
 Katz, Eleonora, 758, 759  
 Katz, Elyssa, 138  
 Kaur, Tejbeer, 723, 819, 820  
 Kavianpour, Sarah, 789  
 Kawai, Hideki, 483  
 Kawano, Satoyuki, 1062  
 Kawasaki, Hiroto, 489, 515  
 Kawase, Tetsuaki, 411, 711  
 Kawashima, Yoshiyuki, 308, 580, 581  
 Kawaura, Mitsuhiro, 952  
 Kazmitcheff, Guillaume, 553  
 Keefe, Douglas, 37, 1021  
 Keine, Christian, 213  
 Kel, Gordana, 712  
 Kelley, Matthew, 353, 669  
 Kelly, John, 306, 424, 825, 911  
 Kemner, Chantal, 1078  
 Kemp, David, 837  
 Kempton, Beth, 439, 828, 865, 872, 873, 878  
 Keniston, Leslie, 496  
 Kennon-McGill, Stefanie, 365  
 Kersigo, Jennifer, 9, 273, 666, 673  
 Ketterer, Angela D., 1045  
 Khalmuratova, Roza, 47  
 Khatri, Vivek, 229  
 Kidd Jr., Gerald, 111  
 Kidd, Ambrose, 590  
 Kidd, Jr., Gerald, 410  
 Kiefer, Susan, 170  
 Kiernan, Amy, 670  
 Kim, Ah Reum, 299  
 Kim, Chang-Hee, 60  
 Kim, Chul-Ho, 437  
 Kim, Duck O., 105, 264, 773, 774  
 Kim, Duk Joong, 200  
 Kim, Ernest, 316  
 Kim, Eun Jung, 866, 989  
 Kim, Eun Yeon, 851  
 Kim, Hee Nam, 178  
 Kim, Hong Lim, 957  
 Kim, Hyo Jeong, 427, 428, 429  
 Kim, Hyoung-Mi, 315  
 Kim, Jae Eun, 71  
 Kim, Jichul, 574  
 Kim, Jin Young, 462  
 Kim, John, 442  
 Kim, Jun, 60  
 Kim, Jun Hee, 231  
 Kim, Ki hyun, 989  
 Kim, Kihyun, 866  
 Kim, Kyunghee X., 447  
 Kim, Mi Joo, 896  
 Kim, Minbum, 178  
 Kim, Namhison, 299  
 Kim, Namkeun, 208  
 Kim, Sang Cheol, 380, 884  
 Kim, Sang Gyooun, 870  
 Kim, Sang Jeong, 60  
 Kim, Sei Eun, 231  
 Kim, Seung Won, 866, 989  
 Kim, Soo-Chan, 896  
 Kim, Sung Huhn, 462  
 Kim, Sung Woon, 877  
 Kim, Sunny, 663  
 Kim, TaeWoo, 896  
 Kim, Un-Kyung, 687, 934  
 Kim, Wandoo, 27  
 Kim, Yeon Joo, 866  
 Kim, Yong-Gyu, 60  
 Kim, Youn Ju, 989  
 Kim, Young Chul, 963  
 Kim, Young Ho, 963, 989  
 Kim, Young-Jin, 323  
 Kimitsuki, Takashi, 133  
 Kindt, Katie, 579  
 King, Andrew J., 472, 1053  
 King, Ericka, 298  
 Kinoshita, Makoto, 326  
 Kirjavainen, Anna, 1063  
 Kirkegaard, Mette, 336  
 Kirkwood, John E, 552  
 Kishline, Lindsey, 90  
 Kispert, Andreas, 423  
 Kitajiri, Shin-ichiro, 451  
 Kitamura, Ken, 333, 857, 931  
 Kitani, Rei, 182  
 Kitterick, Pádraig Thomas, 77  
 Klein, Barbara, 305  
 Klein, Ronald, 305  
 Kleine Punte, Andrea, 14  
 Kleinjung, Tobias, 887  
 Kline-Schoder, Robert, 846  
 Klinge, Astrid, 629  
 Kliš, Sjaak, 1029  
 Klump, Georg M., 527, 629, 653, 795  
 Knipper, Marlies, 216, 718, 886  
 Koay, Gimseong, 844  
 Kobayashi, Toshimitsu, 411, 711  
 Koch, Kelly-Jo, 1045  
 Koch, Ursula, 237  
 Kodama, Takashi, 49  
 Koehler, Karl, 354, 356  
 Koehler, Seth, 86, 252  
 Koester, Daniel, 202  
 Koh, Seung Hyun, 380, 884  
 Kohrman, David, 940  
 Kok, Melanie, 497  
 Koka, Kanthaiiah, 119, 123, 597, 964  
 Kol, Nitzan, 928  
 Kolesnikova, Olga, 52  
 Kollmar, Richard, 915  
 Kommareddi, Pavan, 432  
 Komune, Shizuo, 133  
 Kondoh, Hisato, 265  
 Kong, Jee-Hyun, 296, 754, 755  
 Kong, Soo-Keun, 845  
 König, Reinhard, 470  
 Konishi, Masakazu, 120  
 Konrad-Martin, Dawn L., 36, 401, 635, 842  
 Kopco, Norbert, 655  
 Kopecky, Benjamin, 9, 666, 673, 835  
 Kopke, Richard, 163, 228, 720, 726, 731  
 Koppel, Scott, 905  
 Kopp-Scheinflug, Cornelia, 236, 239, 241  
 Köpfschall, Iris, 718  
 Kopun, Judy, 95  
 Korn, Matthew, 905  
 Korrapati, Soumya, 692  
 Korte, Megan, 1009  
 Korzyukov, Oleg, 94  
 Koullich, Elena, 319  
 Koviuniemi, Andrew, 21  
 Kozlov, Serguei, 1007  
 Kral, Andrej, 3, 24, 381, 505, 793  
 Kramer, Florian, 240  
 Kraus, Nina, 72, 76, 91, 108, 223, 225  
 Krause, Eike, 1020  
 Krefft, Heather, 628  
 Krenmayr, Andreas, 14  
 Kreuzer, Peter, 887  
 Krey, Jocelyn, 453, 578  
 Krishnamoorthy, Gayathri, 948, 949  
 Krishnan, Ananthanarayan, 218, 222, 226  
 Krishnan, Lakshmi, 643  
 Kristiansen, Arthur, 996  
 Kriwacki, Richard, 345  
 Krug, Edward, 1069  
 Ku, Jeffrey, 1065  
 Kuenzel, Thomas, 243  
 Kuhn, Maggie, 275  
 Kuhn, Stephanie, 718  
 Kujawa, Sharon G, 316  
 Kumar, Rishi, 194  
 Kumar, Sukhbinder, 531, 1074, 1075  
 Kumaraguru, Anand, 781  
 Kunz, Lars, 209  
 Kuo, Bryan, 344, 1068  
 Kurabi, Arwa, 880  
 Kuriki, Shinya, 518  
 Kurima, Kiyoto, 308, 311, 580, 581  
 Kurioka, Takaomi, 717  
 Kuriyavar, Satish I., 163  
 Kurt, Simone, 463  
 Kuster, Kael, 283  
 Kuthanova, Lada, 923  
 Kuttva, Sudhagar, 476  
 Kuwada, Shigeyuki, 105, 264, 773, 774  
 Kwak, Eunyee, 856  
 Kwak, Sangyeop, 856  
 Kwan, Kelvin Y., 349, 1001  
 Kwon, Bomjun, 16  
 Kwon, Hyun Ja, 966  
 Kwon, See Youn, 851  
 La Brecque, Brian, 997  
 Labay, Valentina, 580, 581  
 Laborde, Marie-Laurence, 18  
 Lacour, Michel, 809  
 Ladak, Hanif, 128  
 Ladrech, Sabine, 332, 1030  
 Laflen, Brandon, 13  
 Lai, Edwina, 552  
 Lakemeyer, Gerhard, 640  
 Laker, David, 58  
 Lamas, Veronica, 504  
 Lamers, Alyssa, 369  
 Land, Rüdiger, 24  
 Landgrebe, Michael, 887  
 Landry, Tom, 2  
 Landsberger, David M., 394, 395  
 Lang, Hainan, 355, 1069  
 Langers, Dave, 82, 87  
 Langguth, Berthold, 887  
 Laos, Maarja, 1063  
 Larabee, Patti, 317  
 Larrain, Barbara, 439, 872  
 Larsen, Deb, 594  
 Larson, Chuck, 94  
 Larsson, Christina, 320  
 Laske, Roman, 662  
 Lasker, David, 54, 56, 277  
 Lau, Bonnie K., 1061  
 Laudanski, Jonathan, 217  
 Lauer, Amanda, 329  
 Lauxmann, Michael, 1022  
 Lavner, Yizhar, 367  
 Lawler, Jack, 137  
 Le, Linda, 881  
 Leake, Patricia, 555, 557, 619  
 LeBel, Carl, 998  
 Lee, Adrian K. C., 110, 484, 637  
 Lee, Daniel J., 570, 606, 903  
 Lee, Duk-Gyu, 845  
 Lee, Eun Ji, 896  
 Lee, Hyun Jae, 869  
 Lee, Il-Woo, 845  
 Lee, Jaewook, 612  
 Lee, Jianyi, 917  
 Lee, Jone Dae, 877  
 Lee, Jong Bin, 866  
 Lee, Jun Ho, 27, 315  
 Lee, Jungmee, 100, 403, 841, 850  
 Lee, Jungwha, 100, 841, 850  
 Lee, Kyu Yup, 308, 934  
 Lee, Mi Hye, 437  
 Lee, Roger, 591  
 Lee, Sang Yeon, 231  
 Lee, Won-Sang, 341  
 Lee, Yi-Ching, 420  
 Léger, Agnès C., 416  
 Lehmann, Jessica, 506  
 Lehnert, Simon, 115, 237  
 Lehtimäki, Jarmo, 883  
 Lei, Debin, 590, 733  
 Leibold, Christian, 115, 237  
 Leijon, Arne, 843  
 Lelli, Andrea, 580  
 Leman, Marc, 561  
 Lenarz, Minoo, 793  
 Lenarz, Thomas, 22, 156, 621, 793, 867  
 Lengyel, Mate, 487  
 Lenoir, Anne, 1066  
 Lenoir, Marc, 332, 1030  
 Lentz, Jennifer, 827, 1057  
 Lentz, Danielle R., 1007  
 Lepczyk, Laura, 586, 587, 589, 885  
 LePrell, Colleen, 164  
 Lescanne, Emmanuel, 503  
 Lesperance, Marci, 298  
 Leung, Johahn, 1055, 1076  
 Lev, Dorit, 928  
 Levano, Soledad, 821  
 Levitt, Pat, 921  
 Levy, Suzanne Carr, 409, 565  
 Lewicki, Michael, 545  
 Lewis, Morag, 302, 938  
 Lewis, Richard, 570  
 Lewis, Rick, 572  
 Li, Chaoying, 686  
 Li, Chuan-Ming, 312  
 Li, Gang, 812  
 Li, Geng-lin, 292  
 Li, Hongzhe, 976  
 Li, Huawei, 153, 985  
 Li, Ji, 781  
 Li, Jun, 298  
 Li, Ming, 74  
 Li, Na, 772  
 Li, Shuang, 359  
 Li, Shufeng, 762, 763  
 Li, Song-Zhe, 982  
 Li, Wei, 163, 228, 720, 726  
 Li, Xiangming, 458  
 Li, Xiantao, 735  
 Li, Yizeng, 197  
 Liang, Chun, 142, 143, 174, 307  
 Liaw, Eric, 1067, 1068  
 Liberman, Charles, 137, 290, 355, 749, 753, 956  
 Liberman, Tamara, 109  
 Licastro, Danilo, 300  
 Lichtenhan, Jeffery, 1025  
 Lighthall, Jessyka, 873  
 Lim, David J., 435, 436, 874  
 Lim, Hubert H., 783, 784, 793  
 Lim, Hyun Woo, 232  
 Lim, Keoun, 572  
 Lim, Rebecca, 48, 739  
 Limb, Charles, 93, 389  
 Limjoco, Alexander, 167, 457  
 Lin, Chia-Cheng, 898  
 Lin, Frank, 73, 528  
 Lin, Harrison, 996  
 Lin, Kuang-Yi, 206  
 Lin, Shuh-Yow, 747, 748  
 Lin, Shu-Wha, 169  
 Lin, Vincent, 340  
 Lin, Xi, 157, 420, 539, 985, 990  
 Lin, Yin-Hung, 169, 420  
 Linbo, Tor, 444  
 Linden, Jennifer F., 360, 499, 510, 526  
 Lindgren, Magnus, 464  
 Linley, Deborah, 80  
 Listyo, Alwin, 821  
 Litovsky, Ruth, 4, 369, 382, 383, 384, 385, 386, 642  
 Litvak, Leonid, 613  
 Liu, Hong, 979  
 Liu, Jianzhong, 729, 730, 964  
 Liu, Li Qian, 461  
 Liu, Lijie, 152  
 Liu, Lily, 748  
 Liu, Liqian, 1034  
 Liu, Puzhao, 74  
 Liu, Qing, 1036  
 Liu, Robert, 528, 908  
 Liu, Wenke, 702, 1026  
 Liu, Xiao-Peng, 363  
 Liu, Xiao-Ping, 812  
 Liu, Xue, 542  
 Liu, Yi-Wen, 206  
 Liu, Yuming, 30  
 Liu, Zada, 90  
 Liu, Zhiyong, 344, 682  
 Liu, Zhyong, 694  
 Livingston, Christine, 256  
 Llano, Daniel, 334  
 Lobarinas, Edward, 588, 959  
 Locastro, Michael, 529  
 Loebach, Jeremy, 377  
 Loera, Katie, 392  
 Loewenheim, Hubert, 734  
 Loizou, Philip, 612  
 Lokensgard, James, 168  
 Lokakin, Oleg, 263  
 Lomber, Stephen G., 478, 493, 497, 511, 513  
 Long, Glennis, 101, 102  
 Longenecker, Ryan, 592  
 Longo-Guess, Chantal, 309  
 Lonsbury-Martin, Brenda, 97, 98, 836, 840  
 Loper, Adam, 628, 631

- Lopez, Ivan, 986  
Lopez-Gonzalez, Monica, 93  
López-Paullier, Matias, 366  
Lopez-Poveda, Enrique A., 623, 625  
Lorente, Beatriz, 145, 302  
Lorenzen, Sarah, 684  
Lorenzi, Christian, 23, 368, 416, 1050  
Lortejije, Jeannette, 257  
Lou, Kristina, 903  
Lou, Xiangxin, 346  
Lovell, Jonathan, 480  
Lovett, Michael, 1065  
Lu, Cindy, 246, 1001  
Lu, Guang-Jin, 174  
Lu, Jianzhong, 228, 726  
Lu, Jingqiao, 539  
Lu, Na, 153  
Lu, Thomas, 558  
Lu, Xiaowei, 270, 917  
Lu, Yan, 716  
Lu, Ying-Chang, 169, 420, 930  
Lu, Yong, 238, 254  
Lu, Zhongmin, 445  
Luan, Hongge, 287  
Lucas, Jeffrey, 770  
Ludin, Katia, 929  
Luebke, Anne, 44, 136  
Luethy, Kirsten M., 271  
Luk, Lauren, 442  
Lundberg, Yunxia (Yesha), 62, 280, 281, 282  
Luo, Hao, 589  
Luo, Xin, 12  
Lupo, J. Eric, 597  
Lustig, Laurence, 557, 862, 939, 957, 970  
Lysakowski, Anna, 812, 1010  
Lyxell, Björn, 464  
Ma, Ketao, 950  
Maas, Paige, 73  
MacArthur, Carol, 439, 828, 865, 872, 873, 878  
MacKinnon, Robert, 1081  
MacNeilage, Paul, 571  
Machpherson, Ewan, 651  
Maddox, Ross K., 110  
Maftoon, Nima, 129  
Magin, Robert, 192  
Mahendrasingam, Shanthini, 707  
Mahrt, Elena, 909  
Maier, Hannes, 423  
Maiorano, Domenico, 160  
Maison, Stéphane F., 137, 956  
Majczenko, Karen, 298  
Makishima, Tomoko, 283, 580, 581  
Maklad, Adel, 46  
Maldonado, Natalia, 229  
Malkavaara, Kari, 883  
Mangosing, Sara, 748  
Manis, Paul, 230, 1036  
Manley, Geoffrey, 953  
Mann, David, 317  
Mann, Mary Ann, 286  
Mann, Scott, 284, 285  
Manneberg, Otto, 997  
Mannell, Robert, 15  
Manning, Michael, 304  
Mannström, Paula, 336  
Manohar, Senthilvelan, 83, 508, 781  
Mansour, Suzanne, 686  
Manzo, Amy, 186  
Manzoor, Nauman, 361, 362  
Mao, Zhongping, 79  
Mappus, Rudolph, 528  
Marano, Robert, 335  
Marchetti, Gregory, 898  
Marcotti, Walter, 718  
Margoliash, Daniel, 550  
Maricich, Stephen M., 592, 667, 906  
Marimuthu, Vijay Mohan Raaja, 15  
Mark, Paul, 932  
Markovitz, Craig D., 783  
Marler, Jeffrey A., 933  
Marmel, Frederic, 80, 632  
Maro, Isaac, 846  
Marquardt, Torsten, 116, 205, 602, 776  
Marrone, Nicole, 412  
Martin, Cathy, 337  
Martin, Donna, 683  
Martin, Glen, 97, 98, 840  
Martinelli, Giorgio P., 50, 51  
Martinez-Monedero, Rodrigo, 135  
Martins, Ana Raquel, 524  
Marx, Mathieu, 18  
Masaki, Kinuko, 613  
Mason, Christine, 111, 410  
Massing, Thomas, 988  
Massoudi, Roohollah, 494  
Masuda, Masatsugu, 675  
Masutomi, Keiko, 1077  
Matic, Agnella, 551, 609  
Matic, Agnella Izzo, 608  
Matsui, Jonathan, 443  
Matsumoto, Nozomu, 133  
Matsunaga, Tatsuo, 173  
Matsunobu, Takeshi, 717  
Matsuoka, Akihiro, 356  
Matsuta, Naohiro, 644  
Mattley, Jane, 499  
Matui, Toshie, 1079  
Mauermann, Manfred, 96  
May, Bradford, 244  
Mayko, Zachary, 788  
Mc Laughlin, Myles, 558  
McAlpine, David, 116, 121, 258, 602, 776  
McCaffrey, Kate, 827  
McCall, Andrew, 903  
McCombie, W. Richard, 538  
McCullar, Jennifer, 351  
McDermott Jr, Brian M., 577  
McDermott, Daniel, 401  
McDermott, Josh H., 107, 374, 535, 546, 1049, 1059, 1077  
McGee, JoAnn, 139, 325, 696, 1009  
McKay, Colette M., 606  
McKenna, Charles, 996  
McKenna, Michael, 316, 996  
McLean, Julie, 962  
McMenomey, Sean, 563  
McMillan, Ameer J., 478, 511  
McMillan, Garnett P., 36, 842  
Medina-Ferret, Eduardo, 109, 366  
Meech, Robert, 728  
Meehan, Daniel, 166, 457, 919, 920  
Meenderink, Sebastiaan, 149, 450, 460  
Megerian, Cliff, 175  
Mehraei, Golbarg, 637  
Mellado Lagarde, Marcia M, 144, 682  
Mellott, Jeffrey, 785  
Meltser, Inna, 165  
Menardo, Julien, 160, 332  
Merchán, Miguel A., 504  
Merchant, Gabrielle R., 863  
Merchant, Saumil N., 455, 863, 954  
Meredith, Frances, 284, 285  
Meredith, M. Alex, 496  
Merfeld, Daniel, 570, 572  
Mescher, Mark J, 316  
Mesgarani, Nima, 474  
Metherate, Raju, 465, 483  
Metzger, Brian, 405  
Meyer zum Gottesberge, Angela Maria, 988  
Micarelli, Alessandro, 70  
Michaels, Leslie, 910  
Michalski, Nicolas, 295  
Michel, Christophe, 332  
Micheyl, Christophe, 404, 532, 628, 631  
Micucci, Joseph, 683  
Middlebrooks, John C., 114, 641  
Middleton, Jason W., 486  
Mighell, Taylor, 696  
Migliaccio, Americo, 53  
Mikiel-Hunter, Jason, 121  
Mikosz, Andrew, 354  
Miikuriya, Takefumi, 328, 438, 973  
Milenkovic, Ivan, 213  
Mill, Robert, 795  
Miller, Christopher, 620, 900  
Miller, Danielle, 432  
Miller, Josef, 164  
Miller, Kimberly E., 90  
Miller, Richard, 337  
Minami, Shujiro, 173  
Minekawa, Akira, 699  
Minh, Zayer, 329  
Minoda, Ryosei, 434, 676, 912  
Minor, Lloyd B., 807, 904  
Minowa, Osamu, 699  
Miroir, Mathieu, 553  
Mishra, Srikanta, 99  
Miura, Mauricio, 915  
Miwa, Toru, 434  
Miwa, Tory, 676  
Miyachi, Motohiko, 931  
Mizutari, Kunio, 355  
Mochizuki, Hideki, 699  
Moghadam, Setareh, 49  
Mohr, Ian, 275  
Moiseenkov-Bell, Vera, 186  
Molina, Ramon, 997  
Molis, Michelle R., 635  
Monahan, Jodi, 924  
Monahan, Kelly, 308  
Monksfield, Peter, 712  
Moon, Il Joon, 323, 851  
Moon, In Seok, 341, 884  
Moon, Sung K., 435, 436, 874  
Mooney, Chance, 183  
Moore, Brian, 75, 416, 632  
Moore, David R., 406, 407, 849, 1072, 1081  
Moore, Ernest, 475  
Morales, Marti, 1034  
Moran, John, 88, 358  
Mori, Susumu, 834  
Morino, Michiharu, 68  
Morisono, Tetsuo, 864, 983  
Morley, Barbara, 750  
Morley, John, 719  
Morris, Ken A., 666  
Morrison, Annie, 311  
Morse, Susan, 303  
Mortensen, Amanda H., 309  
Morton, Cynthia C., 934  
Moser, Tobias, 573, 1035  
Moshi, Ndeserua, 846  
Moss, Cynthia, 545, 643  
Motallebzadeh, Hamid, 26  
Mountain, David, 196, 200, 1016  
Mueller, Marcus, 734  
Muench, Gerald, 719  
Muhammed, Louwai, 220  
Mukherjee, Debashree, 723, 819, 820  
Mukherjee, Jogeshwar, 483  
Mulavara, Ajitkumar P, 900  
Mullen, Lina, 675  
Müller, Susanne, 330, 525  
Mulvaney, Joanna, 681  
Mun, Joung Hwan, 323  
Mun, Seog-Kyun, 856  
Munguia, Raymundo, 507  
Münkner, Stefan, 744  
Munnamalai, Vidhya, 665  
Murai, Aya, 322, 847  
Murakami, Haruka, 931  
Murata, Junko, 674  
Murillo-Cuesta, Silvia, 433  
Musicant, Alan, 658  
Musiek, Frank, 846  
Musolino, Mark, 898  
Mustain, William, 46, 893  
Mutai, Hideki, 173  
Mutnal, Manohar, 168  
Mylius, Judith, 480  
Nadaraja, Garani, 308, 442  
Nagle, Stephanie, 846  
Nair, Thankam, 432  
Naka, Kikuko, 847  
Nakagawa, Seiji, 518, 596  
Nakagawa, Takashi, 864, 983  
Nakagawa, Takayuki, 346, 352, 701, 814, 816, 914, 967, 1062  
Nakai, Akira, 438  
Nakajima, Hideko H., 863, 903, 1023  
Nakamura, Masaya, 995  
Nakaya, Kazuhiro, 711  
Nakayama, Masahiro, 977, 978  
Nakmalia, Don, 720, 731  
Nam, Jong-Hoon Nam, 191  
Nam, Sung-Il, 796  
Namba, Kazunori, 173  
Nandur, Vuday, 601  
Napolitano, Bianca, 70  
Nara, Takeshi, 699  
Narayanan, Rekha, 784  
Narins, Peter, 149  
Nation, Javan, 589  
Navaratnam, Dhasakumar, 187, 188, 189, 735, 736, 743  
Nayagam, Bryony, 826  
Nayak, Shruti, 275, 767  
Neely, Stephen, 95, 839, 1024  
Negandhi, Jaina, 233  
Neilans, Erikson, 1044  
Nelson, Mark, 164  
Neng, Lingling, 945, 947  
Nerlich, Jana, 213  
Neuman, Arlene, 393  
Newlands, Shawn, 287  
Nguyen, Kimanh, 895  
Nguyen, Tot, 695  
Nguyen, Yann, 553, 994  
Nguyen-Huynh, Anh, 30, 392  
Ni, Jing-Tian, 363  
Nibu, Ken-ichi, 146, 172  
Nichols, David, 926  
Nichols, Michael, 180  
Nicholson, Hilary, 606  
Nicoletti, Michele, 559  
Nicolson, Teresa, 274, 579  
Nie, Kaibao, 23  
Nie, Liping, 738  
Niesner, Thomas, 791  
Niesten, Marlien, 903  
Nihira, Tomoko, 699  
Nik, Atefeh M., 422  
Nilsson, Michael, 409, 565  
Nishimura, Koji, 346, 701  
Nishio, Ayako, 333, 857  
Nishitani, Allison, 272  
Nishizaki, Kazunori, 179, 322, 847, 875  
Niu, Yuguang, 781  
Noda, Tetsuo, 699  
Nodal, Fernando, 472  
Noguchi, Yoshihiro, 333, 857, 931  
Nolte, Ingo, 621  
Norena, Arnaud, 536  
Norman-Haignere, Samuel, 535  
Norris, Andrew, 476  
Nourski, Kirill, 489, 515  
Nowotschin, Sonja, 677  
Nusse, Roel, 1068  
Nuttall, Alfred L., 30, 193, 207, 704, 709, 740, 944, 946, 951, 968, 1008, 1015, 1017, 1019  
Nyc, Mary Ann, 870  
Ó Maoiléidigh, Dáibhid, 199  
Ochi, Atsushi, 638  
O'Connell, Samantha, 223  
Oertel, Donata, 246, 1041  
Oesterle, Elizabeth, 351  
Ogata, Erika, 313  
Ogawa, Kaoru, 671, 952, 995  
Ogino, Eriko, 352  
O'Gorman, David E., 779  
Ogorodnikov, Dmitri, 50, 51  
Ogun, Oluwaseye Ayoola, 62  
Oh, Sejo, 435, 436, 874  
Oh, Seung Ha, 27  
Oh, Seung-Ha, 299  
Ohashi, Mitsuru, 133  
Ohl, Frank, 802  
Ohi, Frank W., 482  
Ohlemiller, Kevin K., 822, 942, 982  
Ohyama, Takahiro, 921  
Oishi, Naoki, 150, 958, 974  
Ojima, Hisayuki, 471  
Okada, Hiroko, 699  
Okano, Hideyuki, 674, 952, 995  
Okano, Hirota, 995  
Okano, Hirota James, 952  
Okano, Mitsuhiro, 875  
Olds, Kevin, 834  
O'Leary, Stephen, 600, 712, 826  
Oleskevich, Sharon, 725  
Oline, Stefan N., 245  
Oliver, Douglas, 771  
Olafsson, Ake, 843  
Olshausen, Bruno, 545  
Olson, Elisabeth, 29, 130, 1011  
O'Malley, Jennifer, 954  
Omelchenko, Irina, 709, 740, 968  
O'Neill, William, 652, 656, 657  
Ono, Munenori, 771  
Orban, Gergo, 487  
Ornitz, David, 267  
Oron-Karni, Varda, 928  
Ors, Marianne, 464  
Orton, Llwyd, 780  
Oshima, Hidetoshi, 711  
Oshima, Kazuo, 662  
Oshima, Takeshi, 711  
Oshima-Takago, Tomoko, 573  
Otsuka, Asuka, 518  
Otsuka, Sho, 400  
Otsuki, Naoki, 172  
Ottaviani, Fabrizio, 70  
Otto, Kevin, 21  
Ouyang, Jessica, 586, 587  
Overath, Tobias, 374, 531, 1077  
Owen, Thomas, 682  
Oxenham, Andrew J., 624, 628, 631  
Oya, Hiroyuki, 489, 515  
Ozmeral, Erol, 639  
Paasche, Gerrit, 156, 867  
Pace, Edward, 88, 586, 587, 589, 885  
Padilla, Monica, 394, 395  
Pagani, Marco, 70  
Paige, Gary, 652, 656, 657  
Pak, Kwang, 675, 821, 880  
Palan, Vikrant, 964  
Palmer, Alan, 114, 516, 803  
Palmiter, Richard, 695, 909  
Pals, Carina, 390  
Pan, Ning, 9, 666, 673  
Pan, Wei, 670  
Panford-Walsh, Rama, 886  
Pankow, James, 305  
Pankratz, Nathan, 305  
Papal, Samantha, 1064  
Paparella, Michael, 179, 876  
Papatzamos, Georgios, 320  
Pararas, Erin E, 316  
Parbery-Clark, Alexandra, 72, 76, 91  
Parikh, Malav, 782  
Park, Albert, 317  
Park, Ga Young, 323  
Park, Hee Sung, 851

- Park, Hong Ju, 966  
 Park, Hong-Joon, 934  
 Park, Hun Yi, 437, 866, 989  
 Park, Keehyun, 437  
 Park, Keun Ha, 722, 984  
 Park, Kye Hoon, 721  
 Park, Kyoung Ho, 700, 957  
 Park, Moo Kyun, 877  
 Park, Se Ra, 341, 462  
 Park, Sera, 615, 884  
 Park, Shi-Nae, 957  
 Park, Su-Kyoung, 848  
 Park, Sung-Hwan, 845  
 Park, Yong-Ho, 963  
 Parker, Andrew, 303  
 Parker, Kathryn, 767  
 Parker, Mark, 703  
 Parnitzke, Timo, 629  
 Parpaite, Thibaud, 741  
 Parsa, Arya, 140  
 Parsons, Carl, 719  
 Parthasarathy, Aravindakshan, 338  
 Parzefall, Thomas, 928  
 Pass, Johanna, 306  
 Patel, Aniruddh, 1080  
 Patel, Chirag, 364  
 Patel, Minal, 965  
 Patthy, Laszlo, 934  
 Patton, Kyle A., 668  
 Pau, Henry, 725  
 Pavlinkova, Gabriela, 923  
 Pawlowski, Karen, 319  
 Pearson, Ben, 1074  
 Pearson, Selina, 145, 306, 938  
 Pecka, Jason, 190  
 Pecka, Michael, 117, 259  
 Pedemonte, Marisa, 109, 366  
 Pedersen, Nancy L., 858  
 Pellieux, Lionel, 649  
 Peng, Anthony, 446  
 Penninger, Richard, 561  
 Perachio, Adrian, 283  
 Pereira, Fred A., 186, 339  
 Peretz, Isabelle, 1049  
 Perez, Enrique, 714  
 Perkel, David, 788, 909  
 Perkins, Guy, 946  
 Perkins, Rodney, 565  
 Perreau, Ann, 563  
 Perrier, Thomas, 992  
 Perry, Trevor, 16  
 Peters, Brian T., 900  
 Petit, Christine, 295  
 Petrillo, Marco, 153  
 Pettingill, Lisa, 2  
 Pfannenstiel, Travis, 964  
 Pflugst, Bryan E., 379, 618, 690  
 Phillips, Jannel, 500  
 Pienkowski, Martin, 488, 507  
 Pierce, Marsha, 1009  
 Pierstorff, Erik, 993  
 Pike, John M., 713, 1043  
 Pilati, Nadia, 236  
 Pineda, Mario, 964  
 Pinsky, Peter, 574  
 Pirastu, Nicola, 302  
 Piron, Cristiano, 356  
 Pirvola, Ulla, 1063  
 Pisoni, David, 377  
 Pitt, Mark, 92  
 Pitynski, Dori, 787, 792  
 Piu, Fabrice, 617, 998  
 Plack, Christopher, 80, 220, 622, 632  
 Platt, Michael, 318  
 Plinkert, Peter K., 314  
 Plontke, Stefan, 617  
 Poeppel, David, 374  
 Poling, Gayla, 100, 841  
 Politanski, Piotr, 727  
 Pollak, George, 772  
 Polley, Daniel, 521, 1048  
 Popelka, Gerald, 855, 999  
 Porsov, Edward, 1014  
 Portfors, Christine, 788, 909  
 Potter, Paul, 303  
 Powers, Richard, 575  
 Pradhan, Gaurav, 897  
 Praetorius, Mark, 314  
 Pressnitzer, Daniel, 537  
 Prieskorn, Diane, 164  
 Priesol, Adrian, 572  
 Prieve, Beth, 101  
 Profant, Oliver, 78  
 Prosolovich, Ksenia, 393  
 Psaltis, Demetri, 154  
 Pu, Lichun, 79  
 Pu, Ye, 154  
 Puel, Jean-Luc, 160, 332, 992, 1030  
 Pujol, Remy, 2  
 Puligilla, Chandrakala, 353, 669  
 Purcell, Erin, 1034  
 Purdy, Suzanne, 1076  
 Puria, Sunil, 25, 203, 208, 409, 565, 574  
 Pyott, Sonja, 746, 751  
 Pysanenko, Kateryna, 514  
 Qian, Dong, 269  
 Quesnel, Alicia, 996  
 Rabbitt, Richard D., 46, 155, 276, 286  
 Radja, Asja, 460  
 Radomskij, Paul, 476  
 Radtke-Schuller, Susanne, 529  
 Raft, Steven, 927  
 Rahman, Mehdi A., 57, 58, 59, 279, 834  
 Rahmen, Irfan, 724  
 Raible, David, 444  
 Rajadinakaran, Gopinath, 1000  
 Rajguru, Suhrud, 276, 551, 607, 608, 609  
 Rajkowska, Elzbieta, 727  
 Ramachandran, Ramnarayan, 797  
 Ramage, Erin, 860  
 Ramakrishnan, Neeliyath A., 171  
 Ramamoorthy, Sripriya, 193, 1019  
 Ramekers, Dyan, 1029  
 Ramkumar, Vickram, 723, 819, 820  
 Ramnarine, Kiran, 229  
 Randle, James, 707  
 Raphael, Robert, 183, 184  
 Raphael, Yehoash, 235, 343, 432, 618, 690, 691, 818, 940  
 Raphan, Theodore, 50, 52  
 Rasetshwane, Daniel, 1024  
 Rask-Andersen, Helge, 350  
 Ratanapongleka, Mayryl, 719  
 Rathbone, Graeme, 17  
 Ratnanather, J. Tilak, 500  
 Rau, Thomas, 867  
 Rauchman, Michael, 170  
 Ravicz, Michael, 127  
 Ravicz, Mike, 126  
 Raynor, Graham, 630  
 Razak, Khaleel, 517  
 Reamer, Elyse, 683  
 Reavis, Kelly M., 36, 842  
 Rebillard, Guy, 332  
 Rebscher, Stephen, 557  
 Redfern, Mark, 898  
 Redmond, Sharon, 335  
 Reed, Charlotte, 614  
 Rees, Adrian, 780  
 Regele, Oliver, 21  
 Rehman, Zarin, 823  
 Reichenbach, Tobias, 459  
 Reif, Roberto, 704  
 Reimann, Katrin, 948, 949  
 Reiss, Lina, 1, 392, 563  
 Rellinger, Erin A., 942  
 Remme, Michiel, 121  
 Ren, Chongyu, 227  
 Ren, Dong-Dong, 269  
 Ren, Tianying, 946  
 Ren, Tianying, 1013, 1014  
 Rennie, Katherine, 284  
 Rennie, Katie, 285  
 Retzlöff, Kurt, 317  
 Reuter, Guenter, 621  
 Rewerska, Anna, 727  
 Rhee, Chung-Ku, 721  
 Ricci, Anthony J., 198, 296, 442, 446, 574, 754, 755, 756  
 Richards, Virginia, 1070  
 Richardson, Rachael, 826  
 Richter, Claus-Peter, 519, 551, 607, 608, 609, 610  
 Rigo, Frank, 827  
 Rinaldi Barkat, Tania, 521  
 Ringdahl, Erik, 860  
 Rinzel, John, 121, 794  
 Riquimaroux, Hiroshi, 644  
 Ritzl, Eva K., 904  
 Rivetta, Alberto, 188  
 Robb, Mallory, 402  
 Roberts, Daniel, 943  
 Roberts, Larry E., 889  
 Roberts, Michael, 122  
 Robertson, Nahid G., 934  
 Robertson, Sara, 500  
 Robinson, Alan, 551  
 Robinson, Sue, 239  
 Rocha-Sanchez, Sonia, 139, 696  
 Roche, Jennica, 898  
 Rockefeller, Nicholas, 158  
 Rode, Thilo, 793  
 Rodrigues De Andrade, Leonardo, 927  
 Rodríguez-Contreras, Adrián, 214, 229  
 Rodríguez-de la Rosa, Lourdes, 433  
 Roehm, Pamela, 275, 767  
 Rogers, Rick, 729, 997  
 Rohbock, Karin, 718  
 Roland, Peter S., 319  
 Roongthumskul, Yuttana, 450  
 Roos, Matthew, 244  
 Rössli, Christof, 28, 125  
 Rosen, Merri, 1047  
 Rosowski, John J., 28, 124, 125, 126, 127, 131, 863  
 Ross, Hayley, 285  
 Ross, Mark, 897  
 Roth, Jerome, 430  
 Röthlisberger, Benno, 929  
 Rothwell, Clayton, 373  
 Rottier, Robbert, 670  
 Rouchka, Eric, 1000  
 Roussel, Martine, 694  
 Roux, Kyle J., 1007  
 Roux, Sylvie, 503  
 Roy, Alexis, 389  
 Roy, Sitikantha, 575  
 Rozental, Abraham J., 768  
 Rubel, Edwin W., 238, 241, 255, 444, 695, 909  
 Ruben, Robert, 1054  
 Rubinstein, Jay T., 23, 562, 611, 1056  
 Rubio, Maria, 248  
 Rubsamen, Rudolf, 213  
 Ruder, Charlotte, 500  
 Rudnick, Eric, 164  
 Ruggles, Dorea, 219  
 Ruhland, Janet, 647, 659  
 Rupprecht, Laura, 1016  
 Russo, Andrew F., 710  
 Rust, Marco, 216  
 Rutherford, Mark, 291, 757, 1035  
 Rutledge, Joseph, 170  
 Rüttiger, Lukas, 216, 718, 886  
 Ryan, Allen F., 675, 821, 880  
 Ryan, Claire, 628  
 Rybak, Leonard P., 723, 819, 820  
 Ryugo, David, 2, 329  
 Sachs, Matthew, 93  
 Sadeghi, Soroush, 746  
 Saeed, Shakeel, 689  
 Saffran, Jenny, 369  
 Saffieddine, Saaid, 295  
 Sagi, Elad, 393  
 Sagong, Borum, 687  
 Sahani, Maneesh, 526  
 Sahlén, Birgitta, 464  
 Sahota, Raguwinder, 725  
 Sakai, Yoshihisa, 742  
 Sakamoto, Shuichi, 411  
 Sakamoto, Takashi, 313, 331, 451  
 Sakamoto, Tatsunori, 1062  
 Sakuraba, Mayumi, 674  
 Salamati, Ehsan, 128  
 Saicher, Rolf, 867  
 Saldaña, Enrique, 250  
 Saleur, Aurélie, 40  
 Saliu, Aminat, 214, 229  
 Sallin, Michelle, 311  
 Salt, Alec N., 617, 620, 832  
 Saltzman, W. Mark, 163  
 Salvi, Richard, 83, 119, 147, 159, 430, 508, 588, 959, 979, 980  
 Samani, Abbas, 128  
 Samson, Fabienne, 372  
 Samuvel, Devadoss, 1069  
 San Roman, Cecilia, 894  
 Sangi-Haghpeykar, Haleh, 900  
 Santi, Peter, 357, 829, 831, 835  
 Santos-Sacchi, Joseph, 187, 188, 189, 296, 421, 735  
 Santurette, Sebastien, 654  
 Sarampalis, Anastasios, 390  
 Sarwar, Azeem, 591  
 Sasse, Anja, 988  
 Sato, Mika, 411  
 Saulnier, Patrick, 992  
 Saunders, Thom, 432  
 Sautter, Nathan, 882  
 Savall, Joan, 999  
 Savel, Sophie, 649  
 Scarborough, John, 310  
 Schachner, Patricia, 179, 876  
 Schachner, Melitta, 971  
 Schacht, Jochen, 337, 974, 981  
 Schachtele, Scott, 168  
 Schaefer, Stefan, 988  
 Schaeffe, Roland, 360  
 Schaffner, Adam, 50  
 Schatzer, Reinhold, 14  
 Scheckmann, Martin, 887  
 Scheetz, Laura, 696  
 Scheffer, Deborah, 925, 1001  
 Scheich, Henning, 466  
 Schendel, Dillon, 784  
 Schepher, Verena, 22, 867  
 Scherer, Elias, 391  
 Scherer, Steve, 301, 935  
 Schick, Bernhard, 718  
 Schillaci, Orazio, 70  
 Schilp, Soeren, 714  
 Schimmang, Thomas, 718  
 Schleiss, Mark, 168  
 Schmitz, Heather, 357, 831, 835  
 Schnee, Michael E., 296, 755, 756  
 Schnitzer, Mark, 999  
 Schnupp, Jan W., 472, 1053  
 Schofield, Brett, 785  
 Schönhof, Uwe, 63  
 Schörmich, Sven, 103, 104  
 Schraner, Michael, 103  
 Schraven, Sebastian, 598  
 Schreiner, Christoph, 481, 547  
 Schrode, Katrina, 1046  
 Schroeder, Charles, 509  
 Schubert, Michael C., 53, 54, 892, 901  
 Schultz, Alan, 1059  
 Schulze, Holger, 467, 501, 502, 745  
 Schwarz, Douglas M., 1045  
 Schweizer, Michaela, 423  
 Scrabble, Heidi, 941  
 Seidman, Michael, 321  
 Selezneva, Elena, 466  
 Selvakumar, Dakshnamurthy, 1004  
 Selvaskandan, Haresh, 236  
 Semaan, Maroun, 175  
 Semal, Catherine, 1052  
 Semple, Malcolm, 262  
 Seo, Jin Kyung, 232, 966  
 Seonwoo, Hoon, 866  
 Sepulveda, Rosalinda, 997  
 Serrador, Jorge, 67  
 Setz, Cristian, 821  
 Seunghyun, Koh, 871  
 Sewell, William F., 316, 996  
 Seymour, Michelle L., 339  
 Sha, Su-Hua, 150, 958, 969, 981  
 Shackleton, Trevor, 114, 516  
 Shaffer, Lauren, 402  
 Shah, Hetel, 765  
 Shah, Priyanka, 321  
 Shaheen, Luke, 260, 1033  
 Shahn, Antoine, 92  
 Shalev, Stavit, 928  
 Shamma, Shihab A., 473, 487, 491, 522, 529, 537, 636, 1075  
 Shanbhag, Sharad, 490  
 Shanthakumar, Prashanthini, 303  
 Shapiro, Ben, 591  
 Shapiro, Mikhail, 610  
 Sharma, Mridula, 1076  
 Shea-Brown, Eric, 611  
 Shearer, A. Eliot, 540, 935  
 Shearer, Eliot, 301  
 Sheehan, Kelly, 723, 819, 820  
 Sheets, Lavinia, 274  
 Sheikh, Ahmad, 707  
 Shelat, Anang, 345  
 Shen, Jun, 747, 925, 1001  
 Shen, Li, 794  
 Shen, Yi, 1073  
 Shen, Zuolian, 582  
 Shepard, Kathryn, 908  
 Shepherd, Gordon M. G., 486  
 Shepherd, Rob, 600  
 Shepherd, Robert, 4, 599, 826  
 Shera, Christopher A., 201, 399, 838  
 Shi, Fuxin, 355, 703  
 Shi, Jianrong, 74  
 Shi, Lijuan, 152  
 Shi, Wei, 254  
 Shi, Xiaorui, 704, 709, 945, 946, 947, 951, 968, 1008  
 Shibata, Seiji, 235, 618  
 Shibata, Shinsuke, 674, 995  
 Shibata, Shumei, 921  
 Shih, Jonathan, 547  
 Shim, Hyun joon, 890  
 Shimizu, Takahiko, 326  
 Shimogori, Hiroaki, 41, 42, 328, 438, 902  
 Shin, Jung-Bum, 454, 578  
 Shin, Minyoung, 49  
 Shinn-Cunningham, Barbara G., 219, 484, 637  
 Shintaku, Hirofumi, 1062  
 Shiotani, Akihiro, 717  
 Shivatzki, Shaked, 1007  
 Shnyder, Yelizaveta, 158  
 Shohat, Mordechai, 928  
 Shomron, Noam, 928  
 Shore, Susan, 86, 234, 235, 252, 782  
 Shpargel, Karl, 308  
 Shrestha, Bibesh, 475  
 Shreve, Lauren, 234  
 Shu, Yilai, 153  
 Siddiq, Aiysha, 1075  
 Siegel, Bianca, 321

- Siegel, Jonathan, 32, 100, 396, 397, 398, 841, 850
- Sihn, Choong Ryoul, 427, 429
- Sihn, Choongryoul, 428
- Silverman, Joshua, 903
- Sim, Jae Hoon, 1022
- Simmons, Dwayne D., 750, 822
- Simogoori, Hiroaki, 973
- Simon, Jonathan Z., 491, 530, 636
- Simoncelli, Eero, 107
- Simonoska, Rusana, 852, 853
- Simpson, Brian D., 373, 376
- Singer, Wibke, 718, 886
- Sinha, Ghanshyam P., 141
- Sininger, Yvonne, 498
- Sinkkonen, Saku, 662
- Sipe, Conor, 270
- Sirimanna, Tony, 176
- Siveke, Ida, 117, 259
- Skoe, Erika, 225
- Slama, Michaël, 260, 1033
- Slattery, William, 993
- Slayman, Clifford, 188
- Slee, Sean, 778, 790
- Sliwinka-Kowalska, Mariola, 727
- Sloan, David M., 250
- Slowik, Amber, 697
- Sly, David, 600
- Smalt, Christopher J., 218, 222, 226
- Smans, Joleit, 1032
- Smeds, Henrik, 320
- Smith, Benn, 897
- Smith, Elliot, 19
- Smith, Felicia L., 766, 1027
- Smith, Kristen, 500
- Smith, Lynette, 696
- Smith, Michael, 1000
- Smith, Rachel, 370
- Smith, Richard, 301, 540, 935, 937
- Snik, Ad, 660, 1060
- Snyder, Joel, 404, 405, 860
- Snyder, Russell, 613
- Soares, Danny J., 171
- Sohn, Inkyung, 866
- Sokolowski, Bernd, 742
- Sokolowski, Sophia, 742
- Solanki, Krupa, 1047
- Son, Eun Jin, 663
- Song, Haiyan, 74
- Song, Jae-Jun, 877
- Song, Lei, 421
- Song, Mee Hyun, 615
- Song, Won Joon, 27
- Songer, Jocelyn, 812
- Sonntag, Mandy, 213
- Sorensen, Janna, 148
- Soto, Enrique, 425, 808
- Sotta, Gonzalo, 894
- Soucek, Sava, 910
- Soukup, Garrett, 325, 924, 1009
- Souter, Melanie, 712
- Spector, Alexander, 575
- Spencer, Nathaniel, 113
- Spiden, Sarah, 145
- Spinelli, Kateri, 1002
- Spirou, George, 215
- Srinivasan, Arthi G., 394, 395
- Srinivasan, Nirmal, 548
- Srinivasan, Ramya, 186
- Srinivasan, Varadamurthy, 941
- Staecker, Hinrich, 365, 593, 693
- Stagner, Barden, 97, 98, 840
- Stakhovskaya, Olga, 555, 557, 619
- Stange, Annette, 117, 259
- Stankovic, Konstantina M., 154, 318, 943, 972
- Stare, Jerneja, 706
- Stark, Thomas, 202, 391
- Starr, Arnold, 627
- Stebbing, Kevin, 334
- Stecker, G. Christopher, 648
- Steel, Karen P., 145, 302, 306, 937, 938
- Steele, Charles, 203, 208, 574
- Stefanovic, Aleksandra, 459
- Steffes, Georg, 145
- Steigelman, Katherine A., 682, 1064, 1066
- Steiner, Claudia A., 312
- Steinschneider, Mitchell, 489, 515, 532
- Stepanek, Jan, 897
- Stepanyan, Ruben, 141, 585, 962
- Stephan, Thomas, 103
- Sterkers, Olivier, 553, 994
- Stewart, Charles, 726, 731
- Stewart, Colin L., 1007
- Steyger, Peter, 419, 443, 975, 976
- Stimmler, Sarah, 139
- Stift, Iain, 48
- Stock, Stuart, 551
- Stoelb, Corey, 384
- Stoelv, Martin, 75
- Stoller, Michelle L., 668
- Stone, Jennifer, 695, 1065
- Stöver, Timo, 22
- Strahl, Stefan B., 618, 1029
- Strait, Dana, 223
- Straka, Malgorzata, 784
- Streeter, Timothy, 111
- Strelyck, Olaf, 1050
- Strenzke, Nicola, 757
- Strickland, Elizabeth, 626
- Strimbu, Elliott, 460
- Strömbäck, Karin, 320
- Strome, Scott, 308, 311
- Su, Gina L., 618
- Su, Yi-Ning, 169
- Suarez, Alejo, 894
- Suarez, Hamlet, 894
- Subhash, Hreshesh M., 30, 1017
- Sugahara, Kazuma, 41, 42, 328, 438, 902, 973, 987
- Sugahara, Satoko, 265
- Sugamura, Mayumi, 864, 983
- Suh, Myung-Whan, 721
- Sullivan, Sarah C., 376
- Sullivan, Susan, 256
- Sultemeier, David, 39, 986
- Summerfield, A. Quentin, 77
- Sumner, Chris, 798
- Sun, Hong, 979
- Sun, Huifang, 1000
- Sun, Sean, 575
- Sun, Shuting, 996
- Sun, Wei, 147, 781
- Sun, Willy, 685
- Sun, Xiao-Ming, 861
- Sun, Yuxiang, 339
- Sunami, Kishiko, 66, 68
- Sung, Yolin, 498
- Sunghuhn, Kim, 871
- Surguchev, Alexei, 735, 736, 743
- Suri, Ranjan, 176
- Surlykke, Annemarie, 545
- Suta, Daniel, 514
- Sutton, Griffin, 860
- Suzuki, Mitsuya, 331
- Suzuki, Yo-iti, 411
- Svedbrant, Johan, 852
- Svirsky, Mario, 13, 393
- Swanson, Brett, 15
- Sweeney, Alex, 186
- Swiderski, Donald L., 818
- Syda, Josef, 78, 514, 923
- Tabei, Ken-Ichi, 471
- Tabuchi, Keiji, 977, 978
- Tada, Hirobumi, 674
- Tadros, Melissa, 739
- Taira, Masato, 471
- Takahashi, Masatoki, 333
- Takase, Hisamitsu, 864
- Takekuma, Chihiro, 417, 1079
- Taketo, Makoto, 344
- Takubo, Keiyo, 681
- Talamo, Maria Victoria, 715
- Talavage, Thomas M., 222
- Talmadge, Carrick, 101
- Tam, William, 786
- Tan, Chin-Tuan, 13, 393
- Tan, Hongyang, 95
- Tanaka, Chiemi, 392
- Tanaka, Masashi, 931
- Tang, Jie, 190
- Tang, Tanye, 39
- Tang, Wenxue, 420, 539, 985
- Tang, Xuehui, 46
- Tang, Yong, 332, 1030
- Tang, Zheng-Quan, 254
- Taniguchi, Mirei, 352
- Tanimoto, Hitoshi, 146
- Tapp, Rachel, 151
- Tateya, Ichiro, 918
- Tateya, Tomoko, 918
- Taylor, Ruth, 689
- Teki, Sundeep, 1074, 1075
- Telisch, Fred F., 162, 714
- Tellers, Philipp, 506
- Tempel, Bruce L., 239, 241
- Theorell, Töres, 375, 854
- Thomas, Holly, 849
- Thomas, Jessica M., 90
- Thomas, Lisa, 101
- Thomas, Paul, 461
- Thompson, Eric R., 111, 376, 410
- Thoreson, Wallace, 293
- Thornton, Jennifer, 119, 123
- Thorp, Elias, 1071
- Thorpe, Roland, 73
- Tian, Chunjie, 866
- Tickner, Jennifer, 335
- Tideholm, Bo, 320
- Tierney, Adam, 91
- Tillein, Jochen, 24, 381, 505
- Tobias, Moser, 757
- Todd, Dylan, 710
- Todd, N Wendell, 132
- Tokita, Joshua, 765
- Tollin, Daniel, 119, 123, 261, 597
- Tomoriova, Beata, 655
- Tong, Ling, 695, 909
- Torii, Hiroko, 914
- Toupet, Michel, 899
- Towers, Emily, 825
- Toyota, Hideki, 41, 42, 973
- Tozer, Adam, 239
- Trachte, George, 456
- Trahiotis, Constantine, 634
- Tran, Vy M., 155
- Trattner, Barbara, 209
- Travo, Cécile, 40
- Treviño-Villareal, Humberto, 997
- Trexler, Maria, 934
- Trinh, Le, 664
- Trowe, Mark-Oliver, 423
- Trujillo, Michael, 517
- Trune, Dennis, 439, 828, 865, 872, 873, 878, 882, 946
- Trussell, Laurence, 242
- Tsuchihashi, Takatoshi, 671
- Tsuda, Junko, 328
- Tsuprun, Vladimir, 876
- Tsuyuguchi, Naohiro, 68
- Tsuzaki, Minoru, 417, 1079
- Tucci, Debara L., 5
- Tuft, Bradley, 762, 763
- Turcan, Sevin, 137
- Turner, Christopher, 1, 563
- Turner, Jeremy, 334, 590, 594
- Tward, Daniel J., 500
- Ty, Sida, 351
- Tziridis, Konstantin, 501, 502, 745
- Tzounopoulos, Thanos, 359, 486
- Uchikawa, Masanori, 265
- Uemaetomari, Isao, 978
- Uhlén, Inger, 664
- Ulfendahl, Mats, 336, 769
- Ulrich, Felicitas, 867
- Undurraga, Eduardo, 1059
- Urban, Zsolt, 933
- Urdang, Zachary, 951
- Uribe, Phillip, 443
- Urness, Lisa, 686
- Ushio, Munetaka, 891
- Usubuchi, Hajime, 956
- Vachhani, Jay J., 635
- Valentin, Nicolas S., 55
- Valentine, Marc, 682, 1064
- Valko, Yulia, 572
- Valverde, Ángela, 433
- van Barneveld, Denise, 660
- Van de Heyning, Paul, 14
- Van De Water, Thomas, 162, 714, 715
- van der Heijden, Marcel, 257, 1012, 1032
- van Dijk, Pim, 82, 87
- Van Ee, Raymond, 1078
- van Grootel, Tom, 660
- Van Hoorebeke, Luc, 134
- van Opstal, John, 494, 660, 1060, 1078
- Van Waes, Carter, 161
- van Wanrooij, Marc, 494, 660, 1060
- van Wetter, Sigrid, 494
- VandeBerg, John, 342
- Vandevord, Pamela, 586, 587, 885
- Vanpoucke, Filiep, 556
- Vanya, Robert, 64
- Varela-Nieto, Isabel, 433
- Varvares, Alexis, 166
- Varvares, Tessa, 167
- Vauchel, Thomas, 553
- Vazdarjanova, Almira, 534
- Vega, Rosario, 425
- Vélez-Ortega, A. Catalina, 141
- Velkey, J. Matthew, 1034
- Vellinga, Dirk, 556
- Velluti, Ricardo, 109, 366
- Venselaar, Hanka, 934
- Verhey, Jesko L., 408, 414, 1058
- Verhoeven, Kristien, 620
- Verhulst, Sarah, 34, 106
- Verhulst, Steven, 728
- Verma, Rohit U., 606
- Vermeire, Katrien, 14, 561
- Verschooten, Eric, 1028
- Versnel, Huib, 494, 1029, 1078
- Versteegh, Corstiaen P.C., 1012, 1032
- Vetter, Douglas, 137
- Viberg, Agneta, 165
- Videhult Pierre, Pernilla, 858
- Vielsmeier, Veronika, 887
- Viemeister, Neal, 112
- Villarreal, Sebastian, 610
- Villaume, Karin, 888
- Trujillo, Daniel, 14
- Viswanathan, Sarada, 485
- Vlaming, Marcel, 1081
- Vogel, Joseph, 868
- Volkenstein, Stefan, 552
- Vollmer, Maïke, 564
- Vollrath, Melissa, 706
- von Gersdorff, Henrique, 292
- von Mentzer, Cecilia, 464
- von Unge, Magnus, 350
- Voormolen, Maurits, 14
- Vozzi, Diego, 300
- Vriend, Gert, 934
- Vu, Ly, 162
- Wada, Hiroshi, 1062
- Wagner, Hermann, 506, 640
- Wagner, Jan, 705
- Wahlberg, Magnus, 103
- Wakabayashi, Ken-ichiro, 952
- Wakefield, Gregory, 111
- Walker, Kerry, 472
- Wallace, Mark, 803
- Wallace, Matthew, 789
- Wallmeier, Ludwig, 104
- Walsh, Edward, 139, 325, 696, 1009
- Walsh, Tom, 541
- Walters, Brad, 342
- Walters, Brandon, 682, 694
- Walton, Joseph, 327
- Wan, Eric A., 401
- Wan, Guoqiang, 749
- Wang, Han Chin, 760
- Wang, Jian, 152, 960
- Wang, Jianjun, 985
- Wang, Jing, 160, 332, 992, 1030
- Wang, Kevin, 443
- Wang, Le, 582, 775
- Wang, Lingyan, 677, 678, 740
- Wang, Qi, 419, 443, 975
- Wang, Qiong, 273, 710
- Wang, Ruikang, 30, 704, 1017
- Wang, Tian, 419, 1067, 1068
- Wang, Wenyang, 427
- Wang, Xiaobo, 998
- Wang, Xiaoqin, 533, 549
- Wang, Yimin, 74
- Wang, Yong, 227, 317
- Wang, Yuan, 238, 241, 255
- Wang, Yunfeng, 985
- Wang, Zhengming, 153
- Wangemann, Philine, 458, 948, 949
- Warchol, Mark, 267, 698, 1065
- Ward, Bryan K., 807, 904
- Washizawa, Shihoh, 633
- Watabe, Takahisa, 671
- Watanabe, Yoshiaki, 644
- Watson, Bracie, 256
- Watson, Richard P. W., 1053
- Watts, Melissa M., 618
- Wayne, Rachel, 371
- Webster, Paul, 140, 874
- Wei, Benjamin P., 177
- Wei, Min, 287
- Wei, Shun-Hwa, 65
- Wei, Vincent, 1055
- Wei, Wei, 893
- Weichert, Rachel M., 347, 702
- Weinberger, Norman, 468, 483
- Weiner, Benjamin D, 85
- Weintraub, David, 404, 405
- Weisz, Catherine, 135, 752
- Welgampola, Miriam, 895
- Wells, Gregg B., 198
- Wells, Sara, 303
- Wells, Toby, 798
- Wen, Bo, 1031
- Wensel, Theodore, 186
- Wenstrup, Jeffrey, 490, 801, 1042
- Werner, Lynne, 1056, 1061
- Wersinger, Eric, 751, 810
- Westendorf, Sarah, 44
- Westerlund, Hugo, 375
- Weston, Michael D, 661
- Wheaton, Melissa, 101
- Whitcomb, Carolyn, 147
- White, Mark, 600
- White, Patricia, 724
- Whitton, Donna S., 768
- Whitmer, William, 646
- Whitney, Susan, 898
- Whitton, Jonathon, 1048
- Wickesberg, Robert, 413
- Wiegner, Armin, 564
- Wiegrebe, Lutz, 103, 104
- Wilch, Ellen, 932
- Williams, Anthony, 787, 792
- Williams, Deborah, 1075
- Williams, Diane, 454
- Wilson, Angus, 275
- Wilson, Blake, 5
- Wilson, Teresa M., 193, 709, 740, 865, 968
- Windsor, Alanna, 903
- Winkowski, Daniel, 522
- Winter, Ian M., 1058

- Wisby, Laura, 303  
Wise, Andrew, 2, 826  
Wismer, Zachary Q, 766  
Wohlgemuth, Melville, 643  
Wojtczak, Magdalena, 624  
Woldorff, Marty, 5  
Wolf, Michael, 640  
Won, Jong Ho, 23, 562, 1056  
Wong, Hiu Tung, 690, 691, 818  
Wong, Jau-Min, 420  
Woo, Jeong-Im, 435, 436, 874  
Wood, Scott, 63, 64, 67, 283  
Woodfield, Alexandra, 415  
Wright, Beverly A., 412  
Wright, Charles G., 319  
Wright, David, 139  
Wright, Samantha, 246  
Wrzeszcz, Antonina, 621  
Wu, Calvin, 475  
Wu, Chen-Chi, 169, 420, 930  
Wu, Doris, 265, 580, 581, 680, 927  
Wu, Jonathan, 215  
Wu, Julie, 921  
Wu, Ling, 663, 687  
Wu, Sean, 84  
Wu, Tao, 193, 740  
Wu, Xuewen, 979  
Wynne, Dwight, 627  
Xia, Anping, 344, 1067, 1068  
Xia, Jing, 418  
Xiang, Yongqing, 50  
Xie, Jing, 974  
Xie, Ruili, 230  
Xing, Yazhi, 1069  
Xiong, Hao, 886  
Xu Parks, Xiaorong, 43  
Xu, Helen, 761, 936  
Xu, Jishu, 298  
Xu, Li, 378  
Xu, Linjing, 762, 763  
Xu, Yinfang, 280, 281, 282  
Xu, Yougou, 893  
Xu-Friedman, Matthew, 251  
Yakushin, Sergei B., 50, 51, 52  
Yamagishi, Takayuki, 671  
Yamamoto, Hidefumi, 66, 68  
Yamamoto, Norio, 352, 814, 816, 914, 967  
Yamane, Hideo, 66, 68  
Yamano, Takafumi, 864, 983  
Yamashita, Daisuke, 146, 172  
Yamashita, Hiroshi, 41, 42, 328, 438, 902, 973, 987  
Yamasoba, Tatsuya, 313, 326, 331, 638, 891  
Yamoah, Ebenezer N., 422, 427, 428, 429  
Yang, Amy, 1034  
Yang, Bin, 881  
Yang, Guang, 378  
Yang, Hua, 251  
Yang, Hyungchae, 732  
Yang, Jun, 582  
Yang, Liping, 281  
Yang, Shiming, 584, 716  
Yang, Sungchil, 85  
Yang, Tian, 273  
Yang, Wanwan, 993  
Yang, Weiyang, 716  
Yang, Won Sun, 615  
Yang, Xin, 154  
Yang, Yue, 968  
Yang, Yuqin, 419, 944, 950  
Yang, Ziheng, 234, 235  
Yao, Jun, 519  
Yasin, Ifat, 414, 622  
Yasuda, Akimasa, 995  
Yasui, Takuya, 313  
Yatteau, Andrew, 681  
Ye, Keqiang, 990  
Yeo, Sang Won, 700, 957  
Yin, Haifeng, 266  
Yin, Ping-Bo, 537  
Yin, Shan-Kai, 378  
Yin, Tom, 647, 659  
Ylikoski, Jukka, 883  
Yoder, Joshua, 151  
Yoon, Heejei, 663  
Yoshida, Atsuhiko, 914, 967  
Yoshida, Shuhei, 42, 438  
Young, Eric, 778, 786, 790  
Yrttiaho, Santeri, 883  
Yu, Ah Ram, 896  
Yu, Cathy, 728  
Yu, Heping, 175, 310, 881  
Yu, Lu-Ming, 206  
Yu, Ning, 716  
Yu, Qing, 990  
Yu, Yiling, 682  
Yu, Zitian, 794  
Yuan, Yasheng, 355  
Yue, Wei Ying, 764  
Yumoto, Masato, 518  
Zachariah, Nishant, 790  
Zacharias, Norman, 470  
Zahorik, Pavel, 105, 264, 548  
Zallocchi, Marisa, 166, 919, 920  
Zappala, David, 897  
Zarate, Jean M., 374  
Zecker, Steve, 108, 850  
Zeng, Chunhua, 234, 235  
Zeng, Fan-Gang, 558, 627  
Zenisek, David, 297  
Zenner, Hans-Peter, 598  
Zha, Dingjun, 1015, 1017, 1019  
Zhai, Suoqiang, 716  
Zhang, Fawen, 20  
Zhang, Hongyu, 365  
Zhang, Hui, 280  
Zhang, Huiming, 364  
Zhang, Jinsheng, 84, 88, 358, 586, 587, 589, 885  
Zhang, Kang, 7  
Zhang, Kechen, 533, 786  
Zhang, Lei, 348  
Zhang, LingLi, 144, 682, 694, 1006, 1066  
Zhang, Ming, 859  
Zhang, Qian, 325, 584  
Zhang, Wenjing, 945, 946, 947  
Zhang, Xiangming, 31, 879  
Zhang, Xueguo, 84, 88, 358, 589, 885  
Zhang, Yan, 280, 281, 881  
Zhang, Yang, 112  
Zhang, Yuan, 1017  
Zhang, Yu-Xuan, 407, 1072  
Zhao, Hong-Bo, 142, 143, 174, 307  
Zhao, Hongyu, 454  
Zhao, Ken, 607  
Zhao, Lijun, 79  
Zhao, Wei, 224  
Zhao, Xing, 280, 281  
Zheng, Jing, 138, 192, 913  
Zheng, Lili, 452, 583  
Zheng, Qing, 175, 881  
Zheng, Qing Yin, 310  
Zheng, Ye, 310  
Zheng, Yi, 383  
Zheng, Yiqing, 881  
Zheng, Yuxi, 175  
Zhi, Zhongwei, 704  
Zhong, Sheng, 187  
Zhou, Binfei, 985  
Zhou, Ning, 378, 379  
Zhou, Wu, 46, 893  
Zhou, Xiang, 393  
Zhou, Yufeng, 188  
Zhu, Hong, 46, 893  
Zhu, Juhong, 1069  
Zhu, Na, 84  
Zhu, XiaoXia, 327, 616  
Zhu, Yan, 142, 143, 174, 307  
Zierhofer, Clemens, 14  
Zindy, Frederique, 694  
Zoefel, Benedikt, 408  
Zong, Liang, 143, 174, 307  
Zorrilla de San Martín, Javier, 758  
Zosuls, Aleks, 1016  
Zou, Junhuang, 582  
Zuccotti, Annalisa, 718, 886  
Zuk, Patricia, 986  
Zuniga, M. Geraldine, 892, 895, 901  
Zuo, Jian, 144, 342, 344, 345, 682, 694, 1006, 1064, 1066, 1068

**Association for Research in Otolaryngology**

Executive Offices  
19 Mantua Road  
Mt. Royal, NJ 08061

Phone: (856) 423-0041

Fax: (856) 423-3420

E-mail: [headquarters@aro.org](mailto:headquarters@aro.org)

Website: [www.aro.org](http://www.aro.org)